Petroleum Geology of North Africa

edited by D. S. Macgregor, R. T. J. Moody and D. D. Clark-Lowes

Geological Society
Special Publication
No. 132

Published by The Geological Society

Petroleum Geology of North Africa

Geological Society Special Publications

Series Editor A. J. FLEET

GEOLOGICAL SOCIETY SPECIAL PUBLICATION NO. 132

Petroleum Geology of North Africa

EDITED BY

D. S. MACGREGOR
BP Indonesia

R. T. J. MOODY
Moody-Sandman Associates, Kingston, UK

and

D. D. CLARK-LOWES
Imperial College, University of London, UK

1998

Published by

The Geological Society

London

THE GEOLOGICAL SOCIETY

The Society was founded in 1807 as The Geological Society of London and is the oldest geological society in the world. It received its Royal Charter in 1825 for the purpose of 'investigating the mineral structure of the Earth'. The Society is Britain's national society for geology with a membership of around 8000. It has countrywide coverage and approximately 1000 members reside overseas. The Society is responsible for all aspects of the geological sciences including professional matters. The Society has its own publishing house, which produces the Society's international journals, books and maps, and which acts as the European distributor for publications of the American Association of Petroleum Geologists, SEPM and the Geological Society of America.

Fellowship is open to those holding a recognized honours degree in geology or cognate subject and who have at least two years' relevant postgraduate experience, or who have not less than six years' relevant experience in geology or a cognate subject. A Fellow who has not less than five years' relevant postgraduate experience in the practice of geology may apply for validation and, subject to approval, may be able to use the designatory letters C Geol (Chartered Geologist).

Further information about the Society is available from the Membership Manager, The Geological Society, Burlington House, Piccadilly, London W1V 0JU, UK. The Society is a Registered Charity, No. 210161.

Published by The Geological Society from:
The Geological Society Publishing House
Unit 7, Brassmill Enterprise Centre
Brassmill Lane
Bath BA1 3JN
UK
(*Orders*: Tel. 01225 445046
Fax 01225 442836)

First published 1998
Reprinted 2001

British Library Cataloguing in Publication Data
A catalogue record for this book is available from the British Library.

ISBN 1-86239-004-5

Typeset and printed by Alden Group, Oxford, UK.

Distributors
USA
AAPG Bookstore
PO Box 979
Tulsa
OK 74101-0979
USA
(*Orders*: Tel. (918) 584-2555
Fax (918) 560-2652)

Australia
Australian Mineral Foundation
63 Conyngham Street
Glenside
South Australia 5065
Australia
(*Orders*: Tel. (08) 379-0444
Fax (08) 379-4634)

India
Affiliated East-West Press PVT Ltd
G-1/16 Ansari Road
New Delhi 110 002
India
(*Orders:* Tel. (11) 327-9113
Fax (11) 326-0538)

Japan
Kanda Book Trading Co.
Tanikawa Building
3-2 Kanda Surugadai
Chiyoda-Ku
Tokyo 101
Japan
(*Orders*: Tel. (03) 3255-3497
Fax (03) 3255-3495)

Contents

Introduction

DUNCAN S. MACGREGOR

BP Exploration Operating Co. Ltd, Kuningan Plaza, S. Tower, P.O. Box 2749, Jakarta 12940, Indonesia

This Special Publication of the Geological Society documents a series of papers collected on the petroleum geology of Morocco, Algeria, Tunisia, Libya and the western part of Egypt. This region contains some 4% of the world's remaining oil and gas reserve (Table 1), placing the area above more traditional producing regions, including Europe, the USA and SE Asia, in its importance as a future petroleum producer. In addition to these considerable proven reserves, North Africa is now one of the world's most active exploration areas. This was reflected, for instance, in more new oil reserves being 'booked' in Algeria in 1994 than in any other country in the world.

The importance of the region to the petroleum industry is, of course, not reflected in the volume of geological literature available on the area, particularly that in English. This volume represents the first such attempt at a compilation of the petroleum geology of this region. The main objectives of this book are thus to increase the level of documentation towards that appropriate for such major petroleum provinces and to facilitate the application of analogues between North African countries and beyond.

Table 1. *North African petroleum reserves and their global significance*

Rank	Country	Reserves (10^9 BBO)
Oil reserves (remaining)		
1	Saudi Arabia	261.2
2	Iraq	100.0
3	United Arab Emirates	98.1
4	Kuwait	96.5
5	Iran	88.2
6	Venezuela	64.5
7	Mexico	49.8
8	Russia*	49.0
9	USA*	29.6
10	*Libya*	*29.5 (2.9% of world total)*
11	China	24.0
12	Nigeria	20.8
13	*Algeria**	*9.2 (0.9% of world total)*
–	*Egypt (inc. Gulf of Suez)*	*3.9 (0.4% of world total)*
–	*Tunisia*	*0.4 (<0.1% of world total)*
Rank	Country	Reserves (10^{12} SCF)
Gas reserves (remaining)		
1	Russia*	1700
2	Iran	742
3	Oman	250
4	United Arab Emirates	205
5	USA*	164
6	Venezuela	140
7	*Algeria**	*128 (2.6% of world total)*
8	Nigeria	110
9	Iran	110
10	Indonesia	69
19	*Libya*	*46 (0.9% of world total)*
–	*Egypt (inc. Gulf of Suez)*	*22 (0.4% of world total)*

*Areas with significant Palaeozoic–Triassic reservoired component to reserves.
Source: *BP Statistical Review of World Energy, 1996*, data as at end 1995. BBO, Billion barrels of oil; SCF, standard cubic feet.

MACGREGOR, D. S. 1998. Introduction. *In*: MACGREGOR, D. S., MOODY, R. T. J. & CLARK-LOWES, D. D. (eds) 1998. *Petroleum Geology of North Africa*. Geological Society, London, Special Publication No. 132, 1–6.

It has been our mission, in seeking papers for this volume, to try to obtain a full and representative set of papers covering different regions and themes. Thus we sought both full coverage of the stratigraphic column (Fig. 1) and as wide as possible geographical coverage (Fig. 2). Particular encouragement was given to authors from North Africa to submit previously unpublished material on the oilfields and gas fields of the region. In this regard, we particularly acknowledge the contribution from Sonatrach, which, with six papers, is overwhelmingly the predominant contributor to the volume.

As the aims of this book are to encourage the use of analogues over national boundaries, we have avoided grouping the papers geographically. Instead, we have first split the papers stratigraphically into 'Palaeozoic and sub-salt' and 'Mesozoic–Cenozoic' sections (Fig. 2). This division is justified both by the structural history of the area, which would suggest a partition at the Hercynian unconformity (Fig. 3), with a modification to this boundary suggested by reviewing source–reservoir associations, such that discussions on the sub-salt Triassic reservoir of Algeria are most rationally included in the 'Palaeozoic' category. Overview papers are presented for each of the two stratigraphic sections thus defined and are followed in each case by regional papers, covering topics such as petroleum systems, stratigraphy and regional structure, and those relating to individual reservoirs, fields and play fairways. Because of its unique structural history and play types, the Atlas region is assigned a separate sub-section within the Mesozoic–Cenozoic category. The Gulf of Suez and Nile Delta petroleum provinces are not strictly included in the region covered by this book, but are touched on in some papers, particularly that by **Keeley & Massoud**.

Palaeozoic and sub-salt

The North Africa region is perhaps best known in international geological circles for its Palaeozoic reservoirs and source rocks (Figs 1 and 3). The Palaeozoic and sub-salt contribute nearly half the oil (43%) and the vast majority (84%) of the gas reserves of the region (Figs 4 and 5), with most of this petroleum originating from Silurian and Devonian source beds (Fig. 3).

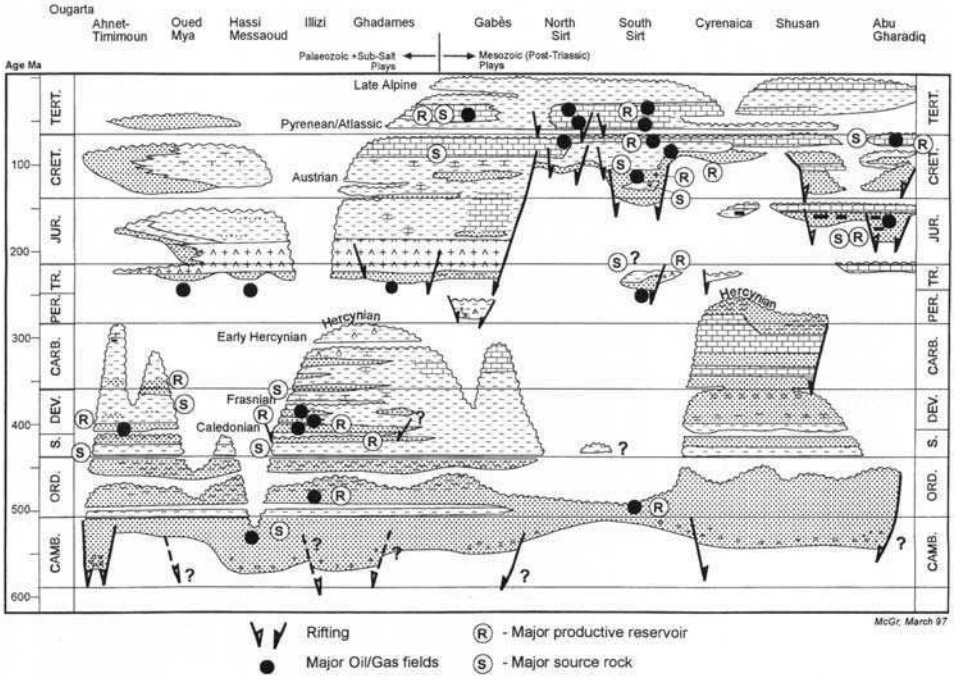

Fig. 1. Chronostratigraphy of the Phanerozoic of the main North African petroleum provinces, as compiled from various papers in this volume. The most significant oilfields, reservoirs and source rocks are labelled. Papers in this volume are split into those pertinent to the petroleum systems below the salt in the west of the region and those on the Mesozoic systems in the east of the region. (For line of section, see Fig. 2.)

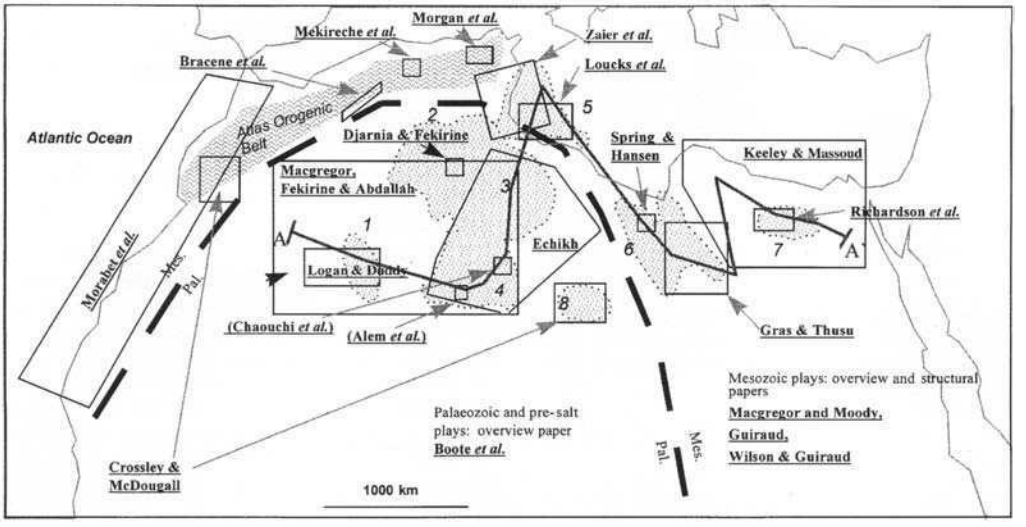

Fig. 2. Geographical coverage of the papers in this volume. The main petroleum basins are stippled and numbered as follows: 1, Ahnet; 2, Oued Mya; 3, Ghadames; 4, Illizi; 5, Gabes–Pelagian; 6, Sirt; 7, Abu Gharadiq; 8, Murzuq.

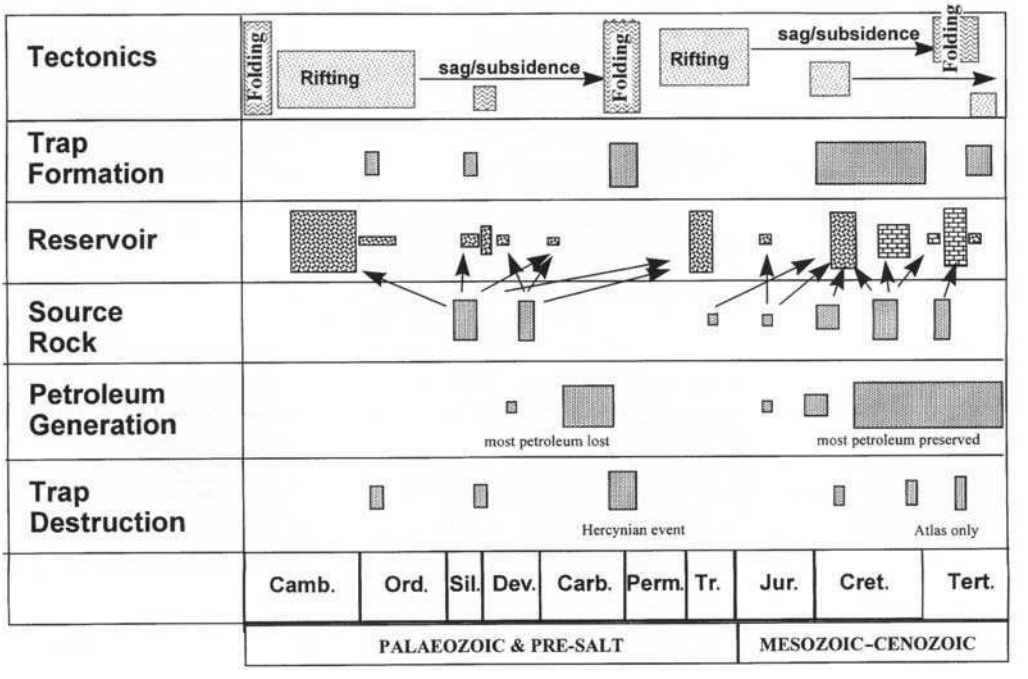

Fig. 3. Composite petroleum system diagram for the North African provinces. The boxes are sized according to the relative importance of the various reservoirs, source rocks and events. It is possible to differentiate two main plate tectonic cycles, Cambrian to Carboniferous and Triassic to Recent, which are also reflected in cycles of petroleum generation, entrapment and destruction.
*Existing hydrocarbon-bearing traps only.

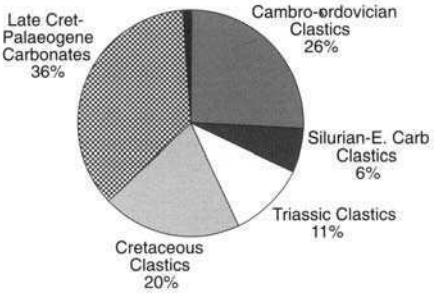

Fig. 4. Pie chart illustrating distribution of oil reserves amongst the main reservoir fairways of North Africa. The predominance of Mesozoic–Cenozoic reservoirs should be noted.

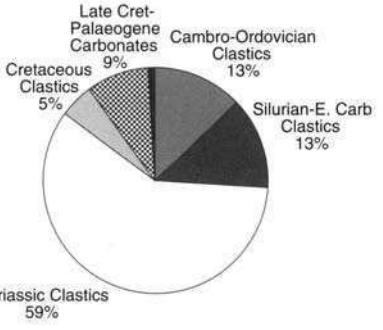

Fig. 5. Pie chart illustrating distribution of gas reserves amongst the main reservoir fairways of North Africa. The predominance of Palaeozoic and Triassic reservoirs should be noted. The more gas-prone nature of these reservoirs is related to the state of maturity of Palaeozoic source and rocks, and timing relationships between that maturity and the formation of traps.

With the exception of the Amal and a few associated fields in the Sirt Basin (**Gras & Thusu**), Palaeozoic production comes almost exclusively from the western part of the region, particularly Algeria (Figs 1 and 2). **Boote *et al.*** open this section with a comprehensive overview of Palaeozoic petroleum systems, based on a series of detailed play maps delineating the main producing plays in the Cambro-Ordovician, Early Devonian and Triassic, sourced mainly from the Early Silurian and Late Devonian. **Traut *et al.*** then detail the long exploration history of these plays. In another overview paper, devoted mainly to the largest petroleum fields within these Palaeozoic petroleum systems, **Macgregor** examines regularities in the main producing fields, and considers the possible nature of the giant fields that may still lie undiscovered in this region. **Fekirine & Abdallah** concentrate on the stratigraphic development and sequence stratigraphy of the Algerian Palaeozoic, work which emphasizes the unusually strong role that eustasy plays in controlling facies development in this cratonic area. A complementary paper by **Echikh** attempts a similar understanding of the Ghadames Basin; this study extends into Libya and notes a number of key differences with the parts of Algeria reviewed by **Fekerine & Abdallah**, particularly the more significant role of the Caledonian event in the Ghadames area. The extension of the Palaeozoic petroleum systems productive in Ghadames and Illizi into the frontier basins to the west is the subject of a paper by **Logan & Duddy**, who emphasize the significance in these areas of timing of generation relative to trap formation. This paper emphasizes the contribution that modern techniques, in this case apatite fission track analysis, can make to frontier exploration in North Africa. The interpretation by these authors of a late-stage heating event of large regional extent is one which has major significance for our view of the prospectivity of western Algeria.

Cambro-Ordovician clastic reservoirs contribute 26% of the oil and 13% of the gas in North Africa (Figs 4 and 5), with the region having higher reserves in rocks of this age than any other region of the world. **Crossley & McDougall** open the review of Palaeozoic reservoirs by summarizing some of the key points controlling reservoir quality and distribution in the Lower Palaeozoic, based on literature and their own outcrop studies in Morocco. These authors also emphasize the potential for subtle trap discoveries in the future, on grounds independent of those used by **Macgregor**.

Most of the Cambro-Ordovician reserves lie in a single field, Hassi Messaoud. The controls on the producibility of these reservoirs in the area of that field are reviewed by **Djarnia & Fekirine**. This work illustrates the importance of clay mineralogy as a control on permeability, and identifies relationships to clay type and content similar to those described in the Rotliegendes of the Southern North Sea.

The clastic section ranging from latest Silurian to Early Carboniferous delivers 11% of North African oil and 13% of gas (Figs 4 and 5), with most of this contribution coming from the Early Devonian of the Illizi area (Fig. 2). These reservoirs are addressed by three papers. In each case, reservoir quality is shown to be sporadic and generally facies controlled, although in his overview of these reservoirs, **Echikh** also emphasizes the importance of diagenetic pro-

cesses, for instance the favourable influence of grain coating chlorite. The F6 reservoir of the Tin Fouyé–Tabankort field, which straddles the Silurian–Devonian boundary, is the subject of a paper by **Alem *et al.*** In addition to sedimentological controls, the key feature of this hydrocarbon occurrence is the hydrodynamic influence on oil entrapment. A further subtle trap analogue in the Middle Devonian of the Alrar stratigraphic trap is presented by **Chaouchi *et al.***: here facies variations control not only the distribution of reservoir quality but also entrapment itself.

There is no specific paper in this volume dealing with the sub-salt Triassic fluvial reservoir system, which delivers 11% of the oil and a staggering 59% of the gas of the region. The giant Hassi R'Mel field is here the main contributor. Most of the key controls on this fairway are, however, covered in the overview and regional papers, with **Boote *et al.*** summarizing the petroleum system involved, **Macgregor** the features of the main fields and **Echikh** the regional sedimentary model for these reservoirs and the sourcing model for the recent finds in the central Ghadames Basin. This model of long-distance migration from Silurian and Devonian subcrops to the Hercynian unconformity forms an important analogue for other areas which might not appear prospective at first glance.

Mesozoic–Cenozoic section

The Mesozoic section agains opens with an overview paper (**Macgregor & Moody**), aimed at introducing the reader to the Mesozoic–Cenozoic tectonic cycle and the basics of its petroleum geology. Mesozoic prospectivity extends over all coastal and offshore areas of North Africa and over the Atlas belt, which is dealt with in a separate sub-section. The structural history of Mesozoic basins is better controlled than for the Palaeozoic and is presented in two complementary papers by **Guiraud** and **Wilson & Guiraud**. These papers provide invaluable compilations of our understanding of the rifting patterns which led to the Mesozoic basin and the associated volcanism, and will be invaluable references for these involved in predicting the deep stratigraphy of many basins and the history of heat flow development within these. These two papers are followed by two structural and petroleum system overviews, covering northeast Africa (Egypt, Eastern Libya) and northwest Africa (Morocco) respectively. These two papers, by **Keeley & Massoud** and **Morabet *et al.***, respectively, document the established petroleum systems of these two relatively underexplored parts of North Africa and highlight many new potential plays.

The Mesozoic reservoirs and fields section describes many of the features, problems and opportunities specific to the two main fairways within the Mesozoic cycle, namely the Early Cretaceous–Cenomanian clastic deposits, productive in Libya and Egypt, and the Late Cretaceous–Paleogene carbonates, productive in the Tethyan margin basins (Fig. 2) extending from Egypt to Tunisia. These reservoirs form part of a large-scale transgressive cycle overlying the rifts described by **Guiraud** (Figs 2 and 3). The clastic rocks, which seem to be sourced primarily from underlying syn- or post-rift sources, contribute 20% of North African oil and 6% of gas, whereas the carbonates contribute 36% of North African oil and 9% of gas (Figs 4 and 5). These reservoir papers are ordered from east to west (Fig. 2), following a general trend of productivity in progressively younger portions of the stratigraphic column (Fig. 1) and from clastic deposits to carbonates.

Richardson *et al.* focus on the key control of fault seal in the clastic fairways of the Egyptian Western Desert. Other important factors in this area are presented in the regional overview by Keeley & Massoud. By far the predominant area of Mesozoic clastic production, however, is the eastern Sirt Basin, which is reviewed by **Gras & Thusu**. This paper compiles many of the new concepts proposed for this region in recent years, including the probability of contributing lacustrine source rocks in the Triassic and the Early Cretaceous, the recent assignment of much of the productive reservoir section in the giant Amal field to the Triassic (rather than Cambro-Ordovician) and the possibilities for new structural plays in features such as relay ramps.

Late Cretaceous–Paleogene carbonates are the predominant producers in a belt extending from the northern Sirt Basin through offshore Tunisia into the Atlas. Two papers deal with the complex reservoir models for these carbonates, emphasizing the wide variety of environments under which these carbonates are deposited, the complexities in reservoir distribution and the contribution that sequence stratigraphy and sedimentological studies can make to identifying areas of reservoir development. **Spring & Hansen** examine the multitude of environments within a Paleocene carbonate sequence in northern Libya and outline reservoir distribution models pertinent to the two types of margin observed in the region, ramps and rimmed carbonate margins. **Loucks**

et al. describe and interpret the depositional environment of and reservoir development with the Eocene nummulitic limestones of offshore Tunisia, these being the main producing reservoir in that country and in its largest field, Ashtart. The paper by **Zaier *et al.*** is also concerned with this region, concentrating on the structural controls on sedimentary patterns that influence both reservoir and source rock development at Paleogene level.

Despite a not inconsiderable exploration effort over the years, large discoveries have not materialized in the Atlas, and this region does not even feature in the statistics presented in Figs 4 and 5. As pointed out by **Macgregor & Moody**, a revitalization of interest may occur in this region following recent successes in directly analogous regions of the Alpine belt in Europe, particularly in the Apennines. It is therefore now critical to understand why the wells drilled in this region to date have failed. The three papers presented on the region contribute to this understanding, as does the previously mentioned overview of Morocco by **Morabet *et al.*** The papers by **Morgan *et al.*** and **Bracène *et al.*** deal with the alternative tectonic models of thin- and thick-skinned tectonics applicable to the surface anticlines that have been the focus for much of the drilling to date. This distinction is fundamental not only to whether wells penetrated valid closures at depth but also to the deep stratigraphy, including reservoirs and source rocks, that can be expected below such potential traps. Both groups of authors conclude by identifying different mechanisms for their individual study areas but acknowledging that different models apply in different parts of the Atlas. In other words, there is no commonly applicable model or easy solution to the issue. In the final paper, **Mekireche *et al.*** focus on many of the problems concerned with reservoir development and petroleum systems which must be addressed while exploring this region. The overall message of these papers for the petroleum industry is that it is only with improved seismic definition, together with the application of modern exploration techniques and concepts, that the barriers to success in the Atlas will be broken.

We hope this volume, in addition to increasing interest in the region, will help provoke international debate on many ill-understood issues affecting the petroleum geology of the region. Examples of such issues highlighted in this volume include the potential for subtle traps throughout the region and stratigraphic column, the structural origin of many of the Palaeozoic basins, the possibility of deeper plays associated with precursor rifts to Sirt and other 'Cretaceous rifts', the relationship between timing and trap formation in many regions, the debate between thin- and thick-skinned tectonics in the Atlas, and the complex depositional and diagenetic controls on many of the key reservoirs. We hope this volume will be the first of many attempts to discuss these and other issues openly and to facilitate debate between workers from North Africa itself and those working the region from elsewhere.

We close by thanking all the authors for their efforts, particularly those from North Africa itself, together with the many reviewers of the papers. Because of language problems and lack of drafting support, many of the papers were rewritten and/or redrafted by the editors, and D.M. acknowledges the support of the BP Indonesia and Algeria assets in this regard, particularly the efforts of Misran and Krisnandi in the BP Indonesia drafting office. Malika Hamraoui of BP's Algiers office is thanked for her hard work in co-ordinating the submission of papers from Algeria. In addition to financial contributions from many authors themselves, the following are thanked for financial contributions towards drafting for authors who required assistance in this regard: BP (Algeria asset), the Petroleum Group, Fina, ARCO and Leeds University. Amina Mabrouk is thanked for her help with the French proof-reading.

Palaeozoic petroleum systems of North Africa

DAVID R. D. BOOTE[1], DANIEL D. CLARK-LOWES[2,3] & MARC W. TRAUT[1]

[1]*Occidental Oil and Gas Corporation, 1200 Discovery Drive, P.O. Box 12021, Bakersfield, CA 93389, USA*

[2]*Geology Department, Imperial College of Science, Technology and Medicine, Prince Consort Road, London SW7 2BP, UK*

[3]*Present address: Clark-Lowes Consulting, Oak Court, Silver Street, Wiveliscombe, Taunton TA4 2PA, UK*

Abstract: The Palaeozoic petroleum systems of North Africa contain five large giant (> 1 billion barrels of oil equivalent) and 24 giant (> 250 million barrels of oil equivalent) oil and gas fields with total recoverable reserves discovered to date of more than 46 billion barrels of oil equivalent. This article presents a classification of these petroleum systems based upon their productivity and maturity. Productivity of each system has been estimated from the associated hydrocarbon reserves and maturity from an analysis of their geological history ranging from initial genesis to maturity, destruction and final extinction. Key factors controlling both productivity and maturity include hydrocarbon charge, style of drainage and entrapment, and intensity of post-entrapment tectonic, thermal and hydrodynamic destructive processes.

The regionally extensive Lower Silurian Tanezzuft Formation is the origin of 80–90% of Palaeozoic sourced hydrocarbons, with a further 10% from the Upper Devonian Frasnian shales, charging a number of intra-Palaeozoic and basal Triassic reservoirs. Triassic fluvial sands are the most important of these, hosting just over half of the total reserves, while Cambro-Ordovician and Lower Devonian F6 sandstone reservoirs are the second and third most significant, respectively.

Three categories of Palaeozoic petroleum systems have been identified:

(1) Mesozoic to early Tertiary charged systems with Triassic–Liassic shale and evaporite seals in the Mesozoic sag or 'Triassic' Basin of the northern Sahara Platform. These include > 78% of the total discovered reserves, with > 56% in the supergiants, Hassi R'Mel and Hassi Messaoud fields

(2) Mesozoic to early Tertiary charged systems with intra-Palaeozoic shale seals in basins of south and east of the Triassic Basin. These include > 18% of the total discovered reserves, mostly in the prolific Illizi Basin.

(3) Now largely extinct Palaeozoic charged systems with intra-Palaeozoic seals in basins of southwest Algeria and Morocco with 3% of discovered reserves.

The productivity of these systems varies considerably. Hassi R'Mel and Hassi Messaoud are classified as super-productive, located on the crests of broad Palaeozoic arches which encouraged extremely efficient lateral migration focusing, and a very high impedance entrapment style. Other petroleum systems within the Triassic Basin are of high productivity with somewhat less effective migration focusing and impedance characteristics. Because of a regional evaporite seal and minimal late stage modification, these systems are all preserved in a mature phase of evolution.

Basins south and east of the Triassic Basin are in various stages of destruction with variable productivities reflecting both less robust seals and post-entrapment modification by Austrian and mid-Tertiary uplift, tilting, remigration, spillage and freshwater flushing. The Illizi Basin is the least affected by these late stage destructive processes with some 15% of total discovered reserves still remaining.

The Palaeozoic charged systems of southwest Algeria and Morocco were largely destroyed by Hercynian, Austrian and mid-Tertiary deformation. Only the high relief Hercynian anticlines of the Ahnet–Gourara Basin retained their trapping integrity and still reservoir a very significant amount of gas. Apart from scattered hydrocarbon shows and a few small residual accumulations the other basins in this region now all appear to be extinct.

Since the first discovery in 1953, more than 1100 new field wildcat wells have been drilled to test the Palaeozoic basins of North Africa, with the discovery of more than 46 billion barrels of oil equivalent (BBOE) in over 300 separate pools. The hydrocarbon productivity of the petroleum systems within these basins varies widely from non-productive to extremely prolific. This paper

BOOTE, D. R. D., CLARK-LOWES, D. D., TRAUT, M. W. 1998. Palaeozoic petroleum systems of North Africa. *In:* MACGREGOR, D. S., MOODY, R. T. J. & CLARK-LOWES, D. D. (eds) 1998. *Petroleum Geology of North Africa.* Geological Society, London, Special Publication No. 132, 7–68.

attempts to define the key stratigraphic and structural variables which govern their differing productivity.

The North African Platform experienced a complex and polyphase history (Fig. 1). Initially part of a regionally continuous, clastic-dominated Gondwana passive margin, it was progressively segmented into broad forelands and intracratonic basins and swells during late Devonian to late Carboniferous collision with Laurasia. Uplift and erosional truncation of the deformed platform during late Carboniferous to early Permian was followed by a phase of rifting. This was succeeded by opening of the Tethyan seaway during the Mesozoic, when a regional transgression extended far south across the peneplaned Hercynian unconformity commencing in the late Permian and continuing through to the mid-Cretaceous. The Palaeozoic basins were buried beneath a Tethyan passive margin wedge of continental clastic deposits, evaporites and carbonates. During the later Cretaceous, the opening of the Atlantic seaway and change in relative plate motion between Africa and Eurasia were associated with periods of structural inversion, extension and development of local rift-associated depocentres on and along the flanks of the North African platform. Tertiary sedimentation was largely confined to the northern margin of the platform where the effects of collision between Africa and Eurasia were manifested in the Eocene through to the Miocene by Atlassic inversion and subsequent Maghrebian (Rif–Tellian) thrusting and nappe emplacement (Ziegler 1988). The influence of this compressional event extended back across the North African Platform with the development of a shallow foreland sag above the more inboard Palaeozoic basins and uplift of bounding highs, tilting and partial unroofing of those beyond.

Palaeozoic sourced hydrocarbon accumulations are widely distributed across the western part of the Saharan Platform, reservoired in various sandstones ranging from Cambro-Ordovician to basal Triassic in age. This review attempts to group these accumulations into discrete petroleum systems, each sharing a common generative area or pod of source rock and common reservoir(s) with broadly similar charging history (Magoon & Dow 1994). The more important systems have been described in a series of maps (Fig. 2), schematic cross-sections and critical element analyses, developed from the approach suggested by Demaison & Huizinga (1994) and Magoon & Dow (1994). These highlight the key stratigraphic and structural variables that appear to govern the distribution of oil and gas accumulations within each system, including source, reservoir and sealing facies, peak expulsion, preferred migration directions and post-charge modification such as basin tilting and flushing. Precise descriptive and analytical information is generally very limited and it was often not possible to constrain these variables directly. Instead, they were frequently inferred indirectly from regional structural and stratigraphic control. Critical uncertainties included the following:

(1) Defining generative areas or pods: although organic-rich Lower Silurian and Upper Devonian shales are now widely recognized as the primary source of Palaeozoic hydrocarbons in the region (Tissot *et al.* 1984; Daniels & Emme 1995) it was rarely possible to link reservoired oil or gas directly with discrete generative areas. These had generally to be inferred from the structural relationship between hydrocarbon accumulations and nearby source rocks.

(2) Critical period: because of the polyphase history of the region, source rocks within individual basins often experienced two periods of burial and maturation separated by significant uplift and unroofing. Consequently, it was frequently difficult to reconstruct the charge history with any precision. This was commonly extrapolated from structural history and the relationship between source, reservoired hydrocarbon maturities and time of trap formation.

(3) Migration drainage and entrapment style: sufficient stratigraphic information was available to define the more obviously important lateral migration conduits. Vertical migration conduits were inferred from the stratigraphic distribution of hydrocarbon accumulations and their relationship with lateral conduits, faults and erosional windows in intra-formational seals. Preferred migration drainage directions were then extrapolated from structural configuration. Entrapment style or impedance was estimated from the geometry of the primary conduit, seal continuity and structural complexity.

(4) Preservation time: the preservation time of each system was reconstructed from its structural history and relative timing between trap charge and late-stage events including uplift, tilting and hydrodynamic flushing.

(5) Relative importance of the stratigraphic and structural factors responsible for each system: although significant amounts of hydrocarbons must certainly remain to be discovered, exploration in the region is now at a fairly mature level and the reserves so far established for each system are considered at least a relative estimate of their ultimate productivity or efficiency in entrapping and retaining oil and gas. This in turn provides an independent and semi-

quantitative measure to compare the relative importance of the factors responsible for each system.

The analysis relied upon a wide variety of proprietary and published sources including Claret and Tempere (1967), Aliev *et al.* (1971), Bishop (1975), Chiarelli (1978), Hammuda (1980), Hamouda (1980*a*, *b*), Tissot *et al.* (1984), Van de Weerd & Ware (1994), Daniels & Emme (1995), Thomas (1995), Gumati *et al.* (1996), Macgregor (1996*b*). Many of the interpretations presented in this paper are dependent upon the accuracy of data and interpretations from a variety of published and proprietary sources. These were sometimes contradictory and required pragmatic selection and simplification. Wherever possible the final interpretations were constrained by independent evidence but geological inference and extrapolation were sometimes necessary and the resulting synthesis is inevitably rather speculative. Nevertheless, we believe this empirical approach proved adequate to measure and rank the relative importance of the critical variables which control the productivity of each system.

Tectono-stratigraphic evolution of the North African Platform

The North African Platform lies yoked between the African Shield in the south, with its Eglab, Hoggar, Tibesti, Jebel Awaynat and Nubian Precambrian massifs, and the Atlassic–Maghrebian fold belts and East Mediterranean Basin in the north (Fig. 2). The varied structural style of this platform is illustrated by a series of predominantly north–south schematic cross-sections, illustrating the Palaeozoic intra-cratonic basins of Morocco, Algeria and Libya, and the later Mesozoic sag and rift basins of eastern Algeria, Libya and Egypt (Figs 3–7). The underlying Precambrian basement evolved as part of Pangaea, formed from the collision and suturing of several cratons and intervening island arcs during the Pan-African orogeny. This subsequently evolved into a stable Gondwana and later Tethyan passive continental margin, interrupted by Hercynian deformation in the late Carboniferous, rifting during the Mesozoic and Atlassic-Maghrebian orogenesis in mid–late Tertiary. A widespread Hercynian unconformity divides the sedimentary cover into a lower Gondwana Super-Cycle of mildly deformed Palaeozoic clastic deposits and an upper Tethyan Super-Cycle of Mesozoic–Tertiary clastic deposits, evaporites and carbonates.

Gondwana Super-Cycle

During the early part of the Gondwana Super-Cycle, the North African Platform was blanketed by a regionally extensive succession of high-lati-

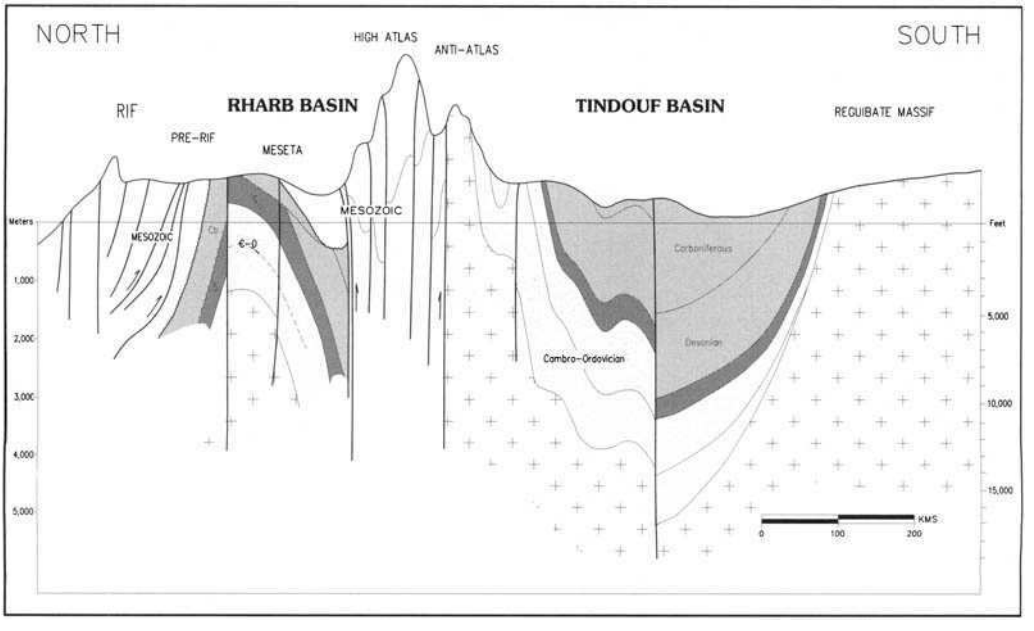

Fig. 3. Generalized structural cross-section across the Rharb and Tindouf Basins. (See Fig. 2 for location.) Partly adapted from Peterson (1986).

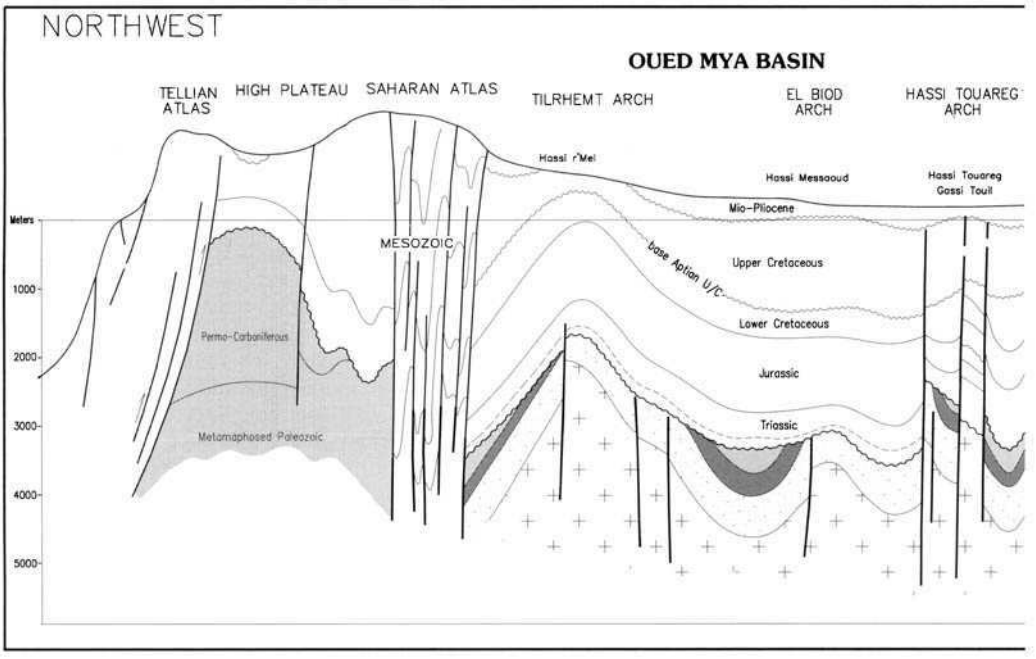

Fig. 4. Generalized structural cross-section across the Oued Mya and Illizi Basins. The Mesozoic foreland (1982).

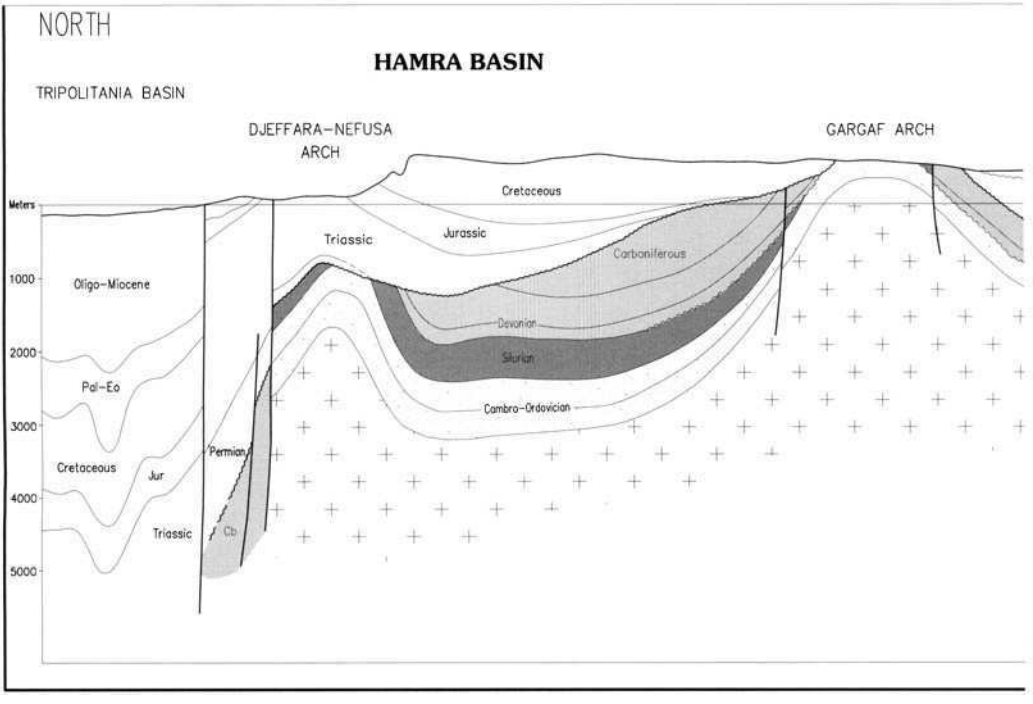

Fig. 5. Generalized structural cross-section across the Hamra and Murzuq Basins. (See Fig. 2 for location.) Partly

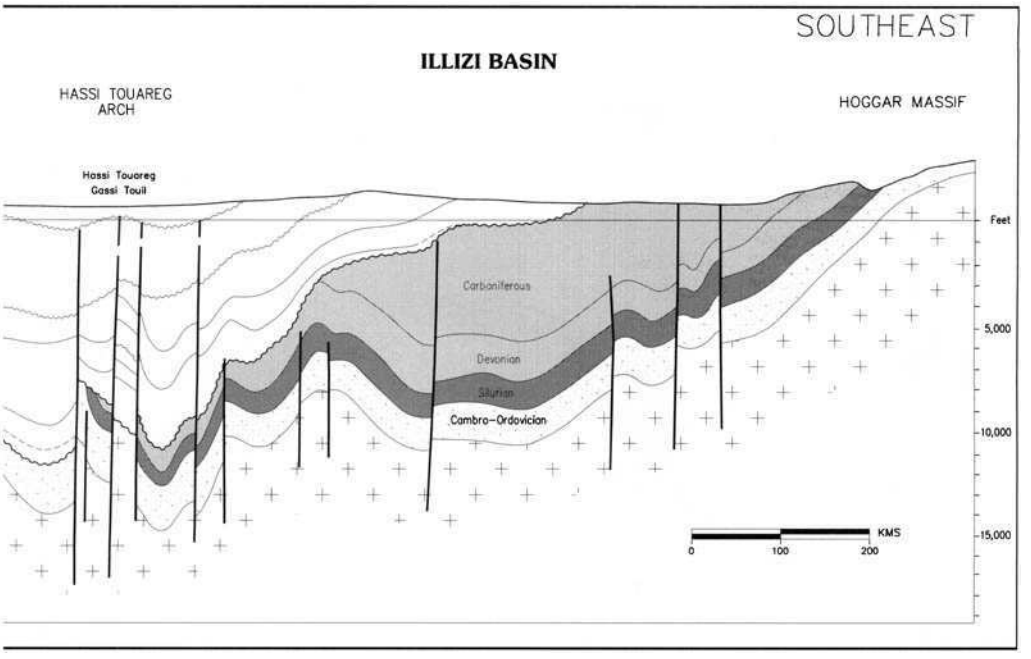

depocentre of the Saharan Platform is also illustrated. (See Fig. 2 for location.) Partly adapted from Peterson

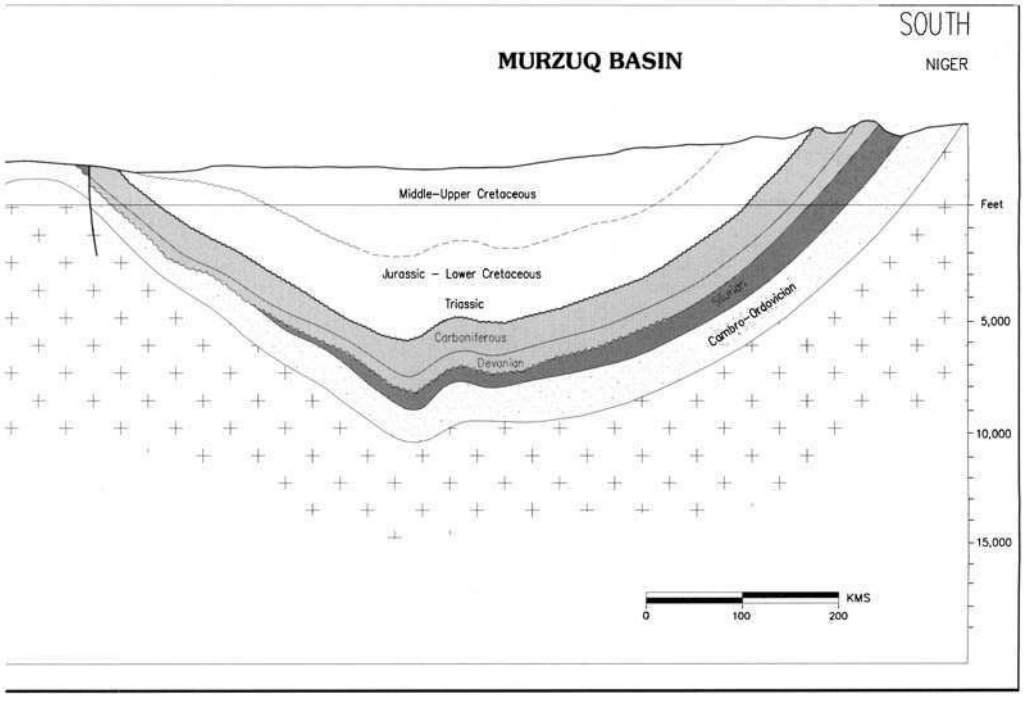

adapted from Pallas (1980) and Peterson (1982).

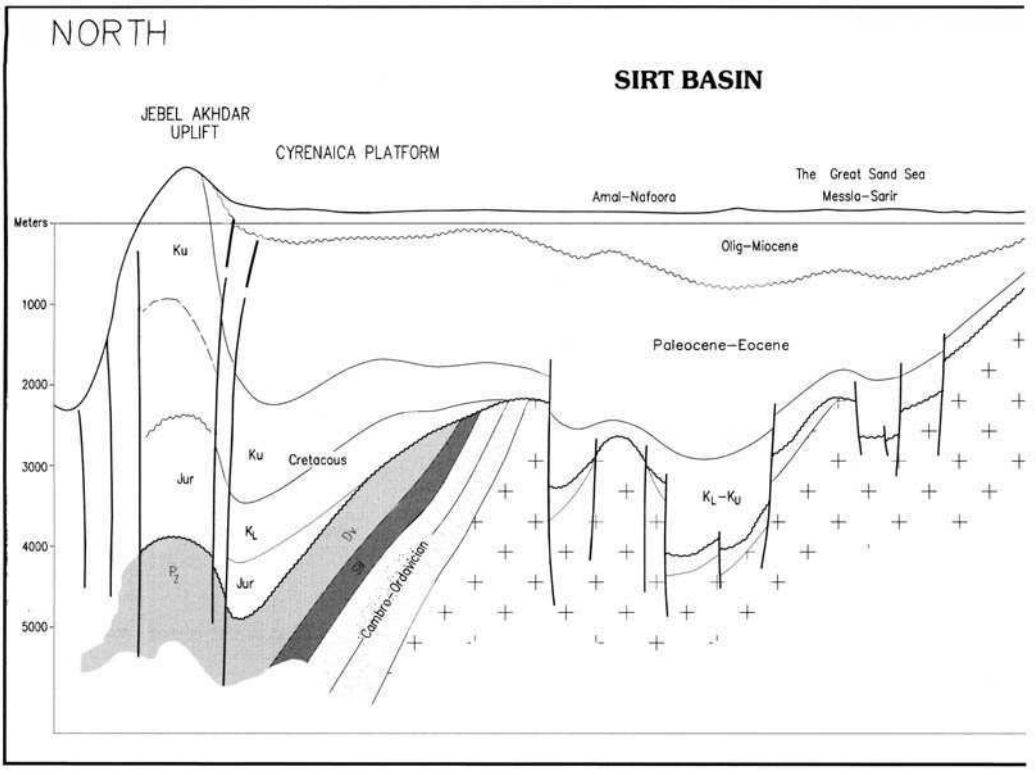

Fig. 6. Generalized structural cross-section across the Sirt and Kufrah Basins. (See Fig. 2 for location.) Partly

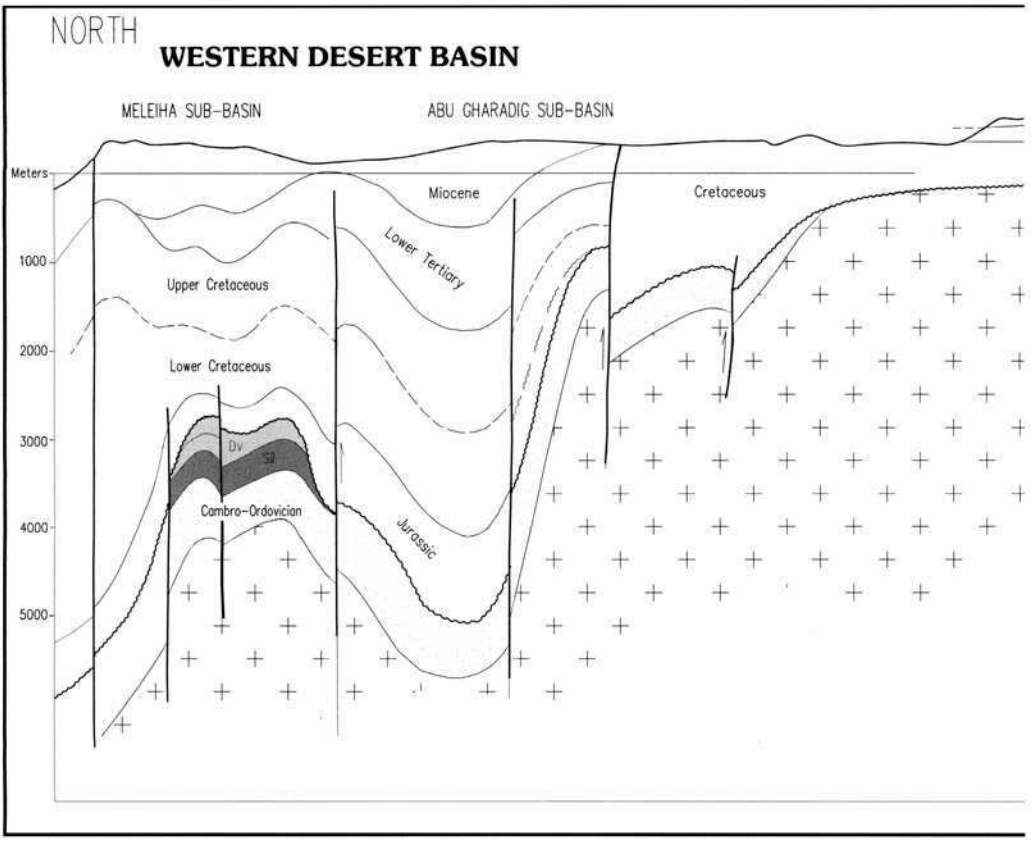

Fig. 7. Generalized structural cross-section across the Western Desert Basin and southern Egyptian platform. The (See Fig. 2 for location.) Partly adapted from Peterson (1982).

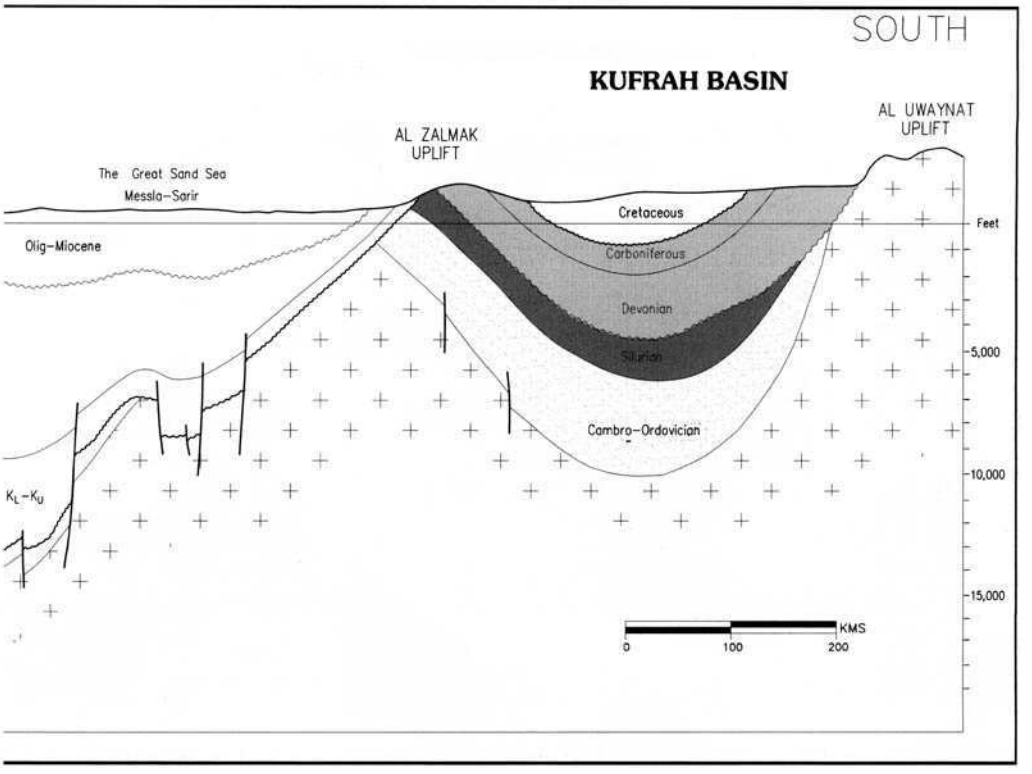

adapted from Peterson (1982).

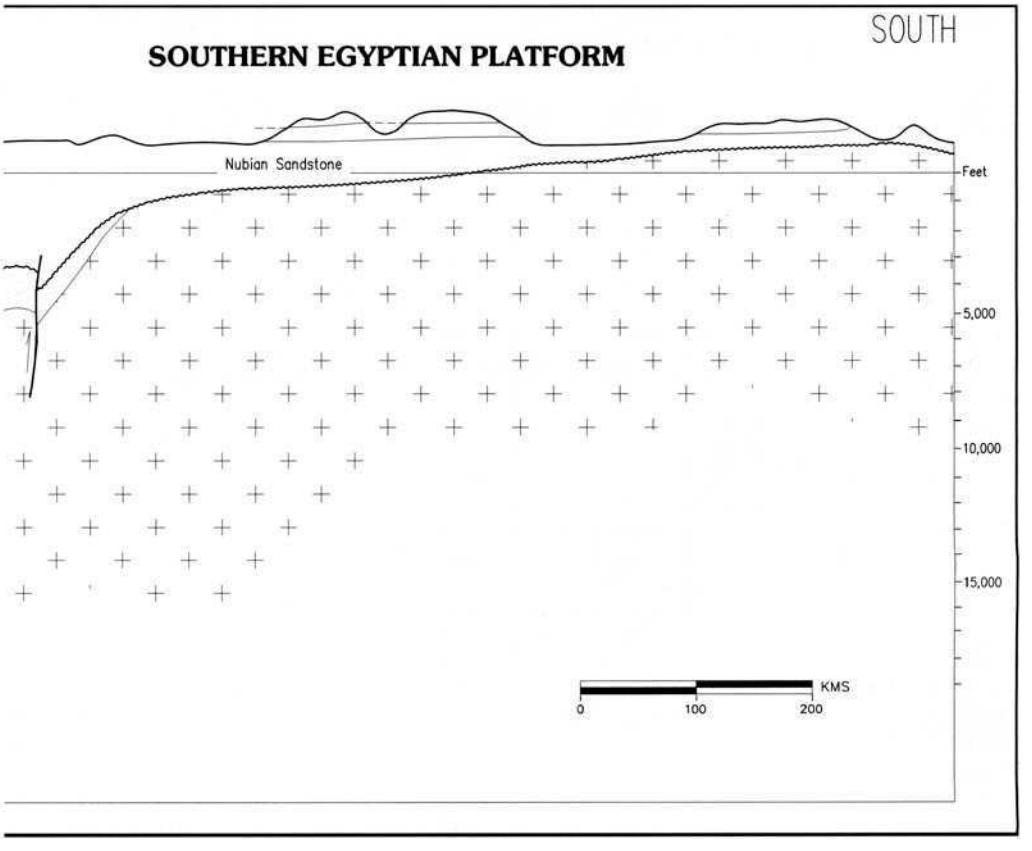

structure of the southern platform is weakly constrained and Palaeozoic sub-basins may underlie the Mesozoic.

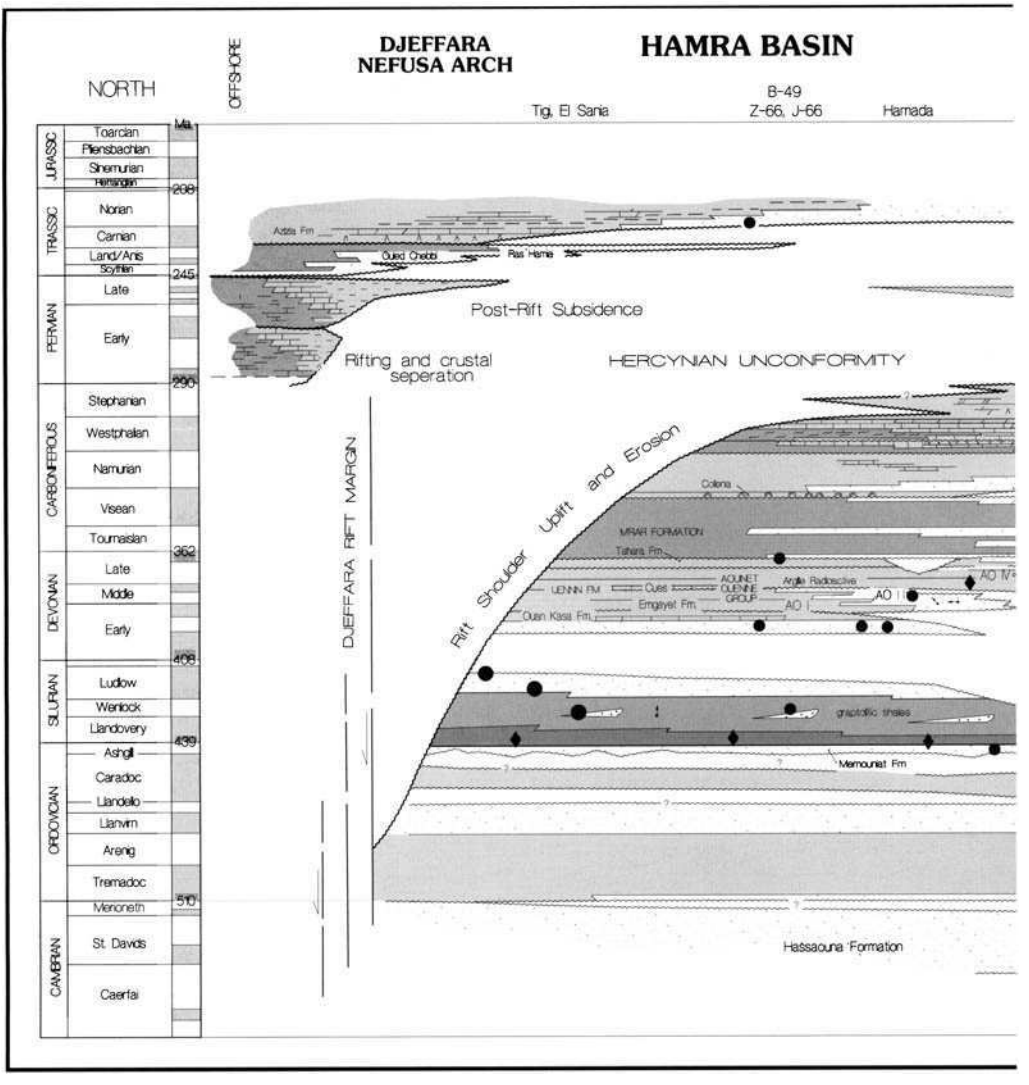

Fig. 8. Generalized Palaeozoic chronostratigraphy of western Libya, illustrating the more important stratigraphic Devonian 'Argile Radioactive' are highlighted with lozenges. Partly based upon information from Busson & Conrad *et al.* (1986), Kilani-Mazraoudi *et al.* (1990) and Rigo (1995).

tude platform sequences. Progressive collision with Laurussia commenced in late Devonian (Ziegler 1989) with mild uplift of positive areas in the platform interior. Depositional systems were increasingly influenced by local intra-platform highs with a marked decrease in regional stratigraphic continuity in the upper part of the Super-Cycle (Fig. 8).

Lower Gondwana Cycle. The Cambrian to lower Ordovician Hassaouna succession is dominated by cyclic sequences of thick, regionally extensive, transgressive, fluvial and estuarine sands which pass up into shallow marine sandstones and maximum flooding shales (Achebyat Formation). Highstand facies are subordinate or absent. The transgressive sands provide reservoirs in the Hassi Messaoud, El Gassi, El Agreb and Rhourde al Baguel fields located respectively on the Hassi Messaoud and El Biod Arches and the Hassi Touareg Axis (Fig. 2). Sandstone matrix porosity is generally low but secondary dissolution immediately below the Hercynian unconformity and fracturing induced by Austrian inversion have locally improved reservoir quality significantly (Clark-Lowes 1988; Crossley

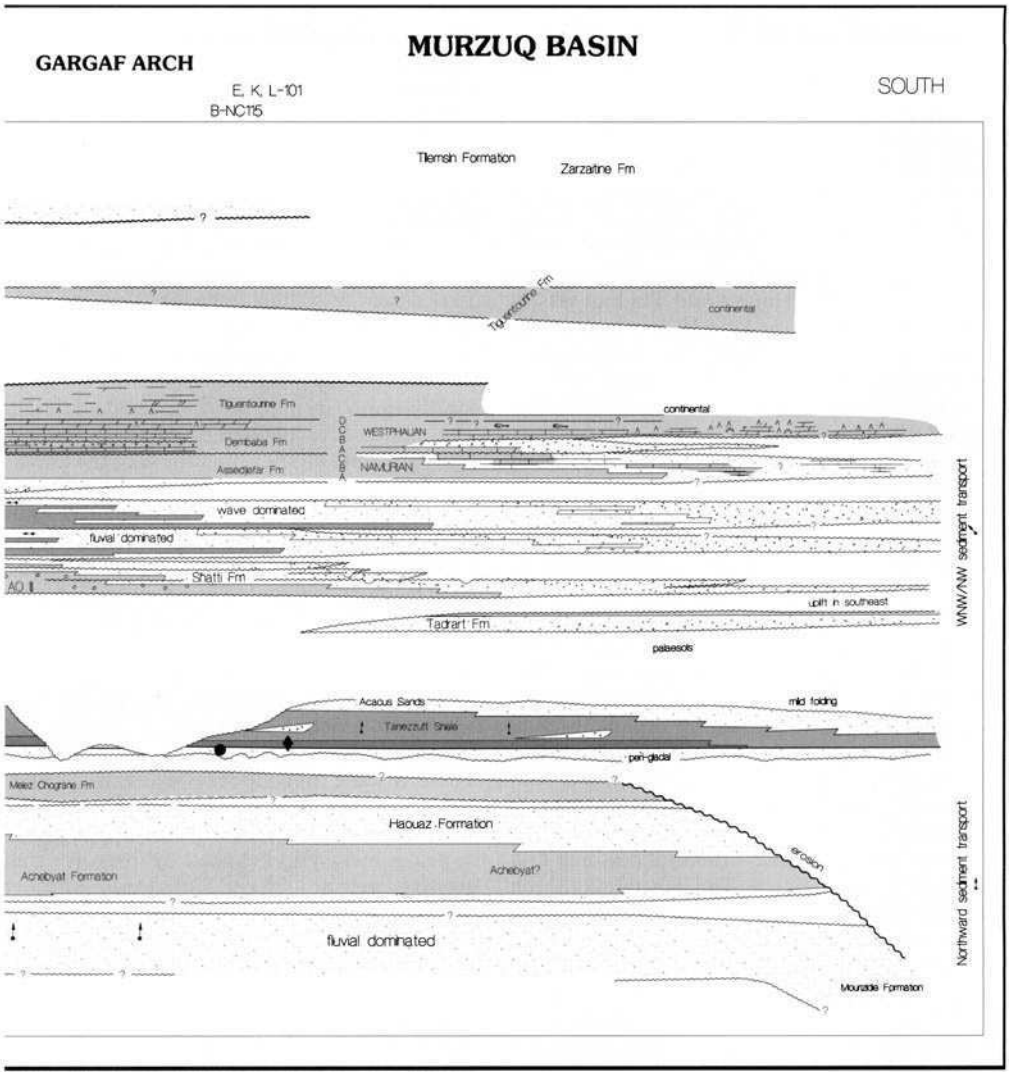

sequences and bounding unconformities in a simplified fashion. The organically-rich Tanezzuft Shales and Upper Burollet (1973), Massa & Beltrandi (1975), Jaeger *et al.* (1975), Bellini and Massa (1980), Fatmi *et al.* (1980), & McDougall this volume; Djarnia & Fekerine this volume).

Stacked regressive dominated sequences characterize the overlying Ordovician Arenig to Llandeilo Haouz Formation, typically with a thin basal transgressive lag passing up into marine graptolitic shales and coarsening-up delta front–delta top highstand sandstone facies (Vos 1981*a*). These generally have very low matrix porosity. The succeeding Llandeilian-Caradoc Melez Chograne shales extend across a wide area of the North African Platform, clearly represent a major flooding sequence, and may sometimes form a poor-quality source.

Unconformities interrupt the Ordovician succession at the base of the Haouz and Melez Chograne Formations. These reflect epeirogenic reactivation of heterogeneities in the underlying Pan-African basement. They tend to be local and confined to elongate intra-platform structural highs, with a generally pronounced NW–SE to N–S alignment. The most important include the Ougarta, Amguid–El Biod, Tihemboka, Gargaf, Calanscio–Al Uwaynat (Klitzsch 1981) and Al Uwaynat–Bahariyah (Keeley 1989) Arches of Algeria and Libya.

By the Ashgill, the North African Platform was positioned near the South Pole (Scotese *et al.* 1979) and a short-lived icecap developed over much of Africa and South America (Arbey 1978; Hargraves & Van Houten 1985; Brenchley *et al.* 1994). The glacigene Memouniat Formation was probably deposited towards the end of this glacial cycle as the icecap retreated. Deeply incised palaeovalleys with fluvio-glacial sediment fill have been recognized in the southern Saharan Platform passing north into glaciomarine facies in the Hamra and Tindouf Basins and the Atlas range beyond (Beuf *et al.* 1971). Fluvial sandstones within the palaeovalleys form significant reservoirs in parts of the Murzuq Basin, often in traps enhanced by differential compaction.

The Memouniat represents a basal lowstand system of the Silurian Tanezzuft–Acacus depositional sequence. Initial marine transgression is marked by an erosional ravinement surface sometimes overlain by residual shallow marine sands. These pass up into the black radioactive shales of the Lower Tanezzuft, deposited during post-glacial flooding across much of the North African and Arabian platforms. The shales form the most important source rock on the Sahara Platform with total organic carbon (TOC) content of between 2% and 17%. Original organic quality and richness appears to have been fairly consistent throughout Algeria and western Libya. However, it is locally influenced by intra-platform structural features first active in the Ordovician. The Tihemboka Arch was a trough at this time with a relatively thick organic-rich sequence extending south into the Hoggar, Niger and perhaps even Chad. In contrast, source quality deteriorates onto contemporaneous positive structural axes, such as the central part of the adjacent Murzuq Basin and perhaps across the ancestral Tibesti–Sirt Arch of central Libya (Klitzsch 1966). In the Kufrah Basin further to the southeast, the Tanezzuft is present, and although largely unknown, is reported to have some source potential (Keeley & Massoud this volume). In western Egypt, Silurian source potential is generally poor (Keeley 1989; Keeley & Massoud this volume).

Regional flooding of the North African Platform during early Llandovery (Berry & Boucot 1973; Bellini & Massa 1980) was followed by a pro-delta and delta top highstand system of the upper Tanezzuft and Acacus Formations which prograded northwards from late Llandovery to the Ludlow. Thin turbidite, shelf and distal delta sands of this sequence provide moderate- to poor-quality reservoirs in several western Libyan and Tunisian accumulations.

This sequence was terminated by a regionally extensive unconformity reflecting an episode of rifting and crustal separation along the Gondwana margin in the late Silurian (Harland *et al.* 1990). The succeeding transgressive-dominated sequence includes the Tadrart–Ouan Kasa and F6–F5–F4 Formations of Pridoli to Emsian–Eifelian age. The Tadrart–F6 sandstone reservoir consists of up to four transgressive cycles, each with a basal fluvial sand passing up into distal tidal offshore facies (Clark-Lowes & Ward 1991, Alem *et al.* this volume). This appears to have been part of a vast, regionally continuous fluvial system, reminiscent of the Cambrian Hassaouna, thinning regionally to the north and locally onto intra-platform structural arches. The sands were derived from a southeasterly source and are coarser than those of the underlying Acacus Formation. The F6–Tadrart is an important reservoir in the Illizi, Ghadames and Hamra Basins of Algeria and western Libya.

Increasing epeirogenic activity in the mid to late Devonian is reflected by an increase in stratigraphic complexity. Intra-Eifelian–base Givetian uplift and erosion terminated the Tadrart–Ouan Kasa sequence. This was followed by a widespread marine transgression, grading up into a series of stacked depositional cycles, each strongly influenced by intra-platform highs. These Middle and Upper Devonian cycles are made up of regressive, fluvial-dominated delta systems each with an erosional upper surface, in places incised and capped by extensive transgressive marine shales, limestones and iron oolites (Van Houten & Karasek 1981; Karasek 1981; Vos 1981*b*; Clark-Lowes 1988).

In the Murzuq Basin Middle Devonian sediments are thin or absent (Aouinet Ouenine Formations I and II) whereas in the Hamra Basin the Middle Devonian is represented by the Emgayet Formation. The Illizi–Ghadames equivalent comprises regressive sequences which form significant reservoirs in a number of the Illizi Basin fields (most notably the F3 sand; see Chaouchi *et al.* this volume).

Upper Gondwana Cycle. Mid to Upper Devonian intra-platform epeirogenic movements reflect the initial collision between Gondwana and Laurussia and progressive reassembly of Pangaea during the Late Palaeozoic. Deformation commenced along the northwestern promontory of the North African Platform and subsequently propagated eastwards to encompass the entire Atlas region by late Namurian. Foreland basins developed immediately south of this Mauretanide–Variscan orogenic belt, and major northwest aligned structural axes in the interior

platform collapsed to be replaced by northeast-trending arches. The Tibesti–Tripoli (Brak–Ghanimah) and Calanscio–Al Uwaynat Arches subsided whereas the Tibesti–Sirt uplift became a dominant feature (Klitzsch 1971).

The basal Upper Devonian Frasnian unconformity reflects the most significant of the intra-Devonian epeirogenic movements, with clear evidence of deep erosional truncation over parts of the Ougarta and Gargaf Arches. A regional transgression followed during the Frasnian with the deposition of a widespread organic-rich shale, the 'Argile Radioactive', across much of the North African Platform. These shales, comparable with the basal Tanezzuft radioactive unit, are a major source rock in the Ghadames and Illizi Basins with TOC values ranging between 2% and 14%. Their distribution is less well defined elsewhere but they appear to have extended at least as far as the Western Desert of Egypt.

The overlying late Frasnian to early Tournaisian succession is dominated by relatively thin, cyclic, platform deltaic deposits of the upper Aouinet Ouenine (III and IV)–Ouenine–Shatti sandstone formations in Libya and the F2 sequence of the Illizi–Ghadames region. These sandstones and those of the overlying Tahara Formation (Karasek 1981) provide significant reservoirs in the Illizi and Hamra Basins.

Deltaic deposition dominated the Carboniferous across much of the North African Platform. Sedimentation patterns were strongly influenced by intra-platform highs and by the developing fold and thrust belt, with its associated flanking foreland basins, to the northwest. In the greater Ghadames area, Whitbread & Kelling (1982) interpreted the Visean M'rar Formation as a series of stacked fluvial-dominated deltaic cycles becoming more wave dominated upwards in the succession. This sequence was terminated in the early Namurian by a regionally widespread transgression and deposition of the Lower Assedjefar fluvio-deltaic systems tract. These deltaic deposits are overlain by marine shales and paralic algal stromatolitic limestones of the upper Assedjefar Formation above. Sandstones within this Lower Carboniferous succession form significant reservoirs in the Illizi and Ahnet Basins and to a lesser extent in the Ghadames–Hamra region. Clastic-dominated depositional systems transgressed southwards in the middle to late Carboniferous and gave way to shallow-marine carbonates and evaporites during the Westphalian (Dembaba Formation). By late Westphalian, the rising Hercynian orogenic belt had isolated the central and western Saharan Platform where sedimentation was dominated by continental sands and shales were deposited while carbonate platform deposition prevailed to the east.

Mauretanide–Variscan orogenesis culminated in the mid to late Westphalian with regional uplift and transpression in the Atlas and Anti-Atlas. The interior platform was deformed into a series of broad intracratonic sags, foreland basins, and intervening saddles and arches as far east as western Egypt. Intra-platform structural axes first established in the early Palaeozoic were once again uplifted. The Ougarta, Reguibate and El Biod Arches, and the Meharez and Oued Namous Domes all become strongly positive at this time, as did the Tilrhemt Dome and Dahar Arch (together forming the Talemzane Arch) and the Libyan Gargaf Arch. These were subsequently erosionally truncated and peneplaned during the early Permian to form the residual Palaeozoic basins now subcropping the Hercynian unconformity (Figs 9 and 10).

Tethyan Super-Cycle

With the disassembly of Pangaea in late Palaeozoic–early Mesozoic, the North African Platform became a broad Tethyan-facing passive continental margin (Wildi 1983; Ziegler 1988, 1989; Stampfli *et al.* 1991). A thick succession of Triassic to early Cretaceous sediments was deposited in a vast interior sag basin, the 'Triassic Basin' of eastern Algeria, southern Tunisia and western Libya. Mid to late Cretaceous sediments extend more widely across the Saharan Platform with major rift-related depocentres in the Sirt and Western Desert Basins of eastern Libya and Egypt. Lower Tertiary sedimentation was largely confined to the northern margins of the platform and by Mid-Tertiary Maghrebian orogenesis, and collision with Eurasia, brought the Super-Cycle to a close. The Mesozoic and Cenozoic tectonic and stratigraphic evolution of North Africa is discussed in this volume by Guiraud, Wilson & Guiraud and Macgregor & Moody.

Lower Tethyan Cycle. Late Carboniferous to early Permian rifting and crustal separation was the first step in the break-up of Pangaea with the opening of the Permo-Tethyan seaway and the East Mediterranean Basins (Stampfli *et al.* 1991). Synrift Permian clastics and reefal carbonates were deposited north of the Talemzane–Djeffara Arch (Rigo 1995; Rigby *et al.* 1979), while associated rift shoulder uplift shed continental Tiguentourine clastic deposits south onto the Saharan Platform. Rifting and crustal

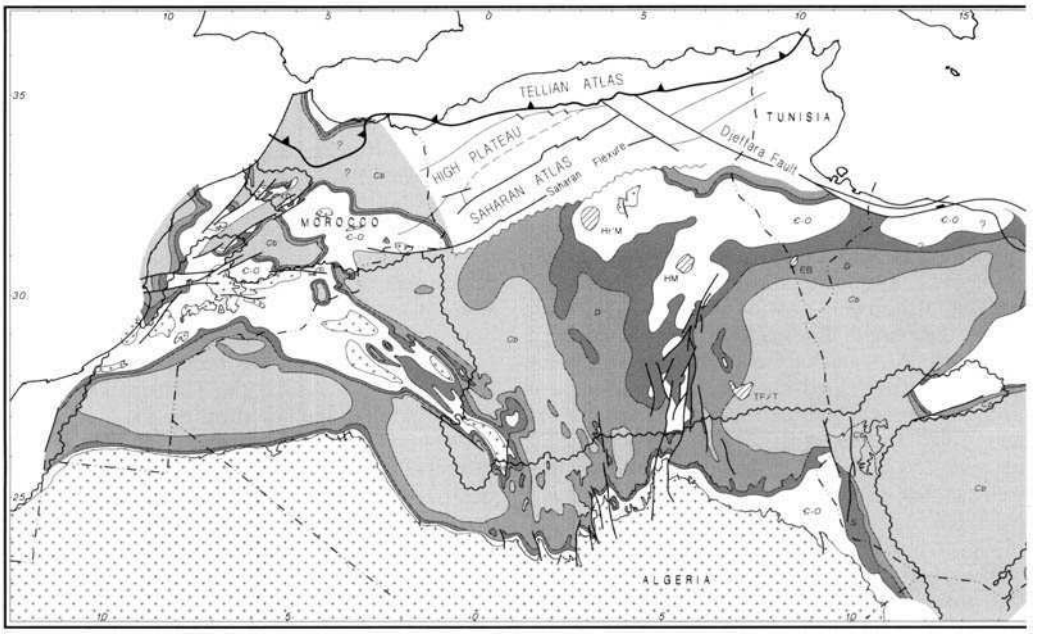

Fig. 9. Palaeozoic outcrop and subcrop distribution below the Hercynian unconformity. The present-day the Ougarta Ridge. Talemzane and Hassi Messaoud Arches. the Gargaf High and the Tibesti–Sirt Arch. modified distribution in the Algerian Atlas and north of the Djeffara fault trend is uncertain and not shown on this map.

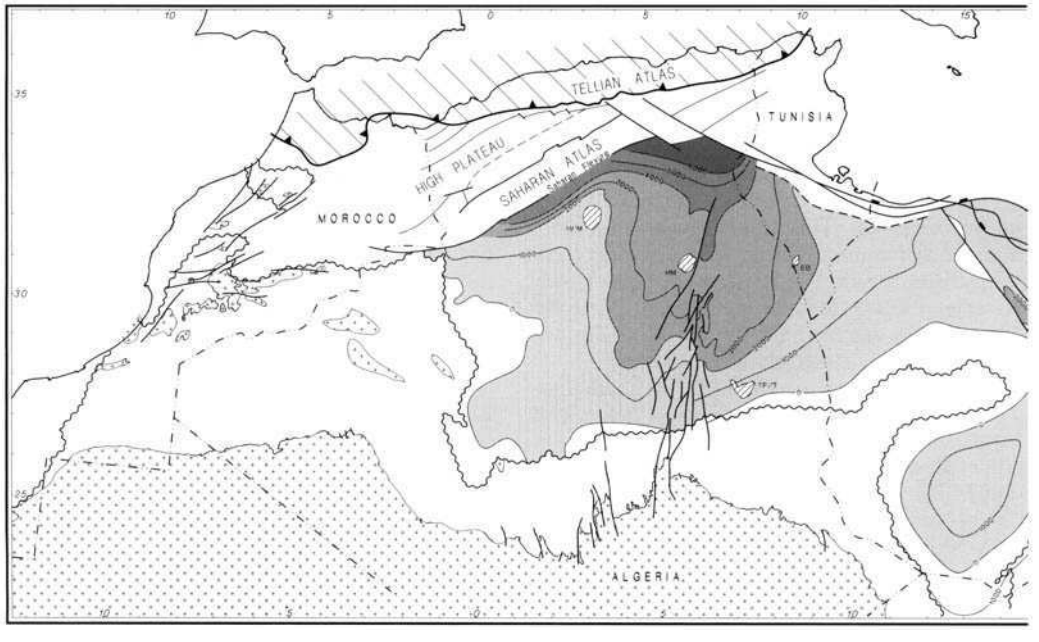

Fig. 10. Generalized structure of Hercynian unconformity. highlighting the Mesozoic 'Triassic Basin' depocentre

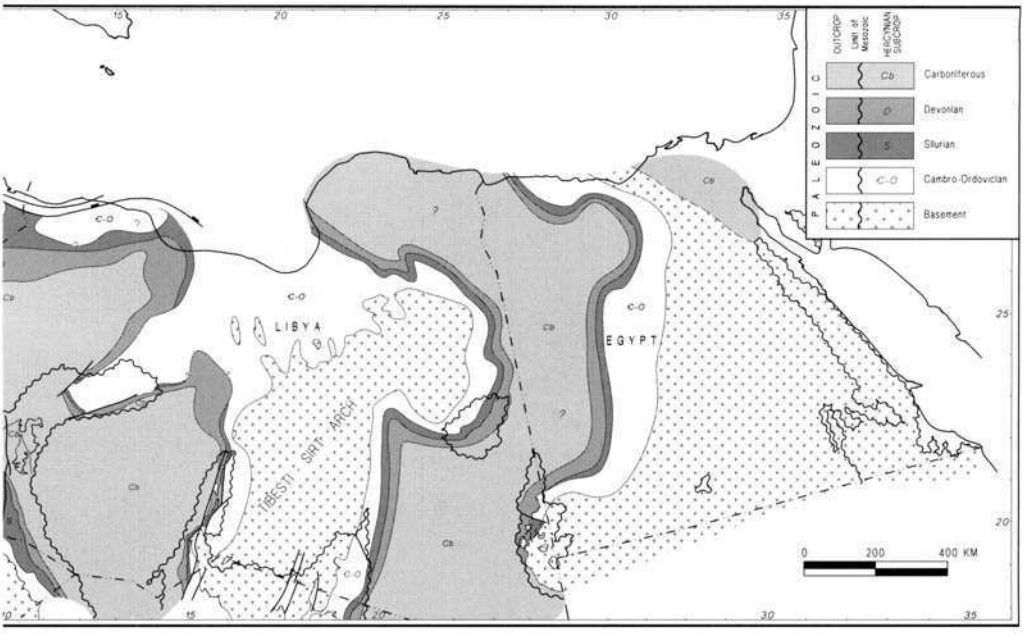

distribution of Palaeozoic basins on the North African Platform is a result of late Hercynian uplift and erosion of by later Mesozoic and early Tertiary subsidence associated with rifting and local transpression. Palaeozoic

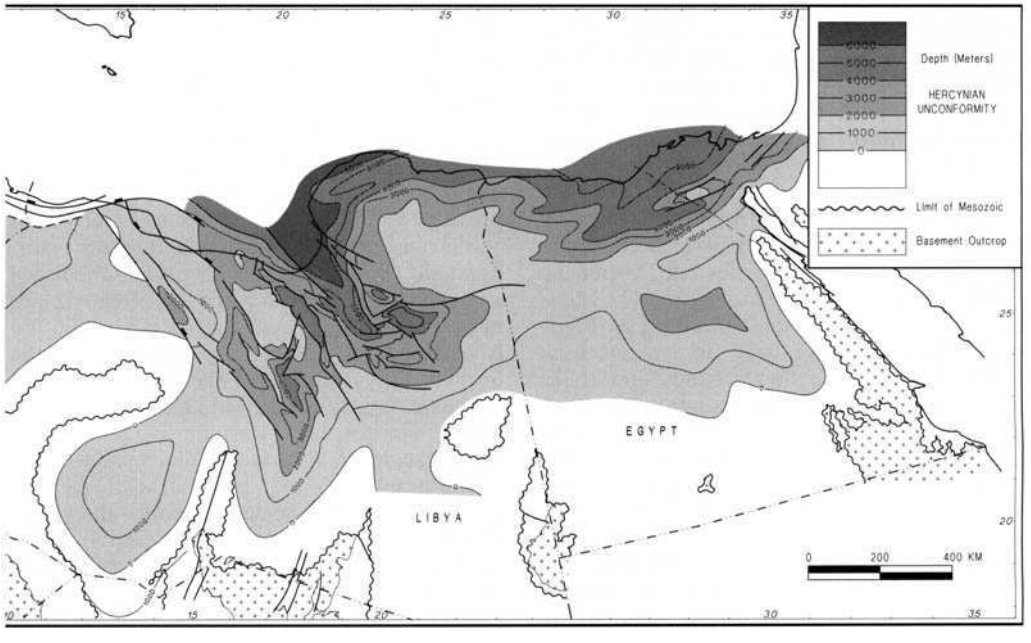

of Algeria and Cretaceous rift basins of Libya and Egypt.

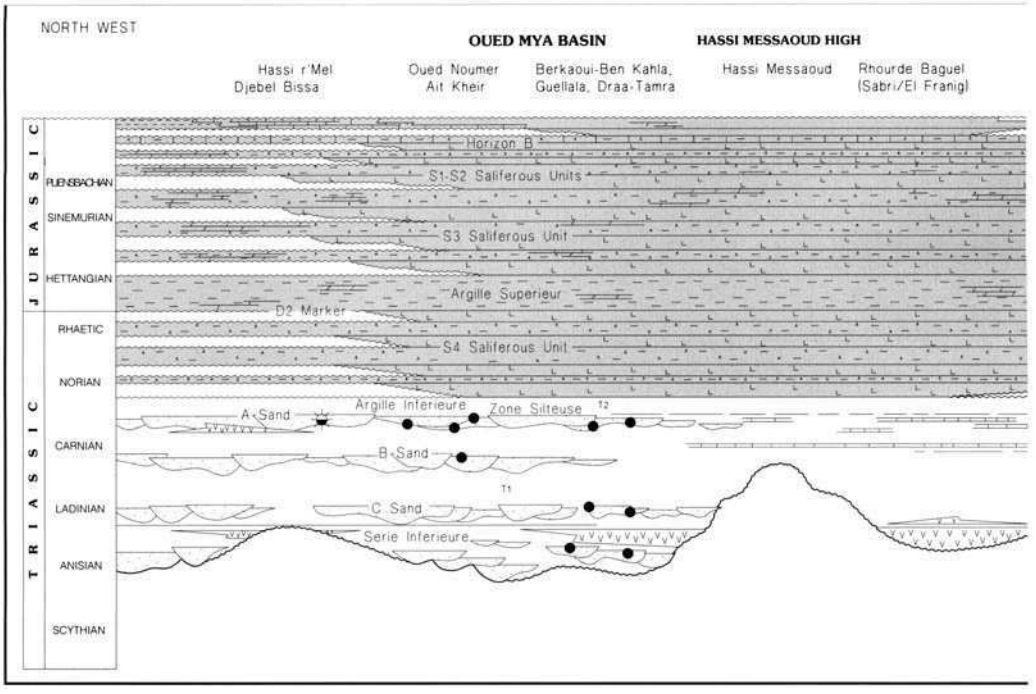

Fig. 11. Generalized lower Mesozoic chronostratigraphy of eastern Algeria. The diagram provides a tentative eastern Algeria and illustrates the diachronous relationship with the Hercynian unconformity surface and the consequently is very approximate. Partly based on information from Claret & Tempere (1967), Ali (1973), Assaad

stretching propagated westwards across the Mauretanide–Variscan orogen during the Triassic with diffuse crustal extension (Andrieux *et al.* 1989; Favre & Stampfli 1992). This was followed by more localized rifting in the High, Middle and Saharan Atlas and along the western margin of the platform during the early Jurassic. Crustal separation followed in mid-Jurassic with the opening of Alpine Tethys and the Central Atlantic.

As rifting waned, the North African Platform subsided and was blanketed by a succession of continental clastics, evaporites and carbonates during the subsequent Mesozoic (Fig. 11). Initial late Permian transgression from the East Mediterranean basin gave way to an extensive sequence of Triassic fluvial sands and shales which transgressed southwards across the peneplaned Hercynian unconformity. These now form the most important reservoir in the 'Triassic Basin' of northeast Algeria and southern Tunisia. The basal 'Triassic Argilo-greseux Inferieur' (TAGI) member of this sequence, and its lateral equivalent in the Hassi Touareg area (Claret & Tempere 1967), forms an extensive braided fluvial sheet sand over a large part of the Ghadames Basin passing laterally to the northwest, into shales and volcanic rocks. It grades upwards into mudstones, lacustrine carbonates and a second sandstone member, the 'Triassic Argilo-greseux Superieur' (TAGS) (Claret & Tempere 1967), laterally equivalent of the late Triassic S4 mudstones and salts (Ali 1973; Busson & Burollet 1973) (Fig. 11) to the north.

A roughly equivalent basal fluvial sand and shale sequence is developed to the northwest and north of the Hassi Messaoud Arch where it provides the reservoir for the north Oued Mya and Hassi R'Mel accumulations. Its precise stratigraphic relationship with the Ghadames sequence is unclear but it may be slightly older in part. The lower basal sand member (Unit C) is confined to erosional irregularities on the unconformity surface but the succeeding sand members (Units A and B) are more widespread, passing upwards into alluvial muds and evaporites of the upper Triassic S4 saline member.

This basal clastic sequence is strongly diachronous grading into Liassic sandstones and shales onlapping the Hercynian unconformity to the south and north into a thick cyclic succession of anhydrites, salts (S1, S2 and S3) and interbedded muds. The sandstones may represent highstand system tracts alternating with low stand evaporite precipitation and desiccation in

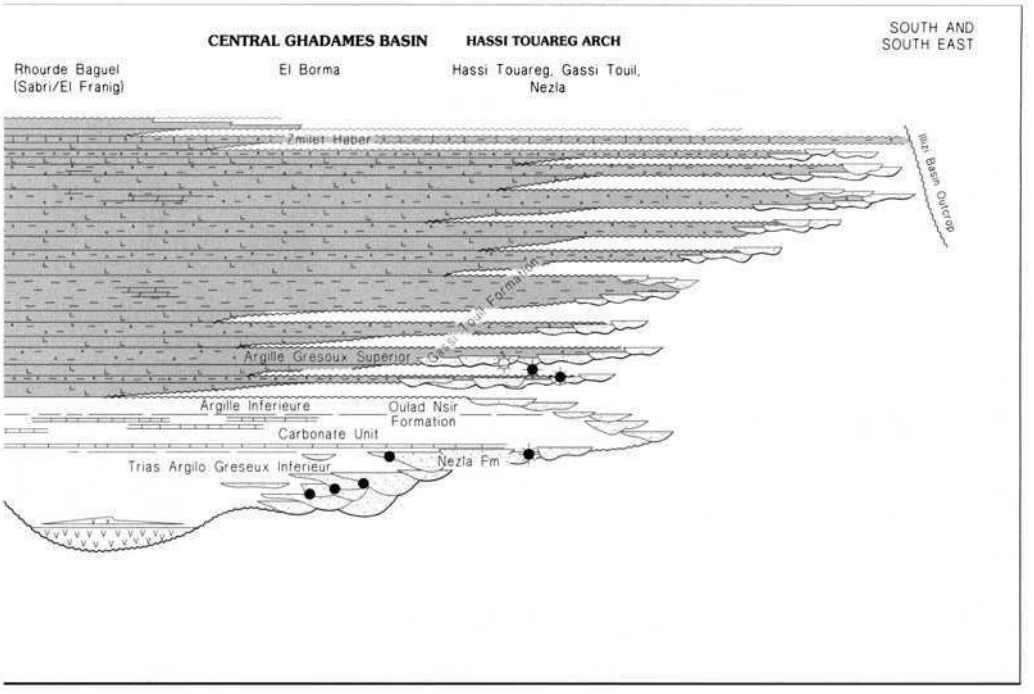

chronostratigraphic correlation of the more important basal Triassic sandstone reservoirs of the 'Triassic Basin' of overlying late Triassic–Liassic evaporite sequence. It is based upon very imprecise chronostratigraphic control and (1981), Megerisi & Mamgain (1980) and Bentahar & Ethridge (1991).

a broad alluvial basin, partially restricted from the open Tethyan seaway to the northeast.

Evaporite deposition had largely ended by the late Liassic and the Middle and Upper Jurassic is represented by a backstepping sequence of transgressive marine shales, carbonates and fringing deltaic sands. Regression followed in the Lower Cretaceous with a widespread deltaic system. This was terminated by an early Aptian phase of deformation developed in response to crustal separation and seafloor spreading in the South Atlantic (Guiraud & Maurin 1991; Guiraud 1992). Transpressional wrenching and uplift occurred along pre-existing Palaeozoic and Pan-African crustal heterogeneities with locally intense faulting and uplift. The north–south trending Amguid–Hassi Touareg structural axis was formed at this time and the Tihemboka Arch bounding the southeastern flank of the Illizi Basin and western Murzaq Basin experienced significant faulting and uplift.

Upper Tethyan Cycle. Platform sedimentation continued into the Upper Cretaceous. Intra-platform rifting was renewed in the Abu Gharadig Basin of Egypt and a phase of very rapid subsidence took place in the Sirt rift system during the Senonian. A change in relative plate motion (Savostin *et al.* 1986) between Africa and Eurasia at this time was reflected by mild inversion in the Atlas Basins, Cyrenaica and western Egypt. The platform subsequentially became relatively positive and only very thin successions of lower Tertiary sediments are present over much of the western North African Platform, at least partially as a consequence of later uplift and unroofing. Western Tethys began to close during the early to mid Tertiary with inversion of the Atlas Basin in the early Eocene (Courbouleix *et al.* 1981; Laville 1981; Van Stets & Wurster 1981; Vially *et al.* 1994), coincident with the initial collision of Africa and the Kabylie Block. Convergence with Eurasia accelerated during late Oligocene–Miocene, culminating in Maghrebian folding and nappe emplacement in northern Morocco, Algeria and Tunisia (Caire 1953; Wildi 1983)). A shallow foreland basin developed in the proximal part of the adjacent platform with fault reactivation, uplift of intra-platform highs, tilting and erosional unroofing of the intra-cratonic Palaeozoic basins in the region beyond. Further reactivation and uplift of the inverted Atlas Rift basins occurred during the late Pliocene–Pleistocene in response to dextral wrenching along the South Atlas fracture.

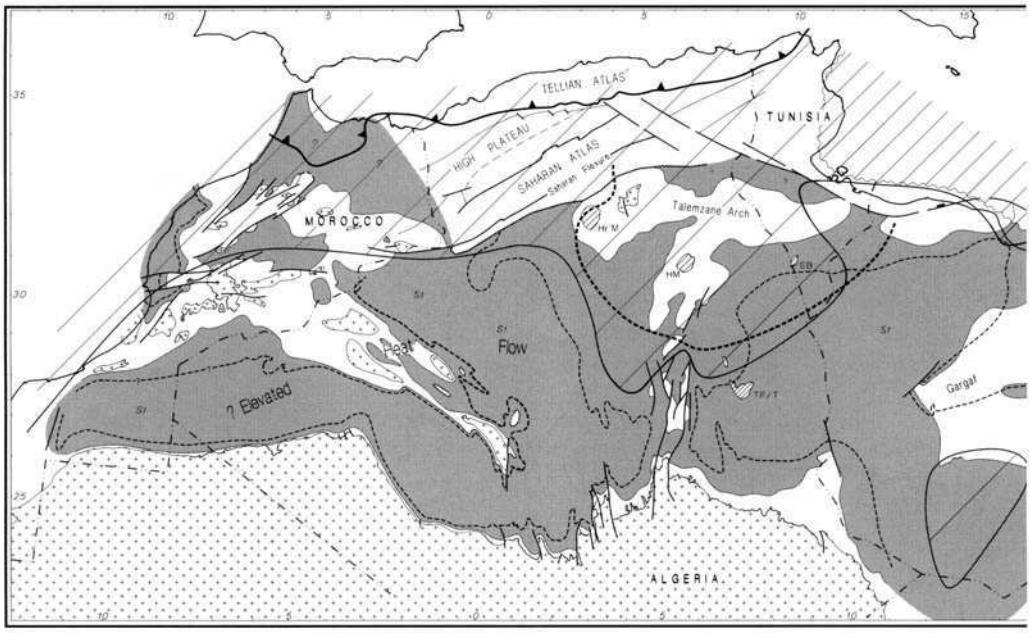

Fig. 12. Regional stratigraphic and structural controls governing the distribution of Palaeozoic petroleum evaporite seals and areas of significant post-Hercynian subsidence are highlighted. With the exception of the Illizi strong positive correlation with these three factors. Pre-Hercynian petroleum systems were probably active in the thus generated were largely dispersed by late Hercynian uplift and unroofing.

Palaeozoic petroleum systems

Introduction

The most significant Palaeozoic-sourced petroleum accumulations of the North African Platform lie in Algeria and western Libya. Within this large area, there is a variety of discrete petroleum systems of widely different hydrocarbon productivity, reservoired in intra-Palaeozoic and basal Triassic sandstones and sealed by intra-Palaeozoic shales or late Triassic–Liassic evaporites. The regional stratigraphic and structural factors responsible for these systems are illustrated in Fig. 12 and include the following.

Distribution of Lower Silurian and Upper Devonian source rocks. Although shales within the Ordovician and Middle Devonian have some limited source potential, the Tanezzuft and Frasnian bituminous mudstones are overwhelmingly the most important Palaeozoic source rocks on the North African Platform. Both were deposited over a wide area of the platform during regional flooding events and their present distribution, preserved within Palaeozoic intra-cratonic depressions, is a result of gentle Hercynian deformation, uplift and erosion.

Presence of intra-Palaeozoic and basal Triassic fluvial sandstone reservoirs. Sandstone reservoirs occur throughout the Palaeozoic, and are of varying quality depending upon facies, age and post-depositional diagenesis. Basal Triassic reservoirs are best developed in the 'Triassic Basin' of Algeria and Western Libya onlapping onto the Hercynian unconformity to the south.

Distribution of intra-Palaeozoic and Triassic seals. Regionally developed shales are commonly developed throughout the Palaeozoic sequence. The Tanezzuft and Middle Devonian are the most significant of these, acting as primary seals for Cambro-Ordovician and Lower Devonian (F6) reservoired petroleum systems. They are limited to the intra-cratonic Palaeozoic depressions and eroded locally allowing migration into lower or higher reservoirs. The Trias–Liassic evaporite sequence provides the primary seal for the basal Triassic reservoired systems. It is confined to the 'Triassic Basin' on the northern part of the Saharan Platform, grading southwards into more proximal clastic facies.

Depocentres capable of maturing and generating hydrocarbons from the Tanezzuft and Frasnian source rocks. The Palaeozoic appears to have

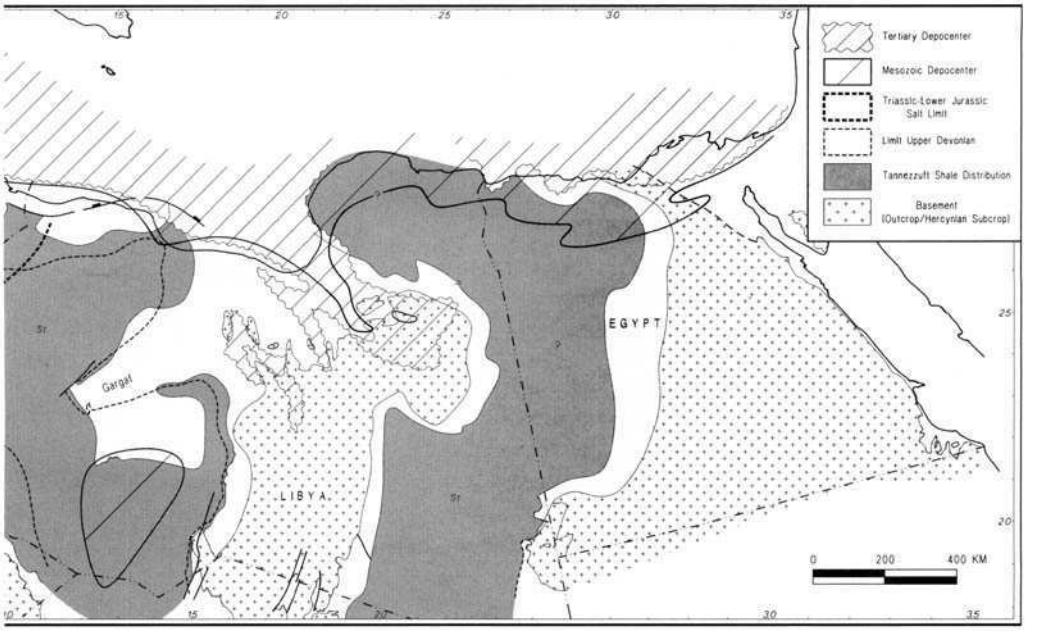

systems. The distribution of the Silurian Tanezzuft and Upper Devonian Frasnian source rocks, Triassic–Liassic Basin, which lacks Triassic reservoir and seal, all the high-productivity Palaeozoic systems of North Africa show a western and southwestern Palaeozoic basins, partly in response to regionally elevated heat flow. Hydrocarbons

thickened regionally towards the west and southwest before Hercynian uplift and erosion, with more rapidly subsiding depocentres developed locally. The Tanezzuft and Frasnian Shales achieved very high maturities in places, as a consequence of increased overburden and regionally elevated heat flow associated with Hercynian igneous activity. Very significant amounts of oil and gas were generated at this time. However, much of this was subsequently dissipated with Hercynian unroofing and residual gas accumulations were only preserved locally. The exhumed basins were never buried deeply enough again to renew generation and much of the western part of the North African Platform is unprospective as a result.

Virtually all the currently active petroleum systems in the region are directly associated with the Mesozoic sag basin ('Triassic Basin') of eastern Algeria.

Migration conduits. Regional continuity of the intra-Palaeozoic and basal Triassic sandstones and seal facies encouraged sometimes very long distance lateral migration and dispersion within the mildly deformed basinal areas. However, fault-related vertical migration is important locally along intra-basinal structural axes and bounding highs, reactivated during the Cretaceous.

Presence of adequate hydrocarbon traps. A wide variety of trapping closures were formed on the Saharan Platform at different times. These range from tight anticlinal folds of the Ahnet Basin to the broad regional domes of Hassi Messaoud and Hassi R'Mel, formed during the Hercynian deformation, to the very high relief wrench fault structures and very subtle low-relief closures of the Ghadames and Oued Mya Basins formed by Austrian and possibly later deformation.

Post-charge dispersal processes. Mid to late Tertiary plate margin orogenesis was responsible for significant uplift and local erosion of the Saharan Platform. This was particularly severe in the south where regional tilting and unroofing encouraged meteoric invasion with increased water flow through intra-Palaeozoic and Triassic aquifers. Mature petroleum systems affected by this late-stage event, were partially and sometimes completely dispersed by spillage, remigration and flushing.

It is the varying effect of these factors upon the petroleum systems in the region that is responsi-

Table 1. *Mesozoic to early Tertiary-charged petroleum systems with Triassic–Liassic evaporite seals*

Basin/area	System Representative fields	Field size	Reserves/system
Super-productive petroleum systems			
Hassi Messaoud Arch	**Tanezzuft/Cambrian**		**10 000 MMBOE**
	Hassi Messaoud (1956)	LG	
Hassi R'Mel	**Tanezzuft/Triassic**		**18 000 MMBOE**
	Hassi R'Mel (1956)	LG	
High productivity petroleum systems			
Ghadames Basin	**Tanezzuft/Triassic**		**750 MMBOE**
	El Borma (1964)	G	
	Keskessa (1969)	S	
	Debbech (1979–81)	S	
	Larich (1979–81)	S	
	Makhrouga (1979–81)	S	
	Frasnian/Triassic		**+2250 MMBOE**
	Bir Rebaa complex (1990)	G	
	Berkine East (1994)	G	
	Hassi Berkine (1994)	G	
	Bir Berkine (S) (1993)	L	
	El Merk (1993)	L	
	Rhourde El Krouf (1992)	L	
	Wadi el Teh (1976)	M	
	Ech Chouech	S	
	Chouech Essaida	S	
Oued Mya Basin	**NE Tanezzuft/Triassic**		**1080 MMBOE**
	Haoud Berkaoui (1965)	G	
	Guellala (1969)	G	
	Ben Khalala (1966)	G	
	Haniet El Beida (1978)	M	
	Draa El Temra (1971)	M	
	N'Goussa (1975)	M	
	NW Tanezzuft/Triassic		**120 MMBOE**
	Oued Noumer (1969)	M	
	Ait Kheir (1971)	S	
El Biod Arch	**Tanezzuft/Cambrian**		**630 MMBOE**
	El Agreb (1960)	G	
	Zotti (1959)	L	
	El Gassi (1958)	L	
Amguid–Hassi Touareg Axis	**Tanezzuft/Triassic (South)**		**2550 MMBOE**
	Rhourde Nouss (1962)	LG	
	Hamra (1959)	G	
	Rhourde Chouff (1963)	L	
	Rhourde Adra (1964)	L	
	Tanezzuft/Triassic (Central)		**950 MMBOE**
	Gassi Touil (1961)	G	
	Brides (1964)	G	
	Hassi Touareg (1960)	L	
	Hassi Chergui (1963)	S	
	Tanezzuft/Cambro-Ordovician (North)		**870 MMBOE**
	Rhourde El Baguel (1963)	G	
	Nezla (1960)	L	
	Messdar (1967)	M	

Notes to Table 1. Petroleum systems are grouped according to their relative productivity and representative fields are listed by size with their discovery date indicated. Approximate total estimated ultimately recoverable reserves are given for each system based upon existing discoveries, and are therefore a minimum amount. Additional discoveries and improved recoveries may increase these figures considerably. A field with significant reserves in secondary reservoirs may be listed under more than one petroleum system. The boundary between the Illizi–Ghadames and the Hamra Basins is taken along the boundary between Libya and Algeria–Tunisia save for D1-52 (Alrar extension) and the giant A1 NC169/Alwafa (adjacent to Alrar), which are taken as part of the Illizi Basin. The division adopted in this table between systems with either Mesozoic or Palaeozoic seals is difficult to apply to the Amguid–Hassi Touareg multiple-reservoir systems. For simplicity, these systems are grouped together on the basis that a salt seal is present within this province. MMBOE, million barrels of oil equivalent; bbls, barrels; LG, large giant fields (recoverable reserves greater than 1000 MMBOE); G, giant fields (greater than 250 MMBOE); L, large field (greater than 100 MMBOE); M, medium-sized field (greater than 25 MMBOE); S, small field (less than 25 MMBOE). The conversion factor used for gas was 5.8 billion cubic feet gas = 1 MMBOE. The definition of a giant field varies widely but the one used here is consistent with Macgregor & Moody (this volume).

ble for their wide range in productivity, from extremely prolific to non-productive or extinct. Each of these systems is reviewed in the following section and the relative influence of the controlling factors is examined in more detail. Emphasis is placed upon the high-productivity petroleum systems, while moderate to non-productive systems are described in less detail. However, a fuller account is given of one of the non-productive or extinct basins, the Tindouf Basin to provide a more complete perspective.

Hydrocarbon productivity was estimated very approximately from reserves so far discovered in each system as listed in Tables 1–3. Inevitably these will increase with new discoveries and enhanced recovery techniques but nevertheless they do provide a relative and semi-quantitative measure, sufficient to permit a general comparison of each system.

The main characteristics of the petroleum systems identified are tabulated in Table 4 and described in the following section. This review is based upon information displayed in the accompanying diagrams constructed from both published sources (cited in the figure captions) and proprietary data/interpretations. Definitions of field size (large giant, giant, medium) referred to in the text and tables are given in the footnotes to Table 1.

Mesozoic to early Tertiary charged systems with Triassic–Liassic seals

Ghadames Basin.

The Ghadames Basin forms part of a broad intra-cratonic Palaeozoic depression east of the Hassi Touareg structural axis and south of the Talemzane Arch (Figs 2 and 13). It plunges northwards unconformably beneath a thick Mesozoic wedge of clastics, carbonates and evaporites which provide reservoir and seal for a number of large accumulations (Van de Weerd & Ware 1994; Echikh this volume). Recent exploration has proven it especially prolific, with reserves of over 3 BBOE and potential for significantly more (Table 1; Macgregor this volume). Much of this is concentrated in the central and northeastern part of the basin in generally subtle low-relief structures. Although it has not been possible to differentiate oils reservoired in the area into discrete families (Daniels & Emme 1995), the regional stratigraphic architecture of the basin suggests the presence of two petroleum systems defined by the relative contribution of the Tanezzuft and Frasnian source rocks. These subcrop the Hercynian unconformity to the west and north, charging basal Triassic sands below Upper Triassic to Liassic shale and evaporite seals. A shaly basal Triassic facies limits the effectiveness of the Tanezzuft in the northwest, separating a Tanezzuft sourced–Triassic reservoired system to the northeast and a Frasnian–Triassic system in the central part of the basin. Regional dip at the unconformity level encouraged long distance, lateral migration through the basal Triassic sands towards the south and east, where the sealing facies grade into continental clastic deposits and both systems are limited by water washing, flushing and dispersion to the surface (Fig. 13).

Tanezzuft–Triassic petroleum system. The Tanezzuft Shale in the Ghadames area ranges in thickness from less than 200 m to over 500 m, thinning over the Ahara Arch and to the northeast. The organically richest interval is a basal 30 m radioactive unit with as much as 17% TOC of predominantly type I–II kerogen (Daniels & Emme 1995). Although the deepest part of the Palaeozoic depocentre is now very mature, it is unlikely to have contributed much to the Triassic petroleum system because of the intervening Devonian and Carboniferous. Instead this was charged by the section immediately below the unconformity, either directly

Table 2. *Mesozoic to early Tertiary-charged petroleum systems with intra-Palaeozoic shale seals*

Basin/area	System Representative fields	Field size	Reserves/system
High productivity petroleum systems			
Illizi Basin	**Lower Tanezzuft/Cambro–Ordovician (I)**		**1500 MMBOE**
	Zarzaitine (1957)	LG	
	Tin Fouye–Tabankort (1961)	LG	
	Edjeleh (1956)	G	
	Alwafa (1991)	G	
	Ohanet (1960)	L	
	Tiguentourine (1956)	M	
	La Reculee (1957)	M	
	Dome a Collenias–Ouan Taredert (1958)	S	
	Upper Tanezzuft/Lower Devonian (II)		**3500 MMBOE**
	Zarzaitine (1957)	LG	
	Tin Fouye–Tabankort (1961)	LG	
	Alrar (1960)	G	
	Edjeleh (1956)	G	
	Alwafa (1991)	G	
	Dimeta Ouest (1979)	G	
	Tin Zemane (1981)	G	
	Stah (1971)	G	
	Timedratine (1961)	L	
	Mereksene (1974)	M	
	Tiguentourine (1956)	M	
	Acheb (1963)	M	
	Dome à Collenias/Ouan Taredert (1958)	S	
	Frasnian/Upper Devonian–Carboniferous (III)		**2000 MMBOE**
	Zarzaitine (1957)	LG	
	Alrar (1960)	G	
	In Amenas Nord (1958)	G	
	Edjeleh (1956)	G	
	Dimeta Ouest (1979)	G	
	Stah (1971)	G	
	Ohanet (1960) (Lower Devonian reservoir)	L	

The petroleum systems and their representative fields are listed as in Table 1. Abbreviations as in Table 1.

from the subcropping shale, or more diffusely through Upper Silurian–Lower Devonian and Cambro-Ordovician sands on either side and vertically via nearby faults and fractures. Peak expulsion is estimated to have occurred during the later Cretaceous and early Tertiary.

The basal Triassic clastic unit, TAGI, is a regionally extensive sheet sand, discontinuous or absent in the northwest and thickening south and east to over 100 m. Porosities range from 17 to 20% and permeabilities between 100 and 450 mD (Boudjema 1987). It formed an excellent conduit and, once charged, encouraged lateral migration towards the southwest for distances of 50 kms and occasionally up to 100 km. Structural relief is very gentle at the unconformity level, with minor perturbations capable of focusing significant amounts of migrating hydrocarbons. The El Borma field is an exception because of its unique position on the culmination of a broad regional high. Although Ghenima (1995) and others have argued that this was charged from the Devonian, its position structurally downdip from the Frasnian subcrop, suggests the Tanezzuft as a more likely source. Elsewhere, accumulations are small in low-relief features draped over deeper Palaeozoic structures. Such traps were especially sensitive to mid–late Tertiary tilting associated with uplift of the Djeffara–Nefusa Arch. Scattered oil and gas shows, and some possible residual oil columns are common in the area, suggesting that pre-existing accumulations may have spilled some or all of their entrapped hydrocarbons during uplift, perhaps accounting for the small size of the fields characteristic of the area. The system is estimated to reservoir 750 MMBOE of which 700 MMBOE. is in El Borma.

Frasnian/Triassic Petroleum System. The Frasnian source rock ranges from less than 25 m to

Table 2. *Continued*

Basin/area	System Representative fields	Field size	Reserves/system
High productivity petroleum systems (continued)			
	Mereksene (1974)	M	
	Tiguentourine (1956)	M	
	El Adeb Larache (1958)	M	
Moderate to low productivity systems			
Hamra Basin	**(North) Tanezzuft/Acacus**		**65 MMBOE**
	NC 100 discoveries (1982–1986)	M	
	Bir Tlacsin (1959)	S	
	Tigi (1961)	S	
	Es Sania (1961)	S	
	(Central) Tanezzuft/Devonian		**250 MMBOE**
	Gazeil (A-1-26) (1959)	M	
	NC005A (O66-Z) (1961)	M	
	O26-Q-001 (Q-1-26) (1965)	M	
	NC007-AA (1981)	M	
	North Gazeil (1960)	S	
	Kabir (1979)	S	
	(South) Tanezzuft/Lower Devonian		**635 MMBOE**
	El Hamra Pools (1960–1962)	G	
	Emgayet (1959)	M	
	O66-LL (1962)	M	
	O66-E (1960)	S	
Murzuq Basin	**Tanezzuft/Cambro–Ordovician**		**600 MMBOE**
	NC 115 discoveries (including Murzuq Field) (1984)	G	
	NC 101 discoveries (1984)	L	
	NC 174 discovery (1993)	S	
Extinct systems			
Kufrah Basins	Immature–marginally mature and flushed		

greater than 100 m in thickness, displaying similar lateral variations to the Tanezzuft. Values of up to 8–14% TOC of oil-prone type I–II kerogen have been reported in a basal radioactive interval, with quality improving to the north. Its maturity generally mirrors the Silurian but at slightly less elevated levels. As in the case of the Tanezzuft, the overlying Triassic sands were probably charged most efficiently from the section immediately below the unconformity, both directly from the subcropping shale and more diffusely through Devonian sands on either side. Because of their relatively higher porosities, this process may have been more efficient than was the case for the Tanezzuft–Triassic system. Furthermore, the Frasnian subcrop lies some distance southeast from the shaly basal Triassic facies responsible for the reduced effectiveness of the Tanezzuft and was ideally positioned to charge the overlying conduit. Perhaps most importantly, a series of fault splays extending northeast from the Hassi Touareg structural axis across the central part of the basin promoted vertical migration through the Carboniferous, directly into Triassic traps above. Two Triassic fluvial sands are present in the area, the basal TAGI and the overlying TAGS reservoirs. As in the Tanezzuft–Triassic system, these encouraged long distance lateral migration towards the southeast. Most of the larger accumulations in the system occur in very low relief traps, a relatively short distance updip of the Frasnian subcrop. This apparent concentration may reflect more efficient local migration focusing by subtle perturbations at the Triassic sand level. As regional structural relief above the unconformity is extremely gentle, these would have become less effective with increasing distance from the subcrop, tending to disperse hydrocarbons widely towards the southeast. Unlike the

Table 3. *Palaeozoic-charged petroleum systems with intra-Palaeozoic shale seals*

Basin/area	System Representative fields	Field size	Reserves/system
Productive systems			
Ahnet/Gourara Basins	**Tanezzuft/Devonian (Cambro–Ordovician)**		**1250 MMBOE**
	In Salah (1958)	G	
	Krechba (1957)	G	
	Teguentour (1973)	L	
	Hassi Moumene (1990)	L	
	Hassi M' Sari (1990)	L	
	Gour Mahmoud (1989)	M	
	Garet El Guefoul (1991)	M	
	Djebel Berga (1953)	M	
	Tit (1956)	S	
Sbaa Basin	**Tanezzuft/Devonian (Cambro–Ordovician)**		**100 MMBOE**
	Hassi Sbaa (1980)	M	
	Oued Tourhar (1991)	M	
	Hassi Ilatou (1983)	S/M	
	Azzene (1959)	S	
	Frasnian/Devonian (Carboniferous)		**50 MMBOE**
	Hassi Sbaa (1980)	M	
	Hassi Ilatou (1983)	S/M	
	Decheira (1987–89)	S	
Extinct systems			
Tindouf Basin	Extremely high maturity—exhumed and flushed		
Reggane Basin	Extremely high maturity—exhumed and flushed		

The petroleum systems and their representative fields are listed as in Table 1. Abbreviations as in Table 1.

Tanezzuft–Triassic system, the Frasnian-sourced accumulations were largely unaffected by mid–late Tertiary tilting and retained their trap integrity to the present time. As a consequence, the system is extremely prolific, with approximately 2250 MMBOE discovered so far and the probability of more to be found.

A number of relatively small Palaeozoic accumulations are also present in the area. The Devonian F6 sand is perhaps the most important reservoir with significant reserves in the Tin Zemane and Bir Rebaa fields. These were probably charged by fault-controlled migration vertically upwards from the Silurian. In contrast, the small Cambro-Ordovician Ain Romana pool was presumably charged by downloading from the basal radioactive member of the Tanezzuft.

Northern Oued Mya–Hassi R'Mel–Hassi Messaoud Province.

The greater Oued Mya Basin is an elongate Palaeozoic cratonic sag, west of the El Biod–Amguid axis, lying unconformably beneath a northeasterly thickening wedge of Mesozoic sediments (Figs 2 and 14). The central and southern part of the basin is unproductive but the northern arm is fairly prolific, with a number of fields reservoired in basal Triassic sandstones sealed by late Triassic evaporites. The super–giant Hassi R'Mel and Hassi Messaoud accumulations lie to the northwest and southeast on flanking Lower Palaeozoic arches (Table 1).

In the northern Oued Mya Basin, the Devonian source rock interval has been entirely removed by Hercynian erosion and all the fields in the province have been charged by Tanezzuft shales still preserved within the basin. Four distinct petroleum systems can be identified, two in the northern Oued Mya limited by deteriorating reservoir updip to the south, and the Hassi R'Mel and Hassi Messaoud systems situated on broad regional structural highs. A fifth petroleum system, the El Biod system, is also included here although it is not certain from which area it received its charge (Figs 14a and 15a).

Tanezzuft–Triassic (NE Oued Mya) system. The Tanezzuft Shale subcrops the Triassic over much of northeast Oued Mya, in an ideal position to charge the overlying sands (Hamouda 1980*a*,*b*). A 20–70 m basal radioactive unit is

the richest part organically of the shale, with an average 3–12% of oil-prone kerogen. Accurate reconstruction of its thermal history is difficult because of the uncertain amount of Hercynian erosion. However there is little evidence of significant pre-Hercynian generation and peak oil expulsion is estimated to have occurred during the late Cretaceous to early Tertiary.

The overlying basal Triassic sequence is composed of several stacked fluvial sands interbedded with shales and volcanic rocks (Ali 1973). Porosities range from between 11 and 15% and permeabilities from 130 to 150 mD. Shale and volcanic interbeds acted as intra-formational seals locally but are sufficiently discontinuous to allow migration up into higher sands, while gentle regional dip encouraged long distance lateral migration to the northwest and southeast. Within the central part of the depression, migration was more locally focused along low-relief northeast–southwest trending structural highs. These first developed during a mid-Cretaceous deformational episode and were sometimes enhanced by mid-Tertiary reactivation. Subtle culminations along these axes now provide traps for a series of stacked accumulations culminating with the Hassi Berkaoui field to the south.

Hydrocarbon expulsion from the Tanezzuft source was almost certainly terminated by Miocene uplift and unroofing with little further post-uplift burial capable of renewing generation. Structural readjustment at this time was very gentle and apart from some possible local spillage and remigration, the fields appear to have retained their trapping integrity to the present. The petroleum system is of moderate to high productivity with 1080 MMBOE reserves.

Tanezzuft–Triassic (NW Oued Mya) petroleum system. A number of relatively small oil and gas accumulations occur clustered together in low-relief closures on the northwestern flank of the Oued Mya Basin. The hydrocarbons are reservoired in Triassic sands resting unconformably upon the Cambro-Ordovician and were clearly charged by long distance lateral migration from subcropping Tanezzuft Shale, 20–40 km to the southeast. There is a greater proportion of gas in this system compared with the northeast Oued Mya, reflecting their differing charge history. The area was strongly influenced by the growth of the Hassi R'Mel culmination during the later Mesozoic, when expulsion and migration from the subcropping source rock to the southeast was at its peak. Subtle changes of dip on an otherwise very gentle regional surface may have induced significant changes in preferred migration direction, perhaps responsible for the later charging of the northwestern fields at a time of more elevated source maturity. Only some 120 MMBOE are attributed to this system. It is not clear whether this reflects limited trap size or volume, or relatively ineffective migration focusing.

Hassi R'Mel petroleum system. The Hassi R'Mel gas field lies on the culmination of the broad regional Talemzane Arch, flanked by the Benoud Trough–Atlas Foredeep to the north and the northern Oued Mya depression to the southeast (Magloire 1970). Hydrocarbons are reservoired in three basal Triassic sands (A, B and C) below upper Trias and Liassic evaporites (Hamel 1990). Reservoir continuity is variable, particularly in the lower two sands, reflecting both erosional topography on the unconformity surface and local facies changes. Porosities range up to 20–22% with permeabilities as high as several darcies (Magloire 1970).

The area was part of a southeasterly dipping monocline in the Jurassic and it was only later in the Cretaceous, after the subsidence of the Benoud and Oued Mya basins that the modern closure developed. During the subsequent later Cretaceous and early Tertiary it formed the culmination of a very gently deformed arch, ideally positioned to focus hydrocarbons migrating updip from two large fetch areas to the north and southeast. It is this combination of circumstances which is responsible for its enormous size.

Although predominantly gas, the accumulation includes an oil rim with greater than 300 MMBOE reserves. Subtle changes in the geochemical character of this oil across the field suggest northwesterly migration from the Oued Mya Basin. In contrast, the gas appears to have come from very mature Tanezzuft and possible Upper Devonian source rocks in the Benoud Trough on the northern side of the Talemzane Arch. The system reservoirs 18 000 MMBOE almost entirely within the Hassi R'Mel field itself with a few very small flanking accumulations.

Hassi Messaoud petroleum system. The Hassi Messaoud oil field lies on the culmination of a regional, north–south trending Palaeozoic arch, buried unconformably beneath basal Triassic silts, clays and evaporites (Balducchi & Pommier 1970; Bacheller & Peterson, 1991). Hydrocarbons are reservoired in Cambrian Ra Unit sandstones which subcrop the unconformity in the area of the field. There is also minor production from the R2 unit just below. These sands are usually impermeable and their quality has only been enhanced locally in the Hassi Messaoud area by weathering during Hercynian erosion and exposure. The reservoir is layered, with a

Table 4. *North African Palaeozoic petroleum systems; summary of key factors controlling productivity*

Productivity	Area/basin	Systems	Stage	Trap	
				Style	Age
Mesozoic–Early Tertiary charge; Mesozoic evaporite or shale seal					
Super	Tilrhemt Dome	Tanezzuft/Triassic	Late Mature	L, A	Aust?
	Hassi Messaoud	Tanezzuft/Cambrian	Early Mature	L, A	Herc
High	Ghadames Basin	Tanezzuft/Triassic	Early Mature	L, F	Aust
		Frasnian/Triassic	Early Mature	L, F	Aust
	North Oued Mya Basin	NE Tanezzuft/Triassic	Early Mature	M, F	Herc/Aust
	El Biod Arch	Tanezzuft/Cambrian	Early Mature	L, F	Herc
	Amguid Hassi Touareg Rhourde Chouff	Tanezzuft/Triassic	Late Mature	H, F	Aust
	South Hassi Touareg	Tanezzuft/Triassic	Late Mature	H, F	Aust
	North Hassi Touareg	Tanezzuft/Cambro–Ordovician	Late Mature	H, F	Aust
Mod	North Oued Mya Basin	NW Tanezzuft/Triassic	Early Mature	L, F	Herc/Aust
Mesozoic–Early Tertiary Charge; Palaeozoic shale seal					
High	Illizi Basin	Lower Tanezzuft/ Cambro–Ordovician	Early Destructive	M, F	Herc/Aust
		Upper Tanezzuft/ Lower Devonian	Early Destructive	M, F	Herc/Aust
		Frasnian/Upper Devonian (Cb)	Early Destructive	M, F	Herc/Aust
Mod–low	Hamra Basin	(North) Tanezzuft/Acacus	Early Destructive	M. F	Herc/Aust
		(Central) Tanezzuft/Devonian	Early Destructive	L, F	Herc
		(South) Tanezzuft/Devonian	Late Destructive	L, F	Herc
	Murzuq Basin	Tanezzuft/Cambro–Ordovician	Late Destructive	L	Herc
Extinct	Kufrah Basin	Tanezzuft/Cambro–Ordovician	Extinct	L	Herc?
Palaeozoic charge; Palaeozoic shale seal					
High	Ahnet-Gourara	Tanezzuft/Lower Devonian (Є-O)	Late Destructive	H, A	Herc
Mod–low	Sbaa Basin	Tanezzuft/Devonian (Є-O)	Late Destructive	M, F	Herc
		Frasnian/Devonian (Cb)	Late Destructive	M, F	Herc
Extinct	Tindouf Basin	Tanezzuft/Lower Devonian (Є-O)	Extinct	M, F	Herc
	Reggane Basin	Tanezzuft/Lower Devonian	Extinct	M, F	Herc

Three groups of Palaeozoic-sourced petroleum systems are recognized on the North African Platform: (1) Mesozoic-charged systems with Triassic evaporite seals, (2) Mesozoic-charged systems with intra-Palaeozoic seals and (3) Palaeozoic-charged systems with intra-Palaeozoic shale seals. The key factors governing their productivity are tabulated. The relative effectiveness of each petroleum system can be estimated approximately from the total recoverable reserves (in oil equivalent) reservoired within it. This is a minimum number and may increase with future discoveries and increased recovery efficiencies. Notes: (a) trap style refers to the general structural relief and

Migration drainage	Peak oil expulsion	Phase oil–gas	Impedance	Entrapment style	Post-charge modification	Reserves (MMBOE)
L	K_u–T	Gas >> oil	HI	Ex salt seal large domal closure	Miocene tilting and remigration of oil	18,000
L	K_u–T	Oil >> gas	HI	Ex salt seal large domal closure	Minor Miocene uplift	10,000
L >> V	K_m–T	Oil >> gas	MI	Ex salt seal moderate structure	Minor freshwater flushing	750
L > V	T	Oil >> gas	MI	Ex salt seal moderate structure	Minor freshwater flushing	2250
V > L	K_u–T	Oil >> gas	MI	Gd volcanic seal moderate structure	Minor Miocene uplift	1080
V + L	K_u–T	Oil >> gas	HI	Ex shale seal moderate structure	Minor Miocene uplift	630
V	J–K_L	Gas >> oil	MI	Gd salt seal intense structure	Miocene uplift: Mio–Pliocene subsidence	2550
V	J–K_L	Gas > oil	MI	Gd salt seal intense structure	Miocene uplift: Mio–Pliocene subsidence	950
V + L	J–K_L	Oil > gas	MI	Gd salt seal intense structure	Miocene uplift: Mio–Pliocene subsidence	870
L	K_u–T	Oil > gas	LI	Ex salt seal major structure	Miocene tilting and remigration of oil	120
L + V	T_R–T Pre-Herc?	Gas > oil	MI	Gd shale seal moderate structure	Tertiary tilting, spillage, remigration, freshwater flushing	1500
L + V	T_R–T Pre-Herc?	Oil > gas	MI	Gd shale seal moderate structure	Tertiary tilting, spillage, remigration, freshwater flushing	3500
L + V	K_L–T	Oil ≈ gas	MI	Gd shale seal moderate structure	Tertiary tilting, spillage, remigration, freshwater flushing	2000
V > L	K_L–T	Oil >> gas	LI	F shale seal minor structure	Major Tertiary tilting, spillage, remigration, freshwater flushing	65
L	K_L–T	Oil >> gas	LI	F shale seal minor structure	Tertiary tilting, spillage, remigration, freshwater flushing	250
L > V	K_L–T	Oil >> gas	LI	F shale seal minor structure	Major Tertiary tilting, spillage, remigration, freshwater flushing	635
L	K_u–T	Oil >> gas	MI	Ex shale seal minor structure	Tertiary uplift, spillage remigration, freshwater flushing	600
L?	T?	Oil?	LI	P shale seal minor structure	Tertiary uplift, spillage remigration, freshwater flushing	–
V	Herc	Gas >> oil	HI	Gd shale seal major structure	Hercynian uplift, thermal event; Tertiary uplift	1250
V	Herc	Oil >> gas	MI	Gd shale seal moderate structure	Hercynian uplift, Tertiary flushing	100
V	Herc	Oil >> gas	MI	F shale seal moderate structure	Hercynian uplift, Tertiary flushing	50
V + L	Herc	Gas >> oil	LI	F shale seal moderate structure	Hercynian uplift, thermal event; Tertiary uplift	–
V	Herc	Gas >> oil	LI	F shale seal moderate structure	Hercynian uplift, thermal event; Tertiary uplift	–

character of the traps where relief is indicated as high (H), moderate (M) or low (L), and further qualified as being either anticlinal (A) or faulted (F); (b) important trap-forming orogenic phases are indicated as Hercynian (Herc) and Austrian (Aust); (c) migration drainage is indicated as vertical (V) or lateral (L); (d) the critical period of peak oil generation is estimated; (e) the impedance of each petroleum system is indicated as high (HI), moderate (MI) or low (LI), and further qualified by the intensity of structural deformation and the general lithology and nature of the seal (Ex, excellent; Gd, good; F, fair; P, poor).

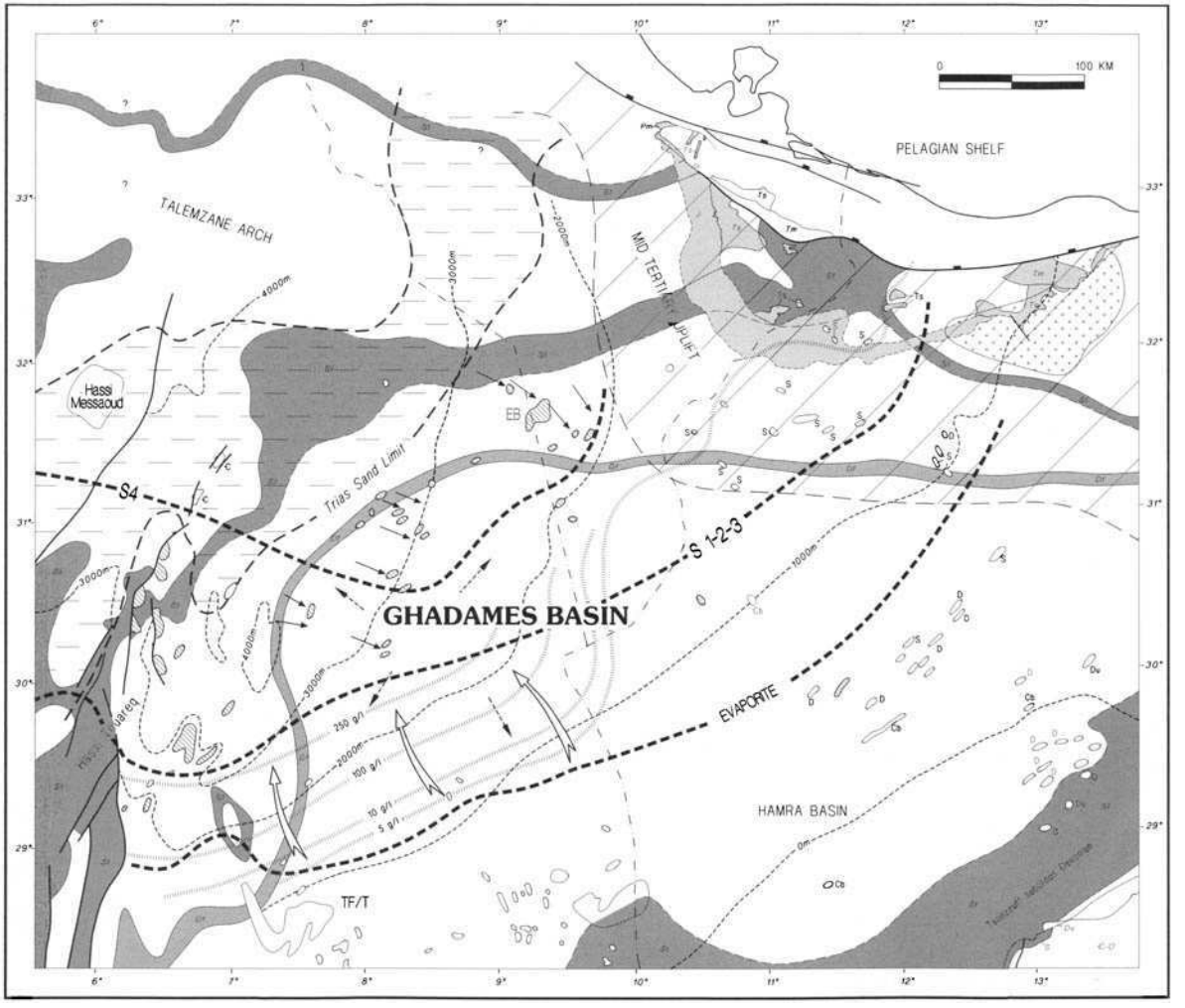

Fig. 13. (**a**) Ghadames Basin petroleum systems summary map (see Fig. 2 for location). Two petroleum systems are recognized in the Ghadames area reservoired in Triassic sands, one in the central part of the basin charged by Frasnian shales and a second to the northeast charged by the Tanezzuft. The subcrop of the Tanezzuft and Frasnian source rocks to the Hercynian unconformity is highlighted and preferential migration directions within the Triassic sandstone conduit are indicated by arrows (see depth contours on Hercynian unconformity). Oil and gas accumulations reservoired in the Triassic are shown by a hachured pattern. The systems are limited by basal Triassic shale facies to the northwest, and loss of Triassic–Liassic evaporite seals by lateral facies change to the south. Preferential intra-Palaeozoic migration directions are indicated by broken arrows. Late-stage meteoric invasion and freshwater flushing from the south are suggested by open arrows and isosalinity contours (after Chiarelli 1978). (Refer to the legend for further detail.) Partly based on information from Bishop (1975), Sonatrach (1979), Hamouda (1980), Bentaher & Ethridge (1991), Emme & Sunderland (1991), van de Weerd and Ware (1994), Daniels & Emme (1995), Gauthier *et al.* (1995).

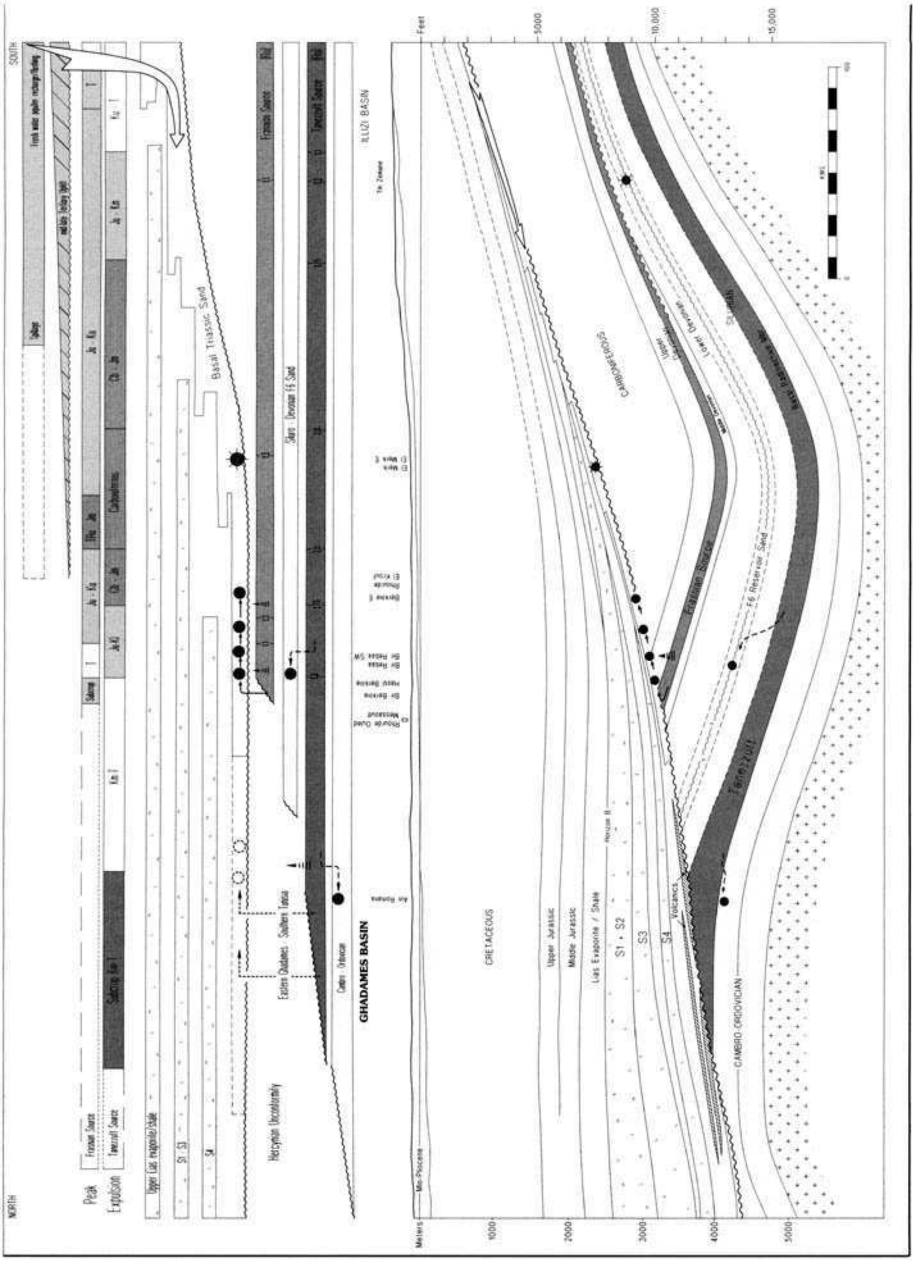

Fig 13. (**b**) Critical elements analysis for Ghadames Basin petroleum systems, illustrating the spatial relationship and relative timing of critical structural, stratigraphic and thermal variables controlling hydrocarbon distribution in the basin and highlighting their relative timing. Although Tanezzuft and Frasnian sources matured early within the deepest part of the Palaeozoic basin, most of the hydrocarbons reservoired in the two systems were probably generated later from the subcropping shales directly into overlying Triassic conduits and via porous units above and below. The main phase of charging is estimated to have started in mid-Cretaceous with short to long distance, high-impedance lateral migration towards the southwest. Prospectivity decreases to the south with the loss of seal and late Tertiary meteoric invasion. (Refer to the legend for more detail.) It should be noted that petroleum system data from out of the line of section are displayed with dashed lines.

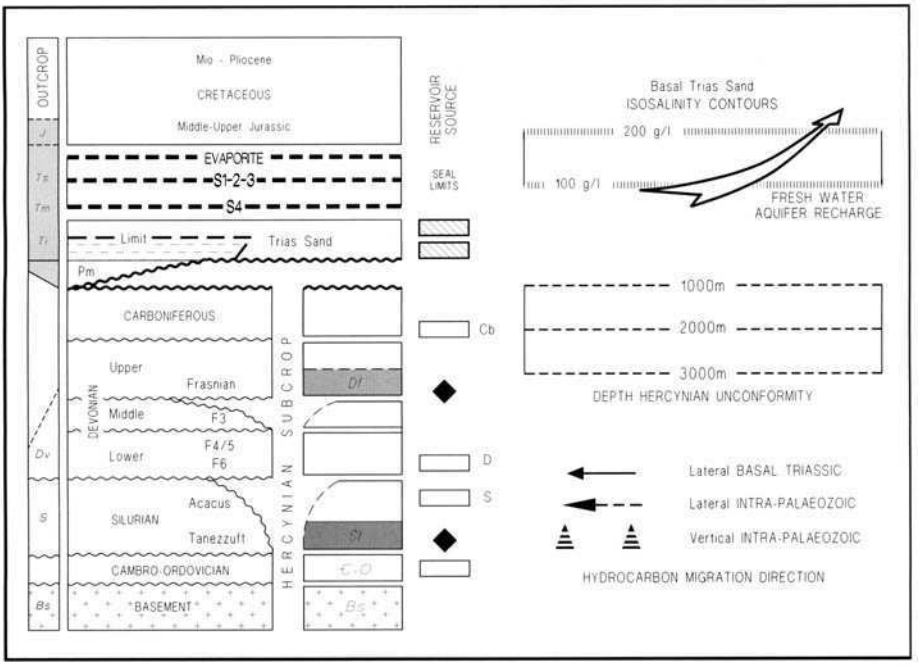

Fig 13. Legend. Ghadames Basin petroleum systems. Schematic stratigraphy (divided into outcrop map notation on left and subcrop notation on right), illustrates main source rocks (lozenge symbols) and main reservoir rocks (rectangles), the reservoir of the primary play being hachured.

thin impermeable cap at the unconformity surface passing down into sands with variable porosities and permeabilities ranging between 2 and 11% (average 8%) and 0 to 1000 mD.

The field was charged by long distance migration from Tanezzuft Shale in the Oued Mya Basin (Bacheller & Peterson 1991). With few structural barriers, migration was very efficiently focused by the Hassi Messaoud Arch, first through Triassic sands and then perhaps along the weathered unconformity surface towards the crest of the structure where these pass into shales. Basal Triassic incised sand-filled fluvial channels may have enhanced this process significantly. The field was unaffected by mid-Cretaceous deformation and later Tertiary uplift and erosion, with little or no subsequent loss of trap integrity. Some 10 000 MMBOE are reservoired in the accumulation.

El Biod petroleum system. The El Agreb, Zotti and El Gassi oil fields are clustered together to form a second discrete petroleum system further south along the Hassi Messaoud Arch (Figs 14a, and 15). They are similar to the Hassi Messaoud field, with Cambrian reservoirs and a Triassic shale and silt seal (Ali 1975). Charging may have been southwards by spillage from Hassi Messaoud or more laterally from Tanezzuft Shale preserved in a separate Palaeozoic depression immediately to the east. Approximately 630 MMBOE are reservoired in the three accumulations.

North Talemzane Arch. Four oil and gas condensate fields (including Sabri and El Franig) have been discovered in southern Tunisia, on the northern flanks of the Talemzane Arch (Cunningham 1988; Rigo 1996). One is reservoired in basal Triassic sands and sealed by shales and evaporites, and the others are reservoired within fractured Ordovician sandstones unconformably beneath Triassic shales. All four accumulations were clearly sourced from mature Tanezzuft shales which subcrop the Hercynian unconformity in the immediate area. Although they are very small they are significant, proving the presence of an active petroleum system(s) on the north side of the Arch. It is possible that further exploration may extend the system to the west although it is limited in the east by the Djeffara–Nefusa Uplift (Rigo 1996).

Amguid Spur–Hassi Touareg Axis.
The Amguid Spur–Hassi Touareg Axis is a complex north-plunging ridge of en echelon horsts and faulted anticlines, bounded by the El Biod Arch and Oued Mya Basin to the west and the

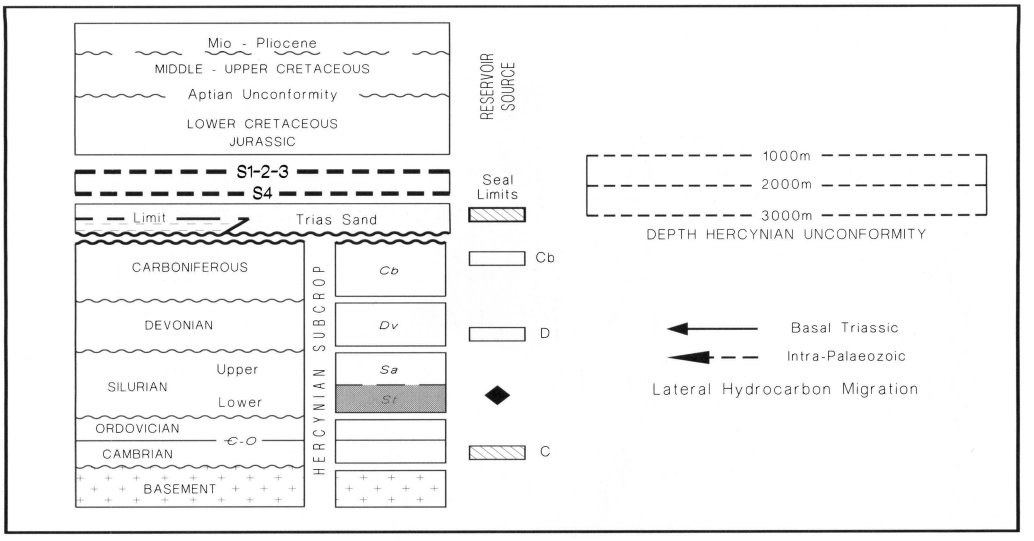

Fig. 14. Legend. North Oued Mya, Hassi R'Mel and Hassi Messaoud-El Biod Arch petroleum systems.

Ghadames Basin in the east (Figs 2 and 15). The ridge developed during the mid-Cretaceous Austrian phase of transpressional wrench deformation and very pronounced high relief structural traps were formed at this time. These reservoir large gas, gas condensate and oil accumulations in Triassic and fractured Palaeozoic sands, sealed by overlying and across-fault shales and evaporites (Table 1). The accumulations were charged by Tanezzuft Shale from a depocentre flanking the eastern side of the axis. Peak oil expulsion maturities were reached before mid-Cretaceous deformation over much of this depression and the Austrian-aged traps were charged later with gas and gas condensate and lesser amounts of oil as maturities increased during the later Cretaceous and early Tertiary. Unlike petroleum systems in the neighbouring basins, large displacement faulting encouraged vertical migration, and multiple stacked reservoirs are common. In some parts of the Hassi Touareg trend faulting has been too severe, offsetting reservoir against Cretaceous sands and limiting trap volume.

Three petroleum systems can be distinguished, a Tanezzuft–Cambrian one to the north and two Tanezzuft–Triassic systems along the southern part of the Hassi Touareg Axis and southeast in the Rhourde Chouff area (Figs 2 and 15).

Rhourde Chouff Tanezzuft–Triassic petroleum system. There are several large gas condensate and oil accumulations on the Rhourde Chouff structural alignment reservoired in basal Triassic sands. These occur within high-relief Austrian aged structural traps charged by relatively long distance lateral migration from the north and perhaps by vertical migration via faults from the underlying Tanezzuft. The southern boundary of the system is defined by the stratigraphic limit of the Triassic–Liassic evaporite seal. It reservoirs some 2550 MMBOE.

South Hassi Touareg Tanezzuft–Triassic petroleum system. The southern Hassi Touareg accumulations are trapped within very high relief mid-Cretaceous fault blocks. Hydrocarbons are reservoired in two stacked basal Triassic fluvial sands charged by vertical and short distance lateral migration from subcropping Tanezzuft Shale nearby. The reservoir sand grades into alluvial silts, shales and mudstones immediately to the north, which define the limit of the system (Claret & Tempere 1967).

The combined reserves of the accumulations within this system are only 950 MMBOE despite the very large structures, because effective trap volume has been limited by across fault seals.

Tanezzuft–Cambro-Ordovician petroleum system. Two oil and gas fields, Messdar and Rhourde El Baguel, are located along the northern part of the Amguid Spur–Hassi Touareg ridge, trapped within wrench-generated horst blocks. In contrast to the accumulations further south, the hydrocarbon phase in both fields is dominated by oil (with subsidiary gas), reservoired in fractured Cambrian sandstones. The stratigraphic architecture of the area surrounding the two fields suggests they were charged by long distance lateral migration immediately

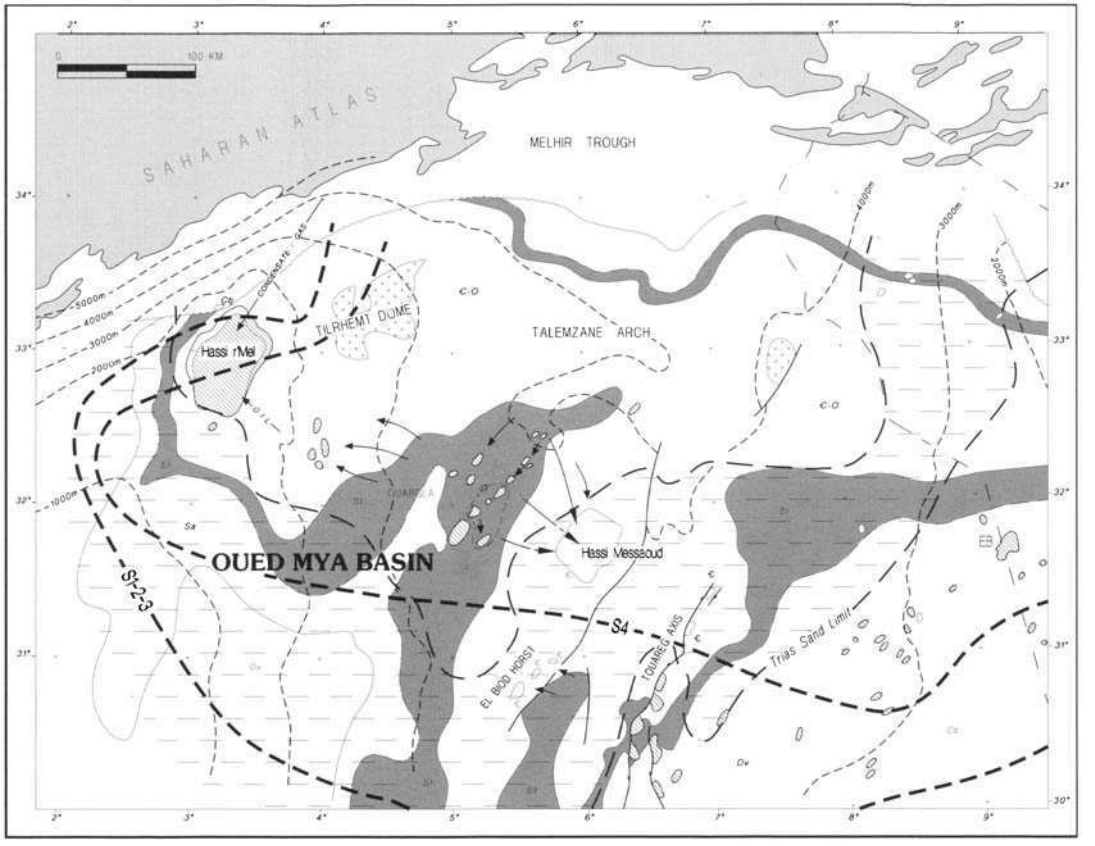

Fig. 14. (a) North Oued Mya, Hassi R'Mel and Hassi Messaoud–El Biod Arch petroleum systems (See Fig. 2 for location). Five petroleum systems are recognized in the northern Oued Mya Basin and adjacent areas: (1) the northeastern Oued Mya Basin system with basal Triassic reservoirs charged directly from unconformably underlying Tanezzuft Shale, (2) the northwestern Oued Mya System with Triassic reservoirs charged by long distance lateral migration from the southeast, (3) Hassi R'Mel gas field with a Triassic sandstone reservoir charged by gas and condensate from the northern Benoud Trough and oil from the southeast in late Cretaceous–early Tertiary, (4) the Hassi Messaoud oilfield with a weathered Cambrian reservoir sealed by Triassic shales unconformably above and charged by long distance migration from the Oued Mya Basin and (5) the El Biod system with Cambrian reservoirs charged by a Tanezzuft depression to the east or possibly by spillage from the Hassi Messaoud accumulation (Fig. 15b). A group of fields in southern Tunisia on the northern margin of the Talemzane Arch demonstrates the existence of another, poorly known petroleum system(s). The Tanezzuft subcrop within the northern Oued Mya Basin is highlighted and the stratigraphic limits of the Triassic reservoir sandstone and overlying sealing evaporite units are indicated. The distribution of a Triassic volcanic and shale sequence which forms an intraformational seal in the northeastern part of the Oued Mya Basin is also shown. (Refer to the legend for more detail.) Partly based on information from Balducchi & Pommier (1970), Magloire (1970), Aliev *et al.* (1971), Ali (1973), Ali (1975), Hamouda (1980*a*), Hamouda (1980*b*), Assaad (1981), Bacheller & Peterson (1991), Benamrane *et al.* (1993) and Yahi and Khatir (1995).

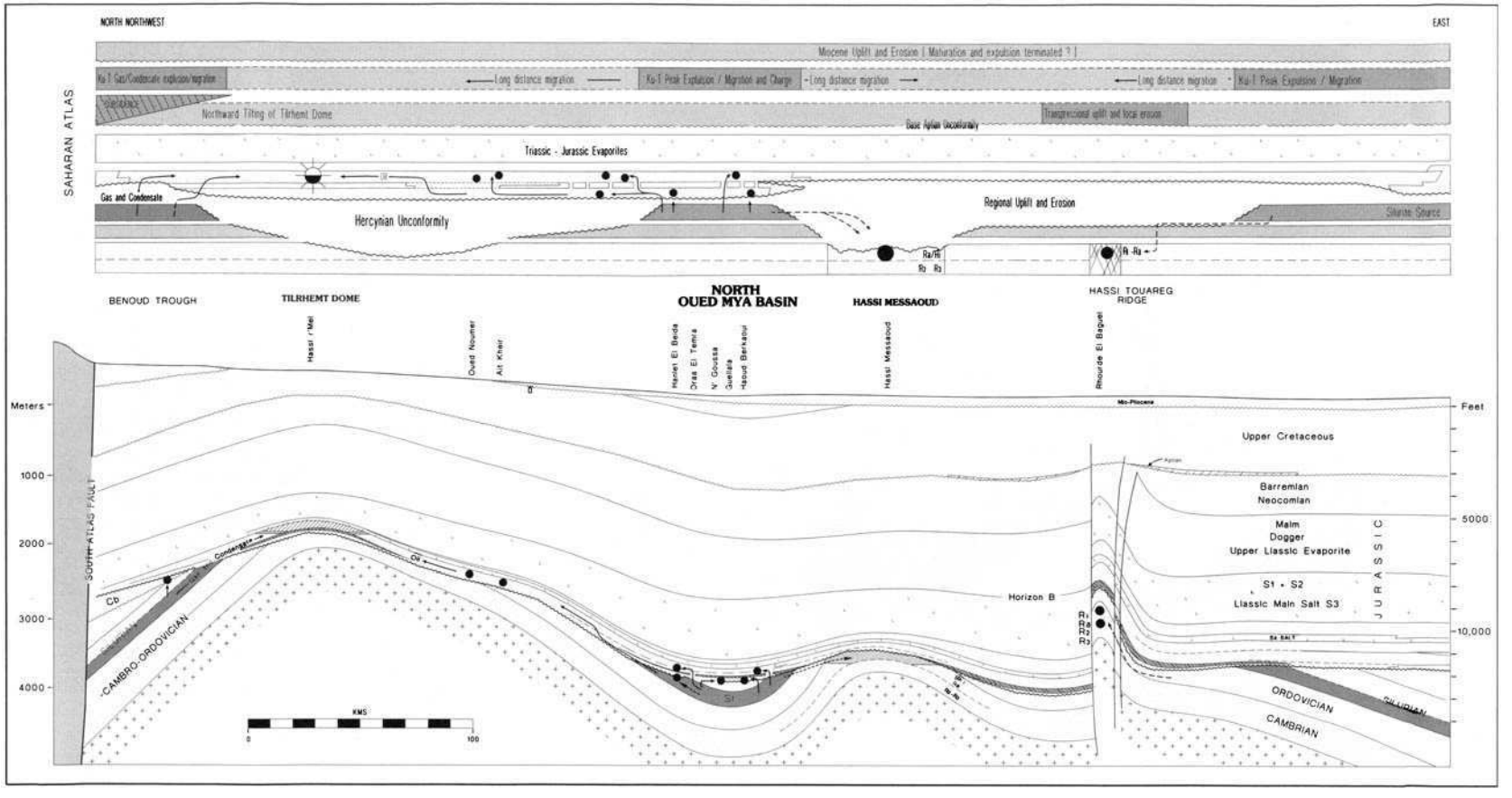

Fig. 14 (b) Critical elements analysis for North Oued Mya, Hassi R'Mel and Hassi Messaoud–El Biod petroleum system, illustrating the spatial relationship and relative timing of key structural, stratigraphic and internal factors controlling hydrocarbon distribution in the area. The five systems recognized in this area were all charged by high-impedance short to long distance lateral migration with only a minor component of vertical migration.

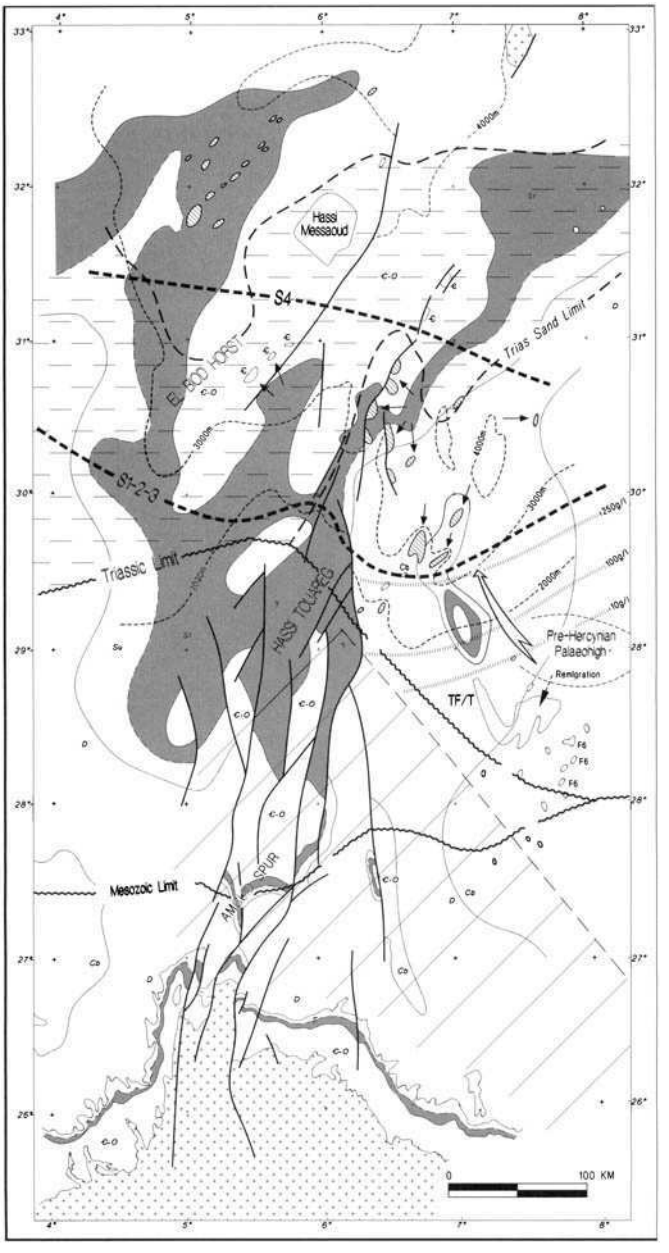

Fig. 15. (**a**) Amguid–Hassi Touareg Ridge petroleum systems summary map (see Fig. 2 for location). Three petroleum systems are recognized along the mid-Cretaceous (Austrian) Amguid–Hassi Touareg Ridge, all in high-relief structural traps sealed by overlying and across-fault Triassic and Jurassic shales and evaporites. These are (1) a southern Triassic reservoired system on the Rhourde Chouff Alignment (140 km NW of TF-T) charged by subcropping Tanezzuft Shale to the north and locally by vertical migration from the Silurian below, (2) a Triassic reservoired system along the southern part of the Hassi Touareg horst complex charged locally by Tanezzuft Shale and (3) a Cambrian reservoired system along the northern part of the Hassi Touareg axis (Fig. 14b). The north–south trending mid-Cretaceous ridge with its bounding faults is shown schematically. Triassic sandstone reservoir and evaporite seals limits are highlighted. Triassic reservoired oil and gas fields are indicated with a hachured pattern and postulated migration directions are indicated with arrows. (Refer to the legend for more detail.) Partly based on information from Claret & Tempere (1967), Aliev *et al.* (1971) and Ali (1975).

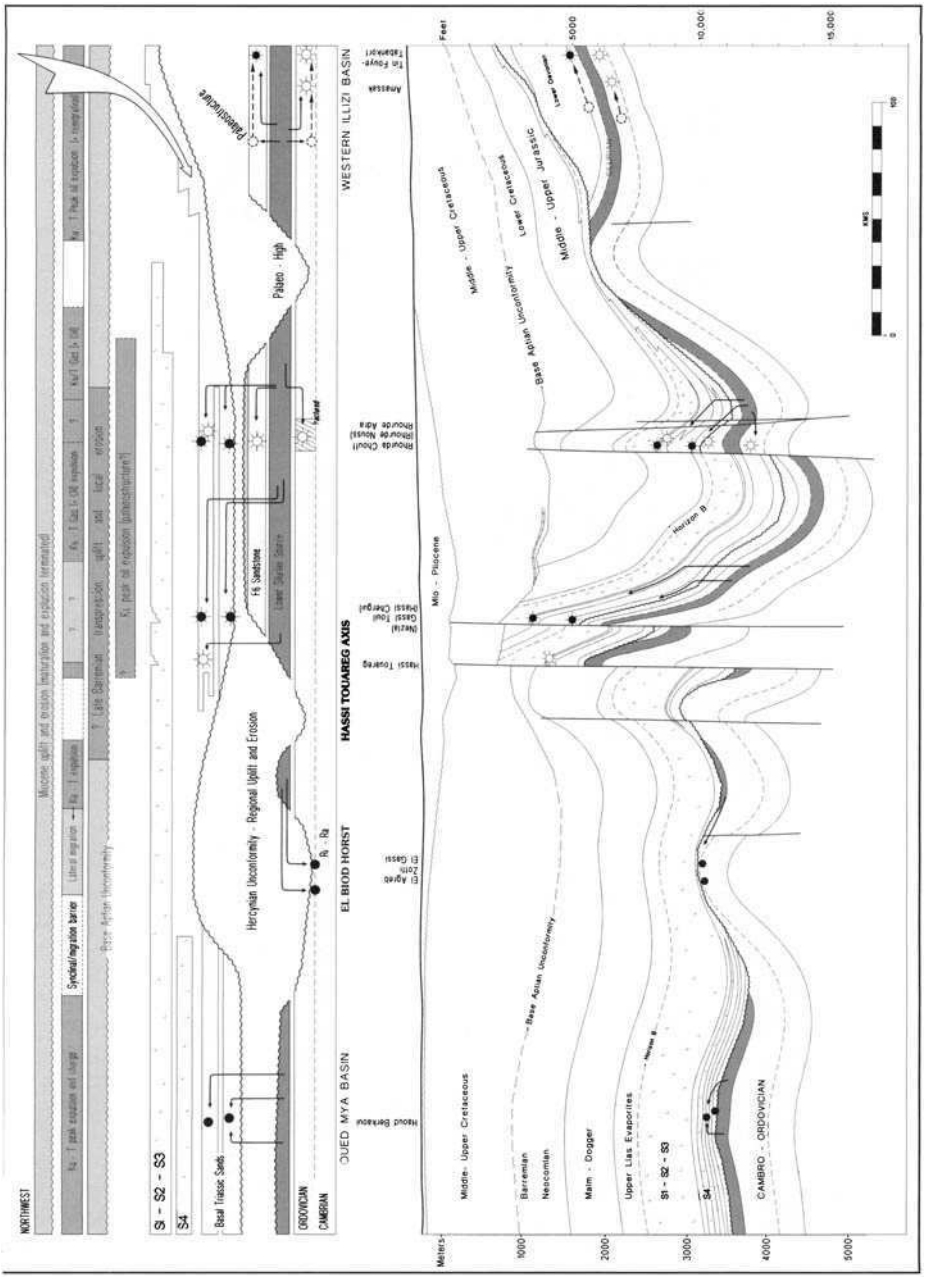

Fig. 15 (b) Critical elements analysis for Amguid–Hassi Touareg Ridge petroleum systems, illustrating the spatial relationship and relative timing of key structural, stratigraphic and thermal variables controlling hydrocarbon distribution along the Amguid–Hassi Touareg structural ridge (adapted from Claret & Tempere (1967)). Burial history analysis suggests that peak oil generation occurred before the mid-Cretaceous transpressional deformation responsible for the structural axis, and traps formed at that time were subsequently charged by high-maturity gas and oil in later Cretaceous and early Tertiary. The southern two systems were charged by lateral migration from subcropping Tanezzuft source rocks to the east with significant vertical migration locally up trap bounding faults (and underlying Tanezzuft). The northern system was charged by long distance lateral migration from the east along the unconformity surface and perhaps thin sands above. Preferred migration directions are indicated.

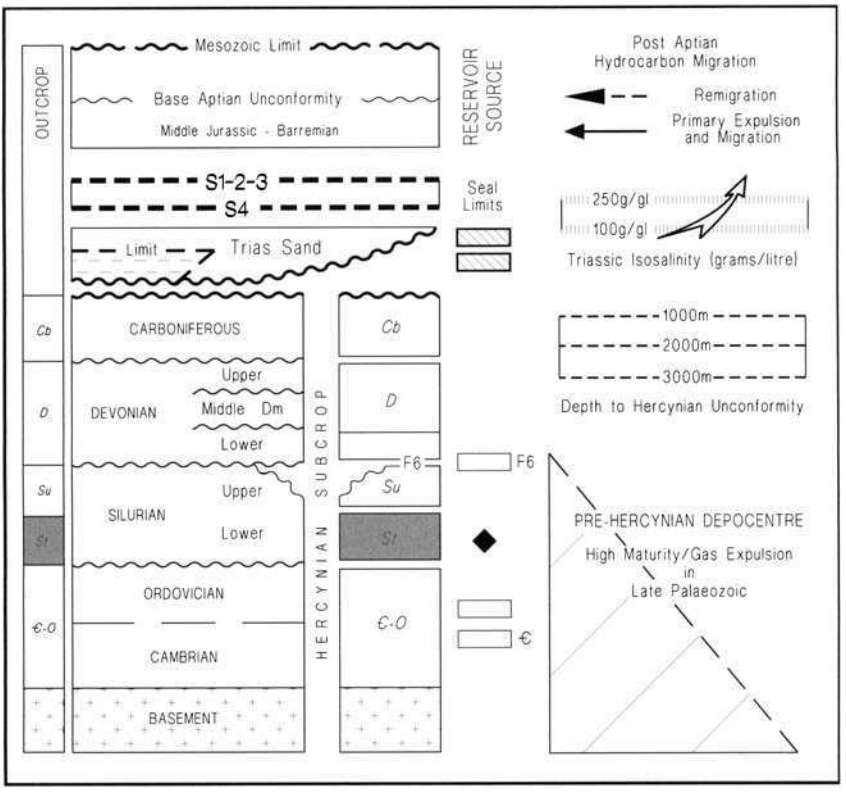

Fig. 15. Legend. Amguid–Hassi Touareg Ridge petroleum systems.

along the Hercynian unconformity surface, from Tanezzuft Shale some distance to the east. The system appears to be trap limited, with only 870 MMBOE reserves discovered so far.

Mesozoic to early Tertiary charged systems with Palaeozoic shale seals

Illizi Basin.

The Illizi Basin (Figs 2 and 16) forms the southern part of a broad intra-cratonic Palaeozoic depression extending over the greater Ghadames–Hamra region. It is flanked by the Amguid Spur to the west and the Tihemboka Arch to the east. The Palaeozoic crops out to the south towards the Hoggar Massif and plunges north below a thin unconformable Mesozoic cover. Its northern boundary is generally defined as the proximal limit of the Liassic evaporite sequence.

The basin is extremely prolific with eight fields of over 250 MMBOE and total reserves of approximately 7 BBOE (Table 2). As in the Ghadames area to the north, the Tanezzuft and Frasnian source rocks are both preserved in the basin, charging fluvial, estuarine and shallow marine sandstone, ranging from Cambro-Ordovician to Carboniferous in age (Chiarelli 1978; Tissot *et al.* 1984; Van de Weerd & Ware 1994; Daniels & Emme, 1995). Interbedded marine shales provide seals of varying effectiveness. The area is only very gently deformed and regional stratigraphic continuity tended to encourage long distance lateral migration. However, vertical migration was important locally through erosional windows in intra-formational shale seals, and also in proximity to the Tihemboka Arch, where faulting was more common.

The basin experienced a long but relatively simple history, punctuated by Hercynian, Austrian and mid–late Tertiary deformational events. During the Palaeozoic, a thick sequence of sediments accumulated in a depocentre immediately southwest of the modern basin (Tissot *et al.* 1984). Tanezzuft shales within this depocentre achieved very high maturities (+1.75% *Ro*) before the Hercynian and generated large

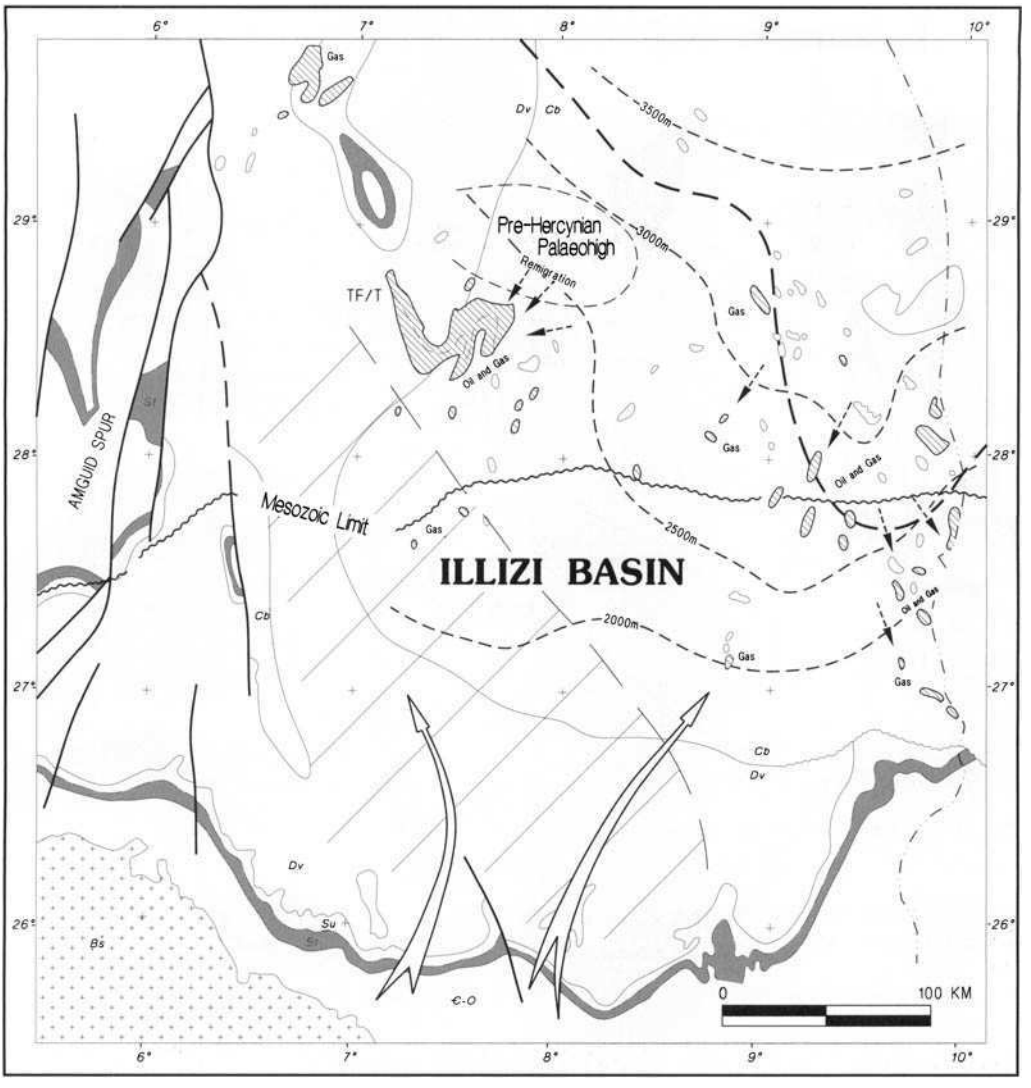

Fig. 16. (a) Illizi Basin: Lower Silurian/Cambro-Ordovician Petroleum System I (see Fig. 2 for location). Three active and one extinct petroleum systems are recognized in the Illizi Basin: (1) a late Palaeozoic system charged from a depocentre to the southeast and subsequently dispersed during Hercynian (and Austrian) uplift and unroofing, (2) a Cambro-Ordovician system (System I) charged by the Lower Tanezzuft, (3) a Lower Devonian reservoired system (System II) charged by Upper Tanezzuft Shale and (4) an Upper Devonian–Lower Carboniferous reservoired system (System III) charged by Frasnian shales, from the northeastern depocentre and flanking areas to the northeast. The outcrop and Mesozoic subcrop of the Lower Tanezzuft source rock responsible for System I are indicated. Cambro-Ordovician oil and gas accumulations are highlighted with a hachured pattern and preferred lateral migration directions are shown by dashed arrows. The estimated present-day oil–gas maturity transition within the Mesozoic depocentre is shown by a dashed line and the exhumed pre-Hercynian depocentre southwest of the basin is indicated by diagonal lines. Source rocks in this area are thought to have charged palaeo-highs on the adjacent platform which subsequently remigrated into new structures after Austrian uplift and tilting. Late-stage meteoric invasion and flushing from the south is suggested by open arrows. Partly based on information from Chiarelli (1978), Tissot *et al.* (1984), van de Weerd & Ware (1994) and Gauthier *et al.* (1995).

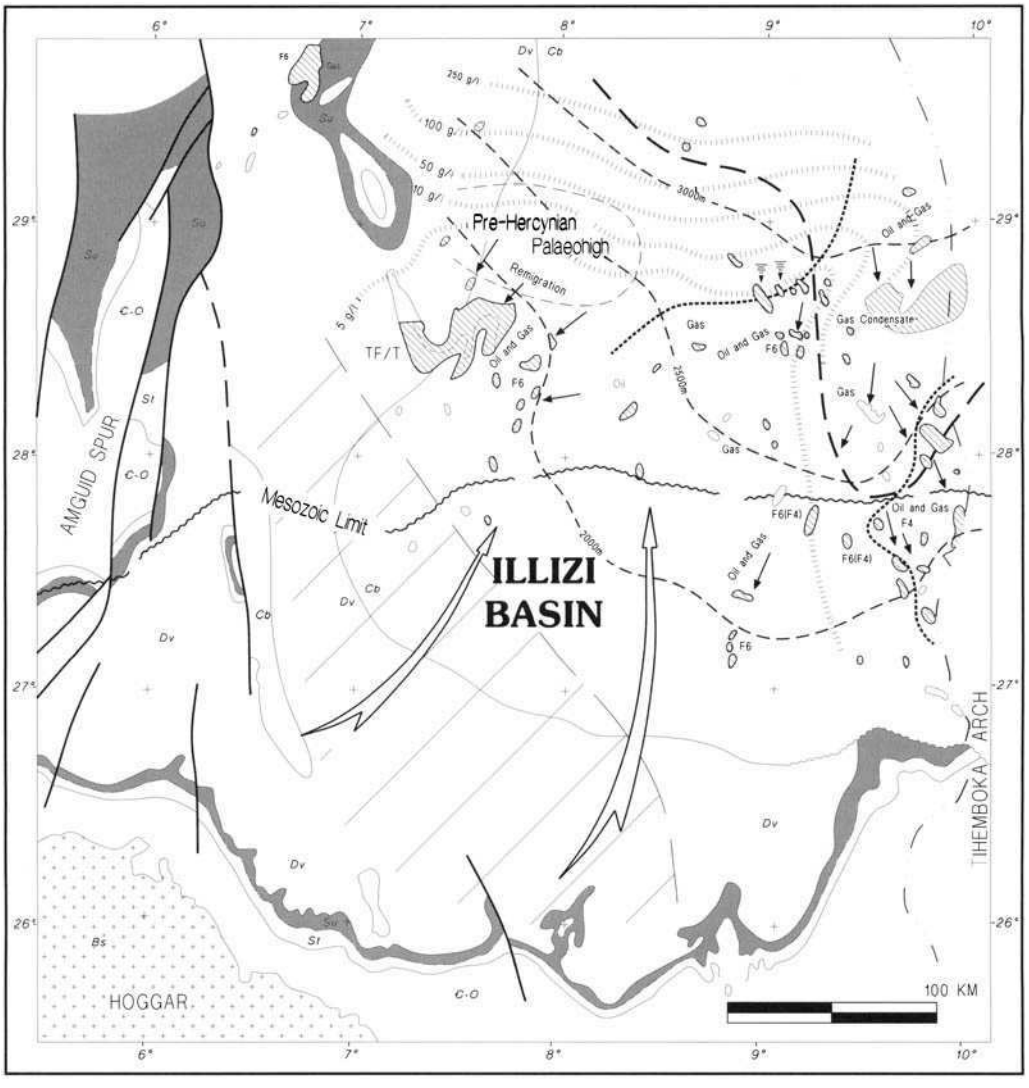

Fig. 16 (**b**) Illizi Basin: Silurian/Lower Devonian F6–F4 Petroleum System II (see Fig. 2 for location). The outcrop and Mesozoic subcrop of the upper Tanezzuft source rock responsible for this system is indicated. Lower Devonian accumulations are highlighted with a hachured pattern and preferred lateral migration directions are shown by arrows. Erosional windows in the F6 shale seal allowing upward migration into F4 reservoirs on the Talemzane Arch and downward migration of Frasnian oil into F6 reservoirs in the Ohanet area are outlined by short dashed lines. The estimated present-day oil–gas maturity transition is shown with a long dashed line. The exhumed pre-Hercynian depocentre is shown by diagonal lines and possible remigration from Palaeozoic charged palaeo-accumulations into later post-mid-Cretaceous closures are indicated (after Tissot *et al.* (1984)). Late Tertiary meteoric invasion and flushing from the south is suggested by open arrows and F6 Sand isosalinity contours (after Chiarelli (1978)).

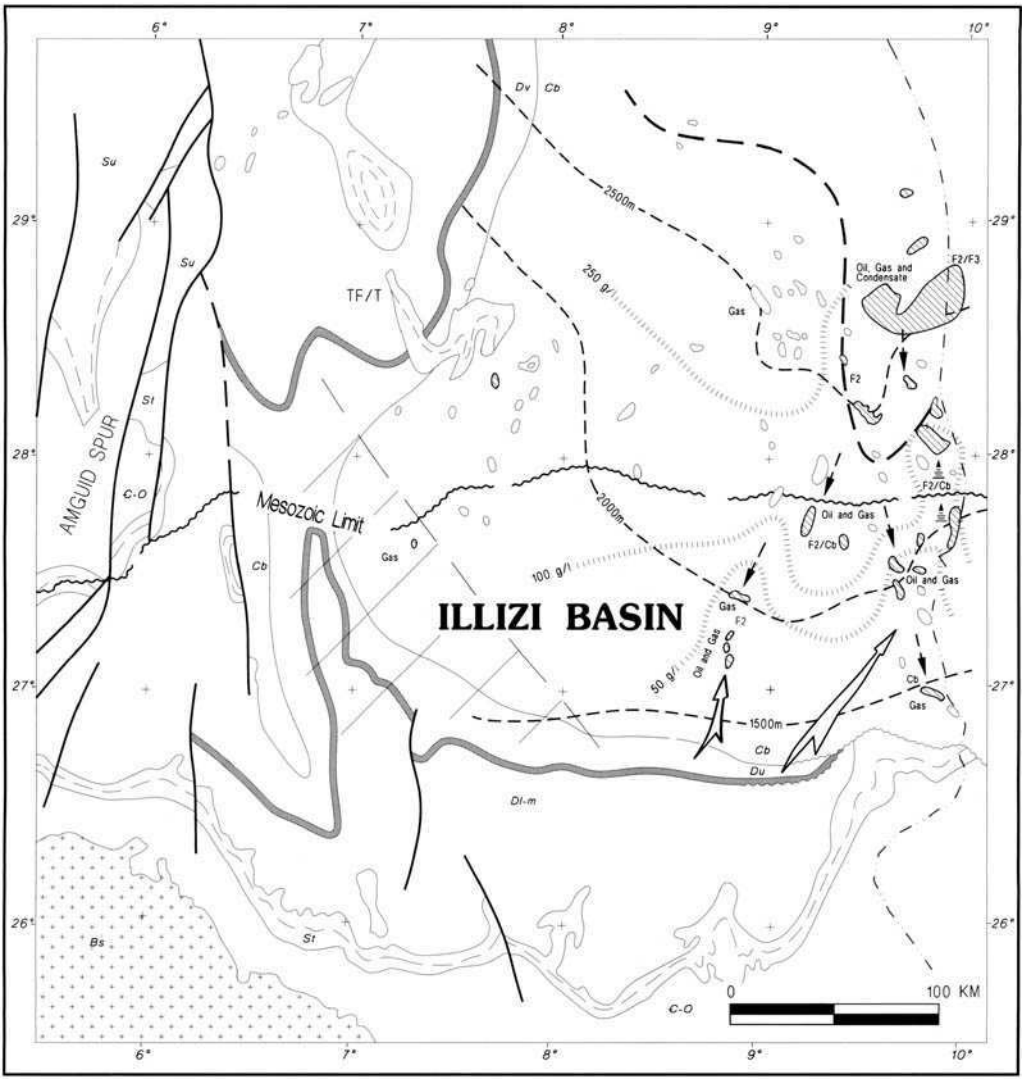

Fig. 16. (c) Illizi Basin: Frasnian/Upper Devonian to Lower Carboniferous System III (Figure 2 for location). The outcrop and Mesozoic subcrop of the Frasnian source rock responsible for the Upper Devonian-Carboniferous system is indicated. Upper Devonian/Lower Carboniferous accumulations are highlighted by a hachured pattern and preferred lateral and vertical migration directions are shown by dashed arrows. Late Tertiary meteoric invasion and flushing from the south is suggested by open arrows and Upper Devonian isosalinity contours (after Chiarelli (1978)). (Refer to the legend for more detail.)

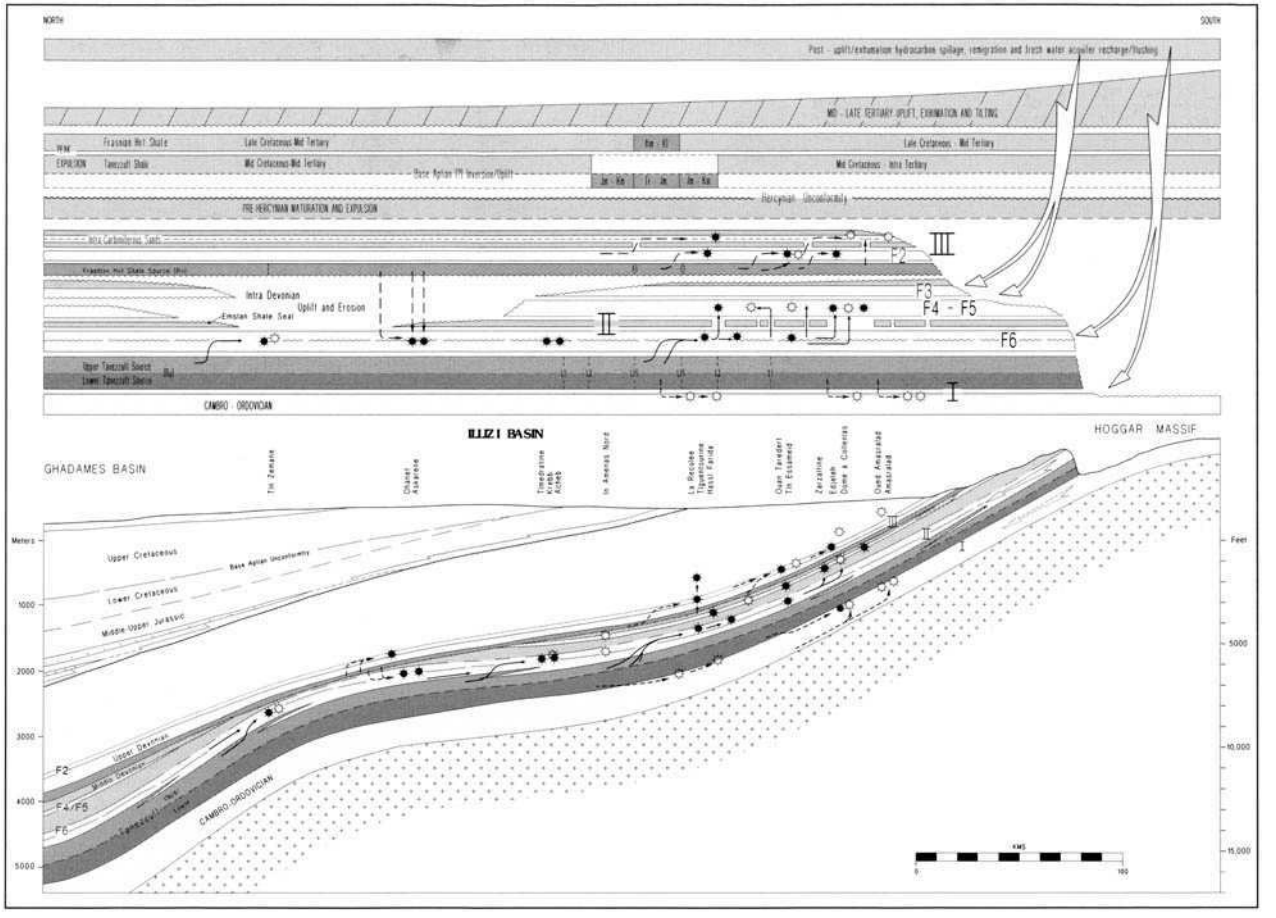

Fig. 16 (d) Critical elements analysis for Illizi Basin petroleum systems, illustrating the spatial relationship and relative timing of critical structural, stratigraphic and thermal variables controlling hydrocarbon distribution in the Illizi Basin. Generation and expulsion from the Tanezzuft and Frasnian source within the Mesozoic depocentre started in the north and moved progressively south during the Cretaceous and early Tertiary. Preferred short to long distance moderate-impedance migration directions are indicated.

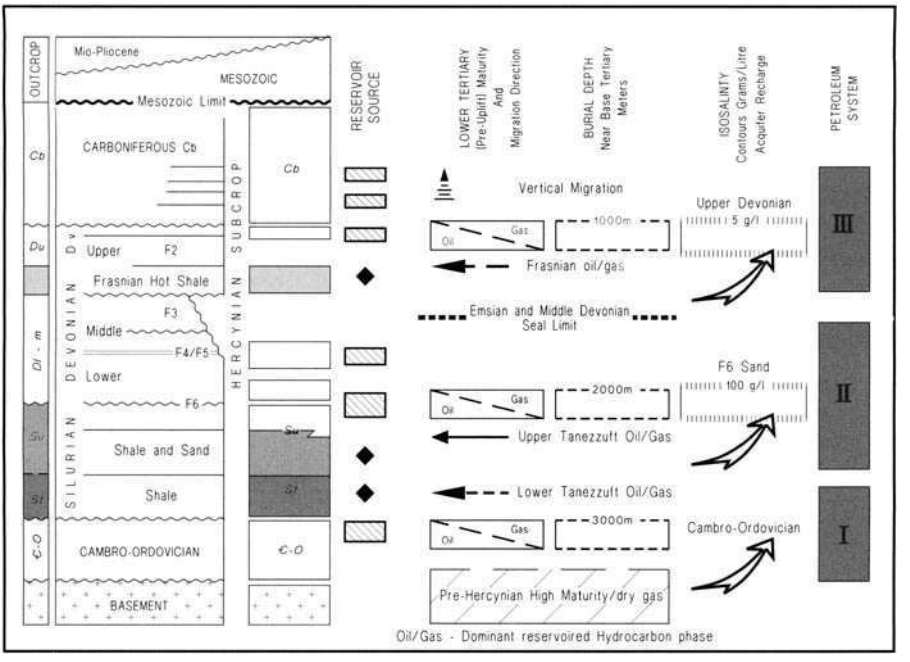

Fig. 16. Legend. Illizi Basin petroleum systems.

volumes of oil and gas, which must subsequently have migrated northeast towards the central part of the Illizi Basin. Expulsion was terminated by Hercynian uplift and unroofing, and hydrocarbons generated at this time were largely dissipated. However there is some evidence (Tissot *et al.* 1984) suggesting a very significant amount may have been preserved in a large palaeo-high just north of the Tin Fouye–Tabankort field.

During the Mesozoic, the Illizi Basin gradually subsided to the north and a second depocentre developed to the northeast along the flank of the Tihemboka Arch. Tanezzuft and Frasnian shales in this depocentre become mature in the Jurassic and early Cretaceous, first to the north and then progressively southwards. Oil and gas generated in the depocentre migrated out to charge low-relief structural closures on the flanking platform, while gentle regional structural axes encouraged longer distance migration, along the Tihemboka Arch to the south and west towards the Tin Fouye–Tabankort area. Austrian deformation followed with uplift and unroofing of the Amguid Spur, Hoggar Massif and southern Tihemboka Arch. The north Tin Fouye–Tabankort palaeostructure was tilted out of closure at this time, and may have spilled entrapped hydrocarbons southwards to charge the Tin Fouye–Tabankort field and flanking structures (Tissot *et al.* 1984).

Generation continued during the later Cretaceous and early Tertiary with increasing amounts of gas migrating from the Mesozoic depocentre to the northeast, whereas the exhumed southwestern Palaeozoic depocentre remained inactive. Many of the deeper reservoirs were partially and sometimes completely gas flushed at this time (Macgregor 1996*a*,*b*), and oil and gas remigrated far to the south. Generation was terminated by regional mid-Tertiary uplift, unroofing and northward tilting. Renewed hydrodynamic flow and freshwater recharge followed with flushing, spillage and partial dissipation of entrapped hydrocarbons (Chiarelli 1978). However, this destructive phase so far appears to have been gentle and most accumulations remain only slightly to moderately affected.

As a result of this polyphase history, a number of petroleum systems developed in the basin at different times. Tissot *et al.* (1984) identified three families of reservoired oil, which they correlated with the lower and upper Tanezzuft (Lower Acacus) and Frasnian shales. The two Silurian sourced oils are very similar and differ only in their maturity (Daniels & Emme 1995). However, their distribution and stratigraphic position justifies the distinction. Based upon this oil–source correlation, it is possible to distinguish three petroleum systems still active in the basin and one extinct one as follows:

Extinct Tanezzuft–intra-Palaeozoic system. Tanezzuft shales within the southwestern Palaeozoic depocentre achieved very high maturities before the Hercynian, when they must have generated very significant amounts of oil and gas. Although speculative, it is probable this would have migrated outward to charge traps on the surrounding platform. Accumulations formed during this period would have been dispersed by Hercynian and Austrian unroofing. However, there is limited evidence to suggest that hydrocarbons spilled from some of these palaeo-fields remigrated later into Austrian aged closures nearby.

Lower Tanezzuft–Cambro-Ordovician System I (Fig. 16a and d). The Tanezzuft Shale extends over the entire basin varying in thickness from 200 to 500m and locally thinning over structural highs. As further to the north, the lowest part of the formation appears to be the most organically rich and is the source of hydrocarbons in the underlying Cambro-Ordovician accumulations. Original TOC content of this interval was probably fairly high throughout the basin but was subsequently reduced in areas of more elevated maturities. It now varies from less than 2% in the east rising to 4% in the north and 8% in the west (Daniels &Emme 1995). Maturities range from 1.1% *R*o equivalent in the central part of the basin to 1.75% *R*o in the southwest and northeast. Local very high maturities are associated with laccolith intrusions (Daniels & Emme 1995).

As well as a source, the Tanezzuft provides an excellent regional seal for underlying Cambro-Ordovician sandstone reservoirs (porosities 7–14% and permeabilities up to 250 mD). Although of rather poor quality, their regional continuity has encouraged long distance lateral migration to the west, southwest and south along the flank of the Tihemboka Arch during later Mesozoic and early Tertiary. Pools in the Tin Fouye–Tabankort area were partially charged by high-maturity oil and gas spilled from pre-Hercynian traps during the Austrian deformational event. Charge and migration ceased with mid-Tertiary uplift and unroofing to be followed by freshwater aquifer recharge and flushing from the south. The system is very prolific, with some 1500 MMBOE reserves.

Tanezzuft–Lower Devonian F6, F4 System II (Fig. 16b and d): Hydrocarbons in the Lower Devonian F6 and F4 sands were sourced from the upper part of the Tanezzuft Shale and perhaps interbedded shales within the overlying Acacus Formation. Although inferior in quality compared with the rich basal member of the Tanezzuft, they form a very prolific source rock because of their thickness, regional extent and interdigitation with the Acacus which facilitated very efficient primary migration.

The Devonian F6 sands provide an excellent reservoir with porosities of 18–25% and permeabilities of a few darcies (Alem *et al.* this volume). Their stratigraphic continuity and position directly above the Acacus sands encouraged long distance lateral migration to the west and southwest. However, the overlying F6 shale seal was eroded along the flanks of the Tihemboka Arch, thus allowing southerly migrating hydrocarbons to pass up into F4 reservoir sands above. Further west in the Tin Fouye–Tabankort area, oil and gas migrating from the northeast probably mixed with higher-maturity hydrocarbons from pre-Hercynian palaeo-accumulations.

Mid-Tertiary uplift brought primary migration to a close and was followed by very active aquifer recharge and flushing. Fresh to brackish water and strong hydrodynamic flow are observed in the F6 sands across a large area in the central part of the basin. Accumulations in that area were strongly affected. Both Chiarelli (1978) and Alem *et al.* (this volume) have suggested that the Tin Fouye–Tabankort accumulation is trapped hydrodynamically. Alternatively it may represent an originally structurally trapped accumulation now in the first phases of flushing and destruction. The petroleum system is extremely prolific, with 3500 MMBOE reserves.

Frasnian to Upper Devonian–Carboniferous System III (Fig. 16c and 16d): The Frasnian shales extend across the central and northeastern part of the basin, outcropping to the south and subcropping the Mesozoic to the west. They vary in thickness between 25 and 110 m thinning locally onto structural highs. Organic carbon content ranges from less than 2% in the southeast to 4–6% in the north and west. The kerogen is predominantly oil prone (although a mixed kerogen facies becomes more dominant to the southeast). Present-day maturities increase northwards from 1.1 R_0 in the central part of the basin to 1.3 R_0 in the northeastern depocentre.

Peak oil expulsion is timed at early Cretaceous to mid-Tertiary and has charged overlying reservoirs in the Upper Devonian and Lower Carboniferous including the F2 sands, Tahara Sandstone and sands interbedded with the M'rar Formation. Porosities in the F2 reservoir typically range from 15 to 22% with permeabilities of 50–300 mD. The overlying Tahara and Carboniferous sandstones have rather poorer reservoir quality.

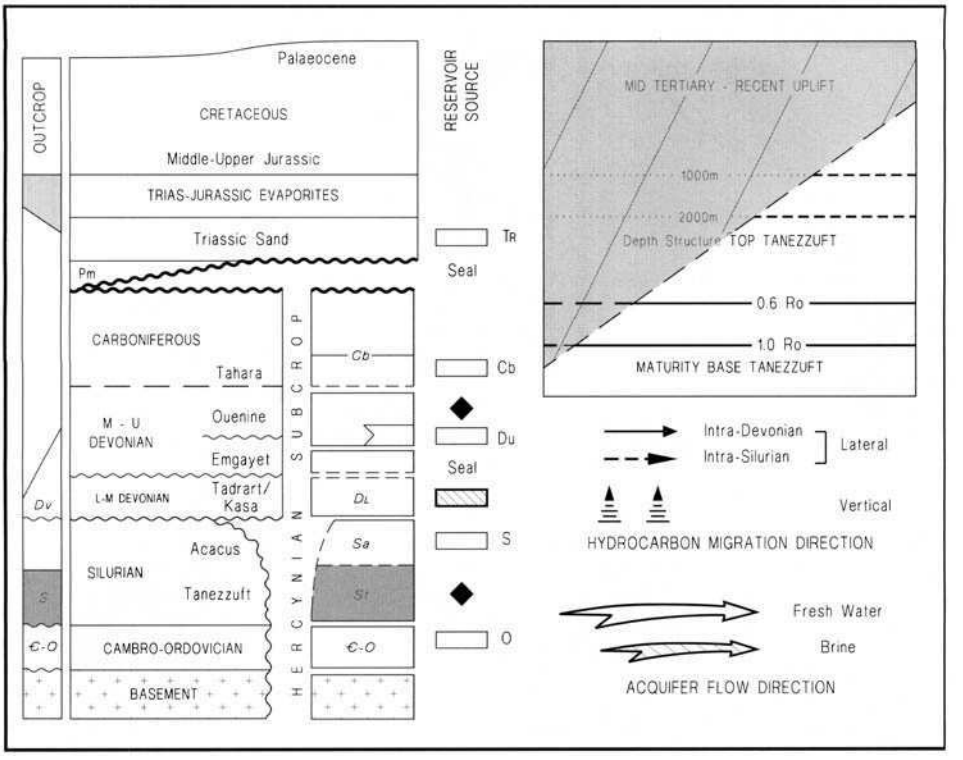

Fig. 17. Legend. Hamra Basin petroleum systems.

Migration was dominantly lateral, southwards along low-relief structural axes. There also appears to have been a significant vertical component of migration through Austrian aged faults on the flank of the Tihemboka Arch. To the north of the basin, a local erosional window in the Middle Devonian shales allowed the Frasnian source to charge F6 reservoirs in the Ohanet area (Tissot *et al.* 1984) and F3 sands at Alrar (Chaouchi *et al.* this volume).

As in the other sytems, mid-Tertiary uplift and unroofing appears to have terminated primary migration and charging. However hydrodynamic flushing was less severe than in the underlying F6 sands, perhaps because of lower stratigraphic continuity and proximity to the Tihemboka Arch. The system is very prolific, with total reserves of approximately 2000 MMBOE.

Hamra Basin.

The Hamra Basin (Figs 2 and 17) forms the eastern extension of the greater Ghadames intra-cratonic Palaeozoic sag, buried beneath a north thickening wedge of Mesozoic clastics, carbonates and evaporites (Gumati *et al.* 1996; Echikh this volume). The basin is only moderately productive, with 950 MMBOE reserves in a large number of small to very small accumulations (Table 2). These all appear to have been sourced from the Tanezzuft Shales with perhaps only a minor contribution from the largely immature Upper Devonian Ouenine Formation. The Tanezzuft is thickly developed in the central part of the basin, subcropping the Mesozoic in the north on the Djeffara–Nefusa Arch, and the Lower Devonian Tadrart sands in the south, on the flanks of the Gargaf High. Peak oil expulsion is timed at late Cretaceous to early Tertiary, charging a number of sandstone reservoirs ranging in age from Cambro-Ordovician to Triassic.

Mid-Tertiary uplift of the Nefusa and Gargaf Arches had a very profound effect upon hydrocarbon accumulations within the basin. Tilting and pervasive meteoric invasion and flushing which occurred at this time are probably responsible for the small field size characteristic of the basin. Oil and gas fields are clustered in three areas, representing discrete petroleum systems, each with slightly different charge histories (Fig. 17).

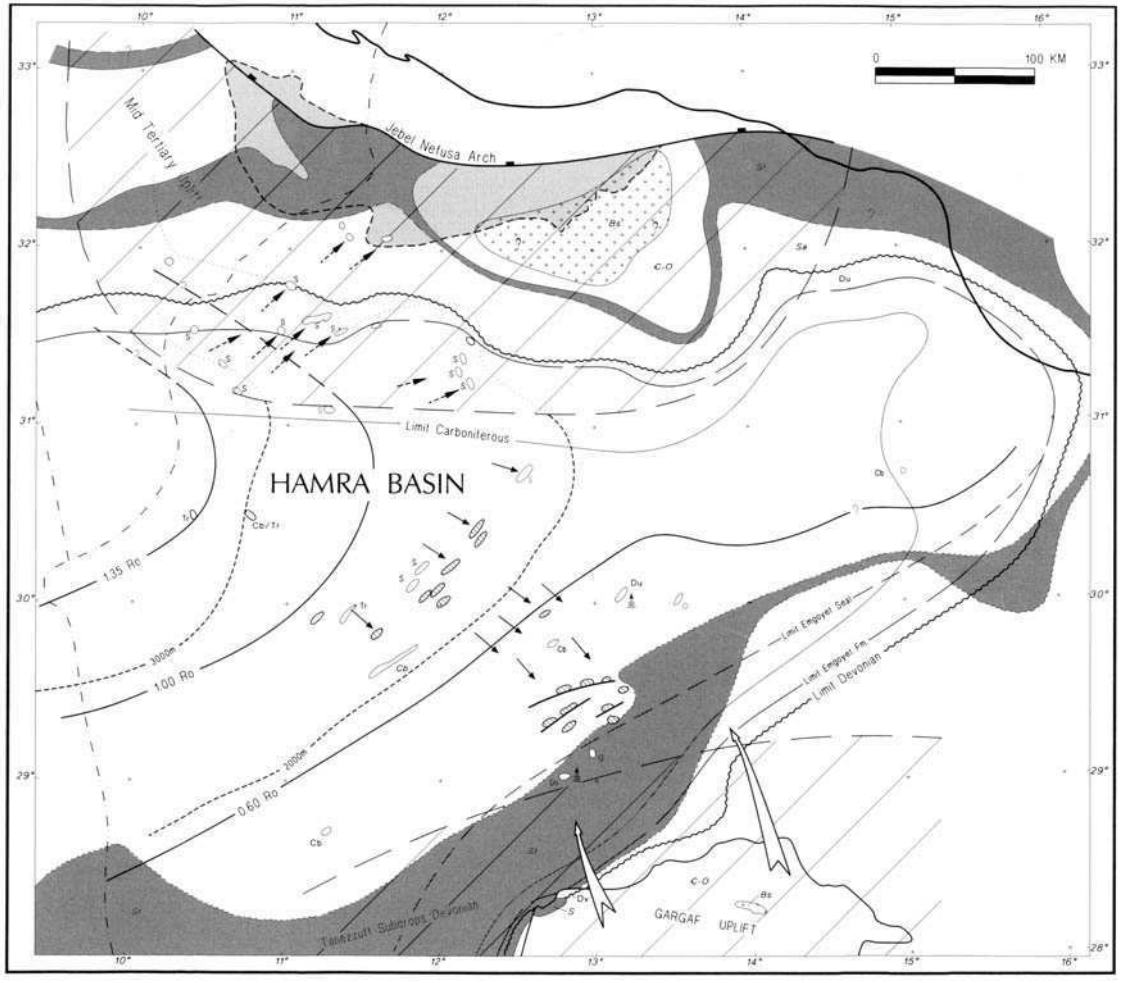

Fig. 17. (a) Hamra Basin petroleum systems (see Fig. 2 for location). Three broadly defined petroleum systems are recognized in the Hamra Basin: (1) in the north, a system reservoired by Upper Silurian Acacus sands (and occasionally in Lower Devonian sandstones) in small fault and unconformity traps charged by Tanezzuft Shale, (2) a second system in the central part of the basin reservoired in Acacus and Lower Devonian sandstones (with some vertical leakage into Lower Carboniferous sandstones) and (3) a southern system with Lower Devonian reservoirs charged by long distance migration from Tanezzuft Shale to the north. The Lower Devonian shale seal (Emgayet Formation) is increasingly sandy towards the south and allowed migration up into overlying sands and ultimately to the surface. Minor downloading of Tanezzuft hydrocarbons into Cambro-Ordovian reservoirs also occurred locally. The distribution of the Tanezzuft source rock subcrop is highlighted. In the north, subcrop is to the Permian Bir Jaja Shale and Triassic; to the south, subcrop is to the Devonian. Preferred migration directions (lateral and vertical) are shown by small arrows. Areas of mid-Tertiary uplift and unroofing are shown by diagonal lines; late Tertiary meteoric invasion and flushing by open (fresh) and hachured (brackish) arrows (adapted from Pallas 1980). Small Triassic accumulations in the west central part of the basin were probably sourced by long distance migration from Frasnian source rocks to the west. (Refer to the legend for more detail. Partly based upon information from Bishop (1975), Hammuda (1980), Pallas (1980), Gumati *et al.* (1996).

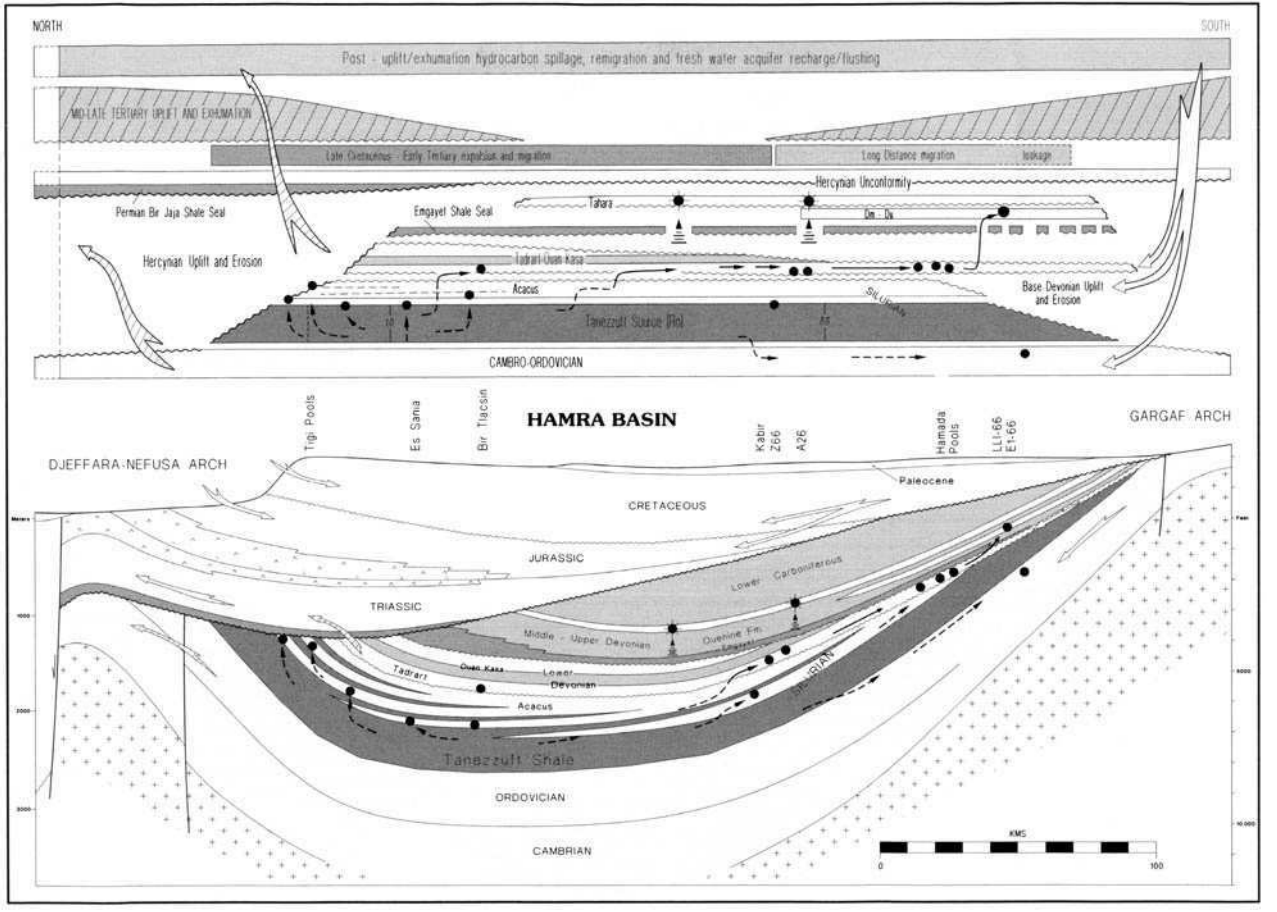

Fig. 17. (b) Critical elements analysis for Hamra Basin petroleum system, illustrating the spatial relationship and relative timing of key stratigraphic, structural and thermal factors controlling hydrocarbon distribution in the Hamra Basin (adapted in part from Pallas (1980)). Preferred migration directions from the Tanezzuft into the Acacus and Lower Devonian Tadrart sands above are indicated by arrows. Meteoric invasion and fresh to brackish water hydrodynamic flow which followed mid-Tertiary uplift and unroofing is shown by open hachured arrows.

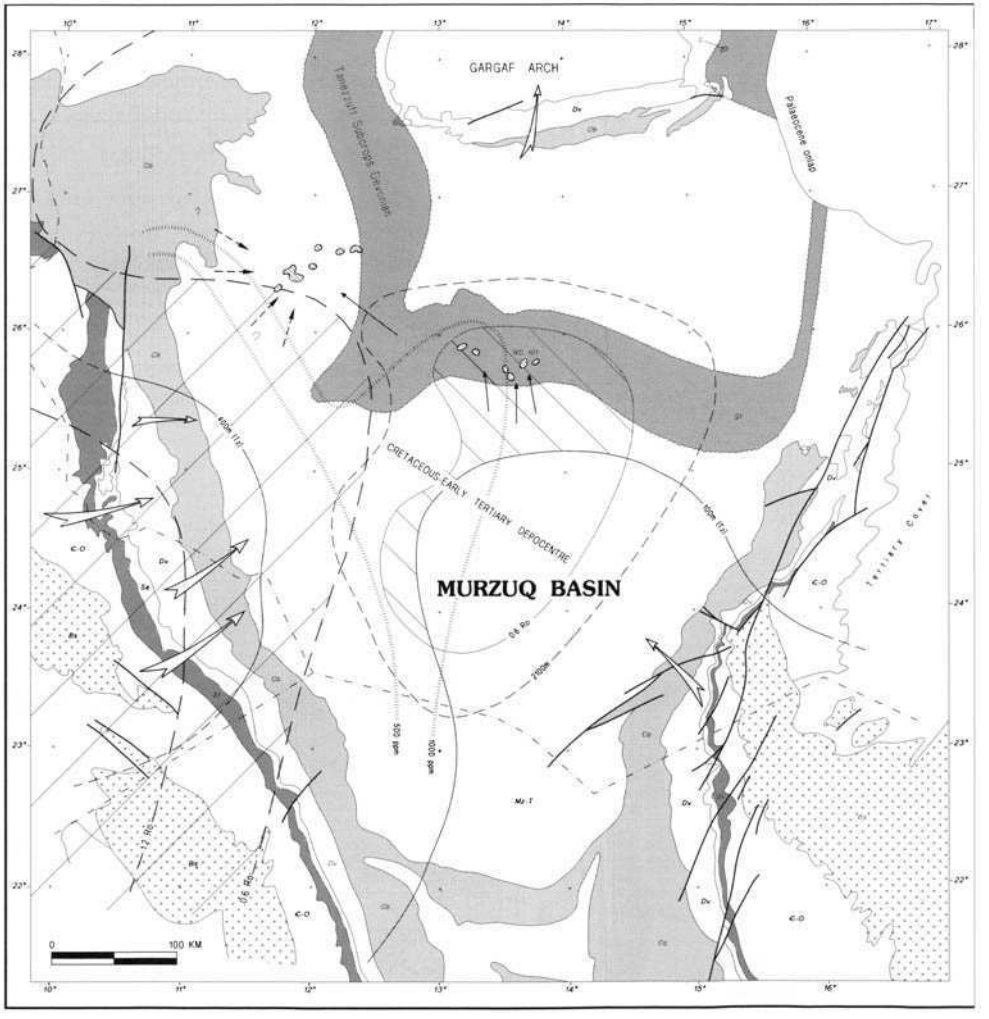

Fig. 18. (a) Murzuq Basin petroleum system summary map (see Fig. 2 for location). One Tanezzuft-sourced petroleum system is recognized in the Murzuq Basin, reservoired within Ordovician sandstones. The Silurian outcrop and Tanezzuft subcrop below the Devonian is highlighted. Decreased source quality to the southeast is suggested by the 100 m Tanezzuft isopach contour. An exhumed Palaeozoic depocentre is shown by diagonal lines. Cretaceous and early Tertiary migration directions are indicated by arrows. Possible remigration from pre-Austrian palaeo-accumulations is shown with dashed arrows. Late-stage meteoric invasion is suggested by isosalinity contours. (Refer to the legend for further detail.) Partly based on information from Bellini & Massa (1980), Dubuy (1980), Lorenz (1980), Pallas (1980), Clark-Lowes (1985), Clark-Lowes and Ward (1991), Meister *et al.* (1991), Pierobon (1991) and Thomas (1995), Gumati *et al.* (1996).

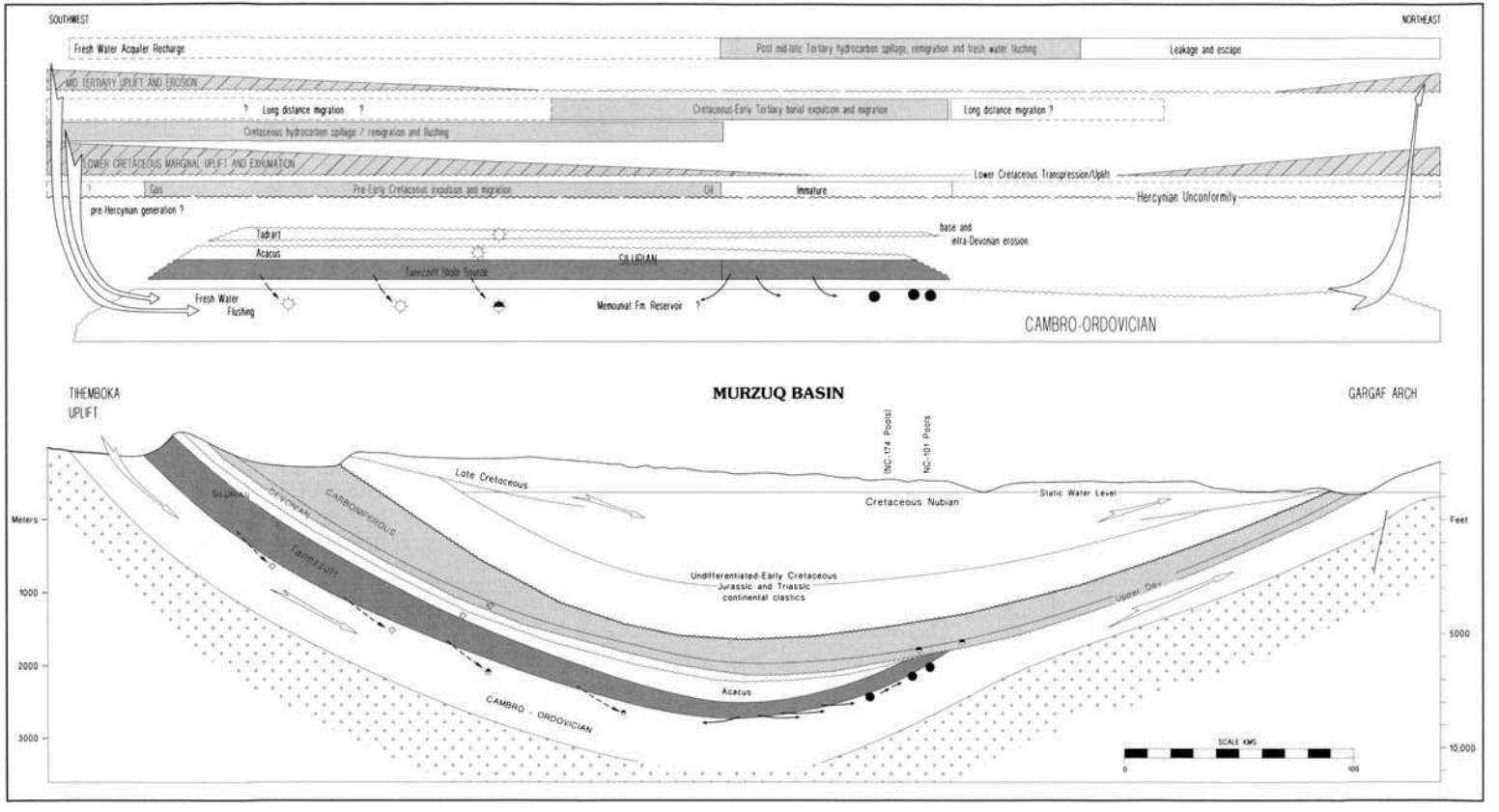

Fig. 18. (**b**) Critical elements analysis for Murzuq Basin petroleum system, illustrating the spatial relationship and relative timing of key structural, stratigraphic and thermal variables controlling hydrocarbon distribution in the Murzuq Basin. Stratigraphic relationships suggesting Austrian uplift and unroofing superimposed upon the Hercynian deformational event are illustrated. Pre- and post-uplift migration directions are suggested by dashed and solid arrows.

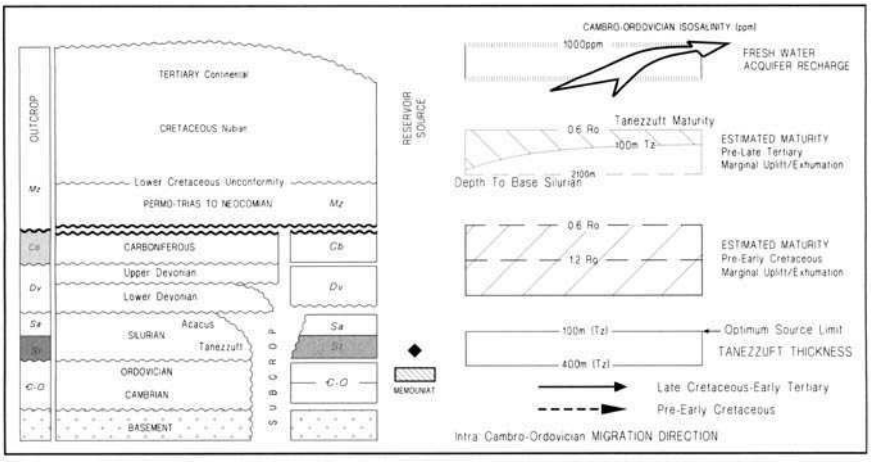

Fig. 18. Legend. Murzaq Basin petroleum system.

(North) Tanezzuft–Acacus system. Nearly all the fields in the northern part of the basin are reservoired in Acacus sandstones with only minor production from the Lower Devonian. Most are trapped by small fault closures with across-fault intra-formational shale seals charged by relatively short distance lateral and vertical migration. However, the Tigi pools appear to be unconformity traps, sealed below the Permian Bir Jaya Shale. Mid-Tertiary uplift and tilting of the Djeffara–Nefusa Arch, associated with spillage and pervasive hydrodynamic flushing, left only small remnants of what once might have been quite large accumulations (see Chiarelli 1978). The system now reservoirs some 65 MMBOE reserves.

(Central) Tanezzuft–Devonian system. Hydrocarbon pools in the central part of the basin are reservoired in Lower Devonian Tadrart sands with lesser amounts in the Silurian, Carboniferous and Triassic. Traps are generally low-relief structural closures charged by vertical and short distance lateral migration through the Acacus sandstones. The Carboniferous Tahara sands were charged by vertical migration from the Lower Devonian through stratigraphic gaps in the intervening Emgayet shales. Two small basal Triassic pools in the axis of the basin may have been charged by relatively long distance migration from subcropping Upper Devonian shales to the west. Meteoric invasion is particular severe in this part of the section and the fields may owe their preservation to the stratigraphic nature of the traps. The system includes some 250 MMBOE reserves approximately.

(South) Tanezzuft–Lower Devonian system. The small Hamada fields in the southern part of the basin are trapped in low relief culminations along northeast–southwest trending fault systems. Lower Devonian Tadrart sandstones are the main reservoir and appear to have been charged by relatively long distance lateral migration from the central part of the basin. The effectiveness of the overlying Emgayet seal deteriorates towards the south, allowing leakage into middle–upper Devonian sandstones. Much of this was probably dispersed during mid-Tertiary uplift but one small pool remains. As elsewhere in the basin, late Tertiary meteoric invasion and flushing appears to have been fairly destructive. The system now reservoirs some 635 MMBOE reserves.

Murzuq Basin.

The Murzuq Basin (Figs 2 and 18) is a symmetrical intra-cratonic sag bounded by the Hoggar, Gargaf and Tibesti uplifts. The Palaeozoic now crops out around the margins and is buried unconformably beneath undifferentiated Triassic–Cretaceous continental clastic deposits in the central part. The Palaeozoic succession is similar to that further north and northwest. However, it becomes increasingly sandy and dominated by terrestrial facies towards the south, with reduced seal integrity. This is compounded by several late Silurian–Devonian erosional unconformities, which developed in response to uplift of the surrounding structural highs. As a result, significant petroleum systems never appear to have developed in the post-Tanezzuft section. In contrast, significant reserves have been discovered within underlying Ordovician clastic deposits, charged and sealed

by basal Tanezzuft Shale on the northern flank of the basin. The associated accumulations are clustered in two distinct areas, but appear sufficiently similar to be considered as part of one system (Fig.18).

Tanezzuft–Ordovician Petroleum system. The Tanezzuft Shale is organically rich in the northern part of the basin with TOC content of up to 8%. It thins to the south and southeast across a Lower Palaeozoic arch, with a corresponding deterioration in organic quality and thickens significantly northwestwards towards a now exhumed Palaeozoic depocentre, where maturities of greater than 1.2 *R*o were achieved before Hercynian and Austrian uplift and unroofing. During the later Cretaceous and early Cenozoic, the Tanezzuft was buried to sufficient depth only in the central part of the basin, where moderate maturities of *R*o 0.6–0.7% were reached. Hydrocarbons generated in this area migrated northwards through the Ordovician to charge the NC 101 fields. The NC 115 pools (including the Murzuq field) lie some distance to the northwest, and it is possible they were charged both by long distance migration from the late Mesozoic depocentre and by remigration from pre-Austrian palaeo-accumulations to the south and southwest.

Ordovician sandstone reservoir quality varies greatly. However porosity as high as 20% has been observed. Although largely secondary and often tectonically induced, it is at least partially controlled by depositional facies. Glacial and peri-glacial clastic deposits of the Memouiat Formation provide the best reservoirs, infilling incised north–south aligned palaeo-valleys in the NC 101 region. These may have acted as efficient migration conduits into traps formed by updip facies changes and differential compaction. The northwestern NC 115 pools appear to be trapped within low-relief fault structures of Austrian age. Mid to late Tertiary uplift of the basin margins terminated further expulsion and encouraged extensive meteoric invasion and flushing. The system reservoirs approximately 600 MMBOE reserves.

Palaeozoic charged systems with Palaeozoic shale seals

Gourara and Ahnet Basins.

The southern Gourara and Ahnet Basins (Figs 2 and 19) form part of a strongly deformed Palaeozoic depression, bounded by the Azzene High and Azel Matti Swell to the west and the Idjerane Horst to the east (Conrad & Lemosquet 1984; Aliev *et al.* 1971; Pelet & Tissot 1970; Rahmani *et al.* 1994). It was once part of a much larger depocentre subsequently uplifted, folded and erosionally truncated during the late Hercynian deformational episode. The Palaeozoic now crops out around the southern margins of the Ahnet Basin and unconformably subcrops a thin veneer of late Jurassic to Cretaceous sediment to the north.

Important reserves of gas have been discovered in large anticlinal traps mostly reservoired in Devonian sandstones but with lesser amounts in the Ordovician and Carboniferous. These accumulations are all considered part of a single petroleum system, charged by extremely mature Lower Silurian shales (Fig. 19).

Tanezzuft–Devonian (Carboniferous, Ordovician) system. Tanezzuft shales preserved within the depression have TOC content ranging up to 4%. They are extremely mature as a consequence of deep burial and a regionally elevated thermal event, generally linked to widespread Hercynian igneous activity (Cawley *et al.* 1995; Takherist *et al.* 1995). Logan & Duddy (this volume) have argued that this occurred somewhat later, towards the end of the Triassic or early Jurassic, based upon apatite fission track analysis. However, the complete absence of liquid hydrocarbons in the associated accumulations indicates that the shales had already reached high maturities by the time the anticlinal traps had formed in late Palaeozoic and supports an earlier event.

The Devonian reservoir sandstones are developed in a rather more distal marine facies than further east in the Illizi Basin, with lower porosities averaging 12% but locally as high as 24%. They are sealed by intra-formational Siegenian and Eifelian shales. Charge and migration are assumed to have occurred rapidly where vertical migration along faults filled growing anticlinal structures. It appears probable that significant amounts of gas generated and trapped at this time were dispersed during the final phase of Hercynian uplift and unroofing. Later Mesozoic and early Tertiary burial was followed by late-stage uplift and erosion with further dispersal of hydrocarbons. The reserves discovered to date for this system are 1250 MMBOE. The large volume of hydrocarbons still retained suggests the pre-Hercynian petroleum system was very prolific with robust shale seals (Table 3).

Sbaa Basin.

The Sbaa Basin (Fig. 19a) is a small Palaeozoic sag yoked between the Ougarta Arch and the Azzene High (Aliev *et al.* 1971; Baghdadli 1988). The present basin formed as a result of Hercynian uplift and erosional truncation, and was subsequently buried unconformably beneath

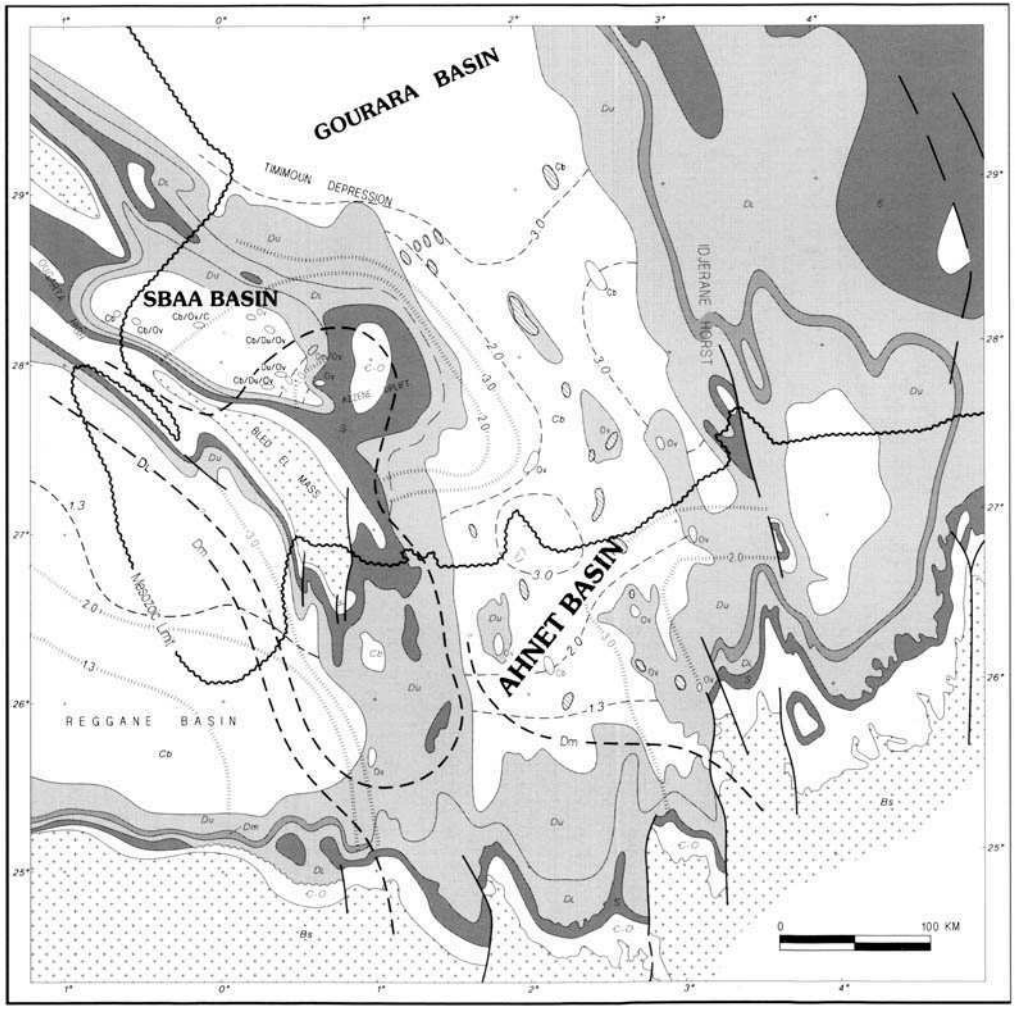

Fig. 19. (a) Gourara Ahnet and Sbaa Basins petroleum systems summary map (see Fig. 2 for location). One Tanezzuft-sourced petroleum system is recognized in the Gourara- Ahnet depression reservoired in Devonian sandstones with subsidiary oil and gas in the Cambro-Ordovician and Carboniferous (from a possible Devonian source). Two systems are distinguished in the Sbaa Basin, an Upper Devonian-sourced system reservoired in Carboniferous sandstones and a Lower Tanezzuft system with Cambro-Ordovician reservoirs. Lower Devonian reservoired accumulations are hachured, and Palaeozoic outcrop and subcrop below the Mesozoic is highlighted. Tanezzuft and Frasnian source rocks achieved very high maturities during the late Hercynian. Reflectance equivalent contours are indicated, adapted from Logan & Duddy (1997). Partly based on information from Pelet & Tissot (1970), Aliev *et al.* (1971), Conrad & Lemosquat (1984), Conrad *et al.* (1986), Baghdadli (1988), Cawley *et al.* (1995) and Takherist *et al.* (1995).

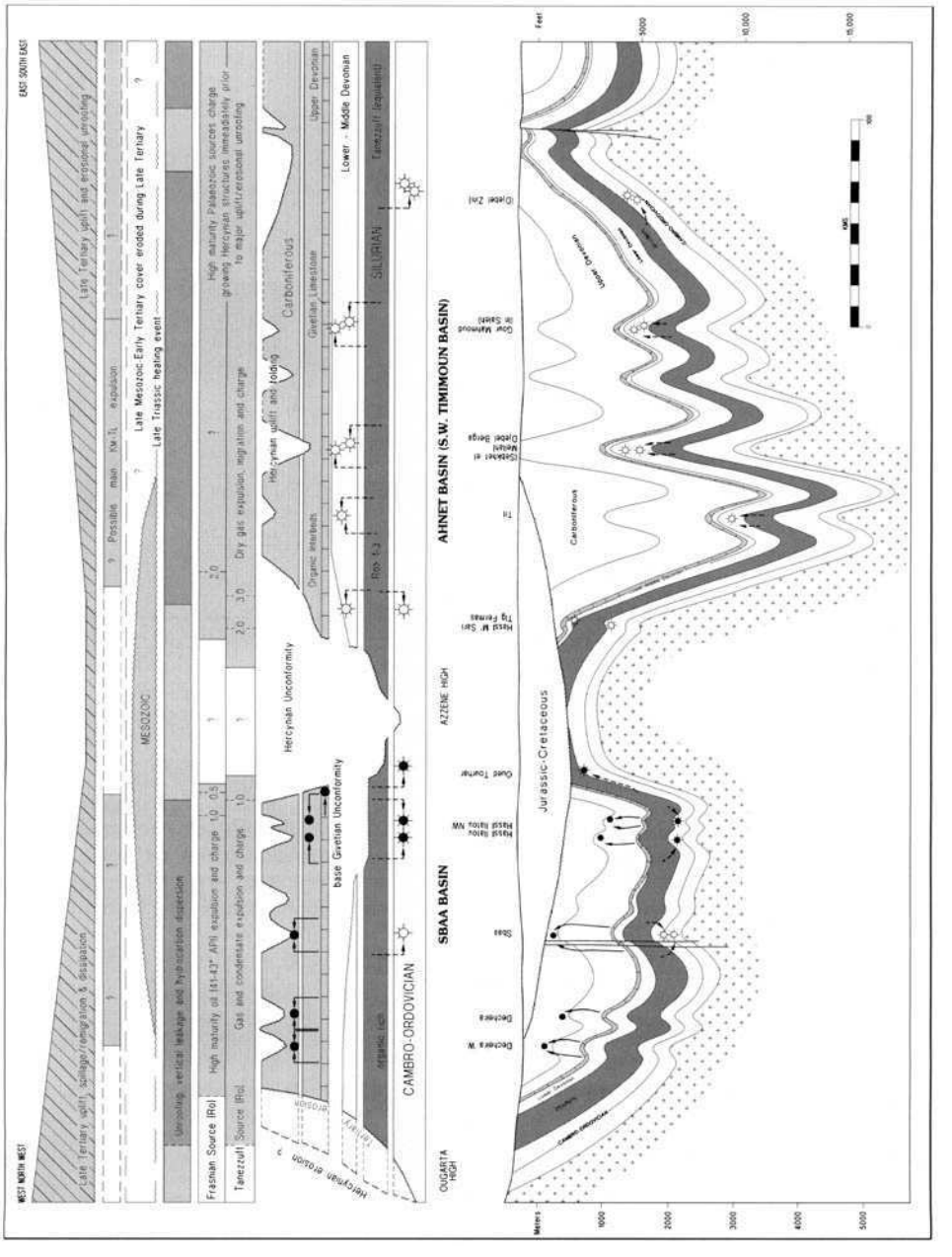

Fig. 19. (b) Critical elements analysis for Gourara–Ahnet and Sbaa petroleum systems, illustrating the spatial relationship and relative timing of key structural, stratigraphic and thermal factors controlling hydrocarbon distribution. Migration and charging in both Sbaa and Gourara–Ahnet Basins occurred during late Hercynian deformation before the final phase of uplift and unroofing. Vertical migration was dominant, and is illustrated by arrows with dashed lines (Tanezzuft) and with continuous lines (Upper Devonian). A possible late Triassic heating event (after Logan & Duddy, this volume) is acknowledged, but further discussion is given in the text.

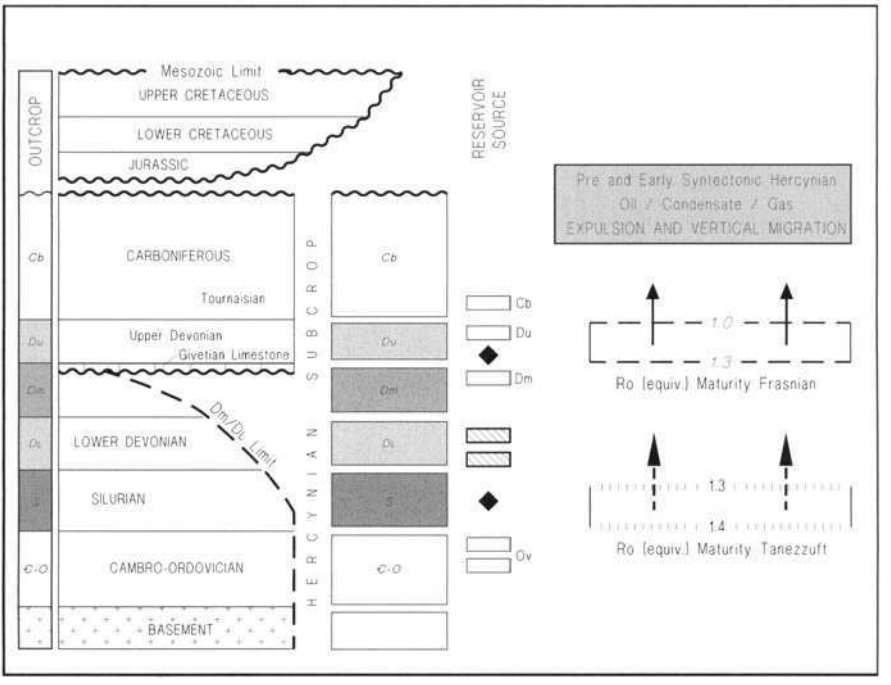

Fig. 19. Legend. Gourara–Ahnet and Sbaa Basins petroleum systems.

a thin blanket of late Jurassic and Cretaceous sediment. Partial unroofing in the mid to late Tertiary exposed the Palaeozoic in outcrop over the western part of the basin.

Only moderate amounts of oil and gas have so far been discovered, in highly faulted anticlinal traps, draped over basement blocks (Baghdadli 1988). Two petroleum systems have been distinguished, one charged by Upper Devonian shales with Strunian and Tournaisian sandstone reservoirs and a second Lower Silurian sourced system, reservoired in Cambro-Ordovician sandstone (Fig. 19).

Sbaa Basin petroleum systems. The Sbaa Basin initially developed as part of the larger Ahnet–Gourara Palaeozoic depression, but was never buried as deeply. As a result, the Lower Silurian and Upper Devonian source rocks preserved within it are significantly less mature. Both systems were active immediately before and during the late Hercynian deformational event, charging growing structures by vertical migration through syntectonic bounding faults. The Upper Devonian sourced system has estimated reserves of 50 MMBOE. The more mature Lower Silurian source has charged underlying Cambro-Ordovician sands with some 100 MMBOE. of gas and condensate reserves (Table 3).

Tindouf Basin.

The Tindouf Basin (Figs 2 and 20) is the westernmost of the North African Palaeozoic basins, bounded by the Anti-Atlas Mountains and Ougarta Arch to the north and the Reguibate Massif in the south (Aliev *et al.* 1971). Although once covered unconformably by a blanket of Mesozoic to early Tertiary sediments, the Palaeozoic now crops out over much of the region, preserved in an asymmetric depression with a broad gentle southern flank and steeply dipping more structurally complex northern margin.

A number of well-placed exploratory tests have been drilled in the basin without success. The black bituminous basal member of the Tanezzuft shale extends over a wide area of the basin, buried beneath a thick sequence of Devonian and Carboniferous rocks. It is now highly mature, but could once have generated a considerable amount of oil and gas. Hydrocarbon shows are fairly widespread and it is likely that these represent the remnants of one or more pre-Hercynian petroleum systems, destroyed during late Hercynian or Tertiary unroofing. A speculative reconstruction of the region suggests that two or three may once have been active in the basin. The most significant of these was prob-

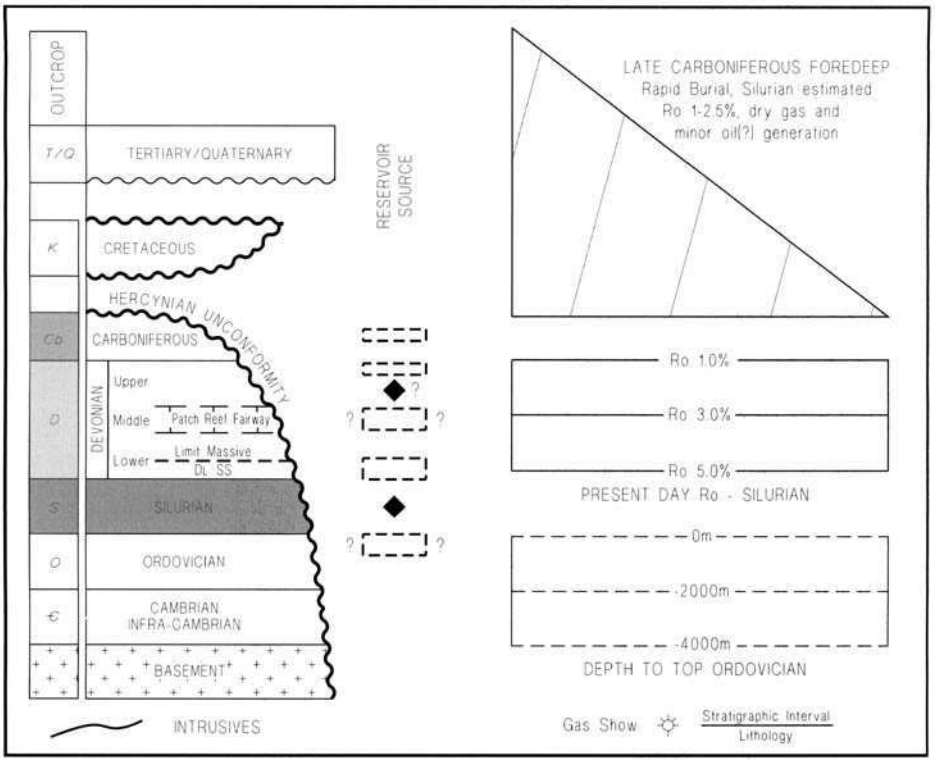

Fig. 20. Legend. Tindouf Basin extinct petroleum systems.

ably the Tanezzuft–Devonian (Carboniferous) system (Fig. 20).

Extinct Tanezzuft–Devonian (Carboniferous) petroleum system. Early Hercynian orogenesis commenced in late Devonian to earliest Carboniferous with the uplift of the Anti-Atlas and Ougarta Ranges and active subsidence of the Tindouf Basin. During the Carboniferous, the Tanezzuft within this foredeep was buried beneath a thick wedge of detritus shed from the rising orogen. By late Carboniferous, it achieved maturities of 1.0–2.5% R_0 along the northern flank with significant generation of oil and gas. There are few porous conduits in the overlying Silurian and Lower Devonian but fractures and faults associated with growing syn-orogenic structures may have encouraged vertical migration into Upper Devonian and Lower Carboniferous reservoirs above. Residual hydrocarbon shows now present in these structures are thought to represent palaeo-accumulations formed during this time.

As in the northern margin of the basin, the Tanezzuft on the southern flank must have generated considerable volumes of oil and gas. However, in contrast to the north, a Lower Devonian sandstone sequence is well developed in this part of the basin and could have provided an efficient lateral hydrocarbon conduit to charge low-relief fault closures further south.

As intensity of deformation increased during the late Hercynian, the Tanezzuft Shale in the foredeep reached an extremely high level of maturity (> 3.0% R_0). It appears too high to be explained by overburden alone and is probably related to regionally elevated heat flow associated with widespread igneous intrusive activity. At these elevated temperatures, reservoired hydrocarbons in the deeper northern part of the basin would have been thermally destroyed, and with continuing deformation, uplift and unroofing, structural traps must surely have been breached. Maturities of the Tanezzuft Shale along the southern flanks of the basin are also believed to have increased at this time (0.6–3.0% R_0) in response to the regionally elevated heat flow. Expulsion and lateral migration may have continued to charge fault traps to the south with increasingly higher maturity oil and gas. Residual gas shows found in the Devonian and Ordovician may be the remnants of such accumulations.

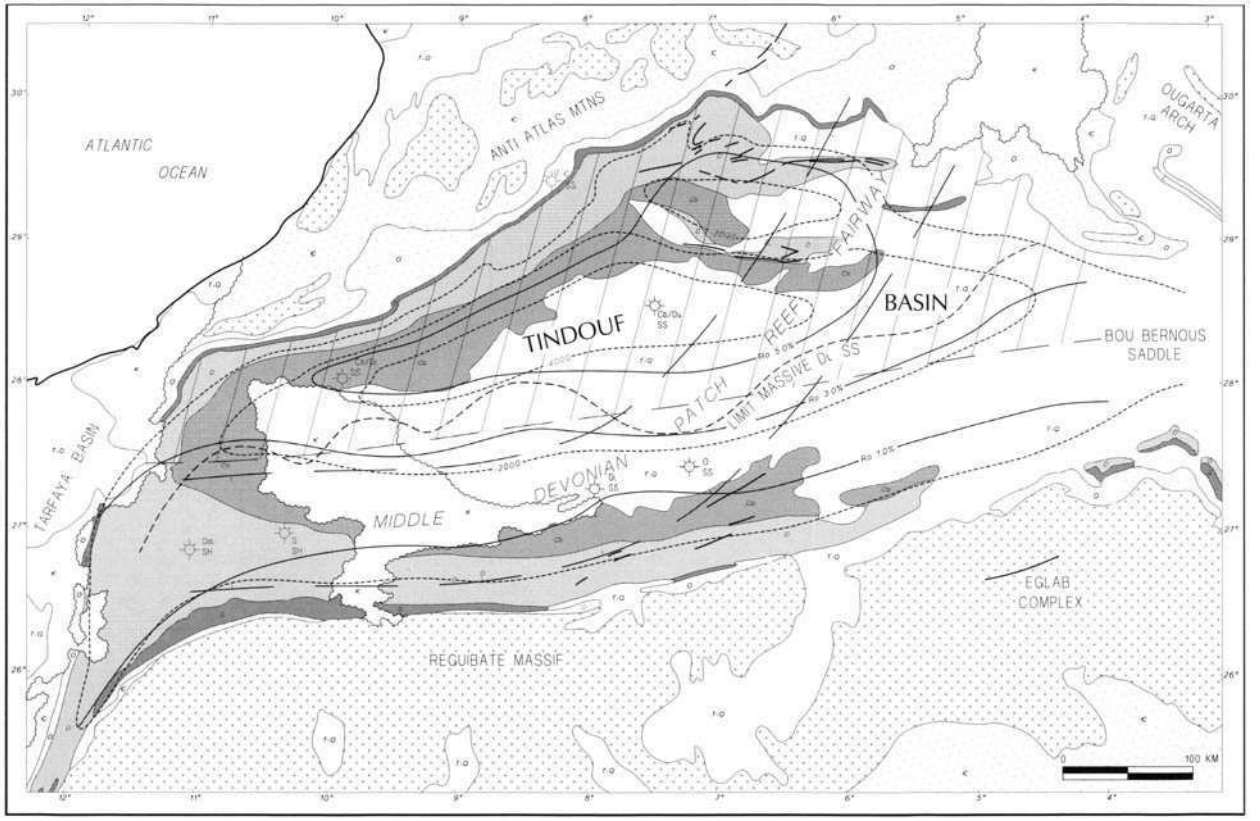

Fig. 20. (a) Tindouf Basin, extinct Palaeozoic petroleum system summary map (see Fig. 2 for location). Residual hydrocarbon shows suggest one or more petroleum systems were active in the Tindouf Basin before Hercynian uplift and unroofing. These palaeo-accumulations are presumed to have been sourced from Tanezzuft Shale (with perhaps a minor contribution from the Upper Devonian), now very mature throughout the basin as a result of Late Devonian Carboniferous burial and regionally elevated heat flow. The distribution of the postulated Tanezzuft source rock is defined by the mapped outcrop. Hydrocarbons generated on the northern side of the basin probably migrated vertically via syntectonic faults into Upper Devonian Lower Carboniferous sandstones, whereas a more widespread Lower Devonian sandstone may have provided a conduit for hydrocarbons migrating laterally to the south. A Devonian patch reef trend projected across the basin from outcrops on either side may have been associated with a second system.

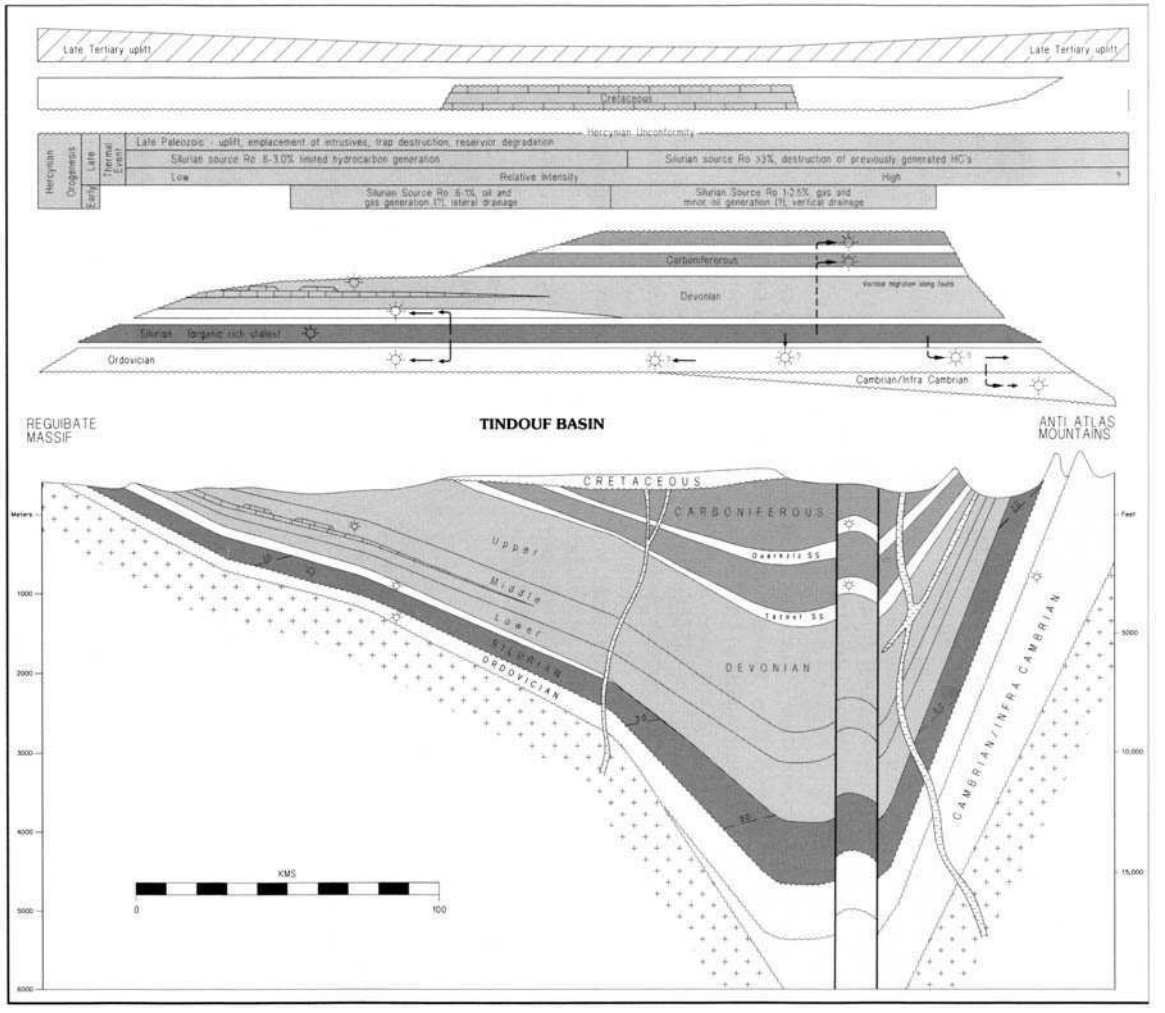

Fig. 20 (**b**) Critical elements analysis for extinct Tindouf Basin petroleum system(s), illustrating the spatial relationship and relative timing of critical stratigraphic, structural and thermal factors which may have been responsible for hydrocarbon entrapment and subsequent dispersal in the Tindouf Basin. Maximum Tanezzuft Shale maturities are highlighted and postulated preferred vertical and lateral migrations directions are suggested.

Late Hercynian deformation culminated with uplift and erosional unroofing, exposing the Lower Palaeozoic in outcrop around the margins of the basin. Any significant accumulations still preserved at this time would finally have been destroyed by fault breaching and late tilting of trap closures, water washing, flushing and biodegradation. The subsequent Mesozoic to early Tertiary cover appears to have been fairly thin and the Tanezzuft Shale never again achieved depths sufficient to renew expulsion. Further late Tertiary uplift and unroofing associated with renewed freshwater aquifer flow, must have dispersed any remaining hydrocarbons in the basin.

Tanezzuft–Ordovician and Intra-Devonian palaeo-petroleum systems. Gas shows encountered in the Ordovician and middle to late Devonian shales may represent the remnants of other extinct petroleum systems. It is possible Ordovician reservoirs were charged by downloading from a basal Tanezzuft Shale source, and a postulated middle Devonian carbonate trend was certainly well positioned to receive hydrocarbon charge from organic rich shales immediately above. However both possibilities are weakly constrained and must remain speculative.

Reggane Basin.
The Reggane Basin (Figs 2 and 19) is a large intra-cratonic Palaeozoic depression bounded by the Eglab (Hoggar) Shield in the south and Ougarta Arch to the north (Aliev *et al.* 1971; Morabet *et al.* this volume). It formed in response to Hercynian uplift and erosional truncation and was subsequently buried beneath a thin sequence of Cretaceous sediment. Much of this was stripped away during mid-Tertiary uplift, and the Palaeozoic now crops out around the margin of the basin.

As in the Ahnet Basin nearby, Lower Silurian and Upper Devonian shales within the depression are extremely mature (Logan & Duddy this volume) as a result of deep burial and a regional late Palaeozoic thermal event. The scattered oil shows and a small gas accumulation encountered in the northern part of the basin (Boudjema *et al.* 1990) may be the remnants of a pre-Hercynian petroleum system(s) later dispersed during Hercynian and mid-Tertiary uplift and unroofing. The relative frequency of hydrocarbon shows within Lower Devonian sandstones of the basin suggests these may once have provided the reservoir for a Lower Silurian sourced system. However, other porous sands are developed in the Cambro-Ordovician and Carboniferous and could also have been important.

Marginal to non-productive basins

Moroccan Basins.
A Silurian-sourced petroleum system is present in the Essaouira Basin, and could once have existed in the Doukkala, Tadla (Jabour & Nakayama 1988), Rharb, Boudenib–Bechar and Tarfaya Basins (Morabet *et al.* this volume). Located along the northwest margin of Africa, these intra-cratonic sag basins lie west, north and northeast of the Tindouf Basin (see Fig. 2 for location; the Tadla Basin lies east of Doukkala). All except the southerly located Boudenib–Bechar and Tarfaya Basins have been extensively modified by Mesozoic Cenozoic compressional tectonics (see Fig. 12). Deep pre-Hercynian burial of the Silurian source rock generally resulted in Palaeozoic maturation and expulsion. Hydrocarbons generated at this time had a low preservation potential because of the strength and complexity of subsequent tectonic events (see Fig. 3), and effects of uplift and freshwater flushing. In the south an intrusive-related thermal event contributed to high levels of maturity (Logan & Duddy this volume).

The small Triassic oil and wet gas Meskala accumulation of the Essaouira Basin was sourced from Silurian shales. These subcrop the Hercynian unconformity immediately below the accumulation and charged a silty fluvial sandstone reservoir by vertical fault-controlled migration. Evidently Silurian source capacity was not entirely destroyed by Hercynian deformation and subsequent Mesozoic burial was sufficient to renew generation during the late Cretaceous or early Tertiary. The accumulation is clearly the result of several perhaps unique factors but it is possible that similar fields may be present in areas where the Silurian source has been protected from over-maturity, such as on the more gently deformed offshore shelf.

Eastern Libya–Egypt.
The potential for Palaeozoic petroleum systems in eastern Libya and Egypt has been identified on the southern platform of Egypt, in the Kufrah Basin and in Cyrenaica (Figs 2, 6 and 7).

The Kufrah Basin is a large intra-cratonic depression bounded by the Tibesti Massif to the west and the Jebel Awaynat High in the east (Bellini & Massa 1980; Pallas 1980; Turner 1980; Bellini *et al.* 1991; Gumati *et al.* 1996). The Palaeozoic succession was once part of the regionally extensive Gondwana platform sequence with very similar facies to the Murzuq. The basin first developed as an intracratonic sag during the late Hercynian phase of

deformation and was subsequently buried unconformably beneath poorly dated Jurassic(?) and Cretaceous continental Nubian clastic deposits. Later mid-Tertiary uplift and erosional unroofing of the surrounding highs exposed the Palaeozoic in outcrop around the basin margins.

Although very lightly explored, with only four deep exploration tests, the basin is considered unprospective. The Tanezzuft Shale equivalent sequence appears significantly more silty than elsewhere, and is difficult to distinguish from the Acacus Sandstone Formation. A full geochemical analysis of its source capacity is not available but published lithological descriptions suggest it is probably fairly lean (Bellini *et al.* 1991). Furthermore, it was never deeply buried and probably only reached maturity locally in the deepest part of the basin (Keeley & Massoud this volume). Any early crudes generated before mid-Tertiary uplift and unroofing were probably dispersed by the very extensive meteoric invasion and flushing which followed.

In coastal Cyrenaica, northeast Libya, a Palaeozoic petroleum system has been suggested by the drilling of well B1–2 (Sola & Ozcicek 1990). Non-commercial gas in Late Carboniferous reservoir sands was generated from Carboniferous gas-prone shales buried deeply offstructure to the north (Keeley & Massoud this volume). Intraformational shales provide the seal for this trap which was charged from the Late Jurassic onwards. The system is believed to extend eastwards into offshore Egypt.

Discussion

Petroleum system characteristics

Despite the relative geological simplicity of the Saharan Platform, the Palaeozoic-sourced petroleum systems it harbours vary widely in character and productivity (Tables 1–4). This reflects differences in source charging efficiency, migration drainage style, critical period and degree of impedance or dispersal (Demaison & Huizinga 1994) as described below.

Charge factor. The Tanezzuft and Frasnian source rocks responsible for these petroleum systems are regional in extent, and local variations of thickness and quality appear too small to have much direct effect on their charge factor. However, charge is strongly influenced by drainage area. Extremely efficient charging was facilitated by proximity of large volumes of mature source rock with regionally continuous intra-Palaeozoic and basal Triassic migration conduits. Efficient charge was further enhanced locally by fracturing and faulting offsetting source rock intervals against primary carrier beds.

Migration drainage style. The exceptional stratigraphic continuity of the Palaeozoic and basal Triassic succession provided multiple regionally continuous migration conduits. In less structurally deformed parts of the Saharan Platform this allowed lateral migration to occur over very long distances. Vertical migration was significant only in faulted and deformed areas such as the Ahnet–Gourara depression, the Amguid–Hassi Touareg axis and perhaps formerly in the Tindouf and Reggane Basins before their uplift and unroofing.

Critical period. The relative timing of trap charge varies widely. Although speculative, it seems likely that most of the pre-Hercynian accumulations in the Tindouf and Ahnet–Gourara Basin, and elsewhere, were predominantly gas and gas condensate. A tentative reconstruction of their history suggests that the Tanezzuft source rock had reached relatively high maturities by the time associated traps had begun to form. Consequently, a significant part of their charge was probably late stage.

The relative timing of charge and formation of post-Hercynian traps is not always well constrained. Nevertheless, the Hassi Messaoud closure is clearly Hercynian, although later enhanced by differential subsidence of the flanking basins. Certainly, it was well timed to receive an oil charge. In contrast Hassi R'Mel achieved closure only during the later Cretaceous, some time after its primary generative pod in the Benoud Trough had reached gas-generating maturities.

Further to the south, the Hassi Touareg and Rhourde Chouff area accumulations developed in Austrian aged traps after the Tanezzuft source in the adjacent basin had passed through the oil generating phase. At least some structures in the Illizi Basin developed early during the Hercynian, either forming closures at that time or later, after Austrian uplift and regional tilting. Certainly they existed throughout the main period of expulsion from the Tanezzuft and Frasnian source rocks in late Jurassic to Cretaceous and were available to receive both oil and later gas. Based upon limited information, the recently discovered Ghadames Basin accumulations appear to be trapped in very low relief Austrian (and perhaps Jurassic) aged closures, and were charged in the late Cretaceous.

Entrapment style. In this region of high-continuity sand conduits and robust shale and evaporite seals, entrapment style, or impedance, was largely dependent upon basin geometry and degree of structural deformation. In the less deformed parts of the platform, broad regional arches such as the Tilrhemt and Hassi Messaoud Domes focused migration very efficiently and the associated petroleum systems are of very high impedance. In contrast, the gentle synclinal form of adjacent depressions encouraged dispersal and only local focusing along intra-basin structural axes. With very subtle low-relief closures, both the Oued Mya and Ghadames petroleum systems were probably of moderate impedance, with large volumes of hydrocarbons escaping to the south beyond the evaporite seal. Structural traps are more common in the Illizi Basin, where the petroleum systems may have been of rather higher overall impedance as a result. Although sealed by shales rather than evaporites, they were only very mildly deformed and so largely retained their trapping integrity. Even where faults or local erosional windows in intraformational seals allowed hydrocarbons to move up into overlying conduits, still higher shales were present to act as new seals.

In structurally more deformed areas with greater frequency of high-amplitude traps, associated petroleum systems were of relatively high impedance locally, and seal integrity has sometimes been maintained to the present. This appears to have been the case in the Ahnet–Gourara depression. Elsewhere, large displacement faulting, such as at the southern end of the Hassi Touareg horst, rendered the Triassic–Liassic evaporite seal locally ineffective by offsetting reservoir against Cretaceous sandstones. As a result, the associated petroleum system is less productive than in the structurally similar but less faulted Rhourde Chouff area further south.

Post-charge destruction processes. Pre-Hercynian petroleum systems in the Tindouf and Reggane Basins, and elsewhere, were all largely destroyed by Hercynian or later Austrian unroofing. However, significant gas accumulations still remain in the Ahnet–Gourara depression. At least some of the hydrocarbons originally reservoired in this basin must have been dispersed by spillage or vertical leakage through faults and hydrodynamic flushing along the basin margin while anticlinal traps in the central part have preserved their sealing integrity.

Austrian deformation and uplift almost certainly had a very significant impact upon petroleum systems initiated earlier in the Mesozoic and Late Cretaceous gas flushing appears to have been significant in deeper reservoirs of the northern Illizi area. However, these earlier destructive processes were overshadowed by mid-Tertiary uplift and unroofing, which had a profound influence upon the entire region. Its effect was fairly mild in the central and northern part of the Triassic Basin. The large regional culminations of Hassi R' Mel and Hassi Messaoud were entirely unaffected, with only minor spillage and remigration from low-relief accumulations in adjacent depressions. However, the eastern flank of the Ghadames Basin was strongly tilted in response to uplift along the Djeffara–Nefusa Arch and although the broad El Borma structure retained its closure, smaller low-relief pools nearby were partially or completely dispersed by spillage and hydrodynamic flushing. The region to the south and west beyond the Triassic–Liassic evaporites was even more strongly affected. Hydrodynamic flushing was especially severe in the Hamra Basin as a result of uplift and unroofing to both north and south, and accumulations in the Illizi Basin are in various phases of dispersal as a result of regional tilting and flushing. However, large volumes of oil and gas are still retained in this basin suggesting the process of dispersal is only in a very early phase.

Hydrocarbon productivity; controlling factors

With broadly equivalent charge factors and multiple reservoirs, seals and traps, differences in productivity between Palaeozoic-sourced petroleum systems of the North African Platform appear to be directly related to migration and entrapment style and post-charge destructive processes. These can be considered in three broad categories.

Mesozoic to early Tertiary charged systems with Triassic–Liassic evaporite seals (Tables 1 and 4). The Hassi R'Mel and Hassi Messaoud fields contain *c.* 56% of the reserves in the entire province. They owe their enormous size to their position on large regional structural arches, with extremely high impedance trapping style. In contrast, the Northeast Oued Mya and Frasnian sourced Ghadames Basin systems rely upon very local migration focusing along gentle intra-basinal structural axes immediately above or just updip of the subcropping source. The Triassic sands form excellent conduits in both basins, largely unaffected by faulting. These systems appear to be of rather lower impedance, allowing large volumes of hydrocarbons to dis-

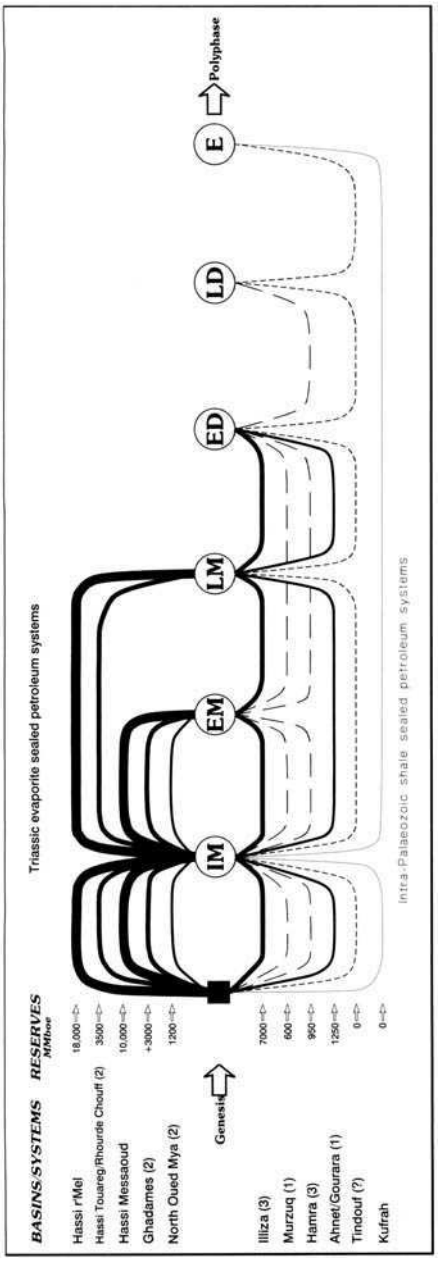

Fig. 21. Evolution of North African Palaeozoic petroleum systems; a working model illustrating the evolution of the main Palaeozoic-sourced petroleum systems of Algeria and western Libya from initial genesis through immaturity (IM), early maturity (EM), late maturity (LM), early destruction (ED) and late destruction (LD) to extinction (E). The thickness of the lines provides a relative measure of the productivity of the systems.

perse and escape by long-distance lateral migration, except where captured by regional arches.

The small reserves associated with the Northwest Oued Mya system are probably a reflection of limited trap volume as well as inefficient migration focusing. The area is entirely overshadowed by the Tilhremt Dome and may have experienced significant late tilting. The Tanezzuft-sourced system of the eastern Ghadames Basin is dominated by El Borma. This was preserved by a very robust closure on the culmination of a regional arch but other fields in the area are now very small, presumably as a result of post-charge tilting and spillage from once larger accumulations.

Differences in productivity between the three petroleum systems along the Amguid–Hassi Touareg Ridge are thought to be related to the distribution of adequate traps. Despite the frequency of high-amplitude structures along the trend, their trapping effectiveness is often limited by across-fault seals. The southern Tanezzuft–Triassic system is very productive because of relatively lower amplitude structures and more effective fault seals. In contrast, the central Hassi Touareg system is significantly less productive because of higher-amplitude structures and greater fault displacements with more frequent across-fault juxtaposition of reservoir against younger sands. The northern system is also relatively less productive because of poorer reservoir quality and fewer structural traps.

Mesozoic to early Tertiary charged systems with intra-Palaeozoic shale seals (Tables 2 and 4). Petroleum systems in the Illizi Basin, reservoir very large volumes of hydrocarbons. The reason for this high productivity is not entirely clear. However it may reflect the frequency of optimally positioned traps with multiple reservoir–seal pairs, and the effects of efficient migration focusing along low-relief intra-basinal structural axes, immediately updip of the generative area. Although these systems are now undergoing post-charge regional tilting and hydrodynamic flushing, this has been fairly limited so far and most of the hydrocarbons originally trapped are probably still retained.

The Hamra Basin is stratigraphically similar to the Illizi, with similar reservoir and source rocks. However, it is very much less productive. Any estimate of hydrocarbon volume originally reservoired in the basin must remain entirely speculative but it could have been significant. Late-stage basin tilting and hydrodynamic flushing is now very severe, and the small scattered pools which remain may represent the remnants of once much larger accumulations.

The Murzuq Basin to the south is also relatively unproductive. Hercynian and Austrian uplift and unroofing would have dispersed most early generated hydrocarbons from the western palaeo-depocentre, whereas later Cretaceous to early Tertiary burial was limited and only a very small area in the central part of the modern basin reached maturity. Consequently, the Tanezzuft–Cambro-Ordovician system was relatively undercharged. Furthermore, because of the gentle structural relief, significant volumes of hydrocarbons generated in the central part of the basin may have been dispersed by long distance migration to the north or by hydrodynamic flushing in the west.

Palaeozoic-charged systems with intra-Palaeozoic shale seals (Tables 3 and 4). Once fairly prolific petroleum systems probably existed in the southwestern and western intra-cratonic basins of Algeria and Morocco, to be destroyed by later uplift and unroofing. The Ahnet-Gourara depression was strongly folded with many large anticlinal traps, and probably always reservoired far larger volumes of hydrocarbons than the less deformed Reggane and Tindouf Basins. Significant reserves still remain, although these may represent the remnants of an originally more prolific system(s). The relative frequency and size of traps, combined with the still very robust shale seals, point to a relatively high impedance system(s). Furthermore, their high amplitudes, would have tended to reduce the effects of later Mesozoic and Tertiary tilting and hydrodynamic flushing.

Accumulations in the neighbouring Sbaa Basin are very small and as in the Ahnet–Gourara depression, may represent once larger accumulations now partially destroyed by later tilting and flushing.

Conclusion

Large volumes of hydrocarbons have been generated, trapped and sometimes dispersed on the North African Platform since the Late Palaeozoic. Petroleum systems charged by Lower Silurian Tanezzuft and Upper Devonian source rocks developed around discrete sedimentary depocentres, first in the Palaeozoic and later during the Mesozoic and early Tertiary. Most of the hydrocarbons generated during the Palaeozoic were dispersed by later uplift and unroofing, whereas all the Mesozoic charged petroleum systems now lie directly beneath or around the Mesozoic sag basin of eastern Algeria, southern Tunisia and western Libya.

In this structurally simple region with highly continuous reservoirs and seals, intimately associated with excellent source rocks, productivity of active petroleum systems varies according to migration style and effectiveness of migration focusing, degree of impedance and stage of maturity. The petroleum systems range from those of the enormous Hassi Messaoud and Hassi R'Mel accumulations (56% of the total reserves in the region), characterized by broad regional culminations with very efficient migration focusing and high-impedance entrapment style, to the Hamra Basin systems (2% of total reserves) with small scattered pools now largely dispersed by hydrodynamic flushing.

Each of these systems is ephemeral in various stages of an evolutionary cycle from initial genesis, to maturity, destruction and final extinction (Fig. 21). The Triassic–Liassic evaporite sealed systems of the northern 'Triassic Basin' are all now in a mature phase of evolution. Hassi Messaoud and the Ghadames and Oued Mya systems are in early (oil-dominant) maturity, whereas Hassi R'Mel and the Hassi Touareg and Rhourde Chouff systems bypassed this phase and are now in late (gas-dominant) maturity because of later trap development. The southern intra-Palaeozoic shale sealed systems are in a more advanced stage in their evolutionary cycle, because of their position on the flanks of the Mesozoic depocentre away from the evaporite seal. Petroleum systems in the Illizi Basin appear to have passed through maturity and are now just starting to disperse, whereas those in the Hamra and Murzuq Basins moved directly from early maturity to a more advanced phase of destruction. The majority of the pre-Hercynian petroleum systems once active in the Tindouf, Reggane and Moroccan Basins are now extinct. Only the Ahnet–Gourara gas dominated system has been preserved into late maturity–early destruction, since its charge in the Late Palaeozoic.

From an initially very simple concept this paper expanded almost uncontrollably into its present size. A number of people helped to make it possible. J. Kidd, J. Means, W. Stewart and S. Elcano as well as others in the Occidental draughting department converted very obscure scribblings into legible illustrations. Without their creativity and persistence these very complicated diagrams would not have been practical. K. Alvarez typed the manuscript (and retyped it many times) and D. Monckton improved the English. Their support, patience and encouragement over what seemed like an interminable length of time is very much appreciated. S. Mills and D. Macgregor reviewed the text and suggested significant improvements. The management of Occidental International Exploration

and Production Company is thanked for approving its publication. Imperial College Geology Department is thanked for its assistance in providing one of the authors with a research fellowship on North Africa. Assistance is also gratefully acknowledged from Anglo Siberian Oil Company with the preparation of some of the numerous drafts of this text and for some of the figures.

References

ALEM, N., ASSASSI, S., BENHEBOUCHE, S. & KALDI, B. 1998. Controls on hydrocarbon occurence and productivity in the F6 reservoir, Tin Fouyé–Tabankort Area, N. W. Illizi Basin. *This volume.*

ALI, O. 1973. Stratigraphy of Lower Triassic sandstone of northwest Algeria Sahara, Algeria. *Bulletin of the American Association of Petroleum Geologists*, **57**, 528–540.

—— 1975. El Agreb–El Gassi oil fields, central Algerian Sahara. *Bulletin of the American Association of Petroleum Geologists*, **59**, 1676–1684.

ALIEV, M., AIT LAOUSSINE, N., AUROV, V., ALEKSINE, G., BAROULINE, G., MAZANOV, V., MEDEUDEV, E., *et al.* 1971. *Geological Structures and Estimation of Oil and Gas in the Sahara in Algeria.* Atamira-Rotopress, Spain.

ANDRIEUX, J., FRIZON DE LAMOTTE, D. & BRAUD, J. 1989. A structural scheme for the western Mediterranean area in Jurassic and Early Cretaceous times. *Geodinamica Acta (Paris)*, **3**(1), 5–15.

ARBEY, F. 1978. Sedimentological and ecological effects of glacioeustatic sea level changes on Saharan Siluro-Ordovician north-west rim (N. Africa). Conservation of detrital pyrite in cold climates. *International Congress Sedimentological Meeting, 9–14 July, Vol. 1, 10th International Congress on Sedimentology, Jerusalem*, International Association of Sedimentologists, 28–31.

ASSAAD, F. A. 1981. A further geological study on the Triassic formations of north-central Algeria with special emphasis on halokinesis. *Journal of Petroleum Geology*, **4**(2), 163–176.

BACHELLER, W. D. & PETERSON, R. M. 1991. Hassi Messaoud Field, Algeria; Trias Basin, Eastern Sahara Desert. *In*: FOSTER, N. H., *et al.* (eds) *Structural Traps V*, American Association of Petroleum Geologists, Treatise of Petroleum Geology, Atlas of Oil and Gas Fields, 211–225.

BAGHDADLI, S. M. 1988. Sbaa Basin: a new oil producing region in Algeria. *Bulletin of the American Association of Petroleum Geologists*, **72**(18), 985 (abstract.).

BALDUCCHI, A. & POMMIER, G. 1970. Cambrian oil field of Hassi Messaoud, Algeria. *In*: HALBOUTY, M. T. (ed.) *Geology of Giant Petroleum Fields.* American Association of Petroleum Geologists, Memoir, **14**, 477–488.

BELLINI, E. & MASSA, D. 1980. A stratigraphic contribution to the Palaeozoic of the Southern Basin of Libya. *In*: SALEM, M. J.& BUSREWIL, M. T. (eds) *The Geology of Libya, Vol. 1*, Academic Press, London, 3–56.

——, GIORI, I., ASHURI, O. & BENELLI, F. 1991. Geology of Al Kufrah Basin, Libya. *In*: SALEM, M. J., SBETA, A. M. & BAKBAK, M. R. (eds) *The Geology of Libya, Vol. 6.* Elsevier, Amsterdam, 2155–2184.

BENAMRANE, O., MESSAOUDI, M. & MESSELLES, H. 1993. Geology and hydrocarbon potential of the Oued Mya Basin, Algeria. *Bulletin of the American Association of Petroleum Geologists*, **77**(9), 1607 (abstract).

BENTAHAR, H. & ETHRIDGE, F. G. 1991. Depositional environments of Upper Triassic sandstones, El Borma oil field, southwestern Tunisia. *Bulletin of the American Association of Petroleum Geologists*, **75**(3), 541 (abstract).

BERRY, W. B. N., & BOUCOT, A. J. 1973 Glacio-eustatic control of Late Ordovician–Early Silurian platform sedimentation and faunal changes. *Geological Society of America Bulletin*, **84**, 275–284.

BEUF, S., BIJU-DUVAL, B, DE CHARPAL, O., ROGNON, P., GARIEL, O. & BENNACEF, A. 1971. *Les Grès du Paléozoique Inférieur au Sahara.* Editions Technip, Paris. Publications de l'Institut Français du Pétrole, Science et Technique du Pétrole, **18**, 464 pp.

BISHOP, W. F. 1975. Geology of Tunisia and Adjacent Parts of Algeria and Libya. *Bulletin of the American Association of Petroleum Geologists*, **59**, 413–450.

BOUDJEMA, A. 1987. Evolution structuralé du bassin petrolier—triasique—du sahara nord oriental (algerie) (Structural evolution of the petroleum (Triassic) basin of northeastern Sahara (Algeria)). Doct. en sciences 1987. Universite de Paris XI.

——, HAMEL, M., MOHAMEDI, A., LOUNISSI, R. 1990. Petroleum potential of the Reggane Basin, Algeria. *Bulletin of the American Association of Petroleum Geologists*, **74**(5), 616 (abstract).

BRENCHLEY, P. J., MARSHALL, J. D., CARDEN, G. A. F., ROBERTSON, D. B. R., LONG, D. G. F., MEIDLA, T., HINGS, L. & ANDERSON, T. F. 1994. Bathymetric and isotopic evidence for a short-lived Late Ordovician glaciation in a greenhouse period. *Geology (Boulder)*, **22**, 295–298.

BUSSON, G. & BUROLLET, P. F. 1973. La limite Permien–Trias sur la Plate-Forme Saharienne (Algerie, Tunisie, Libye), *Canadian Society of Petroleum Geologists, Memoir*, **2**, 74–88.

CAIRE, A. 1953. *Allochtone Sud-Telliene et Autochtone Presaharien au Nord du Hodna.* SN REPAL Internal Report.

CAWLEY, S. J., WILSON, N. P., PRIMMER, T. & OXTOBY, N., KHATIR, B. 1995. Palaeozoic gas charging in the Ahnet–Timimoun Basin, Algeria. *Bulletin of the American Association of Petroleum Geologists*, **79**(8), 1202 (abstract).

CHAOUCHI, R., MALLA, M. S. & KECHOU, F. 1998. Sedimentological evolution of the Giventian-Eifelian (F3) Sand Bar of the West Alrar Field, Illizi Basin, Algeria. *This volume.*

CHIARELLI, A. 1978. Hydrodynamic framework of eastern Algerian Sahara—Influence on hydrocarbon occurrence. *Bulletin of the American Association of Petroleum Geologists*, **62**(4), 667–685.

CLARET, J. & TEMPERE, C. 1967. Une nouvelle region productrice au Sahara Algérien: l'anticlinorium

de Hassi Touareg. *Proceedings, 7th World Petroleum Congress 2*, **81–100.**

CLARK-LOWES, D. D. 1985. Aspects of Palaeozoic cratonic sedimentation in southwest Libya and Saudi Arabia. PhD thesis, London University.

—— 1988. Similarities in the Palaeozoic successions of North Africa and Arabia and implications for petroleum exploration. *In*: *AAPG Mediterranean Basins Conference, Nice, France*, Abstract.

—— & WARD, J. 1991. Palaeoenvironmental evidence from the Palaeozoic 'Nubian Sandstones' of the Sahara. *In*: SALEM, M. J. *et al.* (eds) *The Geology of Libya vol. 6*. Elsevier, Amsterdam, 2099–2153.

CONRAD, J. & LEMOSQUET, Y. 1984. Du craton vers sa marge: évolution sédimentaire et structurale du bassin Ahnet–Timimoun–Bechar (Sahara algérien) au cours du Carbonifère: donnés paléoclimatiques. *Bulletin de la Société Géologique de France, 7*, **XXVI**(6), 987–994.

——, MASSA, D. & WEYANT, M. 1986. *Late Devonian regression and Early Carboniferous transgression on the Northern African Platform*. Ministry of Economic Affairs, Administration of Mines, Belgian Geological Survey, *Annales de la Société Géologique de Belgique*, **109**, 113–122.

CROSSLEY, R. & MCDOUGALL, N. 1998. Lower Palaeozoic reservoirs of North Africa. *This volume*.

CUNNINGHAM, S. M. 1988. Gothlandian source rock discovered north of the Talemzane Arch, central Tunisia. *Bulletin of the American Association of Petroleum Geologists*, **72**, 996–997 (Abstract).

DANIELS, R. P. & EMME, J. J. 1995. Petroleum system model, eastern Algeria, from source rock to accumulation: when, where and how? *Proceedings of the Seminar on Source Rocks and Hydrocarbon Habitat in Tunisia*. ETAP Memoir, **9**.

DEMAISON, G. & HUIZINGA, B. J. 1994. Genetic classification of petroleum systems using three factors: charge, migration and entrapment. *In*: *The Petroleum System–from Source to Trap*. American Association of Petroleum Geologists, Memoir, **60**, 73–89.

DJARNIA, M. R. & FEKERINE, B. 1998. Sedimentological and diagenetic controls on Cambro-Ordovician reservoir quality in the south Hassi-Messaoud Area (Sahara Platform, Algeria). *This volume*.

DUBUY, L. 1980. Ground water in Wadi ash Shatí, Fazzan–a case history of resource development. *In*: SALEM, M. J. & BUSREWIL, M. J. (eds) *The Geology of Libya Vol. 2*. Academic Press, London, 611–627.

ECHIKH, K. 1998. Geology and hydrocarbon occurences in the Ghademes Basin, Algeria, Tunisia, Libya. *This volume*.

EMME, J. J. & SUNDERLAND, B. L. 1991. Regional stratigraphy and petroleum potential, Ghadames Basin, Algeria. *Bulletin of the American Association of Petroleum Geologists*, **75**(3), 569 (abstract).

FATMI, A. N., ELIAGOUBI, B. A. & HAMMUDA, O. S. 1980. Stratigraphic nomenclature of the pre-Upper Cretaceous Mesozoic rocks of Jabal Nafusah, N.W. Libya. *In*: SALEM, M. J. & BUSREWIL, M. T. (eds) *The Geology of Libya* Vol. 1. Academic Press, London, 57–66.

FAVRE, P. & STAMPFLI, G. M. 1992. From rifting to passive margin: the examples of the Red Sea, Central Atlantic and Alpine Tethys. *Tectonophysics*, **215**, 69–97.

GAUTHIER, F. J., BOUDJEMA, A. & LOURUS, R. 1995. The structural evolution of the Ghadames and Illizi Basins during the Palaeozoic, Mesozoic and Cenozoic: petroleum implications. *Bulletin of the American Association of Petroleum Geologists*, **79**(8), 1214 (abstract).

GHENIMA, R. 1995. Hydrocarbon generation and migration in the Ghadames Basin: application to the filling history of the El Borma oil field. *Proceedings of the Seminar on Source Rocks and Hydrocarbon Habitat in Tunisia*. ETAP Memoir, **9**.

GUIRAUD, R. 1992. Early Cretaceous rifts of Western and Central Africa: an overview. *Tectonophysics*, **213**, 153–168.

—— 1998. Mesozoic rifting and basin inversion along the Northern African Tethyan margin: an overview. *This volume*.

—— & MAURIN, J. C. 1991. Le rifting en Afrique au Cretace inférieur: synthèse structurale, mise en évidence de deux phases dans la genèse des bassins, relations avec les ouvertures océaniques peri-africaines. *Bulletin de la Société Géologique de France*, **5**, 811–823.

GUMATI, Y. D., KANES, W. H. & SCHAMEL, S. 1996. An evaluation of the hydrocarbon potential of the sedimentary basins of Libya. *Journal of Petroleum Geology*, **19**(1), 95–112.

HAMEL, A. 1990. Geological study of the Triassic reservoirs of the Hassi R'Mel gas condensate field, Algeria. *Bulletin of the American Association of Petroleum Geologists*, **74**(5), 668 (abstract).

HAMMUDA, O. S. 1980. Geologic factors controlling fluid trapping and anomalous freshwater occurrence in the Tadrart Sandstone, Al Hamadah al Hamra area, Ghadames Basin. *In*: SALEM, M. J. & BUSREWIL, M. T. (eds) *The Geology of Libya, Vol. 2*. Academic Press, London, 501–507.

HAMOUDA, A. 1980*a*. Petroleum potential-Ouargla Region Triassic Basin, Algeria. *In*: HALBOUTY, M. T. (ed.) *Giant Oil and Gas Fields of the Decade: 1968–1978*. American Association of Petroleum Geologists, Memoir, **30**, 539–541.

—— 1980*b*. Oil and gas potential of Algeria's Ouargla region. *Oil and Gas Journal*, **78**(11), 206–224.

HARGRAVES, R. B. & VAN HOUTEN, F. B. 1985. *Palaeogeography of Africa in Early-Middle Palaeozoic: Palaeomagnetic and Stratigraphic Constraints and Tectonic Implications*. Occasional Publication, International Centre for Training and Exchanges in the Geosciences, **3**, 160–161.

HARLAND, W. B., ARMSTRONG, R. L., COX, A. V., CRAIG, L. E., SMITH, A. G. & SMITH, D. G. 1990. *A Geologic Time Scale 1989*. Cambridge University Press, Cambridge.

VAN HOUTEN, F. B. & KARASEK, R. M. 1981 Sedimentologic framework of Late Devonian Oolitic Iron Formation, Shatti Valley, West–Central Libya. *Journal of Sedimentary Petrology*, **51**, 415–428.

JABOUR, H. & NAKAYAMA, K. 1988. Basin modelling of Tadla Basin, Morocco, for hydrocarbon potential. *Bulletin of the American Association of Petroleum Geologists*, **72**(9), 1059–1073.

JACKSON, J. S., MOORE, S. R. & QUARLES, A. I. 1995. Tethys and Atlas-related deformations in the Triassic Basin, Algeria. *Bulletin of the American Association of Petroleum Geologists*, **79**(8), 1223 (abstract).

JAEGER, H., BONNEFOUS, J. MASSA, D. 1975. Le Silurian en Tunisie; ses relations avec le Silurian de Libye nord-occidentale. *Bulletin de la Société Géologique de France, 7*, **XVII**(1), 68–77.

KARASEK, R. M. 1981. *Structural and stratigraphic analysis of the Palaeozoic Murzuk and Ghadames basins, western Libya.* Thesis South Carolina, USA.

KEELEY, M. L. 1989. The Palaeozoic history of the Western Desert of Egypt. *Basin Research*, **2**, 35–48.

—— & MESSOUD, M. S. 1998. Tectonic controls on the petroleum geology of North East Africa. *This volume.*

KILANI-MAZRAOUDI, F., RAZGALLAH-GARGOURI, S. & MANNAI-TAYECH, B. 1990. The Permo-Triassic of southern Tunisia–biostratigraphy and paleoenvironment. *Review of Palaeobotany and Palynology*, **66**, 273–291.

KLITZSCH, E. 1966. Geology of the northeast flank of the Murzuk Basin (Djebel Ben Ghnema–Dor el Gussa). *In*: WILLIAMS, J. J. (ed.) *South–Central Libya and Northern Chad: a guidebook to the Geology and Prehistory. 8th Annual Field Conference.* Petroleum Exploration Soc. Libya, Tripoli, 19–32.

—— 1971. The structural development of parts of North Africa since Cambrian time. *In*: GRAY, C. (ed.) *Symposium on the Geology of Libya, Tripoli*, University of Libya, 253–262.

—— 1981. Lower Palaeozoic rocks of Libya, Egypt and Sudan. *In*: HOLLAND, C. H. (ed.) *Lower Palaeozoic of the Middle East, Eastern and Southern Africa and Antarctica.* John Wiley, New York, 131–163.

LOGAN, P. 1998. An investigation of the thermal history of the Ahnet and Reggane Basins, Central Algeria, and the consequences for hydrocarbon generation and accumulation. *This volume.*

LORENZ, J. 1980. Late Jurassic–Early Cretaceous sedimentation and tectonics of the Murzuq Basin, southwestern Libya. *In*: SALEM, M. J. & BUSREWIL, M. T. (eds) *The Geology of Libya, Vol. 2*, Academic Press, London, 383–392.

MACGREGOR, D. S. 1996*a*. Factors controlling the destruction or preservation of giant light oilfields. *Petroleum Geoscience*, **2**, 197–217.

—— 1996*b*. Hydrocarbon systems of North Africa. *Marine and Petroleum Geology*, **13**(3), 329–340.

—— & MOODY, R. T. J. 1998. Mesozoic and Cenozoic petroleum systems of North Africa. *This volume.*

MAGLOIRE, P. R. 1970. Triassic gas field of Hassi er R'Mel, Algeria. *In*: *Geology of Giant Petroleum Fields.* American Association of Petroleum Geologists, Memoir, **14**, 489–501.

MAGOON, L. B. & DOW, W. G. 1994. The petroleum system. *In*: MAGOON, L. B. & DOW, W. G. (eds) *The Petroleum System–from Source to Trap.* American Association of Petroleum Geologists, Memoir, **60**, 3–24.

MASSA, D. & BELTRANDI, M. 1975. Sédimentologie du Silurien de Libye Occidentale. *IXth Congrès International de Sédimentologie, Nice, 1975, Vol. I*, Blackwell, 113–118.

MEGERISI, M. & MAMGAIN, V. D. 1980. Stratigraphic nomenclature of the pre-Upper Cretaceous Mesozoic rocks of Jabal Nafusah, N.W. Libya. *In*: SALEM, M. J. & BUSREWIL, M. T. (eds) *The Geology of Libya Vol. 1.* Academic Press, London, 57–66.

MEISTER, E. M., ORTIZ, E. F., PIEROBIN, E. S. T., ARRUDA, A. A. & OLIVEIRA, M. A. M. 1991. The origin and migration fairways in the Murzuq Basin, Libya: an alternative exploration model. *In*: SALEM, M. J., BUSREWIL, M. T. & BEN ASHOUR, A. M. (eds) *The Geology of Libya Vol. 7.* Elsevier, Amsterdam, 2725–2742.

MORABET, A. & JABBOUR, H. 1998. Mesozoic and Cenozoic petroleum systems of Morroco. *This volume.*

PALLAS, P. 1980. Water resources of the Socialist People's Libyan Arab Jamahiriya. *In*: SALEM, M. J. & BUSREWIL, M. J. (eds) *The Geology of Libya, Vol. 2*, Academic Press, London, 539–594.

PELET, R. & TISSOT, B. 1970. Étude geochimique du Silurien (Argiles à Graptolites) de la Bordure Nord du Hoggar. *Revue de l'Institut Français du Pétrole*, **25**(5), 543–574.

PETERSON, J. A. 1982. *Geology and Petroleum Resources of North–Central and North-Eastern Africa.* US Geological Survey Open File Report, 85–709.

—— 1986. *Geology and Petroleum Resource Assessment of Onshore Northwestern Africa.* US Geological Survey Open File Report, 86–183.

PIEROBON, E. S. T. 1991. Contribution to the stratigraphy of the Murzuk Basin, Southwest Libya. *In*: SALEM, M. J. & BELAID, M. N. (eds) *The Geology of Libya, Vol. 5.* Elsevier, Amsterdam, 1769–1784.

PRATSCH, J. C. 1995. New play indicates promise in central onshore Tunisia. *Oil and Gas Journal*, **93**(32), 69–72.

RAHMANI, A., YAHI, N. & ISSAD, M. 1994. Source rock identification and hydrocarbon generation related to trap formation of Allal High, Algerian Sahara. *Bulletin of the American Association of Petroleum Geologists. AAPG–SEPM Annual Meeting Abstracts*, 240.

RIGBY, J. K., NEWELL, N. D. & BOYD, D. W. 1979. Marine Permian rocks of Tunisia. *Bulletin of the American Association of Petroleum Geologists*, **63**(3), 516 (abstract).

RIGO, F. 1995. Overlooked Tunisia reef play may have giant field potential. *Oil and Gas Journal*, **93**(1), 56–60.

—— 1996. North Tunisian Sahara hosts giant Triassic, Lower Palaeozoic prospects. *Oil and Gas Journal*, **94**(3), 52–57.

SCOTESE, R. C., BAMBACH, R. K., BARTON, C., VAN DER VOO, R. & ZEIGLER, A. M. 1979. Paleozoic base maps. *Journal of Geology*, **87**, 217–277.

SOLA, M. & OZCICEK, B. 1990. On the hydrocarbon prospectivity of North Cyrenaica region, Libya. *Petroleum Research Journal (Tripoli, GSPLAJ)*, **2**, 25–41.

SONATRACH 1979. Geology of Algeria, the hydrocarbon-bearing provinces. *Schlumberger Algeria Well Evaluation Conference, Algeria Proceedings*, I-1–I-26.

STAMPFLI, G., MARCOUX, J. & BAUD, A. 1991. Tethyan margins in space and time. *Palaeogeography, Palaeoclimatology, Palaeoecology*, **87**, 373–409.

VON STETS, J. & WURSTER, P. 1981. Zur Strukturgeschichte des Hohen Atlas in Marokko. *Geologische Rundschau*, **70**(3), 801–841.

TAKHERIST, D., AREZKI, A. & MOUAICI, R. 1995. Characterization and evolution of Palaeozoic source rock organic matter in Algerian Central Sahara. *Bulletin of the American Association of Petroleum Geologists*, **79**(8), 1251 (abstract)

THOMAS, D. 1995. Libya basins, Part 1: Geology, Murzuk oil development could boost S.W. Libya prospects. *Oil and Gas Journal Specia*, **93**(10), 6 March, 41–46.

TISSOT, B., ESPITALE, J., DEROO, G., TEMPERE, C. & JONATHAN, D. 1984. Origin and migration of hydrocarbons in the eastern Sahara (Algeria). *In*: *Petroleum Geochemistry and Basin Evaluation*. American Association of Petroleum Geologists, Memoir, **35**, 315–324.

TRAUT, M. W., BOOTE, D. R. D. & CLARK-LOWES, D. D. 1998. Exploration history of the Palaeozoic petroleum systems of North Africa. *This volume*.

TURNER, B. R. 1980. Palaeozoic sedimentology of the southeastern Part of Al Kufrah Basin, Libya: a model for oil exploration. *In*: SALEM, M. J. & BUSREWIL, M.T. (eds) *The Geology of Libya, Vol. 2*. Academic Press, London, 351–374.

VAN DE WEERD, A. A. & WARE, P. L. G. 1994. A review of the east Algerian Sahara oil and gas province (Triassic, Ghadames and Illizi Basins). *First Break*, **12**(7), 363–373.

VIALLY, R., LETOUZEY, J., BENARD, F., HADDAD, N., DESFORGES, G., ASKRI, H. & BOUDJEMA, A. 1994. Basin inversion along the North African Margin. The Sahara Atlas (Algeria). *In*: ROURE, F. (ed.) *Peri-Tethyan Platforms*. Editions Technip, Paris, 79–118.

VOS, R. G. 1981*a*. Sedimentology of an Ordovician fan dalta complex, western Libya. *Sedimentary Geology*, **29**, 153–170.

—— 1981*b*. Deltaic sedimentation in Devonian of western Libya. *Sedimentary Geology*, **29**, 67–88.

WHITBREAD, T. & KELLING, G. 1982. Mrar Formation of Western Libya–evolution of an Early Carboniferous delta system. *Bulletin of the American Association of Petroleum Geologists*, **66, 1091–1107.**

WILDI, W. 1983. La chaîne tello-rifaine (Algérie, Maroc, Tunisie): structure stratigraphique et évolution du Trias au Miocene. *Revue de Géologie Dynamique et de Géographie Physique, Numéro spécial. Chaîne Tello-Rifaine*, **24**, 201–298.

WILSON, M. & GUIRAUD, R. 1998. Late Permian to recent magmatic activity of the African-Arabian Margin of Tethys. *This volume*.

YAHI, N. & KHATIR, B. 1995. Source rock identification and basin modelling, Mouydir Oued Mya Basin, central Algeria. *57th EAGE Conference; Extended Abstract Poster, Vol. 2*, 53.

ZIEGLER, P. A. 1988. Laurussia—the Old Red Continent. *In*: MCMILLAN, N. J., EMBRY, A. F. & GLASS, D. J. (eds) *Devonian of the World*. Canadian Society of Petroleum Geologists, Memoir, **14**(1), 15–48.

—— 1989. *Evolution in Laurussia*. Kluwer,Dordrecht.

Exploration history of the Palaeozoic petroleum systems of North Africa

MARC W. TRAUT[1], DAVID R. D. BOOTE[1], & DANIEL D. CLARK-LOWES[2,3]

[1]*Occidental Oil and Gas Corporation, 1200 Discovery Drive, P.O. Box 12021, Bakersfield, CA 93389, USA*

[2]*Geology Department, Imperial College of Science, Technology and Medicine, Prince Consort Road, London SW7 2BP, UK*

[3]*Present address: Clark-Lowes Consulting, Oak Court, Silver Street, Wiveliscombe, Taunton TA4 2PA, UK*

Abstract: Subsurface exploration of the Palaeozoic petroleum systems of Libya, Algeria, Tunisia and Morocco began in the early 1950s after the discovery of a large prospective Palaeozoic basin in the Sahara Desert province of North Africa. The first exploration well to test this concept was drilled in Algeria in 1952. A non-commercial find in 1953 was followed by major discoveries in 1956. Since that time approximately 1100 new field wildcats have been drilled to test Palaeozoic and basal Triassic reservoir targets in a variety of discrete petroleum systems. This resulted in the discovery of approximately 330 Palaeozoic-sourced accumulations in the Algerian, Libyan and Tunisian portions of the Sahara Desert. By the end of 1996 ultimate recoverable reserves in oil equivalent for these discoveries were estimated to be just over 46 billion barrels. Using measures of activity and reserves discovered, it is seen that the history of exploration of this province has followed a normal cycle, familiar to the petroleum industry, which can be divided into five major periods. They are: Pre-Discovery, Discovery, post-Discovery Boom, post-Boom and Revival. It is anticipated that future advances in technology will result in new ideas and more effective exploration, and ultimately in the future discovery of significant oil and gas reserves.

Subsurface exploration of the Palaeozoic hydrocarbon systems of the Sahara Desert province of Libya, Algeria, Tunisia and Morocco began in the early 1950s. Petroleum exploration was undertaken after the recognition, in the 1930s and 1940s, that a large Palaeozoic basin was present in the Sahara Desert of North Africa which was potentially prospective for hydrocarbons. The first petroleum exploration drilling to test this concept took place in Algeria during 1952 and the first discovery was made in 1953. At the end of 1996, the estimated ultimate recoverable reserves in oil equivalent for discoveries associated with the Palaeozoic hydrocarbon systems were just over 46 billion barrels (BBBL). The proven areal extent of the Palaeozoic petroleum systems associated with these reserves consists of two fairly large domains encompassing parts of Algeria, Libya, and Tunisia (Fig. 1).

The focus of this review is on the history of exploration concepts, methods and tools that have combined to give us our present understanding of the Palaeozoic petroleum systems of North Africa. In addition, a review of the history of discovery of petroleum systems is revealing for what we can learn about the way in which accepted intellectual paradigms drive exploration activity and how often-unexpected discoveries change perceptions and create a new paradigm, which takes over until it, in turn, is exhausted or replaced. The development of technology and exploration play concepts, and their effectiveness in achieving results, cannot be divorced from the commercial and political history of the period, a brief description of which is also included. Boote *et al.* (this volume) provides a description and analysis of these petroleum systems; Figs 13–20 and Tables 1–4 of that paper contain information that will help the reader of this paper with background on the various petroleum systems, basins and provinces. The known productive Palaeozoic systems involve hydrocarbon accumulations in both Palaeozoic and Triassic reservoirs, sourced and charged by Silurian (Tanezzuft Shale) or Devonian shales.

Exploration history

Five distinct periods can be recognized in the chronology following an early phase of field studies suggesting the existence of a large Palaeozoic basin in the Sahara Desert province of North Africa (see Fig. 2, below). These are (1) a Pre-Discovery period, when operators studied the region and acquired acreage in prospective areas, (2) a period of initial discoveries, defining in outline a number of prospective Palaeozoic systems, (3) a discovery 'Boom' period when exploration activity was at its peak, (4) a

TRAUT, M. W., BOOTE, D. R. D. & CLARK-LOWES, D. D. 1998. Exploration history of the Palaeozoic petroleum systems. *In*: MACGREGOR, D. S., MOODY, R. T. J. & CLARK-LOWES, D. D. (eds) 1998. *Petroleum Geology of North Africa*. Geological Society, London, Special Publication No. 132, 69–78.

mature or post-Boom cycle of exploration, and (5) a Revival period when activity and success increased above the baseline established by maturity.

Early exploration (late nineteenth century to 1945)

Petroleum exploration in North Africa began in the late nineteenth century with a focus on oil seeps associated with Tertiary measures in the Gulf of Suez–Red Sea region of Egypt and in coastal portions of the Atlas Province of northwest Africa (Fig. 1). The latter area was proximal to the growing market for petroleum products in Europe and it offered good exposures of Tertiary and Mesozoic strata with numerous documented oil seeps. The first reported 'commercial' oil discovery in North Africa was the Gemsa find in 1909 which is located in the southern Gulf of Suez coastal region of Egypt and which produced small quantities of oil from shallow Miocene reservoirs. After this discovery further exploration during this period in the Gulf of Suez region was only modestly successful. Early exploration attempts in Morocco, Algeria and Tunisia, on the other hand, were all failures, and it was not until 1923 that the first commercial hydrocarbon discovery was made. This discovery was the Ain Hamra find situated in the Rharb Basin of northern Morocco. Subsequent exploration of this region during this period was unsuccessful.

At this time the vast interiors of Libya, Tunisia, Algeria, Morocco and Spanish Sahara received virtually no attention for their hydrocarbon potential as a consequence of their remoteness. However, between 1920 and 1940 teams of Italian and French geologists ventured into the interior of their respective colonies (Tenaille *et al.* 1975). The outbreak of the Second World War brought a halt to surface exploration and reconnaissance of these interior regions.

Pre-Discovery period 1946–1952. After the Second World War, the French Government created the Bureau de Recherches des Pétroles (BRP), charged to ensure a long-term supply of petroleum from its colonial territories (Grayson 1981). The BRP formed the Société Nationale de Recherche et d'Exploitation des Pétroles en Algérie (SNREPAL) with the Algerian colonial government in 1946 to pursue exploration in Algeria. Initially, SNREPAL concentrated on the Tertiary and Mesozoic of northern Algeria, leading to the discovery of the rather modest Oued Gueterine Field in 1949. During the same period SNREPAL also evaluated the Saharan interior, building on earlier reconnaissance surveys, and by 1949 had defined a regionally extensive Palaeozoic basin immediately south of the Saharan Atlas, stretching from western Libya to the Spanish Sahara. This regional work highlighted the possibility of significant hydrocarbon potential in both the Triassic and Palaeozoic (Tenaille *et al.* 1975)

In 1949 SNREPAL and Compagnie Française de Pétroles-Algérie (CFP(A)) filed a joint application for a 300 000 km^2 exploration permit in the northern part of the Algerian Sahara (Tenaille *et al.* 1975). Early results from analogue reflection seismic surveys over the permit area were disappointing (Bouchon *et al.* 1959). However, results of a 1952 refraction survey across a large northeast-plunging surface structure in the Ghardaia region were more promising. The group was finally awarded the permit in 1952 and shortly thereafter drilled a stratigraphic well near the village of Berriane, approximately 40 km north of Ghardaia (Figs 1 and 2) to evaluate the anomaly. BE-1 encountered a 200 m section of Triassic sand with gas shows at 2306 m immediately below a Mesozoic evaporite sequence. Although it flowed salt water at high rates with only traces of gas, the presence of reservoir and hydrocarbons was considered very encouraging. Subsequently the group went on to drill another 20 wells with no success (Tenaille *et al.* 1975).

During this period two additional groups applied for exploration permits. In 1953, Shell as Companie Pétrole d'Algérie (CPA) was awarded a 240 000 km^2 permit in the southwest part of the province and Compagnie de Recherche et d'Exploitation de Pétrole au Sahara (CREPS), a consortium of Régie Autonome des Pétroles (RAP), Shell, BRP and SNREPAL, was granted a 190 000 km^2 block on the northern flank of the Hoggar (Tenaille *et al.* 1975).

Discovery period (1953–1956). During this 4 year period, some 50 exploratory wells were drilled on Palaeozoic prospects, defined by field mapping and photogeology, refraction seismic and, to a lesser extent, analogue reflection seismic surveys. This resulted in some 12 discoveries with estimated ultimate recoverable reserves of 27.6 billion barrels oil equivalent (BBOE), mostly in two enormous accumulations (Figs 1 and 2).

The first discovery was made by the CREPS group in the Ahnet Basin during 1953 (Guillemot *et al.* 1955). The discovery well Djebel Berga 1 was drilled on a surface anomaly, approximately 80 km southwest of In Sallah, encountering a

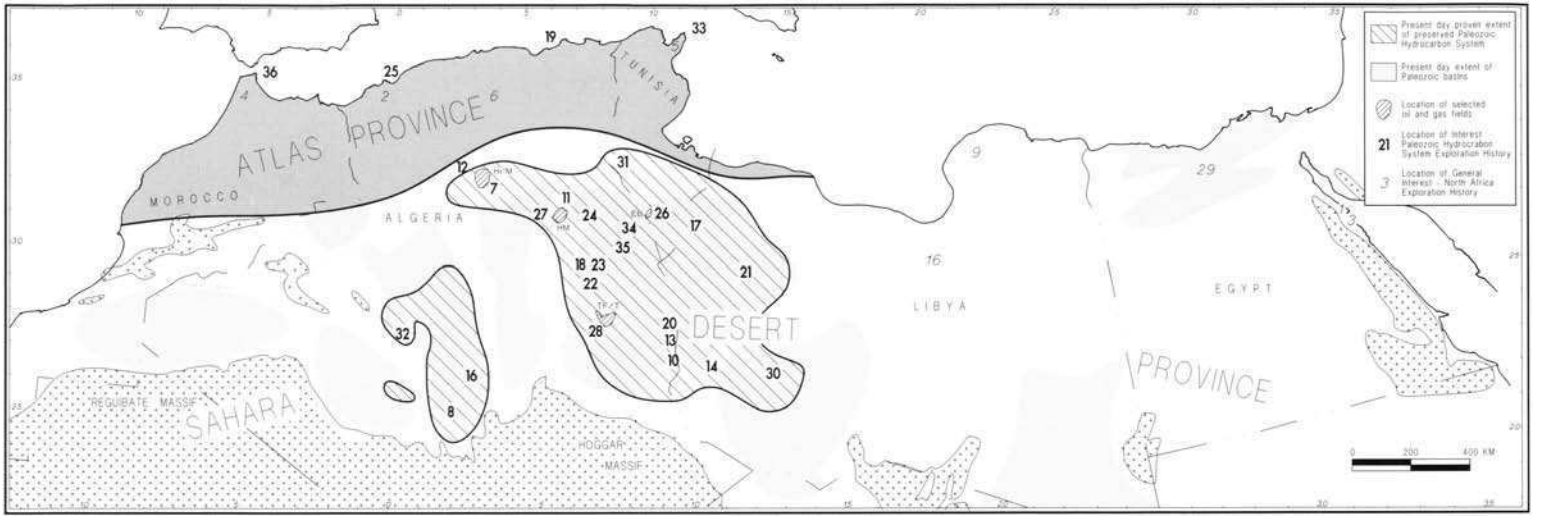

Fig. 1. Index map and chronology of key events, highlighting the location of points of interest in the early exploration history of North Africa and in the subsequent exploration history of the Palaeozoic petroleum systems of the Sahara Desert. The reference (first) number for each of the listed events corresponds to a matching location on the map. **1**. 1886, first exploration well in North Africa. **2**. 1892, first exploration well in NW Africa. **3**. 1909, first commercial oil discovery in North Africa, Gemsa (Mio.). **4**. 1923, first discovery in NW Africa, Ain Hamra (Mio.). **5**. 1948, first discovery in Tunisia, Cap Bon (Cret.). **6**. 1949, first discovery in Algeria, Oued Gueterini (Eoc.). **7**. 1952, first Palaeozoic test drilled in Sahara. **8**. 1953, first Palaeozoic gas discovery, Djebel Berga (Dev.). **9**. first exploarion well in Libya. **10**. 1956, first Palaeozoic oil discovery, Edjeleh (Carb.–Dev.). **11**. 1956, Hassi Messaoud (Cambro-Ord.). **12**. 1956, Hassi R'Mel (Trias.). **13**. 1957, Zarzaitine (Carb.–Dev.). **14**. 1957, first oil discovery in Libya, Atshan (Dev.). **15**. 1958, In Sallah (Dev.). **16**. 1959, first major discovery in Sirt Basin, Zelten (Palaeoc.). **17**. 1959, Tlacsin (Sil.). **18**. 1959, Hassi Touareg and Hamra (Trias.). **19**. 1959, first oil pipeline from Hassi Messaoud to Mediterranean. **20**. 1960, Alrar (Carb.–Dev.). **21**. 1960, El Hamra (Dev.). **22**. 1961, Gassi Touil (Trias.). **23**. 1962, Rhourde Nouss (Trias.). **24**. 1962, Rhourde El Baguel (Cambro-Ord.). **25**. 1963, first gas pipeline from Hassi R'Mel to Mediterranean. **26**. 1964, El Borma (Trias.). **27**. 1965, Haoud Berkaoui (Trias.). **28**. 1966, Tin Fouye–Tabankort (Ord.). **29**. 1966, first discovery in Western Desert, El Alamein (Cret.). **30**. 1984, first discovery in Murzuq Basin (Ord.). **31**. 1979, Sabria Nord (Ord.). **32**. 1980, first oil discovery in Sbaa Basin, H. Sbaa (Carb.–Dev.). **33**. 1981, first trans-Mediterranean gas pipeline, Algeria to Italy. **34**. 1990, Bir Rebaa Nord (Trias.). **35**. 1994, Berkane Est (Trias.). **36**. 1996, second trans-Mediterranean gas pipeline, Algeria to Spain.

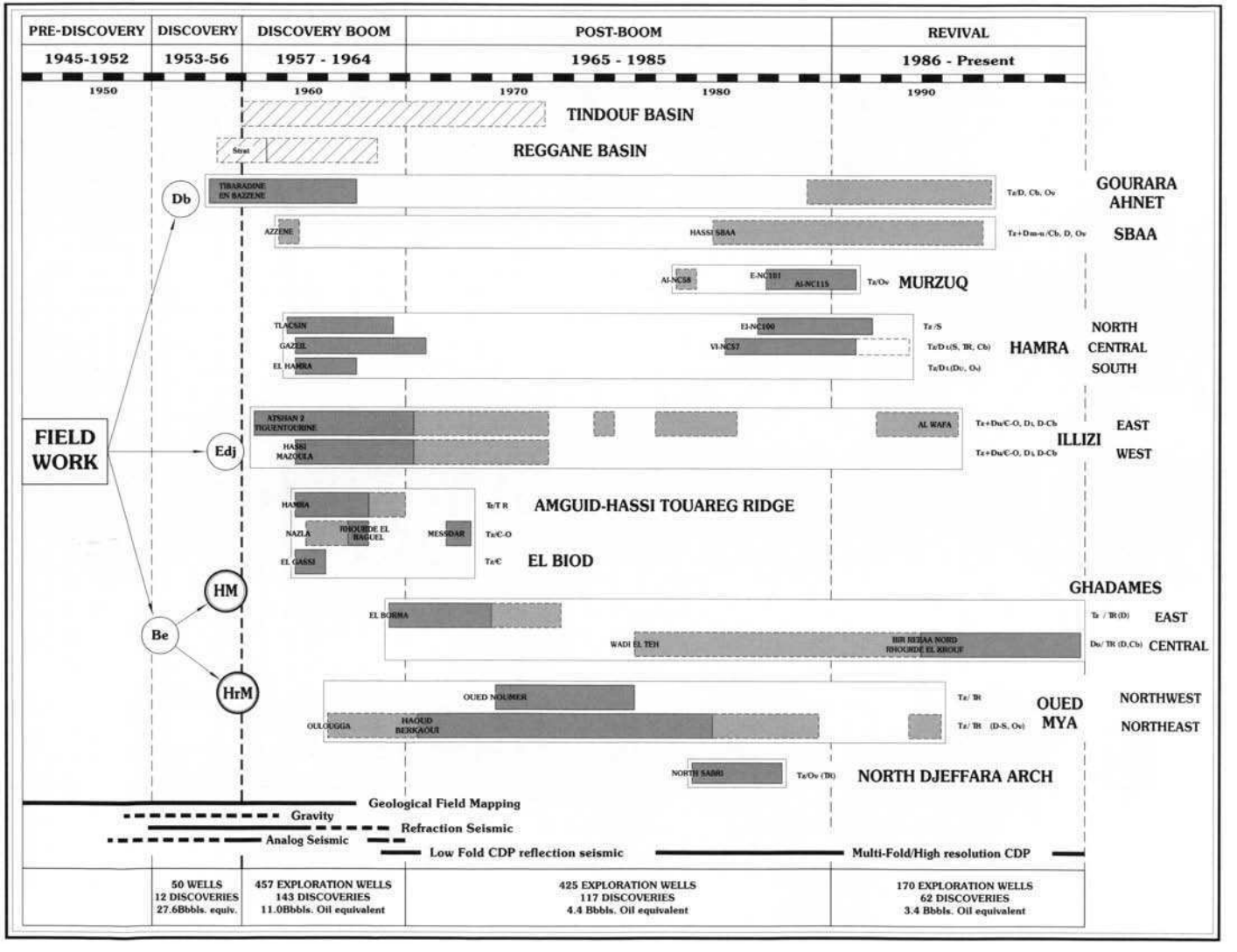
PRE-DISCOVERY
1945-1952
DISCOVERY
1953-56
DISCOVERY BOOM
1957 - 1964
POST-BOOM
1965 - 1985
REVIVAL
1986 - Present
1950
1960
1970
1980
1990
TINDOUF BASIN
REGGANE BASIN
Strat
FIELD WORK
Db
Edj
Be
HM
HrM
TIBARADINE
IDN BAZZENE
AZZENE
HASSI SBAA
GOURARA
AHNET
SBAA
Tz/D, Cb, Ov
Tz+Dm-u /Cb, D, Ov
Al-NC58
E-NC101
Al-NC115
Tz/Ov
MURZUQ
TLACSIN
GAZEIL
EL HAMRA
E3-NC100
VI-NC57
Tz /S
Tz/D t.(S, TR, Cb)
Tz/D t.(Du, Ou)
HAMRA
NORTH
CENTRAL
SOUTH
ATSHAN 2
HOUENTOURINE
HASSI
MAZOULA
AL WAFA
Tz+Du/C-O, D t, D-Cb
ILLIZI
EAST
WEST
HAMRA
NAZLA
RHOUDDE EL
BAGUEL
MESSDAR
EL GASSI
Tz/T R
Tz/C-O
Tz/C
AMGUID-HASSI TOUAREG RIDGE
EL BIOD
GHADAMES
EL BOSMA
WADI EL TEH
IHR REDAA NORD
RHOUDDE EL KROUF
Tz / TR (D)
Du/ TR (D,Cb)
EAST
CENTRAL
OUED NOUMER
OULOUGGA
HAOUD
BERKAOUI
Tz/ TR
Tz/ TR (D-S, Ov)
OUED
MYA
NORTHWEST
NORTHEAST
NORTH SADRI
Tz/Ov (TR)
NORTH DJEFFARA ARCH
Geological Field Mapping
Gravity
Refraction Seismic
Analog Seismic
Low Fold CDP reflection seismic
Multi-Fold/High resolution CDP
50 WELLS
12 DISCOVERIES
27.6Bbbls. equiv.
457 EXPLORATION WELLS
143 DISCOVERIES
11.0Bbbls. Oil equivalent
425 EXPLORATION WELLS
117 DISCOVERIES
4.4 Bbbls. Oil equivalent
170 EXPLORATION WELLS
62 DISCOVERIES
3.4 Bbbls. Oil equivalent

medium sized dry gas accumulation in a Lower Devonian sandstone (Figs 1 and 2; also see Fig. 19 of Boote *et al.* this volume). It was not viewed as economically significant at the time because of its remote location. However, it did validate the Devonian sand as an exploratory target in the province and it provided the impetus for further exploration in the Ahnet, Gourara, Sbaa, Reggane and Tindouf Basins.

In early 1956, the CREPS DL-101 well was drilled to test a surface structure on the Tihemboka Arch along the eastern flank of the Illizi Basin. It encountered multiple oil and gas pays in Devonian and Carboniferous reservoirs between 400 and 800 m. The discovery was named Edjeleh with initial estimated reserves of some 280 MMBOE. The well highlighted the Palaeozoic prospectivity of the Illizi Basin and triggered a very aggressive exploration programme in the region over the following few years (Figs 1 and 2; also see Fig. 16 of Boote *et al.*, this volume).

Further north, a regional seismic refraction survey acquired by the SNREPAL–CFP(A) group in 1955 revealed a large deep-seated arch, southwest of Ouargla. Preliminary mapping suggested it was some 120 km across (Bouchon *et al.*; Balducchi & Pommier 1970). With minimal control, SNREPAL spudded MD-1 in January 1956. The well encountered a section of Mesozoic evaporites and reddish mudstones above a 300 m section of oil-saturated Cambrian sandstone. This interval tested at rates in excess of 1000 barrels of oil per day (Tenaille *et al.* 1975; Bacheller & Peterson 1991). Subsequent seismic surveys and delineation drilling confirmed the presence of an enormous oil accumulation, the Hassi Messaoud Field, initially estimated to reservoir some 2 BBBL oil. Through time this estimate has been increased. Today it is considered to hold as much as 10 BBOE reserves. The field marked the first major Palaeozoic discovery in North Africa and became the cornerstone of the petroleum industry in Algeria (Figs. 1 and 2; see also Fig. 14 of Boote *et al.*, this volume).

SNREPAL quickly followed up the Hassi Messaoud discovery with HR-1. This well was spudded in September 1956 to evaluate a large anomaly defined by refraction seismic survey, on structural trend with the BE-1 stratigraphic test drilled in 1952. It encountered wet gas-bearing Triassic sands below 2132 m testing at 18 MMCF (million cubic feet) per day with a 170 g/m3 condensate yield. Subsequent drilling defined an enormous accumulation of some 2600 km^2 areal extent, the Hassi R'Mel Field (Magloire 1970). Present estimates of reserves are 90 TCF (trillion cubic feet) gas and 3 BBBL condensate or 18 BBOE (Figs 1 and 2; see also Fig. 14 of Boote *et al.*, this volume).

Boom period (1957–1964). The Algerian war of independence (1954–1962) started as the pace of exploration increased in the Sahara (Heggoy 1981) and the discovery of important oil and gas reserves greatly accentuated French interest in the country (Smith 1978). However, military activity was confined to northern Algeria and did not dampen the tremendous interest stimulated by the Hassi Messaoud and Hassi R'Mel discoveries. Together with the Djebel Berga and Edjeleh finds, these discoveries loosely defined a vast, highly prospective region in central Algeria and western Libya. Once commercial development of these vast fields was assured, it became obvious they would provide the infra structure necessary to support other projects in this remote region. The first major crude oil pipeline linking Hassi Messaoud with the port of Bougie was completed in 1959 and a gas line between Hassi R'Mel and Arzew was completed in 1963 (Tiratsoo 1983).

Industry interest quickly focused upon scheduled relinquishments first by SNREPAL–CFP in 1957 and later by CREPS and CPA in 1958. By 1960 more than 20 companies had acquired exploration acreage in Algeria (Tenaille *et al.* 1975). A number of operators also attempted to extend the new Palaeozoic play west into the Tindouf Basin and east into southern Tunisia and western Libya.

Fig. 2. Exploration history of North African Palaeozoic petroleum systems. Exploration periods between 1945 and 1996 are shown along the top of the figure. For each petroleum system, grouped by basin or province, the key discoveries are shown and, at the base of the figure, evolution of technology responsible for the successful discovery of these systems is illustrated. The most active exploration phase of each system is shaded. (See Boote *et al.* (this volume) for a description of each system.) Abbreviations (in this figure and other figures and in the text): Be, Berriane, Db, Djebel Berga, Edj, Edjeleh, HR'M, Hassi R'Mel, HM, Hassi Messaoud; Tz–Dl petroleum system, Tanezzuft source–Lower Devonian reservoir, Du–Cb petroleum system, Upper Devonian (Frasnian) source–Carboniferous reservoir; Dm, Middle Devonian, Ov, Ordovician, C-O, Cambro-Ordovician. Recoverable reserves are quoted in barrels of oil equivalent (BOE), barrels (BBL) or cubic feet (CF); in trillions (T), billions (B) or millions (MM). Field sizes are as follows: giant (greater than 250 MMBOE), large (greater than 100 MMBOE), medium (greater than 25 MMBOE), small (less than 25 MMBOE).

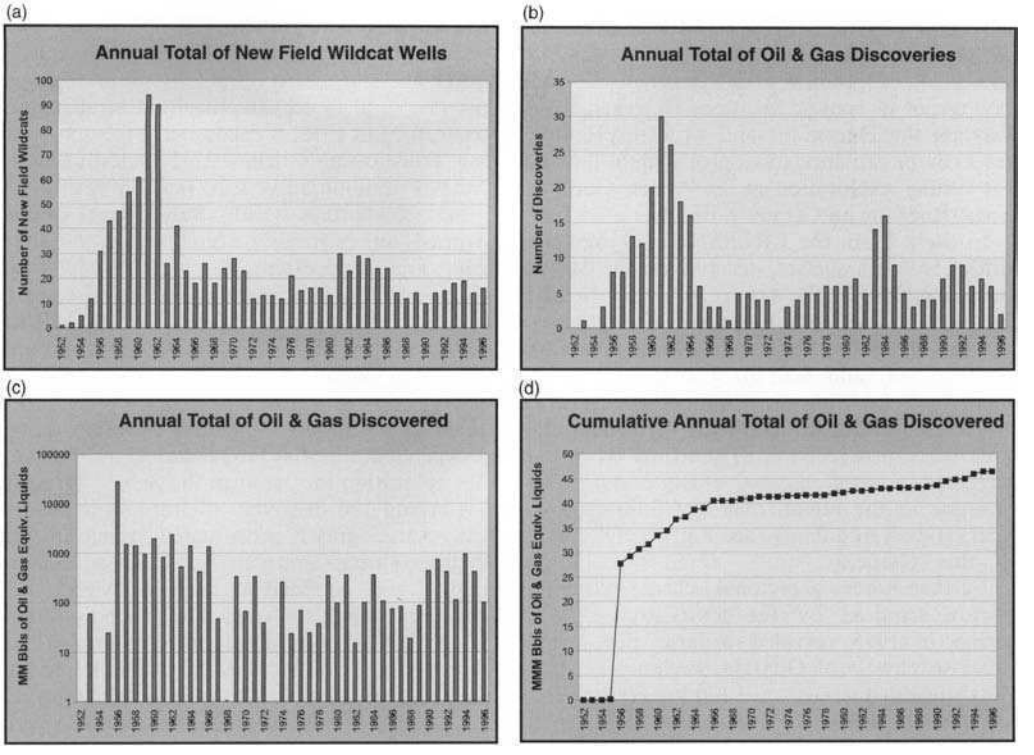

Fig. 3. Exploration statistics for Palaeozoic petroleum systems of North Africa, including all Saharan Palaeozoic basins of Morocco, Algeria, Tunisia and Libya. Well statistics and reserves relate to Palaeozoic and basal Triassic sandstone reservoirs only. (**a**) Annual total of new field wildcats. In the peak year (1961), 94 exploratory wells were drilled. It should be noted that since the end of the boom period (1964) between 10 and 30 exploration wells have been drilled each year. The cumulative number of exploration wells is approximately 1100. (**b**) Annual total of oil and gas discoveries, including both commercial and non-commercial discoveries. In the peak year (1961), 30 discoveries were made. Spikes for 1983 and 1984 represent successful activity in the Libyan Hamra and Murzuq Basins. The cumulative number of discoveries is approximately 330. (**c**) Yearly total of oil and gas discovered (MMBOE). In the peak year (1956), 27.6 BBOE were discovered. (**d**) Cumulative estimated ultimately recoverable oil and gas reserves. At the end of 1996 estimated total recoverable reserves were just over 46 BBOE. The relatively flat segment between 1964 and 1990 should be noted.

Over this 8 year period, some 457 exploratory wells were drilled to test prospects defined by field mapping and photogeology; coupled with gravity, refraction and analogue reflection seismic surveys, the low-fold common depth point seismic technique was introduced towards the end of the period. Activity peaked in 1961 with 94 new field wildcats. Success followed quickly, with 143 discoveries for an average exploration success rate of 29%. Cumulative estimated ultimate recoverable reserves found at this time were 11 BBOE, an average of 77 MMBOE per discovery (Fig. 3).

Exploration activity was most intense in Algeria, most notably in the Illizi Basin. Triggered by the CREPS Edjeleh and Tiguentourine finds in 1956 and Exxon's Atshan 2 small discovery close by in Libya in 1957, the Illizi area was rapidly explored in the following few years. Interest initially focused on the southwest part of the basin with the Tin Essameid find in 1957, followed by El Adeb Larache, In Amenas North, Zarzaitine, La Reculée and Dome à Collenias between 1957 and 1959, moving progressively northwards with time. The Alrar, Krebb and Ohanet finds were made in 1960, and Timedratine, In Akamil Nord and Timadanet in 1961; further to the west, Hassi Mazoula was discovered in 1959, followed by Oued Zenani in 1960 and the Tin Fouye–Tabankort complex between 1961 and 1966. By 1964 most of the more significant fields in the region had been delineated (Fig. 2; see also Table 2 of Boote *et al.*, this volume).

Early success in the Illizi Basin and at Hassi

Messaoud encouraged exploration along the intervening Hassi Touareg and El Biod High (Figs 1 and 2; see also fig. 15 in Boote *et al.*, this volume). Starting with El Gassi in 1958 and Hamra in 1959, a series of large discoveries followed, including Gassi Touil in 1961, Rhourde Nouss and Rhourde El Baguel in 1962.

Exploration success elsewhere was more chequered. Several significant Palaeozoic gas discoveries were made in the Ahnet and Gourara Basins, extending the play first established by the Djebel Berga find into an area where a large number of surface structures offered clearly defined drilling prospects. These included the En Bazzene and Tiraradine finds in 1955, Djebel Mouhadrine in 1956, Tirechoumene and the Gourara Basin Tineldjane and Krechba fields further north in 1957, and In Sallah in 1958. However, reserves remained insufficient for commercial development and interest in the area waned by 1964. Gas was found on the flank of the neighbouring Sbaa Basin during 1959 (Azzene Field) but the small size of the find discouraged further exploration there. At the same time a very ambitious 25 well drilling programme in the Tindouf Basin was singularly unsuccessful encountering only a few isolated sniffs of gas (Fig. 2; see also Fig. 20 of Boote *et al.*, this volume).

The Palaeozoic exploration play was opened up in 1957 in Libya with Exxon's Atshan 2 Devonian small discovery located on the southwest extension of the Gargaf Arch. Interest subsequently focused on the Hamra Basin, where some 47 discoveries were made during the following few years. These included Bir Tlacsin (1959) and Tigi (1960) to the north, Gazeil (1959) and Z-1–66 (1961) in the central area, the southern El Hamra field complex between 1959 and 1962, and the Alar field extension, D-1–52, in 1964 (Fig. 2). However, enthusiasm for the basin faded as it became apparent that the finds were generally small and, with Exxon's Zelten discovery in 1959, attention shifted towards the developing Cretaceous and early Tertiary play in the Sirt Basin of central Libya.

Agip's El Borma find was the first significant discovery in the Ghadames Basin, establishing a new basal Triassic sandstone play (Fig. 2; see also Fig. 13 of Boote *et al.*, this volume). Well EB-1 was spudded in December 1963 on a low-relief structural prospect, first defined by surface mapping and later confirmed by seismic survey (Perrodon & Dumon 1975). The well encountered a massive 110 m oil-saturated sandstone section at 2382 m, resting unconformably upon the Palaeozoic. This field, with reserves of 700 MMBOE was later extended into Algeria.

Post-boom period (1965–1985). The Algerian war of independence drew to a close in 1962 with the Evian Accords settlement. The agreement included conditions perpetuating existing hydrocarbon exploration and production contracts. As a result, the initial impact of the change in government was relatively minor (Naylor 1992). However, in 1963, the first president of the new Democratic Republic of Algeria, Mr Ahmed Ben Bella, signed decree 63–491, establishing a state company, SONATRACH, to manage transportation and marketing of hydrocarbons. Its responsibilities were expanded in 1966 by President Houori Boumedine to encompass exploration and production activity. Over the next few years various segments of the petroleum industry were nationalized, including Sinclair's Rhourde el Baguel field in 1969, Shell's CREPS equity in 1970 and various French assets in 1971. Prior to nationalization SONATRACH controlled 33% of Algeria's oil and gas resources; by 1981 SONATRACH controlled 100% of Algerian oil and gas production (Mezier & Valentin 1994).

As part of the nationalization process, the Government revised its hydrocarbon legislation, introducing more onerous terms and limiting new exploration contracts with foreign companies to a duration of 3–5 years. The Government also stipulated that the foreign partner in any joint venture would pay for all exploration costs, that SONATRACH would assume operatorship during production and oil produced was to be split 51% 49% in favour of the Government. Foreign companies entering into crude oil purchase contracts were required to spend 35 cents on exploration for each barrel lifted. Several joint-venture agreements, notably with Amoco, Shell, TOTAL, SOHIO, Texaco, Deminex, Hispanoil, Agip, Braspetro and Cepsa, were established under these terms between 1971 and 1985.

Digital common depth point reflection seismic technology was introduced in 1963–1964, opening up new and increasingly subtle plays that had been difficult to discern with the analogue reflection and refraction seismic techniques used previously. However, the new contractual terms discouraged exploration and activity declined significantly. Only some 425 new field wildcat wells were drilled between 1965 and 1985. These established 4.4 BBOE additional reserves, spread across 117 discoveries, with an average success rate of 27% (Fig. 3).

Twenty of these discoveries were made in the Illizi Basin province, extending the Palaeozoic play, established earlier, further to the north. The most notable of these were the giant fields,

Stah (1971), Mereksene (1974), Dimeta Ouest (1979) and Tin Zemane (1981).

Further west continuing exploration along the Hassi Touareg trend led to the Messdar discovery in 1967. Even further west there was little activity in the Gourara and Ahnet Basins during this period. SONATRACH made a medium-sized oil find in 1980, Hassi Sbaa 1, in the neighbouring Sbaa Basin, and although this was considered significant in an otherwise gas-dominated region, its relatively small size together with the follow-up Hassi Ilatou (1983) and Hassi Ilatou NE (1986) discoveries, confirmed the limited potential of the basin.

One of the more significant exploration highlights during this period was the discovery of the Oued Mya petroleum province. Most exploration in the basin before 1965 had been focused on surface anticlines to the south with no success. Cities Service first established a Triassic oil play in the northern Oued Mya in 1961 with its Oulougga discovery. However the find was small and non-commercial. In 1965 CFP(A) spudded the OK-101 well on a prospect defined by common depth point reflection seismic survey. The well encountered multiple oil-bearing Triassic sands below a thick evaporitic section, in what subsequently become the Haoud Berkaoui Field with reserves of 300 MMBOE. Further exploration of the play resulted in 21 discoveries including the giants, Ben Khala (1966) and Guellala (1969). Draa El Temra (1971) and Guellala Nord Est (1972) were also discovered in the northeastern part of the basin, and Oued Noumer (1969) Ait Kheir (1971) and Dhjorf (1974) were found to the northwest (Fig. 2).

Exploration activity in western Libya led to a string of small finds in the northern and central Hamra Basin between 1980 and 1986. Further south in the Murzuq Basin, Boco and Rompetrol followed up a 1978 Braspetro non-commercial discovery to make a series of Ordovician discoveries between 1982 and 1985, most of which were medium-sized to small but, in the Murzuq Field, a collection of pools is grouped as a giant field (Figs 1 and 2; see also Figs 17 and 18 of Boote *et al.*, this volume).

The 1964 El Borma discovery in the northeastern part of the Ghadames Basin was followed up with only limited success. Its western extension into Algeria was established in 1969 and a number of small accumulations were subsequently made nearby, over the next 10 years. These included Hassi Keskessa (1969) in Algeria and Chouech Essaida (1972), Larich (1979) and Debbech (1980) in southern Tunisia. Further north, Amoco extended the Palaeozoic play into central Tunisia with the small El Franig, Sabri Nord and Baguel discoveries between 1980 and 1983. Although they proved the existence of a Palaeozoic petroleum system on the northern flank of the Talemzane Arch, and suggested the possibility of further discoveries in the region, they were very modest in size with combined reserves of only 20 MMBOE.

Revival (1986–1996): In 1986 the Algerian Government modified its hydrocarbon legislation quite significantly, providing production-sharing contracts and allowing foreign companies to retain operatorship through production. A number of new concessions were awarded between 1986 and 1992, and pre-existing contracts were modified to incorporate the terms available under the revised legislation.

At the same time, the petroleum infrastructure was expanding. Algeria's gas production capacity had been increased with additional LNG facilities and completion of the first trans-Mediterranean pipeline, linking Hassi R'Mel to the large Italian market in 1981. A second trans-Mediterranean gas pipeline from Hassi R'Mel to Spain via Morocco and the Straits of Gibraltar was completed in December 1996. In addition exploration for increasingly subtle plays was becoming increasingly practical with improvements in technology and especially in enhanced imaging capability offered by high resolution multi-fold seismic survey. As a result, exploratory activity gradually increased. A total of 170 exploration wells were drilled in the 10 year period between 1986 and 1996, establishing some 3.4 BBOE reserves in a total of 62 discoveries (Fig. 3).

By far the most significant new finds made during this period were concentrated in the northern part of the Ghadames Basin. Earlier exploration in the area had yielded only shows and a few non-commercial oil finds. With improved seismic resolution it became possible to define subtle basal Triassic structures, previously masked by an almost impenetrable evaporite sequence. The result was an impressive extension of the Triassic sandstone play first highlighted by El Borma in 1964 and Wadi el Teh in 1976. The most notable of these discoveries were the giant and large discoveries at Bir Rebaa Nord made in 1990, Rhourde el Krouf in 1992, Hassi Berkine Nord in 1994 and Berkine East in 1994 (Fig. 2).

Elsewhere there was little significant success, with a few additional gas discoveries in the Ahnet and Gourara Basins, including the medium-sized discovery Gour Mahmoud in 1989, the large field Hassi Moumene in 1990

and the medium field, Garet el Guefoul in 1991. Further east in the Hamra Basin, Sirte Oil's 1991 A-1–NC169 (Alwafa) discovery, 15 km northeast of Alrar encountered oil and gas pay in Devonian sandstones, reviving interest in that area. Reserves are estimated to be 400MMBOE. Additional reserves in the Murzuq Basin were added by Lasmo.

Western Libya's infrastructure was significantly improved with the 1996 completion of a pipeline linking the Murzuq Basin with the coast.

Conclusion

Since 1952 when the first exploration well was drilled in the Saharan Desert province of North West Africa more than 1100 exploratory test wells have been drilled to test prospects which are associated with the various Palaeozoic petroleum systems in the region. This exploratory drilling has resulted in the discovery of approximately 330 hydrocarbon accumulations with cumulative estimated ultimate reserves of more than 46 billion barrels of oil.

Using measures of activity and reserves discovered it is seen that the history of exploration of this province has followed a normal cycle, familiar to the petroleum industry, which can be divided into five major periods. Each of these has its own characteristics and is influenced by creativity, technology, success, economics, and politics of the period. The majority of the reserves in the province were discovered early in the Discovery and Discovery Boom periods when the more favourable areas and plays were identified and aggressively pursued with existing technology. There followed the Post-Boom period characterized by a rapid decline in exploration activity and in reserves discovered as opportunities associated with the various proven plays were depleted or met with failure. This mature state of exploration has been impacted by second order exploration 'Booms' as new technology has been employed, as old paradigms were challenged, as new concepts were developed and tested, and as the known areas of the productive hydrocarbon systems were expanded through rank wildcat drilling. The Revival period, which began in 1986, represents a significant second order exploration boom.

Those who explore this oil-rich region today are faced with a variety of technical challenges. Overcoming these challenges can be rewarding, as evidenced by the success of the industry in this region during recent years. The potential for opportunity continues to grow as technological advances become available (i.e. high resolution 2D seismic, 3D seismic, coherency cube, etc.) which allow for the identification of structure which was previously unrecognized and for detailed reservoir characterization which will aid the search for subtle stratigraphic traps. These advances will result in new ideas and more effective exploration, and ultimately in the future discovery of significant oil and gas reserves.pt >

We would like to thank S. Mills and D. Macgregor, who reviewed the text and offered helpful comments and encouragement. A special acknowledgement goes to J. Kidd, J. Means and S. Elcano, who prepared the figures. We also appreciate the approval and support from the management of Occidental International Exploration and Production Company to publish this paper.

References

BACHELLER, W. D. & PETERSON, R. M. 1991. Hassi Messaoud Field—Algeria, Trias Basin, Eastern Sahara Desert. *In*: FOSTER, N. H. & BEAUMONT, E. A. (eds) *Treatise of Petroleum Geology Atlas of Oil and Gas Fields, Structural Traps*. American Association of Petroleum Geologists, Tulsa, OK.

BALDUCCHI, A. & POMMIER, G. 1970. Cambrian oil field of Hassi Messaoud, Algeria. *In:* HALBOUTY, M. T. (ed.) *Geology of Giant Petroleum Fields*. American Association of Petroleum Geologists, Memoir, **14**, 477–488.

BOOTE, D. R. D., CLARK-LOWES, D. D. & TRAUT, M. W. 1998. Palaeozoic petroleum systems of North Africa. *This volume*.

BOUCHON, R., LAPPARENT, C. de, ORTYNSKI, H. I. & POMMIER, G. 1959. Le developpement de la sismique refraction dans l'interpretation geologique du Sahara Nord; son role dans la decouverte et l'etude du champ d'Hassi Messaoud. *In*: *Proceeds of the Fifth World Petroleum Congress*. John Wiley & Sons, Chichester, pp. 729–746.

GRAYSON, L. E. 1981. *National Oil Companies*. John Wiley & Sons, Chichester.

GUILLEMOT, A., MICHEL, P. & TRUMPY, D. 1955. La Prospection du Paléozoique au Nord du Hoggar (Sahara). *4th World Petroleum Congress Proceedings, Section 1*, Applied Science, New York, USA, 243–249.

HEGGOY, A. A. 1981. *Historical Dictionary of Algeria*. Scarecrow Press, NJ, USA.

MAGLOIRE, P. R. 1970. Triassic Gas Field of Hassi R'Mel, Algeria. *In*: *Geology of Giant Petroleum Fields*. American Association of Petroleum Geologists Memoir, **14**, 489–501.

MEZIER, C. & VALENTIN, N. 1994. SONATRACH-an International Petroleum Group. Régie Sud Méditerranée-Alger.

NAYLOR, P. C. 1992. French–Algerian relations 1980–1990. *In*: ENTELIS, J. P. & NAYLOR, P. C.

(eds) *State and Society in Algeria*, Westview Press, Boulder, CO.

PERRODON, A. & DUMON, E. 1975. Tunisia. *In*: OWEN, E. W. (ed.) *Trek of the Oil Finders, A History of Exploration for Petroleum*. American Association of Petroleum Geologists Memoir, **6**, 1445–1449.

SMITH, T. 1978. *The French Stake in Algeria, 1945–1962*. Cornell University Press, Ithaca, NY.

TENAILLE, M., BURGER, J. & PERRODON, A. 1975. Algeria. *In*: OWEN, E. W. (ed.) *Trek of the Oil Finders, A History of Exploration for Petroleum*. American Association of Petroleum Geologists Memoir, **6**, 1450–1471.

TIRATSOO, J. N. H. (ed.) 1983. *World Pipelines and International Directory of Pipeline Organizations and Associations*. Gulf Publishing, Houston, TX.

Giant fields, petroleum systems and exploration maturity of Algeria

DUNCAN S. MACGREGOR

BP Exploration Operating Co. Ltd, Kuningan Plaza, S. Tower, P.O. Box 2749, Jakarta 12940, Indonesia

Abstract: The giant petroleum fields of eastern Algeria can be divided into six significant petroleum systems. More than 60% of the giant fields and 80% of the reserves within them lie in a specific setting in reservoirs immediately below or above the Hercynian unconformity, and below the Liassic salt seal. The second main reservoirs are Early Devonian sandstones. Timing of generation and preservation potential, as controlled by tectonic history, seal type and source rock burial, are key controls on the distribution of petroleum in these giant fields, particularly for oil. Field size distributions within the six petroleum systems can be related to structural style and to differing levels of exploration maturity within each system. Comparisons can be made between the productive trap types and petroleum systems of Algeria and analogous but more heavily drilled basins elsewhere in the world. Such comparisons suggest that further giant fields lie undiscovered in Algeria, particularly in subtle forms of traps, and in the 250–500 MMBOE (million barrels oil equivalent) reserves range. The Ghadames petroleum system may be the system which carries the highest yet-to-find, as predicted from a range of criteria, including discovery trends, drilling density, field size distribution and source rock supply analysis. The challenge to the oil industry in Algeria is to identify the locations of the missing giant fields suggested by this analysis.

The prime objective of this paper is to assess the potential for, and possible nature of further giant field discoveries through the use of a range of objective techniques involving the use of analogues. The first step in the analysis presented is to subdivide the proven giant fields of Algeria into a number of different petroleum systems, based on key factors such as reservoir and source age and trap type. Assessments are then attempted of the degree of exploration maturity of the identified petroleum systems, based on a comparison of field size distributions and trap types with analogous, but more heavily drilled petroleum systems. 'Giant fields', for the purposes of this paper, are defined as those indicated from available data to contain more than 250 MMBO (million barrels oil) or 1.5 TCF (trillion cubic feet) of recoverable petroleum reserves. Fields which contain less than these of each individual phase, but contain more than 250 million barrel oil equivalent total reserves (5.8 BCF = 1 MMBO) are also included.

According to the compilation of Attar & Hammat (1993), the recoverable reserves of Algeria total 16400 MMBO and 130 TCF, spread across 207 fields. There is at least an additional 6000 MMBO of condensate, giving a total for the country of 45000 MMBOE (million barrels oil equivalent), placing the province in the world's largest ten petroleum provinces (Macgregor this volume). As in other areas of the world (Roadifer 1987), the majority of these reserves lie in 'giant' fields. Although full details are not available, particularly for the smaller fields, it would appear that least 90% of Algeria's gas reserves and at least 80% of oil reserves lie in 'giants', of which the two largest, Hassi Messaoud and Hassi R'Mel, have reserves of 9300 MMBO (c. 58% of country's oil total) and 60–65TCF (c. 46–50% of country's gas total), respectively. Practically all the country's reserves, and all of its giant fields, lie in eastern Algeria (Fig. 1), despite the fact that the source rocks and reservoirs concerned are known to extend over much larger portions of the country. This paper will concentrate on this productive area, covering the Oued Mya, Ghadames and Illizi Basins together with adjoining ridges, and more briefly, the less well-documented Ahnet Basin. Comments will also be made on the factors that may control giant field occurrence in frontier areas.

Reserve assessments form a key element of this paper. It is emphasized that the figures used are neither Sonatrach nor BP internal figures, but have been derived or deduced from a number of public sources. These include a published oil- and gas-in-place compilation by Attar & Hammat (1993), published figures for some fields (e.g. Claracq *et al.* 1963; Balbucchi & Pommier 1970; Magliore 1970; Odeh Ali 1975; Hamouda 1980; Perrodon 1983), press releases, and figures quoted verbally in presentations at American Association of Petroleum Geologists (AAPG) and Geological Society conferences. Undoubtedly, there are error bars on each estimate shown in Fig. 2. The highest uncertainties lie in the most recent discoveries in the Gha-

MACGREGOR, D. S., 1998. Giant fields, petroleum systems and exploration maturity of Algeria. *In*: MACGREGOR, D. S., MOODY, R. T. J. & CLARK-LOWES, D. D. (eds) 1998. *Petroleum Geology of North Africa*. Geological Society, London, Special Publication No. 132, 79–96.

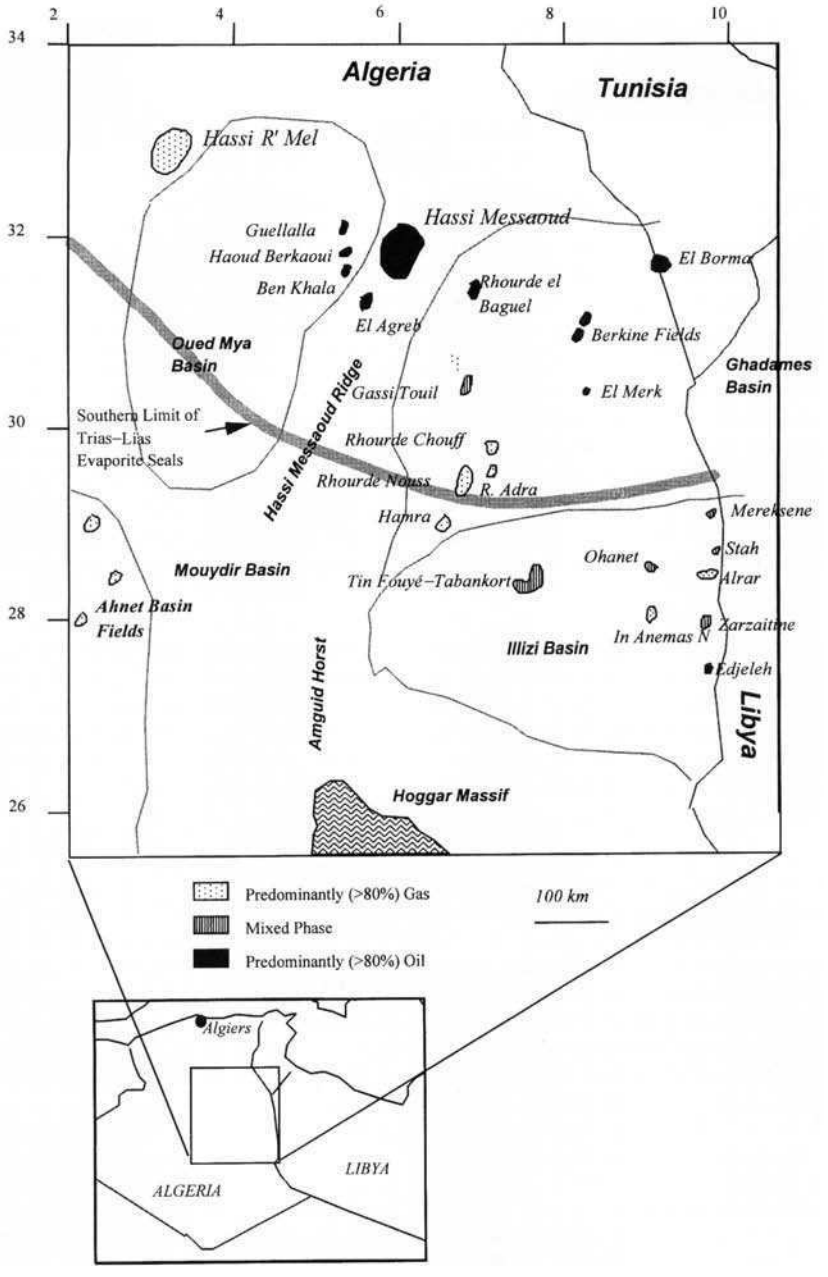

Fig. 1. Location and phase of giant fields, Eastern and Southern Algeria

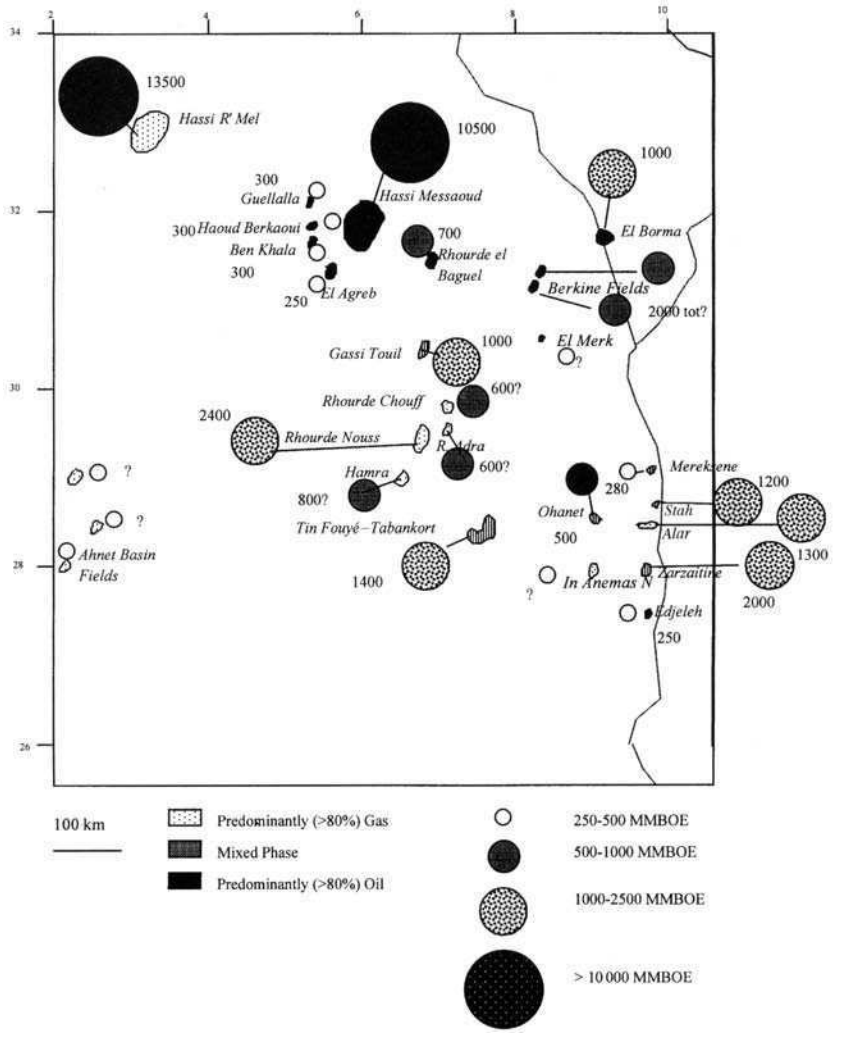

Fig. 2. Estimated reserves in million barrels oil equivalent (5.8 BCF = 1 MMBO) for the Algerian giant fields. (For sources of reserve figures, see text.) The low number of 250–500 MMBOE fields in the east of the region compared with the Oued Mya area should be noted.

dames Basin, where field reserves have not been published; indeed, some of these fields are still undergoing appraisal. On the basis of press releases and predicted production profiles, it is apparent that a number of these new fields must have reserves exceeding 250 MMBOE and it is assumed for the purposes of the analysis in this paper that the three following discoveries are of giant status: Hassi Berkine North, Hassi Berkine South and El Merk. Very large uncertainties exist on reserves distributions in the Ahnet Basin, where fields are still being appraised. As these fields are geographically separated from others considered in this paper, they have not been included in the analysis of reserves distributions.

It should additionally be noted that, as recoverable reserves form the basis for the analysis, there is a resulting bias towards the more economically attractive oil phase and towards reservoirs which flow at commercial rates. Discoveries such as Tiguentourine (tight Ordovician reservoir) and Tin Zemane (Devonian undeveloped gas discovery) may well move into the giant category as defined in this paper if an economic development scheme for these can be proposed.

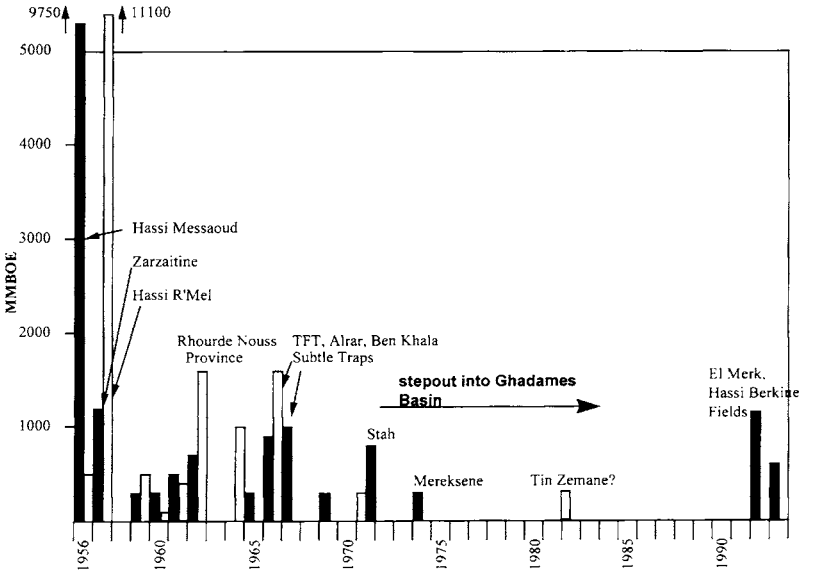

Fig. 3. Reserves in giant fields separated for oil and gas (condensate not included) and plotted v. time (black represents oil, white represents gas). Discoveries seem to have become more 'difficult' since 1965, and thereafter are concentrated in subtle traps and in regions in which accurate seismic definition was required. The latter factor was probably the reason for the long delay in finding fields such as the Berkine fields. The sequence of discoveries in the Illizi and later Ghadames systems show a south-to-north trend.

Figure 3 illustrates that the vast majority of the reserves in giant fields (85%) were discovered in the 12 years from 1956 to 1967. Exploration results in the period 1968–1992 were relatively disappointing in comparison, leading to a perception that significant numbers of further giant field discoveries were unlikely. The declining trend was, however, arrested by the discovery of the new Ghadames Basin oilfields in 1993. This paper tries objectively to assess whether these new discoveries will be the first of many, or whether they are merely anomalies along a trend of decline.

Petroleum systems and trap types

The first section of this paper presents a compilation of data on the geological features of the established giant fields and attempts a basic understanding of the petroleum systems involved. As will be shown later, this understanding is necessary to interpret the statistical trends shown by the giant fields. For these purposes, the giant fields of the region are broken down into six main petroleum systems (Fig. 4), using factors such as common features in reservoir age, structural style of traps and timing of key events (trap formation, sourcing etc.) The systems identified do not necessarily correspond to the basin boundaries illustrated in Fig. 1, and because of the mixing of hydrocarbons between different sources, their boundaries cannot be sharply defined. Some of the datasets created may be too small for meaningful analysis, and in some of the elements of the analysis it has been necessary to combine systems. The number of systems identified is hence a compromise between the need to differentiate key features of the structural and source systems involved and the requirement to maintain reasonably sized datasets.

Reserves within each system are often spread between a variety of reservoirs and may have been derived from multiple source rocks, e.g. Ghadames and Illizi systems. As a result, the chronostratigraphic nomenclature for petroleum systems proposed by Magoon & Dow (1994), which is most applicable to situations where the bulk of reserves tie to specific source rock and reservoir formations, has not been attempted. A brief summary of each individual system and of the giant fields within them follows. The emphasis is on the features of the systems most relevant to the following discussions on exploration maturity and yet-to-find estimation, particularly the ease of recognition of traps and the likely efficiency of the petroleum systems involved.

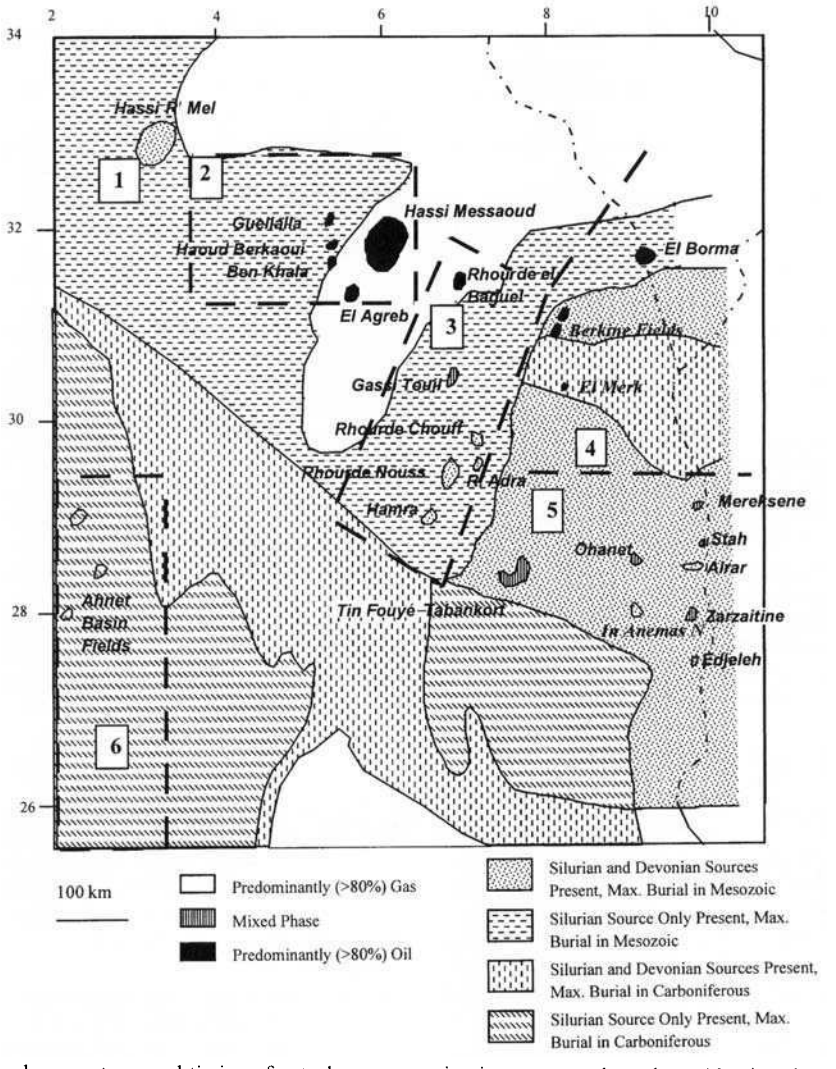

Fig. 4. Petroleum systems and timing of petroleum generation in eastern and southern Algeria. The petroleum systems described in the text are numbered. A good relationship is apparent between giant field occurrence and kitchens that reach maximum depth of burial in the Mesozoic.

(1) Hassi R'Mel system

The Hassi R'Mel system contains a single giant gas field developed in the pinchout of Triassic fluviatile sands on a major structural arch (Magliore 1970). The field thus forms a classic combination structural–stratigraphic trap and is sealed by Liassic evaporites. The gas column, and minor associated oil leg, is believed to be sourced from highly mature Palaeozoic source rocks below the Saharan Atlas. Closure was not formed until the Turonian (Magliore 1970), thus gas emplacement clearly is timed as post-dating this event. Most of the earlier oil charge in this region may well have been lost.

(2) Oued Mya–Hassi Messaoud system

Fields assigned to this system are those believed to be sourced from a kitchen in the Oued Mya depocentre (Fig. 4). Attar & Hammat (1993) reported oil-in-place of 47 BBO (billion barrels oil) in the area, though reported recoverable reserves (in giants) are only 10.2 BBO, largely because of unfavourable reservoir conditions in Hassi Messaoud. There is little doubt here that

the main effective source rock is the c. 30 m thick basal Silurian graptolitic shale (Benamrane *et al.* 1993; Chaouchi *et al.* 1995), because the Devonian is eroded out on the Hercynian unconformity in the catchments of these fields. The fields concerned fall into two groups; (1) fields reservoired in the Triassic and located in the Oued Mya depocentre (Hamouda 1980), which are generally small and often are associated with sand pinchouts; (2) the broad low-relief structural traps developed in Cambro-Ordovician quartzite reservoirs on the adjoining Hassi Messaoud Arch (Balbucchi & Pommier 1970; Odeh Ali 1975). It is apparent that the key control on hydrocarbon occurrence in this area is not reservoir age but the positioning of these reservoirs below the Liassic evaporites and at the Hercynian unconformity, which controls both petroleum migration and entrapment. The Oued Mya depocentre contains a paucity of large structures capable of holding the large amounts of oil generated and, as a result, excess oil migrated onto the Hassi Messaoud Ridge. This model, which sources the majority of Hassi Messaoud reserves from the west, is supported by the similarities in the oils and gas–oil ratios to those in the Triassic reservoired fields further west and by the absence of Silurian or Devonian source rocks over much of the Hassi Messaoud catchment area to the east (Figs 4–6). In addition, the kitchens to the southeast of the field (Figs 5 and 6) are in the late oil–gas window (Daniels & Emme 1995) and thus, if any significant component of charge came from this direction, the field would not be expected to be undersaturated with gas, as is observed. The oil charge clearly post-dates the formation of closure at Hassi Messaoud in the late Jurassic–early Cretaceous (Balbucchi & Pommier 1970) and probably occurred during deposition of the thick pile of Late Cretaceous sediments over the Oued Mya depocentre. The continuous Liassic salt seal that extends across the system seems to have played a crucial role in preventing any leakage of petroleum: no oil has been encountered in the post-salt (A. Boudjema, pers. comm. 1992) and no seeps are recorded in this area.

(3) Rhourde Nouss System

The Rhourde Nouss petroleum system comprises a trend of Early Cretaceous structures formed through wrench-related reactivation of an earlier Triassic–Liassic extensional system (Claret & Tempere 1967; Boudjema 1987). The fields in this trend are formed in steep structures of compressional origin (the transtensional Rhourde el Baguel structure being an exception), and with the exception of the Cambrian reservoir at Rhourde el Baguel, are reservoired in Triassic sands sealed by the Liassic evaporite section or equivalent. A key difference from the Oued Mya system discussed above seems to be the availability of numerous steep easily detectable structural traps. Study of the Hercynian subcrop pattern (Fig. 4) suggests the Silurian to be the main source, with the Devonian 'hot shale' absent through subcrop in the vicinity of the fields. These structures are predominantly gas filled with a total of 25 TCF in place (c. 20 TCF recoverable) (Attar & Hammat 1993), practically all of which is believed to lie in giant fields, of which the largest, Rhourde Nouss, contains at least 40% of these reserves. Oil reserves, in contrast, are modest, being confined to the northern fields in the trend, particularly Gassi Touil and Rhourde el Baguel. The model applied to the observed phase distribution is that the oil charge from the Silurian possibly preceded the formation of the traps during the Austrian inversion, i.e. is pre-Aptian in age (Claret & Tempere 1967; Boudjema 1987).The presence of oil in the northern part of the trend may indicate lower maturities (Fig. 5) and or different timing relationships in that area.

(4) Ghadames System

The Ghadames system has been analysed in detail by Daniels & Emme (1995) and by Echikh (this volume). The Ghadames Basin evolved in four main structural phases: (a) as a Palaeozoic basin, (b) a period of uplift and often deep erosion in the Hercynian, (c) superimposition of a Mesozoic extensional basin, and (d) local inversion in the Early Cretaceous and, to a lesser extent, the Tertiary. As Palaeozoic reservoirs are often very deep, exploration has concentrated on the Triassic, and it is in the Triassic play of the Ghadames Basin that most recent discoveries have been made. The model proposed for most of the fields is long-distance migration along the Hercynian surface from subcrops of the Devonian and Silurian source beds (Daniels & Emme 1995; Echikh this volume). The system shows similarities to the Rhourde Nouss Triassic-reservoired system described above, but has been differentiated because of a number of key differences, namely: (a) the distribution of the fields relative to the subcrops (Figs 5 and 6), plus the comparison in terms of phase or maturity, suggests that the Devonian is the main source in this region. The two sources cannot be differentiated using biomarkers (Daniels & Emme 1995).

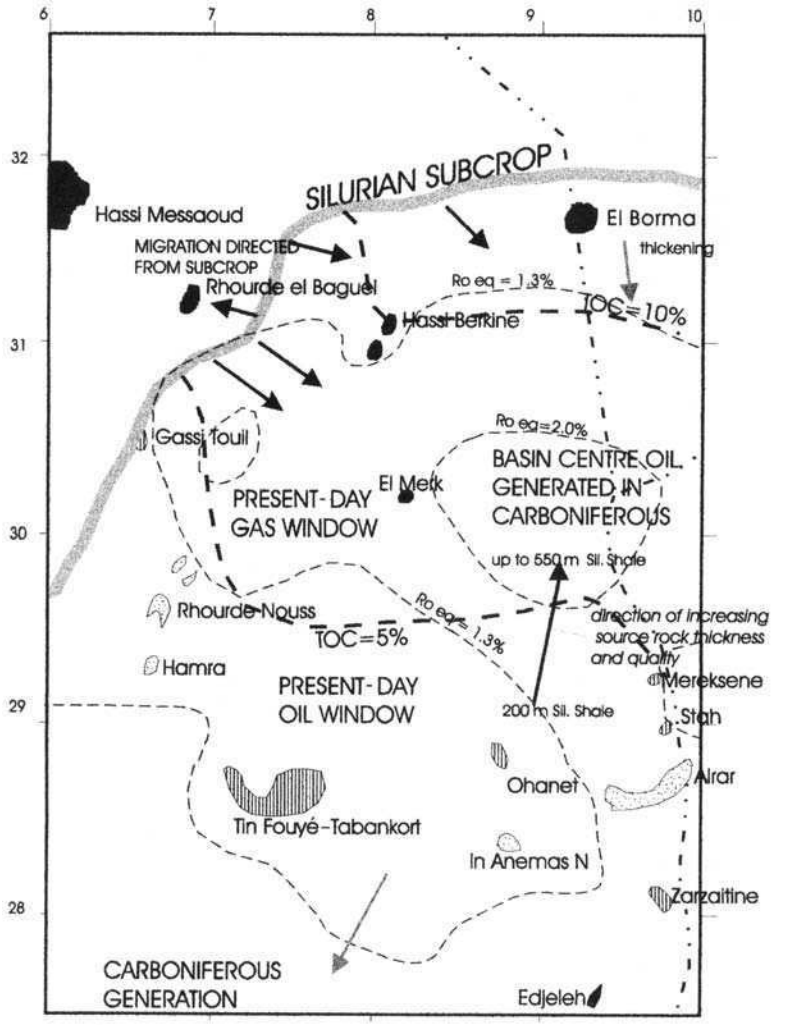

Fig. 5. Geochemical summary of the Silurian source rock in the Ghadames–Illizi area, based on data and maps of Daniels & Emme (1995). TOC (total organic carbon) contours represent maximum values in the basal Silurian 'hot shale', whereas thicknesses quoted refer to the shale interval as a whole. The Silurian is probably the main source for the Illizi fields and for certain fields further north, though a contribution from this area to Hassi Messaoud seems unlikely.

(b) Structures appear to be lower relief than Rhourde Nouss, with many largely unaltered Triassic–Liassic extensional traps (Echikh this volume). Aptian and Pyrenean inversion structures (e.g. El Borma (Bishop 1975; Echikh this volume)) appear to be gentler and less faulted. (c) A significant component of generation from the source rocks in this deep basin was probably pre-Hercynian (Figs 5 and 6). (d) There are many non-geological differences between the two regions, particularly a lower degree of exploration maturity in Ghadames (see later discussion).

(5) Illizi system

The Illizi system contains a number of major fields, most with a significant gas fill, in a series of reservoirs ranging from Ordovician to Carboniferous, that are charged by multiple source rock systems in the Silurian and Devonian (Tissot *et al.* 1984; Daniels & Emme 1995). There are numerous producing reservoir horizons with several cases of stacked pools (e.g. Stah, Tin Fouyé–Tabankort, Mereksene), of which the predominant in terms of reserves is

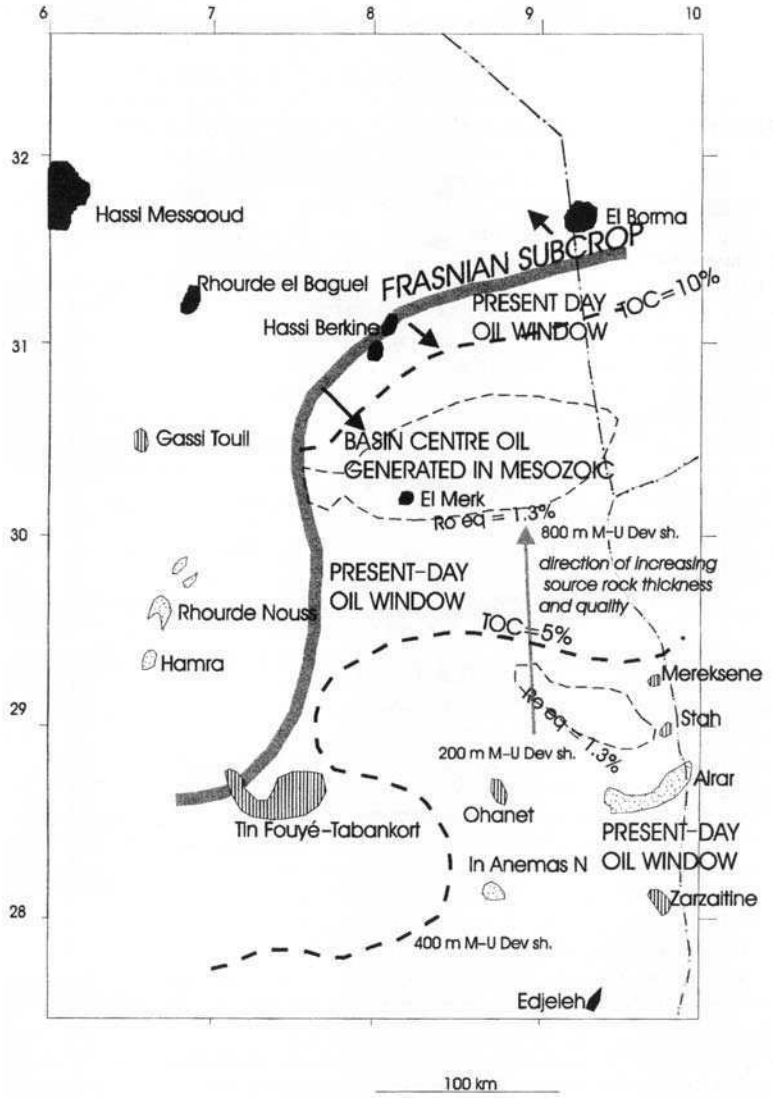

Fig. 6. Geochemical summary of the Mid–Late Devonian source rock in the Ghadames–Illizi area, based on data and maps of Daniels & Emme (1995). TOC contours represent maximum values in the Frasnian 'hot shale', whereas thicknesses quoted refer to the shale interval as a whole. Feeding of Devonian-sourced hydrocarbons into the Triassic reservoir at the Hercynian subcrop surface is the most likely source model for the Hassi Berkine and other recent discoveries.

the Late Silurian–Early Devonian F6 reservoir (Echikh this volume). Structural traps are generally of Hercynian or pre-Hercynian origin, including fault blocks (e.g. Zarzaitine, Boudjema 1987) and compressional–inversion features (e.g. Ohanet, Claracq *et al.* 1963). There are also two major occurrences of giant fields in subtle trap: a hydrodynamic trap at Tin Fouyé-Tabankort (Chiarelli 1978), which may be the world's largest field of this type, and a sand pinchout trap at Alrar. The Liassic salt seal is not present over the Illizi portion of the system, where seals are provided by intraformational Palaeozoic shales.

Again, the two source levels have proven impossible to distinguish by biomarkers. On the basis of stratigraphic proximity and ease of communication path to the main reservoirs (Early Devonian and younger), it is likely that the Silurian is the main source. Over most of the region, the reservoired volumes of gas and associated condensate exceed those of oil, consistent with the observation that most Palaeozoic source rocks, particularly the deeper Silurian source rock, now lie within the gas window. In many Illizi fields, oil is seen only as high API (American Petroleum Institute) oil rims to large gas caps (e.g. Alrar: Chaouchi *et al.* this volume) and with the notable exception of Tin Fouyé–Tabankort, seems to be virtually absent in the Cambro-Ordovician reservoir. This suggests that much of an original oil charge may have been gas flushed, a hypothesis supported by the higher proportion of oil seen in regions most distant from the current depocentre (Macgregor 1996). Additional destructive processes evidenced in the Illizi area that may have caused dissipation of an early oil charge include trap tilting, predicted to occur in the Late Cretaceous as the Hoggar massif was uplifted, and hydrodynamic flushing (Chiarelli 1978).

Timing of generation has been documented to be a critical control in this region. Tissot *et al.* (1984) identified two phases of oil charge from the Palaeozoic sources, in the Carboniferous and in the Late Jurassic–Paleogene, the timing varying between individual regions in the manner roughly shown in Figs 4–6. A good relationship is observed between giant field occurrence and the locations of kitchens active in the Mesozoic, implying that the Carboniferous charge either did not reach traps, or more probably, the Hercynian orogeny destroyed most pre-existing traps.

(6) Ahnet System

The gas fields of the Ahnet Basin of Algeria lie in Devonian and Early Carboniferous reservoirs within steep anticlinal trapping geometries (Cawley *et al.* 1995; Logan & Duddy this volume). Gas pools are again often stacked. The main source rock is believed to be the Silurian, by virtue of its higher source rock quality than the Devonian, and its more favourable stratigraphic position relative to the main Early Devonian reservoirs, though the Mid–Late Devonian source may charge the highest reservoir sand in the Tournaisian. The amount of gas-in-place in these fields is reported to be large (17 TCF according to Attar & Hammat (1993)). The fields are still, however, under appraisal and reserves are uncertain: for these reasons the fields are not included in the field size distributions discussed later in this paper. It seems probable, however, that at least three of the fields will prove to be of giant scale.

There are many similarities between this system and the traps and reservoirs of the Illizi system. However, there appears to be a fundamental difference in the timing of generation of the petroleum present. The Ahnet fields lie below a major erosional Hercynian unconformity and have since lain in an intracratonic platform setting, with no evidence for any significant Mesozoic reburial. Maximum burial was therefore undoubtedly attained in late Carboniferous time, immediately before the Hercynian movements (Cawley *et al.* 1995; Logan & Duddy this volume; Takherist *et al.* 1995). There are problems, however, in linking generation associated with this maximum burial phase to the age of the inversion anticlines forming the traps. These are believed to have formed during the Hercynian event (Cawley *et al.* 1995), i.e. to post-date maximum burial. Apatite fission track analysis suggests the existence of a heat pulse, interpreted variously as being either synchronous with (Cawley *et al.* 1995) or post-dating (Logan & Duddy this volume) trap development. Cawley *et al.* (1995) and Takherist *et al.* (1995) placed this heat pulse at 300 Ma (late Carboniferous), whereas Logan & Duddy (this volume) placed it in the Late Triassic–Early Jurassic. In either case, the fields seem to be considerably older than those elsewhere in Algeria or indeed any other giant fields in North Africa. They therefore form important analogues for future exploration in a number of frontier Palaeozoic basins in Algeria and beyond.

Controls on giant field occurrence

The geographical distribution of the giant fields in Algeria and of the reserves within them is illustrated against a number of key factors in Figs

2–5, allowing discussion of the importance of individual controlling factors on giant field occurrence.

Structural style

As discussed above, around half the oil and gas reserves of Algeria lie in two fields, both situated on broad arches that presumably tap areally large surrounding kitchens. A smaller proportion lies in fairways with steeper structures and narrower structural wavelengths, with the reserves present spread over several fields, e.g. Rhourde Nouss, Ahnet, Illizi. Areas with gentler structures generally show smaller field sizes, with a tendency towards more subtle forms of trap and smaller reserves. A prospectivity ranking is therefore apparent on the basis of structural style, with broad arches with large structural wavelengths ranked above regions of dense, steep structures and finally relatively structureless regions.

Hercynian unconformity

Most of Algeria's oil and gas reserves are trapped at or very closely below the Liassic evaporite seal, in a variety of reservoirs ranging from Cambrian to Triassic. Out of the 27 giant fields, 17 lie at this level, containing over 80% of giant field reserves. One probable key control on this trend is that traps associated with the Liassic seal may have higher preservation potential than those elsewhere. An absence of shows above the seal (A. Boudjema, pers. comm. 1992) testifies to its influence on preservation potential. A further influencing factor is the significance of the unconformity surface as a migration conduit, with long-distance migration proven in a number of areas.

Source development and timing

With the exception of the Ahnet Basin gas fields, all giant fields occur close to kitchens where at least one of the main Palaeozoic source levels is present and is modelled to have attained maximum burial in the Late Mesozoic (Fig. 4). Areas of maximum burial in the Carboniferous are generally those of little exploration success, e.g. southern Illizi and Mouydir Basins. Exceptions are the Ahnet fields, where a late-stage heating event of uncertain geographical extent is required, and the central Ghadames Basin (Fig. 5), where Triassic oil overlies an overcooked Palaeozoic kitchen. The answer in the latter case seems to lie in a model of long-distance migration at Triassic level from the subcrop of the source rocks, within a region in which generation occurred in the Mesozoic (Daniels & Emme 1995; Echikh this volume).

Perhaps surprisingly, there is not a good relationship between reserves distribution and number of active source rock levels or source rock thickness. This is particularly true for oil. The concentration of oil reserves lies in the Oued Mya–Hassi Messaoud system, which shows a single and relatively thin source rock level, and the reserves of the Illizi system exceed those of the Ghadames, despite a trend of improving source quality and thickness northwards (Figs 5 and 6). The reasons for this will be explored later in this paper.

Exploration maturity analysis

This second part of the paper uses the observations on the giant fields of Algeria presented in the discussion above, and compares them against similar observations on analogues, to estimate the level of exploration maturity of the different systems identified. A variety of techniques are attempted: it is probable that none of these are sufficiently exact in themselves to derive valid conclusions. However, when analysed together, as attempted in the discussion at the end of this section, they are believed to form powerful tools. The analyses below cover, in every case, the good data areas of eastern Algeria (east of Hassi R'Mel). Because of uncertainties on reserve volumes and distribution, the Ahnet Basin is only reviewed under drilling density and briefly on trap type analysis.

A range of analogues have been considered in this analysis. In the interests of brevity, only one of the most geologically representative analogues, the Permian Basin of West Texas, is presented here. The geology and petroleum resources of this analogue have been described by Bureau of Economic Geology (1957), Holmquest (1965), Galloway *et al.* (1983), Hills (1984) and Horak (1984, 1985). Similarities between Algeria and the Permian Basin include the classification of the basins in both areas as Palaeozoic post-rift sags, reservoir age (Cambrian to Trias in Algeria compared with Ordovician to Permian in the Permian Basin), concentrations of reserves in both on structural arches, presence in both of a regional evaporite seal, and oil generation at similar times, from Carboniferous to Cretaceous. Differences include the higher proportion of carbonate reser-

voirs and the presence of many subtle trapping geometries in the Permian Basin, though the latter may be partly a consequence of its far greater level of exploration maturity. Exploration well density in the Permian Basin, as discussed below, is around 100 times that of the Algerian basins.

The results of each technique are now summarized

Exploration drilling density

Attar & Hammat (1993) emphasized the low drilling density in Algeria compared with most other major petroleum provinces, quoting a figure of seven wells per 10 000 km^2 of sedimentary surface, compared with a world average of 95 and a North American average of 500. In contrast, the North Sea has around 90 wells per 10 000 km^2. Attar's low figure is partly a consequence of the inclusion of the large unexplored basin areas of western Algeria; a more typical figure for the productive basins considered in this paper is around 15–20 exploration wells per 10 000 km^2, with a maximum of 29 in Illizi (Attar and Hammat 1993). The Oued Mya Basin and the Rhourde Nouss province are also relatively well drilled. On the basis of drilling density, the least explored regions covered within the systems reviewed here seem to be the Ghadames Basin, particularly areas within the Grand Erg sand sea, and the Ahnet Basin, both with 5 wells or less per 10 000 km^2.

Depth range of discovered fields

A general trend observed in most mature provinces is for exploration to penetrate deeper, and make deeper discoveries, with time. Average and maximum giant field depth should give a rough measure of maturity as measured on this aspect.

The average giant field depth in Algeria lies close to the global average of 2100 m (Macgregor 1996) and is actually deeper than the Permian Basin average of 1300 m. The deepest giant field in Algeria, however, lies at 3450 m (Guellala), and is surprisingly an oilfield; the deepest oil or gas production in Algeria from smaller fields lies at 3830 m (International Petroleum Encyclopedia 1990). This compares with the deepest giant (gas) field in the Permian Basin (Brown–Bassett) at 6000 m and with the deepest giant oilfield in the world (Cardenas in Mexico at 5400 m; Macgregor 1996). The suggestion from these analogues is that untapped potential may exist in Algeria in deeper sedimentary sections such as the Cambro-Ordovician of the Central Ghadames depocentre, though the Permian Basin analogue and the considerations on age of petroleum system suggest a predominance of gas–condensate in such plays.

Trap or play type distribution

A further trend against which exploration maturity may be measured is the well-known tendency for an initial phase of exploration in structural traps to be followed by a phase of exploration for subtle and stratigraphic traps. To aid the discussion here, the Algerian and analogue basin fields have been classified into three categories: (1) 'structural' traps, with four-way or three-way and fault closure mapped on the sealing surface; (2) 'mixed' or 'combination' traps, representing traps formed in anticlines or arches that are closed on most flanks by structural dip, but also contain a subordinate element of permeability pinchout or other non-structural trapping style; (3) 'subtle' traps, which are not associated with anticlines or arches and rely mainly on non-structural forms of trapping (Fig. 7). The objective of this classification is to represent the ease of detection inherent in each trap type, with structural traps clearly the most easily, and subtle traps the least easily, imaged. The subtle category is chosen to represent fields that are found deliberately only after exploration techniques have advanced beyond simple delineation of anticlines (though some are usually found serendipitously at an earlier stage). Of the world's current listing of giant oilfields, its is estimated that only 8% are in the subtle category (Macgregor 1996).

The three regions illustrated in Fig. 8, Algeria, the Permian Basin and the North Sea, contain very similar numbers of giant fields (24 with Ahnet excepted, 25 and 25), though they are all at very different levels of exploration maturity in terms of drilling density. Each of the fields within them has been categorized as described above and the cumulative numbers of each are plotted against the order of discoveries. The North Sea shows the classic trend. Here, all giant fields discovered before 1975 were essentially in structural traps (Forties being a serendipitous 'mixed' discovery, though it was drilled as a structural test), whereas practically all post-1975 discoveries are in subtle traps, in this case deep-water sand pinchouts and hanging wall traps. There are therefore now seven 'subtle' giants in the North Sea (or 28% of giant fields),

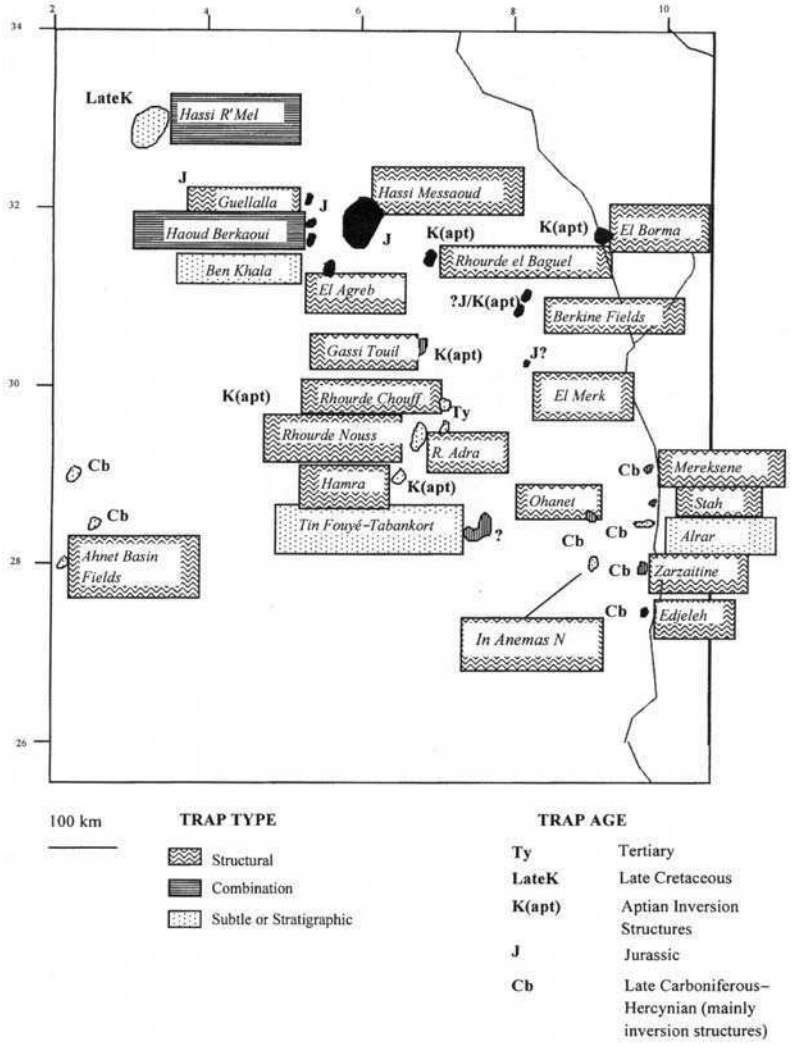

Fig. 7. Trap types and ages for Algerian giant fields. The three categories identified for trap type–exploration maturity analysis are shown. 'Subtle' traps are found only in the relatively well drilled areas of Oued Mya and Illizi.

all found at a time at which drilling density had exceeded the present level in the Algerian basins.

The Permian Basin is, as discussed above, a rather better geological analogue, and shows a similar trend of increasing proportion of subtle traps with time. If the carbonate build-up at Scurry is included as a subtle trap, then 16% of the giant fields are assessed to be subtle, again most being found when drilling density had far exceeded that in Algeria. Both this and the North Sea analogue suggest that the global average in discovered fields of 8% subtle giants substantially under-represents the actual population, with subtle fields remaining undiscovered world wide. A further interesting feature in the Permian Basin is a late burst of very deep giant gas discoveries in structural traps, representing a late stage of new play types opened up by improved seismic and drilling technology. This emphasizes that structural plays can still contain undiscovered giants in mature basins, in cases where improved seismic or drilling technology becomes available to delineate or drill these: the key requirement here is that a technology barrier must be broken.

With these analogies in mind, the discovery history of Algeria can be readily categorized. The corresponding analysis is illustrated in

Fig. 8, which again excludes the Ahnet basin fields. Early discoveries, up till about 1965, were heavily concentrated in structural traps (Fig. 2). The discoveries of the fields on the large obvious arches of Hassi Messaoud and Hassi R'Mel stimulated the drilling of the smaller but steeper anticlines, many in inversion structures, and many with surface expression, e.g. in Illizi (Zarzaitine, Ohanet) and Rhourde Nouss. From 1965 to 1969, more intensive exploration in Oued Mya and Illizi resulted in the discovery of a higher proportion of subtle and mixed traps, such as Tin Fouyé–Tabankort, Alrar and the Triassic pinchout traps of Oued Mya (Figs 7 and 8). At the end of this period, the proportion of giant fields in subtle traps stood at 17%, possibly representing a moderate level of maturity in the regions explored up till that time. The most recent five giant field discoveries represent a step-out of exploration from Illizi northwards into the more difficult terrain of the Ghadames depocentre (Fig. 2), and the continuous improvement in seismic imaging of structural traps in a sandy desert area. Discoveries at Stah (1971) and Mereksene (1974) were followed by a large, possibly giant, gas discovery at Tin Zemane (1981), and then after a long gap by the El Merk, Hassi Berkine and other nearby discoveries of the 1990s. The proportions of giant subtle traps in Algeria has, in this period, dropped to 12.5%.

With the danger that datasets may become too small to conduct a rational analysis, it is possible to conduct such an analysis of trap type for each of the petroleum systems identified. The subtle and combination traps that have been found in Algeria all lie in the Oued Mya and Illizi systems, corresponding to the most densely drilled systems. As a local analogue, Illizi, with its pinchout trap at Alrar, mixed hydrodynamic–structural traps at Tin Fouyé–Tabankort and further smaller discoveries with subtle or mixed styles (e.g. a diagenetic trap at Tiguentourine; Echikh this volume), is perhaps the best illustration of the trap type distribution of a mature Algerian province. The Rhourde Nouss, Ahnet and Ghadames systems currently contain no giant fields in either the mixed or subtle category.

This analysis clearly points out potential for further subtle traps in Algeria, particularly in the regions in which large fields in structural traps are still being found. The potential for further subtle traps discoveries throughout the provinces considered here in favourable clastic-dominated reservoir systems, with strata containing an abundance of unconformities, is considered to be high. Ford & Muller (1995) quoted examples of undrilled giant-sized subcrop traps in the Palaeozoic of this region, one of the many types of subtle trap that could be expected to feature in new discoveries. Echikh (this volume) emphasizes the degree of lateral facies variations within the Triassic fluvial system, particularly towards the northern part of Ghadames Basin. Ultimately, therefore, the proportion of subtle giants in Algeria could rise towards the figures seen in mature basins such as the North Sea and Permian Basin.

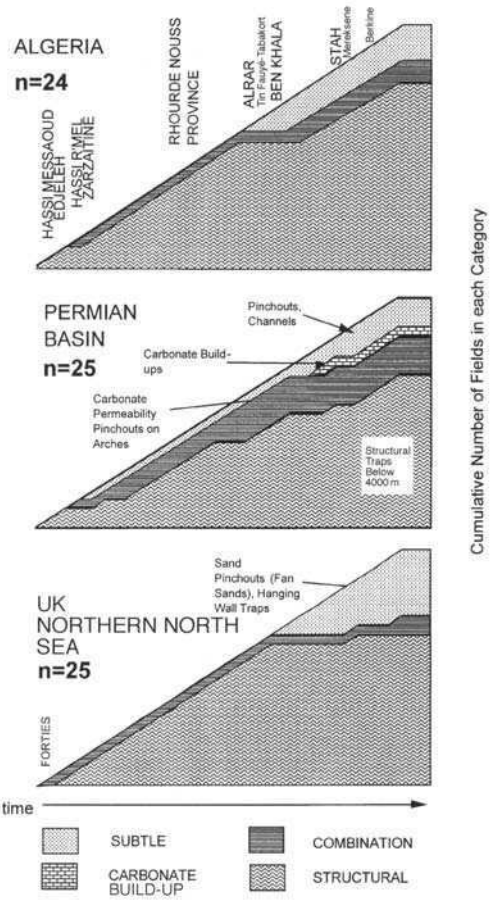

Fig. 8. History of discovery of giant fields plotted by cumulative number found in Algeria, the Permian Basin and the North Sea. The much more highly drilled analogues suggest that subtle giant field discoveries can still be expected in Algeria. Analysis of the Algerian distribution suggests that some areas may have gone through into a subtle trap stage in the 1960s (e.g. Oued Mya, southern Illizi) but others, particularly the Ghadames system, are still in a stage of structural trap exploration.

The Ahnet Basin is not covered in the analysis in Fig. 6. However, it is known that all large fields in this area lie in structural traps. This region has therefore yet to progress beyond the structural trap stage. In terms of structural style and stratigraphy, there are strong similarities to the Illizi segment of the Ghadames–Illizi system, and it can be therefore be proposed, by analogy, that pinchout and hydrodynamic traps may also occur in Ahnet.

Field size distributions

Another common manner of yet-to-find estimation is to compare statistical field size distributions in well- and lightly drilled basins. Many well-drilled basins have log-normal field size distributions (e.g. the North Sea, onshore Netherlands, onshore USA), approximated by a straight-line trend when the logarithm of the frequency of occurrence of fields of a certain minimum reserves is plotted against the logarithm of reserve size (Fig. 9). The deviation of the distribution from flatness (when plotted on log–log paper) can be taken as an indicator of the degree of exploration maturity of any basin. A common technique of estimating yet-to-find is to 'flatten' the proven field size distribution on a log–log distribution by addition of whatever number of fields of different sizes is necessary to do so. These assumed new fields can then be added to calculate an estimated yet-to-find for that basin.

When applied in ignorance of the characteristics of the petroleum system and of the structural style of the basin concerned, this approach is considered hazardous. Several petroleum systems do not show log-normal distributions, for which two possible reasons may be proposed (Macgregor, 1995). First, the structural style may be such that most of the generated petroleum may be focused into a single structural high and a concentration of reserves in one or two very large fields may then result. This model seems applicable for the Oued Mya–Hassi Messaoud system (Figure 9), which clearly does not show a log-normal distribution, yet is assessed to be mature on other criteria. Second,

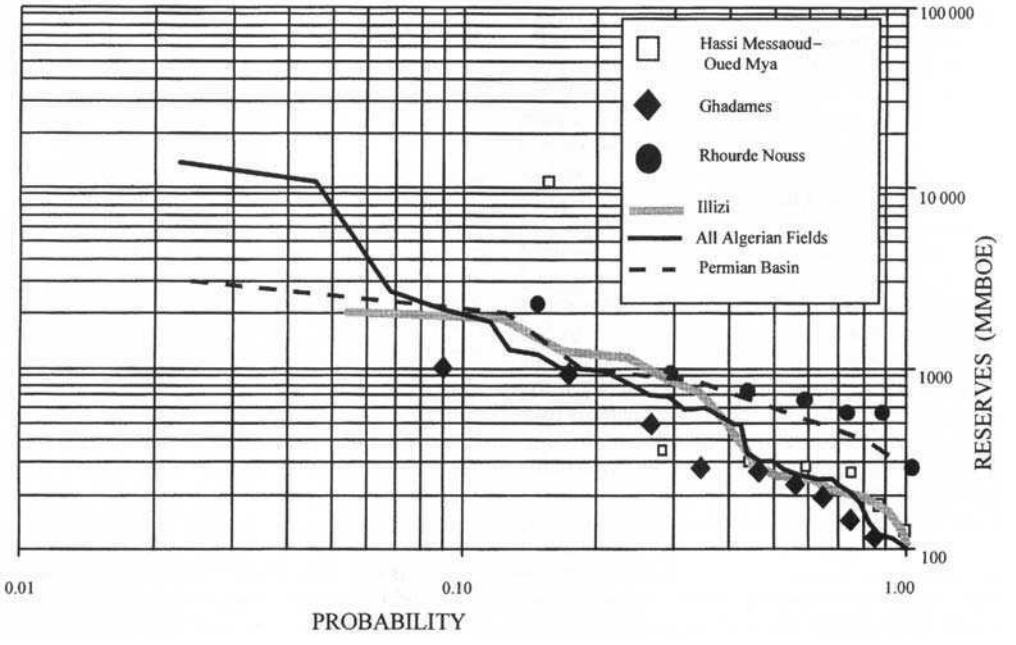

Fig. 9. A comparison of field size distributions of Algerian systems v. the mature Permian Basin analogue, which shows near log-normal behaviour. Lines are used to display systems with a significant number of data points. Where only points are shown, the amount of data is deemed to be insufficient to confidently identify a trend. The 'true' trend is believed to be displayed by the Permian analogue and by the 800–2500 MMBOE segments of the Illizi and all Algerian distributions. The departure from log-normal behaviour in Illizi, and probably also in Ghadames, may indicate a significant yet-to-find in 250–800 MMBOE fields.

a log-normal field size distribution may have once existed but has since been destroyed by selective destruction of some fields, particularly during uplift and erosion of part of the basin. Given the nature of these exceptions, the technique is perhaps most applicable to systems which have not been significantly uplifted and in which there is a high degree of fragmentation of structures, traps and kitchens, such that petroleum can then become more randomly spread around the system. Figure 9 illustrates the distributions obtained for the analysis for Algeria as a whole (Ahnet again not included) and for the individual identified petroleum systems. Where a reasonable number of data points exist, the resulting trend is shown as a continuous line. Otherwise, where the trends are suspect because of small datasets, only the relevant points are shown. The analysis has been extended to fields in the 100–250 MMBOE range.

The field size distribution for giant fields in Algeria can first be compared against that of the Permian Basin. The Permian Basin distribution approaches the expected flatness for a mature province, whereas the Algerian distribution has three components to it, two very large fields, a flat segment between about 2500 and 600–800 MMBOE, and a sharp downwards step thereafter to fields of 250–300 MMBOE. Only the middle segment follows a similar gradient to the Permian Basin distribution. To correct the distribution to one similar to that in the Permian Basin, several new fields need to be discovered in the 250–600 MMBOE range, plus a more limited number in the 600–800 MMBOE range. The two largest fields in Algeria are regarded as anomalies for the reasons discussed above.

It may be more meaningful to examine the field size distributions, despite the small size of the datasets, for the individual systems. The Oued Mya–Hassi Messaoud system, as has already been discussed, does not follow log-normal behaviour, for reasons proposed above. The Rhourde Nouss distribution is the closest to flatness and can be interpreted as a mature field size distribution, at least for fields in excess of 500 MMBOE. The Illizi distribution for fields larger than 1000 MMBOE mirrors that for Algeria as a whole and that for the Permian Basin, but deviates substantially from the expected flat line for smaller fields, suggesting missing fields in the range 250–1000 MMBOE. The Ghadames distribution is most difficult to interpret, but appears immature. On this technique, therefore, the Ghadames and Illizi systems are highlighted as ones in which further large discoveries can be expected, despite the apparent maturity of the former on other criteria.

Geochemical supply analysis

Some workers have suggested that source supply volumetrics provide a possible manner of calculating ultimate yet-to-find reserves in a basin (e.g. Katz & Kahle 1988). Making estimates on this basis alone will always be hazardous as their accuracy will rely not only on the availability of sufficient data on the source rock to accurately calculate amounts generated, but also an estimation of the efficiencies of the system concerned. This requires accurate prediction of the amounts of oil retained in source rocks and lost through migration path staining, seepage and post-accumulation trap destruction. Geochemists typically use figures in the range of 10–20% for source rock and migration efficiency in making predictions of source supply, usually without applying variations for the nature of the petroleum system. I submit that consideration of factors such of age of petroleum system, tectonic history and seal type need to be integrated into any estimation of system efficiency (Macgregor 1996). This technique is therefore the most uncertain of those considered in this paper.

The efficiency of a number of potential analogue systems has been estimated and published, as calculations of generation–accumulation efficiency (GAE), a parameter defined as the proportion of oil reservoired in traps to that estimated to have been generated (Magoon & Dow 1994). Estimates of GAE in different basins world wide range from several cases of under 1% to maxima of 30–33% (Magoon & Dow 1994). Acknowledging the errors involved in GAE calculation, Magoon & Dow gave three categories of GAE in terms or order-of-magnitude variations: very efficient (GAE > 10%), moderately efficient (GAE 1–10%); inefficient (GAE < 1%).

Daniels & Emme (1995) have performed calculations of the amounts of hydrocarbon generated from the combined areas of the Ghadames, Illizi and Rhourde Nouss systems, and estimated that 2100 BBOE of petroleum was generated from the Devonian and Silurian source rocks in the region, of which c. 1500 BBOE were generated in the Mesozoic and the remainder in the Palaeozoic. This compares with a reservoired (in place) figure of around 25 BBOE, indicating a minimum GAE (ignoring yet-to-find) of c. 1%. As proven reserves are concentrated in the Illizi area, and source rock thickness and quality is maximized in central Ghadames (Figs 5 and 6), this implies a GAE in Ghadames of well under 1%, i.e. generated petroleum is more than two orders of magnitude above that discovered.

There are no published GAE calculations on Oued Mya. However, a rough calculation, based on areal productivities for the Silurian source rock established for Ghadames by Daniels & Emme (1995), indicates a much higher GAE for the Oued Mya system, in the region of 10–16%. The only estimate available for GAE in the Permian Basin is for the relatively minor Simpson–Ellenburger petroleum system (Katz *et al.* 1994), which has an estimated GAE of 10%, the highest published for any system involving Palaeozoic source rocks. Even in younger systems, there are relatively few cases of GAEs exceeding 15%. The GAE figure estimated for Oued Mya, based on proven reserves, thus seems close to a figure which would be consistent with the basin's age, seal type, structural style and geology.

Although this technique is too inexact to formulate firm conclusions, the indications are that a very large yet-to-find does not exist in Oued Mya, but may well do so in the Ghadames. Some compensation needs to be made for the differences in the ages of the Oued Mya and Ghadames systems, particularly in discounting the amount of the petroleum generated before the destructive Hercynian event. However, an ultimate efficiency in the range of 5–10% does seem credible, and would imply that several times the existing proven reserves of oil and gas still lie undiscovered.

Conclusions

None of the techniques described above can be considered as conclusive in their own right. Nevertheless, the techniques, when applied together and properly integrated with an understanding of structural style, existing giant fields, and the nature and history of the petroleum systems involved, do provide an objective manner of objectively assessing exploration maturity. On this basis, the exploration maturity of the petroleum-bearing basins of Algeria can be shown to vary, but to be generally low compared with other established petroleum provinces with large proven reserves.

The region shown most consistently by different techniques to be immature is the Ghadames Basin, where many technological barriers to exploration have only recently been broken. This region is still in a structural trap stage of exploration, has an immature field size distribution and abundant supplies of petroleum from source rocks. A high proportion of the yet-to-find may be gas–condensate, with many deep reservoirs untapped. The Ahnet Basin is also in an immature structural trap stage, similar to the state of exploration in the analogous Illizi Basin in the early 1960s.

The other major petroleum systems of Algeria, e.g. Illizi, Oued Mya and Rhourde Nouss, appear, on this overview, to be in a relatively more advanced state of exploration maturity. In general, these systems show higher drilling densities, a higher proportion of subtle traps, more mature field size distributions and more limited remaining geochemical potential. However, it should be noted that these areas still lie far short of the degree of exploration maturity attained in other major petroleum provinces. Analogies to more heavily drilled analogues suggest that further subtle and deep gas-bearing structural traps can still be expected. The majority of undiscovered giants in all Algerian systems are most likely to be in the 250–1000 BBOE range.

Finally, a third group of lightly drilled basins in western Algeria, currently devoid of giant discoveries and not covered in this review, needs mention. The controls identified on giant field occurrence in the productive areas and the nature of the sedimentary fill to these frontier basins suggest that the major control on prospectivity in that region will be the relationship between timing of petroleum generation, trap formation and destructive episodes. Further study of this key factor, similar to that conducted in the Ahnet Basin, is required, to focus exploration where the chances of success are maximized.

Several researchers attending at the North Africa symposium contributed to the information base on the giant fields on which this paper is based. I acknowledge the co-operation of Sonatrach, particularly information given by M. Attar at the Mediterranean Oil and Gas Conference in Malta, 1992, and by the late A. Boudjema in many fruitful discussions. BP Exploration gave permission to publish this paper and a fruitful review was given by D. Roberts.

References

ATTAR, M. & HAMMAT, M., 1993. Hydrocarbon potential of Algeria. *In: Proceedings of the Mediterranean Oil & Gas Conference (MOEX), Valletta, Malta, 1993.*

BALBUCCHI, A. & POMMIER, G. 1970. Cambrian oilfield of Hassi Messaoud, Algeria. *In:* HALBOUTY, M. T. (ed.) *Geology of Giant Petroleum Fields.* American Association of Petroleum Geologists, Memoirs, **14**, 477–488.

BENAMRANE, O, MESSAOUDI, M. & MESSELLES, H. 1993. Geology and hydrocarbon potential of the Oued Mya Basin, Algeria. *Bulletin, American Association of Petroleum Geologists*, **77**(9), 1607 (abstract).

BISHOP, W. F. 1975. Petroleum Geology of Tunisia and adjacent parts of Libya and Algeria. *Bulletin, American Association of Petroleum Geologists*, **59**(3), 413–450.

BOUDJEMA, A. 1987. *Évolution structurale du Bassin Pétrolier Triassique du Sahara Nord-Oriental (Algérie)*. PhD thesis, Université Paris-Sud.

BUREAU OF ECONOMIC GEOLOGY 1957. *Occurrence of Oil and Gas in West Texas, Bureau of Economic Geology*. University of Texas at Austin, Publication **5716**.

CAWLEY, S. J., WILSON, N. F., PRIMMER, T., OXTOBY, N. H. & KHATIR, B. 1995. Palaeozoic gas charging in the Ahnet–Timimoun Basin, Algeria. *Bulletin, American Association of Petroleum Geologists*, **79**(8), 1202 (abstract).

CHAOUCHI, R. & SADAOUI, M. 1995. Geochemical characteristics of Silurian source rocks of Oued Mya and Mouydir basins. *In: Hydrocarbon Geology of North Africa, Abstracts Booklet, Geological Society Petroleum Group Conference, 1995*.

CHAOUCHI, R., MALLA, M. S. & KICHOU, F. 1998. Sedimentological evolution of the Givetian–Eifelian (F3) sand bar of the West Alrar field, Illizi Basin, Algeria. *This volume*.

CHIARELLI, A. 1978. Hydrodynamic framework of Eastern Algerian Sahara—influence on hydrocarbon occurrence. *Bulletin, American Association of Petroleum Geologists*, **62**(4), 667–685.

CLARACQ, P., COURAUD, P. C. & AYMON, J. 1963. Le Devonien Inférieure du Bassin de Fort Polignac, un champ typique de la CREPS. *6th World Petroleum Congress*, **1**, 14, PD3, 773–794.

CLARET, J. & TEMPERE, C. 1967. Une nouvelle région productice au Sahara Algérien: l'anticlinorium d'Hassi Touareg. *In: 7th World Petroleum Congress, Mexico*, **2** Elsevier, Amsterdam, pp. 81–100.

DANIELS, R. P. & EMME, J. J. 1995. Petroleum system model, Eastern Algeria, from source rock to trap: when, where and how. *In: Sonatrach Symposium on the Ghadames Basin, Hassi Messaoud, 1995*.

ECHIKH, K. 1998. Geology and hydrocarbon occurrences in the Ghadames Basin, Algeria, Tunisia, Libya. *This volume*.

FORD, G. W. & MULLER, W. J. 1995. Potential Silurian and Devonian truncation traps across the Ahara Arch, southwest Ghadames Basin, Algeria. *In: Hydrocarbon Geology of North Africa, Abstracts Booklet, Geological Society Petroleum Group Conference, 1995*.

GALLOWAY, W. E., EWING, T. E., BARRETT, C. M., TYLER, N., & BEBOUT, D. G. 1983. *Atlas of Major Texas Oil Reservoirs*. Bureau of Economic Geology, University of Texas at Austin, Publication **78712**.

HAMOUDA, A. 1980. Petroleum Potential—Ouargla Region, Triassic Basin, Algeria. *American Association of Petroleum Geologists, Memoir*, **30**, 539–541.

HILLS, J. M. 1984. Sedimentation, tectonism and hydrocarbon generation in Delaware Basin, West Texas and Southeastern New Mexico. *Bulletin, American Association of Petroleum Geologists*, **68**(3), 250–267.

HOLMQUEST, H. J. 1965. Deep plays in Delaware and Val Verde Basins. *In: Fluids in Subsurface Environments*. American Association of Petroleum Geologists, Memoir, **4**, 257–279.

HORAK R. L. 1984. Sequential tectonism and hydrocarbon distribution in the Permian Basin. *In: The Geological Evolution of the Permian Basin, Symposium Abstracts*, SEPM (Permian Basin Section), Midland, TX, 25–26 April 1984.

—— 1985. Tectonic and hydrocarbon maturation history in the Permian Basin. *Oil & Gas Journal*, 27 May, 124–128.

International Petroleum Encyclopedia, 1990 edn, Pennwell, Tulsa, OK.

KATZ, B. J. & KAHLE, G. M. 1988. Basin evaluation, a supply side approach to resource assessment. *Proceedings of the Indonesian Petroleum Association*, **17**, 135–168.

——, ROBISON, V. D., DAWSON, W. C. & ELROD, L. W. 1994. Simpson–Ellenburger petroleum system of the Central Basin Platform, West Texas, USA. *In*: MAGOON, L. B. & DOW, W. G. (eds) *The Petroleum System—From Source to Trap*. American Association of Petroleum Geologists, Memoirs, **60**, 453–462.

LOGAN, P. 1995. A possible reconstruction for the tectonic and thermal history of the Timimoun, Ahnet, Reggane and Sbaa Basins. *In: Hydrocarbon Geology of North Africa, Abstracts Booklet, Geological Society Petroleum Group Conference, 1995*.

—— & DUDDY, I. 1998. An investigation of the thermal history of the Ahnet and Reggane Basins, central Algeria, and the consequences for hydrocarbon generation and accumulation. *This volume*.

MACGREGOR, D. S. 1995. Hydrocarbon habitat and classification of inverted rift basins. *In*: BUCHANAN, J. G. & BUCHANAN, P. G. (eds) *Basin Inversion*, Geological Society, London, Special Publications, **88**, 83–93.

—— 1996. Factors controlling the destruction and preservation of giant light oilfields. *Petroleum Geoscience*, **2**(3), 197–217.

—— 1998. Introduction. *This volume*.

MAGLIORE, P. R. 1970. Triassic gas field of Hassi R'Mel, Algeria. *In: Geology of Giant Petroleum Fields*. American Association of Petroleum Geologists, Memoirs, **14**, 489–501

MAGOON, L. B. & DOW, W. G. (eds) *The Petroleum System—From Source to Trap*. American Association of Petroleum Geologists, Memoir, **60**.

ODEH ALI 1975. El Agreb-El Gassi Oilfields, Central Algerian Sahara. *Bulletin, American Association of Petroleum Geologists*, **59**, 9.

PERRODON, A. 1983. *Dynamics of Oil and Gas Accumulations*. Centre of Exploration and Production Research, Elf-Aquitaine, Memoir, **5**.

ROADIFER, R. E. 1987. Size distributions of the world's largest known oil and tar accumulations. *In*: MEYER, R. F. (ed.) *Exploration for Heavy Crude*

Oil and Natural Bitumen. American Association of Petroleum Geologists, Studies in Geology, **25**, 3–24.

TAKHERIST, D., AHMAD, A. & RABAH, M. 1995. Characterisation and evolution of Palaeozoic source rock organic matter in Algerian Central Sahara. *Bulletin, American Association of Petroleum Geologists*, **79**(8), 1251 (abstract).

TISSOT, B., ESPITALIE, J., DEROO, G., TEMPERE, C. & JONATHAN, D. 1984. Origin and migration of hydrocarbons in the Eastern Sahara (Algeria). *In*: DEMAISON, G. & MURRIS, R. (eds) *Petroleum Geochemistry and Basin Evaluation*. American Association. of Petroleum Geologists, Memoirs, **35**, 315–324.

Palaeozoic lithofacies correlatives and sequence stratigraphy of the Saharan Platform, Algeria

B. FEKIRINE[1] & H. ABDALLAH[2]

[1]*Sonatrach CRD, Ave. 1er Novembre 35000 Boumerdès, Algeria*
[2]*Sonatrach Exploration, 2, Rue Capitaine Azzoug, HUSSEIN-DEY, Algiers, Algeria*

Abstract: This paper attempts to unravel the interacting effects of eustacy, subsidence and sediment supply in controlling facies distributions in the Palaeozoic of the Algerian craton. These strata, particularly the Cambro-Ordovician section, contain no diagnostic index fossils, and the identification of sequence boundaries is therefore of paramount importance in defining a stratigraphic framework for the region. The wealth of outcrop and subsurface data in the Algerian Palaeozoic enables us to recognize six major sequences, the boundaries of which correspond to major events such as Taconic and Hercynian tectonism, the Ordovician glaciation and global-scale sea-level falls. Formations within these sequences exhibit thickness variations and lateral facies changes that are traceable and predictable in the subsurface. Unconformities of regional extent generally tie to significant facies changes and to inflection points on the global sea-level curve. These trends stem from the high sensitivity of this area, which was structurally stable over most of its Palaeozoic history, to eustatic sea-level fluctuations. The Cambro-Ordovician strata feature a high proportion of coarse clastic rocks, with subtle lateral and vertical facies variations, which were deposited within continental fluvial and shallow marine environments. The Silurian, Devonian and Early Carboniferous sequences show a typical pattern of marginal shallow marine sand belts, which migrate with changing sea-level and pass rapidly into deep marine shales, many of which are organic rich. The Upper Carboniferous strata consist of sediments deposited in continental and restricted basin settings, created as a result of tectonic movements heralding the Hercynian event. With respect to the occurrence of petroleum, the most important reservoirs are found in lowstand tracts in the Cambro-Ordovician and Siluro-Devonian sequences. Thick radioactive marine Silurian and Devonian black shales deposited during major transgressions provide both source and cap-rocks.

This paper attempts an understanding of the sedimentary section within the Palaeozoic of the Saharan Platform in the context of sequence stratigraphy (*sensu* Vail *et al.* 1977). The main emphasis of the paper is placed on the role and importance of unconformity bounded sediment packages. Additional objectives are the identification and interpretation of transgressive–regressive alternations and the assessment of the effect of global variations in eustatic sea-level in controlling lithofacies development. The study utilizes well logs, subsurface cores and outcrop observations across the area, covering all of the Saharan Platform area. Biostratigraphic control is poor or imprecise across the region (Boumendjel 1987; Paris & Robardet 1990; Oulebsir 1992). The region is an ideal one to apply seismic stratigraphy as the successions concerned are fully exposed on either side of the Saharan Platform (Figs 1 and 2) and the primary depositional architecture is only slightly deformed. Much outcrop information is obtained from the Ougarta ranges (Fig. 1) in the west, within strata thought to have been deposited in a Cambro-Ordovician aulacogen and later inverted in the Hercynian orogeny (Nedjari 1994). Most sedimentary units are relatively easily distinguished as they exhibit progressive rather than sharp lateral facies changes and can thus be correlated over long distances (Figs 3–8).

It should be noted that the framework presented here is the first attempt at applying sequence stratigraphic concepts to this section and, in view of the scale of the study, should not be construed to be accurate in its fine detail. Some correlations will undoubtedly change through time and more detailed subdivision should ultimately become possible.

Geological framework

The Saharan Platform represents the northern part of the African Precambrian platform and contains Palaeozoic and Meso-Cenozoic sedimentary successions of variable thickness and composition (Fig. 2). The Platform represents a relatively stable cratonic domain where sedimentary basins have subsided continuously since the Cambrian. The most rapid subsidence occurred in the western portion of the region (e.g. Ougarta aulacogen). The most important tectonic phases

FEKIRINE, B. & ABDALLAH, H. 1998. Palaeozoic lithofacies correlatives and sequence stratigraphy of the Saharan Platform, Algeria. *In*: MACGREGOR, D. S., MOODY, R. T. J. & CLARK-LOWES, D. D. (eds) 1998. *Petroleum Geology of North Africa*. Geological Society, London, Special Publication No. 132, 97–108.

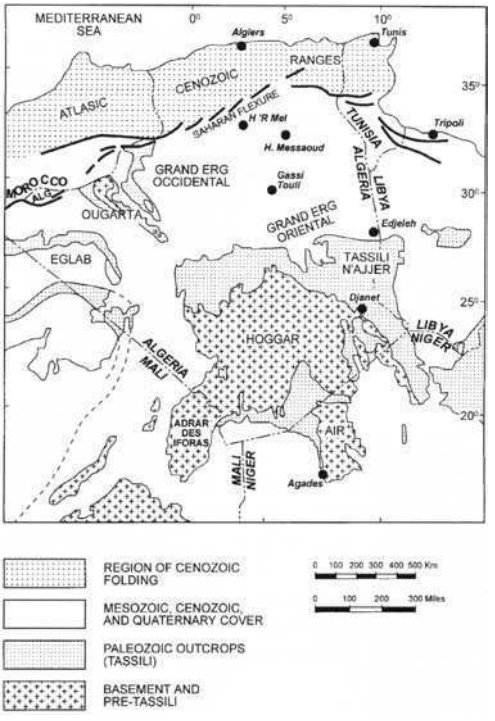

Fig. 1. Generalized geological map of Algeria and adjacent countries, showing the distribution of Precambrian, Palaeozoic and Mesozoic to Quaternary rocks (from Bennacef *et al.* 1971).

caused uplifts, which have shaped the present structural geometry of the region. Most major structural features were formed before the Palaeozoic and were reactivated many times.

During the Cambro-Ordovician, a number of events (Arenig and Taconic events) caused uplift with slight structuring, with local erosion. Many basins subsided at this time, e.g. the Ougarta aulacogen. The Caledonian (Siluro-Devonian) movements represent the first major phase of tectonic activity. During this time, several important zones of uplift and block-tilting occurred, causing sediment thickness reductions, zones of erosion and a number of regional sedimentary hiatuses. The basic style of the Saharan Platform, namely several depressions separated by highs (Fig. 2), was formed at this time. The Late Carboniferous (Hercynian) represents a period of intense tectonic activity, followed by erosion, with such events generally accentuating the main structural features of the Palaeozoic sedimentary basins.

The sedimentary cover of the Saharan Platform is conveniently separated into the Palaeozoic section and the Meso-Cenozoic section at the Hercynian unconformity (Fig. 2). The Palaeozoic sediments thus lie unconformably over Precambrian basement and are unconformably overlain by the Mesozoic. The age of the youngest preserved Palaeozoic sediments is controlled by the degree of erosion on the Hercynian unconformity, with erosion extending as deep as the Cambrian in the north and northeastern Sahara (Fig. 2).

General sediment features

The Palaeozoic strata consist almost entirely of siliciclastics, with significant carbonates and evaporites developed only in the Late Carboniferous. The sediments concerned generally show an uncomplicated structure and commonly show a cyclical nature, with individual facies and formations often very laterally extensive. Variations that occur tends to be gradual and can usually be related to basement and tectonic configurations (e.g. epeirogenic warping, fault block movement, etc.). These patterns are characteristic of a cratonic domain.

Overall, the Palaeozoic strata are believed to have been deposited in an area highly sensitive to eustatic fluctuations. The resulting sediments are cyclic, this cyclicity often being best seen in outcrop as the repeated occurrence of broad tabular rock bodies. Such sediments bear clear evidence of transgressions and regressions, reflected in local unconformities.

Sequences

The sequence stratigraphic study of the Palaeozoic strata across the Platform defined six major second-order sequences (Figs 3–8). Sequence boundaries were initially interpreted on subsurface sections, where the stratigraphic record is often more complete, and were then correlated to outcrops on either side of the Saharan Platform (Fig. 2), where bounding unconformities are particularly well expressed. From a hierarchical point of view, the sequences defined are of low order, representing eustatic cycles of long duration (c. 15–80 Ma).

Sequence 1: Cambrian–Early Ordovician (Fig. 3)

The base of Sequence 1 lies at the Panafrican unconformity, which is traceable over the whole of the Sahara. The underlying Precambrian basement consists of acidic volcanic rocks

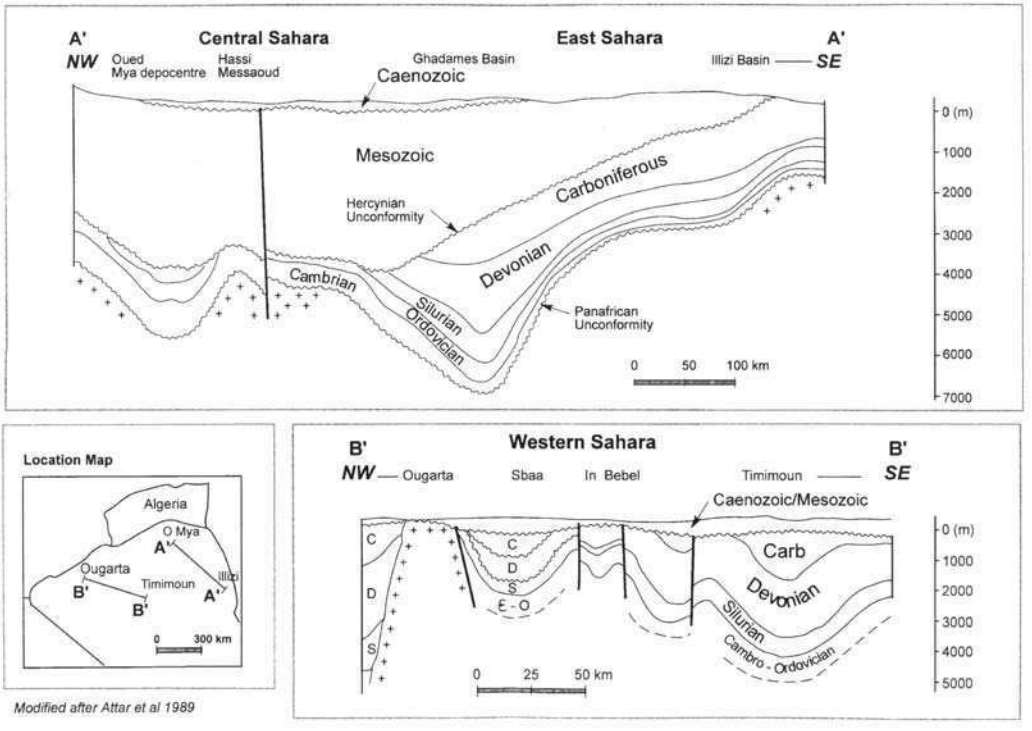

Modified after Attar et al 1989

Fig. 2. Geological cross-sections across Algeria, modified after Attar *et al.* (1989). The maximum preservation of Palaeozoic section occurs in synclines where erosion is minimized on the Hercynian unconformity.

and ignimbrites in the Ougarta ridge and of sandstone, arkoses or crystalline limestones overlying granites in the Tassili area. The lower part of Sequence 1 consists of lowstand deposits (LD), which are generally coarse in nature. The Tassili outcrops consist of an interval of coarse-grained and cross-bedded sandstone, with interbeds of finer-grained sandstones and shales. In the Ougarta Ridge outcrop, the basal Sebkhat El-Mellah Formation contains similar medium-grained and cross-bedded arkosic sandstones. The Sebkhat El-Mellah arkoses pass upwards into well-sorted and clean quartzose sandstone of the Ain Nechaa Formation. A sharp top to this formation is defined by the 'Lingula Flag' bed, and the appearance of the first body fossils. In the subsurface, equivalent lowstand deposits are composed of four units, which are, from base up, R3, R2, Ra and Ri (Fig. 3). The interval cleans and fines upward, with the Ra unit having the best reservoir quality. These basal sandstones contain fossil tracks and trails, with burrows generally becoming more abundant upward, and including *Skolithus*, *Cruziana*, *Vexillum* and *Harlania*.

Throughout the area, cross-stratified sandstone facies occur in the lowstand deposits. The cross-stratification consists of large trough sets ('gouttières') within coarse-grained sandstones showing normal grading and very thin shale drapes. Shale clasts are absent. The clay present, both detrital and diagenetic, is almost entirely kaolinite, with relict feldspars almost completely absent, suggesting an environment involving subaerial leaching. The sandstones are silica cemented, with the intensity of silicification increasing with decreasing grain size. These features, together with the bioturbation patterns, suggest a high-energy fluvial environment at the base, passing upwards into nearshore or very shallow–marginal marine.

The transgressive deposits (TD) are present only in the central and western Saharan subsurface and in the Ougarta outcrop. The Alternation Zone, the Miribel Sandstone and the lower portion of the Foum Tineslem shales (Fig. 3) represent the TD deposits in wells TG-1, UC-101 and in the Ougarta respectively. The Alternation Zone consists of bioturbated fine-grained hummocky cross-stratified sandstone and black to

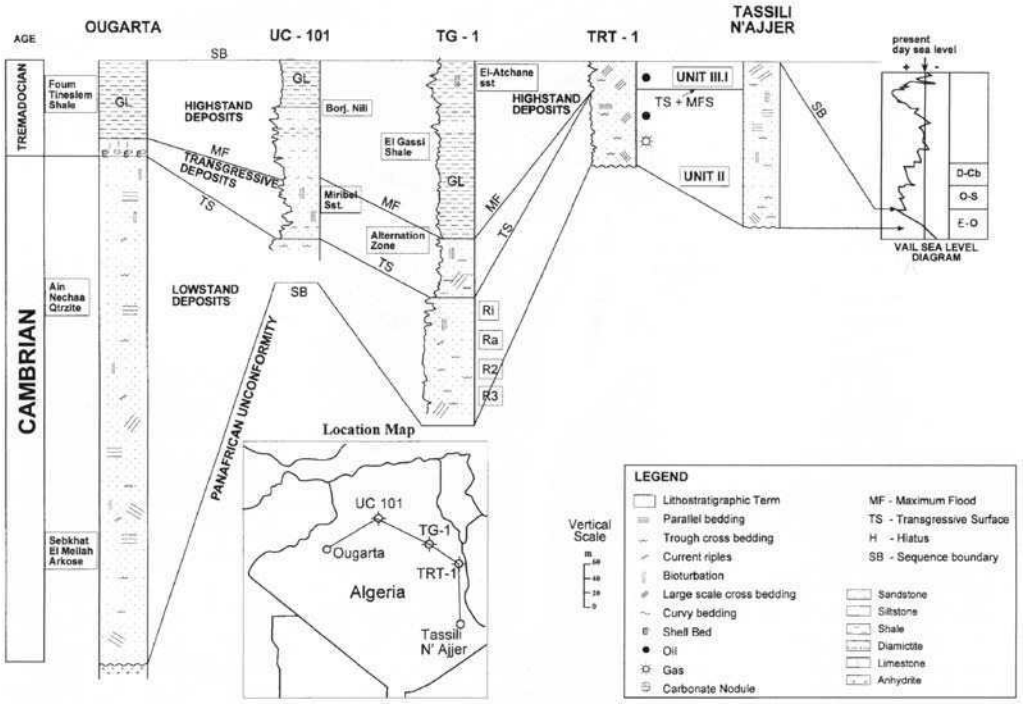

Fig. 3. Correlation of Sequence 1: Cambrian to Early Ordovician. The section illustrates the basal amalgamated sandstone facies, the fining up through the sequence as a whole and the thickening into the basin. The thick sequence in the Ougarta is related to rapid subsidence and sediment influx at this time.

greyish black silty shales. The Miribel Sandstone is made up of an alternation of thick quartzose sandstone beds and black silty and glauconitic shales. In the Ougarta, the lower portion of the Foum Tineslem Formation consists of dark sandy micaceous glauconitic silty shales.

The transgressive deposits are bounded below by a transgressive surface (TS) and above by a maximum flood surface (MFS). In the Ougarta outcrop, the transgressive surface is marked by the 'Lingula Flag' bed mentioned above, representing a lag deposit formed during transgression.

The TS appears on cores as a bioturbated surface overlain by heavily bioturbated interbedded shale and siltstone beds. These fine upwards, indicating that the rate of sea-level rise outpaced sedimentation. No erosional lag is present in the subsurface, suggesting low-energy conditions during transgression. Everywhere below the transgressive surface, the sandstones contain abundant *Skolithus*, suggesting a slowly rising sea-level. In the Tassili N'Ajjer, the transgressive deposits are not recognized and a sedimentary hiatus is interpreted. The MFS in the Ougarta lies over a condensed section containing glauconite and phosphate minerals. In the subsurface, the condensed zone ranges to <4 m thickness west of TG-1. The transgressive surface and the overlying MFS merge onto a single surface over which the progradational Unit III.1 sands are deposited (Fig. 3). The shoreline during the maximum flood probably lay to the south, over the present-day Hoggar Massif, where the equivalent shallow marine environments have since been removed by erosion.

The upper interval of highstand deposits (HD) is well developed in the subsurface. In well TG-1 they are made up of thick black deep marine glauconitic shales, passing upward into alternating fine-grained shaly sandstone and silty shale. The sandstones coarsen and thicken upward, marking the progradational component of the highstand stage. Rare hummocky and planar to wavy cross-stratification, with sharp sandstone bases, indicates sufficiently shallow water for storm and wave action to rework the substrate. Overall, the indicated depositional pattern is

one of progressive shallowing from deep marine to storm and wave action dominated shelf environments. These intervals correspond to the El Gassi Shale and the El-Atchane Sandstone Formations.

In well UC-101, the HD consist of shaly glauconitic and quartzose sandstone with interbeds of silty shale (Borj Nili Fm), passing upwards into black silty and glauconitic shales (El Gassi Shale), and shaly fine-grained glauconitic sandstone (El-Atchane). This interval can be divided into two paracycles, the lower of which is thought to represent deposition in an aggrading inner to mixed shelf, and the upper deposition in an episodically starved open marine environment. A sedimentary hiatus is indicated at the top of the El-Atchane. In the Eastern Sahara, the equivalent interval contains fine- to medium-grained rippled and trough cross-bedded sandstone with dark shale and siltstone interbeds, termed the Unit III.1, and was deposited in a prograding marginal marine environment. Bioturbation is common to all the facies in this area. A shallow marine to nearshore environment is indicated by the sedimentary structures and the fauna. The Ougarta equivalents are thick, homogeneous dark open marine shales of the Foum–Tineslem Formation. Thus a distinct trend of progressively more marine sediments occurs from southeast to northwest across the area, with the shoreline lying close to the Tassili region.

Sequence 2: late Early to early Late Ordovician (Fig. 4)

This sequence shows all its component tracts developed across the region, with the exception of the basal LD in well UC-101, where a temporary hiatus was formed. The lower sequence boundary is well expressed, both in outcrop and in the subsurface. In the Ougarta Ridge outcrops, a clear erosional surface is observed capped by a ferruginous interval, including ooliths and argillaceous pebbles. In the Tassili outcrop, the equivalent boundary is the flat base of a massive sandstone, overlying a rippled and trough cross-bedded sandstone. In well logs (e.g. TG-1, Figure 4), the boundary is taken at a sharp increase in gamma-ray response, tied to the sharp base of a massive sandstone interval.

The LD in each area comprise an interval of massive to rarely planar bedded, medium-grained sandstone, often containing a number

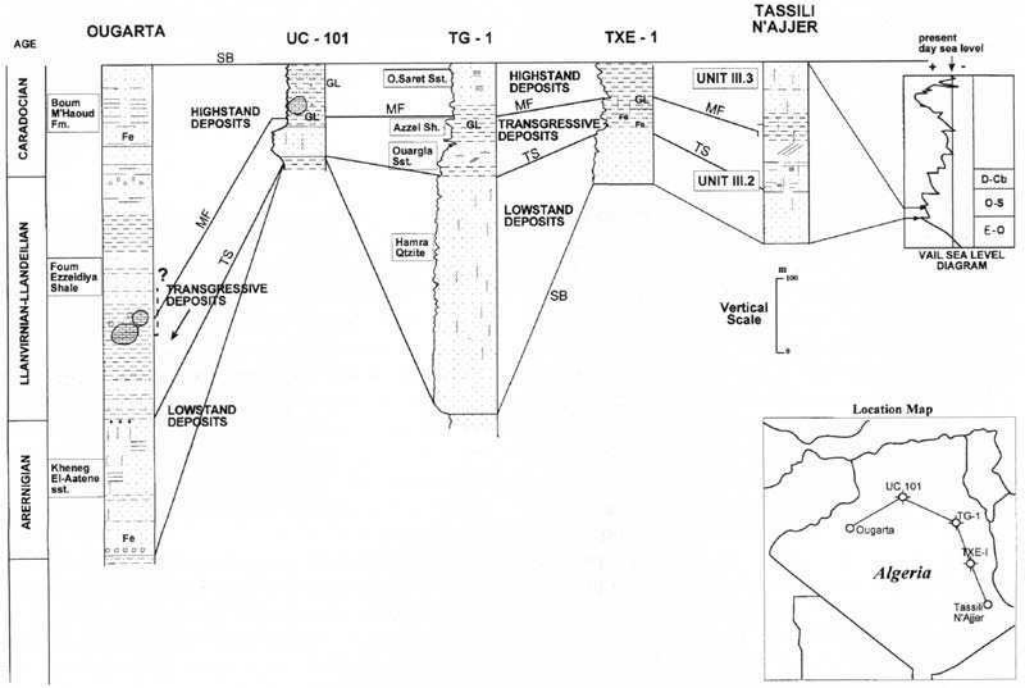

Fig. 4. Correlation of Sequence 2: late Early to early Late Ordovician. The base of the sequence is a significant regressive event. Many of the features of Sequence 1 persist. A shallow sea covered most of the area at this time, allowing the build-up of thick sandstone facies.

of subtly fining upward cycles. *Skolithus* burrows increase in intensity up the section. The sandstone of this tract is remarkably similar in appearance over a large area including the Tassili area outcrops and many subsurface wells, and reaches its maximum thickness in well TG-1. This sandstone corresponds to the Unit III.2 and the Hamra Quartzite formations in the Tassili region and in the subsurface, respectively. The equivalent lithofacies in the Ougarta ridge are represented by the Kheneg El-Aatene Formation, which is made up of ferruginous sandstone at the base, grading upward into quartzose sandstones with abundant *Skolithus* burrows.

The striking homogeneity of the LD in all areas, their high degree of mineralogical and textural maturity, highly silicified character, sedimentary structures, trace fossils and grain size are all indicative of a shallow high-energy nearshore environment such as an epicontinental sea. With the exception of well UC-101, where there is a hiatus, there is very little indication of any significant tectonic control on sedimentation at this time. Source areas to the south must have been very mature at this time.

The TD generally consist of fine alternations of sandstone and shales, with increasing shale content up the section. In the Tassili region, fine alternations of bioturbated sandstone and shale pass up into shales, with the degree of bioturbation increasing upwards. In the subsurface, the transgressive deposits are composed of fine cross-bedded sandstone at the base, passing up into alternations of fine sandstone and shale. The maximum flood is marked here by a thin interval of black glauconitic shales. In UC-101, a hiatus is present at the base of the sequence. The interval in the Ougarta outcrop commences with a ferruginous horizon, followed by an interval of silty shales and fine shaly sandstone beds and finally a thick shale sequence containing carbonate lenses. This reflects reduced terruginous influx during the MF.

From the Tassili to the Ougarta, the transgressive event is therefore correlated through a surface of intense bioturbation, a surface of slight burrowing and marked deepening of facies, a hiatus and a ferruginous level. The maximum flood is correlated from intervals of glauconitic black shale to the interval of carbonate nodules in the Ougarta. The overall sedimentary environment, as suggested by the sedimentary structures, is that of a progressively deepening tide-dominated shelf, with a low sedimentation rate. The shoreline must have again migrated progressively to the south.

The HD show a reversal of fining and log trends from the Tassili through the subsurface to the Ougarta outcrop. Sandstones predominate in this section and clean upward. In well UC-101, the correlative sediments are made up of black silty shale with common fine glauconitic sandstone beds indicating sedimentation in an anoxic offshore environment, with episodic starving. In the Ougarta area, the HD consist of clays with sandstone lenses. The sediments become sandier upwards, with ferruginous levels indicating paracycles involving shallowing or exposure. The upper sequence boundary is marked by an influx of conglomerates.

In the eastern Sahara subsurface and in the limited areas of preservation in the Tassili, the HD comprise black shales with thin fine sandstone beds. The sandstones thicken upward and are arranged in a distinctive progradational stacking pattern, suggesting basin infilling. Hummocky cross-stratifications are common along with soft sediment deformation structures (convolute bedding, load and gutter cast structures, microfaulting) and slight bioturbation. This suggests storm activity in an inner shelf with unstable sea-floor conditions, possibly resulting from structural movements heralding the Taconic event. In the central Sahara subsurface, the highstand deposits consist of black shales passing up into thickening and coarsening upwards sandstones with shale interbeds. Again, a progradational stacking pattern is evident. Hummocky and inclined cross-stratifications are present, suggesting an environment similar to that for the sandstones in the eastern Sahara.

Sequence 3: Ashgill–Early Llandovery (Fig. 5)

This sequence (Fig. 5) is distinct in that its lower boundary corresponds to an incised valley network in the Tassili region. Here, the base of the sequence cuts down into underlying sediments to the point that, in some instances, it directly lies on the basement in the nearby subsurface. This erosion is tied to the Taconic event of the literature. Synsedimentary tectonics during the deposition of Sequence 2 may have exerted a control on palaeovalley incision at this time. In the Ougarta outcrop, the equivalent sequence boundary is taken at the base of a conglomerate bed, which often overlies an angular discordance. In the subsurface, the boundary is marked by a conglomeratic layer, which is in turn overlain by a transgressive carbonate bed and by the Microconglomeratic Shales.

The LD in the Tassili area are composed of incised valley fills. These are coeval with a channel–levee complex and a prograding complex

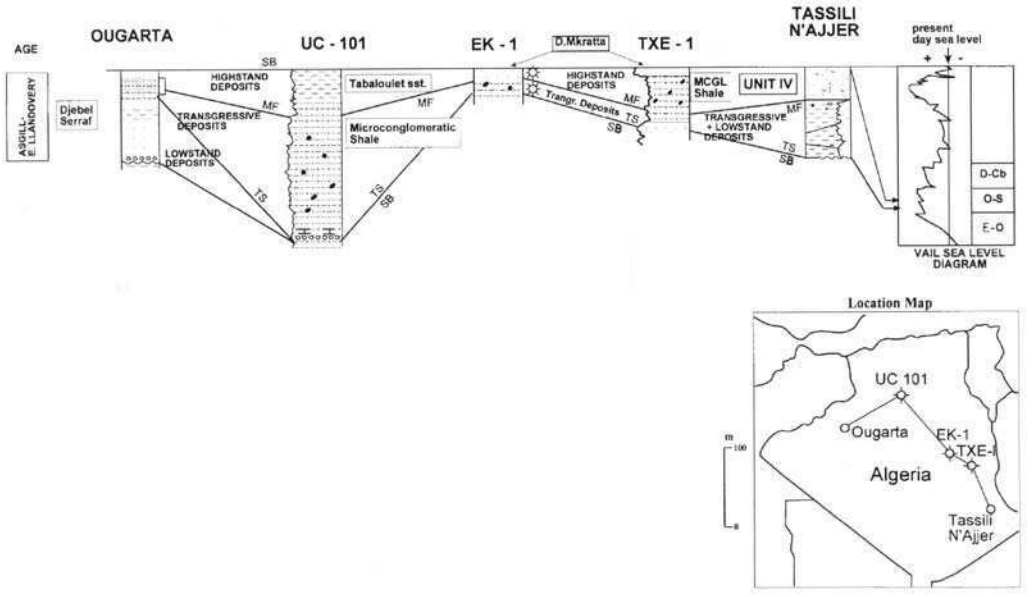

Fig. 5. Correlation of Sequence 3: Ashgill to Llandovery. The sequence consists of a single glacio-eustatic cycle fill induced by the Late Ordovician glacial event. The sequence boundaries are readily picked at major glacial–tectonic (Taconic) and transgressive events, respectively. In the east of the region, the lower sequence boundary is enhanced by tectonic uplift and ensuing valley incision.

(Posamentier *et al.* 1991) in the nearby subsurface (e.g. La Reculée and Oued-Saret Fields, Taredert and El Golea Sandstones). In the Ougarta ridge, the LD contain a conglomeratic layer at the base overlain by sandstone.

The TD consist of monotonous black mudstones with dispersed rock fragments, pebbles, and rounded clasts and quartz grains. The mudstones, commonly known as 'Microconglomeratic Shales', are present over all the Saharan Platform and show a homogeneous composition but varying thickness. In outcrop, these facies appear light grey and greenish yellow as a result of weathering. In the Central Saharan subsurface, the typical facies consists of black to greyish black shales with minor, regularly distributed rounded medium to coarse sandstone clasts. In the Ougarta ridge, the equivalent shales are green to greenish yellow, and contain quartz grains and silty lenses.

The HD are made up of compact, massive, fine- to coarse-grained quartzose sandstones, containing silica, carbonate and sometimes kaolinite cements. In the Illizi Basin subsurface, the sandstone is cut by vertical fissures filled with clean sandstone, reminiscent of sandstone dyke structures ('les grès à mârbrures'). In the central Saharan subsurface, the equivalent is the the M'kratta Plate formation ('Dalle de M'kratta'), whereas in well UC-101, the Tabaloulet Sandstones are the equivalent. These consist of grey or white fine-grained quartzose sandstone with shale stringers. In the Tassili region, the sandstones include two members, a lower member made up of medium- to coarse-grained, shaly and micaceous sandstones which fill the palaeotopography over incised valleys, and an upper member consisting of coarse-grained sandstone. In the Ougarta area, the sandstone unit of the Djebel Serraf Formation represents the HD.

The lower sequence boundary, LD and TD sections are tied to a major glacial event and associated lowstand, whereas the sequence as a whole represents the fill of a glacio-eustatic cycle. Detailed studies by earlier workers, e.g. Bennacef *et al.* (1971) and Fabre (1976), documented a major continental glaciation during the Late Ordovician in the Algerian Sahara. The evidence for glacial origin is best indicated by the diamictite–dropstone association within the transgressive deposits. Whereas diamictites can be formed in several ways, dropstone facies must have a glacial origin (Ojakangas 1985; Robardet & Dore 1988).

Sequence 4: Silurian (Fig. 6)

This sequence was initiated by the major eustatic trangression that followed the Late Ordovician

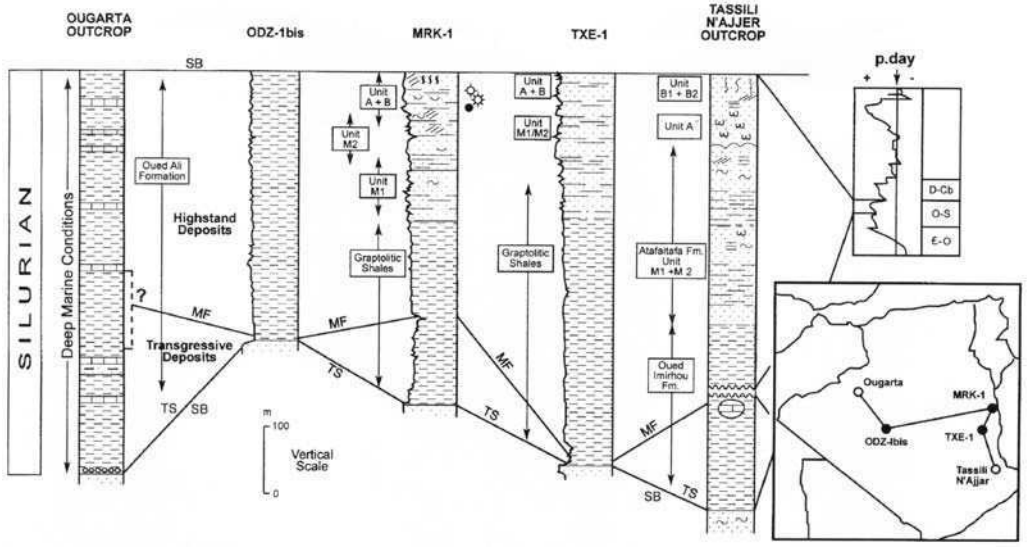

Fig. 6. Correlation of Sequence 4: Silurian. A very rapid transgression at the base of this system precludes the deposition of the transgressive deposits seen in other sequences. This was controlled both by rapid sea-level rise and subsidence. Deep marine conditions are marked by the deposition of the anoxic graptolite shale facies. A slow eustatic fall in sea level towards the end of the interval on the eastern side of the basin led to the deposition of sands in that area.

glacio-eustatic regression. The boundaries of the sequence correspond almost exactly to the onset and end of the Silurian Period. The lower sequence boundary is a transgressive surface over the highest sandstone of the previous sequence (Fig. 6). In the Tassili region, it is marked by intense bioturbation. In the Ougarta outcrop, a thin conglomeratic bed, representing a transgressive lag deposit, marks the sequence boundary. In the central and northern Saharan subsurface, the Silurian graptolitic shales directly overlie the Upper Ordovician sandstone. The surface here seems to be smooth without any evidence of marine reworking.

The Silurian transgression may have happened quickly, with rapid sea-level rise and subsidence rates leading to a rapid increase in water depth. As a result, transgressive legs and sands may never have been developed in many areas, and the LD unit observed in other sequences is absent. The lowest deposits observed are thus those of the transgressive systems tract and are composed of fissile mudstones commonly referred to as the graptolitic or black shales. These are rich in pyrite and composed of nearly equal amounts of kaolinite and illite. These TD are reduced in thickness in the platform interior and expanded in thickness in both outcrop areas. In the Tassili region, the maximum flooding event is marked by a bed of carbonate nodules. In the subsurface, it is easily recognizable as a gamma-ray peak. In the Ougarta, the section was deposited in deep marine conditions throughout and no clear maximum flood event is obvious.

The HD overlie the maximum flood event and make up the bulk of the sequence over the entire Sahara. These are highly euxinic and carbonaceous shales, and form the prime source rocks for hydrocarbons in the region (Chaouche 1992). The deposits become progressively sandier upwards, so that at the top of the sequence, only coarse-grained sandstones are represented in the eastern Sahara (Fig. 6). These sandstones pinch out basinward. Coarsening and thickening upward patterns suggest progradation, shallowing, and basin infilling in the eastern Sahara region at the end of the Silurian.

Sequence 5: Early Devonian–Namurian (Fig. 7)

This sequence contains the greatest thicknesses of sediment, reaching in excess of 1300 m in well MRK-1 (Mereksene field). Its lower boundary is taken at the Caledonian unconformity, which is in turn tied to tectonism related to the closure of the Iapetus Ocean. By European standards, this is not, however, a major tectonic event

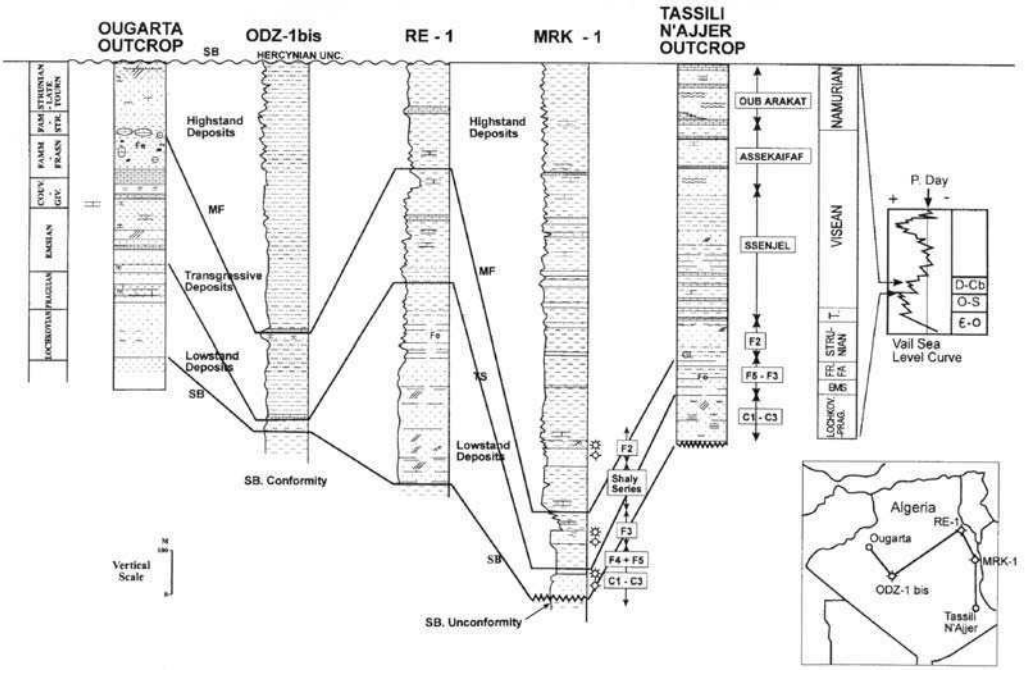

Fig. 7. Correlation of Sequence 5: Early Devonian–Namurian. The base of the sequence ties to Caledonian uplift and to emergence of much of the sediment supply area to the south. An influx of coarse-grained sand is seen in the transgressive deposits. Lateral facies variations at this time are related to uplift and block tilting. Much of the sequence is truncated by the Hercynian unconformity.

in this region. The unconformity shows a slight angular discordance in the Tassili region and appears on cores from Mereksene as a clear erosional surface. In the western Saharan subsurface (e.g. well ODZ-1bis), however, there is neither physical nor biostratigraphic evidence for a break in sedimentation. Similarly, in the Ougarta area, there seems to be no clear unconformity and the base of the sequence is taken at a facies change.

The LD comprise coarse-grained sandstones with red shale interbeds, interpreted as of terrigenous origin. The iron content increases upward, with a high iron content believed to indicate proximity to the seashore. In the western Sahara, the LD contain interbedded shallow marine sandstone and shales deposited in a shallow marine setting with, in the Ougarta outcrop, the presence of thin carbonates overlying sandstone beds indicating marine incursions. The more frequent lateral facies changes in this tract appear to be related to tectonic activity, usually local uplift and block-tilting, rather than being responses to eustatic effects.

The TD also show the effects of syndepositional tectonics, expressed as thickness as well as facies changes. An example is the F3 reservoir formation (Middle Devonian) of the Illizi basin, which shows a rapid pinchout to the south and west from its maximum development in the northeast of the basin. The oscillations between sand-dominated and shale-dominated units at this level may be indicative of a number of small-scale relative sea-level rises and falls. A general decrease in sand/shale ratio is observed from the Tassili area, through well ODZ-1bis to the Ougarta outcrop (Fig. 7), with significant carbonate content apparent in the latter. This facies pattern indicates a trend from shallow- to deep-water environments, probably associated with a sea-level rise or a backstepping shoreline. The maximum flood event is marked in the Tassili by a glauconitic horizon, and in the eastern and western Sahara subsurface by a gamma-ray peak commonly referred to as the radioactive peak. The equivalent in the Ougarta is the top of the condensed section represented by the 'calcaire griottes' facies.

The HD are represented by interbedded sandstone and shales, with the shales generally predominant. In the central Saharan subsurface, the sequence is truncated by the Hercynian unconformity, such that it only shows partial preservation. Overall, the facies evolution and the

stacking pattern of these facies indicate an upward shallowing and basin infilling, heralding the approach of a sequence boundary. The most complete stratigraphic record of the sequence occurs in the eastern Tassili outcrop where, following the final transgressive event, the appearance of alternating sandstone and carbonate stromatolites indicates episodes of shoreline progradation. This section is termed the 'Mushroom Sandstones' ('grès à champignons') and Collenia Limestones (blue–green algal stromatolites). The upper sequence boundary is interpreted as corresponding to the large rapid global eustatic sea-level fall at the Serpukhovian–Bashkirian boundary, and it is expressed by fluvial entrenchment and incision. In the Ougarta area the Hercynian unconformity coincides with the upper sequence boundary.

The eustatic curve of Vail *et al.* (1977) indicates a minor eustatic sea-level fall near the base of the Tournaisean, preceding the larger fall in the Namurian. This is tentatively correlated with an apparent transgression at the top of the F2 reservoir in the Tassili region (Fig. 7). The F2 reservoir itself contains a number of coarsening and shallowing upward sandstone paracycles, with the overlying transgressive shale marking a return to deep-water conditions.

Sequence 6: Late Carboniferous (Fig. 8)

A sequence boundary in the Early Carboniferous is reflected in the deposition of fluvio-deltaic sediments in the western Sahara and local fluvial entrenchment and/or erosion in the eastern Sahara (Fig. 8). This event is interpreted as a eustatic marine regression correlatable with the first Early–Middle Carboniferous glaciation. The lower sequence boundary is a surface of subaerial exposure, fluvial entrenchment and erosion in the Tassili region. In the Ougarta outcrop, the boundary is taken at the appearance of channelized ferruginous sandstone. In the central Sahara, the sequence is completely truncated by the Hercynian unconformity.

The earliest events of the Hercynian orogeny began during Sequence 6. The structural setting of the platform during Sequence 6 time was a transition between that of a eustacy-sensitive platform area in the east of the region and a rapidly subsiding foreland domain in the west (Latreche 1982). The development of a foreland basin was controlled by the uplifting Maghrebian chain to the northeast. In the eastern Sahara, the rejuvenation of originally Precambrian lineaments led to the differentiation of a number of more or less independent basins, separated by

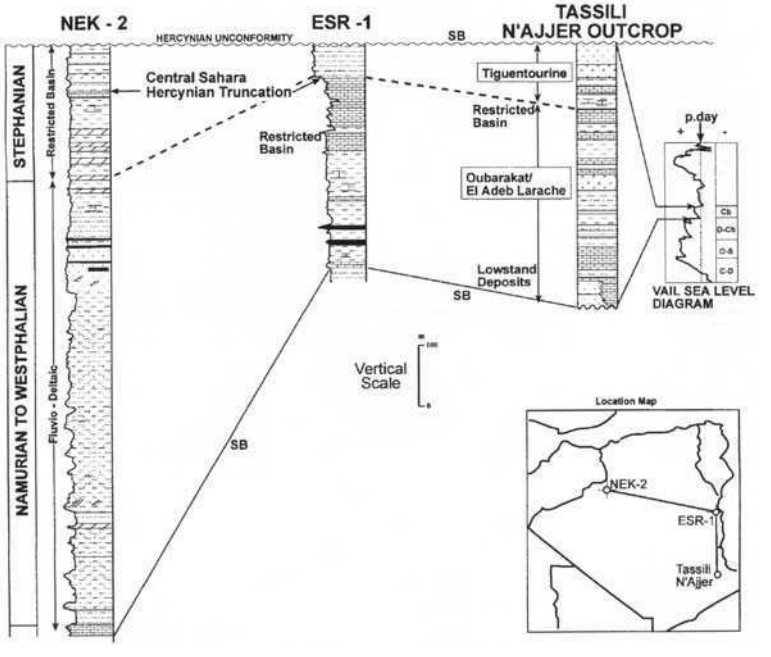

Fig. 8. Correlation of Sequence 6: Late Carboniferous. The base of the sequence is marked by valley cuts and an influx of fluviomarine sands in the western Sahara.

high zones. A major regression is observed during the Late Carboniferous (Namurian), the shoreline retreating from west to northeast. In the western Sahara, the sediments consist of fluvio-deltaic sandstone and shales followed by coal seams. The upper part of the sequence contains shales, carbonates and evaporites laid down under restricted basin conditions (Fig. 8). This restriction resulted from the withdrawal of the sea to the south, accompanied by the rise of the Maghrebian chains. In the Eastern Sahara, the equivalent section is condensed and contains mainly carbonates, shales and evaporites, with some fluvial sandstones at the top. The upper sequence boundary is the Hercynian unconformity in all areas.

Hydrocarbon associations

Numerous productive reservoir horizons occur in the Palaeozoic deposits of the Saharan Platform. The most prolific reservoirs lie in Sequence 1 (Cambro-Ordovician) and in Sequences 4 and 5 (Late Silurian–Early Devonian). Sequence 6 (Carboniferous) contains the fewest hydrocarbon occurrences, which may be attributed to shallow burial, absence of reservoirs and stratigraphic separation from source rocks (Fig. 9: Chaouche,1992). Most productive reservoirs tie to lowstand events. The transgressive and highstand deposits contain more minor and nearly equal amounts of hydrocarbons.

The highstand deposits in the Silurian (graptolitic hot shales) and the Upper Devonian form the most prolific source rocks, and additionally act as good seals.

Conclusions

The Palaeozoic deposits of the Saharan Platform can be subdivided into six sequences. The majority of the events picked as sequence boundaries tie to significant eustatic events that are correlatable on a global scale, many related to glaciation. Other sequence boundaries tie to tectonic events. With the exception of the top Sequence 6 boundary (Hercynian event) and the base Sequence 3 boundary (Taconic event), both of which comprise major eustatic and tectonic events, the amount of erosion on the sequence boundaries is minor, leading to preservation of most parts of the stratigraphic record. Preservation was also favoured by high sedimentation rates and generally slow rates of eustatic sea-level fall. It is to be noted that sedimentation rate here is considered with regard to internal sequence organization and not to thickness of the stratigraphic pile.

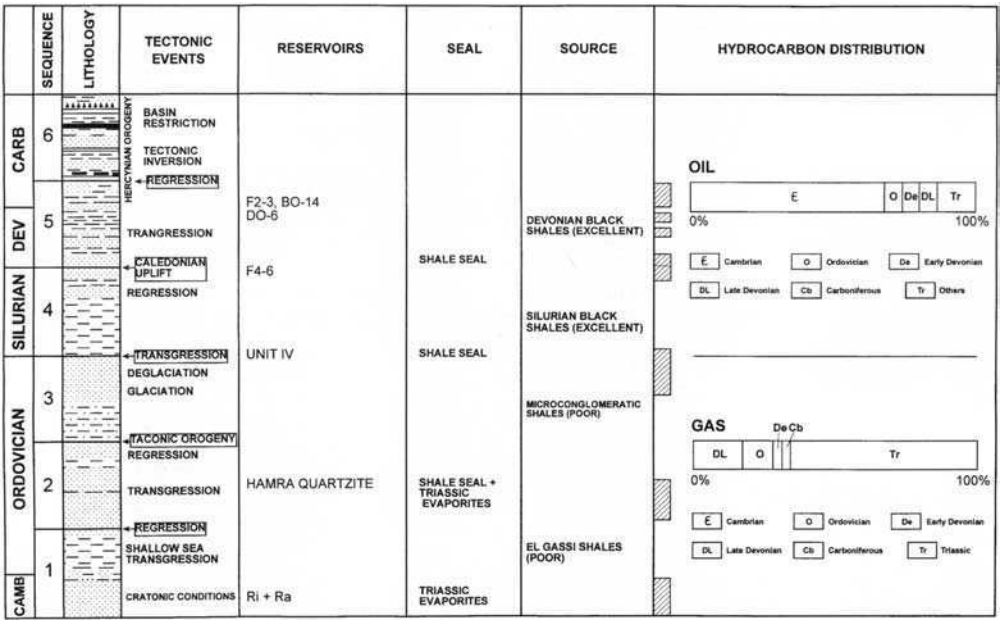

Fig. 9. Relation of sequences to hydrocarbons.

All the sequences dip and thicken northward, which suggests a southern source area throughout the Palaeozoic. The thickest deposits are thus observed in the western foredeep–Ougarta aulacogen area. The depositional regime varied so that sometimes the sediment influx dominated, whereas at other times eustacy was the dominant control on depositional patterns. Tectonics played an important role only at a few limited times. The most sand-prone sequences are those of Cambro-Ordovician age (Sequences 1–3), whereas Sequences 4–6 are more mud prone, particularly Sequence 4 (Silurian). Sequence 6 (Late Carboniferous) is characterized by high-frequency paracycles and has the most diverse lithologies. Sands are thickest and coarsest in the lowstand deposits in the lower parts of the various sequences.

The typical facies geometry developed throughout the Palaeozoic consists of a marginal amalgamated sand-dominated belt, grading out basinward into shales. The sequences thus exhibit a general pattern of basin centre thickening accompanied by diminishing grain size. Backstepping component analysis indicates that sea-level rises were slow, such that no marine erosion surfaces are formed.

References

ANON. 1964. *Essai de nomenclature lithostratigraphique du Cambro-Ordovicien Saharien.* Mémoires hors séries, Société Géologique de France, **2**.

ATTAR, BAGHDADLI, S. M, & CHAOUCHE, A. 1989. Origine et distribution des hydrocarbures en Algérie. 2ème Conférence sur l'Exploration en Algérie. Sonatrach Internal Report.

BENNACEF, A., BOEUF, S., BIJU-DUVAL, B., CHARPAL, O. de, ROGNON, P. & GARIE, O. 1971. *Les grès du Paléozoique inférieur au Sahara—sédimentation et discontinuités—évolution structurale d'un craton.* Publications de l'Institut Français du Pétrole Collège Science et Technique du Pétrole, **18**.

BOUMENDJEL, K. 1987. *Les chitinozoaires du Silurien supérieur et Dévonien du Sahara algérien (cadre géologique–systématique–biostratigraphique).* PhD Thesis, Université de Rennes.

CHAOUCHE, A. 1992. *Genèse et mise en place des hydrocarbures dans les bassins de l'Erg Oriental (Sahara Algérien).* PhD thesis, Université Michel de Montaigne–Bordeaux.

FABRE, J. 1976. *Introduction à la géologie du Sahara Algérien et des régions voisines.* Société nationale d'édition et de diffusion, **334–373**.

LATRECHE, S. 1982. *Evolution structurale du Bassin d'Illizi (Sahara Oriental Algérian) au Paléozoique superieur.* DES thesis, Université Sciences et Techniques d'Aix Marseilles.

NEDJARI, A. 1994. *Images et évènements fini-hercyniens de l'ouest du Maghreb (Algérie, Maroc).* Mémoires du Service Géologique de l'Algérie, **6**, 13–40.

OJAKANGAS, R. W. 1985. Glaciation: an uncommon mega-event as a key to intracontinental and intercontinental correlation of Early Proterozoic basin fill, North America and Baltic cratons. *In*: KLEINSPEHN, K. L & PAOLA, C. (eds.) *New Perspectives In Basin Analysis*, 431–444.

OULEBSIR, L. 1992. *Chitinozoaires et palynomorphes dans l'Ordovicien du Sahara algérien: biostratigraphie et approche des paléo-environnements.* PhD Thesis, Université de Rennes.

PARIS, F. & ROBARDET, M. 1990. Early palaeobiogeography of the Variscan regions. *Tectonophysics*, **177**, 193–213.

POSAMENTIER, H. W., ERSKINE, R. D. & MITCHUM, R. M., Jr 1991. Models for submarine fan deposition within a sequence-stratigraphic framework. *In*: WEIMER, P. & LINK, M. M. (eds) *Seismic Facies and Sedimentary Processes of Submarine Fans and Turbidite Systems.* Springer-Verlag, New York, pp. 127–136.

ROBARDET, M. & DORE, F. 1988. The late Ordovician diamictic formations from southwestern Europe: North-Gondwana glaciomarine deposits. *Palaeogeography, Palaeoclimatology, Palaeoecology*, **66**, 19–31.

VAIL, P. R., MITCHUM, R. M. Jr. & THOMPSON, S., III 1977. Seismic stratigraphy and global changes of sea-level, Part four: global cycles of relative changes of sea-level. *In*: Payton, C. E. (ed.) *Seismic stratigraphy—Application to Hydrocarbon Exploration.* American Association of Petroleum Geologists, Memoirs, **26**.

Geology and hydrocarbon occurrences in the Ghadames Basin, Algeria, Tunisia, Libya

K. ECHIKH

Petroleum Exploration Consulting Ltd, 20–22 Bedford Row, London WC1R 4EN, UK

Abstract: The Ghadames Basin is a large intra-cratonic basin, covering portions of Algeria, Tunisia and Libya. The three countries are independently conducting petroleum exploration in their portions of the basin, using different play concepts and consequently obtaining different exploration results. This paper presents the first published basin-wide view of petroleum stratigraphy and play types. Some 700 exploratory wells have been drilled in the basin, resulting in the discovery of at least 150 oil pools with 9500 MMBO (million barrels of oil) in place. Most wells were located in the structurally higher parts of the basin, with deeper portions being less explored because of shifting dune conditions and an expectation of reservoir thinning into the basin centre. Silurian and Devonian source rocks occur across large parts of the basin and have generated volumes of hydrocarbon orders of magnitude above those discovered. The numerous structural phases (Taconic, Caledonian, Hercynian and Austrian) that have affected the basin have had important implications for depocentre migration, structural style, and for patterns of trap formation, alteration and destruction. The erosion pattern and topography developed on the Hercynian unconformity is a key control on petroleum systems within the basin, controlling the preservation of Palaeozoic hydrocarbons, communication between source and higher reservoirs and patterns of long-distance migration in the Triassic reservoir. For each of the producing plays, an analysis is presented of the geological factors controlling the habitat of hydrocarbons (e.g. the effect of various tectonic phases, the influence of basin-scale facies variations on reservoir quality, and the source rock–reservoir relationship), and is related to the variations that have been observed in exploration success rate and producibility. It is believed that a substantial volume of hydrocarbons still remains undiscovered in a range of trap and play types.

The Ghadames Basin is a large intra-cratonic basin, covering portions of Algeria, Tunisia and Libya, and extending over 350 000 km^2. The basin contains up to 6 000 m of Palaeozoic and Mesozoic sediments. It is bounded to the north by the Dahar–Naffusah High, to the south by the Qarqaf Uplift (Libya) and the Hoggar Shield (Fig. 1), and its western limit is represented by the Amguid–El Biod Arch. The eastern boundary is not well defined, being overlapped by the western flank of the younger Sirt Basin. The region often termed the 'Illizi Basin' is included, for the purposes of this paper, in the Ghadames Basin.

Some 700 exploratory wells have been drilled in the three countries, resulting in the discovery of 160 oil pools with at least 9 500 million barrels of oil (MMBO) in place (c. 3500 MMBO recoverable). These figures exclude recent discoveries in central Ghadames and those in the extreme west of the basin (Rhoude Nouss and Gassi Touil regions). Most wells were located in the structurally higher parts of the basin. The deeper parts of the basin are underexplored because of hazards presented by shifting sand dunes, and because of a previous perception that Palaeozoic reservoirs will thin or shale out in this region, a view that will be challenged in this paper. Silurian and Devonian source rocks occur across large parts of the basin, and are estimated to have generated volumes of hydrocarbon far greater than the volumes discovered in traps to date, suggesting that a great volume of oil remains to be discovered in the Ghadames Basin. In the Algerian portion of the basin alone, Daniels & Emme (1995) calculated that 2100 billion barrels (BBO) have been generated. The oil in place established in known oilfields is less than 1% of this figure.

Algeria, Tunisia and Libya are conducting exploration activities in adjoining parts of the same basin, concentrating on the reservoirs that have proven most productive in each country. This paper attempts to integrate all previous studies into a regional synthesis of the geological factors controlling the habitat of hydrocarbons in the most important plays. Particular emphasis is given to two aspects, (1) the correlation of the main producing reservoirs and their regional facies trends, and (2) the effects of the tectonic history of the basin on reservoir development and hydrocarbon preservation.

Structural setting

The present-day structural configuration of the Ghadames Basin is represented by the structural contour map for the latest Ordovician (Fig. 1). This map highlights the major tectonic elements

ECHIKH, K. 1998. Geology and hydrocarbon occurrences in the Ghadames Basin, Algeria, Tunisia, Libya. *In*: MACGREGOR, D. S., MOODY, R. T. J. & CLARK-LOWES, D. D. (eds) 1998. *Petroleum Geology of North Africa*. Geological Society, London, Special Publication No. 132, 109–129.

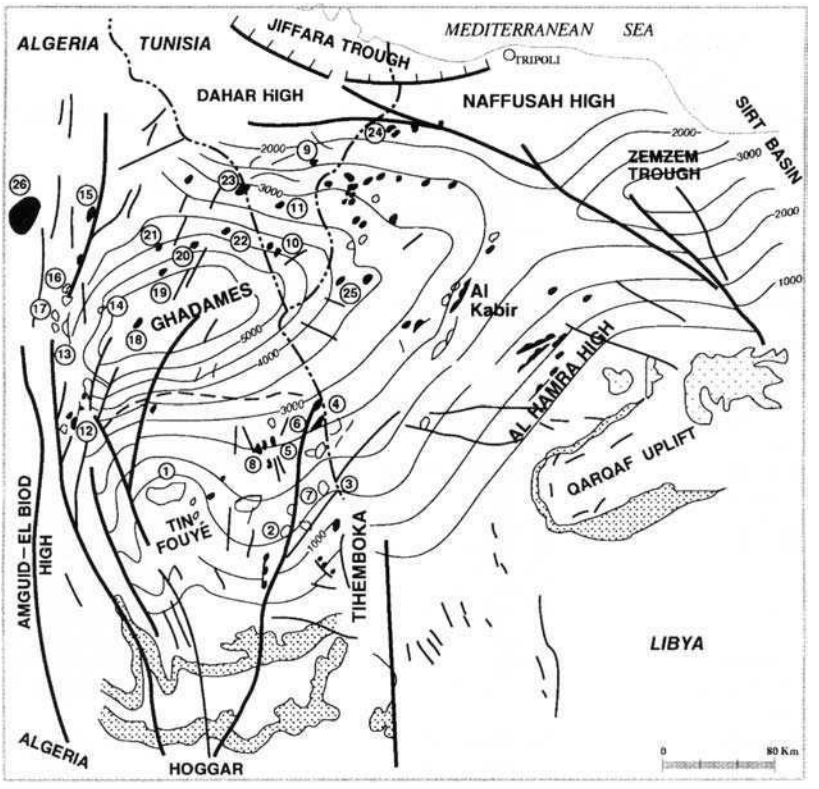

Fig. 1. Structural contour map: latest Ordovician. Infilled polygons are oilfields; non-filled polygons are gas fields. Fields: 1, Tin Fouyé–Tabankort; 2, Tiguentourine; 3, Alrar; 4, Mereksene; 5, Dimeta; 6, Stah; 7, Zarzaitine; 8, Ohanet; 9, Makhrouga; 10, Chouech Essaida; 11, Larich; 12, R. Nouss; 13, G. Touil; 14, Brides; 15, Rhoude el Baguel; 16, Nezla; 17, H. Touareg; 18, Wadi El Teh; 19, Bir Berkine; 20, Bir Rebaa; 21, R. Messaoud; 22, R. El Rouni; 23, El Borma; 24, Tigi; 25, F9O; 26, H. Messaoud.

bounding the basin, i.e. the Amguid–El Biod Arch, the Dahar–Naffusah High and the Qarqaf Uplift. The southern flank is complicated by several second-order structural highs, e.g. the Tin Fouyé, Tihemboka and Al Hamra Highs.

The evolution of this basin occurred in three phases: (1) initiation through reactivation of Pan-African fault systems of a subsiding Palaeozoic basin; (2) uplift and erosion of much of the basin during the Hercynian phase; (3) a northwest tilting and superimposition of a Mesozoic extensional basin.

The present structural framework of the Ghadames Basin was produced by the successive effects of tectonic movements related to the Taconic, Caledonian, Hercynian and Austrian phases. As a consequence, there is a wide variety of structural styles, fault patterns and structural trap types present, and depocentres have tended to migrate with time.

Palaeozoic tectonic events

Taconic phase

Early Ordovician time was characterized by a tectonic instability (Attar 1987) indicated by the absence of the Cambrian over the main uplifts, e.g. the Ahara Uplift and the Tihemboka Arch. Peak activity occurred during Llandeilo time, when there was substantial activity, particularly on the southern rim of the Ghadames Basin, in Illizi and close to the Qarqaf Uplift. Active fault uplifts caused erosion and the creation of a series of overlapping deep erosional troughs, which were later filled by periglacial deposits. The folds created at this time are broad, with active faulting controlling thickness and facies distribution in syn- and post-tectonic formations. The Taconic unconformity is illustrated by a cross-section though the Dahar High (Fig. 2), where successive units of the Early Ordovi-

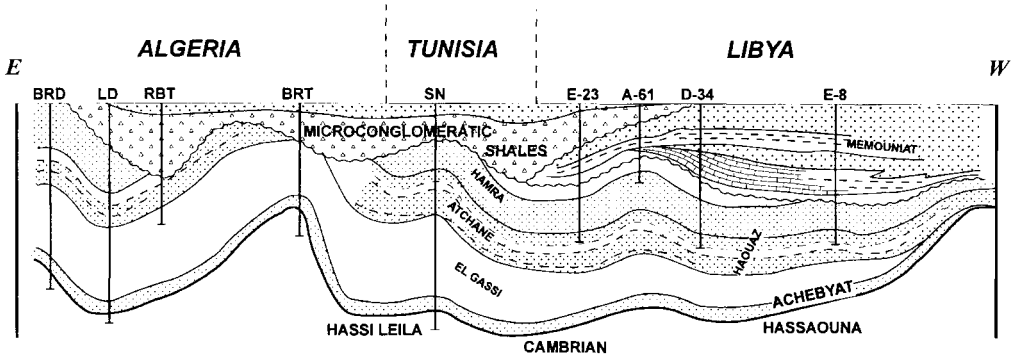

Fig. 2. Geological cross-section: Ordovician formations. Datum: latest Ordovician. This section illustrates the erosional effects of the Taconic event.

cian are seen to be overlain by the Late Ordovician Microconglomeratic Shales.

The presence of volcanic layers in the Brides area (western flank of basin) and in Illizi (Mereksene, Stah and Dimeta fields) is also related to this tectonic activity. In Libya, deep troughs were formed close to the Qarqaf Uplift (Echikh 1992) and were filled with the periglacial facies of the Bir Tlacsin and Memouniat Formations (Unit IV of Algeria). These unconformably overlie older Ordovician strata (Fig. 2). An erosional phase is also noted in southern Tunisia (Chandoul 1992).

Caledonian phase

A significant Caledonian tectonic event was initiated during the Přídolí–Gedinnian as a result of the collision between West Africa and North America. This caused the uplifting and erosion of the southwestern and southern flank of the Ghadames Basin, where the Lower Devonian (Tadrart) is seen to directly overly the Upper Silurian (basal Acacus). Figure 3 illustrates the progressive truncation of the various Acacus (Upper Silurian) units from NE to SW on this unconformity. In Algeria (Illizi) only the lowermost part of Acacus Formation is preserved (Fig. 4). Again, there are few indications of significant high-amplitude folding during this phase, except in NW Libya and over the Al Kabir trend (Echikh 1992) and in Illizi (Sonatrach-Beicip 1975; Attar 1987; Boudjema 1987). In these regions, seismic data may show folding of the Silurian section below flat-lying Devonian deposits (Fig. 5, 1)

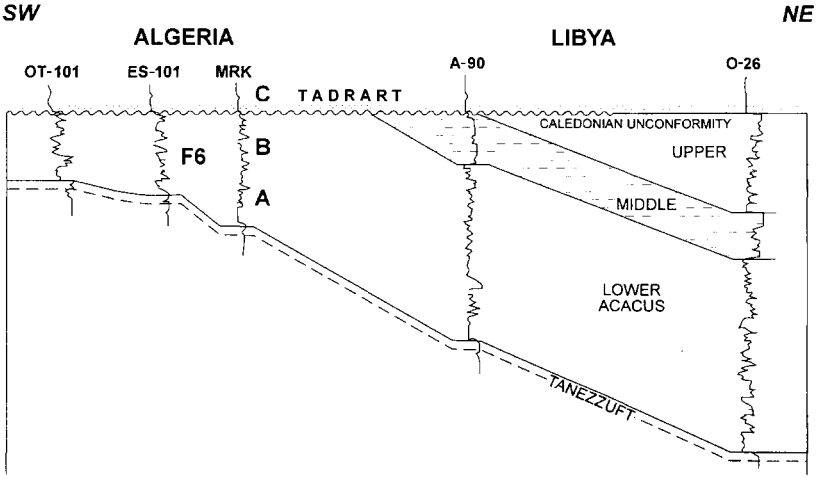

Fig. 3. Log correlation showing progressive erosion of Acacus units towards Algeria on the Caledonian unconformity. (For location, see Fig. 4).

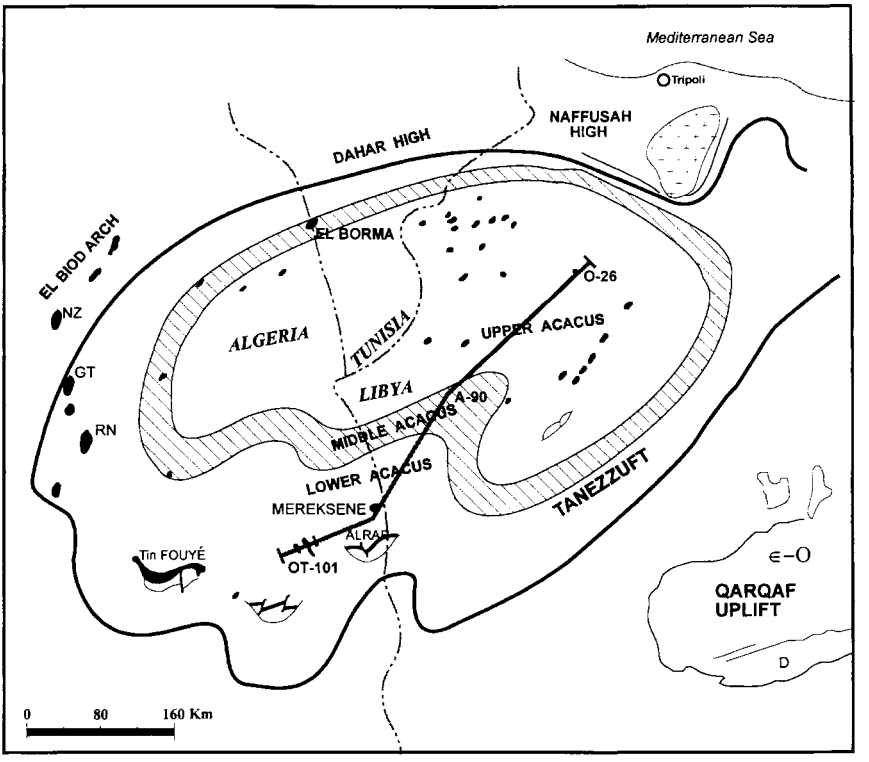

Fig. 4. Subcrop map: latest Silurian (Caledonian unconformity), illustrating the basin-scale erosion of Acacus units.

Two additional unconformities are observed higher in the Devonian, particularly over the southern flank of the Ghadames Basin, representing Late Caledonian tectonic phases. These unconformities are observed at the top of the Emsian (Sonatrach-Beicip 1975; Abdesselam Rouighi 1991; Echikh 1992) and at the base of the Frasnian radioactive carbonate-shale layer (Sonatrach-Beicip 1975). In Libya, biostratigraphic hiatuses occur in the Givetian and Frasnian (Echikh 1987 1992).

Hercynian phases

Two major tectonic events occurred during the Carboniferous, representing the Hercynian tectonic movements that terminate the Palaeozoic cycle:

Early Hercynian phase. The thickness distribution of the Tournaisian–Lower Viséan sediments in the Illizi basin, their partial erosion over some local structures in the Tihemboka Arch (Boudjema 1987) and the absence of the Early Tournaisian over the entire basin (as proven by biostratigraphy) all clearly indicate the existence of a regional early Hercynian tectonic event.

Main Hercynian phase. The Late Westphalian–Early Permian Hercynian movements initiated the uplifting of the El Biod, Dahar and Naffusah Highs, resulting in the intensive erosion of Palaeozoic rocks, in some cases as deep as the Cambrian. The effects of the earliest movements of the main Hercynian phase on structure are well illustrated in the Illizi basin, e.g. over the Edjeleh structure, where Westphalian carbonates are observed to unconformably overlie subcropping Namurian units (Sonatrach-Beicip 1975; Attar 1987).

Mesozoic tectonic events

Trias–Jurassic period

An extensional event affected the area in the Triassic–Liassic, related to the rifting of Tethys

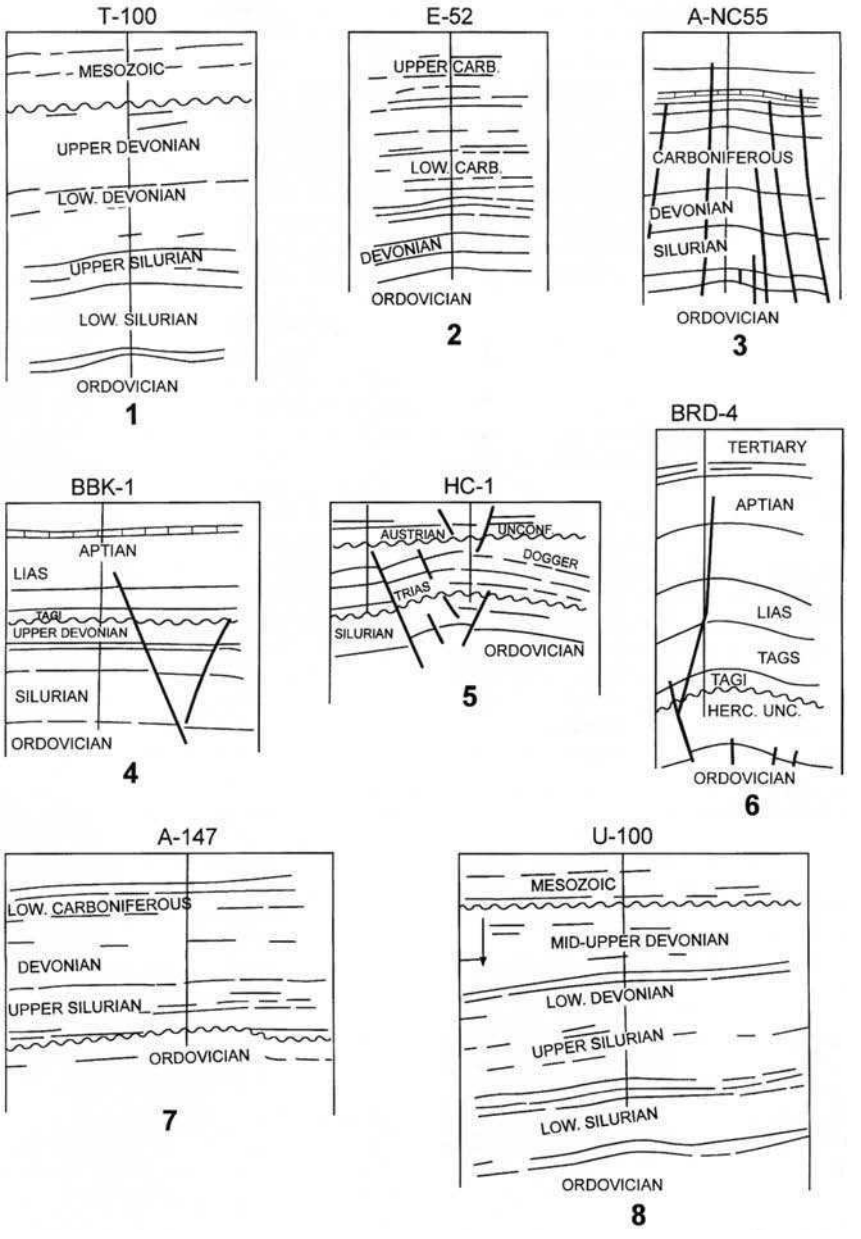

Fig. 5. Examples of different generations of structural traps in the Ghadames Basin. 1, Structural growth up to Silurian; 2, structural growth up to Late Devonian; 3, structural growth up to Hercynian; 4, Triassic–Liassic extensional; 5, Austrian compressional; 6, Pyrenean compressional; 7, structural related to glacial palaeotopography: 8, structure reopened during Late Devonian–Carboniferous subsidence.

and the opening of the Atlantic (Guiraud this volume). This led to the development of a series of en echelon normal faults and tilted blocks, with associated volcanism, in the northwestern part of the Ghadames Basin and southern Tunisia. These fault sets can be demonstrated to control thickness and facies changes within Triassic sediments. Peak activity probably occurred during the Lias (Hettangian, Boudjema 1987). The Bir Berkine (Fig. 5), Si Fatima and Wadi el Teh tilted fault block traps were formed at this time.

Cretaceous period

At the end of the Barremian, the tectonic movements tied to the Austrian phase occurred. These were pronounced over the El Biod Arch and its eastern flank (Boudjema 1987), with east–west compression producing high-amplitude structures along north–south-trending reverse faults. In Algeria, structures such as the Hassi Chergui, Hassi Touareg, Rhourde Nouss and Ain Romana anticlines were initiated during this phase. The Hassi Chergui example is illustrated in Fig. 5, where flat-lying Cretaceous strata is seen to overlie folded Jurassic deposits.

Tertiary tectonic events

Latest Eocene (Pyrenean phase) movements, which are significant in the Atlas area, affect the Saharan platform with less intensity. The distal effects of this compressive event led to accentuation and remodelling of Austrian structures (Boudjema 1987), inversion of Hercynian or Liassic normal faults (producing traps such as the Bir Rebaa, Rhourde El Rouni and El Borma structures) and the formation locally of some new structures, such as the Brides, Ain Romana and Rhourde Adra features. A typical Tertiary aged structure is illustrated in Fig. 5.

Local structural styles and ages

Analysis of seismic data over the Ghadames Basin indicates the existence of a wide variety of structural types of different ages. Many structures and traps have grown successively throughout geological time. It is therefore difficult to classify structures in discrete timing categories, but the following broad groupings can be made: (1) Structures which grew in pre-Silurian times only; these include traps related to Early Ordovician glacial palaeotopography (Taconic phase); (2) Structures which grew in pre-Devonian and Devonian times only; (3) Palaeozoic structures which continued to grow until the Hercynian event; (4) Structures produced by Liassic extensional movements; (5) Structures formed during the Austrian phase during the latest Barremian, often by inversion of earlier faults; (6) Structures formed by Tertiary (Pyrenean, Alpine) structural phases, again often by inversion. Implications of each of these for the formation of structural traps will be discussed later.

It can be noted that in many cases, structural culminations have shifted with time. The Austrian event in particular played a significant role in causing lateral migration of the culminations of Palaeozoic aged structures. It can be noted that the location of structural culminations can consequently differ at the levels of the Liassic anhydrite seismic marker and the Triassic reservoir. In the northern part of the basin, it is possible to identify early structures on which closure has been destroyed through structural tilting related to Mesozoic subsidence. The failure of many dry wells in the basin can be related to the resulting problems of accurately locating structural crests at reservoir level from mapping on higher seismic markers.

Reservoirs and petroleum results

Different stratigraphical nomenclatures currently apply in each of the three countries. A correlation between these for the Palaeozoic section is attempted in Fig. 6. The most important reservoirs are summarized below for each geological period.

Ordovician reservoirs

The Ordovician section is seen to have a significant sand content in the marginal and structurally highest parts of the basin. A few penetrations in the deepest part of the basin indicate the presence of a more shaly facies.

In the Algerian part of the Ghadames Basin, the Ordovician has been subdivided into several reservoir-bearing formations, namely the Oued Saret, Ouargla, Hamra Quartzites and El Atchane Formations. The Ordovician lies very deep over much of the Algerian portion of the basin and is penetrated only on its western flank, where it contains wet gas (Brides and Gassi El Adem fields). In Illizi, the Ordovician has been subdivided into two Units: III and IV. The most prolific reservoirs, such as those of Tin

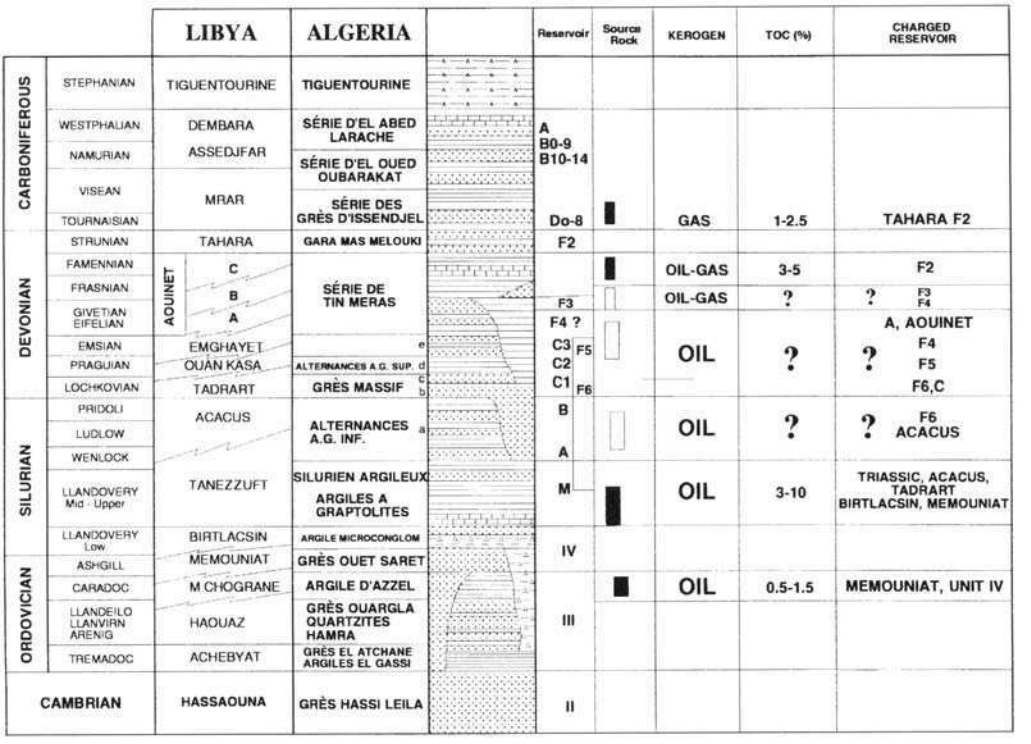

Fig. 6. Stratigraphical correlation chart of the Palaeozoic of Algeria and Libya, illustrating the different reservoir and source rock terminologies. sources for Libya: Massa (1988), Echikh (1992); sources for Algeria: Attar (1987), Bekkouche (1992).

Fouyé–Tabankort, lie in Unit IV, corresponding to the Memouniat Formation in Libya. These sands are glacial in origin (Fekirine & Abdallah this volume). The petrophysical proprieties of Unit IV show rapid lateral and vertical variations, with porosities ranging between 6 and 10%, except for some levels with values reaching 12%. Gas columns occur with oil rings in wells on the Tin Fouyé, Tiguentourine and Tihemboka Highs.

In Libya, the Cambro-Ordovician has been penetrated by only a few wells, with most of these terminating at the top of the Memouniat. The main producing reservoir lies in the Memouniat quartzitic sands (equivalent to Unit IV in Algeria). Available data suggest a similar facies distribution pattern to that established in Algeria (Fig. 7), passing from sandy periglacial deposits in the south, close to the Qarqaf Uplift, to a marine shaly sequence in the central and northern parts of the basin. Several oilfields have been found by AGOCO and AGIP over the Al Hamra High. In the central and northern parts of the basin, and at Larich in Tunisia, only wet gas has been tested.

Silurian reservoirs

The main regional reservoir of Silurian age is the Acacus Formation, equivalent to the lower part of the F6 in Algeria (Fig. 8). The Acacus has been subdivided into three formations, Lower, Middle and Upper, by Massa (1988), which are well represented in the northern parts of the basin, within Libya. On the southern margin, Caledonian erosion (Echikh 1984, 1992) has removed the upper two members and only the Lower Acacus Formation (reservoir units M, A, B1 and B2 of the lower F6 in Algeria) is present. In the basin centre, the Silurian has yet to be reached by drilling. The Lower Acacus and equivalent reservoirs show maximum sand development on the southern flank (Fig. 8), passing progressively into a more shaly facies in central and northwestern areas. This trend is sometimes broken by the incoming of sands orientated along SW–NE trends, related probably to an intra-basin high that was active in the Caledonian. This palaeohigh is evidenced in some wells by the presence of a local unconformity within the Acacus Formation and follows a simi-

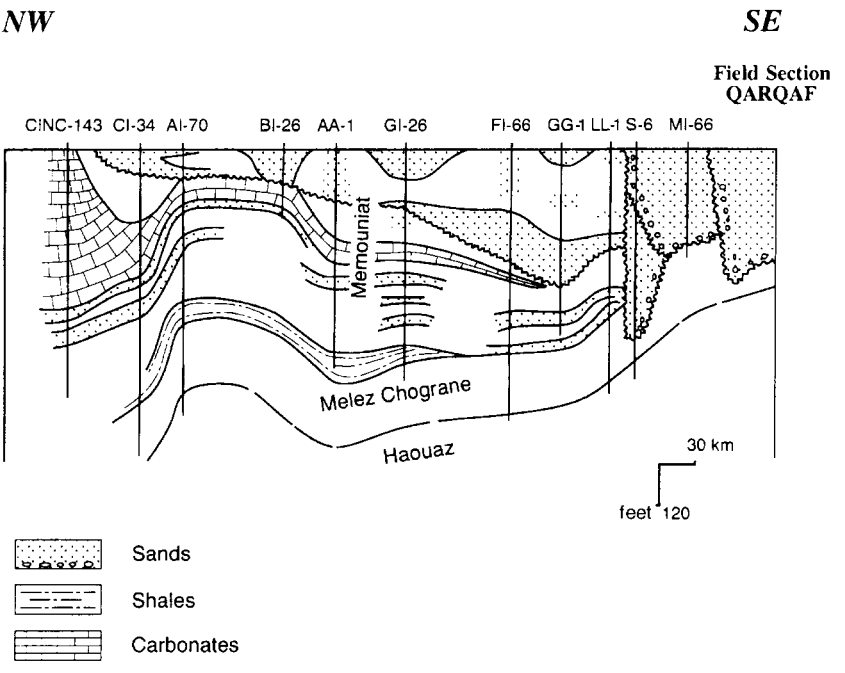

Fig. 7. Regional facies variation of Memouniat (Unit IV) Formation in Libya. The southern part is the area of maximum sand development, where sediments of peri-glacial origin were deposited in deep erosional troughs. The facies in central and northern areas is shalier. (Note the presence of a palaeohigh around the BI–26 and AI–70 wells, probably initiated by Taconic movements, close to the Nafussah High.)

lar orientation to the Amguid–El Biod Arch in Algeria. Both features are suggested here to be essentially features of Caledonian rather than, as has previously been suggested, Hercynian age.

Within the Illizi Basin, Silurian sands show fair to good reservoir quality, with porosities ranging between 10 and 15% (maximum 20%) and permeability around 100 mD. Over the El Biod Arch and in the Rhourde Nouss field, the reservoir deteriorates, with porosities of 8–12% and permeabilities not exceeding 10–50 mD. Within Libya, the Acacus sands show good petrophysical properties in the productive areas in southern and central parts of the basin, with porosities of 20–25%, rising locally to 30%. A deterioration in petrophysical proprieties occurs from the south towards the northwestern part of the basin, where porosities do not exceed 12–15%.

The Lower Acacus has proven to be a prolific producer in Libya, with flowing oil in the central and northwestern parts of the basin. Twenty-two oilfields and three gas fields have been found in this region. In Algeria, the Silurian is productive only in Illizi, with the lower parts of the F6 (M, B and A units) producing gas with oil in the Merksene, Stah, Dimeta, Ohanet and In Anemas fields. The low productivity in Algeria seems to be related to seal, rather than reservoir, issues, as will later be discussed.

Lower Devonian reservoirs

Within Libya, there are two discrete producing reservoirs in the Lower Devonian, the Tadrart and Ouan Kasa Formations. These are respectively equivalent to the upper part of the F6 and the F5 in Algeria (Fig. 6). The Tadrart–F6 reservoir can be correlated throughout the basin, and consists in practically all areas of clean, medium- to coarse-grained sandstones deposited as widespread channelled sheets. The Ouan Kasa Formation is more difficult to correlate, because of facies changes and the erosional effects of a mid-Devonian (Frasnian) unconformity in Algeria, particularly over the Ahara and Tihemboka Highs. Over these highs, Middle and Upper Devonian strata directly overlie the lowermost sections of the F6 (Acacus).

Although showing a remarkably constant facies throughout the basin, the Tadrart shows

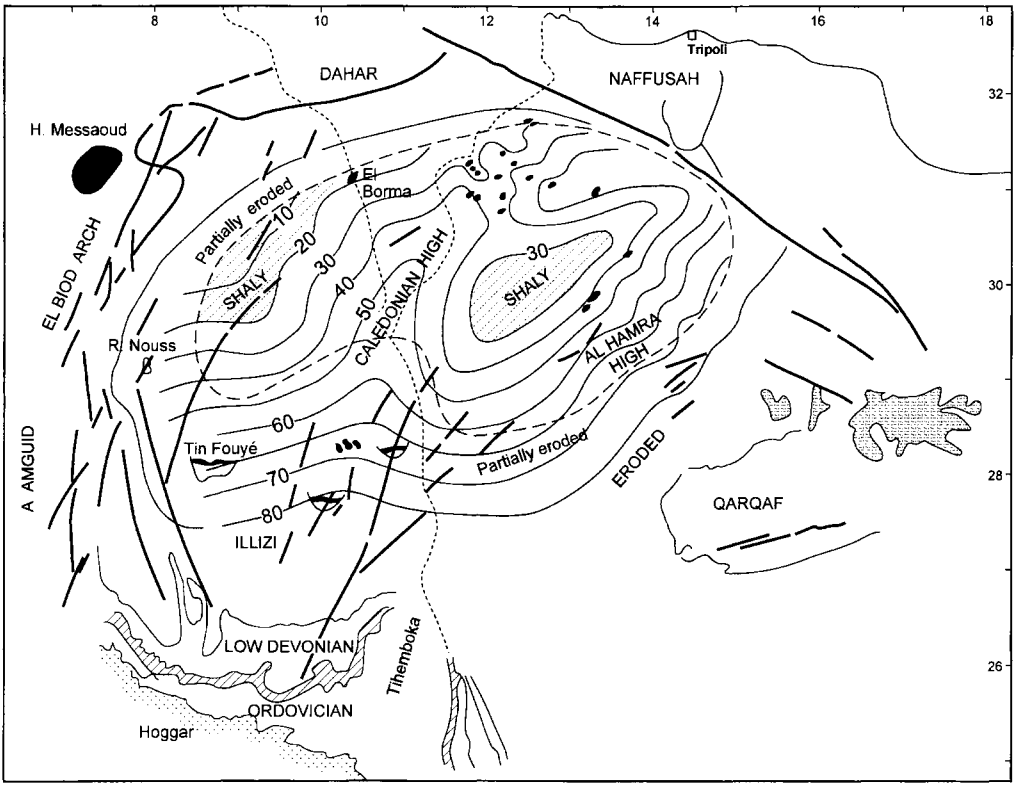

Fig. 8. Sand content (percentage) of Lower Acacus Formation. (Note the presence of a Caledonian high in the central part of the basin, with an associated SW–NE trending sand-rich belt.)

significant regional porosity variation, attributed to burial and diagenetic effects. The highest porosities are seen in the south, where they range from 15 to 20%. Porosity falls into the central and deepest parts of the basin, where it does not exceed 8–10%, but then increases again towards the northwest, where values of 11–14% are seen (Bir Rebaa, Rhourde Messaoud and Bir Berkine fields). The Tadrart–F6 reservoir is a prolific producer over the southern part of the basin (see Fig. 10, below), producing mainly oil in Illizi (Algeria) and on the Al Hamra high (Libya). The recent intensification of exploration activities on the Algerian side resulted in the discovery of several new oilfields (e.g. Bir Rebaa, Rhourde Messaoud and Bir Berkine), upgrading the potential of the western flank of the Ghadames Basin at this level.

The Ouan Kasa can be subdivided into two members, Lower and Upper. The Lower Member shows substantial facies variation, passing from a very sandy succession in the south to shaly with carbonate layers in the northern part of the basin. The Upper Member, in contrast, is of fairly uniform composition throughout the basin, consisting of an alternation of sands, silts and shales. It is of markedly less significance as a producing reservoir.

Middle and Upper Devonian reservoirs

Reservoir quality in the Middle and Upper Devonian is considerably more irregular than in the Early Devonian, with reservoir units thinner and generally associated with local highs. The Middle–Upper Devonian reservoirs also generally do not show good petrophysical characteristics, except in some areas of shallow burial and proximity to source areas close to the Tihemboka, Ahara and Al Hamra Highs. The F4 reservoir produces oil in Illizi, the F3 gas in the Alrar field (Chaouchi *et al.* this volume) and the Aaouinet Formation oil in the Al Hamra area (Libya). The Tahara (F2 in Algeria) reservoirs seem to be more gas prone and are productive as such over a large area of the central part of the Ghadames Basin.

Triassic reservoirs

Sands, often non-marine in origin, are present at Triassic level over all three countries. These are termed the Trias Argilo Greseux in Algeria, the Ras Hamia Formation in Libya and the Kirchaou Formation in Tunisia. These form the highest-quality and most prospective reservoirs in the northern parts of the basin, particularly in Algeria and Tunisia.

The Triassic is characterized by significant vertical and lateral facies variations, which can be related to the topography developed on the Hercynian unconformity (Benrabah *et al.* 1991). Triassic sediments were supplied from the major palaeohighs such as the El Biod, Dahar (Algeria) and Naffusah (Libya) in the manner shown in Fig. 9. Deposition took place on the flank of these palaeohighs within braided fluvial systems characterized by a high sand/shale ratio, leading to the development of sheet sands with good lateral continuity and petrophysical properties. In the northeastern part of the Ghadames Basin, conditions of deposition change to a meandering fluvial system flowing SW to NE. A more shaly facies is observed in this area, with sands developed as elongated lens-shaped bodies, e.g. in the Rhourde El Rouni, El Borma and Makhrouga (Tunisia) field areas. Further to the NE, the depositional environment passes into fluvio-deltaic and sand development becomes highly irregular.

The Triassic reservoirs are prolific oil and gas producers (Fig. 10), particularly over the El Biod Arch (Gassi Touil, Rhourde Nouss, Nezla, Hassi Chergui fields) and over the western flank of the Ghadames Basin, where a number of more recent oil discoveries have been made (e.g. Wadi el Teh, Bir Berkine, Bir Rebaa and Rhourde El Rouni fields, plus the recent Anardarko, Cepsa and AGIP discoveries). In Tunisia, Triassic oil is produced from El Borma, Makhrouga, Chouech Essaida and Larich fields.

Hydrocarbon occurrence

This section analyses the distribution of hydrocarbons in the basin in terms of stratigraphic distribution, depth and trap type. Statistics are compiled on oil in place and illustrated in a series of charts (Figs 10–14). The fields in the extreme west of the basin (Gassi Touil and Rhourde Nouss areas) are not included in these figures. Recent downwards revisions of the reserves and oil in place of the Illizi Basin fields have been taken into account.

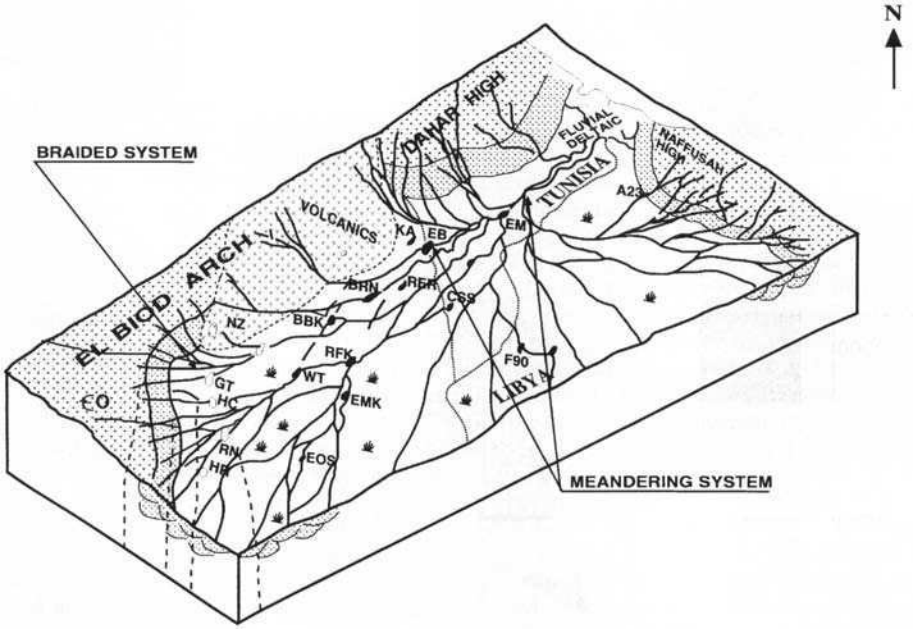

Fig. 9. Sedimentological framework of Triassic deposits, with braided and meandering fluvial systems merging into fluvial–deltaic systems towards the northeastern part of Tunisia. Most major oilfields at this level are located in the braided fluvial belt and are characterized by high reservoir quality.

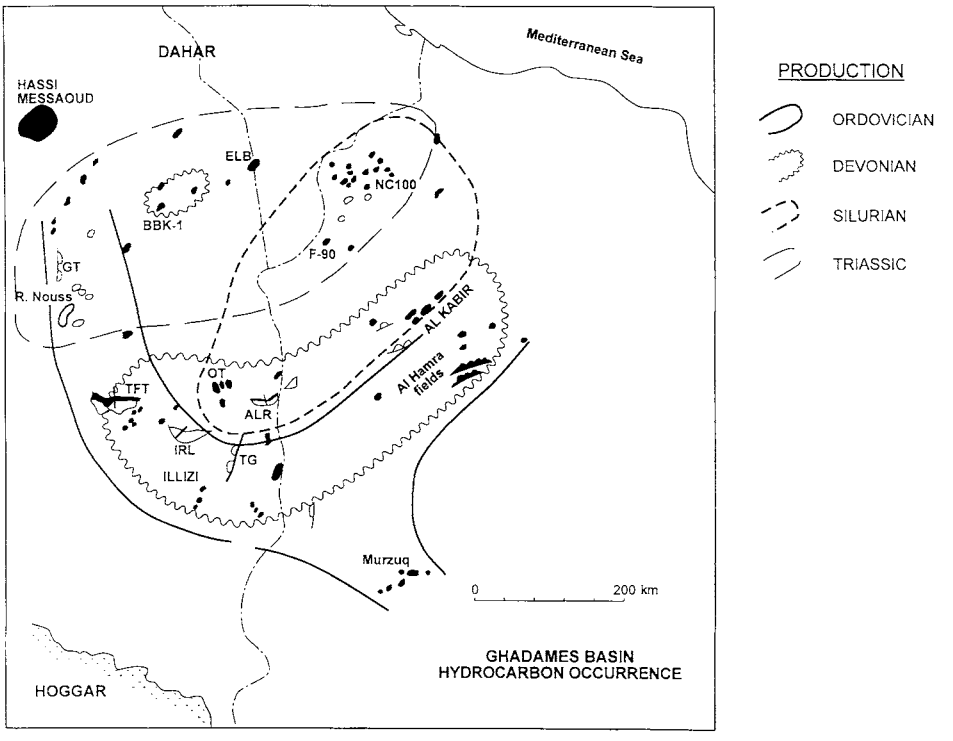

Fig. 10. Regions ('fairways') in which the different reservoir levels are productive. (Note the substantial geographical differences, which are caused by many geological factors, as discussed in the text.)

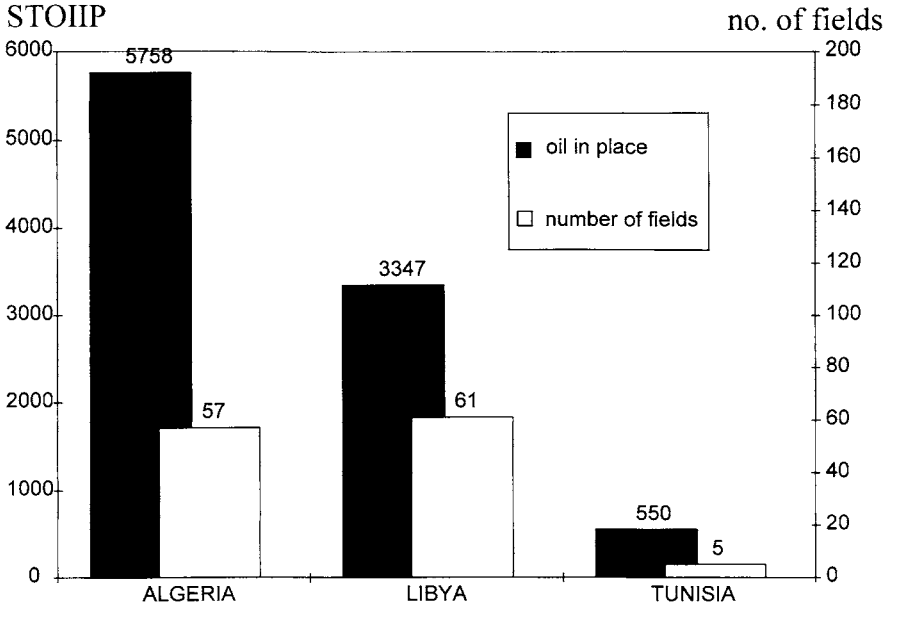

Fig. 11. Oil in place (STOIIP) and numbers of oilfields within the Ghadames Basin, by country. Libya has the highest number of fields but Algeria the highest oil volume.

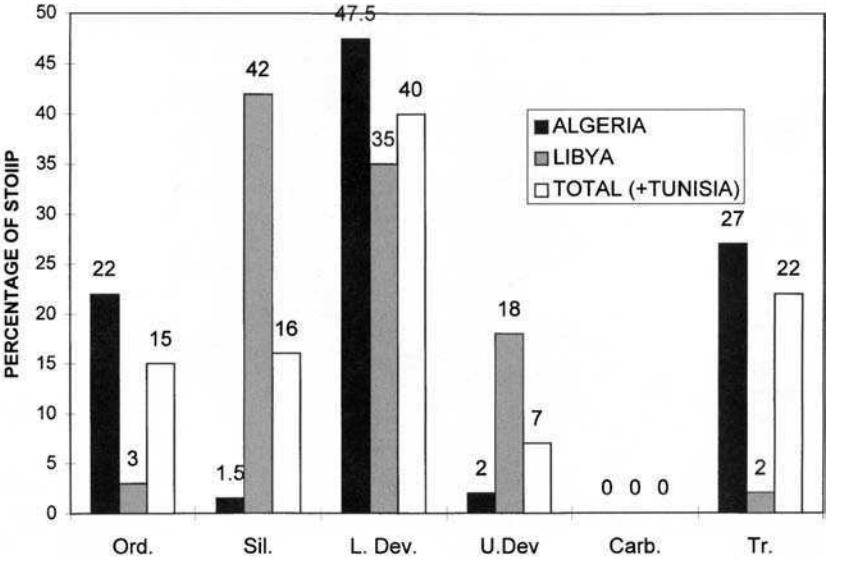

Fig. 12. Oil in place distribution within the Ghadames Basin by reservoir age.

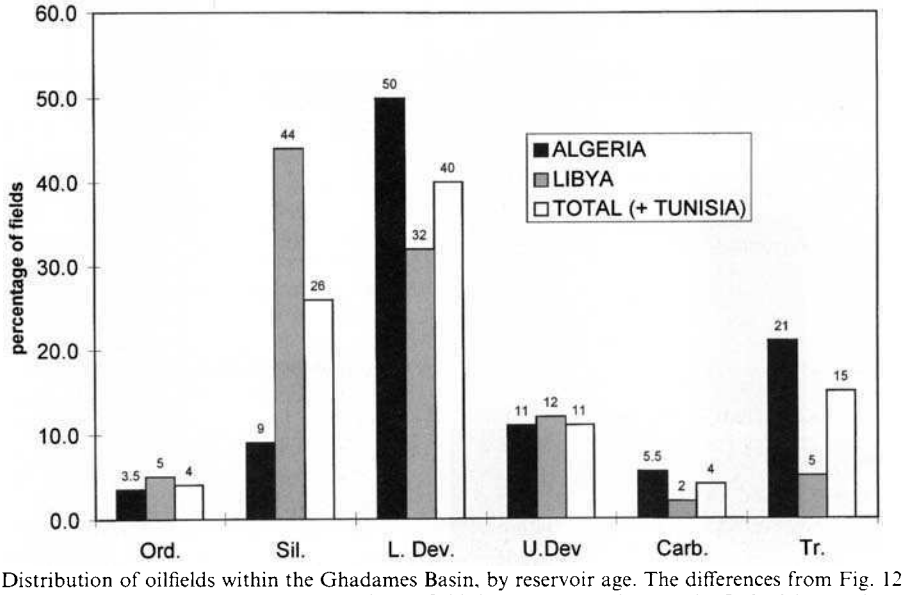

Fig. 13. Distribution of oilfields within the Ghadames Basin, by reservoir age. The differences from Fig. 12 are caused by the tendency towards a small number of large fields in some reservoirs (e.g. the Ordovician) and towards a large number of small fields in others (e.g. the Silurian).

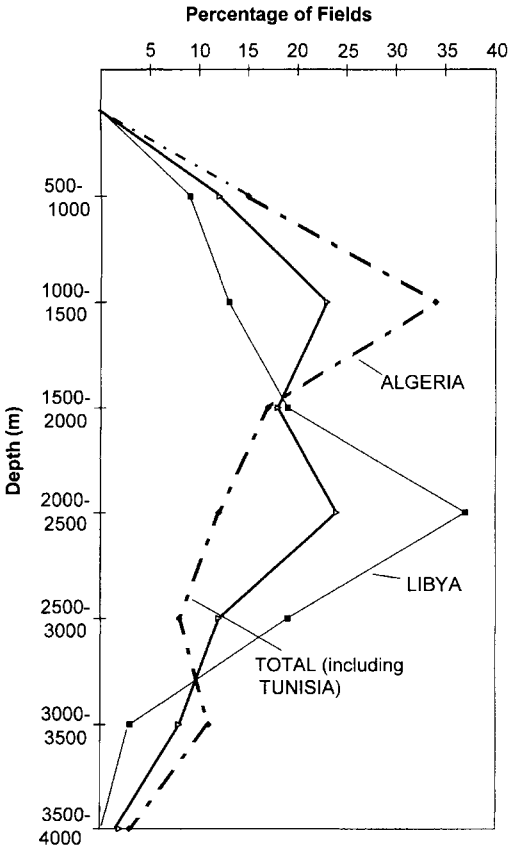

Fig. 14. Depth distribution of proven oilfields in the Ghadames Basin. The fall-off of number of discoveries below 2500 m is noteworthy, and is particularly marked for Algeria. This suggests that many deep fields may lie undiscovered.

Areal distribution

The geographical extent of the productive 'fairways' at the various reservoir levels described above is illustrated in Fig. 10. The older reservoirs (Ordovician and Devonian) are good producers over the southern and western flanks of the Ghadames Basin, whereas the Silurian fairway extends over the northwestern part of the basin (Al Kabir), extending into the Illizi area. Triassic production is centred in Algeria and southern Tunisia. These geographical trends can be related primarily to patterns of reservoir distribution and quality, although the lower density of drilling of the deeper reservoirs may also play a role.

The largest number of oil pools has been discovered in Libya (49%), just above that of Algeria (46%, Fig. 11). However, proven oil in place within these pools is substantially higher in Algeria, despite the use here of conservative figures, implying that average field size in Algeria is considerably higher than in Libya. This is primarily due to the occurrence of a small number of very large fields in the Illizi area. It should also be noted in interpreting these statistics that most of the smaller Libyan discoveries lie in the Silurian fairway of the Al Kabir area. The southern portion of the Ghadames Basin in Libya is less explored than the southern Algerian portion (Illizi). Tunisia contributes only 4% of the discovered pools in the basin.

Stratigraphic distribution

The Lower Devonian is the most productive horizon in the Ghadames Basin in terms of both number of oil pools (Fig. 12) and total oil in place (Fig. 13), with 40% of each parameter. Roughly half of the Algerian reserves and pools and about a third of the Libyan occur at this level. It is followed in importance by the Triassic (22% of oil in place in 15% of fields, figures which can be expected to rise as the latest discoveries are added), the Silurian (16% of oil in place in 26% of fields) and the Ordovician (15% of oil in place in only 3.5% of fields).

Triassic fields are heavily concentrated in Algeria, whereas the play is thought to be underexplored in Libya, where identical reservoirs and seals are present. More detailed study of the Ras Hamia reservoir will probably lead to further discoveries at this level. In contrast, Silurian fields are the dominant producers in Libya (42%), where they show a tendency towards small field sizes, but are insignificant in Algeria. This is largely because of the depths reached by the Silurian over much of Algeria and to the absence of a good sealing formation within the late Silurian. Many pools at Silurian level may have been drilled but not detected by log analysis, as it is now known that this reservoir often gives a low resistivity response when hydrocarbon bearing. Significant Ordovician reserves are found only in a few large fields in Algeria, particularly Tin Fouyé–Tabankort. The Ordovician represents a promising but still ill-understood frontier play over much of the region, particularly in Libya.

Depth distribution

There is no discrete trend of oilfield occurrence against depth for the basin as a whole (Fig. 14).

A peak at around 1000 m for Algerian fields represents the predominantly shallow Illizi group of fields. Elsewhere, in the Algerian portion of the central part of the basin, discoveries are spread over a wide depth range, ranging down to 3500 m. In Libya, oil pools are concentrated between 2000 and 3000 m. The sharp fall-off in number of discovered pools below 3000 m may be attributed at least partly to lack of deep drilling.

Trapping mechanism

Structural traps. Most of the discovered oil accumulations occur in structural traps. As previously discussed, the complex structural history of the region has produced a wide variety of structural traps of differing ages. Known structural traps fall into the following categories, with examples shown in Fig. 15:

(1) Simple anticlines (unfaulted) of pre-Hercynian age. This trap type is present mainly in northwest Libya (e.g. Silurian oilfields of concession NC100) and in the central part of the Ghadames Basin. Such anticlines are generally broad low-relief structures and were formed during the Silurian and Devonian (Caledonian and Frasnian events).

(2) Normal faulted structures of Hercynian age. These are related to basement vertical movements during the Hercynian event. Examples of this trap types are observed in north and northwest Libya and in Illizi (e.g. Zarzaitine, Tin Fouyé, J-100, TNC7 fields).

(3) Reverse faulted structures. These are observed along the western flank of the basin (e.g. Brides field), the El Biod Arch (Gassi Touil, Hassi Touareg and Rhourde Nouss fields) and the Al Hamra High in Libya. This form of trap was produced by compressional movements related to the Austrian and Pyrenean phases.

(4) Uplifted faulted blocks of Liassic age. In this form of trap, entrapment was achieved by the uplifting of blocks through faults initiated during the Liassic distensional movements. Examples occur in the central Algerian part of the basin, e.g. Bir Berkine, Wadi el Teh and Rhourde Messaoud

Stratigraphic traps. Two forms of stratigraphic trap have been observed (Fig. 16):

(1) Updip shale-outs. The most significant example is the Alrar field (Chaouchi *et al.* this volume), located close to the boundary between the Ghadames and Illizi Basins. A large trap is here created through an abrupt updip sand

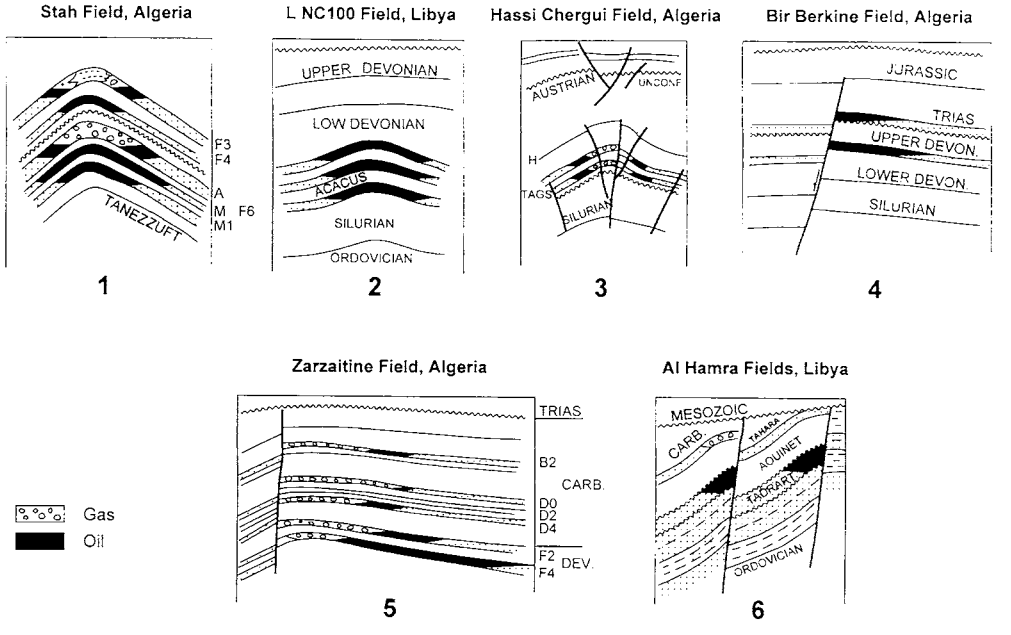

Fig. 15. Sketch sections across type examples of different structural traps: 1, 2, Simple anticlines; 3, 6, Reverse faulted structures of Austrian/Pyrenean age; 4, normal faulted structure of Trias-Jurassic age; 5, normal faulted structure of Hercynian age. Al Hamra field after Hammuda (1980). Zarzaitine field after Echikh (1975).

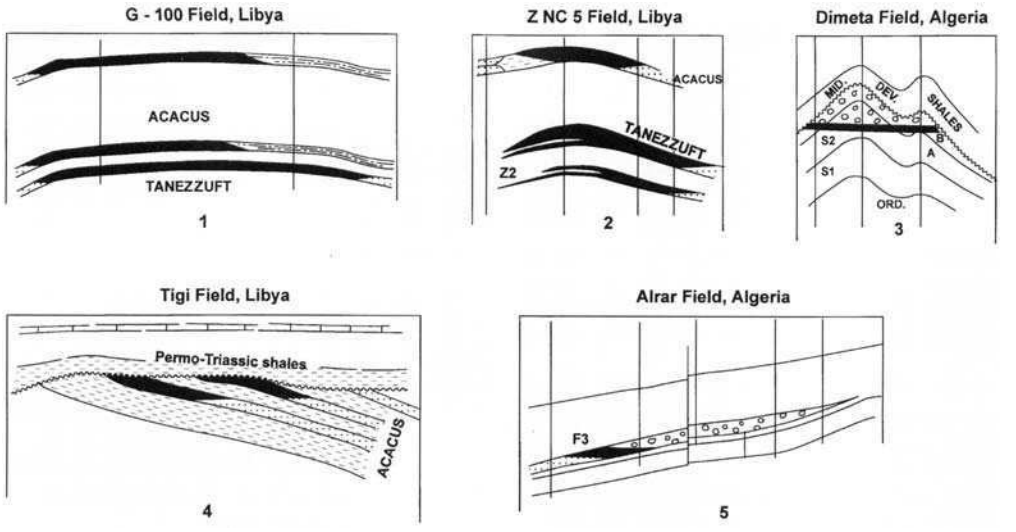

Fig. 16. Sketch sections across type examples of different combination and stratigraphic traps: 1, 2, structural trap enhanced by pinchout within the closure; 3, unconformity trap; 4, subcrop trap; 5, pinchout trap.

pinchout. Other oilfields, such as Wadi el Teh (at Triassic level) and Al Kabir also show elements of this trap type.

(2) Stratigraphical truncation (on unconformity). This trap type has been proven to date only in the northwestern part of Libya. Hydrocarbons are trapped in the subcrop of the Acacus (Silurian) reservoirs below Triassic shales (e.g. Tigi field, Fig. 16). It is likely that further examples of this play type lie undiscovered in the basin, e.g. over various arches in Algeria (Ford & Muller 1995).

Structural–stratigraphic combination traps. A number of fields shows elements of both structural and stratigraphic trapping. In Libya, good examples are the Z and G-100 fields (Fig. 16), where entrapment is accentuated by rapid facies changes in the Acacus (Silurian) reservoir over the crest of the structure.

In Algeria, an example is the Dimeta field. The seal to the Upper Silurian (A, B) reservoir is provided here on an unconformity surface by Upper Devonian shales, the Early Devonian having been removed by Frasnian erosion. The field, though essentially structural, does therefore show some features of a subcrop trap.

Permeability barrier. The Tiguentourine field in Illizi provides an example of a diagenetic trap, with a lateral seal provided by increased quartzification within the Cambrian II reservoir. The TG-1 well encountered a 600 m gas column, whereas wells only a few kilometres to the south and east penetrated a tight, very compact, quartzite at reservoir level.

Hydrodynamic and combination structural-hydrodynamic traps. The Late Silurian–Early Devonian pools of the Tin Fouyé–Tabankort field are well known hydrodynamic traps (Alem *et al.* this volume). Other fields in the same area have variable hydrodynamic components.

Factors controlling habitat of hydrocarbons

Hydrocarbon richness varies widely across the Ghadames Basin, depending on several key geological controls. The most important of these controls are believed to be reservoir facies and diagenetic tranformation, communication with source, and the influence of the numerous tectonic phases on patterns of hydrocarbon migration, accumulation and preservation.

Reservoir facies changes

Ordovician and Devonian reservoirs both show sandier facies and improved petrophysical properties on the southern flank of the Ghadames Basin. Reservoir quality deteriorates towards the central and northeastern parts, where open marine shale-prone environments predominate (Echikh 1992). Most production from the Ordovician and Devonian thus comes from the southern flank of the basin.

The Silurian reservoirs follow similar environmental and sand thickness trends. However, there is not such a good relationship between reservoir thickness and exploration success, as the net/gross value is so high in the southern area as to preclude the formation of effective intraformational seals, The Silurian sands (Acacus) thus communicate directly with the Early Devonian (Tadrart) sandstones. The most productive areas at Silurian level are thus located in the northwestern part of Libya, where Caledonian erosion is minor, net/gross values are lower and effective intraformational seals are thus developed.

Because of their continental origin and consequently complex depositional patterns, reservoir quality and productivity within Triassic reservoirs varies widely. Productivity may change rapidly within the same structure, as has been established by the delineation wells over some oilfields (e.g. Wadi el Teh, Rhourde Messaoud, Rhourde El Rouni). Reservoir quality and productivity are maximized within areas where the sands were deposited as laterally continuous braided fluvial sand sheets or as point bars. Quality deteriorates rapidly towards the flood-plain environments, which show high shale and silt contents.

Reservoir diagenetic transformation

Ordovician reservoirs decrease in quality with burial depth, as a result of the effects of compaction and quartzification. Permeability can be improved through fracturing, close to intensively faulted areas, such as the El Biod High.

Lower Devonian reservoirs also show increasing quartzification with depth. Sonatrach analytical reports (e.g. Bekkouche 1992) conclude that Lower Devonian reservoir quality can be related to three separate diagenetic processes, as follows:

(1) The presence of primary chlorite cement coating quartz grains inhibits the deposition of quartz cement, and so leads to preservation of anomalously high permeabilities. Where chlorite cement is thin or absent, quartzification and feldspar alteration usually lead to the blocking of pore throats and a consequent loss of both porosity and permeability.

(2) Carbonate cement may also block pore throats, and carbonate may also replace other minerals. On the other hand, should the carbonate cement be dissolved at a late stage, anomalously high porosities may result.

(3) Clay mineral type seems to have a major influence on permeability. Pore filling by kaolinite may reduce porosity but not materially affect permeability. The presence of fibrous illite, however, usually is associated with a considerable loss in permeability, through the blocking of pore throats. This is also a significant factor for the Cambro-Ordovician reservoir (Djarnia *et al.* this volume).

Data concerning the effects of diagenetic processes on reservoir quality of the Upper Devonian and Triassic reservoirs are not available at this time.

Communication of reservoirs with source

The presence of hydrocarbons in effective traps is clearly dependent on communication with one or more of the two main source rocks in the basin, namely the Silurian and the Upper Devonian shales. The observed distribution of hydrocarbons would indicate that communication can occur in one of three ways:

(a) Through direct contact of Silurian and or Upper Devonian source rocks with potential reservoirs, either through stratigraphic proximity or through juxtaposition on unconformity surfaces, particularly the Hercynian. Migration distances in this model are usually short.

(b) By long-distance updip migration (generally eastwards) from the Hercynian subcrop of the various source rocks, following the regional dip of the Hercynian unconformity surface.

(c) By vertical migration through fault systems.

Model (a) is applicable to most Palaeozoic petroleum occurrences. Within Illizi, the distribution of hydrocarbons within reservoirs shows a strong relationship to proximity to source rocks, with the most prolific reservoirs being the Tadrart–F6 and the Ordovician, which respectively overlie and underlie the Silurian source rock. Communication with the Tadrart is facilitated here by erosion on the Caledonian unconformity. The same trend is true in Libya, where Silurian (Acacus) sands are those in closest proximity to source, with seals within and above these preventing significant vertical migration to higher reservoirs. Carboniferous sands, which are normally significantly separated from the source rocks are, with a few notable exceptions, usually devoid of hydrocarbons.

Model (b) is applicable particularly to Triassic reservoirs directly overlying the Hercynian unconformity (Fig. 17). Over the Algerian central parts of the basin, the productive basal Triassic reservoirs are separated from the Upper Devonian and Silurian sources by a thick shaly Carboniferous section (Figs 18 and 19). Since Cretaceous time, both source rocks in this region are believed to have been in the gas

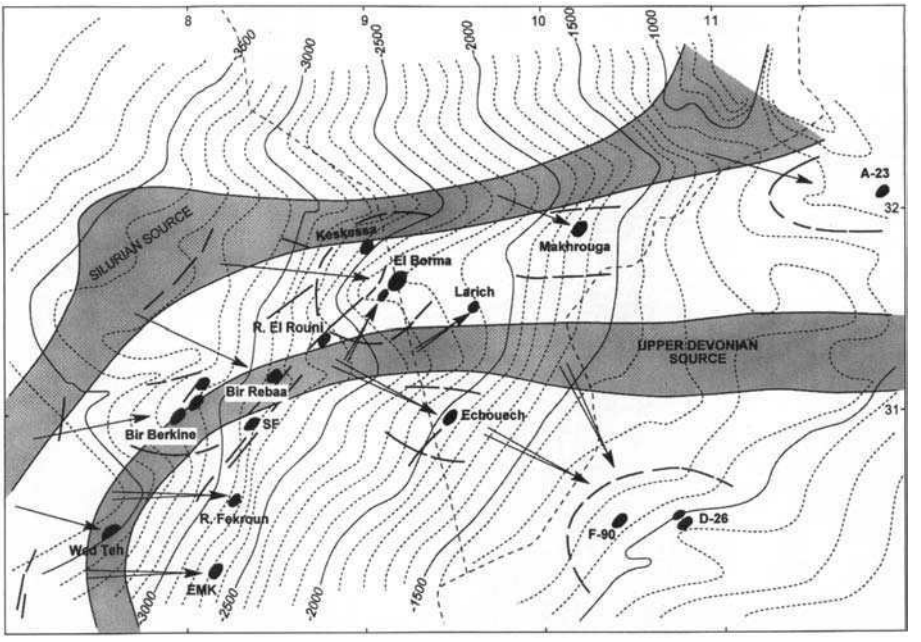

Fig. 17. Structure contour map on the Hercynian unconformity over the central Ghadames Basin. Interpreted long-distance migration paths on the Triassic reservoir are illustrated, originating from the Silurian and Devonian source rock subcrops. Triassic oilfields also tend to be located over structural noses and highs at this level.

window (Chaouche 1991; Taylor 1991; Ghenima & Espitalie 1992; Daniels & Emme 1995). The answer would appear to lie in a model of long-distance migration from the source rock subcrops to the west and northwest, derived from a kitchen that is still in the oil window at the present day (Fig. 17). The proposed migration pathways and spill chains extend many hundreds of kilometres into fields of biodegraded Triassic oil within Libya.

The vertical migration model (c) is supported by the study of the distribution of the Early Devonian oil pools in many areas of significant faulting. Within the central–northern part of the basin, oil is found in the Devonian only in structures that are characterized by the presence of dense fault systems (e.g. Bir Berkine, Rhourde Messaoud and Bir Rebaa fields). These fields are penetrated by a series of faults that cut both the reservoir units and the deeper Silurian source rocks. In other areas of central Algeria and northeastern Libya, where tectonic activity was weak, the Early Devonian has tested only water.

In the Bir Rebaa field, different hydrocarbon compositions are observed within stacked oil pools in the Early Devonian, with the oil in the deeper (Tadrart equivalent) pool lighter than that in the overlying (Ouan Kasa equivalent) pool. A model of active charging up the bounding fault system may here be invoked to explain this.

Influence of tectonic phases

Each of the major tectonic phases has had significant direct or indirect influence on the hydrocarbon habitat of the Ghadames Basin. Some of the main influences are as follows.

Caledonian movements. In late Silurian time, the western and the southern flanks of studied area were uplifted and partially eroded. Subsequent deposition led to the Silurian sands being placed in direct contact with Devonian (Tadrart, lower F6). As a result, Silurian (Acacus) reservoirs often lack a seal. In some fields, such as Mereksene and Stah, Early Devonian (Tadrart) and Silurian (Acacus) reservoirs have common oil–water contacts. This is essentially the main reason why the Early Devonian is the main productive reservoir in Illizi, whereas the Late Silurian is the most productive over large areas of Libya.

Hercynian movements. Hercynian tectonic movements were significant in limiting the extent of

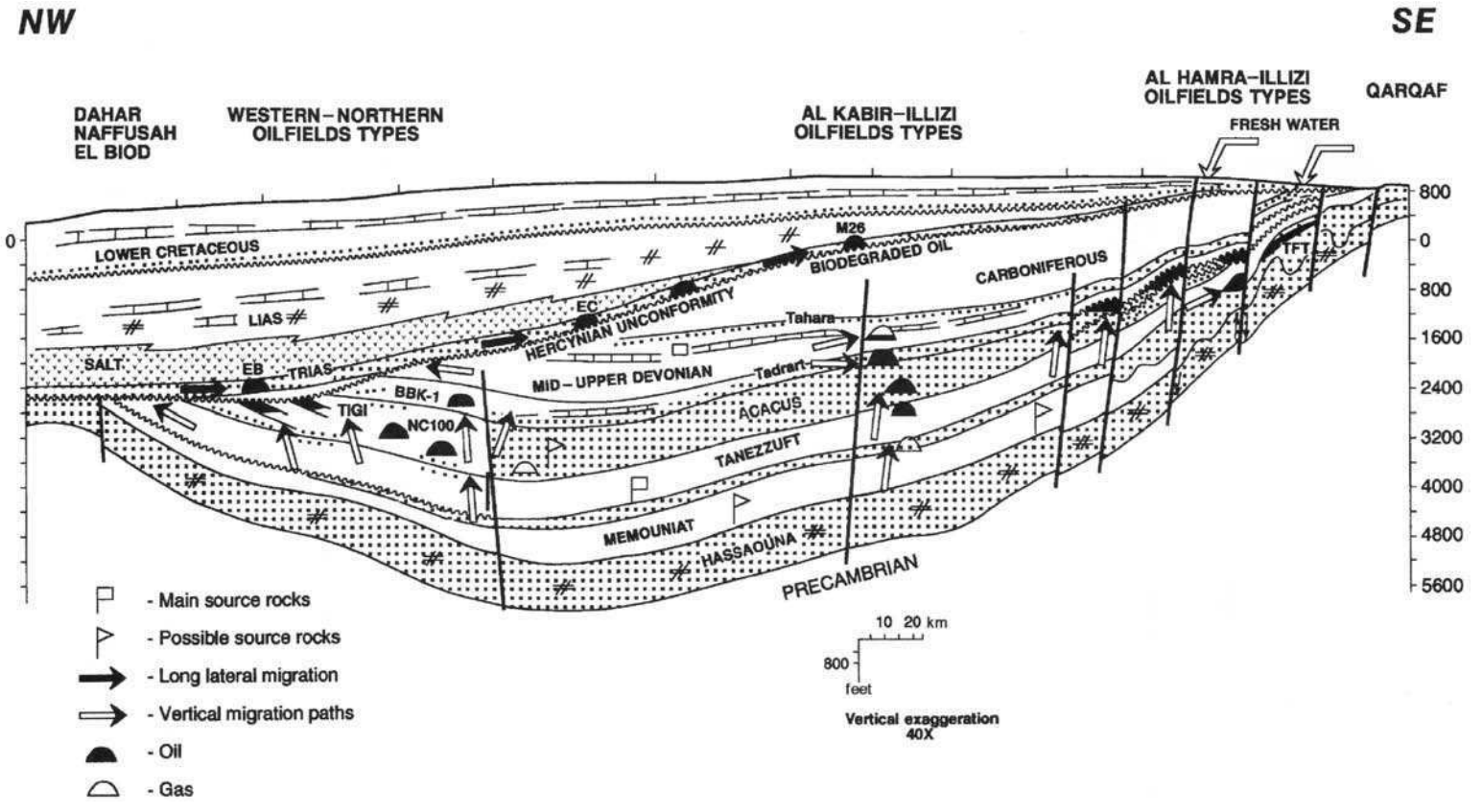

Fig. 18. Sketch summary of play concepts in the Ghadames Basin, illustrating proven and possible source rocks, reservoirs and trap type. Also shown are directions of water influx, which has caused biodegradation of the M-26 oilfield.

the Silurian and Devonian source rocks though erosion and in placing Palaeozoic source rocks and Triassic reservoirs in direct contact over significant areas. The topography developed on the Hercynian unconformity seems to form an important control on migration patterns. Most major Triassic oilfields are located over palaeohighs on the unconformity surface (Fig. 17).

In addition, it is believed that large scale destruction took place of pools filled during Carboniferous time. Various workers (e.g. Daniels & Emme 1995) have modelled generation from Silurian source rocks in central parts of the basin before the Hercynian, and presumably pools were formed in pre-Hercynian structures at this time. In both Libya and Algeria, the Lower Devonian reservoirs are unproductive when partially eroded or not sealed by Upper Devonian and Carboniferous rocks. In such situations, only water and traces of heavy oil have been found.

Figure 19 illustrates the distribution of oil volume across the basin according to various stratigraphic relationships resulting from the Hercynian erosion pattern. It can be seen that the productivity of the Lower Devonian and other Palaeozoic reservoirs increases markedly with increasing stratigraphic separation from the unconformity. The inference drawn from this is that oil pools filled before the Hercynian event have been destroyed in areas of deep erosion. Additionally, during the second (Mesozoic) pulse of generation and migration, oil has tended to migrate up into the Triassic in areas of reduced stratigraphic separation, rather than be trapped in less well-sealed Palaeozoic reservoirs.

For the Triassic reservoirs, it can be noted that the largest number of fields occurs in areas where the Triassic strata are in contact with, or in close stratigraphic proximity to, the Silurian source. This relationship is less well marked, however, because of the effects of long-distance migration mentioned above.

Austrian movements. The Cretaceous movements related to the Austrian phase resulted in the remodelling of Hercynian structural features. This caused the redistribution, through new faults, of hydrocarbons previously entrapped in Hercynian structures in the western flank of the Ghadames Basin (Sonatrach-Beicip 1991).

Hydrodynamic factors

Hydrodynamic regime plays a key role locally on the basin flanks, in areas close to present and former reservoir subaerial exposure. The uplift of the Hoggar (Algeria) and the Al Hamra and Qarqaf Highs (Libya) during the Late Cretaceous led to the exposure of, and freshwater influx into, the Upper Palaeozoic and Trias–Jurassic reservoirs. This influx of meteoric water is of greatest significance for the Lower Devonian, this being the most permeable reservoir in this region. The lower permeability Cambro-Ordovician reservoirs are not as seriously affected.

The meteoric water invasion at Lower Devonian level created a steep hydrodynamic gradient on the southern flank of the Illizi Basin (Chiarelli 1978), probably causing the flushing of low-relief structures in this region. The region of existing large fields in Illizi and Al Hamra (Hammuda 1980; Echikh 1984) seems to have encountered a less intense hydrodynamic gradient, insufficient to flush the high-relief structures present (Echikh 1992). The hydrodynamic traps in the Tin Fouyé-Tabankort region should, however, be noted (Chiarelli 1978; Alem *et al.* this volume).

Within the Triassic reservoirs, fresh water (salinity less than 500–1000 ppm) is observed in the southern part of the basin, passing into brackish water in the F-90 area, and to brine further north. Further evidence of freshwater invasion is given by the presence of biodegraded oil in the Al Kabir area of Libya (Fig. 19).

Conclusions

The present structural framework of the Ghadames Basin was produced by tectonic movements related to the Taconic, Caledonian, Hercynian and Austrian phases. This complex structural history has produced a wide variety of structural styles and trap types. The main factors controlling hydrocarbon habitat are: (1) the effects of these main tectonic phases and the resulting basin topography (particularly at Hercynian level) on stratigraphic column, seal preservation and consequently migration; (2) basin scale reservoir facies variations; (3) diagenetic processes. Different reservoir levels are prospective within fairways covering differing parts of the basin. Ordovician and Devonian reservoirs have the best petrophysical properties on the southern basin flank but decrease in quality into the basin because of increased shaliness and diagenetic effects associated with deeper burial. The Silurian is the most prolific reservoir in northwestern Libya, in a region where source–reservoir–seal relationships are optimized, largely because of preservation of seals below the Caledonian unconformity. Triassic reservoir

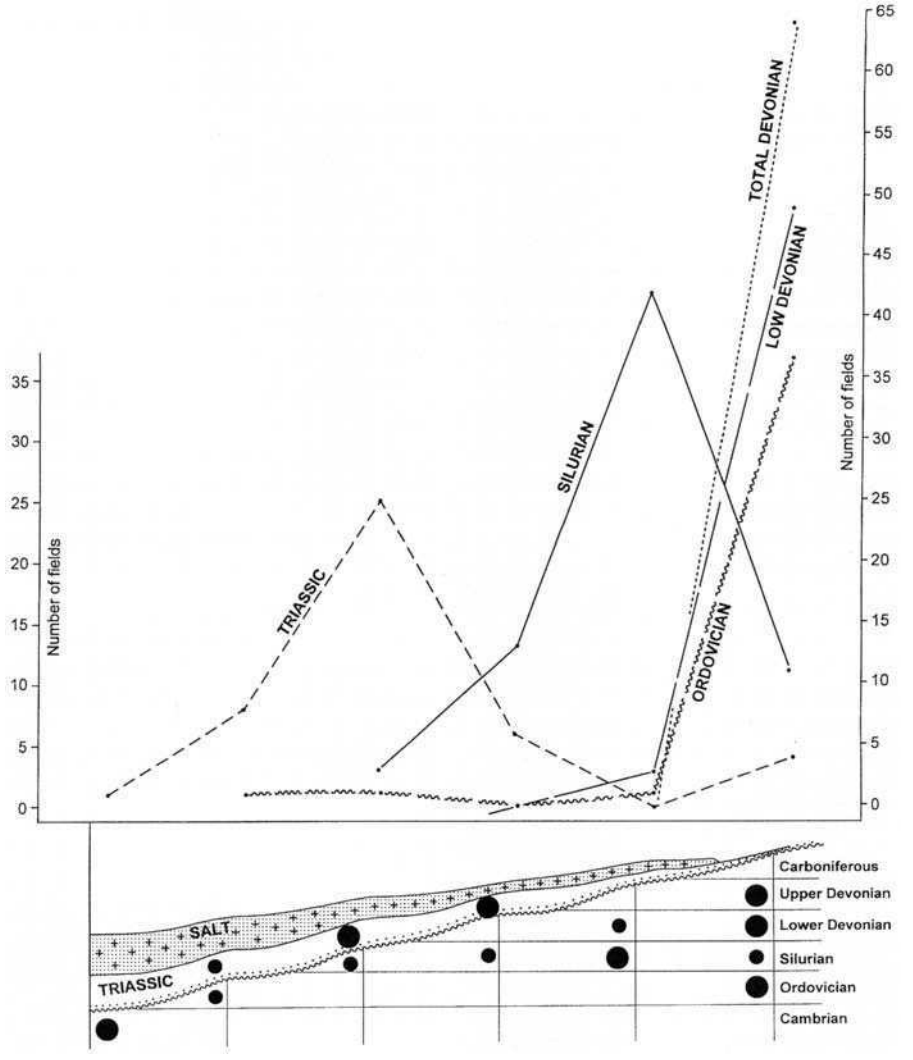

Fig. 19. Relationship between hydrocarbon occurrence and stratigraphic relationships across the Hercynian unconformity. Most Devonian and other Palaeozoic-reservoired oilfields are found in regions where the degree of erosion on the unconformity is light. Substantial destruction of Palaeozoic oilfields may have occurred in areas of deeper erosion.

productivity is controlled mainly by depositional facies, with the braided fluvial facies favoured. Communication with source at this level is controlled by the subcrop pattern on the Hercynian unconformity. Migration distances along this unconformity can be very long.

The recent successes obtained by foreign companies in partnership with Sonatrach in the Algerian portion of the Ghadames Basin confirm the high potential of this region. Further exploration potential in the basin may exist in the various reservoirs, plays and regions, as follows:

(1) The central parts of the basin are still poorly understood, with seismic data quality poor. The Triassic–Liassic evaporite layers in this region prevent the penetration of much of the seismic energy to the Palaeozoic section. If this problem can be resolved, many new traps may be identified. Recent oil discoveries at depths of more than 3500 m in Algeria suggest that much untapped potential may exist in Silurian and Devonian reservoirs in the basin deeps.

(2) The central part of the basin in Libya is still poorly explored, with low seismic and drilling

coverage, because of previous expectations of poor reservoir quality. The successes in Algeria, particularly at Triassic level, upgrade this region.

(3) Whereas the Algerian Illizi basin has a high drilling density and can be considered to be well explored, the analogous southern flank of the basin in Libya is considerably less densely drilled. Further discoveries can be expected in this region.

(4) Discoveries such as the Al Fatah field in Libya, related to sand pinchout, plus the occurrence of a number of subcrop traps, such as Tigi, indicate that the basin has a high potential for further discoveries in stratigraphic traps. Improved understanding of the basin's seismic sequence stratigraphy is required to realize this.

References

ABDESSELAM-ROUIGHI, F. 1991. Biostratigraphie des spores, acritarches et chitinozoaires de Dévonien du Sahara oriental (Algeria). *IIème Séminaire de géologie pétrolière*, Sonatrach 21–23 October, Boumerdès.

ALEM, N., ASSASSI, S. BENHEBOUCH, S. & KADI, B. 1998. Controls on hydrocarbon occurrence and productivity in the F6 reservoir, Tin Fouyé–Tabankort area, NW Illizi Basin. *This volume.*

ATTAR, A. 1987. Evolution structurale du bassin d'Illizi. Internal Exploration Report **2575**, Sonatrach, Algiers.

BEKKOUCHE, A. 1992. *Le Silurien–Dévonien inférieur du Bassin de Ghadamès (Sahara oriental): Lithostratigraphie, Sédimentologie et Diagenèse des réservoirs gréseux.* Doctoral thesis, Université Joseph Fourier, Grenoble .

BENRABAH, B., KERDJIJI, K. & BENCHIEDH, S. 1991. A propos des charactéristiques roches mères de certains niveaux de Trias. *IIème Séminaire de géologie pétrolière*, Sonatrach 21–23 October, Boumerdès.

BOUDJEMA, A. 1987. *Évolution structurale du bassin pétrolier triasique du Sahara nord-oriental (Algérie).* PhD thesis, Université Paris-Sud.

CHANDOUL, H. 1992. Paléogéographie du Paléozoïque dans le sud de la Tunisie et son implication sur le potentiel pétrolièr de la région. *3èmes Journées de l'Exploration Pétrolière en Tunisie*, ETAP, Tunis.

CHAOUCHE, A. 1991. Corrélation huile/roche-mère dans les bassins sédimentaires sahariens. *IIème séminaire de géologie pétrolière*, Sonatrach, 21–23 October, Boumerdès.

CHAOUCHI, R., MALLA, M. S. & KECHOU, F. 1998. Sedimentological evolution of the Givetian-Eifelian (F3) sand bar of the West Alrar field, Illizi Basin, Algeria. *This volume.*

CHIARELLI, A. 1978. Hydrodynamic framework of Eastern Algeria: influence on hydrocarbon occurrence. *Bulletin, American Association of Petroleum Geologists*, **62**(4), 667–685.

DANIELS, R. P. & EMME, J. J. 1995. Petroleum system model, Eastern Algeria, from source to accumulation - when, where and how. *Sonatrach Symposium on Ghadames Basin, Hassi Messaoud, Algeria.*

DJARNIA, M. R. & FEKIRINE, B. 1998. Sedimentological and diagenetic controls on Cambro-Ordivician reservoir quality in the southern Hassi Messaoud area (Saharan Platform, Algeria). *This volume.*

ECHIKH, K. 1975. *Géologie des provinces pétrolifères de l'Algérie.* SNED, Algiers.

—— 1984. *Sedimentological conditions of deposition and petroleum evaluation of Acacus–Tanezzuft reservoirs.* Internal Report, National Oil Company of Libya (NOC),Tripoli.

—— 1987. Geology and habitat of hydrocarbons in western Libya. *Third Symposium on Geology of Libya*, Tripoli University, Tripoli, Libya.

—— 1992. *Geology and hydrocarbon potential of Ghadamis basin.* Internal Report, National Oil Company of Libya (NOC), Tripoli.

FEKIRINE, B. & ABDALLAH, H. 1998. Palaeozoic lithofacies correlatives and seqence stratigraphy of the Saharan Platform, Algeria. *This volume.*

FORD, G.W. & MULLER, W. J. 1995, Potential Silurian and Devonian truncation traps across the Ahara Arch, southwest Ghadames Basin, Algeria. *In: Hydrocarbon Geology of North Africa, Abstracts Booklet*, Geological Society Petroleum Group Conference 1995.

GHENIMA, R. & ESPITALIE, J. 1992. Génération et migration des hydrocarbures dans le bassin de Ghadames. *3èmes Journées de l'Exploration Pétrolière en Tunisie*, ETAP, Tunis.

GUIRAUD, R. 1998. Mesozoic rifting and basin inversion along the northern African Tethyan margin: an overview. *This volume.*

HAMMUDA, O. 1980. Geological factors controlling fluid trapping and anomalous freshwater occurrence in the Tadrart Sandstone, Al Hamada Al Hamra area, Ghadames Basin. *In: Geology of Libya, Vol. 2.* Academic Press, London, 501–507.

MASSA, D. 1988. *Paléozoïque de Libye occidentale: stratigraphie et paléogéographie.* PhD thesis, Université de Nice.

SONATRACH-BEICIP 1975. *Étude structurale et cartographique de bassin d'Illizi, Môle d'El Biod.* Internal Exploration Report, Sonatrach, Algiers.

—— 1991. *Bassin de Ghadames—évaluation pétrolière.* Internal Exploration Report, Sonatrach, Algiers

TAYLOR, M. 1991. An integrated approach to evaluation of geochemical data in the Illizi and Ghadames Basins (Algeria). *IIèmes séminaire de géologie pétrolière*, Sonatrach, 21–23 October, Boumerdes.

This page intentionally left blank

An investigation of the thermal history of the Ahnet and Reggane Basins, Central Algeria, and the consequences for hydrocarbon generation and accumulation

PAUL LOGAN[1] & IAN DUDDY[2]

[1]*BHP Petroleum, Neathouse Place, London SW1V 1LH, UK*
[2]*Geotrack International, 37 Brunswick West, Victoria 3055, Australia*

Abstract: In an attempt to better understand the thermal history of the Ahnet and Reggane Basins, the techniques of apatite fission track analysis and zircon fission track analysis were employed on samples from a number of exploration wells previously drilled in the study area. The results indicated clear evidence for a major heating event at *c.* 200 Ma, overprinted on the effects of heating caused by simple burial before the Hercynian uplift. It is proposed that at least two major phases of hydrocarbon generation took place within the study area; an early, pre-Hercynian phase, in which chiefly liquid hydrocarbons were expelled and a later phase, associated with a 'heat spike' at *c.* 200 Ma, in which significant quantities of dry gas were generated and expelled.

This paper arises from an investigation carried out by BHP and Sonatrach into the hydrocarbon potential of the Ahnet, Timimoun and Reggane Basins of central Algeria. The study encompassed the area shown in Fig. 1. Geographically, the area is located in the Sahara Desert of central Algeria, immediately to the north of the Hoggar and Eglab Massifs. Numerous gas discoveries have been made in the Ahnet and Timimoun Basins of District 3, whereas the Reggane Basin of District 7 has been explored to a lesser degree and to date, only a few wells on the northern fringe of the basin have encountered gas with minor oil shows. Adjacent to the northern part of District 3, on the western side, is the area known as the Cuvette de Sbaa, which contains several proven oilfields, none of which are yet in production.

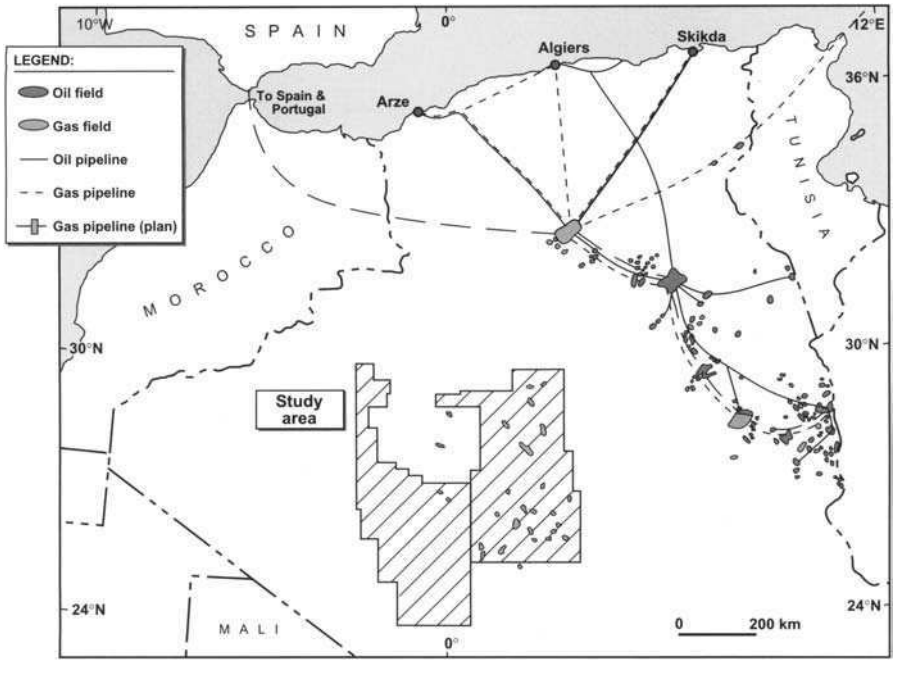

Fig. 1. Location map.

LOGAN, P. & DUDDY, I. 1998. An investigation of the thermal history of the Ahnet and Reggane Basins, Central Algeria, and the consequences for hydrocarbon generation and accumulation. *In*: MACGREGOR, D. S., MOODY, R. T. J. & CLARK-LOWES, D. D. (eds) 1998. *Petroleum Geology of North Africa*. Geological Society, London, Special Publication No. 132, 131–155.

A key aim of the study was to investigate the thermal histories of these basins and to determine the consequences of those histories for the generation, migration and accumulation of significant volumes of hydrocarbons in the study area. BHP and Sonatrach were also keen to investigate the relationship (if any) between the study area and the small oilfields encountered in Palaeozoic reservoirs in the Cuvette de Sbaa. To this end it was decided to employ the techniques of apatite fission track analysis (AFTA) and zircon fission track analysis (ZFTA) in an attempt to shed light on the thermal history of these basins.

Regional geology

The main structural elements and major basin lineaments relevant to the study area are shown in Fig. 2. The Ahnet Basin is one of a series of north–south trending basins and basement highs that exist in central and southern Algeria. The basin is northerly dipping with Cretaceous and Tertiary-Quaternary cover to the north and the Precambrian Hoggar Mountains to the south. It contains thick Palaeozoic sequences of Cambrian to Carboniferous age which include potential hydrocarbon reservoirs, source rocks and seals, together providing an excellent setting for a hydrocarbon-bearing basin.

The structural trend in the basin is dominantly north–south controlled by major sub-vertical basement lineaments. To the north of the outcrop area, the basin exhibits a more significant northwesterly trend. The structures take the form of large, elongate anticlines and domes formed compressionally, probably as a result of the Austrian tectonic event or possibly Variscan compression.

The generalized stratigraphy of the Ahnet and Reggane Basins is shown in Fig. 3. In both basins, the thickness of the preserved sedimentary sequence has been considerably modified by erosion associated with Hercynian, Austrian and Tertiary (Atlassic) earth movements.

In the Ahnet and southern Timimoun Basins, the pre-Hercynian sequence comprises Cambrian to Visean and possibly Early Namurian rocks. The thickest sequence is preserved in the north of the Ahnet Basin, with over 3000 m of Palaeozoic sediments overlying Precambrian basement at a depth of some 4000 m. The Hercynian unconformity cuts down the sequence from north to south, with only some 2000 m of Palaeozoic section having been preserved in the south of the basin (Fig. 4).

In the Reggane Basin, the pre-Hercynian sequence also comprises Cambrian to Early Namurian rocks. The basin is an asymmetric syncline (Fig. 5), with a heavily faulted northern margin, and is bounded to the north by a reverse fault complex marking the edge of the uplifted

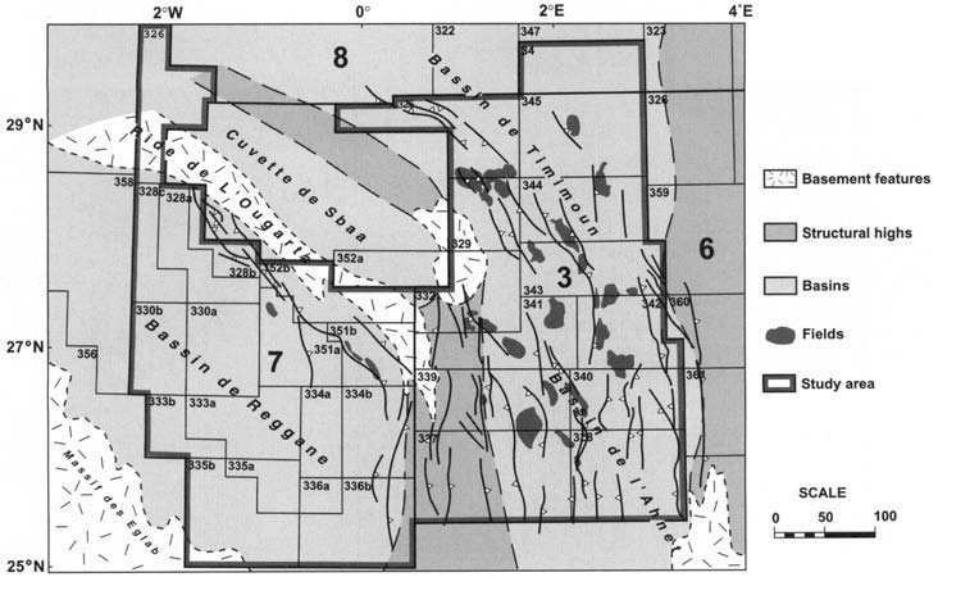

Fig. 2. The main tectonic elements of the Reggane and Ahnet Basins.

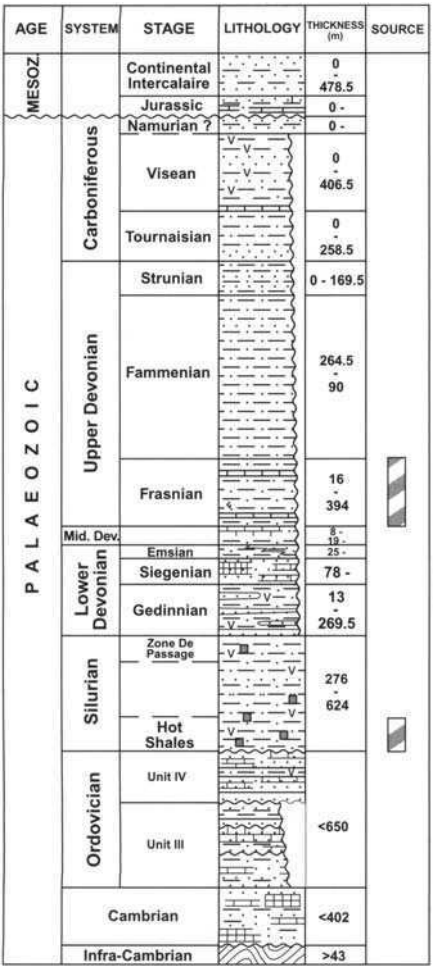

Fig. 3. Stratigraphic column

Ougarta Ridge. The thickest sequence occurs in the north of the Reggane Basin, where over 5000 m of Palaeozoic sediments are known to be present and where the Precambrian is estimated to be at a depth in excess of 6000 m.

In both basins, basement of Precambrian–Early Cambrian age is overlain by a Cambro-Ordovician sequence of both marine and continental sediments for which well control is sparse. This is overlain by thick, Silurian marine shales which in the Reggane Basin, may exceed 800 m in thickness, although no well has yet reached the base of the sequence in the basin depocentre. In the Ahnet Basin, a maximum thickness of 1000 m of Silurian sediments have been penetrated.

During the Silurian, restricted anoxic conditions led to the deposition of highly radioactive 'hot shales' which reach a maximum thickness of 70–80 m in the Ahnet Basin and may exceed 100 metres in the north of the Reggane Basin (Fig. 6). These 'hot shales' are known to have formed a significant hydrocarbon source rock for the Reggane and Ahnet Basins, as will be discussed below.

Towards the end of Silurian times, the Caledonian orogeny resulted in local uplift and the formation of significant local topography with a general tilt to the north. The sea retreated to the north and northwest, and the resulting shallow marine–continental conditions persisted throughout Lower and Middle Devonian times.

The Late Devonian succession was deposited in fully marine conditions which spread across the entire area, resulting in the deposition of a thick sequence of claystones. During the Late Devonian, the Reggane and Ahnet Basins were the principal depocentres in southern and central Algeria. During Frasnian times, continued uplift of the basin margins resulted in the development of restricted anoxic conditions leading to the deposition of a series of radioactive 'hot shales'. The Frasnian sequence reaches a maximum thickness of almost 700 m in the west of the Ahnet Basin and a little over 400 m in the Reggane Basin. The 'hot shales' occur in the lower part of the Frasnian sequence and are generally at least 50–100 m in thickness. They are best developed in the eastern and central parts of the Ahnet Basin, reaching a maximum thickness of some 300 m (Fig. 7), and are believed to be important hydrocarbon source rocks. In the Reggane Basin, the Frasnian 'hot shales' appear to be less well developed, with a maximum thickness of 231 m encountered in the sparsely drilled centre of the basin.

Mud-dominated marine deposition continued throughout the remainder of the Upper Devonian in both the Ahnet and Reggane Basins. During Strunian times, a major period of regression associated with the Bretonian phase of the Hercynian orogeny resulted in a return to shallow marine conditions. Uplift occurred on basin margins and at this time, the Ougarta region became a significant high.

Shallow marine conditions persisted throughout the Tournaisian and Visean, whereas in the Reggane Basin, the Visean sequence is also considerably affected by the presence of igneous sills, particularly in the Djebel Heirane area.

The end of the Visean seems to have been marked by a pronounced lowering of sea level and a consequent regressive phase in the Namurian. Rapid deposition continued in the Reggane Basin where up to 1000 metres of Namurian sedi-

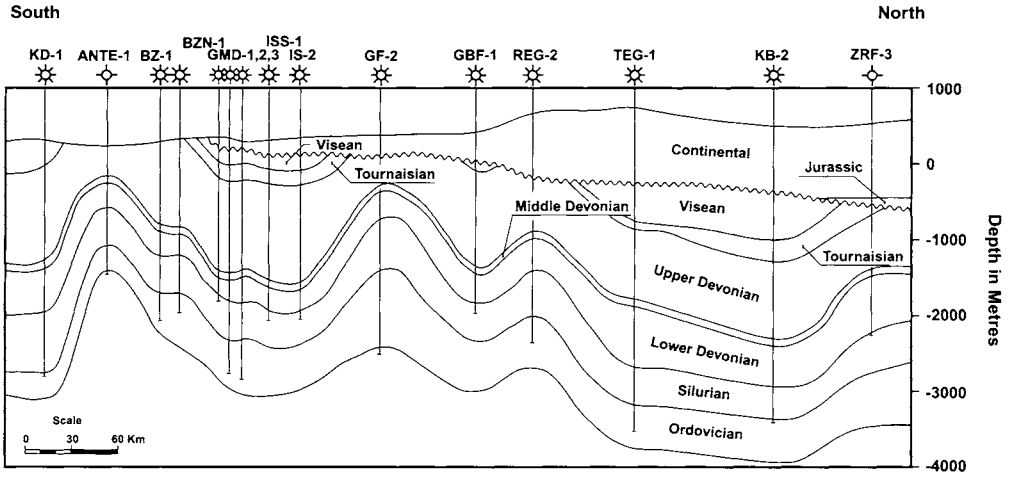

Fig. 4. Schematic cross-section of the Ahnet Basin.

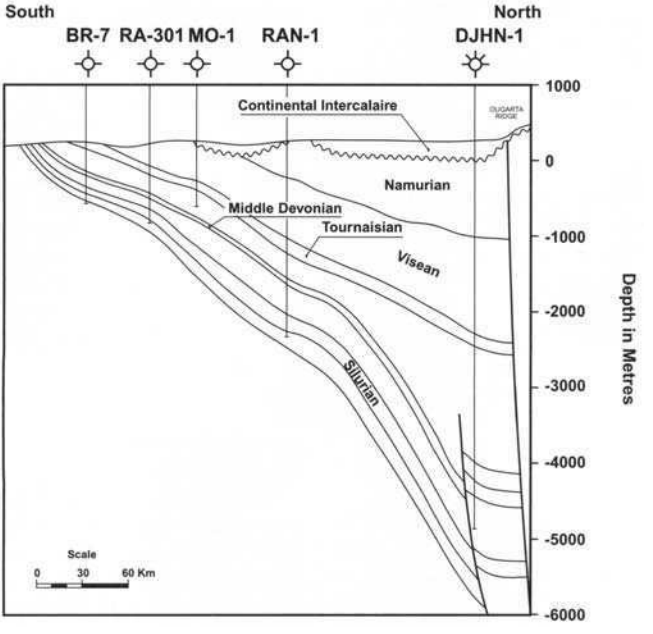

Fig. 5. Schematic cross-section of the Reggane Basin.

ments are preserved. In the Ahnet Basin, the Namurian section appears to be restricted to a northwest–southeast trending trough in the north of the basin. Drilling has shown that over 400 m is preserved in some areas.

At the end of Carboniferous times, the Hercynian orogeny resulted in some uplift, folding and faulting. The uplift caused considerable erosion of the existing stratigraphy. As will be discussed below, the magnitude of this unconformity was significantly increased by later periods of uplift and deformation. As shown in Fig. 4, the enhanced Hercynian Unconformity cuts down the sequence from north to south and with the exception of the extreme northeast of the Ahnet Basin, is overlain by the Cretaceous Continental Intercalaire or younger Tertiary rocks. Many areas, including the Ougarta Ridge, which continued to rise, remained areas of non-deposition until the present day.

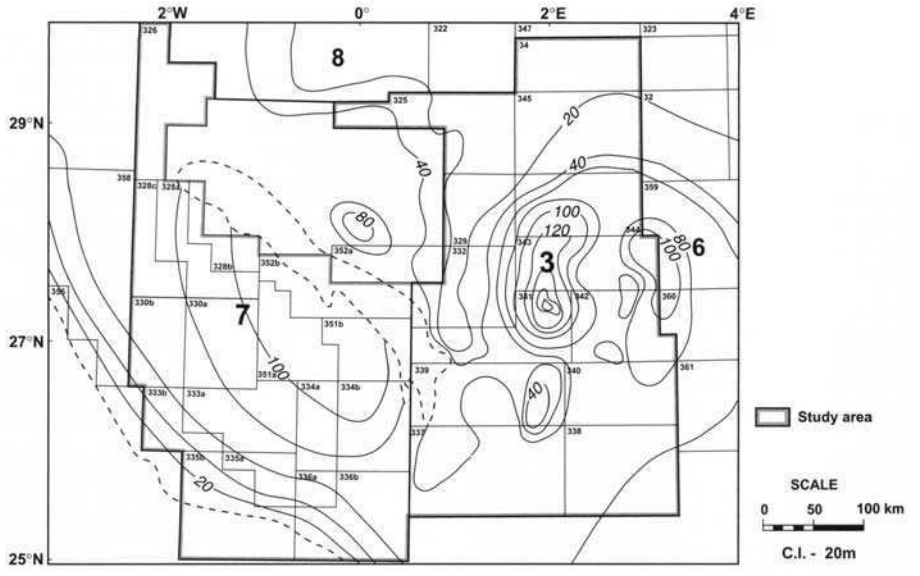

Fig. 6. Silurian hot shale isopach map.

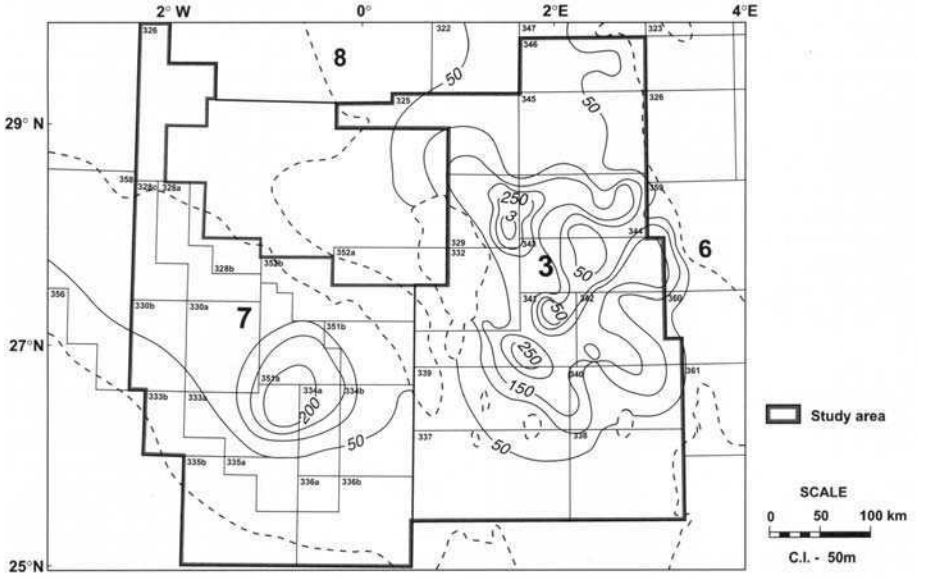

Fig. 7. Frasnian hot shale isopach map.

No sediments of Permo-Triassic age are known from the Ahnet and Reggane Basins. In the north of the Ahnet Basin, however, some 200–230 m of assumed Early–Middle Jurassic sediments were encountered, comprising claystones with some thin sands at the top of the succession. These were in turn overlain by 600–700 m of Early Cretaceous sandstones, succeeded by 260–300 m of Cenomanian–Turonian mudstones.

Discussion

In previous reviews of the burial history of the Palaeozoic section in both the Ahnet and Reggane Basins, it has been widely accepted

that this history was dominated by the Hercynian orogeny, which, it was assumed, resulted in considerable uplift and erosion at the end of the Carboniferous. It was previously considered that the basins achieved maximum burial at this time and thus the source rocks reached their present state of maturity before the Hercynian and later episodes of uplift. Data resulting from the apatite and zircon fission track analyses carried out by Geotrack Inc on behalf of BHP and BP, together with associated organic reflectance measurements, have revealed the possibility of a far more complex thermal history for these basins.

Present-day heat flow is considerably greater in central Algeria and in the Ahnet Basin in particular, than in the rest of northwest Africa. It is also clear that present geothermal gradients are relatively low at 34–45°C/km in the Ahnet Basin and 26–30°C/km in the Reggane Basin when compared with palaeogeothermal gradients, which in some cases, reached 60–70°C/km. These very high heat flows undoubtedly contributed to the advanced state of maturation which is seen in the Lower Palaeozoic section.

As the timing of maximum palaeotemperatures within sequences containing prospective hydrocarbon source rocks generally coincides with maximum hydrocarbon generation, good control on the timing is a critical factor in assessing regional hydrocarbon prospectivity. Areas where the main phase of hydrocarbon generation occurred after structures were formed will clearly be more prospective than areas where structures post-date hydrocarbon generation.

To investigate the evidence of past thermal events in the rock record, it was decided to employ the techniques of AFTA and ZFTA, together with a study of whatever organic maturity data could be obtained from wells previously drilled in the study area.

Methods

AFTA and ZFTA rely on analysis of radiation damage features ('fission tracks') in detrital apatite and zircon grains, respectively, within sedimentary rocks. Fission tracks are produced continuously through geological time, as a result of the spontaneous fission of U impurity atoms. Once formed, tracks are shortened (annealed) at a rate which depends on temperature, and the final length of each individual track is determined by the maximum temperature which that track has experienced. Therefore as the temperature to which an apatite or zircon grain is subjected increases, all existing tracks shorten to a length determined by the prevailing temperature, regardless of when they are formed. After the temperature has subsequently decreased, all tracks formed before the thermal maximum are 'frozen' at the degree of length reduction they attained at that time.

For apatite, rocks which have been heated to a maximum palaeotemperature less than ≈110°C (the precise value depends on the chlorine content of the apatite grain) at some time in the past and subsequently cooled will contain two populations of tracks: a shorter component formed before the thermal maximum and a longer component representing tracks formed after cooling. The length of the shorter component indicates the maximum palaeotemperature, and the proportion of short to long tracks indicates the timing of cooling in relation to the total duration over which tracks have been retained. More complex thermal histories result in more complex distributions of track length. If the maximum palaeotemperatures exceeds ≈110°C, all tracks are totally annealed, and tracks are only retained once the sample cools below this temperature once more.

In zircon, fission tracks are more stable, and maximum paleotemperature must exceed ≈300°C (corresponding to vitrinite reflectance values of at least 5% R_0(max) before all tracks are totally annealed, with the time of cooling below ≈300°C indicated by the number of tracks accumulated since cooling began.

The annealing kinetics of fission tracks in apatite during geological thermal histories is well understood, onon the basis of study of the response of fission tracks to elevated temperatures both in the laboratory (Kaslett *et al.*, 1982, 1987; 1989*b*; Green *et al.* 1986; Duddy *et al.* 1988; Green, 1988) and in geological situations (Gleadow & Duddy 1981; Gleadow *et al.* 1986; Green *et al.* 1989*a*). Natural apatites essentially have the composition $Ca_5(PO4)_3(F,OH,Cl)$. The amount of chlorine in the apatite lattice exerts a subtle compositional control on the degree of annealing, with apatites richer in fluorine being more easily annealed than those richer in chlorine. The result of this effect is that in a single sample, individual apatite grains may show a spread in the degree of annealing, and the data are interpreted using proprietary multi-compositional kinetic equations based both on laboratory annealing studies on a range of apatites with different Cl contents, and on observations of geological annealing in apatites from a series of samples from exploration wells in which thermal histories are simple and well understood.

In studies such as that described in this paper, AFTA and ZFTA thermal history evaluation provides direct determination of the timing (as well as the magnitude) of maximum palaeotemperatures. When combined with conventional maturity indicators, particularly vitrinite reflectance (VR), AFTA and ZFTA allow identification and characterization of the major episodes of heating and cooling that have affected a sedimentary sequence. Specifically, the technique of thermal history reconstruction provides the following information: magnitude of maximum palaeotemperatures in individual samples; timing of cooling from maximum palaeotemperatures; the style of cooling from maximum palaeotemperatures (fast or slow); characterization of mechanisms of heating and cooling; palaeogeothermal gradients; section removed by uplift and erosion (where appropriate); reconstructed thermal and burial/uplift histories based on these factors. Using

this information the thermal history of likely hydrocarbon source rocks can be reconstructed with confidence, on the basis of measured variables, rather than relying on modelled results which often have little rigorous basis. The resulting improvement in assessment of hydrocarbon prospectivity is clearly beneficial in reducing exploration risk.

A key element in the thermal history reconstruction is the interpretation of the palaeotemperature profile (i.e. the palaeogeothermal gradient), which allows the mechanisms of heating (e.g. deeper burial, elevated heat floor or fluid movements) and cooling (uplift and erosion, decrease in heat flow, or cessation of fluid flow) to be deduced (Duddy et al. 1991, 1994; Bray *et al.* 1992; Green *et al.* 1995).

Two typical end-member cases are illustrated in Fig. 8. A measured palaeogeothermal gradient the same as the present-day geothermal gradient but displaced to higher temperatures is indicative of heating caused by deeper burial followed by uplift and erosion (see Fig. 8a). A measure, palaeogeothermal gradient higher than the present-day geothermal gradient that intersects the present-day ground surface at a palaeotemperature similar to the present-day surface temperature is indicative of heating caused predominantly by higher heat flow with cooling caused by decline in heat flow (see Fig. 8b). In detail, the timing of cooling determined using AFTA or ZFTA is critical in allowing the absolute magnitude of uplift and erosion to be attributed to a particular unconformity and quantified.

Although this technique allows the main elements of a basin's thermal history to be reconstructed, thermal history techniques in general (i.e. fission track analysis, VR, biomarkers, hydrocarbon generation, etc.) cannot currently give quantitative information on either the duration of heating or the thermal history before time of maximum palaeotemperatures, as illustrated in Fig. 9.

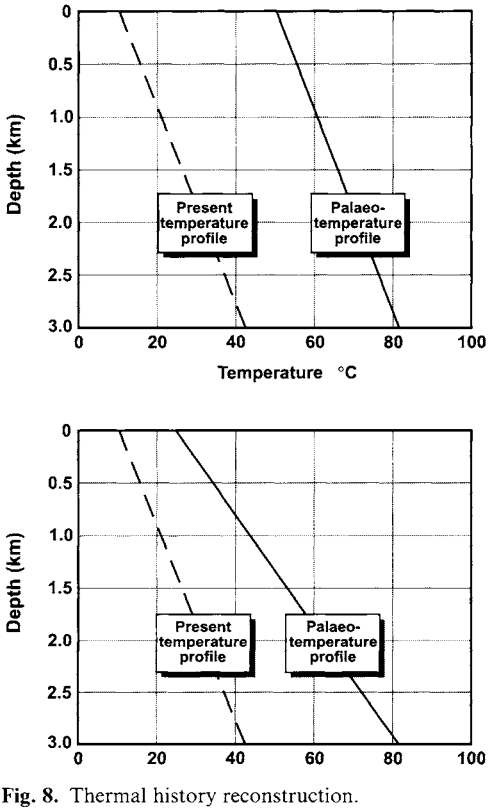

Fig. 8. Thermal history reconstruction.

Results

The results of the AFTA and ZFTA studies have identified a major period of heating at about 200 Ma (Late Triassic–Early Jurassic) which affected the Palaeozoic section. This heating event involved very high geothermal gradients over a large part of the study area, which implies a phase of regional heating.

In summary, the principal events in the burial and thermal histories of the Reggane and Ahnet Basins are thought to be as follows:

(1) Modest geothermal gradients during Devonian–Carboniferous times. Increased burial led to the onset of thermal maturation in the Lower Palaeozoic sequence with early oil generation and possibly gas generation from Ordovician, Silurian and Devonian source rocks in deeper parts of the Ahnet and Reggane Basins and in the Sbaa Basin.

(2) Hercynian uplift was probably relatively minor over much of the area, significant effects being largely confined to the Sbaa Basin and the northern Ahnet Basin (Table 1). A modest increase in heat flow, accompanied by deposition and increased depth of burial before the uplift, was followed by a cooling phase and a suspension of hydrocarbon generation.

(3) During the Permo-Triassic, little or no deposition occurred and no further generation of hydrocarbons took place during this period.

(4) In Late Triassic times, a major thermal event took place. Igneous rocks were extensively intruded in the Reggane Basin, as discussed above, and in the north of the Ahnet Basin, increased heat flow resulted in very high geothermal gradients in excess of 100°C/km! The causes, magnitude and duration of this heat pulse are unknown, but it was probably related to continental 'under-plating' or introduction of hot material into the crust beneath central Algeria. Although this event was probably of relatively short duration, the thermal effects were considerable. Source rocks were rapidly heated beyond the threshold for hydrocarbon generation, and existing liquid hydrocarbons were cracked to

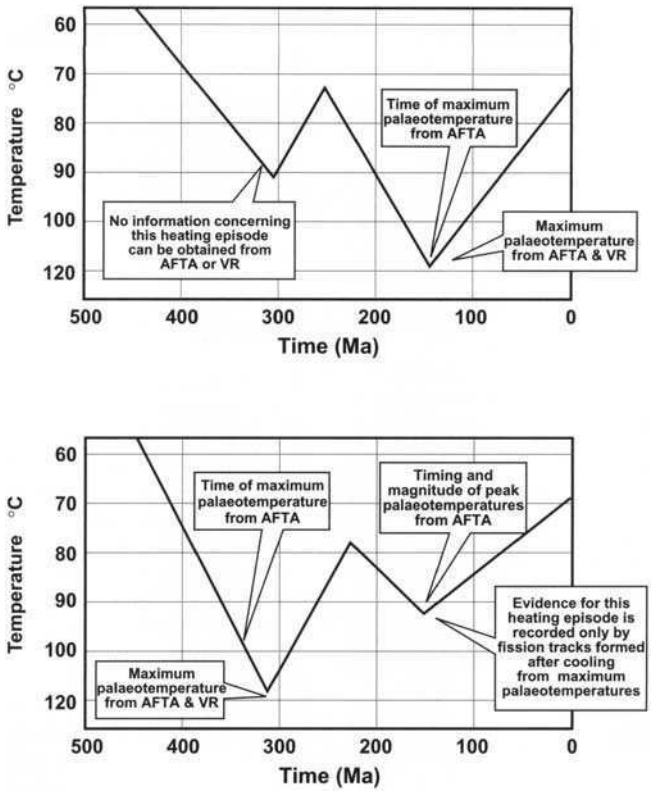

Fig. 9. Cooling history plots.

gas. It seems likely that the Sbaa Basin remained structurally high after the Hercynian event and was therefore not affected by this Late Triassic event. It is probable that no further maturation took place in the Sbaa Basin.

(5) The thermal event was followed by a Late Triassic–Early Jurassic phase of deformation which folded the recently intruded sills and increased the amount of uplift and erosion at the existing Hercynian unconformity.

(6) Further deposition in the Jurassic and Early Cretaceous may have been confined to the northwest of the Ahnet Basin, but was, in any case, modified by a further phase of uplift in mid-Cretaceous times, which resulted in the removal of yet more section at the Hercynian unconformity.

(7) post mid-Cretaceous deposition resulted in modest burial and heating of the section, insufficient to increase maturity.

(8) Finally, Tertiary inversion led to uplift and erosion of Cretaceous sediments.

The location of the geochemical study wells is shown in Fig. 10, and the paleotemperature profiles obtained for some of the study wells are given in Figs 11–14.

These profiles, which show present geothermal gradient, together with the estimates of palaeotemperature derived from AFTA, ZFTA and vitrinite reflectance measurements, give clear evidence in each case of the sampled section having cooled from elevated palaeotemperatures after deposition. In the case of reflectance measurements, it should be noted that, as land plants appeared in the Late Devonian–Carboniferous, true vitrinite cannot be identified in sections older than this. Measurements in the older Palaeozoic section, therefore, rely on other organic matter. In this study, reflectance measurements were made on graptolites, which appear to overestimate palaeotemperature, and on chitinous material, which appears to underestimate palaeotemperature.

The highest estimates of palaeotemperature occur in wells ECF-1 and ZRFW-1 (Figs 11 and 12) where palaeotemperatures in excess of 300°C are recorded. It is equally clear that in the west of the Ahnet Basin, for example at

Table 1. *Estimates of removed sections for major events in the thermal history of central Algeria*

Well	Removed section estimates		
	Hercynian (m)	Early Jurassic (m)	Tertiary (m)
Area A: Timimoun–N Ahnet Basin			
AFF-1	No evidence	1243 (648–2792)	600
KB-2	No evidence	849 (418–1555)	1400
MJB-1	No evidence	1181 (533–2566)	600
TEG-1	No evidence	906 (679–1261)	480 (193–1079)
ZRFW-1	No evidence	690 (590–799)	800
ECF-1	> 2500	874 (369–1294)	> 895
Area B: Eastern Ahnet Basin			
IS-2	No evidence	1059 (802–1387)	600
Area C: Southern Ahnet Basin			
ANT-1	No evidence	740 (637–911)	1000
BH-3	No evidence	1812 (1066–3438)	1350
Area D: Western Ahnet Basin			
MSR-1	No evidence	No quantitative analysis possible	740 (395–1426)
OTLH-1	No evidence	896 (686–1254)	84 (< 441)
Sbaa Basin			
OTRA-1	840 (545–2003)	925 (> 112)	321 (107–1119)
Reggane Basin			
RG-1	No evidence (4527–1890)	702	> 446

OTLH-1, much lower palaeotemperatures were experienced, leading to a somewhat less mature section, as will be discussed below.

In the Reggane Basin, paleotemperature profiles, as in the case of RG-3, have been locally severely modified by the effect of Late Triassic intrusions, which are common in the central and northern parts of that basin (Fig. 13).

Data from OTRA-1 in the Sbaa Basin (Fig. 14) indicates that palaeotemperatures were generally much lower than in the surrounding basins, probably because of the continued relative elevation of this area since Silurian times.

Figures 15–18 show the reconstructed thermal histories of a number of wells within the study area. In each case, the AFTA–ZFTA data provide evidence for two important phases of heating, or more correctly, cooling. These correspond to the Late Triassic–Early Jurassic event at about 200 Ma and the Late Cretac-

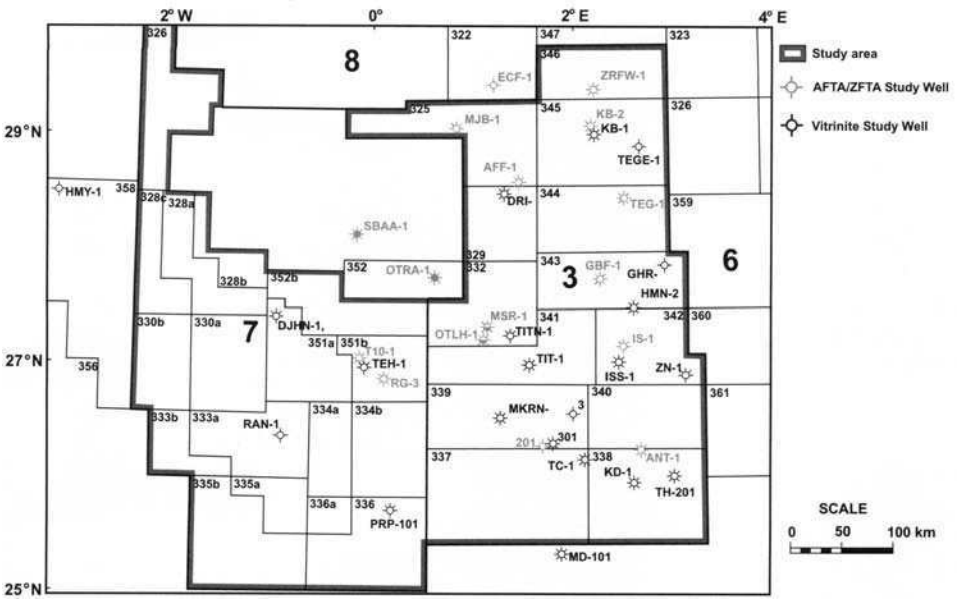

Fig. 10. Well database map.

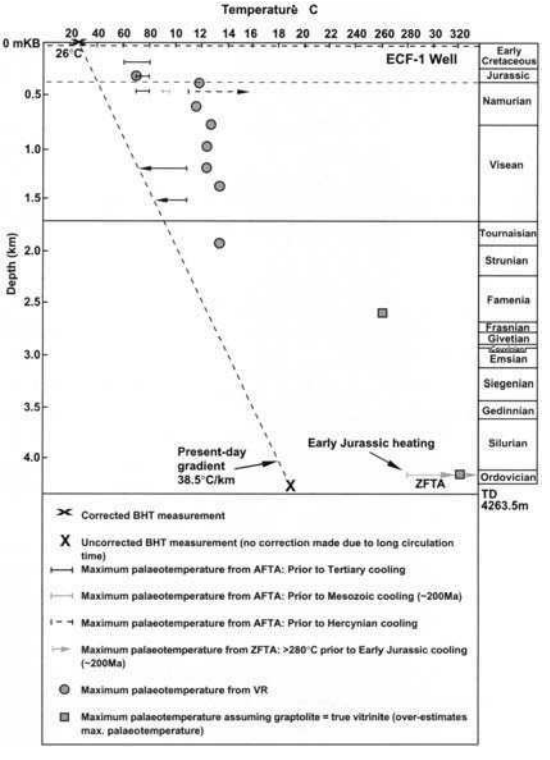

Fig. 11. Palaeotemperature profile for well ECF-1. TD, Total depth.

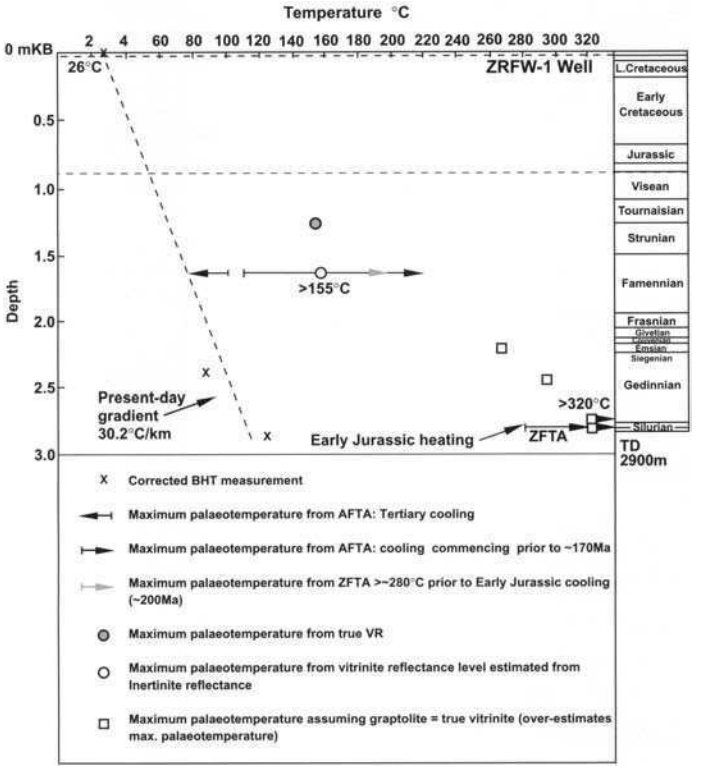

Fig. 12. Palaeotemperature profile for well ZRFW-1.

eous–Early Tertiary event, as mentioned in the summary above. In some cases, evidence exists for a possible early event, the 'Hercynian event'.

As discussed above, it had previously been assumed that the major heating event to affect the Ahnet and Reggane Basins had occurred before Hercynian uplift and erosion, implying a mid–late Carboniferous timing with the consequence of significant oil and gas generation and migration having occurred before this event.

This hypothesis was given currency by an earlier AFTA study carried out by BP. Because of the high degree of Tertiary heating observed in the wells analysed in this study, the AFTA data gave virtually no control on the timing of this early event, other than to identify it as pre-Cretaceous. It was clear, however, that a pre-Cretaceous heating event had occurred and this was assumed to be earlier than the Hercynian uplift. In particular, ZFTA results from a single sample in well MJB-1 (Fig. 16) gave an age of 310 ± 31 Ma. This was seen as compatible with the assumed timing of Hercynian tectonism and was interpreted as a complete overprinting of the zircon system, with cooling at that time.

Wells chosen for the BHP study had experienced less Cretaceous burial and heating and therefore provided better data on the timing of this early event, which complemented the BP data set. Clear evidence was obtained from wells TEG-1 and ZRFW-1 showing the youngest fission track ages to be *c.* 200 Ma, in Late Triassic times (Figs 17 and 18). Figure 19 shows that the Reggane Basin is considered to have undergone a similar thermal history to the Ahnet and Timimoun Basins. It is now considered, therefore, that although a Hercynian event occurred, it was of less significance, in terms of regional heating, than the Late Triassic event at 200 Ma, which was followed by Early Jurassic tectonism.

Evidence from well OTRA-1 (Fig. 20) in the Sbaa Basin indicates that the measured maturity levels may be attributed to heating before the known Hercynian uplift. This was due to either post-Namurian burial by up to 2000–2500 m of section which was subsequently removed with the Hercynian uplift, or a similar amount of uplift which took place between the Silurian and the Namurian to remove an older unknown section. Thus the observed maturities may have

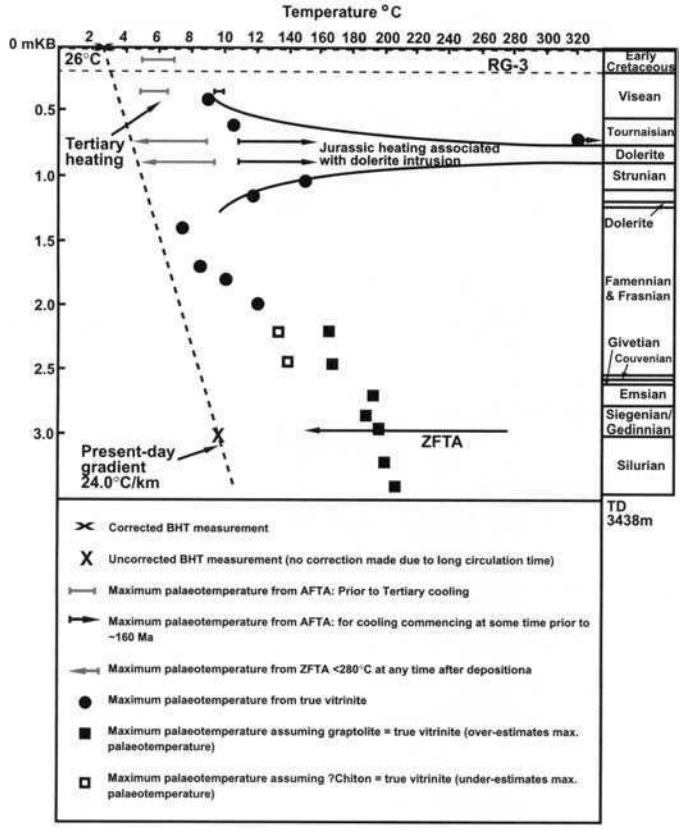

Fig. 13. Palaeotemperature profile for well RG-3.

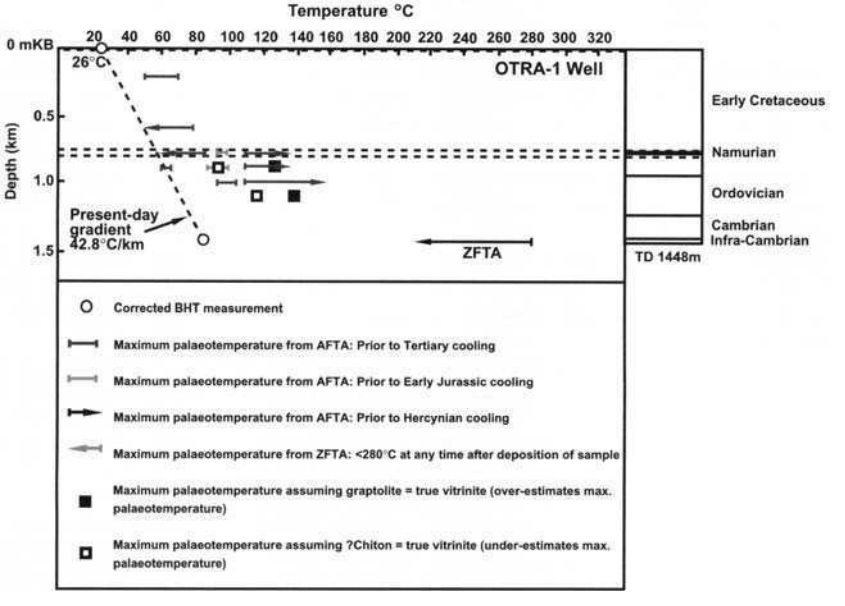

Fig. 14. Palaeotemperature profile for well OTRA-1.

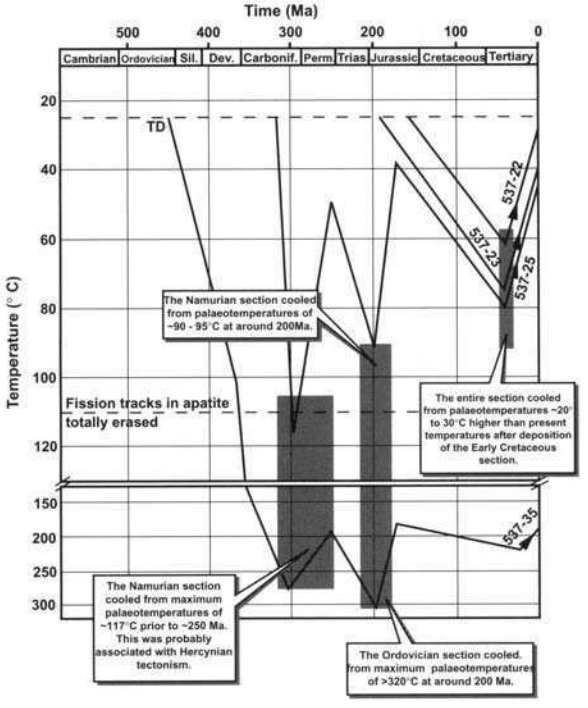

Fig. 15. Schematic illustration of the thermal history reconstruction for well ECF-1 based on AFTA, VR and ZFTA data.

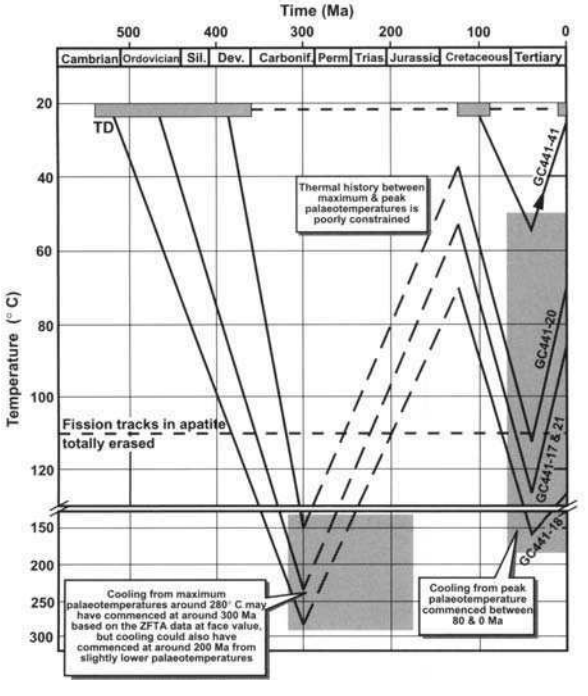

Fig. 16. Schematic illustration of the thermal history reconstruction for well MJB-1 based on AFTA, VR and ZFTA data.

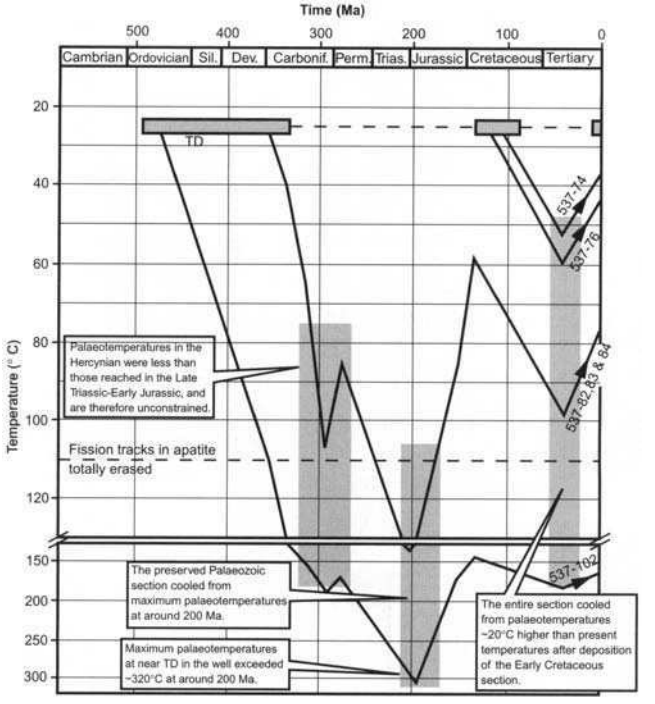

Fig. 17. Schematic illustration of the thermal history reconstruction for well TEG-1 based on AFTA, VR and ZFTA data.

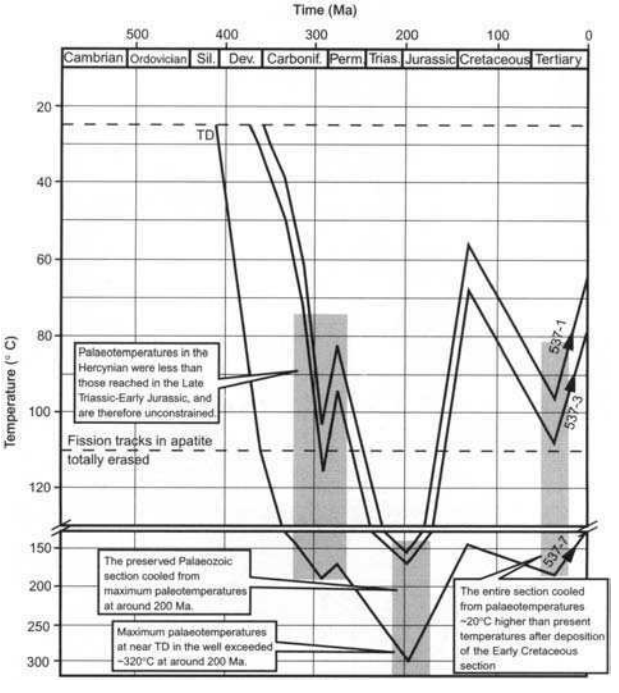

Fig. 18. Schematic illustration of the thermal history reconstruction for well ZRFW-1 based on AFTA, VR and ZFTA data.

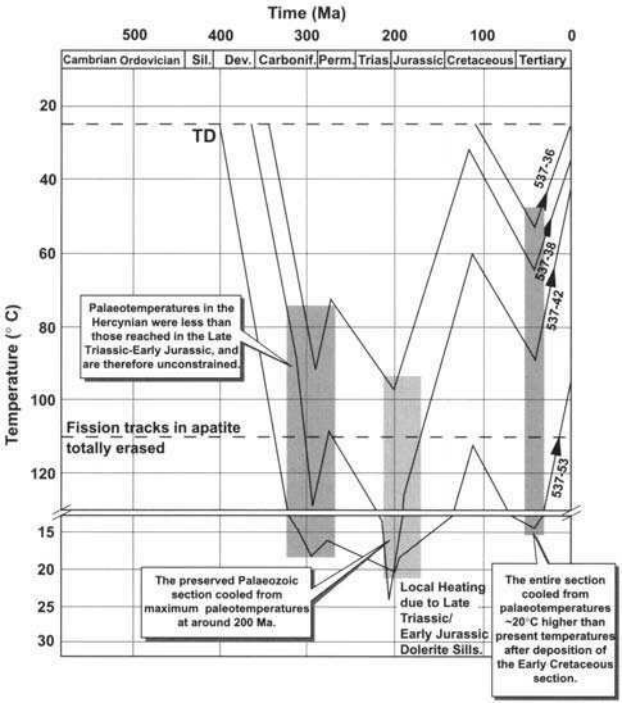

Fig. 19. Schematic illustration of the thermal history reconstruction for well RG-3 based on AFTA, VR and ZFTA data.

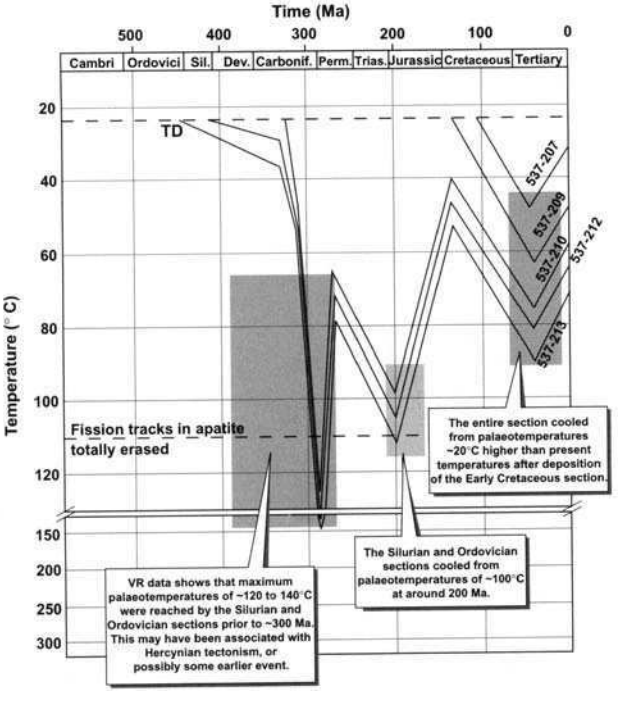

Fig. 20. Schematic illustration of the thermal history reconstruction for well OTRA-1 based on AFTA, VR and ZFTA data.

been achieved in some otherwise unknown post-Silurian, pre-Hercynian event, although this seems unlikely.

The strong evidence for the late Triassic heating event from the majority of study wells indicates that this was an important, regional event. Figure 21 shows the constraints on the palaeogeothermal gradients associated with this event. Values in the range 60–80°C/km are typical, representing a considerably greater heat flow than at present.

Determining the cause of this important event is problematic. Stratigraphic evidence suggests that it was probably not accompanied by major deposition and significant increased burial, and no Triassic rocks are known from the area, even where the Jurassic is thought to be preserved. Two possible explanations present themselves. Either the region underwent a large increase in basal heat flow or the heating was linked to the voluminous emplacement of intrusive igneous rocks in the Reggane Basin. As mentioned above, doleritic intrusions are common throughout the Reggane Basin and local heating effects are clearly visible from the geochemical data, as in the case of RG-3 (Fig. 13). No such intrusive rocks are known from the Ahnet Basin, although the high levels of thermal maturity seen in some of the northern wells, with coke textures being observed in organic material from some wells, may indicate underlying intrusions.

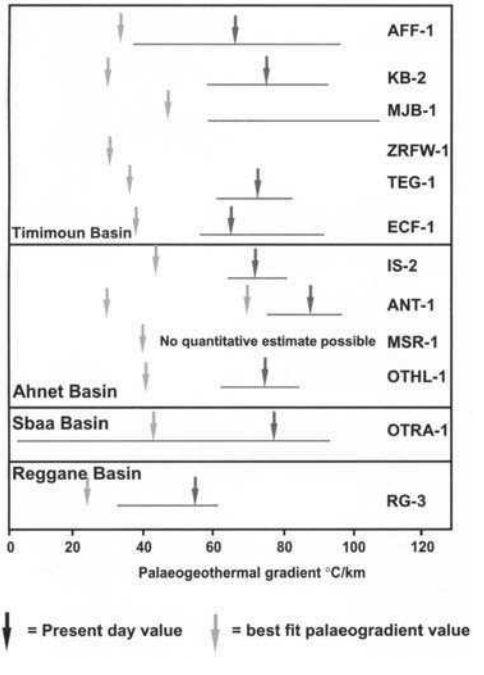

Fig. 21. Late Triassic–Early Jurassic palaeogeothermal constraints.

It should also be noted that raised geothermal gradients alone are insufficient to explain the estimated palaeotemperatures, which are often of the order of *c.* 10–120°C at the Hercynian unconformity. It is clear that considerable additional burial, followed by uplift and erosion, would be required to achieve the observed degree of maturity. The estimates of uplift and erosion are given in Table 1. The estimated amount of section removed is typically about 1 km and is likely to be related to a Late Triassic–Early Jurassic phase of uplift superimposed on an earlier Hercynian uplift. Evidence of this early Mesozoic phase of deformation is also provided by the presence of folded intrusive rocks in the southern part of the Ahnet Basin.

Good evidence for the later, Tertiary heating event is provided by a number of wells which show consistent evidence for cooling from a period of elevated palaeotemperatures at *c.* 50–30 Ma. The interpreted small degree of post-Cretaceous heating is confirmed by the limited vitrinite reflectance data from the Cretaceous section in the wells analysed. The relative similarity of Tertiary and present-day geothermal gradients suggests that post-Cretaceous heating was due to simple burial.

Figures 22–25 provide summaries of the thermal histories for the different regions of the study area. In each case, with the exception of the Sbaa Basin, the temperature histories are dominated by a heat 'spike' at 200 Ma.

Conclusions: maturity and hydrocarbon generation

At present, the organic maturities of older Palaeozoic rocks at even modest depths of burial usually exceed the level required for the generation of dry gas (2% R_0 equivalent), whereas those in the younger Palaeozoic (Carboniferous) beneath the Hercynian Unconformity typically lie within the oil window (or lower). This uniform pattern of maturities would appear to be an effect of the consistent Late Triassic heating of the basins. The current observed maturities of the two principal source rocks in the basin, the Silurian and Frasnian hot shales, are shown in map form in Fig. 26 and Fig. 27 respectively. These maps are based on measured and computed maturities, based

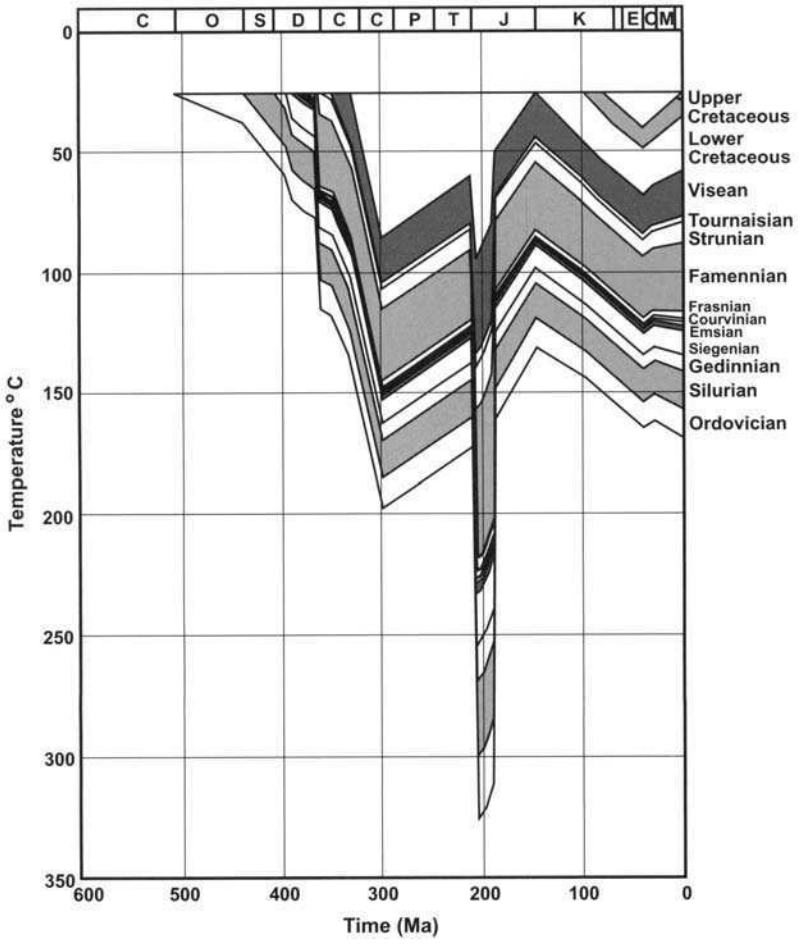

Fig. 22. Temperature–time history of the northern Ahnet–Timimoun Basin (TEG-1).

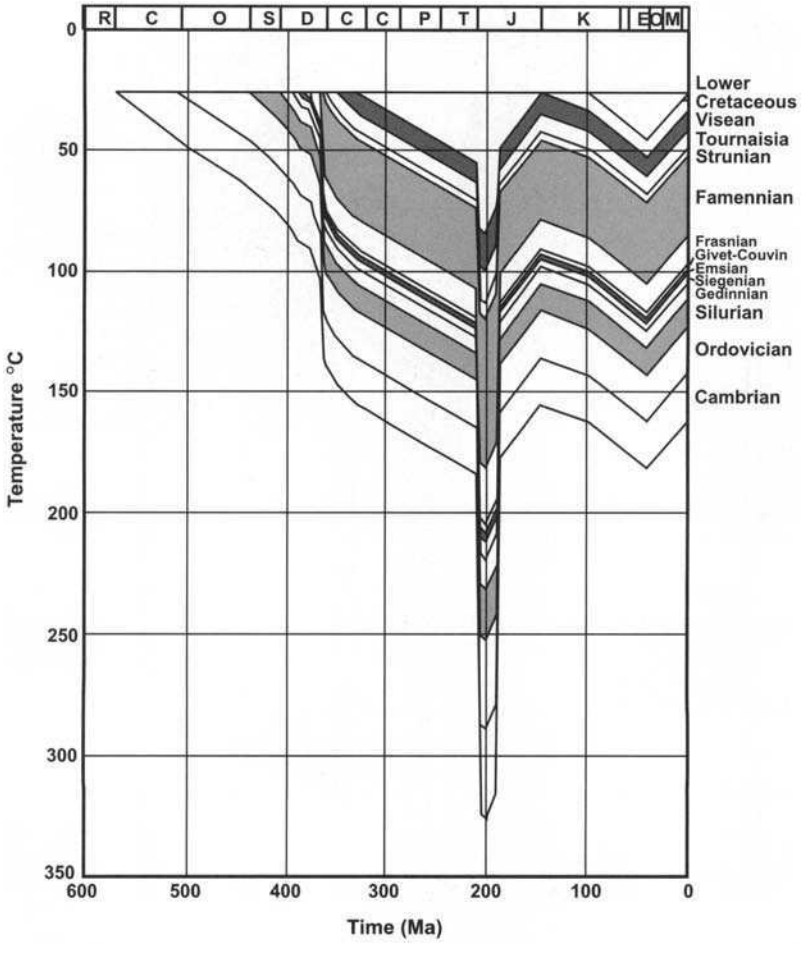

Fig. 23. Temperature–time history of the eastern Ahnet Basin.

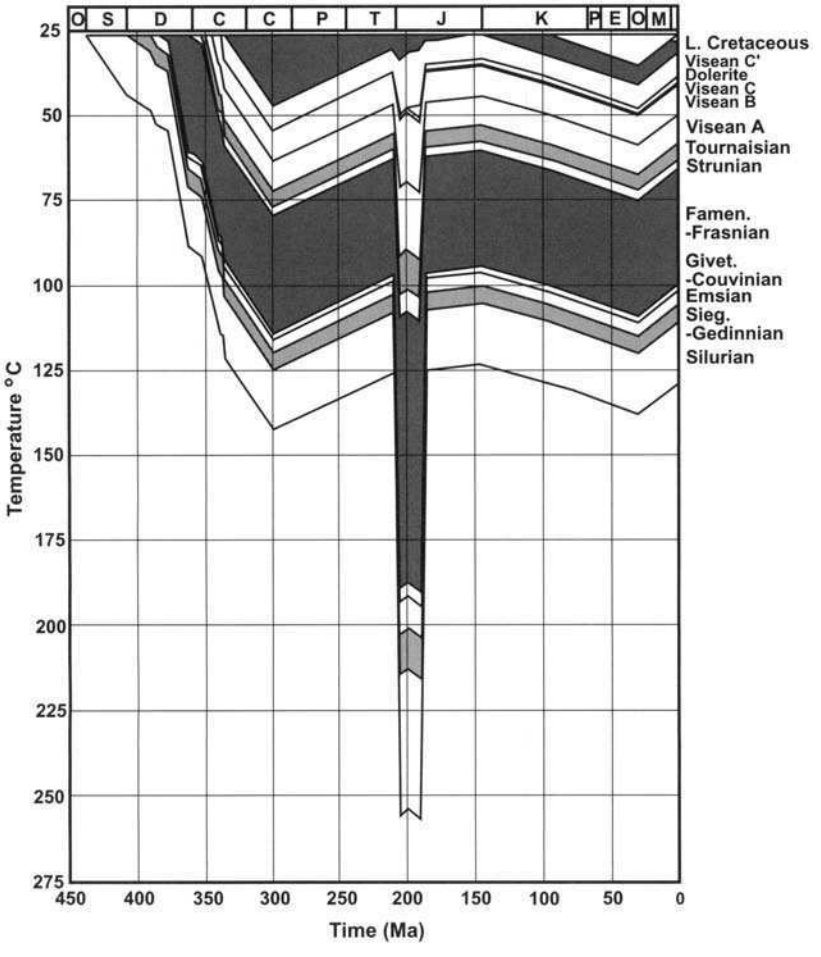

Fig. 24. Temperature–time history of the Reggane Basin (RG-3).

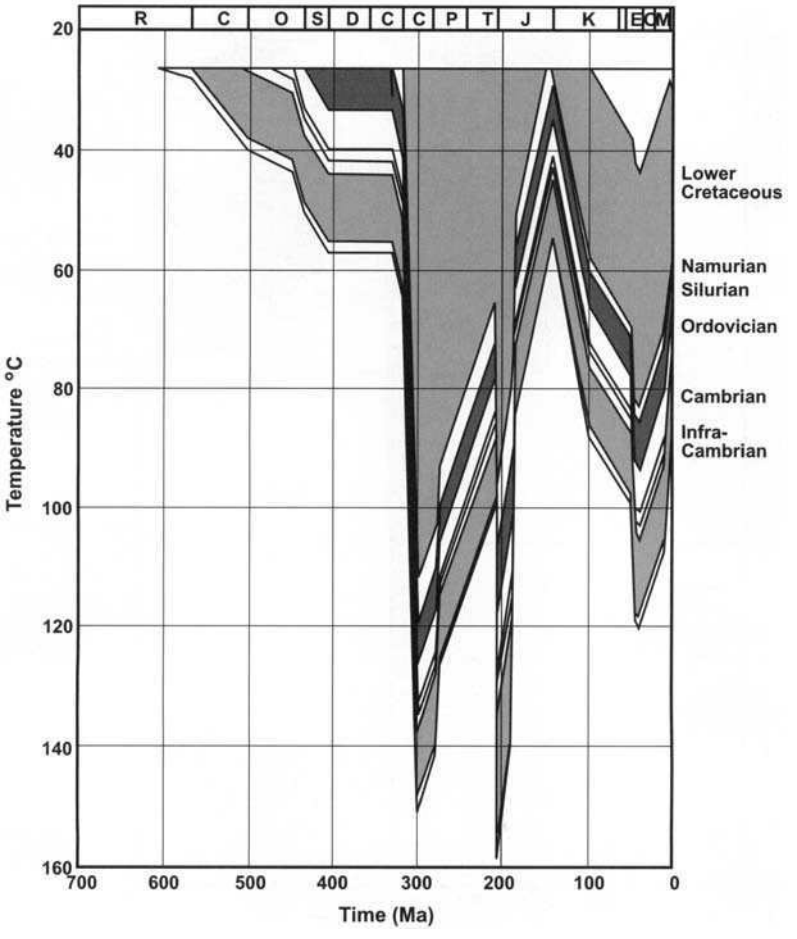

Fig. 25. Temperature–time history of the Sbaa Basin (OTRA-1)

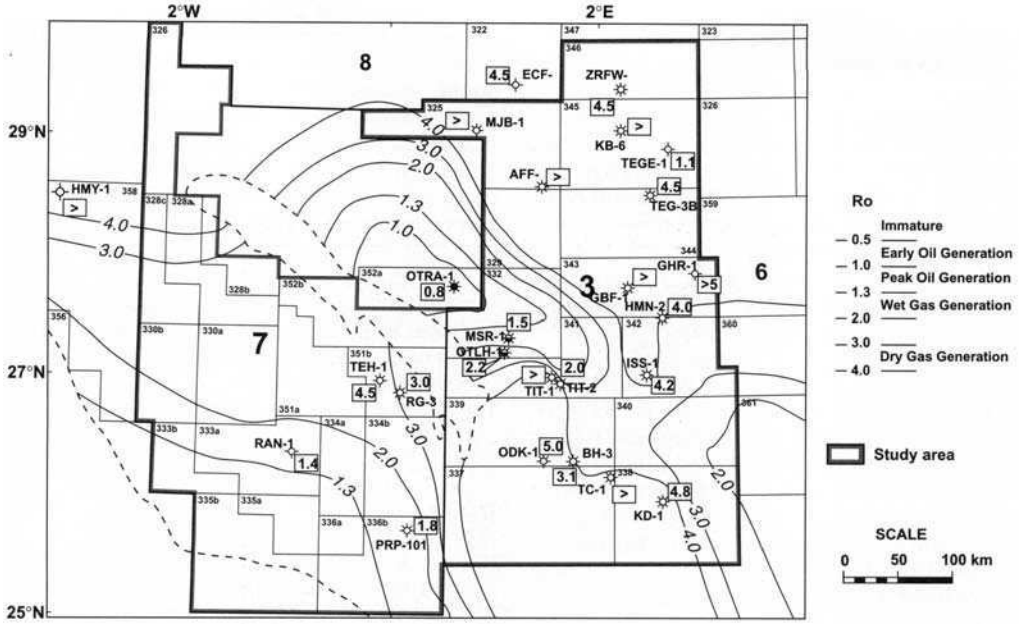

Fig. 26. Estimated maturity (R_0 equivalent) of Silurian hot shale.

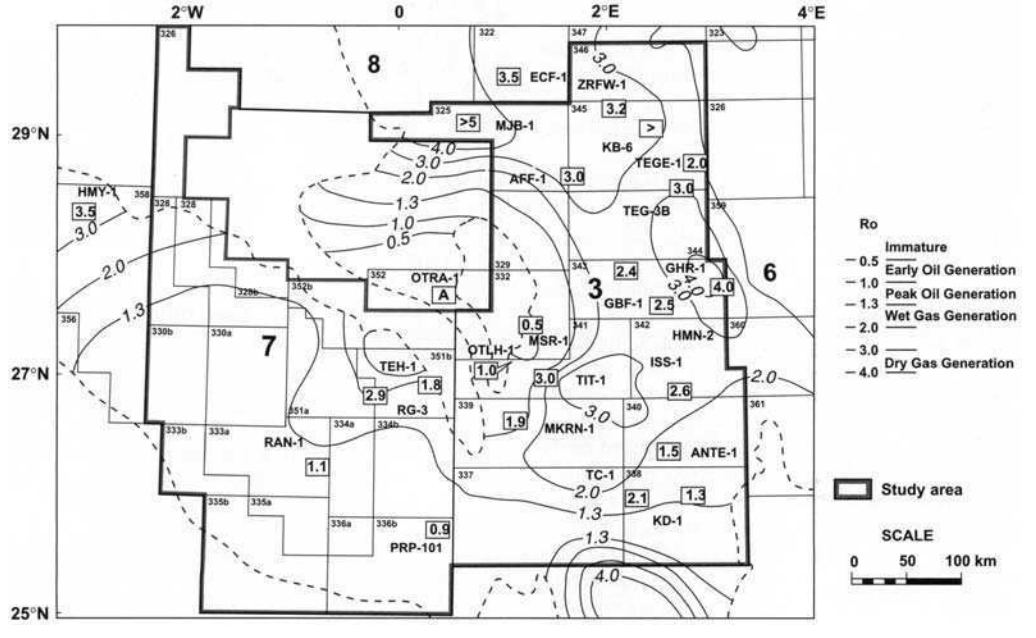

Fig. 27. Estimated maturity (R_0 equivalent) of Frasnian hot shale.

on the thermal histories derived from the analytical data.

As is to be expected, the Silurian hot shale is mature for dry gas generation throughout the area, with the exception of the Sbaa Basin and the centre of the Reggane Basin. In these cases, the admittedly limited data from OTRA-1 in the Sbaa Basin and from RAN-1 and PRP-101 in the Reggane Basin suggest that these areas lie within the oil window and wet gas window respectively. In the case of the Frasnian hot shale, a variety of states of maturity are suggested by the data. Some areas of the Ahnet Basin, particularly the north and extreme south, are mature for dry gas, with high levels of reflectance. On the western flank, however, and in the Sbaa and central Reggane Basins, the interval remains within the oil window.

Figures 28–30 provide burial history curves for wells TEG-1 (Ahnet Basin), RG-3 (Reggane Basin) and OTRA-1 (Sbaa Basin). In the case of TEG-1 it is likely that Silurian and Devonian source rocks were probably sufficiently mature to have generated oil before the Hercynian event. During the Late Triassic event, they would have been heated through the gas window and any previously reservoired oil would have been cracked. On the less deeply buried flanks of the basin, however, for example at OTLH-1, maturity is somewhat less and it is possible that oil generation, particularly from Devonian source rocks, could have occurred in the relatively recent past. This is supported by the presence of oil shows in OTLH-1 and nearby wells.

The history of maturation for RG-3 is similar to that for TEG-1, although the overall maturity is rather lower. Evidence suggests that heating effects caused by the emplacement of intrusions are very localized and these have been excluded from the modelling.

Well OTRA-1, in the Sbaa Basin, indicates that the Silurian source rocks have not yet reached the gas window and reached a state of oil generation before the Hercynian event, since which time, maturity has not been significantly increased. Thus oil generated from these source rocks would have been available for expulsion and migration before Hercynian tectonism. It seems unlikely that these oils have remained entrapped in reservoirs since the Carboniferous, although this is not impossible. It seems more likely, however, that the oil currently found in the Sbaa Basin has been generated on the western flank of the Ahnet Basin in Mesozoic or later times and has migrated updip to the elevated Sbaa Basin.

It would seem therefore that the study area was affected by two principal phases of heating and hydrocarbon generation. The first, before Hercynian tectonism and uplift, involved heating because of simple burial. During this phase, liquid hydrocarbons were generated in the Sbaa, Reggane and deeper parts of the Ahnet Basin. The second phase, in Late Triassic times, elevated maturities to the gas window in deeper parts of the Ahnet and Reggane Basins, accompanied by cracking of previously reservoired oils. The Sbaa Basin was relatively unaffected by this heating event, and no significant increase in maturation took place. Generation of liquid hydrocarbons continued on the less mature flanks of the Ahnet Basin until relatively recently in geological time.

References

BRAY, R. K., GREEN, P. F. & DUDDY, I. R. 1992. Thermal history reconstruction using apatite fission track analysis and vitrinite reflectance: a case study from the UK East Midlands and Southern North Sea. *In*: HARDMAN, R. P. F. (ed.) *Exploration Britain: Geological Insights for the Next Decade*. Geological Society Special Publication, **67**, 3–25.

DUDDY, I. R., GREEN, P. F., BRAY, R. J. & HEGARTY, K. A. 1994. Recognition of the thermal effects of fluid flow in sedimentary basins. *In*: PARNELL, J. (ed.) *Geofluids: Origin, Migration and Evolution of Fluids in Sedimentary Basins*. Geological Society Special Publication. **78, *325–345.***

——, ——, HEGARTY, K. A. & BRAY, R. J. 1991. Reconstruction of thermal history in basin modelling using apatite fission track analysis: what is really possible? *Proceedings of the First Offshore Australia Conference (Melbourne)*, III-49–III-61.

——, —— & LASLETT, G. M. 1988. Thermal annealing of fission tracks in apatite 3. Variable temperature behaviour. *Chemical Geology (Isotope Geoscience Section)*, **73**, 25–38.

GLEADOW, A. J. W. & DUDDY, I. R. 1981. A natural long-term track annealing experiment for apatite. *Nuclear Tracks*, **5**. 169–174.

——, ——, GREEN, P. F. & LOVERING, J. F. 1986. Confined fission track lengths in apatite—a diagnostic tool for thermal history analysis. *Contributions to Mineralogy and Petrology*, **94**, 405–415.

GREEN, P. F. 1988. The relationship between track shortening and fission track age reduction in apatite: Combined influences of inherent instability, annealing anisotropy, length bias and system calibration. *Earth and Planetary Science Letters*. **89**, 335–352.

——, DUDDY, I. R. & BRAY, R. J. 1995. Applications of thermal history reconstruction in inverted basins. *In*: BUCHANAN, J. G. & BUCHANAN, P. G. (eds) *Basin Inversion*. Geological Society Special Publications. **88**, 149–165.

——, ——, GLEADOW, A. J. W. & LOVERING, J. F. 1989*a*. Apatite fission track analysis as a paleotemperature indicator for hydrocarbon exploration. *In*: NAESER, N. D. & MCCULLOH, T. (eds.) *Thermal History of Sedimentary Basins—Methods and Case Histories*. Springer-Verlag, New York, 181–195.

——, ——, ——, TINGATE, P. R. & LASLETT, G. M. 1986. Thermal annealing of fission tracks in apatite 1. A qualitative description. *Chemical Geology (Isotope Geoscience Section)*, **59**, 237–253.

——, ——, LASLETT, G. M., HEGARTY, K. A., GLEADOW, A. J. W. & LOVERING, J. F. 1989*b*. Thermal annealing of fission tracks in apatite 4. Quantitative modelling techniques and extension to geological timescales. *Chemical Geology (Isotope Geoscience Section)* **79**, 155–182.

LASLETT, G. M., GREEN, P. F., DUDDY, I. R. & GLEADOW, A. J. W. 1987. Thermal annealing of fission tracks in apatite 2. A quantitative analysis. Chemical Geology (Isotope Geoscience Section) **65**, 1–13.

——, KENDALL, W. S., GLEADOW, A. J. W. & DUDDY, I. R. 1982. Bias in measurement of fission track length distributions. *Nuclear Tracks*, **6**, 79–85.

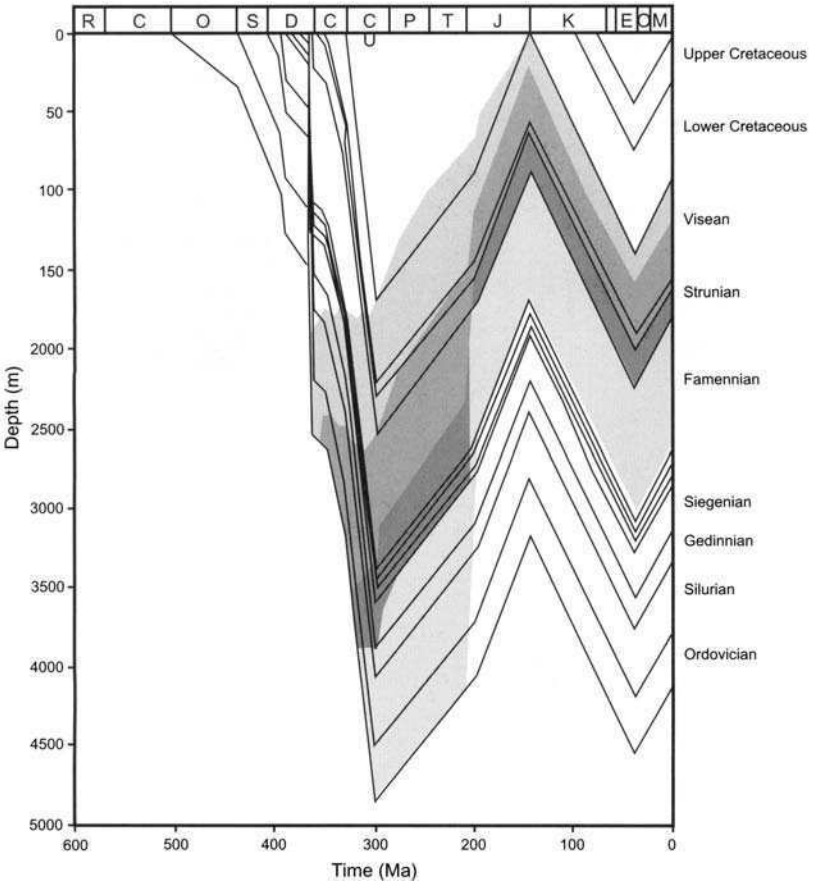

Fig. 28. Reconstructed burial history of well TEG-1.

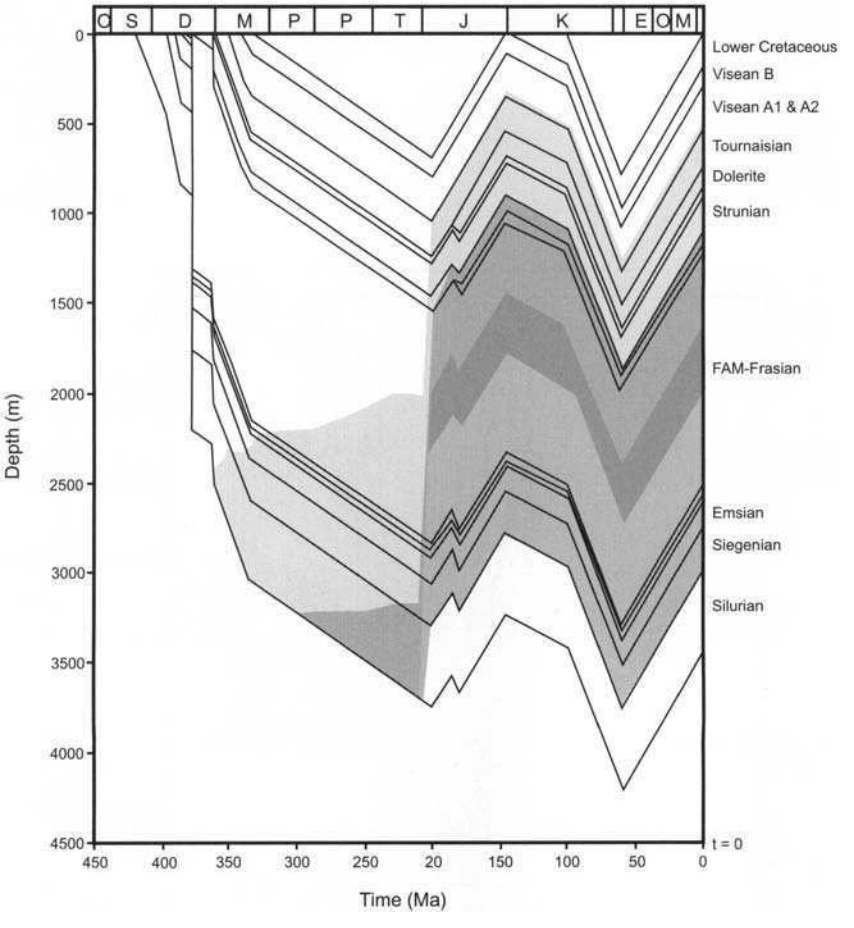

Fig. 29. Reconstructed burial history of well RG-3.

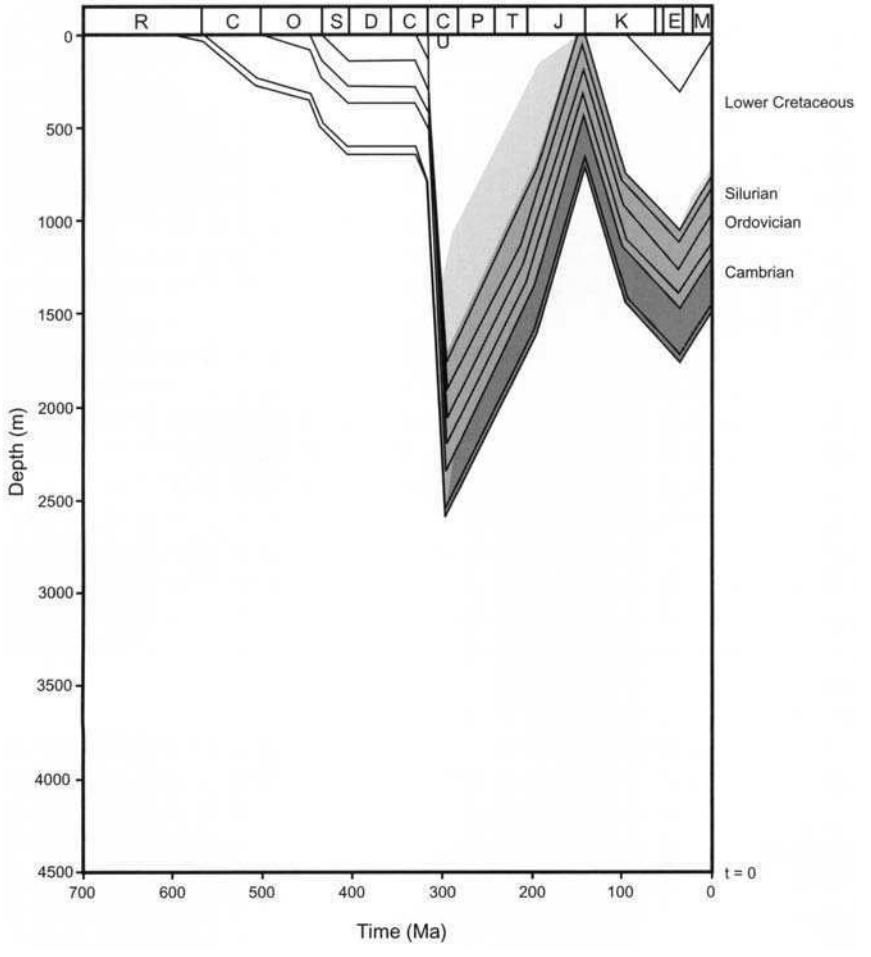

Fig. 30. Reconstructed burial history of well OTRA-1.

This page intentionally left blank

Lower Palaeozoic reservoirs of North Africa

ROB CROSSLEY & NEIL McDOUGALL

Robertson Research International Ltd, Llandudno, Conwy LL30 1SA, UK

Abstract: This paper provides an overview of features considered significant in the exploration and development of Lower Palaeozoic reservoirs of North Africa. Information is derived from a review of literature on the Lower Palaeozoic successions of north Africa, combined with outcrop observations from the Anti Atlas mountains of Morocco. The focus of the exploration-oriented part of the review is on identification of potential traps other than two-way structural dip closure. Stratigraphic elements described include depositional models of reservoir facies, tectonic unconformities and possible eustatic unconformities. Cases of established or potential trapping by post-depositional faulting, by diagenesis and by hydrodynamic flow are examined. Development-related topics highlighted include the impact on reservoir matrix quality of burial diagenesis and of palaeo-weathering at the Hercynian unconformity. Other issues discussed which additionally affect producibility from the reservoir matrix include tectonic fracturing, palaeotopography and unloading fracturing at the Hercynian unconformity, and induced fracturing within the present stress regimes.

The Cambrian to Silurian sequences of Algeria, Libya and Tunisia form one of the world's greatest concentrations of Lower Palaeozoic reservoirs. Algeria contains the largest number of fields discovered to date, including the giant field of Hassi Messaoud (Fig. 1). Libya also has substantial production from the Lower Palaeozoic, which is in the process of being boosted by new fields under development in the Murzuq Basin. Minor but potentially significant relatively deep discoveries have also been made in Tunisia. Equivalent sequences in Egypt, Morocco (including former Western Sahara), Niger and Chad might also have hydrocarbon potential (see below).

To date, exploration for Lower Palaeozoic prospects has mainly focused on structural highs. As a consequence there are large areas, even close to producing fields, which remain undrilled. Most producing fields are situated on convincing

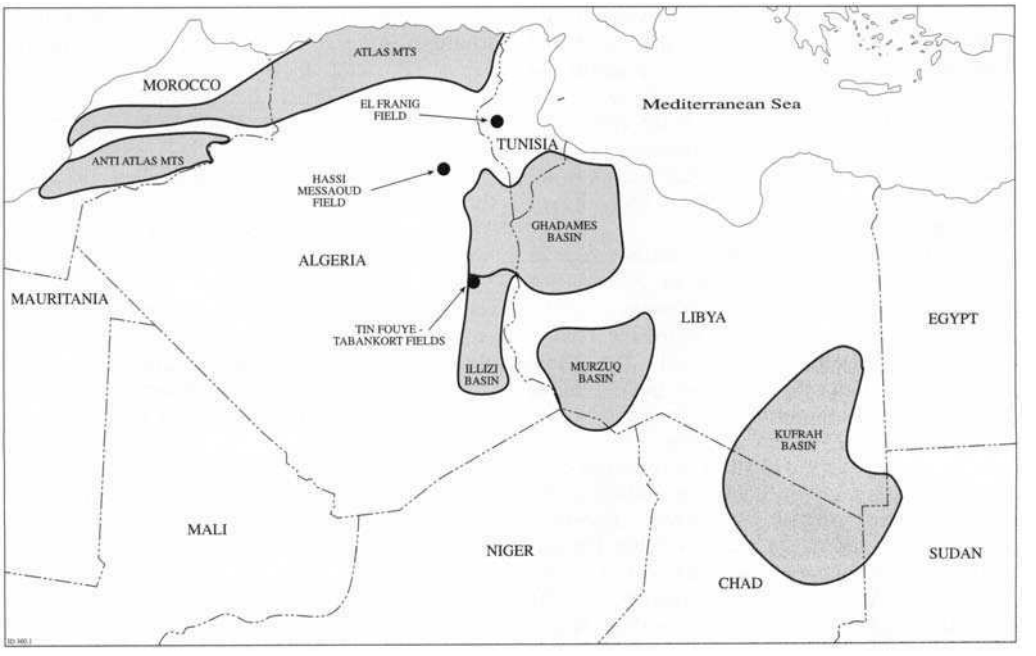

Fig. 1. North Africa locality map.

CROSSLEY, R. & MCDOUGALL, N. 1998. Lower Palaeozoic reservoirs of North Africa. *In*: MACGREGOR, D. S., MOODY, R. T. J. & CLARK-LOWES, D. D. (eds) 1998. *Petroleum Geology of North Africa*. Geological Society, London, Special Publication No. 132, 157–166.

structural closures, but evidence for the complete structural closure of some other fields is not compelling. Once the possibility of trapping by stratigraphic pinchout, by fault seal, diagenetic seal, or hydrodynamic seal is admitted, then prospectivity in the Lower Palaeozoic of North Africa is significantly increased. A similar conclusion, regarding the relative immaturity of exploration in the region, has been arrived at through the comparative study of analogue hydrocarbon provinces (Macgregor this volume). The quest for these more subtle traps requires a better understanding of the geology of these basins and their reservoirs.

Data sources

We attempt in this paper to integrate some of the extensive literature available from outcrop work and from published subsurface information.

The outcrops of Lower Palaeozoic rock in Algeria, Libya, Egypt, northern Sudan and Jordan (Selley 1972; Bellini & Massa 1980; Klitzsch 1981; Klitzsch & Squyres 1990) mainly represent palaeo-highs. Consequently, they have developed sand-rich facies which are often different from the sequences in adjacent basin fill successions, for example in the Murzuq Basin (Bellini & Massa 1980; Pierobon 1991) or in parts of Algeria (Balducchi & Pommier 1970). Age-diagnostic macrofossils and microfossils are relatively uncommon in such arenaceous outcrops. Historically, the resulting absence of reliable dating caused a confusing mixture of lithostratigraphies which were summarized by Whiteman (1971). With continued research, the stratigraphic significance of these outcrops is becoming clearer in Algeria (Legrand 1985b), Libya (Klitzsch 1981) and Egypt (Klitzsch & Squyres 1990).

In contrast, the Lower Palaeozoic outcrops in the Atlas–Anti Atlas fold belt of NW Africa mainly comprise basin-fill successions which have been exposed by erosion following Hercynian and Tertiary deformation. As these sequences tend not to represent palaeo-highs, they are useful analogues for hydrocarbon-bearing basinal sequences in Algeria, Libya, and Tunisia, and have good biostratigraphic age control (Destombes *et al.* 1985). In addition, the unconformable relations between deformed Lower Palaeozoic rocks and overlying Permo-Trias to Mesozoic sediments, are well exposed in the Atlas–Anti Atlas. Consequently, the 3D geometries of Lower Palaeozoic reservoir facies, their diagenesis, structures and fractures, and their modification at the Hercynian unconformity and under the present erosional regime, are unambiguously displayed.

Most palaeogeographical reconstructions place the Iberian craton of Spain–Portugal adjacent to the northern margin of Gondwana during the Lower Palaeozoic (Scotese & McKerrow 1991, Trench & Torsvik 1992). Consequently, the outcrops in Iberia provide an additional source of data to help understanding of the sequences in north Africa (Julivert *et al.* 1980; McDougall *et al.* 1987; McDougall 1988; Aramburu 1995).

Depositional models of reservoir facies

The lowermost Palaeozoic in North Africa infills topography eroded into a variety of metasedimentary and volcanic rocks last folded during the late Precambrian (Caby *et al.* 1981). In most proximal areas these basal deposits are pebbly, arkosic, cross-bedded sandstones associated with an extensive fluvial braidplain (e.g. Hassaouna Formation of Libya, Menkel Formation of eastern Algeria; Fig. 2). These basal fluvial deposits can be hundreds of metres thick (Klitzsch 1981, Pierobon 1991).

The basal deposits are typically overlain by a succession of fine- to medium-grained shallow marine, estuarine, deltaic and fluvial sediments including, for example, the Hamra Quartzite and Haouaz Formations of Libya (Vos 1981). Such sediments are identified at outcrop in southern Algeria (Beuf *et al.* 1971), southern Libya (Burollet & Byramjee 1969, Bellini & Massa 1980, Turner 1980; Klitzch 1981, Vos 1981, Clark-Lowes & Ward 1991), northern Sudan (Klitzsch & Wycisk 1987), eastern Egypt (Seilacher 1990) and Jordan (Selley 1972). In the subsurface of eastern Algeria and southern Tunisia, several distinctive offshore mudstone horizons, such as the El Gassi and Azzel Shales, also occur within the Ordovician (Hmidi *et al.* 1991). At the top of the Ordovician sequence, there are laterally discontinuous conglomeratic sandstones, pebbly and sandy mudstones, and mudstones (e.g. Memouniat, Melez Chograne, Jeffara Formations of Libya). In different areas, these are interpreted as fluvial or fluvio-glacial (Biju-Duval 1974) to fluvio-marine with dropstones (Pierobon 1990), and as glacial tills (Klitzsch 1981) or periglacial deposits (Collomb 1962; Beuf *et al.* 1969).

Through much of the Silurian, in contrast, more fully marine conditions prevailed in most areas as relative sea level rose across the latest Ordovician erosion surface. Thick graptolitic, locally organic-rich shales (the Tanezzuft For-

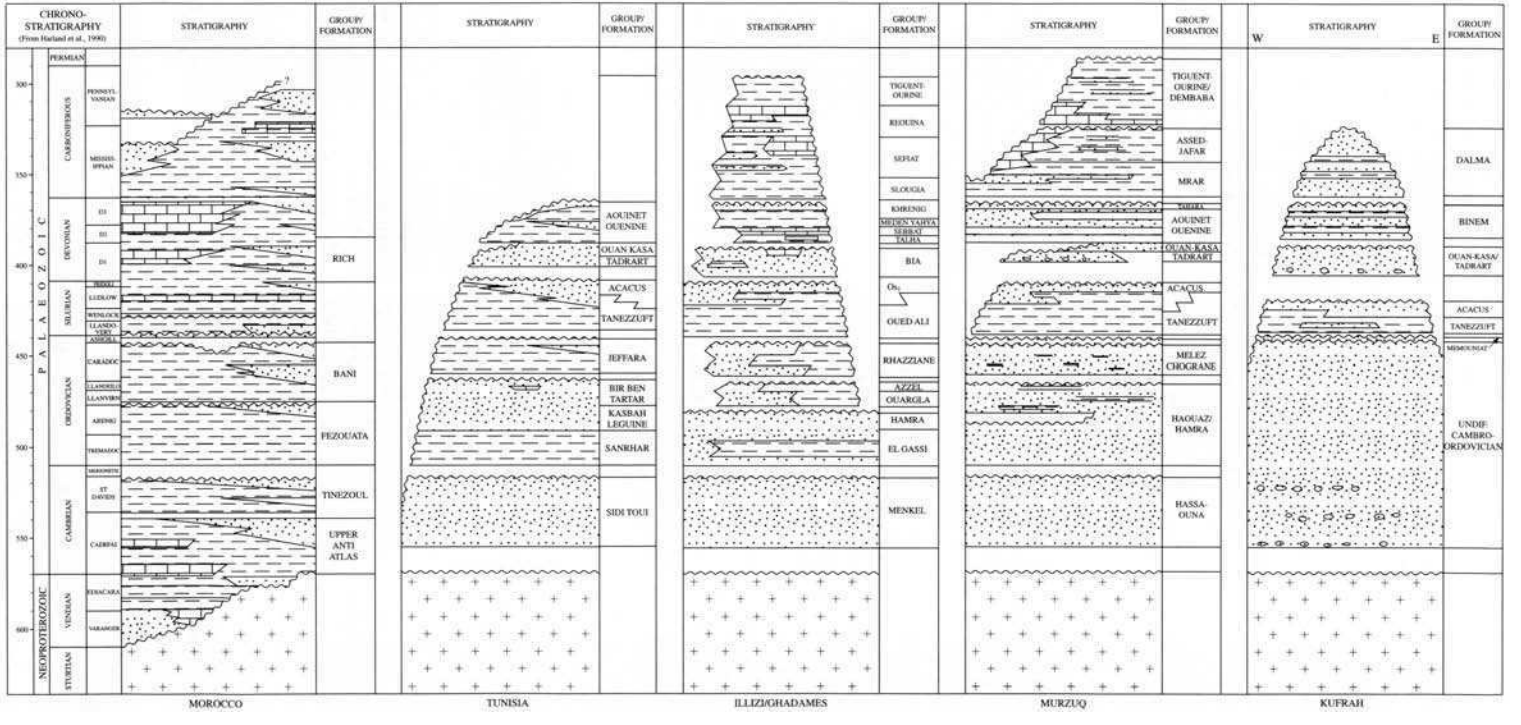

Fig. 2. Simplified Lower Palaeozoic lithostratigraphy for selected North African locations. Modified after Hmidi *et al.* (1991) and Simon Petroleum Technology (1994).

mation in Libya) initially accumulated across the area, forming a regional seal and source rock unit (Berry & Boucot 1973). During the middle Silurian, northwards progradation of the shoreline led initially to the limited deposition of storm-emplaced sand, both below and above storm wave base (e.g. Castro *et al.* 1991). These sediments in Libya form the lowermost Acacus Formation which, overall, displays an upwards increase in sand deposition, accompanying a return to shallow marine, shoreface, estuarine and fluvial deposition (e.g. Bracaccia *et al.* 1991, Castro *et al.* 1991).

The more basinal setting of the Moroccan Anti Atlas sequence results in fluvial deposition being largely restricted to the Lower Cambrian. The Middle Cambrian and Ordovician sandstones, which typically form less than 30% of these mudstone-dominated sections, comprise repeated coarsening-upwards sequences representing shoreline progradation across a muddy shelf. Storm-emplaced sandstones interbedded with shelfal mudstones represent the lowest parts of each sandy sequence and are typically overlain in turn by shallow shelf sand sheets, and shoreface and estuarine deposits. Channelized fluvial conglomerates occur locally at the top of the Ordovician section. Destombes (1968) reported occasional glacial striations at this stratigraphic level, and possible iceberg keel marks occur in shallow marine sandstones close to the top of the Ordovician in the southern Anti Atlas. The Silurian section of the Anti Atlas is almost entirely mudstone with thin beds of turbiditic sandstone.

Unconformities within the Lower Palaeozoic

This section draws heavily upon major syntheses by Klitzsch (1981) for southern Libya, Legrand (1985*b*) for Algeria, and Destombes *et al.* (1985) for the Anti Atlas. Additional publications are referred to where appropriate. Several erosive contacts are reported within the outcrops of southern Algeria and southern Libya. These significant erosive intervals, transgressed by basal Ordovician, by basal Silurian, and by Devonian, can also be traced in the subsurface of Algerian and Libyan basins (Castro *et al.* 1991, Pierobon 1991). The Late Cambrian and Latest Ordovician erosive contacts are also displayed in the Anti Atlas outcrops. In view of the regional extent of these erosive events, it is tempting to invoke a eustatic origin, particularly as the Latest Ordovician erosive phase is coeval with the cessation of the Upper Ashgill glaciation (Brenchley 1984). However, although a glacio-eustatic cause is probable for some Late Ordovician unconformities, outcrop evidence generally indicates a tectonic origin for the most significant erosive episodes.

Latest Cambrian

On the eastern side of the Murzuq basin in southern Libya, Ordovician (locally Upper Ordovician; cf. Turner 1991) rests with marked angular unconformity, of 30°, on Cambrian. Klitzsch suggested that the difference in dips is principally due to horst development which started within the Cambrian. Legrand (1985*b*) reported that much of the Upper Cambrian also appears to be missing beneath the equivalent erosive contact in Algeria. He cited faunal evidence that onset of the subsequent transgression may have started locally towards the end of the Cambrian. Angular unconformities are also reported within parts of the Cambrian to lowermost Ordovician succession in some southern Algerian outcrops, and not in others. This has led, in the absence of biostratigraphic control, to debate about stratigraphic equivalence. Some of the apparent contradictions raised by this approach might, however, be due to local dip and fold development on horst margins.

In the Anti Atlas, the entire Upper Cambrian appears to be absent and Destombes *et al.* (1985) ascribed the Moroccan pre-Ordovician erosion surface to 'epeirogenic' uplift. However, total thickness changes of several hundred metres occur within the Cambrian section across the margins of faulted basement highs, so it is likely that vertical movements occurred in large fault-bounded blocks before deposition of the Ordovician.

A similar picture emerges from the palaeogeographically adjacent Iberian craton. Here, Lower Ordovician Sandstones (the so-called 'Armorican Quartzite Group'; see McDougall *et al.* 1987; MacDougall 1988), equivalent in age to the Hamra Quartzite, commonly rest unconformably on Lower to Upper Cambrian, and even on Precambrian, sediments (Julivert *et al.* 1980). The magnitude of the unconformity, which is often marked by a dip discordance, tends to reach a maximum where associated with palaeo-highs but passes laterally into effectively conformable sequences. Observations from the Lower Ordovician (Arenig) sandstones, in both northwestern and central Iberia, also reveal the presence of lower-order unconformities within the sequence (e.g. McDougall 1988;

Aramburu & Garcia-Ramos 1993; Aramburu 1995). Overall, it is apparent that the distribution, sedimentary character and thickness of the Lower Ordovician and also later Ordovician deposits, were actively controlled by the movements of fault blocks. Within the Iberian, and possibly in the wider north Gondwanan context, these movements are thought to have been related to transpressive and transtensional episodes associated with major strike-slip systems (Lefort & Ribeiro 1980, Silva & Ribeiro 1985).

On a regional scale, the Upper Cambrian of northern Gondwana and adjacent cratonic areas, appears to have been characterized by differential vertical movements on fault-bounded blocks of various scales, accompanied by erosion. This was followed by subsidence and transgression, giving rise in many cases to a basal Ordovician marine mudstone. If this level can be successfully imaged on seismic records within the basins, then a model might be developed for predicting fault seals and the distribution of reservoir sands offering stratigraphic traps around the margins of uplifted areas.

Latest Ordovician

In the Murzuq basin of Libya, NW–NNW striking horsts continued, after initial uplift in the Cambrian, to be sites of reduced deposition and periodic erosion within and at the end of the Ordovician. Late Ordovician sandstone in places unconformably overlies Middle or Lower Ordovician rocks (Klitzsch 1981), and the sandstone sequence as a whole is terminated erosively and transgressed by lower Silurian claystones, commonly known as the Tanezzuft Shale. The scale of cumulative lower Palaeozoic uplift on some south Libyan structures is large and can be illustrated by the fact that, locally, the Silurian unconformably overlies the Cambrian Hassaouna Formation and oversteps onto a horst of metamorphic basement (Klitzsch 1981).

In Algeria, a similar phase of tectonic instability occurred, with uplifted areas often being eroded to Cambrian and Precambrian basement levels. The stratigraphy of coarse clastic rocks at latest Ordovician contains various unconformities, and this complexity continues into the base of the transgressive Silurian. Farther west, in Morocco, a similar scenario occurs, with substantial uplifts commencing in the early Ashgill. In the eastern Anti Atlas, the Silurian locally rests unconformably on upper Caradoc sediments, indicating the loss of perhaps 100 m of section.

A very similar situation, with late Ordovician faulting, erosional unconformities near latest Ordovician, and Silurian 'hot shales' overstepping onto Lower Ordovician sandstones, occurs in the subsurface in Tunisia (Hmidi *et al.* 1991).

It seems surprising, given the stratigraphic evidence across the region for truncation of structural uplifts, that slumped and reworked sediments representing the Caradoc and older Ordovician, are not widely recognized. Either regional relative base level fell so much that all these erosion products were transported beyond existing outcrops and wells, or the erosion products are represented in part by some of the heterogeneous and contorted Ashgill sediments, of for example the Memouniat and Jeffara Formations, which are usually interpreted as periglacial and glacial deposits (e.g. Bellini & Massa 1980, Pierobon 1991).

Consequently, with successful seismic imaging of fault block margins, downthrown wedges of reworked sand with stratigraphic and fault trapping might be identified in off-structure locations. This issue is of particular importance because the immediately overlying Silurian includes world-class source rocks for petroleum exploration; hence risk associated with charge and seal is minimal.

The stratigraphic complexity seen at outcrop in Morocco and Algeria, with variably channelized upper Ashgill conglomeratic sandstones, with basal Silurian transgressive sandstones resting locally with slight angular discordance on the Ordovician, and with local development of channelized sandstones up to 125 m thick within the basal part of the Silurian, offers additional prospects for combined stratigraphic and structural traps near the base of the regional oil-prone Silurian claystone.

Latest Silurian

A further phase of horst-crest erosion was particularly active in the Murzuq basin during late Silurian times. Similarly, on the western margin of the Kufrah basin, sandstones of the widespread Acacus Formation, close to latest Silurian, wedge out northwards because of late Silurian–early Devonian erosion, and are unconformably overlain by Devonian Tadrart sandstone.

An overall upwards increase in the proportion of sandstones through the Silurian occurs in many parts of southern Libya and Algeria. Where biostratigraphic control is available, it appears that a variety of relatively isolated sandstone bodies of differing ages have developed.

Minor unconformities are noted in the upper part of the Silurian and in places Devonian sandstones rest with marked angular unconformity on upper Silurian sandstones.

In the western part of the Anti Atlas, the end of the Silurian is characterized by a minor development of sandstones and local discordances, but in general no major tectonic event of proven late Silurian age has been identified. In contrast, the central and northern segments of the Iberian craton reveal a major depositional hiatus and local discordances where Devonian sandstones truncate the Silurian succession and in some cases directly overlie the Ordovician (Julivert *et al.* 1980; Aramburu 1995).

Scenarios clearly exist therefore, particularly in the upper Silurian of Algeria and Libya, for stratigraphic trapping of sandstone reservoirs. However, the youngest of these runs the risk of breaching into overlying sand-rich Devonian successions.

Post-depositional faulting and implications for fault seal trapping

Differential movement of fault blocks continued in places through the Upper Palaeozoic. In parts of the western Anti Atlas, lower to middle Devonian uplift and erosion exposed upper Ordovician rocks which were subsequently transgressed by upper Devonian carbonates. Such faulting could add to the prospects for trapping latest Ordovician sandstones laterally against downthrown Silurian source rocks. Published cases of this specific trap situation include wells in the El Franig Field of Tunisia (Nelson & Hsu 1993).

Diagenesis and implications for diagenetic traps

Quartz cementation is the main diagenetic cause of porosity reduction in the Lower Palaeozoic sandstones of North Africa. For example, Balducchi & Pommier (1970) quoted quartz cement percentages of 9–14% in oil-producing sandstone reservoirs at Hassi Messaoud. Similarly, Hmidi *et al.* (1991) quote quartz cement abundances of 10–15% in sandstones of Lower Ordovician age in southern Tunisia. Diagenetic clays consist mainly of kaolinite, locally associated with illite (Balducchi & Pommier 1970; Hmidi *et al.* 1991; Ben Amrane 1993; Gellati & Sentoun 1993). Despite published matrix porosities of only 2–12% (average 8–10%; e.g. Hmidi *et al.* 1991), permeabilities may reach 100 mD in matrices not damaged by diagenetic clay (e.g. Nelson & Hsu 1993). These high permeability to porosity ratios may be due to microfractures (Nelson & Hsu 1993) but could be a consequence of smooth planar pore throats caused by the abundance of quartz overgrowths.

A further consequence of the abundance of quartz overgrowths is the support against compaction provided by this cement during burial. Relatively large primary pores can therefore be preserved at burial depths of 4 km, such as in the Hamra Quartzite and El Atchane Sandstone of southern Tunisia (Hmidi *et al.* 1991).

The hypothesis has developed amongst some groundwater scientists (Burdon 1980; Dubay 1980) that the small-scale processes of near-surface silica reprecipitation (Hea 1971) have in time resulted in extensive silica cementation in North Africa's Palaeozoic sandstones. Burdon's inference arose from the observation, while drilling shallow boreholes in latest Ordovician sandstones, that the rocks at outcrop or near outcrop are more tightly cemented than sandstones taken to be equivalent in the shallow subsurface. We have seen that marked lateral changes occur in facies and stratigraphy at 'latest Ordovician', so it is probable that the tight and the less cemented sandstones are not necessarily the same at every location. Hydrocarbon drilling has also shown that tight quartzitic sandstones at 'Latest Ordovician' are not confined to outcrops or near-outcrop locations. In addition, Hercynian structures post-date quartzite formation in the Anti Atlas (see below), so extensive quartz cementation is taken to be a deep-burial geological process rather than the result of recent shallow- level weathering or groundwater processes.

There can be marked lateral variations in the abundance of quartz cement, with some rocks being rendered effectively impermeable (see below, and Balducchi & Pommier 1970) in the absence of an open fracture network. If the basis for quartz cementation can be modelled, then there may be a basis for predicting diagenetic traps. This topic at present remains poorly understood.

Hydrodynamic traps

On the north side of the Murzuq basin (south side of the Gargaf arch), Dubay (1980) described a Cambrian aquifer sandstone at least 350 m thick, which is unconformably overlain by Devonian sandstones. The produced water is fresh

(total dissolved solids 510 mg/l) and weakly acid (pH 6.6). Dead oil traces are frequently found, though mainly in sandstones within the Devonian. In contrast, groundwater in Cambro-Ordovician aquifers on the northwest side of the Gargaf arch, on the margins of the Illizi and Hamra (Ghadames) basins, is highly saline. The interpretation placed on these observations is that meteoric water has flushed Cambro-Ordovician and Devonian sandstones, at least to depths penetrated in the groundwater studies (up to about 300 m), and that the Gargaf arch area acted as a barrier to these meteoric waters. If this hydrodynamic model is valid then the possibility exists, in parts of the basin with low structural dips, for hydrodynamic trapping.

In the adjacent Illizi Basin of Algeria, Chiarelli (1978) interpreted a large hydrodynamic and water chemistry dataset as providing evidence of flushing of aquifers by meteoric water at Cambrian, Ordovician and upper Silurian to lower Devonian levels. The chemical data are interpreted as indicating limited flushing at Cambro-Ordovician levels, implying relatively low aquifer connectivity. The converse is that Cambro-Ordovician strata may offer relatively high potential for stratigraphic or other subtle traps.

Upper Silurian to Lower Devonian strata in the Tin Fouyé-Tabankort fields display a gradual south to north deepening of oil–water contacts of about 130 m over a 30 km distance along an apparently unclosed northward-plunging structure. This oil–water contact slope is compatible with the hydrodynamic gradient and so is interpreted as evidence of hydrodynamic trapping. If the hydrodynamic trapping model is rejected, then an alternative subtle trapping mechanism must be sought. In either case, prospectivity in unclosed structures is demonstrated.

Post-depositional faulting and fracturing

Relationships at the Hercynian unconformity, between Palaeozoic and Permo-Trias to Cretaceous successions, show that high-amplitude–low-wavelength deformation in the Anti Atlas pre-dated the unconformity. Geometrical relationships between Hercynian folds, fractures and minor faults indicate that the sandstones were brittle before deformation. Much of the quartz cementation is therefore inferred to predate the Hercynian deformation event.

The Hercynian fracture sets can be modelled in relation to fold geometries in terms of brittle slab folding with bed slip, and with simultaneous development of extensional fractures and shear fractures in different geometric positions in the folded competent units (e.g. Stearns & Linscott 1993). These fracture sets are widespread and so, in the subsurface, most probably play an important role in 'bleeding' hydrocarbons from the sandstone matrix into the main permeability conduits. However, in terms of fracture analogues for subsurface reservoirs, other factors make the situation more complex.

Many of the larger structures in the Anti Atlas, which are of a scale comparable with those recognized in seismic surveys and subsequently drilled in Algeria and Libya, have in addition suffered transpressional and transtensional stresses. These stresses have resulted in near-vertical faults and associated fracture sets, which although areally restricted, would in the subsurface play an important role in controlling permeability conduits near the crestal areas of such structures. Modelling these fracture sets is problematic.

First, modest changes of strike along the structure can result in a change from tight transpressional structures ('restraining bend') to gaping transtensional structures ('releasing bend'), within one overall stress regime. Modern stress regimes in the Atlas mountains (Gomez *et al.* 1996) provide a good example of the potential complexity that could develop.

Second, some of the Atlas–Anti Atlas structures appear to have been reactivated, with structural expression during the Hercynian, again during the Mesozoic, and again in the Tertiary. The overall stress regimes were different at each stage, so at any one location a complex mixture of cross-cutting transtensional and transpressional structures can result.

Third, these fossil fracture sets may not coincide with the preferred direction of fracture within the current stress regime (e.g. the direction in which an induced fracture stimulation might develop).

Fourth, bedding-parallel stylolites are commonly developed in the sandstones and quartzites of North Africa (e.g. Nelson & Hsu 1993), and present further complexity for permeability modelling.

Finally, there are likely to be further complications in the fracture systems where, such as around Hassi Messaoud, Palaeozoic reservoirs subcrop at the Hercynian unconformity and have suffered erosional unloading (see below).

The Atlas/Anti Atlas outcrop analogues therefore indicate that a large number of complex factors influence fracture systems developed in North African Palaeozoic reservoirs and simple fracture models for the subsurface should be treated with some scepticism.

The Hercynian unconformity

Palaeotopography and matrix reservoir quality

Palaeozoic successions in the Anti Atlas region are composed of alternations of sandstone and mudstone, with sandstone typically representing less than 30% of the total thickness. Quartzitic sandstones are the main scarp formers, but these are not normally the top of the sandstone succession. The matrix of the quartzites tends to be so completely cemented that they are impermeable to weathering processes except along fracture planes. The overlying less-cemented sandstones show weathering effects, including feldspar dissolution, which may enhance matrix porosity by a few per cent in some cases.

Where structurally flat, the less-cemented, less-resistant sandstones are either completely eroded, or are partly preserved set back from the main scarp cliff. In this situation, drilling the apex of the topographic feature yields the greatest chance of encountering less-cemented sandstone above the tight quartzite. Where structurally dipping, the less-cemented sandstones above the quartzites are exposed low on the dip slope and are fully preserved beneath shales at the foot of the dip slope. This clearly carries different implications for optimal drilling of reservoir above the quartzite.

Erosional unloading and gravity slide fractures

Exhumed examples of the Palaeozoic Hercynian surface in the Anti Atlas show that erosional unloading results in pervasive opening of pre-existing fracture sets. Other fractures are opened on hills and scarps by gravitational sliding of quartzite or sandstone slabs and blocks. The unloading and gravity slide fractures can be held open by natural proppant in the form of aeolian sand, fluvial sand, and colluvial debris. Some opened fractures may become partly to completely infilled by surficial siliceous, ferruginous, carbonate or sulphate cements, but overall the net impact of exposure on Palaeozoic reservoirs appears to improve, rather than decrease, reservoir potential. The El Franig Field of Tunisia is a published case where enhanced Lower Palaeozoic reservoir properties are associated with subcrop against the Hercynian unconformity (Nelson & Hsu 1993).

Results from groundwater investigations

The latest Cambrian sequence of quartz-cemented sandstones 50–75 m thick on the northern margin of the Murzuq basin has in several groundwater tests proved impermeable, but the underlying less-cemented Cambrian sandstones show high permeabilities (Dubay 1980). Flow tests are interpreted as indicating laterally variable dual permeability systems, with flow dominantly from fractures. Total water production rates of 155×10^6 m^3/year have been reported for this area by Pallas (1980).

On the western side of the Murzuq basin, Burdon (1980) reported six boreholes drilled into Ordovician sandstones through 100 m of Silurian shale which yielded groundwater, with best flows coming from sandstones which were interpreted as fractured. Total water production rates of 8×10^6 m^3/year have been reported for this area by Pallas (1980).

The groundwater data clearly demonstrate that, even at near-surface conditions, quartz cementation can be sufficient to render parts of the Lower Palaeozoic sandstone succession impermeable. However, considerable fluid storage capacity can also be shown by less-cemented parts of the sequence, and high production rates can be achieved, with the benefit of erosional-unloading opening of fracture sets. The fact that the rocks respond to lithostatic load reduction in this brittle way, rather than by more ductile deformation, is, however, encouraging for prospects of enhancing production rates in hydrocarbon reservoirs by induced fracturing.

Conclusions

Review of outcrop and subsurface information shows that the Lower Palaeozoic succession is dominated by marine to marginal marine–fluvial sandstones interbedded with marine mudstones. Such sequences offer potential for stratigraphic trapping and for trapping by Palaeozoic and post-Palaeozoic faulting of sandstone against mudstone.

Several unconformities are identified within the Lower Palaeozoic succession and some of these are associated with tectonic events that locally resulted in fault block rotation. These circumstances offer possibilities of combined structural and stratigraphic traps.

Some sandstones are totally cemented by quartz, so potential exists for diagenetic trapping. Some fields without structural closure are known and these have been interpreted as products of hydrodynamic trapping.

Tectonic fractures are important for improving reservoir permeability in some places, and erosional unloading and weathering associated with the Hercynian unconformity is known to improve reservoir properties of some Lower Palaeozoic reservoirs.

Trapping by stratigraphic pinchout, by fault seal, by diagenetic seal and by hydrodynamic seal therefore all occur in North African Lower Palaeozoic basins. We have noted that abundant quartz overgrowths offer potential for maintaining permeable moderate- to low-porosity reservoirs to burial depths of at least 4 km. The existence of subtle trapping, combined with maintenance of reservoir quality with compaction, suggests that the Lower Palaeozoic reservoir plays of North Africa are at present underexplored.

References

ARAMBURU, C. 1995. El Precambrico y Paleozoico Inferior. *In*: ARAMBURU, C. & BASTIDA, F. (eds) *Geologia de Asturias*. Ediciones Trea, 35–51

—— & GARCIA-RAMOS, J. C. 1993. La sedimentacion Cambro-Ordovicica en la Zona Cantabrica (NO de Espana). *Trabajos de Geologia*. Universidad de Oviedo, **19**, 45–73.

BALDUCCHI, A. & POMMIER, G. 1970. Cambrian oil field of Hassi Messaoud, Algeria. *American Association of Petroleum Geologists Memoirs*, **14**, 477–488.

BELLINI, E. & MASSA, D. 1980. Palaeozoic sedimentology of the southeastern part of Al Kufrah Basin, Libya: a model for oil exploration. *In*: SALEM, M. J. & BUSREWIL, M. T. (eds) *The Geology of Libya. Vol. 1*. Academic Press, London, 3–56.

BEN AMRANE, O. 1993. Etude des grès réservoirs fissures du Cambrien de Hassi-R'mel. *In*: BEN HASSINE, K. & EL BORGI, M. (eds) *Fractured Reservoir Seminar* (Tunis, 1–4 September 1993), ETAP, Tunis, 29–39.

BERRY, W. B. N. & BOUCOT, A. J. 1973. Correlation of the African Silurian rocks, *American Association of Petroleum Geologists Special Paper*, **147**, 83.

BEUF, S., BIJU-DUVAL, B., DE CHARPAL, O., ROGNON, P., GARIEL, O. & BENNACEF, A. 1971. Les grès du Paléozoïque inférieur au Sahara. *Science Technologie Pétrole*, **18**, 1–464.

——, ——, STEVAUX, J. & KULBICKI, G. 1969. Extent of 'Silurian' glaciation in the Sahara. Its influence and consequences upon sedimentation. *In*: KANES, W. H. (ed.) *Geology, Archaeology and Prehistory of Southwestern Fezzan, Libya*. Petroleum Exploration Society of Libya, 11th Annual Field Conference, 103–116.

BIJU-DUVAL, B. 1974. Exemples de dépôts fluvio-glaciaires dans l'Ordovicien supérieur et le Précambrien supérieur du Sahara central. *Bulletin du Centre de Recherches de Pau*, **8**, 209–226.

BRACACCIA, V., CARCANO, C. & DRERA, K. 1991. Sedimentology of the Silurian-Devonian series in the southeastern part of the Ghadamis basin. *In*: SALEM, M. J. & BELAID, M. N. (eds) *The Geology of Libya. Vol. 5*. Academic Press, London, 1727–1744.

BRENCHLEY, P. J. 1984. Late Ordovician extinctions and their relationshp to the Gondwana glaciation. *In*: BRENCHLEY, P. J. (ed) *Fossils and Climate*. John Wiley, Chichester, 291–315.

BURDON, D. J. 1980. Infiltration conditions of a major sandstone aquifer around Ghat, Libya. *In*: SALEM, M. J. & BUSREWIL, M. T. (eds) *The Geology of Libya. Vol. 2*. Academic Press, London, 595–609.

BUROLLET, P. F. & BYRAMJEE, R. 1969. Sedimentological remarks on Lower Paleozoic sandstones of south Libya. *In*: KANES, W. H. (ed.) *Geology, Archaeology and Prehistory of Southwestern Fezzan, Libya*. Petroleum Exploration Society of Libya, 11th Annual Field Conference, 91–102.

CABY, R., BERTRAND, J. M. & BLACK, R. 1981. Pan-African ocean closure and continental collision in the Hoggar-Iforas segment, central Sahara. *In*: KRONER, A. (ed.) *Precambrian Plate Tectonics*. Elsevier, Amsterdam, 407–434.

CASTRO, J. C., DELLA FAVERA, J. C. & EL-JADI, M. 1991. Tempestite facies, Murzuq basin, Great Socialist People's Libyan Arab Jamahiriya: their recognition and stratigraphic implications. *In*: SALEM, M. J. & BELAID, M. N. (eds) *The Geology of Libya. Vol. 5*. Academic Press, London, 1757–1765.

CHIARELLI, A. 1978. Hydrodynamic framework of eastern Algerian Sahara - influence on hydrocarbon occurrences. *Bulletin, American Association of Petroleum Geologists*, **62**, 667–685.

CLARK-LOWES, D. D. & WARD, J. 1991. Palaeoenvironmetal evidence from the Palaeozoic 'Nubian Sandstones' of the Sahara. *In*: SALEM, M. J. & BUSREWIL, M. T. (eds) *The Geology of Libya. Vol. 6*. Academic Press, London, 2099–2154.

COLLOMB, G. R. 1962. Etude géologique du Jebel Fezzan et de sa bodure Paléozoïque. *Notes, Mém. Comp. Fr. Pétrole*, **1**, 1–26.

DESTOMBES, J. 1968. Sur la nature glaciaire des sédiments du groupe 2ème Bani, Ashgill supérieur de l'Anti Atlas, Maroc. *Comptes Rendus de l'Academie des Sciences*, **267**, 684.

——, HOLLARD, H. & WILLEFERT, S. 1985. Lower Palaeozoic rocks of Morocco. *In*: HOLLAND, C. H. (ed.) *Lower Palaeozoic of North-western and West-Central Africa*. John Wiley, New York, 91–336.

DUBAY, L (1980. Ground water in Wadi ash Shati, Fazzan—a case history of resource development. *In*: SALEM, M. J. & BUSREWIL, M. T. (eds) *The Geology of Libya. Vol. 2*. Academic Press, London, 611–627.

FEKERINE, B. & ABDALLAH, H. 1998. Palaeozoice lithofacies correlatives and sequence stratigraphy of teh Saharan Platform, Algeria. *This volume*.

GELLATI, N & SENTOUN, R. 1993. Fracturation et diagenèse des réservoirs Cambro-Ordoviciens de la regio de Garet el Guefoul (Ahnet). *In*: BEN

HASSINE, K. & EL BORGI, M. (eds) *Fractured Reservoir Seminar* (Tunis, 1–4 September 1993), ETAP, Tunis, 29–39.

GOMEZ, F., BARAZANGI, M. & BENSAID, M. 1996. Active tectonism in the intracontinental Middle Atlas Mountains of Morocco: synchronous crustal shortening and extension. *Journal of the Geological Society, London*, **153**, 389–402.

HARLAND, W. B. ARMSTRONG, R. L., COX, A. V., CRAIG, L. E., SMITH, A. G. & SMITH, D. G. 1990. *A Geologic Time Scale 1989*. Cambridge University Press, Cambridge.

HAVLICEK, V. & MASSA, D. 1973. Brachiopodes de l'Ordovicien supérieur de Libye occidentale; implications stratigraphiques régionales. *Geobios*, **6**, 267–290.

HEA, J. P. 1971. Petrography of the Palaeozoic-Mesozoic sandstones of the southern Sirte basin, Libya. *In*: GRAY, C. (ed.) *Symposium on the Geology of Libya*. Faculty of Science, University of Libya, Tripoli, 107–125.

HMIDI, Z., SADRAS, W. *et al.* 1991. Ordovician. *In*: CHARNOCK, G., GAMBLE, S. & CHARNOCK, A. (eds) *Tunisian Exploration Review*. ETAP, Tunis; Schlumberger.

JULIVERT, M., MARTINEZ, F. J. & RIBEIRO, A. 1980. The iberian segemnt of the European Hercynian foldbelt. *In*: COGNE, J. & SLANSKY, M. (eds) *Geology of Europe: From the Precambrian to the Post-Hercynian Sedimentary Basins*. Mémoirs du BRGM, **108**, 132–158.

KLITZSCH, E. 1981. Lower Palaeozoic rocks of Libya, Egypt, and Sudan. *In*: HOLLAND, C. H. (ed.) *Lower Palaeozoic of the Middle East, Eastern and Southern Africa, and Antarctica*. John Wiley, New York, 131–164.

—— & SQUYRES, C. H. 1990. Paleozoic and Mesozoic geological history of northeastern Africa based upon new interpretation of Nubian strata. *Bulletin, American Association of Petroleum Geologists*, **74**, 1203–1211.

—— & WYCISK, P. 1987. Geology of sedimentary basins of northern Sudan and bordering areas. *Berliner geowissenschaftliche Abhandlungen, A*, **75**, 97–136.

LEFORT, J. P. & RIBEIRO, A. 1980. La faille Porto–Badajoz–Cordove a-t-elle contrôlé l'évolution de l'océan paléozoïque sud-armoricain? *Bulletin de la Société Géologique de France*. **23**, 455–462.

LEGRAND, PH. 1985*a*. Lower Palaeozoic rocks of Tunisia. *In*: HOLLAND, C. H. (ed.) *Lower Palaeozoic of North-western and West-central Africa*. John Wiley, New York, 1–3.

—— 1985*b*. Lower Palaeozoic rocks of Algeria. *In*: HOLLAND, C. H. (ed.) *Lower Palaeozoic of North-western and West-central Africa*. John Wiley, New York, 5–89.

MACGREGOR, D. S. 1998. Giant fields, petroleum systems and exploration maturity of Algeria. *This volume*.

McDOUGALL, N. D. 1988. The sedimentology of the Armorican Quartzite Group in Portugal. PhD thesis, University of Liverpool.

——, BRENCHLEY, P. J. REBELO, J. A. & ROMANO, M. 1987. Fans and fan-deltas-precursors to the Armorican Quartzite (Ordovician) in western Iberia. *Geological Magazine*. **124**, 347–359.

NELSON, R. A. & HSU, M. Y. 1993. Fractures in the Ordovician sandstones of the Sabria and El Franig structures, Tunisia. *In*: BEN HASSINE, K. & EL BORGI, M. (eds) *Fractured Reservoir Seminar*, Tunis, 1–4 September 1993, ETAP, Tunis, 29–39.

PALLAS, P. 1980. Water resources of the Socialist People's Libyan Arab Jamahiriya. *In*: SALEM, M. J. & BUSREWIL, M. T. (eds) *The Geology of Libya. Vol. 2*. Academic Press, London, 539–594.

PIEROBON, E. S. T. 1991. Contribution to the stratigraphy of the Murzuq basin, SW Libya. *In*: SALEM, M. J. & BELAID, M. N. (eds) *The Geology of Libya. Vol. 5*. Academic Press, London, 1767–1784.

SCOTESE, CH. R & MCKERROW, W. S. 1991. Ordovician plate tectonic reconstructions. *In*: BARNES, R. & WILLIAMS, S. H. (eds) *Advances in Ordovician Geology*. Geological Survey of Canada Paper, **90**(9), 271–282.

SEILACHER, A. 1990. Palaeozoic trace fossils in Egypt. *In*: SAID, R. (ed.) *The Geology of Egypt*. Balkema, Rotterdam, 649–670.

SELLEY, R. C. 1972. Diagnosis of marine and nonmarine environments from the Cambro-Ordovician sandstones of Jordan. *Journal of the Geological Society*, **128**, 135–150.

SILVA, A. F. D. & RIBEIRO, A. 1985. Thrust tectonics of sardic age in the Alto Douro region (Northeastern Portugal. *Comunicacoes dos Servicos Geologicos de Portugal*, **71**, 151–157.

SIMON PETROLEUM TECHNOLOGY (1994) Regional exploration guide—North Africa.

STEARNS, D. W. & LINSCOTT, J. P. 1993. The influence of in situ shear stress on fracture permeability in folded reservoirs. *In*: BEN HASSINE, K. & EL BORGI, M. (eds) *Fractured Reservoir Seminar*, Tunis, 1–4 September 1993, ETAP, Tunis, 3–17.

TRENCH, A. & TORSVIK, T. H. 1992. Palaeomagnetic constraints on the Early-Middle Ordovician palaeogeography of Europe: Recent advances. *In*: WEBBY, B. D. & LAURIE, J. R. (eds) *Global Perspective on Ordovician geology*. Balkema, Rotterdam, 255–259.

TURNER, B. R. 1980. Palaeozoic sedimentology of the southeastern part of Al Kufrah basin, Libya: a model for oil exploration. *In*: SALEM, M. J. & BUSREWIL, M. T. (eds) *The Geology of Libya. Vol. 2*. Academic Press, London, 351–374.

—— 1991. Palaeozoic deltaic sedimentation in the southeastern part of Al Kufrah basin, Libya. *In*: SALEM, M. J. & BUSREWIL, M. T. (eds) *The Geology of Libya. Vol. 5*. Academic Press, London, 1713–1726.

VOS, R. G. 1981. Sedimentology of an Ordovician fan delta complex, western Libya. *Sedimentary Geology*, **29**, 153–170.

WHITEMAN, A. J. 1971. 'Cambro-Ordovicien' rocks of Al Jazair (Algeria)—A review. *Bulletin, American Association of Petroleum Geologists*, **55**, 1295–1335.

Sedimentological and diagenetic controls on Cambro-Ordovician reservoir quality in the southern Hassi Messaoud area (Saharan Platform, Algeria)

MOHAMED ROBERT DJARNIA & BERRACHED FEKIRINE

CRD-Sonatrach, Avenue du 1er Novembre, 35000 Boumerdès, Algeria

Abstract: The Cambro-Ordovician reservoirs of the Hassi Messaoud area comprise quartzitic sandstones, which rest unconformably on granitic basement and are capped by the Hercynian unconformity. Two sequence stratigraphic cycles are identified: a lower cycle of lowstand, transgressive and highstand deposits, and an upper cycle in which only lowstand deposits are preserved below the Hercynian unconformity. Sandstone of the greatest thickness and highest porosity and permeability occur within the lowstand deposits of the two sequences. Petrographic and scanning electron microscope studies were conducted in two wells in the southern Hassi Messaoud area on five sandstone units, to which the following chronostratigraphic terms are applied, from base to top: Ra + Ri lithozones (which contain the bulk of the reserves), Alternance Zone, El Atchane Sandstones and Hamra Quartzite. Reservoir quality is found to bear a strong relationship to clay content and mineralogy. All reservoirs are characterized by an extensive quartz cementation, which reduces porosities to generally below 10%. Permeability is related to clay content and type, with effective permeabilities generally limited to the quartz- and kaolinite-rich Ra lithozone. Permeability is lowest in reservoirs rich in fibrous illite and/or chlorite, such as the Hamra Quartzite. As porosity shows a less direct relationship to matrix mineralogy, there is a poor statistical relationship observed between porosity and permeability. Comparative diagenetic studies carried out within both the oil-bearing and the water-bearing parts of the reservoirs have determined that all the secondary processes occurred under freely operating diagenesis, pre-dating oil emplacement in the structure.

Production within the giant Hassi Messaoud oilfield is concentrated within the central part of the field. In contrast, the wells drilled in the peripheral parts of the field have low or uneconomic production rates and have often even been dry, despite the presence above the oil–water contact of some moderately porous sandstone reservoirs. The objective of this paper is to seek geological explanations for these trends, either in the primary sedimentary fabric of the reservoirs concerned or in their subsequent diagenetic alteration. This study is concentrated in the southern part of the Hassi Messaoud field, particularly on wells HGA-1 and SG-1 (Fig. 1).

The Hassi Messaoud field is the largest oilfield in Algeria, containing in excess of 9 billion barrels recoverable reserves, within a series of Cambro-Ordovician reservoirs sealed on the Hercynian unconformity by Triassic evaporites (Balbucchi & Pommier 1970). The Hassi Messaoud palaeomorphological trap was progressively formed during a series of Palaeozoic tectonic events, ranging from the Sardian (intra-Cambrian, *c.* 500 Ma), through the Taconic (Ordovician, 440 Ma) to the Hercynian (Carboniferous, 324 Ma).

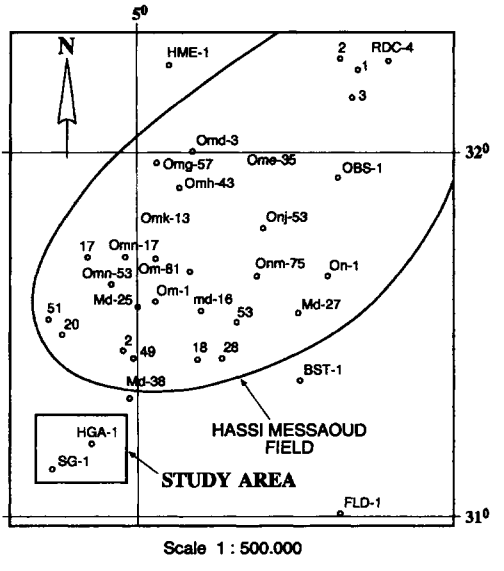

Fig. 1. Location map of the Hassi Messaoud area showing the study area relative to the main producing field. Scale 1:500 000.

DJARNIA, M. R. & FEKERINE, B. 1998. Sedimentological and diagenetic controls on Cambro-Ordovician reservoir quality in the southern Hassi Messaoud area. *In*: MACGREGOR, D. S., MOODY, R. T. J. & CLARK-LOWES, D. D. (eds) 1998. *Petroleum Geology of North Africa*. Geological Society, London, Special Publication No. 132, 167–174.

Chrono-stratigraphy and sequence stratigraphy

Five reservoir units are distinguished in the Hassi Messaoud oilfield, all of which were penetrated by the two wells (Fig. 2). These reservoirs range in age from Upper Cambrian (Ra + Ri) to Tremadoc–Arenig (Alternance Zone, El Atchane Sandstone and Hamra Quartzite). The bulk of production comes from the Ra, whereas other reservoirs are only locally productive. Reservoir depth lies between 3450 and 3150 m. The field OWC lies within the Ra in the productive well HGA-1 but roughly corresponds to the top of the main Cambrian reservoirs (Ri) in the structurally lower and unproductive well SG-1 (Fig. 2). The overlying Ordovician Hamra Quartzite, positioned above the field OWC, gives some oil shows but has proven unproductive because of low permeability.

The Cambro-Ordovician section of the Sahara Platform can be subdivided into three major sequences (Fekirine & Abdallah this volume). As a regional generalization, formations exhibit thickness variations and lateral facies changes that are traceable and predictable in the subsurface, reflecting the existence of a wide shelf primarily influenced by eustatic sea-level rises and falls. This regional sequence stratigraphy can be correlated into the sections of wells HGA-1 and SG-1 and provides an alternative means of viewing reservoir stratigraphy (Fig. 3). In this correlation, the Ra lithozone ties to the lowstand systems tract of the first sequence, the Ri lithozone to the transgressive systems tract and the El Atchane to the top of the highstands tract, whereas the Hamra Quartzite ties to the lowstand tract of the second sequence.

Cements and clay content

Scanning electron microscope observations have determined the nature of the clay mineral and quartz overgrowths that are seen in varying amounts in all reservoirs (Figs 4 and 5), and have allowed an assessment of the relative timing of different cements. The following summarizes the characteristics of each cement type.

Quartz

Quartz overgrowths form in very regular shapes, with the extent of these overgrowths being the prime control on porosity preservation. Such quartz cements are thought to form at temperatures exceeding 90 °C and can theoretically continue after oil emplacement (Bjørlykke & Egeberg 1993). Quartz overgrowths from similar Cambrian sandstones in nearby outcrop at Hassi Bir Rebaiz are thought to have formed at temperatures of 95–130 °C. Such formation temperatures will have certainly been attained in the Mesozoic and possibly in the Carboniferous.

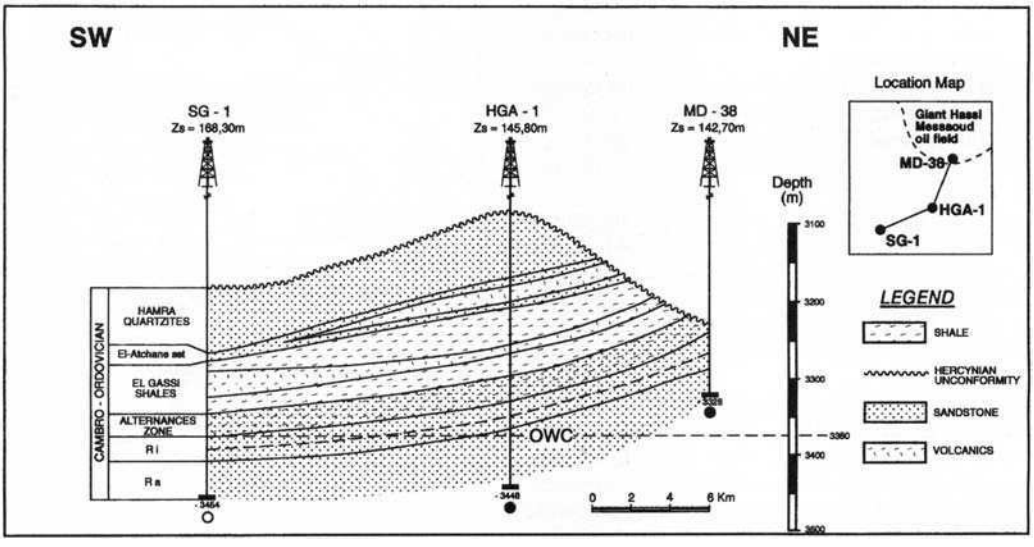

Fig. 2. Structural geological cross-section through the Cambro-Ordovician reservoirs of wells SG-1 . HGA-1 and a productive Hassi Messaoud well. Producibility of these wells is strongly connected to the presence of the Ra unit above the field OWC.

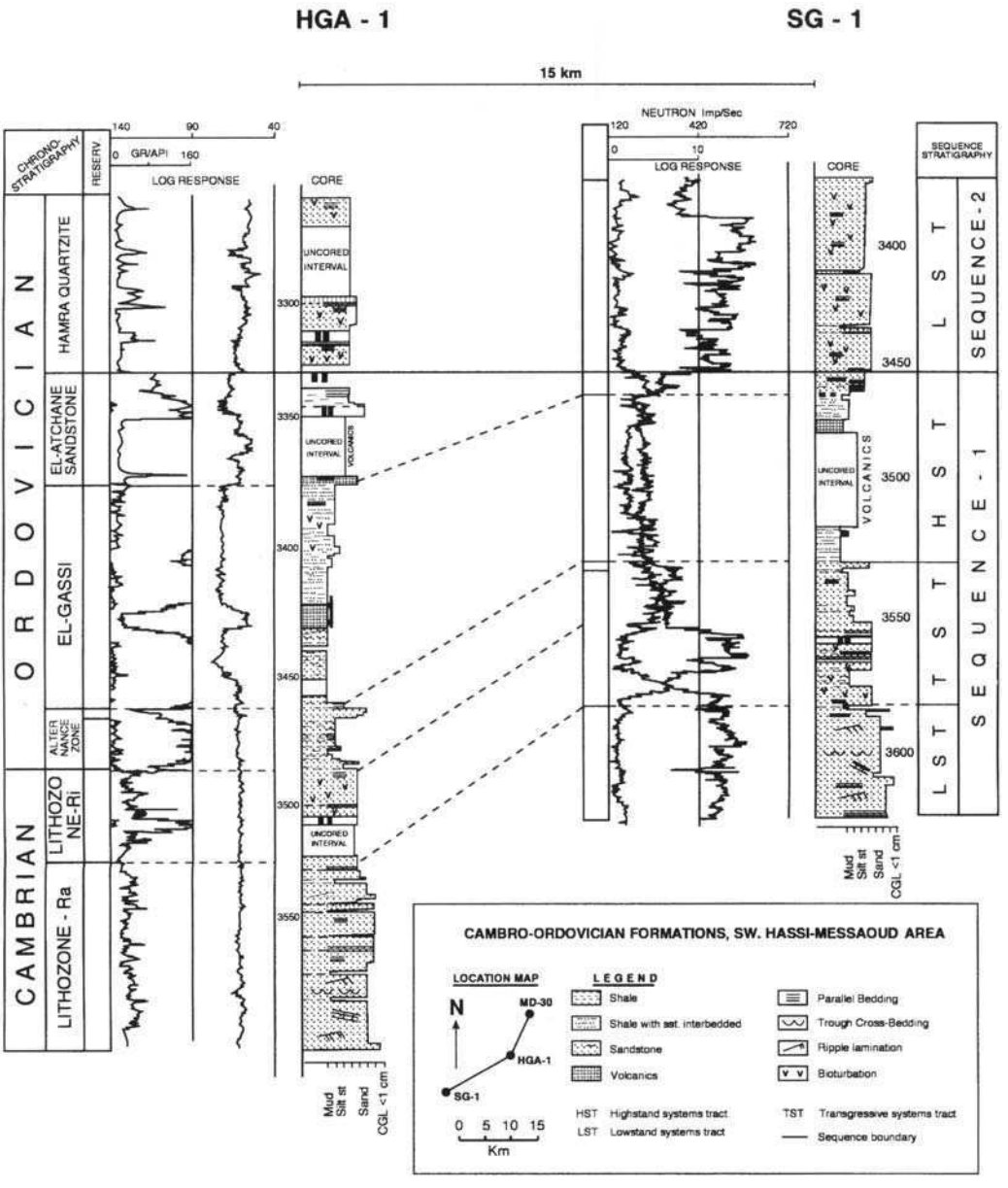

Fig. 3. Stratigraphic correlation between HGA-1 and SG-1, illustrating the sequence stratigraphy applied in this paper.

The latter date would be more consistent with the interpreted Permian date of the later illite cement.

The most likely origins for the silica cement are illitization of K-feldspars and mica or kaolinization of feldspars. Quartz may be produced also by the pressure-solution of quartz grains or mineral reactions involving the release of silica from amorphous silica (biogenic, volcanic, opal, etc.). The breakdown of K-feldspar to illite and quartz is evidenced through scanning electron microscope studies on Triassic and Cambro-Ordovician sediments in the Hassi R'Mel field (Djarnia, 1991). Some samples here show adjoining altered K-feldspar and fibrous illite.

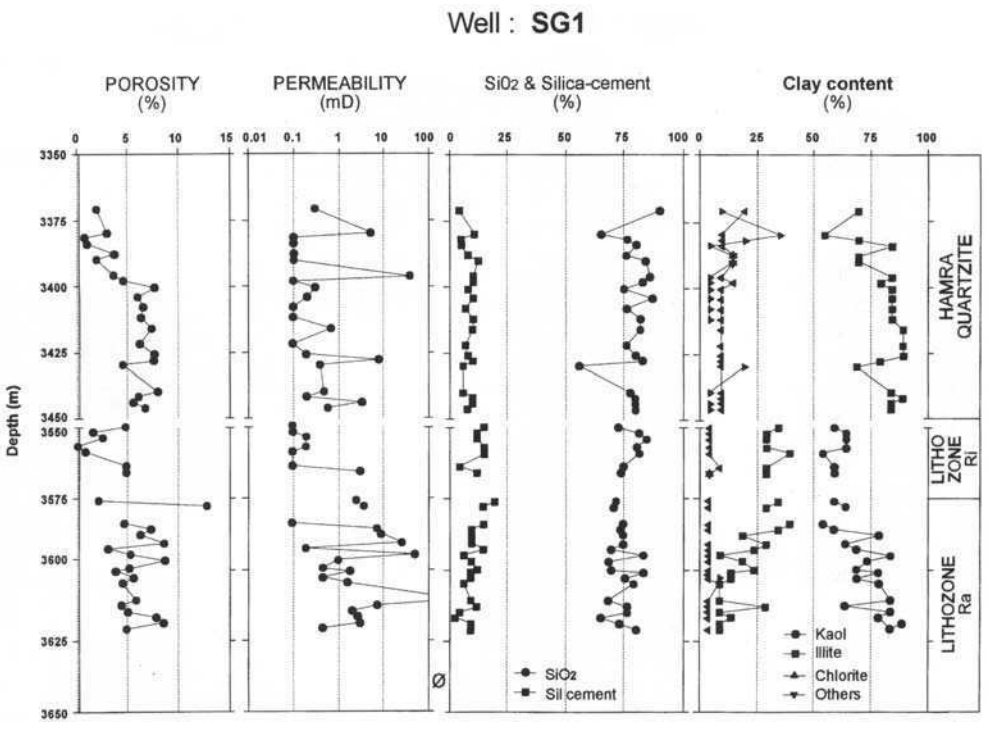

Fig. 4. Graphical distribution of porosity, permeability, quartz cement and clay content in well SG-1

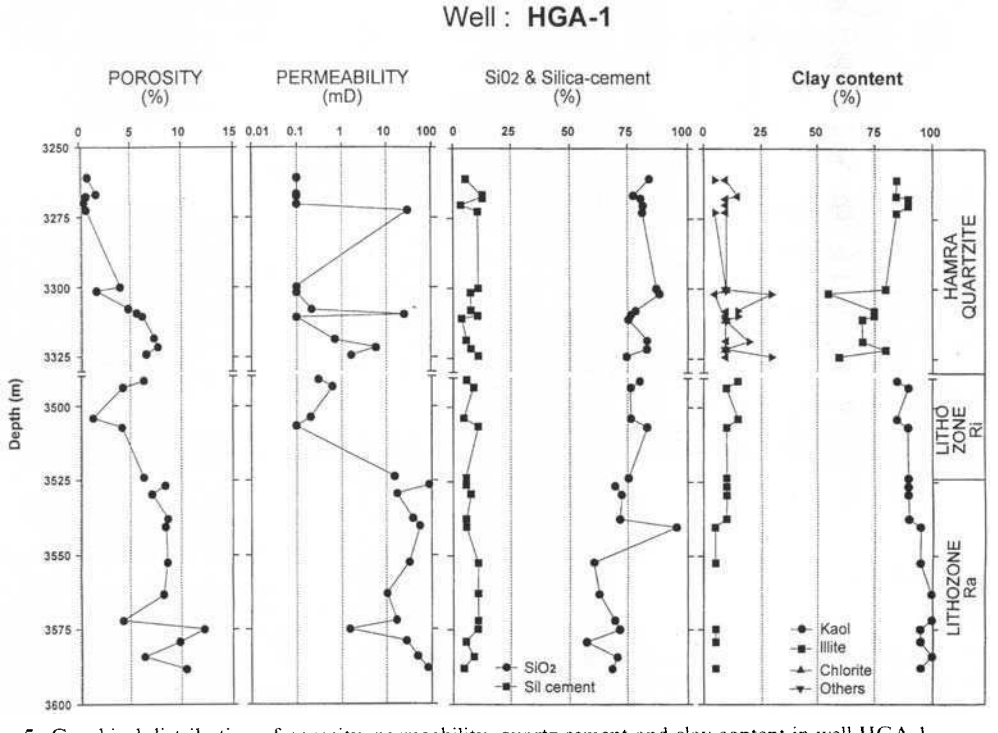

Fig. 5. Graphical distribution of porosity, permeability, quartz cement and clay content in well HGA-1

Kaolinite

Clay minerals present are normally secondary in origin, forming as microcrystals over the earlier quartz overgrowths. Kaolinite is common in all Cambrian reservoirs, normally taking a hexagonal form. In well HGA-1, however, it takes a different crystalline form throughout the Cambrian reservoir, and may possibly be dickite (Kulbicki *et al.*, 1961). In many sandstones, the kaolinite fills what would appear to be secondary pores and in some of these, particularly in the Ra and Ri, it constitutes 60–95% of the cement (Fig. 6). Kaolinite cements post-date quartz overgrowths but pre-date the formation of illite cements. The most likely origin for the formation of kaolinite is considered to be the breakdown of feldspars and micas.

Illite

Illite is the latest diagenetic clay formed in Ri + Ra reservoirs. There are several generations of illite, the most significant of which is a late-stage fibrous illite. In the Ra of both the studied wells, this illite, when present in significant quantities, has a major downgrading effect on permeability.

Illite may form as a product of the breakdown of a wide variety of primary minerals, including feldspar (see discussion on quartz, above), mica, kaolinite, smectite, detrital alumino-silicates and glauconite. The formation of fibrous illite is the latest observable diagenetic event before oil emplacement in the Ra and Ri of Hassi Messaoud, though in other water wet reservoirs, a later alteration to chlorite may be observed (see below). Although this has not been studied in Hassi Messaoud itself, the timing of formation of the fibrous illite cement in Cambro-Ordovician reservoirs has been the subject of a number of studies in other areas of Algeria, aimed at providing control on the timing of oil emplacement. The best data comes

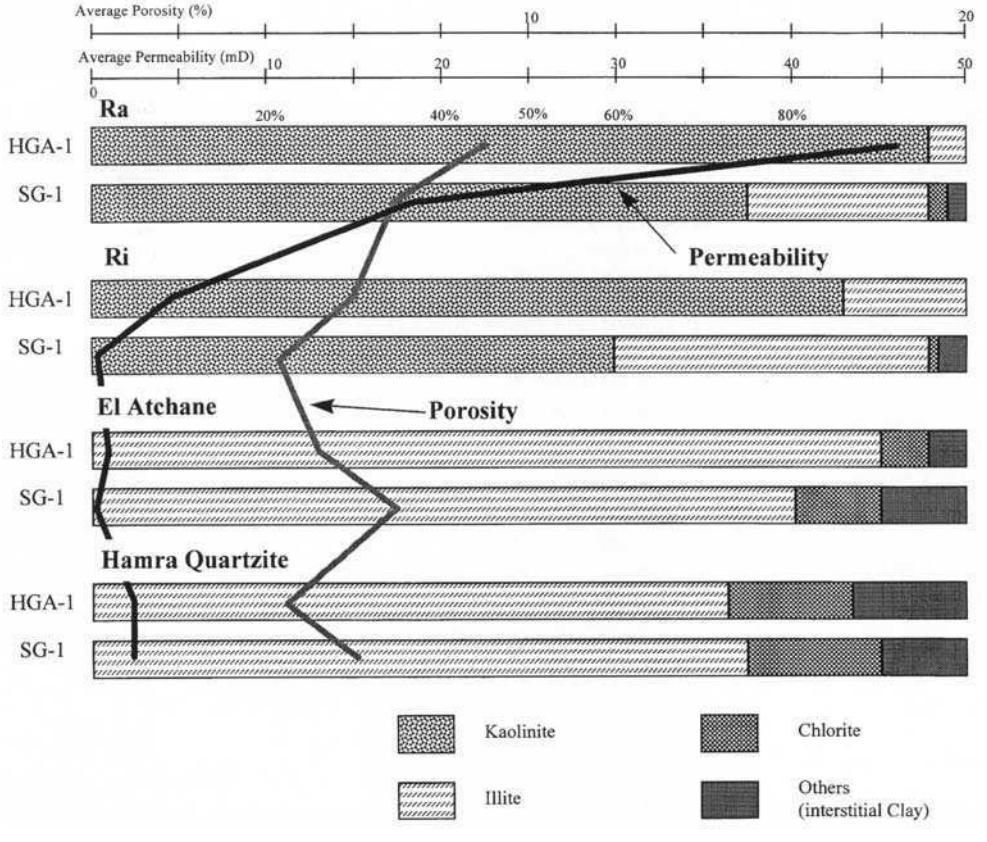

Fig. 6. Simplification of Figs 4 and 5, showing average porosities, permeabilities, quartz and clay content for the various reservoirs of the two wells. (Note the clear relationships between permeability and clay type.)

again from the Cambro-Ordovician of the Hassi R'Mel field (well HR22), where K–Ar dating has established an age of 324 Ma (Carboniferous) for the fibrous illite (Djarnia ,1991). Durfee (1995) has also attempted to date the illite at the well EHT-1, where an average age of 273 Ma (Permian) was recorded. These dates would suggest a tie to Hercynian tectonic events, which may have caused major changes in patterns of fluid flow in these reservoirs, particularly as a result of subaerial exposure on the Hercynian unconformity.

Chlorite

In the Hamra Quartzite, much of the illite appears to be partly transformed to chlorite. Chlorite is, however, rare in the Ra and Ri.

Controls on clay mineralogy

The relative timing of clay cements observed in these wells is consistent with that observed in the main part of the Hassi Messaoud field. Here, three main stages of clay formation are suggested; (1) kaolinite, (2) illite (3) the transformation of illite to chlorite, the latter being largely confined to the Hamra Quartzite.

By and large, there is a statistical correlation (Fig. 6), by which sandstones rich in one cement tend to be poorer in another cement type. A decrease in quartz cement may thus be associated with an increase in kaolinite and a decrease in kaolinite with an increase in illite. Many sandstone units are therefore polarized in terms of their relative clay mineral content, being composed almost entirely of one clay mineral type. This is believed to be a result of pH control on clay mineral formation. The formation of kaolinite requires low-pH near surface free water circulation conditions, whereas formation of illite is favoured by more confined and alkaline conditions at depth. The change from acidic to alkaline conditions with depth may be extremely rapid, such that no zone permits the formation of a mixed set of clay minerals.

Reservoir quality and relationship to cements and clays

Cambrian reservoirs

The emphasis in this study is on the main Cambrian reservoirs of the lowstand sequence tract of Sequence 1 (Ra + Ri lithozones), and on relationships observed between permeability, clay mineralogy and diagenetic features. Porosity within these units varies between 3 and 12% (Figs 6–8), with little variation seen between the two zones. Porosity reduction has occurred through quartz overgrowth, and through plugging of pores by illite and kaolinite cement. As observed in scanning electron micrographs, significant secondary intercrystalline microporosity is developed where authigenic hexagonal kaolinite and/or fibrous illite are abundant. As illustrated in Figs 7 and 8, the relationship between porosity and permeability is poor for these wells. This is the result of variations in cement type and its implications for the relative amounts of intergranular macroporosity and

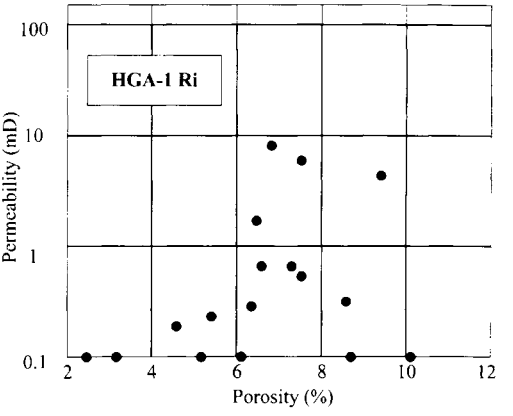

Fig. 7. Porosity v. permeability for the Ra unit of well HGA-1. Net pay cut-off can be taken as low as 6% here, though there is a strong dependence on clay mineralogy.

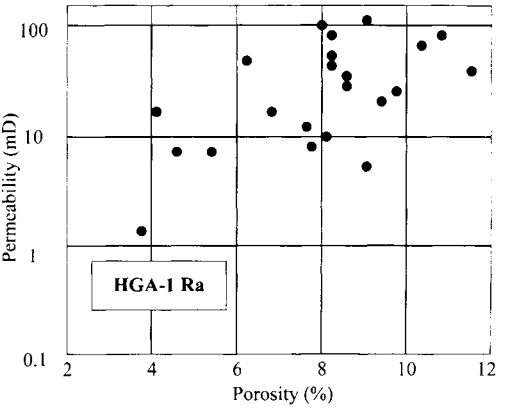

Fig. 8. Porosity v. permeability for the Ra unit of well HGA-1. (Note the differences in trend compared with Fig. 7, attributable to a lower clay and particularly illite content in this unit.)

intercrystalline microporosity, permeability being generally associated with the former. General trends that are apparent in Figure 6 are as follows: (a) Sandstones with a high proportion of secondary porosity filled with fibrous illite often show appreciable porosity but nearly always show low permeability (e.g. Ri of well SG-1); (b) within the Ra, the highest permeabilities (> 10 mD) occur in clay- (and particularly illite)-poor quartz cemented sandstones, with a range of porosity between 5 and 9%; (c) contents of chlorite are insufficient in the Ra and Ri to significantly influence porosity and permeability development.

Ra reservoirs show an average permeability of 46 mD in the kaolinite-rich and illite-poor section at well HGA-1 and 17 mD in well SG-1, with an overall range of 1 to > 100 mD. Cross-plotting for the Ra of well HGA-1 shows the correlation coefficient between porosity and permeability to be low, at < 0.2 (Fig. 7). The overlying more illite-rich Ri unit shows poorer reservoir quality, with an average permeability of around 4.5 mD in well HGA-1 and only 0.4 mD in a particularly illite-rich interval in well SG-1.

In summary, variations in reservoir quality within both Cambrian reservoirs indicate clearly the effect of the relative proportions of kaolinite, illite and silica cements in controlling permeability. The failure of well SG-1 at this level can be attributed to the absence of any permeable illite-poor reservoir intervals above the OWC, with the only instances of permeability greater than 10 mD occurring in the Ra, below the OWC.

Ordovician reservoirs

High allogenic clay content accounts for reservoir quality impairment within the El Atchane Sandstones and the Alternance Zone in well SG-1 and HGA-1 (Fig. 6). Average permeability within these units is only around 0.2 mD. despite porosities in the El Atchane of around 7%.

The Hamra Quartzite, representing the lowstand deposits of Sequence 2, shows extensive quartz overgrowths, which have drastically reduced porosity to around 4–6%. Kaolinite is almost completely absent in this unit whereas fibrous illite and chlorite are abundant, as is interstitial clay. The combined effect of these clays is to reduce permeabilities to well below those for equivalent porosities in the Ra reservoir (Fig. 6) and therefore to make this unit ineffective as an oil reservoir. Porosity and permeability again show a relatively poor relationship in this unit.

Conclusions

Two geological controls are observed on reservoir development in the southern Hassi Messaoud field: sequence stratigraphy and diagenesis. The thickest and highest-quality reservoirs of the Ra lithozone and Hamra Quartzite represent the lowstand deposits of two Palaeozoic sequences.

Diagenesis is a very important controlling factor on permeability development in the reservoirs of the Hassi Messaoud field. The main cements present are quartz, kaolinite and illite, deposited in that order. Specific formations and intervals are usually dominated by a single clay type, with the controlling factor on that clay type probably being pH. A distinct relationship is seen between presence and amount of clay cement, particularly pore throat blocking fibrous illite, and permeability. The highest permeabilities consequently occur in the sandstone intervals with a high proportion of quartz cement and low clay content, where most of the clay present is kaolinite. These are concentrated in the Cambrian Ra lithozone. The more clay-rich sandstones of the Ri lithozone, Alternance Zone and El Atchane tend to be tight as a result of high illite content. Poor reservoir quality in the Hamra Quartzite seems to be related to a high illite and chlorite content. Because of the lowering of permeability in these upper reservoirs, many wells, such as SG-1, are unproductive where the kaolinite-rich and clay-poor Ra lithozone falls below the OWC.

The authors wish to acknowledge the Director of CRD-Sonatrach for the permission to publish this work.

Ph. Karcher from the Institute of Geology, Strasbourg, France, was responsible for the SEM work. BP are thanked for their assistance in drafting the figures.

References

BALBUCCHI, A. & POMMIER, G. 1970. Cambrian oilfield of Hassi Messaoud, Algeria. *In*: HALBOUTY, M. T. (ed.) *Geology of Giant Petroleum Fields, American Association of Petroleum Geologists, Memoirs*, **14**, pp. 477–488.

BJØRLYKKE, K & EGEBERG, P. K. 1993. Quartz cementation in Sedimentary Basins. *Bulletin, American Association of Petroleum Geologists*, 77(9), pp.1538–1548).

DJARNIA, M. R. 1991. *Étude des conditions de formation d'un eventuel anneau à huile dans le gisement de Hassi R'Mel, Algérie*. Thèse de Doct. ès Sci., Université Louis Pasteur, Strasbourg.

—— 1995. Les argiles des réservoirs Cambro-ordoviciens impact de l'aggradation diagénètique sur la

porosité. *1ères J.S.T de l'Institut Algérien du Pétrole, Boumerdès.*

—— & FEKIRINE, B. 1995. New microscopic vision of the diagenetic effect within the Cambro-Ordovician reservoirs of the SW Hassi-Messaoud Area. *In*: *10èmes Séminaire National des Sciences de la Terre, Algiers.*

DURFEE, B. A. 1995. *Diagenetic evolution of Cambrian sandstones, Hassi Bir Rekaiz Area, Algeria.* Arco Internal Report.

FEKIRINE, B. & ABDALLAH, H. 1998. Palaeozoic lithofacies correlatives and sequence stratigraphy of the Saharan Platform, Algeria. *This volume.*

KULBICKI, J. *et al.* 1961. Les oligo-élements de la série argilo-grèseuse de l'Ordovician et du Mésozoique inférieure de la région de Hassi Messaoud. *Mémoire de la Société Géologique de France.* **39**(88).

Controls on hydrocarbon occurrence and productivity in the F6 reservoir, Tin Fouyé–Tabankort area, NW Illizi Basin

N. ALEM, S. ASSASSI, S. BENHEBOUCHE & B. KADI

Sonatrach, Centre de Recherche et Dévelopment, Boumerdès, Algeria

Abstract: Several oil accumulations of various sizes have been found within the F6 reservoir of Upper Silurian–Lower Devonian age in the Tin Fouyé region of the Illizi Basin, about 1500 km from Algiers. Lithologically, the F6 consists of interbedded sandstones and shales and is subdivided into units: M1, M2, A, B1, B2, C1, C2 and C3, the upper units often being missing through erosion. These reservoirs, which were deposited in offshore coastal bars and tidal channels, show a high degree of lateral and vertical facies variation. Reservoir quality is maximized in medium- to coarse-grained clay-poor bar sands within units C1 and B2, which contain significant secondary porosity. Hydrodynamic activity is very important in controlling the distribution of hydrocarbons. Study of the hydrology of the F6 reservoir shows that connate water and oil have been frequently flushed by fresh water in the most permeable units, particularly C1 and B2. This finding is supported by hydrochemical data, by the inclination of oil–water contacts and by a high observed hydraulic gradient. This mechanism has led to the flushing of some oil from the Tin Fouyé Est (TFE) structural trap and a concentration of oil in an accumulation with a tilted contact on the Tin Fouyé Nord structural nose. Many kinds of traps have been recognized in this region. These include a simple structural trap at Tin Fouyé, a combination hydrodynamic–stratigraphical–structural trap at Tin Fouyé Nord, a hydrodynamic–structural trap at TFT-2 and a pure hydrodynamic trap at TFT 8. Hydrodynamic activity is not favourable for the accumulation of hydrocarbons in low-amplitude structures but can lead to significant accumulations in favourably orientated structural noses, even when these lack closure.

This paper describes the petroleum geology of the 'F6' reservoir in the Tin Fouyé–Tabankort region of the northwestern part of the Illizi Basin (Fig. 1). This field produces from the Ordovician as well as the F6 reservoir. The F6 pools are some of the most unusual and complex in the region, showing a distinct hydrodynamic control, together with a complex reservoir and poroperm distribution. This paper summarizes the factors controlling hydrocarbon distribution and reservoir production in this Upper Silurian–Lower Devonian reservoir.

The first exploration in the Tin Fouyé region was conducted by CFPS in the late 1950s. Seismic data were acquired in 1958–1959, and led to the drilling of the first well in 1960, which discovered the Tin Fouyé field in a simple structural trap (see Fig. 3, below). It was not until 6 years later that exploration stepped out to the north into the area termed 'Tin Fouyé–Tabankort'. The TFT-101 well (see Figs 3, 9) discovered the first of a series of F6 oil pools in this northern region, within traps which are clearly not primarily structurally controlled. The pool found by TFT-101 is termed 'Tin Fouyé Nord' in this paper. A number of smaller pools have since been found by later appraisal and development drilling, much of which was primarily directed at the deeper Ordovician reservoir. The Tin Fouyé region commenced production in 1963 and TFT (Tin Fouyé Nord pool) in 1967. Chiarelli (1978) described the results of drilling in the field up to that time, and this paper is essentially an update of his work, based on the results of further development drilling, which have considerably improved our knowledge of oil distribution in the region and the geological controls on productivity.

Reservoir stratigraphy and structure

The F6 reservoir is subdivided into eight reservoir units (Fig. 2). The highest (Early Devonian) units are frequently eroded out on an overlying unconformity and the highest reservoir, Unit C3, is completely missing over the area. The units distinguished can be grouped into two series and tied to the palynological zonation of Lanzoni & Magloire (1968; Fig. 2). A good correlation also exists with outcrops to the south.

The isobath map at the top of the F6 reservoir (Fig. 3) illustrates the structure resulting from the Hercynian and earlier orogenies. A broad N–S anticlinal nose crosses the area, with several second-order narrow anticlines formed along a series of NNW–SSE trending inversion faults (e.g. between TFT-104 and TFTN-2). These faults were initially active as normal faults during the Frasnian tectonic movements and were inverted during the Hercynian orogeny.

ALEM, N., ASSASSI, S., BENHEBOUCHE, S. & KADI, B. 1998. Controls on hydrocarbon occurrence and productivity in the F6 Reservoir, Tin Fouyé–Tabankort area, NW Illizi Basin. *In*: MACGREGOR, D. S., MOODY, R. T. J. & CLARK-LOWES, D. D. (eds) 1998. *Petroleum Geology of North Africa*. Geological Society, London, Special Publication No. 132, 175–186.

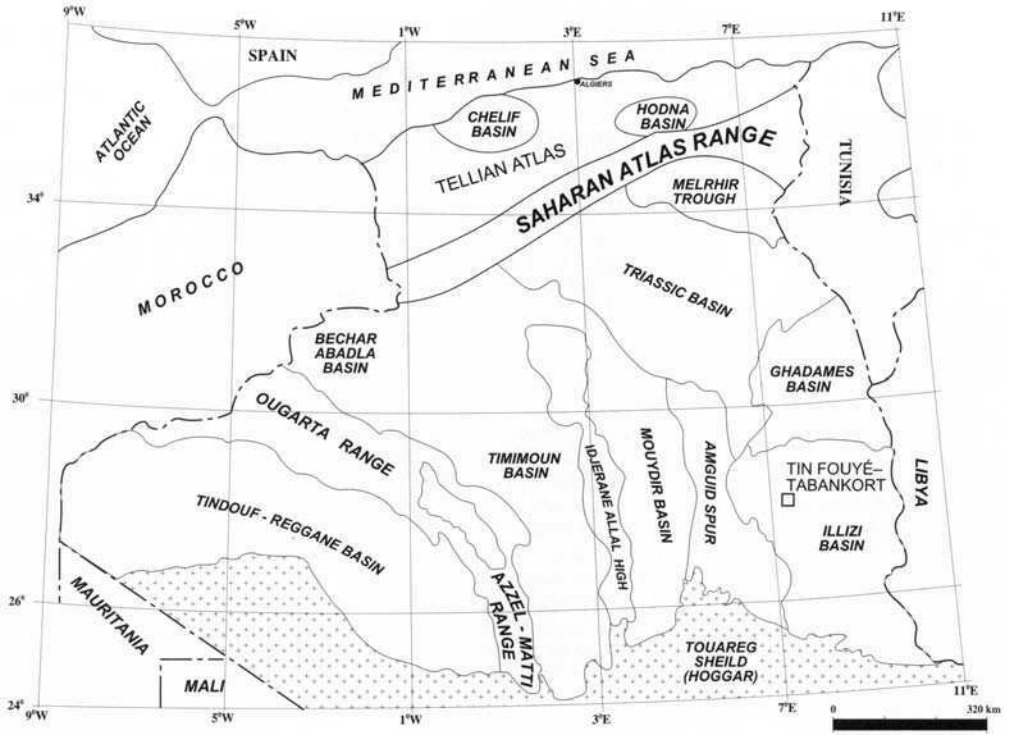

Fig. 1. Location of Tin Fouyé–Tabankort area.

F6 reservoir sedimentology and reservoir quality

The reservoir has been correlated as eight electrosequences, which are related to chronostratigraphic units in the manner shown in Figs 2 and 4. Unfortunately, electrosequences rarely tie exactly to the main reservoir units. This division is based on log correlations tied to core descriptions and outcrops. The electrosequences themselves usually show coarsening-up log profiles, though individual sand bodies may show both fining-up and coarsening up-profiles. The correlation of individual sand bodies from well to well is poor, indicating a high degree of lateral facies variation.

Reservoir quality is controlled by both the primary sedimentary fabric and through secondary diagenetic alteration. Table 1 summarizes the petrophysical parameters, as measured from cores, recorded in the various sandstone units.

Most production in the Tin Fouyé–Tabankort region comes from Units C2, C1 and the upper part of Unit B2 (equivalent to electrosequences F, G and H). Individual sand bodies within these units were deposited as shoreface bars, tidal bars and tidally influenced channels. Individual sands range up to 10 m in thickness, with the greatest thicknesses encountered within unit C1. Despite the high level of lateral facies variation, a single oil-bearing reservoir is present with a free water level dipping to the NNW.

Petrographic study of the F6 reservoir has revealed a complex diagenetic history, summarized in Fig. 5. The main diagenetic controls apparent are: (a) the development of silica overgrowths that destroy primary porosity but inhibit the compaction process; (b) later dissolution of the silica cement, creating significant secondary porosity; this may be related to periods of elevated temperature and pressure; (c) development of other later cements (illite, carbonate, pyrite, ferruginous) that generally reduce porosity and permeability.

Porosity and permeability maps are given for the two main productive zones, the C1 and B2 reservoirs (electrosequences G–H and E–F–G respectively; Figs 6 and 7). The C1 reservoir shows high permeabilities across the field, increasing from a minimum of around 50 mD close to the erosion limits of the reservoir to in excess of 500 mD in the Tin Fouyé Nord area.

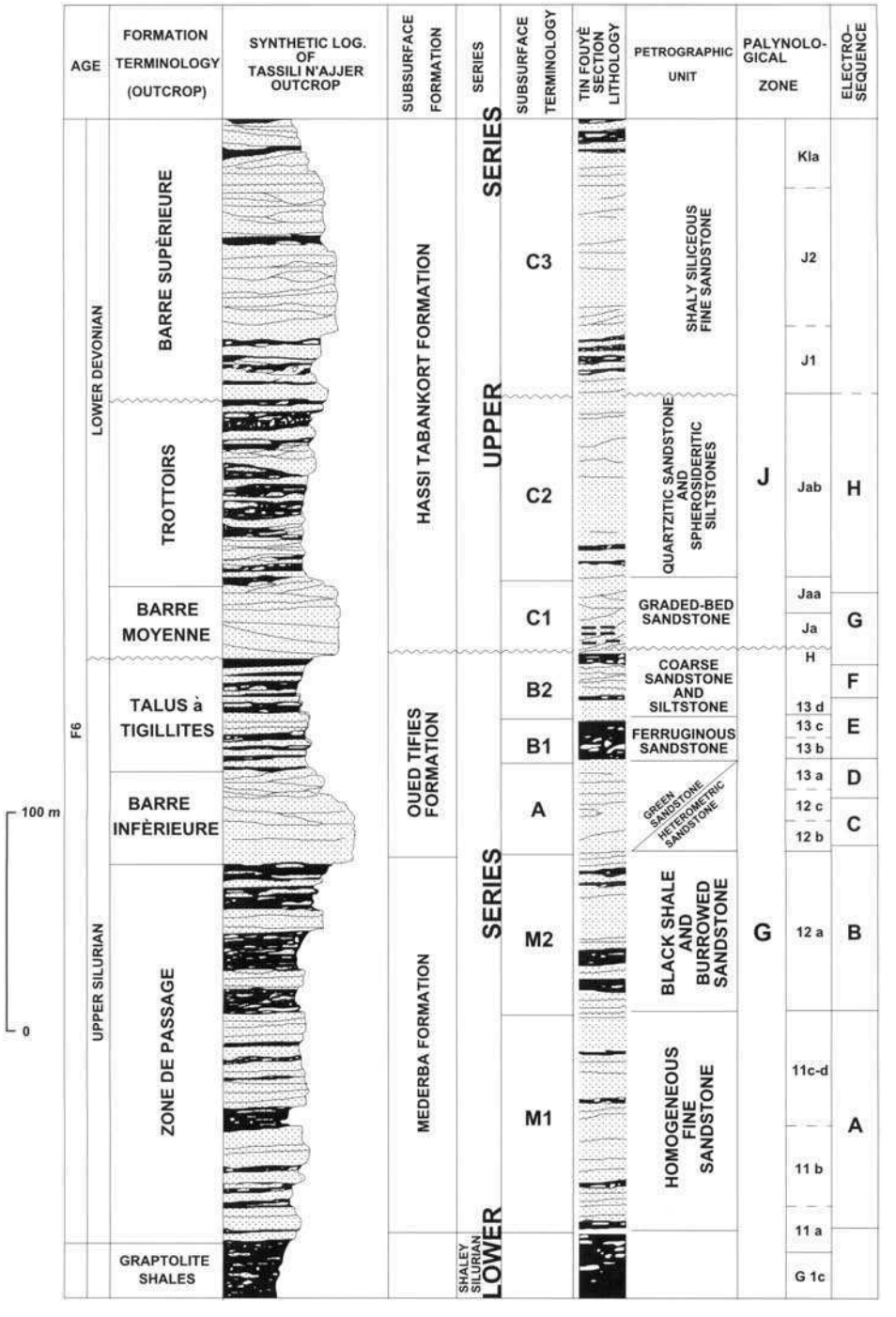

Fig. 2. Correlation of Tin Fouyé–Tabankort cored reservoir section with outcrop and with palynological zones and electrosequences. It should be noted that most of the Lower Devonian (C1–C3) section is missing on an unconformity over large parts of the region.

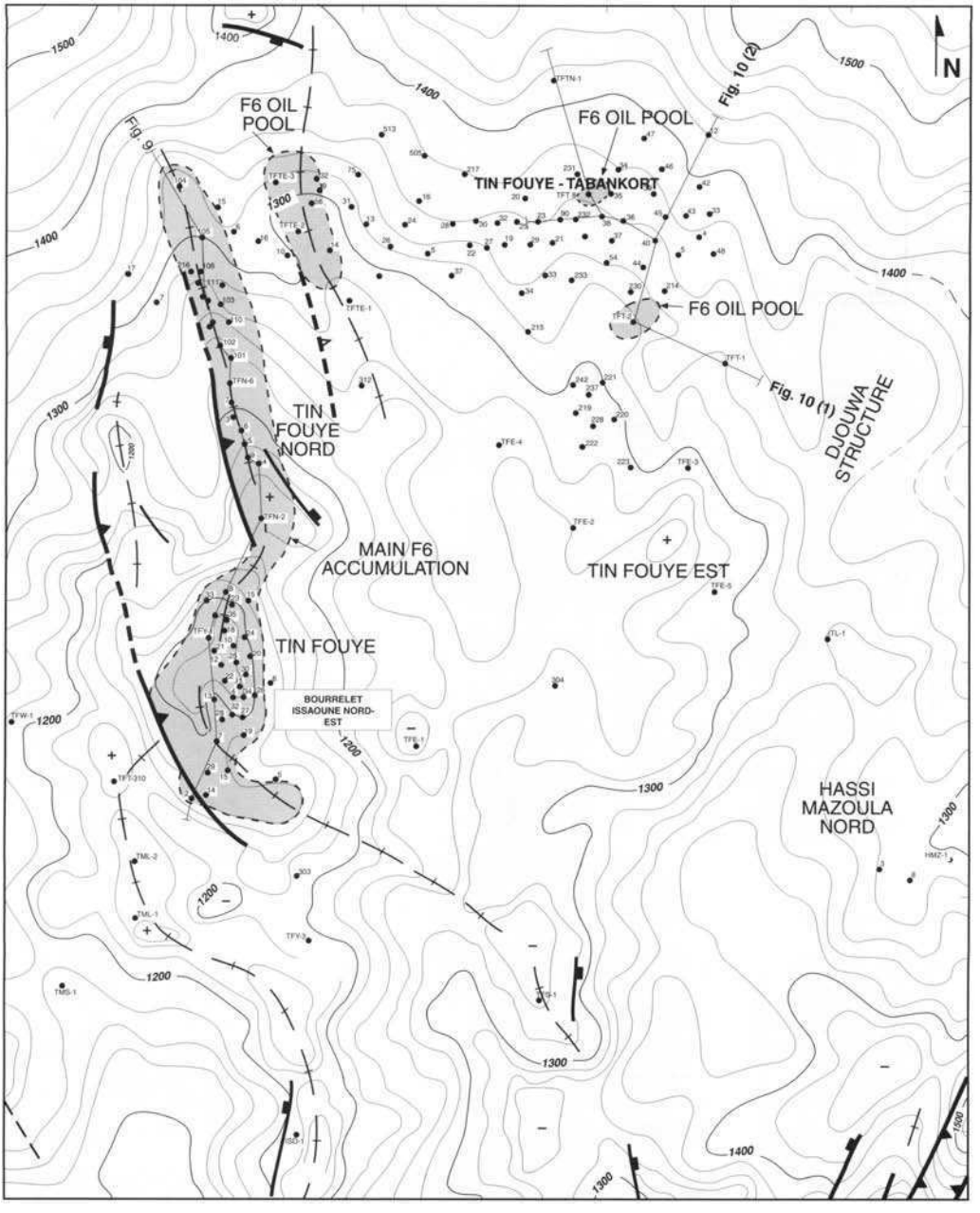

Fig. 3. Isobath map at the top of the F6 reservoir. Schematic outlines of oil accumulations at F6 level are shown and the general lack of correspondence to structural closure can be noted. The well pattern illustrated here is more indicative of hydrocarbon occurrence at Ordovician level.

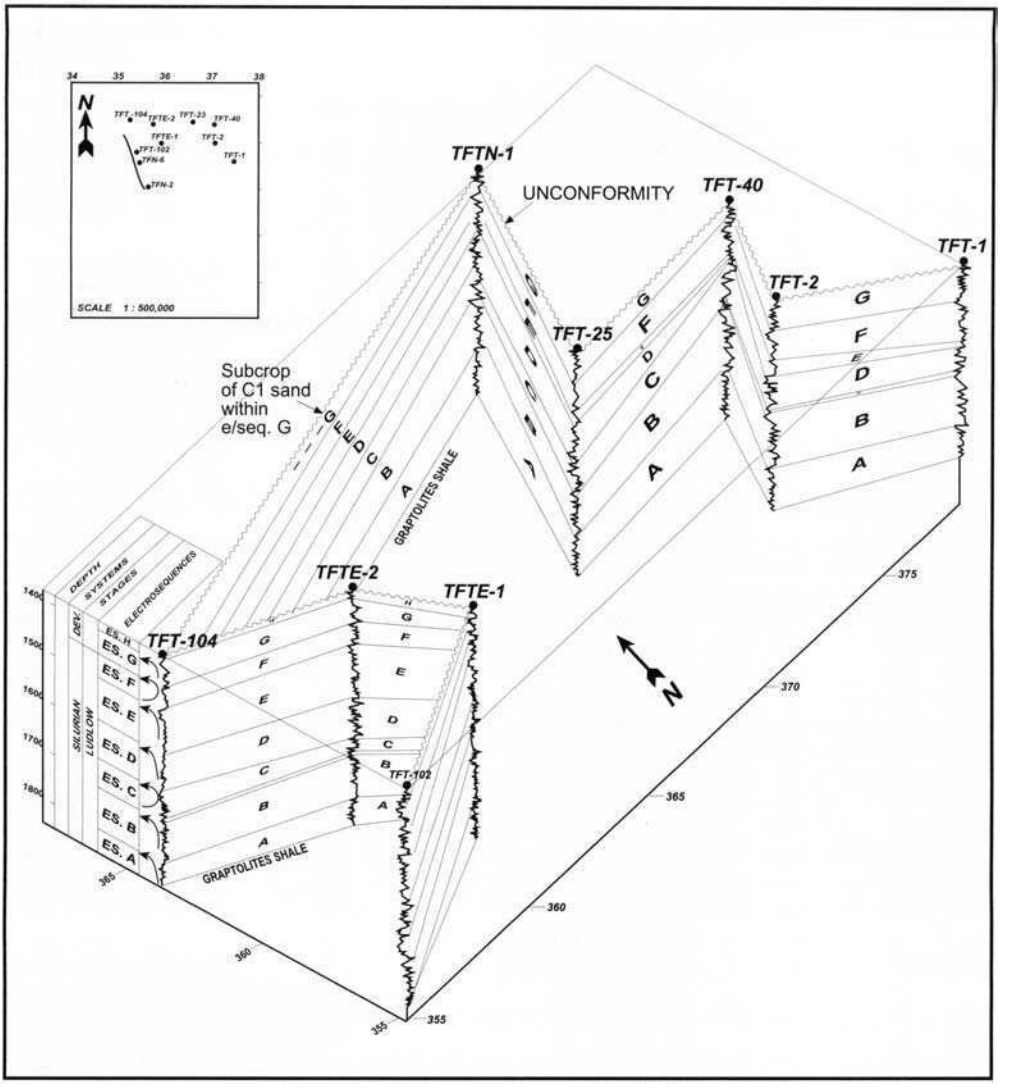

Fig. 4. Electrosequence correlation of Tin Fouyé–Tabankort wells. The presence of a full Devonian electrosequence G only in the west of the area should be noted. The C1 reservoir lies at the top of this unit and is subcropped between TFT-104 and TFTN-1.

The main controls on poroperm appear to be clay content and type, and the development of secondary porosity (Table 1). An indirect link is also indicated to grain size, with the coarsest (medium- to coarse-grained) sands tending to be low in clay with significant solution porosities. These coarsest units correlate both with the tops of barrier bar sequences (the tops of coarsening-up profiles on logs) and with the base of channels (base of fining-up sequences on logs). The predominant clay is illite, which when present in significant quantities, has a major downgrading effect on permeability. Because of the disproportionate effect of illite development on permeability and its minor effect on porosity, the most permeable reservoirs are not necessarily the intervals of highest porosity. Secondary (dissolution) porosity would appear to be most significant in faulted areas in the west of the area (Tin Fouyé Nord) and is least well developed in the northeast of the study area. Reasons for this are currently unclear.

Within Unit B2, reservoir quality is notably concentrated along an E–W trend crossing the

Table 1. *Reservoir quality of sandstone units, F6 reservoir*

Reservoir unit	Porosity developed	Porosity range (%)	Permeability range (mD)
C1	Intergranular porosity only	11–15	50–200
	Intergranular + dissolution porosity	15–20	100–500
B2	Intergranular porosity only	7–10	50–150
	Intergranular + dissolution porosity	10–14	50–500
B1	Intergranular porosity only	5–10	0.1–100
	Intergranular + dissolution porosity	15–25	100–1000
A	Intergranular porosity only	10–20	1–10
	Intergranular + dissolution porosity	25–30	10–1000
M2		10–15	0.1–2
M1		2–10	0.1–10

field (Fig. 7), probably reflecting sedimentological and grain-size controls. This trend follows the interpreted orientation of the offshore bars that are believed to be the predominant depositional environment of this unit. The relationship between porosity and permeability is again irregular.

The finer-grained sandstones of units A and B1 units are generally unproductive because of their position below the field oil–water contacts (OWCs), despite often good reservoir quality (Table 1). Unit M1 gives shows in the eastern and central parts of the field (TFT 1, TFT 2 and TFTE 2), which may indicate the existence of intraformational seals within the F6 reservoir. The M reservoirs, however, have high clay contents and low permeabilities, and these intervals did not flow on testing.

Hydrogeology

It is apparent from the outlines of the oil pools in the F6 reservoir shown in Fig. 3, that there is a poor relationship in the Tin Fouyé region between structure and hydrocarbon occurrence. The C1, B2, and A reservoirs are in pressure communication and form a single hydraulic unit characterised by pore pressures lower than or equal to hydrostatic. Mapping of pressures reveals a general flow direction from SSE to NNW (Fig. 8), a direction which is also thought to correspond to the direction of progradation of the bar facies of the reservoir.

The measured hydraulic gradient increases from east to west across the study area, averaging 0.008 in the east and 0.02 in the west. A substantial though irregular tilt in the OWC is seen (Figs 9 and 10) and represents the main reason why oil reserves are developed on the Tin Fouyé Nord structural nose (Fig. 3) as well as in the main anticlinal closure (TFY) further south (Figs 3 and 9). The angle of tilt of the OWC is greater in the northwest, where it reaches 1 m 100 m, consistent with the higher hydraulic gradient in that area.

Water circulation is also clearly affected by faults and by permeability distribution. These controls are most apparent in the Tin Fouyé Nord (TFN) area, where the fault shown in Fig. 8 clearly acts as a barrier. In addition, a change of flow directions between TFT-101 and TFN-3 (Fig. 8) suggests the occurrence of a permeability barrier in that area. Both of these effects undoubtedly contribute to trapping in this region.

It is now possible to identify the trapping style for each of the significant oilfields in the region. The main Tin Fouyé Nord pool is a combination hydrodynamic–structural trap located on a structural nose, with structural closure provided to the north, east and west. The southern limit to the trap is provided by hydrodynamic mechanisms, and a secondary element of stratigraphic trapping is also apparent (Figs 3 and 9). A similar trap is present in the TFTE-2 and -3 area. The small pool penetrated by TFT-2 is also a combination structural–hydrodynamic trap located on a small structural nose favourably orientated with respect to the hydraulic gradient. Another small pool at TFT-8 is located on an area of a steady northern structural dip, with trapping apparently entirely provided by hydrodynamic mechanisms, specifically by local variations in hydraulic gradient.

In contrast, the Tin Fouyé Est (TFE) pool is essentially a structural trap, with only minor var-

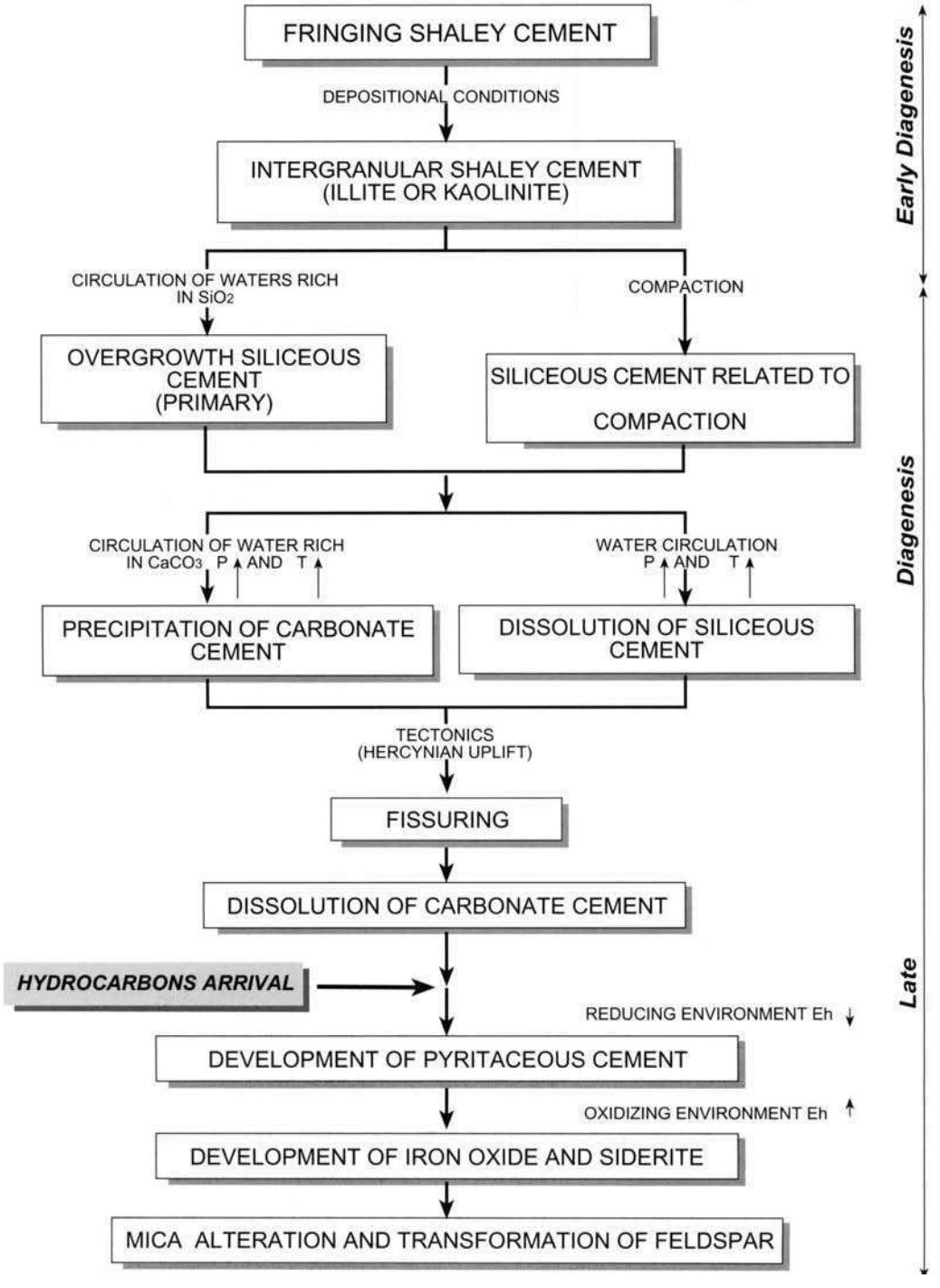

Fig. 5. Sequence of diagenetic events in the F6 reservoir, as determined from petrographic work in the field.

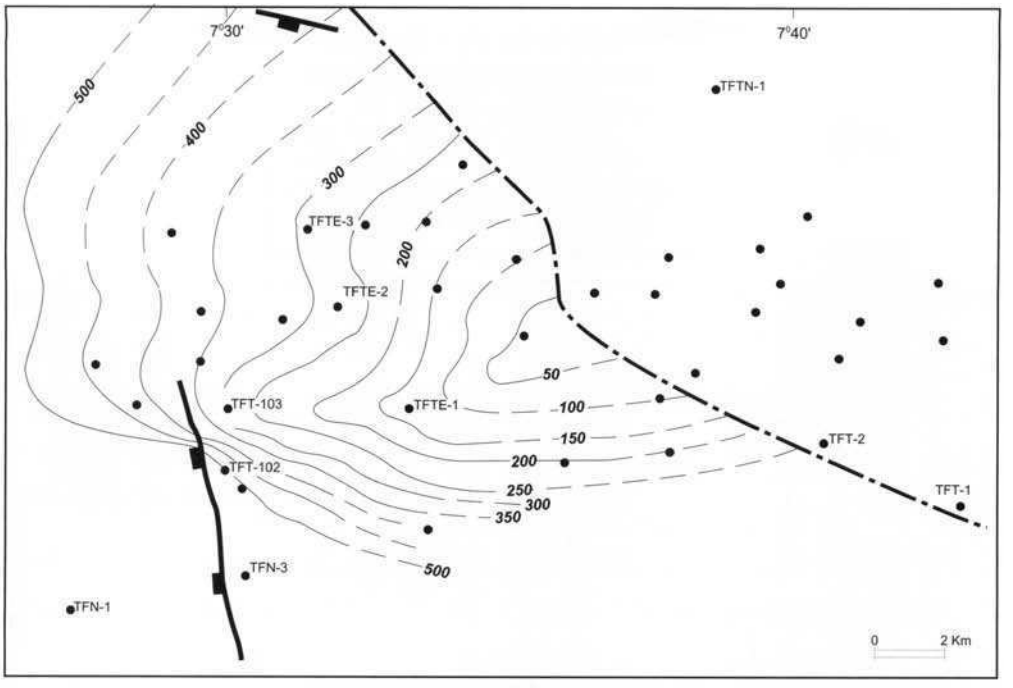

ISOPERMEABILITY - UNIT C1 (mD)

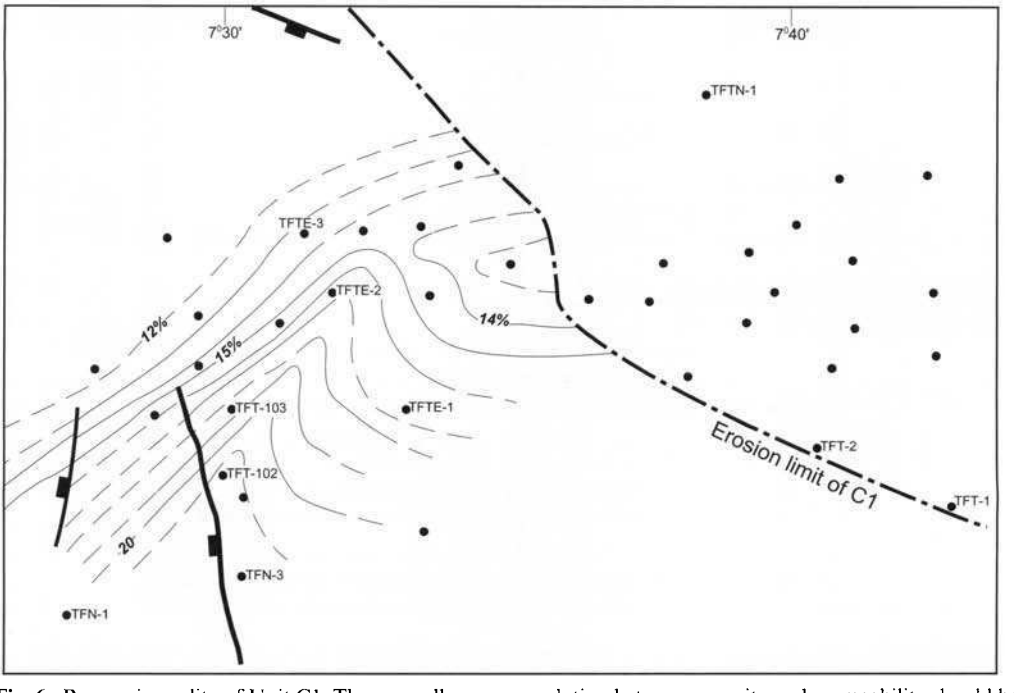

Fig. 6. Reservoir quality of Unit C1. The generally poor correlation between porosity and permeability should be noted. Reservoir quality is highest in the west, because of an increased level of dissolution of silica cement.

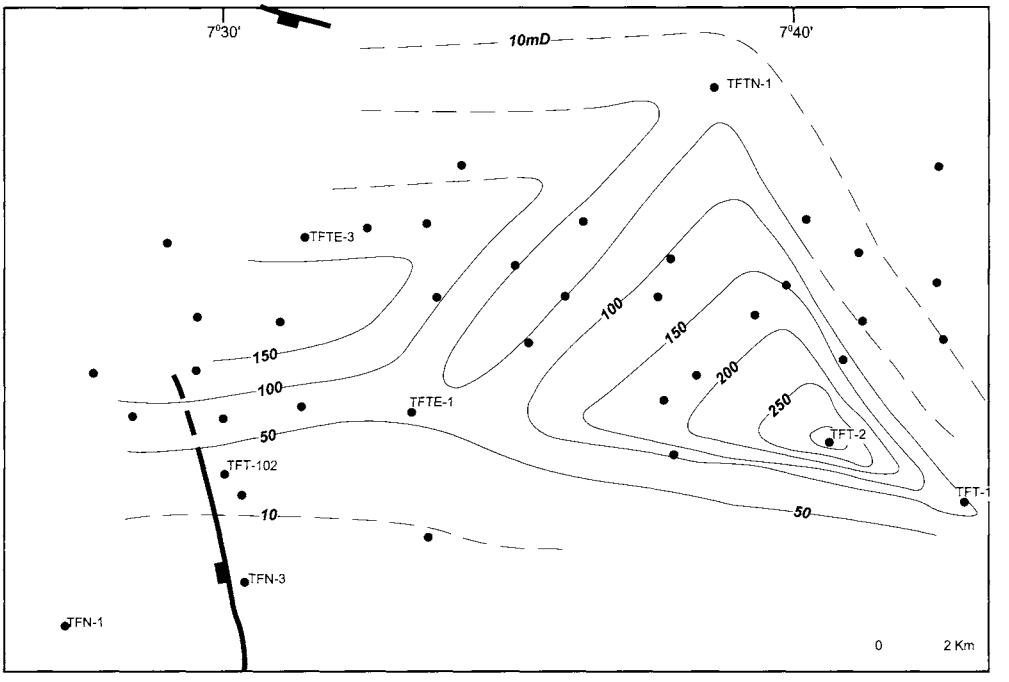

ISOPERMEABILITY UNIT B2 (mD)

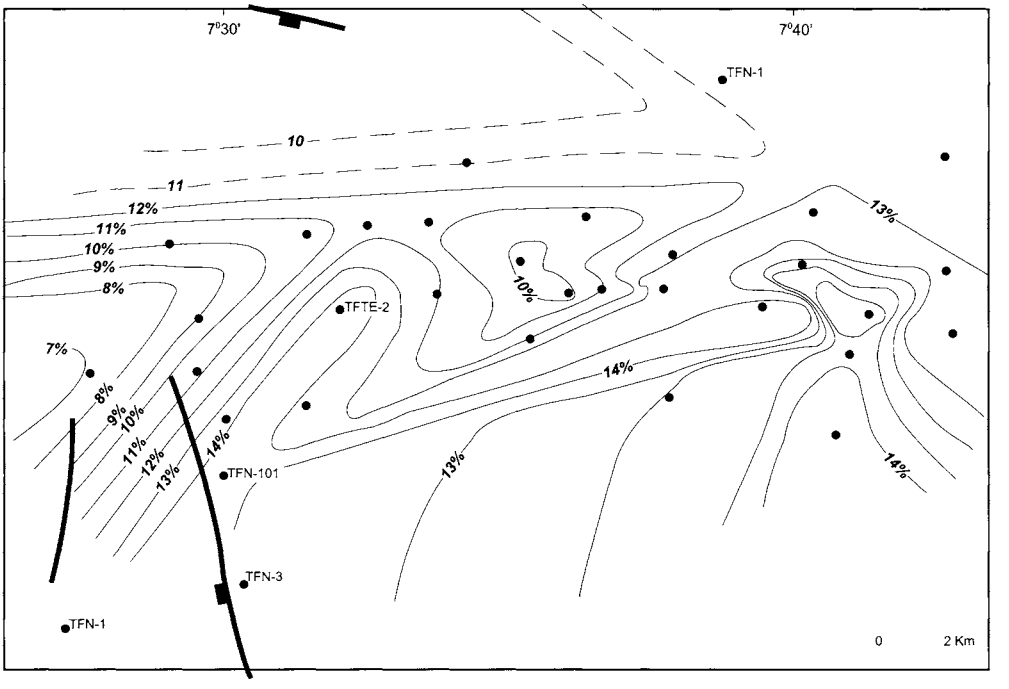

Fig. 7. Reservoir quality of Unit B2. The correlation between porosity and permeability is again poor. An east–west trend is evident.

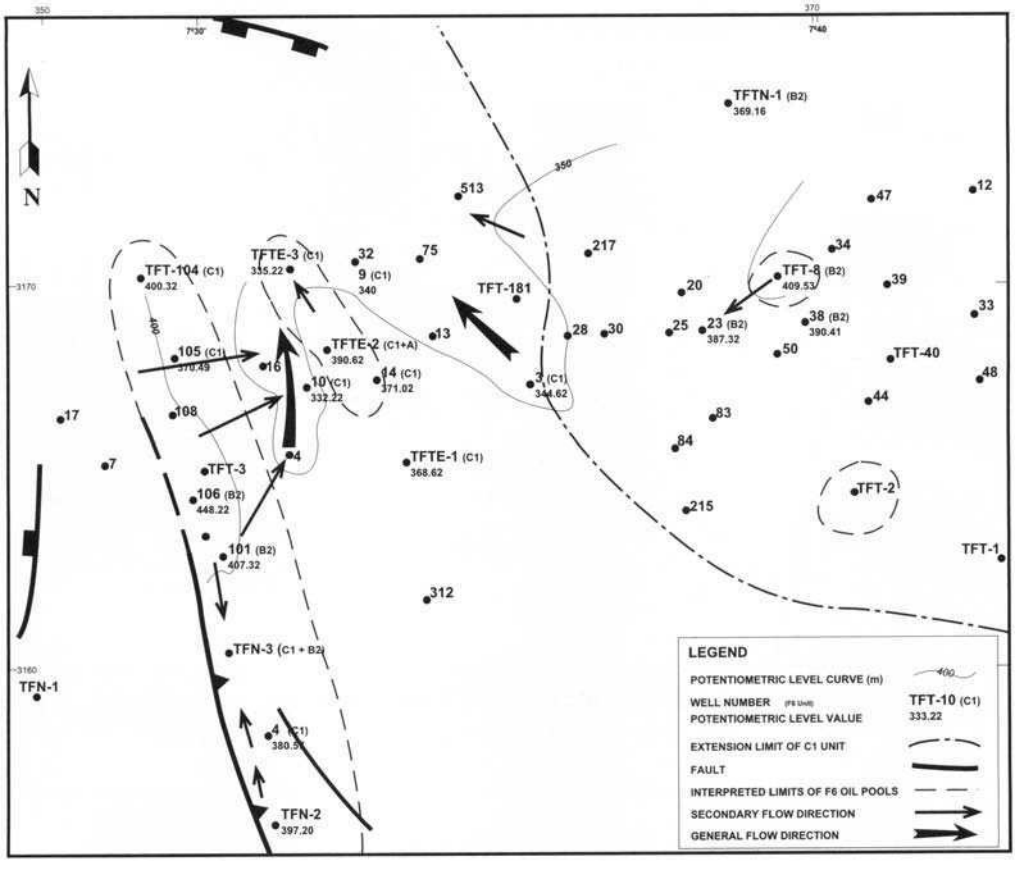

Fig. 8. Potentiometric map for formation waters within the F6 reservoir. It should be noted that the general flow is in a SSE–NNW direction, parallel to the TFN structural nose, which controls hydrodynamic trapping on that feature. Also noteworthy is the local flow in the TFT-8 area, responsible for a local trap at that well.

iations observed in the level of the OWC. However, even here, hydrodynamic effects are evident, in that some wells within structural closure (TFE-5 and -6) are completely flushed with fresh water. Oil flushed in this manner has presumably remigrated downdip into the Tin Fouyé Nord structural nose.

Hydrochemistry

Salinities are low (0.2–6 g/l) throughout the C2 and B2 reservoirs, showing no relationship to depth and providing further evidence for active hydrodynamic flow. Chemical analyses show the waters to be rich in sodium hydrocarbonate, calcium and chlorine. In the M1 reservoirs, salinities of 50–59 g/l have been recorded, indicating this lower reservoir unit not to be in communication with the main reservoir. It is thus clear that the fresh water has preferentially invaded the more permeable reservoir units.

Conclusions

The Tin Fouyé–Tabankort region show a complex hydrocarbon, reservoir and poroperm distribution at the level of the F6 reservoir. Reservoir quality is essentially confined to reservoir Unit C1 (locally absent through erosion) and the top of Unit B2. The highest-quality reservoirs correspond to coarse intervals of sandstone deposited in E–W trending offshore bars and, to a lesser extent, tidally influenced channels. Illite content and the dissolution of silica

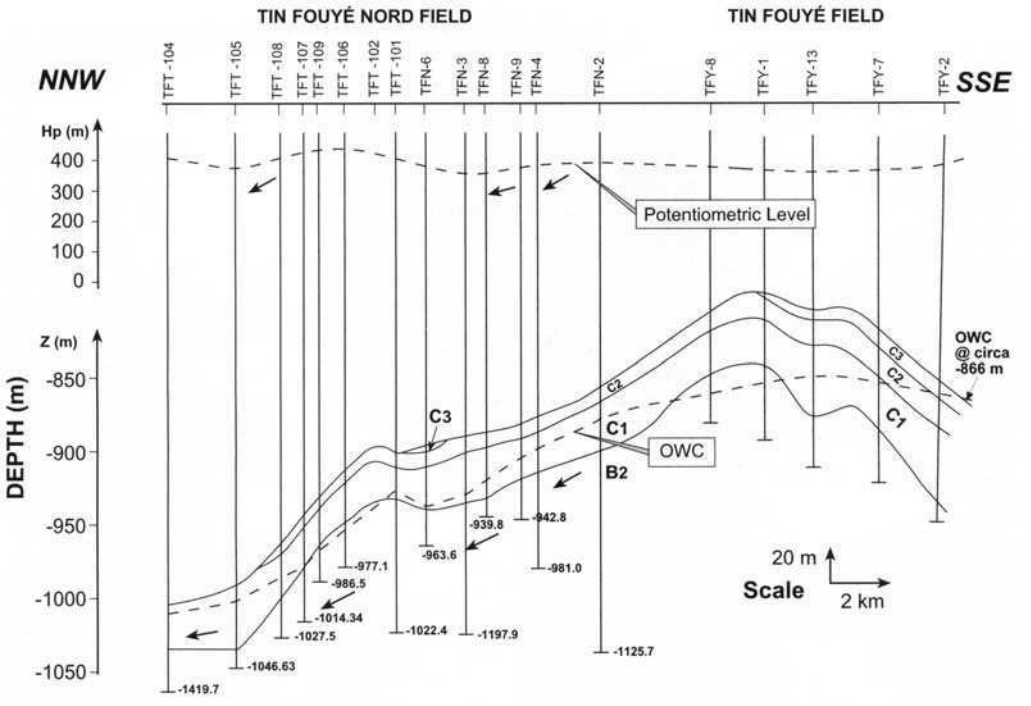

Fig. 9. Cross-section at the level of the F6 reservoir along the TFN–TFT structural nose and oil accumulation. The high dip on the OWC in TFN should be noted, contrasting with the relatively even level of the OWC at TFY. (For line of section, see Fig. 3.)

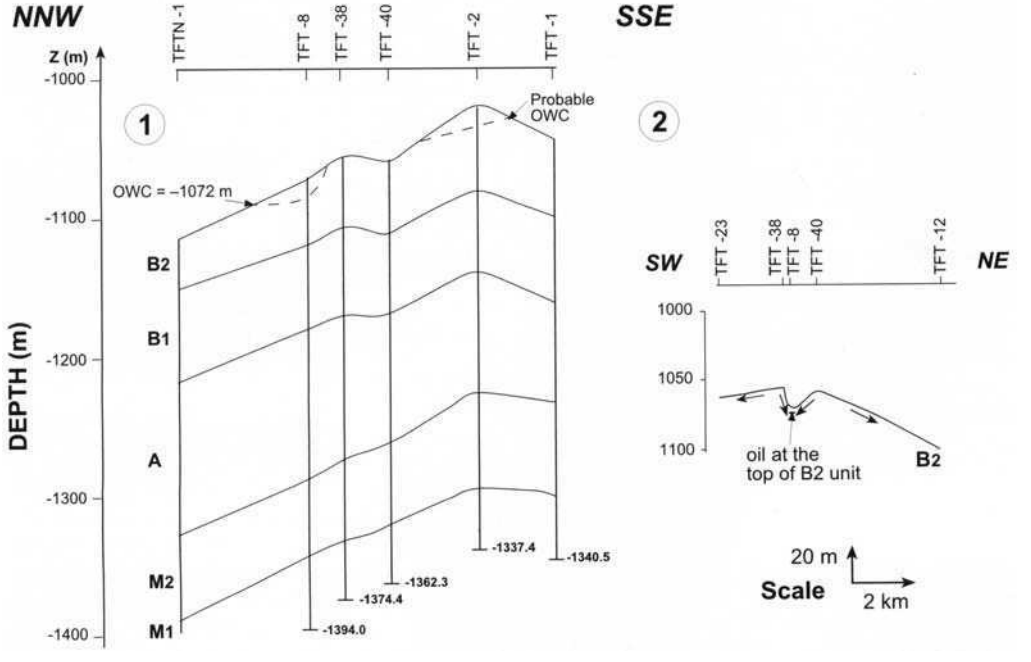

Fig. 10. Cross-section at the level of the F6 reservoir in the TFT-8 and TFT-2 discovery areas. The lower and more variable dip on the OWC, representing a lower and more variable hydraulic gradient in this region should be noted. (For line of section, see Fig. 3.)

cement are significant controls on permeability and producibility. Unit M1 gives shows in only two wells and, on the basis of formation water salinity, seems not to be in communication with the other reservoir units.

Hydrodynamic activity has a major impact on oil distribution in the region. The existence of a strong SSE–NNW hydrodynamic drive has led to the trapping of the largest oil accumulation at this level on a structural nose without mapped closure. A variety of productive trap types are present in the region, ranging from pure hydrodynamic traps, as at TFT-8, through several mixed structural–hydrodynamic–stratigraphic traps to an essentially pure structural trap at TFE. These provide important analogues for exploration for further hydrodynamically influenced traps in similar settings elsewhere in Algeria.

References

CHIARELLI, A. 1978. Hydrodynamic framework of Eastern Algerian Sahara—influence on hydrocarbon occurrence. *Bulletin, American Association of Petroleum Geologists*, **62**(4), pp. 667–685.

LANZONI, E. & MAGLOIRE, L. 1968. *Synthèse palynologique du Silurien Supérieur–Dévonien Inférieur du Nord du Bassin d'Illizi (Polignac, Réservoir F6)*. SN-REPAL Report, Laboratoire de Géologie.

Sedimentological evolution of the Givetian–Eifelian (F3) sand bar of the West Alrar field, Illizi Basin, Algeria

RABAH CHAOUCHI[1], M. S. MALLA[2] & F. KECHOU[2]

[1]*National Institute for Hydrocarbons and Chemistry, Boumerdès, Algeria*
[2]*Exploration Division, Sonatrach, Hussein-Dey, Algiers, Algeria*

Abstract: Commercial accumulations of hydrocarbons depend on several factors, among which sedimentological conditions are of prime importance. Such sedimentological factors are of particular importance in controlling both entrapment and reservoir quality in the western part of the Alrar field, within the F3 sandstone reservoir of Givetian–Eifelian age. Recent well results have shown facies and reservoir quality distribution to be more complex and generally more favourable than previously predicted. A series of tidally influenced littoral bars are now believed to have existed in the Alrar area at the time of deposition of the reservoir, these being elongated in a NW–SE direction in the West Alrar area, with an interbar area in the vicinity of well DZ-1. The highest reservoir quality is largely confined to this bar facies and understanding its distribution is therefore vital to locating development wells. Four possible sedimentological interpretations of the extension of the F3 reservoir to the south and west have been developed. In most areas, the pinchout seems to be gradual, but in other areas where the transition to lagoonal shale is sharp, fault control may apply. Significant uncertainties however remain in predicting this shale-out in undrilled areas.

The Alrar field is located in the southeastern part of the Algerian Sahara within the Illizi Basin (Figs 1 and 2). The field lies 230 km. north of the town of In Amenas, and straddles the border with Libya. In contrast to most other major fields in this region, entrapment at the Alrar field is highly dependent on facies changes, particularly the sedimentary pinchout of the main reservoir against a steady monoclinal structural dip (Fig. 3). In addition to the influence of sedimentological conditions on the extent of the field, there are also large variations observed over the field in reservoir quality and thickness. Despite the drilling of a large number of development wells, the distribution of the main Eifelian–Givetian (F3) clastic reservoir over the Alrar field is still poorly understood. The objective of this paper is to update and revise existing sedimentological models for the field in the light of the most recent data, and consider the implications of various models for the areal extent and pinchout of the main reservoir unit. This is the first publication on this field.

The area studied in this paper is the western structural segment of the field ('West Alrar'), though reference is also made to models resulting from the earlier development of other portions of the Alrar field.

The Alrar gas–condensate field was discovered in 1961 by the AL-1 well (Fig. 3). The field was slowly appraised and developed throughout the next decade, with 16 wells having been completed by 1970. All of these with the exception of ALB-1, the discovery well for West Alrar, were drilled in the eastern part of the field. The AL-03 well established fluid contacts for the eastern segment, with a gas–oil contact (GOC) at −1948.5 m and an oil–water contact (OWC) at −1958.5 m (Fig. 3). The discovery of the nearby Stah oilfield in 1971 (Fig. 2) led to a reduction of activity on Alrar, with further drilling not resuming until 1976. In 1978, a major development programme began, initially focused on East Alrar, but spreading to West Alrar in the period 1982–1993, when 23 wells were drilled on that segment of the field. All except three of these wells were successful in flowing gas–condensate, the exceptions being AL-37 (reservoir absent), AL-39 (water bearing) and ALC-1 (thin poor quality reservoir). Gas–water contacts are now known to vary between different fault segments of West Alrar (Fig. 3). Oil has only been encountered in West Alrar in one downdip well, which encountered a very thin oil column in poor-quality sands near the base of the F3 reservoir. The West Alrar hydrocarbon reserves are currently estimated at 55×10^9 m^3 gas (*c.*1.85 trillion cubic feet (TCF)) and 12.2×10^6 tonnes condensate (*c.* 110 million barrels condensate (MMBC)).

Stratigraphy and local structural framework

Fig. 4 illustrates the stratigraphic column observed in the Alrar area. Two main sedimentary cycles are observed, separated by the Hercynian unconformity. Other regional

CHAOUCHI, R., MALLA, M. S., KECHOU, F. 1998. Sedimentological evolution of the Givetian–Eifelian (F3) sand bar of the West Alrar field, Illizi Basin, Algeria. *In*: MACGREGOR, D. S., MOODY, R. T. J. & CLARK-LOWES, D. D. (eds) 1998. *Petroleum Geology of North Africa*. Geological Society, London, Special Publication No. 132, 187 200.

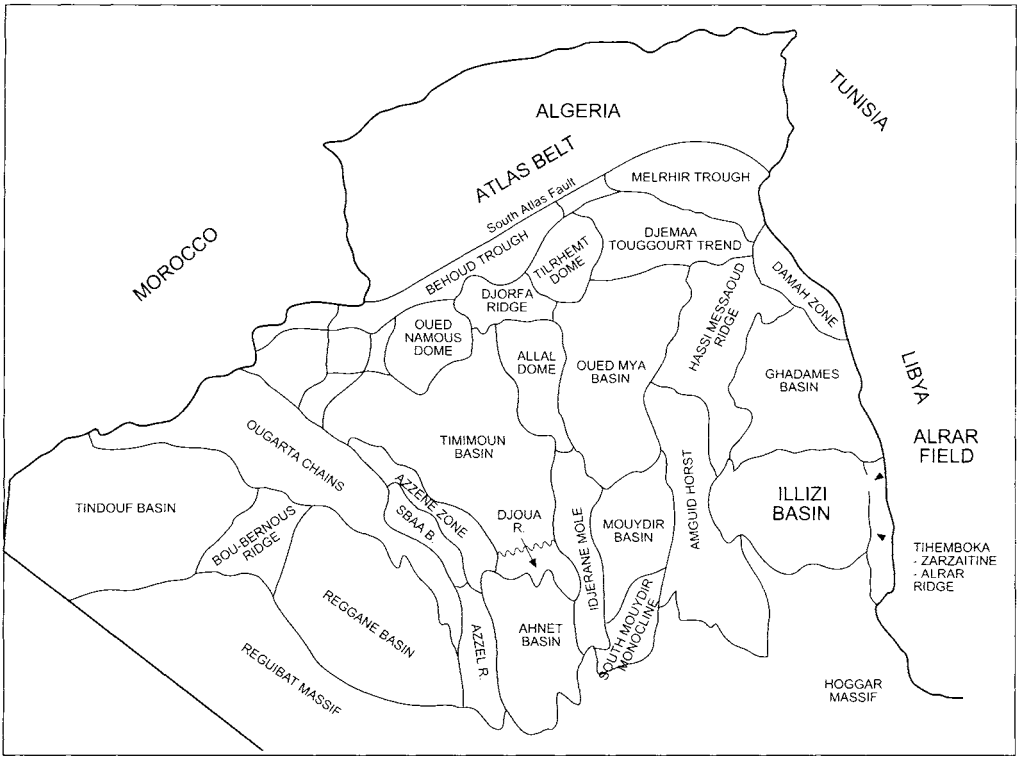

Fig. 1. Location of Alrar field within the Illizi Basin

unconformities of Ordovician, Devonian and Cretaceous age can be used to subdivide the section further into megasequences (Attar 1987; Fekirine & Abdallah this volume).

The zone of economic interest in the Illizi Basin lies in the Palaeozoic, with all sandstone units ranging from Ordovician to Carboniferous age productive in the region. The primary reservoir in the Alrar field is of Givetian–Eifelian age and is termed, using the basin-wide reservoir nomenclature illustrated in Fig. 4, the F3 reservoir. This reservoir lies close to and below one of the main regional unconformities, of Frasnian age.

The overall dip pattern of the Devonian over Alrar is that of a steady northwards dip (Fig. 3). The structure of the region is complicated by numerous faults and flexures, active from Frasnian to Late Carboniferous–Permian times, which generally trend north–south (Fig. 5). In West Alrar, these faults clearly act as seals, segmenting the field into a number of compartments in which different fluid contacts are developed.

F3 reservoir stratigraphy and facies

Figure 6 shows a section of the F3 reservoir, representative of the West Alrar area. The F3 interval throughout the field shows a trend of upward bed thickening and coarsening, with a range in total thickness from 29 to 48 m. To the west and south of the study area, significant facies changes occur, with the F3 equivalent typically composed of a dolomite bed capped by an interval of thinly bedded sandstone and shale with carbonate nodules at the base. The reservoir in the field area has been subdivided by previous workers (Sommer 1979; BEICIP 1987) into three informal units as described below. The nomenclature of Sommer (1979) will be maintained in this paper, although certain aspects of the terms used can be misleading. The chief problem here lies in the application of the term 'sandy bars' to a variety of time-equivalent arenaceous facies. To prevent confusion the 'sandy bars' will be described as a unit, included in which may be 'bar', 'sheet sand' and other facies.

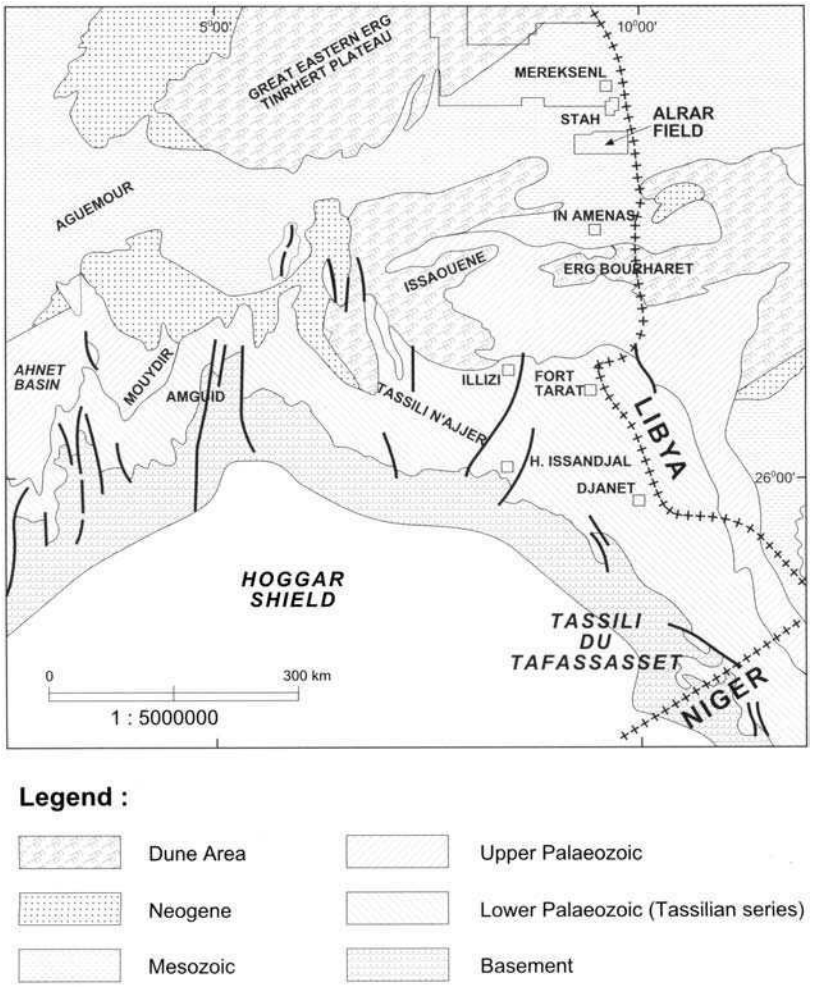

Fig. 2. Geological map of Illizi Basin and Hoggar Shield. Alrar and associated Devonian-reservoired fields such as Stah and Mereksene lie on the north dipping slope of the Illizi Basin.

'Progradation sequence'

The lower part of the reservoir, or 'progradation sequence' conformably overlies the pteropod shales that cap the underlying 'F4' reservoir. This unit is continuous over the field, ranging from 1 to 6m in thickness. The base of the interval consists of bioclastic black shale, with numerous shell fragments, passing upwards into bioturbated argillaceous sandstones, again rich in shell fragments. Each sandstone–shale layer in this section shows a fining-up cycle and a sharp base. Laminations are horizontal at the base, becoming wavier higher in the succession. Bioturbation is most frequently associated with the upper sections of the upward fining cycles.

The black shales concentrated close to the base are believed to represent very low energy deposits, with the presence of bioclasts indicating weak storm influences. The upward grading cycles are interpreted to represent alternations between storm and quiet water deposits, with bioturbation occurring predominantly during the quieter water periods. Thicker sandstone beds could represent periods of increased fluvial input from the source area to the west (Sommer 1979; BEICIP 1987).

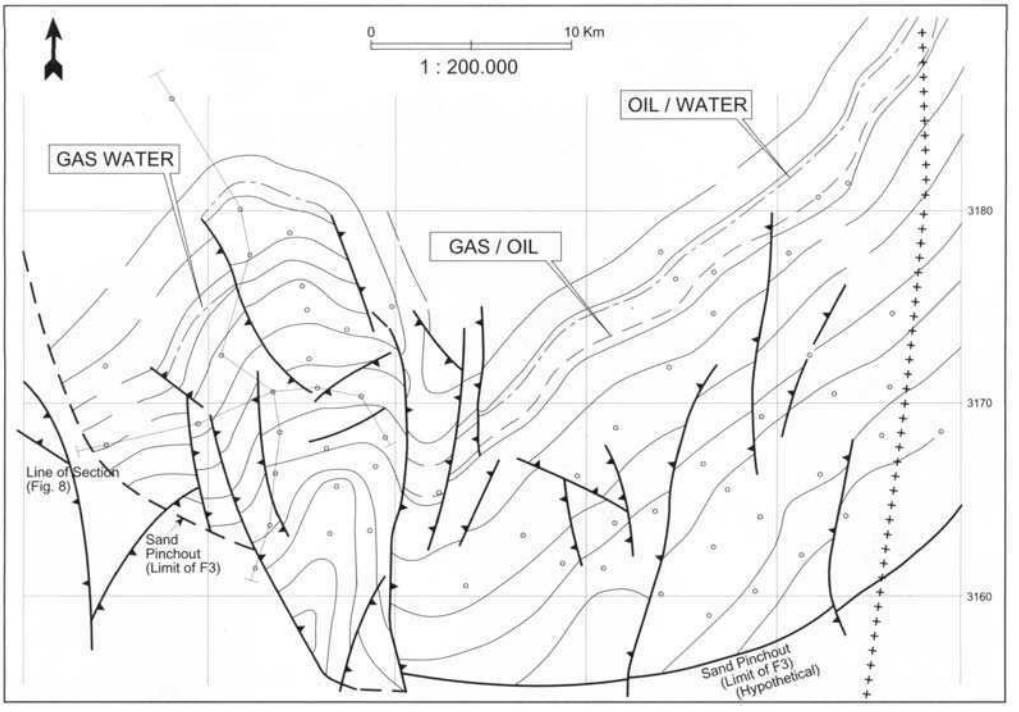

Fig. 3. Structural contours in metres on uppermost F3 reservoir. The southern limit of the field, controlled through pinchout, is still poorly defined by well control. The more severe degree of fault segmentation and differences in fluid contacts within West Alrar should be noted.

'Shale and sandstone complex'

The middle unit of the F3 reservoir consists of an interbedded succession of sandstones and shales that is continuous over the field but varies significantly in thickness. The unit shales out to the west and south, being represented by thin sandstones and shales in well AL-37 see Fig. 10, below. Average thickness is 11 m. The interval commences with a coarse grained sandstone, pebbly at the base, which is marked by high-angle cross-stratification. This passes rapidly upwards into fine-grained quartzitic sandstones that are in turn overlain by an interval of medium-grained sandstone with low-dip cross-stratification. The sandstones are lenticular and argillaceous, and are often interbedded with black shales, with flaser bedding common.

The lower coarse-grained sandstone is believed to represent distributary channel deposits, whereas the medium-grained sandstone interval with low-angle cross-stratification is believed to represent deposition in submarine dunes (Sommer 1979; BEICIP 1987).

Sandy bar unit

The highest unit of the F3 reservoir consists in most Alrar wells of thick, coarse-grained sandstone, with high-angle cross-stratification developed almost throughout. Occasional thin intervals occur of finer-grained sandstone with stylolites and rare flaser bedding. Thickness varies from 10 to 25 m. This facies is interpreted to have been deposited within high-energy barrier bars and the F3 sequence as a whole is consequently thought to represent a prograding coastline sequence (Sommer 1979; BEICIP 1987). This facies is referred to in the rest of this paper as the 'bar' facies.

In some other wells, e.g. DZ-1 (Fig. 7), and in areas to the northwest of the field, a different sandstone facies has been penetrated. Here, the sandy bar unit consists of a fine carbonate-cemented sandstone with carbonate nodules at the top, overlain by dolomitic and sandy shale and underlain by shaly dolomitic sandstone with crystalline dolomite at the base. This 'sheet sand' facies is believed to be representative

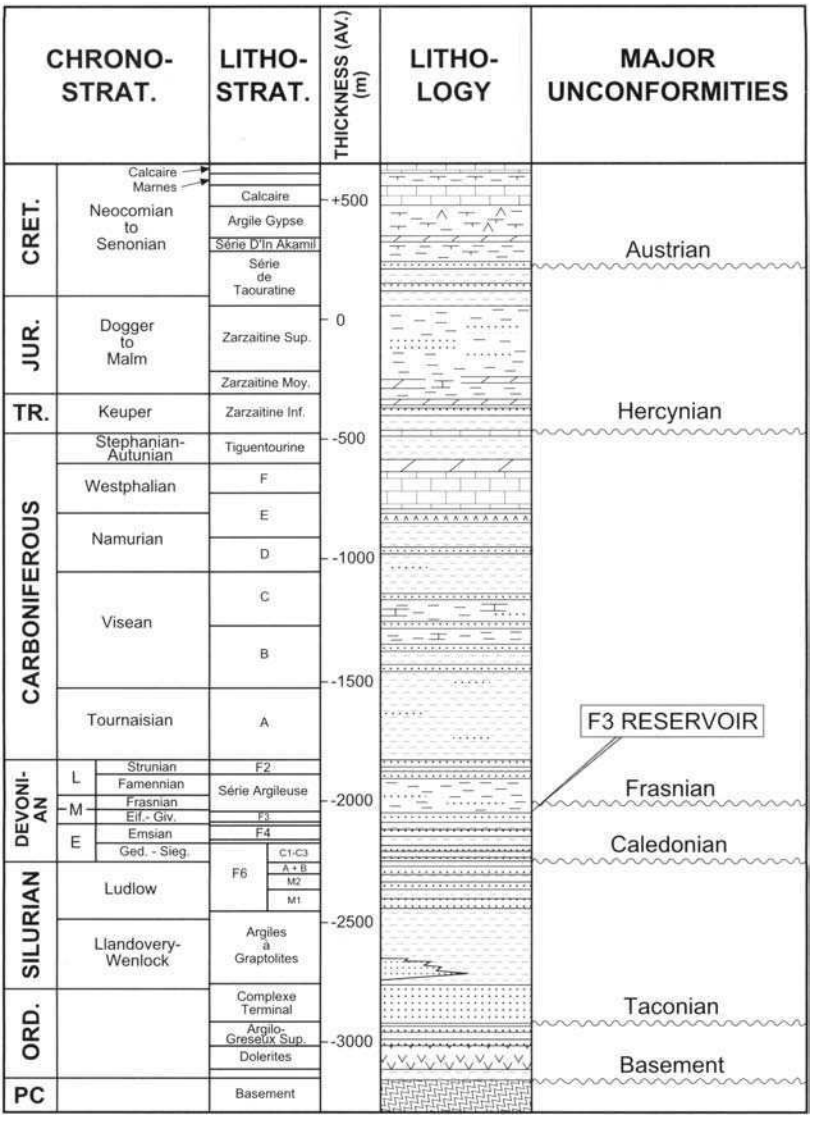

Fig. 4. Stratigraphic column of the northeastern part of the Illizi Basin. The main Devonian reservoir sands, which are correlatable from field to field, may possibly be tied to regressive events.

of interbar areas. The sandy bar unit shales out completely to the west and south (e.g. AL-37, Fig. 7; ALC-1, Fig. 8). The nature of this shale-out has been the subject of some controversy and is discussed below.

Sandy bar unit facies distribution

Facies variations within the F3 reservoir, and particularly within the sandy bar unit, play two important roles in Alrar. The shale-out of the sandstone controls the entrapment of hydrocarbons and the extent of the field towards the south and west, and producibility of the reservoir is heavily related to facies development in the sandy bar unit.

Sommer (1979) performed a comprehensive sedimentological study of the F3 reservoir over a wide area of the Illizi Basin. His main conclusions related to the Alrar field can be summarized as follows:

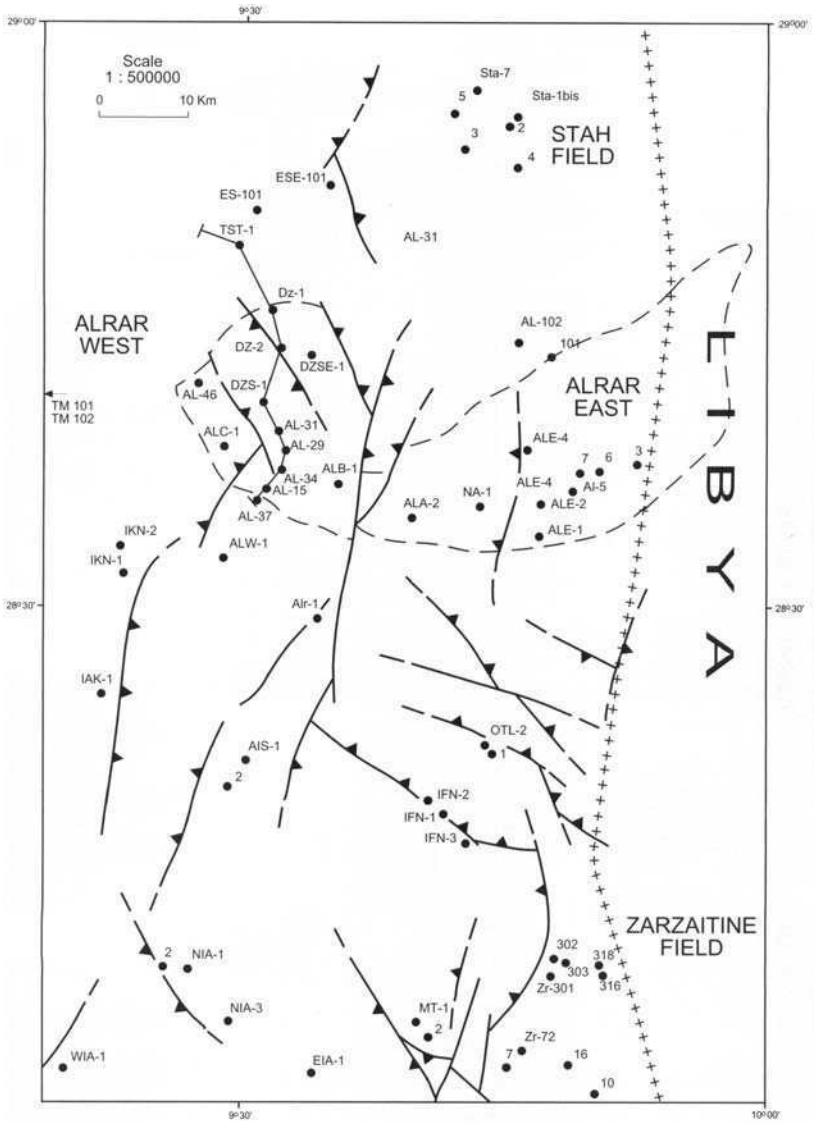

Fig. 5. Structural framework of the eastern part of the Illizi Basin. Faults were active from Frasnian to Early Permian (Hercynian) and play a significant role in segmenting the West Alrar field.

(1) The F3 sand was deposited in a gulf-shaped embayment (Fig. 9).

(2) The main source area of the sand was probably the Ahara High (Figs 9 and 10), where the older F6 sand was probably subject to erosion.

(3) Bar facies were interpreted over the East Alrar field, the focus of much of the drilling at that time, being cut by a channel in the AL-3 area. The coarse sand material in these bars was transported from the source area by longshore drift. The local channel deposits contained finer grained material, believed to be characteristic of a local source.

(4) Sheet sand deposits were interpreted in most other areas, including the West Alrar field, which had been penetrated only by two wells at that time (Fig. 10). This interpretation was based largely on the facies observed in core in the DZ-1 well. The negative implication of this interpretation for reservoir quality was one of the factors which led to the delayed development of West Alrar.

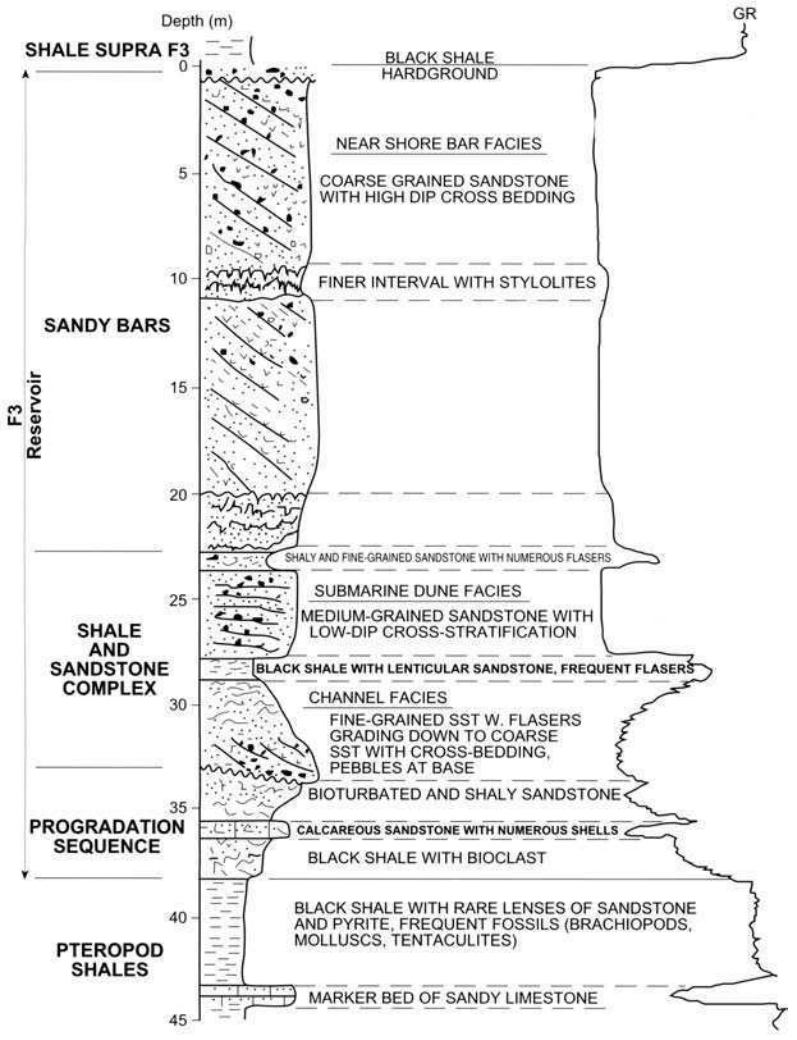

Fig. 6. Schematic section of the F3 reservoir in the Alrar area (after Sommer 1979), showing the unit terms used in this paper.

Since Sommer performed his work, 24 further development wells have been drilled in West Alrar. Although most of these were not cored, it is apparent from log signatures, dipmeter analysis and the relationship of these to cored sections that most of these (e.g. DZS-1, DZ-2, AL-28, AL-36) penetrated a bar facies. The revised interpretation of facies distribution within the sandy bar unit (Fig. 11) is thus considerably more favourable than that predicted by Sommer (1979).

Dipmeter interpretation of these wells (Fig. 12) aids the prediction of the extent of bar facies in undrilled areas. Rose diagrams are illustrated for three wells, showing both the predominant dips within bar facies sands (assumed perpendicular to shoreline and bar orientation) and for distributary or tidal channels in the subtidal units in the shale and sandstone complex. The former shows an east–west dip for the cross-beds of the bar facies in AL-28 and a NE–SW trend for wells DZ-2 and DZS-1. Dips in the channel deposits in the lower unit of the F3 reservoir vary considerably. These patterns are interpreted (Elliot 1986; Johnson & Baldwin 1986) as indicative of the presence of a barrier bar trending NW–SE, perhaps swinging slightly towards N–S in the AL-28 area. Integration

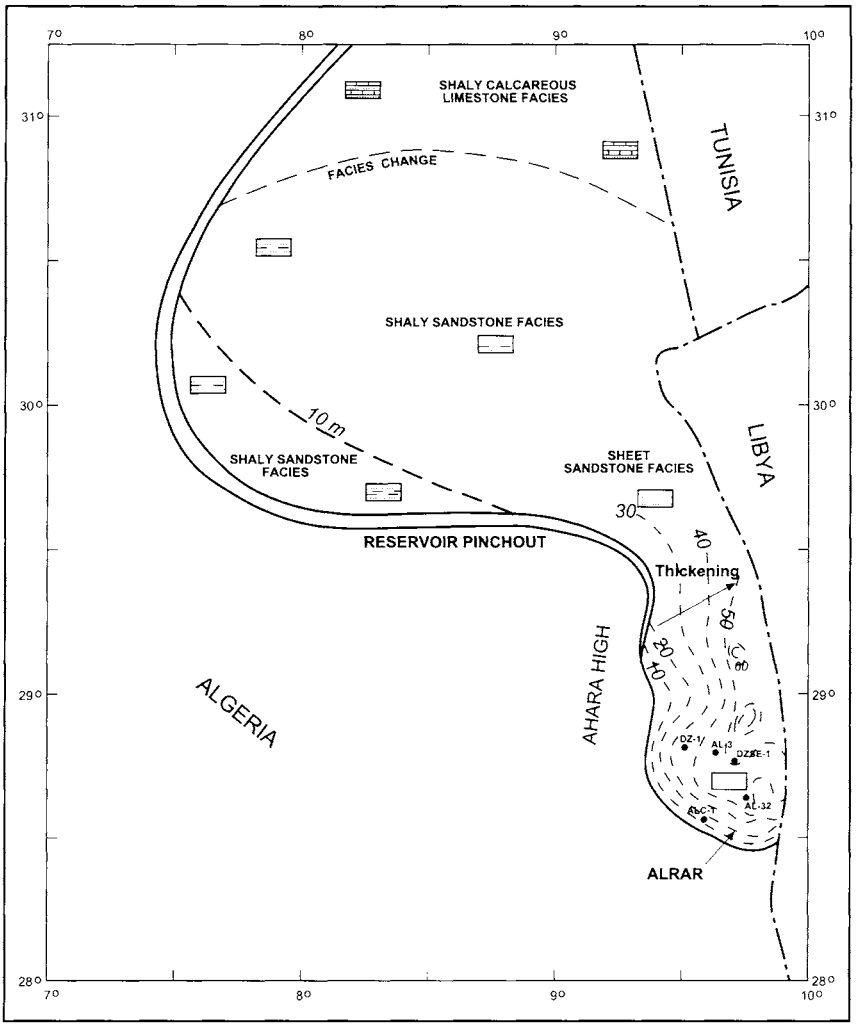

Fig. 9. F3 reservoir isopach map over the Illizi and Ghadames basins. Good sands are present only in the Alrar area.

with similar analysis for other wells and the facies analysis of well DZ-1 indicates that several such bars were present in the Alrar area, broken by interbar areas and channels (Fig. 11).

Controls on sand and facies distribution

A further study of the F3 reservoir was undertaken by BEICIP (1987). Their work was limited to wells within a radius of 30 km of the field. With the data then available, BEICIP attempted to predict sand thickness variations in undrilled areas and suggested four possible models, all with different implications for reservoir thickness variation, as illustrated in Fig. 13. Model 1 invokes a steady increase in sand thickness, controlled by a west east progradation. Model 2 invokes a sharper thickening, a pattern which tends to be favoured by well data over a wider part of the field. Model 3, involving rapid thickening of the reservoir over faults, is favoured in limited areas, particularly between the AL-37 and AL-34 wells (Figs 3 and 7). Model 4, involving non-deposition in some areas because of the presence of a syn-sedimentary structural spur, is also favoured in some northern areas of the field, where evidence exists for such a feature. However, it was accepted at the time of BEICIP's work that the well coverage was insufficient over

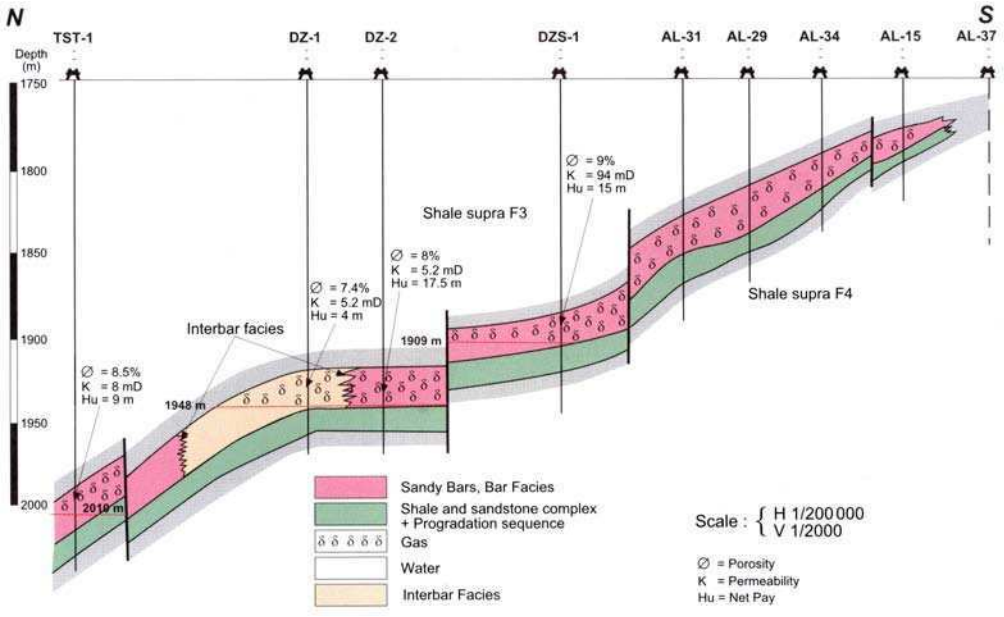

Fig. 7. Structural section from north to south across West Alrar (location shown in Fig. 3). Noteworthy features are the differences in fluid contacts across segments, the presence of poor reservoir quality in a sheet sand facies at DZ-1 and the rapid shale-out of the entire reservoir between AL-34 and AL-37.

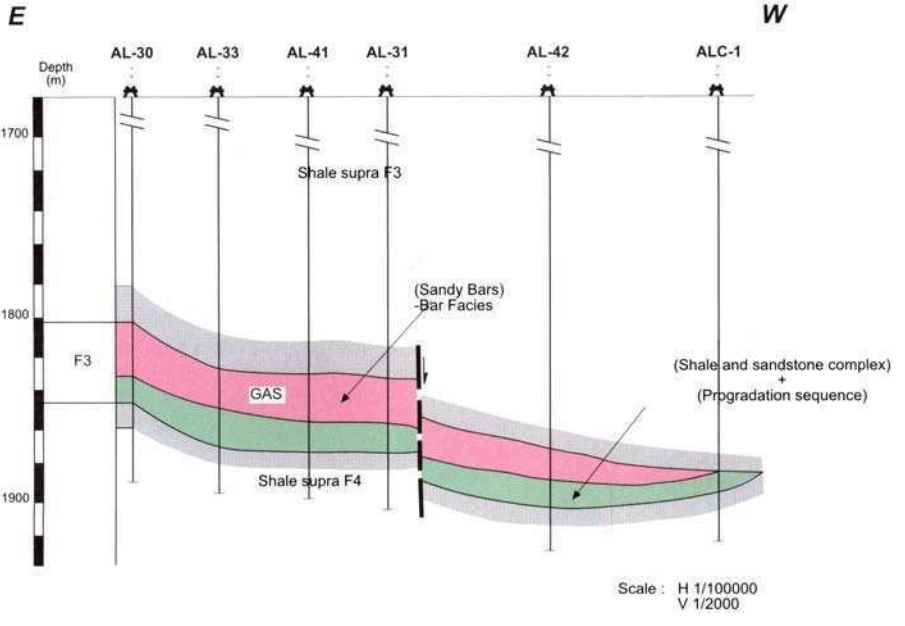

Fig. 8. Structural section from east to west across West Alrar (location shown in Fig. 3). The more gradual thinning of the reservoir on this section should be noted. The sandy bar unit has been lost at ALC-1, which therefore failed because of poor reservoir quality.

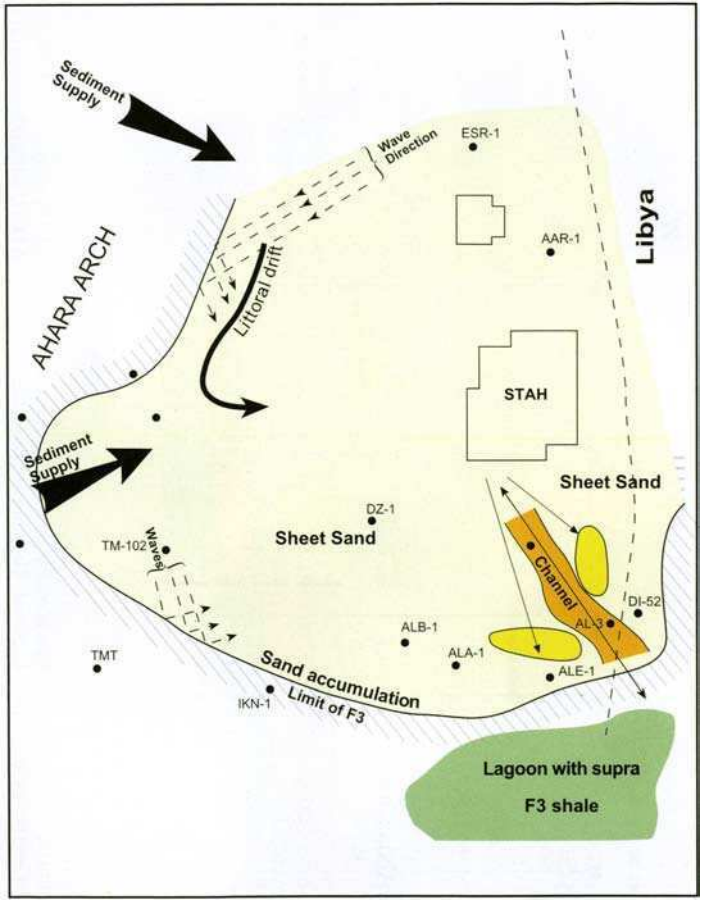

Fig. 10. Original sedimentary model for the F3 reservoir proposed in June 1979 by Sommer. A poor-quality sheet sand facies was predicted over most of West Alrar on the basis of the DZ-1 facies interpretation.

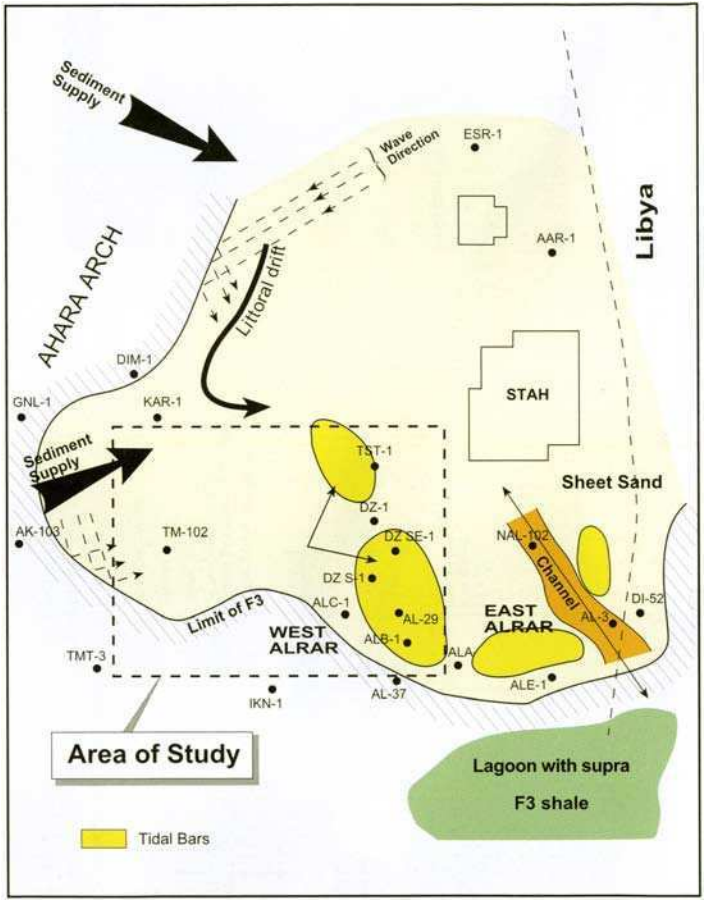

Fig. 11. Modified sedimentary model, post-drilling of West Alrar development wells. Two additional bars are now indicated, whose orientation is established from well control and dipmeter patterns. Further bars may well exist in undrilled areas to the north.

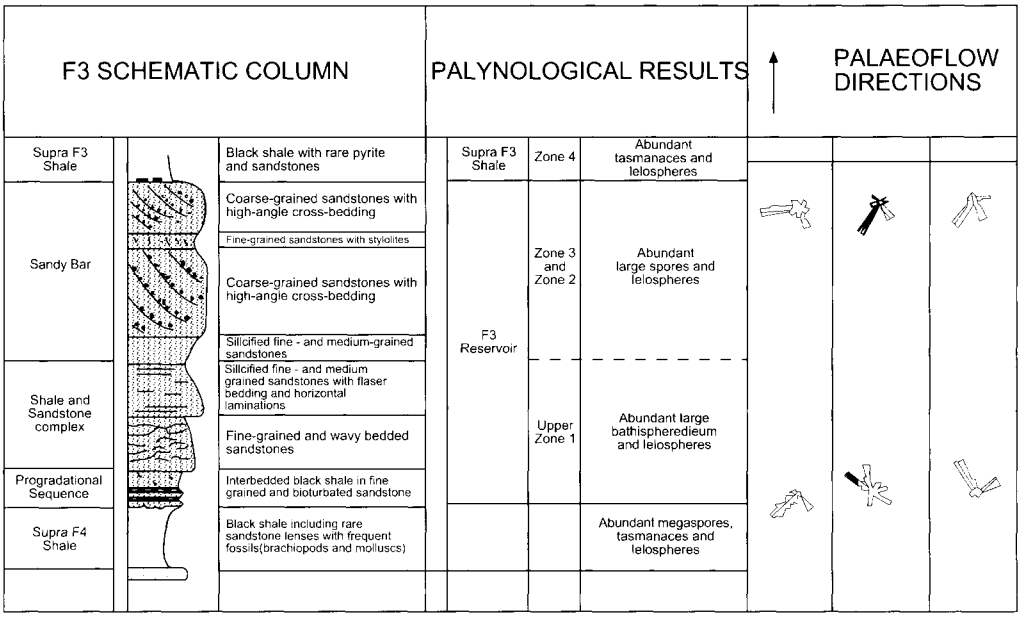

Fig. 12. Dipmeter patterns observed in West Alrar. When compared with interpreted facies, the trends observed can be rationally explained. The E–W to NE–SW dips in the cross-beds in the bar facies indicate the direction of subaerial dunes and can be assumed to be perpendicular to the trend of bars.

most areas of the field to confidently identify any of these models as the predominant controlling factor.

A further model was suggested at an early stage by workers from SNEA (Elf), who proposed that an erosional unconformity existed at the top of the F3 reservoir. In this case, erosion could account for the disappearance of the reservoir to the south and west, making the field an unconformity trap. Such an unconformity does indeed exist at this level in the Stah and Mereksene fields (Abdallah & Bryl 1988). However, this interpretation seems to have been discredited by the latest well correlations.

Considerable additional well data have become available in recent years, particularly on West Alrar. Correlations between wells, hung on horizons above and below the reservoir, now strongly suggest that the sandy bar unit passes laterally into a thickened lower portion of the supra-F3 lagoonal shale. This is illustrated by the correlation between DZS-1 and ALC-1 (Figs 14 and 15). DZS-1 shows a typical F3 section with 17m of coarse barrier bar facies overlying about 23 m of fine shaly sandstone (mainly 'shale and sandstone complex'), whereas ALC-1, 7 km to the west, contains only 'shale and sandstone complex', with the apparent equivalent of the sandy bar unit being 17 m of lagoonal shale. In addition, the correlation from AL-15 to AL-37 (Fig. 7) shows that the underlying 'shale and sandstone complex' also shales out. The multiple well correlations that can now be established suggest that the thinning of the sandstone units is usually gradual (as in Fig. 8, Models 1 and 2 of BEICIP above). The sharp thickening between AL-34 and AL-37 (Fig. 7) would appear to be the exception rather than the rule.

It has always proven difficult to predict the extent and quality of the Alrar reservoir, and even with the current dense drilling pattern, significant uncertainties remain on the extent of the sands, and of the field, to the west and south. The western and southern field limits shown in the figures thus remain schematic, being controlled by well data only in the AL-37 and ALC-1 areas. Further drilling may be necessary to firmly resolve these problems.

Reservoir quality

Reservoir quality within the F3 reservoir shows a strong relationship to grain size, and the highest

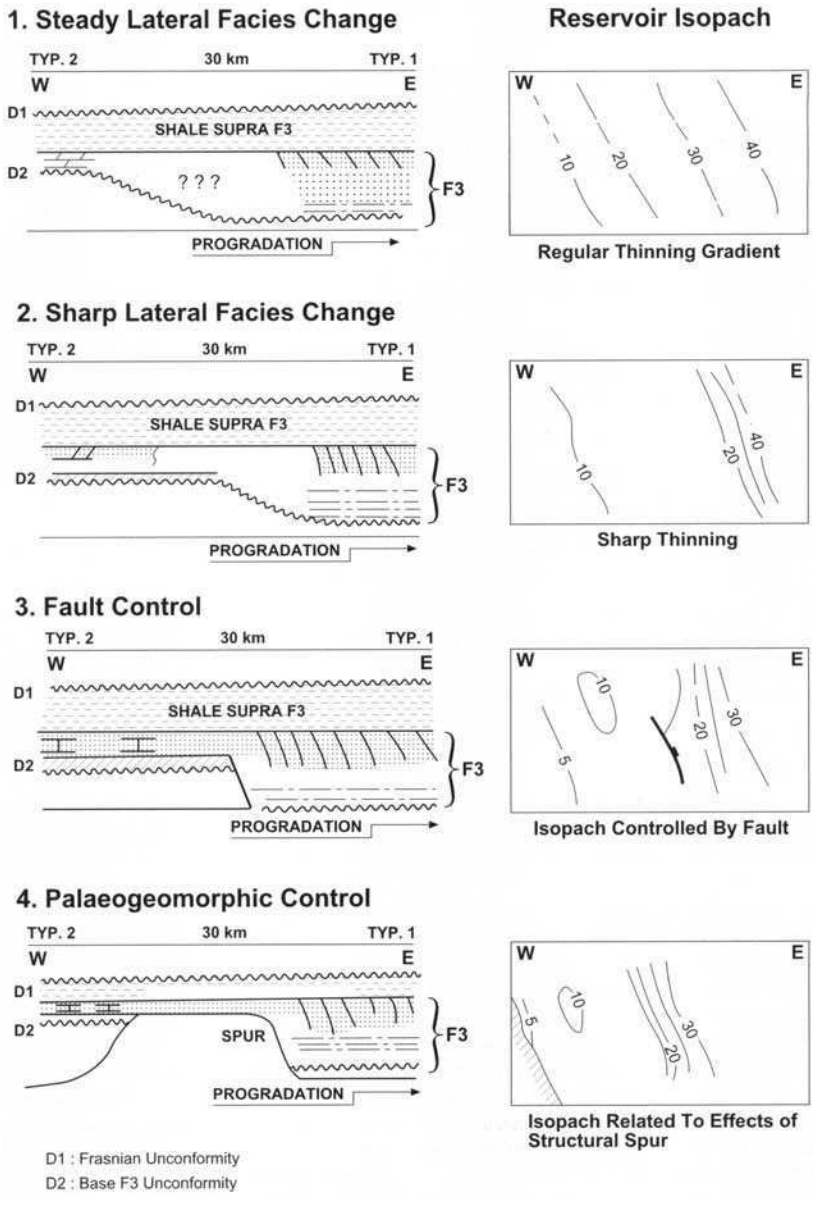

Fig. 13. Models proposed by BEICIP (1987) as possible explanations for east to west facies variations in the F3 reservoir. Type 1 refers to the Alrar-type F3 illustrated in Fig. 6, and Type 2 refers to a poorer-quality dolomitic F3 seen in wells 30 km east of the field. Well control is still insufficient to fully distinguish between these models, though Model 2 is currently favoured. Model 3 could explain areas of sharper facies change (e.g. AL-37), but there are few data with which to prove this.

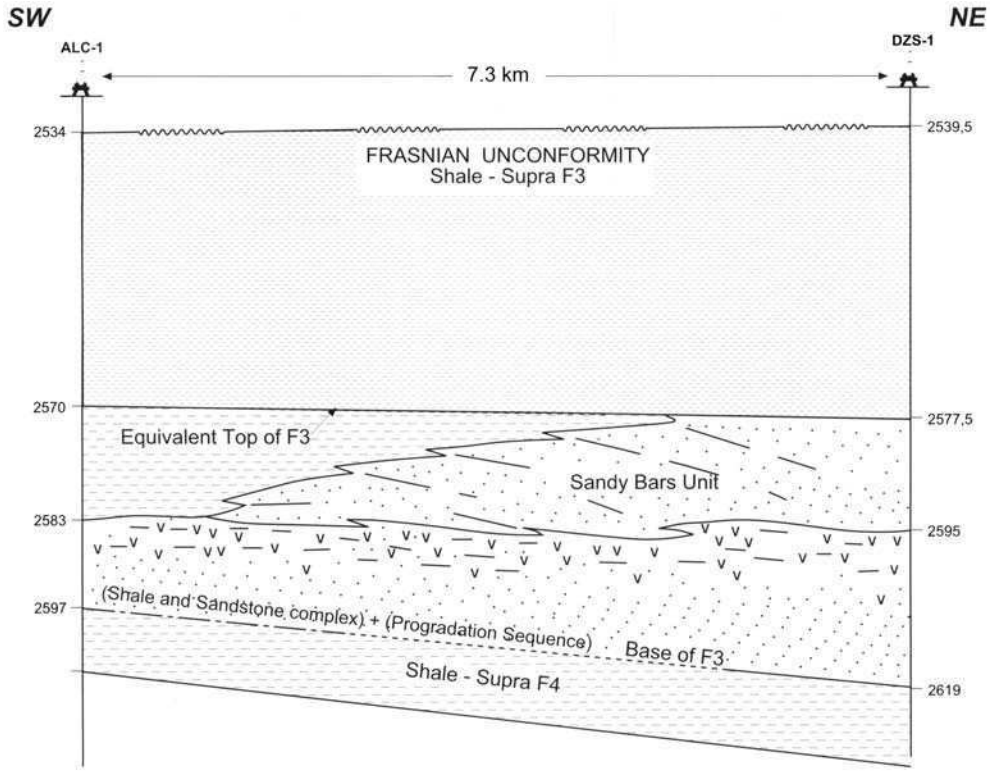

Fig. 14. Reservoir correlation between ALC-1 and DZS-1. Reference to marker horizons above and below the reservoir seem to establish that the disappearance of the main reservoir unit at ALC-1 is due to facies variations, with lagoonal shales representing the time equivalent of the sandy bar unit.

reservoir quality is almost entirely concentrated in the sandy bar unit (Fig. 7). In addition, the sheet sand–interbar facies, as penetrated by well DZ-1, is of considerably poorer quality than the bar facies. DZ-1 contains only 4 m of pay, concentrated at the very top of the F3 reservoir, as compared with ranges of 11–25 m pay for bar facies penetrations in West Alrar. Equivalent figures for other petrophysical parameters are 7.4% porosity, 5.2 mD permeability and 61% gas saturation in DZ-1, as opposed to 7–15% porosity, 5–43 mD permeability and 65–93% gas saturation in typical bar facies.

Conclusions

The F3 reservoir in the Alrar field was formed as a coastal deposit, with the main and highest-quality reservoir unit corresponding to a series of tidally influenced barrier bars. In West Alrar, two such bars are present, which follow a NW–SE elongation as interpreted from dipmeter data. A poorer-quality sheet sand was deposited in an interbar area in the DZ-1 well area. In East Alrar, the bars are also cut by channels. Understanding the distribution of the tidal bars is critical to locating development wells on the field.

The nature of the shale-out of the F3 reservoir to the south and west, which provides the trapping mechanism to the field, is still poorly understood, though improved well coverage and correlations do seem to have established that the shale-out is due to lateral facies change. In most regions, a gradual loss in reservoir thickness related to gradual progradation is suggested, whereas in more limited areas a structural control is evident.

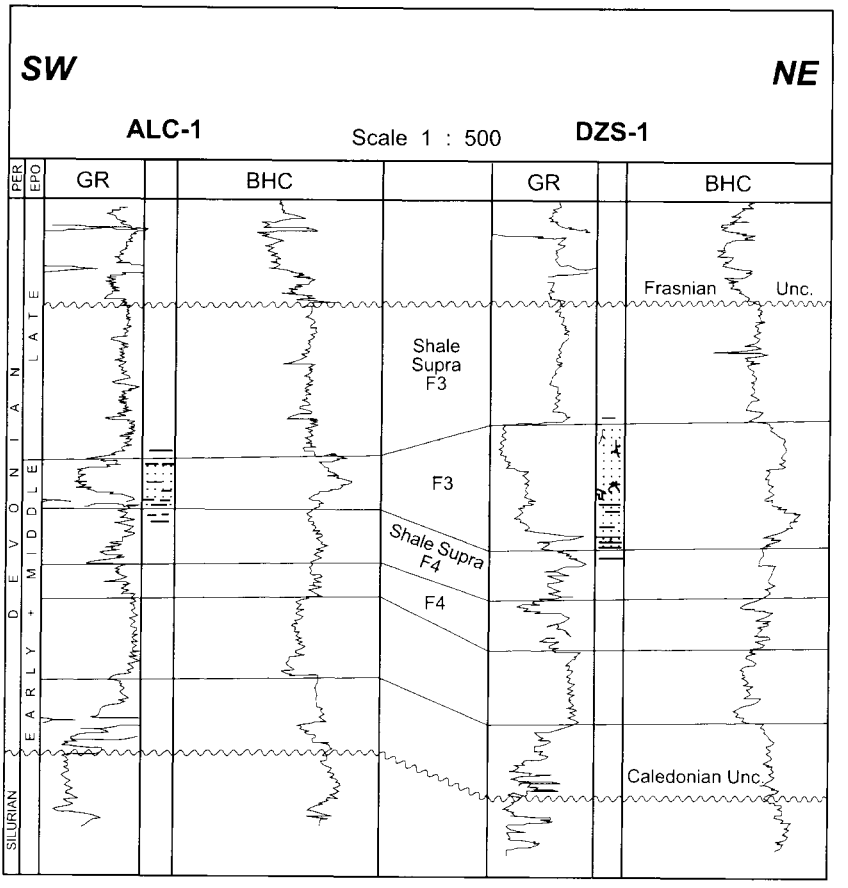

Fig. 15: Log correlation between ALC-1 and DZS-1. The excellent coarsening up profile seen at DZS-1 should be noted. The low GR sands at the top of this section, which correspond to the bar facies, are clearly absent at ALC-1.

BP are thanked for redrafting many of the figures and paying for colour reproduction costs.

References

ABDALLAH, H. & BRYL, T. 1988. *Mise au point sur le réservoir F3 (Dévonien Moyen) dans la partie Nord Orientale du bassin d'Illizi et la dépression de Ghadamès.* Unpublished Internal Exploration Report, Sonatrach.

ATTAR, A. 1987. *Évolution structurale du bassin d'Illizi.* Unpublished Internal Exploration Report, Sonatrach.

BEICIP 1987. *Le biseau du réservoir F3 à l'ouest d'Alrar.* Unpublished Report prepared for Sonatrach Exploration Department.

ELLIOT, T. 1986. Siliciclastic shorelines. *In:* READING, H. G. (ed.) *Sedimentary Environments and Facies.* Department of Earth Sciences, University of Oxford, 165 188.

FEKIRINE, B. & ABDALLAH, H. 1997. Palaeozoic lithofacies correlations and sequence stratigraphy of the Saharan Platform, Algeria. *This volume.*

JOHNSON, H. D. & BALDWIN, C. T. 1986. Shallow siliciclastic seas. *In:* READING, H. G. (ed.) *Sedimentary Environments and Facies.* Department of Earth Sciences, University of Oxford, 229 282.

SOMMER, F. 1979. *Le Réservoir F3 du Champ d'Alrar, Mise à jour des connaissances.* Unpublished Internal Exploration Report, Total Algeria.

Mesozoic and Cenozoic petroleum systems of North Africa

DUNCAN S. MACGREGOR[1] & RICHARD T. J. MOODY[2]

[1]*BP Exploration Operating Co. Ltd, Kuningan Plaza S. Tower, P.O. Box 2749, Jakarta 12940, Indonesia*

[2]*Moody-Sandman Associates, 47 Arundel Road, Kingston upon Thames, Surrey KT1 3RX*

Abstract: The Mesozoic and Tertiary petroleum systems of North Africa have formed in a suite of extensional basins developed along the Atlantic and Tethyan margin. Petroleum is unevenly spread across the region of Mesozoic basin development, with one world-class petroleum province developed (the Sirt Basin of Libya), and several more modest developments of reserves in Western Egypt and offshore Libya–Tunisia. A set of these extensional basins were later subject to compression on the Atlas and Syrian trends, with generally unfavourable effects for the preservation of the petroleum systems affected. The Moroccan passive margin is also a region of currently low exploration success. Productive reservoirs are spread throughout the Mesozoic section, though, with the exception of the prolific Early Cretaceous clastic deposits and the Paleogene carbonates, are generally not seen to correlate between basins. Effective source rock development is heavily concentrated in the Late Cretaceous and Eocene. Recent evidence also suggests an additional contribution from lacustrine source rocks of Early Cretaceous and older age in the southeastern Sirt Basin. Patterns of maturity on these main source levels, and timing of that maturity relative to trap formation, seem to be the main controls on basin success and failure, with preservation an additional key factor in inverted basins. The Mesozoic basins of North Africa are generally lightly explored compared with basins of similar petroleum productivity elsewhere in the world. Exploration to date in the Sirt Basin, for instance, has barely progressed beyond the structural trap stage, with application of analogues suggesting undrilled potential in various types of subtle trap. Further exploration remains necessary in the Atlas trend and Moroccan margin, focused on plays with more favourable timing relationships between generation and structural development than those drilled to date.

This paper provides an overview of the Mesozoic petroleum systems of North Africa, similar to that provided for the Palaeozoic by Boote *et al.* (this volume). The main objectives of the paper are to explain patterns of success and failure across the region within the Mesozoic and Tertiary sections and to contribute to the development of new exploration plays. The region covered extends from southern Morocco to the Western Desert of Egypt and does not therefore attempt to analyse the Neogene petroleum provinces of the Gulf of Suez and Nile Delta. The paper also concentrates on petroleum systems in which reservoir, source and trap are all provided within the Mesozoic–Recent section (Table 1) and discussions in the text will be centred on these. Petroleum systems with a partial Mesozoic component (e.g. the Triassic reservoired but Palaeozoic sourced system of Eastern Algeria), plus relevant systems in adjoining areas, are, however, shown for comparison in the figures. Detailed discussion of these is presented in the corresponding Palaeozoic overview (Boote *et al.* this volume)

Figures 1 and 2 illustrate the distribution of known hydrocarbon resources across the region. The contrast in exploration success between the eastern and western halves of North Africa is immediately apparent. Also apparent is the dominance of the Sirt Basin, which is the sixth largest oil province in the world and contains the majority of the proven reserves considered in this paper. Significant petroleum reserves are nevertheless developed in the Gabes–Pelagian province of offshore Tunisia and Libya and in the Western Desert of Egypt.

Structural history

The region under review forms the northern margin of the African plate, bounded by the Atlantic to the northwest, the Mediterranean to the north and the Arabian plate to the east (Fig. 1). With the exception of the Atlasic domains accreted in the Hercynian (Late Carboniferous) and Alpine (Tertiary) events, the region has formed part of a single plate throughout the Phanerozoic. This removes the need to use plate reconstructions for the maps attached to this paper (Figs 1–9) and these are therefore, for reasons of clarity, plotted on present-day geogra-

MACGREGOR, D. S. & MOODY, R. T. J. 1998. Mesozoic and Cenozoic petroleum systems of North Africa. *In*: MACGREGOR, D. S., MOODY, R. T. J. & CLARK-LOWES, D. D. (eds) 1998. *Petroleum Geology of North Africa*. Geological Society, London, Special Publication No. 132, 201–216.

Table 1. *Summary of North African Mesozoic petroleum provinces*

Province or system	*Age of source(s)*	*Source environment*	*Main reservoirs*	*Estimated reserves, oil* ($\times 10^9$ *BBL*)	*Estimated reserves, gas* ($\times 10^{12}$ *SCF*)
1. Mesozoic reservoir and source systems					
Southern Sirt	1. Cenomanian–Turonian 2. Early Cret. 3. ?Triassic	Marine Lacustrine Lacustrine	1. Early Cret. 2. Triassic-Cambro-Ordovician 3. Precambrian	24 (Barsoum 1995) 9 (Parsons *et al.* 1983)	8.6
Central/Western Sirte	1. Late Cret. 2. Paleocene	Marine Marine	1. Late Cret. carbonates 2. Paleogene Cabonates	21 (Barsoum 1995) 14 (Parsons *et al.* 1983)	~3
Abu Gharadiq	1. Middle Jurassic 2. Late Cretaceous	Marine	1. Late Cret.	0.2	3.5
Gulf of Gabès	1. Eocene carbonates 2. Late Cret. carbonates	Marine	1. Late Cret. 2. Eocene 3. Triassic-Liassic 4. Early Cret.	~1.5	~1
Tellian Atlas	1. Eocene 2. Late Cret.	Marine	1. Eocene carbonates	< 0.1	–
Saharan Atlas	1. Early Cret. 2. Late Cret.	Marine	1. Early Cret. carbonates	~0.1	
Rharb	1. Late Cret.	Marine		< 0.1	< 0.1
Essaouria	1. Mid-Late Jurassic 2. Carboniferous coals	Marine	1 Jurassic 2. Triassic	small (< 0.1??)	small (c. 0.1??)
Tarfaya	1. Middle Jurassic	Marine	1. Late Jurassic carbonates	< 0.1	0
2. Other North African petroleum sysems with a partial Mesozoic component					
Triassic Basin, Algeria	1. Silurian 2. Devonian	Marine	Triassic (sub-salt)	~4	~90

phy. On the older time slices, it is necessary, however, to remove later accreted terranes such as the Khabylis microcontinents.

Two large-scale Phanerozoic tectonic cycles can be identified affecting the area, each involving regional-scale extension followed by compression, the latter in both cases being concentrated in the northwest of the region (Macgregor this volume). The first such cycle (Palaeozoic) ended with the Hercynian event in the Atlas area, resulting from a plate collision with Europe. The second cycle (Permian–Recent) commenced with a phase of regional extension, leading to the development of a series of rifts along what was to become the eastern margin of the Atlantic and the southern margin of the Tethys Ocean (Mengoli & Spinicci 1985; Guiraud this volume). Rifting began on the Atlantic margin in the Triassic (Fig. 3), spread to the Atlas area in the Liassic (Fig. 4) and into the

Estimated reserves, total ($\times 10^9$ BBL equivalent)	*Largest field*	*Trap types*	*Age of generation–oilfield filling*	*Comments*	*References*
24 (Barsoum 1995) 11 (Parsons *et al.* 1983)	Sarir	1. Fault Blocks 2. Updip pinchout	Mainly Neogene	High preservation system	Gumati & Schamel 1988, Parsons *et al.* 1983 Gras & Thusu (this volume)
24 (Barsoum 1995) 17 (Parsons *et al.* 1983	Gialo	1. Drape anticlines 2. Carbonate build-ups	Paleogene in Western Basins, Paleogene–Neogene in Eastern basins	High preservation system	Gumati & Schamel 1988 Parsons *et al.* 1983
0.8	Abu Gharadiq	1. Inversion anticlines (L. Cret. age) 2. Fault Blocks	Tertiary		Awab 1984 Keeley *et al.* 1990, Bagge & Keeley 1994
~2	Bouri	1. Carbonate build-ups 2. Carbonate permeability pinchout 3. Inversion anticlines	Neogene		Zappaterra (1995) Bishop 1975
< 0.1	Oued Gueterini	Thrust anticlines	Neogene		
~0.1	Douleb	Inversion anticlines (Alpine)	Tertiary		Bishop 1975
< 0.1		1. Thrust anticlines 2. Sand pinchouts	Neogene		Morabet *et al.* (this volume)
< 0.1	Meskala				Broughton & Treppanier 1993
< 0.1	Cap Juby	Carbonate build-up	?		Morabet *et al.* (this volume)
~20	Hassi R'Mel	1. Pinchout traps on arches 2. Inversion anticlines 3. Fault blocks	Late Jurassic–Paleogene		Boudjema 1987 Attar *et al.* 1993

eastern Mediterranean around the Middle Jurassic (Dixon & Robertson 1984). Spreading was consequently initiated in the Middle and Late Jurassic in the Atlantic and Western Mediterranean (Fig. 5) and in the Early Cretaceous in the Eastern Mediterranean (Fig. 6). A trend of Mesozoic passive margin basins and failed rifts was thus created extending from the Moroccan margin through the Atlas and Pelagian Basins to the Abu Gharadiq Basin in Egypt (Awad 1984; Keeley & Massoud this volume). Oblique extension during the drift phase affected much of the North African margin, and led to development of occasional transpressional structures. The opening of the Eastern Mediterranean in the Late Jurassic–Early Cretaceous led to the formation of the multi-phase rift and transtensional structures of the Sirt and Abu Gharadiq Basins (Guiraud & Maurin 1992), although recent evidence suggests precursor rifts may have existed

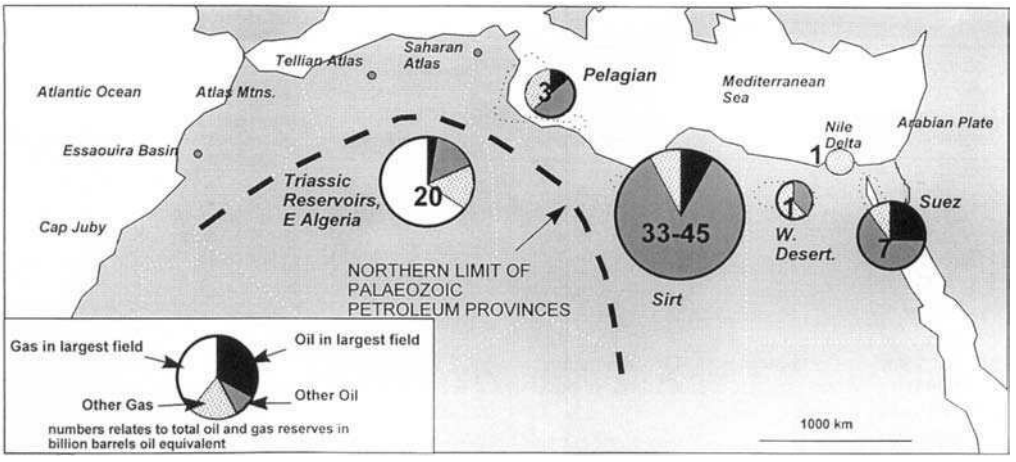

Fig. 1. Distribution of reserves within the Mesozoic and Tertiary petroleum provinces of North Africa. (Note the predominance of the Sirt province of Libya as the largest system sourced and reservoired by Mesozoic strata.) The Triassic reservoired system of Algeria is sourced from Palaeozoic source rocks.

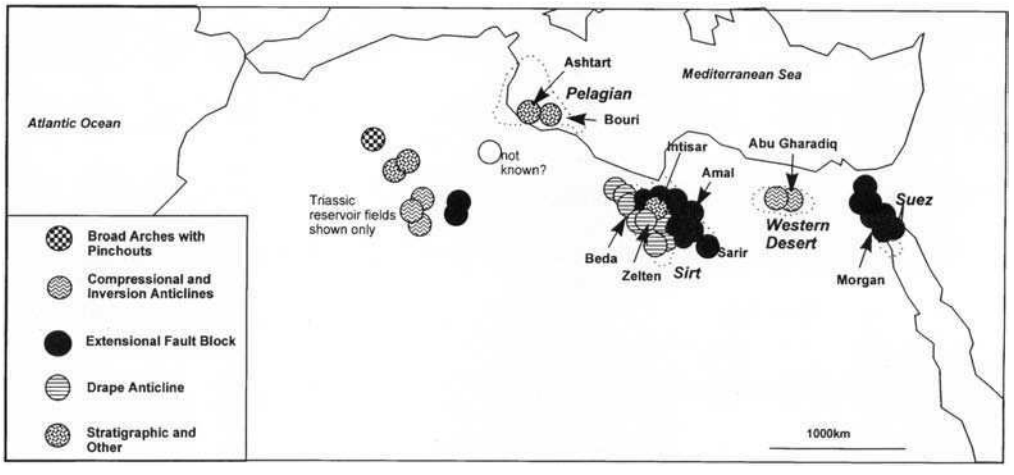

Fig. 2. Trap types of giant oilfields within Mesozoic and Tertiary reservoirs, with main fields labelled.

in these regions in the Permo-Triassic (Guiraud this volume). Movement on interior transform faults in the Aptian led to localized structural inversions within the Ghadames–Triassic Basin (Boudjema 1987; Echikh this volume), whereas a change in the relative movements of Africa and Europe in the Late Cretaceous (Fig. 7) led to more regional-scale inversions, particularly in the Atlas and Syrian Arc (Western Desert) areas (Mengoli & Spinicci 1985). All these Cretaceous tectonic events were significant in creating traps in the basins concerned (Figs 2–7).

The effects of the Alpine orogeny were largely confined to the Atlas area and adjoining basins. Thrusting and nappe formation occurred in the northern Atlas (Fig. 8) passing into milder inversions in the northern Pelagian Basin (Bishop 1975, Morgan *et al.* this volume) with additional minor effects in the Ghadames–Triassic area. The remainder of North Africa, protected by the Apulian promontory (Italy), was largely unaffected by Alpine events. A final isolated event was the rifting of the Gulf of Suez in the Miocene (Fig. 9), which can be interpreted as the onset of a further tectonic cycle.

This paper will show the petroleum systems of the region to be related intimately to the tectonic processes described above.

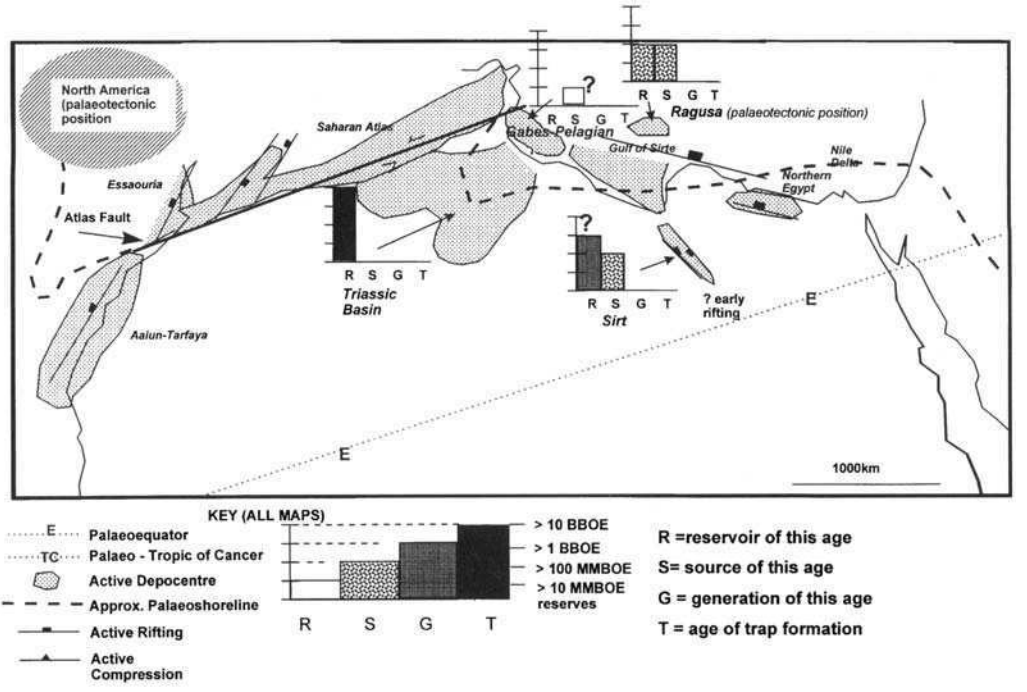

Fig. 3. Triassic events of significance to petroleum systems. Main event of significance is initiation of Triassic Basin. (Note sparsity of source rocks of this age.) Major oil- or gas-bearing reservoirs are developed of this age in Algeria, but are sourced from underlying Palaeozoic strata. Key applies to all figures.

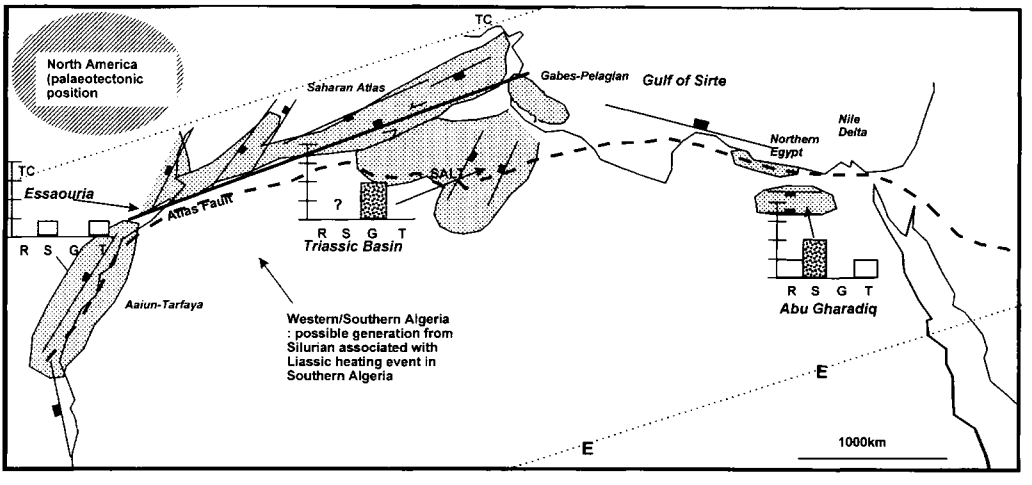

Fig. 4. Early–Middle Jurassic events of significance to petroleum systems. Rifting is established over wide areas, leading to eventual spreading. There are few known occurrences of source rocks, however, associated with this rifting phase.

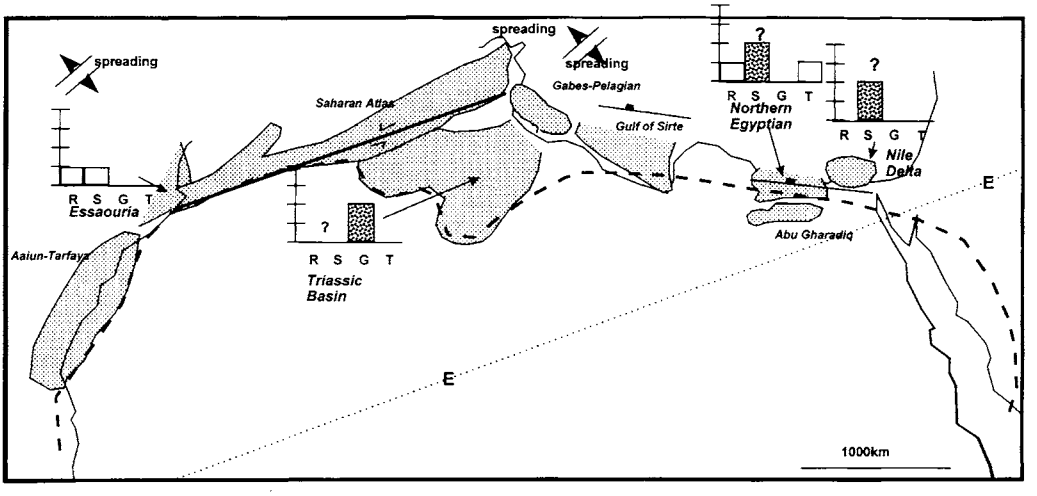

Fig. 5. Late Jurassic events of significance to petroleum systems. Spreading is now established along Tethyan margins. Source rocks are deposited associated with transgressions in northern Egypt.

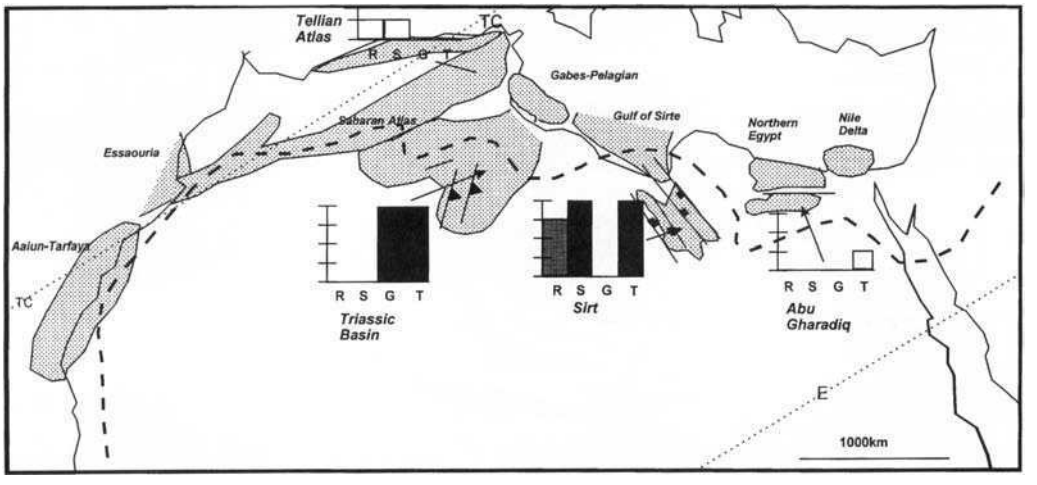

Fig. 6. Early Cretaceous events of significance to petroleum systems. Active extension is developed in Libya, Tunisia and Egypt, together with transpression in eastern Algeria, associated with opening of Tethys and African rift systems. Main associated events of significance to petroleum systems are deposition of syn-rift lacustrine source rocks in Sirt and trap formation through inversion in Algeria.

Stratigraphy and reservoirs

Facies development in the Tethyan margins (Fig. 10) is essentially a response to the tectonic regime described above, passing from rift to passive margin settings, and locally into collision and foreland development.

Non-marine Triassic reservoirs (Fig. 3) are developed in eastern Algeria and in the extension of the Ghadames Basin into Algeria. Reservoir development seems to be lost in a marine setting further north. Triassic non-marine reservoirs have also recently been recognized in the Amal Formation of the Sirt Basin (Gras & Thusu this volume)

The Jurassic (Figs 4 and 5) is a period of relatively deficient reservoir development, particularly of clastic deposits, along the developing Tethyan margin. Carbonates form potential reservoirs in a belt parallel to the palaeoshoreline, but are often of poor quality. The main reservoirs for the Essaouria and Tarfaya Basins

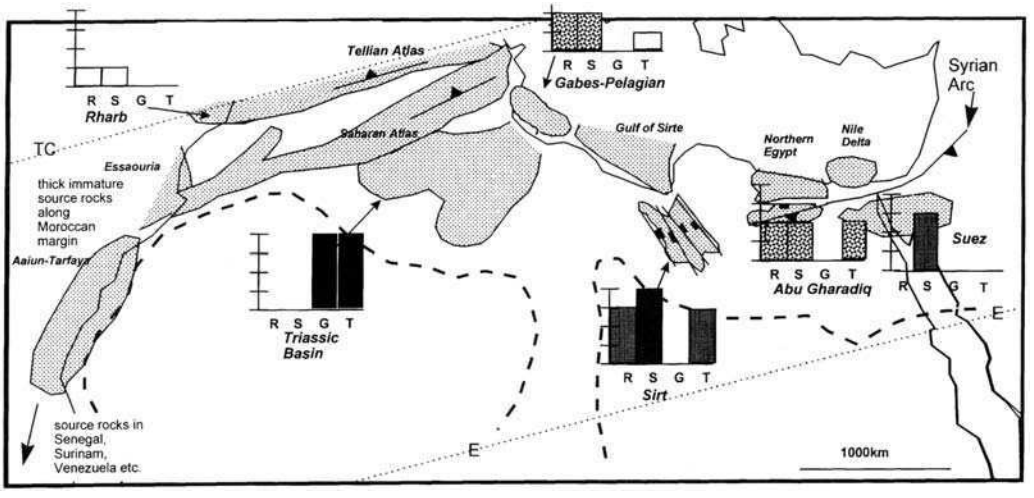

Fig. 7. Late Cretaceous events of significance to petroleum systems. Source rocks associated with upwelling, transgression and marine anoxia are developed along the entire Tethyan margin; generation from these is controlled largely by Tertiary patterns of burial and maturity. Structural inversion affects the Atlas and Syrian trends with generally negative effects on hydrocarbon preservation.

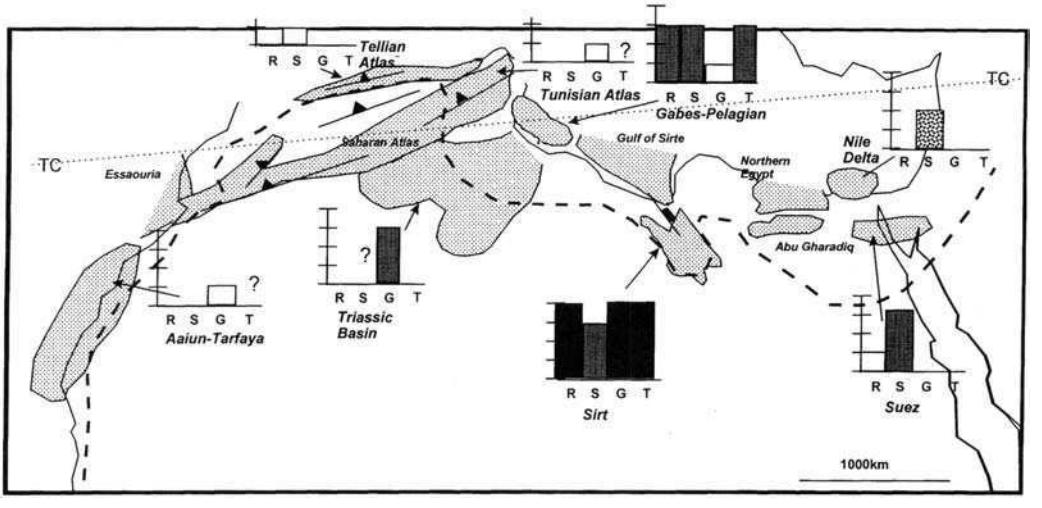

Fig. 8. Paleogene events of significance to petroleum systems. In addition to the deposition of further areally widespread source rocks in the Eocene, the Paleogene is a major period of generation and entrapment.

are of Triassic–Jurassic and Late Jurassic age, respectively, and the main traps are carbonate build-ups. Coarse clastic rocks are confined within locally subsiding basins. The M'Rabtine sands (Oxfordian–Tithonian) are one of the two known reservoirs of the Essaouia field in the Gulf of Gabès. They are the age equivalent of upper part of the Nara Formation (Upper Jurassic), which is also a minor reservoir in the same area. Syn-rift Mid–Late Jurassic sands are now an exploration objective in various regions of the Western Desert (Keeley & Massoud this volume).

Early Cretaceous clastic deposits are the main producers in the southern part of the Sirt Basin and in western Egypt (Fig. 6). Thomas (1995) recorded that the late Jurassic–early Cretaceous crustal collapse in north–central Libya resulted in a NW–SE orientated intracratonic rift system, over which 7000 m of Mesozoic–Tertiary sediments accumulated in the deeper segments of the Sirt Basin. Early rifting resulted in the deposi-

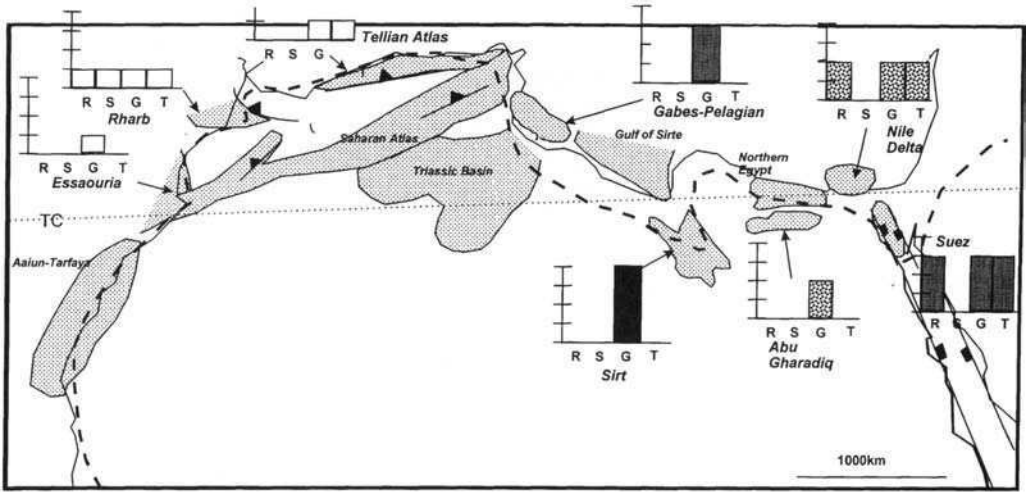

Fig. 9. Neogene events of significance to petroleum systems. Generation and entrapment of oil and gas continues as Late Cretaceous and Eocene sources are further buried below Neogene overburdens.

tion of the alluvial fan and fluviatile deposits of the Sarir or Nubian Sand Group in the south-east. The initial sediments filled syn-rift grabens (Gras & Thusu this volume) subsequently being overlain by marine shales and carbonates of the Tagrifet and Sirt Shale Formations, the distribution of which was also controlled by a localized palaeogeography. Erosion may have removed part of the Sarir Group in the southern and central areas but up to 3000 ft of sediment is recorded in the eastern areas of the basin, and Sarir sandstone is regarded as the principal reservoir for this giant oilfield. Sandstones of the late Jurassic–early Cretaceous Amal Formation occur on the eastern flank of the Sirt Basin.

Lower Cretaceous siliciclastics also occur in Egypt, southern and central Tunisia and in the Hodna Basin of Algeria (Mekireche *et al.* this volume). The Tunisian and Western Desert deposits are associated with erosion of the Saharan block. In Egypt the massive sands of the Bahariya and Abu Roash Formations (Cenomanian–Santonian) contain over 90% of known reserves (Richardson *et al.* this volume). Similar age deposits constitute ideal potential reservoirs in Tunisia but a major problem exists with sealing. In the Hodna Basin the clastic deposits are of Apto-Albian age and the potential seal is Vraconian shales. Known fields within these areas are usually less than 50 MMBOE (million barrels oil equivalent).

Upper Cretaceous siliciclastic deposits overlying fractured Cambro-Ordovician quartzites constitute a major play in the platform areas of the Sirt Basin (Thomas 1995). The sandstones of the Bahi Formation are derived from the underlying Gargaf quartzites and although seldom more than 100 m thick, are the major reservoirs for the Nafoora Augila, Waha, Raguba and Hateiba fields.

Late Cretaceous carbonate reservoirs are most significant in northern Sirt and of more minor importance elsewhere, particularly in Tunisia (Fig. 7). In Tunisia, where our understanding of these reservoirs is perhaps best, most of the Cretaceous reservoirs are found in ramp carbonate sequences. These carbonates are essentially developed north of the Gafsa Fault which extends NW–SE into the offshore region. In the lower part of the section production is restricted to the Serdj Formation (Aptian) onshore (Douleb, Semmama and Tamesmida) and the Zebbag Formation (Albian Cenomanian) in the Gulf of Gabès (Ezzaouia).

The Isis Formation (Cenomanian) is the lateral equivalent of the upper part of the Zebbag and the rudist–bioclastic limestones are a reservoir offshore. There is some controversy over the dating of these carbonates and those of the R1 Member, which is the main reservoir of the Miskar gas field. Isotope dating suggests that these carbonates are Apto-Albian in age, the equivalent of the Serdj Formation. The R1 is divided into three units (Knott *et al.*,1995) with the main reservoir in coarse, shallow water, bioclastic limestones. Reserves within the Miskar field are estimated at 1 trillion cubic feet (TCF). Rudist-rich, oolitic and shallow water foraminif-

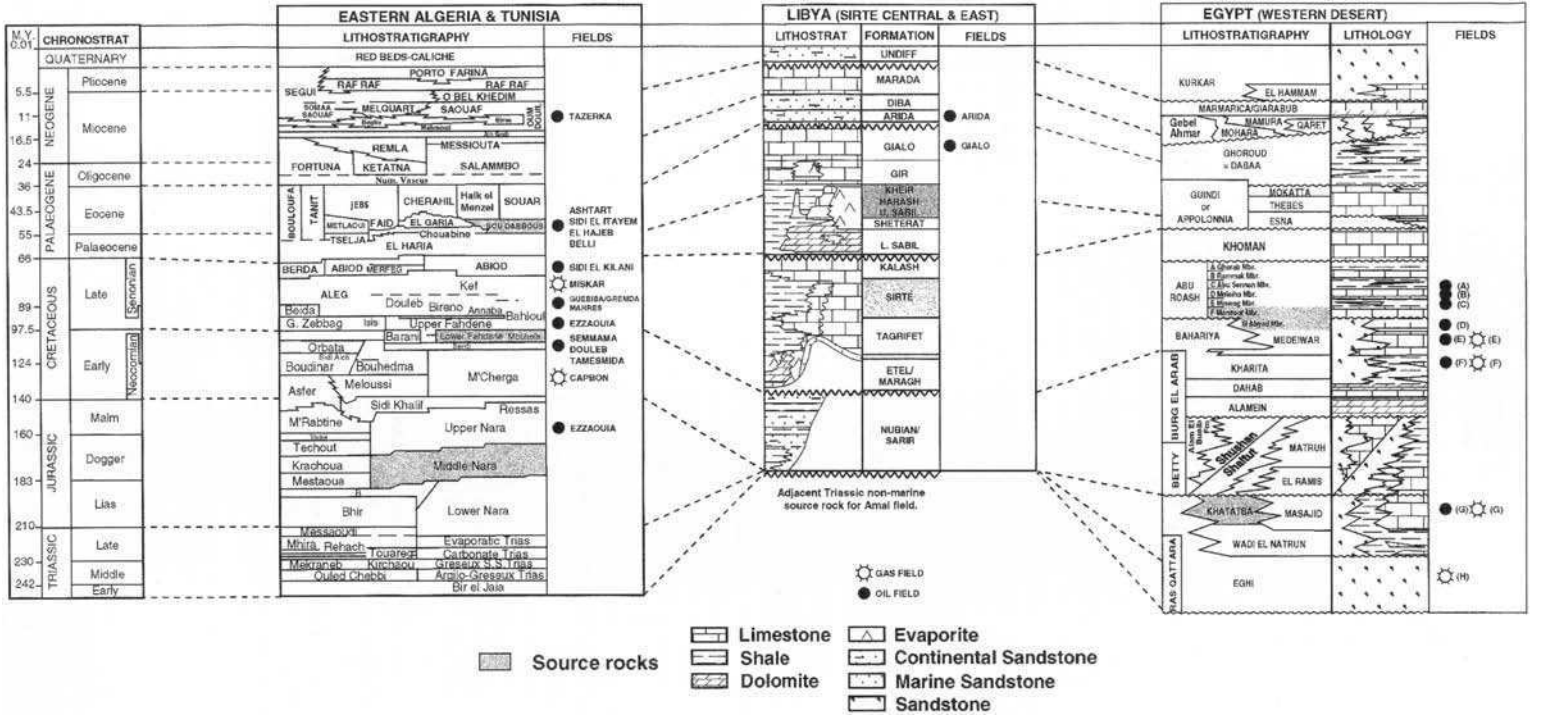

Fig. 10. Stratigraphic correlation along the Tethyan margin from west to east. The good correlation of the main source rocks (in grey) should be noted.

eral limestones make up the Bireno Formation (Turonian) as an important reservoir in the Sfax area, onshore in central Tunisia and offshore in the Gulf of Gabès. This reservoir and the Coniacian Douleb oolitic limestones are sealed by the overlying Aleg shales. The latter are overlain by the chalky limestones of the Abiod Formation, which constitute the fractured reservoir of the Sidi El Kilani field in onshore central Tunisia and the secondary target in the giant Miskar gas field.

The Kalash Formation of the Sirt Basin is the lateral equivalent of the Abiod chalks of Tunisia (Fig. 10). According to Thomas (1995), the structural highs of the Sirt Basin were mostly covered by Maastrichtian time, with extensive Paleocene carbonate banks building on a Kalash substrate. The carbonates were part of a regressive system with coral–algal accumulations present in the western, central and southern regions. Large cor-algal reefs occur in the Zelten, Defa and Beda fields. High-energy shallow water carbonates rich in miliolids and algae occur to the west. These sediments are referred to the Beda Formation and constituent members, and are major reservoirs for the Ora, Meem, Sabah Mabruk and Dahra–Hofra fields (Thomas 1995).

These Late Cretaceous carbonate sequences continue into the Paleogene in both northern Libya and Tunisia, where they form the main producing reservoirs. Paleocene–Eocene post rift limestones thicken into the northern section of the Sirt Basin. Nummulitic limestones occur at the top of the Paleocene and in the Middle Eocene. In the eastern Sirt Basin the bioclastic, coral-rich boundstones and grainstones of the Upper Sabil Formation form the main reservoir (Spring & Hansen this volume). Shoal carbonates and pinnacle reefs are the respective reservoirs of the Zelten and Intisar fields. Nummulitic reservoirs are recorded in the western area of the Sirt Basin on the axis of the Adegabia Trough (Thomas 1995). The limestones of the giant Gialo field are of Middle Eocene age, where known reserves in place total 14 billion barrels. The giant offshore Bouri field, close to the Libyan–Tunisian border, also has an Eocene nummulitic reservoir. The carbonate reservoirs of the Paleocene and Lower Eocene are sealed by the shales of the Kheir Formation in Libya and by the Souar–Cherahil Formation (Lutetian) in Tunisia.

Comparatively small fields of Eocene age are recorded in the Dor Al Beida and Zella troughs of the western Sirt Basin in the Facha dolomites.

The Lower Eocene of Tunisia is marked by regression and the deposition of ramp carbonates with the nummulitic limestones of the Ypresian El Garia Formation (Loucks *et al.* this volume) the reservoir for the Ashtart, Didon, Zarat and onshore Sidi El Itayem fields. Gas has been discovered in Sidi Behara and c. 10 MMBO have been produced from the down-dip, locally chalky limestones of the Bou Dabbous Formation (Ypresian, lateral equivalent) in the Grombalia Trough, northern Tunisia. Intra Middle Eocene nummulitic accumulations are the known reservoir for the Cercina field in the Gulf of Gabès (3500 barrels of oil per day (BOPD)).

Oligocene–Miocene sedimentation in the Gabes–Pelagian and Sirt regions is dominated by sandstones and shales, which are of relatively minor commercial importance, although the Ain Grab Formation carbonates provide the reservoir for the Maamoura (3000 BOPD) and Yasmin fields (2390 BOPD) in the Gulf of Hammamet. The more prolific reservoirs in this area of northern Tunisia are found in the Birsa sands of the Tarzarka field. Time equivalent sediments may constitute a major reservoir in the unexplored area of northwest Tunisia, with generation having occurred during the last 4–8 Ma.

Source rocks

In contrast to the spread of reserves through different trap types and reservoir levels, there is a concentration of reserves attributed to a few key source rock levels. This is a similar level of stratigraphic concentration to that seen in the Palaeozoic (Macgregor 1996; Boote *et al.* this volume).

The older part of the Mesozoic section seems to be relatively deficient in oil-prone source rocks. The predominantly non-marine nature of Permo-Triassic strata is clearly unfavourable to marine source rock development and few effective source rocks are known from this level (Fig. 3). Lacustrine source rocks of Triassic age are known from Tunisia and in failed rifts along the facing Atlantic margin of the USA, but none of these seem to have the potential to be quantitatively significant petroleum generators. A possible exception may be the Triassic lacustrine section now suggested to occur, at least locally, in the Sirt Basin (Fig. 3; Gras & Thusu this volume). The Toarcian may show regional but thin source rock development (Fig. 4), represented by a highstand event that ties to a phase of thin source rock deposition in the Atlas rifts of Morocco and in many European basins. Middle Jurassic sources are locally developed in the lacustrine coal section of the Western Desert (Bagge & Keeley 1994; Keeley & Mas-

soud this volume; Figs 4 and 10) and in the lacustrine deposits of the Middle Nara succession of Tunisia, and intra-shelf carbonates of the same age are suspected to be the source of the degraded oil accumulation at Cap Juby, Morocco. Oxfordian shales are the source for the small oil reserves of the Essaouira Basin in Morocco (Fig. 5, Broughton & Trepanier 1993), and late Jurassic shales may contribute in the Western Desert and Nile Delta. Puzzlingly, these relatively minor source occurrences (in terms of reserves tied) seem to be the only North African representatives among a large number of highly significant Late Jurassic source rocks world wide: the reasons for this relative deficiency are unknown.

Early Cretaceous lacustrine source rocks (Fig. 6) are now believed to be a significant source for much of the oil in the pre-Upper Cretaceous Clastic rocks (PUCC) in the southeastern portion of the Sirt Basin, Libya (Gras & Thusu this volume). Such an interpretation aids the explanation of the waxy nature of the oil in many of the fields in this region, including Libya's largest field, Sarir (Fig. 2, Sanford 1970).

Thin Upper Barremian (Sidi Khalif Formation) and Albian (Mouelha Formation) marine source rocks are known from central and northern Tunisia, developed within a small Cretaceous rift, and these may represent the first of several 'anoxic events' across the North African margin, marked by widespread but often thin source facies developments.

As shown in Figs 6 and 7, the vast majority of North African Mesozoic reserves derive from source rocks in two short stratigraphic intervals: in the Late Cretaceous (particularly Cenomanian–Turonian) and Eocene. These do not, however, mark single 'anoxic events', as source facies development is not fully time-correlative over the region. The trend of source rock development at these times extends along the Central Atlantic and Mediterranean margins and can, in fact, be seen on larger palaeo-plate reconstructions to continue along the entire south Tethyan margin from Venezuela to Iraq (Klemme & Ulmishek 1991). The most productive source rocks included within the Late Cretaceous grouping are the Cenomanian–Turonian 'Sirt Shales' and 'Rakb Shales' of the Sirt Basin (Shardanov 1983; Gras & Thusu this volume), the Santonian Brown Limestone of the Gulf of Suez, and the strongly laminated marine sediments of the Bahloul Formation in the Constantine and Gabès–Pelagian Basins (Bishop 1988; Nacer Bey *et al.* 1995). The thickness of source rocks varies widely, with the thickest development probably represented by a 50 m (gross) interval of immature Turonian black shales in the onshore Aaiun–Tarfaya Basin of Morocco, with total organic carbon (TOC) values of 6–10% (Einsele & Wiedmann 1982). It is likely that a variety of processes combined to favour the development of these source rocks: many correlate with transgressions associated with sea-level rises at this time, there is clear evidence for oceanic anoxia and of upwelling systems (phosphates), and the Sirt development can clearly also be tied to the formation of a tectonically controlled marine restriction.

Eocene source rock developments seem to occur along a similar trend to the Late Cretaceous sources (Fig. 8). The Eocene trend appears to have a stronger upwelling control with source rocks more frequently associated with phosphate development. The greater discontinuity of the Eocene level as productive source rocks is probably tied to the frequent immaturity of this level. The most significant Eocene source rock contributions occur where the source is buried beneath thick Neogene overburdens in the Gabès–Pelagian (Ashtart area) and Suez Basins. Thrust loading is a possible mechanism by which this source level can be locally matured (e.g. Tellian Atlas, Algeria).

A further feature which can be noted is the tendency for most productive basins to have generated their petroleum in relatively recent times, as represented by the peaks on the generation histograms on the more recent time slices. This is a trend that is particularly marked for Palaeozoic source systems in Eastern Algeria, effective generation and entrapment from these occurring mainly in Cretaceous times (Macgregor 1996, Figs 6–7).

Petroleum systems and play types

Ghadames and Triassic Basins (Triassic reservoirs)

This major petroleum system is only briefly described here, as more complete discussions are presented in the Palaeozoic papers in this volume (Boote *et al.* this volume; Echikh this volume; Macgregor this volume). Daniels & Emme (1995) recorded that within the Ghadames Basin, Triassic rocks rest on an eroded Palaeozoic section with a major trangression related to Triassic rifting. They also stated that hydrocarbons have moved updip to the west and north, in the Palaeozoic section, with the Triassic reservoirs charged with hydrocarbons sourced from less mature areas. The major field is that at Hassi R'Mel with c. 65–70 TCF and 2600 mil-

lion barrels condensate (MMBC) recoverable reserves in the Triassic reservoir sub-salt.

Triassic reservoirs in Tunisia are essentially confined to the northern section of the Ghadames Basin. The major field is at El Borma, where poorly dated, coarse sandstones probably of Ladinian age (Kirchaou–Ras Hamia Formations) rest on Palaeozoic siliciclastic deposits. Ghenima & Lafargue (1995) noted that the main field is sourced from Silurian and Devonian rocks with the so-called tar mat deposits of the SE part of the field sourced from Silurian only. The tar mat deposits are the probable product of deasphalting before the Miocene orogeny with maximum expulsion from Devonian rocks occurring post-orogeny.

Sirt Basin

The Sirt Basin represents the largest concentration of oil reserves in North Africa (Figs 1 and 2) and contains about 70% of the proven hydrocarbons in the region within the Mesozoic section (excluding the Triassic reserves of Algeria). The basin is believed to be essentially an assemblage of late Jurassic–early Cretaceous rift basins (Guiraud & Maurin 1992; Guiraud this volume), younging from south to north, although recently it has been suspected that precursor rifts may have existed in Triassic times (Gras & Thusu this volume). The main sedimentary fill to the basin ranges from Early Cretaceous to Neogene, again with a tendency to young northwards, as do the ages of the main reservoirs. At least two major petroleum systems can be distinguished and it is probable that several smaller ones also exist (Table 1). The largely non-marine reservoirs of the pre-Upper Cretaceous clastic rocks (PUCC) seem to be charged from multiple sources, including the lacustrine facies of the Early Cretaceous Middle Sarir Formation Shale and the Cenomanian–Turonian Sirt and Rakb Shales. The latter source, which is younger than the reservoir, probably contributes when juxtaposition is established on the hanging walls of faults. The PUCC reservoirs themselves range in age from Cambro-Ordovician through Triassic (e.g. Amal field) to Early Cretaceous (Sarir and Messlah fields), but are nearly always developed immediately above or below the basal Cretaceous unconformity, which is believed to form the main conduit for migration (Shardanov 1983). Productive traps within this system (Fig. 2) include footwall blocks (e.g. Sarir, Sanford 1970; Amal, Roberts 1970) and pinchout traps (e.g. Messlah).

Younger reservoirs consist almost entirely of carbonates, with the Paleocene–Eocene section being the most productive. Reservoir facies include shoal carbonates (located over deeper footwall blocks (e.g. Zelten field) and pinnacle build-ups (e.g. Intisar). These reservoirs are believed to be sourced from the laterally extensive source rocks of the Cenomanian–Turonian Sirt Shales, with a secondary contribution, where mature, from the Paleocene Heria Shales. The major trap types are low-relief drape anticlines and pinnacles enveloped in shales (Fig. 2).

Timing of generation and entrapment of the oils is assessed as ranging from Late Paleogene to Neogene in the eastern rifts (Gumati & Schamel 1988), which are at maximum burial at present day, and as tying to a Paleogene heating event in the western rifts, which were uplifted in the late Paleogene and are no longer at maximum burial. The petroleum systems present seem to show all the characteristics of a high state of preservation. The oilfields lie between 800 m depth, at which point only mild indications of biodegradation are seen, and 4100 m, where oil is still preserved in the absence of a gas phase (Parsons *et al.* 1980). The reservoir temperature range observed ranges from 52 to 152 C, with the only case of a gas filled trap tying to the highest temperature of 152 C. A major influence here seems to be a low geothermal gradient, which at an average of 25.5 C 1000 m (Parsons *et al.* 1980), allows only a small volume of Early Cretaceous to enter the gas window (> 150 C), whereas the 60 C limit of biodegradation lies high in the section, despite the low geothermal gradient, partly because of the effect of a high surface temperature. Additionally, there is little indication of significant amounts of oil migrating upwards towards surface, because of the effectiveness of the thick, laterally extensive, and in the case of post-Cretaceous horizons, unfaulted nature of the main regional seals (Parsons *et al.* 1980). The high petroleum productivity of the Sirt Basin can therefore be attributed to a coincidence of several favourable factors, including multiple source rock development, ease of communication between source rocks and reservoirs, traps developed close to kitchens, well-developed regional seals and a high state of preservation.

There have been few reported large new finds in the Sirt Basin for over 10 years (Thomas 1995). However, a comparison between the discovered fields of the basin and those in the analogous structural setting of the North Sea (Fig. 11), indicates that the basin is still is a relatively low state of exploration maturity. The exploration well density in the North Sea is around three times that in the Sirt Basin, with the finds in

the later two-thirds of wells lying largely within 'subtle traps', e.g. stratigraphic traps and hanging wall closures. The potential for large stratigraphic traps may be less than in the North Sea, because of a less favourable sedimentological setting (most North Sea stratigraphic traps are deep-water fan and channel sands, whereas most Sirt reservoirs may be more laterally extensive), but there is no reason not to expect the more subtle forms of fault-associated traps (e.g. hanging wall closures such as Brae, plus the relay ramps suggested by Gras & Thusu (this volume)) to be absent. The key to future success in the Sirt Basin may therefore lie in a refocusing of exploration towards more subtle forms of trap.

Western Egypt

Reviews of the petroleum geology of this region have been given by Keeley *et al.* (1990) and Keeley and Massoud (this volume). The region consists of several small rift basins, some of which date back to the Permian, but the majority of which can be considered to have initiated in the Late Jurassic–Early Cretaceous, contemporaneously with creation of the Mediterranean basin and with the southernmost Sirt rifts (Guiraud this volume). In contrast to the Sirt Basin, however, extensional tectonic activity was terminated in the Late Cretaceous by the Syrian Arc inversion phase.

Two well-defined petroleum systems are identified, an oil-prone Late Cretaceous system and a largely gas-prone Jurassic coal-derived system. Smaller systems may also act locally, as described by Keeley & Massoud (this volume). Laterally extensive Late Cretaceous source rocks are identified in the Abu Gharadiq, Faiyum and Shoesan Basins, but are mature only in the deepest portions of these rifts (Awad 1984). The largest oilfields, including the Abu Gharadiq field itself, noticeably concentrate around these small oil kitchens. The pre-rift Jurassic section contains lacustrine coals, which seem to be major contributors to gas reserves and minor contributors to oil reserves (Bagge & Keeley 1994). It seems to be largely because of the gas-prone nature of these coals that the hydrocarbons discovered to date in the basin consist predominantly of gas. Pre-Cretaceous reservoirs appear to have suffered from a major hydrodynamic flushing event associated with Late Cretaceous uplift and exposure on the Syrian inversion trend (Awad 1984).

There are no oilfields of giant (> 250 MMBO) scale in the region though at least one field, or probably two fields contain equivalently large gas reserves. The multiple pool Abu Gharadiq field is the largest in the region, both in terms of oil and gas reserves, and is developed in a Santonian inversion anticline. Other trap types

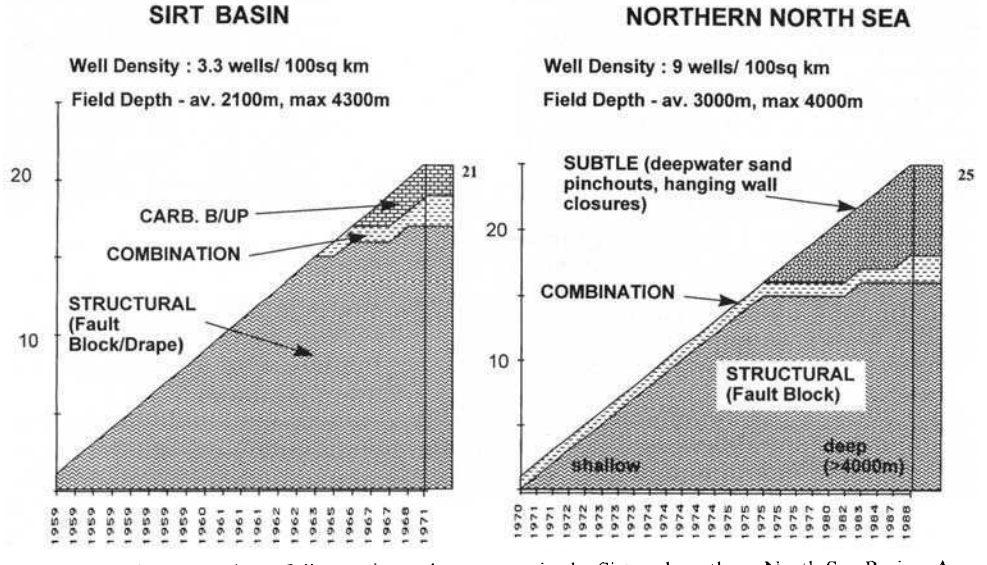

Fig. 11. Comparison over time of discoveries and trap types in the Sirt and northern North Sea Basins. A noteworthy feature is the large portion of subtle traps discovered at a late stage in the North Sea, a stage that has not apparently yet been reached, according to the drilling density statistics in the Sirt Basin.

developed in the region include fault blocks, although success in these seems to be determined largely by the nature of the potential sealing lithologies juxtaposing the reservoir on faults (Richardson *et al.* this volume).

Offshore Tunisia–Libya

The giant fields of offshore Libya and Tunisia are the Bouri field in the Gulf of Sirte and the Ashtart and Miskar fields in the Gulf of Gabès. The Bouri field with 5 BBOE and 2.5 TCF of gas is the supergiant of the region, but although the reservoir facies extends into Tunisian waters, Ashtart, with > 720 MMBOE, is the biggest discovery to date in that country. Ashtart is drilled on a palaeohigh, though the trap is partly stratigraphic in nature. The Ypresian nummulitic reservoir is sourced from the laterally equivalent off-ramp Bou Dabbous Formation. The same source–reservoir relationship is proposed for the smaller Hajeb and Sidi El Itayem fields onshore.

Atlas trend

The Atlas fold belt falls into two segments, the Saharan Atlas, comprising a severely inverted and deformed set of Mesozoic rift basins, and the Tellian Atlas, a later fold and inversion belt resulting from the accretion of the Khabylis microcontinents to the North African margin in the Miocene (Dixon & Robertson 1984). The region is one of low exploration success: despite the drilling of over 50 exploration wells in the region, there have been no discoveries of more than 30 MMBO reserves. The region is richer in reported surface seeps than any other part of North Africa (Macgregor 1993), thus absence of source rocks does not seem to be an issue. The lack of success of wells drilled to date can to a large extent be attributed to unfavourable timing relationships between generation, trap formation and destructive events (Mekireche *et al.* this volume). There has been a tendency to drill the largest and most obvious structures, which probably tend also to tie to the youngest phase of structure development and therefore are the ones least likely to have been in existence during periods of maximum source rock burial and generation. High vitrinite reflectances at surface, around or in some cases above those of the oil window, testify that kitchens over most of the region are no longer generating. Many structures have also been eroded to a level such that both mature source rocks and potential reservoirs are exposed in many anticlinal crests, i.e. traps have been unroofed. Such features may be largely responsible for the large numbers of reported seeps.

Although relatively well drilled with respect to other frontier African basins, exploration well densities (generally less than 1 well 1000 km^2) are considerably lower than in many European basins in which significant late-stage discoveries have been made. Examination of such European analogues gives some hope for basins where timing seems to be the main explanation for failures to date. The heavily inverted Cimmerian basins of NW Europe (e.g. Wessex Basin, Broad Fourteens, West Netherlands basins) had already been considerably explored with limited success before the Wytch Farm giant was found in a deep reservoir on a palaeostructure that had survived inversion in an unaltered form. This experience suggests that a search for undeformed palaeostructures in some of the inverted Mesozoic basins might provide dividends. The High Plateau represents one area where such features may be preserved.

The recent successes in the sub-nappe areas of the Southern Apennines (d'Andrea *et al.* 1993; Mattavelli *et al.* 1993), in an area directly on trend with the Tellian Atlas, demonstrate the value of perseverance in structurally complex areas such as the Atlas. It can now be seen that success on the Alpine trend, associated with a variety of source rocks, seems almost entirely to be associated with generation from Neogene depocentres; examples are the Southern Apennines sub-nappe and foreland areas, the Po Valley and the Vienna Basin. This aspect clearly highlights potential along the Tellian trend of Algeria, where Late Cretaceous and or Eocene source rocks should have been matured by thrust loading, and possibly also in the Rif sub-nappe area of Morocco.

Moroccan Passive Margin

The trend of passive margin basins extending from the Rharb foreland to the Aaiun Basin is another area where, despite considerable exploration effort, no large discoveries have been made. Oil and gas finds have been limited to two regions of minor finds in the Rharb and Essaouria Basins and a degraded heavy oil accumulation near Cap Juby in the Tarfaya Basin. This lack of success mirrors that in the contiguous passive margin of the Atlantic coast of the USA.

As most areas are at maximum source rock maturity at the present day, timing of maximum maturity from Mesozoic sources does not seem to be the issue. The paucity of shows over wide areas would instead suggest that the general failure to date of exploration in this region is due to an absence of mature source rocks, an explanation which has also been considered for the failure of the lesser number of wells drilled to date on the US Atlantic margin. Source quality is probably suitable at the levels corresponding to the most prolific source rocks in North Africa, i.e. Silurian and Late Cretaceous, but many of these basins may have been doubly unfortunate in containing overmature Palaeozoic source rocks (or those which generated before the Hercynian event) and an immature Late Cretaceous section.

The region still contains significant undrilled or sparsely drilled areas. The key to future success is likely to lie in working the source issue harder, e.g. by using seismostratigraphic techniques to identify sections in which mature source rocks may lie, or in modelling regions in which Palaeozoic source rocks could have generated in post-Hercynian times. The Aaiun–Tarfaya Basin may have some potential associated with the latter model (T. Kilenyi, pers. comm. 1995).

Conclusions

Exploration success within the Mesozoic section in North Africa appears to be controlled by several factors, including thick source development, maturity of source rocks, timing of generation relative to trap formation and possible destruction of oil pools during inversion events. The last two factors are heavily influenced by tectonic history, with a continued extensional setting favoured over those subject to late-stage compression and inversion. Reservoir development is present at most levels, though the most productive reservoirs, and those which can most readily be correlated between basins, are the Early Cretaceous clastic deposits and Late Cretaceous–Eocene carbonates. This trend seems to be related to the proximity of these reservoirs to the main source rocks in the Late Cretaceous and, where mature, the Eocene.

Remaining exploration potential is perceived to be good, although it needs to be guided more by the factors considered above than has often been the case in the past. Exploration in the most productive basin, the Sirt Basin, seems to have barely progressed beyond the stage of seeking structural traps, and attention now needs to be moved towards more subtle forms of trap. In addition, a search for early formed traps on the Atlas trend, and for restricted areas of mature source rock development on the Atlantic margin, may well lead to success in these currently unproductive regions.

References

ATTAR, M. & HAMMAT, M. 1993. Hydrocarbon potential of Algeria. *In*: *Proceedings of the Second Mediterranean Oil and Gas Conference (MOEX), Valletta, Malta.*

AWAD, G. M. 1984. Habitat of oil in Abu Gharadiq and Faiyum Basins, Western Desert, Egypt. *Bulletin, American Association of Petroleum Geologists*, **68**(5), 564–573.

BAGGE, M. A. & KEELEY, M. L. 1994. The oil potential of Middle Jurassic coals in Northern Egypt. *In*: SCOTT, A. J. & FLEET, A. J. (eds) *Coal and Coal-Bearing Strata as Oil-Prone Source Rocks*, Geological Society, London, Special Publications, **77**, 183–200.

BARSOUM, T. K. 1995. Factors controlling the deposition of the pre-Upper Cretaceous clastics and hydrocarbon accumulation in the Sirt Basin, Libya. *In*: *Abstract Booklet of First Symposium on the Hydrocarbon Geology of North Africa*, 28–30 November 1995.

BISHOP, W. F.,1975, Petroleum Geology of Tunisia and adjacent parts of Libya and Algeria, *Bulletin, American Association of Petroleum Geologists*, **59**(3), 413–450.

— — 1988. Petroleum geology of East Central Tunisia, *Bulletin, American Association of Petroleum Geologists*, **72**(9), 1033–1058.

BOOTE, D., TRAUT, M. & CLARKE-LOWES, D. D. 1998 Palaeozoic petroleum systems of North Africa. *This volume.*

BOUDJEMA, A. 1987. *Évolution structurale du Bassin petrolier triasique du Sahara Nord-Oriental (Algérie)*. PhD thesis, Université Paris-Sud.

BROUGHTON, P. & TREPANIER, A. 1993. Hydrocarbon Generation in the Essaouira Basin of Western Morocco. *Bulletin, American Association of Petroleum Geologists*, **77**(6), 999–1015.

D'ANDREA, S., PASI, R., BERTOZZI, G., DATTILO, P. 1993. Geological model, Advanced methods help unlock oil in Italy's Apennines. *Oil & Gas Journal*, 23 August, 53–56.

DANIELS, R. P. & EMME, J. J. 1995. Petroleum system model, eastern Algeria from source rock to accumulation: when, where and how? *Proceedings of the Seminar on Source Rocks and Hydrocarbon Habitat in Tunisia.* Mémoire de l'ETAP, **9**, 101–124.

DIXON, J. E. & ROBERTSON, A. H. F. (eds) 1984. *The Geological Evolution of the Eastern Mediterranean*, Geological Society, London, Special Publications, **17**.

ECHIKH, K. 1998 Geology and hydrocarbon occurrences in the Ghadames Basin, Algeria, Tunisia, Libya. *This volume.*

EINSELE, G. & WIEDMANN, J. 1982. Turonian Black Shales in the Moroccan Coastal Basins. *In*: VON RAD, U. *et al.* (eds) *Geology of the Northwest African Continental Margin*. Springer-Verlag, Berlin, 396–414.

GHENIMA, R. & LAFARGUE, E. 1995. Hydrocarbon generation and migration in the Ghadames Basin. Application to the filling history of the El Borma Oil Field. *Proceedings of the Seminar on Source Rocks and Hydrocarbon Habitat in Tunisia*. Mémoire de l'ETAP, **9**, 3–16.

GRAS, R. & THUSU, B. 1998. Trap architecture of the Early Cretaceous Sarir sandstone in the eastern Sirt Basin, Libya. *This volume*.

GUIRAUD, R. 1998. Mesozoic rifting and basin inversion along the northern African Tethyan margin: an overview. *This volume*.

—— & MAURIN, J.-C. 1992. Early Cretaceous Rifts of Western and Central Africa, an overview. *Tectonophysics*, **213**, 153–168.

GUMATI, Y. D. & SCHAMEL, S. 1988. Thermal Maturity History of the Sirt Basin, Libya. *Journal of Petroleum Geology*, **11**(2), 205–218

HARDING, T. P. 1983. Graben hydrocarbon plays and structural styles. *In*: KAASCHIETER, J. P. H. & REIJER, T. J. A. (eds) *Petroleum Geology of the Southeastern North Sea and the Adjacent Onshore Areas*. Geologie en Mijnbouw, **62**, 003–023.

KEELEY, M. L. & MASSOUD, M. S. 1998 Tectonic controls on the petroleum geology of NE Africa. *This volume*.

——, DUNGWORTH, G., FLOYD, C. S., FORBES, G. A., KING, C., MCGARVA, R. S. & SHAW, D. 1990. The Jurassic System in Northern Egypt. 1. Regional stratigraphy and implications for hydrocarbon prospectivity. *Journal of Petroleum Geology*, **13**(4), 397 420

KLEMME, H. D. & ULMISHEK, G. F. 1991. Effective petroleum source rocks of the world: stratigraphic distribution and controlling depositional factors. *Bulletin, American Association of Petroleum Geologists*, **75**(12), 1809–1851.

KNOTT, I., MOODY, R. T. J. & SANDMAN, R. I. 1995. The Coniacian Turonian carbonates of the Miskar Field Offshore Tunisia. *American Association of Petroleum Geologists, International Conference, Nice* (abstracts).

LOUCKS, R. G. MOODY, R. T. J., BELLIS, J. K. & BROWN, A. A. 1998. Regional depositional settling and pore network systems of the El Garia Formation (Metlaoui Group, Lower Eocene), offshore Tunisia. *This volume*.

MACGREGOR, D. S. 1993. Relationships between seepage, tectonics and subsurface petroleum reserves. *Marine & Petroleum Geology*, **10**(6), 606–619.

—— 1996. The hydrocarbon systems of North Africa. *Marine & Petroleum Geology*, **13**(3), 329 340.

1996. Introduction. *This volume*.

MATTAVELLI, L., PIERI, M. & GROPPI, G. 1993. Petroleum exploration in Italy, a review. *Marine & Petroleum Geology*, **10**(5), 410 425.

MEKIRECHE, K., SABAOU, N. & ZAZOON, R.-S. 1998. Critical factors in the exploration of an Atlas intramontane basin: the Western Honda Basin of northern Algeria. *This volume*.

MENGOLI, S. & SPINICCI, G.1985. Tectonic evolution of North Africa (from North Sinai to Algeria). *In*: *Proceedings of the Seminar on Source and Habitat of Petroleum in the Arab Countries, Kuwait, October 1984*. OAPEC, 119–174.

MORABET, A. M., BOUCHTA, R. & JABBOUR, H. 1998. An overview of the petroleum systems of Morocco. *This volume*.

MORGAN, M. A., GROCOTT, J. & MOODY, R. T. J. 1998. The structural evolution of the Zaghouan–Ressas Structural Belt, northern Tunisia. *This volume*.

NACER BEY, R., BERGHEUL, M. & GUELLAL, S. 1995. Étude et charactérisation des roches mères crétacées du bassin sud-est constantinois. *In*: *Proceedings of the Seminar on Source Rocks and Hydrocarbon Habitat in Tunisia*. Memoire de l'ETAP, **9**, 29 43.

PARSONS, M. G., ZAGAAR, A. M., & CURRY, J. J. 1980. Hydrocarbon occurrences in the Sirt Basin, Libya. *In*: MAILL, A. D. (ed.), *Facts and Principles of World Petroleum Occurrence*. Canadian Society of Petroleum Geologists, Memoir, **6**, 723–732.

RICHARDSON, S. M., VIVIAN, N., COOK, R. J., WILKES, M. & HUSSAIN, H. 1998. Application of fault seal analysis techniques in the Western Desert, Egypt. *This volume*.

ROBERTS, J. M. 1970. Amal Oil Field, Libya. *In*: HALBOUTY, M. T. (ed.), *Geology of Giant Petroleum Fields*. American Association of Petroleum Geologists, Memoirs, **14**, 438–448.

SANFORD, R. M. 1970. Sarir Field Desert Surprise. *In*: HALBOUTY, M. T. (ed.) *Geology of Giant Petroleum Fields*. American Association of Petroleum Geologists, Memoirs, **14**, 449 476.

SHARDANOV, A. N. 1983. Regional hydrocarbon migration as a factor in the formation of major petroleum accumulation zones. *International Geology Review*, **25**, 5.

SPRING, D. & HANSEN, O. P. 1998. The influence of platform morphology and sea level on the development of a carbonate sequence: the Harash Formation, Eastern Sirt Basin, Liby. *This volume*.

THOMAS, D. 1995. Exploration limited since '70s in Libya's Sirt basin. *Oil & Gas Journal*, 99 104.

ZAPPATERRA, E. 1995. The Pelagian Block (Central Mediterranean), exploration and new opportunities (abstract). *Bulletin, American Association of Petroleum Geologists*, **79**(8), 1258.

Mesozoic rifting and basin inversion along the northern African Tethyan margin: an overview

R. GUIRAUD

Laboratoire de Géophysique et Tectonique, case 060, Université de Montpellier II, 34095 Montpellier Cedex 5, France

Abstract. The northern African Tethyan margin registered three major rifting episodes from the latest Palaeozoic–earliest Mesozoic to the earliest Cenozoic. Break-up of Gondwana was initiated in the late Carboniferous. Along the northern African–Arabian plate margin rifting propagated westward from the northeastern Arabian margin to Morocco during the Permian and Triassic, and was accompanied by Mid–Late Triassic–earliest Liassic extensive alkaline flow basalts. Rifting continued during the Liassic, e.g. in the Moghrebian Atlas troughs. A second stage of rifting occurred in the Late Jurassic and continued into, or was rejuvenated during, the Early Cretaceous. Along the east Mediterranean margin, some large E–W trending rifts formed, often with associated volcanism, e.g. southern Sirt and Abu Gharadig. Most researchers believe the oceanization of the eastern Mediterranean basin occurred at this time. Flexural subsidence affected the Moghrebian Atlas, including the Riffian–Tellian domain, where a thick flysch series was deposited. Two short-lived, but widespread and tectonically important, compressional or wrench-dominated events occurred during the Santonian and the latest Maastrichtian. From Morocco to Oman, most sedimentary basins were folded and inverted at these times. The Santonian event resulted from onset of the collision between the African–Arabian and Eurasian plates. New stress-fields favoured NE–SW extension along the African plate margin, generating or rejuvenating some rifts, e.g. in the Euphrates trough and in the Libya–Tunisia region (northwestern Sirt, Pelagian Sea). Rifting and magmatism continued in these regions into the Paleocene. During the Mesozoic, therefore, the northern margin of the African–Arabian plate registered both rifting resulting in the oceanization of the Tethys and rifting resulting from the initiation of the closure of the Tethys. The intraplate domain exhibited echoes of the tectonic events affecting the margin.

The aim of this paper is to document the phases of rifting and basin inversion which affected the northern African margin of Tethys from the late Carboniferous to the early Paleocene (Figs 1 and 2). The major geodynamic events which have been recognized in Africa, often extending into Arabia, will be described. Magmatic activity, which may accompany rifting, will be mentioned (see details given by Wilson & Guiraud (1992) and elsewhere in this volume). More detailed palaeogeographical analysis can be found in the *Atlas Tethys Palaeoenvironmental Maps* of Dercourt *et al.* (1993).

Late Carboniferous–Liassic rifting episodes

Following the Variscan orogeny, the break-up of Gondwana occurred in the late Carboniferous (Lambiase 1989; Stampfli *et al.* 1991; Guiraud & Bellion 1995). Along the northern African–Arabian plate margin rifting propagated westward during the Permian and Triassic from the northeastern Arabian margin to Morocco (Figs 3 and 4). The Neotethys ocean was formed in the Late Permian (Baud *et al.* 1993*a*, and *b*; Stampfli 1996), south of the Cimmerian continental blocks, which thereafter moved rapidly northward.

Along the northern African–Arabian margin, several rift basins were active during late Carboniferous or Permian–Triassic times, including the following: the Palmyra Basin (Lovelock 1984); the Erez graben along the coastal margin of Israel (Hirsch *et al.* 1995); small-scale grabens of western Jordan (Powell & Khalil Mohamed 1993); half-grabens of northern Egypt (Keeley 1994); small-scale grabens of south east Sirt (Thusu & Mansouri 1995); the Jeffara Basin of Tunisia–Libya (Burollet *et al.* 1978); some basins along the Tunisian Atlas, the Saharan Atlas (Stampfli & Pillevuit 1993), the Moroccan Middle Atlas and High Atlas (Laville & Piqué 1991) troughs; the Moroccan Atlantic margin rifts, which belong to the very active Triassic Central Atlantic province, extending south to the Senegal margin.

Some activity also occurred southwards, in the continental domain, e.g. in the Erdis Basin of northwestern Sudan (Klitzsch & Wycisk 1987) and along the roughly N–S trending fault zones of the Algerian–Malian–Nigerian Sahara (Marcoux *et al.* 1993*a–d*).

GUIRAUD, R. 1998. Mesozoic rifting and basin inversion along the northern African Tethyan margin: an overview. *In*: MACGREGOR, D. S., MOODY, R. T. J. & CLARK-LOWES, D. D. (eds) 1998. *Petroleum Geology of North Africa*. Geological Society, London, Special Publication No. 132, 217–229.

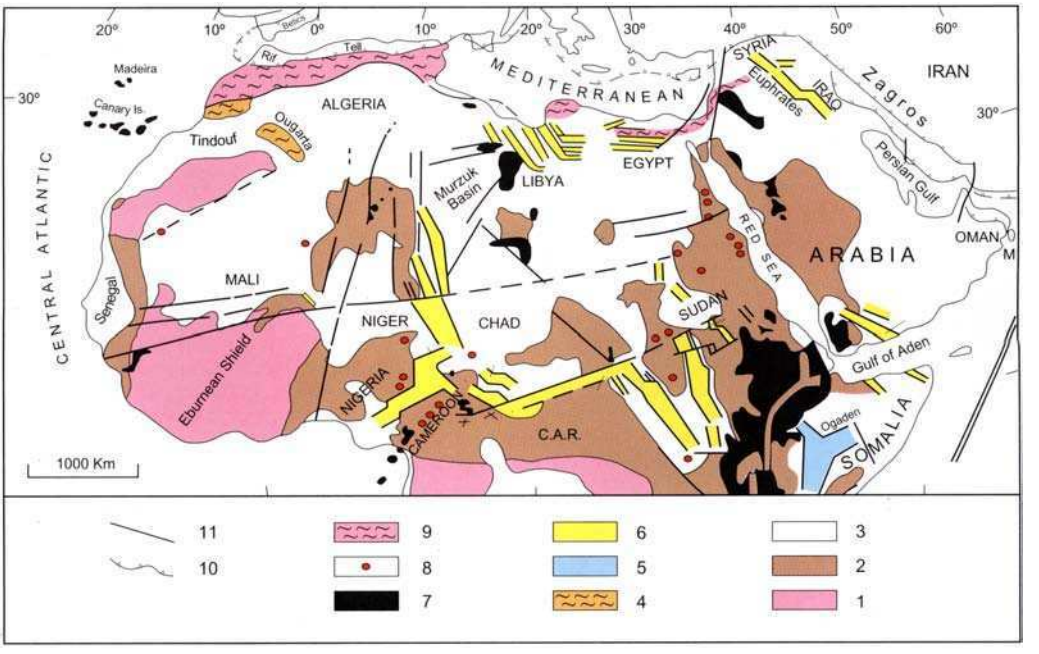

Fig. 1. Location map with tectonic features of northern Africa, central Africa and Arabia. 1, Archaean cratonic area; 2, Proterozoic belt (mainly Pan African); 3, Phanerozoic; 4, Variscan fold belt; 5, Karroo rift; 6, Mesozoic and/or Cenozoic rift; 7, Mesozoic or Cenozoic magmatism; 8, Late Carboniferous Early Paleocene alkaline ring complex; 9, Phanerozoic fold belt; 10, Alpine thrust front; 11, major fault zone.A, Abyad; B, Bornu; B-B, Birao-Bagarra; Be, Benue; Bo, Bongor; C, Çyrenaica; CAFZ, Central African Fault Zone; CAR, Central African Republic; D, Darfur; Dj, Djerem; EB, El Biod High; E.G., Equatorial Guinea; G, Gargaf High; H.M., Hassi Messaoud; K, Khartoum; M, Massirah Island; Mb, Mbere; Me, Melut; Mu, Muglad; M-S, Marib–Shabwa; P, Palmyrides; S, Sinai; Soc., Socotra Island; T, Tarfaya; Te, Tenere; Tib., Tibesti; U, Uweinat.

During the Liassic, large rift basins and troughs were formed and/or developed along the northwestern African margins. Active rifting occurred along the Moghrebian–Iberian margins and throughout the Central Atlantic domain (Stampfli 1996), in relation to a general sinistral transtensional movement along the Newfoundland–Gibraltar–Sicily transform zone. This latter feature was initiated in Triassic times and was active until the Late Cretaceous (Lemoine 1985; Ziegler 1989). The Saharan Atlas, the High Atlas and the Middle Atlas troughs developed as sets of pull-apart basins, as proposed by Mattauer *et al.* (1977) and later illustrated by many workers, e.g. Aït Ouali & Delfaud (1995) (Fig. 5).

Strong magmatic activity occurred during these times, both along the margins and within the intraplate domains. Permian magmatism was mainly expressed as alkaline anorogenic intrusion complexes located along major intraplate fault zones. During the Triassic and the Liassic extensive alkaline flow basalts were extruded, particularly in the Levant, in the Sirt area, and in the Moghreb and the Taoudenni Basin–Central Atlantic province. These extrusions peaked at *c.* 200 Ma, whereas alkaline intrusions occurred throughout this period (Wilson & Guiraud this volume).

The late Carboniferous–Liassic rifting resulted in the thinning of the lithosphere, causing the major magmatic activity. For some workers, break-up of the continental crust occurred in the East Mediterranean Basin as early as the Late Permian (Stampfli *et al.* 1991; Stampfli & Pillevuit 1993; Stampfli 1996; Vai 1996). Others consider that this phenomenon could be younger (see below, and discussion of this problem by Robertson *et al.* (1996)). In the Central Atlantic domain, spreading occurred in approximately Bajocian times (Klitgord & Schouten 1986).

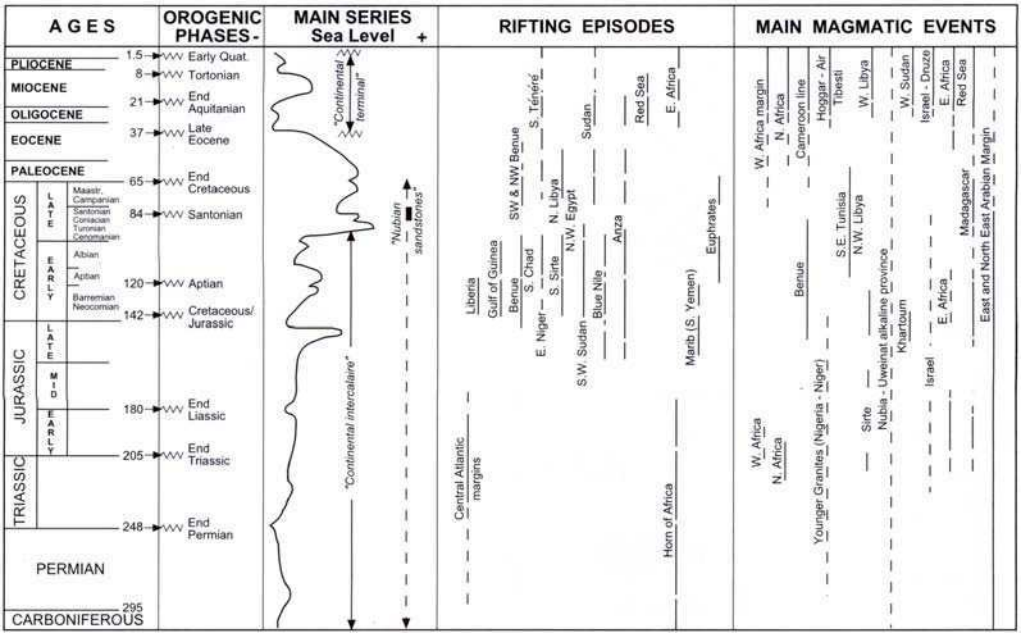

Fig. 2. Late Carboniferous to Recent tectonosedimentary and magmatic events in northern Africa, central Africa and Arabia. Modified from Guiraud & Bellion (1995). Chronostratigraphic scale from Berggren *et al.* (1995).

Late Jurassic-Early Cretaceous rifting episodes

Late Jurassic

During the Late Jurassic a further stage of rifting or subsidence occurred. Along the northern African margin, earlier generated rifts registered regional, flexural subsidence: e.g. the Levant margin troughs (Hirsch *et al.* 1995), the Saharan Atlas Trough (Vially *et al.* 1994), the Aures Trough (Guiraud 1990) and some basins along the Riffian–Tellian troughs (Wildi 1983; Cattaneo & Gélard 1989). Rifting occurred in some small basins, such as southeastern Sirt and northwestern Egypt. Active rifting was concentrated further southwards, within the intraplate domain, where some large rift-basins were formed (Figs 1 and 6a): e.g. the Upper Benue (Nigeria), the Blue Nile–Khartoum (Sudan) and the Marib (Yemen) rift-basins (reviewed by Guiraud & Bellion (1995)).

Along the Tethyan margin, some magmatism occurred in the Levant area, in the Riffian–Tellian belt (basalts and peridotites which could imply the existence of oceanic crust), and in the Moroccan High Atlas (gabbros and basalts) (reviewed by Wilson & Guiraud (this volume)). Intraplate rifting was accompanied by strong magmatic activity (basalts, tuffites) in the Upper Benue and Khartoum areas.

Within many basins, the Jurassic–Cretaceous transition exhibits hiatuses and unconformities in the series (Fourcade *et al.* 1993*a*, *b*). These phenomena may be associated with the sharp drop in global sea level in the Late Tithonian (Fig. 2). However, they are also locally associated with uplift, block tilting and sometimes slight folding caused by local transpression: a latest Jurassic tectonic event the (the 'Cimmerian event') is recognized in Israel and Sinai (Bartov *et al.* 1980), in northern Egypt (Keeley & Wallis 1991), in the Tellian Atlas (Obert 1984), in the Saharan Atlas (Kazi-Tani 1986), in Morocco (Demnati 1996), the High Atlas (Laville & Piqué 1992) and around the Horn of Africa, from Yemen to Tanzania. These deformations represent the distal effects of stronger tectonic activity, including thrusts, which occurred in southeastern Europe and has been termed the (Mid-) 'Berriasian orogenic event' by Nikishin *et al.* (1996).

Neocomian-earliest Aptian

By the earliest Cretaceous a new stage of active rifting began along the northern African–Ara-

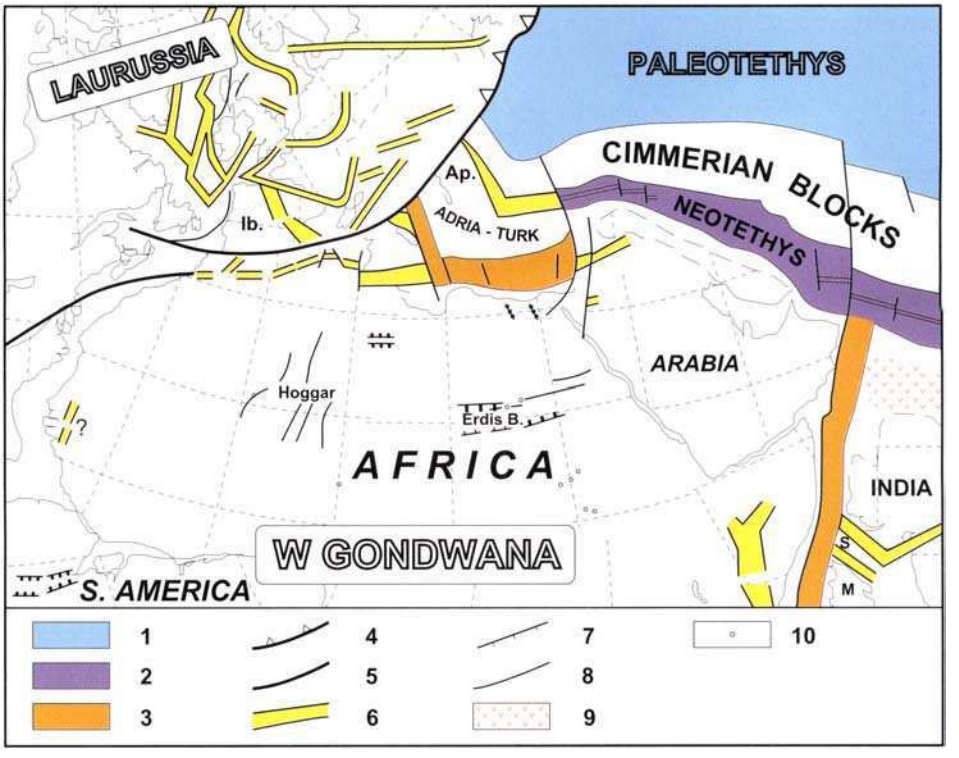

Fig. 3. Schematic map of Late Carboniferous -Permian rifting in northern Africa, Arabia and adjacent regions.

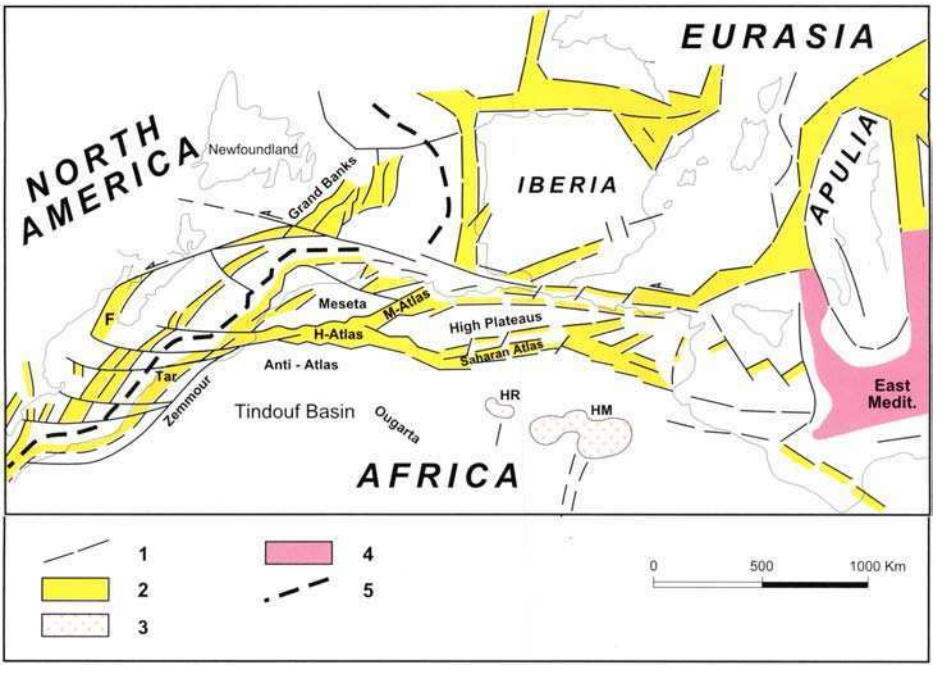

Fig. 4. Schematic map of Triassic rifting along the northwestern African margin and adjacent areas.

bian margin and within the intraplate domain (Guiraud & Maurin 1991, 1992). Numerous rift-basins appeared, and some earlier rifts were reactivated. Along the Egyptian–Libyan margin several E–W to ENE–WSW trending half-grabens (Fig. 7) showed strong subsidence during Neocomian–Barremian times, notably the Abu Gharadig and Shushan in the northern Western Desert of Egypt (Bayoumi & Lotfy 1989; Taha 1992; Breman & Rinehart 1995) and the Hameimat and Sarir in the southeastern Sirt (AGOCO 1980; Rossi *et al.* 1992; Gras & Thusu this volume). This set of roughly E–W rifts appears as a double horse-tail pattern, in relation to the southern damping of the major NNW–SSE and approximately N–S fault zones delimitating the East Mediterranean Basin, which developed further and possibly oceanized at this time (Dercourt *et al.* 1986; Masse *et al.* 1993).

Along the Moghrebian margin this period also saw E–W rifting in Tunisia, and subsidence along the Saharan Atlas–Aures troughs (Guiraud 1990; Vially *et al.* 1994) and the Riffian–Tellian troughs (Wildi 1983). Southwards, in the Algerian Sahara, the major roughly N–S trending El Biod fault zone acted as a sinistral strike-slip, with a reverse component (Boudjema 1987; Guiraud & Maurin 1991, 1992). Several drag folds, associated with this fault zone, are unconformably overlain by the mid-Aptian carbonates: examples are the structures containing the Gassi Touil–Hassi Touareg oilfields. Finally, the huge intraplate Central African Rift System, which extends from the Gulf of Guinea to eastern Kenya (Fig. 8), was formed or reactivated at this time (Guiraud & Maurin 1991, 1992). The development of this rift system, synchronous with the development of the South Atlantic margins rifts, resulted in disruption of the African–Arabian and South American plates into four plates, sub-plates or blocks. Rift geometries as well as synsedimentary tectonic analyses show that the Arabian–Nubian block (Guiraud & Maurin 1991) was moving northward during this Neocomian–earliest Aptian stage.

A high level of magmatic activity occurred at this time (1) along the Levant fault zone and in the Sirt area, probably in relation to the opening of the East Mediterranean Basin; (2) along the Moroccan Middle and High Atlas; (3) along the Benue Trough (Wilson & Guiraud this volume).

Aptian–Albian

A new rifting or subsidence episode, occurred in the Early Aptian, as evidenced by the presence of an unconformity within many basins (Guiraud & Maurin 1991, 1992). Along the northern African–Arabian margin, rifting and related volcanism (flow basalts) is observed from the Euphrates Trough to Tunisia, through the Palmyrides, Northern Egypt and to the Sirt area (Guiraud & Bellion 1995). In the Moghrebian Atlas, troughs deepened and some pull-apart basins were activated, e.g. in the Oranese flysch basin (Ciszak 1993). Southwards, in the intraplate domain, the huge Tenere troughs and other Central African rifts developed.

During this stage, the role of major NW–SE trending normal faults, often relayed by roughly E–W dextral strike-slips, was significant. This resulted, in particular, in the northeastward displacement of the Arabian–Nubian block (Guiraud & Maurin 1991 1992) (Fig. 6b). Finally, it should be noted that the initiation of this rifting stage corresponds precisely to the beginning of the 'Cretaceous Normal Magnetic Quiet Zone', and that the end of the CNMQZ corresponds to the initiation of basin inversion in Santonian times (see below) (Guiraud & Bosworth 1997).

Fig. 3. Schematic map of Late Carboniferous–Permian rifting in northern Africa, Arabia and adjacent regions. Reconstruction stage is Late Murgabian (*c.* 264 Ma), inspired from Baud *et al.* (1993*a*), Stampfli & Pillevuit (1993) and Stampfli (1996). 1, Paleotethys ocean; 2, Neotethys ocean; 3, thinned continental crust due to active rifting (and possibly locally oceanized crust along the East Mediterranean Basin); 4, active margin; 5, plate scale fault zone; 6, rift; 7, major normal fault; 8, major fault; 9, Penjal traps; 10, alkaline ring complex. Ap, Apulia; Ib, Iberia; M, Madagascar; S, Seychelles.

Fig. 4. Schematic map of Triassic rifting along the northwestern African margin and adjacent areas. Reconstruction stage is Late Norian (*c.* 212 Ma). Modified from Marcoux *et al.* (1993*a*), Favre (1995) and Stampfli (1996). 1, Major fault; 2, rift; 3, northern Algerian Sahara effusive province (trachybasalts, andesites); 4, thinned continental crust, possibly locally oceanized (East Mediterranean Basin); 5, future plate limit. F, Fundy Basin; HM, Hassi Messaoud; HR, Hassi R'Mel; Tar, Tarfaya Basin.

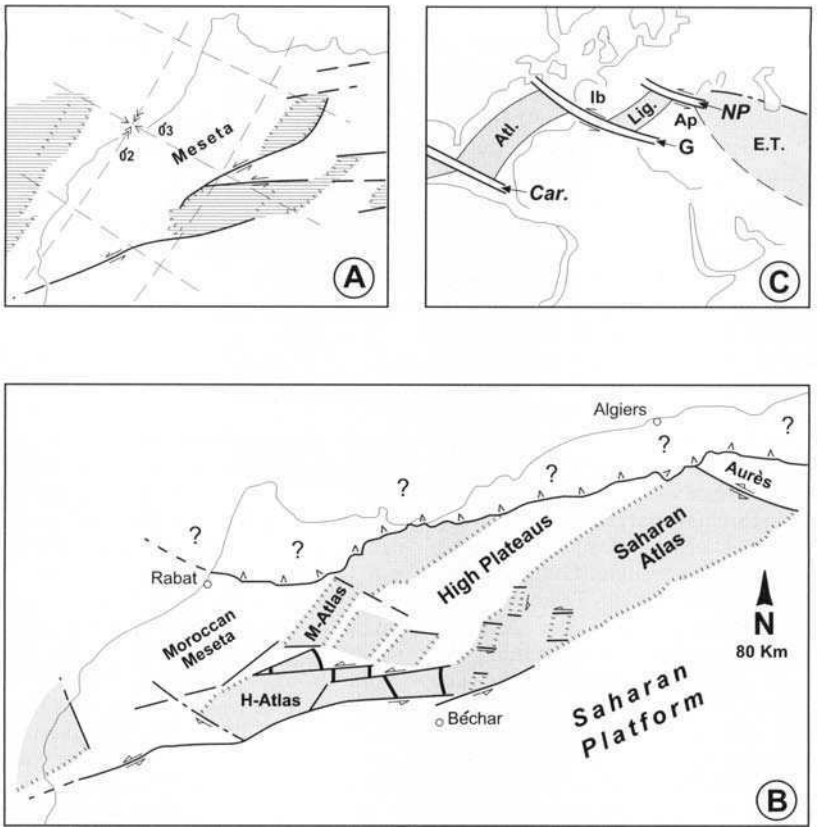

Fig. 5. The Liassic stage of basin subsidence along the Moroccan and Algerian Atlas. Models of pull-apart basin development proposed by Mattauer *et al.* (1977) (**a**) and Aït Ouali & Delfaud (1995) (**b**), in relation to a general sinistral strike-slip movement along the Moghrebian–Iberian margins (**c**). (**c**) gives a Late Jurassic sketch, after Lemoine (1985). Ap, Apulian–Adriatic continental block; Atl., Central Atlantic; Car., Caribbean Tethys; ET, Eastern Neotethys; G, Gibraltar-Sicily transform zone; Ib, Iberia; Lig., Ligurian Tethys; NP, North Penninic transform zone.

Late Santonian basin inversion

The rifting episode described above was followed during the Mid Cretaceous by a tectonically quiet period. Tectonic activity was limited to localized slight folding or subsidence, which may have occurred along the northern African margin. Thereafter, during the Early Senonian and more markedly in the Late Santonian, a compressional episode occurred, resulting in folding and inversion of many basins along the African–Arabian Tethyan margin as well as those within the Central African Rift System (Guiraud *et al.* 1987, 1992). Some major intraplate fault zones were also rejuvenated (Fig. 8). A detailed review of this major tectonic event has been given in a recent paper by Guiraud & Bosworth (1997), from which the following summary is presented.

Along the northern African–Arabian margin an initial episode of (slight) folding and basin inversion of the Syrian Arc *sensu lato* fold belt occurred during Santonian times, extending from the Palmyrides to northern Egypt and the Cyrenaica–NE Libya region (Bartov *et al.* 1980; Röhlich 1991; Sehim 1993). Westwards, the Moghrebian alpine fold belts were also initiated, including the following domains: the north–south structural axis of central Tunisia and the Tunisian Atlas (Letouzey & Trémolières 1980; Ben Ferjani *et al.* 1990); the Saharan Atlas and, very locally, the Aures along the Algerian foreland (Guiraud 1990); the Pre-Atlasic Chain of Algeria (Guiraud 1975, 1990); the Moroccan

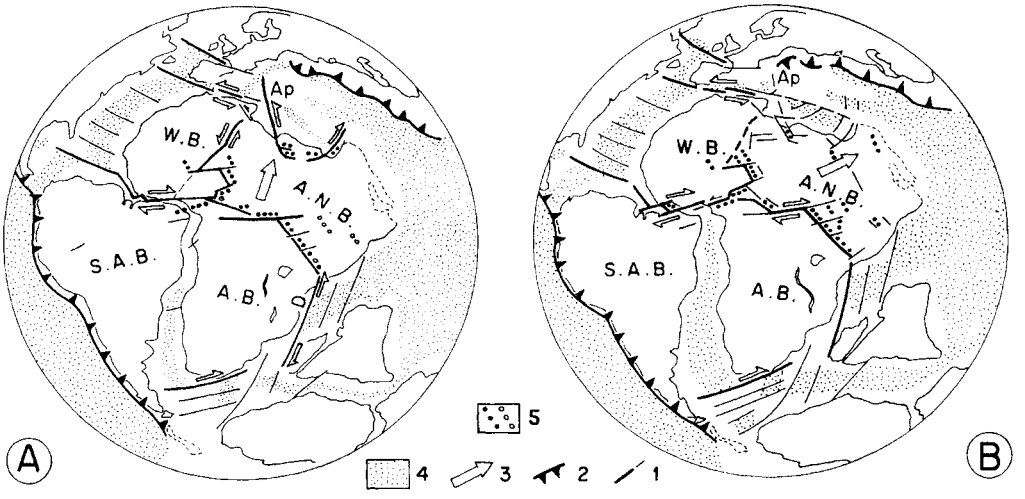

Fig. 6. Late Jurassic–Early Cretaceous break-up of western Gondwana. (**a**) Barremian (reconstruction *c.* 122 Ma). (**b**) Albian (reconstruction *c.* 107 Ma). Slightly modified from Guiraud and Bellion (1995). 1, Fault or strike-slip fault; 2, subduction zone; 3, relative motion of the Arabian-Nubian block; 4, oceanic crust; 5, main northern and central African Late Jurassic (○) and Early Cretaceous (●) rifts. A.B., Austral block; A.N.B., Arabian-Nubian block; S.A.B., South American block; W.B., Western block; Ap, Apulia; D, Davie Ridge.

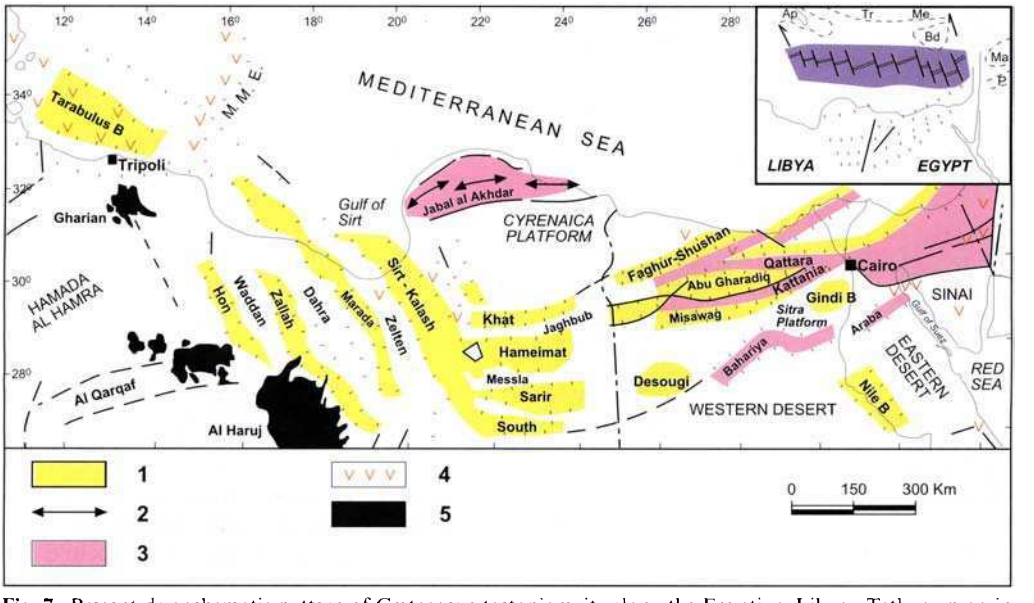

Fig. 7. Present-day schematic pattern of Cretaceous tectonic units along the Egyptian–Libyan Tethyan margin, modified from Guiraud & Bosworth (1997). 1, Cretaceous rift or subsiding basin; 2, anticline axis; 3, Senonian inverted belt; 4, Cretaceous magmatic occurrence; 5, Miocene to Recent volcanism. M.M.E., Misratah–Malta escarpment. Schematic diagram shows the horsetail pattern of the Neocomian–Barremian rifts, in relation to the opening of the East Mediterranean Basin. Time reconstruction is Early Aptian, after Masse *et al.* (1993). Ap, Apulia; Bd, Bey Daglari; Ma, Mardin Island; Me, Menderes; P, Palmyrides; Tr, Tripolitza.

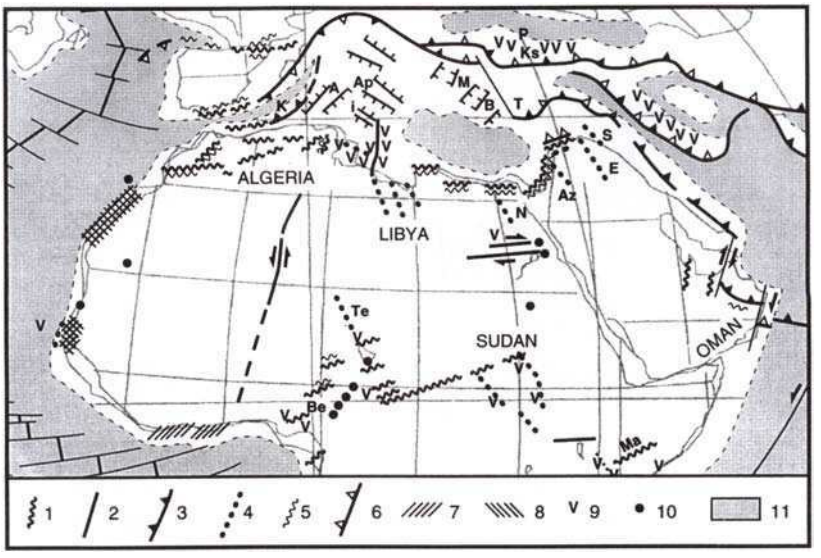

Fig. 8. Senonian tectonic map of northern Africa-Arabia and adjacent regions. Reconstruction is Cretaceous–Paleocene transition times (*c.* 65 Ma). After Guiraud & Bosworth (1997).1, Late Santonian fold belt; 2, major Late Santonian fault; 3, Late Santonian thrust (Early Campanian for Zagros); 4, Campanian–Maastrichtian rift or trough; 5, latest Maastrichtian fold belt; 6, latest Maastrichtian thrust; 7, Santonian–Campanian unconformity; 8, Maastrichtian–Paleocene unconformity; 9, Senonian volcanism; 10, Senonian alkaline anorogenic complex; 11, oceanic crust or thinned continental crust. A, Apenninic platform; Ap, Apulia; Az, Azraq; B, Bey Daglari; Be, Benue; E, Euphrates–Anah; I, Iblean domain; K, Kabylie; Ks, Kirsehir; M, Menderes; Ma, Mandera; N, Nile; P, Pontides; S, Sinjar; T, Taurides; Te, Tenere.

High Atlas and Middle Atlas (Laville *et al.* 1977; Brede *et al.* 1992); the Internal and External zones of the Riffian–Tellian belt, where strong deformations and metamorphism occurred (e.g. Maluski *et al.* 1979; Obert 1984; Ciszak 1993).

Along these Moghrebian belts, the presence in the sedimentary series of Mid–Late Triassic salt layers, acting as décollement levels, facilitated folding and basin inversion.

Within the intraplate domain, the E–W trending Guinean–Nubian lineaments (Guiraud *et al.* 1985) were rejuvenated in Egypt–Sudan, and acted as dextral strike-slip faults with associated drag folds (Issawi 1971). Small displacements also occurred along the sinistral, N–S trending El Biod fault-zone. Southwards the Central African Senonian Fold Belt formed, extending, with interruptions, from the Benue (Nigeria) to the Mandera Belt (Somalia–Ethiopia region) (Guiraud *et al.* 1987; Boccaletti *et al.* 1988; Benkhelil 1989; Genik 1993).

Most of these belts, trending approximately E–W to NE–SW, resulted from a NW–SE compression or dextral transpression during the Late Santonian. They are synchronous with similar fold belts described in the Eurasian plate (Ziegler 1989). The synchroneity with and similarity to European features arise from the fact that the Santonian compressional event corresponds to the first stage of the collision of the African–Arabian and Eurasian plates, and of the closure of the Neotethys ocean. These in turn result from plate motion changes caused by rapid alteration of Central Atlantic, South Atlantic and North Atlantic ocean opening directions (Guiraud *et al.* 1992; Janssen *et al.* 1995; Ziegler *et al.* 1995). This change occurred around Anomaly 34 (*c.* 84 Ma) and corresponds to a global event that is synchronous with the end of the CNMQZ (Guiraud & Bosworth 1997).

Late Senonian rifting

Along the northern African–Arabian margin, rifting recommenced in the Early Campanian and continued to the Late Maastrichtian or the Paleocene (reviewed by Guiraud & Bosworth (1997)). The main Late Senonian rifts trend roughly NW–SE and are located between the

Euphrates basin and the Tunisian platform (Fig. 8). Proceeding from east to west, the rift basins are: the Sinjar, Euphrates–Anah and Azraq grabens, around the Palmyrides (Lovelock 1984; May 1991; Alsdorf *et al.* 1995); the Nile Basin of Middle Egypt (Abdel Halim 1995); the Abu Gharadig basin, rejuvenated as a pull-apart along dextral strike-slip faults (Sehim 1993); the Sirt–Kalash, Marada, Tagrifet–Zellah and Hon troughs of northern Libya (Massa & Delort 1984; Van der Meer & Cloetingh 1993); the Tarabulus basin, along the northwestern offshore region of Libya (Hammuda *et al.* 1992).

Along the Moghrebian Riffian–Tellian margin flysch basins, including thick synsedimentary breccia formations, developed within a set of roughly E–W trending troughs separated by narrow highs (Wildi 1983; Camoin *et al.* 1993 *a, b*; Ciszak 1993).

Within the intraplate domain, large NW–SE trending rift basins were rejuvenated during Late Senonian–Paleocene times, e.g. the Tenere–Termit trough of northern Niger (Genik 1993), the Abu Gabra–Muglad, White Nile and Blue Nile rifts of Sudan, and the Anza rift of Kenya (Bosworth 1992).

Some Late Senonian magmatic activity is recorded, mainly in the Tunisian–Sicilian–Libyan region (Hammuda *et al.* 1992; Camoin *et al.* 1993*a* , *b*) and along the E–W trending Nubian fault swarm of southern Egypt–northern Sudan (Wilson & Guiraud this volume).

In terms of plate tectonics, the overall NW–SE orientation of the major Late Senonian rifts suggests a general NE–SW extension of the African plate. A slight decrease of the roughly NW–SE shortening that occurred during the previous Santonian event causes the alteration in stress-field to that which prevailed in Late Senonian times.

Latest Maastrichtian compressional event

The Cretaceous–Cenozoic transition often exhibits unconformities, denoting a tectonic event. Along the northeastern African–Levant margin, a compressional event occurred in latest Maastrichtian times, continuing into the early Paleocene. Major thrusting took place in the Palmyrides (Salel & Séguret 1994), as well as obduction of ophiolitic massifs along the southeastern Turkey to northwestern Iran Alpine margin (Camoin *et al.* 1993*a, b*) (Fig. 8). The Syrian Arc folds developed, from Lebanon to Cyrenaica (reviewed by Guiraud & Bosworth (1997)). Some deformation occurred along the Moghrebian Alpine fold belts, with local thrusting in the Moroccan High Atlas.

The intraplate domain also showed evidence of fault rejuvenation, e.g. along the dextral Nubian fault swarm (Issawi 1971; Guiraud *et al.* 1985), the Upper Benue (Benkhelil 1989) and some roughly E–W trending accommodation zones in the Sudan–Kenya troughs (Bosworth 1992).

Conclusions

From the late Carboniferous to the latest Cretaceous, three main stages of rifting, with substages, occurred along the northern African–Arabian Tethyan margin. Synchronous rift basins also developed within the African intraplate domain along some zones of weakness, the largest of which was the huge Central African Fault Zone.

Magmatic activity commonly accompanied or immediately followed rifting. Both rifting and magmatism developed along major, pre-existing crustal discontinuities (Maurin & Guiraud 1993).

During Late Santonian times, the onset of the collision of the African–Arabian and Eurasian plates provoked the initiation of folding and inversion of most of the sedimentary basins along the northern margin of Africa–Arabia, as well as the approximately E–W trending Central African fold belt (Guiraud & Bosworth 1997). The collision resulted in the creation of new stress-fields in the plate. From this stage to Recent times, each change in the plates motions has provoked compressional or wrench-dominated events, with alternating folding or rifting episodes (Fig. 2) (Ziegler 1989; Guiraud *et al.* 1992; Guiraud & Bellion 1995; Janssen *et al.* 1995).

In conclusion it can be said that during the late Carboniferous–mid Cretaceous times the northern African–Arabian plate margin showed multiple phase rifting resulting in the oceanization of Neotethys, whereas from Late Senonian times, rifting resulted from the multiple phase closure of Neotethys.

I would like to thank the Convenors of the Symposium on the Hydrocarbon Geology of North Africa, who invited me to London in November 1995 and gave me the opportunity of fruitful discussions with many participants. Review and suggested improvements by M. Anketell were greatly appreciated. BP is also specially thanked for helping in drafting some of the illustrations of this paper; and G. Daniel is thanked for typing the manuscript. This paper is a contribution to IGCP Project 369 'Comparative Evolution of PeriTethyan Rift Basins'.

References

ABDEL HALIM, M. 1995. Oil and gas exploration in Egypt. Past, present, and future. *American Association of Petroleum Geologists International Conference and Exhibition, Nice, 10–13 September 1995*, Abst. 1A.

AGOCO (Arabian Gulf Oil Company, Exploration Staff) 1980. Geology of a stratigraphic giant - the Messlah oil field. *In*: SALEM, M. J. & BUSREWIL, M. T. (eds) *Geology of Libya, Vol. 2*. Academic Press, London, 521–536.

AIT OUALI, R. & DELFAUD, J. 1995. Les modalités d'ouverture du bassin des Ksour au Lias dans le cadre du «rifting» jurassique au Maghreb. *Comptes Rendus de l'Académie des Sciences*, **320**, 773–778.

ALSDORF, D., BARAZANGI, M., LITAK, R., SEBER, D., SAWAF, T. & AL-SAAD, D. 1995. The intraplate Euphrates fault system-Palmyrides mountain belt junction and relationship to Arabian plate boundary tectonics. Annali di Geofisica, **38**, 385–397.

BARTOV, Y., LEVY, Z., STEINITZ, G. & ZAK, I. 1980. Mesozoic and Tertiary stratigraphy, paleogeography and structural history of the Gebel Areif en Naqa area, eastern Sinai. *Israel Journal of Earth-Sciences*, **29**, 114–139.

BAUD, A., MARCOUX, J., GUIRAUD, R., RICOU, L. E. & GAETANI, M. 1993*a*. Late Murgabian (266 to 264 Ma). *In*: DERCOURT, J., RICOU, L. E. & VRIELYNCK, B. (eds) *Atlas Tethys Palaeoenvironmental Maps. Maps*. BEICIP-FRANLAB, Rueil-Malmaison.

—— 1993*b*. Late Murgabian (266 to 264 Ma). *In*: DERCOURT, J., RICOU, L. E. & VRIELYNCK, B. (eds) *Atlas Tethys Palaeoenvironmental Maps. Explanatory notes*. Gauthier-Villars, Paris, 9–20.

BAYOUMI, A. I. & LOTFY, H. I. 1989. Modes of structural evolution of Abu Gharadig Basin, Western Desert of Egypt, as deduced from seismic date. *Journal of African Earth Sciences*, **9**, 273–287.

BEN FERJANI, A., BUROLLET, P. F. & MEJRI, F. 1990. *Petroleum Geology of Tunisia*. ETAP, Tunis.

BENKHELIL, J. 1989. The origin and evolution of the Cretaceous Benue Trough (Nigeria). *In*: ROSENDAHL, B. R., ROGERS, J. J. W. & RACH, N. M. (eds) *African Rifting*, Special Volume, *Journal of African Earth Sciences*, **8**, 251–282.

BERGGREN, W. A., KENT, D. V., AUBRY, M.-P. & HARDENBOL, J. (eds) 1995. *Geochronology, Time scales and Global, Stratigraphic Correlation*. SEPM (Society for Sedimentary Geology) Special Publication, **54**.

BOCCALETTI, M., DAINELLI, P., ANGELUCCI, A., *et al.* 1988. Folding of the Mesozoic cover in SW Somalia: a compressional episode related to the early stages of Indian Ocean evolution. *Journal of Petroleum Geology*, **11**, 157–168.

BOSWORTH, W. 1992. Mesozoic and early Tertiary rift tectonics in East Africa. *In*: EBINGER, C. J., GUPTA, H. K. & NYAMBOK, I. O. (eds) *Seismology and related Sciences in Africa*, Special Volume, *Tectonophysics*, **209**, 115–137.

BOUDJEMA, A. 1987. *Évolution structurale du bassin pétrolier «triasique» du Sahara nord oriental (Algérie)*. Thèse Sciences, Université Paris-Sud.

BREDE, R., HAUPTMANN, M. & HERBIG, H.-G. 1992. Plate tectonics and intracratonic mountain ranges in Morocco—the Mesozoic Cenozoic development of the Central High Atlas and Middle Atlas. *Geologische Rundschau*, **81**, 127–141.

BREMAN, E. & RINEHART, C. 1995. Source rock maturity and structure growth using Zycor backstripping, Khalda Concession, Western Desert, Egypt. *Geological Society of London, Petroleum Group, First Symposium on the Hydrocarbon Geology of North Africa*, 28–30 November 1995, London, Abstract P. 13.

BUROLLET, P. F., MUGNIOT, J. M. & SWEENEY, P. 1978. The geology of the Pelagian block: the margins and basins of southern Tunisia and Tripolitania. *In*: NAIRN, A. E. M. & KANES, W. H. (eds) *The Ocean Basins and Margins, Vol. 4B, The Western Mediterranean*. Plenum Press, New York, 331–359.

CAMOIN, G., BELLION, Y., BENKHELIL, J., *et al.* 1993*a*. Late Maastrichtian (69.5 to 65 Ma). *In*: DERCOURT, J., RICOU, L. E. & VRIELYNCK, B. (eds) *Atlas Tethys Palaeoenvironmental Maps. Maps*. BEICIP-FRANLAB, Rueil-Malmaison.

——, ——, DERCOURT, J., *et al.* 1993*b*. Late Maastrichtian (69.5 to 65 Ma). *In*: DERCOURT, J., RICOU, L. E. & VRIELYNCK, B. (eds) *Atlas Tethys Palaeoenvironmental Maps. Explanatory Notes*. Gauthier-Villars, Paris, 179–196.

CATTANEO, G. & GELARD, J. P. 1989. Le fonctionnement de la marge africaine de la Téthys maghrébine au Jurassique supérieur-Crétacé basal: son enregistrement dans les systèmes sédimentaires de l'Avant-pays rifain oriental. *Comptes Rendus de l'Académie des Sciences*, **309**, 109–114.

CISZAK, R. 1993. Évolution géodynamique de la chaîne tellienne en Oranie (Algérie occidenale) pendant le Paléozoïque et le Mésozoïque. *Strata*, **2**(20), 1–513.

DEMNATI, A. 1996. The Peri-Tethys Programme and some possible links to the ongoing exploration projects in Morocco. *In*: *Peri-Tethys Programme Annual Meeting, Amsterdam, 10–11 June 1996*, Abstracts volume, p. 16.

DERCOURT, J., RICOU, L. E. & VRIELYNCK, B., (eds) 1993. *Atlas Tethys Palaeoenvironmental Maps. Gauthier-Villars*.

——, ZONENSHAIN, L. P., RICOU, L. E., *et al.* 1986. Geological evolution of the Tethys belt from the Atlantic to the Pamir since the Lias. *Tectonophysics*, **123**, 241–315.

FAVRE, P. 1995. Analyse quantitative du rifting et de la relaxation thermique de la partie occidentale de la marge transformante nord-africaine: le Rif externe (Maroc). Comparaison avec la structure actuelle de la chaîne. *Geodynamica Acta*, **8**, 59–81.

FOURCADE, E., AZEMA, J., CECCA, F., *et al.* 1993*a*. Late Tithonian (138 To 135 Ma). *In*: DERCOURT, J., RICOU, L. E. & VRIELYNCK, B. (eds) *Atlas Tethys Palaeoenvironmental Maps. Maps*. BEICIP-FRANLAB, Rueil-Malmaison.

——, ——, ——, *et al.* 1993*b*. Late Tithonian (138 to 135 Ma). *In*: DERCOURT, J., RICOU, L. E. & VRIE-

LYNCK, B. (eds) *Atlas Tethys Palaeoenvironmental Maps. Explanatory notes*. Gauthier-Villars, Paris, 113–134.

GENIK, G. J. 1993. Petroleum geology of Cretaceous–Tertiary rift basins in Niger, Chad, and Central African Republic. *Bulletin, American Association of Petroleum Geologists*, **77**, 1405–1434.

GRAS, R. & THUSU, B. 1997. Trap architecture of the Early Cretaceous Sarir sandstone in the eastern Sirt Basin, Libya. *This volume*.

GUIRAUD, R. 1975. L'évolution post-triasique de l'avant-pays de la chaîne alpine en Algérie, d'après l'étude du bassin du Hodna et des régions voisines. *Revue Géographie physique et Géologie dynamique*, **17**, 427–446.

— — 1990. *Évolution post-triasique de l'avant-pays de la chaîne alpine en Algérie, d'après l'étude du bassin du Hodna et des régions voisines*. Geological Survey of Algeria, Memoir 3.

— — & BELLION, Y. 1995. Late Carboniferous to Recent geodynamic evolution of the West Gondwanian cratonic Tethyan margins. *In*: NAIRN, A., DERCOURT, J. & VRIELYNCK, B. (eds) *The Ocean Basins and Margins, Vol. 8, The Tethys Ocean*, Plenum, New York, 101–124.

—— & BOSWORTH, W. 1997. Senonian basin inversion and rejuvenation of rifting in Africa and Arabia: synthesis and implications to plate-scale tectonics. *Tectonophysics*, in press.

— — & MAURIN, J. C. 1991. Le rifting en Afrique au Crétacé inférieur: synthèse structurale, mise en évidence de deux phases dans la genèse des bassins, relations avec les ouvertures océaniques péri-africaines. *Bulletin de la Société Géologique de France*, **5**, 811–823.

— — & — — 1992. Early Cretaceous Rifts of Western and Central Africa: an overview. *In*: ZIEGLER, P. A. (ed.) *Geodynamics of Rifting, Vol. II. Case History studies on Rifts: North and South America, Africa–Arabia. Tectonophysics*, **213**, 153–168.

— —, BELLION, Y., BENKHELIL, J. & MOREAU, C. 1987. Post-Hercynian tectonics in Northern and Western Africa. *In*: BOWDEN, P. & KINNAIRD, J. (eds) *African Geology Reviews. Geological Journal*, **22**, 433–466.

— —, BINKS, R. M., FAIRHEAD, J. D. & WILSON, M. 1992. Chronology and geodynamic setting of Cretaceous–Cenozoic rifting in West and Central Africa. *In*: Ziegler, P.A. (Editor), *Geodynamics of Rifting, Vol. II, Case History Studies on Rifts: North and South America, Africa–Arabia. Tectonophysics*, **213**, 227–234.

——, ISSAWI, B. & BELLION, Y. 1985. Les linéaments guinéo-nubiens: un trait structural majeur à l'échelle de la plaque africaine. *Comptes Rendus de l'Académie des Sciences*, **300**, 17–20.

HAMMUDA, O. S., VAN HINTE, J. E. & NEDERBRAGT, S. 1992. Geohistory analysis mapping in central and southern Tarabulus Basin, northwestern offshore Libya. *In*: SALEM, M. J., HAMMUDA, O. S. & ELIAGOUBI, B. A. (eds) *The Geology of Libya, Vol. 5*, Elsevier, 1657–1680.

HIRSCH, F., FLEXER, A., ROSENFELD, A. & YELLIN-DROR, A. 1995. Palinspastic and crustal setting of the Eastern Mediterranean. *Journal of Petroleum Geology*, **18**, 149–170.

ISSAWI, B. 1971. Geology of Darb el Arbain, Western Desert. *Annals of the Geological Survey of Egypt*, **1**, 53–92.

JANSSEN, M. E., STEPHENSON, R. A. & CLOETINGH, S. 1995. Temporal and spatial correlations between changes in plate motions and the evolution of rifted basins in Africa. *Bulletin, Geological Society of America*, **107**, 1317–1332.

KAZI-TANI, N. 1986. *Évolution géodynamique de la bordure nord-africaine: le domaine intraplaque nord-algérien. Approche mégaséquentielle*. Thèse Doct. Sci., Université de Pau et Pays de l'Adour.

KEELEY, M. L. 1994. Phanerozoic evolution of the basins of Northern Egypt and adjacent areas. *Geologische Rundschau*, **83**, 728–742.

— — & WALLIS, R. J. 1991. The Jurassic system in northern Egypt: II. Depositional and tectonic regimes. *Journal of Petroleum Geology*, **14**, 49–64.

KLITGORD, K. D. & SCHOUTEN, H. 1986. Plate kinematics of the central Atlantic. *In*: VOGT, P. R. & TUCHOLKE, B. E. (eds) *The Western North Atlantic Region*. The Geology of North America, Geological Society of America, **M**, 351–378.

KLITZSCH, E. & WYCISK, P. 1987. Geology of the sedimentary basins of northern Sudan and bordering areas. *Berliner Geowissenschaftliche Abhandlungen*, **A75**, 97–136.

LAMBIASE, J. J. 1989. The framework of African rifting during the Phanerozoic. *Journal of African Earth Sciences*, **8**, 183–190.

LAVILLE, E. & PIQUÉ, A. 1991. La distension crustale atlantique et atlasique au Maroc au début du Mésozoïque: le rejeu des structures hercyniennes. *Bulletin de la Société Géologique de France*, **162**, 1161–1171.

—— & — — 1992. Jurassic penetrative deformation and Cenozoic uplift in the Central High Atlas (Morocco): a tectonic model. Structural and Orogenic inversions. *Geologische Rundschau*, **81(1)**, 157–170.

— —, LESAGE, J. L. & SÉGURET, M. 1977. Géométrie, cinématique (dynamique) de la tectonique atlasique sur le versant sud du Haut Atlas marocain. Aperçu sur les tectoniques heryniennes et tardi-hercyniennes. *Bulletin de la Société Géologique de France*, **3**, 527–539.

LEMOINE, M. 1985. Structuration jurassique des Alpes occidentales et palinspastique de la Téthys-Ligure. *Bulletin de la Société Géologique de France*, **1**, 127–138.

LETOUZEY, J. & TRÉMOLIÈRES, P. 1980. Paleo-stress fields around the Mediterranean since the Mesozoic derived from microtectonics: comparisons with plate tectonic data. *In*: AUBOUIN, J., DEBELMAS, J. & LATREILLE, M. (Coordinators) *Geology of the Alpine Chains Born of the Tethys*. Mémoires du Bureau de Recherches Géologiques et Minières, **115**, 261–273.

LOVELOCK, P. 1984. A review of the tectonics of the northern Middle East region. *Geological Magazine*, **125**, 577–587.

MALUSKI, M., LEPVRIER, C. & BIARDEAU, V. 1979. Epimétamorphisme syntectonique d'âge 85 M.A. dans les zones nord-telliennes (Algérie). *Comptes Rendus de l'Académie des Sciences*, **288**, 1583–1586.

MARCOUX, J., BAUD, A., RICOU, L. E., *et al.* 1993*a*. Late Norian (215 to 212 Ma). *In*: DERCOURT, J., RICOU, L. E. & VRIELYNCK, B. (eds) *Atlas Tethys Palaeoenvironmental Maps. Maps*. BEICIP-FRANLAB, Rueil-Malmaison.

——, ——, ——, *et al.* 1993*b*. Late Anisian (237 to 234 Ma). *In*: DERCOURT, J., RICOU, L. E. & VRIELYNCK, B. (eds) *Atlas Tethys Palaeoenvironmental Maps. Maps*. BEICIP-FRANLAB, Rueil-Malmaison.

——, ——, ——, *et al.* 1993*c*. Late Norian (215 to 212 Ma). *In*: DERCOURT, J., RICOU, L. E. & VRIELYNCK, B. (eds) *Atlas Tethys Palaeoenvironmental Maps. Explanatory notes*. Gauthier-Villars, Paris, 35–53.

——, ——, ——, *et al.* 1993*d*. Late Anisian (237 to 234 Ma. *In*: DERCOURT, J., RICOU, L. E. & VRIELYNCK, B. (eds) *Atlas Tethys Palaeoenvironmental Maps. Explanatory notes*. Gauthier-Villars, Paris, 21–33.

MASSA, D. & DELORT, T. 1984. Evolution du bassin de Syrte (Libye) du Cambrien au Crétacé basal. *Bulletin de la Société Géologique de France*, **26**, 1087–1096.

MASSE, J. P., BELLION, Y., BENKHELIL, J., *et al.* 1993. Lower Aptian (114 to 112 Ma). *In*: DERCOURT, J., RICOU, L. E. & VRIELYNCK, B. (eds) *Atlas Tethys Palaeoenvironmental Maps. Maps*. BEICIP-FRANLAB, Rueil-Malmaison.

MATTAUER, M., TAPPONNIER, P. & PROUST, F. 1977. Sur les mécanismes de formation des chaînes intracontinentales. L'exemple des chaînes atlasiques du Maroc. *Bulletin de la Société Géologique de France*, **3**, 521–526.

MAURIN, J.-C. & GUIRAUD, R. 1993. Basement control in the development of the Early Cretaeous West and Central African Rift System. *Tectonophysics*, **228**, 81–95.

MAY, P. R. 1991. The eastern Mediterranean Mesozoic Basin: Evolution and Oil Habitat. *Bulletin, American Association of Petroleum Geologists*, **75**, 1215–1232.

NIKISHIN, A., BARABOSHKIN, E., BOLOTOV, S., *et al.* 1996. Late Paleozoic-Mesozoic-Cenozoic history of the southern part of the Eastern Europe. *Peri-Tethys Programme Annual Meeting, Amsterdam 10–11 June 1996*, Abstracts Volume, 44–45.

OBERT, D. 1984. Géologie des Babors (Algérie): importance de la paléotectonique alpine dans l'orogenèse tellienne. *Revue de Géologie dynamique et Géographie physique*, **25**, 99–117.

POWELL, J. H. & KHALIL MOHAMED, B. 1993. Structure and sedimentation of Permo-Triassic and Triassic rocks exposed in small-scale horsts and grabens of pre-Cretaceous age: Dead Sea margin, Jordan. *Journal of African Earth Sciences*, **2**, 131–143.

ROBERTSON, A. H. F., DIXON, J. E., BROWN, S., *et al.* 1996. Alternative tectonic models for the Late Palaeozoic-Early Tertiary development of Tethys in the Eastern Mediterranean region. *In*: MORRIS, A. & TARLING, D. H. (eds) *Palaeomagnetism and Tectonics of the Mediterranean Region*, Geological Society, London, Special Publications, **105**, 239–263.

RÖHLICH, P. 1991. Tectonic development of Jabal al Akhdar. *In*: SALEM, M. J. & BUSREWIL, M. T. (eds) *The Geology of Libya, Vol. 3*, London, Academic Press, 923–931.

ROSSI, M. E., TONNA, M. & LARBASH, M. 1992. Latest Jurassic-Early Cretaceous Deposits in the Subsurface of the Eastern Sirt Basin (Libya): Facies and Relationships with Tectonics and Sea-Level Changes. *In*: SALEM, M. J., SBETA, A. M. & BAKBAK, M. R. (eds) *The Geology of Libya, Vol. 6*. Elsevier, Amsterdam, 2211–2226.

SALEL, J. F. & SÉGURET, M. 1994. Late Cretaceous to Palaeogene thin-skinned tectonics of the Palmyrides belt (Syria). *Tectonophysics*, **234**, 265–290.

SEHIM, A. 1993. Cretaceous tectonics in Egypt. *Egyptian Journal of Geology*, **37**, 335–372.

STAMPFLI, G. M. & PILLEVUIT, A. 1993. An Alternative Permo-Triassic reconstruction of the Kinematics of the Tethyan realm. *In*: DERCOURT, J., RICOU, L. E. & VRIELYNCK, B. (eds) *Atlas Tethys Palaeoenvironmental maps. Explanatory notes*. Gauthier-Villars, Paris, 55–62.

——, MARCOUX, J. & BAUD, A. 1991. Tethyan margin in space and time. *Palaeogeography, Palaeoclimatology, Palaeoecology*, **87**, 373–409.

STAMPFLI, G. M. 1996. The Intra-Alpine terrain: a Paleotethyan remnant in the Alpine Variscides. *Eclogae geologicae Helveticae*, **89**, 13–42.

TAHA, M. A. 1992. Mesozoic rift basins in Egypt. Their southern extension and impact on future exploration. *In*: *The Egyptian General Petroleum Corporation, Proceedings of the Eleventh Exploration & Production Conference, Cairo, November 1992. Exploration Volume*, **2**, 1–19.

THUSU, B. & MANSOURI, A. 1995. Reassignment of the Upper Amal Formation to Triassic and its implications for exploration in southeast Sirte, Libya. *In*: *First Symposium on Hydrocarbon Geology of North Africa, London, 28–30 November 1995. Abstracts*, p. 48.

VAI, G. B. 1996. Interim report about the preparation of the Moscovian and Artinskian maps (PTP). *In*: *Peri-Tethys Programme Annual Meeting, Amsterdam, 10–11 June 1996. Abstracts Volume*, p. 54.

VAN DER MEER, F. & CLOETINGH, S. 1993. Intraplate stresses and the subsidence history of the Sirte Basin (Libya). *Tectonophysics*, **226**, 37–58.

VIALLY, R., ASKRI, H., BENARD, F., BOUDJEMA, A., DESFORGES, G., HADDADI, N. & LETOUZEY, J. 1994. Basin Inversion along the North African Margin. The Saharan Atlas (Algeria). *In*: ROURE, F. (ed.) *Peri-Tethyan Platforms*. Technip, Paris, 79–118.

WILDI, W. 1983. La chaîne tello-rifaine (Algérie, Maroc, Tunisie): structure stratigraphique et évolution du Trias au Miocène. *Revue de Géologie Dynamique et de Géographie physique*, Numéro spécial, *Chaîne Tello-Rifaine*, **24**, 201–298.

WILSON, M. & GUIRAUD, R. 1992. Mesozoic–Cenozoic magmatism associated with the West and Central African Rift System. *In*: ZIEGLER, P. A. (ed.) *Geodynamics of Rifting, Vol. II, Case History Studies*

on Rifts: North and South America, Africa–Arabia. Tectonohysics, **213**, 203–225.

—— & —— 1996. Late Permian to Recent magmatic activity on the African–Arabian margin of Tethys. *This volume.*

ZIEGLER, P. A. 1989. Geodynamic model for Alpine intra-plate compressional deformation in Western and Central Europe. *In*: COOPER, M. A. & WILLIAMS, G. D. (eds) *Inversion Tectonics*. Geological Society, London. Special Publications, **44**, 63–85.

——, CLOETINGH, S. & VAN VEES, J.-D. 1995. Dynamics of intra-plate compressional deformation: the Alpine foreland and other examples. *Tectonophysics*, **252**, 7–59.

This page intentionally left blank

Late Permian to Recent magmatic activity on the African-Arabian margin of Tethys

M. WILSON[1] & R. GUIRAUD[2]
with assistance from C. MOREAU[3] & Y. J.-C. BELLION[4]

[1]*School of Earth Sciences, Leeds University, Leeds LS2 9JT, UK.*
e-mail: m.wilson@earth.leeds.ac.uk
[2]*Laboratoire de Géophysique et Tectonique, Case 060, Université Montpellier II Sciences et Techniques, 34095 Montpellier Cedex 5, France*
[3]*Departement des Sciences de la Terre, Université de la Rochelle, 17042 La Rochelle Cedex 1, France*
[4]*Laboratoire de Géologie, Faculté des Sciences, 33 rue Louis Pasteur, 84000 Avignon, France*

Abstract: Magmatic activity on the African–Arabian margin of Tethys has fluctuated significantly during the past 250 Ma in response to major phases of mantle plume activity and to extensional stresses within the African plate related to periods of continental break-up. A series of maps have been compiled, based upon stratigraphic constraints and K–Ar and ^{40}Ar–^{39}Ar age determinations, to illustrate the changing patterns of igneous activity since the Late Permian. These are divided into five stages: I, Late Permian (256 Ma)–Latest Triassic (208 Ma); II, Early Jurassic (208 Ma, Liassic)–Mid Jurassic (157 Ma, Dogger); III, Late Jurassic (157 Ma)–Earliest Aptian (120 Ma); IV, Mid Aptian (119 Ma)–Mid Eocene (42 Ma); V, Late Eocene (42 Ma)–Recent. Extensive tholeiitic basaltic magmatism at *c.* 200 Ma, preceding continental break-up in the Central Atlantic, is attributed to upwelling of the Cape Verde mantle plume beneath the West African craton. Contemporaneous magmatic activity in the Levant is related to the break-up of the Eastern Mediterranean margin. Early Cretaceous alkaline magmatism around the margins of the Equatorial Atlantic and within the Levant may also be plume related. During Neogene–Recent times there was a major change in the convection pattern within the upper mantle, generating extensive magmatism across the entire margin. Magmatism appears to be extremely long lived in a number of areas (e.g. Sudan, Air), with volcanic centres located along major basement fault zones, such as the Guinean–Nubian lineaments.

Introduction

A wide spectrum of magmatic activity has been associated with the geodynamic evolution of the African–Arabian margin of Tethys since the Late Permian. This includes major phases of magmatism related to mantle plume activity accompanying the break-up of Pangaea–Gondwana and more localized magmatic activity within intra-plate rifts in which crustal stretching is a response to plate boundary forces. To understand the geodynamic setting of this magmatism it is clearly important to establish regional correlations for the onset of magmatic activity and to establish its relationship with major phases of basin subsidence, basement uplift and intra-plate deformation. This has fundamental implications for our understanding of the thermal evolution of the lithosphere which, in turn, has important implications for hydrocarbon exploration.

Considerable progress has been made in recent years in understanding the processes involved in the formation of sedimentary basins and passive continental margins by lithospheric extension. Individual basins may be magmatic or non-magmatic depending upon the amount of extension and whether thermally anomalous mantle (a mantle plume) is upwelling beneath the rift (Wilson 1993*a*). Extension of the continental lithosphere with subsequent plate separation to form a new ocean basin necessarily involves the ascent of asthenospheric mantle material towards the surface. In most cases this is a passive response to plate boundary forces (*passive rifting*), although it may be enhanced by the upwelling of a deep mantle plume (*active rifting*) from a major thermal boundary layer within the deep mantle (670 km discontinuity or the core–mantle boundary). It is now widely accepted that mantle plumes have played an important role in continental break-up throughout the Phanerozoic (e.g. White & McKenzie 1989, 1995; Storey *et al.* 1992; Storey 1995). Plumes may range from a few hundred kilometres to 2000 km in diameter as they spread out at the

WILSON, M. & GUIRAUD, R. 1998. Late Permian to Recent magmatic activity on the African-Arabian margin of Tethys. *In*: MACGREGOR, D. S., MOODY, R. T. J. & CLARK-LOWES, D. D. (eds) 1998. *Petroleum Geology of North Africa*. Geological Society, London, Special Publication No. 132, 231–263.

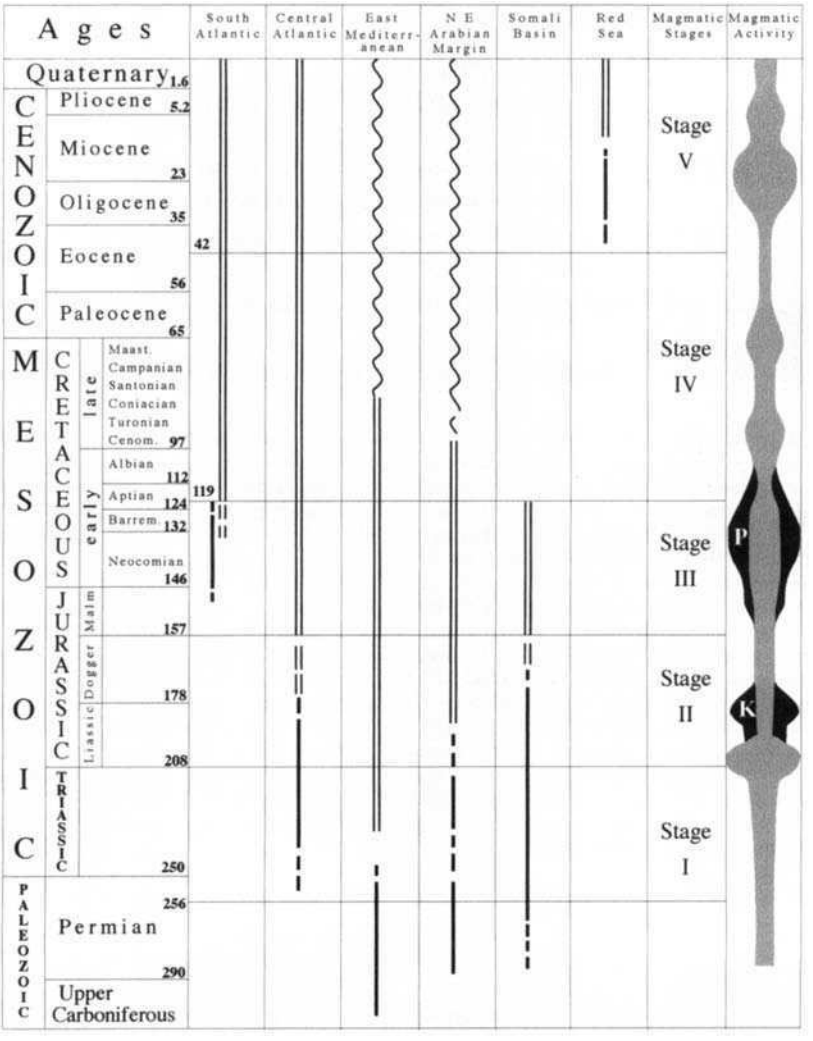

Fig. 2. Geodynamic framework of the Late Permian to Recent magmatic activity of the African–Arabian margin of Tethys. Time-scale from Harland *et al.* (1990); Permo-Triassic boundary placed at 250 Ma after Claoué-Long *et al.* (1991). Heavy vertical line, major periods of rifting; parallel vertical lines, periods of ocean opening; wavy line, periods of ocean closure and compression. K, Karoo magmatic event in Southern Africa; P, Parana–Etendeka flood basalts.

base of the lithosphere; they are not necessarily symmetrical although they are frequently shown schematically as such. Passive rifting models predict that the onset of magmatic activity should occur after the initiation of rifting. In contrast, in the case of active rifting above a mantle plume, domal basement uplift and magmatism should precede the onset of rifting. In practice, however, the recognition of the relative timing of rifting and associated magmatic activity is often complicated by the diachronous development of individual sub-basins within a particular rift and by the cover of younger volcanic and sedimentary rocks which tend to obscure the early rift sequences. Nevertheless, recognition of regional domal uplift of basement rocks associated with magmatic activity provides strong support for the involvement of a mantle plume.

A wide compositional spectrum of magmatic activity may be associated with rifting of the continental lithosphere. The geochemical characteristics of the primary, mantle-derived, mafic magmas, ranging from silica-undersaturated

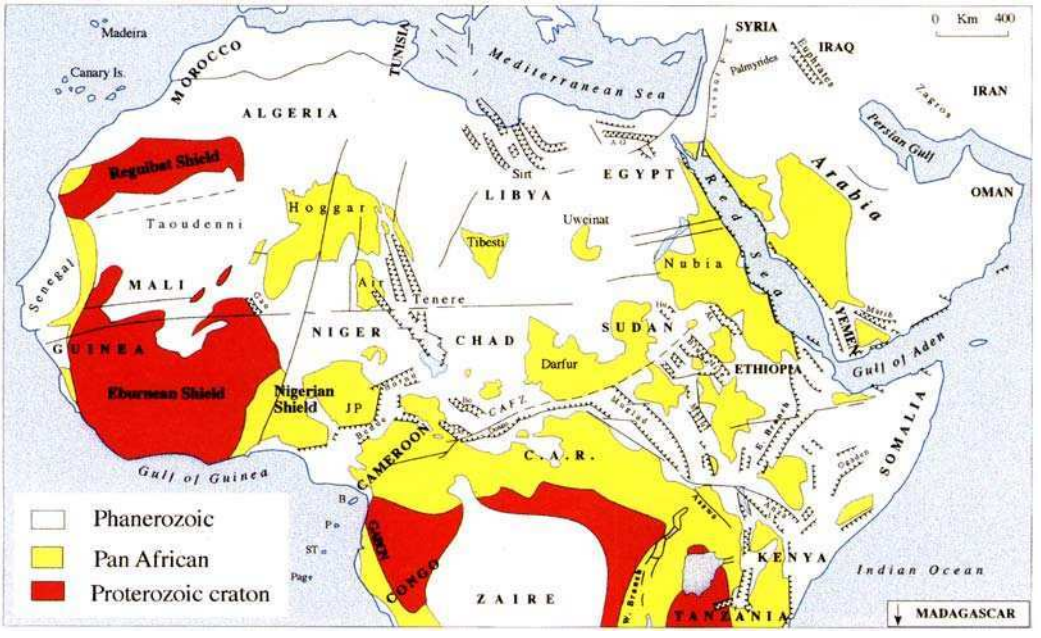

Fig. 1. The Afro-Arabian margin of Tethys. Map illustrates the distribution of Pan African basement domains, Proterozoic cratons, Mesozoic–Cenozoic rift basins and major fault systems. Abbreviations as in Table 1.

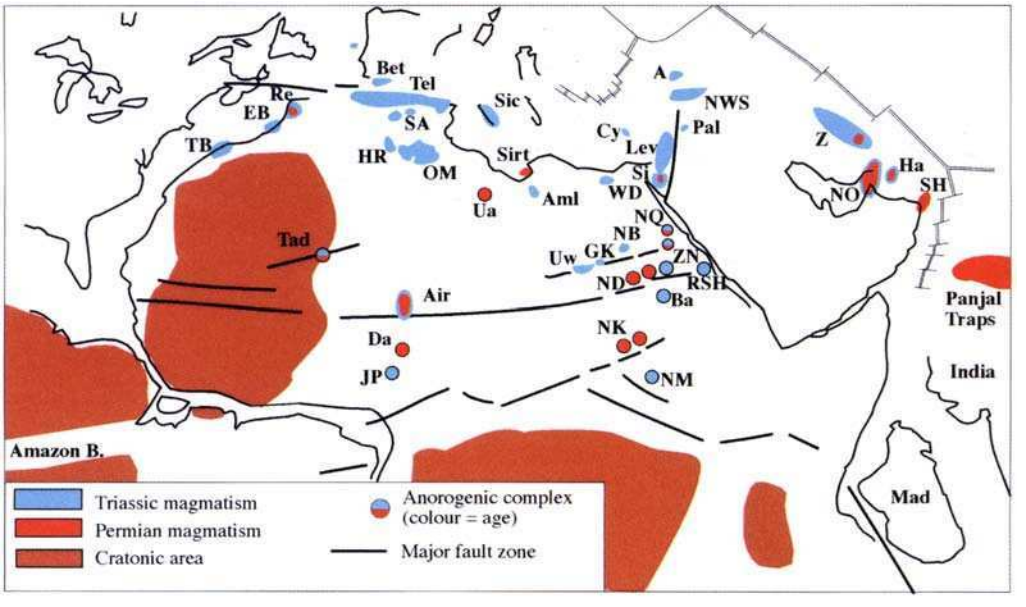

Fig. 3. Stage I: Late Permian (256 Ma)–latest Triassic (208 Ma). Plate reconstruction according to Dercourt *et al.* (1993). Abbreviations listed in Table 1.

Table 1. *List of abbreviations used in figures*

A	Antalya	HK	Hama Koussou	Pel	Pelagian Shelf
AA	Anti Atlas	Hog	Hoggar	Pot	Potiguar
AD	Ala Dag	HR	Hassi Rumel	Re	Rehamna
Ada	Adamawa	Hu	Humar basin	Rec	Recife
Am	Amapa	Iv.C	Ivory Coast	RGN	Rio Grande do Norte
Aml	Amal	JP	Jos Plateau	Ri	Rif
Anz	Anza	K	Kizildag	Ric	Richat Dome
B	Bioko	Ken	Kenya Basin	Ro	Rhonda
Ba	Bayuda Desert	Kor	Kordofan	RSH	Red Sea Hills
Bar	Barreirinhas	Kr	Krause seamount	Run	Rungwe
BB	Baër Bassit	La	Lamu embayment	SA	Saharan Atlas
Bet	Betics	Leo	Leona	Sar	Sardinia
Bi	Bihendula	Ler	Lere	SBT	Southern Benue
Biu	Biu Plateau	Lev	Levant		Trough
BNR	Blue Nile Rift	Lib	Liberia	SCB	Somali Coastal Basin
Bon	Bongor	LK	Little Kabylia	Se	Semail
BT	Benue Trough	Los	Los Island	Sey	Seychelles
Can	Canary Islands	Lu	Luwegu	SH	Saïh Hatat
CAR	Central African	MA	Middle Atlas	Si	Sinai
	Republic	Mad	Madagascar	Sic	Sicily
CL	Cameroon Line	Mar	Maranhão	Sirt	Sirt Trough
Com	Comores	Mas	Masirah	SL	Sierra Leone
CVA	Cape Verde	Mbe	Mbeya	SLR	Sierra Leone Rise
	Archipelago	Md	Mardin Plateau	SS	South Sudan
CVP	Cape Verde Peninsula	Mdr	Madeira	ST	Saõ Tomé
Cy	Cyprus	Mei	Meidob Hills	T	Troodos
D	Delgo	Mel	Melut	Tac	Tacutu
Da	Damagaram	Mta	Malta	Tad	Tadhak
Dar	Darfur	Mud	Mudugh	TB	Tarfaya Basin
DEG	Dor El Goussa	Mug	Muglad	TCB	Tanzania Coastal Basin
Dos	Doseo	NB	Nusab el Balgum	Te	Ténéré
DP	Demerara Plateau	NBT	Northern Benue	Tef	Tefidet
Dr	Druse		Trough	Tel	Tellian Trough
EB	Essaouira Basin	ND	Nubian Desert	Tib	Tibesti
ED	Eastern Desert	NK	North Kordofan	Ua	Uaddan
Elb	Elborz	NM	Nuba Mountains	Uw	Uweinat
Fu	Fuerteventura	NO	North Oman	WD	Western Desert
Gh	Ghana	NQ	Nasb el Qash	WK	Wanakum Hills
GK	Gebel Kamil	NWS	Northwestern Syria	WN	Wadi Natash
Gn	Garian High	OHP	Oranes High Plateau	Z	Zagros
Gus	Gebel Umm Shaghir	OM	Oued Mya	Ze	Zelten
HA	High Atlas	P	Principe	ZN	Zargat Naam
Ha	Hawasina	Pal	Palmyrides		
Har	Haruj	Pag	Pagalú		

alkaline magmas (nephelinites, basanites, alkali basalts) through transitional basalts to subalkaline continental tholeiites, reflect varying degrees of partial melting of both asthenospheric and lithospheric mantle sources (Wilson 1989, 1993*a*,*b*). Any of these parental magma types may then differentiate at crustal levels to produce a diverse range of more evolved (more silica-rich) magma types. It is generally accepted that anomalously hot asthenosphere must be involved in the generation of large volumes of subalkaline (tholeiitic) basalts. Alkaline mafic magmas (alkali basalts, basanites, nephelinites) may be generated by extension alone, although in many cases the involvement of mantle plumes may be demonstrated, particularly when magmatism is accompanied by doming of the lithosphere.

Mantle plumes and the break-up of Gondwana

The Mesozoic break-up of the supercontinent Gondwana clearly represents a radical change in the plate tectonic regime, the causes of which have been a subject for vigorous debate. Three main phases may be recognized (Storey 1995):

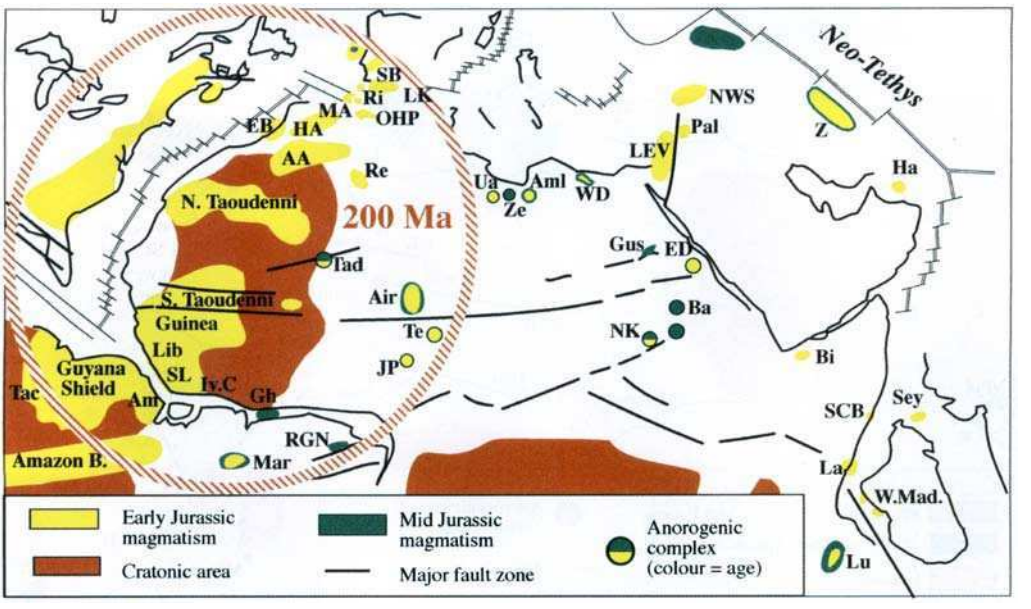

Fig. 4. Stage II: Early Jurassic (208 Ma, Liassic)–Mid Jurassic (157 Ma, Dogger). Abbreviations listed in Table 1. Circle marks the location of the postulated 200 Ma mantle plume head.

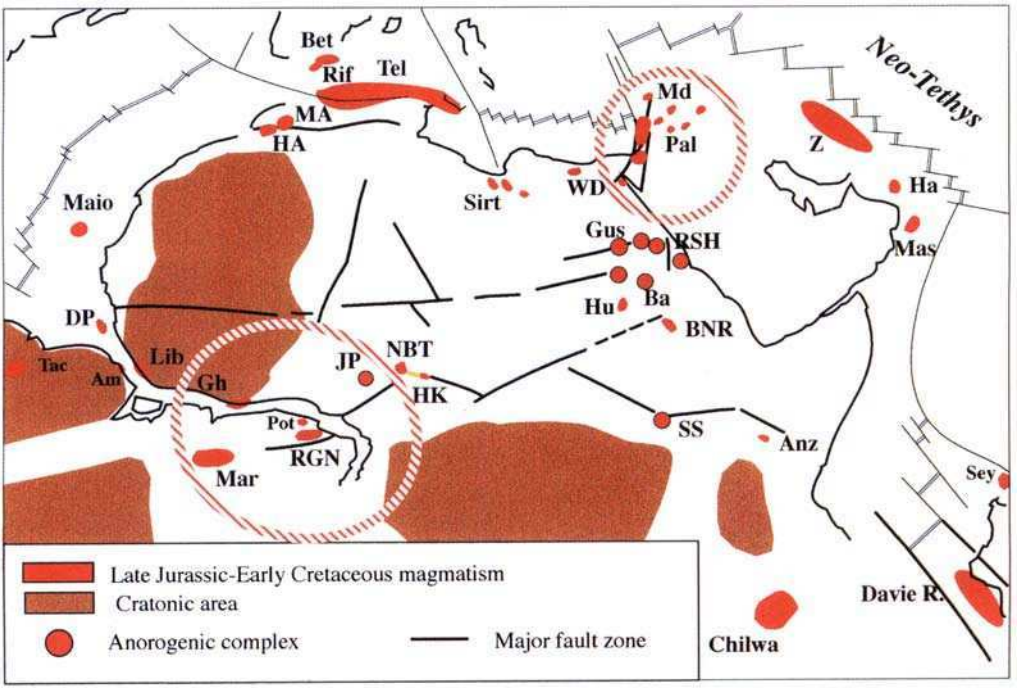

Fig. 5. Stage III: Late Jurassic (157 Ma)–earliest Aptian (120 Ma). Abbreviations listed in Table 1. Circles mark the locations of postulated Early Cretaceous mantle plume heads.

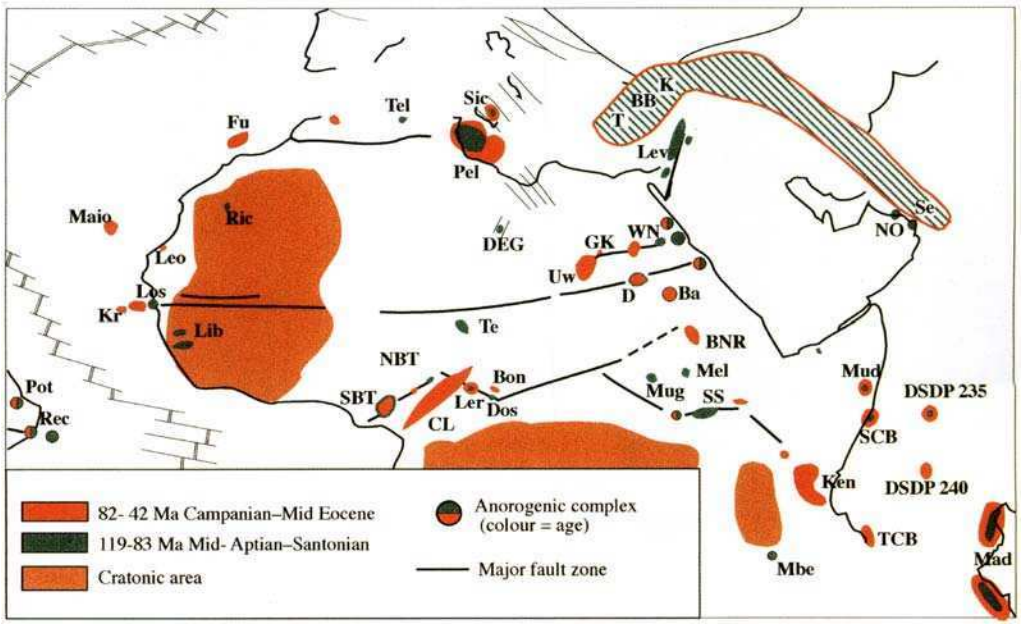

Fig. 6. Stage IV: Mid Aptian (119 Ma)–Mid Eocene (42 Ma). Abbreviations listed in Table 1.

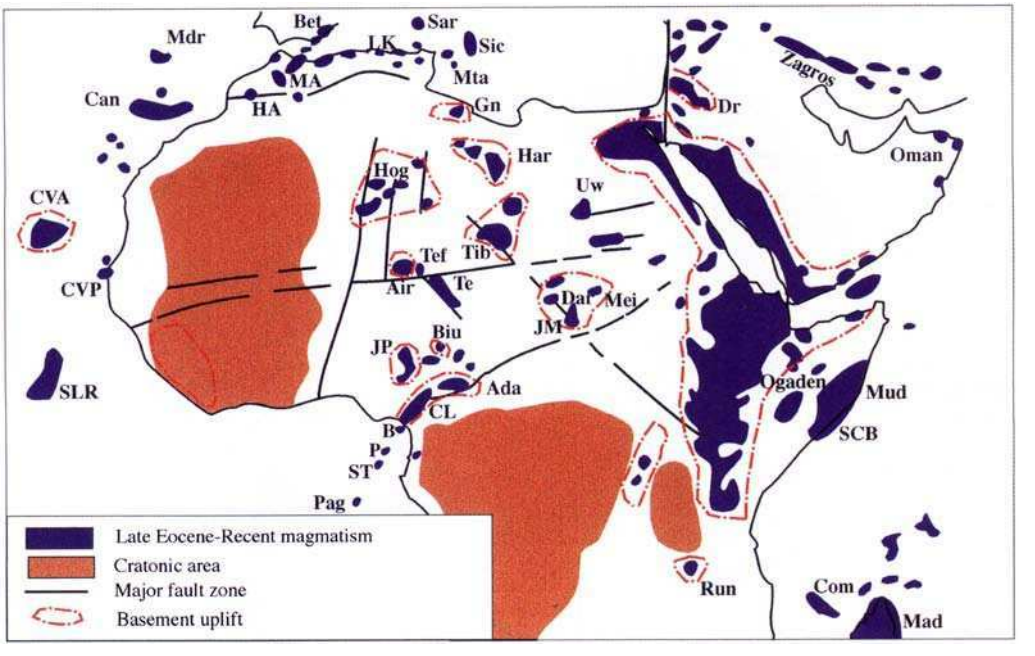

Fig. 7. Stage V: Late Eocene (42 Ma)–Recent. Abbreviations listed in Table 1.

(1) *Late Triassic-Early Jurassic.* Rifting initiated between West Gondwana (South America and Africa) and East Gondwana (Antarctica, Australia, India and New Zealand). The Central Atlantic Ocean started to open with the resultant separation of North America and Africa. The northern (Tethyan) margin of Gondwana appears to have changed from a convergent to a passive margin in Triassic times as a consequence of the rifting off of the Cimmerian continent (parts of Turkey, Afghanistan, Iran, Tibet, China and Indo-China) from Gondwana and the opening of the Neo-Tethys ocean (Sengör 1990; Sengör *et al.* 1993). Emplacement of voluminous Early Jurassic tholeiitic flood basalts (Central Atlantic, Karoo, Levant) suggests that large areas of the shallow mantle were anomalously hot. This may reflect 'incubation' of mantle plumes upwelling beneath Gondwana (Kent *et al.* 1992) with the heat unable to escape because of the insulating effect of the supercontinent.

(2) *Early Cretaceous.* South America started to separate from Africa–India and India separated from Antarctica.

(3) *Late Cretaceous.* Australia and New Zealand started to separate from Antarctica; Madagascar separated from the Seychelles and India and migrated northwards away from Africa and Antarctica.

Globally, major plume-related magmatic events appear to be periodic with a time frequency of *c.* 50–75 Ma. The most important events occur at the Permo-Triassic boundary (250 Ma), in the Early Jurassic (200 Ma), Early Cretaceous (145–135 Ma) and at the Cretaceous–Tertiary boundary (65 Ma). Earlier events have been recognized in the Late Carboniferous (300 Ma) and in the Late Devonian (375–350 Ma).

In an attempt to distinguish plume-related magmatic events from more localized magmatism related to lithospheric extension within the Afro-Arabian margin of Tethys (Fig. 1) we have divided the Late Permian to Recent magmatic activity into five major stages, I–V (Fig. 2). These stages correspond broadly to major tectonic cycles related to the opening and subsequent evolution of the Neo-Tethys, Atlantic and Indian Oceans (Guiraud & Bellion 1995).

Stage I: Late Permian (256 Ma)–latest Triassic (208 Ma);

Stage II: Early Jurassic (208 Ma, Liassic)–Mid Jurassic (157 Ma, Dogger);

Stage III: Late Jurassic (157 Ma)–earliest Aptian (120 Ma);

Stage IV: Mid Aptian (119 Ma)–Mid Eocene (42 Ma);

Stage V: Late Eocene (42 Ma)–Recent.

A series of maps have been produced (Figs 3–7) showing the distribution of magmatic activity for each stage, based on the time-scale of Harland *et al.* (1990). In producing these maps we have used a combination of stratigraphical constraints and Rb–Sr, K–Ar and ^{40}Ar–^{39}Ar ages to determine the age range of volcanism at a particular locality. It is important to recognize, however, that whole-rock K–Ar ages for basalts are frequently unreliable as a consequence of Ar loss or gain and overprinting by later thermal events (e.g. Baker *et al.* 1996*a*). The ^{40}Ar–^{39}Ar step-heating technique overcomes many of these problems, and as more samples are analysed by this method it is becoming clear that in many provinces magmatism actually occurred over a much narrower time interval compared with that deduced on the basis of K–Ar geochronology.

In general, we have cited the most recent publications concerning magmatic activity in a given area, focusing on those which comprehensively review earlier publications. Readers are directed to the bibliographies of these publications as a source of additional references.

Stage I: Late Permian (256 Ma)–latest Triassic (208 Ma)

Magmatism during Stage I (Fig. 3) is mostly concentrated on the northern margin of Afro-Arabia and is mainly Triassic in age with localized occurrences of Permian activity. Rifting and associated magmatism migrates from east (northern India) to west (Central Atlantic). In general, there is little magmatism within the African plate apart from scattered anorogenic ring complexes which may be the subvolcanic root zones of former central volcanoes. The preceding Palaeozoic period was not strongly magmatic in the Gondwanian domain apart from intra-plate activity in the Air (Vail 1989) and Nilotic (Nuba Mountains, Kordofan, Bayuda Desert and Uweinat inlier) provinces.

North African–Arabian margin

Widespread magmatism, of Late Triassic to Early Jurassic age, is associated with the development of Triassic rift basins along the North African margin. Basalts occur in the Tellian–Riffian Trough (Caire 1957; Michard 1976), in the Moroccan and Algerian Mesetas and Atlas (Lapierre *et al.* 1984; Baudelot *et al.* 1990) and in the Essaouira (Ziegler 1990) and Tarfaya basins (Michard 1976). More differentiated volcanics

(trachybasalts and trachyandesites) are known from the Northern Algerian Sahara (Busson 1970; Boudjema 1987), and acidic lava flows and dykes of Permian–Triassic age have been reported from the Rehamna area of the Moroccan Meseta (Muller *et al.* 1991). Some caution must, however, be exercised in interpreting the age of this magmatism; much of the activity may be related to the widespread 200 Ma tholeiitic magmatic event described in Stage II (Sebai *et al.* 1991*a*; Piqué & Laville 1995).

Further east, in the Sirt basin of Libya, Mid–Late Permian basalts have been drilled offshore (Almond 1992). Cahen *et al.* (1984) and Massa & Delort (1984) reported Permian–Triassic granites (256 Ma) and granodiorites (230–180 Ma) from the Uaddan horst, and basalts (213–218 Ma and 251 Ma) and microsynenite sills (245 Ma) from the Amal horst. In the northern Western Desert of Egypt Triassic dolerite intrusions have been recorded by Schlumberger (1984).

In central Sinai basaltic lava flows and dykes give ^{40}Ar–^{39}Ar ages ranging from 273 to 240 Ma (Steinitz *et al.* 1992). Meneisy (1990) reported a K–Ar age of 238 ± 3 Ma for an olivine basalt from Farsh El Azraq. Triassic–Liassic magmatism also occurs along the Levant–Syrian–Turkish margin (Sengör *et al.* 1993), much of which is of probable Early Jurassic age and is therefore described in more detail under Stage II. Searle (1994) noted the occurrence of a thin early Carnian volcanic horizon in the northern Palmyrides, which are otherwise volcanically inactive at this time. Baer *et al.* (1995) reported ^{40}Ar–^{39}Ar ages of 209.6 ± 3.8 Ma and 213.6 ± 3.8 Ma for a transitional basaltic sill from Makhtesh Ramon in southern Israel, confirming magmatic activity close to the Jurassic–Triassic boundary.

The Mamonia Complex in SW Cyprus contains Triassic lavas (Robertson & Xenophontos 1993). Similar rocks are exposed in Greece, SW Turkey (Antalya complex), Syria (Baer-Bassit) and Oman. The Mammonia complex represents a highly tectonized Late Triassic–Mid-Cretaceous passive continental margin sequence (Malpas *et al.* 1993). More than 80% of the Mamonia volcanic rocks are mid-ocean ridge basalt (MORB)-like tholeiitic pillow lavas. Interpillow voids are filled with uppermost Triassic calcilutite, providing important constraints for the age of the magmatism. The remaining volcanic rocks are predominantly alkali basalts which may have developed as oceanic islands or seamounts upon a tholeiitic ocean crust basement. The magmatic rocks are considered to be remnants of a much more widespread, extension-related, Late Triassic volcanism in a series of small ocean basins along the northern margin of Gondwana, south of the Palaeo-Tethys ocean. This may represent the initial stages of opening of the Neo-Tethys ocean (Stampfli 1996).

Sengör (1990) considered that the Neo-Tethys ocean opened as a back-arc basin above a long-lived (Carboniferous–Late Triassic) subduction system dipping to the SW beneath the Arabian passive margin of Palaeo-Tethys. Extension probably began in the Early Permian, with the main phase of magmatism during the Late Permian–Late Triassic. By the Early Triassic there may have been an extensional basin extending from Oman to southern Turkey.

The Zagros province was magmatically active from Permian to Dogger whereas the Oman margin was active from Permian to Liassic (Sengör *et al.* 1993). Late Permian to Late Triassic alkaline to tholeiitic pillow lavas occur in northern Oman (Robertson *et al.* 1990a; Sengör *et al.* 1993), and the Hawasina nappes (Bechennec *et al.* 1990). Late Permian volcanic intercalations, including pyroclastic deposits and andesite and rhyodacite lavas, occur in the South Oman Saïh Hatat autochthon (Rabu *et al.* 1990). Mid-Triassic carbonatites have also been reported from this area (Ziegler *et al.* 1991).

On the northern Indian margin Mid–Late Permian (270–250 Ma) tholeiitic flood basalts (Panjal Traps) were erupted (Gaetani & Garzanti 1991; Stampfli *et al.* 1991; Baud *et al.* 1993).

Intra-plate domain

Pan African suture. The Tadhak province (Mali), located on a major Panafrican suture along the eastern margin of the West African craton, is characterized by 100 Ma of within-plate magmatic activity during Permian–Jurassic times (Liégeois *et al.* 1991; Black & Liégeois 1993). The intrusion of alkaline igneous complexes appears to have been strongly influenced by the location of older tectonic lineaments. The Adrar Tadhak and Tirkine complexes give Rb–Sr isochron ages of 262 ± 7 Ma and 215 ± 11 Ma respectively. Further south, along the margins of the Gao Trough, dolerite dykes have reported K–Ar ages of 260 275 Ma (Lay & Reichelt 1971).

Niger–Nigeria province. In Northern Niger, the occurrence of volcanic shards and analcimolites in the Izeguandane and 'Grès d'Agadès' series could indicate some magmatic activity in the Air province at this time (Valsardieu 1971;

Forbes 1989). Further south the province of Damagaram Mounio (Niger) includes some ring complexes of Permian age; the Matsena massif has an Rb–Sr isochron age of 258 ± 5 Ma (Rahaman *et al.* 1984). The Jos Plateau of northern Nigeria is characterized by a 400 km long N-S trending zone of Mesozoic alkali granite ring complexes (Younger Granites) which decrease in age from north to south. The oldest complex (Dutse) gives an Rb–Sr age of 213 ± 7 Ma (Vail 1989). Structurally, the Air, Damagaram and Jos Plateau intrusions are located on a major, Late Precambrian, N–S fracture zone, which may have facilitated the intrusion of the magmas (Maurin & Guiraud 1993).

Nilotic Province. The Uweinat region, at the border of Sudan, Egypt and Libya, is magmatically active with a basaltic neck dated at 235 ± 5 Ma by K–Ar (Meneisy 1990). The adjacent Gebel Kamil area has volcanism at 233 ± 9 and 240 ± 7 Ma (Franz *et al.* 1987). The Nusab El Balgum alkali rhyolitic subvolcanic complex gives an Rb–Sr age of 216 ± 5 Ma (Schandelmeier & Darbyshire 1984). In the Eastern Desert of Egypt trachytic plugs at Nasb El Qash and Zargat Naam give Rb–Sr isochron ages of 245 ± 15 Ma and 247 ± 13 Ma, respectively (Meneisy 1990). Further south, intrusive alkaline complexes (alkali granites, quartz syenites, gabbros and undersaturated nepheline syenites) of Late Permian to Late Triassic age are widespread in Sudan. Höhndorf *et al.* (1994), on the basis of new Rb–Sr isochron ages and a summary of previously published data, concluded that there is a peak of intrusive activity between 270 and 220 Ma. The main intrusive centres are in the Nuba Mountains (251–222 Ma), North Kordofan (280–206 Ma), Bayuda Desert (238–233 Ma), Nubian Desert (297–229 Ma) and northern Red Sea Hills (232 Ma). The northern magmatic areas are located in the swarm of the Guinean–Nubian lineaments (Fig. 1; Guiraud *et al.* 1985) whereas the North Kordofan and Nubia Mountains magmatic centres are located in the vicinity of the Central African Fault Zone.

Stage II: Early Jurassic (208 Ma) –Mid Jurassic (157 Ma)

This is a period of major lithospheric extension involving the opening of the Neo-Tethys (on the Arabia–India Gondwana margin), the Mediterranean rift and the Central Atlantic rift, all accompanied by extensive tholeiitic magmatism, and by alkaline intra-plate magmatism in Nubia and Niger–Nigeria (Fig. 4). A widespread tholeiitic magmatic event at 200 Ma preceding the opening of the Central Atlantic Rift is clearly plume related.

West African and Central Atlantic margins

A widespread tholeiitic magmatic event at *c.* 200 Ma along the conjungate passive continental margins of Africa and North America is closely associated with the opening of the Central Atlantic Ocean and may be related to the activity of a thermally and chemically anomalous mantle plume which influenced an area more than 5000 km SW–NE and 1500 km E–W (Wilson 1997; Fig. 4). Correlatives of this magmatic event occur as far north as the Iberian peninsula and as far south as the Amazon basin in Brazil. The magmatism is expressed as mafic dykes, sills, lava flows and rare layered plutons of tholeiitic affinity, similar in chemistry to continental flood basalts world-wide. Some SW–NE trending dykes have considerable lengths (e.g. Messejana dyke, Iberian peninsula, 530 km; Ksi-Ksou dyke, western Algeria, 800 km; Sebai *et al.* 1991*a*). Lava flow remnants are restricted to Triassic–Early Jurassic (Liassic) rift basins, although fissure-fed flows may originally have been more extensive.

Continental rifting began in the Late Triassic (225–230 Ma), following the trend of the Permo-Carboniferous Alleghanian–Hercynian orogenic belt (Piqué & Laville, 1995), with sea-floor spreading initiating in the early Middle Jurassic (170–175 Ma; White & McKenzie 1989; Hill 1991). Combined stratigraphic and geochronological data indicate that most of the basaltic magmatism along the North American margin (NAM) was restricted to an extremely short time interval between 200 and 202 Ma (McHone 1996). Klitgord & Schouten (1986) considered that the onset of sea-floor spreading was more or less simultaneous from Florida to the Gibraltar fracture zone, a distance of some 2700 km.

The widespread occurrence of magmatism concurrent with continental rifting led White & McKenzie (1989) to propose that there was a broad asthenospheric temperature anomaly beneath the NAM at this time. This was attributed to the activity of the Cape Verde mantle plume, which they placed some 1000 km to the NW within the continental interior. Subsequently, Hill (1991) proposed that the axis of the plume was actually located much further to

the south, in the vicinity of Florida, on the basis of the radial orientation of dykes along the east coast of North America, the NW coast of Africa and the coast of Brazil. Recently, McHone (1996) has proposed that the NAM should be considered as one of the worlds large igneous provinces (LIPS). By analogy with many other LIPS it seems likely, therefore, that the magmatism is indeed plume related. The lateral extent of magmatic rocks across the conjugate Central Atlantic margins indicates a marked asymmetry between Africa and North America, with a much wider distribution of magmatic rocks on the African side (Fig. 4). This strongly suggests that if the magmatism is indeed plume related then the location of the plume axis is much more likely to have been beneath Africa than North America (Wilson 1997).

Correlatives of the Early Jurassic magmatic event also occur within South America. Intense basaltic magmatic activity occurred during the Late Triassic–Early Liassic in the Guyana Shield, the Amazon basin and the Parnaiba–Maranhão basin (Asmus 1984). In the Tacutu Trough (Guyana Shield) tholeiitic basalts give ages ranging from 146 to 208 Ma (Asmus 1984). The N–NW trending tholeiitic Amapa dyke swarm of northern Brazil (250–180 Ma) is temporally and spatially related to the opening of the Central Atlantic Ocean (Oliveira *et al.* 1990). Individual dykes within this swarm can attain several hundreds of metres in width and can be traced over distances exceeding 250 km. Fodor & McKee (1986) reported whole-rock K–Ar ages of 185–126 Ma for tholeiitic basaltic rocks cored in the offshore Amapa basin, northern Brazil. In pre-drift reconstructions of South America and Africa the Brazil–Guyana dykes are parallel to those of similar age in Liberia, Sierra Leone and the Ivory Coast. Huge diabase sills, dykes and some basaltic flows have been recognized in numerous oil wells in the Amazon basin. The total thickness of these interbedded igneous formations is more than 600 m (Bigarella 1973). Their K–Ar ages range between 170 and 220 Ma (Cunha *et al.* 1994). Montes-Lauar *et al.* (1994) reported Ar–Ar ages of 197 Ma for tholeiitic basalts from the Anari and Tapirapuã formations of western Brazil, in the Parecis–Alto Xingu basin to the south of the Amazon basin. Previously published K–Ar ages for these formations (155–117 Ma) are almost certainly unreliable. Triassic–Jurassic flood basalts (K–Ar ages: 200–170 Ma; Bellieni *et al.* 1990; Fodor *et al.* 1990) have been described from the western Maranhão province of NE Brazil. In Rio Grande do Norte there are Middle Jurassic dykes (179–161 Ma) and rare (180–169 Ma) lava flows (Horn *et al.* 1988; Bellieni *et al.* 1992). Within the Upper Amazon Solimões basin, intrusion of Triassic–Jurassic sills (*c.* 200 Ma) appears to have generated high levels of thermal maturity within Upper Devonian petroleum source rocks (Mello *et al.* 1994). These intrusions mark the SW limit of the 200 Ma magmatic event.

Extensive dyke swarms occur in Mauritania, Mali and Liberia, the most important being in the Taoudenni area in northern Mali. Sill complexes are prevalent in southwest Mali and Guinea and southern Morocco. Sebai *et al.* (1991*a*) report $^{40}Ar/^{39}Ar$ ages between 203 and 197 Ma for dykes from Taoudenni (Mali) and lava flows from Morocco, and use ^{40}Ar–^{39}Ar age spectra to constrain an age of *c.* 200 Ma for the Messejana (Iberia), Foum Zguid (Morocco) and Ksi-Ksou (Algeria) giant dykes. Bertrand & Villeneuve (1989) described early Jurassic dolerite dykes and sills from Guinea, which give K–Ar ages of 180–200 Ma. Mesozoic dolerite dykes, locally associated with sills and rare lava flows, are widespread in Liberia. These give K–Ar ages of 173–201 Ma where they intrude Pan-African crust (Dupuy *et al.* 1988; Mauche *et al.* 1989) but anomalously old K–Ar ages where they intrude the 2700 Ma West African craton, most probably as a consequence of inheritance of excess ^{40}Ar (Mauche *et al.* 1989). Doleritic basalts of 162 Ma have been reported from the coastal basin of Ghana by Akpati (1978). Kimberlites of inferred Mesozoic age occur in the southern part of the West African craton (Taylor *et al.* 1994). Their age is not well constrained, although the similar erosional levels of exposed kimberlite clusters in Sierra Leone, Liberia and Guinea suggest that they may represent a single age province; it is possible that they could be Early Jurassic in age, although they are generally considered to be Cretaceous (*c.* 115 Ma).

Fiechtner *et al.* (1992) described tholeiitic lava flows from the Middle and High Atlas of Central Morocco, intercalated with Triassic–Liassic continental red beds, deposited in elongated NE–SW striking basins which give ^{40}Ar–^{39}Ar ages in the range 210–196 Ma. Late Triassic to Early Jurassic volcanism is also known from the Essaourira Basin of Morocco (Baudelot *et al.* 1990). Lapierre *et al.* (1984) described tholeiitic basaltic flows intercalated with pyroclastic deposits from the Oranese High Plateau, west Algeria, stratigraphically constrained to the Triassic-Jurassic boundary or slightly younger. In Little Khabylia Early Jurassic ophiolites have been reported (Boullin *et al.* 1977)

Central–Eastern Mediterranean

Keeley & Wallis (1991) considered that the present continental margin to Egypt formed during a period of west propagating crustal rifting of Neo-Tethys from late Pliensbachian (*c.*190 Ma) to Bathonian (*c.* 160 Ma). A range of magmatic activity is associated with this rifting. In northern Libya granodiorites (230–180 Ma) are known from the Uaddan horst, granodiorite (207 Ma), basalt (164 Ma), rhyolite (161 Ma) and microsyenite (159 Ma) from the Amal horst, and rhyolite (160 Ma) from the Zelten horst (Cahen *et al.* 1984; Massa & Delort, 1984). Magmatic rocks have also been penetrated in oil wells in the northern Western Desert of Egypt; basalts dated at 178 Ma have been mentioned by Meneisy (1990), and Early Bathonian (*c.* 165 Ma) interbedded basic volcanic rocks by Keeley & Wallis (1991).

In the Levant province, including Sinai, extensive Liassic tholeiitic basaltic volcanism is associated with the later stages of the rifting event which produced the passive continental margin of the Levant Basin of the Eastern Mediterranean (Garfunkel, 1989; Hirsch *et al.* 1995). In northern Israel this phase (Asher volcanic series) includes up to 2.8 km of transitional to alkaline basalt flows and pyroclastic deposits, with minor felsic intercalations and associated intrusive rocks, encountered in a number of deep boreholes (Dvorkin & Kohn 1989; Garfunkel 1989). The age of the Asher volcanic series in the Mount Carmel area of northern Israel is well constrained at *c.* 200 Ma on the basis of stratigraphy, ^{40}Ar–^{39}Ar and K–Ar dating (Gvirtzman *et al.* 1990; Kohn *et al.* 1993). Minor Mesozoic volcanism is also known from the Palmyride trough of Syria (Best *et al.* 1993). Robertson & Xenophontos (1993) considered that Triassic–Jurassic rifting and sea-floor spreading resulted in the formation of a small ocean basin in the Cyprus area but there is no evidence for any Jurassic–Early Cretaceous ocean floor volcanism.

East African and Indian margins

Late Triassic to Early Jurassic basaltic flows are known from Bihendula in northern Somalia (Bosellini 1992). Liassic volcanics also occur in the Somali Coastal Basin and the Lamu Embayment (Coffin & Rabinowitz 1988). Sea-floor spreading between Africa and the Madagascar–India–Seychelles block initiated during the Jurassic Magnetic Quiet Zone (*c.* 156 Ma; Bosellini 1992). Hankel (1993) noted the occurrence of basaltic flows interbedded with Karoo continental clastic deposits in the Luwegu (Selous) Basin in southern Tanzania, with K–Ar ages ranging between 164 and 186 Ma. On the western Madagascan margin, some Liassic basalt flows have been drilled offshore (Coffin & Rabinowitz 1988). Luger *et al.* (1994) have provided a useful summary of the Jurassic and Cretaceous stratigraphy of Somalia and Madagascar.

Voluminous tholeiitic flood basalt magmatism (Karoo) occurs in Southern Africa, during Stage II. Two major episodes of basaltic volcanism at 193 ± 5 Ma and 178 ± 5 Ma have been recognized within the Karoo province (Cox, 1992). Recent ^{40}Ar–^{39}Ar dating (Hooper *et al.* 1993), however, has suggested that the peak-magmatic event was actually rather short at 182 ± 2 Ma. Plummer (1995) reported Early Jurassic (*c.* 190 Ma) layers of devitrified ash from the Seychelles which may be correlated with the widespread Karoo flood basalt volcanism in southern Africa.

Intraplate domain

Within the Tadhak Permian–Jurassic magmatic province of eastern Mali the Anezrouf syenitic complex has an Rb–Sr isochron age of 184 ± 14 Ma and the Tidjerazraze–In Imanal intrusion gives 161 ± 5 Ma (Liégeois *et al.* 1991). In the Jos Plateau of Nigeria intrusion of alkali granitic complexes began with the Dutse complex (213 ± 7 Ma), Zaranda complex (186 ± 15 Ma) and Ningi-Burra complex (183 ± 7 Ma) (Vail 1989). Further north, in the western Ténéré, granites dated at 190 ± 7 Ma have been drilled (Genik 1992). The presence of volcaniclastic sediments in the Tim-Mersoi basin (Valsardieu 1971; Forbes 1989) may indicate a continuation of magmatic activity in the Air province at this time. Anorogenic alkaline igneous complexes also occur in northern Kordofan (206–163 Ma), the Bayuda Desert (159 Ma) and the Eastern Desert of Egypt (191 Ma) (Höhndorf *et al.* 1994). Alkali olivine basalts of the Gebel Umm Shaghir area have been dated by K–Ar at 155 ± 4 Ma and 157 ± 4 Ma (Schandelmeier *et al.* 1987*a*.).

Stage III: Late Jurassic (157 Ma)–Earliest Aptian (119 Ma)

Magmatic activity during this stage (Fig. 5) is considerably reduced compared with Stage II. The main tectono-magmatic events are related to the separation of South America and Africa, accompanied by the decoupling of Africa into

three blocks (western, Arabian–Nubian, southern) and the opening of the Indian Ocean, separating West Gondwana from East Gondwana. Extensive, plume-related tholeiitic flood basalt magmatism occurred in South America (Parana province of Brazil) as a precursor to the opening of the South Atlantic Ocean. In the Equatorial Atlantic, the St Helena mantle plume may have played an important role in the extension of the Benue Trough and subsequent continental break-up, although it did not generate extensive magmatism (Wilson 1992). In the Levant regional doming of the basement and widespread erosion accompanied by alkali basaltic magmatism suggests upwelling of a thermally anomalous mantle plume beneath the area. Continued emplacement of plutonic complexes in Sudan and Egypt may have been controlled by the Guinean–Nubian lineaments.

West African margin and Equatorial Atlantic opening

West Africa. In the Cape Verde Archipelago tholeiitic pillow basalts on Maio island have been dated at 157± 4 Ma (Mitchell *et al.* 1983), whereas intercalated sedimentary layers in their upper part provide micropalaeontological evidence for an early Valanginian (*c.* 140 Ma) age (Fourcade *et al.* 1990). These probably represent an uplifted part of the earliest oceanic crust formed by Central Atlantic sea-floor spreading. Martin (1982) has documented the occurrence of basaltic lavas of very Late Jurassic–Early Cretaceous age along the Liberian margin. Along the Ghanean margin 120–125 Ma volcaniclastic deposits have been mentioned by Reyre (1984).

South America. In northeastern Brazil there are widespread occurrences of magmatic rocks which can be correlated with the various phases of opening of the Central and Equatorial Atlantic oceans. Tholeiitic and alkaline magmatism, synchronous with Early Cretaceous rifting in Brazil and west-central Africa, has been related to the activity of the St Helena mantle plume by Wilson & Guiraud (1992). Neocomian volcanic activity is known along the eastern Demerara Plateau escarpment (Benkhelil *et al.* 1995). In the Tacutu Trough (Guyana Shield) thick tholeiitic basalts have reported ages ranging from 208 to 114 Ma (Asmus 1984). Tholeiitic basalts, dated at 126.5 Ma, have been cored within the offshore Amapa basin (Fodor & McKee, 1986). Basic dykes dated *c.*120–140 Ma are known both onshore and offshore in the Potiguar basin (Araripe & Feijo, 1994; Magnavita *et al.* 1994). E–W to NE–SW trending tholeiitic dykes from the Rio Grande de Norte and Ceará provinces are of Early Cretaceous (145–125 Ma) age (Horn *et al.* 1988; Bellieni *et al.* 1992). It should be noted that there are also Middle Jurassic (Stage II) dykes in the same area. In the eastern part of the Maranhão basin there are 130–120 Ma tholeiitic sills and dykes (Bellieni *et al.* 1990; Fodor *et al.* 1990). The main magmatic activity in Brazil during this period is essentially restricted to a zone south of 16 S in the Parana basin and the coastal basins, where voluminous flood basalt volcanism related to the activity of the Tristan da Cunha mantle plume peaked at 127–137 Ma (Turner *et al.* 1994).

North African–Arabian margin

North African margin. The Moroccan Middle Atlas and High Atlas rift basins were intruded by basic dykes during this stage (Hailwood & Mitchell 1971; Charroud *et al.* 1993; Souhel *et al.* 1993); gabbro dykes have been dated from the Middle Atlas (119 ± 3 Ma), High Atlas (119–125 Ma) and central High Atlas (173–119 Ma). Submarine oceanic volcanism is known in several areas of the Riffian–Tellian Trough and eastward up to the Sicilian margin. Early Kimmeridgian basalts (Cecca *et al.* 1993) and Berriasian serpentinites (Boullin, 1983) occur in Great and Little Kabylia. Oxfordian–Early Kimmeridgian tuffites occur in northern Tunisia (Alaouani, 1993) and Early Kimmeridgian volcanic rocks occur offshore from Sicily (Dercourt *et al.* 1985).

Serpentinized peridotite, either massive or detrital, occurs in the eastern External Rif (Beni Malek) at the base of the Jurassic–Lower Cretaceous succession (Michard *et al.* 1992). The serpentinites are considered to represent a slice of a serpentinite ridge from the North African rifted continental margin incorporated into a thrust pile during the Tertiary Iberia–Africa collision. They are distinct from the other Betic–Maghrebide peridotite bodies (e.g. Beni Bousera and Ronda). Pearson *et al.* (1993) have recently suggested that the Beni Bousera peridotites represent slices of asthenospheric mantle from above a Late Cretaceous subduction zone which were tectonically emplaced into the crust at *c.*21 Ma.

Further eastward, magmatism occurred in some of the Libyan Sirt troughs and rift shoulders. Latest Jurassic Early Cretaceous granite intrusions (152–122 Ma) and basic–intermediate volcanic rocks (148–127 Ma) have been

reported by Cahen *et al.* (1984), Massa (1988) and Rossi *et al.* (1992). In NE Egypt basalts have been dated by K–Ar from 115 to 125 Ma (Meneisy 1990).

Arabian margins. Everywhere in NE Africa and the Levant a major break, from mid-Tithonian to mid-Berriasian (*c.* 150–142 Ma), separates the Jurassic and Cretaceous sequences. This 'Cimmerian' event (Keeley & Wallis 1991) is characterized by regional tilting, uplift and erosion, folding and widespread alkali basaltic volcanic activity (Guiraud this volume; Laws & Wilson, 1997). As this coincides with a worldwide sea-level lowstand, however, care must be taken not to attribute the poor sedimentary record beneath the 'Cimmerian' unconformity exclusively to uplift and erosion. Uplift is least in the north and increases southward, indicating a regional tilt.

The Eastern Mediterranean Mesozoic basin extends from the Western Desert of Egypt some 2000 km eastward through northern Egypt, Israel, Lebanon and Jordan, then northeastward through Syria to southeastern Turkey and northern Iraq (May 1991). From the Syrian coast eastward it is bounded by the Taurus–Zagros fold belt. The basin is considered to have originated by the separation of a continental block, Apulia, from Africa and Arabia. Rifting initiated during the Late Carboniferous–Early Permian (Stampfli *et al.* 1991; Stampfli 1996; Guiraud this volume) and sea-floor spreading may have generated a small ocean basin by the Late Permian (Stampfli, 1996) or earliest Cretaceous (Dercourt et al, 1985; May 1991). This view conflicts with that of Hirsch *et al.* (1995), who considered that the Eastern Mediterranean is floored by thinned continental and not oceanic crust.

Magmatic rocks occur in a N–S trending region in the Levant extending from NW Syria and Lebanon through Israel to southern Sinai (Garfunkel 1989; Laws & Wilson, 1997). Both extrusive rocks and hypabyssal intrusions are found within Early Cretaceous and older sediments in exposures and in the subsurface. Early Cretaceous basalt flows cover wide zones in the Mardin Plateau and Palmyrides domains of Syria, and within the shoulders of the Euphrates graben of Iraq (unpublished data from Elf Aquitaine and Total). K–Ar dating of basalts from Israel has yielded ages mostly in the range 140–120 Ma (Lang & Steinitz 1989). During the period of igneous activity the long-term subsidence of the region was interrupted and uplift formed a broad swell from which 1000 m or more of sediments were eroded (Garfunkel & Derin, 1988). Basalts dominate the magmatic activity and range from weakly subalkaline to alkaline in composition. This province also includes (115–125 Ma) basalts from the Gulf of Suez area (Meneisy, 1990).

The Zagros margin of Iran is intruded by granodiorites, diorites and gabbros of Late Jurassic–Early Cretaceous age (Sengör 1990; Sengör *et al.* 1993). The magmatic activity may be subduction related, although the geodynamic setting is not well constrained.

Storey (1995) considered that continental rifting, commencing in the Early Jurassic (*c.* 180 Ma), resulted, by Late Jurassic times, in the formation of a seaway between West Gondwana (South America and Africa) and East Gondwana (Antarctica, Australia, India and New Zealand) and to sea-floor spreading in the Somali and Mozambique basins, where the oldest known sea-floor magnetic anomalies are *c.*156 Ma. The Late Jurassic–Early Cretaceous Masirah ophiolite, which was obducted shortly after its formation, provides evidence for the age of onset of sea-floor spreading along the eastern Oman margin. The Hawasina deep basin exhibits alkaline magmatism of Late Tithonian (*c.* 150 Ma)–Early Berriasian (*c.* 145 Ma) age (Bechennec *et al.* 1990). Further to the southeast gabbros (126–158 Ma), granites (124–146 Ma) and alkaline basalts (123 Ma), now preserved on Masirah Island, were emplaced in the 'proto-Owen Basin' and margin (Smewing *et al.* 1991).

East Africa–Madagascar

The separation of Madagascar from Africa in the Late Jurassic led to the development of extensional basins along the east coast of Somalia and Kenya and NNW-trending basins in Sudan (Bosworth 1992; Reynolds 1993). In southern Malawi the Chilwa alkaline province, consisting of syenite and alkali granite plutons, basanite–nephelinite volcanic rocks and carbonatites, gives ages ranging between 138 and 105 Ma (Eby *et al.* 1995). On the western Madagascar margin, Late Jurassic and Early Cretaceous volcanic rocks (basalt flows, rhyolites and pyroclastics) have been drilled offshore (Coffin & Rabinowitz 1988). This magmatism may be correlated with transcurrent movements along the Davie Ridge. Plummer (1995) has reported basic dykes (*c.* 135 Ma) and lava flows at 124–113 Ma from the Seychelles. The tholeiitic flood basalt Rajmahal Traps of eastern India are also of this age (117 Ma; Kent *et al.* 1992). This latter event has been related to the upwelling of the Kerguelen mantle plume.

African intra-plate domain

Niger–Nigeria Province. The southern part of the Jos Plateau was active during the latest Jurassic–earliest Cretaceous with the emplacement of the youngest 'Newer Granite' intrusions, Mada (145 Ma) and Afu (141 Ma) (Vail 1989). Vannucci *et al.* (1989) have reported a K–Ar age of 157 ± 5 Ma for basaltic lavas and dykes located at the margin of the Cretaceous–Paleocene Sokoto embayment of the Iullemeden basin in NW Nigeria.

Volcanic activity in the Benue Trough (Nigeria) was particularly important during this period and took place in several phases contemporaneous with the opening and infilling of the trough. The first phase, restricted to the Northern Benue, during the latest Jurassic–early Cretaceous (147–106 Ma; Maluski *et al.* 1995), is related to the main extensional tectonic regime which affected the trough (Guiraud & Maurin 1992). Transitional basalts occur as lava flows and dykes accompanied by smaller volumes of rhyolite. In the Burashika district the volcanism (147–138 Ma) is bimodal. The Burashika volcanics are the oldest igneous activity known from the Benue Trough and were emplaced synchronously with the southernmost, youngest ring complex on the Jos Plateau (Vail 1989). Eastward, in northern Cameroon, basalt flows interbedded within Barremian shales are known in the small Hama Koussou half-graben (Maurin & Guiraud, 1990).

Sudan. Within central and northern Sudan and southern Egypt abundant alkali intrusive complexes were intruded throughout the Late Jurassic and Early Cretaceous with a peak between 165 and 120 Ma (Vail, 1989; Schandelmeier *et al.* 1993; Höhndorf *et al.* 1994). Most of these complexes are associated with E–W to ENE–WSW trending faults of the Nubian and Central African lineaments and local pre-exisiting N–fault zones. In NE Sudan N-S trending alkali dyke swarms are associated with syenitic igneous centres (Vail 1993). In southern Sudan three alkali ring complexes, located at the junction of the W Muglad–Assoua fault zone and the E–W trending South Sudan shear, gave K–Ar ages of 140–110 Ma (Reynolds, 1993).

Locally, contemporaneous volcanic activity is preserved in Mesozoic sedimentary basins, whereas in general the alkaline complexes are located outside the rifts. In the Khartoum (Blue Nile) and Humar basins up to 1000 m of latest Jurassic–earliest Aptian (145–120 Ma) alkali basalt lava flows and tuffs are interbedded with clastic sediments (Wycisk *et al.* 1990; Reynolds 1993). In Southern Egypt alkali olivine basalts in the Gebel Umm Shaghir area give K–Ar ages of 155–157 Ma (Schandelmeier *et al.* 1987*a*).

Stage IV: Late Aptian (119 Ma)–Mid Eocene (42 Ma)

This period is not characterized by any major magmatic activity on a regional scale (Fig. 6). Intra-plate alkaline magmatism occurs at scattered localities within the Mesozoic rift basins of west and central Africa, Nubia, Sudan and the Somalia–Madagascar region. The Cameroon Volcanic Line initiates as a major tectono-magmatic feature during this stage. Magmatism on the West African margin and in Sudan appears closely linked to the E–W trending Guinean–Nubian lineaments. There is strong magmatic activity associated with NW–SE trending fault zones in Tunisia, Libya and Sicily in the so-called *Mediterranean Seuil* (High) (Dercourt *et al.* 1993). Scattered magmatism is associated with the Levant fault zone. Stage IV is also a period of major ophiolite formation and obduction along the Neo-Tethyan margin of the Arabian Peninsula and in the Eastern Mediterranean. A major plume-related flood basalt event occurs in India with the eruption of the Deccan Traps at the K–T boundary.

Along the Equatorial Atlantic margins continental break-up occurred by the latest Albian (Mascle *et al.* 1988), whereas the South Atlantic had been opening since the Mid-Aptian. A major regional compressive event occurred in the Santonian, followed by the onset of magmatism along the Cameroon Volcanic Line and rejuvenation of magmatism in the Mediterranean Seuil (High). This period ends with a regional compressive event related to the collision of Africa–Arabia and Eurasia.

West African margin and Equatorial Atlantic opening

West Africa. Magmatism in West Africa appears to be closely linked to the Guinean–Nubian lineaments (Guiraud *et al.* 1985). In Guinea intrusive rocks from Los Island give an Rb–Sr isochron age of 104.5 ± 1.6 Ma (Demaiffe & Moreau, unpublished data). Within the Precambrian Guinea shield dykes and pipes of kimberlite may have been emplaced between 120 and 83 Ma (Haggerty 1982), although the age constraints are not particularly reliable. Palaeocene alkaline volcanic rocks and flood basalts have been recognized on the southern margin of the

offshore Guinea Plateau, which give ^{40}Ar–^{39}Ar ages of 59 Ma (Bertrand *et al.* 1989, 1993). Similar Paleocene alkaline volcanism is known from the Krause seamount on the northern Sierra Leone Rise (Bertrand *et al.* 1993). In the Cape Verde Archipelago, pillow basalts of *c.*100, 73 and 63–42 Ma have been reported from Maio island by Mitchell *et al.* (1983). In the Canary Islands, the oldest basaltic dykes of Fuerteventura give ages ranging between 48 and 35 Ma (Le Bas *et al.* 1986). Magmatism may, however, have initiated earlier in the Senonian with submarine volcanic rocks and plutons still undated (Le Bas *et al.* 1986). Bertrand *et al.* (1993) have described a 3000 m high seamount, the Nadir seamount, on the southern Guinea margin which is of the same age as the Krause seamount. This consists of hyaloclastite breccias and subaerial alkali basalts dated by ^{40}Ar–^{39}Ar dating of biotite phenocrysts at 58.6 Ma. On the northern Senegal margin, the Leona microsyenite intrusion is inferred to be Late Campanian–Early Maastrichtian in age, according to stratigraphic constraints (Bellion 1989). Further north, the Richat dome of central Mauritania is a 45 km diameter annular structure located at the intersection of two sets of fractures oriented N 10–20 E and N 70–80 E (Netto *et al.* 1992). Magmatic rocks include gabbro–dolerite intrusions and carbonatite necks and veins. A carbonatite vein was dated at 85 ± 5 Ma by apatite fission track dating (Netto *et al.* 1992).

*South Americ*a. In the onshore coastal Potiguar basin, 83 ± 6 Ma dykes of alkali diabase have been reported by Araripe & Feijo (1994). Alkaline intrusive complexes and acid volcanic rocks (Ipojuca Fm) are known in the Recife area, northeastern Brazil, both onshore and offshore. They have been dated between 90 and 114 Ma (de Almeida *et al.* 1988; Mabesoone & Alheiros 1988) and could denote a rejuvenation of the Pernambuco fault. Southwestward, dolerite dykes intruding the Precambrian basement east of the Tucano rift give a K–Ar age of 105 ± 9 Ma (Magnavita *et al.* 1994). Westward, 115–122 Ma hypabyssal intrusions are known in the eastern part of the Maranhão basin (Fodor *et al.* 1990), and in the Tacutu basin volcanism may end at *c.*114 Ma (Asmus 1984). Mid-Aptian diabases and basalts have been reported in the coastal Ceará basin (Beltrami *et al.* 1994).

North African–Arabian margin

Little magmatic activity is known during this stage in the Alpine domain of North Africa. Michard (1976) has reported nephelinitic basic sills and dykes (aiounites) from northern Morocco dated at 57–37 Ma. Obert (1981) mentioned dolerites and diorites from the Algerian Tellian Trough (Babors) which are pre-Albian and probably Aptian in age. In contrast, the eastern Tunisian and northwestern Libyan Tethyan margin was magmatically very active. Abundant Aptian to Paleocene volcanics have been penetrated by oil wells (Hammuda *et al.* 1992; Laridhi-Ouazaa 1994). Southward, in the S Sirt, trachytes have been dated at 103 Ma (Cahen *et al.* 1984). This magmatic province is clearly elongated NW–SE and is associated with the very active Early Cretaceous and/or Late Cretaceous–Paleocene rifting on the Pelagian Shelf (Guiraud & Maurin 1991; Van der Meer & Cloetingh, 1993; Guiraud, this volume). By the Mid-Late Cretaceous, especially during the Maastrichtian, the neighbouring southern Central Mediterranean domain (Apulian sub-plate sensu lato) exhibits a strong NE–SW extension, accompanied by magmatism in southern Sicily (Camoin *et al.* 1993).

The Levant province was active during the Mid–Late Cretaceous. Basalt flows and some pyroclastic deposits of Aptian–Santonian age are known from southern Israel to northwestern Syria (Ponikarov *et al.* 1967; Garfunkel 1989; Lang & Steinitz 1989). This magmatic activity demonstrates the play of the Levant fault zone swarm. In northern Sinai volcanic ashes interbedded in Albian strata were recently discovered in Gebel Maghara (J. Kuss, pers. comm. 1995).

Ophiolites and ophiolitic melange generated during the Cenomanian–Turonian were obducted in the Coniacian–Campanian (90–80 Ma) in an arcuate belt from Cyprus and southern Turkey to northeastern Oman (Bechennec *et al.* 1990; Rabu *et al.* 1990; Robertson & Searle 1990; Robertson *et al.* 1990*a*, *b*; Sengör *et al.* 1993). Dilek & Eddy (1992) suggested that the ophiolites represent remnants of the Neo-Tethys ocean, which evolved as a result of Mesozoic sea-floor spreading north of Afro-Arabia. The Cretaceous Peri-Arabian ophiolite belt (Troodos, Baër-Bassit, Kizildag, Ispendere-Kömürhan, Gevas-Guleman, Cilo, Kermanshah, Neyriz, Semail) crops out discontinuously along the Bitlis–Zagros suture zone in the eastern Mediterranean. Regional studies indicate that the Neo-Tethys ocean may have had multiple strands floored with oceanic crust and separated by continental fragments which were rifted blocks from Afro-Arabia. The lack of evidence for any significant emplacement-related tectonic deformation of the ophiolite massifs and their sedimentary cover, at least for Troodos and Kizildag, suggests that they did not experience

any large-scale tectonic transport and therefore that they probably represent fragments of the southernmost strand of Neo-Tethys immediately north of Afro-Arabia. The Semail ophiolite is Middle Cretaceous in age (90–95 Ma; Gnos & Peters, 1993). The Troodos ophiolite is believed to have formed at a spreading axis above a subduction zone in the Late Cretaceous (Malpas *et al.* 1993; Robertson & Xenophontos 1993). There is, however, no direct evidence of the orientation or location of this subduction zone. In northern Oman alkali basalt flows and diabase sills dated at 92–109 Ma (K-Ar on biotite and hornblende) occur on the shelf edge–slope boundary (Robertson *et al.* 1990*a,b*). These may be related to regional crustal extension immediately preceding or accompanying the genesis of the Semail ophiolite.

East African–Madagascan margin

Highly altered basalt flows of Maastrichtian to latest Paleocene–Early Eocene age have been drilled in the Mudugh basin (Central Somalia), the Somali Coastal Basin, and DSDP (Deep Sea Drilling Project) wells 235 and 240 (Piccoli *et al.* 1986; Coffin & Rabinowitz 1988; Bosellini 1992). An extensive province of Late Cretaceous intrusions exists in the Kenya Basin and its flanks, according to Reeves *et al.* (1987). Trachytes and basalts of Late Cretaceous age intruded the Tanzanian Coastal Basin (Kajato 1982). In southwestern Tanzania, carbonatite intrusions from the Mbeya area gave ages ranging between 90 and 120 Ma (Cahen *et al.* 1984).

Much stronger magmatic activity occurred on the northern, western and eastern Madagascan margins, both onshore and offshore. Magmatism, consisting mainly of basalts, trachytes and pyroclastic deposits, continued from Aptian to Lutetian times (Besairie, 1970; Coffin & Rabinowitz, 1988; Storetvedt *et al.* 1992; Luger *et al.* 1994), with the bulk of the activity during the Late Cretaceous. This coincides with the separation and early drifting of India from Madagascar because of the opening of the Mascarene basin, as registered in the Seychelles block tholeiitic basalts (*c.* 82–65 Ma; Plummer 1995). Storetvedt *et al.* (1992) have reported K–Ar ages of 94.5 ± 1.2 Ma for dolerite dykes from the east coast of Madagascar, coincident with the earliest phase of Cretaceous magmatism on the island. On the basis of stratigraphic constraints, the main magmatic event occurred between 90 and 74 Ma; extensive tholeiitic and alkaline basalts may have blanketed most of the island but are now principally preserved along the east and west coasts and offshore (Mahoney *et al.* 1991). The volcanism may be diachronous, younging towards the south.

In Late Cretaceous and Tertiary times India migrated rapidly northwards, with sea-floor spreading taking place in the Mascarene basin rather than in the existing Mozambique basin, resulting in the separation of Magagascar from India (Storey 1995). An extensive flood basalt event at 88 Ma is attributed to the influence of the Marion plume (Storey *et al.* 1995). After about 63 Ma spreading ceased in the Mascarene basin but was replaced by a spreading system, the Carlsberg Ridge, that split the Seychelles away from the Indian mainland and created the eastern part of the Somali basin (White & McKenzie 1989). The eruption of the Deccan continental flood basalt province at 69 65 Ma (Hooper 1990) has been related to the migration of the northward-moving Indian microplate over the upwelling Réunion mantle plume.

African intra-plate domain

Central African Rift System and Cameroon Volcanic Line. In the Southern Benue Trough Cenomanian to Santonian (97–81 Ma) alkaline igneous activity includes basalts, dolerites, phonolites, trachytes, tephrites, rhyolites and lamprophyres, mainly as high-level intrusions (Maluski *et al.* 1995). This is followed by a second, again dominantly subvolcanic, magmatic phase of Late Maastrichtian to Eocene (68 49 Ma) age, which changes from alkaline to tholeiitic with decreasing age. The oldest Stage IV activity in the Southern Benue is the Mount Ikuyen rhyolite dome, dated by the Rb–Sr method at 113 ± 3 Ma (Umeji & Caen-Vachette 1983). There was little magmatic activity in the Northern Benue Trough at this time apart from the 106 Ma basalts of Gwol (Maluski et al, 1995).

In northern Cameroon and southwestern Chad basaltic dykes have K Ar ages ranging between 43 and 87 Ma (R. Guiraud & M. Wilson, unpublished data). In southern Chad, a dolerite sill, dated at 52–56 Ma, has been drilled in the Bongor basin, and basaltic sills of 97–101 Ma in the Doseo basin (Genik 1992). Some rhyolitic and basaltic dykes and dolerite sills, ranging in age between 85 and 95 Ma, were drilled in the Ténéré trough (Genik 1992). Further north, alkali basalts dated at 99 ± 4.5 Ma outcrop in the Dor El Goussa fault zone of southwestern Libya (Massa 1988).

The 700 km NE–SW trending Cameroon Volcanic Line to the southeast of the Benue Trough

straddles the West African continental margin and is characterized by Maastrichtian–Recent alkaline magmatism. It is partly superimposed upon a pre-existing fracture zone, the Central African Shear Zone, which cuts across a broad post-Cretaceous uplift, the Adamawa Uplift. Magmatic activity has been reactivated several times along the length of the line. From the Maastrichtian to the end of the Eocene (73–35 Ma) anorogenic ring complexes of granite and syenite, with less abundant gabbro and occasional remnants of trachyte and rhyolite were emplaced (Fitton 1987; Déruelle *et al.* 1991). In north and central Cameroon these are generally older (73–60 Ma) than in central and south Cameroon (45–35 Ma), although there are insufficient data to confirm space–time relationships. Two main periods of emplacement can be distinguished at 60 Ma and 35–40 Ma. According to Moreau *et al.* (1987), the Cameroon Line corresponds to a bundle of 'en echelon' megatension gashes associated with Cenozoic left lateral transcurrent movement along the Central African Shear Zone.

Sudan. In the Blue Nile rift of Sudan, Wycisk *et al.* (1990) noted the existence of volcanic activity at *c.*80 and 38 Ma. In southern Sudan, alkaline basalts dated at 105–95 Ma are known from oil wells in the Muglad Trough (Reynolds, 1993) and a dolerite sill of 82 ± 8 Ma (McHargue *et al.* 1992), whereas Senonian andesitic tuffs were found in the central Melut basin (McHargue *et al.* 1992). Anorogenic complexes associated with the Aswa fault zone range between 140 and 110 Ma (Reynolds, 1993).

Nilotic province. In southeastern Egypt and northeastern Sudan several fields of magmatic activity are known. Magmatism appears to be continuous from the Early Cretaceous (or older) up to the Mid-Eocene (Ressetar *et al.* 1981; Vail 1989; Meneisy 1990).

In northeast Sudan the Umm Shibrick complex has an Rb–Sr isochron age of 94 ± 16 Ma, whereas further south in the Bayuda Desert ring complexes have yielded ages of 74–62 Ma (Cahen *et al.* 1984). Small shallow intrusions (dykes, plugs), flows, pyroclastic deposits and some ring complexes with K–Ar and Rb–Sr ages of 48–40 Ma (Eocene), occur sporadically in the Jebel Uweinat area (Cahen *et al.* 1984; Franz *et al.* 1987; Schandelmeier *et al.* 1987*a*, *b*; Meneisy, 1990). To the northeast in Gilf Kebir 80 Ma basalts occur (Meneisy 1990). In the Delgo area of Sudan, north of the Humar rift in the Nubian Desert, Franz *et al.* (1993) have described a 200 km × 150 km igneous province (87–47 Ma) containing volcanic rocks (mainly basalts, but also trachyte, phonolite and ignimbrite), subvolcanic rocks (mainly felsic dykes, minor basaltic dykes) and syenite intrusions, associated with an uplift of the Late Proterozoic basement.

The 100–80 Ma Wadi Natash–Aswan field of southern Egypt (Cahen *et al.* 1984; Franz *et al.* 1987; Schandelmeier *et al.* 1987*a*,*b*; Saradeth *et al.* 1989; Vail 1989) extends from near the Red Sea to west of the Nile. Over most of the field igneous activity is recorded by subvolcanic to hypabyssal intrusions (plugs, dykes and ring complexes; Vail 1993). The absence of volcanic rocks from most of the field and the general presence of hyperbyssal intrusions strongly suggests that there has been widespread uplift and erosion. Most of the volcanic rocks and intrusions are of alkali basalt although more differentiated compositions are also present.

Stage V: Late Eocene (41 Ma)–Recent

During Stage V (Fig. 7) magmatic activity became widespread in Africa on a regional scale and extensive basaltic volcanic fields formed in north Africa and Arabia. This major volcanic flare-up is recognized across both the European and African margins of Tethys and may reflect a fundamental reorganization of the convection system within the upper mantle associated with the Alpine–Himalayan collision. Major phases of volcanism occur in the Early Miocene and in the Late Miocene. Cenozoic magmatism was relatively rare before about 30 Ma. The volcanic fields are generally concentrated in Pan-African mobile belt zones which have experienced tectonothermal events within the past 650 Ma; these generally have higher heat flow and thinner lithosphere than the adjacent cratons. In some instances, volcanism is closely associated with zones of earlier Cretaceous rifting (e.g. Benue Trough). Many of the volcanic fields, however, lie outside the Mesozoic rift basins (Guiraud & Bellion 1995).

A new rifting regime in East Africa (Red Sea, Gulf of Aden, Ethiopia–Kenya), Sudan and Ténéré (Niger), is marked by widespread alkaline and tholeiitic mafic magmatism. Extensive outpourings of tholeiitic flood basalts in Yemen and Ethiopia are undoubtedly related to the activity of mantle plumes. Domally uplifted areas within the African plate (e.g. Hoggar, Tibesti, Jebel Marra, Adamawa, Biu Plateau) are also volcanically active and may be plume related. Along the West African margin alkaline volcanism occurs in the Cape Verde Archipelago,

Canary Islands and Madeira, and onshore in the Cape Verde Peninsula. Subduction and diachronous continent–continent collision along the Zagros–Bitlis suture, initiated in the latest Cretaceous (Alavi 1994), resulted in calc-alkaline volcanism along an arcuate zone from Iran to Turkey, followed by Miocene–Quaternary alkaline volcanism (Yilmaz 1990; Seyitoglu & Scott 1992).

The bulk of the magmatism appears to be associated with extension within the Alpine chain, forelands and intra-plate domains postdating a major phase of Aquitanian–Burdigalian (*c.* 20 Ma) compression induced by the Alpine collision. Major fault zones, for example, the E–W trending Guinean–Nubian lineaments (Guiraud *et al.* 1985), the NW–SE trending Aswa–Tibesti Fault Zone and the N–E trending Trans-Saharan Fault Zone (Maurin & Guiraud 1993), appear to exert a strong control on the location of the magmatic activity, which is particularly common in areas in which two or more differently oriented crustal lineaments or faults intersect (e.g. Hoggar). Partial melting appears to be triggered by adiabatic decompression of upwelling asthenospheric mantle.

West African margin

An extensive magmatic province extends along the West African continental margin from the Madeira Archipelago south to the latitude of Guinea. The individual magmatic areas are located in the transition zone between continental and oceanic crust and may be associated with Atlantic transform fault zones. Halliday *et al.* (1992) have suggested that the mantle source of the magmas may be oceanic lithosphere enriched at the time of continental break-up.

In the Canary Islands the main phase of subaerial volcanism began between 15 and 20 Ma ago and continues to the present day (Ancochea *et al.* 1990). Volcanic activity appears to have occurred in pulses on the different islands of the group. On Gran Canaria there was an intense shield-building stage *c.*14 Ma, whereas in Tenerife the bulk of the volcanism has occurred in the last 7 Ma. On Fuerteventura basaltic dykes were intruded between 48 and 20 Ma (Féraud 1981; Le Bas *et al.* 1986).

The Cape Verde Archipelago, located 500 km off the west coast of Africa, includes ten major volcanic islands underlain by uplifted Late Jurassic oceanic crust (Gerlach *et al.* 1988). Magmatic activity is mostly Mid-Miocene–Recent (Mitchell *et al.* 1983), although activity may have occurred on Maio as early as the Oligocene. Historical volcanism has occurred on the islands of Fogo and Brava at the SW end of the archipelago. The Cape Verde Rise is one of the highest oceanic swells in the world, rising over 2000 m above the adjacent ocean floor. Courtney & White (1986) considered that the dynamic uplift of the swell is caused by an ascending mantle plume. The magmas are alkaline mafic (basanites, alkali basalts, melilitites) and their differentiates. In the Cape Verde Peninsula (Senegal) several magmatic events, of undersaturated basic alkaline type, occur between 36 and 1 Ma (Crevola *et al.* 1994).

North African margin

Neogene magmatic activity occurs along the whole western Mediterranean margin, from Morocco to Tunisia. This is clearly linked geodynamically to the Alpine collision and to the subsequent opening of the Western Mediterranean basin. It exhibits many similarities to contemporaneous magmatism in the Betic Cordillera of Southern Spain (Hernandez *et al.* 1987). Bellon (1981), on the basis of K–Ar age determinations, considered that there were four distinct periods of magmatic activity, at 30–15 Ma, 15–10 Ma, 10–5.3 Ma and 5–1.5 Ma. It is doubtful, however, whether such a detailed subdivision would hold if samples were reanalysed using the more reliable ^{40}Ar–^{39}Ar technique.

The Atlas system of North Africa is an active, 2000 km long, intracontinental mountain belt which developed in the foreland of the Cenozoic Alpine collision. Both the Middle and High Atlas are inverted Mesozoic rift systems. Uplift of the Middle Atlas began in the Neogene, probably in the Late Miocene. The NW flank of the Middle Atlas, the so-called Tabular Middle Atlas, is covered by a veneer of Quaternary (1.5–0.5 Ma) alkali basalts and basanites (Morel & Cabanis 1993; Gomez *et al.* 1996). Basaltic magmatism also occurs on the High Moulouya Rise on the SW flank and locally within the folded Middle Atlas and further to the west in the Moroccan Meseta. Du Dresnay (1988) noted that the volcanic centres are aligned in a NNW–SSE direction parallel to the trend of the present-day maximum principal stress field.

Calc-alkaline magmatism appears to have initiated in northeastern Algeria by the Early Miocene (*c.* 25 Ma) and subsequently extended all along the margin (Girod & Girod 1977). Magmatism has been continuous to the Quaternary, becoming progressively more alkaline with time (Bellon 1981). Belanteur *et al.* (1995), on the basis of K–Ar ages supported by micropalaeon-

tological data, have provided evidence for two calc-alkaline magmatic episodes, at 16–15 Ma and 14–12, Ma within the narrow coastal strip east of Algiers. Along the northwestern coast of Algeria Louni-Hacini *et al.* (1995) have obtained K–Ar ages of 11.7–7.2 Ma for calc-alkaline to shoshonitic andesites and dacites, post-dated by 4 Ma alkali basalts. There is some evidence for an even older alkaline magmatic phase in northern Morocco involving the emplacement nephelinite sills and dykes (aiounites and mestigmerites) dated at 57–37 Ma (Michard, 1976). Nephelinites with a K–Ar age of 35 Ma are known on the northern margin of the High Atlas (Harmand & Cantagrel, 1984). The Miocene calc-alkaline episode is considered by some workers to be post-collisional (Hernandez & Lepvrier, 1979), whereas others link it directly to subduction (Tricart *et al.* 1994). Zeck *et al.* (1992) proposed that subduction in the western Mediterranean occurred in Cretaceous times followed by slab detachment in the Tertiary. Monié *et al.* (1992) have reported ages of 15–17 Ma for granitic intrusions in the Edough massif, Algeria, which they related to a major extensional episode in the Early Miocene which may be associated with slab detachment.

The central Mediterranean Hyblean–Maltese Platform is part of the Pelagian block of the African plate and occupies a critical site between two neotectonically active structural zones (Pedley & Grasso 1992). To the south, in the Sicily Channel, lies the Malta Graben, which is part of the larger Pantelleria rift system. To the north lies a broad thrust belt generated by Africa–Europe plate convergence. Early Miocene NE–SW oriented highs are associated with volcanism from Late Tortonian (*c.* 7 Ma) to recent times. In northwest Libya (Gharian) basalts have been dated at 30–12 Ma (Cahen *et al.* 1984), but magmatism may have started as early as Early Eocene.

North and East Arabian margin

Widespread, extension-related, intra-plate alkali basaltic volcanism of Late Miocene–Pliocene to Recent age occurs throughout the Middle East in Israel, Turkey, Syria and eastward within the Zagros collision zone (Garfunkel 1989; Sawaf *et al.* 1993; Sengör *et al.* 1993; Alavi 1994). East of the Levant Fault Zone, the 50 000 km^2 Jebel Druze–Golan volcanic field extends some 500 km along a NW trend (Giannerini 1988). The southern part comprises mostly Middle Miocene volcanic rocks (9–13 Ma) whereas the northern part is Pliocene to Quaternary in age. In NE Oman, Shackleton *et al.* (1990) have mapped the occurrence of localized Tertiary basaltic volcanism, probably linked with the NE–SW Masirah fault line. Southwest of Muscat akali olivine basalt dykes intrude Paleocene sediments (Al-Harthy *et al.* 1991).

East African margin

Extensive flood basalts of Late Oligocene–Early Miocene and locally Pliocene age occur in the Mudugh Basin and Somali Coastal Basin (Piccoli *et al.* 1986; Bosellini 1989). On Madagascar strong Oligocene to Recent volcanic activity affects all the island (Coffin & Rabinowitz 1988). The Comores Archipelago is a WNW trending, 5–0 Ma volcanic lineament at the northern entrance to the Mozambique Channel (Nougier *et al.* 1986), which may be plume related.

Red Sea province

Magmatic activity in Saudi Arabia, associated with the early opening of the Red Sea, produced voluminous intra-plate alkali basalts between 27 and 28 Ma and tholeiitic to transitional dyke swarms and plutons parallel to the Red Sea rift axis between 21 and 24 Ma (Coleman & Vaughn McGuire, 1988; Féraud *et al.* 1991; Sebai *et al.* 1991b). NW–SE trending dykes are also known from the Eastern Desert of Egypt, the Gulf of Suez and Sinai (Eyal *et al.* 1981; Baldridge *et al.* 1991). The tholeiitic magmatic event affected a linear zone some 1700 km long along the Red Sea margins. Its age is comparable with the emplacement age of the Zabargad Island peridotite in the Red Sea at 18–21 Ma, based on U–Pb zircon dating (Oberli *et al.* 1987). Lotfy *et al.* (1995) obtained ^{40}Ar–^{39}Ar ages of *c.*22 Ma for basalts near Cairo, although the spectra are somewhat disturbed. Some basaltic sills or flows dated at 20–24 Ma have recently been drilled along the Red Sea coast of Sudan (Schroeder, pers. comm.). Late Oligocene basalt flows have been reported from this area by Montenat *et al.* (1990).

Extensive alkaline to transitional basaltic magmatism occurs throughout western Saudi Arabia (Camp *et al.* 1991, 1992), ranging in age from 11 Ma to Recent. Holocene alkaline basaltic volcanism occurs within a zone of highly attenuated continental crust in the axial zone of the southern Red Sea (Rogers 1993) in the Zubair and Hanish-Zukur island groups and there is active tholeiitic basalt volcanism on the island of Jebel-at-Tair.

The distribution of Oligocene to Holocene alkaline volcanism is asymmetric about the Red Sea, as is the pattern of basement uplift. North of Ethiopia, alkaline volcanism is primarily confined to the Arabian peninsula, which is also a little higher than the Nubian side (Bohannon *et al.* 1989; Bord & Bertrand, 1995). Uplift and lithospheric thinning adjacent to the Red Sea rift began 5–10 Ma after rifting. This suggests that the Red Sea is a passive rift that formed because of 2–D plate motions, rather than as a consequence of mantle upwelling. A possible cause for the stress in the plate might have been the change in plate motions in the Indian Ocean that resulted from the collision of India with Eurasia (McGuire & Bohannon 1989). The Oligocene–Recent evolution of the stress field in the western border of the Arabian plate, deduced from the analysis of dyke swarms and volcanic cone alignments, was described by Giannerini (1988) who demonstrated a three-stage clockwise rotation in response to the tectonic evolution of the Gulf of Aden, Red Sea, Dead Sea and Palmyride zones.

Yemen

The onset of basaltic continental flood volcanism in Yemen is well constrained by ^{40}Ar–^{39}Ar dating at between 31 and 29 Ma (Baker *et al.* 1996*a*). This is followed by bimodal basaltic-rhyolitic volcanism from 29 to 26 Ma. The relatively short duration of the volcanic episode (< 5 Ma) contrasts with the wide range (> 50 Ma) of K–Ar ages previously obtained for this province. Baker *et al.* (1996a) considered that only 25% of the K–Ar ages previously obtained for the Yemen volcanic rocks are reliable and that most samples have disturbed Ar systematics. Clin (1991) reported K–Ar ages of 8–13 Ma for rhyolites and ignimbrites from the Afar triple junction, indicating that volcanism continued for over 20 Ma in this region.

Continental flood volcanism in Yemen was preceded by an episode of broad uplift which resulted in a change from Palaeocene shallow marine sedimentation to the development of lateritic paleosols (Baker *et al.* 1996*a*). The sequence of events (surface uplift, flood magmatism (31–26 Ma) and subsequent extension (26–20 Ma)) in Yemen is consistent with the involvement of a mantle plume at the Afro-Arabian triple junction. Sr–Nd–Pb isotopic studies of continental flood basalts from Ethiopia, Djibouti and Yemen suggest that magma generation occurred within the upwelling Afar mantle plume, although magmas have interacted with the lithosphere en route to the surface (Vidal *et al.* 1991; Chazot & Bertrand, 1993; Baker *et al.* 1996*b*). The location of the plume axis at the Afro-Arabian triple junction is consistent with the large volumes of magma erupted there in contrast to the rest of the Gulf of Aden and Red Sea rift margins. An interesting problem is why flood volcanism in Yemen apparently ceased during upper-crustal extension, which should have actually triggered further melting, as it did in Ethiopia.

East African Rifts

The East African rift system comprises two main segments, the Kenyan or Gregory rift and the Main Ethiopian rift. Faults bounding the main rifts transect older Mesozoic rift basins of the Central African rift system at the borders of Ethiopia, Kenya, Sudan and Uganda in the Turkana Depression (Fig. 1; Ebinger & Ibrahim, 1994). Both rifts are situated on topographic plateau 800–1000 km in diameter, which appear to be dynamically supported by mantle convection (Ebinger *et al.* 1989*a*). The East African rift lies in the middle of the African continent which is entirely surrounded by mid-ocean ridges and the Alpine continental collision zone to the north. As a consequence, East Africa is actually under compression, dominated by ridge push from the Red Sea–Gulf of Aden spreading centres (Bosworth *et al.* 1992).

Bonavia *et al.* (1995) noted that the magmatism becomes progressively younger to the southwest, consistent with the idea that the rift is propagating southward. They considered that the magmatic activity of the rift is related to the NE migration of the African plate over a deep mantle plume which initially impinged beneath Nubia–Arabia at 84 Ma and is now under the Tanzania craton. Variants of this model have previously been discussed by Camp & Roobol (1992) and Schilling *et al.* (1992).

Main Ethiopian rift. The Ethiopian province is a classic example of plume-related magmatism in an area of active extension (Mohr & Zanettin 1988), above the Afar mantle plume. Stratigraphic studies and radiometric age determinations indicate that there are two main phases of magmatic activity in Central Ethiopia, one pre-rift and the second syn-rift (Behre *et al.* 1987; Gasparon *et al.* 1993). During the first phase (50–15 Ma) extensive fissure-fed flood basalt eruptions were succeeded by ignimbrites and the building of several shield volcanoes. Ebinger *et al.* (1993*a*) used a combination of K–Ar and ^{40}Ar–^{39}Ar dating to distinguish a widespread episode of flood basaltic volcanism at 45–35 Ma,

with later episodes at 34–28 Ma and 18–12 Ma affecting smaller regions. The second phase (15–0 Ma) consists mainly of silicic volcanic and pyroclastic rocks, and subordinate basalts. There was a climax of volcanic activity between 9.5 and 3 Ma associated with central volcanoes developed along rift parallel faults. The Miocene to Recent basalts are more alkaline than the tholeiitic Oligocene and Eocene flood basalts. Baker *et al.* (1996*a*), on the basis of a technique for screening previously published K–Ar age data for their reliability, have concluded that much of the published whole-rock K–Ar data for the Ethiopian flood basalt province is erroneous. They have inferred two phases of flood volcanism in Ethiopia and Eritrea at 38–30 Ma and *c.*20 Ma. The older phase is equivalent to that in Yemen whereas the younger phase is related to Red Sea–Gulf of Aden rifting and the intrusion of tholeiitic dyke swarms parallel to the Red Sea (Féraud *et al.* 1991; Sebai *et al.* 1991b). The limited ^{40}Ar–^{39}Ar data for the Ethiopian flood basalt province gives an age range of 33–28 Ma for samples from within 100 m of the base of the volcanic sequence (Drury *et al.* 1994).

Extension across the main Ethiopian rift occurred between 18 and 14 Ma (Ebinger *et al.* 1993*a*,*b*) whereas extension in the Red Sea may have commenced at 30–34 Ma (Omar & Steckler, 1995). Little or no extension accompanied the first and most voluminous phase of flood basalt volcanism. Pliocene eruptive centres, in contrast, are restricted to basins bounded by N–S faults and Quaternary volcanic centres to seismically active basins bounded by NNE and N–S faults.

Stewart & Rogers (1996) considered that the pre-rift basalts were primarily derived by partial melting of the mantle lithosphere which was heated by conductive heat transport from the mantle plume; subsequent melting was triggered by adiabatic decompression within the plume head as the lithosphere thinned under extension, and the resultant syn-rift basalts were largely plume derived.

Kenya (Gregory) rift. Volcanism in Kenya began about 30 Ma ago, spreading progressively southwards from Lake Turkana in northern Kenya (Kampunzu & Mohr 1991; Latin *et al.* 1993), and continues to the present. Magmatic activity within the rift zone is bimodal (60% basic, 40% felsic) and predominantly alkaline. There is a decrease in the alkalinity of the basaltic rocks with time and, during the Neogene, a north to south increase in alkalinity. Basaltic activity on the western flanks of the rift began in the Miocene and has been strongly alkaline, including basanites, nephelinites, melilitites and carbonatites. On the eastern flank of the rift the volcanism is Plio-Quaternary in age and somewhat less alkaline than on the western flank (nephelinites, basanites and alkali basalts). The total volume of basalt generated over a 30 Ma period has been estimated at over 900 000 km^3 (Latin *et al.* 1993), consistent with a mantle plume, similar to that beneath Hawaii, decompressing beneath thinned lithosphere. Seismic tomography (Green *et al.* 1991) suggests that the asthenospheric upper mantle may upwell to depths of 70 km beneath the rift. The large volumes of silicic volcanic rocks suggest that large volumes of mafic magma must have been added to the lithosphere beneath the rift. In the Turkana area and the northern part of the Kenya rift, phonolitic activity occurred at 9–7 Ma (Baker *et al.* 1971; Tiercelin *et al.* 1987).

Western rift (Zaire). The western branch of the East African rift in Uganda and Zaire developed in a sigmoidal shape (Fig. 1) within Proterozoic mobile belts which surround the Tanzanian Archaean craton. Magmatic activity is characterized by strongly ultrapotassic magmas, which are most probably derived by partial melting of enriched domains within the lithospheric mantle (Rogers *et al.* 1992). Sedimentation started in the Upper Miocene; throughout the Cenozoic, volcanic deposits are interbedded with lacustrine and fluviatile sediments, which together with K–Ar and ^{40}Ar–^{39}Ar dating provide good age constraints for the stratigraphic succession (Ebinger *et al.* 1989*b*). In Zaire–Burundi (Kivu) and Tanzania (Rungwe) volcanism is not older than 10 Ma (Pasteels *et al.* 1989).

African intra-plate domain

Egypt–Sudan. In the Jebel Uweinat area intrusive complexes of alkali granite, syenite and carbonatite, and phonolite plugs may have been emplaced between 46 and 33 Ma, on the basis of available K–Ar data (Vail 1989). To the northeast, olivine basalt plugs in the Gilf Kebir area gave K–Ar ages of *c.*38 Ma (Schandelmeier *et al.* 1987*a*). Further south, in northernmost Sudan, similar plugs gave 26–20 Ma K–Ar ages (Schandelmeier *et al.* 1987*a*). The location of these magmatic centres appears to be controlled by the faults of the E–W trending Guinean–Nubian lineaments (Guiraud *et al.* 1985).

The Darfur volcanic province in western Sudan is an area 400 km × 100 km of Tertiary–Holocene volcanic and sub-volcanic activity

associated with a major Late Cretaceous domal uplift of the basement (Franz *et al.* 1994). On the basis of available K–Ar age determinations, Franz *et al.* (1994) demonstrated that magmatic activity commenced at 36 Ma at the centre of the dome. The most important phases of magmatism ocurred in the Marra Mountains (14–10 Ma) and the Tagabo Hills (16–11 Ma). Volcanism resumed at *c.* 7 Ma in the Meidob Hills and at 4.3 Ma in the Marra Mountains, and continued until the late Quaternary. The formation of the Deriba Crater of the Jebel Marra volcano (2 Ma to Holocene; Davidson & Wilson 1989) represents the climax of the second volcanic phase. The magmas range in composition from basanite to phonolite–trachyte. In the nearby Muglad basin some pyroclastic rocks of *c.* 4 and 2 Ma could be linked with the activity of Jebel Marra (Wycisk *et al.* 1990; Wilson & Guiraud 1992).

Tibesti–Jebel Al Haruj. The Tibesti massif in northern Chad and Jebel Al Haruj in western Libya are areas of domally uplifted basement rocks capped by Tertiary–Quaternary volcanic rocks. The Tibesti massif has been the site of intense volcanic activity from Middle Eocene to Quaternary times (Vincent 1970). Although the timing of initiation of basement uplift is not well constrained, it is thought to be pre-Early Cretaceous. The initial phase of activity in Tibesti involved the eruption of mildly alkaline plateau basalts and their differentiates. In the central part of the massif these are surmounted by four large shield volcanoes which erupted subalkaline basalts and their differentiates. These were followed by large-scale eruptions of alkali rhyolitic ignimbrite. The final phase of Quaternary volcanism involved the eruption of silica-poor potassic alkali basalts and their differentiates. Jebel Al Haruj may have a similar volcanic history to Tibesti. Both areas are, however, poorly known and have received limited attention since the original fieldwork of Vincent (1970) on Tibesti.

Air-Ténéré-Tefidet. Neogene–Quaternary magmatism in eastern Niger has been related to intra-plate extension along NW–SE trending structural lineaments which extend from Hoggar to Lake Chad (Wilson & Guiraud 1992). Much of the activity is concentrated in an area in which these lineaments intersect the E–W trending Guinean–Nubian lineaments (Guiraud *et al.* 1985). In southern Air and central Ténéré volcanism began in the Oligocene (Pouclet *et al.* 1994). The magmatism is predominantly alkaline involving nephelinites, basanites, alkali basalts, transitional basalts and their differentiates. Two volcanic phases have been recognized on the basis of geomorphology and K–Ar dating. During the Oligocene to early Miocene (35–21 Ma) dykes of nephelinite and domes of trachyte and phonolite were intruded. From the Late Miocene to the Pleistocene (9–1.5 Ma) dykes, necks and flows of nephelinite and basanite were emplaced, along with domes of evolved lavas. The magmatic activity is similar to that of Hoggar and the Cameroon Line, with a near-synchronous onset of volcanism at 35 Ma in all three areas. The new magmatic cycle may be linked to a major post-Eocene change in the orientation of the principal stress regime from NE–SW to NW–SE in response to collision events in the Alpine belt.

Hoggar. Domal basement uplift (1000 km in diameter) of the Hoggar swell has been attributed to thermo-mechanical erosion of the lithosphere above a mantle plume during the Cretaceous (Dautria & Lesquer 1989; Aït Hamou & Dautria 1994), although the timing is not well constrained. Magmatism commenced in the Mid Eocene with the eruption of voluminous (300–700 m thick; 1000 km^3) fissure-fed transitional tholeiitic basalts in the centre of the swell (K–Ar ages of 44–35 Ma), followed by emplacement of annular intrusive complexes (35–22 Ma). After a period of quiescence, Mio–Pliocene–Quaternary eruptions of basanite, nephelinites and alkali basalts and their differentiates occurred in peripheral areas (Dautria & Girod, 1991). The Miocene–Quaternary volcanism of the Hoggar indicates the important control reactivated basement faults may have on the location of volcanism (Guiraud *et al.* 1987; Dautria & Lesquer 1989; Wilson & Guiraud 1992).

Mali. Some enigmatic rocks of the Lake Faguibine area, called 'daounites', are supposed to be of volcanic origin and could provide evidence for recent magmatic activity linked with the play of the Guinean–Nubian lineaments (Guiraud *et al.* 1985; El Abbass *et al.* 1993).

*Cameroon Volc*anic Line. The Cameroon Line is a 1600 km long alignment of oceanic and continental volcanic massifs, comprising alkali basalts, basanites and their differentiates, and anorogenic plutonic complexes extending N30 from Pagalú island to Lake Chad (Fitton 1987; Déruelle *et al.* 1991). Several models have been proposed to explain the origin of the Cameroon Line. These include membrane tectonics (Freeth 1979), a reworking of a Mesozoic plume head (Halliday *et al.* 1990; Wilson 1992) and rejuvena-

tion of a major translithospheric fracture zone (Moreau *et al.* 1987). Lee *et al.* (1994) have recently proposed that the magmatism results from a sublithospheric enriched hot zone, periodically fed by deep mantle plumes, part of which represents reactivated mantle previously enriched during the Mesozoic break-up of the Equatorial Atlantic above the St Helena plume. Alkaline volcanic activity commenced around 35 Ma and has continued intermittently to the present day (Fitton 1987). There are 12 major volcanic centres, of which the only currently active volcano is Mount Cameroon, situated on the boundary between oceanic and continental volcanic sectors. Both the oceanic and continental sectors appear to have been active since the end of the Cretaceous and there is no evidence for any consistent migration of volcanic activity with time along the line. Two basaltic plateau Biu and Adamawa, mark the continental termination of the volcanic line. The Adamawa Plateau is an asymmetrical horst upon which two large volcanoes, Tchabal Nganha and Tchabal Djinga, are constructed (Nono *et al.* 1994). Volcanic rocks from Tchabal Nganha give K–Ar ages of 7.2–9.8 Ma.

Benue Trough–Biu Plateau. During the Tertiary basaltic magmas were emplaced throughout the Benue Trough with the greatest concentration in the northeast (trachytes and phonolites, 22–11 Ma; Maluski *et al.* 1995). More than 500 volcanic necks occur in this region, associated with the eruption of extensive alkali basalt lava flows on the Biu Plateau (23–7 Ma and 3–0 Ma; Guiraud *et al.* 1987). Volcanism of this age also occurs on the nearby Jos Plateau and in the Cameroon Volcanic Line. In the Biu Plateau the distribution of volcanic necks appears to be controlled by a N–S alignment of Tertiary faults. Intrusives of 41 Ma have been mentioned in the Kerri-Kerri Formation of the Gongola Branch (N. Benue) by Adegoke *et al.* (1986).

Summary

The level of magmatic activity within the Afro-Arabian margin of Tethys has clearly varied considerably during the past 250 Ma, related to changing patterns of mantle convection and to changing stress fields within the African plate (Guiraud & Bellion 1995; Janssen *et al.* 1995). On the basis of our compilation of the ages of Mesozoic–Cenozoic magmatic activity during five time stages (Stage I, 256–208 Ma; Stage II, 208–157 Ma; Stage III, 157–120 Ma; Stage IV, 119–42 Ma; Stage V, 42 Ma–Recent) there appear to be two major peaks in activity (210–200 Ma and 30 Ma–Recent), which may be attributable to partial melting within thermally anomalous mantle plumes upwelling beneath Africa–Arabia. Elsewhere, magmatism may be dominantly extension related, associated with the development of the Neo-Tethyan margin, or locally subduction related associated with the Alpine collision.

A widespread phase of Liassic tholeiitic flood basalt volcanism (Stage II, 210–200 Ma) is closely associated with rifting and continental break-up in the Central Atlantic and the Eastern Mediterranean. The emplacement of high-degree partial melts (tholeiites) within the West African craton provides conclusive evidence for the involvement of a thermally anomalous mantle plume in this initial phase of Gondwana break-up. The voluminous Karoo tholeiitic flood basalt event in southern Africa is, in part, synchronous, although new data indicate that the peak of magmatic activity may actually be as young as 182 Ma.

The Early Cretaceous is recognized globally as a time of intense mantle plume activity, of which the greatest expression in the African–South American plates is the upwelling of the Tristan plume beneath Brazil, generating the extensive Parana flood basalt province. Continental break-up within the South Atlantic occurred shortly after the peak of the Parana volcanism. Within the Afro-Arabian margin of Tethys, we suggest that Early Cretaceous plume-related magmatism occurs in the Levant and in the Equatorial Atlantic. The Mesozoic St Helena plume may have played an important role in the opening of the Benue Trough and continental break-up in the Equatorial Atlantic, weakening the base of the lithosphere over a broad zone by conduction of heat and transport of volatiles from the plume head. There is, however, no voluminous flood basalt event in this area, suggesting that the upwelling plume may have become cooled by entrainment of upper mantle before its impact on the base of the plate.

Late Oligocene to Recent magmatism within the African plate is widespread and reflects a change in the plate tectonic regime induced by the Alpine collision. Magmatism is frequently associated with domal uplifts of the basement which vary from 500 to over 1000 km in diameter. Available geophysical data suggests that these uplifts are dynamically supported by the upwelling of hot asthenospheric mantle beneath the base of the plate. Large-scale mantle plumes upwelling from the deep mantle appear to be the cause of the voluminous flood basalt volcanism within Ethiopia and Yemen, which closely

precedes the opening of the Red Sea and Gulf of Aden.

Certain areas within the African plate (e.g. Sudan, Air) are notable for the longevity of their magmatic activity. In Sudan there has been an almost continuous record of intrusive and extrusive activity for the past 250 Ma, although distinct peaks in activity parallel those in the rest of the plate. Focusing of magmatic activity in both Sudan and Air may be related to their proximity to a system of E–W trending deep basement faults, the Guinea–Nubian lineaments, which may channel magmas towards the surface. In other areas, such as the Hoggar massif, long-lived magmatism may also be focused by trans-lithospheric fault systems.

If we are to use the distribution of magmatic activity to provide constraints on mantle dynamic processes, the importance of obtaining high-quality ^{40}Ar–^{39}Ar ages for magmatic rocks must be emphasized. It is now clear that many K–Ar ages are erroneous and that when detailed ^{40}Ar–^{39}Ar studies are made of particular provinces the age range of the magmatic activity is drastically reduced. This also has important implications for the hydrocarbon industry as regional thermal gradients may be dramatically enhanced during major periods of magmatic activity and it is clearly important to constrain the timing of such thermal events.

Discussions with colleagues, too numerous to mention individually, have, over the years, contributed to our understanding of the magmatic evolution of the African plate. We thank them for their interest and encouragement in the pursuit of what turned out to be a massive task. Any errors and omissions are of course ours.

References

ADEGOKE, O. S., JAN DU CHENE, R. E., AGUMANU, A. E., BENKHELIL, J. & AJAYI, P. O. 1986. New stratigraphic, sedimentologic and structural data on the Kerri-Kerri Formation, Bauchi and Borno States, Nigeria. *Journal of African Earth Science*, **5**, 249–277.

AÏT HAMOU, F. & DAUTRIA, J. M. 1994. Le magmatisme cénozoique du Hoggar: une synthèse des données disponibles. Mise au point sur l'hypothèse d'un point chaud. *Bulletin du Service Géologique de l'Algérie*, **5**, 49–68.

AKPATI, B. N. 1978. Geological structure and evolution of the Keta Basin, Ghana, West Africa. *Geological Society of America Bulletin*, **89**, 124–132.

ALAOUANI, R. 1993. Les échanges chimiques dans une séquence siliceuse à reccurrences volcaniques durant la diagenèse et le métamorphisme. Exemple des radiolarites du Jebel Ichkeul (NE Tunisien). *In*: *14th Regional Meeting of Sedimentology, Marrakesh, 27–29 April*, 28.

ALAVI, M. 1994. Tectonics of the Zagros orogenic belt of Iran: new data and interpretations. *Tectonophysics*, **229**, 211–238.

AL-HARTHY, M. S., COLEMAN, R. G., HUGHES-CLARKE, M. W. & HANNA, S. S. 1991. Tertiary basaltic intrusions in the Central Oman Mountains. *In*: PETERS, Tj. *et al.* (eds) *Ophiolite Genesis and Evolution of the Oceanic Lithosphere*, Kluwer Academic, Dordrecht, Boston, 675–682.

ALMOND, D. C. 1992. Anorogenic magmatism in Northeast Africa. *In*: SALEM, M. J. (ed.) *The geology of Libya*. Elsevier, Amsterdam, 2495–2510.

ANCOCHEA, E., FUSTER, J. M., IBARROLA, E., *et al.* 1990. Volcanic evolution of the island of Tenerife (Canary Islands) in the light of new K–Ar data. *Journal of Volcanology and Geothermal Research*, **44**, 231–249.

ARARIPE, P. T. & FEIJO, F. J. 1994. Bacia Potiguar. *Bulletin Geosciences PETROBRAS*, **8** (1), 127–141.

ASMUS, H. E. 1984. Geologia da margen continental brasileira. *In*: SCHOBBENHAUS, C. *et al.* (eds) *Geologia do Brasil: explanatory text of geological map of Brazil and adjoining ocean floor including mineral deposits, 1:2 500 000*. DNPM, 443–472.

BAER, G., HEIMANN, A., ESHET, Y., WEINBERGER, R., MUSSETT, A. & SHERWOOD, G. 1995. The Saharonim Basalt: a Late Triassic–Early Jurassic intrusion in southeastern Makhtesh Ramon, Israel. *Israel Journal Earth-Sciences*, **44**, 1–10.

BAKER, B. H., WILLIAMS, L. A. J., MILLER, J. A. & FITCH, F. J. 1971. Sequence and geochronology of the Kenya rift volcanics. *Tectonophysics*, **11**, 191–215.

BAKER, J., SNEE, L. & MENZIES, M. 1996*a*. A brief Oligocene period of flood volcanism in Yemen: implications for the duration and rate of continental flood volcanism at the Afro-Arabian triple junction. *Earth and Planetary Science Letters*, **138**, 39–55.

BAKER, J. A., THIRLWALL, M. F. & MENZIES, M. A. 1996*b*. Sr–Nd–Pb isotopic and trace element evidence for crustal contamination of a mantle plume: Oligocene flood volcanism in western Yemen. *Geochimica et Cosmochimica Acta*, **60**, 2559–2581.

BALDRIDGE, W. S., EYAL, Y., BARTOV, Y., STEINITZ, G. & EYAL, M. 1991. Miocene magmatism of Sinai related to the opening of the Red Sea. *Tectonophysics*, **197**, 181–201.

BAUD, A., MARCOUX, J., GUIRAUD, R., RICOU, L. E. & GAETANI, M. 1993. Late Murgabian (266 to 264 Ma). *In*: DERCOURT, J., RICOU, L. E. & VRIELYNCK, B. (eds) *Atlas Tethys Palaeoenvironmental Maps. Explanatory Notes*. Gauthier-Villars, Paris, 9–20.

BAUDELOT, S., CHARRIERE, A., OUARHACHE, D. & SABAOUI, A. 1990. Données palynologiques nouvelles concernant l'Ordovicien et le Trias–Lias du Moyen-Atlas (Maroc). *Géologie Méditerranéenne*, **XVII**(3–4), 263–277.

BECHENNEC, F., LEMETOUR, J., RABU, D. BOURDILLON-DE-GRISSAC, CH., DE WEVER, P., BEURRIER, M. & VILLEY, M. 1990. The Hawasina nappes: stratigra-

phy, palaeogeography and structural evolution of a fragment of the south-Tethyan passive continental margin. *In*: ROBERTSON, A. H. F., SEARLE, M. P. & RIES, A. C. (eds) *The Geology and Tectonics of the Oman region*. Geological Society, London, Special Publications, **49**, 213–223.

BEHRE, S. M., DESTA, B., NICOLETTI, M. & TEFERRA, M. 1987. Geology, geochronology and geodynamic implications of the Cenozoic magmatic province in W and SE Ethiopia. *Journal of the Geological Society, London*, **144**, 213–226.

BELANTEUR, O., BELLON, H., MAURY, R. C., *et al.* 1995. Le magmatisme miocène de l'Est Algérois, géologie, géochimie et géochronologie ^{40}K–^{40}Ar. *Comptes Rendus de l' Académie des Sciences, Série IIa*, **321**, 489–496.

BELLIENI, G., MACEDO, M. H. F., PETRINI, R., *et al.* 1992. Evidence of magmatic activity related to Middle Jurassic and Lower Cretaceous rifting from northeastern Brazil (Ceará-Mirim): K/Ar age, palaeomagnetism, petrology and Sr–Nd isotope characteristics. *Chemical Geology*, **97**, 9–32.

——, PICCIRILLO, E. M., CAVAZANNI, G., *et al.* 1990. Low- and high-TiO_2 Mesozoic tholeiitic magmatism of the Maranhão basin (NE-Brazil): K/Ar age, geochemistry, petrology, isotope characteristics and relationships with Mesozoic low- and high-TiO_2 flood basalts of the Paraná basin (SE-Brazil). *Neues Jahrbuch für Mineralogie Abhand lungen*, **162**, 1–33.

BELLION, Y. 1989. *Histoire géodynamique post-paléozoque de l'Afrique de l'Ouest d'après l'étude de quelques bassins sédimentaires (Sénégal, Taoudenni, Iullemmeden, Tchad)*. CIFEG, Publ. occasionelles, **17**.

BELLON, H. 1981. Chronologie radiométrique (K–Ar) des manifestations magmatiques autour de la Méditerranée occidentale entre 33 et 1 Ma. *In*: WEZEL, F. C. (ed.) *Sedimentary Basins of Mediterranean margins*, Tectonoprint, Bologna, 341–360.

BELTRAMI, C. V., ALVES, L. E. M. & FEIJO, F. J. 1994. Bacia do Ceará. *Bulletin Geosciences PETROBRAS*. **8**, 117–125.

BENKHELIL, J., MASCLE, J. & TRICART, P. 1995 The Guinea continental margin: an example of a structurally complex transform margin. *Tectonophysics*, **248**, 117–137.

BERTRAND, H. & VILLENEUVE, M. 1989. Témoins de l'ouverture de l'atlantique central au début du jurassique: les dolérites tholéiitiques continentales de Guinée (Afrique de l'Ouest). *Comptes Rendus Hebdomadaires des Séances de l'Académie des Sciences, Serie II*, **308**, 93–98.

——, FÉRAUD, G. & MASCLE, J. 1993. Alkaline volcano of Paleocene age on the Southern Guinean margin: mapping, petrology, ^{40}Ar–^{39}Ar laser probe dating, and implications for the evolution of the Eastern Equatorial Atlantic. *Marine Geology*, **114**, 251–262.

——, MASCLE, J., VILLENEUVE, M., ROBERT, C., COUSIN, M. & LE GROUPE EQUAMARGE 1989. Le volcanisme de la marge sud guinéenne, implications pour l'ouverture de l'Atlantique équatorial: résultats de la campagne Equamarge II. *Comptes Rendus Hebdomadaires des Séances de l'Académie des Sciences, Série II*, **309**, 1703–1708.

BESAIRIE, H. 1970. Précis de géologie de Madagascar. *Service Géologique de Madagascar, Tananarive*, **36**.

BEST, J. A., BARAZANGI, M., AL-SAAD, D., SAWAF, T. & GEBRAN, A. 1993. Continental margin evolution of the Northern Arabian Platform in Syria. *Bulletin, American Association of Petroleum Geologists*, **77**, 173–193.

BIGARELLA, J. J. 1973. Geology of the Amazon and Parnaiba basins. *In*: NAIRN, A. E. M. & STEHLI, F. G. (eds) *The Ocean Basins and Margins, Vol. 1 The South Atlantic*. Plenum, New York, 25–86.

BLACK, R. & LIÉGEOIS, J.-P. 1993. Cratons, mobile belts, alkaline rocks and continental lithospheric mantle: the Pan-African testimony. *Journal of the Geological Society London*, **150**, 89–98.

BOHANNON, R. G., NAESER, C. W., SCHMIDT, D. L. & ZIMMERMANN, R. A. 1989. The timing of uplift, volcanism, and rifting peripheral to the Red Sea: a case for passive rifting? *Journal of Geophysical Research*, **94**, 1683–1701.

BONAVIA, F. F., CHOROWICZ, J. & COLLET, B. 1995. Have wet and dry Precambrian crust largely governed Cenozoic intraplate magmatism from Arabia to East Africa? *Geophysical Research Letters*, **22**, 2337–2340.

BORD, C. & BERTRAND, H. 1995. Géochimie du volcanisme alcalin récent d'Arabie Saoudite: signification dans le cadre du 'rifting' de la Mer Rouge. *Comptes Rendus Hebdomadaires des Séances de l'Académie des Sciences, Série IIa*, **320**, 31–38.

BOSELLINI, A. 1989. The continental margins of Somalia: their structural evolution and sequence stratigraphy. *Memorie Sci. Geol. Padova*, **XLI**, 373–458.

—— 1992. The continental margins of Somalia. *In*: WATKINS, J. S. *et al.* (eds) *Geology and Geophysics of Continental Margins*. American Association of Petroleum Geologists, Memoirs, **53**, 185–200.

BOSWORTH, W. 1992. Mesozoic and Early Tertiary rift tectonics in East Africa. *Tectonophysics*, **209**, 115–137.

——, STRECKER, M. R. & BLISNIUK, P. M. 1992. Integration of East African palaeostress and present-day stress data: Implications for continental stress field dynamics. *Journal of Geophysical Research*, **97**, 11851–11865.

BOUDJEMA, A. 1987. *Évolution structurale du bassin pétrolier 'triasique' du Sahara nord oriental (Algérie)*. Thèse, Université de Paris-Sud.

BOULLIN, J. P., KORNPROBST, J. & RAOULT, J. F. 1977. Données préliminaires sur le complexe volcano-sédimentaire de Rekkada Metletine (ex-Texenna), en Petite Kabylie (Algérie). *Bulletin de la Société Géologique de France*, **XIX**(4), 805–813.

BOULLIN, J. P. 1983. Nouvelles hypothèses sur le structure des Maghrébides. *Comptes Rendus Hebdomadaires des Séances de l'Académie des Sciences*, **296**, 1329–1332.

BUSSON, G. 1970 *Le Mésozoque saharien. 2e partie: essai de synthèse des données des sondages algéro-tunisiens*. Publications du Centre de Recherche sur les Zones arides, CNRS, **11**(2).

CAHEN, L., SNELLING, N. J., DELHAL, J. & VAIL, J. R. 1984. *The Geochronology and Evolution of Africa*. Clarendon Press, Oxford.

CAIRE, A. 1957. *Etude géologique de la région des Biban (Algérie)*. Publication des Service de la Carte géologique d' Algérie, Nouvelle série, Bulletin 16.

CAMOIN, G., BELLION, Y., DERCOURT, J. *et al.* 1993. Late Maastrichtian (69.5 to 65 Ma). *In*: DERCOURT, J., RICOU, L. E. & VRIELYNCK, B. (eds) *Atlas Tethys Palaeoenvironmental Maps. Explanatory Notes*. Gauthier-Villars, Paris, 225–242.

CAMP, V. E. & ROOBOL, M. J. 1992. Upwelling asthenosphere beneath western Arabia and its regional implications. *Journal of Geophysical Research*, **97**, 15255–15271.

——, —— & HOOPER, P. R. 1991. The Arabian continental alkali basalt province: 2. Evolution of Harrats Khaybar, Ithnayn, and Kura, Kingdom of Saudi Arabia. *Geological Society of America Bulletin*, **103**, 363–391.

——, —— & —— 1992. The Arabian Continental Alkali Basalt Province. 3. Evolution of Harrat Kishb, Kingdom of Saudi Arabia. *Geological Society of America Bulletin*, **104**, 379–396.

CECCA, F., AZEMA, J., FOURCADE, E., BAUDIN, F., GUIRAUD, R., RICOU, L. E. & DE WEVER, P. 1993. Early Kimmeridgian (146 to 144 Ma). *In*: DERCOURT, J., RICOU, L. E. & VRIELYNCK, B. (eds) *Atlas Tethys Palaeoenvironmental Maps. Explanatory Notes*. Gauthier-Villars, Paris, 97–111.

CHARROUD, A., CHARROUD, M. & FEDAN, B. 1993. La ride de Tichoukt, un exemple de ride moyen atlasique (Maroc), active durant le Méso-Cénozoïque. *In*: *14th Regional Meeting of Sedimentology, Marrakesh, 27–29 April*, 102–103.

CHAZOT, G. & BERTRAND, H. 1993. Mantle sources and magma–continental crust interactions during early Red Sea–Gulf of Aden rifting in southern Yemen: elemental and Sr–Nd-Pb isotope evidence. *Journal of Geophysical Research*, **98**, 1819–1835.

CLAOUÉ-LONG, J. C., ZANG ZICHAO, MA GUOGAN & DU SHAOHUA. 1991. The age of the Permian–Triassic boundary. *Earth and Planetary Science Letters*, **105**, 182–190.

CLIN, M. 1991. Evolution of eastern Afar and the Gulf of Tadjura. *Tectonophysics*, **198**, 355–368.

COFFIN, M. F. & RABINOWITZ, P. D. 1988. Evolution of the conjugate east African–Madagascan margins and the Western Somali Basin. *Geological Society America Special Paper*, **226**.

COLEMAN, R. G. & VAUGHN MCGUIRE, A. 1988. Magma systems related to the Red Sea opening. *Tectonophysics*, **150**, 77–100.

——, DE BARI, S. & PETERMAN, Z. 1992. A-type granite and the Red Sea opening. *Tectonophysics*, **204**, 27–40.

COURTNEY, R. C. & WHITE, R. S. 1986. Anomalous heat flow and geoid across the Cape Verde Rise: evidence for dynamic support from a thermal plume in the mantle. *Geophysical Journal of the Royal Astronomical Society*, **87**, 815–868.

COX, K. G. 1992. Karoo igneous activity and the early stages of the break-up of Gondwanalad *In*: STOREY, B. C., ALABASTER, T. & PANKHURST, R. J. (eds) *Magmatism and the Causes of Continental Break-up*. Geological Society, London, Special Publications, **68**, 137–148.

CREVOLA, G., CANTAGREL, J.-M. & MOREAU, C. 1994. Le volcanisme cénozoique de la presqu'île du Cap-Vert (Sénégal): cadre chronologique et géodynamique. *Bulletin de la Société géologique de France*, **165**, 437–446.

CUNHA, P. R. C., GONZAGA, F. G., COUTINHO, L. F. C. & FEIJO, F. J. 1994. Bacia do Amazonas. *B. Geoci. PETROBRAS*, **8**(1), 47–55.

DAUTRIA, J. M. & GIROD, M. 1991. Relationship between Cainozoic magmatism and upper mantle heterogeneities as exemplified by the Hoggar volcanic area (Central Sahara, Southern Algeria). *In*: KAMPUNZU, A. B. & LUBALA, R. T. (eds) *Magmatism in Extensional Structural Settings*. Springer-Verlag, Berlin 250–269.

—— & LESQUER, A. 1989. An example of the relationship between rift and dome: recent geodynamic evolution of the Hoggar swell and of its nearby regions (Central Sahara, Southern Algeria and Eastern Niger). *Tectonophysics*, **163**, 45–61.

DAVIDSON, J. P. & WILSON, I. R. 1989. Evolution of an alkali basalt–trachyte suite from Jebel Marra volcano, Sudan, through assimilation and fractional crystallization. *Earth and Planetary Science Letters*, **95**, 141–160.

DE ALMEIDA, F. F. M., CARNEIRO, C. D. R., MACHADO, D. L., JR & DEHIRA, L. K. 1988. Magmatismo ps-Paleozico no nordeste oriental do Brasil. *Revista Brasileira de Geociências*, **18**, 451–462.

DERCOURT, J., RICOU, L. E. & VRIELYNCK, B. 1993. *Atlas Tethys Palaeoenvironmental Maps. Explanatory Notes*. Gauthier-Villars, Paris.

——, ZONENSHAIN, L. P., RICOU, L. E. *et al.* 1985. Présentation de 9 cartes paléogéographiques au 1.20.000.000e s'étendant de l'Atlantique au Pamir pour la période du Lias à l'Actuel. Bulletin Société géologique de France, **1** (5), 637–652.

DÉRUELLE, B., MOREAU, C., *et al.* 1991. The Cameroon Line: a review. *In*: KAMPUNZU, A. B. & LUBALA, R. T. (eds) *Magmatism in Extensional Structural Settings*. Springer-Verlag, Berlin, 274–326.

DILEK, Y. & EDDY, C. A. 1992. The Troodos (Cyprus) and Kizildag (S. Turkey) ophiolites as structural models for slow-spreading ridge segments. *Journal of Geology*, **100**, 305–322.

DRURY, S. A., KELLEY, S. P., BERHE, S. M., COLLIER, R. E. L. & ABRAHA, M. 1994. Structures related to Red Sea evolution in northern Eritrea. *Tectonics*, **13**, 1371–1380.

DU DRESNAY, R. 1988. Recent data on the geology of the Middle Atlas (Morocco). *In*: JACOBSHAGEN, V. (ed.) *The Atlas System of Morocco*. Springer-Verlag, Berlin, 293–320.

DUPUY, C., MARSH, J., DOSTAL, J., MICHARD, A. & TESTA, S. 1988. Asthenospheric and lithospheric sources for Mesozoic dolerites from Liberia (Africa): trace element and isotopic evidence. *Earth and Planetary Science Letters*, **87**, 100–110.

DVORKIN, A. & KOHN, B. P. 1989. The Asher Volcanics, northern Israel: petrography, mineralogy and

alteration. *Israel Journal of Earth-Sciences*, **38**, 105–123.

EBINGER, C. J. & IBRAHIM, A. 1994. Multiple episodes of rifting in Central and East Africa: a re-evaluation of gravity data. *Geologische Rundschau*, **83**, 689–702.

——, BETCHEL, T. D., FORSYTH, D. W. & BOWIN, C. O. 1989*a*. Effective elastic plate thickness beneath the East African and Afar Plateaus and dynamic compensation of the uplifts. *Journal of Geophysical Research*, **94**, 2883–2901.

——, DEINO, A., DRAKE, R. & TESHA, A. L. 1989*b*. Chronology of volcanism and rift propagation: Rungwe Volcanic Province. *Journal of Geophysical Research*, **94**: 15785–15803.

——, REX, D. C., YEMANE, T. & KELLEY, S. 1993*a*. Volcanism and extension between the Main Ethiopian and Gregory rifts. *In*: THORWEIHE, U. & SCHANDELMEIER, H. (eds) *Geoscientific Research in Northeast Africa*. Balkema, Rotterdam 301–304.

——, YEMANE, T., WOLDEGABRIEL, G., ARONSON, J. L. & WALTER, R. C. 1993*b*. Late Eocene–Recent volcanism and faulting in the southern main Ethiopian rift. *Journal of the Geological Society, London*, **150**, 99–108.

EBY, G. N., RODEN-TICE, M., KRUEGER, H. L., EWING, W., FAXON, E. H. & WOOLEY, A. R. 1995. Geochronology and cooling history of the northern part of the Chilwa Alkaline Province, Malawi. *Journal of African Earth Sciences*, **20**, 275–288.

EL ABBASS, T., PERSON, A., GERARD, M., ALBOUY, Y., SAUVAGE, M., SAUVAGE, J.-F. & BERTIL, D. 1993. Arguments géophysiques et géologiques en faveur de manifestations volcaniques récentes dans la région du lac Faguibine (Mali). *Comptes Rendus Hebdomadaires des Séances de l' Académie des Sciences, Série II*, **316**, 1303–1310.

EYAL, M., EYAL, Y., BARTOV, Y. & STEINITZ, G. 1981. The tectonic development of the western margin of the Gulf of Elat (Aqaba) rift. *Tectonophysics*, **80**, 39–66.

FÉRAUD, G. 1981. *Datation de réseaux de dykes et de roches volcaniques sous-marines par les méthodes K–Ar et ^{40}Ar–^{39}Ar. Utilisation des dykes comme marqueurs de paléocontraintes*. Thèse Sciences, Université de Nice.

——, ZUMBO, V. & SEBAI, A. 1991. $^{40}Ar/^{39}Ar$ age and duration of tholeiitic magmatism related to the early opening of the Red Sea rift. *Geophysical Research Letters*, **18**, 195–198.

FIECHTNER, L., FRIEDRICHSEN, H. & HAMMERSCHMIDT, K. 1992. Geochemistry and geochronology of Early Mesozoic tholeiites from Central Morocco. *Geologische Rundschau*, **81**, 45–62.

FITTON, J. G. 1987. The Cameroon Line, West Africa: a comparison between oceanic and continental alkaline volcanism. *In*: FITTON, J. G. & UPTON, B. G. J. (eds) *Alkaline Igneous Rocks*. Geological Society, London Special Publications, **30**, 273–291.

FODOR, R. V. & MCKEE, E. H. 1986. Petrology and K–Ar ages of rift-related basaltic rocks, offshore northern Brazil, 3°N. *Journal of Geology*, **94**, 585–593.

——, SIAL, A. N., MUKASA, S. B. & MCKEE, E. H. 1990. Petrology, isotope characteristics and K-Ar ages of the Maranhão, northern Brazil, Mesozoic basalt province. *Contributions to Mineralogy and Petrology*, **104**, 555–567.

FORBES, P. 1989. Rôles des structures sédimentaires et tectoniques, du volcanisme alcalin régional et des fluides diagénétiques–hydrothermaux pour la formation des minéralisations à U–Zn–V–Mo d'Akouta (Niger). *Géologie et Géochimie d'Uranium, Mémoires*, **17**, 1–375.

FOURCADE, E., AZEMA, J., DE WEVER, P. & BUSNARDO, R. 1990. Contribution à la datation de la croûte océanique de l'Atlantique Central: âge valanginien inférieur des basaltes océaniques et âge néocomien des calcaires Maiolica de Maio (Iles du Cap Vert). *Marine Geology*, **95**, 31–44.

FRANZ, G., HARMS, U. & DENKLER, T. 1993. Late Cretaceous igneous activity in the Delgo uplift (Northern Province, Sudan). *In*: THORWEIHE, U. & SCHANDELMEIER, H. (eds) *Geoscientific Research in Northeast Africa*. Balkema, Rotterdam, 227–230.

——, PUCHELT, H. & PASTEELS, P. 1987. Petrology, geochemistry and age relations of Triassic and Tertiary volcanic rocks from SW Egypt and NW Sudan. *Journal of Afican Earth Sciences*, **6**, 335–352.

——, PUDLO, D., URLACHER, G., HAUßMANN, U., BOVEN, B. & WEMMER, K. 1994. The Darfur dome, western Sudan: the product of a subcontinental mantle plume. *Geologische Rundschau*, **83**, 614–623.

FREETH, S. J. 1979. Deformation of the African plate as a consequence of membrane stress domains generated by post-Jurassic drift. *Earth and Planetary Science Letters*, **45**, 93–104.

GAETANI, M. & GARZANTI, E. 1991. Multicyclic history of the northern India continental margin (northwestern Himalaya). *Bulletin, American Association of Petroleum Geologists*, **75**, 1427–1446.

GARFUNKEL, Z. 1989. Tectonic setting of Phanerozoic magmatism in Israel. *Israel Journal of Earth Sciences*, **38**, 51–74.

—— & DERIN, B. 1988. Reevaluation of Latest Jurassic–Early Cretaceous history of the Negev and the role of magmatic activity. *Israel Journal of Earth Sciences*, **37**, 43–52.

GASPARON, M., INNOCENTI, F., MANETTI, P., PECCERILLO, A. & TSEGAYE, A. 1993. Genesis of the Pliocene to Recent bimodal mafic–felsic volcanism in the Dbre Zeyt area, central Ethiopia: volcanological and geochemical constraints. *Journal of African Earth Sciences*, **17**, 145–165.

GENIK, G. J. 1992. Regional framework and structural aspects of rift basins in Niger, Chad and the Central African Republic (C.A.R.). *Tectonophysics*, **213**, 169–185.

GERLACH, D. C., CLIFF, R. A., DAVIES, G. R., NORRY, M. & HODGSON, N. 1988. Magma sources of the Cape Verdes archipelago: isotopic and trace element constraints. *Geochimica e Cosmochimica Acta*, **52**, 2979–2992.

GIANNERINI, G. 1988. *Propagation des phénomènes*

tectoniques et magmatiques intraplaques liés aux zones de rifting: exemple de la plaque arabique. Thèse Sciences, Université de Nice.

GIROD, M. & GIROD, N. 1977 Contribution de la pétrologie la connaissance de l'évolution de la Méditerranée occidentale depuis l'Oligocène. *Bulletin de Société géologique de France*, **XIX(3)**, 481–488.

GNOS, E. & PETERS, T. 1993. K-Ar ages of the metamorphic sole of the Semail ophiolite: implications for ophiolite cooling history. *Contributions to Mineralogy and Petrology*, **113**, 325–332.

GOMEZ, F., BARAZANGI M. & BENSAID, M. 1996. Active tectonism in the intracontinental Middle Atlas Mountains of Morocco: synchronous crustal shortening and extension. *Journal of the Geological Society, London*, **153**, 389–402.

GREEN, W. V., ACHAUER, U. & MEYER, R. P. 1991. A three-dimensional seismic image of the crust and upper mantle beneath the Kenya rift. *Nature*, **354**, 199–203.

GUIRAUD, R. 1997. Mesozoic rifting and basin inversion along the northern African Tethyan margin: An overview. *This volume*.

—— & BELLION, Y. 1995. Late Carboniferous to Recent geodynamic evolution of the West Gondwanian cratonic Tethyan margins. *In*: NAIRN, A., DERCOURT, J & VRIELYNCK, B. (eds) *The Ocean Basins and Margins, Vol. 8, The Tethys Ocean*. Plenum, New York, 101–124.

—— & MAURIN, J. C. 1991. Le rifting en Afrique au Crétacé inférieur: synthèse structurale, mise en évidence de deux étapes dans la genèse des bassins, relations avec les ouvertures océaniques péri-africaines. *Bulletin de la Société géologique de France*, **162**, 811–823.

—— & —— 1992. Early Cretaceous rifts of Western and Central Africa: an overview. *Tectonophysics*, **213**, 153–168.

——, BELLION, Y., BENKHELIL, J. & MOREAU, C. 1987. Post-Hercynian tectonics in Northern and Western Africa. *In*: BOWDEN, P. & KINNAIRD, J. (eds) *African Geology Reviews. Geological Journal*, **22**, 433–466.

——, ISSAWI, B. & BELLION, Y. 1985. Les linéaments guinéo-nubiens: un trait structural majeur l'échelle de la plaque africaine. *Comptes Rendus Hebdomadaires des Séances de l'Académie des Sciences*, **300**, 17–20.

GVIRTZMAN, G., KLANG, A. & ROTSTEIN, Y. 1990. Early Jurassic shield volcano below Mount Carmel: new interpretation of the magnetic and gravity anomalies and implication for Early Jurassic rifting. *Israel Journal of Earth-Sciences*, **39**, 149–159.

HAGGERTY, S. E. 1982. Kimberlites in Western Liberia: an overview of the geological setting in a plate tectonic framework. *Journal of Geophysical Research*, **87**, 10811–10826.

HAILWOOD, E. A. & MITCHEL, J. G. 1971. Paleomagnetic and radiometric dating results from Jurassic intrusions in South Morocco. *Geophysical Journal of the Royal Astronomical Society*, **24**, 351–364.

HALLIDAY, A. N., DAVIDSON, J. P., HOLDEN, P., DEWOLF, C., LEE, D. C. & FITTON, J. G. 1990. Trace-element fractionation in plumes and the origin of HIMU mantle beneath the Cameroon line. *Nature*, **347**, 523–528.

——, DAVIES, G. R., LEE, D.-C., TOMMASINI, S., PASLICK, C. R., FITTON, J. G. & JAMES, D. E. 1992. Lead isotope evidence for young trace element enrichment in the oceanic upper mantle. *Nature*, **359**, 623–626.

HAMMUDA, O. S., VAN HINTE, J. E. & NEDERBRAGT, S. 1992. Geohistory analysis mapping in central and southern Tarabulus Basin, northwestern offshore of Libya. *In*: SALEM, M. J. (ed.) *The Geology of Libya*. Elsevier, Amsterdam, 1657–1680.

HANKEL, O. 1993. Depositional cycles and palynostratigraphy of the Permo-Triassic and Early to Middle Jurassic of East Africa and Madagascar. *In*: THORWEIHE, U. & SCHANDELMEIER, H. (eds) *Geoscientific Research in Northeast Africa*. Balkema, Rotterdam, 351–355.

HARLAND, W. B., ARMSTRONG, R. L., COX, A. V., CRAIG, L. E., SMITH, A. G. & SMITH, D. G. 1990. *A Geologic Time Scale 1989*. Cambridge University Press, Cambridge.

HARMAND, C. & CANTAGREL, J. M. 1984. Le volcanisme alcalin Tertiaire et Quaternaire du Moyen Atlas (Maroc): chronologie K Ar et cadre géodynamique. *Journal of Africa Earth Sciences*, **2**, 51–55.

HERNANDEZ, J. & LEPVRIER, C. 1979. Le volcanisme calco-alcalin miocène de la région d'Alger (Algérie): pétrologie et signification géodynamique. *Bulletin de la Société géologique de France*, **XXI**, 73–86.

——, DE LAROUZIERE, F. D., BOLZE, J. & BORDET, P. 1987. Le magmatisme néogène bético-rifain et le couloir de décrochement trans-Alboran. *Bulletin de la Société géologique de France*, **III**(2), 257–267.

HILL, R. I. 1991. Starting plumes and continental break-up. *Earth and Planetary Science Letters*, **104**, 398–416.

HIRSCH, F., FLEXER, A., ROSENFELD, A. & YELLIN-DROR, A. 1995. Palinspastic and crustal setting of the Eastern Mediterranean. *Journal of Petroleum Geology*, **18**, 149–170.

HÖHNDORF, A., MEINHOLD, K.-D. & VAIL, J. R. 1994. Geochronology of anorogenic igneous complexes in the Sudan: isotopic investigations in North Kordofan, the Nubian Desert and the Red Sea Hills. *Journal of African Earth Sciences*, **19**, 3–15.

HOOPER, P. R. 1990. The timing of crustal extension and the eruption of continental flood basalts. *Nature*, **345**, 246–249.

——, REHACEK, J., DUNCAN, R. A., MARSH, J. S. & DUNCAN, R. A. 1993. The basalts of Lesotho, Karoo Province, Southern Africa. *Abstract 1993 American Geophysical Union Fall Meeting. EOS*, **74**, 553.

HORN, P., MULLER-SOHNIUS, D. & SCHULT, A. 1988. Potassium–Argon ages on a Mesozoic tholeiitic dike swarm in Rio Grande do Norte, Brazil. *Revista Brasiliera de Geociências*, **18**, 50–53.

JANSSEN, M. E., STEPHENSON, R. A. & CLOETINGH, S. 1995. Temporal and spatial correlations between changes in plate motions and the evolution of rifted basins in Africa. *Geological Society of America Bulletin*, **107**, 1317–1332.

KAJATO, H. K. 1982. Gas strike spurs search for oil in Tanzania. *Oil & Gas Journal*, **80**, 123–131.

KAMPUNZU, A. B. & MOHR, P. 1991. Magmatic evolution and petrogenesis in the East African Rift System. *In*: KAMPUNZU, A. B. & LUBALA, R. T. (eds) *Magmatism in Extensional Structural Settings. The Phanerozoic African Plate*. Springer-Verlag, Berlin, 85–136.

KEELEY, M. L. & WALLIS, R. J. 1991. The Jurassic system in northern Egypt: II. Depositional and tectonic regimes. *Journal of Petroleum Geology*, **14**, 49–64.

KENT, R. W., STOREY, M. & SAUNDERS, A. D. 1992. Large igneous provinces: sites of plume impact or plume incubation? *Geology*, **20**, 891–894.

KLITGORD, K. D. & SCHOUTEN, H. 1986. Plate kinematics of the central Atlantic. *In*: VOGT, P. R. & TUCHOLKE, B. E. (eds) *The Geology of North America, Vol. M, The Western North Atlantic Region*. Geological Society of America, Boulder, CO, 351–378.

KOHN, B. P., LANG, B. & STEINITZ, G. 1993. ^{40}Ar–^{39}Ar dating of the Atlit-1 volcanic sequence, northern Israel. *Israel Journal of Earth-Sciences*, **42**, 17–28.

LANG, B. & STEINITZ, G. 1989. K–Ar dating of Mesozoic magmatic rocks in Israel: a review. *Israel Journal of Earth-Sciences*, **38**, 89–103.

LAPIERRE, H., MANGOLD, C., ELMI, S. & BROUXEL, M. 1984. Deux successions volcano-sédimentaires dans le 'Trias' d'Oranie (Algérie occidentale); témoins de la fracturation d'une plate-forme continentale. *Revue de Géologie dynamique et de Géographie physique*, **25**, 361–373.

LARIDHI-OUAZAA, N. 1994. *Étude minéralogique et géochimique des episodes magmatiques Mésozoques et Miocènes de la Tunisie*. Thesis Doctorat-des-Sciences Géologiques, University of Tunis II.

LATIN, D., NORRY, M. J. & TARZEY, R. J. E. 1993. Magmatism in the Gregory Rift, East Africa: Evidence for melt generation by a plume. *Journal of Petrology*, **34**, 1007–1027.

LAWS, E. & WILSON, M. 1997. Tectonics and magmatism associated with Mesozoic passive margin development in the Middle East. *Journal of the Geological Society, London*, **154**, 459–464.

LAY, C. & REICHELT, R. 1971. Sur l'âge et la signification des intrusions de dolérites tholéitiques dans le bassin de Taoudenni (Afrique Occidentale). *Comptes Rendus de l'Académie des Sciences*, **272**, 374–376.

LE BAS, M. J., REX, D. C. & STILLMAN, C. 1986. The early magmatic chronology of Fuerteventura, Canary islands. *Geological Magazine*, **123**, 287–298.

LEE, D.-C., HALLIDAY, A. N., FITTON, J. G. & POLI, G. 1994. Isotopic variations with distance and time in the volcanic islands of the Cameroon Line: evidence for a mantle plume origin. *Earth and Planetary Science Letters*, **123**, 119–138.

LESQUER, A., VILLENEUVE, J. C. & BRONNER, G. 1991. Heat flow data from the western margin of the West African craton (Mauritania). *Physics of the Earth and Planetary Interiors*, **66**, 320–329.

LIÉGEOIS, J. P., SAUVAGE, J. F. & BLACK, R. 1991. The Permo-Jurassic alkaline province of Tadhak, Mali: geology, geochronology and tectonic significance. *Lithos*, **27**, 95–105.

LOTFY, H. I., VAN DER VOO, R., HALL, C. M., KAMEL, A. & ABDEL AAL, A. Y. 1995. Palaeomagnetism of Early Miocene basaltic eruptions in the areas east and west of Cairo. *Journal of African Earth Sciences*, **21**, 407–419.

LOUNI-HACINI, A., BELLON, H., MAURY, R. C., *et al.* 1995. Datation ^{40}K–^{40}Ar de la transition du volcanisme calco-alcalin au volcanism alcalin en Oranie au Miocène supérieur. *Comptes Rendus de l' Académie des Sciences*, **321**, 975–982.

LUGER, P., GRÖSCHKE, M., BUSSMANN, M., DINA, A., METTE, W., UHMANN, A. & KALLENBACH, H. 1994. Comparison of the Jurassic and Cretaceous sedimentary cycles of Somalia and Madagascar: implications for the Gondwana breakup. *Geologische Rundschau*, **83**, 711–727.

MABESOONE, J. M. & ALHEIROS, M. M. 1988. Origem da Bacia sedimentar costeira Pernambuco–Paraiba. *Revista Brasiliera de Geociências*, **18**, 476–482.

MAGNAVITA, L. P., DAVISON, I. & KUSZNIR, N. J. 1994. Rifting, erosion and uplift history of the Recncavo–Tucano–Jatob rift, northeast Brazil. *Tectonics*, **13**, 367–388.

MAHONEY, J., NICOLLET, C. & DUPUY, C. 1991. Madagascar basalts: tracking oceanic and continental sources. *Earth and Planetary Science Letters*, **104**, 350–363.

MALPAS, J., CALON, T. & SQUIRES, G. 1993. The development of a late Cretaceous microplate suture zone in SW Cyprus. *In*: PRICHARD, H. M., ALABASTER, T., HARRIS, N. B. W. & NEARY, C. R. (eds) *Magmatic Processes and Plate Tectonics*. Geological Society, London Special Publications, **76**, 177–195.

MALUSKI, H., COULON, C., POPOFF, M. & BAUDIN, P. 1995. $^{40}Ar/^{39}Ar$ chronology, petrology and geodynamic setting of Mesozoic to early Cenozoic magmatism from the Benue Trough, Nigeria. *Journal of the Geological Society, London*, **152**, 311–326.

MARTIN, G. 1982. Geologie des Küsten-gebietes von Nordwest-Africa südlich der Sahara. Neue Erkenntnisse aus der Erdölexploration. *Giessener Geologische Schriften*, **30**, 160 S.

MASCLE, J., BLAREZ, E. & MARINHO, M. 1988. The shallow structures of the Guinea and Ivory Coast–Ghana transform margins: their bearing on the Equatorial Atlantic Mesozoic evolution. *Tectonophysics*, **188**, 193–209.

MASSA, D. 1988. *Paléozoque de Libye occidentale: stratigraphie et paléogéographie*. Thèse Sciences, University of Nice.

—— & DELORT, T. 1984. Evolution du bassin de Syrte (Libye) du Cambrien au Crétacé basal. *Bulletin de*

la Société géolologique de France, **XXVI**(6), 1087–1096.

MAUCHE, R., FAURE, G., JONES, L. M. & HOEFS, J. 1989 Anomalous isotopic compositions of Sr, Ar and O in the Mesozoic diabase dykes of Liberia, West Africa. *Contributions to Mineralogy and Petrology*, **101**, 12–18.

MAURIN, J.-C. & GUIRAUD, R. 1990. Relationships between tectonics and sedimentation in the Barremo-Aptian intracontinental basins of Northern Cameroon. *Journal of Africa Earth Sciences*, **10**, 331–340.

—— & —— 1993. Basement control in the development of the Early Cretaceous West and Central African Rift System. *Tectonophysics*, **228**, 81–95.

MAY, P. R. 1991. The Eastern Mediterranean Mesozoic Basin: Evolution and oil habitat. *Bulletin, American Association of Petroleum Geologists*, **75**, 1215–1232.

MCGUIRE, A. V. & BOHANNON, R. G. 1989. Timing of mantle upwelling: evidence for a passive origin for the Red Sea Rift. *Journal of Geophysical Research*, **94**, (B2), 1677–1682.

MCHARGUE, T., HEIDRICK, T. & LIVINGSTON, J. 1992. Tectonostratigraphic development of the Interior Sudan Rifts, Central Africa. *Tectonophysics*, **213**, 187–202.

MCHONE, J. G. 1996. Broad-terrane Jurassic flood basalts across northeastern North America. *Geology*, **24**, 319–322.

MELLO, M. R., KOUTSOUKOS, E. A. M., MOHRIAK, W. U. & BACOCCOLI, G. 1994. Selected petroleum systems in Brazil. *In*: MAGOON, L. B. & DOW, W. G. (eds) *The Petroleum System–from Source to Trap*. American Association of Petroleum Geologists, Memoirs, **60**, 499–512.

MENEISY, M. Y. 1990. Vulcanicity. *In*: SAID, R. (ed.) *The Geology of Egypt*. Balkema, Rotterdam, 157–172.

MICHARD, A. 1976. Eléments de Géologie Marocaine. *Notes et Mémoires du Service géologique du Maroc*, **252**.

——, FEINBERG, H., EL-AZZAB, D., BOUYBAOUENE, M. & SADDIQI, O. 1992. A serpentinite ridge in a collisional paleomargin setting: the Beni Malek massif, External Rif, Morocco. *Earth and Planetary Science Letters*, **113**, 435–442.

MITCHELL, J. G., LE BAS, M. J., ZIELONKA, J. & FURNES, H. 1983. On dating the magmatism of Maio, Cape Verde Islands. *Earth and Planetary Science Letters*, **64**, 61–76.

MOHR, P. & ZANETTIN, B. 1988 The Ethiopian flood basalt province. *In*: MACDOUGALL, J. D. (ed.) *Continental Flood Basalts*. Kluwer, Dordrecht, 63–110.

MONIÉ, P., MONTIGNY, R. & MALUSKI, H. 1992. Age burdigalien de la tectonique ductile extensive dans le massif de l'Edough (Kabylie, Algérie). Données radiométriques ^{39}Ar–^{40}Ar. *Bulletin de la Société géologique de France*, **163**, 571–584.

MONTENAT, C., ANGELIER, J., BEAUDOIN, B., BOLZE, J., BUROLLET, P.-F., ORSAG-SPERBER, F. & RICHERT, J.-P. 1990. La marge occidentale de la mer Rouge au nord de Port-Soudan. *Bulletin de la Société géologique de France*, (8), **VI**(3), 435–446.

MONTES-LAUAR, C. R., PACCA, I. G., MELFI, A. J., PICCIRILLO, E. M., BELLIENI, G., PETRINI, R. & RIZZIERI, R. 1994. The Anari and Tapirapuã Jurassic formations, western Brazil: paleomagnetism, geochemistry and geochronology. *Earth and Planetary Science Letters*, **128**, 357–371.

MOREAU, C., REGNOULT, J. M., DERUELLE, B. & ROBINEAU, B. 1987. A new tectonic model for the Cameroon Line, Central Africa. *Tectonophysics*, **139**, 317–334.

MOREL, J.-M. & CABANIS, B. 1993. Mise en évidence d'une association magmatique dans le volcanisme plio-quaternaire du Moyen-Atlas marocain. *Comptes Rendus Hebdomadaires des Séances de l'Académie des Sciences, Série II*, **316**, 537–362.

MULLER, J., CORNEE, J. J. & EL KAMEL, F. 1991. Evolution tectono-sédimentaire d'un bassin molassique postorogénique: l'exemple des séries conglomératiques stéphano-triasiques de Mechra ben Abbou, Rehamna, Maroc. *Géologie Méditerranéenne*, **XVIII**(1–2), 109–122.

NETTO, A. M., FABRE, J., POUPEAU, G. & CHAMPENOIS, M. 1992. Datation par traces de fission de la structure circulaire des Richat (Mauritanie). *Comptes Rendus Hebdomadaires des Séances de l'Académie des Sciénces, Série II*, **314**, 1179–1186.

NONO, A., DERUELLE, B., DEMAIFFE, D. & KAMBOU, R. 1994. Tchabal Nganha volcano in Adamawa (Cameroon): petrology of a continental alkaline lava series. *Journal of Volcanology and Geothermal Research*, **60**, 147–178.

NOUGIER, J., CANTAGREL, J. M. & KARCHE, J. P. 1986. The Comores archipelago in the western Indian Ocean: volcanology, geochronology and geodynamic setting. *Journal of African Earth Sciences*, **5**, 135–145.

OBERLI, F., NIAFLOS, T., MEIER, M. & KURAT, G. 1987. Emplacement age of the peridotites from the Zabargad island (Red Sea), a zircon U–Pb isotopes study. *Terra Cognita*, **7**, 334.

OBERT, D. 1981. *Étude géologique des Babors orientaux (Domaine tellien, Algérie)*. Thèse Sciences, Université de Paris VI.

OLIVEIRA, E. P., TARNEY, J. & JOAO, X. J. 1990. Geochemistry of the Mesozoic Amapa and Jari dyke swarms, northern Brazil: plume-related magmatism during the opening of the central Atlantic. *In*: PARKER, A. J., RICKWOOD, P. C. & TUCKER, D. H. (eds) *Mafic Dykes and Emplacement Mechanisms*. Balkema, Rotterdam, 173–183.

OMAR, G. I. & STECKLER, M. S. 1995. Fission track evidence on the initial rifting of the Red Sea: two pulses, no propagation. *Science*, **270**, 1341–1344.

PASTEELS, P. M., VILLENEUVE, P., DE PAEPES, P. & KLERKX, J. 1989. Timing of the volcanism of the southern Kivu province: implications for the evolution of the western branch of the East African Rift system. *Earth and Planetary Science Letters*, **94**, 353–363.

PEARSON, D. G., DAVIES, G. R. & NIXON, P. H. 1993. Geochemical constraints on the petrogenesis of diamond facies pyroxenites from the Beni Bousera

peridotite massif, North Morocco. *Journal of Petrology*, **34**, 125–172.

PEDLEY, H. M. & GRASSO, M. 1992. Miocene synteconic sedimentation along the western margins of the Hyblean–Malta platform: a guide to plate margin processes in the Central Mediterranean. *Journal of Geodynamics*, **15**, 19–37.

PICCOLI, G., BOCCALETTI, M., ANGELUCCI, A., ROBBA, E., ARUSH, M. A. & CABDULQAADIR, M. M. 1986. Geological history of central and southern Somalia since the Triassic. *Memorie della Società Geologica Italiana*, **31**, 415–425.

PIQUÉ, A. & LAVILLE, E. 1995. L'ouverture initiale de l'Atlantique central. *Bulletin de la Société géologique de France*, **166**, 725–738.

PLUMMER, Ph. S. 1995. Ages and geological significance of igneous rocks from Seychelles. *Journal of African Earth Sciences*, **20**, 91–101.

PONIKAROV, V. P., KAZMIN, V. G., MIKHAILOV, I. A., *et al.* 1967. *Explanatory notes Part I, The Geological Map of Syria, scale 1:500 000*. Ministry of Industry, Damascus.

POUCLET, A., AHMED, Y., BAUBRON, J.-C., BELLON, H. & MOREL, A. 1994. Age et mise en place du volcanisme cénozoque dans le graben du Téfidet (système de rift du Niger oriental). *Comptes Rendus Hebdomadaires des Séances de l'Académie des Sciences, Série II*, **318**, 683–690.

RABU, D., LE METOUR, J., BECHENNEC, F., BEURRIER, M., VILLEY, M. & BOURDILLON-JEUDY DE GRISSAC, C. 1990. Sedimentary aspects of the Eo-Alpine cycle on the northeast edge of the Arabian Platform (Oman Mountains). *In*: ROBERTSON, A. H. F., SEARLE, M. P. & RIES, A. C. (eds) *The Geology and Tectonics of the Oman Region*. Geological Society, London Special Publications, **49**, 49–68.

RAHAMAN, M. A., VAN BREEMEN, O., BOWDEN, P. & BENNETT, J. N. 1984. Age migrations of anorogenic ring-complexes in northern Nigeria. *Journal of Geology*, **92**, 173–184.

REEVES, C. V., KARANJA, F. M. & MACLEOD, I. N. 1987. Geophysical evidence for a failed Jurassic rift and triple junction in Kenya. *Earth and Planetary Science Letters*, **81**, 299–311.

RESSETAR, R., NAIRN, A. E. M. & MONRAD, J. R. 1981. Two phases of Cretaceous–Tertiary magmatism in the Eastern Desert of Egypt: Paleomagnetic, chemical and K–Ar evidence. *Tectonophysics*, **73**, 169–193.

REYNOLDS, P. O. 1993. Plate tectonic aspects of continental rift basin formation in Central and West Sudan. *In*: THORWEIHE, U. & SCHANDELMEIER, H. (eds) *Geoscientific Research in Northeast Africa*. Balkema, Rotterdam, 207–212.

REYRE, D. 1984. Remarques sur l'origine et l'évolution des bassins sédimentaires africains de la côte atlantique. *Bulletin de la Société géologique de France*, **6**, 1041–1059.

ROBERTSON, A. H. F. & XENOPHONTOS, C. 1993. Development of concepts concerning the Troodos ophiolite and adjacent units in Cyprus. *In*: PRICHARD, H. M., ALABASTER, T., HARRIS, N. B. W. & NEARY, C. R. (eds) *Magmatic Processes and Plate Tectonics*. Geological Society, London, Special Publications, **76**, 85–119.

ROBERTSON, A. H. F. & SEARLE, M. P. 1990. The northern Oman Tethyan continental margin: stratigraphy, structure, concepts and controversies. *In*: ROBERTSON, A. H. F., SEARLE, M. P. & RIES, A. C. (eds) *The Geology and Tectonics of the Oman Region*. Geological Society, London, Special Publications, **49**, 3–25.

——, BLOME, C. D., COOPER, D. W. J., KEMP, A. E. S. & SEARLE, M. P. 1990*a*. Evolution of the Arabian continental margin in the Dibba Zone, Northern Oman Mountains. *In*: ROBERTSON, A. H. F., SEARLE, M. P. & RIES, A. C. (eds) *The Geology and Tectonics of the Oman Region*. Geological Society, London, Special Publications, **49**, 251–284.

——, KEMP, A. E. S., REX, D. C. & BLOME, C. D. 1990*b*. Sedimentary and structural evolution of a continental margin transform lineament: the Hatta Zone, Northern Oman Mountains. *In*: ROBERTSON, A. H. F., SEARLE, M. P. & RIES, A. C. (eds) *The Geology and Tectonics of the Oman region*. Geological Society, London Special Publications, **49**, 285–305.

ROGERS, N. W. 1993. The isotope and trace element geochemistry of basalts from the volcanic islands of the southern Red Sea. *In*: PRICHARD, H. M., ALABASTER, T., HARRIS, N. B. W. & NEARY, C. R. (eds) *Magmatic Processes and Plate Tectonics*. Geological Society, London, Special Publications, **76**, 455–467.

——, DE MULDER, M. & HAWKESWORTH, C. J. 1992. An enriched mantle source for potassic basanites: evidence from Karisimbi volcano, Virunga volcanic province, Rwanda. *Contributions to Mineralogy and Petrology*, **111**, 543–556.

ROSSI, M. E., TONNA, M. & LARBASH, M. 1992. Latest Jurassic–Early Cretaceous deposits in the subsurface of the eastern Sirt basin (Libya): facies and relationships with tectonics and sea-level changes. *In*: SALEM, N. J., SBETA, A. M. & BAKBAK, M. R. (eds) *The Geology of Libya Vol. 6*. Elsevier, Amsterdam, 2212–2225.

SARADETH, S., SOFFEL, H. C., HORN, P., MÜLLER-SOHNIUS, D. & SCHULT, A. 1989. Infra-Cambrian and Phanerozoic pole positions and potassium–argon ages from the East Sahara craton. *Geophysical Journal*, **97**, 209–221.

SAWAF, T., AL-SAAD, D., GEBRAN, A., BARAZANGI, M., BEST, J. A. & CHAIMOV, T. A. 1993. Stratigraphy and structure of eastern Syria across the Euphrates depression. *Tectonophysics*, **220**, 267–281.

SCHANDELMEIER, H. & DARBYSHIRE, D. P. F. 1984. Metamorphic and magmatic events in the Uweinat–Bir Safsaf uplift (Western Desert/Egypt). *Geologische Rundschau*, **73**, 819–831.

—— & RICHTER, A. 1991. Brittle shear deformation in Northern Kordofan, Sudan: late Carboniferous to Triassic reactivation of Precambrian fault systems. *Journal of Structural Geology*, **13**, 711–720.

——, HUTH, A., HARMS, U., FRANZ, G. & BERNAU, R. 1987*a*. The East Saharan craton in southern Egypt and northern Sudan: lithology, metamorph-

ism, magmatism, geochronology and structural development. *Berliner geowissenschaftlichen Abhandlungen*, A, **75**, 25–48.

——, KLITZSCH, E., HENDRICKS, F. & WYCISK, P. 1987*b*. Structural development of North-East Africa since Precambrian times. *Berliner geowissenschaftlichen Abhandlungen*, **75**, 5–24.

——, REYNOLDS, P. O. & KUSTER, D. 1993. Spatial and temporal relationship between alkaline magmatism and early rifting in north/central Sudan. *In*: THORWEIHE, U. & SCHANDELMEIER, H. (eds) *Geoscientific Research in Northeast Africa*. Balkema, Rotterdam, 221–225.

——, RICHTER, A. & FRANZ, G. 1983. Outline of the geology of magmatic and metamorphic units from Gebel Uweinat to Bir Safsaf (SW-Egypt/NW-Sudan). *Journal of African Earth Sciences*, **1**, 275–283.

SCHILLING, J. G., KINSLEY, R. H., HANAN, B. B. & MCCULLY, B. L. 1992. Nd–Sr–Pb isotopic variations along the Gulf of Aden: Evidence for Afar mantle plume–continental lithosphere interaction. *Journal of Geophysical Research*, **97**, 10927–10966.

SCHLUMBERGER 1984. *WEC Egypt, Well Evaluation Conference*.

SEARLE, M.P. 1994. Structure of the intraplate eastern Palmyride fold belt, Syria. *Geological Society of America Bulletin*, **106**, 1332–1350.

SEBAI, A., FERAUD, G., BERTRAND, H. & HANES, J. 1991*a*. $^{40}Ar/^{39}Ar$ dating and geochemistry of tholeiitic magmatism related to the early opening of the Central Atlantic rift. *Earth and Planetary Science Letters*, **104**, 455–472.

——, ZUMBO, V., FÉRAUD, G., BERTRAND, H., HUSSAIN, A. G., GIANNERINI, G. & CAMPREDON, R. 1991*b*. $^{40}Ar/^{39}Ar$ dating of alkaline and tholeiitic magmatism of Saudi Arabia related to early Red Sea rifting. *Earth and Planetary Science Letters*, **104**, 473–487.

SENGÖR, A. M. C. 1990. A new model for the late Palaeozoic–Mesozoic tectonic evolution of Iran and implications for Oman. *In*: ROBERTSON, A. H. F., SEARLE, M. P. & RIES, A. C. (eds) *The Geology and Tectonics of the Oman Region*. Geological Society London, Special Publications, **49**, 797–831.

——, CIN, A., ROWLEY, D. B. & NIE, S. Y. 1993. Space–time patterns of magmatism along the Tethysides: a preliminary study. *Journal of Geology*, **101**, 51–84.

SEYITOGLU, G. & SCOTT, B. C. 1992. Late Cenozoic volcanic evolution of the northeastern Aegean region. *Journal of Volcanology and Geothermal Research*, **54**, 157–176.

SHACKLETON, R. M., RIES, A. C., BIRD, P. R., FILBRANDT, J. B., LEE, C. W. & CUNNINGHAM, G. C. 1990. The Batain Melange of NE Oman. *In*: ROBERTSON, A. H. F., SEARLE, M. P. & RIES, A. C. (eds) *The Geology and Tectonics of the Oman Region*. Geological Society, London Special Publications, **49**, 673–696.

SMEWING, J. D., ABBOTTS, I. L., DUNNE, L. A. & REX, D. C. 1991. Formation and emplacement ages of the Masirah ophiolite, Sultanate of Oman. *Geology*, **19**, 453–456.

SOUHEL, A., CANEROT, J., BOUCHOUATA, A., CHAFIKI, D., EL HARIRI, K. & GHARIB, A. 1993. Le rift atlasique sur la transversale de Beni-Mellal (Haut Atlas Central). *In*: *14th Regional meeting of Sedimentology, Marrakesh, 27–29 April*, 305–306.

STAMPFLI, G. M. 1996. The Intra-Alpine terrain: a Paleotethyan remnant in the Alpine Variscides. *Eclogae Geologicae Helveticae*, **89**, 13–42.

——, MARCOUX, J. & BAUD, A. 1991. Tethyan margins in space and time. *Palaeogeography, Palaeoclimatology, Palaeoecology*, **87**, 373–409.

STEINITZ, G., BARTOV, Y. & EYAL, M. 1992. K–Ar and Ar–Ar dating of Permo-Triassic magmatism in Sinai and Israel initial results. *In*: *Israel Geological Society, Annual Meeting*, 147.

STEWART, K. & ROGERS, N. 1996. Mantle plume and lithosphere contributions to basalts from southern Ethiopia. *Earth and Planetary Science Letters*, **139**, 195–211.

STOREY, B. C. 1995. The role of mantle plumes in continental break-up: case histories from Gondwanaland. *Nature*, **377**, 301–308.

STOREY, M., MAHONEY, J., SAUNDERS, A. D., DUNCAN, R. A., KELLEY, S. P. & COFFIN, M. F. 1995. Timing of hot-spot related volcanism and the breakup of Madagascar and India. *Science*, **267**, 852–855.

——, ALABASTER, T. & PANKHURST, R. J. (eds) 1992. *Magmatism and the Causes of Continental Breakup*. Geological Society, London, Special Publications, **68**.

STORETVEDT, K. M., MITCHELL, J. G., ABRANCHES, M. C., MAALOE, S. & ROBIN, G. 1992. The coast-parallel dolerite dykes of east Madagascar: age of intrusion, remagnetization and tectonic aspects. *Journal of African Earth Sciences*, **15**, 237–249.

TAYLOR, W. R., TOMPKINS, L. A. & HAGGERTY, S. E. 1994. Comparative geochemistry of West African kimberlites: evidence for a micaceous kimberlite endmember of sublithospheric origin. *Geochimica et Cosmochimica Acta*, **58**, 4017–4037.

TIERCELIN, J. J., VINCENS, A. & COLL, X. 1987. Le demi-graben de Baringo-Bogoria, Rift Gregory, Kenya. 30000 ans d'histoire hydrologique et sédimentaire. *Bulletin des Centres Recherches Exploration–Production Elf-Aquitaine*, **11**(2), 249–540.

TRICART, P., TORELLI, L., ARGNANI, A., REKHISS, F. & ZITELLINI, N. 1994. Extensional collapse related to compressional uplift in the Alpine Chain off northern Tunisia (Central Mediterranean). *Tectonophysics*, **238**, 317–329.

TURNER, S., REGELOUS, M., KELLEY, S., HAWKSWORTH, C. J. & MANTOVANI, M. 1994. Magmatism and continental break-up in the South Atlantic: high precision 40Ar-39Ar geochronology. *Earth and Planetary Science Letters*, **121**, 333–348.

UMEJI, A. C. & CAEN-VACHETTE, M. 1983. Rb Sr isochron from Gboko and Ikynen rhyolites and its implications for the age and evolution of the Benue Trough, Nigeria. *Geological Magazine*, **120**, 529–533.

VAIL, J. R., 1989. Ring complexes and related rocks in Africa. *Journal of African Earth Sciences*, **8**, 19–40.

—— 1993. The dyke swarms of north-eastern Sudan. *In*: THORWEIHE, U. & SCHANDELMEIER, H. (eds) *Geoscientific Research in Northeast Africa*. Balkema, Rotterdam, 127–131.

VALSARDIEU, C. 1971. *Etude géologique et paléogéographique du bassin du Tim Merso*. Thèse Sci., Université de Nice.

VAN DER MEER, F. & CLOETINGH, S. 1993. Intraplate stresses and the subsidence history of the Sirte basin (Libya). *Tectonophysics*, **226**, 37–58.

VANNUCCI, R., CALVINO, F., CORTESOGNO, L. & TOLOMEO, L. 1989. Jurassic volcanism findings in Sokoto State (NW-Nigeria). *Journal of African Earth Sciences*, **9**, 245–258.

VIDAL, P., DENIEL, C., VELLUTINI, P. J., PIGUET, P., COULON, C., VINCENT, J. & AUDIN, J. 1991. Changes of mantle sources in the course of rift evolution: the Afar case. *Geophysical Research Letters*, **18**, 1913–1916.

VINCENT, P. M. 1970. The evolution of the Tibesti volcanic province, Eastern Sahara. *In*: CLIFFORD, T. & GASS, I. G. (eds) *African Magmatism and Tectonics*, Oliver & Boyd, Edinburgh, 301–319.

WHITE, R. & MCKENZIE, D. 1989. Magmatism at rift zones: The generation of volcanic continental margins and flood basalts. *Journal of Geophysical Research*, **94**, 7685–7729.

—— 1995. Mantle plumes and flood basalts. *Journal of Geophysical Research*, **100**, 17543–17585.

WILSON, M. 1989. *Igneous Petrogenesis: a Global Tectonic Approach*. Chapman & Hall, London.

—— 1992. Magmatism and continental rifting during the opening of the South Atlantic Ocean: a consequence of Lower Cretaceous super-plume activity? *In*: STOREY, B. C. ALABASTER, T. & PANKHURST, R. J. (eds) *Magmatism and the Causes of Continental Break-up*. Geological Society, London, Special Publications, **68**, 241–255.

—— 1993*a*. Magmatism and the geodynamics of basin formation. *Sedimentary Geology*, **86**, 5–29.

—— 1993*b*. Geochemical signatures of continental and oceanic basalts: a key to mantle dynamics? *Journal of the Geological Society, London*, **150**, 977–990.

—— 1997. Thermal evolution of the Central Atlantic passive margins: –continental break-up above a Mesozoic super-plume. *Journal of the Geological Society, London*, **154**, 491–498.

—— & GUIRAUD, R. 1992. Magmatism and rifting in Western and Central Africa, from Late Jurassic to Recent times. *Tectonophysics*, **213**, 203–225.

WYCISK, P., KLITZSCH, E., JAS, C. & REYNOLDS, O. 1990. Intracratonal sequence development and structural control of Phanerozoic strata in Sudan. *Berliner Geowissenschaftlichen Abhandlungen*, **120**, 45–86.

YILMAZ, Y. 1990. Comparison of young volcanic associations of western and eastern Anatolia formed under a compressional regime: a review. *Journal of Volcanology and Geothermal Research*, **44**, 69–87.

ZIEGLER, P. 1990. *Shell Atlas of Europe*, 2nd edn.

ZIEGLER, U., STOSSEL, F. & PETERS, Tj., 1991. Meta-carbonatites in the metamorphic series below the Semail Ophiolite in the Dibba Zone, Northern Oman Mountains. *In*: PETERS, Tj. *et al.* (eds) *Ophiolite Genesis and Evolution of the Oceanic Lithosphere*, Kluwer Academic, Dordrecht, Boston, 627–645.

ZECK, H. P., MONIE, P., VILLA, I. M. & HANSEN, B. T. 1992. Very high rates of cooling and uplift in the Alpine belt of the Betic Cordilleras, southern Spain. *Geology*, **20**, 79–82.

This page intentionally left blank

Tectonic controls on the petroleum geology of NE Africa

M. L. KEELEY[1] & M. S. MASSOUD[2]

[1]*Emerald Energy Plc, 2 Ashley Avenue, Epsom, Surrey KT18 5AL, UK*
[2]*Geology Department, College of Science, University of Kuwait, PO Box 5969, Kuwait 13060*

Abstract: During the Palaeozoic and early Mesozoic, the NE sector of the African craton remained an entire, integral part of Gondwanaland. It experienced two episodes of intracratonic sagging and marginal cratonic rifting, linked to episodes of strike-slip affecting both the craton interior and its northern margins. Source kerogens accumulated during Palaeotethyan highstands within these sags, across which reservoir clastics prograded during the corresponding lowstands. Such source–reservoir associations are known from the Silurian, Devonian and Carboniferous. The fragmentation of the NE African margin with Mesotethys took place over the period Mid Triassic–Bathonian. From Palestine to Cyrenaica, a rift propagated westwards, detaching crustal terranes along shears that later formed Asia Minor. Deep marine shales within this rift have some proven oil-generating potential. However, the principal Jurassic oil kerogen is found associated with coal swamp–delta clastics, deposited during the Bathonian lowstand, in basins formed between the shears along the new cratonic edge. There is also now evidence for a Mid-Triassic rift penetrating the Sirt Basin from the northwest. Sinistral strike-slip associated with these Mesotethyan shears penetrated deeper into NE Africa during the Late Cretaceous, with subsidence reaching a maximum in the Jebel el Akhdar, Abu Gharadiq and proto-Clysmic Basins, in which rich oil-prone marine source rocks accumulated during the Turonian–Coniacian lowstand. Inversion followed, as the sense of strike-slip reversed with the onset of 'Syrian Arc' movements, starting in the latest Cretaceous, and proceeding as a series of pulses into the Late Oligocene. The final phase of 'Syrian Arc' tectonics was linked to the opening of the Red Sea and Gulf of Suez Basins, and transtension along the Gulf of Aqaba in the Early Miocene. Falling Miocene sea levels then permitted the accumulation of the restricted 'Globigerina Marls' facies within the active graben system of the Gulf of Suez.

Over the last 50 years, hydrocarbon exploration strategies in NE Africa have developed very much on an ad hoc basis. The discovery of oil at Gemsa in the Gulf of Suez 110 years ago, although at the time little short of a nuisance to the extraction of sulphur, triggered the exploration and development of the small but prolific oil-generating Clysmic (Gulf of Suez) Basin (Fig. 1). Proven and produced reserves here amount to more than 6.5 billion barrels of oil (BBO), equivalent to about 165 thousand barrels of oil (KBO) km^{-3} of gross sediment within the basin.

Although the first oil exploration well in Libya was drilled in 1956 on the crest of the Jebel el Akhdar dome in Cyrenaica, a more complete evaluation of NE Libya was, however, forestalled by the discovery shortly afterwards of vast oil reserves in the Sirt Basin. Yet, it was on the basis of defining the eastward extent into Egypt of this second 'world-class' basin in NE Africa that exploration effort was diverted into the intervening Western Desert (Fig. 1). Only 15 years ago, the entire area west of the Nile was something of an exploration 'graveyard', after the failure to continue the successes in the Abu Gharadiq Basin. However, the development of the Jurassic play in the mid-1980s has rejuvenated this area, leading to a succession of new discoveries.

Notwithstanding this commercial success, our knowledge of the processes that created this abundance has advanced only slowly, as modern geophysical, stratigraphical and geochemical techniques have improved, and the capacity to integrate disparate data has evolved. This has been as much the case with the small and apparently isolated oil and gas discoveries between the Sirt and Clysmic Basins, as with the major basins themselves. Therefore, only now, after the advances of the last 10 years, is it possible to synthesize the four dimensional controls on source, reservoir and seal rock quality and distribution, of the master tectonic mechanisms, and the chronometric control on source rock maturation, migration and trap formation: the petroleum systems. Readers should note that this paper provides a synthesis, and the majority of the references cited include a vast amount of new analytical work based upon material from outcrop and a large number of wells.

KEELEY, M. L. & MASSOUD, M. S. 1998. Tectonic controls on the petroleum geology of NE Africa. *In*: MACGREGOR, D. S., MOODY, R. T. J. & CLARK-LOWES, D. D. (eds) 1998. *Petroleum Geology of North Africa*. Geological Society, London, Special Publication No. 132, 265–281

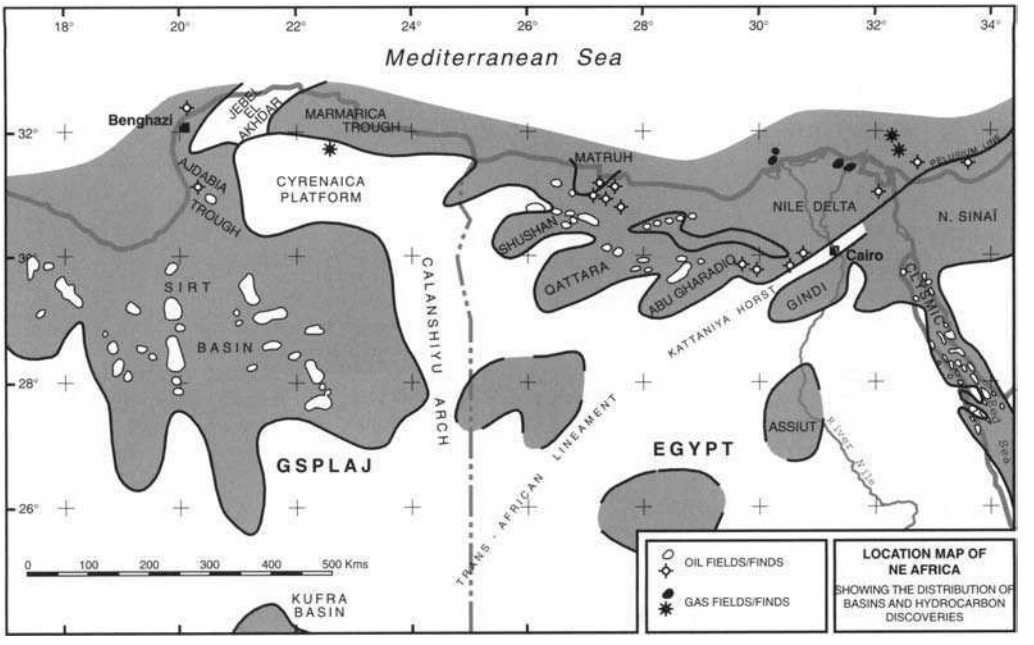

Fig. 1. Location map of NE Africa, showing the distribution of basins, and oilfields and gas fields or finds. GSPLAJ: Great Socialist Peoples' Libyan Arab Jamahariya.

Stratigraphic framework

The relatively new techniques of palynostratigraphy and event or sequence stratigraphy have permitted wide-ranging revisions to be made of basin history in Cyrenaica (El-Arnauti & Shelmani 1985, 1988) and the Western Desert (Gueinn & Rasul 1986; Keeley 1989, 1994; Keeley *et al.* 1990). Sufficient reliable data are only now available for a regional synthesis to be attempted. Differences in approach are apparent on either side of the frontier, but most anomalies arise from the lack of data in the poorly explored sector on either side of the Libyan–Egyptian border (23–26°E).

Such a chronostratigraphic synthesis is presented herein (Fig. 2), passing eastwards from the Adjdabia Trough in Cyrenaica, roughly following 30°N into northern Sinai. The stratigraphic detail bears witness to the twin roles of eustacy in controlling facies, and tectonics in controlling thickness through subsiding basins and rising axes. Post-depositional tectonics, however, are responsible for uplift and erosion, and some complex and overlapping unconformity relationships. Whereas the locations of these tectonic axes are long-standing, important events are represented by the reversal of polarity (from subsidence to uplift, or vice versa) on these axes at about latest Devonian (410 Ma), Early Triassic (245 Ma) and Late Paleocene (60 Ma). These events were interpreted by Keeley (1994) as resulting from changes in the sense of strike-slip along the Trans-African Lineament (TAL), a trans-continental feature first recognized by Neev (1977).

Using the chronostratigraphical control now available, the Phanerozoic can be divided into six episodes characterized by the tectonic and sedimentary processes prevailing, described below.

Ghazalat and Proto-Sirt Basins: 535–365 Ma

Deposition over the period Mid-Cambrian to latest Devonian took place within a stable tectonic environment. A largely regressive depositional system was interrupted by discrete marine flooding events, and by the erosion associated with the Late Ordovician (Ashgill) glaciation. Intra-cratonic sedimentation was centred on the central Western Desert: the Ghazalat Basin (Fig. 3: Keeley 1989). This was separated by the Calanshiyu Arch from a vast shelf area covering central and western Libya, and extending into Algeria (Bellini & Massa 1980, El-Arnauti & Shelmani 1988, Semtner & Klitzsch 1994).

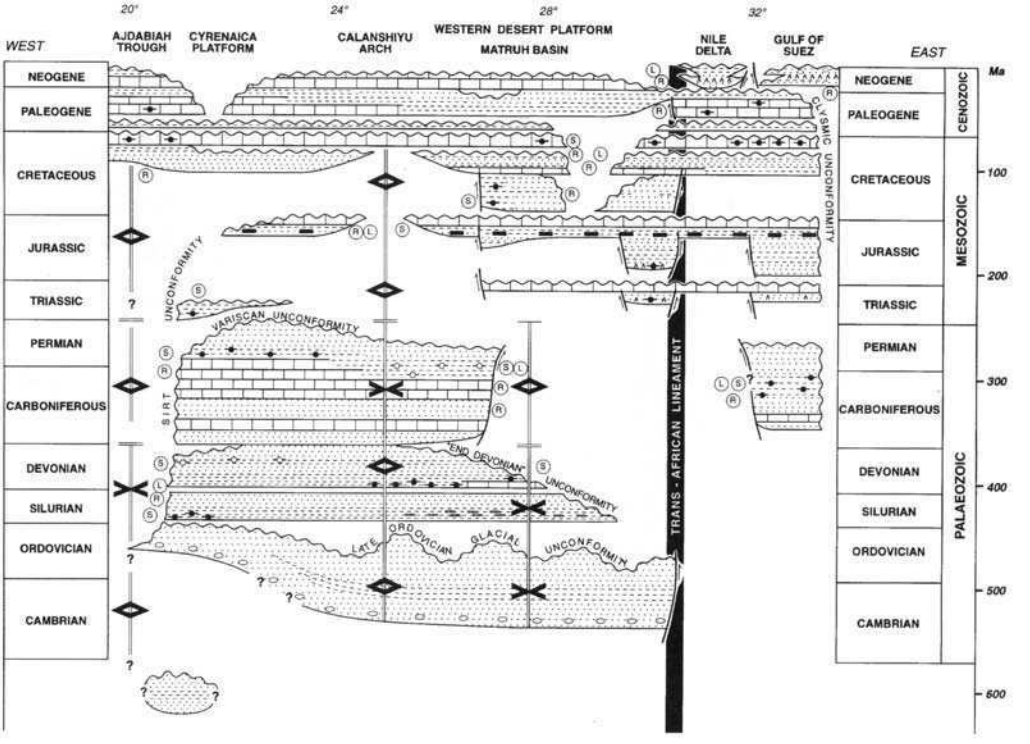

Fig. 2. Chrono-stratigraphic correlation west–east (*c.* 30°N) across NE Africa, from eastern Libya (Cyrenaica) to Sinai (eastern Egypt), true to scale vertically (time, Ma) and horizontally (degrees east of Greenwich). The section broadly follows depositional strike for the Mesozoic and Cenozoic. Dominant bulk lithotypes are shown, and known petroleum source, reservoir and seal rocks are designated S, R and L respectively. The sites and duration of syn-depositional axes and basins are illustrated, together with major erosional events. However, only the most important unconformities are shown in the Cretaceous–Tertiary section, by virtue of the many local complexities. It should be noted that intervals entirely of continental red beds ('Nubian' facies) are omitted throughout.

Gueinn & Rasul (1986) have dated the onset of deposition in the Western Desert as Solvan (Mid-Cambrian), whereas El-Arnauti & Shelmani (1988) found no evidence for Lower Palaeozoic deposition in the Proto-Sirt Basin before the Caradoc (Late Ordovician). This may be indicative of a regional dome preceding formation of the Proto-Sirt Basin (see Fig. 3). However, a Mid-Proterozoic (Riphean) sequence of immature clastics is found on the eastern flank of this arch (El-Arnauti & Shelmani 1988).

Three sedimentary sequences were deposited in the Ghazalat and Proto-Sirt Basins, spanning the intervals Mid-Cambrian to Late Ordovician, Early to latest Silurian, and Early to latest Devonian (Fig. 4). The first sequence contains an undifferentiated mixture of continental and shelf facies, probably arranged as lowstand system tracts, that reflect the interplay between both low sea levels and active local tectonics. The Silurian and Devonian intervals are each represented by single well-developed regressive systems tracts, with a regional maximum flooding surface at the base of each, and separated by a hiatus corresponding to the Přídolí (Keeley 1989).

Tehenu and Proto-Clysmnic Basins: 365–245 Ma

The latest-Devonian unconformity marks a change in basin dynamics, with the inversion of the Ghazalat and Proto-Sirt Basins, followed directly by the subsidence of the intervening Calanshiyu Arch, to form the Tehenu Basin (Keeley 1989). Inversion and erosion down into the Devonian succession increased away from the Calanshiyu Arch, SE towards the TAL (Fig. 2).

Continuous Permo-Carboniferous deposition took place within the Tehenu and Proto-Clysmic Basins, both of which trended NNE, opening

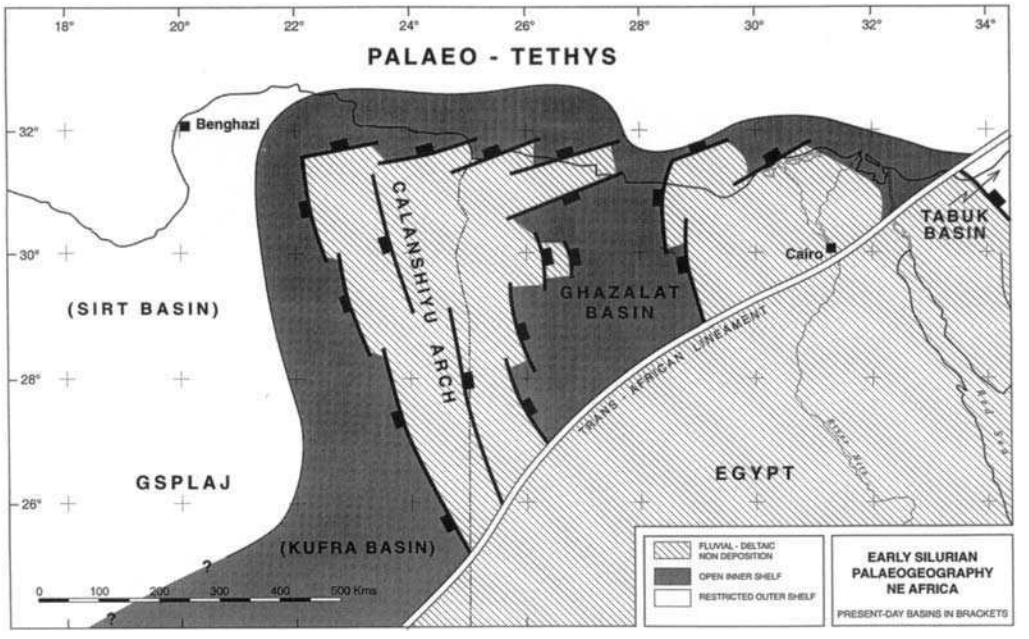

Fig. 3. Early Silurian palaeogeography (present-day basins in parentheses).

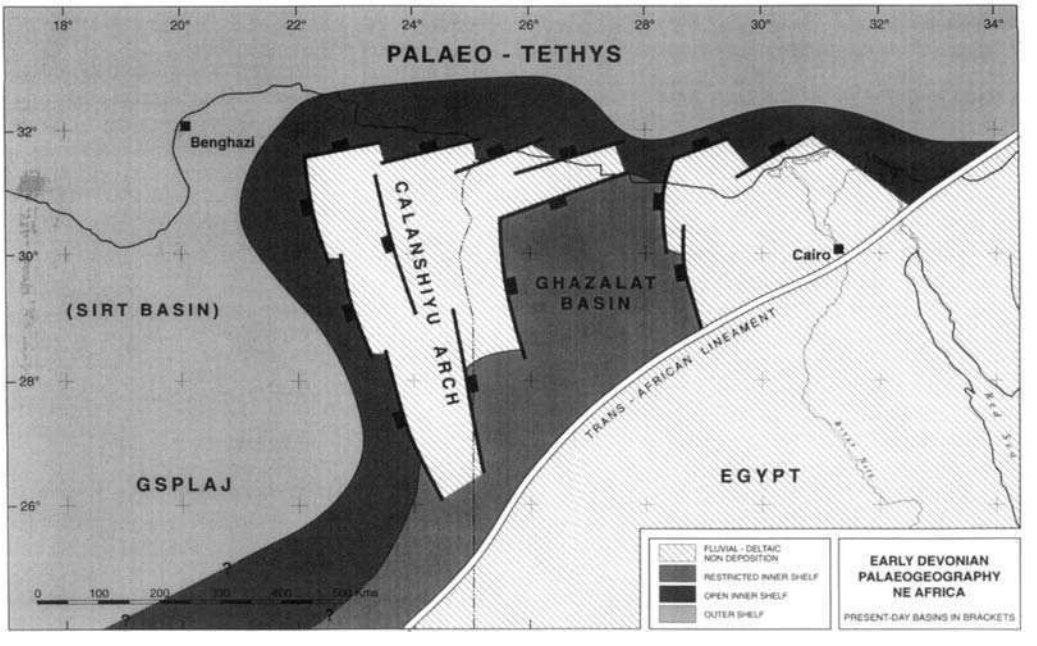

Fig. 4. Early Devonian palaeogeography (present-day basins in parentheses).

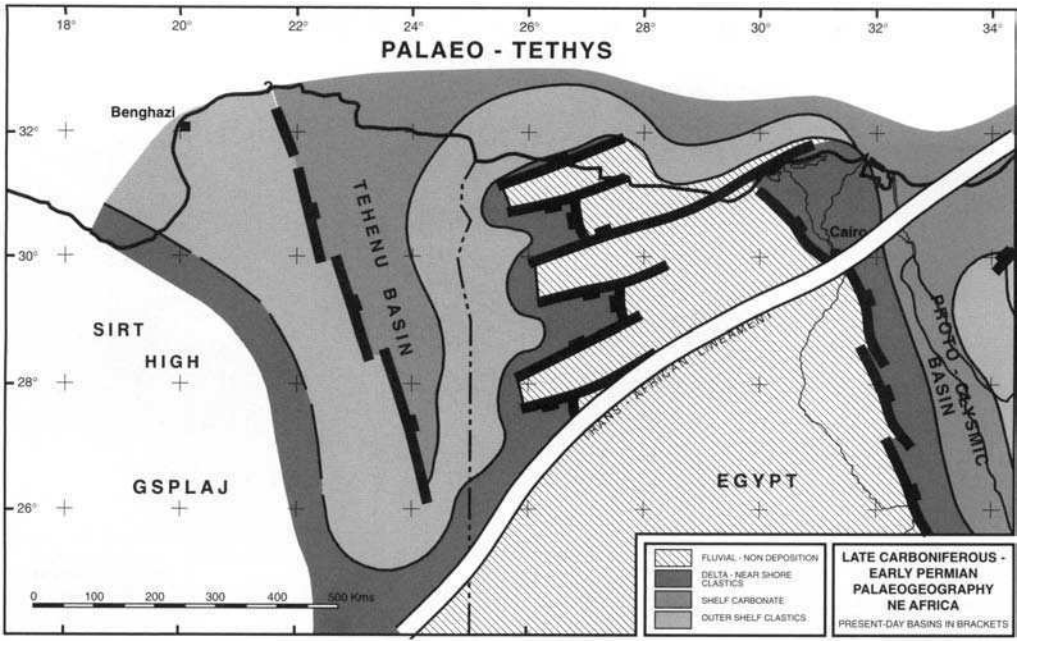

Fig. 5. Late Carboniferous—Early Permian palaeogeography.

into Palaeo-Tethys (Fig. 5). Deposition was dominated by transgressive systems, with several discrete regional flooding events. In northern Cyrenaica and northwesternmost Egypt, no break is apparent in sedimentation from Late Devonian into the Early Carboniferous (El-Arnauti & Shelmani 1988; Keeley 1989).

Throughout the Gulf of Suez, firm evidence is lacking for any Palaeozoic deposition before the mid-Dinantian (Klitzsch 1990); carbonate beds near the sequence base at Gebel en Nukhul in Sinai are dated as Arundian (Brenckle & Marchant 1987). The earliest Dinantian carbonates in the Western Desert are slightly earlier (Chadian), with the main development occurring over the span from latest Dinantian to early Permian, particularly in the more northerly areas (Loboziak & Clayton 1988; Keeley 1989). Biostratigraphical control on the age of the youngest Permian in the Gulf of Suez is poor (Klitzsch, 1990), but in Cyrenaica, the interval Late Permian–Early Triassic is demonstrably missing (Brugman & Visscher 1988).

Failed rift basins: 245–205 Ma

Middle and Upper Triassic strata are poorly represented in NE Africa, comprising continental clastic deposits and restricted marginal marine facies. The usual difficulties are encountered concerning biostratigraphical definition in such facies. A typically mixed clastic–carbonate succession has been recorded from northern Cyrenaica by Brugman & Visscher (1988). It continues eastwards into northern Egypt, beneath the Matruh and Gebel Rissu Basins (Keeley *et al.* 1990), eventually reaching the surface at Arif en Naqa on the Palestine border (Jenkins 1990).

Although Triassic depositional geometry is not clear, it would seem to mark the transition from large intra-cratonic basins to smaller rift basins on a developing continental margin of the type so well developed in Jurassic times and subsequently. The recent recognition of a similar succession beneath the eastern Sirt Basin may also indicate early subsidence along a parallel axis reaching into the craton (Shelmani et al. 1992; see Fig. 6).

Unstable Meso-Tethyan basins: 205–145 Ma

There is a marked hiatus spanning at least the late Hettangian, Sinemurian and early Pliensbachian throughout the region (Keeley et al. 1990); only at one distal site in northern Cyrenaica is there evidence for early Hettangian

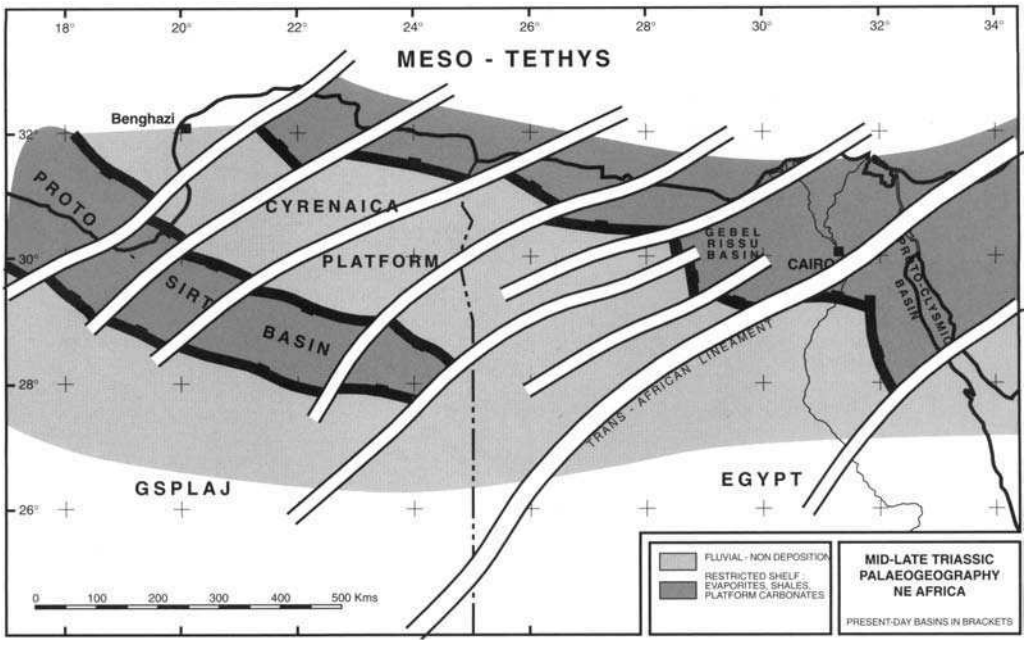

Fig. 6. Mid–Late Triassic palaeogeography.

(Brugman & Visscher 1988). In Palestine and eastern Sinai, this break is represented by weathered flint–clays and laterites (the Mishhor Formation of Goldberg (1964); see also Picard & Hirsch (1987)).

Continuous sedimentation recommenced late in the Pliensbachian, with a marine influx from Meso-Tethys into Palestine and eastern Egypt (east from the Gebel Rissu Basin; Keeley & Wallis 1991). Small basins that first opened towards the north during the Triassic subsided more rapidly, recording at least four regional flooding events. To the west of the Gebel Rissu Basin and into western Libya, continental crustal levels remained buoyant and intact, with little significant deposition. However, early in the Bathonian, this latter area also subsided into a series of small northward-facing basins (Keeley *et al.* 1990), thereby forming the new 'Unstable Margin' to the NE African continent against Meso-Tethys (Said 1962; see also Fig.7).

Although local tectonics continued to control basin subsidence, sea levels rose to a first-order highstand early in the Oxfordian, subsiding thereafter (Keeley & Wallis 1991). The record of latest Jurassic and earliest Cretaceous (Tithonian–Berriasian) sedimentation is obscure, because low sea levels were followed or accompanied by a period of regional uplift, folding, tilting and truncation (El Hawat & Shelmani 1993).

Stable Meso-Tethyan basins: 145–25 Ma

Until the Aptian, sea levels across NE Africa were low. Although subsidence patterns continued from those established during the Jurassic, almost without exception the record is of cyclical prograding fluvio-deltaic systems, dominated by sands, silts and thin vitrinitic coals: the Alam el Bueib Group. This depositional style extended across most of the African craton, and together with more immature and proximal facies has become known as the 'Nubian' facies (Keeley *et al.* 1990; Thusu *et al.* 1988).

The distal margins to this system are known from the coastal Helez region of Palestine (Bein & Sofer 1987), offshore Sidi Barrani, and the Jebel el Akhdar–Marmarica Trough region of NE Cyrenaica (El Hawat & Shelmani 1993). The passage into fine-grained open marine clastic and carbonate deposits appears to have been controlled by a contemporaneous active continental margin; within this distal facies, there may be continuous deposition from the Late Jurassic into the Paleogene. The same facies has also been recorded from the Matruh Basin, on the continental shelf, and is more likely to represent an incised valley or embayment analogous to that at Helez, rather than an ephemeral rift.

The Aptian transgression introduced marine conditions right across NE Africa, and as far

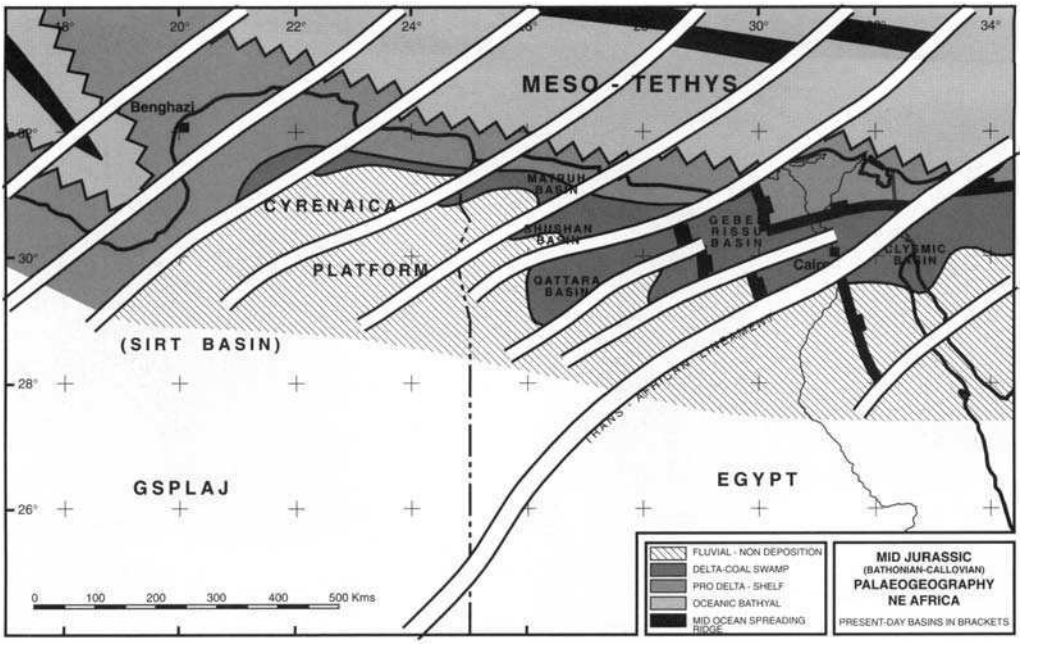

Fig. 7. Mid Jurassic (Bathonian–Callovian) palaeogeography (present-day basin in parentheses).

south onto the craton as 24°N (Said 1990*a*). Repeated cycles of progradation and transgression then followed into the Oligocene, with notable highstands during the Coniacian, Campanian and Paleocene (Said 1990*b*), as carbonate deposition became increasingly significant (Fig. 8). The eustatic signal is confused with discrete pulses of 'Syrian Arc' activity, which reached a climax during the late Oligocene (Keeley 1994). The same faults that controlled subsidence earlier in the Mesozoic became active under repeated strike-slip, following the 'Syrian Arc' trend (NE–SW), parallel to the TAL, but with changing senses of movement. Accordingly, some faults inverted, whereas others subsided more rapidly. In the Abu Gharadiq and Guindi (or Faiyum) Basins, on opposing sides of the TAL (known locally as the Kattanyiah Horst or Pelusium Line), subsidence and inversion alternated (Sestini 1984; Said 1990*b*; Keeley 1994). Subsidence in the Abu Gharadiq Basin reached a maximum during the Late Cretaceous, when the Guindi Basin was emergent, whereas during the Paleocene–Eocene, maximum subsidence in the Guindi Basin coincided with the inversion of the Abu Gharadiq Basin.

The controls on the rapid subsidence experienced in the Jebel el Akhdar area during the Late Cretaceous–Early Paleocene, and its subsequent equally rapid inversion in the Late Paleocene–Early Eocene, are complex and poorly understood (Duronio *et al.* 1991; El Hawat & Shelmani 1993). They do, however, appear to be contemporaneous with, and therefore perhaps genetically linked to, the 'Syrian Arc' movements in Egypt (see below).

In the Late Oligocene, this episode reached its conclusion with the acme of 'Syrian Arc' tectonics (Keeley 1994). This ultimate pulse clearly resulted from the linked movement along the Dead Sea–Aqaba transform and the opening of the Red Sea–Gulf of Suez (Quennel 1984), which generated compressional structures along a NE–SW arcuate trend, through Palestine and into Syria. From NE to SW across Egypt, these include: Arif en Naqa, Gebel el Maghara, Gebel Minshera and other asymmetrical domes in north Sinai, Wadi el Araba on the northern Gulf of Suez, Abu Roash (outside Cairo) and the Oasis of Bahariya. Basement uplift along the margins of the Red Sea–Gulf of Suez rift led to the focusing of northward-draining Nubian fluvial systems into the course of the palaeo-Nile, and also to the eruption of basalts at the northward termination of the rift, in the Cairo–Suez area (Said 1981).

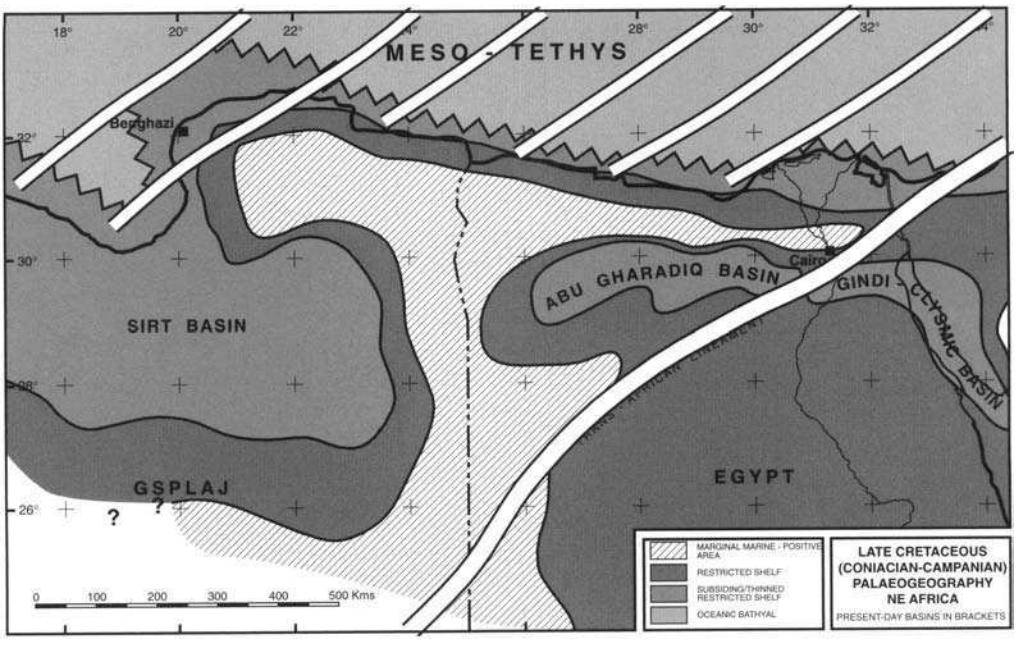

Fig. 8. Late Cretaceous (Coniacian–Santonian) palaeogeography (present-day basin in parentheses).

Neo-Tethyan basins: 25–0 Ma

The latest Oligocene Syrian Arc movements heralded a new system of basin geometry and dynamics, that persists to the present day. The Nile and its delta, together with the Red Sea–Gulf of Suez system, dominate in the east, whereas to the west, the successors of Nubian and Neo-Tethys, the Sahara and the Mediterranean, continue to compete.

Tectonic processes continue, but generally they have been relatively mild. Rapid subsidence has proceeded within the confines of the Nile Delta, and along the course of the Red Sea–Gulf of Suez rift. Within this rift, fault blocks rotated and collapsed, forming sets of opposing polarity, separated by regional cross faults (Meshref 1990; Bosworth 1994). Sedimentary environments within each block were semi-isolated, preserving an entire suite of diachronous facies, from active erosion of basement, through continental clastic deposits, mixed shore-line and shelf clastics and carbonate deposits, into marine anoxic shales (Keeley 1994). The Messinian draw-down led to the accumulation of a thick sequence of evaporites over this rift sequence.

The collapse of the crust beneath the advancing Nile Delta system was no less spectacular. Early–Mid Miocene out-building was also superseded by the effects of the Messinian draw-down, which had the effect of rapidly lowering the fluvial base-level, leading to the incision of a 2.5 km deep canyon in the region north from Cairo (Said 1981), and in the outer delta region, a thin Miocene evaporite sequence was deposited. Plio-Pleistocene out-building then formed the present delta morphology, which has been monitored and influenced by man over the last four millennia (Said 1981).

West of the Nile, as far as Tunisia, post-Oligocene sedimentation has reflected a close balance between deposition and erosion. Aeolian processes, in particular, are active in the desert, whereas on the Marmarica plateau, the outcropping Miocene silicic carbonates resist erosion. However, in the Adjdabia Trough and the offshore sector of the Sirt Basin, thick fine-grained Miocene–Pliocene successions are known.

Associations of source, reservoir and seal rocks

A combination of eustatic and tectonic factors has led on occasion to the close spatial arrangement of source, reservoir and seal rocks, despite very different depositional environments (Fig. 9). The recognition of these associations is

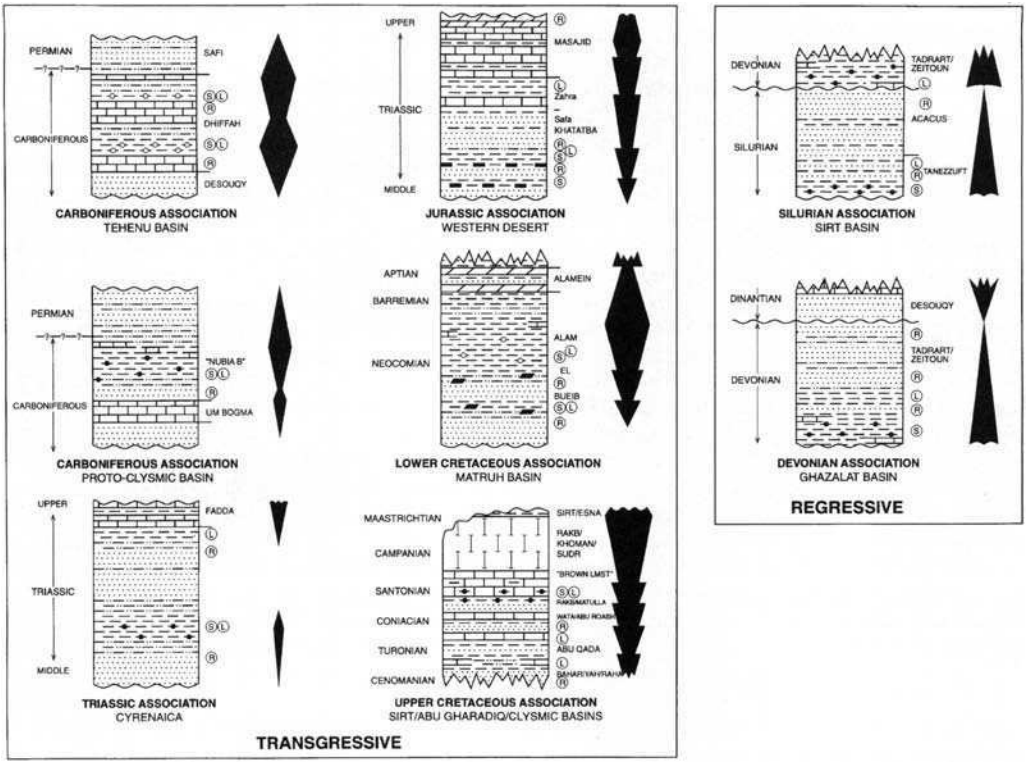

Fig. 9. Source, reservoir and seal rock associations within transgressive and regressive systems tracts. Chronostratigraphy and lithostratigraphy shown along with proven or speculative source (S), seal (L) and reservoir rocks (R).

important to the definition and prediction of petroleum systems, and so there is a need to understand the underlying controlling mechanisms.

By inspection, it is apparent that source, reservoir and seal rocks are found spatially associated in both transgressive and regressive systems tracts. During the Palaeozoic, two well-developed regressive systems tracts are known, corresponding to the Silurian and Devonian periods, respectively. Anoxic marine kerogens however, only accumulated in the area under discussion at the base of the Devonian regressive cycle; there is no Tanezzuft source rock equivalent east of the Adjdabia Trough in Cyrenaica, across Egypt and into Sinai. The subsequent progradation of continental facies provides thick clastic reservoir intervals above. However, a play can only exist when a seal is provided by a fault repeat or by the subsequent flooding event, that is, either by the basal Devonian shales above upper Silurian sands, or by migration beneath the basal Silurian silts into the underlying Cambro-Ordovician sands.

By contrast, transgressive systems tracts are known throughout the Phanerozoic, but reflect a more complex interplay of controls. Sea levels rose across NE Africa during the Carboniferous, providing for the accumulation of shallow marine carbonates and shales rich in both oil- and gas-prone kerogens in the late Dinantian–Namurian, succeeding early Dinantian fluvio-deltaic and shore-face sands. Such associations are well developed in the Tehenu Basin of Cyrenaica and NW Egypt, and in the Proto-Clysmic Basin. Similarly, the world-wide rise in sea levels during the Triassic led to deposition of restricted marine evaporites, carbonates and black shales above continental clastic deposits along the unstable margin with Meso-Tethys, and within the Proto-Sirt Basin.

The transgressive systems tract responsible for the deposition of the Mid-Jurassic oil-prone coals was partly tectonically induced. The final rifting along the continental margin from the Gebel Rissu to Proto-Sirt Basin during the Bathonian led to crustal collapse during a lowstand

(Keeley *et al.* 1990; Keeley & Wallis 1991). Coal swamps built up along the entire coastal facies belt, and eastwards to Sinai, in which liptinitic-rich coals accumulated within a delta-top clastic setting dominated by sandstones and shales (Bagge & Keeley 1994), thereby providing an intra-formational source, seal and reservoir rock association. A very similar association is found within the Lower Cretaceous Alam el Bueib fluvio-deltaic sequence; the coals, however, seem largely to be vitrinitic and gas prone.

Offshore, along the Late Jurassic–Early Cretaceous continental margin, marine anoxic conditions prevailed, in which organic-rich shales were deposited (Bein & Sofer 1987; Picard & Hirsch 1987; Ghori 1991; El Hawat & Shelmani 1993). Immediately inshore, shelf margin carbonate reefs and bedded limestones accumulated, and are overstepped in part by Mid-Cretaceous shales (Keeley *et al.* 1990; Keeley & Wallis 1991). Whereas the reefs so far examined seem to lack sufficient capacity and pore space (Jenkins 1990), the bedded limestones are locally found dolomitized; this transformed them into a potential reservoir.

Commercially, by far the most important association concerns the Sirt, Abu Gharadiq and Gulf of Suez Basins, and the thick organic-rich limestones and shales of Late Cretaceous age therein (Turonian–Coniacian): the Rakb Shale, the Abu Roash 'A', 'C' and 'E' units, and the 'Brown Limestone', respectively (El Ayouti 1990; Fürst 1993; Shaheen *et al.* 1986; Träger 1984). In Egypt, the overlying Campanian–Paleocene chalks provide a top seal, forcing oil into older reservoirs or, as in Abu Gharadiq, maintaining it within interbedded fractured and vuggy Abu Roash limestones.

The Nile Delta progradational system provides for two close associations of clastic reservoir and seal rocks, of Miocene and Pliocene age, separated by the Messinian evaporites (Said 1990*b*). However, geochemical and burial history considerations indicate that oil and gas trapped here must derive from older and deeper source rocks (Deibis *et al.* 1986).

Petroleum systems

It is through the burial, maturation and expulsion of oil from source rocks, and their subsequent migration into traps, that source, seal and reservoir associations can combine to form a petroleum system. These additional chronological and spatial elements can often be very difficult to ascertain with any accuracy, and the only confirmation of a functioning petroleum system rests on its interpretation as a known hydrocarbon occurrence.

Oil and gas sourced from the Tanezzuft kerogens at their eastward depositional or erosional limit beneath the Sirt Basin could have migrated up-dip onto the western margins of the Cyrenaica Platform (Sola & Ozcicek 1990) following Cretaceous and possibly Triassic burial (Fig. 10). Only within the Ghazalat Basin could Devonian and Carboniferous source rocks have become widely mature, in response to Jurassic and Cretaceous burial. The Mid-Carboniferous shales of the Gulf of Suez experienced rapid subsidence and heating during Miocene rifting, and may well have made a contribution toward the charging of the many traps there. Although both Silurian and Devonian shales are both known from the Kufra Basin in SE Libya, they are neither rich enough in organic matter, nor sufficiently deeply buried anywhere but in the very centre of the basin ever to have been active source rocks (Turner 1980).

The only clear case for a Palaeozoic hydrocarbon system in NE Africa hinges on the presence of gas in Late Carboniferous sands on the northern margin of the Cyrenaica Platform, tested by the B1-2 well (Sola & Ozcicek 1990). Ghori (1991) confirmed the extension from NW Egypt of a belt rich in mixed Type III kerogens within interbedded Carboniferous shales (see Keeley 1989). Deep burial off-structure to the north of these shales into the gas window would not have taken place until the Late Jurassic. This same petroleum system extends along the coastal sector into the Western Desert of NW Egypt.

The recognition of dark Triassic shales beneath the Sirt Basin opens up the possibility that some undefined component of Sirt oils, especially those in the SE of the basin, could have derived at least in part from source rocks within this sequence (Shelmani *et al.* 1992).

Recent work has shown the importance of the Mid-Jurassic oil-prone coal petroleum system in charging the oilfields and gas fields around the Shushan and Matruh Basins in NW Egypt (Keeley et al. 1990; Bagge & Keeley 1994). Appreciation of the source to these oils was complicated by the volumetric dilution within the coals and associated carbargillites of oil-prone liptinitic fractions by gas-prone vitrinite (Parker 1982). High gas–oil ratio (GOR) oils began to be generated within these basins as they subsided rapidly under the load of Lower Cretaceous clastic deposits. They then migrated up into subtle structural traps forming within Cenomanian clastic rocks, modified from syn-depositional Jurassic features (Kholeif *et al.* 1988). Recent

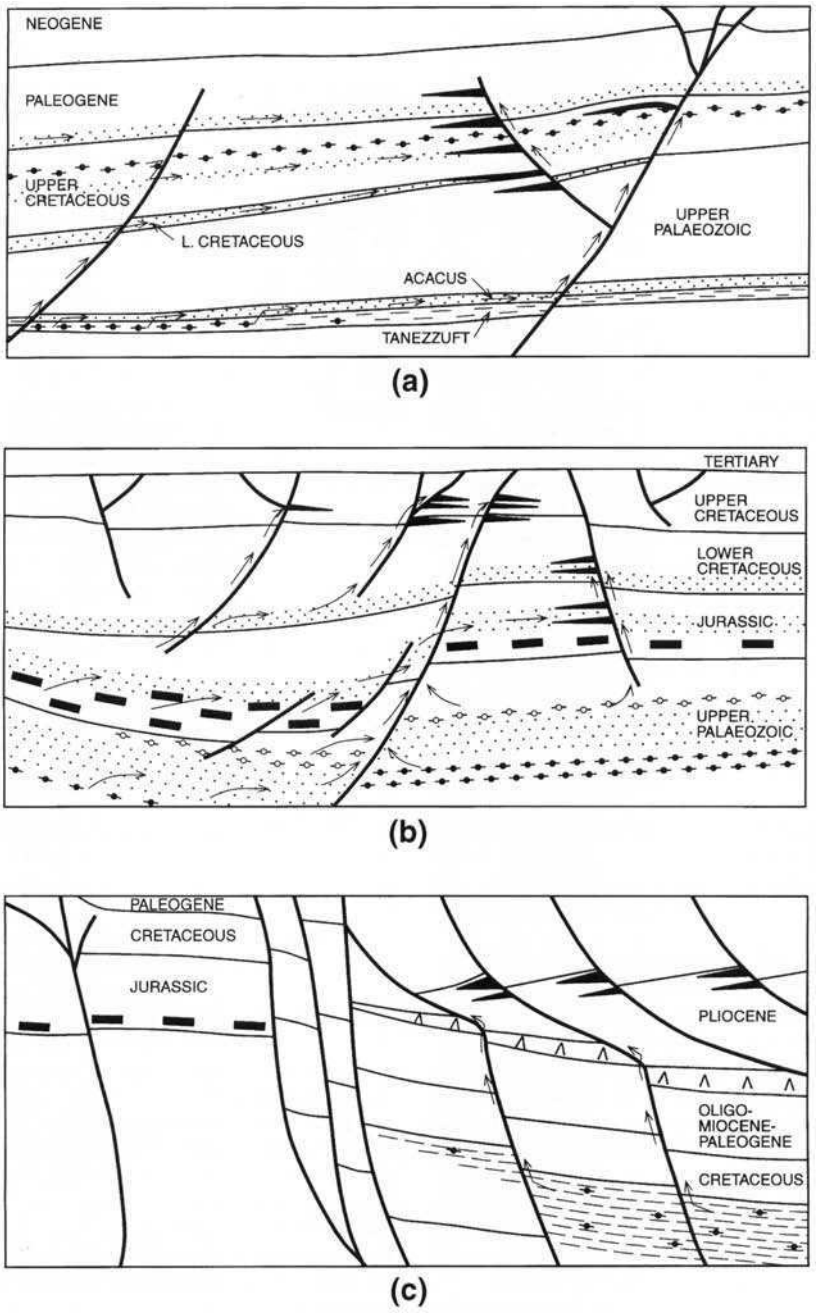

Fig. 10. (**a**) Tanezzuft–Rakb petroleum systems (Sirt). (**b**) Upper Paleocene–Jurassic coal petroleum systems. (**c**) Nile Delta petroleum systems.

exploration has also proven the presence of significant volumes of high-gravity oil and gas at greater depth within the Mid-Jurassic sands themselves, retained by interbedded shales. This petroleum system is delimited by the Mid-Jurassic coal swamp facies belt, to the west along the northern margin of the Cyrenaica Platform (see Sola & Ozcicek 1990; Ghori 1991) and eastwards into the eastern Western Desert, the northern Eastern Desert and into North Sinai.

Although the Helez oils of Israel are demonstrably derived from Late Jurassic–Early Cretaceous deep marine shales (Bein & Sofer 1987), no other hydrocarbons to the west have yet been proven to share a common origin. However, the interpolation of Jurassic basinal shale facies belts, and absence of other suitable source rocks would suggest that the most likely progenitor for gas, condensate and light oils within and adjacent to the Nile Delta and offshore northern Sinai is the overmature Type II kerogen within these Late Jurassic shales (Keeley *et al.* 1990). Although these source rocks may well have first entered the oil window during the Late Cretaceous, only Miocene–Pliocene burial would have brought about thermal maturation sufficient for substantial and principally gas generation and expulsion. A Late Jurassic marine shale petroleum system can be anticipated to follow the Egyptian coastline westwards, and to underlie the Marmarica and Darnah Troughs of northern Cyrenaica (see El-Arnauti & Shelmani 1988, Sola & Ozcicek 1990). There is a risk, however, that along parts of the western Egyptian coast, subsequent burial will not have been sufficient to begin even oil generation.

Localized Lower Cretaceous petroleum systems are thought to function in the Western Desert, within at least the Matruh Basin and the Mireir Trough, which lies adjacent to the Alamein–Yidma–Razzaq trend of fields (El Ayouty, 1990). Delta-front shales and delta-top coals within the Alam el Bueib Formation have generated waxy oils and gas similar in aspect to those of Jurassic origin elsewhere, which makes their definitive recognition problematic. Yet the burial history of these basins, and the apparent absence of Jurassic coals at depth, would support the presence of such an analogous system.

The Upper Cretaceous petroleum system is responsible for the billion barrel fields of the Sirt, Abu Gharadiq and Suez Basins. The prolific Turonian–Coniacian Type I source rocks matured and expelled hydrocarbons at different times, with migration into different reservoirs. In the Sirt Basin, rapid burial of the source rock occurred during the Maastrichtian and Paleogene, over which period most traps were formed (Bezan 1993). The Neogene burial history appears more complex, and certainly involved uplift as well as further burial. In the axial sectors, late-stage generation, especially of gas, continues into the present day.

Rapid burial in the Abu Gharadiq Basin took place at more or less the same time, but episodes of 'Syrian Arc' inversion from the Eocene onwards ensured that further generation was effectively halted. Oil and gas generation here seem to have been broadly contemporaneous. Across the Kattaniyah Horst, the Guindi Basin did not experience rapid burial until the Eocene, so that different reservoirs and trap types were available for charging (Fig. 11).

In response to rapid rift subsidence and the associated heat flow increase during the Early and Mid Miocene (Bosworth 1994), all source rocks in the Gulf of Suez entered the oil window at roughly the same time. However, consistent oil geochemistry points to the overwhelming contribution made by the Turonian–Coniacian 'Brown Limestone' (Salah & Alsharhan 1996).

Mention, albeit mostly speculative, should be made in passing of oil source potential of the Eocene restricted marine shelf carbonates across the coastal sector of NE Africa. Rohrback (1982) cited evidence for a contribution from this level to Gulf of Suez oils, and Said (1962, p. 282) summarized reports of bituminous Eocene limestones from the Cairo region, which are known to extend into Cyrenaica. It would therefore seem possible that these limestones may be found within the early oil generation window along the shelf margin. However, only where deeper burial has taken place subsequently, such as offshore beneath the Nile Delta and in the Marmarica and Darnah Troughs, may a viable Eocene petroleum system exist.

The Lower–Middle Miocene 'Globigerina Marls' of the Gulf of Suez and the northern Red Sea have proven geochemical potential to generate hydrocarbons (Salah & Alsharhan 1996). However, within the Gulf of Suez, the dominance of Type II kerogens and the restricted kitchen area have led to the conclusion that they have only contributed a small fraction to the total volume of hydrocarbons. Further south in the Red Sea, where high geothermal gradients continue to prevail, and other source rocks are absent or eroded, known gas–condensate deposits can be more closely linked to this Miocene interval.

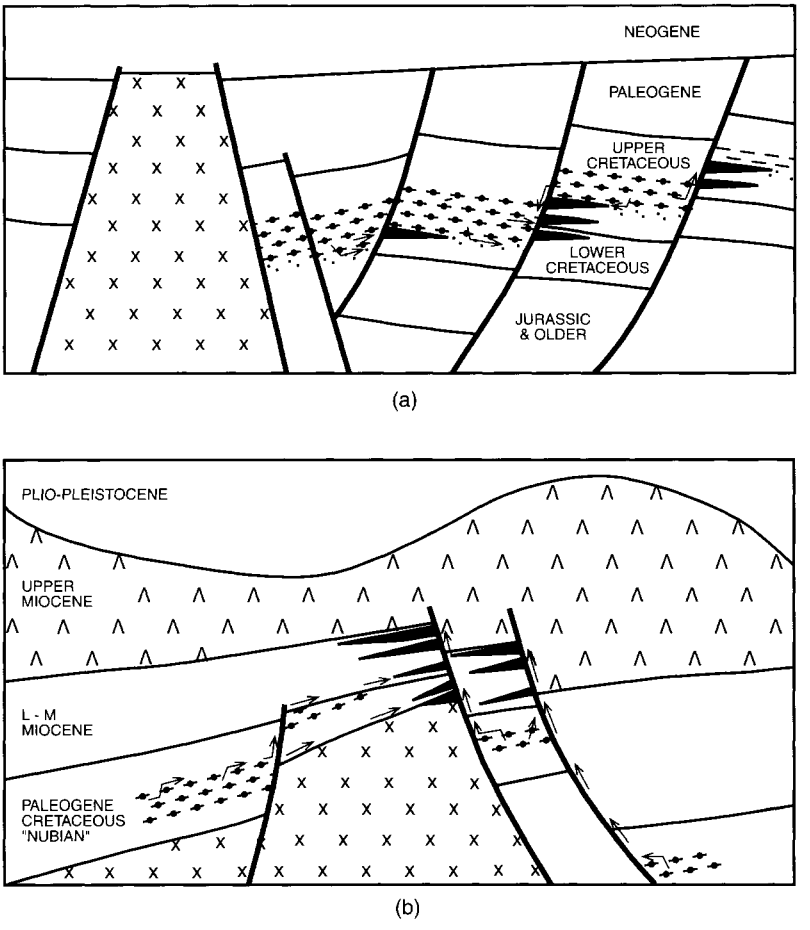

Fig. 11. Upper Cretaceous petroleum systems: (**a**) Abu Gharadig; (**b**) Suez.

Plate tectonics and controls on petroleum distribution

The tectonic processes that gave rise to overlapping areas of basin subsidence and inversion within the NE African craton and along its margin with Palaeo- and Meso-Tethys appear to have been controlled primarily by regional compressive stress systems dispersed and reorientated along major NE–SW 'Syrian Arc' trending fractures, that originated from depth within the craton (Keeley 1994). Before the Mesozoic, these stresses led mostly to transpressive and transtensional strain, inducing phases of rapid basin subsidence followed by inversion, or vice versa. The resulting broad intracratonic basins (> 200 km) permitted the regional accumulation of both sandstone and limestone reservoirs, and kerogen-rich mudstones.

The causes of these strike-slip induced processes remain speculative. These same stress systems continued into the Mesozoic and Cenozoic, but to a less important degree (Fig. 12).

The formation of a new extensional Tethyan margin with continental NE Africa took place over the interval Pliensbachian–Bathonian, propagating by means of crustal rifting from east to west. However, there is now evidence from the Mid–Late Triassic of central Libya for a similar but failed rift processes in the Proto-Sirt Basin, propagating from west to east, but apparently not reaching into Egypt (Shelmani *et al.* 1992). This evidence would also support the presence of a long-lived axis of asthenospheric upwelling, roughly parallel to the present NE African coast, over a period of at least 80 Ma (Mid Triassic–Late Jurassic). The resulting half-graben basins, offset by ancient Syrian Arc

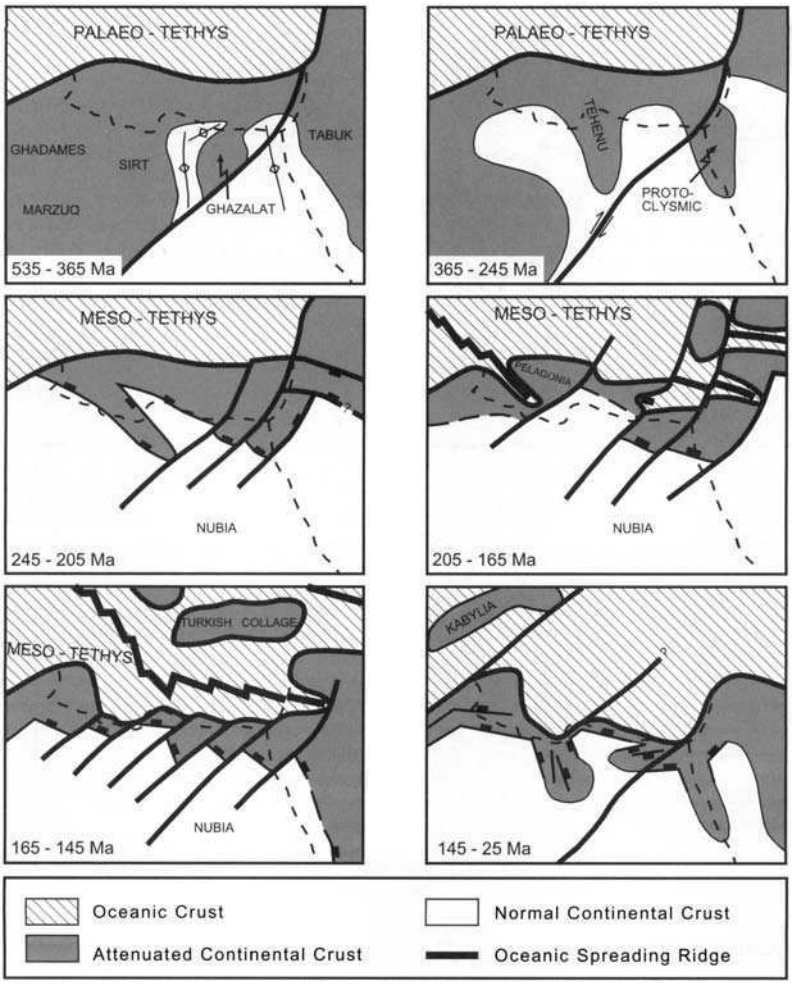

Fig. 12. Plate tectonic evolution of the NE African continental margin with Tethys and its antecedents.

fractures, were much smaller (< 200 kms). However, most of these basins persisted from either the Late Triassic or Mid Jurassic into the Paleogene, despite repeated episodes of inversion and subsidence. The strength of Tethyan eustatic changes ensured that facies belts controlling the distribution of source and reservoir rocks were laterally persistent over hundreds of kilometres.

Of the entire area under study, the Jebel el Akhdar poses the greatest difficulties in tectonic interpretation, and hence in terms of evaluating hydrocarbon potential. The area remains poorly explored, and yet it is clear that thick sequences of mudstone accumulated during Cretaceous and Paleogene subsidence (Shelmani *et al.* 1992; Mansouri *et al.* 1993). However, until a greater understanding of the tectonic controls on this subsidence can be achieved, ideas as to maturation history, and distribution of source and reservoir facies will remain elusive.

There is a close and well-established relationship between tectonics and hydrocarbon potential in the Gulf of Suez. Maturation of the Late Cretaceous source rock was controlled by rapid subsidence of small half-grabens from Early Miocene times onward (Salah & Alsharhan 1996). Within each of these half-grabens, tectonic subsidence and Miocene sea-level fluctuations combined to produce rapid facies changes from alluvial fan clastics, through shallow marine clastics and carbonates, to bathyal mudstones (Keeley 1994). Changes in the polarity of subsidence in these half-grabens influenced the direction of migration of expelled hydrocarbons.

Conclusions

Through a study of the changes in the stratigraphical succession across NE Africa, a greater appreciation has been obtained of the importance not only of eustacy, but also of tectonics in influencing the geological record. A number of basins have evolved, only to be inverted and superseded by basins with different limits and axes. This makes any understanding of facies distribution through time well nigh impossible without first an initial comprehension of the controls on basin subsidence and inversion, and their interaction with sea-level fluctuations. Petroleum potential therefore is influenced not only by the complex distribution of source, seal and reservoir rocks, but also by the effects of burial, uplift and erosion, which all undergo rapid variations in time and space.

Despite great variations in our knowledge base across NE Africa, it has been possible in this study to identify, on a provisional basis at least, those areas where new plays, or those proven elsewhere, await further evaluation. The history of petroleum exploration in NE Africa bears testimony to the role played by fresh ideas, and to their effective implementation to this exciting and, fortunately for us, still poorly understood area. As this analysis shows, much oil and gas must surely remain to be discovered here: in Cyrenaica, in the NW corner of the Western Desert, beneath the southern Nile Delta and between the Delta and the Suez Canal (Fig. 13).

We are grateful for support and encouragement through the last 15 years from many colleagues in Egypt and the UK, particularly to H. Hafez (SUCO, Cairo), M. Ayouti (Cairo), S. S. Ibrahim (AGIBA, Cairo), and the past and present Vice-Chairmen for Exploration and their staff at EGPC in Cairo: M. A. Halim and S. Hafez. In Benghazi (GSPLAJ), M.L.K. benefited from numerous discussions with Dr F. Said, Y. Faituri, Dr M. Shelmani, Dr B. Thusu, S. Ahmed and B. Mohammed, all of AGOCO. M.L.K. would like to thank many UK collaborators, including C. Floyd, G. Forbes, R. McGarva, R. Wallis, C. King, S. Rasul, R. Smout and G. Dungworth. We are both appreciative of the efforts of the conference organisers, and especially D. Clark-Lowes for interest and assistance. The comments of our reviewer, P. Griffiths, were very helpful in improving the manuscript, for which we are grateful. M.L.K. publishes with the permission of Emerald Energy Plc, and M.S.M. thanks the University of Kuwait for financial support.

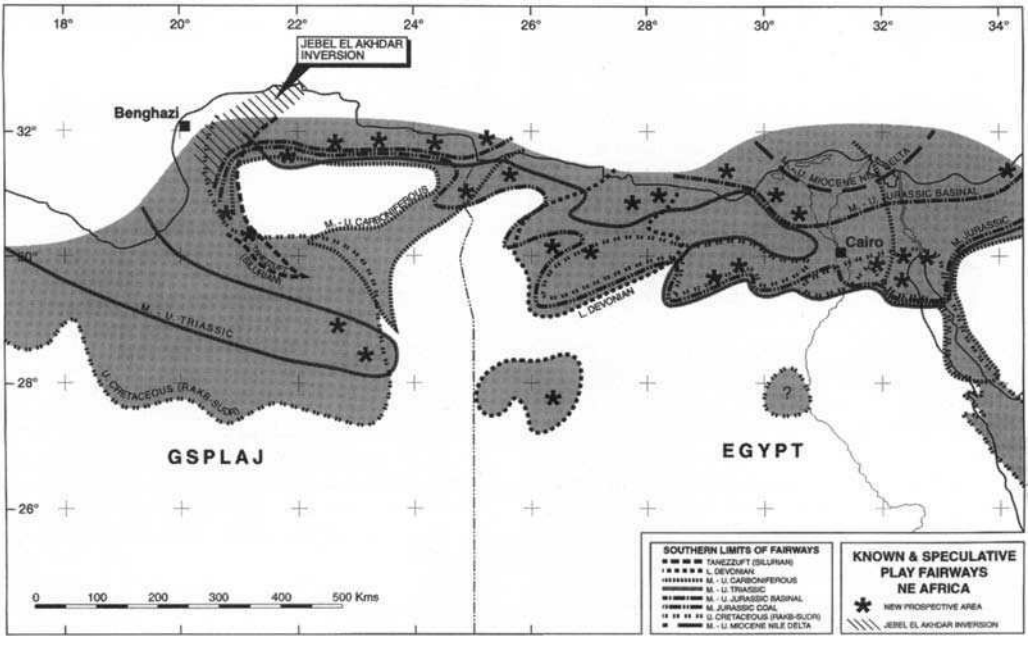

Fig. 13. Known and speculative play fairways.

References

BAGGE, M. A. & KEELEY, M. L. 1994. The oil potential of Mid-Jurassic coals in northern Egypt. *In*: SCOTT, A. C. & FLEET, A. J. (eds) *Coal and Coal-bearing Strata as Oil-prone Source Rocks?* Geological Society, London, Special Publications, **77**, 183–200.

BEIN, A & SOFER, Z. 1987. Origin of oils in Helez region, Israel—implications for exploration in the Eastern Mediterranean. *Bulletin, American Association of Petroleum Geologists*, **71**(1), 65–75.

BELLINI, E. & MASSA, D. 1980. A stratigraphic contribution to the Palaeozoic of the southern basins of Libya. *In*: SALEM, M. J. & BUSREWIL, M. T. (eds) *The Geology of Libya Vol.1* , Academic Press, London, 3–56.

BEZAN, A. M. 1993. Pre-Upper Cretaceous tectonic evolution of Sirt Basin (Abstract). *In*: *Sedimentary Basins of Libya, First Symposium: Geology of Sirt Basin*, Earth Science Society of Libya, Tripoli, GSPLAJ.

BOSWORTH, W. 1994. A model for the three-dimensional evolution of continental rift basins, NE Africa. *Geologische Rundschau*, **83**, 671–688.

BRENCKLE, P. L. & MARCHANT, T. R. 1987. Calcareous microfossils, depositional environments and correlation of the Lower Carboniferous Um Bogma Formation at Gebel Nukhul, Sinai, Egypt. *Journal of Foraminiferal Research*, **17**, 74–91.

BRUGMAN, W. A. & VISSCHER, H. 1988. Permian and Triassic palynostratigraphy of northeast Libya. *In*: EL-ARNAUTI, A., OWENS, B & THUSU, B. (eds) *Subsurface Palynostratigraphy of Northeast Libya*. Garyounis University Publications, Benghazi, Libya, 157–169.

DEIBIS, S., FUTYAN, A. R. J., INCE, D. M., MORLEY, R. J., SEYMOUR, W. P. & THOMPSON, S. 1986. The stratigraphic framework of the Nile Delta and its implications with respect to the region's hydrocarbon potential. *Egyptian General Petroleum Corporation VIII Exploration Conference, Cairo*.

DURONIO, P., DAKSHE, A. & BELLINI, E. 1991. Stratigraphy of Offshore Cyrenaica (Libya). *In*: SALEM, M. J., HAMMUDA, O. S. & ELIAGOUBI, B. A. (eds) *The Geology of Libya Vol. 4*. Elsevier, Amsterdam, 1589–1620.

EL-ARNAUTI, A. & SHELMANI, M. 1985. Stratigraphic and structural setting. *In*: *Palynostratigraphy of northeast Libya. Journal of Micropalaeontology*, **4**, 1–10.

—— & —— 1988. A contribution to the northeast Libya subsurface stratigraphy with emphasis on Pre-Mesozoic. *In*: EL-ARNAUTI, A., OWENS, B & THUSU, B. (eds) *Subsurface Palynostratigraphy of Northeast Libya*. Garyounis University Publications, Benghazi, 1–16.

EL AYOUTI, M. K. 1990. Petroleum geology. *In*: SAID, R. (ed.) *The Geology of Egypt*. Balkema, Rotterdam, 567–600.

EL HAWAT, A. S. & SHELMANI, M. A. 1993. *Short Notes and Guidebook on the Geology of the Jabal al Akhdar, Cyrenaica, NE Libya*. Earth Science Society of Libya, GEOLIBYA, Benghazi.

FÜRST, M. 1993. The palaeogeography of the Sirt basin (Libya) from Upper Cretaceous to Eocene (extended abstract). *In*: THORWEIHE, U. & SCHANDELMEIER, H. (eds) *Geoscientific Research in Northeast Africa. Proceedings of the International Conference on Geoscientific Research in Northeast Africa, Berlin*. Balkema, Rotterdam, 237–242.

GHORI, K. A. R. 1991. Petroleum geochemical aspects of Cyrenaica, NE Libya. *In*: SALEM, M. J., BUSRAWIL, M. T. & BEN ASHOUR, A. M. (eds) *The Geology of Libya Vol. 7*. Elsevier, Amsterdam, 2743–2755.

GOLDBERG, M. 1964. Problems in the Jurassic stratigraphy of Southern Israel. *Israeli Journal of Earth Sciences*, **13**, 169–171.

GUEINN, K. J. & RASUL, S. M. 1986. A contribution on the biostratigraphy of the Palaeozoic of the Western Desert, utilising new palynological data from the subsurface. *Egyptian General Petroleum Corporation VIII Exploration Conference, Cairo*.

JENKINS, D. A. 1990 .North and central Sinai. *In*: SAID, R. (ed.) *The Geology of Egypt*. Balkema, Rotterdam, 361–380.

KEELEY, M. L. 1989. The Palaeozoic history of the Western Desert of Egypt. *Basin Research*, **2**, 35–48.

—— 1994. Phanerozoic evolution of the basins of Northern Egypt and adjacent areas. *Geologische Rundschau*, **83**, 728–742.

—— & WALLIS, R. J. 1991. The Jurassic System in northern Egypt: II. Depositional and tectonic regimes. *Journal of Petroleum Geology*, **14**, 49–64.

——, DUNGWORTH, G., FLOYD, C. S., FORBES, G. A., KING, C., MCGARVA, R. M. & SHAW, D. 1990. The Jurassic System in northern Egypt: I. Regional stratigraphy and implications for hydrocarbon prospectivity. *Journal of Petroleum Geology*, **13**, 397–420.

KHOLEIF, W., WORK, J. G. & SANAD, S. 1988. Meleiha: its history and significance. *VIII Exploration Seminar, Egyptian General Petroleum Corporation, Cairo*.

KLITZSCH, E. 1990. Paleozoic. *In*: SAID, R. (ed.) *The Geology of Egypt*. Balkema, Rotterdam, 393–407.

LOBOZIAK, S. & CLAYTON, G. 1988. The Carboniferous palynostratigraphy of northeast Libya. *In*: EL-ARNAUTI, A., OWENS, B & THUSU, B. (eds) *Subsurface Palynostratigraphy of Northeast Libya*. Garyounis University Publications, Benghazi, 129–155.

MANSOURI, A. L., THUSU, B. & EL-ARNAUTI, A. 1993. Recent advances on the geology of northeast Libya (extended abstract). *In*: THORWEIHE, U. & SCHANDELMEIER, H. (eds) *Geoscientific Research in Northeast Africa. Proceedings of the International Conference on Geoscientific Research in Northeast Africa, Berlin*. Balkema, Rotterdam, 231–235.

MESHREF, W. M. 1990. Tectonic framework. *In*: SAID, R. (ed.) *The Geology of Egypt*. Balkema, Rotterdam, 113–156.

NEEV, D., 1977. The Pelusium Line—a major transcontinental shear. *Tectonophysics*, **38**, 1–8.

PARKER, J. R. 1982. Hydrocarbon habitat of the Western Desert, Egypt. *VIII Exploration Seminar, Egyptian General Petroleum Corporation, Cairo.*

PICARD, L. & HIRSCH, F. 1987. *The Jurassic Stratigraphy in Israel and the Adjacent Countries.* The Israel Academy of Sciences and Humanities, Jerusalem.

QUENNEL, A. M. 1984. The Western Arabian rift system *In*: DIXON, J. E. & ROBERTSON, A. H. F. (eds) *The Geological Evolution of the Eastern Mediterranean.* Geological Society, London Special Publications, **17**, 775–788.

ROHRBACK, B. G. 1982. Crude oil geochemistry of the Gulf of Suez. *Egyptian General Petroleum Corporation VI Exploration Seminar, EPEX Cairo, Vol. 1*, 212–223.

SAID, R. 1962. *The Geology of Egypt.* Elsevier, Amsterdam.

—— 1981. *The Geological Evolution of the River Nile.* Springer-Verlag, New York.

—— 1990*a*. Cretaceous paleogeographic maps. *In*: SAID, R. (ed.) *The Geology of Egypt.* Balkema, Rotterdam, 439–449.

—— 1990*b*. Cenozoic. *In*: SAID, R. (ed.) *The Geology of Egypt.* Balkema, Rotterdam, 451–486.

SALAH, M. G. & ALSHARHAN, A. S. 1996. Structural influence on hydrocarbon entrapment in the northwestern Red Sea, Egypt. *Bulletin, American Association of Petroleum Geologists*, **80**(1), 101–118.

SEMTNER, A.-K. & KLITZSCH, E. 1994. Early Paleozoic paleogeography of the northern Gondwanan margin: new evidence for Ordovician-Silurian glaciation. *Geologisches Rundschau*, **83**, 743–751.

SESTINI, G. 1984. Tectonic and sedimentary history of the NE African margin (Egypt–Libya). *In*: DIXON, J. E. & ROBERTSON, A. H. F. (eds) *The Geological Evolution of the Eastern Mediterranean.* Geological Society, London, Special Publications, **17**, Blackwell, Oxford, 161–176.

SHAHEEN, A. N., SHEBAB, M. M. & MANSOUR, H. F. 1986. Quantitative evaluation and timing of hydrocarbon generation in Abu Gharadig Basin, Western Desert, Egypt. *Egyptian General Petroleum Corporation VIII Exploration Conference, Cairo.*

SHELMANI, M., THUSU, B. & EL-ARNAUTI, A. 1992. Subsurface occurrences of Middle and Upper Triassic sediments in eastern Libya. *In*: SADEK, A. (ed.) *Geology of the Arab World*, **2**, Cairo University, 233–240.

SOLA, M. & OZCICEK, B. 1990. On the hydrocarbon prospectivity of North Cyrenaica Region, Libya. *Petroleum Research Journal*, **2**, 25–41.

THUSU, B., VAN DER EEM, J. G. L. A., EL-MEHDAWI, A. & BU-ARGOUB, F. 1988. Jurassic-Early Cretaceous palynostratigraphy in northeast Libya. *In*: EL-ARNAUTI, A., OWENS, B & THUSU, B. (eds) *Subsurface Palynostratigraphy of Northeast Libya.* Garyounis University Publications, Benghazi, 171–214.

TRÄGER, U. 1984. The oil shale potential of Egypt. *Berliner Geowissenschaftlichen Abhandlungen*, **50**, 375–380.

TURNER, B. R. 1980. Palaeozoic sedimentology of the southeastern part of the Al Kufra Basin, Libya: a model for oil exploration. *In*: SALEM, M. J. & BUSREWIL, M. T. (eds) *The Geology of Libya Vol. 2*, Academic Press, London, 351–374.

This page intentionally left blank

An overview of the petroleum systems of Morocco

AL MOUNDIR MORABET, RABAH BOUCHTA & HADDOU JABOUR

ONAREP, P.O. Box 8030, Rabat, Morocco

Abstract: Magoon & Dow's petroleum system concept is utilized in this paper to evaluate the origin of the proven hydrocarbon resources of Morocco, which lie chiefly in the Essaouira, Prerif and Rharb Basins. Several systems are interpreted, in which the confidence in the source–petroleum tie varies from 'known' to 'speculative', involving charge from Silurian (eastern Essaouira), Lias (Prerif), Oxfordian (western Essaouira), Cretaceous (Ain Hamra) and an intra-Miocene biogenic system in the Rharb Basin. The origin of the Cap Juby heavy oil accumulation in the offshore Tarfaya basin is uncertain, with a Jurassic carbonate source currently the favoured interpretation. The petroleum system concept is extended in this paper to predict further, currently undrilled and unproven systems. These include areas where the proven source systems referred to above are likely to extend, plus additional systems predicted on the basis of analogues to surrounding regions. An example of the latter is a series of postulated Triassic systems developed in lacustrine deposits in offshore half-grabens. Palaeozoic source rocks may be regionally developed and may still be in the oil and gas windows over wide, generally unexplored, regions. Lower to Middle Jurassic source rocks are predicted in lagoonal settings in platform sags and in outer shelf environments, whereas Cretaceous source beds occur in continental rift complexes and passive margins, with maturity likely to be reached in depocentres and below thrusts. Biogenic gas potential is probably confined to Neogene deposits in foreland and divergent margin basins. Further application of the petroleum system concept should help to significantly reduce geological risk, particularly in frontier exploration areas.

Most Moroccan sedimentary basins are still largely unexplored and can justifiably be considered frontier exploration areas. The database so far acquired in the exploration of these basins requires a modern conceptual interpretation. As more geological, geophysical and geochemical information about known petroleum occurrences is acquired, there is a need to adequately document the models pertinent to these proven systems and use these as analogues to accurately and adequately assess the hydrocarbon potential of less explored basins.

Basin evaluation to date in Morocco has relied on analytical studies that emphasize structural evolution and sediment fill, regardless of their relationship to any petroleum deposits. The petroleum system concept, as proposed by Magoon & Dow (1994) is a more holistic approach, which emphasizes the genetic relationship between a particular source rock and the resulting petroleum accumulation. These basic elements include the petroleum source rock, migration path, reservoir rock, seal and trap and an appreciation of the geological processes involved in each of these.

The purpose of this paper is to outline the current level of understanding of the petroleum systems of Morocco, to determine the level of certainty of a specific system and attempt a classification, and additionally to predict where further, currently unproven, petroleum systems may lie elsewhere in the country.

The terminology used in this paper is a composite of that applied by Magoon & Dow (1994), Magoon (1988) and Demaison & Huizinga (1991). Definitions of the key terms used are given below.

An established petroleum system (one in which the occurrence of hydrocarbons is proven) can be identified at three levels of certainty in terms of the geochemical correlation of petroleum and source rocks (Magoon & Dow 1994). These can be listed as follows: (1) a known petroleum system, where a good geochemical match exists between the active source rock and oil or gas accumulations, denoted by (!); (2) a hypothetical petroleum system, where geochemical information is sufficient to identify a source rock but no geochemical match has yet been determined between source and petroleum deposits, denoted by (.); (3) a speculative petroleum system, where the level and nature of the active source rock are postulated entirely on the basis of geological and/or geophysical evidence, denoted by (?). Magoon and Dow proposed naming systems based on the predominant source and reservoir within the relevant system, using lithostratigraphic schemes. The absence of a common accepted lithostratigraphy throughout Morocco presents problems here, therefore, chronostratigraphic terms are used. These have to be used in conjunction with the basin name concerned.

The migration system can be further described

MORABET, A. M., BOUCHTA, R. & JABOUR, H. 1998. An overview of the petroleum systems of Morocco. *In*: MACGREGOR, D. S., MOODY, R. T. J. & CLARK-LOWES, D. D. (eds) 1998. *Petroleum Geology of North Africa*. Geological Society, London, Special Publication No. 132, 283–296.

using the following defined terms: a purebred petroleum system exists in a geological setting in which the structural framework has not changed significantly during the geological life of that system; a hybrid system exists in areas of major structural reorientation, without which the petroleum system would occur in its current form; high-impedance migration systems are characterized by laterally continuous seals coupled with a moderate to high degree of structural deformation; low-impedance migration systems are characterized by either a high degree of regional seal continuity or a low degree of structural deformation. Data available on the petroleum systems of Morocco at this stage are generally not sufficient to estimate charge factor or gross accumulation efficiency (GAE). However, in some cases, observations on trap fill allows an evaluation of whether the system is under, normally- or super-charged.

Basin development, regional stratigraphy and source facies occurrences

A large number of discrete sedimentary basins are recognized in Morocco (Fig. 1), varying in their style from intramontane through inverted rifts to thrust belts, forelands and passive margins. Most these basins remain underexplored, with their potential petroleum systems and resources ill-understood. Production is currently limited to onshore basins in the coastal area of northern and central Morocco. Our current state of knowledge of the history of basin development and stratigraphy of the country is summarized below. Figure 2 presents a summary of the most important tectonic events within a typical onshore Moroccan basin, and a stratigraphic section of the area of fullest control, the Essaouira Basin, is illustrated as Fig. 3.

Palaeozoic

The oldest rocks encountered in Morocco belong to the Precambrian and outcrop in the Anti-Atlas mountains. Lower and Middle Cambrian strata have not been drilled but geophysical data, tied to surface geological control, suggest that the succession varies between 100 and 3000 m thick, containing grey–green shales, sandstones, quartzites, and volcaniclastic deposits. The Ordovician is represented by 1000—2500 m of grey to black shales, siltstones, sandstones and quartzites, and the Silurian by 100—200 m of graptolitic, locally carbonaceous, black shales. Devonian strata are mainly shales, often black, with thin sandstones and deeper water reefal limestones locally developed. The Carboniferous succession, up to 4000 m thick in depocentres, rests unconformably on Devonian strata, and is represented by Visean, Namurian and Westphalian shales, sandstones, conglomerates, turbidites and platform carbonates. Thin carbonaceous shales and coal beds are also present locally. The Carboniferous rocks are bounded by the overlying erosive Hercynian unconformity.

The main potential Palaeozoic source rocks are Silurian sapropelic, radioactive graptolitic black shales, rich in kerogen of Type II; these form the main contributing source bed in Algeria (Boote *et al.* this volume). Black carbonaceous shales also occur frequently in the Upper Ordovician and Lower Devonian, and locally in the Westphalian.

The tectonic evolution of the onshore intracratonic basins, where the Palaeozoïc succession is best represented, is complex and multi-phase (Figure 2). The first main event, the Hercynian orogeny, caused strong deformation of the Palaeozoic sequence. Early Hercynian events commenced at the end of the Devonian with very large scale folding, and strike-slip faulting resulting in the creation of a number of deep Carboniferous basins. Subsequent deformation occurred during the main Hercynian phase, commencing in the Late Westphalian, with tight folding, thrusting, nappe development and strike-slip faulting, associated with dyke emplacement and granite intrusions.

These compressional events have a crucial impact on the maturity history of Palaeozoic source rocks in many of the intracratonic basins of Morocco. In the Tadla Basin, Lower Palaeozoic source rocks are still present within the oil window in uplifted and thrust blocks (Fig. 4), generally in areas which did not suffer from deep Carboniferous burial. It is proposed that recent burial (Tertiary) resulted in renewed hydrocarbon generation in at least some of these basins. Examples are the western Meseta, High Plateau, Prerif, western Tindouf and part of Errachidia–Boudenib areas. In other regions, particularly inverted Carboniferous rifts, Palaeozoic source rocks reached high levels of maturity before the main Hercynian event.

Mesozoic

Triassic grabens and half-grabens associated with the fragmentation of the continents occur throughout Morocco, filled with continental coarse clastic deposits and, red beds and locally by lacustrine deposits (e.g. Brown 1980). Crustal

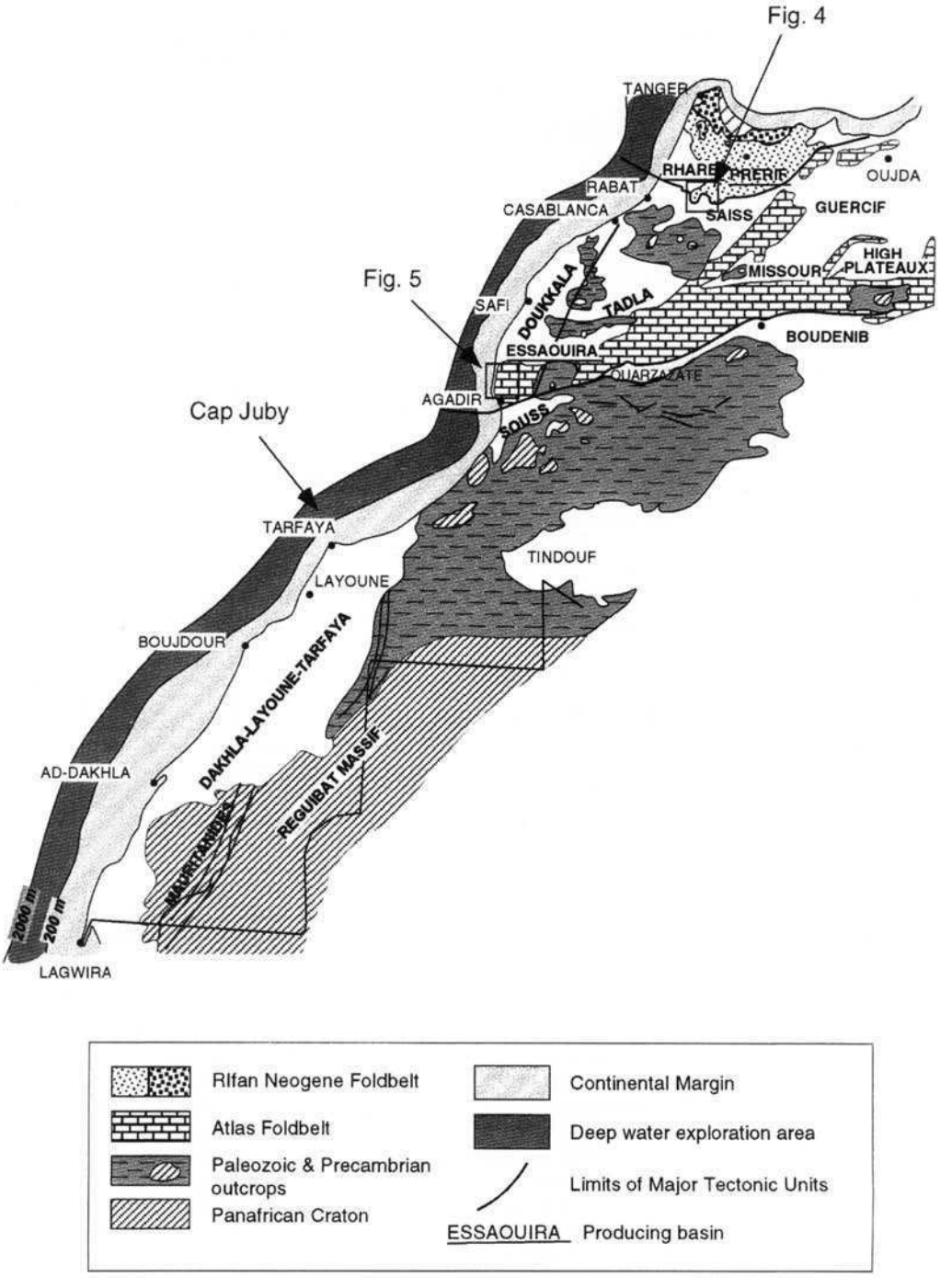

Fig. 1. Main structural units and major sedimentary basins of Morocco.

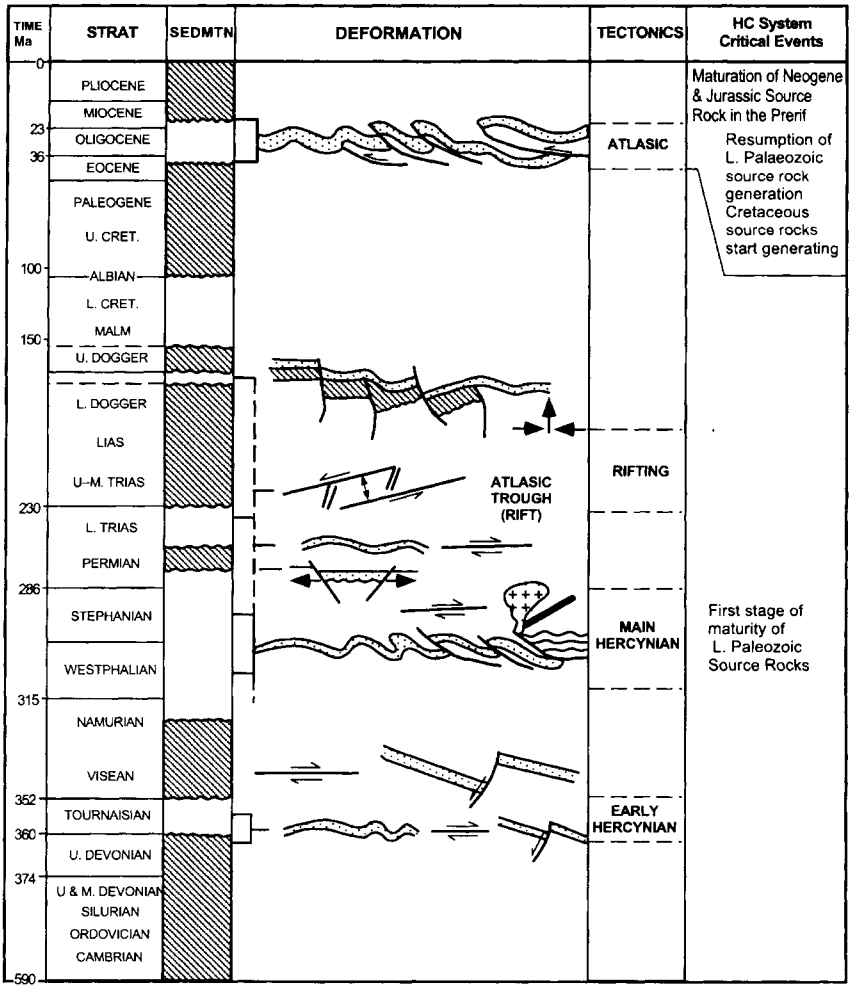

Fig. 2. Tectonic evolution and subsequent critical events of petroleum systems in Morocco, based on the example of the Tadla and other basins bordering the Atlas fold belt.

extension and rifting commenced in the latest Triassic. Alluvial fan and fluvial clastic deposits were then shed from fault margins, Palaeozoïc massifs and Hercynian highs. Transgressive sediments associated with the Tethys seaway spilled into the proto-Atlantic oceanic rift near the end of the Triassic, leading to the development of hypersaline lagoon conditions over a large part of coastal Morocco and the formation of thick salt deposits in, for example, the Essaouira Basin, Prerif and High Plateaux. These should provide excellent seals for hydrocarbons generated from both Palaeozoïc and Triassic source rocks.

The opening of the Atlantic Ocean was preceded by further (Triassic–Lower Jurassic) rifting. This was followed by massive regional subsidence during the Jurassic, as is well illustrated in the Tarfaya region and along the Atlantic shelf. Tethyan-related rifting occurred during the Jurassic in the Atlas (Guiraud this volume). Such Tethyan rifts are often discordant to the Atlantic-related rifts, with the former trending NE–SW and the latter N–S. The Tethyan rift system was later inverted during the Alpine orogeny to form the mountains of the High and Middle Atlas.

Liassic and Dogger (pre-Callovian) sedimentation is dominated by intertidal to supratidal conditions, extending across most of the coastal basins. A sediment pile composed largely of carbonates, anhydrite and red–brown to green

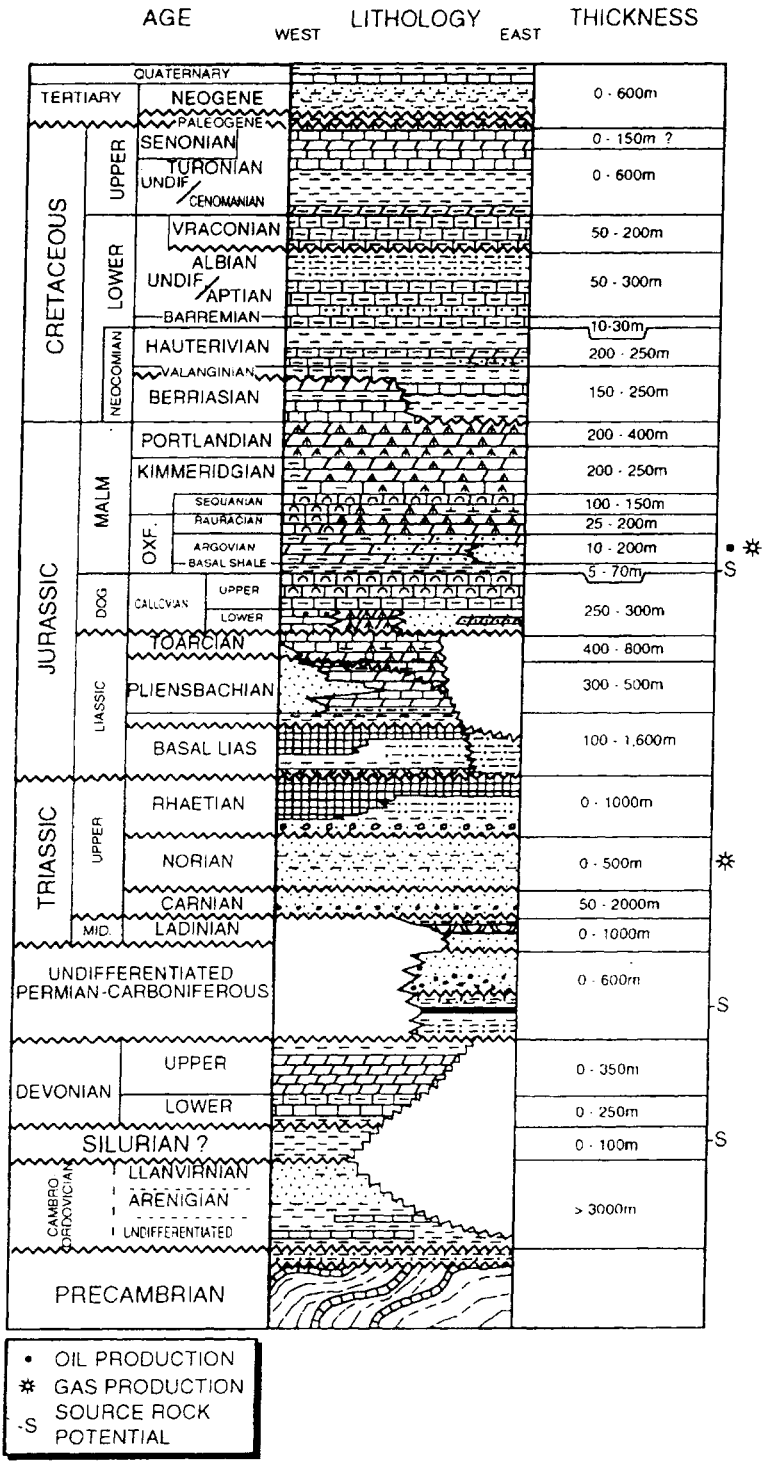

Fig. 3. Stratigraphic column of the Essaouira Basin, after Broughton & Trépanier (1993).

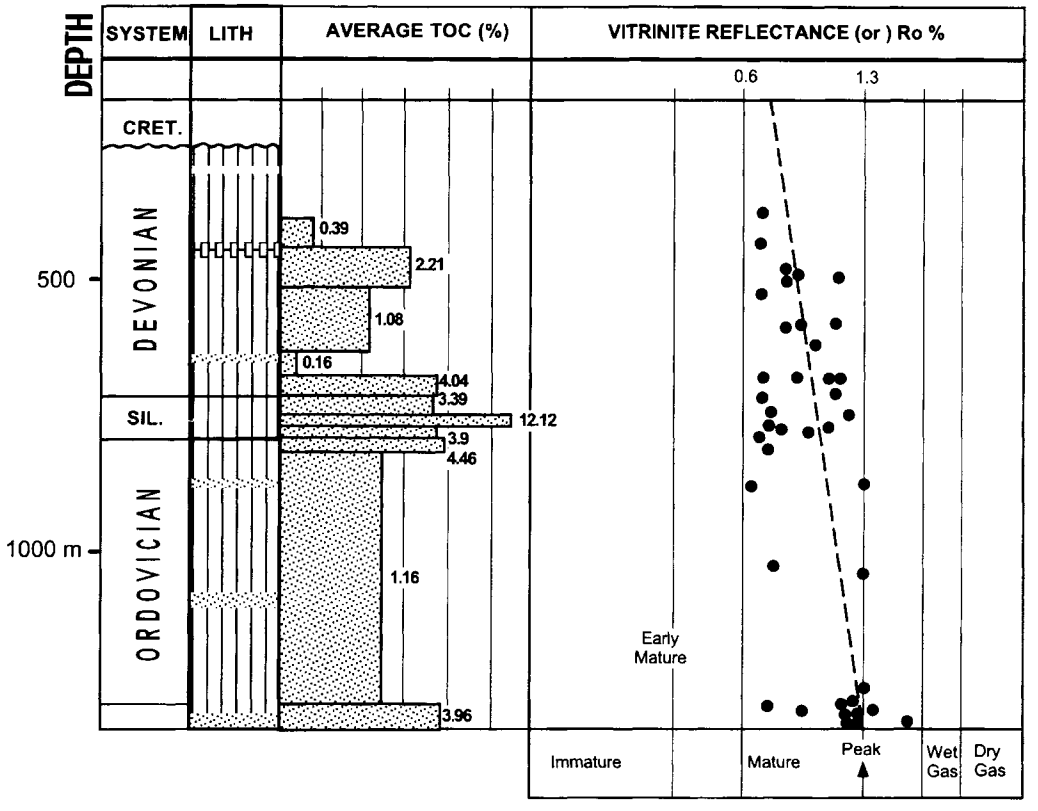

Fig. 4. Geochemical data on the KAT-1 well in the Tadla Basin, illustrating excellent quality Palaeozoic source rocks still within the oil window.

shales accumulated. The Bajocian (Middle Jurassic) is characterized by an important clastic influx, especially in the area of the Prerif ridges. Shelfal carbonates and minor grey shale were deposited during the Callovian and Early Oxfordian times. A gradual regression began in Middle Oxfordian time, resulting in the renewal of intertidal to supratidal facies deposition. This is followed by a marked drop in sea level during the Late Jurassic.

Jurassic potential source rocks range in age from Lower Jurassic (Tarfaya margin, Prerif and the Interatlasic Basins) to Oxfordian (Essaouira Basin). These source rock contain predominantly sapropelic Type II kerogen.

Lower Cretaceous rocks, which are particularly well represented in the Dakhla–Layoune-Tarfaya Basin, are characterized by thick regressive cycles. Thick continental and deltaic clastic deposits accumulated unconformably in that region over Jurassic platform carbonates. The overlying Aptian and Albian succession is composed of a thick interval of shallow marine, lagoonal and intertidal sediments, represented by lithofacies such as shales, sandstones and shelly limestones. Thick marl units, which may locally be rich in organic matter, are also widespread. The Late Cretaceous throughout Morocco is composed of carbonates and shales, with common minor transgressive events. Potential source rock development is tied to these transgressions, with an extensive organic-rich shale recognized in the Turonian (Einsele & Wiedmann 1982) and additional levels in the Albian observed in wells and at offshore Deep Sea Drilling project (DSDP) sites. The Turonian organic shale is seen as a 50m (gross) in the onshore Tarfaya Basin with total organic content (TOC) of 6–10% (Einsele & Wiedmann 1982).

As the Atlantic Ocean widened and deepened, the relative movement between the African and Eurasian plates reversed direction in Late Cretaceous time (Guiraud this volume). Collision and subduction in Early Tertiary time resulted in the Alpine orogeny, which had a major impact on northern Morocco. The Rif Domain

developed Alpine style nappes at this time. Subsidence continued in several marginal sedimentary troughs, associated with continued opening of the Tethys seaway, such as the Prerif ridges and the Moroccoan–Algerian Atlas. A thick Cretaceous sedimentary pile in the Atlas sedimentary trough, which may have subsided along lineaments determined by earlier incipient rifts, was inverted during the Early Tertiary, when the Atlas Mountains were overthrust to the west and south.

Paleocene to Eocene marine clastics are overlain by Oligocene continental clastics. During the Tortonian, the Prerif nappe was emplaced. This appears on seismic reflection profiles as an interval of chaotic internal structures. The nappe, which is up to 3000 m thick, contains Triassic salt and volcanic rocks together with Upper Cretaceous and Lower Tertiary strata. Post-nappe sediments, up to 2000 m thick, are composed of fine-grained clastic rocks, which were deposited in a foreland basin setting. Miocene transgressive sandy carbonates are present in the sub-nappe.

Established petroleum systems (with proven hydrocarbons)

This section of the paper presents the current level of understanding of the established petroleum systems of Morocco (i.e. those where oil and/or gas accumulations have been discovered) and classifies these (Table 1) in terms of our confidence in the source to oil tie, in accordance with the terminology of Magoon & Dow (1994). As geochemical data are available in each instance, but conclusive source to oil ties may be lacking, the majority of these systems fall in the 'hypothetical' or 'speculative' category.

Prerif producing basin

In the Prerif compressional belt, developed basinward of the Rif Nappe, available data are used to define three petroleum systems.

The Cretaceous–Miocene(!) petroleum system lies to the North of the Rharb Basin, and is represented by the first oil discovery in north Africa, Ain Hamra, drilled in 1923. Oil is reservoired in shallow (*c.* 200 m) Upper Miocene sand lenses, within steep compressional structures in the post-nappe series, and has been typed to a Late Cretaceous source. The complex structural setting suggests a hybrid system.

The other two systems occur in the Prerif ridges, as illustrated in Fig. 5. A series of oil occurrences in structures along the NE–SW trending Sidi-Fili fault is reservoired in washed or weathered Hercynian granites and fractured Palaeozoic sandstone reservoirs. The most likely source is the Lower Jurassic and therefore

Table 1. *Petroleum systems (established hydrocarbon accumulations)*

Basin	Petroleum system name (source age/main reservoir age)	Reservoir facies	Representative discovery	Status of geochemical correlation	Migration path
Prerif	Cretaceous–Miocene (!)	Clastic deposits	Ain Hamra	Good	Faults
	Lias–Domerian (!)	Dolomite	Haricha	Good	Faults
	Lias–Paleozoic (.)	Granite + Wash Quartzite	Sidi Fili trend	Fair	Faults
Rharb	Miocene–Miocene (.)	Turbidite sands	Ksiri	Fair	Local expulsion
Essaouira	Oxfordian–Oxfordian (!)	Dolomite	Sidi Rhalem	Good	Lateral Faults, subcrop
	Silurian–Triassic (.) (also Oxfordian reservoir)	Non-marine sands	Meskala	Fair	
Tarfaya	Lias–Upper Jurassic (?)	L. & M. Jurassic carbonate bank	MO–2 heavy oil (Cap Juby)	Poor but carbonate source favoured	Lateral

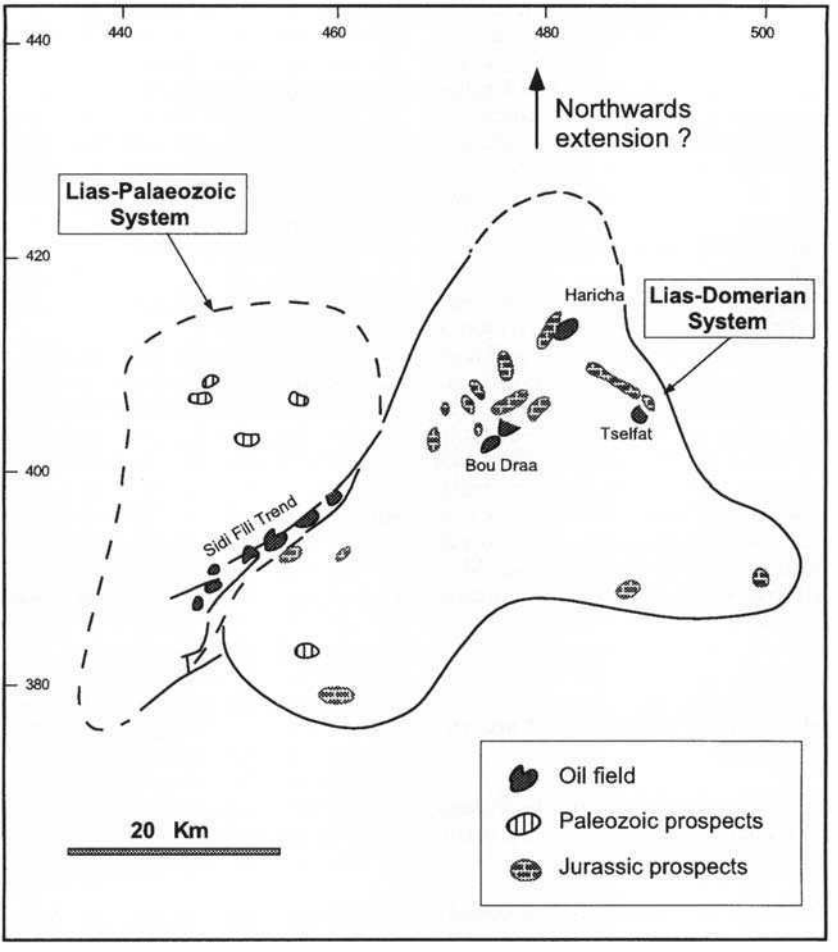

Fig. 5. Map of the two petroleum systems defined in the Prerif ridges area. The Lias–Domerian(!) system may extend to the north.

the system is termed Lias–Palaeozoic (.), though Triassic and Palaeozoic contributions can also be postulated. A hybrid system is suspected.

The Lias–Domerian(!) system occurs in the eastern part of the Prerif (Fig. 4). Oil is sourced mainly from Lower Jurassic and reservoired in Domerian (mid-Jurassic) reefal carbonates and associated arkosic sands. Some oil may also be reservoired in Lower Miocene sandy carbonates. Oil has been produced, so far, from hanging wall anticlines and imbricate ramps at relatively shallow depths. Recent studies suggest that this oil could be a product of dismigration via major faults from deeper accumulations within subthrust anticlines, a possibility as yet not investigated by drilling.

Rharb producing basin

The Rharb Basin is a Neogene foreland basin filled by a thick Miocene–Pliocene clastic series deposited coeval with uplifting of the adjoining Rif and Prerif belts. Palaeozoic and Mesozoic basement outcrops along its southern edge and is deeply buried in the basin centre and in the north-east, where the basin passes into the Prerif folded belt. The deep contains several sub-basins developed along major listric faults.

A significant amount of biogenic gas is reservoired and produced from Tertiary rocks deposited in this foreland basin. This geological setting is classified as a purebred system. Biogenic gas is expelled from thermally immature Miocene

source rock into adjoining medium- to fine-grained, well-sorted Upper Miocene turbidite sand reservoirs. Recent seismic processing techniques have considerably improved the success ratio in exploring for biogenic gas in this petroleum system. More than 80 seismic amplitude anomalies are identified in this region.

Essaouira producing basin

A detailed description of the Essaouira Basin has been provided by Broughton & Trépanier (1993). This basin, which is currently the most important producing basin in Morocco, is a Mesozoic–Cenozoic passive margin basin developed over earlier fault trends. The basin contains numerous extensional salt-related structures.

In the Essaouira Basin two petroleum systems are identified (Figs 3 and 6). Highly mature wet gas in the Meskala–Zelten horsts is thought to be sourced from the Silurian (see Clifford, 1986), and possibly additional Ordovician and Devonian source rocks, and is reservoired below a Triassic salt seal in siliciclastic sediments. The system is termed the Silurian–Triassic(.) and is interpreted to be normally charged. We also favour a Palaeozoic source for the gas fields in the eastern part of the basin, reservoired in fractured Oxfordian dolomites, as these fields are distant from any conceivable Oxfordian gas kitchen.

The oil in the Essaouira Basin is formed in a purebred petroleum system (Oxfordian–Oxfordian(!)). All elements of the petroleum system are confined to Oxfordian stage sediments, with the source developed in the Lower Oxfordian (Broughton & Trépanier 1993), the reservoir in an Upper Oxfordian (Argovian) fractured sandy dolomite reservoir, and the seal by late Oxfordian anhydrite. Data from the Sidi Rhalem oilfield suggest this system to be undercharged. Recent studies, however, suggest a more quantitatively significant charge from a larger kitchen in the west of the basin, where undrilled traps may be associated with salt walls and overhangs (Fig. 6).

Tarfaya Basin (Cap Juby discovery)

Well MO-2 offshore from Cap Juby in the Tarfaya Basin discovered a significant heavy oil (11°API (American Petroleum Institute)) accumulation in a fractured late Jurassic carbonate

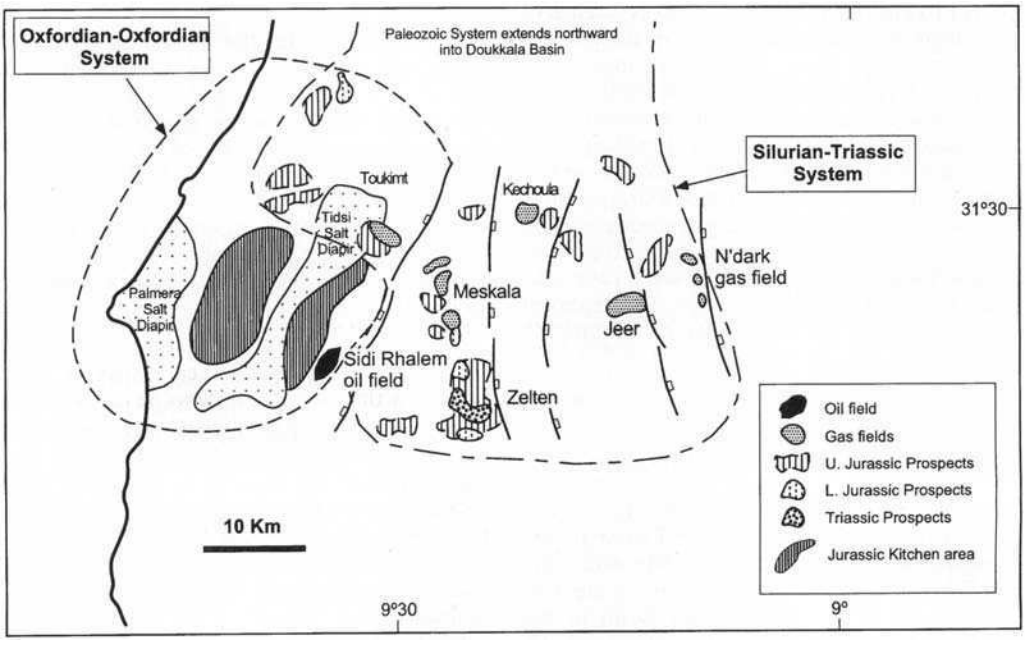

Fig. 6. Map of the two petroleum systems defined in the Essaouira Basin. The Silurian–Triassic (.) system may extend to the north into the Doukkala and Casablanca Basins. (Note the mapping of an additional kitchen in the west of the Oxfordian–Oxfordian (!) system, which has, as yet, no discoveries associated with it.)

bank, which was unfortunately partially breached on an Oligocene shelf collapse unconformity (Hinz 1995). A small amount of light oil was also found in Middle Jurassic reservoirs. Many attempts have been made to determine source to oil correlation, none of which have been conclusive, though the bulk of the evidence tends to favour a Jurassic carbonate source rock. This seems most likely to be developed in the Lower Jurassic in intra-platform sag basins behind the shelf edge. An alternative interpretation of a shalier facies source, located in the present-day adjoining deep water area, cannot, however, be ruled out. Exploration drilling in this area has mainly focused on the Upper Jurassic shelf edge. Recent studies tend to favour Lower and Middle Jurassic objectives surrounding the possible interior platform source rock depocentre, which are less likely to have suffered from reservoir breaching or input of groundwater.

Predicted petroleum systems in frontier basins

This section of the paper presents an interpretation of where further petroleum systems and resources may lie undiscovered in the underexplored basins of Morocco. As the occurrence of petroleum has yet to be proven in these cases, the term 'petroleum system' as applied by Magoon & Dow, cannot strictly be used. Therefore, these interpretations will be presented as 'predicted petroleum systems'. The evidence supporting these includes identification of source rocks from geochemical analyses, extrapolations of source rock extents from palaeogeographical mapping, extrapolations based on regional analogues, basin modelling and, in some cases, the occurrence of shows and/or seeps. The predicted systems are grouped by the age of the inferred source rock.

Predicted Palaeozoic sourced systems

The main regional Palaeozoic source rocks, particularly those in the Silurian and Devonian, are predicted to have extended over Morocco, and are effective source rocks in adjoining areas of Algeria and in the Appalachian Basin of the USA, which originally lay in close palaeotectonic proximity to Morocco. Where stratigraphic data are available, the Silurian source rock can usually be identified, though in a wide range of possible levels of maturity. The highest levels of maturity would be expected to occur over uplifted Carboniferous depocentres (e.g. the Anti-Atlas). The tendency for such areas to present good outcrop data and to therefore be well studied may have contributed to a perception that the Palaeozoic of Morocco is regionally overcooked (e.g. Boote *et al.* this volume). This is clearly not the case in the Essaouira and Tadla (Fig. 4) Basins, and it remains possible that large areas of Morocco contain Palaeozoic source rocks that retained and generated much of their potential in post-Hercynian time (Fig. 2). Such regions include the following.

Tadla Basin. A scarcity of exploration boreholes in this basin (1 well per 3000 km^2) places the emphasis for exploration on geological, geochemical and geophysical evidence. Geochemical analyses show that oil-prone Silurian and Lower Devonian source rocks (TOC up to 12%) are still within the oil window on uplifted blocks (Fig. 4, Jabour & Nakayama 1988). Generation of oil and gas has been modelled to have occurred from Carboniferous to Cretaceous (Jabour & Nakayama 1988). Reservoir objectives occur in basal Triassic and Middle Jurassic siliciclastic deposits, which display excellent reservoir characteristics.

Doukkala Basin. In the Doukkala Basin, a Palaeozoic petroleum system is predicted as an extension of that developed in the Essaouira Basin (Fig. 6). Oil and/or gas produced from Silurian–Lower Devonian source rocks could be reservoired, as in Essaouira, in Permo–Triassic siliciclastic reservoirs. Such a sub-system would be vertically drained and normally charged. A further potential reservoir is a postulated Middle Devonian reef complex, identified by seismic survey.

Casablanca offshore basin. The Doukkala Basin passes northwards into the Casablanca offshore area, in which large structural closures have been defined by seismic survey. No wells have been drilled in this large exploration area. Oil is postulated to be sourced from Silurian–Lower Devonian oil-prone source rocks and to be reservoired in fractured and weathered Ordovician quartizitic sandstones. The system is laterally drained and postulated to be normally charged with a high-impedance entrapment style. The predicted system is very similar in both size and system components to the Hassi Messaoud oil field in Algeria.

Interatlasic Basins. Additional Palaeozoic petroleum systems are predicted In the Interatlasic Basins. Oil and/or gas probably originates from Carboniferous and Silurian source rocks (which are still in the generating stage, particularly on uplifted blocks). Shows have been observed in basal Triassic sands and conglomerates. The oil and/or gas is thought to be vertically drained and sealed by a thick, high-impedance, salt sequence.

The Palaeozoic petroleum system of the Interatlasic Basins may be developed in three areas, namely the High Plateau, the Missour Basin and the Zekkara-Jerada area. No direct correlation has yet been found between the oil and gas seen as shows and seeps and the likely source rock. Currently, no seismic data are available to confidently map the areal extent of these plays, though kitchens can crudely be defined from sparse geochemical data.

Kilenyi (1995) has also suggested that Palaeozoic source rocks may still be in the oil or gas windows below parts of the large Laayoune–Dahkla Basin.

Predicted Triassic sourced systems

The postulated Triassic System is expected to contain lacustrine deposits rich in Type I kerogens similar to those recorded in the coeval basins of Newark, New Jersey, on the opposite Atlantic margin to Morocco (Olsen 1990). This oil-prone source can be expected to charge alluvial fan and fluvial clastic reservoirs in both the hanging wall and the footwall of the half-graben (Fig. 7). Thick Upper Triassic–Lower Liassic salt provides adequate sealing for this system. The Triassic systems are predicted to have the character of purebred systems with a high impedance associated with a mainly vertically drained system. The areal extent of these half-graben systems is very limited, thus the petroleum systems themselves will be of limited extent.

A study integrating seismic, gravity and magnetic data has identified at least eight such buried Triassic half-grabens along segments of the Atlantic margin between Casablanca and Tarfaya.

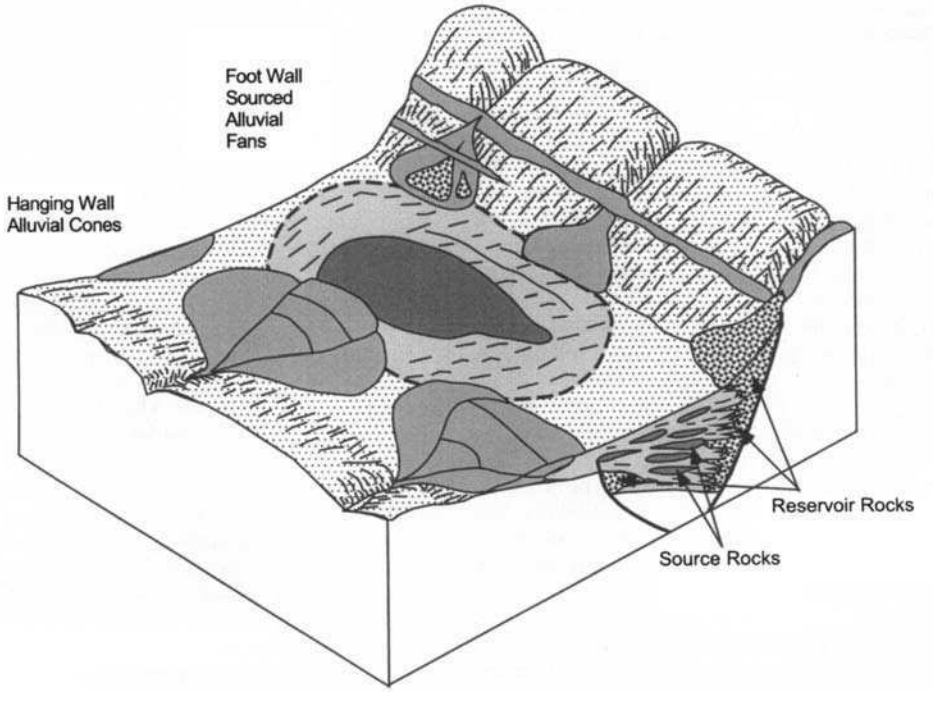

Fig. 7. Sedimentary model of a Triassic Newark-style half-graben, illustrating the various components of the postulated Triassic petroleum system.

Predicted Jurassic sourced systems

Lower Jurassic source rocks, as established in the Tarfaya margin and Prerif, are expected to extend into the Interatlasic Basins, including the southeastern part of the High Plateau, the southeastern and western parts of the Missour Basin, the Guercif Basin and the Zekkara area. Here again, the extent of the kitchens and petroleum systems is speculative, because of lack of seismic coverage.

Predicted Cretaceous sourced systems

Regional source rocks tied to transgressions and oceanic anoxic events are predicted in the Albian and Turonian. Interest is focused on the former because of maturity considerations. The main areas of interest are thus those in which a thick cover is developed above potential Cretaceous source rocks, increasing the chance of maturity being attained. These are the following.

Dakhla–Laayoune Basins. In the Laayoune–Dakhla Basins, Lower Cretaceous source rocks matured below a thick deep-water argillaceous section may charge Albian rollover structures generated along listric faults. In addition, Upper Cretaceous source rocks, if mature, may charge Maastrichian carbonate reservoirs. Such Cretaceous sources may be the origin of the residual oil stains observed in the 51-A-1 well, within Senonian and Eocene carbonates.

Agadir–Essaouira offshore basins. Cretaceous petroleum systems are predicted to exist in the offshore Agadir-Tarfaya segment. Excellent Apto-Albian source rocks, mature basinward, potentially charging a Jurassic faulted and karstified bank edge in Agadir and parts of the Tarfaya offshore basins

In the Agadir–Essaouira offshore area, recent study has developed a new exploration concept. The exploration objective is a faulted carbonate shelf edge, where porosity is enhanced by subareal exposure and consequent karstification. A hypothetical source rock would be Lower Cretaceous shales deposited beyond the Jurassic shelf edge. Geochemical basin modelling has defined a possible kitchen area from which oil is generated. No exploration drilling has yet tested this concept.

Tadla Basin. Rich (up to 13% TOC) oil-prone Cretaceous source rocks are interpreted to enter the oil window under an interpreted low-angle thrust marking the Atlas front. The additional loading and burial acquired is predicted to be sufficient for maturity to be attained. An analogy here may be made to the Ain Hamra discovery in the Prerif.

Predicted Neogene sourced systems

By analogy to the established Neogene hydrocarbon systems of the Rharb and Prerif Basins, shallow biogenic gas systems are predicted in areas of high Neogene sedimentation rate in offshore Rharb, the offshore Mediterranean and Laayoune–Dakhla Basins.

Conclusions

Present geological, geochemical and geophysical coverage has permitted us to predict a number of petroleum systems in Morocco (Table 2) in addition to those identified as the controls on the producing provinces (Table 1). These predicted systems are defined on rather general information over relatively large areas. Any one petroleum system identified on a regional scale may, with additional subsurface data, be found to be subdivided into smaller sub-systems. Furthermore, areas such as the Atlas, Rif, south Atlas and Sahara domains, where little or no seismic coverage has been acquired, will probably provide, once investigated, a large variety of additional petroleum systems.

Several large basins in Morocco still have much unexplored acreage. Drilling to date has tended to concentrate on relatively shallow objectives, drilling large, often recent structures without the modern appreciation of petroleum system concepts or the benefit of high-quality seismic data. Application of petroleum system concepts leads one to concentrate on very specific plays and regions, often unexplored, where petroleum is most likely to have been generated and preserved, e.g. in Palaeozoic-sourced plays over areas not deeply buried in pre-Hercynian times and in regions close to potential Jurassic and Cretaceous kitchens. These may, because of limited source facies extent or maturity considerations, be of limited lateral extent and could easily have been missed by drilling to date. Success in Moroccan exploration may thus prove to be localized, close to 'sweet spots' where the correct geochemical conditions are attained. In this regard, analogies can be made to several large petroleum provinces where success was attained late in the history of the basin, e.g. west of the Shetlands and in the Apennine fold belt.

Very little is known about deep offshore plays. The results so far obtained from the Campos

Table 2. *Predicted Petroleum systems (no discoveries to date)*

Age of proposed source	Basin	Proposed reservoir age	Shows	Comments/critical factors	Proposed migration path
Palaeozoic (Silurian, + ?Devonian, Ordovician)	Tadla	Triassic (Cl.) Middle Jurassic (Cl.) Carboniferous (Cb.)	Shows	Timing of generation	Vertically drained
	Doukkala	Permo-Triassic (Cl.)	Shows	Extension of Essaouira system	Vertically up–faults
		Devonian Build–Ups (Cb.)			Laterally drained
	Casablanca	Fractured Ordovician sst. (Cl.)		Timing + ?overmaturity	Laterally drained
	Boudenib	Devonian carbonates (Cb.)		Timing + ?overmaturity	Vertically drained
Triassic Lacustrine	Coastal Rift half-grabens	Triassic fluvial clastic deposits (Cl.)		Based on Newark rift system analogue	Laterally and vertically drained
Lower Jurassic	Interatlasic Basins (Guercif, Missour, High Plateaux)	Mid Jurassic (Cb.)	Shows Seeps	Timing of generation w.r.t. trap formation	Laterally drained
Cretaceous (Albian + ?Turonian if mature)	Tarfaya	Cretaceous, U. Jurassic (Cb./Cl.)	Shows		Laterally drained
	Agadir	Late Cretaceous (Cb.)	Shows		Laterally drained
	Dakhla	Cretaceous (Cl. + Cb.)	Shows (residual oil in 51-A-1)	No	Up–faults
	Tadla	Late Cretaceous (Cb.)		Maturity predicted below Atlas overthrust	Laterally drained
Neogene biogenic systems	Dakhla	Neogene sand lenses		Compare Rharb analogue	Local generation & expulsion
	Mediterranean	Neogene sand		Compare Rharb analogue	Local generation & expulsion

Cl., Clastic deposits; Cb., carbonates.

Basin on the western side of the Atlantic Ocean illustrate the potential attractiveness of such areas. In salt basins, great strides have been made with new technology in deciphering the architecture of subsalt formations, which will help in exploration for Palaeozoic sourced plays trapped beneath Triassic salt. A better knowledge of the petroleum systems of the Moroccan sedimentary basins should therefore considerably enhance the chances of eventual exploration drilling success.

This work, presented as an oral commmunication during the Hydrocarbon Geology of North African conference held in London (1995) expresses ideas evolved from discussion with several individuals working in both academia and industry. The authors would like to acknowledge the comments of Alton Brown, who refereed the manuscript, and Duncan Macgregor, who made the publication of this work possible. We are grateful to the convenors of the conference for the opportunity to attend and publish this paper.

References

BOOTE, D. TRAUT, M. & CLARK-LOWES, D. D. 1998. Palaeozoic petroleum systems of North Africa. *This volume.*

BROWN, R., 1980, Triassic rocks of the Argana Valley, South Morocco, and their regional structural implications. *Bulletin, American Association of Petroleum Geologists*, **64, 7, 988–1003.**

BROUGHTON, P. & TRÉPANIER, A., 1993, Hydrocarbon generation in the Essaouira Basin of Morocco, *Bulletin, American Association of Petroleum Geologists*, **77**(6), 999–1015.

CLIFFORD, A. C., 1986, African oil past, present and future. *In*: HALBOUTY, M. T. (ed.) *Future Petroleum Provinces of the World*, American Association of Petroleum Geologists, Memoirs, **40**, 339–372.

DEMAISON, G. & HUIZINGA, B. J. 1991, Genetic classification of petroleum systems. *Bulletin, American Association of Petroleum Geologists*, **75**(10), 1626–1643.

EINSELE, G. & WIEDMANN, J., 1982, Turonian Black shales in the Moroccan coastal basins. *In*: VON RAD, U. *et. al.* (eds) *Geology of the Northwest African Continental Margin*. Springer-Verlag, 396–414.

GUIRAUD, R. 1998. Mesozoic riftng and basin inversion along the northern African Tethyan margin: an overview. *This volume.*

HINZ, K. 1995. Morocco. *In*: KULKE, H. (ed.) *Regional Geology of the World, Part II*, Gebrüder Borntträeger, Stuttgart.

JABOUR, H. & NAKAYAMA, K., 1988. Basin modelling of Tadla Basin, Morocco, for hydrocarbon potential, *Bulletin, American Association of Petroleum Geologists*, **72**(9), 1059–1073

KILENYI, T. L. 1995. A re-appraisal of the Tarfaya Basin, Western Morocco. *In*: *Abstracts Booklet, First Symposium of Hydrocarbon Geology of North Africa, Petroleum Group, Geological Society, Seminar, 28 30 November 1995.*

MAGOON, L. B., 1988. The petroleum system—a classification scheme for research, exploration, and resource assessment. *In*: MAGOON, L. B. (ed.) *Petroleum systems of the United States. US Geological Survey Bulletin*, **1870**, 2–15.

—— & DOW, W. G. (eds) 1994. *The Petroleum System—From Source to Trap*, American Association of Petroleum Geologists, Memoirs, **60**, 3–23.

OLSEN, P. 1990. Tectonic, climatic and biotic modulation of lacustrine ecosystems. Example from Newark supergroup of eastern North America. *In*: *AAPG Memoir* 50, *Lacustrine Basin Exploration*, 265–276.

Application of fault seal analysis techniques in the Western Desert, Egypt

S. M. RICHARDSON[1], N. VIVIAN[2], R. J. COOK[3], M. WILKES[1] & H. HUSSEIN[4]

[1]*BG Exploration and Production Ltd, 100 Thames Valley Park Road, Reading, Berkshire RG6 1PT, UK*

[2]*Ranger Oil (UK) Ltd, Ranger House, Walnut Tree Close, Guildford, Surrey, GU1 4US, UK*

[3]*BG R&T, Ashby Road, Loughborough, Leicestershire LE11 3QU, UK*

[4]*BG Egypt S.A., Building 23, Road 216, Digla, Maadi, Cairo, Egypt*

Abstract: The Western Desert is one of Egypt's major hydrocarbon provinces. Most discoveries to date have been in the Cretaceous, with the Jurassic being the most underexplored interval, with the highest potential for new discoveries. Although trap styles vary, the majority are structural fault blocks, requiring fault seal on one or more bounding faults. Despite the number of excellent reservoirs present in the Western Desert, large field sizes are rare, with less than 50 MMBOE STOIIP (million barrels oil equivalent, oil initially in place) being predominant. This apparent failure to regularly prove larger field sizes can be considered a direct function of trap failure resulting from absence of fault seal. A number of fault seal analysis techniques including fault-plane profiles, smear-gouge ratios, incremental strain analysis and structural sections are available to directly address trap integrity. Case histories from the Western Desert are used to demonstrate the use of these techniques, and to highlight potential pitfalls. These case histories show that fault seal techniques allow a more accurate assessment of trap integrity in the Western Desert, provided they are applied iteratively, and integrated with other geological and geophysical data.

Fault seal analysis is a critical component of prospect evaluation for fault-controlled structures with dominantly siliciclastic reservoir sequences. A number of papers have addressed the nature of faults which control hydrocarbon accumulations, how faults seal, and how to assess fault seal integrity as a means to quantitatively rank prospects (Allan 1989; Jev *et al.* 1993; Knott 1993; Gibson 1994 ; Berg & Avery 1995).

The bulk of the reserves in Western Desert fields are found in either four-way dip-closed structures or small fault-controlled structures of low vertical relief. The combination of low-relief structures with complex hydrocarbon contacts and low to moderate field sizes supports the premise that fault seal integrity is of vital importance within the basin (Zein El-Din *et al.* 1990). This paper examines a number of techniques which can be used to assess fault seal integrity, by means of two case studies using geological and geophysical data taken from the Western Desert of Egypt. One of the study areas has already been calibrated by drilling, the other one remains untested. The techniques described in this paper can be applied equally to any other geological province which contains siliciclastic reservoir sequences with structures requiring valid fault seal for success.

Study Areas 1 and 2 (Fig. 1) are located in the northeastern part of the Western Desert. The structural grain in both areas is dominated by WNW–SE to E–W orientated normal, extensional faults, some of which may have experienced a degree of later inversion and subsequent reversal. Study Area 1 contains a normal fault-block tested by Well A, which was abandoned as a dry hole. No further control wells relevant to the tested structure are present within the study area. The tested structure comprises a relatively simple upthrown fault-block with three-way dip closure, with a dependence on one-way fault closure to the south. However, there are a number of smaller faults off the main bounding fault (A–A′ in Fig. 2a), which further complicate the structure. Data from this structure were used as the first case study with which to calibrate the fault seal analysis techniques. The calibrated techniques were then applied to Study Area 2, which also contains an upthrown fault-block, reliant on three-way dip closure and one-way fault closure to the south (B–B′ in Fig. 2b). The structure is currently untested by drilling, but does appear to be less complicated than its counterpart in Study Area 1. Although no wells have been drilled within the area of structural closure itself, well control is present (Wells B and C) on either side of the fault under investigation, which has allowed calibration of both the hanging wall and footwall stratigraphies.

RICHARDSON, S. M., VIVIAN, N., COOK, R. J., WILKES, M. & HUSSEIN, H. 1998. Application of fault seal analysis techniques in the Western Desert, Egypt. *In*: MACGREGOR, D. S., MOODY, R. T. J. & CLARK-LOWES, D. D. (eds) 1998. *Petroleum Geology of North Africa*. Geological Society, London, Special Publication No. 132, 297–315

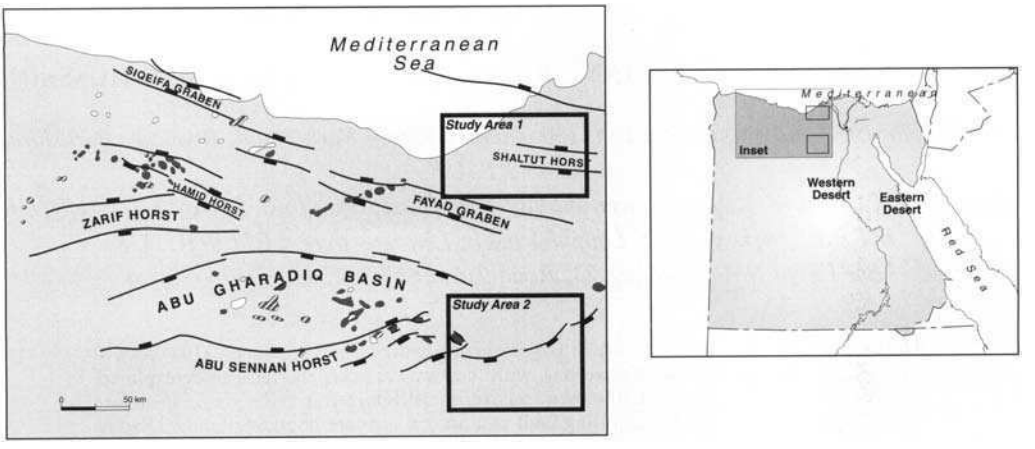

Fig. 1. Location map showing the main structural features of the northern part of the Western Desert and the location of Study Areas 1 and 2.

Within the two study areas examined in this paper, three of the four elements of the petroleum system, namely, reservoir, topseal and source rock, have been proven to be effective by drilling. This leaves only trap integrity, with fault seal effectiveness being the principal cause for concern. As the study areas are immediately east of and adjacent to the prolific Abu Gharadiq Basin in the Western Desert (Fig.1), it is not surprising that the proven plays within the Abu Gharadig Basin have been extended into Study Areas 1 and 2. Reservoir, topseal and source combinations and their impact on prospect evaluation are discussed more fully below, with particular emphasis being placed on the number of interbedded siliciclastic reservoir intervals, and their impact on fault seal effectiveness.

The petroleum system

Reserve distribution

An effective petroleum system has been proven in the Western Desert. However, over half the fields in this area contain less than 50 MMBOE (million barrels oil equivalent, oil initially in place) STOIIP (Egyptian General Petroleum Corporation 1992). Over two-thirds of the proven reserves are in relatively poor-quality Cretaceous reservoirs, and are limited to either three- or four-way dip closed structures. This distribution of reserves reflects the predominance of reservoir sandstones, and the lack of thick regional seals in the petroleum system.

Reservoirs

Mesozoic sediments of the Western Desert were derived from a fluvial system which flowed northwards from the African continent (Said 1990). This fluvial system reached a shallow marine sea within the area studied in this paper, giving rise to deposition in delta and shallow marine conditions. Consequently, the Jurassic and Cretaceous, succession is dominated by shallow marine and fluvial sandstones. Variations in sea level during the Jurassic and Cretaceous, led to the migration of facies belts, and the deposition of similar lithologies across the whole of the study area (Said 1990; Robertson Research International 1982; Hantar 1990; Egyptian General Petroleum Corporation 1992). This depositional model gives rise to laterally extensive sandstone-dominated lithofacies. Thick, porous and permeable sandstones are deposited during regressive phases, such as during deposition of the Kharita Formation (Albian) and the Alam el Bueib Formation (Neocomian–Barremian) (Barakat & Darwish 1988). During transgressive phases, shaly lagoon and delta-top facies are preferentially preserved, and beach barrier sandstones are less well developed. The Cretaceous contains 93% of proven hydrocarbons in the Western Desert Province (Egyptian General Petroleum Corporation 1992), the bulk being reservoired within the Bahariya and Abu Roash Formations (Cenomanian–Santonian), which comprise intercalated massive sandstones, shales and limestones within the two study areas (Fig. 3).

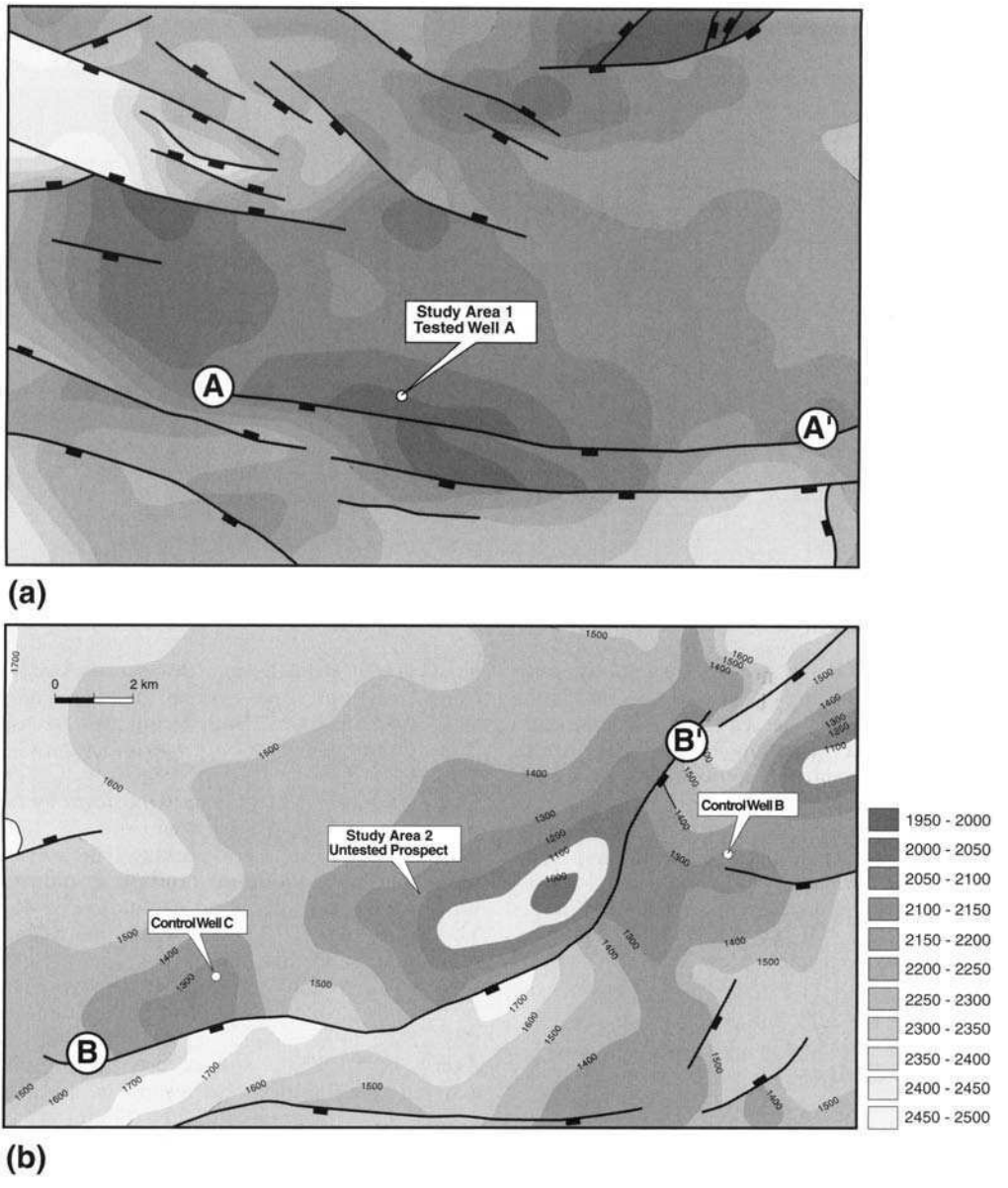

Fig. 2. Structure maps showing the location of control wells and faults A–A′ and B–B′ being analysed for (**a**) Study Area 1 and (**b**) Study Area 2.

Source rocks

Effective source rocks have been identified within the Khatatba (Jurassic), Alam El Bueib, Bahariya and Abu Roash Formations (Parker 1982; Robertson Research International 1982). Source rocks are deposited in lagoonal and deltaic settings in the Western Desert (Bergland *et al.* 1994), and consequently contain Type II, and mixed Type II–III kerogens. Within the two study areas, mature, oil-prone kerogens are present, intercalated within reservoir intervals.

Trapping mechanism

The predominance of reservoir sandstones in the succession leads to juxtaposition of, and communication between sandstones across faults. This explains the reliance on three- or four-way dip closed structures in the Western Desert fields.

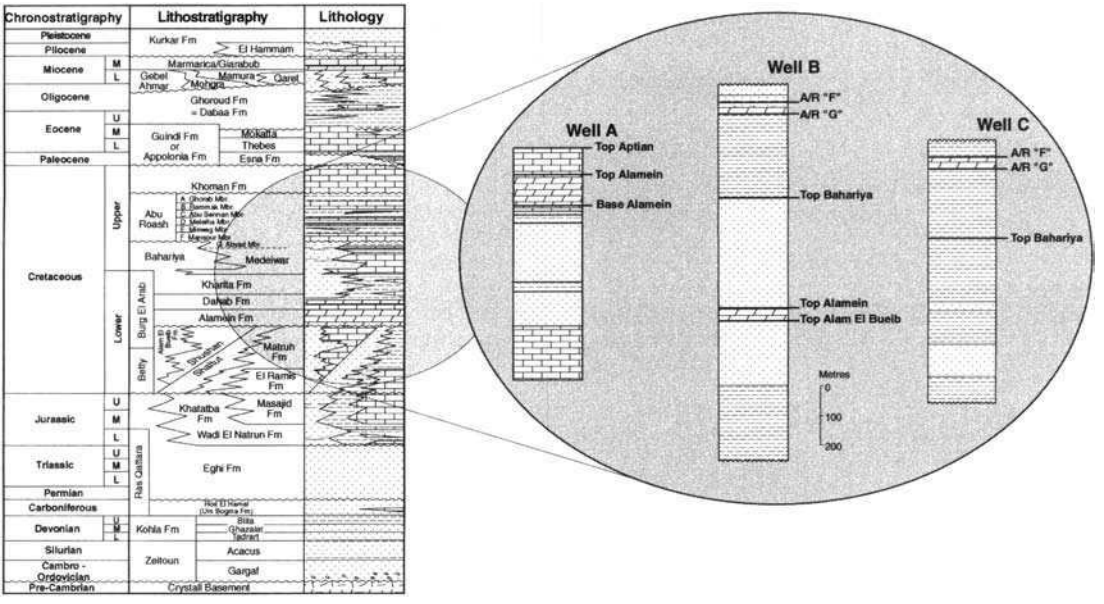

Fig. 3. Generalised Western Desert stratigraphy with specific lithologies for the control wells shown in Fig. 2.

Within more shale- dominated formations, sandstones are less likely to be juxtaposed, and faults are more likely to be sealed by shale smears. However, these formations typically give rise to short, stacked hydrocarbon columns, and small reserve sizes. Hence, four-way dip closed structures form the largest traps in the Western Desert (Abu Gharadiq, Alamein and Abu Sennan–GPT Fields). Large fault-bounded prospects have also proven to be effective (Badr-El-Dar Fields) but are notably less common. This stresses the importance of fault seal analysis in evaluation of prospects within the Western Desert (Zein El-Din *et al*, 1990).

Fault seal analysis

Types of sealing faults considered

Juxtaposition seals. Juxtaposition seals are the most common type of fault-related seals considered, and can result from either normal or reverse fault displacements (Watts 1987). This sort of sealing mechanism is largely independent of the faulting process, and the only fault serves to juxtapose impermeable sealing lithologies (shale) directly against more permeable lithologies (siliciclastic reservoirs) across the fault plane (Fig. 4a). This juxtaposition creates effective cross-fault seal. Juxtaposition seals are more commonly found in shale-dominated sequences, or thin reservoir sequences. Juxtaposition seals are relatively easy to predict once stratigraphy can be accurately defined, and are best assessed by using structural cross-sections in combination with Allan diagrams. Both techniques are discussed in full below.

Shale smear seals. Shale smear seals form by the smearing of shale or claystone into the fault plane during the process of faulting. This reduces the permeability within the fault plane and prevents across-fault migration of fluids (Fig. 4b). These are likely to occur when intercalated shale and sandstone lithologies are present, such as are found in deltaic sequences. Such smear seals have been described in the literature (Jev *et al.* 1993; Lindsay *et al.* 1993; Berg & Avery 1995). Shale smears are most easily assessed quantitatively by means of a smear gouge ratio diagram (SGR), (Smith, 1966, 1980) This technique is discussed more fully below.

Cataclasis Seals. Cataclasis seals (Knipe 1992) occur within clean, massive sandstone sections and form as a series of shear zones (Fig. 4c), which can be closely associated with wrench faults. Although wrench faulting is known to be common in the Western Desert Province, associated with late inversion structures, it is unlikely that these have produced significant cataclasis bands, possibly because of the heterogeneous lithofacies, and general absence of thick massive sandstone sections in the Western Desert. As cataclasis seals are unlikely to be

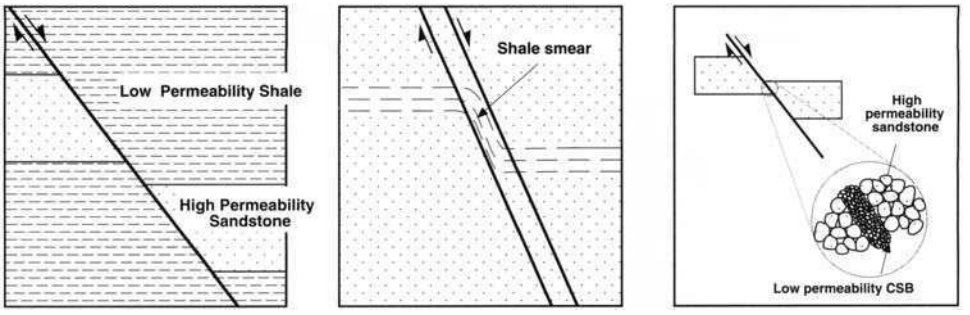

Fig. 4. Illustration of fault seal mechanisms: (**a**) juxtaposition seal; (**b**) shale smear seal; (**c**) cataclasis seal.

responsible for the trapping of major hydrocarbon accumulations in the Western Desert Province, and as graphical fault seal methods discussed below are not appropiate for analysing the sealing potential of faults which are reliant on cataclasis, this type of seal will not be assessed in this paper.

Discussion of graphical methods using case histories

Graphical fault seal methods are those techniques which can be undertaken using basic datasets comprising stratigraphical information (generally geological well data, for calibration purposes), structure contour maps across the fault plane (either depth or two-way travel time, at one or several stratigraphical horizons), and representative seismic lines which traverse the fault plane. The techniques rely on graphically *plotting* data from which conclusions can be made, and are based on the analysis of factors,which are considered to be important as a fault seal prediction tool (Knott 1993), in contrast to statistical techniques, which require large numerical datasets, often acquired as a consequence of drilling.

Geological and geophysical data from Study Areas 1 and 2 have been used to examine fault seal integrity of two faults using a number of graphical techniques which are discussed in full below. Results are then used to qualitatively rank the seal effectiveness of the two faults being examined, and could also be used quantitatively to determine the trap integrity of any prospects being considered for drilling.

Fault displacement diagrams. Before undertaking fault seal analysis, it is important to understand the fault geometry and the validity of the fault interpretation made from seismic data. Any errors incurred at this stage will be carried throughout the fault analysis and may result in incorrect conclusions being reached. Fault-plane displacement diagrams are used to investigate whether a coherent fault correlation had been applied. An idealized fault should show an elliptical fault displacement pattern, with maximum throw in the middle decreasing to zero throw at the tip line. Displacement data are contoured (Fig. 5), and examined for displacement anomalies. Such anomalies in the fault displacement patterns or gradients may be caused by either mis-ties in the seismic interpretation or the incorrect correlation of individual seismic line fault picks.

Results. In Study Area 1, a maximum displacement is seen at the base of the fault (A–A′) along seismic line 2 (Fig. 5a), which decreases away towards the tip lines. There is a small anomaly at the top of the fault around seismic lines 3 and 4, which may indicate either an incorrectly correlated fault or that two faults developed separately and later connected, thus giving two maximum displacements. There are, however, only five seismic lines across the length of the fault, making further analysis of the fault correlation difficult: there is simply not enough information available. Overall, the displacement contours are systematically developed and decrease towards the tip line, suggesting a good fault correlation. It is therefore worth while continuing the fault analysis.

In Study Area 2, the prospect bounding fault (B–B′) shows considerable variation in throw along the fault plane (Fig. 5b). It may be that this is not a single fault but two connected faults. Another possible explanation is that there is a problem with the fault and/or horizon mapping on the seismic lines. The horizon reflectors used to determine fault throw appear to break up some distance short of the fault itself, making accurate measurement of fault throw difficult, and creating anomalies in the fault displa-

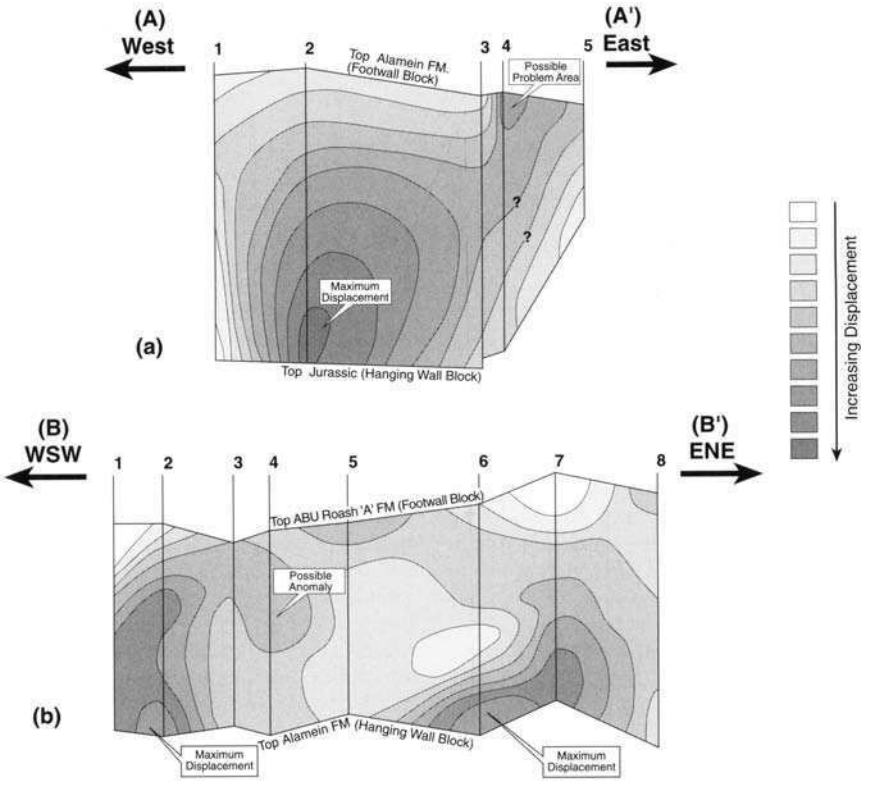

Fig. 5. Contoured fault-plane displacement diagram: (**a**) Study Area 1, showing an anomaly at the intersection with line 4, possibly the result of a mis-pick of the seismic horizon: (**b**) Study Area 2, showing two maxima, indicating that this fault may not be continuous.

cement diagram. For the purpose of this study, analysis was continued without further work on the fault correlation itself, but in practice the fault should be restudied and reinterpreted. This exercise does, however, emphasize how fault displacement diagrams used before drilling can highlight possible problems in structural mapping.

Cross-sections. One of the simplest techniques and often the first tried for examining fault seal integrity is the cross-section (often referred to as a geological or structural cross-section). A cross-section is drawn perpendicular to structures across the fault plane, for a number of stratigraphical horizons, with an interpretation of expected lithology within each zone of interest. The method is principally used to examine the juxtaposition of permeable lithofacies, which makes it a useful screening tool for the early identification of juxtaposition seals.

The technique does have a number of limitations; the most serious of these is its sensitivity to variations in stratigraphy. In particular, it is important to recognize the possibility of stratigraphic variations (changes in facies, net gross ratio and thicknesses) on either side of a fault plane. Fault throw will vary laterally along the fault plane, and the cross-section constructed will not be representative of the entire plane. A number of sections may therefore be required before a confident analysis can be made.

Allan diagrams. Often referred to as fault-plane profiles, Allan diagrams are a graphical method of displaying and examining juxtaposing stratigraphies on both sides of a fault plane (Fig. 6). Allan (1989) first described the technique utilizing fault data in deltaic sequences from the Gulf Coast of the USA.

In contrast to structural cross-sections, which are drawn perpendicular to the fault plane, Allan diagrams are drawn parallel to the strike of a fault. The method therefore automatically takes account of variation of displacement along the length of the fault. Allan diagrams

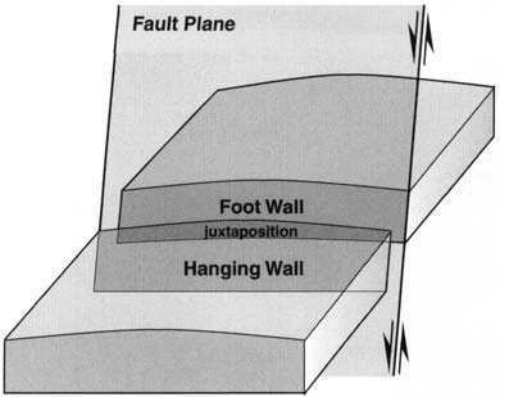

Fig. 6. Illustration of Allan diagram terminology, showing a faulted layer and area of juxtaposition

can be used to indicate where possible leakage routes may exist in any trap. This makes the technique particularly useful when determining which structural closures are likely to seal, and the volume of hydrocarbons these traps could contain (although the technique does not account for additional membrane seal effects). Impermeable beds (generally shales) which have been juxtaposed against permeable beds (generally sandstones) are assumed to provide a (juxtaposition) seal. However, permeable beds which have been juxtaposed against permeable beds are unlikely to seal, thereby providing a conduit for hydrocarbons to spill across the fault. Fault surfaces in Allan's model are assumed to have no properties which affect (positively or negatively) the sealing integrity, therefore the trapping potential of any fault-dependent closure depends primarily on the stratigraphic relationships juxtaposed along the fault boundaries. Unfortunately, the stratigraphic geometry is the most difficult parameter to assess in the absence of dense well control. Lithofacies often need to be correlated over long distances or estimated from the depositional models derived from seismic and subsurface data. Although well control is present within the two study areas presented in this paper, stratigraphic uncertainty remains high. However, this uncertainty can be addressed separately using sensitivity analysis, as discussed below.

One of the key parameters to be considered is the variation of displacement along the strike of the fault, as this in turn will control the position of the cross-fault spill point, and hence the hydrocarbon column-height within the trap. In contrast to geological cross-sections, which are constructed normal to the fault plane, Allan diagrams can automatically compensate for variation of fault throw along strike, within the errors associated with any depth conversion applied. This too is an important sensitivity which will also be discussed later in the paper.

Results. The stratigraphy from Well A (Fig. 3) on the Study Area 1 structure has been used in both the footwall and *hanging wall* of the fault for the Allan diagram. The juxtaposition diagram indicates a large area of sandstone-on-sandstone contact across the fault (Fig. 7a). This degree of sandstone juxtaposition would generally be assumed detrimental to the fault seal integrity, and the fault would be expected to leak.

In Study Area 2, three wells are present in the vicinity of the structure (Figs. 2b and 3), allowing the Allan diagram analysis to consider combinations of stratigraphy from different wells. Initially, only Well B (which is situated in the hanging wall towards the NE tip of the fault) was used to model both the footwall and the hanging wall stratigraphies of the fault. The resultant Allan diagram shows a large area of sandstone-on-sandstone juxtaposition (Fig. 8a) which would indicate a high likelihood of leakage across the fault.

A second variation, using only the stratigraphy of Well C, was applied in both the foot- and hanging wall section. Well C is situated in the footwall of the fault, towards the WSW tip of the fault (Fig. 2b). The Allan diagram of the fault plane indicates that there are only a few instances of sandstone-on-sandstone juxtaposition (Fig. 9a), therefore cross-fault sealing is considered likely. The two variations using different wells, documented above, can be considered 'end-members' of a number of stratigraphic possibilities.

A third, and more realistic case considers the results of two wells. Well B was used to represent the hanging wall, and Well C to represent the footwall. The Allan diagram for this example (Fig. 10a) suggests that there is sandstone-on-sandstone juxtaposition along the entire length of the fault, and therefore the fault is very likely to leak.

A final stratigraphic sensitivity has been included, using a fourth well (Well D), also located in the *hanging wall*, but about 45 km along strike. Using Wells B, C and D, a '3D' stratigraphy has been generated to estimate stratigraphic variations along the fault plane by triangulating stratigraphy from all three wells into the fault plane (Fig. 11). In reality, Well D is too far from the fault to be used to influence the 3D stratigraphy, but the exercise was still carried out to fully test the methods of fault analysis. The Allan diagram constructed using the fault-plane stratigraphy based on all three wells (Fig.

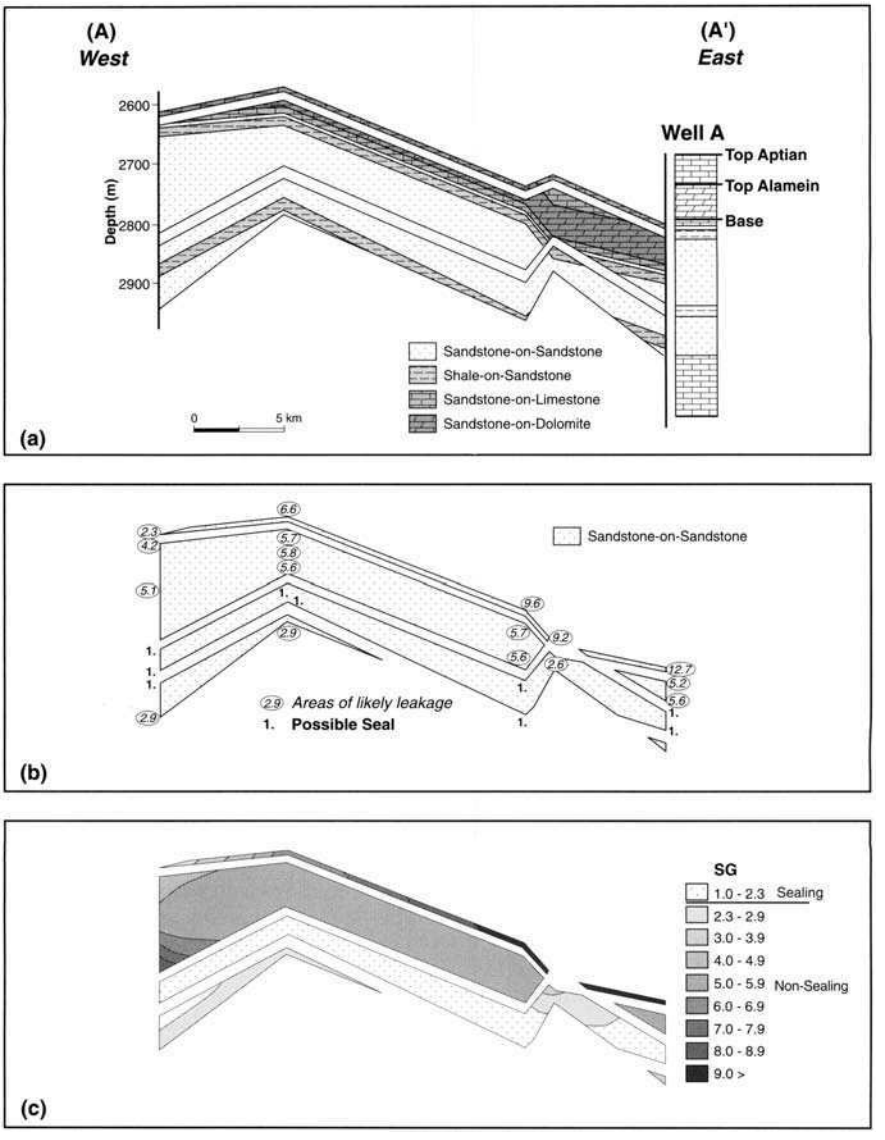

Fig. 7. Study Area 1, fault seal analysis using Well A lithologies. (**a**) Allan diagram which superimposes the footwall and hanging wall lithologies. (**b**) Areas of sandstone–sandstone juxtaposition derived from the Allan diagram with calculated values of SGR; the large amount of cross-fault sandstone juxtaposition indicates the probability of a leaking fault. (**c**) SGR from Fig. 7b contoured and shaded which highlights the lack of shale smear seal in the upper layers.

12a), shows a large area of sandstone-on-sandstone contact at the NE end of the bounding fault. The degree of sandstone-on-sandstone contact decreases towards the WSW end of the fault, reflecting the general change in stratigraphy along the fault plane. The above cases clearly demonstrate that using all available data is critical to the results of the method.

Smear gouge ratios. Areas of the fault that indicate sandstone-on-sandstone juxtaposition can be investigated further using smear gouge analysis, which is a semi-quantitative technique for evaluating fault seal. Shale smears occur on the surfaces of tectonic faults contained within interbedded sandstones and shale intervals. The smear gouge ratio (SGR) is an estimate of the

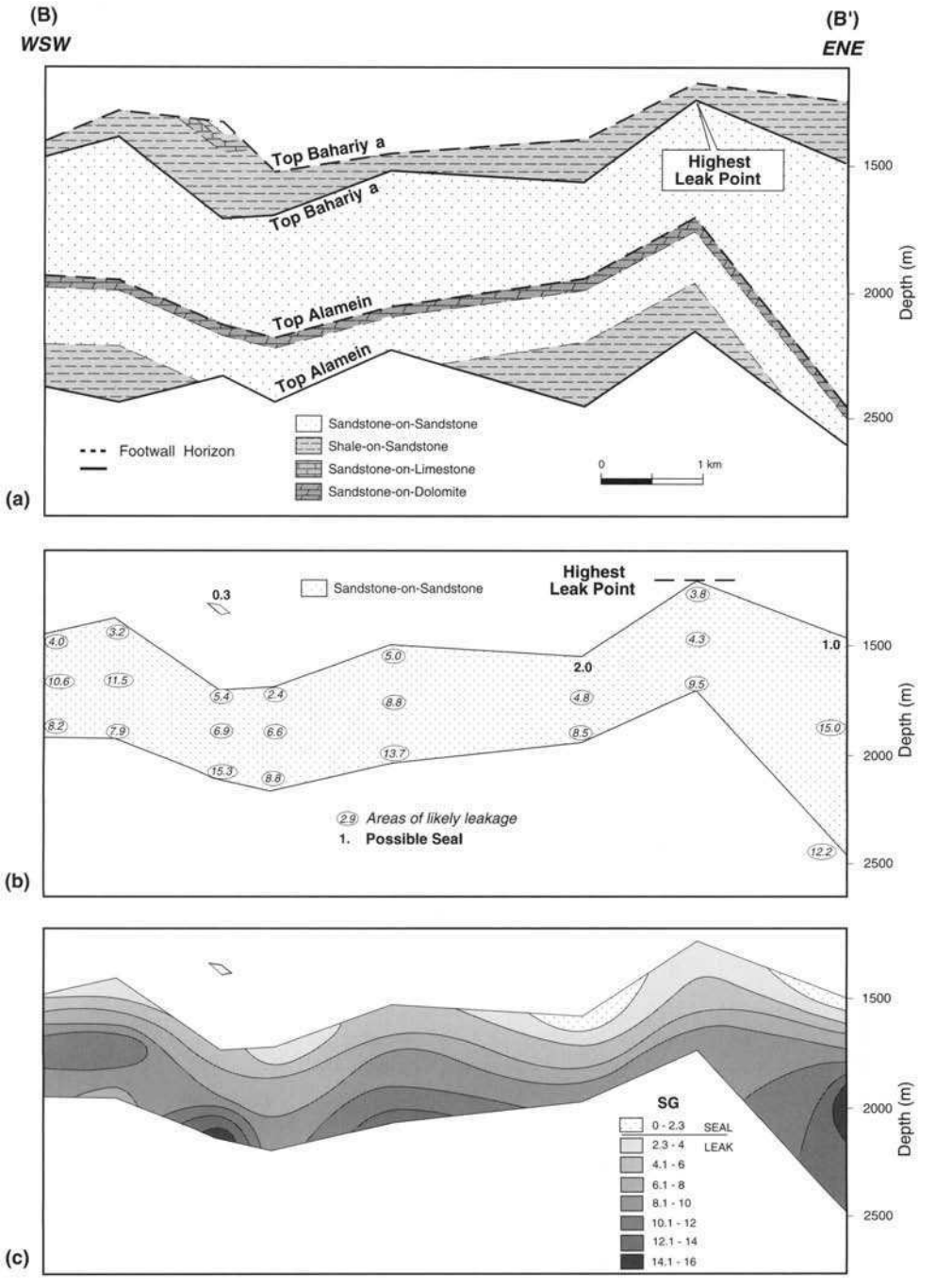

Fig. 8. Study Area 2, fault seal analysis using Well B lithologies. (**a**) Allan diagram which superimposes the footwall and hanging wall lithologies. (**b**) Areas of sandstone–sandstone juxtaposition derived from the Allan diagram with calculated values of SGR; the large amount of cross-fault sandstone juxtaposition indicates the probability of a leaking fault. (**c**) SGR from Fig. 8b contoured and shaded which indicates that shale smear does not contribute any sealing properties to this fault.

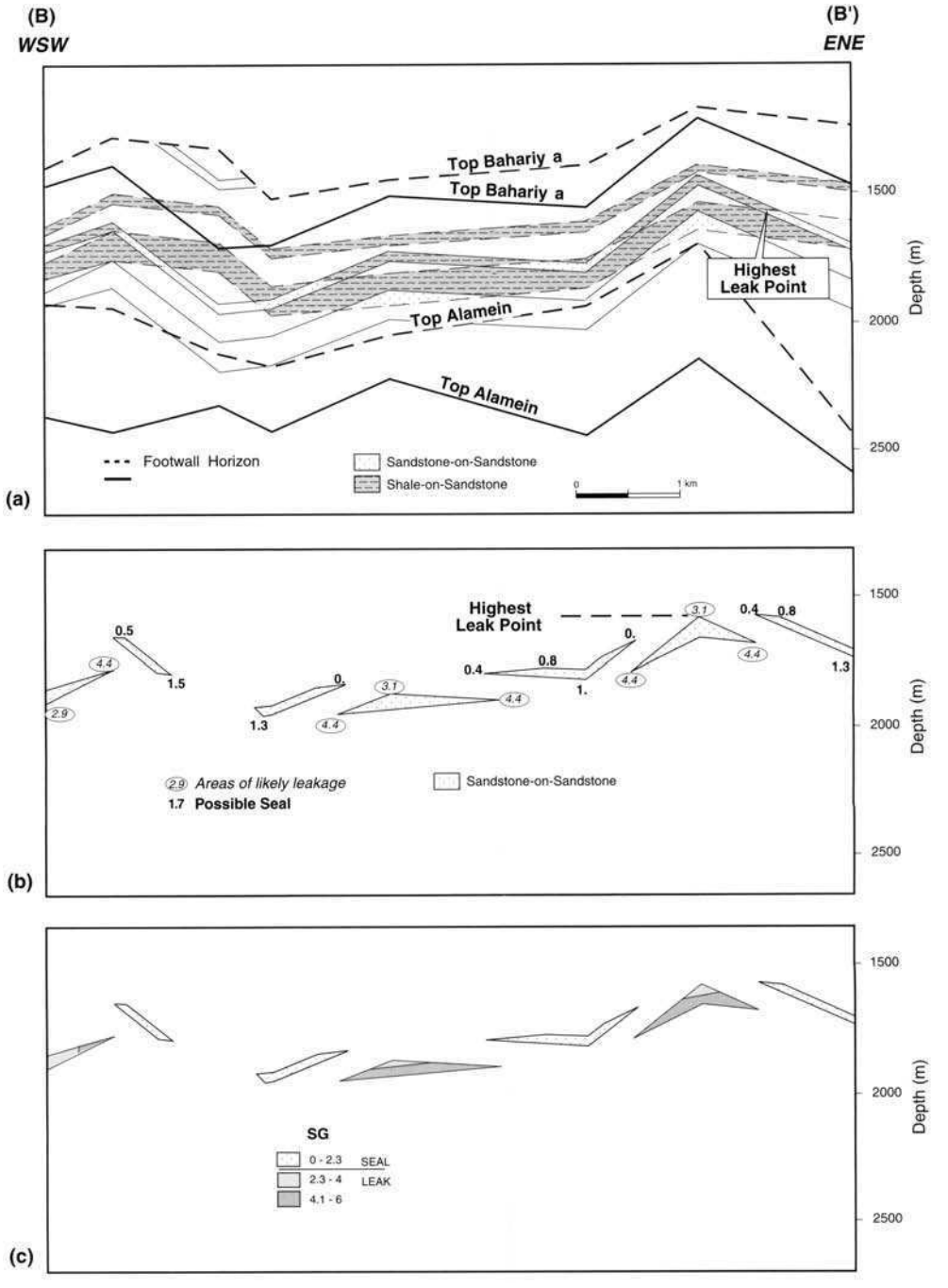

Fig. 9. Study Area 2, fault seal analysis using Well C lithologies. (**a**) Allan diagram which superimposes the footwall and hanging wall lithologies. (**b**) Areas of sandstone–sandstone juxtaposition derived from the Allan diagram with calculated values of SGR; the limited areas of cross-fault sandstone juxtaposition suggest the fault may seal. (**c**) SGR from Fig. 9b contoured and shaded which indicates limited contribution to seal from shale smear.

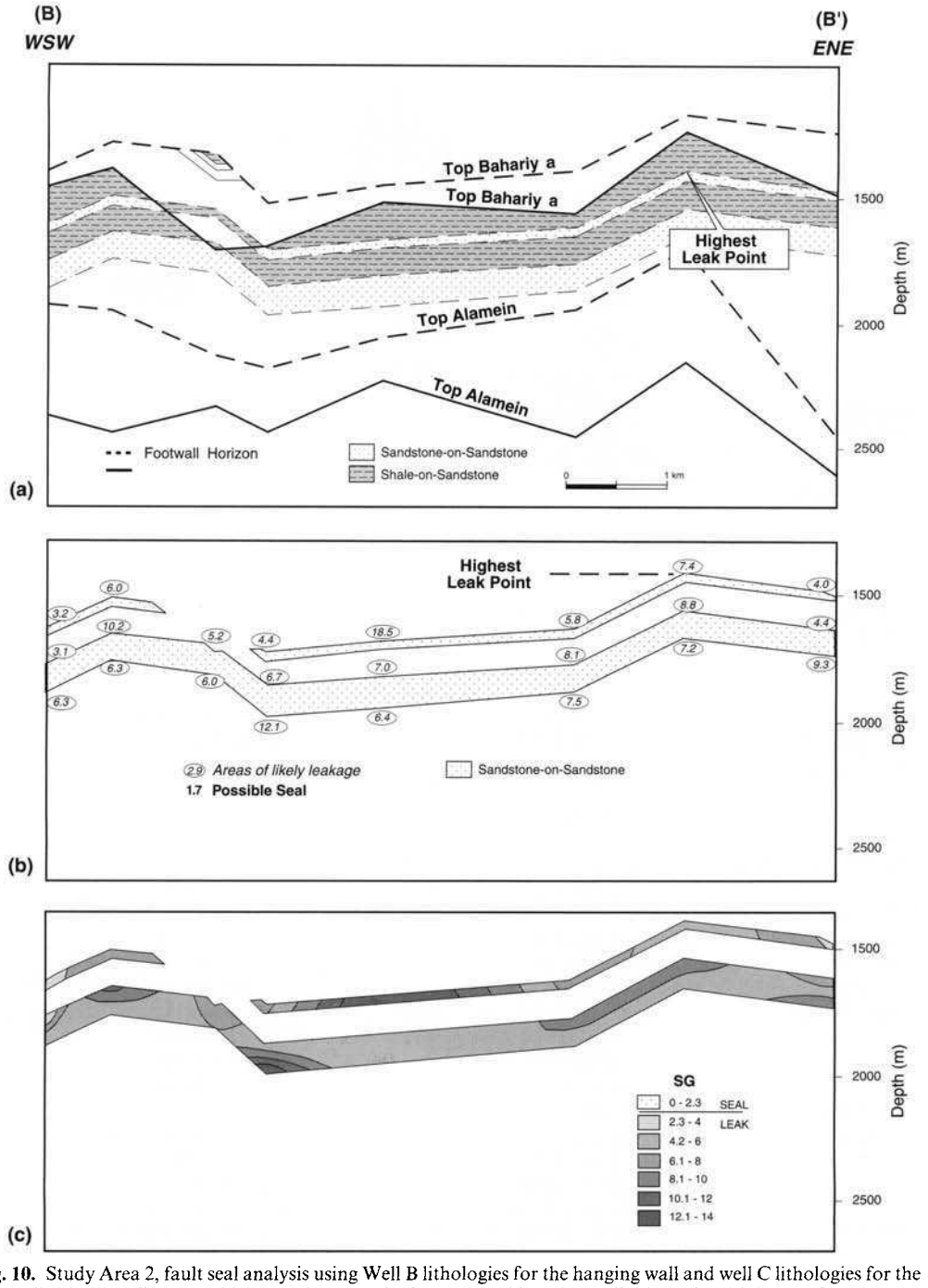

Fig. 10. Study Area 2, fault seal analysis using Well B lithologies for the hanging wall and well C lithologies for the footwall. (**a**) Allan diagram which superimposes the footwall and hanging wall lithologies. (**b**) Areas of sandstone–sandstone juxtaposition derived from the Allan diagram with calculated values of SGR; the large amount of juxtaposition indicates a leaking fault. (**c**) SGR from Fig. 10b contoured and shaded which indicates that shale smear is unlikely to contribute to fault seal.

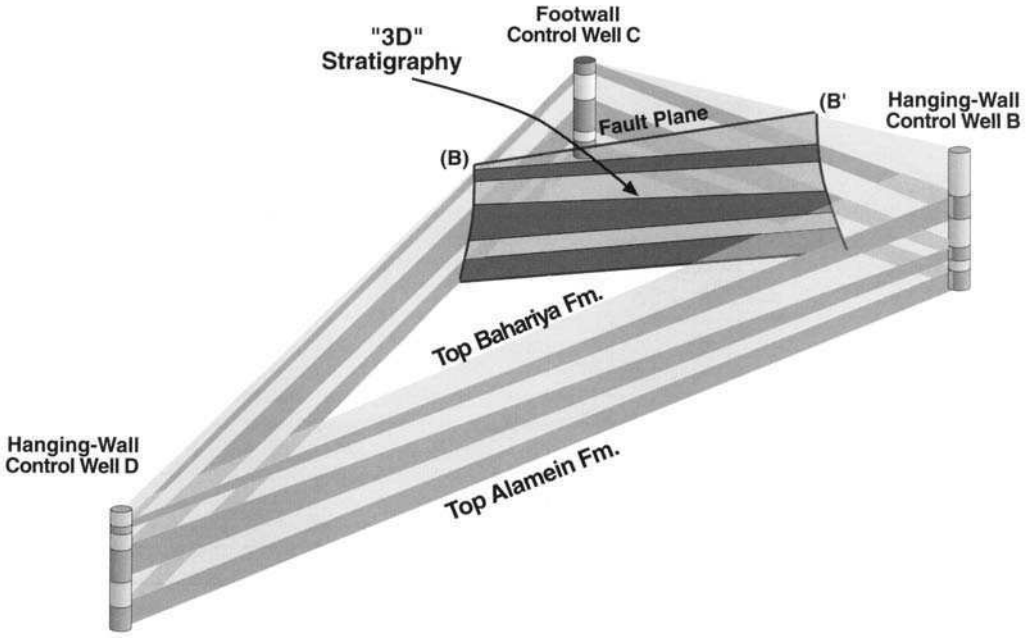

Fig. 11. Study Area 2, triangulation of stratigraphy using an additional well (D, to the southwest of Fig. 2b); the resultant '3D' stratigraphy calculated for the fault plane is shown.

sandstone shale ratio within the fault zone separating two juxtaposed sandstones (Smith 1966, 1980). A high SGR reflects a high sandstone/shale ratio (high permeability) within the fault zone, and therefore increases the likelihood of a leaking fault. In contrast, a low SGR reflects a low sandstone/shale ratio (low permeability) within the fault zone, and increases the likelihood of the fault sealing. SGR will vary along the strike of the fault, in response to varying stratigraphy and fault displacement. The SGR at any point along the strike of the fault is controlled by the sandstone/shale ratio of the entire stratigraphic section that has moved past that point. Therefore it is important to fully understand the stratigraphy of both the footwall and hanging wall sections directly adjacent to the fault to avoid introducing errors.

When estimating fault seal effectiveness, the SGR of the fault being studied is compared with the SGR threshold of the whole basin, using previously calibrated proven sealing and non-sealing faults. The resultant 'threshold' value can then be compared against all other faults within the basin. To calculate this threshold value, the SGR valuesof all faults within the basin are plotted against the number of faults being analysed. A line can then be drawn separating those faults which do seal from those known to leak (Fig. 13a); this line represents the threshold SGR for the basin, and can be used semi-quantitatively. However, as fault displacement may be uncertain, it may be useful to plot a range of SGRs (based on the most likely anticipated stratigraphy) against fault displacement (Fig. 13b), and then apply the previously determined threshold SGR value. This will allow immediate assessment of likely smear gouge sealed faults.

Results. Smear gouge analysis has been carried out on the areas along the fault plane in Study Area 1 that had been identified as having sandstone-on-sandstone juxtaposition (Figs. 7b and c). Well A has tested the structure, but found no hydrocarbon accumulation. This suggests a problem with fault seal at the top of the structure, where the lowest SGR value determined was 2.3 (Fig. 13a and b). The cut-off (or threshold) SGR value was therefore taken as 2.3. The same fault analysis techniques used in Study Area 1 have also been applied to the untested prospect in Study Area 2 using the same leak or seal limit (SGR of 2.3). In addition, the SGR analyses have been carried out using various combinations of fault-plane stratigraphy, based on the three wells within the study area, and already used to model different Allan diagrams. Using these stratigraphic combinations has

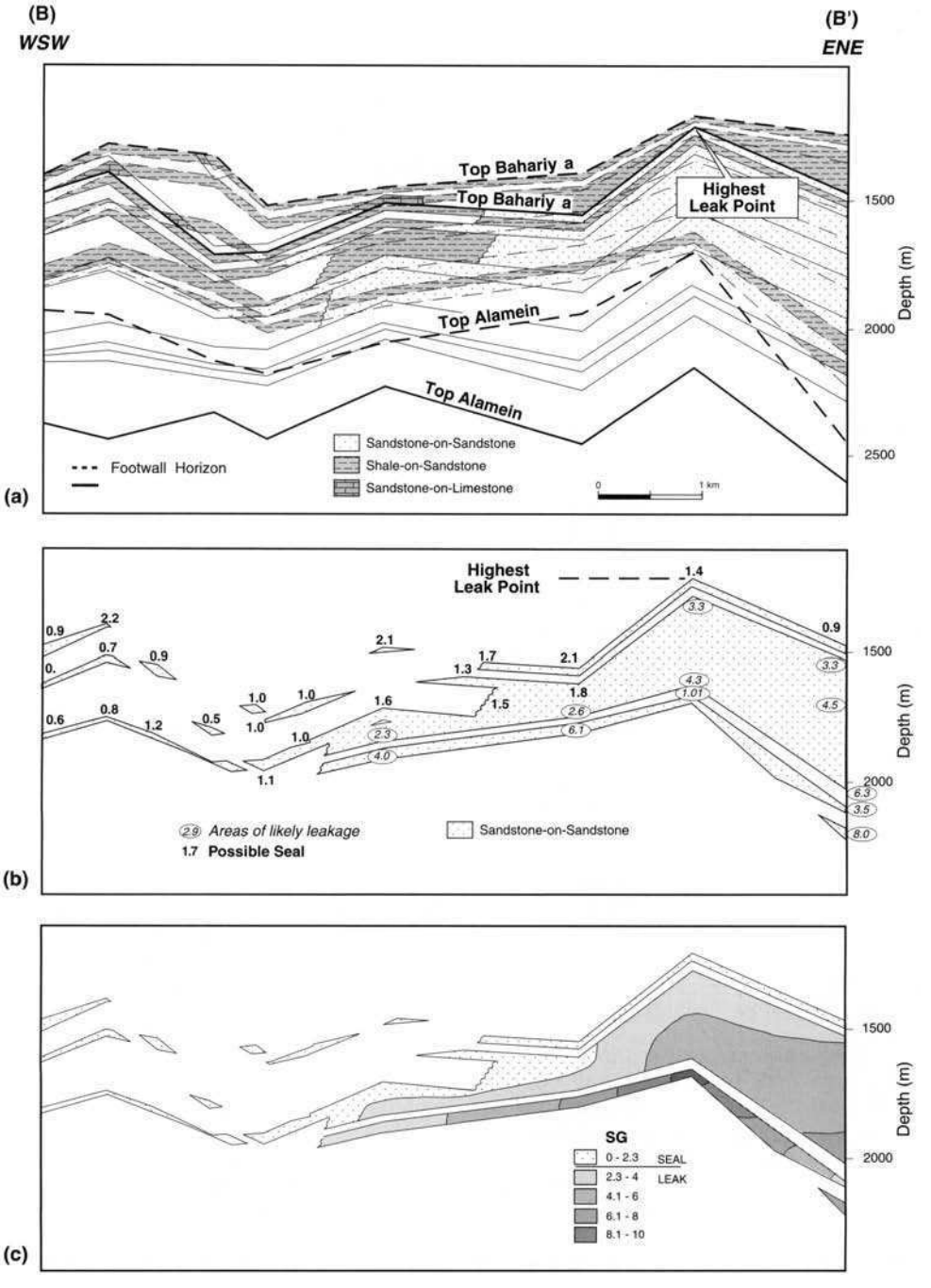

Fig. 12. Study Area 2, fault seal analysis using triangulated lithologies derived from Fig. 11. (**a**) Allan diagram superimposing the footwall and hanging wall lithologies. (**b**) Areas of sandstone–sandstone juxtaposition derived from the Allan diagram with calculated values of SGR; the large amount of sandstone juxtaposition at the ENE culmination indicates a leaking fault. (**c**) SGR from (b) contoured and shaded which indicates that shale smear could make a minimal contribution to fault seal.

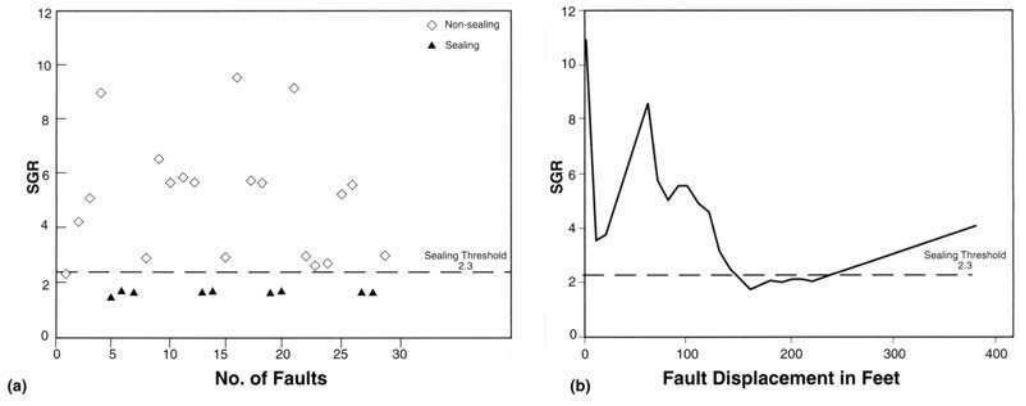

Fig. 13. Study Area 1, smear gouge ratio plots. (**a**) Compilation of SGR values. (**b**) SGR values v. fault displacement (compilation of data from Figs 5a and 7b).

allowed the sensitivity of any fault seal interpretations developed from the methods applied here to be tested.

When calculating SGR based on only Well B, it is clear that the majority of the sandstone-on-sandstone juxtapositions have calculated SGR values above 2.3 and therefore are deemed likely to leak (Fig. 8b and c). Based on this analysis, the highest leak point of this structure would be around 1270 m, whereas the spill point identified directly from the structure mapping is deeper, at 1430 m. The fault seal is therefore shown to be a critical factor, both in terms of trap integrity and reserve estimations.

When the stratigraphy from the footwall only was used (Well C), smear gouge analysis indicates a range of SGR values of between 0.4 and 4.4 (Fig. 9b and c). The highest leak point, determined from the Allan diagram (Fig. 9a), is approximately 1590 m. This is 160 m lower than the spill point as defined by dip (mapped) closure.

The third sensitivity analysed uses the stratigraphy from both the *hanging wall* (Well B) and the footwall (Well C). Smear gouge analysis suggests that in this situation a sealing fault gouge would probably not develop on any of the sandstone-on-sandstone fault surfaces (Fig. 10b and c). Identification of a highest leak point relating to the fault (taken from the Allan Diagram) alone is around 1390 m, *c.* 40 m above the spill point of the structure.

The final sensitivity check uses a combined 'pseudo' stratigraphy based on all three wells within the study area (Figs. 11 and 12a). Smear gouge analysis suggests that the sandstone-on-sandstone contacts towards the WSW end of the fault would be sealed by a fault gouge, but that the fault gouge towards the NE tip of the fault would not act as a seal (Fig.12b and c). The closing contour assuming fault seal would be about 1310 m in this example. These case histories demonstrate that a range of closing contours could easily be selected, ranging from 1270 m to the structural spill at 1430 m.

Strain analysis. Although not strictly a fault seal analysis technique, strain analysis is yet another useful technique for evaluating overall trap integrity. It can be applied to determine the likelihood of failure of a top seal to a reservoir on the basis that strain applied beyond a certain limit or threshold will cause the seal to fracture and thus no longer be able to trap hydrocarbons. An additional use of the technique is the ability to determine whether the timing of the strain (i.e. trap competence) pre-dates or post-dates hydrocarbon charge.

Using measurements made from cross-sections, the amount of incremental strain experienced by a rock layer can be calculated. The result can be compared with a threshold level empirically determined for a specific layer in a basin. To determine this threshold level, it is necessary to study the strain experienced by a variety of tested structures where entrapment of hydrocarbons is controlled by top seal competency.

Incremental and cumulative strain are calculated from the increase in bed length of a rock layer. For the technique to work it is necessary that the selected horizons were, prior to deformation, initially horizontal. Thus for a layer of length a which is stretched to length a' the incremental strain would be $[(a' - a)/a]$. The next incremental strain, where the length increases

from a' to a'', is calculated as $[(a'' - a')/a]$. Cumulative strain is the sum of the contributing incremental strains. Since geological events can be dated, it is also possible to calculate the incremental strain per million years. Displayed graphically, this will clearly show time periods when maximum movement or structuration occurred. Measurements taken along several seismic lines within an area will confirm the consistency of an interpretation, as times of peak strain should coincide.

The start point of the calculation is the measurement of the current horizontal length of the portion of the section being studied, and the measurement of the subsequent older/deeper horizons. The limits of the study area should extend just beyond the area of deformation. This method also requires that compression has not played a major part in the deformation and assumes the layers are pinned and have not been able to slide in or out of the study area. Measurements for the calculation of strain can be taken directly from depth converted cross sections with the same scale in both axes or, with appropriate scaling, seismic sections. This study utilised measurements made from seismic sections which are oriented normal to the fault-plane. There are two problems using seismic time sections for these calculations. One is the difficulty posed in measuring the true length of a line on a seismic section where one dimension is time and the other distance. The second is measuring to the required degree of accuracy of two or more curved lines where the length differences are small. It was decided therefore to calculate the lengths from the deflection seen from a 'baseline' drawn for each horizon across the portion of seismic section being studied. As each measurement is (more or less) only undertaken in one of the two axes, conversion to true length is possible.

Results Fig.14a illustrates the method used while Fig.14b compares this method using seismic without acknowledging the dimension of the vertical axis. In this simple case, strain would be overcalculated by 400%. Fig.15 shows graphically the incremental strain variations along the fault in Study Area 2, which exhibits a remarkably consistent history of maximum strain for all 4 lines. This work has not been extended in the basin beyond these two examples, therefore a regional threshold is not yet available.

Sensitivities

Stratigraphy. Fault-plane stratigraphy is the most difficult of the parameters to estimate for fault seal analysis, and yet can have a profound influence on the outcome of any study. The influence and effects of stratigraphic variation has been fully documented during the discussion of the results of the Allan diagram and SGR analyses using a number of stratigraphic sensitivity models from Study Areas 1 and 2. These results confirm that as much reference as possible needs to be made to seismic, and the nearest available wells to the fault under investigation (Fig.11).

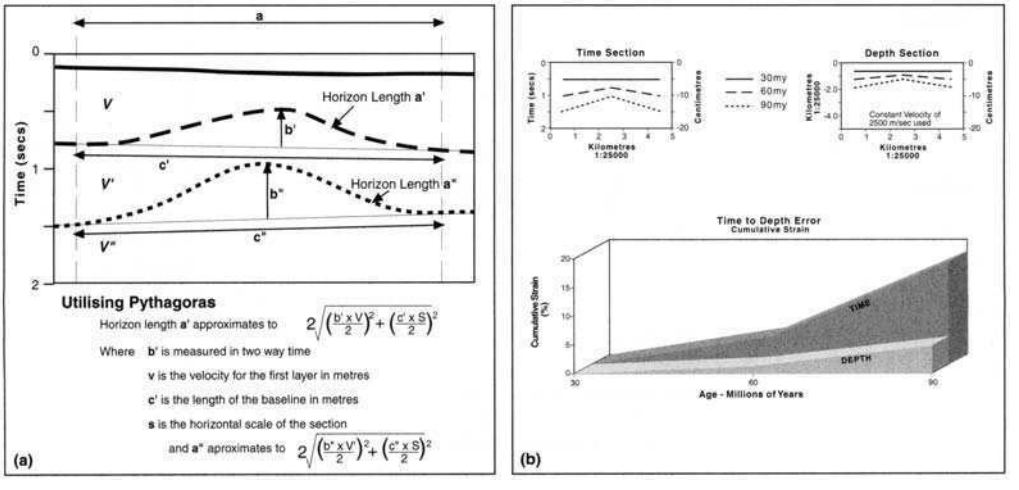

Fig. 14. Calculation of incremental strain. (**a**) The method used to obtain measurements using seismic time sections. (**b**) Possible error introduced by using time sections without applying the method demonstrated in (**a**).

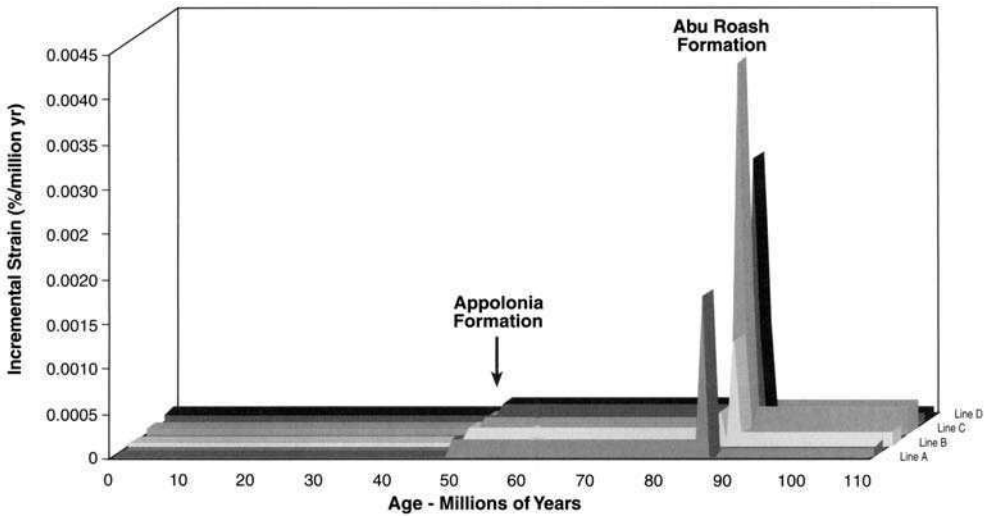

Fig. 15. Study Area 2, incremental strain plot indicating that high levels of strain occurred during Upper Cretaceous (Abu Roash), suggesting that seal failure to older reservoirs may have occurred at that time.

Fault throw and depth conversion. Most fault seal analysis techniques rely on knowledge of the throw and its variation along the fault. With a 2D seismic dataset there are two main areas where errors will be generated: depth conversion and fault-displacement. Faults invariably cause problems with depth conversion, and the technique used will influence the outcome of the calculation of fault throw. Comparisons made in Fig.16 are based on velocities derived from nearby Well A. Even with this close control, the outcomes vary considerably, with (for the deepest horizon), a range of throws from 57 to 88 metres.

In addition, the fault displacement will be dependant on the method of producing the map. Few maps these days are hand contoured where personal styles can affect the outcome; however computer contouring is very dependent, away from control points, on the griding method selected. A study of the input data should be made to ensure the appropriate griding technique

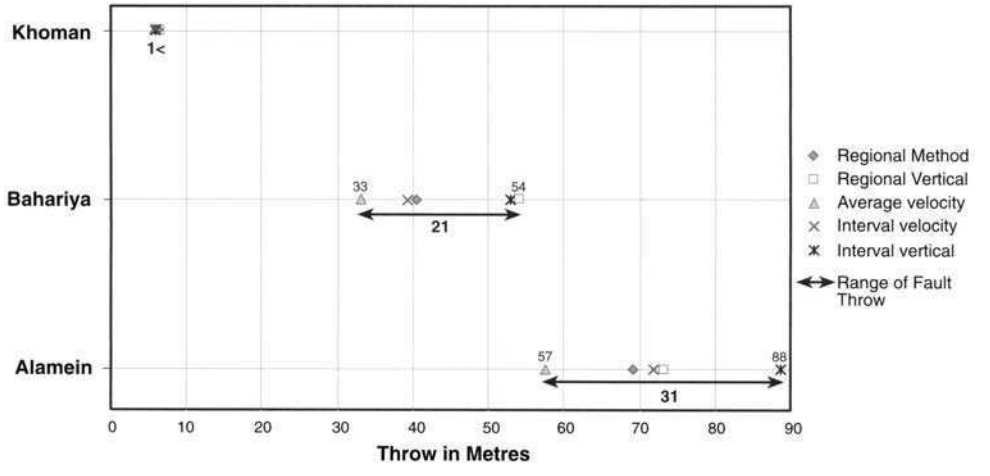

Fig. 16. Study Area 1, variation of calculated fault throw with depth conversion method. This shows the range of fault displacements that could be generated simply by applying different depth conversion methods to the same time map. This would affect the outcome of Allan diagrams, and SGR calculations

is used. Therefore depth conversion and mapping must be properly applied before using many of the methods discussed.

Fault identification. One aspect of fault identification is the difficulty of determining whether a fault mapped on seismic is a discrete single large fault or a series of smaller, sub-seismic faults (Fig. 17). Surface evidence shows that faults often comprise a zone of fracturing rather than a single displacement surface (Knipe, 1992). Seismic data however, cannot resolve horizontally less than the common depth point (CDP) interval, nor vertically much less than ten's of metres, and thus will not show the detail of the fault zone. For smaller faults, this will impact on the usefulness of Allan diagrams and structural cross-sections for determining juxtaposition seals, and will question the application of smear-gouge ratios.

Inversion. The Western Desert Province of Egypt has been subject to a period of early Tertiary transpressional stress, which has resulted in the inversion of Mesozoic fault blocks. Harding and Tuminas (1988, 1989) suggest that reverse faults, or normal faults reactivated by inversion, are more likely to seal than normal faults. They believe that seal capacity increases due to the greater development of shear fractures, cataclasis and fault gouge. Although Allan diagrams can still be constructed, assessment of SGR is more problematic, since the SGR calculation is dependent on the entire stratigraphic section which has moved past that point. Therefore, the fault displacement prior to inversion must be known, together with the amount of inversion that has taken place along the fault in order to determine the stratigraphy that has moved past a point on the fault plane, to allow the SGR to be calculated.

Problem areas

To date, all published work on fault seal analysis describes case histories within extensional tectonic provinces and stratigraphic sequences dominated by siliciclastic lithofacies. However, two major problem areas remain, which must be addressed by future research; these are the influence of inversion (although this has been addressed in the southern North Sea, Knott 1993) and the sealing properties of faulted carbonates.

Carbonates. In the Western Desert, Cretaceous carbonates provide an important reservoir objective, in addition to the intercalated siliciclastic reservoirs (especially within the Abu Roash Formation). Little work has been done on the development of fault-seals in carbonates. Until empirical data sets are available, fault seal prediction in carbonates is difficult. At the present time the problem of fault-sealing in carbonates is perhaps best solved by carrying out field work in the area under study. Further research is required.

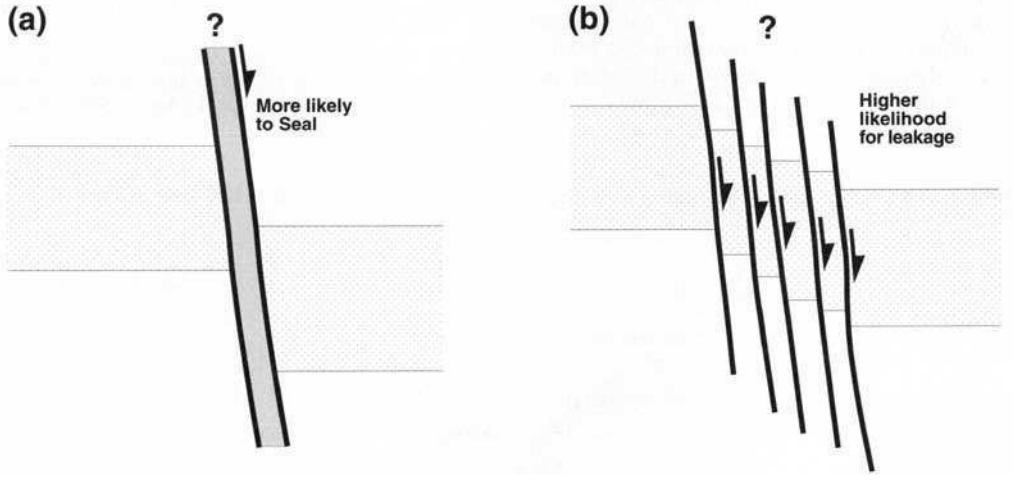

Fig. 17. Fault identification difficulties. (**a**) Faults identified on seismic data are considered to be single displacement. (**b**) If this assumption is incorrect a series of 'sub-seismic' faults will not have the same SGR characteristics and may have complex sandstone-on-sandstone cross-fault juxtapositions.

Conclusions

Two types of fault seals have been investigated applicable to the Western Desert region: (1) Juxtaposition Seals, which occur when shale is displaced against permeable sandstone across the fault plane; (2) Shale Smear Seals, which work by smearing shale into the fault plane, which reduces the effective permeability of the fault plane. These fault seals occur in intercalated sandstone/shale sequences.

Five techniques are available to graphically assess the effectiveness of fault seal, using different datasets. These are summarised in Table 1. Fault displacement diagrams should be used to investigate important faults in exploration and production as they help define the occurrence and size of potential traps. The generation of a fault plane stratigraphy has to be carefully considered however, since it can have a profound effect on spill points taken from Allan diagrams and SGR calculations. Sensitivities therefore always need to be run.

None of these five techniques on their own are likely to provide a unique solution to the problem of fault seal in any geological province. However, any analysis must utilise all available data, preferably calibrated using data from faults with known sealing properties, and must use all five documented techniques. Such data when used collectively can be used to successfully rank undrilled structures within any prospect portfolio, so as to select low risk drilling candidates.

Fault displacement diagrams are useful in defining the occurrence and size of traps. Fault displacement diagrams are relatively simple to construct, and should be carried out routinely for important faults in exploration and production. Allan diagrams are useful in the determination of potential cross-fault leak points, but are highly sensitive to the fault plane stratigraphy. The stratigraphy intersecting the fault plane also has a considerable influence on the SGR, and thus on any leak/seal assumptions about the fault.

This paper has discussed a series of techniques which can be used to describe and analyse fault seal integrity by means of two case histories from the Western Desert of Egypt. However, these techniques are certainly not unique to Egypt, and can be successfully applied to any sedimentary basin in the world, subject to extensional tectonism and dominated by siliciclastic stratigraphic sequences.

The authors would like to thank the Management of BG Exploration and Production Limited for their permission to publish this paper. Our thanks also to Andy Chapman, who produced the figures for this paper.

References

ALLAN, U. 1989. Model for hydrocarbon migration and entrapment within faulted structures. *Bulletin, American Association of Petroleum Geologists*, **73**, 803–811.

BARAKAT, M. G. & DARWISH, M. 1988. Evolution, sedimentary environments and hydrocarbon potentialities of the Kharita Formation (Albian) in the North Western Desert, Egypt. *9th Petroleum Conference for Exploration and Production, Egyptian General Petroleum Corporation*, **9**, 51–73.

BERG, R. & AVERY, A. 1995. Sealing properties of tertiary growth faults, Texas Gulf Coast. *Bulletin, American Association of Petroleum Geologists*, **79**, 375–393.

BERGLAND, L. T., BOCTOR, J., GJELBERG, J., EL MASRY, M. & SKOGEN, J. 1994. The Jurassic hydrocarbon habitat of Ras Kanayes Area, NW Desert,

Table 1. *Summary of fault seal techniques available, data requirements for their use and the order in which the techniques are undertaken*

Technique	Use	Data requirement	Order of analysis
Fault displacement diagrams	Fault interpretation quality control	Seismic data	1
Structural cross-sections	Fault analysis (juxtapositions)	Seismic and well data	2a
Allan diagrams	Fault analysis (juxtapositions)	Structure maps & well data	2b
Smear gouge ratios	Fault analysis when sandstone on sandstone demonstrated	Allan diagrams, well data and seismic	2c
Strain analysis	Topseal analysis	Seismic data	3

Egypt. *12th Petroleum Conference for Exploration and Production, Egyptian General Petroleum Corporation*, **12**, 53–66.

EGYPTIAN GENERAL PETROLEUM CORPORATION. 1992. *Western Desert Oil and Gas Fields (A Comprehensive Overview)*. Publication of the Egyptian General Petroleum Corporation, Cairo.

GIBSON, R. 1994. Fault-zone seals in siliciclastic strata of the Columbus Basin, offshore Trinidad. *Bulletin, American Association of Petroleum Geologists*, **78**, 1372–1385.

HANTAR, G. 1990. North Western Desert. *In*: SAID, R. 1990. *The Geology of Egypt*, Balkema, Rotterdam, Chapter 15, 293–319.

HARDING, T. P. & TUMINAS, A. C. 1988. Interpretation of footwall (low side) fault traps sealed by reverse faults and convergent wrench faults. *Bulletin, American Association of Petroleum Geologists*, **72**, 738–757.

—— & —— 1989. Structural interpretation of hydrocarbon traps sealed by basement normal fault blocks at stable flank of foredeep basins and at rift basins. *Bulletin, American Association of Petroleum Geologists*, **73**, 812–840.

JEV, B., KAARS-SIJPESTEIJN, C., PETERS, M., WATTS, N., & WILKIE, J. 1993. Akaso Field, Nigeria: use of integrated 3-D seismic, fault slicing, clay smearing, and RFT pressure data on fault trapping and dynamic leakage. *Bulletin, American Association of Petroleum Geologists*, **77**, 1389–1404.

KNIPE, R. J. 1992. Faulting processes and fault seal. *In*: LARSEN, R. M., BREKKE, H., LARSEN, B. T., & TALLERAAS, E. (eds) *Structural and Tectonic Modelling and its Application to Petroleum Geology*. NFP Special Publication, **1**, 325–342.

KNOTT, S. 1993. Fault seal analysis in the North Sea. *Bulletin, American Association of Petroleum Geologists*, **77**, 778–792.

LINDSAY, N. G., MURPHY, F. C., WALSH, J. J. & WATTERSON, J. 1993. Outcrop studies of shale smears on fault surfaces. *In*: FLINT, S. S. & BRYANT, I. D. (eds) *The Geological Modelling of Hydrocarbon Reservoirs and Outcrop Analogues*. International Association of Sedimentologists, Special Publication, **15**, 113–123.

PARKER, J. R. 1982. Hydrocarbon habitat of the Western Desert, Egypt. *6th Petroleum Conference for Exploration and Production, Egyptian General Petroleum Corporation*.

ROBERTSON RESEARCH INTERNATIONAL. 1982. *Petroleum Potential Evaluation, Western Desert, The Arab Republic of Egypt. Report and Enclosures*.

SAID, R. 1990. *The Geology of Egypt*, Balkema, Rotterdam.

SMITH, D. A. 1966. Theoretical considerations of sealing and non-sealing faults. *Bulletin, American Association of Petroleum Geologists*, **50**, 363–374.

—— 1980. Sealing and non-sealing faults in Louisiana Gulf Coast salt basin. *Bulletin, American Association of Petroleum Geologists*, **64**, 145–172.

WATTS, N. L. 1987. Theoretical aspects of cap-rock and fault seals for single- and two-phase hydrocarbon columns. *Marine and Petroleum Geology*, **4**, 274–307.

ZEIN EL-DIN, M., ABU EL-KHALIK, M., & MOUSSA, S. 1990. Exploration concepts and reasons for dry holes in the North Western Desert. *Egyptian General Petroleum Corporation 10th Exploration and Production Conference, Egyptian General Petroleum Corporation*, **10**, 71–106.

This page intentionally left blank

Trap architecture of the Early Cretaceous Sarir Sandstone in the eastern Sirt Basin, Libya

RUTGER GRAS[1] & BINDRA THUSU[2]

[1]*Schlumberger GeoQuest, Africa–Mediterranean Region, P.O. Box 362, 92541 Montrouge Cedex, France (e-mail: gras@montrouge.geoquest.slb.com)*

[2]*Arabian Gulf Oil Company, Exploration Department, P.O. Box 263, Benghazi, Libya*

Abstract: The Sarir Sandstone is the principal reservoir for oil accumulations in the eastern Sirt Basin in Libya. The main phase of the rifting in this area took place in the Late Jurassic–Early Cretaceous, during which time the Sarir Sandstone was deposited as a non-marine, intra-continental clastic syn-rift sequence. Although successfully explored from 1959 onwards, the prolific eastern Sirt Basin is in a relatively immature stage of exploration regarding wildcat drilling and 3D seismic data acquisition. The most recent phase of exploration, utilizing 3D seismic techniques, revealed a complex structural development. The trap geometries are often related to E–W trending, basement-controlled fault systems, oblique to the NNW–SSE Sirt Basin trend. The fault systems were active during the Sarir Sandstone deposition, giving rise to structural as well as well as combined structural–stratigraphic traps. An increased understanding of trap architecture has led to both re-evaluation of older fields and new discoveries. Complex structural traps exhibiting four-way dip or fault closures, and combined structural–stratigraphic traps, have been successfully explored in recent years, and will continue to provide exploration opportunities. The prospective areas comprise the faulted basin margins and the Sarir Sandstone depositional and erosional edges. Modern geophysical techniques including high-resolution 3D seismic data acquisition are critical in discovering and developing the remaining potential.

The study area is situated in the eastern part of the prolific Sirt Basin in Libya, between longitude 21° and 24°E and latitude 27° to 30°N (Fig. 1). This region, the centre of which is *c.* 400 km south of Benghazi, consists predominantly of rocky desert plain and sand dunes, with an average ground level of 300 ft above mean sea level.

The Sirt Basin is a Mesozoic and Tertiary rift system, located in the northern central part of Libya. It is the major oil producing region of Libya currently producing some 1.4 million barrels (MMBL) of oil per day, with an estimated original oil in place (OOIP) of 100 billion barrels (BBBL).

In the eastern Sirt Basin Sandstones of Late Jurassic–Early Cretaceous age are the major proven, productive and prospective reservoir. Various lithostratigraphic terms are used to describe these sandstones. In this paper the term Sarir Sandstone is preferred. Reserves within Sarir Sandstone reservoirs are sourced predominantly by the Late Cretaceous Rakb Shales and the intra-Sarir lacustrine to shallow marine source intervals. Regional top seal is provided by the Late Cretaceous Rakb Group shales. These play elements have been proven to be effective in some of the largest fields of the Sirt Basin: the Sarir C-Main field (Sanford 1970), the Messlah field (Arabian Gulf Oil Company (AGOCO), Exploration Staff 1980; Clifford *et al.* 1980), and the Abu Attifel field (Fig. 2), which rank with the world's largest oilfields.

A wealth of recent published data on the Sirt Basin and its petroleum geology is available, as a result of the conference 'Sedimentary Basins of Libya, First Symposium, Geology of the Sirt Basin', held in 1993 in Tripoli. Data presented at this conference have been reviewed for the present paper, using preprint versions of some of the papers, kindly supplied by the authors. Contributions on the petroleum geology of the Sirt Basin are those by El-Ghoul & Hallett (1993), Saenz de Santa Maria (1993), Wennekers *et al.* (1993), and the section devoted to the Sirt Basin by Gumati *et al.* (1996). The petroleum geology of the Sarir Sandstone specifically has been treated by Ibrahim (1987), Rossi *et al.* (1991), El-Hawat (1992), Missallati (1992), El-Hawat & Missallati (1993), Fezzani (1993), among others.

Trap architecture is defined as the sum of the structural and sedimentological elements that define the geometry of a hydrocarbon occurrence. The task of the explorer is to recognize these elements, and thereby, with thorough knowledge of biostratigraphy, sedimentology and structural geology, to understand the trap architecture. The present paper reviews the exploration of the eastern Sirt Basin on the

GRAS, R. & THUSU, B. 1998. Trap architecture of the Early Cretaceous Sarir Sandstone. *In*: MACGREGOR, D. S., MOODY, R. T. J. & CLARK-LOWES, D. D. (eds) 1998. *Petroleum Geology of North Africa*. Geological Society, London, Special Publication No. 132, 317–334.

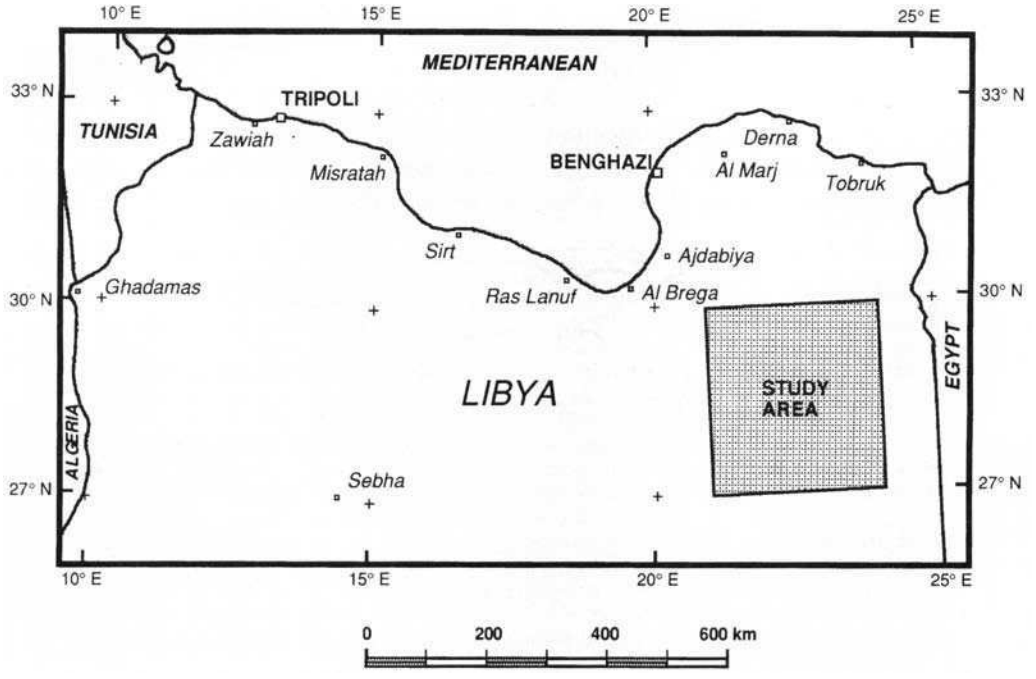

Fig. 1. Location map of study area. This map is no authority on transcriptions of geographical names.

basis of published data and the authors' own experience in the Sirt Basin exploration. An inventory of prospective play types is provided, making use of the latest advances in the Libyan petroleum geology. Furthermore, the major play types considered to hold yet-to-find oil in the eastern Sirt Basin are discussed.

Regional setting and tectonic evolution

The Sirt Basin is a major intra-cratonic rift system in central Libya. The sedimentary succession of the Sirt Basin reflects its tectonic and structural evolution, which is closely related to the opening of the Atlantic Ocean and the convergence of Tethys in Mesozoic and Tertiary times.

The tectonic evolution of the Sirt Basin involved thermal arching and attenuation with multiple phases of rifting, probably starting as early as the Middle Triassic (Thusu 1993). The Triassic rift event with associated volcanism corresponds to the initial break-up of Pangaea. The extension culminated in the Late Jurassic–Early Cretaceous main phase of rifting. The Late Jurassic–Early Cretaceous rift phase, consisting of several sub-stages, is associated with volcanism and has been linked to the opening of the eastern Mediterranean oceanic basin (Guiraud this volume). The evolution of the Sirt Basin resulted in a complex suite of horsts and grabens developed during the polyphase continental fragmentation (Massa & Delort 1984). The Sirt rift system has been interpreted to consist of a triple-point junction that failed to evolve into the spreading stage (Van Houten 1983). The aborted arms are oriented at approximately 120 and have been informally named Sirt, Sarir and Tibesti (Fig. 3). The Sirt arm consists of a series of troughs developed as a result of the conjunctive NNW–SSE trending rifting which culminated during the Campanian, with an estimated stretching factor of 1.7 (El-Ghoul & Hallett 1993). The Sirt arm developed into a major depocentre in the Late Cretaceous–Eocene post-rift or late syn-rift and thermal subsidence stage (Gumati & Nairn 1991). The E–W trending Sarir arm, which covers the study area of the present paper, experienced syn-rift extension during the Late Jurassic–Early Cretaceous. Regional evidence suggests that this main phase of rifting took place during the Neocomian–Barremian (Guiraud & Maurin 1992). The E–W trending fault zones have been demonstrated to have undergone right-lateral divergent wrench-

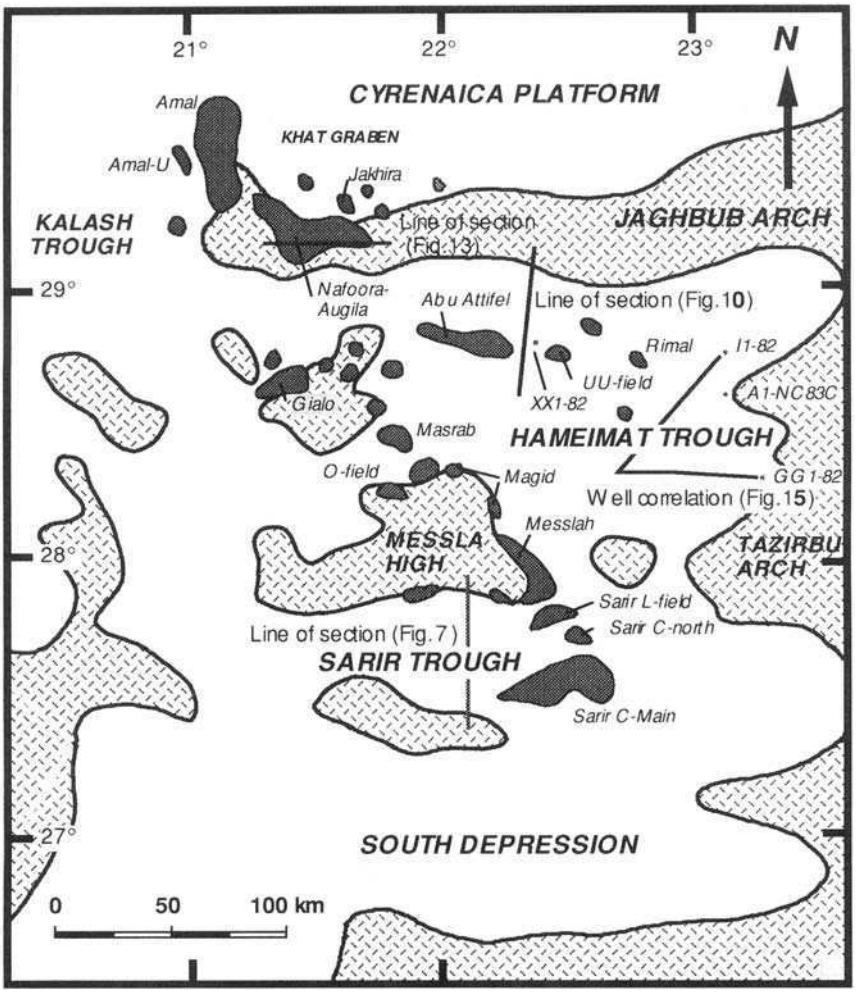

Fig. 2. Eastern Sirt Basin; tectonic elements and oilfields, modified after Ibrahim (1987). This map is no authority on field name transcriptions and field locations, and does not claim to be complete.

ing (transtension), suggesting superposition of the NNW–SSE Sirt arm extension on the pre-existing E–W trend (Gras 1996). The third arm, the NNE–SSW trending Tibesti arm, experienced only minor rifting (Saenz de Santa Maria 1993).

The study area in the Sarir arm of the Sirt Basin consists of a complex arrangement of structural highs which separate the depocentres. The main depocentres are the Sarir Trough and the Hameimat Trough, of which the latter is the deepest basin, with a sedimentary sequence of 25 000 ft (Figs 2 and 3). The Late Cretaceous structure mimics the syn-rift infill. The deepest post-rift troughs coincide with the syn-rift basins (Gras 1997). There is, locally, evidence of reverse reactivation of faults, presumably taking place in the Santonian–Campanian. This is consistent with the Santonian compressional event observed in the Tethyan realm (Guiraud *et al.* 1992).

Exploration history

Exploration in Libya started in 1955 with the adoption of petroleum licensing legislation. The first well in the Sirt Basin was drilled in 1956. Since that time over 1600 exploration wells have been drilled in the Sirt Basin, which covers an area of *c.* 200 000 km^2. These wells have discovered 340 oilfields and gas fields

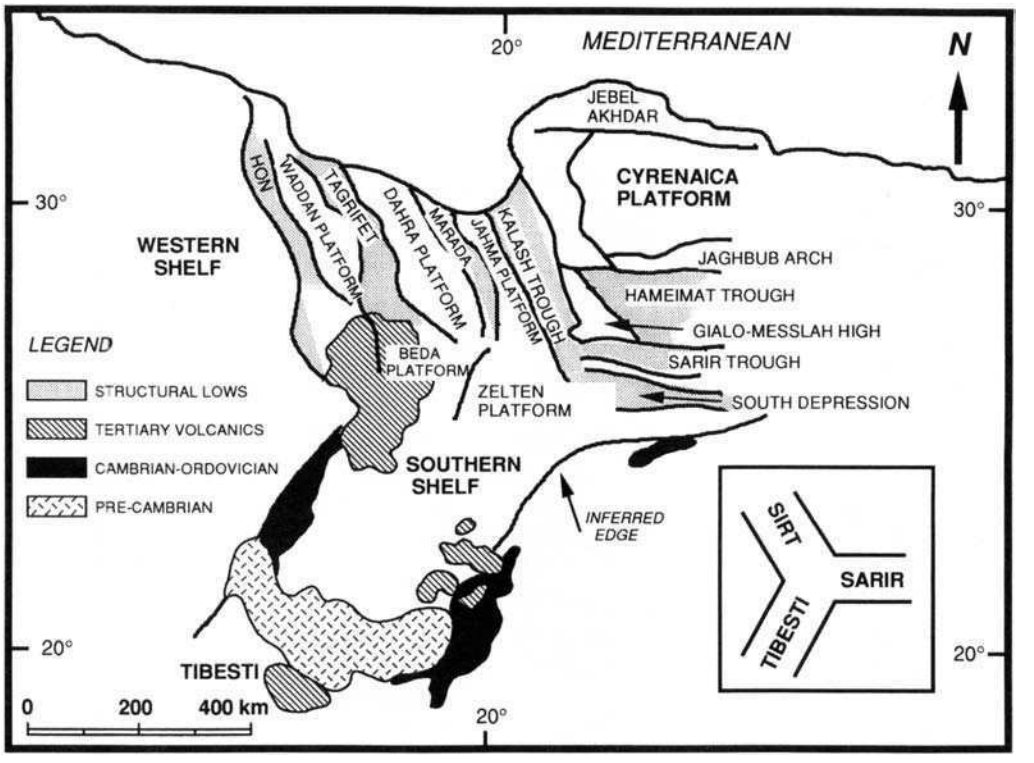

Fig. 3. Tectonic elements of Sirt Basin, showing triple point junction model. Modified after Saenz de Santa Maria (1993).

within 18 reservoirs, with an estimated total of *c.* 100 BBBL OOIP, 50 trillion cubic feet (TCF) of associated gas-in-place (GIIP) and 20 TCF of non-associated GIIP (El-Ghoul & Hallett 1993; Gumati *et al.* 1996), yielding a total of 113 BBBL of original oil-equivalent-in-place. Thomas (1995) estimated that 130 BBBL OOIP has been discovered. El-Ghoul & Hallett (1993) have highlighted that, to date, relatively shallow targets have been explored, as only 10% of the exploration wells have drilled deeper than 10 000 ft.

These exploration statistics have been compared with the Central Graben and Viking Graben in the UK and Norwegian sector of the North Sea, a rift system that shares several characteristics with the Sirt Basin. In the Central Graben and Viking Graben *c.* 3600 exploration wells have been drilled since 1965, in an area of roughly 125 000 km^2. Up to 1994, 78 BBBL of original oil-equivalent was discovered, according to the Brown Book DTI 1994 report (UK) and NPD annual report 1993 (Norway). These statistics indicate that the exploration well density in the North Sea is a factor of three higher than that in the Sirt Basin, yet the original oil discovered per exploration well in the Sirt Basin is approximately three times higher than in the North Sea (Table 1).

In the eastern Sirt Basin, the first discovery was made by well A1-12 in 1959 in the Amal Formation, discovering the Amal field (Roberts 1970). In December 1961, well C1–65 discovered the 'super-giant' Sarir C-Main oilfield (Sanford 1970). Major discoveries in the study area comprise Gialo (1961), Nafoora–Augila (1965–1966), Abu Attifel (1968), and Messlah (1971). The exploration during this period took place using gravity, magnetic, and lowfold 2D seismic techniques, and successfully discovered the largest structures with structural control at basement level. However, many dry exploration wells were drilled during this period, which suggests that the exploration methods at the time failed to identify subtle traps (Sanford 1970). Nevertheless, the major fields which constitute a large proportion of the original oil-in-place were discovered during this period (Ibrahim 1987). These fields, seven of which rank in the 'super-giant' category containing more than

Table 1. *Comparison of exploration statistics, Sirt Basin and North Sea Central Graben (reserves are million barrels of original oil-equivalent-in-place (OOEIP).*

	Sirt Basin	Central Graben/Viking Graben
Exploration start	1960	1965
Area (km^2)	200 000	78 000
Exploration wells	1600	3600
Original oil-equivalent-in-place (MMBBL)	113 000	78 000
Exploration well/km^2	0.008	0.03
OOEIP/exploration well (MMBBL)	71	22
OOEIP/km^2 (MMBBL)	0.6	0.6

1 BBBL OOIP, have often been delineated and developed by means of step-out drilling and low-fold 2D data, and continue to be the most prolific producers today. The exploration largely followed known structural trends (Aburawi 1995). During this period, wells with low flow rates were considered non-commercial and were not appraised fully for development.

Following the initial phase of exploration and subsequent production, a series of smaller discoveries was made from 1970 onwards. Multi-fold 2D seismic data were routinely acquired, mainly using the vibroseis method (Zanati 1994). However, dynamite was occasionally used as a source, with good results. Some of the discoveries, most of which are in the 100–500 MMBBL range, have been developed as satellites to the major fields. Others await development and production facilities.

In the eastern Sirt Basin, 3D seismic data acquisition started around 1990. A number of 3D crews are currently active, both using vibroseis and dynamite as a source. Zanati (1996) presented a discussion on the acquisition parameters for 3D data in the Sirt Basin. As a result of the 3D surveys a number of discoveries has been made in the southeast Sirt Basin. In addition, previous sub-commercial discoveries are now in the stage of appraisal and development.

Thirty-four oil fields and discoveries are known to exist east of 21°E parallel based on a variety of data sources. The major fields are indicated in Fig. 2. An estimation of the field sizes using published data such as those of Thomas (1995) and Gumati *et al.* (1996), reveals that *c.* 65 BBBL OOIP has been discovered in the eastern Sirt Basin. Approximately 92% of the OOIP is contained in the seven giant fields Sarir C-Main, Sarir L-field, Messlah, Gialo, Nafoora–Augila, Abu Attifel and Amal (Fig. 4). The remaining 27 fields, on average, hold 200 MMBBL OOIP. The reservoir for the majority

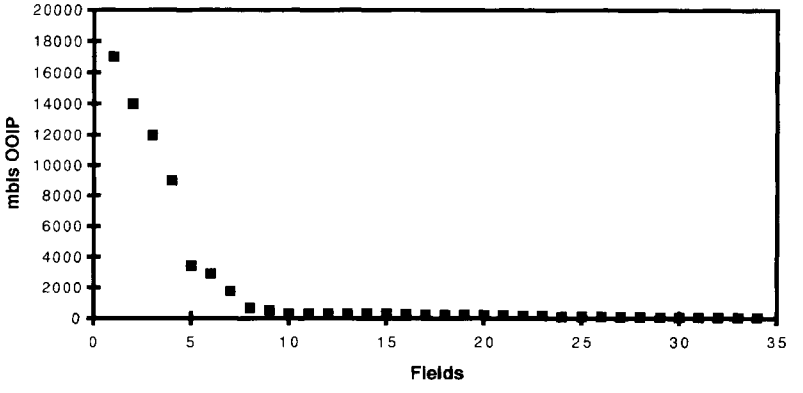

Fig. 4. Field size distribution, eastern Sirt Basin. Field sizes based on published data (Thomas 1995; Gumati *et al.* 1996) and estimations by the authors.

of the fields is the Sarir Sandstone; however, significant exceptions are the giant fields Gialo (Tertiary), Amal (Triassic and Late Cretaceous), and Nafoora–Augila (Late Cretaceous and fractured basement). It is estimated that the Sarir Sandstone in the eastern Sirt Basin holds 24 BBBL OOIP.

Stratigraphy

The stratigraphic succession in the study area, situated in the Sarir arm of the Sirt Basin system, is separated into a pre-rift, early syn-rift, main syn-rift and post-rift sequence (Fig. 5).

The basement pre-rift sequence is composed of igneous and metamorphic rocks. On the Messlah High igneous rocks subcrop in the core, whereas on the margins metaphyllites and quartzites are frequently encountered. The sedimentary pre-rift sequence consists of sandstones and quartzites of the Gargaf Formation.

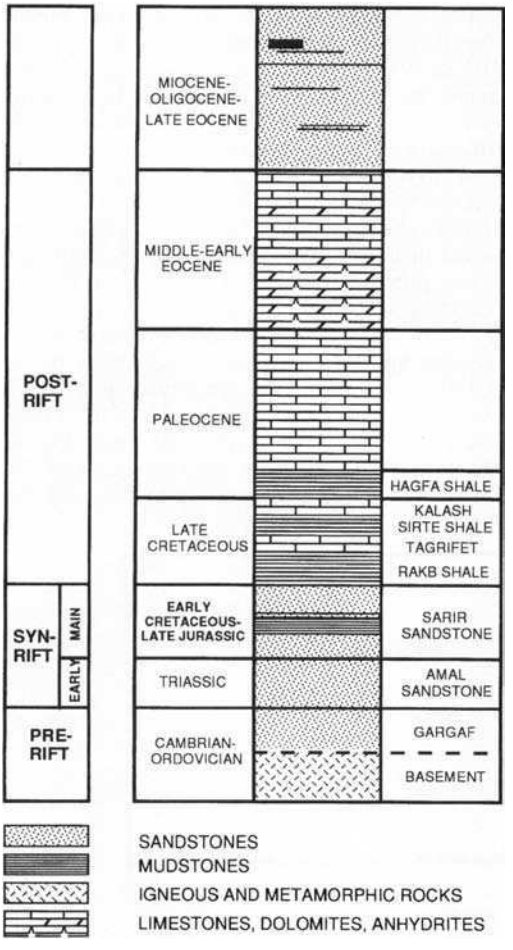

Fig. 5. Summarized stratigraphy of eastern Sirt Basin, showing rift sequences.

In recent years an early or incipient rift stage has been recognized on seismic data. Tentative correlation with scattered well data suggests that Permo-Triassic strata may locally form the earliest rift infill, underlining the polyphase extensional character of the Sirt Basin (Fig. 5; Guiraud & Maurin 1992; Thusu 1993; Van Erve 1993; Thusu & Mansouri 1995). The Amal Sandstone of Triassic age was deposited in the earliest E–W trending rift basins, and has been encountered on the Amal High, in the Maragh Low and in the northern part of the Hameimat Trough. The stratigraphy of the Permo-Triassic strata has been described by El-Arnauti & Shelmani (1998) and Swire (1995).

The main syn-rift sequence comprises a regressive cycle of continental clastic deposits of Late Jurassic-Early Cretaceous age, known as the Sarir Sandstone, Nubian Sandstone, Calanscio or pre-Upper Cretaceous Sandstone. The term Nubian Sandstone is loosely defined (Pomeyrol 1968; Klitsch & Squyres 1990), and the discussion on the validity of this name has become a tradition in the Libyan oil industry, as well as an unresolved dilemma. Nevertheless, the name 'Nubian' is used frequently for clastic intervals. Any sandstone subcropping below the marine Late Cretaceous Rakb Shale is potentially a 'Nubian' Sandstone. The confusion is further compounded by the fact that widespread silica overgrowth of the 'Nubian' Sandstone obscures original sedimentary features, and even leads to confusion with ortho-quartzites from the basement (Hea 1971). Using the term 'Nubian' in the widest sense as 'Pre-Upper Cretaceous' the Triassic Sandstone is included, which is clearly debatable. Van Erve (1993), in a discussion on the stratigraphic nomenclature, suggested using 'Nubian' with an age qualifier. The present authors prefer a lithostratigraphic nomenclature with biostratigraphic control, to be used within a defined geographical context. The term Sarir Sandstone, used for the Late Jurassic–Early Cretaceous sandstones in the eastern Sirt Basin, complies with these rules. In the present paper, the lithostratigraphic name Sarir Sandstone has been selected, in line with other publications by workers from AGOCO on this subject.

Widespread faulting during the syn-rift phase formed structural lows in which the Sarir Sandstones accumulated. The earliest rifting during the Late Jurassic coincides with rhyolitic and basaltic volcanism (El-Ghoul & Hallett 1993). Up to 3000 ft of clastic rocks has been deposited in the grabens and half-grabens of the study area. These are separated by basement horst blocks

with a condensed or absent Sarir section. The top of the Sarir Sandstone is truncated by a major unconformity at the base of the overlying Late Cretaceous marine sequence.

The post-rift sequence comprises marine shales and carbonates, deposited during the thermal subsidence stage. This indicates that extensional tectonics persisted, particularly in the northern parts of the study area. Locally, a basal glauconitic sandstone is developed, which may constitute an additional reservoir. The shale sequence overlying the continental syn-rift clastics is generally named the Rakb Shale. According to the nomenclature of Barr & Weegar (1972), the Late Cretaceous sequence consists of a lower Rachmat Shale, a middle limestone of Campanian age named the Tagrifet, and an upper Sirt Shale. The uppermost Late Cretaceous carbonates are named the Kalash (Fig. 5). The Late Cretaceous strata are conformably overlain by a Paleocene sequence of shales and limestones. In the Late Eocene–Miocene times a return to continental conditions is observed. The post-rift subsidence resulted in an average present-day depth of burial at the top of the Sarir Sandstone ranging between 8500 and 15000 ft below sea level in the study area.

Sarir Sandstone

The principal reservoir in the eastern Sirt Basin is the Sarir Sandstone. The gross isopach map of this reservoir sequence is shown in Fig. 6. A cross-section (in two-way travel time) across the southern part of the Sarir arm highlights the syn-rift nature of these sediments (Fig. 7). Age determinations for these sandstones have yielded Permo-Triassic, Jurassic and Early Cretaceous ages, often as a result of reworking (Thusu *et al.* 1988; B. Thusu, unpublished data). Most of the ages, however point to an Early Cretaceous age, consistent with the Late Jurassic–Early Cretaceous main phase of rifting.

Several facies associations and depositional environments have been interpreted, on the basis of cored wells and log interpretation (Rossi *et al.* 1991; El-Hawat 1992). The depositional environments are predominantly fluvial, ranging from alluvial fans, braided streams and meandering streams to marginal marine, coastal plain and lacustrine. Alluvial 'outwash' sandstones, ranging to conglomerates, occur near the basement highs. Because of the high scale content of the alluvial facies the gross reservoir to interval ratio for these sandstones is in the range of 20–30%. This facies occurs near the Messlah High as well as near the eastern margin of the Hameimat Trough, and is proposed as a type section for the basin margin facies of the Sarir Sandstone (Fig. 8). In the Sarir Trough the sandstones are mostly stacked braided stream facies, with a characteristic blocky log signature. In the Sarir C-Main field the principal producing facies consists of these stacked fluvial channels (Sanford 1970; Fezzani 1993). The stacked fluvial sandstones exhibit good porosities with gross reservoir to interval ratios of 70–80%. The reservoir performance often relies on the facies of the uppermost Sarir Member, subcropping below the Upper Cretaceous uncomformity, and hence can be variable in strongly faulted traps. In the area of the Sarir C-Main field palaeo-current analysis demonstrates a dominant northwards transport direction. The Messlah High is thought to have acted as an additional sediment source. The granite composition of this high is one of the controlling factors for the reservoir quality of the Sarir Sandstone in the Sarir and Hameimat Troughs.

The occurrence of a mudstone-dominated interval has led to various subdivisions of the Sarir Sandstone. El-Hawat (1992) proposed a tripartite subdivision, recognizing an Upper Sarir Sandstone, a middle mudstone-dominated section named the Varicoloured Shale, and the Lower Sarir Sandstone. The subdivision is shown on a type section representing the basinal Sarir Sandstone facies (Fig. 9). The Varicoloured Shale may be the lateral equivalent of the Red Shale, as seen in the Messlah field (Fig. 9). A similar subdivision, using 'Nubian' instead of Sarir, is used by workers focusing on the Hameimat Trough (Rossi *et al.* 1991; Missallati 1992). The upper sandstone ('Upper Nubian Sandstone') is productive in the Abu Attifel field. In this area the Lower Sarir is a separate and prospective reservoir, relying on top seal by the Varicoloured Shale.

A sequence stratigraphic interpretation of the Late Jurassic-Early Cretaceous reservoir sequence has been published by Rossi *et al.* (1991). Recent advances in the study of the Sarir Sandstone result from modern logging techniques such as formation microscanner logs (El-Hawat 1992; Haase 1993). Further correlation on a basin scale within a chronostratigraphic framework and supported by regional seismic lines is required to better understand the distribution and facies of the Sarir Sandstone.

Source rocks

High-resolution biostratigraphy permits the recognition of four source rock type horizons in the Sirt Basin (Bu-Argaub & Thusu 1996).

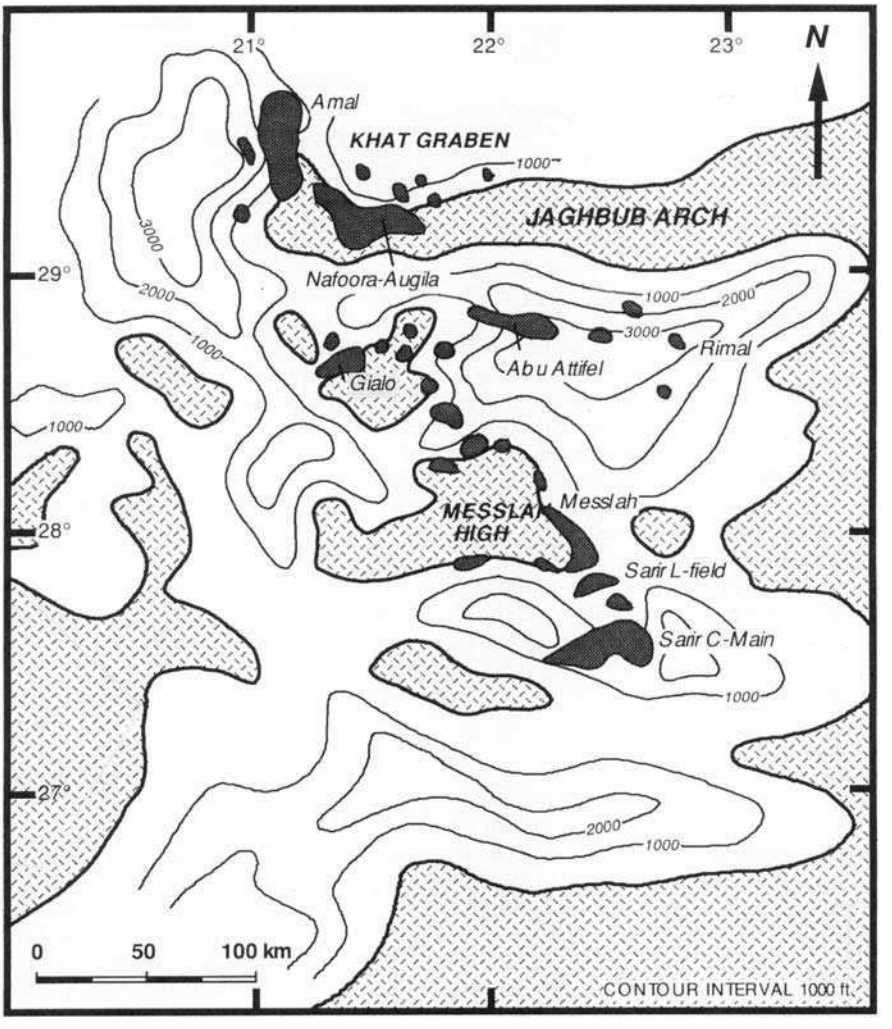

Fig. 6. Sketch isopach map of Sarir Sandstone (including Amal Sandstone), eastern Sirt Basin. Names of major fields and tectonic elements are shown in Fig. 2. Modified after Ibrahim (1987).

Source rock intervals are present in Late Cretaceous (Campanian and Cenomanian–Turonian), Early Cretaceous (Neocomian–Barremian) and Middle Triassic (Scythian–Ladinian) strata. The abundance of mature source intervals, all generating a low-sulphur, waxy type of petroleum, makes the eastern Sirt Basin a prolific oil province. The reservoirs, as far as can be assessed, appear to be full to spilling point, indicating that the presence of a mature source is not a critical element in the eastern Sirt Basin hydrocarbon system.

The Late Cretaceous (Campanian) Rakb Shale, containing kerogen types 1 and 2, is the principal and widespread source rock. The mixture of marine algal and terrestrial organic matter was deposited under restricted conditions in an intrashelf basin. A possible kitchen where the Rakb Shale is mature is in the Hameimat Trough. From here the Sarir C-Main field and Messlah fields are thought to have been partially charged.

The distribution of the Cenomanian–Turonian organic-rich shales is poorly understood, and it is often confused with the Neocomian–Barremian source. Both source intervals have generated high-wax oils. Cenomanian–Turonian shales predominantly contain amorphous marine algae (El-Alami 1993), with significant contribution of type 2 kerogen, deposited in isolated

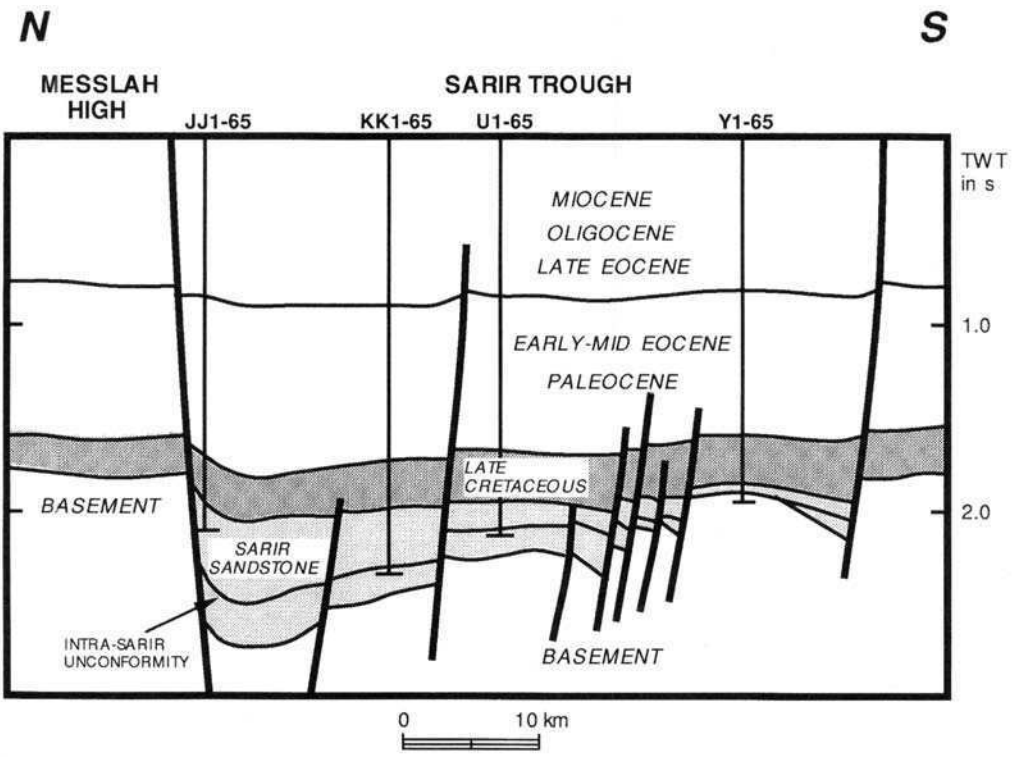

Fig. 7. Cross-section of Sarir Trough, eastern Sirt Basin, based on interpreted seismic section NC171–91–55. (For line location, see Fig. 2.) The age and lithology of the section below the Intra-Sarir unconformity are not known.

basins under anoxic or oxygen-deficient or -depleted conditions. The widespread deposition of source rocks during Cenomanian times in the Tethys region has been attributed to upwelling conditions (Macgregor & Moody this volume). The waxy crude oil of Abu Attifel field is considered to be sourced by the Cenomanian–Turonian source (El-Alami 1993).

The Neocomian–Barremian Varicoloured shale, also named 'Variegated Shale' or 'Middle Nubian Shale', occurs interbedded with the Sarir Sandstone (Fig. 9). These shales were deposited in lagoonal to lacustrine conditions in the deeper parts of the Early Cretaceous basin. The organic matter is predominantly kerogen type 2, with a minor contribution of marine kerogen (type 1). The source rock facies is expected to be restricted to the deep troughs, such as the Hameimat Trough and the deep basin south of the Messlah High. It is expected to be mature for oil generation at the present day wherever it occurs. Only a few exploration wells were drilled in these basinal areas, as a result of which this source interval remains relatively unknown. The communication of these intraformational source rocks with the major oilfields is considered highly effective, requiring updip secondary migration with the Sarir Sandstone acting as a carrier bed.

The Sarir C-Main field is believed to be charged by both a Late Cretaceous and an Early Cretaceous source interval. The oil from the Late Cretaceous source has a reduced wax content, and the increased admixture from this source rock explains the lower wax content in the Messlah field compared with the Sarir C-Main field (respectively 8–10% and 18%). The tar mat, present in Sarir C-Main and Sarir C-North, has been attributed to a miscibility reaction between the two different oils (Sanford 1970). A remaining question pertains to the migration path of the overlying Late Cretaceous source rocks into the Sarir Sandstone, as a downward secondary migration path is generally considered relatively ineffective.

The oldest source rocks identified recently, are Middle Triassic (Scythian–Ladinian) lacustrine shales, interbedded within the Amal Sandstone. These sediments occur as the oldest syn-rift infill, and contain kerogen types 2 and 3. The oil in the Nafoora-Augila field is likely to be at least partly sourced from this shale. Small-scale

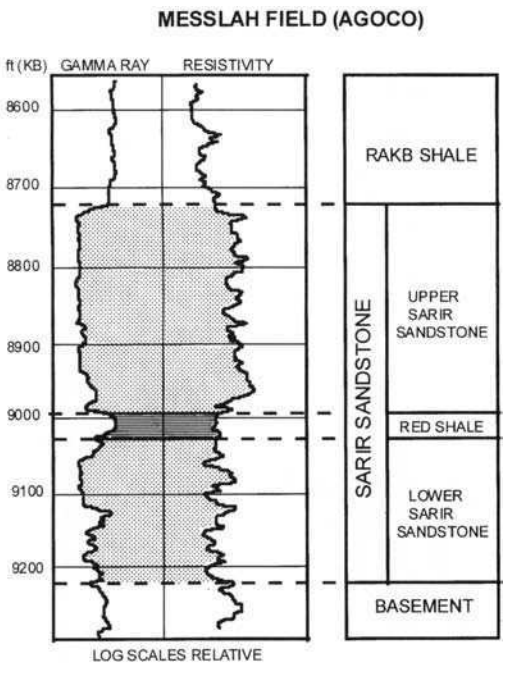

Fig. 8. Sarir Sandstone type section, Messlah field, after Koscec & Gherryo (1993).

half-grabens underlying the Sarir Sandstone, which are locally observed on seismic data, may supply additional source potential in the eastern Sirt Basin.

Trap architecture

The eastern Sirt Basin occupies a separate position in the Sirt Basin at large, in the sense that major structural elements are trending both E–W and NNW–SSE. The unique E–W trending features are interpreted to originate from the E–W Sarir branch of the Late Jurassic–Early Cretaceous triple point extension of the earliest Sirt Basin system (Fig. 3), and are partly reactivated basement faults.

When analysed in detail, using densely spaced 2D or 3D seismic data, complex fault patterns become evident (Skuce 1993; Gras 1996). An interaction of the dominant fault directions has been observed. The most frequently occurring large-scale fault trend is NNW–SSE, parallel to the Sirt arm of the Sirt Basin. However, on a field scale the roughly E–W fault trend appears equally important. With the advent of 3D seismic data, E–W and N–S trending faults ('anti-Sirtic' trends) are increasingly detected. These often play an important role in the generation of prospective structures.

The trap architectures in the eastern Sirt Basin offer a wide range of structural styles commonly related to the extensional and transtensional faulting. The individual fields often line up in distinct linear arrangements, such as the NNW–SSE trend comprising the Sarir C-Main, Sarir C-North, Sarir L-field, Messlah, Magid and Gialo (Fig. 2), stressing the underlying structural control.

Two main classes of traps have been identified (Table 2): traps occurring in basinal settings, and traps occurring in basin margin settings. The fundamental difference between these classes is the thickness and facies of the subcropping Sarir Sandstone reservoir, and a series of trap types for both classes can be recognized. The trap types discriminated are to be regarded as end-members, and some of the fields used as examples may straddle the given trap type definitions.

Table 2. *Overview of trap types in the eastern Sirt Basin*

Trap type	Field
Basinal	
Intrabasinal highs, dip closure	Sarir C-Main
Intrabasinal highs, fault closure	Abu Attifel
Fault blocks	UU1-82, XX1-82, Sarir L-field
Marginal	
Basement highs	Amal, Gialo, Augila Nafoora
Combined structural–stratigraphic traps	Messlah
Tilted fault blocks, relay ramps	Jakhira, Amal-U, Southern Messlah High

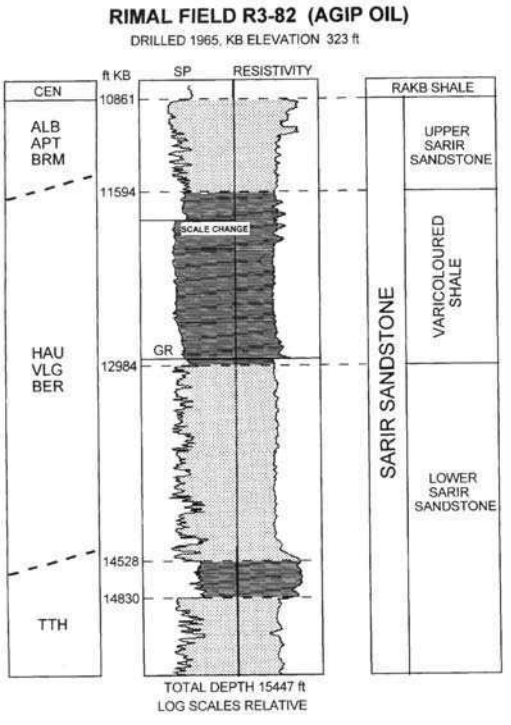

Fig. 9. Sarir Sandstone type section, Rimal field, Hameimat Trough. Tentative ages are derived from sequence stratigraphy by Rossi *et al.* (1991), subdivision of the Sarir Sandstone by Ibrahim (1987).

Trap types occurring in basinal settings

Intrabasinal highs, with predominant dip closure. The main and single example of this kind of trap is the giant Sarir C-Main field in Concession 65. Sarir C-Main was discovered in 1961 and is reported to contain 11–13 BBBL OOIP (Sanford 1970). Although an element of fault closure is present on the flanks of the field, the structure as a whole shows four-way dip closure. The field was discovered using gravity, magnetic and low-fold seismic data (Sanford 1970). Recently, a complex arrangement of boundary and internal faulting has been detected on seismic data. The Sarir Sandstone in the Sarir C-Main field has been discussed in detail by El-Hawat (1992) and Fezzani (1993). It is considered unlikely that intrabasinal highs of the type of Sarir C-Main remain yet to be discovered in the eastern Sirt basin.

Intrabasinal highs, with major fault-bounded closure. The principal example of this trap type is the Abu Attifel in Concession 100. The extension of Abu Attifel in Concession 97 is named Tuama (Kuehn 1993). Abu Attifel was discovered in 1968 with the use of 2D seismic data, and is reported to contain 3.5–4 BBBL OOIP (Thomas 1995; Gumati *et al.* 1996). The field exhibits a general dip towards the north, and is bounded near the southern crest by a major fault zone (Ibrahim 1987). The recent development of the field focuses on the recognition of 3D geometry of the bounding fault zone. Intrabasinal highs of the type of Abu Attifel are unlikely to remain yet to be discovered.

Tilted fault blocks and horst blocks in basinal areas. The tilted fault blocks and horst blocks in basinal areas are smaller structures in terms of oil-in-place, and they are often genetically related to basin-wide fault zones. Examples are the Sarir L-field, Rimal, and the UU1-82 and XX1-82 structures, discovered in the Hameimat Trough east of Abu Attifel. Well UU1-82, spudded in 1990, revealed an 800 ft-oil column in the Upper Sarir Sandstone (Fig. 10; Missallati 1992). The top of the Sarir Sandstone in this well is at a depth of around 15 000 ft.

Missallati (1992) outlined the operational and exploration challenges of exploring in this deep area. The Late Cretaceous overpressured salt section overlying the Sarir Sandstone reservoir causes drilling problems. In addition, porosity and permeability of the Sarir Sandstone in these deep reservoirs is a critical element. Also, the frequent occurrence of volcanic rocks interspersed with the Sarir Sandstone provides an exploration risk for this trap type. Recent exploration and development of this trap type, using 3D seismic data, has focused on the lateral and vertical geometry of the bounding faults. It is expected that relatively small tilted fault blocks and horst blocks developed adjacent to major fault zones remain yet to be found in the eastern Sirt Basin.

Trap types occurring in marginal areas

Traps occurring on basement highs. Basement highs were the first structures to be explored in the eastern Sirt Basin, using gravity and magnetic techniques. Amal, Nafoora–Augila and Gialo are the principal examples of basement highs acting as prolific accumulations.

The Amal field was discovered in 1959, and is estimated to have contained 17 BBBL OOIP (Thomas 1995; Gumati *et al.* 1996). No Sarir Sandstone occurs on the crest of the Amal field basement high; however, fractured quartzites

from a viable reservoir. Traditionally these quartzites were considered to be Cambrian–Ordovician in age; however, recently a Triassic age has been determined and the name Amal Sandstone has been proposed (Thusu 1993). On the flanks of the Amal field production is from pinchout reservoirs of Late Cretaceous age (Roberts 1970).

The Nafoora–Augila field was discovered in 1965, and is estimated to contain 9 BBBL OOIP (Thomas 1995; Gumati *et al.* 1996). Nafoora–Augila consists of a Late Cretaceous diachronous basal clastic unit composed of basement-derived material, grading laterally and upwards into a carbonate shelf facies reservoir, forming a single sedimentary reservoir (Williams 1972). Additional production is from fractured and weathered basement (Fig. 11).

In the Gialo field production is from relatively shallow Tertiary reservoirs. Gialo was discovered in 1961 and is estimated to have contained 14 BBBL OOIP.

The basement highs were the first exploration targets, and were detected with the earliest geophysical methods. They have been positive features throughout geological time, and no Sarir Sandstone was deposited. It is unlikely that additional basement features remain undetected.

Combined structural–stratigraphic traps near structural highs. The Messlah field, in Concessions 65 and 80, is the principal example (Fig. 12; AGOCO 1980; Clifford *et al.* 1980; Kocsec & Gherryo 1993; Gras 1997). The Messlah field was discovered in 1971, and is estimated to contain 3 BBBL OOIP (Thomas 1995; Gumati *et al.* 1996). The Messlah field consists of a shallow dipping wedge of Sarir Sandstone, pinching out against a basement high, the Messlah High. The trapping mechanism of Messlah field relies on a top seal by the Rakb Shale, bottom seal by the basement and lateral dip and fault closures (Fig. 13).

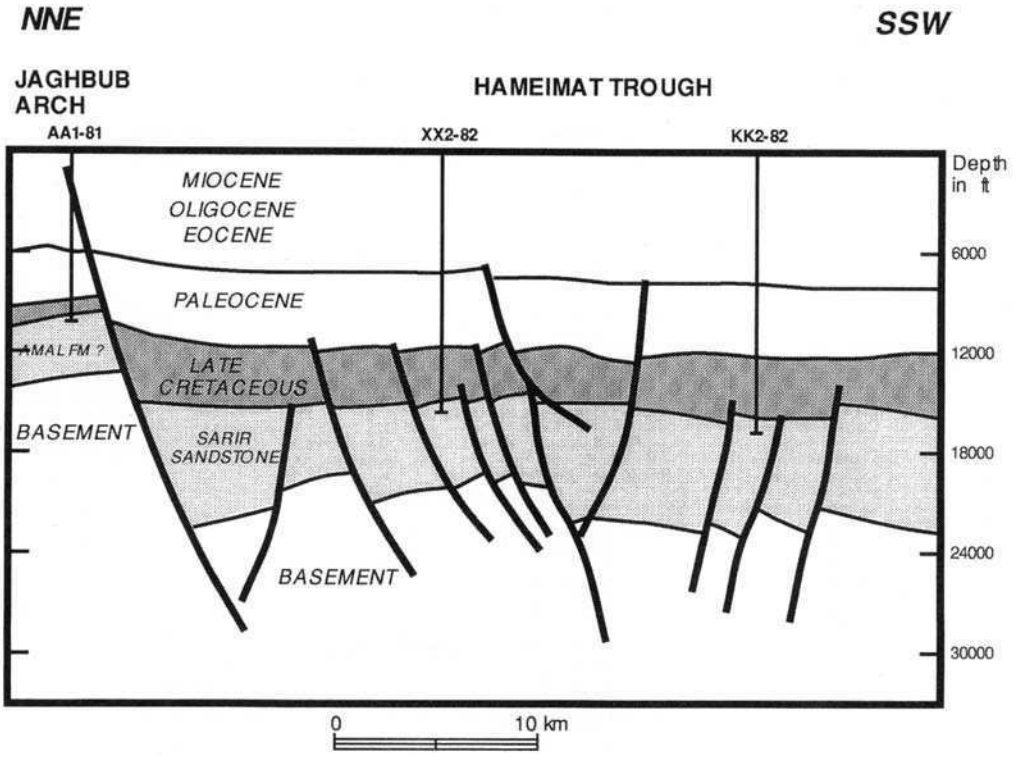

Fig. 10. Cross-section of northern margin of Hameimat Trough, modified after Missallati (1992), showing basinal tilted fault blocks. Sandstone is indicated to be present on the Jaghbub Arch, which comprises the graben shoulder. This Sandstone is likely to be part of the pre- or early rift sequence, and hence it has been tentatively interpreted as the Triassic Amal Sandstone. Location of section shown in Fig. 2.

The critical element in exploration of this trap type is the recognition of the pinch out of the Sarir Sandstone reservoir. This zero-sand line is difficult to resolve on seismic data, as a result of the low angle of the sandstone wedge, as well as the low acoustic impedance contrast between basement and the Sarir Sandstone. Statistical analysis of the Sarir Sandstone in the Messlah field shows a linear geometry of the reservoir wedge, which can be applied in a predictive sense for the exploration of similar traps (Fig. 13).

The play concept of the Messlah field can be applied along the edges of the Sarir Sandstone basin, including the relatively unfaulted margins of the basement highs. Critical elements are the seismic recognition of the truncation and onlap of the Sarir Sandstone below the Late Cretaceous unconformity, and the detection of the lateral structural closure. The combined structural–stratigraphic traps may offer the potential for relatively large traps.

Fault blocks near the margins of structural highs. These traps are medium sized in terms of original oil-in-place, and are related to deep synthetic and antisynthetic faults relative to the main graben-bounding faults. The Amal-U field and Jakhira are examples of this trap type, occurring near the Amal High and Nafoora-Augila High, respectively (Fig. 2; Ibrahim 1987). Many fields occur near the complex faulted margins of the Messlah High. The geometry of the bounding and internal faults in relation to the Sarir Sandstone reservoir development is a critical factor in the recent exploration and development of this trap type. Delineation of the trap geometry, and positioning of exploration and appraisal wells, is now routinely performed using 3D seismic data.

A particular type of fault related play occuring adjacent to the basement highs are relay ramp features. These plays are developed on the downthrown side of normal faults, whereby a pinchout of the Sarir Sandstone is developed in the strike

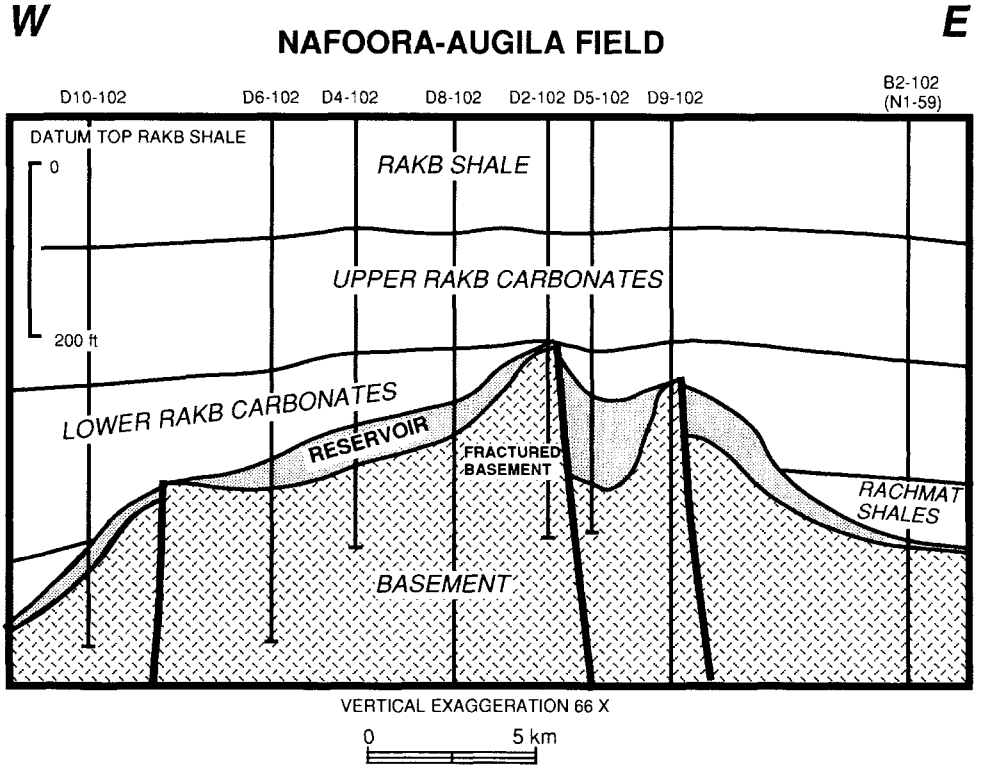

Fig. 11. Stratigraphic cross-section across Augila field (Nafoora-Augila unit) basement high. Production is from transgressive Late Cretaceous reservoirs, consisting of both clastic and carbonate units, as well as fractured and weathered basement. The section has been modified and tentatively interpreted on the basis of Williams (1972); the original Late Cretaceous stratigraphic names used in this paper have been retained. Location of section indicated in Fig. 2.

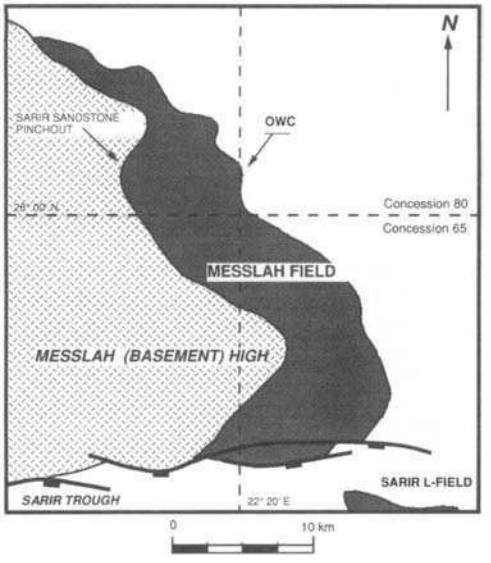

Fig. 12. Schematic overview map of the Messlah field, prototype of a combined structural-stratigraphic trap. Modified after Gras (1997). OWC, Oil–water contact.

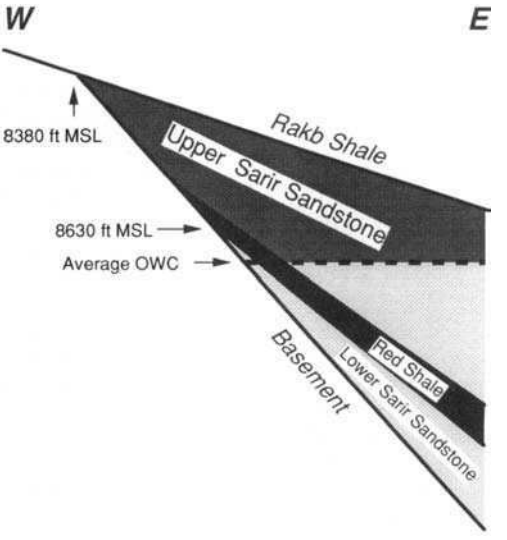

Fig. 13. Sketch of Southern Messlah field geometry, based on statistical analysis of reservoir thickness distribution, modified after Gras (1997).

direction. These occur on the E–W trending southern flank of the Messlah High (Fig. 2; Gras 1996). The pinchouts are interpreted to be caused by deposition of the Sarir Sandstone on a relay ramp, thus providing a stratigraphic component to this trap type (Fig. 14). The fault configuration, consisting of a transfer zone between two overlapping normal faults, was recognized in line with work by Harding (1984, 1985) and Morley *et al.* (1990). The fault pattern is interpreted as Riedel shears, possibly resulting from dextral strike-slip on a deep-seated E–W basement-controlled fault zone (Richard *et al.* 1995). Relay ramp features are an example of complex fault interpretations which may arise from 3D seismic interpretation.

Tilted fault blocks, horst blocks and low-side fault plays such as relay ramps, hosting entrapments with oil-in-place in the range of 100–300 MMBBBL, remain attractive exploration opportunities. With the introduction of 3D seismic acquisition, increasingly complex fault patterns are being recognized in the eastern Sirt Basin. It is anticipated that the detection of these features, especially near the edges of the Sarir Sandstone basin and basement highs, will lead to future discoveries.

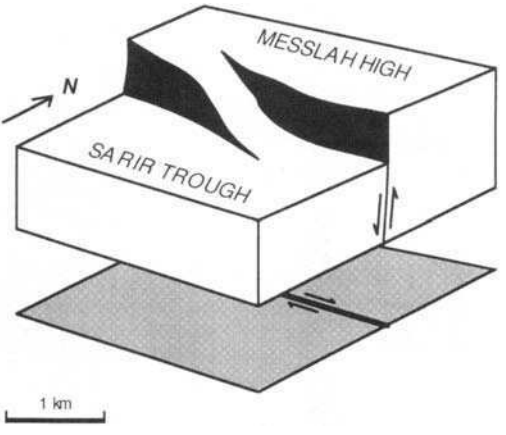

Fig. 14. Relay ramp fault model, southern flank of Messlah High, from Gras (1996). The block diagram shows the pre-rift structure, which has been infilled with the Sarir Sandstone. The thinned Sarir Sandstone developed in the relay ramp (or 'strike ramp') forms a combined structural-stratigraphic trap, as a result of post-rift sagging of the syn-rift basin. Deep-seated wrenching is interpreted to cause the en echelon Riedel shear geometry.

Discussion

The largest trap types, the intrabasinal highs and the basement highs, were discovered early on in the exploration history of the eastern Sirt Basin. These traps host the giant fields, which are generally in an advanced stage of production. Thomas (1995) discussed the potential for secondary and tertiary recovery schemes for these mature fields. Additional discoveries of these types are considered unlikely even with the present-day technology.

The structural component appears to be a requisite for the proven traps of the Sarir Sandstone in the eastern Sirt Basin. However, little exploration effort has been focused on stratigraphic traps. The structural traps rely on the accurate recognition of the geometry of the bounding faults. The lateral resolution of 3D seismic data provided a breakthrough in this respect. The more precise determination of the geometry of the bounding faults has resulted in additional petroleum development. Recent 3D seismic surveys show fault blocks to be frequently arranged en echelon, leading to a better understanding of the trap architecture, and additional prospectivity. Figure 10, based on a section published by Missallati (1992), shows the southern margin of the Jaghbub Arch. It is suggested that the bounding as well as the internal faults may be arranged en echelon. A further step would be the acceptance of pre-stack depth migration as a risk reducing technique for structural traps, such as tilted fault blocks and fault closures. Pre-stack depth migration results in better depth imaging of the fault closures, as the seismic data often suffer from 'fault shadows' near major bounding faults (Fagin 1995).

Combined structural–stratigraphic traps such as the prototype Messlah field and recent relay ramp discoveries are considered to provide future potential (Ibrahim 1987; Aburawi 1995). Potential for stratigraphic trapping exists both below the Late Cretaceous unconformity and within the Sarir sequence, relying on intraformational sealing by the Varicoloured Shale (Fig. 9). Exploring the traps with a stratigraphic component requires state-of-the-art seismic acquisition and processing, particularly focusing on the vertical resolution. Models for trap development in extensional basins, such as those of Leeder & Gawthorpe (1987) and Gabrielsen *et al.* (1995), provide useful analogues to explore for the yet to be found subtle traps in the eastern Sirt Basin. Figure 15, based on a published well correlation diagram by Rossi *et al.* (1991), shows the

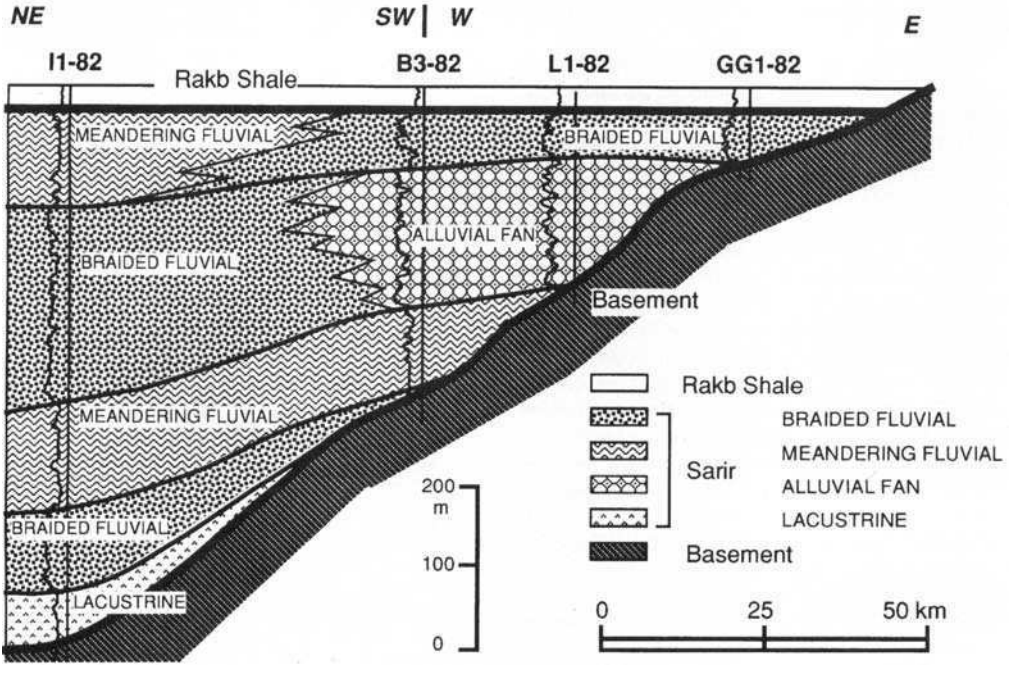

Fig. 15. Log correlation diagram and facies interpretation of Sarir Sandstone, eastern Hameimat Trough, modified after Rossi (1991). Location of well-correlation shown in Fig. 2.

thinning of the Sarir Sandstone towards the eastern basin edge. Wells such as GG1–82 and the nearby A1–NC83C (Fig. 2) penetrated a relatively thin Sarir Sandstone section, similar in facies and thickness to the Sarir Sandstone reservoir of the Messlah field. This underlines the potential for combined structural–stratigraphic traps in the area of the relatively less explored depositional and erosional margins of the Sarir Sandstone basin.

Conclusions

The earliest rifting and collapse of the Sirt arch took place during the Triassic, when the Amal Sandstone was deposited in relatively confined E–W trending basins in the eastern Sirt Basin. The extension culminated during the Late Jurassic–Early Cretaceous main rift phase. The Sarir Sandstone was deposited as an intra-continental clastic syn-rift sequence in the eastern Sirt Basin.

The rifting resulted in a series of approximately E–W trending grabens and half-grabens, in which the Sarir Sandstone accumulated. The Sarir Sandstone hosts the majority of the oilfields in the prolific eastern Sirt Basin. The fields are generally structural traps, although a combined structural–stratigraphic trapping mechanism has been proven to be effective as well. Pure stratigraphic traps remain yet to be identified and explored.

The introduction of 3D seismic acquisition in the eastern Sirt Basin has lead to an increased understanding of the complex trap architectures, resulting in new discoveries and re-evaluation of older fields. Examples of recently detected trap types are structural–stratigraphic traps developed on relay ramps, and tilted fault blocks related to en echelon, Riedel shear zones.

The exploration well density in the eastern Sirt Basin is relatively low, and regarding 3D seismic acquisition for exploration purposes, the area is still in an early stage. Combined structural–stratigraphic traps of the Messlah field prototype provide large future potential in the eastern Sirt Basin. Tilted fault blocks, horst blocks and low-side fault plays such as relay ramps, hosting entrapments with medium-sized oil-in-place, provide further attractive exploration opportunities. The high-graded areas for those prospective trap types in the eastern Sirt Basin are the depositional and erosional edges and faulted boundaries of the Sarir Sandstone basin. Detailed structural interpretation, using modern geophysical technology, is essential in exploring for these prospective traps of the Sarir Sandstone.

The authors wish to extend their thanks to the management of the Arabian Gulf Oil Company (Benghazi), without whom this review would not have been possible. The manager of the Exploration Department, A. Asbali, is thanked for his encouragement and support. Permission to publish this paper by the Arabian Gulf Oil Company (Benghazi) and Schlumberger GeoQuest (Tripoli) is gratefully acknowledged. G. Ambrose, B. Koscec (AGOCO), H. Stelzer, D. Klauser-Baumgärtner (Schlumberger GeoQuest), R. Verdi and P. Tognini (Agip Oil Libya) are thanked for the discussions on the geology of the eastern Sirt Basin. G. M. Peasley (Gulf Canada, Calgary), R. H. C. Robbemond (Darke Taylor Netherlands, The Hague), M. R. Allen (University of Wales, Aberystwyth), R. Guiraud (Université de Montpellier) and the editors of the Geological Society (London) are thanked for critically viewing the manuscript. Although acknowledging the present paper would not have been possible without the fruitful discussions with these and various other workers too numerous to mention, the authors are entirely responsible for any error, omission or inconsistency. The opinions and interpretations expressed in this paper are personal, drawing on the authors' experience in the oil exploration industry in Libya.

References

Note to references: the proceedings of the conference 'Sedimentary Basins of Libya, First Symposium, Geology of the Sirt Basin, Tripoli, 1993' have been published in *The Geology of Sirt Basin* (1996).

ABURAWI, R. 1995. Exploration trends in the Sirte Basin (abstract). *Bulletin, American Association of Petroleum Geologists*, **79**, 1191.

ARABIAN GULF OIL COMPANY (AGOCO), EXPLORATION STAFF. 1980. Geology of a stratigraphic giant–the Messlah oil field. *In*: SALEM, M. Y. (eds) *Geology of Libya Vol. 2*, 521–536.

BARR, F. T. & WEEGAR, A. A. 1972. *Stratigraphic Nomenclature of the Sirte Basin, Libya*. Petroleum Exploration Society of Libya, Tripoli, 1–179.

BU-ARGAUB, F. & THUSU, B. 1996. Stratigraphy and palynofacies character of organic rich sediments in Pre-Campanian Sandstone in southeast Sirt Basin (abstract). *In*: *The Second Middle East Geosciences Conference, Bahrain*.

CLIFFORD, H. J., GRUND, R. & MUSRATI, H. 1980. Geology of a stratigraphic giant–the Messlah oil field. *In*: HALBOUTY, M. T. (ed.) *Giant Oil and Gas Fields of the Decade 1968–1978*. American Association of Petroleum Geologists Memoirs, **30**, 507–524.

EL-ALAMI, M. 1993. Habitat of oil in Abu Attifel area, Sirt Basin, Libya (abstract). *In*: *Sedimentary Basins of Libya, First Symposium, Geology of the Sirt Basin, Tripoli*.

EL-ARNAUTI, A. & SHELMANI, M. 1998. A contribution to the northeast Libyan subsurface stratigraphy

with emphasis on Pre-Mesozoic. *In*: EL-ARNAUTI, A. OWENS, B. & THUSU, B. (eds) *Subsurface Palynostratigraphy of Northeast Libya*. Garyounis University Publication, Benghazi, 1–15.

EL-GHOUL, E. & HALLETT, D. 1993. Oil and gas potential of the deep trough areas in the Sirt basin, Libya (abstract). *In*: *Sedimentary Basins of Libya, First Symposium, Geology of the Sirt Basin, Tripoli*.

EL-HAWAT, A. S. 1992. The Nubian Sandstone sequence in Sirte Basin, Libya: sedimentary facies and events. *Geology of the Arab World*. Cairo University, 317–327.

—— & MISSALLATI, A. A. 1993. The Nubian Sandstone in the Sirt basin and its Correlatives (abstract). *In*: *Sedimentary basins of Libya, First Symposium, Geology of the Sirt Basin, Tripoli*.

FAGIN, S. 1995. Depth imaging's role in structural exploration (part 1). *World Oil*, **216**, 93–96.

FEZZANI, A. 1993. The Sarir group clastics in the Southeast Sirt Basin, Libya (abstract). *In*: *Sedimentary Basins of Libya, First Symposium, Geology of the Sirt Basin, Tripoli*.

GABRIELSEN, R. H., STEEL, R. J. & NOTTVEDT, A. 1995. Subtle traps in extensional terranes: a model with reference to the North Sea. *Petroleum Geoscience*, **1**, 223–235.

GRAS, R. 1996. Structural style of the southern margin of the Messlah High. *In*: SALEM, M. Y. *et al.* (eds) *The Geology of Sirt Basin*, **3**, 201–210.

—— 1997. Statistic analysis of syn-rift sediments; an example from the Sarir Sandstone, Messlah Field, Sirt Basin. Paper presented at First Magrebian Conference on Petroleum Exploration, Ras Lanuf, November 1996 (in press).

GUIRAUD, R. 1998. Mesozoic rifting and basic inversion along the northern African Tethyan margin: an overview. *This volume*.

——& MAURIN, J.-C. 1992. Early Cretaceous rifts of Western and Central Africa: an overview. *Tectonophysics*, **213**, 153–168.

——, BINKS, R. M., FAIRHEAD, J. D. & WILSON, M. 1992. Chronology and geodynamic setting of Cretaceous–Cenozoic rifting in West and Central Africa. *Tectonophysics*, **213**, 227–234.

GUMATI, Y. D. & NAIRN, A. E. M. 1991. Tectonic subsidence of the Sirte Basin. *Journal of Petroleum Geology*, **14**, 93–102.

——, KANES, W. H. & SCHAMEL, S. 1996. An evaluation of the hydrocarbon potential of the sedimentary basins of Libya. *Journal of Petroleum Geology*, **19**, 95–112.

HAASE, G. H. 1993. Formation Microscanner interpretation and caliper measurements in Nubian Sandstones, SE Sirt Basin (abstract). *In*: *Sedimentary Basins of Libya, First Symposium, Geology of the Sirt Basin, Tripoli*.

HARDING, T. P. 1984. Graben hydrocarbon occurrences and structural style. *Bulletin, American Association of Petroleum Geologists*, **68**, 333–362.

—— 1985. Seismic characteristics and identification of negative flower structures, positive flower structures, and positive structural inversion. *Bulletin, American Association of Petroleum Geologists*, **69**, 582–600.

HEA, J. P 1971. Petrography of the Mesozoic Sandstones of the southern Sirte Basin, Libya. *In*: *Geology of Libya, Vol. 4*. 2758–2779.

IBRAHIM, M. W. 1987. Petroleum geology of the Sirt Group Sandstones, eastern Sirt Basin. *In*: *Geology of Libya, Vol. 7*. 2757–2779.

KLITSCH, E. H & SQUYRES, C. H. 1990. Palezoic and Mesozoic geological history of northeastern Nubia based upon new interpretation of Nubian strata. *Bulletin, American Association of Petroleum Geologists*, **74**, 1203–1211.

KOSCEC, B. & GHERRYO, Y. S. 1993. Geology and reservoir performance of the Messlah Oil Field, Libya (abstract). *In*: *Sedimentary Basins of Libya, First Symposium, Geology of the Sirt Basin, Tripoli*.

KUEHN, M. R. 1993. Paleosols as an additional tool defining reservoir characteristics of Pre-Upper Cretaceous section, As Sarah and Tuama oil fields (abstract). *In*: *Sedimentary Basins of Libya, First Symposium, Geology of the Sirt Basin, Tripoli*.

LEEDER, M. R. & GAWTHORPE, R. L. 1987. Sedimentary models for extensional tilt-block/half-graben models. *In*: COWARD, M. P., DEWEY, J. F. & HANCOCK, P. L. (eds) *Continental Extensional Tectonics*. Geological Society, London, Special Publications, **28**, 139–152.

MASSA, D. & DELORT, T. 1984, Évolution du bassin de Sytre (Libye) du Cambrien au Crétacé basal. *Bulletin de la Société Géologique de France*, **6**, 1087–1096.

MACGREGOR, D. S. & MOODY, R. T. J. 1998. Mesozoic and Cenozoic petroleum systems of North Africa. *This volume*.

MISSALLATI, A. A. 1992. Deep exploration drilling in the Central Graben area Concession 82, Southeast Sirt Basin, Libya. *In*: *Geology of the Arab World*. Cairo University, 57–67.

MORLEY, C. K., NELSON, R. A., PATTON, T. L. & MUNN, S. G. 1990. Transfer zones in the east African rift system and their relevance to hydrocarbon exploration in rifts. *Bulletin, American Associations of Petroleum Geologists*, **74**, 1234–1253.

POMEYROL, R. 1968. 'Nubian Sandstone'. *Bulletin, American Association of Petroleum Geologists*, **52**, 589–600.

RICHARD, P. D., NAYLOR, M. A. & KOOPMAN, A. 1995. Experimental models of strike-slip tectonics. *Petroleum Geoscience*, **1**, 71–80.

ROBERTS, J. M. 1970. Amal Field, Libya. *In*: HALBOUTY, M. T. (ed.) *Geology of Giant Petroleum Fields*. American Association of Petroleum Geologists, Memoirs, **14**, 438–448.

ROSSI, M. E., TONNA, M. & LARBASH, M. 1991. Latest Jurassic–Early Cretaceous deposits in the subsurface of the eastern Sirt Basin (Libya): facies and relationships with tectonics and sea-level changes. *In*: SALEM, M. J., SBETA, A. M. & BAKBAK, M. R. (eds) *Geology of Libya, Vol. 6*. Elsevier. Amsterdam. 2211–2225.

SAENZ DE SANTA MARIA, F. 1993. Tectonic and sedimentary evolution of the Sirt Basin, an overview (abstract). *In*: *Sedimentary basins of Libya, First Symposium, Geology of the Sirt Basin, Tripoli*.

SANFORD, R. M. 1970. Sarir oil field, Libya–desert surprise. *In*: HALBOUTY, M. T. (ed.) *Geology of Giant Petroleum Fields*. American Association of Petroleum Geologists, Memoirs, **14**, 449–476.

SKUCE, A. 1993. Transfer zones and compaction structures along the western edge of the central Ajdabiya Trough (abstract). *In*: *Sedimentary Basins of Libya, First Symposium, Geology of the Sirt Basin, Tripoli*.

SWIRE, P. H. 1995. Carboniferous, Permian and Triassic palynostratigraphy of northwestern Libya (abstract). *Bulletin, American Association of Petroleum Geologists*, **79**, 1251.

THOMAS, D. 1995. Exploration limited since '70s in Libya's Sirte basin. *Oil and Gas Journal*, **78**, 99–103.

THUSU, B. 1993. Implication of the discovery of reworked and in-situ Late Palaeozoic and Triassic palynomorphs on the evolution of the Sirt Basin, Libya (abstract). *In*: *Sedimentary Basins of Libya, First Symposium, Geology of the Sirt Basin, Tripoli*.

—— & MANSOURI, A. 1995. Reassignment of the Upper Amal Formation to Triassic and its implications for exploration in southeast Sirte Basin, Libya (abstract). *First Symposium on Hydrocarbon Geology of North Africa, London*. Abstracts.

——, VAN DER EEM, J. G. L. A., EL-MEHDAWI, A. & BU-ARGAUB, F. 1988. Jurassic–Early Cretaceous palynostratigraphy in Northeast Libya. *In*: EL-ARNAUTI, A. OWENS, B. & THUSU, B. (eds) *Subsurface Palynostratigraphy of Northeast Libya*. Garyounis University Publication, Benghazi, 1–15.

VAN ERVE, A. W. 1993. Aspects of Sirt Group stratigraphy (towards the solution of the Nubian problem in Libya) (abstract). *In*: *Sedimentary Basins of Libya, First Symposium, Geology of the Sirt Basin, Tripoli*.

VAN HOUTEN, F. B. 1983. Sirte Basin, North Central Libya: Cretaceous rifting above a fixed mantle hotspot? *Geology*, **11**, 115–118.

WENNEKERS, J. H. N., WALLACE, F. K. & ABUGARES, Y. 1993. Geology of hydrocarbon occurrences of the Sirt Basin a synopsis (abstract). *In*: *Sedimentary Basins of Libya, First Symposium, Geology of the Sirt Basin, Tripoli*.

WILLIAMS, J. J. 1972. Augila Field, Libya: depositional environment and diagenesis of sedimentary reservoir and description of igneous reservoir. American Association of Petroleum Geologists, Memoirs, **16** SEG Special Publication, **10**, 612–632.

ZANATI, M. S. 1994. Vibroseis with short sweeps in the Sirte Basin, Libya. *First Break*, **12**, 91–97.

—— 1996. 3D seismic in the Sirt Basin of Libya. *First Break*, **14**, 169–176.

The influence of platform morphology and sea level on the development of a carbonate sequence: the Harash Formation, Eastern Sirt Basin, Libya

D. SPRING[1,2] & O. P. HANSEN[2,3]

[1]*BHP Petroleum, 120 Collins Street, Melbourne 3000, Vic. Australia*
[2]*Former address: Fina Exploration and Production, 7181 Feluy, Belgium*
[3]*Fina Exploration Norway, PO Box 4055 Tasta, N4004 Stavanger, Norway*

Abstract: The Paleocene section of the Eastern Sirt Basin consists of a carbonate succession which developed in response to subsidence and widespread marine transgression following Cenomanian rifting. Within the study area the principal hydrocarbon reservoir is the Upper Sabil Formation, which is sealed by Harash Formation lime mudstones. Facies analysis and seismic mapping indicate that the Upper Sabil Formation consists of a prograding carbonate shelf with a rimmed platform morphology and palaeo-slopes in excess of 5° along the eastern and western flanks of the Agedabia Trough. To the south, the absence of a lagoonal facies and seismically defined shelf edge indicate a ramp morphology with a palaeo-slope of less than 0.5°. The overlying Harash Formation is characterized by its cyclic nature, relatively high terrigenous mud content and a thickness distribution which shows it to be infilling the pre-existing Upper Sabil shelf topography. The morphology of the Upper Sabil shelf coupled with sea-level fluctuations controlled the distribution of the depositional environments within the Harash Formation. A depositional model for the Harash Formation is proposed which subdivides the formation into five carbonate parasequences (named cycles A–E from base to top). In an exploration context the study facilitated the identification of the distribution of Harash Formation sealing and possible reservoir facies within cycles A and B. Furthermore, the study led to the understanding of the cause of anomalous reflections observed on conventional seismic data within the Paleocene section. Work involved the integration of regional well control with conventional seismic and stratigraphic inversion data. The stratigraphic framework and interpretations derived from this study were ultimately tested and confirmed by an exploration well which was cored through the sections of interest.

This paper outlines the procedures used to develop a stratigraphic framework for the Paleocene section of the Eastern Sirt Basin through the integration of seismic studies, log correlations, detailed (micro) facies analysis and sequence stratigraphic techniques. The study focuses on an area of some 4500 km^2 centred around exploration concession NC171 Block 5 operated by Fina Exploration Libya B.V. (FEL) and located in the Agedabia Trough (Fig. 1). The analysis incorporated data acquired by the FEL-led consortium, traded and open-file data totalling 52 wells and a 2D seismic database of 4700 km as well as seismic stratigraphic inversion data. Access to core data was obtained for 16 wells covering 660 ft of Harash and 600 ft of Upper Sabil Formation (Fig. 2). In addition infill sample material consisting of 200 sidewall cores and 400 ditch cuttings for seven and six wells respectively were analysed.

The onshore Sirt Basin is located in eastern Libya and extends *c.*600 km from north to south and 700 km from east to west (Fig. 1). The current NW–SE configuration of the basin dates from Late Cretaceous time and followed collapse of the Early–Mid Mesozoic Sirt Arch. The basin comprises a distinct series of horsts and grabens formed as a result of subsidence and block faulting which developed in response to reverse dextral shearing along the plate boundary of Africa and Europe (Burke & Dewey 1974). Two main phases of widespread marine transgression are recognized. The first was associated with intense rift-related subsidence throughout the Late Cretaceous and a major rise in sea-level. The second followed thermally driven basinwide subsidence, from Paleocene to Oligocene time (Gumati & Nairn 1991; van der Maer & Cloetingh 1993).

The sedimentary section of the Sirt Basin overlies Precambrian igneous and metamorphic basement rocks. The sediments consist of Lower Palaeozoic clastic rocks unconformably overlain by Lower Cretaceous–Tertiary clastic and carbonate deposits. Because of the asymmetrical architecture of the basin and local differential subsidence during deposition, complex facies relationships exist, with correspondingly compli-

SPRING, D. & HANSEN, O. P. 1998. The influence of platform morphology and sea level on the development of a carbonate sequence: the Harash Formation, Eastern Sirt Basin, Libya. *In*: MACGREGOR, D. S., MOODY, R. T. J. & CLARK-LOWES, D. D. (eds) 1998. *Petroleum Geology of North Africa*. Geological Society, London, Special Publication No. 132, 335–353.

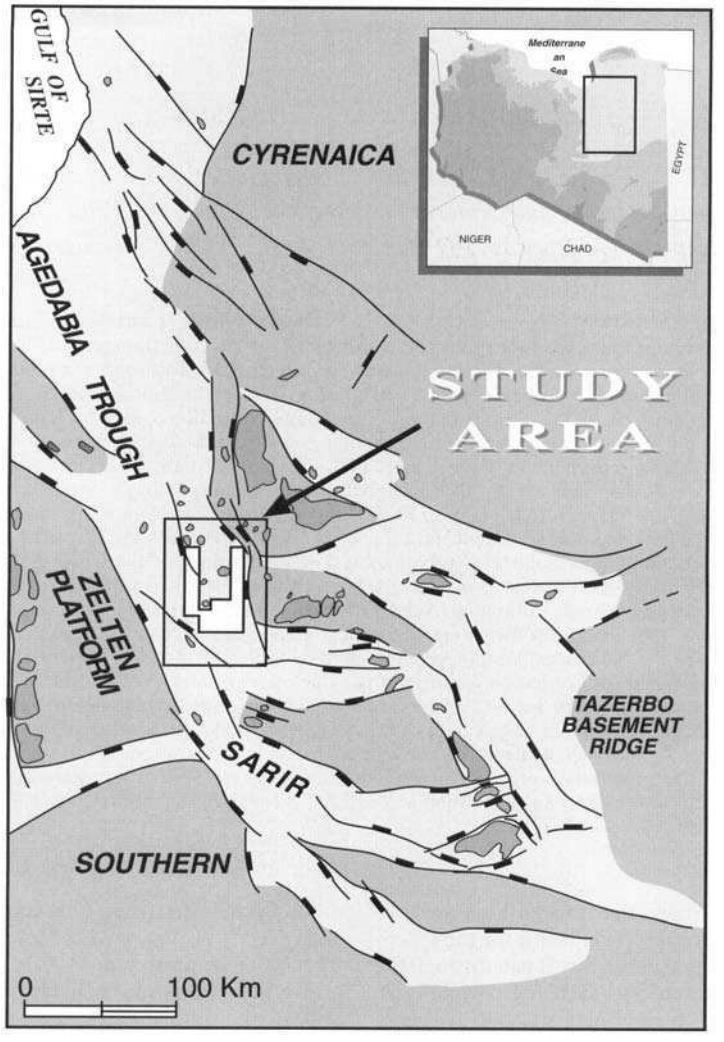

Fig. 1. Tectonic framework of the Eastern Sirt Basin, Libya, showing the position of concession NC171 Block 5 and the study area.

cated Sirt Basin stratigraphic nomenclature. This has been further complicated by the tendency of oil companies to develop their own naming schemes in their area of operations. The stratigraphic nomenclature used here is adopted from the Cretaceous and younger section described by Barr & Weegar (1972) and updated by Banerjee (1980) (Fig. 3).

The Upper Paleocene section discussed here, principally the Upper Sabil and Harash Formations, displays a variety of carbonate facies from shelfal limestones to basinal shales and marls. Although the study was performed over a restricted area, the juxtaposition of rimmed and ramp carbonate shelves, and good geological and geophysical datasets, allow the response of the carbonate system to morphology and sea-level fluctuations to be studied in a sequence stratigraphic framework.

The early graben fill following Late Cretaceous rifting comprised fluviatile sandstones and shales, and alluvial conglomerates and sandstones. Increased tectonic subsidence and a eustatic sea-level rise during the Cenomanian–Turonian caused marine transgression. Marine shales were deposited within the subsiding troughs, and carbonate shelves built on the elevated horsts. Upper Cretaceous Sirt Formation

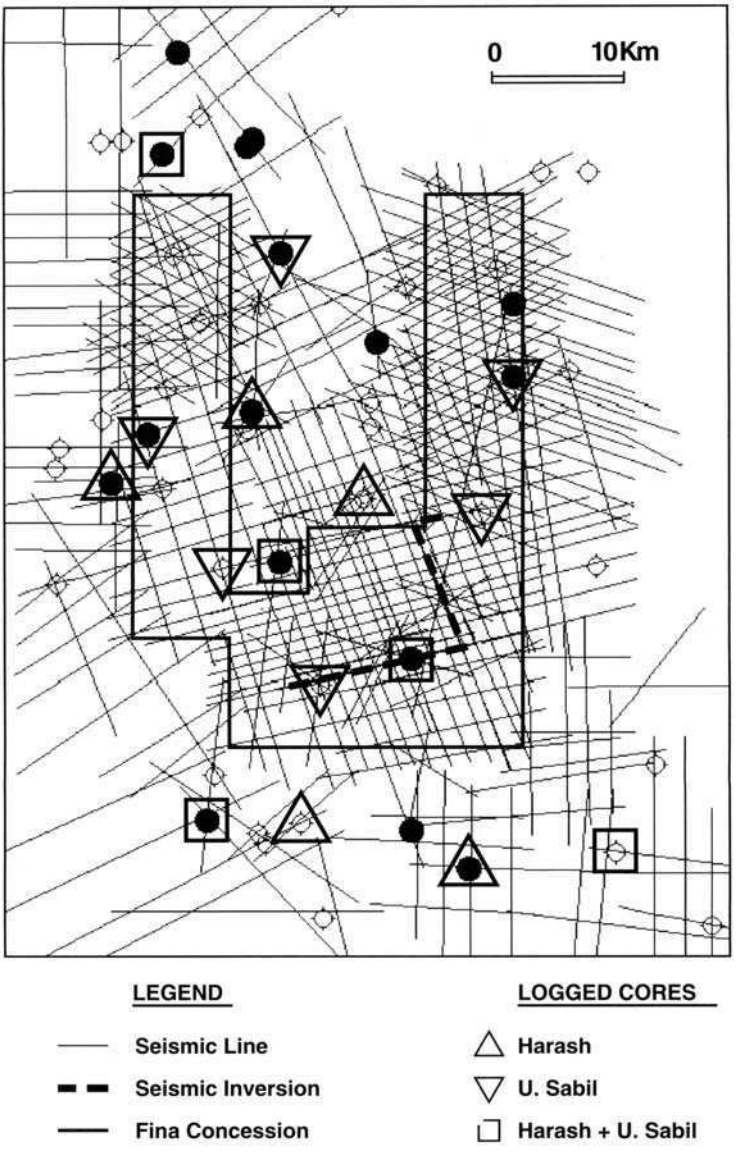

Fig. 2. Extent of NC171 Block 5, study area and geological and geophysical database.

basinal marine shales constitute the principal source rocks within the Sirt Basin and reached peak oil maturity during the Late Eocene to Early Oligocene. Marine conditions and carbonate-dominated deposition within most of the Sirt Basin continued through the Paleocene until the end of the Eocene. Diminishing subsidence and a gradual falling sea-level resulted in marine regression and deposition of continental deposits from the Middle Miocene onwards.

Carbonate sequence stratigraphy

The principles of sequence and seismic stratigraphy were mainly developed through the study of siliciclastic depositional systems and their response to eustatic sea-level changes through mapping stratal geometries on seismic lines (Vail *et al.* 1977*a*, *b*). Continued research has resulted in widespread application of this technology to hydrocarbon exploration in siliciclastic

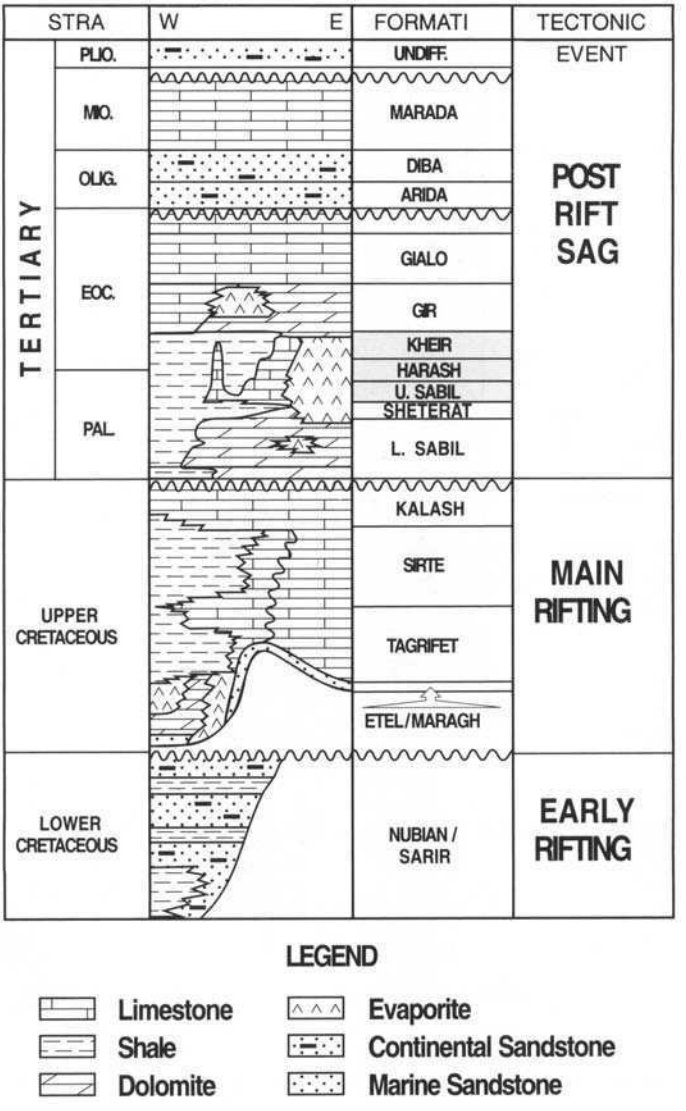

Fig. 3. Lithostratigraphic framework of the Eastern Sirt Basin.

systems. Recently, models of carbonate sequence stratigraphy, which describe the cyclic nature of carbonates in terms of systems tracts and parasequences, have been presented by Sarg (1988), Crevello *et al.* (1989) and James & Kendall (1992). These workers have integrated the siliciclastic-based models of cyclic deposition to carbonates. These models have been applied to outcrop studies (e.g. Goldhammer *et al.* 1991; Tucker *et al.* 1990) which recognize sequence boundaries and systems tracts as physical boundaries related to sea-level fluctuations which can be tied to the global cycle chart of Haq *et al.* (1987). However, application to the subsurface has been more problematic, owing to poor seismic resolution in carbonates and diagenetic alterations that mask the primary lithological response as predicted from wireline logs. This secondary alteration and its effects on porosity and permeability make core to log calibration critical in carbonate sequence stratigraphic analysis.

Although sea-level is recognized as being a major contributor to the vertical and lateral stacking arrangement in carbonates and siliciclastic systems, there are fundamental differences

between the way in which the two systems respond to sea-level change. In siliciclastic depositional systems, clastic input is introduced laterally and eustacy controls the accommodation space and the focus of sedimentation, without directly affecting the amount of sediment supply. In carbonate systems, however, the sediment supply is produced *in situ* and mainly within the highly prolific upper part of the photic zone, the 'carbonate factory'. Sea-level fluctuations determine the health and even existence of the 'carbonate factory' and hence the amount of sediment supply. In addition, environmental controls such as climate, water inflow, salinity and oceanography are major influences that result in carbonate systems responding differently and less predictably to sea-level fluctuations compared with siliciclastic systems. Furthermore, carbonate systems world-wide exhibit two completely different shelf morphologies: the rimmed carbonate platform and the carbonate ramp (Fig. 4). These represent end-members of a range of morphologies and within a basin they may coexist.

As there are numerous classifications used to describe carbonate shelf morphology (e.g. Wilson, 1975; Read, 1985), the following summary defines the terminology used within this paper for clarification.

Rimmed carbonate platform

The rimmed carbonate platform exhibits a flat top, near sea-level, and a distinct break in slope between the shallow water and basinal environments. Slopes are generally steep and may attain angles up to 50°. This profile is characterized by a high-energy environment at the shelf margin, where skeletal shoals and reefs build, forming a wave-resistant barrier behind which a shallow marine, sheltered lagoonal environment is developed. The lagoonal environment, which acts as the main 'carbonate factory', can reach widths of tens of kilometres, resulting in potentially prolific carbonate production.

Carbonate Ramp

The carbonate ramp was first described by Ahr (1973) as an unrimmed shelf which gently slopes, at less than 1°, from the shallow water environment into the basin without a distinct break in slope. Ramps are in equilibrium with the seaward dipping wave base and therefore resemble 'sediment-stuffed' siliciclastic shelves (Schlager 1992). Depositional environments on carbonate ramps are: inner ramp (above fair-weather wave base), mid ramp (between fair-weather wave base and storm wave base) and outer ramp (below storm wave base; Burchette *et al.* 1990). The lack of an adequate wave-resistant barrier results in a non-developed to poorly developed lagoon, and main carbonate production occurs within the inner ramp depositional environment (Buxton & Pedley, 1989).

Because the geometries of the rim and ramp morphology are different and carbonate production is *in situ*, the stacking patterns and geometries of the systems tracts and internal facies distribution will differ significantly for sea-level fluctuations. Figure 5 summarizes the characteristics of each systems tract for the two carbonate profiles.

The responses of the system on a rim and ramp profile during sea-level fluctuations differ most significantly during the highstand (HST) and lowstand systems tracts (LST). During periods of sea-level highstand the entire flat top of a rimmed platform is inundated. Correspondingly, a large area is in the upper photic zone, resulting in prolific carbonate production. Sediments produced during this period may be exported and shed into the basin because of lack of space within the lagoonal environment, a process termed 'highstand shedding' (Schlager 1992). For the ramp profile the width of the sea bed within the upper photic zone is much narrower, leading to lower carbonate production.

For the LST, even during minor sea-level falls the flat-topped, rimmed carbonate platform will be subaerially exposed. Only a narrow band on the steep shelf slope will be in the photic zone, and therefore the carbonate factory will be shut down and carbonate production extremely low. Depending on the degree of early cementation, the platform margin may collapse, forming slope aprons and basin floor fans.

On the monoclinal ramp, the amount of carbonate production will not significantly differ between the HST and the LST, as the width of the sea bed within the upper photic zone remains similar. Ideally, monoclinal ramps therefore have a similar response to siliciclastic shelves to sea-level falls (Schlager 1992), and the LST will be expressed as a forced regression.

Upper Paleocene stratigraphic framework

The principal subject of this paper is the Upper Paleocene section which, in the study area, consists of basinal shales and marls that grade laterally to shallow marine carbonates. The facies distribution is clearly tectonically influenced,

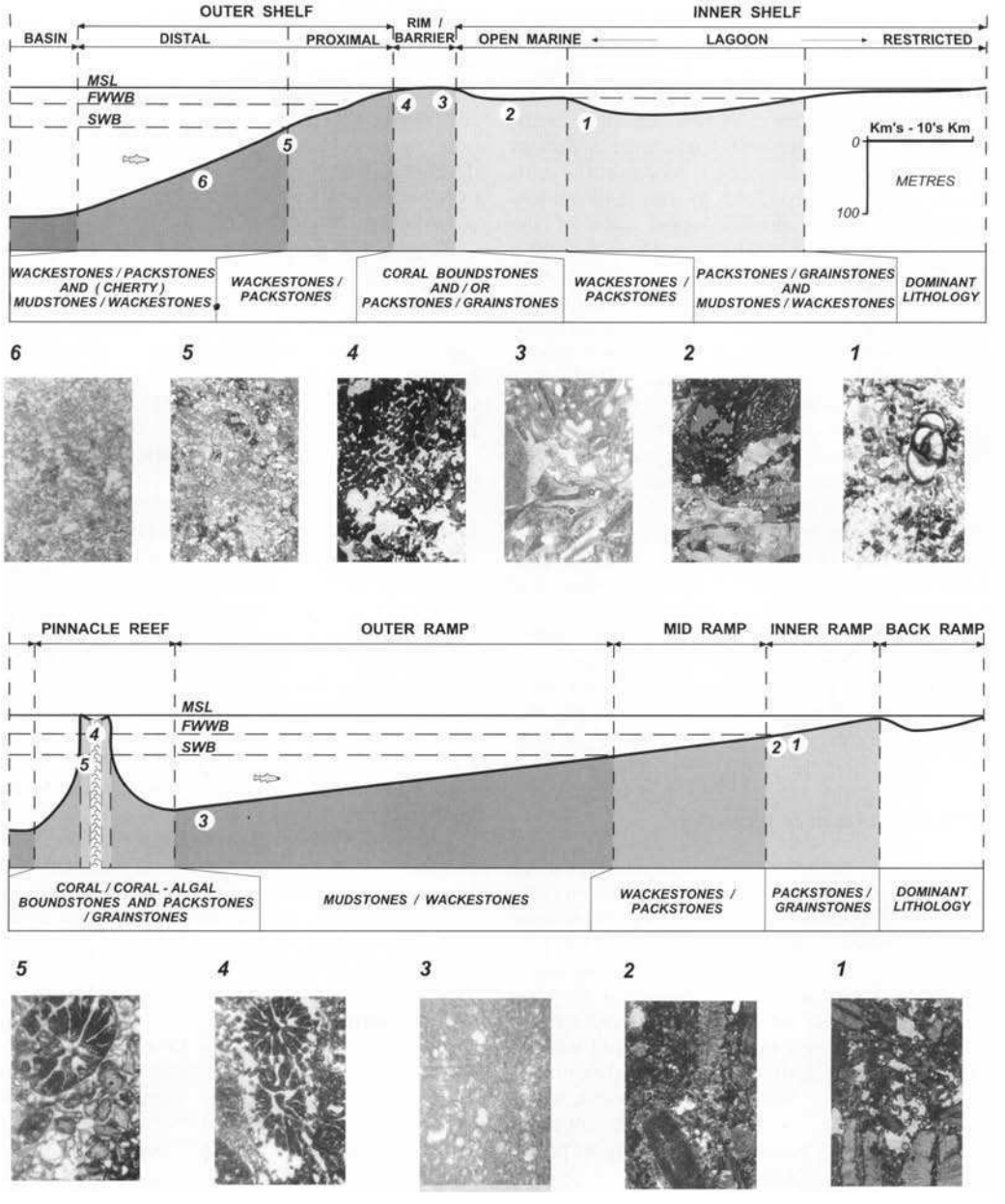

Fig. 4. Morphological profile and lithofacies characteristics of (**a**) rimmed carbonate platforms and (**b**) carbonate ramps.

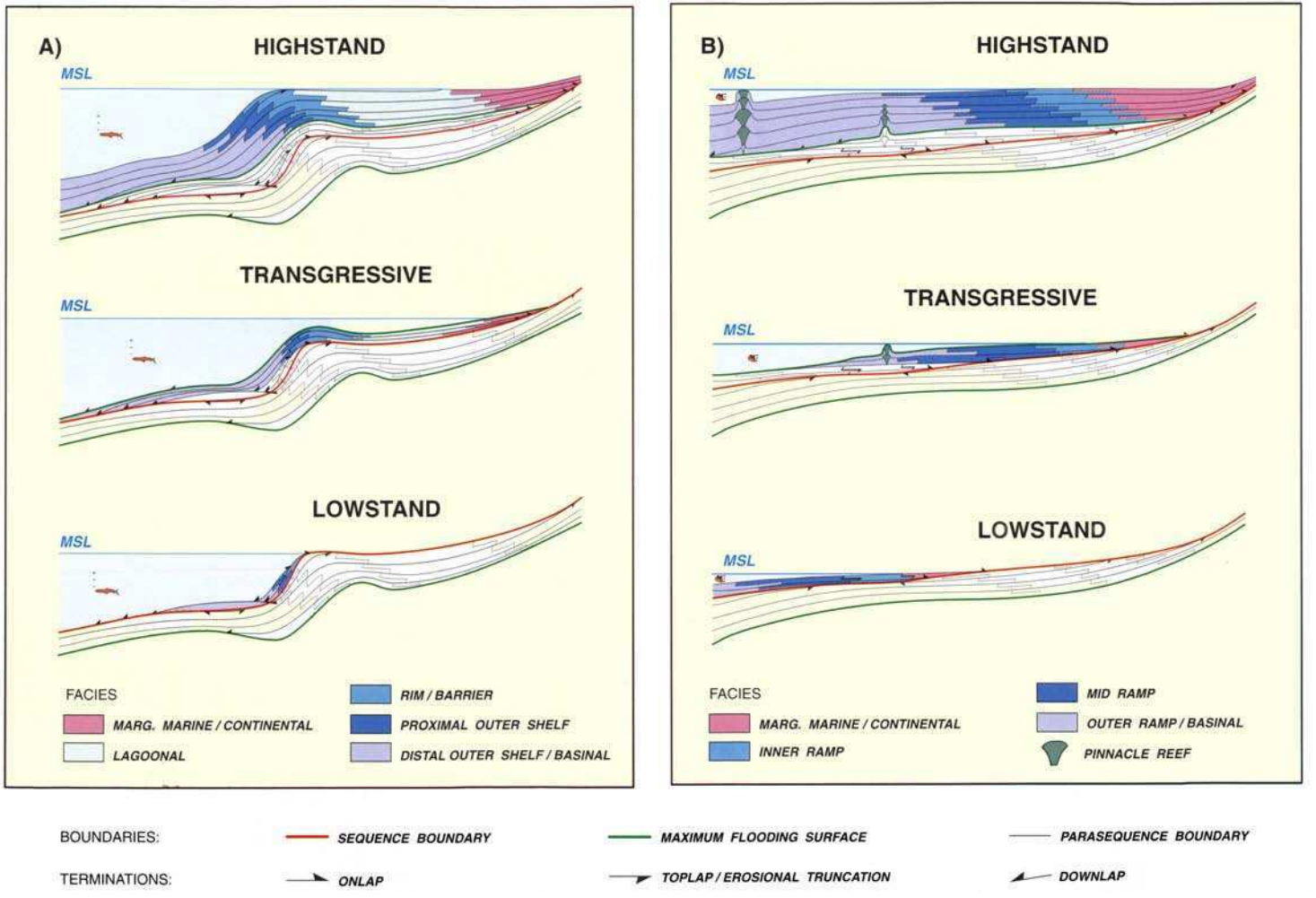

Fig. 5. Geometries and facies distribution for systems tracts on (**a**) rimmed carbonate platforms and (**b**) carbonate ramps.

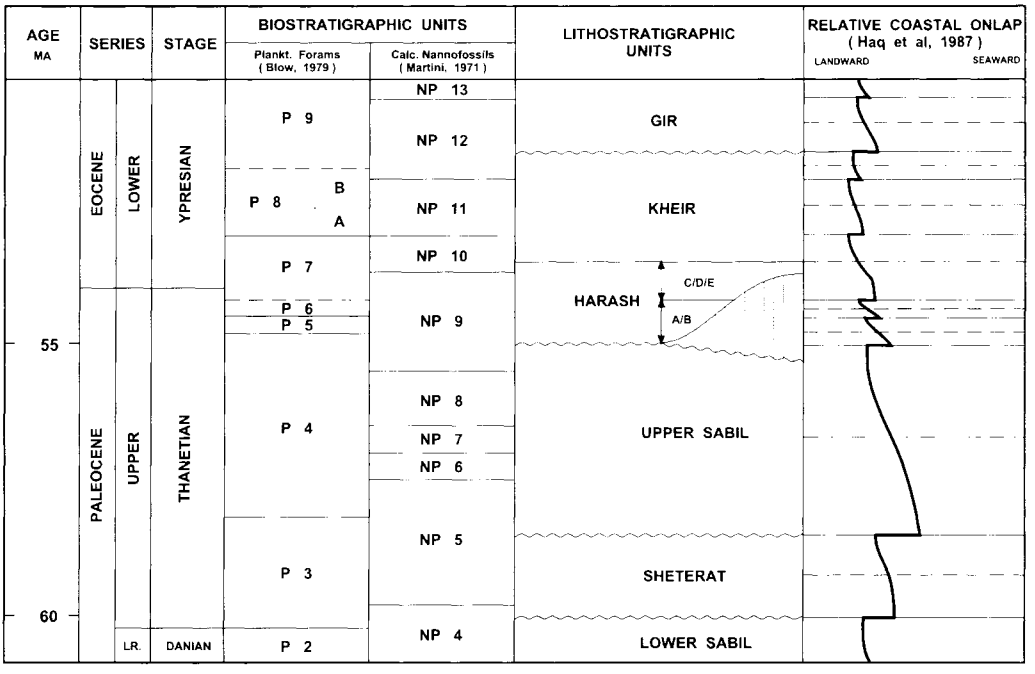

Fig. 6. Chronostratigraphic, biostratigraphic, lithostratigraphic and sequence stratigraphic framework for the Upper Paleocene–Lower Eocene of the Eastern Sirt Basin.

with carbonates developed along the rim of the southernmost extension of the Agedabia Trough, whose limits were influenced by the NW–SE structural framework. Barr & Weegar (1972) have lithostratigraphically subdivided the Upper Paleocene–lowermost Eocene into the Sheterat, Upper Sabil, Harash and Kheir Formations (Fig. 3). The carbonates belonging to the Upper Sabil Formation are interpreted to be overlain by the basinal Kheir and Harash Formations. The exact stratigraphic position of the Harash in relation to the Upper Sabil and Kheir Formations was not clearly defined by Barr & Weegar. Consequently, most studies discussing the Paleocene of the Eastern Sirt Basin have not recognized the Harash Formation and ascribe it to the Kheir Formation as part of an overall deepening succession. Indeed, biostratigraphy often shows the transition between the Harash and Upper Sabil Formation to be characterized by a major deepening event. However, on a regional scale the nature of the stratigraphic break at the top of the Upper Sabil Formation varies and is diachronous. It is our opinion that this break does not represent a 'drowning unconformity' (Schlager 1989) but reflects a sea-level fall followed, after a period of local lowstand deposition, by marine transgression. The Harash Formation is interpreted to be represented by the lowstand and transgressive systems tracts. Evidence for such a sequence boundary at the top of the Upper Sabil Formation is as follows: (1) meteoric leaching and meteoric cements observed in core data suggest subaerial exposure at the top of Upper Sabil shallow marine carbonates; (2) biostratigraphical analyses indicate reworking of pre-Harash Paleocene and Late Cretaceous material within the lower part of the Harash Formation.

On logs, the Harash Formation, where it is thickly developed, is seen to consist of five cycles designated A–E from base to top. Sample analyses show these to represent upward cleaning and shallowing carbonate parasequences. The top of the last cycle (E) corresponds to the base of the basinal shales and marls of the Kheir Formation, and is characterized by a distinct gamma-ray spike representing a maximum flooding surface (MFS). Detailed biostratigraphic analyses, combined with the recognition of a type 1 sequence boundary at the top of the Upper Sabil Formation and a maximum flooding surface at the top of the Harash Formation, have allowed correlation

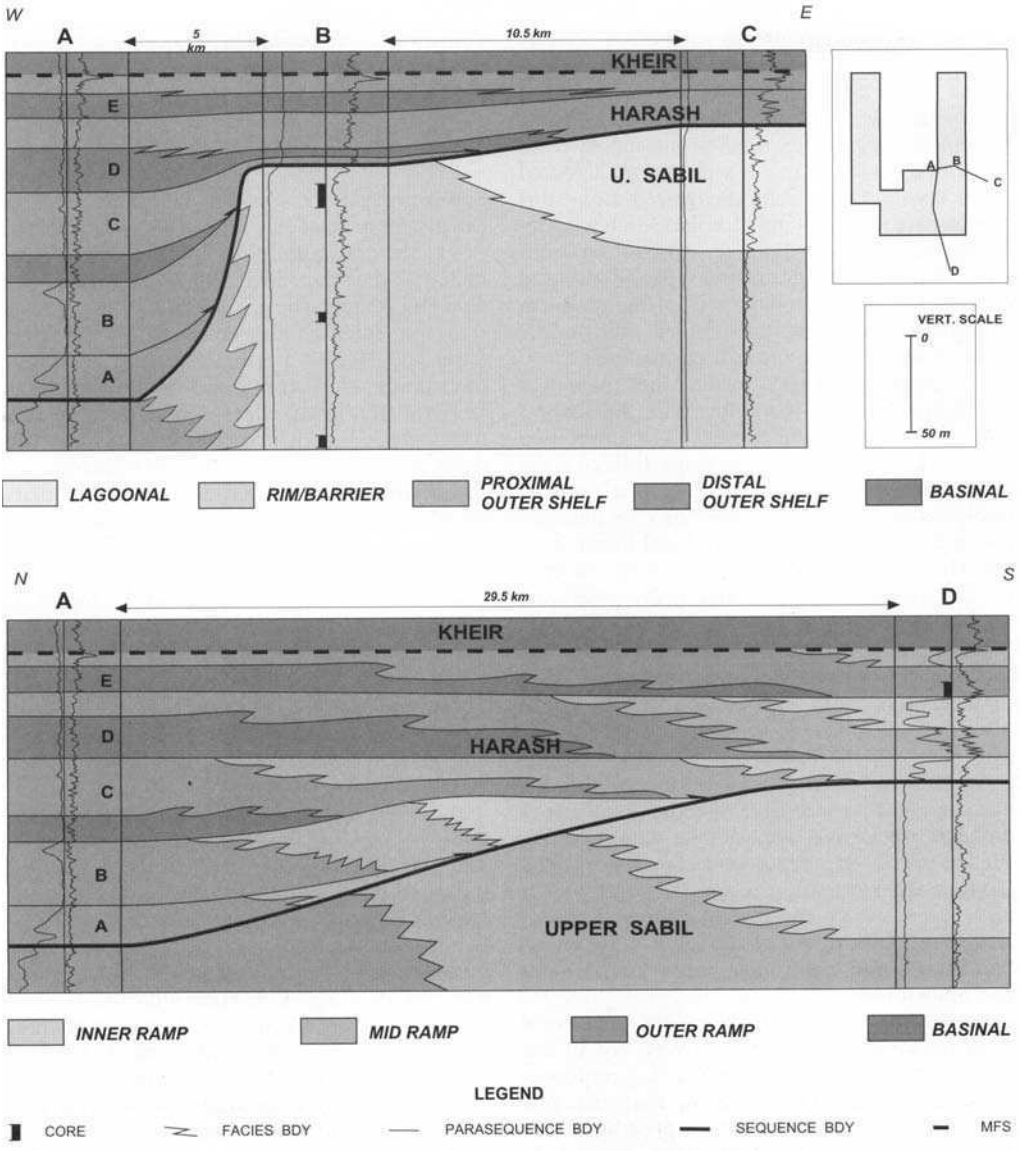

Fig. 7. Upper Sabil and Harash Formation well correlations to show stratigraphic relationships and facies distribution across (**a**) rimmed carbonate platform and (**b**) carbonate ramp in the southern Agedabia Trough.

with the eustatic sea-level curve of Haq *et al.* (1987; Fig. 6). The top of the Upper Sabil Formation probably corresponds to their major sea-level fall at 55 Ma and the MFS to their event at 53.5 Ma. It follows that the overlying Kheir Formation, in the study area consisting of mainly basinal sediments, represents the succeeding HST. Smaller scale-sea-level fluctuations recognized by Haq *et al.* (1987), following the 55 Ma event, could indeed account for the cyclic nature of the Harash Formation.

Upper Paleocene stratigraphic correlation

Stratigraphic correlation

Figure 7 shows east–west and north–south geological well correlations within the study area hung on the maximum flooding surface at the top of the Harash Formation. These illustrate the correlation of the Harash and Upper Sabil Formations using compensated gamma-ray and spontaneous potential wireline logs.

On the east–west cross-section (Fig. 7a), a rimmed carbonate platform geometry is clearly observed. Over a distance of only 5 km the top of the Upper Sabil Formation drops by 130 m from shallow marine to basinal carbonates. Behind the high-energy, shallow marine, skeletal, shoal and reefal facies, a widespread lagoonal facies exists. Facies belts recognized along this transect are miliolid- and alveolinid-rich wackestones and packstones of the lagoonal environment, foraminiferal grainstones–packstones and coral–coralline algal bindstones of the platform rim environment and fine-grained mudstones–wackestones of the slope and basinal facies.

The overlying Harash Formation is thick over the basinal facies of the Upper Sabil Formation and all five cycles are present. The lower two cycles, A and B, onlap the slope facies of the Upper Sabil Formation, leading to a reduced thickness of the Harash Formation over the shallow marine facies of the Upper Sabil Formation. The Harash Formation is notable by the absence of shallow marine facies and hence reservoir-quality carbonates.

On the north–south correlation (Fig. 7b) the top of the Upper Sabil Formation can be seen to drop only 70 m over a distance of 29 km. Microfacies analysis of the Upper Sabil Formation indicates the absence of a well-developed wave-resistant skeletal shoal and/or reefal facies and therefore no well-developed lagoonal environment, suggesting a carbonate ramp profile. Well control on the cross-section shows the Upper Sabil Formation to grade laterally from high- to medium-energy foraminiferal packstones and grainstones of the inner ramp environment to mid and outer ramp wackestones and mudstones.

To the north, where the Harash Formation is most thickly developed (Fig. 7, Well A), all five cycles can be recognized. Wireline log responses and microfacies analysis show that the two lower cycles (A and B) stack in a progradational manner, suggestive of an LST, whereas cycles C–E are retrogradational and belong to the TST (Well A, Fig. 7a and b). A lateral transition from inner ramp to outer ramp carbonates is recognized within cycles C and D both vertically and horizontally. The inner ramp facies of cycles C and D, in fact, form the principal reservoir of the Harash Field (10 km west of Well D, Fig. 7b). Within cycle E, only tight, non-reservoir, outer to mid ramp facies has been encountered by drilling. Before drilling on NC171 Block 5, Harash cycles A and B had only been recognized as poor reservoir quality outer to mid ramp sediments overlying Upper Sabil basinal facies (Well A, Fig. 7). However, the ramp geological model suggests that inner and mid ramp porous, reservoir-quality facies should be developed in suitable up-dip positions of the ramp.

Seismic stratigraphic analysis

Seismic markers mapped in this study to define the distribution of the various Paleocene formations, their stratigraphic limits and structure, included the Top Sheterat, Top Upper Sabil, Top Harash and Top Kheir Formations. In addition, individual parasequences within the Upper Sabil and Harash Formations were interpreted to examine reservoir and seal facies distribution. In particular, onlap edges of Harash Formation parasequences provided critical information for delineating Upper Sabil shelf morphology and the distribution of seal facies. A complete analysis of seismic geometries was also undertaken, which provided diagnostic criteria for mapping facies belts.

Two seismic lines, flattened on the top of the Sheterat Formation and located close to the stratigraphic correlations of Fig. 7, are presented in Fig. 8a and b. These figures display typical reflection geometries and highlight the significant difference in seismic response of the Upper Sabil and Harash Formations in orthogonal sections across rimmed platform and ramp profiles.

A rim geometry is clearly recognized on Seismic Line A (Fig. 8a), oriented east–west, by a steep shelf slope at top Upper Sabil level onlapped by high-amplitude parallel basinal Harash Formation reflectors. Within the Upper Sabil, seismic reflections consist of bidirectional progradational clinoforms representing the high-energy rim and proximal outer shelf facies. This facies is onlapped from the proximal direction by the parallel continuous low- to medium-amplitude reflections of the lagoonal facies and grades basinward into generally low-amplitude parallel and continuous reflectors.

On Seismic Line B (Fig. 8b), there is no seismically defined shelf break and the interpretation of the top of the Upper Sabil is controlled by the correlation of wells located in a proximal environment to the right (south) and basinal to the left (north). It is notable that the profile is not a simple monocline but a series of low-angle terraces dipping basinward. Reflections within the Upper Sabil are continuous, parallel and change amplitude with facies. Within the Harash Formation reflections are lower amplitude and less continuous than on Line A, and contain a high-amplitude anomaly near the onlap edge which represents either tuning or a facies change.

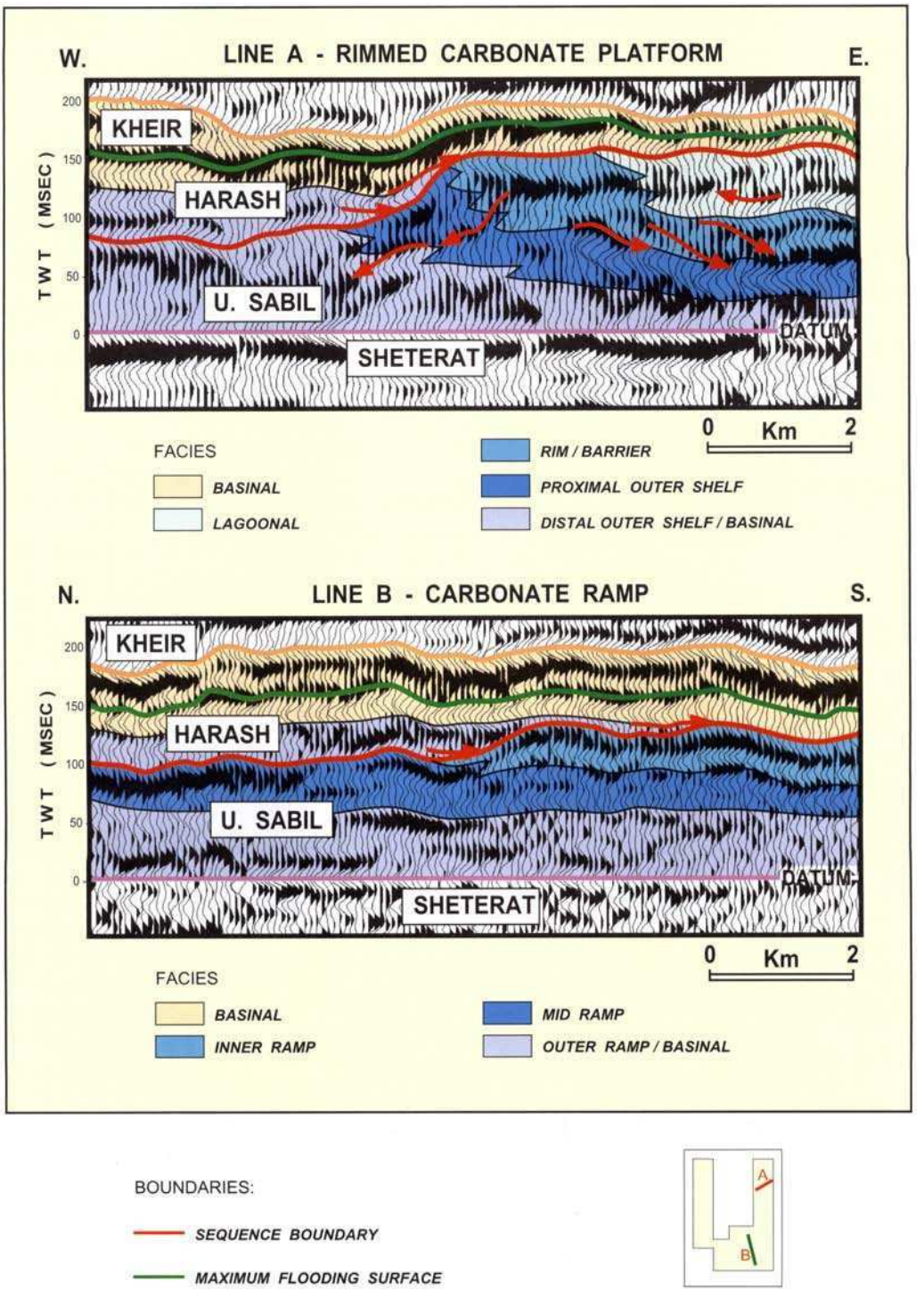

Fig. 8. Conventional seismic interpretation of the Upper Paleocene section to illustrate (**a**) rimmed carbonate platform (Line A) and (**b**) carbonate ramp (Line B) profiles. (Note that both sections are flattened on uppermost Sheterat Formation.)

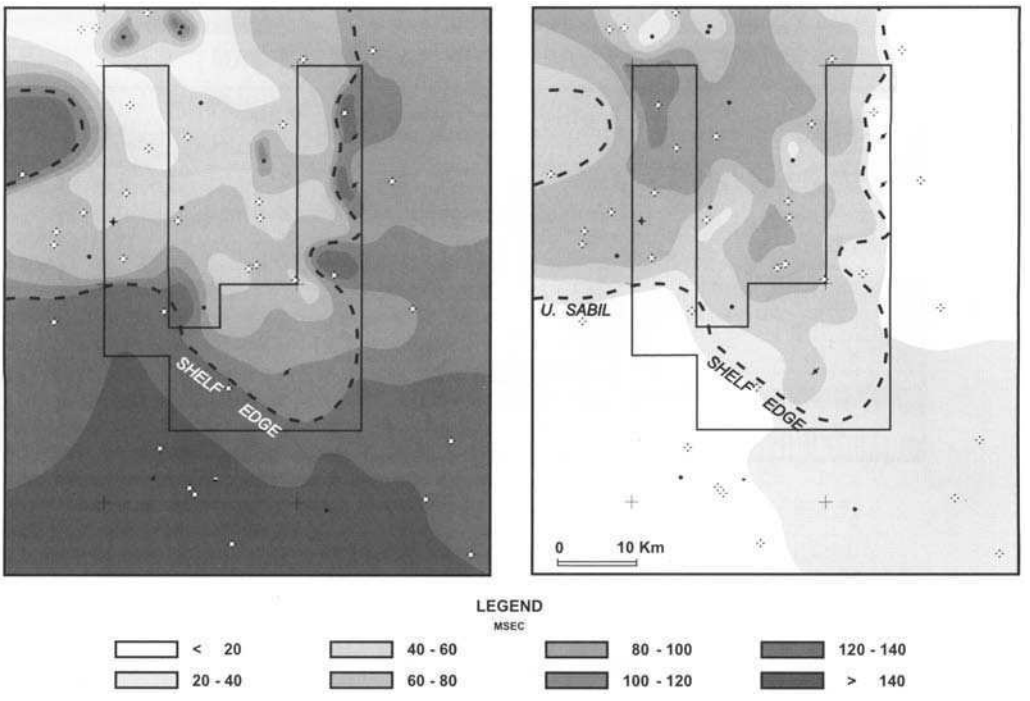

Fig. 9. Regional two-way time thickness maps for (**a**) Upper Sabil Formation and (**b**) Harash Formation.

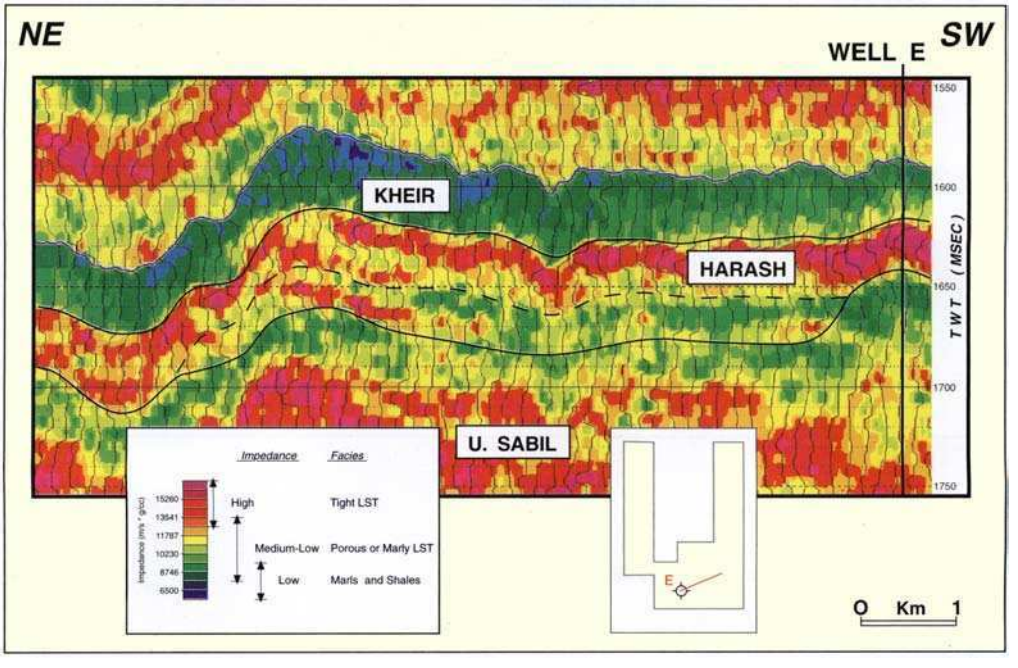

Fig. 10. Pre-drill seismic inversion interpretation for Upper Paleocene seismic anomaly and inversion colour scheme.

On a two-way time (TWT) thickness map of the Upper Sabil Formation (Fig. 9a) a rimmed carbonate platform morphology is recognized on the east and west by a marked thinning, reflecting the transition from outer shelf–/basinal to inner shelf facies; slopes are calculated up to 10°. Along the shelf edge, which was identified by mapping top Harash B onlap and the Upper Sabil internal seismic geometry, localized elongate increases in TWT thickness (>120 msec; 600 ft) represent shelf margin build-ups consisting of coral reefs and skeletal shoals. Seaward of the shelf edge the Upper Sabil Formation regionally thins to less than 20 ms (100 ft), with the localized thickness increases representing pinnacle reefs. In the south the thickness variation is more gradual and the shelf edge poorly defined suggesting a ramp profile. The geometry of the overlying Harash Formation (Fig. 9b) generally reflects infilling of the Upper Sabil morphology. Thick Harash sediments over Upper Sabil basinal facies are seen to thin by progressive onlap onto the Upper Sabil shallow marine facies.

The regional seismic mapping allowed the interpretation of a ramp profile to be developed in both the Upper Sabil and Harash Formation over the southernmost part of the Agedabia Trough. For the Harash Formation it follows that south from well A, for cycles A and B, a series of shallow marine, high energy ramp-related facies belts within a lowstand systems tract could be present. It should be noted that in an easterly direction the development of a steep rimmed platform would preclude the development of differentiated facies belts within cycles A and B. Having identified an area where high-energy facies of cycles A and B could be developed, it remained to locate the presence of porous carbonates by more detailed seismic methods.

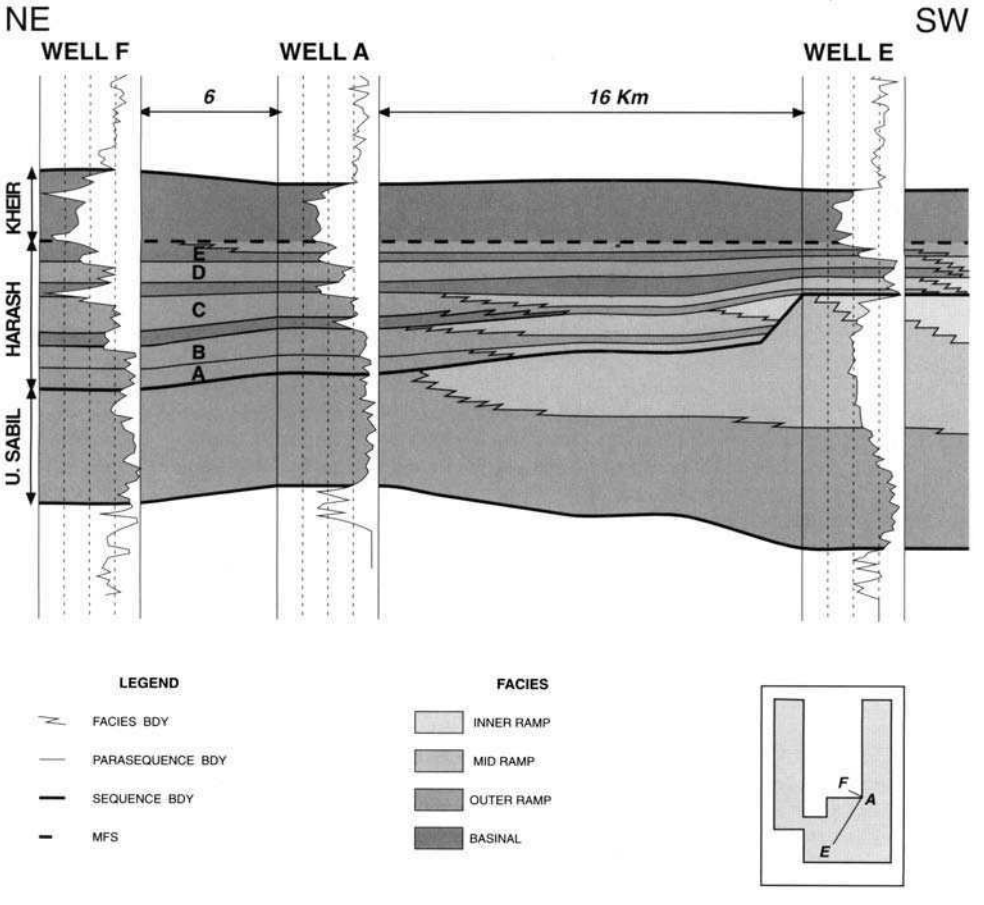

Fig. 11. Acoustic impedance model for the Upper Paleocene of the southern Agedabia Trough.

Seismic inversion studies

Seismic (stratigraphic) inversion was undertaken to investigate the nature of a seismic anomaly identified in the Upper Paleocene section recognized on conventional seismic data within a structure located in the southern part of the study area (Line B, Fig. 8). The objective of seismic inversion studies was to use seismic data to identify and map facies belts, within the Harash and Upper Sabil Formations.

A composite seismic line connecting Well E and Well A, which encountered the Upper Sabil Formation in shallow marine and basinal facies respectively, was processed for true amplitude recovery and stratigraphic inversion. The latter was performed using the STRATA software. Wavelet extraction was performed using wireline log and seismic traces at the well locations to ensure an accurate seismic wavelet for the inversion. The initial geological model, input for low-frequency information, was derived by correlating the Top Kheir Formation marker between the wells, and the underlying Harash and Upper Sabil Formation facies were then linearly interpolated along the line. Inversion was undertaken using a blocky inversion algorithm with 80% weighting on seismic data to minimize the effect of the geologic model. The result is displayed in Fig. 10. Notwithstanding the inherent problems of wavelet stability, band-limited seismic spectrum, noise and the strong influence of the initial geological model on the result, the inversion is considered reliable.

As a guide for interpretation, the stratigraphic model was used to develop an acoustic impedance profile for calibration of the inversion with facies (Fig. 11). The inversion colour scheme highlights that the high-impedance basinal–outer ramp tight limestones and low-impedance basinal shales can be interpreted confidently but ambiguity exists with the low to medium impedance, which can represent either porous or marly limestones (particularly between 1650 and 1700 ms, Fig. 10).

The inversion shows that the anomaly observed on conventional seismic data corresponds to a low- to medium-impedance section encased in high-impedance lithologies (Fig. 10). Based on the inversion there are essentially two ways to correlate the control wells. The Upper Sabil is interpreted high to the north and east of Well E (dashed line: 1650 ms) and the low to medium impedance represents porosity at the top of the Upper Sabil underlain by a tight intercalation. Alternatively, the Upper Sabil shelf edge is located just to the east of Well E (solid line) and the low- to medium-impedance anomaly reflects either porous or marly limestones within the basal part of the Harash Formation.

The geological model suggests a carbonate

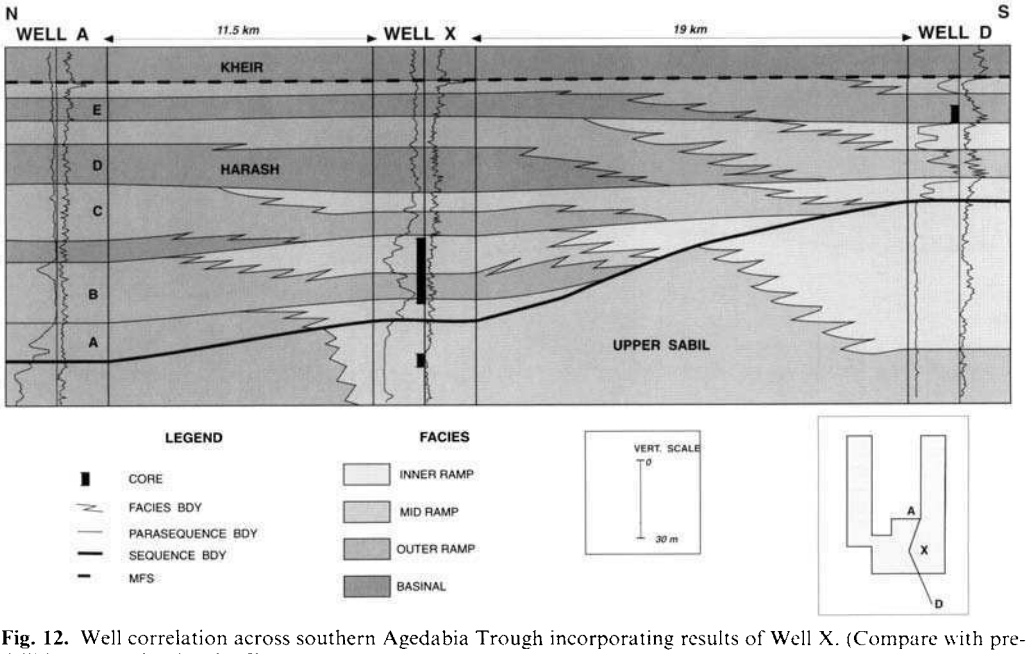

Fig. 12. Well correlation across southern Agedabia Trough incorporating results of Well X. (Compare with pre-drill interpretation in Fig. 7b.)

ramp profile with an axis oblique to the line and the possible development of Harash lowstand porous inner ramp facies, reflected by low to medium impedance within cycles A and B. Thus the second interpretation (low) of the Upper Sabil was considered more likely. The shelf slope is approximately 3° at this location, representing the transition from a rimmed platform to ramp profile from the northeast to south (Fig. 9). The high-impedance section separating the low- to medium-impedance bands is interpreted as tight mid to outer ramp facies within the base of Harash cycles A and B, which onlaps the Upper Sabil slope close to Well E. To the north the low- to medium- impedance section interpreted at the top of Harash B disappears, laterally changing to high impedance, interpreted to reflect a facies change from porous inner–mid ramp to tight mid–outer ramp carbonates.

Results of drilling

In 1994 exploration well X was drilled on the seismic anomaly and was ideally located to test the proposed stratigraphic framework. Figure 12 shows the post-drill stratigraphic correlation of the Upper Sabil and Harash Formations along similar strike to Fig. 7b. This clearly shows a ramp geometry at the Upper Sabil level and the development of an overlying, prograding high-energy facies within cycles A and B of the Harash Formation as a result of a sea-level fall.

Cores were cut through nearly the entire Harash B cycle in Well X and segments are shown in Fig. 13. Analysis of the cores shows the Harash B to comprise a shallowing- and cleaning-up carbonate cycle from outer ramp to mid ramp. The basal outer ramp facies of the Harash B cycle consist of fine-grained mudstones and wackestones, containing mainly indeterminate skeletal debris and occasional small gastropods, planktonic foraminifers, faecal pellets and crinoid fragments. These grade upward into wackestones, which contain mainly fragments of large benthic foraminifers. The presence of reworked shallow marine skeletal debris clearly

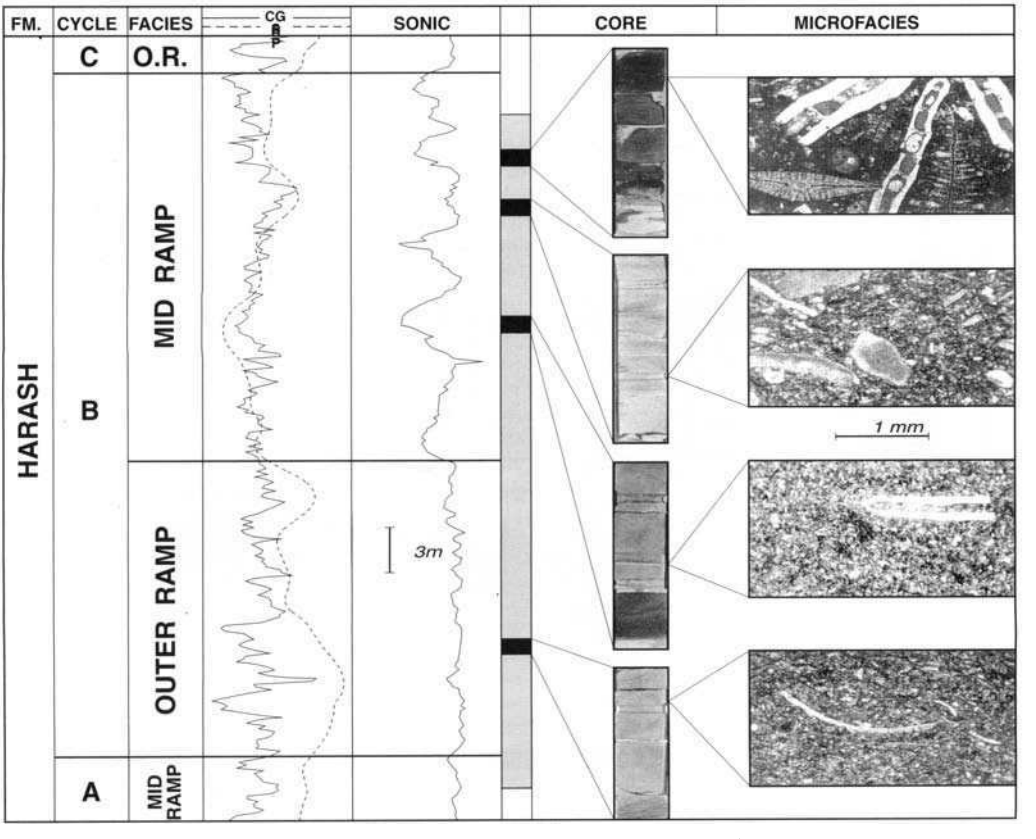

Fig. 13. Log response, core data and microfacies details for Harash cycles A and B in Well X.

reflects deposition within a mid ramp environment of deposition. The upper part of the Harash B consists of medium- to coarse-grained foraminiferal wackestone–packstones. Although the less fragmented nature of the large benthic foraminifers suggests very little reworking, the continued presence of lime mud and rare presence of planktonic foraminifers indicate that the high energy of the inner ramp environment was not attained and that deposition took place in a (proximal) mid ramp setting. As suggested by the seismic inversion study, porosity is indeed developed within the upper part of the Harash B. Although there is a general upward increase in primary porosity to be observed within the Harash B, the porosity variations observed both on wireline logs and cores are largely of secondary origin and can be related to late burial, selective leaching of the lime mud matrix.

Microfacies analysis of the Upper Sabil Formation shows a generally prograding character. The basal 500 ft, deposited in an outer ramp environment of deposition, consist of very fine grained lime mudstones and wackestones containing common planktonic foraminifers. In the overlying section, fine grained wackestones dominate, containing abundant fragments of crinoids and common large benthonic foraminifers. Approximately 300 ft below the top of the Upper Sabil Formation, grainstones containing miliolids and alveolinids are observed over a 100 ft interval. This fossil assemblage is normally characteristic for the lagoonal environment. However, a 21ft core within this section reveals sedimentary features which indicate that the grainstones represent turbidite beds. The upper part of the Upper Sabil Formation is therefore interpreted to have been deposited in a mid ramp setting. The crinoid-rich wackestones were probably sourced along the axis of the ramp profile, whereas the miliolid- and alveolinid-grainstones may reflect 'highstand shedding' from the rimmed carbonate platform developed to the east and west of the well. As suggested by the seismic inversion, the Upper Sabil Formation is porous within its upper part. Microfacies analysis indicates that the porosity is associated with the turbidite-rich mid ramp deposits and is both primary, inter- and intra-granular, and secondary, leached.

Upper Sabil and Harash formation lithofacies distribution

This successful result confirmed the potential of seismic (stratigraphic) inversion as a predictive

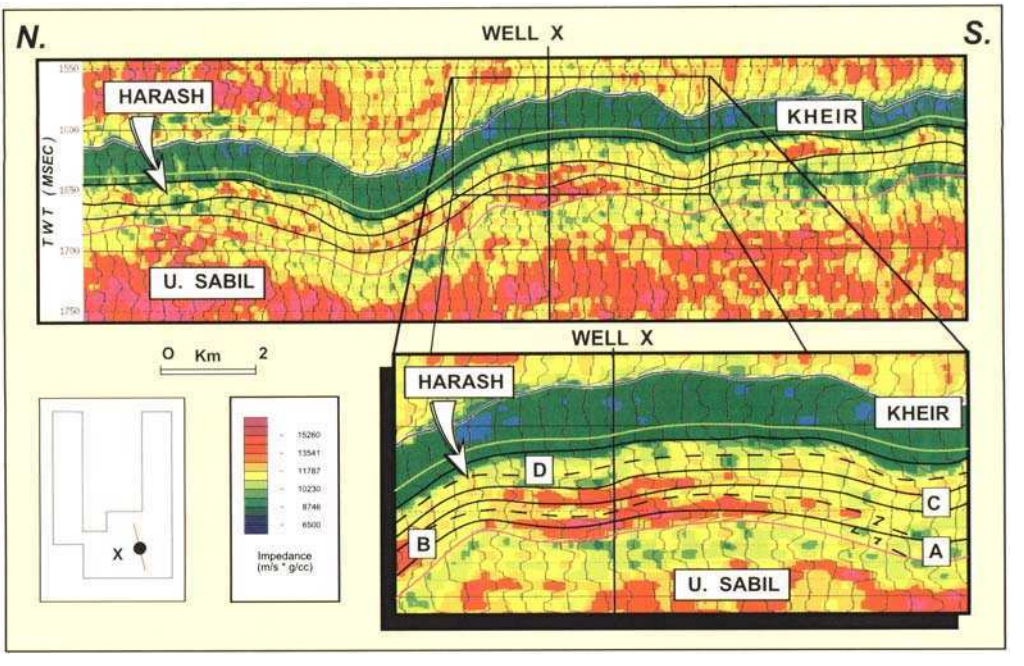

Fig. 14 Post-well seismic inversion interpretation. Inset show details of Harash Formation cycles A–E. (Compare with pre-drill interpretation in Fig. 10.)

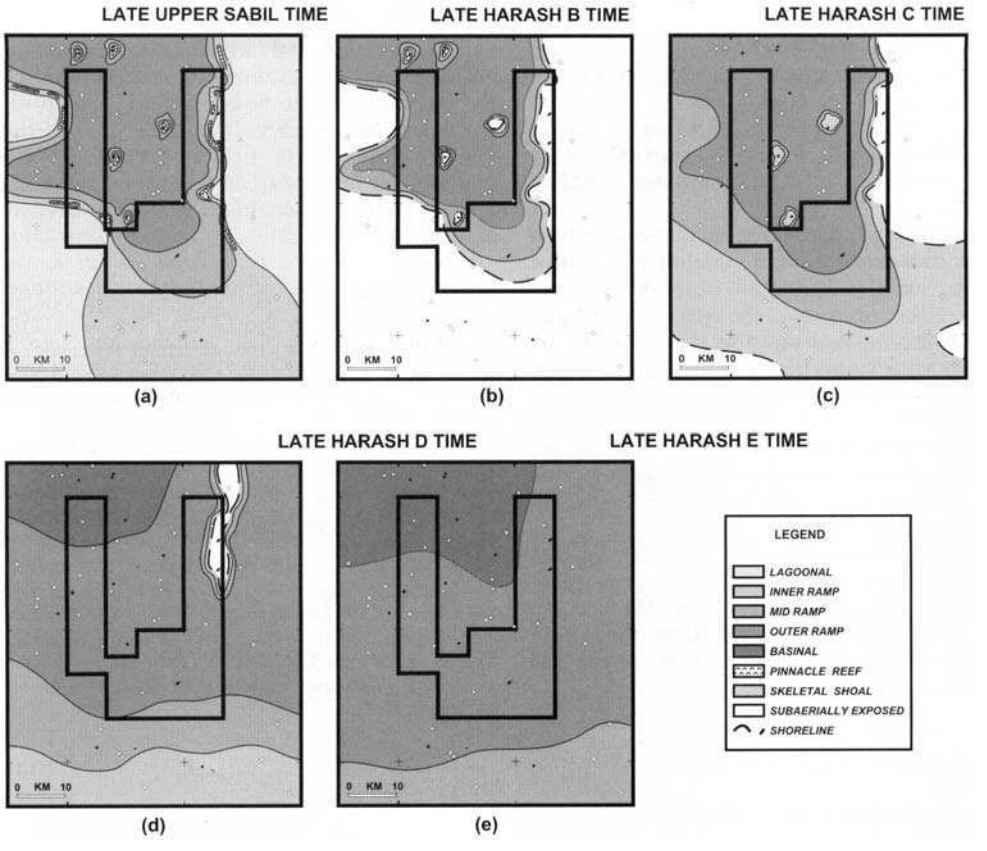

Fig. 15. Late Paleocene lithofacies distribution within the study area.

tool when used with a sound geological model. Having proved the geological concept, regional inversion was undertaken over the Well X structure and surrounding area which allowed confident mapping of individual cycles and facies changes within both the Upper Sabil and Harash Formations. A post-well regional north–south inversion line (Fig. 14) shows the transition of the Upper Sabil high-energy, low- to medium-impedance, porous inner ramp to high-impedance, tight outer ramp limestones. The Harash A and B cycles are represented by tight carbonates basinward which show a lateral transition to porous inner–mid ramp carbonates that onlap the Upper Sabil in a landward (southerly) direction. Over the Well X structure the Harash Formation marine transgression during cycles C–E is represented vertically by high-impedance tight limestones which grade basinward to low-impedance basinal shales.

Application of this technology allows the construction of time-slice lithofacies maps for the Upper Sabil to Harash Formations, as illustrated in Fig. 15. The series of lithofacies distributions clearly show the influence of basin morphology and sea-level on the distribution of depositional environments.

By the end of Upper Sabil time, extensive rimmed carbonate platforms had prograded into the eastern and western parts of the study area (Fig. 15a). Here skeletal shoals and platform margin reefs formed wave-resistant barriers behind which sheltered lagoonal environments developed. Within the southern area a carbonate ramp had gradually prograded northwards. The relatively high lime mud content of the inner to mid ramp deposits suggests relatively moderate energy depositional environments compared with the high-energy shelves developed to the east and west.

A major sea-level fall dated at 55 Ma abruptly ended Upper Sabil deposition and caused subaerial exposure of the shallow marine Upper Sabil facies and proximal pinnacle reefs. Whereas carbonate production in the east and west suddenly ceased, the southern area was

much less affected by the sea-level fall. Because of the nearly constant and low-angle dip of the ramp, the *in situ* carbonate production was not reduced markedly but shifted basinward. This allowed development of a broad northward prograding Harash A and B lowstand wedge across the Upper Sabil mid ramp deposits (Fig. 15b).

The Harash C depositional cycle commenced with a transgressive event which led to marine flooding of the subaerially exposed western Upper Sabil rimmed carbonate platform and most of the exposed ramp to the south. Facies developments comprised thin belts of inner and mid ramp carbonates and basinal shales and marls. Continued transgression through Harash D and E time resulted in marine flooding of the entire study area with deposition of mainly basinal to outer ramp marls and lime mudstones (Fig. 15c and d).

The facies distribution during the late Harash E reflects the end of the last parasequence of the Harash Formation TST. The MFS at the boundary with the overlying Kheir Formation is dated at 53.5 Ma, corresponding to the end of the Paleocene (Fig. 15e).

Conclusions

A major sealevel fall has been documented at the end of Upper Sabil Formation deposition corresponding to the Haq *et al.* (1987) 55 Ma drawdown event. Subaerial exposure of the rimmed carbonate platform in the east and west of the study area occurred, causing the 'carbonate factory' to be largely shut down. In the south, where a carbonate ramp profile existed, forced regression of the high energy inner to mid ramp facies occurred. This geographic variation in the morphology of the Upper Sabil carbonate shelf strongly influenced the facies distribution of overlying basal, lowstand Harash Formation cycles A and B. These sediments form a typical lowstand wedge developed over the area of a pre-existing ramp geometry. They are not represented over areas of rimmed carbonate platform development. Within the Harash lowstand systems tract porous lithologies were developed as foraminiferal wackestone–packstone, representing an inner to mid ramp facies.

The areal distribution of the porous facies within Harash parasequences is critical to the understanding of reservoir and seal relationships. This study has demonstrated the successful use of seismic stratigraphic techniques to interpret these relationships. Although seismic stratigraphic inversion has indeed proved to be a powerful, predictive exploration tool, it does not provide a unique solution. Only with a valid data-derived geological model that allows the interpretation of the inversion data to be constrained, may positive results be expected. The application of the approach used here in the Sirt Basin will undoubtedly help in exploration for the more difficult to find carbonate-reservoired hydrocarbons in other basins.

The authors thank the NC171 Block 5 Joint Venture partners Yukong Ltd, PanCanadian Petroleum Ltd, Numac Energy (Africa) Inc., Chieftain International Inc. and the Libyan NOC for their permission to publish this paper as well as their stimulating technical input throughout the project. We also wish to thank Zueitina and Waha for allowing access to core data. Thanks also are extended to J. Defour for her excellent work on the seismic inversion, T. Lakew for his expertise in carbonate microfacies and sedimentology, and M. Cope for his critical review of the work, editing of the paper and his support. We also thank C. Gobeaux and his drafting department in Petrofina, Belgium, and S.-G. Lea in Fina Exploration Norway for their excellent work in preparing the figures. Finally, we would like to thank Fina Exploration Libya for permission to publish this paper and for their financial support of the colour figures.

References

AHR, W. M., 1973. The carbonate ramp an alternative to the shelf model. *Transactions of the Gulf Coast Association of Geological Societies*, **23**, 221–225.

BARR, F. T. & WEEGER, A. A., 1972. *Stratigraphic Nomenclature of the Sirt Basin, Libya*. Petroleum Exploration Society of Libya.

BANERJEE, S., 1980. *Stratigraphic Lexicon of Libya*. Bulletin of the Department of Geological Research and Mining, Tripoli, **3**.

BURCHETTE, T. P., WRIGHT, V. P. & FAULKNER, T. J. 1990. Oolitic sandbody depositional models and geometries, Mississippian of southwest Britain: Implications for petroleum exploration in carbonate ramp settings. *Sedimentary Geology*, **68**, 87–115.

& 1992. Carbonate ramp depositional systems. *In*: SELLWOOD, B. (ed.) *Ramps and Reefs. Sedimentary Geology*, **79**, 3–57.

BURKE, K. & DEWEY, J., 1974. Two plates in Africa during the Cretaceous. *Nature*, **249**, 313–316.

BUXTON, M. W. N. & PEDLEY, H. M. 1989. A standardised model for Tethyan Tertiary carbonate ramps. *Journal of the Geological Society, London*, **146**, 746–748.

CREVELLO, P., SARG, J. F., READ, J. F. & WILSON, J. L. (eds) 1989. *Controls on Carbonate Platform to Basin Development*. Society of Economic Paleontologists and Mineralogists, Special Publication, **44**.

GOLDHAMMER, R. K., LEHMANN, P. J., TODD, R. G., WILSON, J. L., WARD, W. C. & JOHNSON, C. R. 1991. *Sequence Stratigraphy and Cyclostratigraphy of the Mesozoic of the Sierra Madre Oriental, Northeast Mexico, a Field Guidebook*. Gulf Coast Section, Society of Economic Paleontologists and Mineralogists, Tulsa, OK.

GUMATI, Y. D. & NAIRN, A. E. M., 1991. Tectonic subsidence of the Sirt Basin, Libya. *Journal of Petroleum Geology*. **14**(1), 93–102.

HAQ, B. V., HARDENBOL, J. & VAIL, P. R., 1987. Chronology of fluctuating sealevels since the Triassic: *Science*, **235**, 1156–1166.

JAMES, N. P. & KENDALL, A. C.,1992. Introduction to carbonate and evaporite facies models. *In*: WALKER, R. G. & JAMES, N. P. (eds) *Facies models: Response to Sealevel Change*, 265–275.

READ, J. F. 1985. *Carbonate Platform Facies in Geologic History*. Springer-Verlag, Berlin.

SARG, J. F. 1988. Carbonate sequence stratigraphy. *In*: WILGUS, C. K., HASTINGS, B. S., KENDAL, C. G., ST. C., POSAMENTIER, H. W., ROSS, C. A. & VAN WAGONER, J. C. (eds) *Sea-level Changes: An Integrated Approach*. Society of Economic Paleontologists and Mineralogists, Special Publication, **43**, 155–181.

SCHLAGER, W. 1989. Drowning unconformities on carbonate platforms. *In*: *Controls on Carbonate Platform and Basin Development*. Society of Economic Paleontologists and Mineralogists Special Publication, **44**, 15–25.

—— 1992. *Sedimentology and Sequence Stratigraphy of Reefs and Carbonate Platforms. (A short course)*. Continuing Education Course Note Series, American Association of Petroleum Geologists, **34**.

TUCKER, M. E., WILSON, J. L., CREVELLO, P. D., SARG, J. F. & READ, J. F. 1990. *Carbonate Platforms, Facies, Sequences and Evolution*. International Association of Sedimentologists Special Publication, **9**.

VAIL, P. R., MITCHUM, R. M. & THOMPSON, S. 1977*a*. Seismic stratigraphy and global changes of sealevel, Part 4: Global cycles and relative changes of sea-level. *In*: PAYTON, C. E. (ed.) *Seismic Stratigraphy—Application to Hydrocarbon Exploration*. American Association of American Petroleum Geologists, Memoir, **26**, 83–97.

——, TODD, R. G. & SANGREE, J. B. 1977*b*. Seismic stratigraphy and global changes of sea-level, Part 5: Global cycles and relative changes of sea-level. *In*: PAYTON, C. E. (ed.) *Seismic Stratigraphy—Application to Hydrocarbon Exploration*. American Association of American Geologists, Memoir, **26**, 99–116.

VAN DER MEER, F. D. & CLOETINGH, S. A. P. L. 1993. Late Cretaceous and Tertiary subsidence history of the Sirt Basin (Libya): an example of the use of backstripping analysis. *ITC Journal*, 1993, 68.

WILSON, J. L. 1975. *Carbonate Facies in Geologic History*. Springer-Verlag, Berlin.

This page intentionally left blank

Regional depositional setting and pore network systems of the El Garia Formation (Metlaoui Group, Lower Eocene), offshore Tunisia

R. G. LOUCKS[1], R. T. J. MOODY[2], J. K. BELLIS[3] & A. A. BROWN[1]

[1] *ARCO Exploration and Production Technology, Plano, TX, USA*
[2] *Kingston University, Kingston upon Thames, Surrey, UK*
[3] *ARCO International Oil and Gas Company, Plano, TX, USA*

Abstract: The Metlaoui Group was deposited on a broad ramp that deepened to the northeast into the Tethyan Sea. The ramp contains a series of broad facies belts. The inner-ramp facies belt is composed of three facies tracts: (1) Faid sabkha (most landward) characterised by skeletal-poor dolomudstones and wackestones and interbedded evaporites, (2) Ain Merhotta restricted shallow-lagoon facies composed of sparse skeletal wackestones, packstones, and cross-bedded gastropod grainstones; (3) updip El Garia high-energy shoal complex (most seaward) composed of red algal–discocyclinid grainstones and packstones which are locally cross bedded. The El Garia carbonates in the mid-ramp setting are predominantly composed of large, flat nummulites. Dominant textures are burrowed, mud-poor packstones and poorly sorted or bimodal grainstones. The accumulation was located below fair-weather wave base and above storm wave base, at a water depth estimated to have ranged from 30 to 60 m (middle neritic). The deep-water (deep neritic), outer-ramp Ousselat Member consists of coarse silt- to medium sand-sized nummulithoclastic debris that grades from coarser to finer debris down the ramp. The Bou Dabbous Formation is composed of basinal foraminiferal mudstones, wackestone and packstones deposited by suspension and less commonly by gravity-flow deposition in upper bathyal water depths. Reservoir quality is variable, with most lime packstones and grainstones having moderate to high porosity (related to intraparticle and microporosity), but only poor to fair permeability (generally less than 10 mD). The higher-quality reservoirs have preserved interparticle porosity with permeabilities ranging from tens of millidarcys to several darcys. Permeable nummulitic packstones and grainstones are favoured by the following factors: (1) low abundance of lime mud, (2) low abundance of nummulithoclastic debris, (3) low abundance of echinoderm fragments, (4) moderate sorting, (5) minor precipitation of late burial cements, (6) dolomitization.

The Lower Eocene, Metlaoui Group (Fig. 1) is a well-studied carbonate section in Tunisia where the gross distribution of depositional facies and major rock types is well known. This formation contains proven economic petroleum reserves (Anon 1982; Anz & Ellouz, 1985) and remains an active exploration target. Successful exploration within the El Garia Formation, however, requires an understanding of its depositional history and pore network evolution to assist in estimating risk of encountering reservoir facies and finding adequate reservoir quality for economic production.

There are two depositional-related goals of this study. First, we wish to refine the physiographical setting of the El Garia nummulitic carbonate belt to a greater degree. Several previous studies have presented an interpretation of shallow-shelf platform setting (e.g. Arni, 1965; Decrouez & Laterno 1979 Aigner 1983; Moody 1987; Bailey *et al.* 1989; Moody & Grant 1989) whereas Compte & Lehmann (1974) suggested a ramp morphology. It is clearly important for exploration and development programmes to distinguish ramp from shelf settings, because ramp facies shift laterally with modest relative sea-level changes and facies patterns are generally more interfingered. In contrast, shelf facies tend to aggrade so that a single facies, or stacked, correlatable parasequences are characteristic of the reservoir facies. The second major goal is to address the question of whether the nummulite accumulations are indeed physiographical mounds or banks during deposition. The exploration consequences of this have to do with seismic imaging of facies geometries and the potential for purely stratigraphic traps.

Both of these goals will be addressed by evaluating the data for palaeobathymetry and lateral and vertical facies changes upon which previous interpretations have been based. The focus of this discussion is the main El Garia facies belt. We demonstrate that there is a gradation of El Garia facies from inner to outer ramp, and that most productive El Garia facies were deposited in a mid-ramp setting under tens of metres of water depth, with negligible relief to the nummulite accumulations.

LOUCKS, R. G., MOODY, R. T. J., BELLIS, J. K. & BROWN, A. A. 1998. Regional depositional setting and pore network systems of the El Garia Formation (Metlaoui Group, Lower Eocene), offshore Tunisia. *In*: MACGREGOR, D. S., MOODY, R. T. J. & CLARK-LOWES, D. D. (eds) 1998. *Petroleum Geology of North Africa*. Geological Society, London, Special Publication No. 132, 355–374.

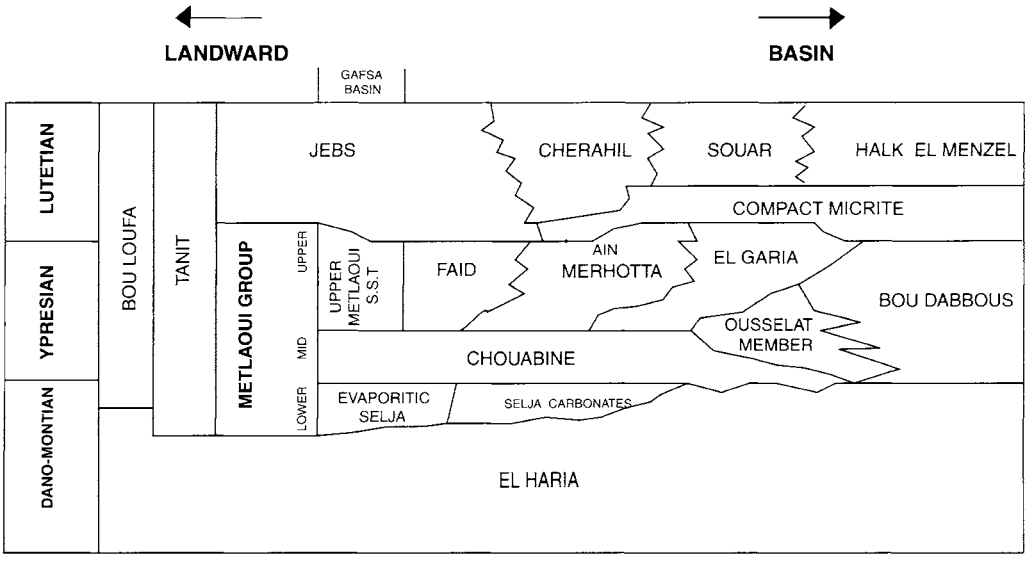

Fig. 1. Lithostratigraphic nomenclature for the Metlaoui Carbonate Group in Tunisia. Modified from Fournie (1975, 1978), Moody & Grant (1989) and Dridi & Sejil (1991).

Another goal of this study is to outline the general diagenetic history of the El Garia nummulite deposits and relate this information to identifying factors controlling the more permeable rock types. Porosities are generally high, but permeability is variable because of the large amount of ineffective intraparticle porosity and microporosity in the pore networks and the loss of effective interparticle porosity by several diagenetic processes.

Data for this study come from cores in the offshore Tunisian Gulf of Gabes area and from outcrops. Outcrops visited cover facies from the updip Faid Formation (southern Cherahil area), through the downdip El Garia Formation (Djebba, Djebel Cherichera, Dar Dakhallate, Djebel es Afair, Kef el Guitoun, El Garia, Kesra, and Sidi Ahmed areas), Ousselat Member (Djebel Goraa, Pont Roman, Cluse Ousselat, and Kef el Guitoun areas), and Bou Dabbous Formation (Kef Bou Dabbous, Pont Roman, Cluse Ousselat, and Bir Bourkana–Oued Fedj areas). Thin-section analysis was extensively used in this study because identifying nummulite A:B ratios and mud- to sand-sized matrix is difficult in outcrop and slabbed core.

Stratigraphy

Regional stratigraphy of the Metlaoui Carbonate Group in the Ypresian section of the Lower Eocene Epoch (Fig. 1) has been summarized by Fournie (1975, 1978), Moody & Grant (1989) and Dridi & Sejil (1991) Five formations make up this group. The Basal Chouabine Formation is presented as being transgressive, and the Faid, Ain Merhotta, El Garia, and Bou Dabbous formations are displayed as being progradational. Phosphatic carbonates of the Chouabine Formation underline the other formations. Faid Formation is the most landward unit and is characterized by fine-grained dolomites and evaporites (Vernet 1971). Bishop (1985, 1988) defined the Ain Merhotta Formation as a gastropod-rich carbonate between the Faid and El Garia formations. Thick nummulitic accumulations make up the El Garia Formation. Moody & Grant (1989) defined the nummulithoclastic facies (silt- and sand-size debris from nummulite disaggregation) as the Ousselat Member of the El Garia Formation. The Bou Dabbous Formation is the most seaward unit.

Regional depositional setting

El Garia carbonates were deposited as a broad belt that deepened to the north and northeast into the Tethyan Sea (Moody 1987; Moody & Grant 1989). South of the carbonate belt are age equivalent, shallow-water evaporites, thin-bedded carbonates and siliciclastic deposits of the Faid and Ain Merhotta formations. Seaward

of the El Garia facies belt are age equivalent deep-water chalks, argillaceous carbonates, and organic-rich carbonates of the Bou Dabbous Formation. The transition from shallow to deep water clearly occurs within the El Garia carbonates.

We propose that the transition is best described as a carbonate ramp (Figs 2 and 3). In our interpretation, the inner ramp consists of the Faid and Ain Merhotta formations, and the landward part of the El Garia Formation. The mid-ramp consists of the main nummulite accumulation in the El Garia Formation. The outer ramp consists of the nummulithoclastic Ousselat Member of the El Garia Formation. Detailed evidence for this interpretation is presented below, but the following lines of evidence form the basis for this interpretation. Grainstone and shoal-water facies are restricted to the landward end of the carbonate tract. The shoal-water facies form a barrier restricting circulation to the shallowest water facies. Both of these features are characteristic of the inner parts of ramps. Most of the mid-ramp facies, which includes the productive facies for most fields, is characterized by an absence of shoaling, and significant evidence for a palaeobathymetry of the order of tens of metres deep, much deeper than is normal for shallow-water carbonate platforms. Finally, the seaward part of the carbonate belt has large-scale interfingering of tongues of Ousselat and El Garia facies (Moody 1987), indicative of major seaward and landward facies shifts on depositional slopes of several degrees, which is not characteristic of platform margins.

Compte & Lehmann (1974) presented a platform model for the Metlaoui carbonates in central Tunisia, in which they show a ramp-like transition from the Faid to the Bou Dabbous formations; however it is not known if they recognized the El Garia strata as mid-ramp deposits. Buxton & Pedley (1989) recognized that nummulite deposits in the Tethyan Tertiary were associated with ramp deposition, but they interpreted the nummulite gravels as having been deposited in a shallow-water, shoaling, inner-ramp environment similar to a coralgal patch-reef belt.

In the following sections, the different parts of the facies belts will be discussed and the key evidence for the ramp and the palaeobathymetric interpretations will be presented and discussed.

Inner-ramp setting

The inner ramp (Figs 2 and 3) is composed of three facies tracts: (1) Faid sabkha (most landward), (2) Ain Merhotta restricted, shallow-water lagoon, and (3) updip El Garia high-energy shoal complex (most seaward). The Faid sabkha, as seen in outcrop, is characterized by skeletal-poor dolomudstones and wackestones and interbedded evaporites (Fig. 4a). Ain Mer-

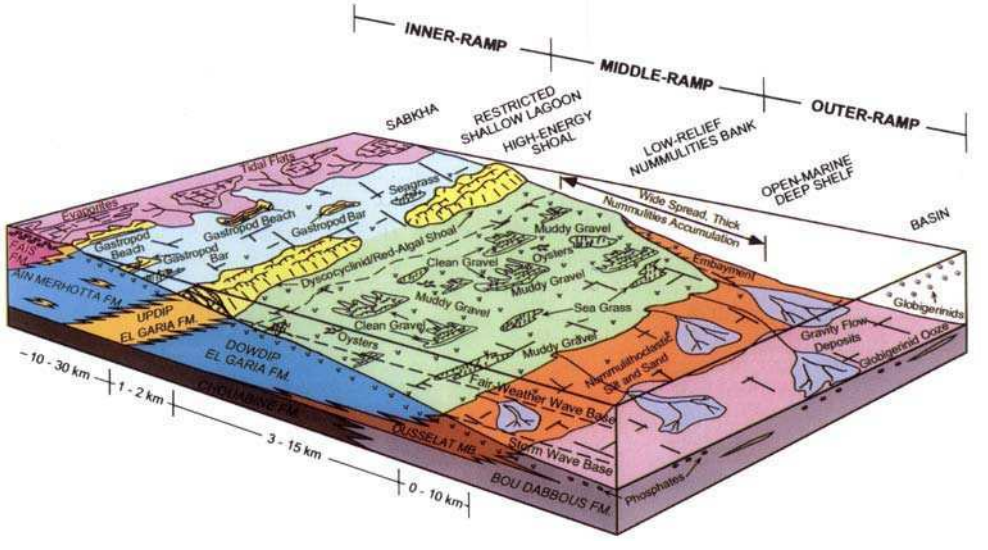

Fig. 2. Regional depositional model of the Metlaoui Carbonate Group. The model shows a well-defined ramp with the main accumulation of nummulites occurring in a mid-ramp position.

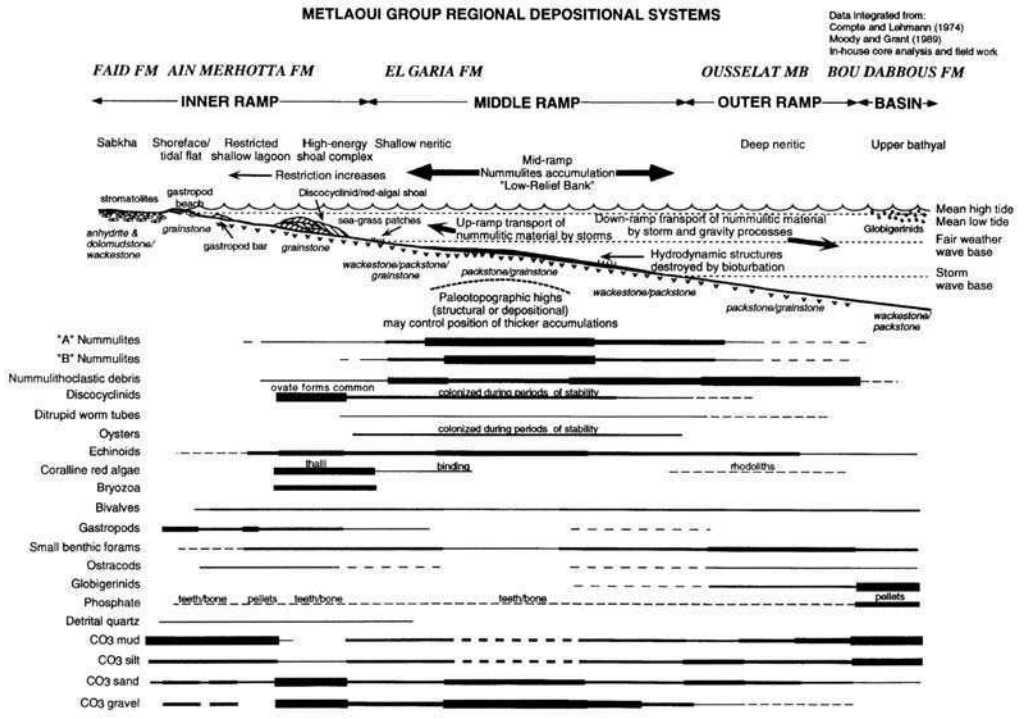

Fig. 3. Two-dimensional model of the Metlaoui Carbonate Group showing general depositional profile and distribution of grain types and textures. Data integrated from Compte & Lehmann (1974), Moody & Grant (1989), in-house core analysis and fieldwork.

hotta restricted, shallow-water lagoonal facies in outcrop are composed of sparse skeletal wackestones, packstones, and cross-bedded gastropod grainstones (Fig. 4b).

Updip El Garia Formation in the outer part of the inner ramp is composed of red algal–discocyclinid grainstones and packstones with nummulites, bryozoan, and echinoid fragments (Figs 3 and 4c). Discocyclinids have an ovate cross-section. According to Hallock & Glenn (1986), thicker forms of larger Foraminifera indicate deposition in high-energy and/or high-light environments. Nummulites are predominantly megalospheric A-types with A:B ratios ranging from 20:1 to 60:1 (Fig. 4d). Large-scale cross-bedding is locally developed (Figs 4e and 4f). Most beds are coarse sand or granule grade, and little fine silt- or mud-sized carbonate occurs in the upper part of the section. These deposits interfinger landward with the wackestones and packstones of the Ain Merhotta Formation. The inner-ramp El Garia facies is interpreted to be a shoal complex. The presence of hydrodynamic sedimentary structures indicates a constant, relatively high-energy setting dominated by marine bar deposition. Some bars may have been in water less than a metre deep at low tide.

Mid-ramp setting

Most of the middle and outer parts of the El Garia facies belt is interpreted to be a mid-ramp deposit. The dominant rock types are mud-poor (Figs 5a and 5b) to mud-rich packstones (Fig. 5c) and poorly sorted or bimodal grainstones (Figs 5d and 5e). Original sediments were sandy pebble- and pebble-sized carbonate gravels (4–25 mm). Nummulites made up most of the sand- and pebble-sized material. Well-sorted grainstones without lime mud or nummulithoclastic debris (coarse silt- and medium sand-sized nummulite fragments) are not as common. These deposits lack the cross bedding and thallose red algae which are common in the inner-ramp shoaling environment. By far the dominant grain type is whole and fragmented nummulites; other larger Foraminifera (mainly flattened discocyclinids; Fig. 5f) are uncommon. Besides larger Foraminifera, grains include echinoid

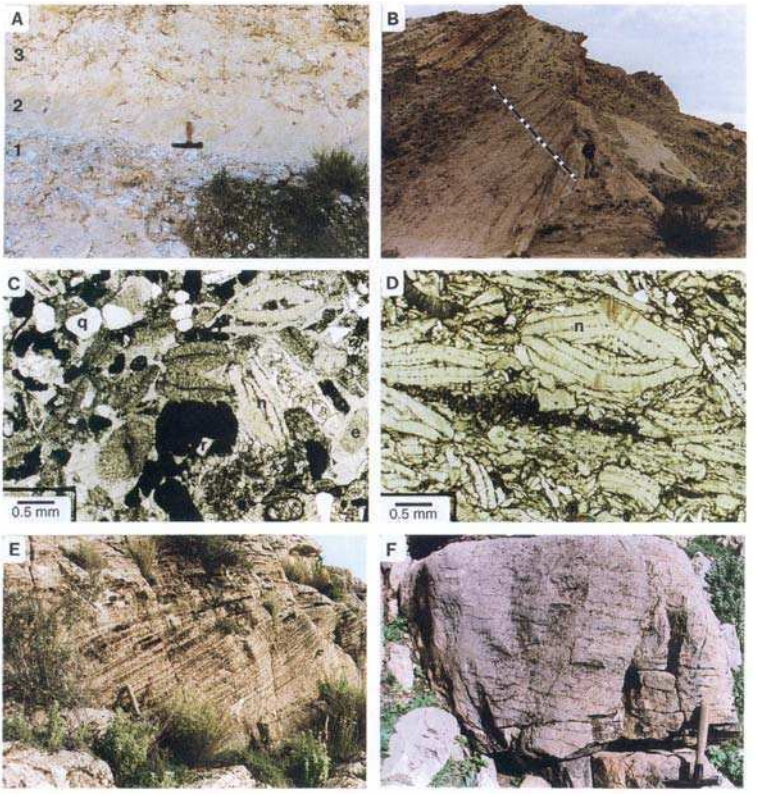

Fig. 4. Photographs of inner-ramp facies. (**a**) Peritidal deposits in the Faid Formation in the southern Cherahil area. Lower part is nodular gypsum (1) deposited in a shallow subtidal environment overlain by deflation-type supratidal flat mudstones (2). Uppermost part is composed of fossiliferous subtidal wackestones (3). (**b**) Cross-bedded gastropod grainstone bar in the Ain Merhotta Formation. The thickness of the bar is shown by the stippled line. (**c**) Inner-ramp El Garia, red algal–discocyclinid grainstone with A-nummulites (n), echinoids (e) & rounded quartz grains (q) from Djebel Cherichera. Red algae are labeled 'r' and discocyclinids are labeled 'd.' (**d**) Inner-ramp El Garia, A-nummulite grainstone with discocyclinids from Djebel Cherichera. Discocyclinids are labeled 'd'. (**e**) Inner-ramp El Garia, thick cross-bedded sequence of nummulithoclastic nummulitic grainstones from Djebel es Afair with coarse rounded-quartz sandstone stringers and discocyclinids. (**f**) Inner-ramp El Garia, thick, avalanche cross-bedding from Djebel Cherichera.

fragments, calcareous worm tubes, oyster shells, small benthic Foraminifera, and rare nautiloids (Fig. 3).

A:B ratios (megalospheric test to microspheric test number ratio) within nummulite accumulations investigated here range between 100:1 and 1:10. A-dominated nummulite deposits appear to be more common than B-dominated nummulite deposits in cores from offshore wells. Some A-dominated nummulite deposits with A:B ratios greater than 10:1 are up to 20 m thick and some B-dominated nummulite deposits with A:B ratios less than 5:1 are up to 14 m thick.

We interpret that these El Garia carbonate gravels were deposited in relatively deep water, below fair-weather wave base and above storm wave base. We estimate average palaeobathymetry in the middle part of this facies tract to be *c.* 30–60 m. This interpretation is supported by three lines of evidence: shape of the larger foraminifer tests, absence of hydrodynamic sedimentary structures, and absence of evidence of large-scale transport of coarse-grained carbonate.

Observations by Biswas (1976) from the South China Sea support the concept that deeper water settings (20–60 m) are more suitable to the Holocene larger benthic species of Foraminifera than shallower, higher-energy settings. In the Gulf of Aqaba, Reiss & Hottinger (1984) noted that Holocene nummulitids occur in a deep-water setting of 20–130 m where they live in a stationary position on soft bottoms or crawl around on

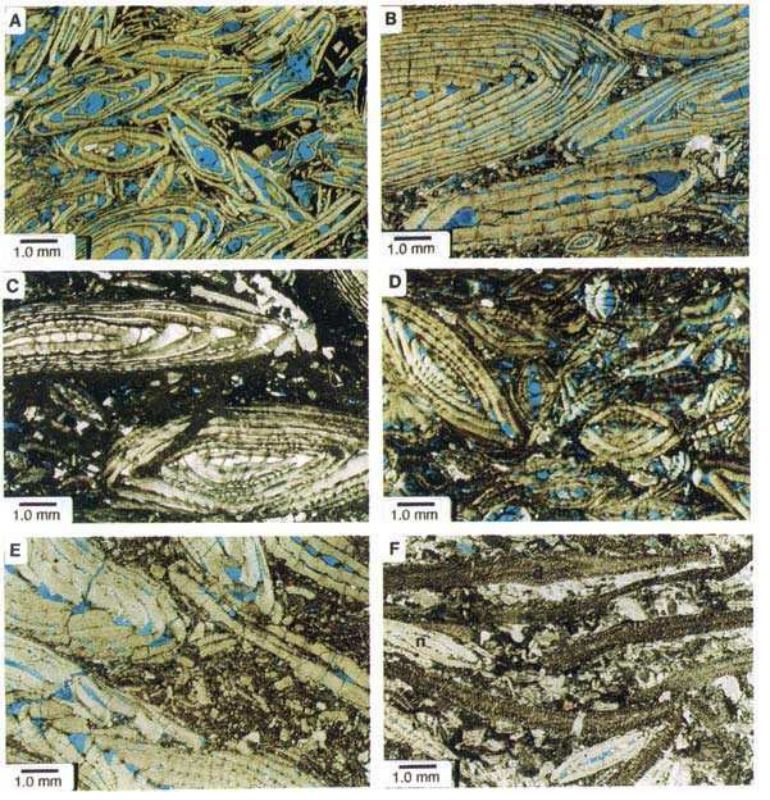

Fig. 5. Rock textures within the mid-ramp El Garia Formation. Samples are from offshore Tunisia. (**a**) A-nummulite mud-poor packstone with abundant intraparticle porosity and some interparticle porosity and microporosity. The mud is probably compacted geopetal fill and it has a very irregular distribution. (**b**) B-nummulite mud-poor packstone with nummulithoclastic debris. The sample has a strong bimodal grain-size distribution. Abundance matrix indicates sediment was not well washed. Pore network of intraparticle porosity and microporosity, and minor interparticle porosity. (**c**) B-enriched nummulite mud-rich packstone. Matrix consists of lime-mud and nummulithoclastic debris. Pore network of microporosity and some intraparticle porosity. Most of the intraparticle pores are cemented. (**d**) Fairly well sorted A-nummulite grainstone with interparticle and intraparticle porosity. (**e**) Nummulithoclastic-rich B-nummulite grainstone. Abundance matrix indicates sediment was not well washed. (**f**) Elongate discocyclinid (d) A-nummulite (n) grainstone. Lack of breakage of the elongated discocyclinids indicates little reworking of the sediment after deposition.

hard substrates. According to Hallock & Glenn (1986), flattened forms of larger Foraminifera indicate deposition in lower-energy and/or lower-light environments. Those workers concluded that on open carbonate shelves (water depths between 40 and 130 meters), large, very flat discoid Foraminifera are common. Hottinger (1983) also noted that the deeper-euphotic, open shelf has been the domain of the flattest nummulitids since the mid-Paleocene. The increase in discocyclinid flatness to the north and northeast within the El Garia Formation indicates, in our interpretation, an increase of water depth to middle neritic bathymetry.

The benthic environment during mid-ramp El Garia deposition is considered to have been similar to the intermediate shelf (20–60 m water depth) in the South China Sea as described by Biswas (1976). These sediments are mainly carbonate sand and gravel with some mud and silt and they are affected daily by mild current agitation and periodically by intense storms. Burrowing (mainly *Thallasinoides* and echinoids) is the only common sedimentary structure in the El Garia carbonates (Figs 6a–c), but most of the strata have the wavy bedding contact and irregular grain orientation indicative of intense bioturbation. Hydrodynamic structures created by storm processes were obliterated by intense bioturbation. No cross-bedding, ripples, or wave

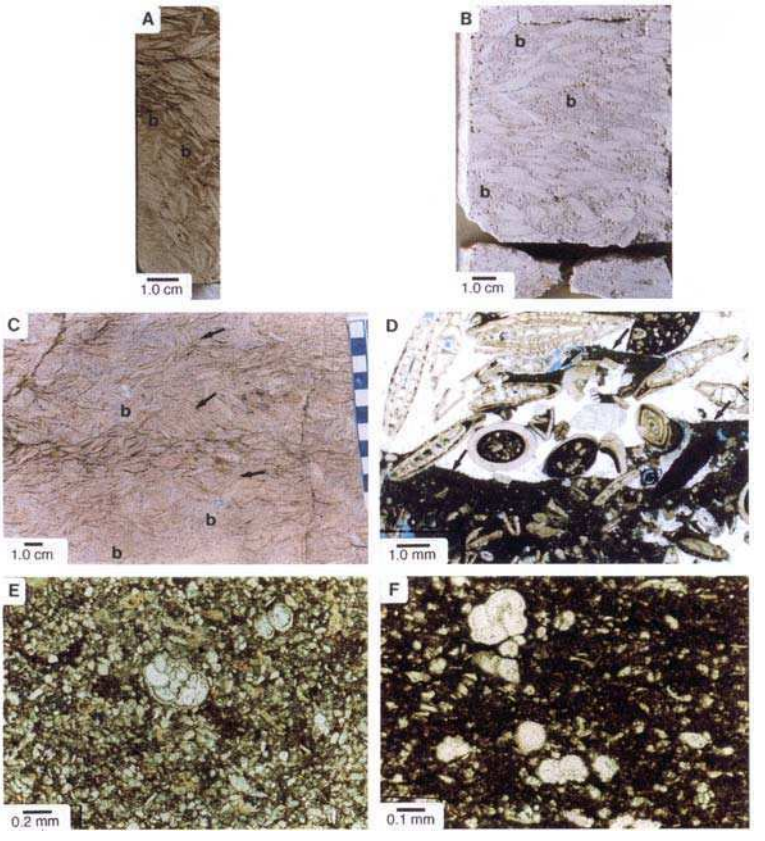

Fig. 6. Examples of mid- to outer-ramp rock textures and fabrics. All photographs are from offshore Tunisia, except (**c**) which is from an outcrop at Kersa. (**a**) Mid-ramp El Garia, B-enriched nummulite grainstone with abundant nummulithoclastic debris. The variable alignment of grains is caused by bioturbation (b). Bioturbation produces some imbrication of grains (arrows). (**b**) Mid-ramp El Garia, nummulithoclastic-rich, B-nummulite grainstone showing burrows (b). Burrows are more nummulithoclastic rich than the matrix. (**c**) Mid-ramp El Garia, B-enriched nummulite grainstone showing bioturbation (b) and multiple directions of grain alignment. Some of the grains appear to be imbricated over a few centimetres laterally (arrows). The imbrication is not laterally extensive enough to be attributed to currents; bioturbation and compaction produced the imbrication. (**d**) Some of the packstones in the mid-ramp El Garia contain geopetal mud (arrows) that filtered into mud-free grainstones. (**e**) Nummulithoclastic mud-poor packstone with globigerinids. Sample is from the outer-ramp Ousselat Member. (**f**) Globigerinid wackestone with some nummulithoclastic debris. Sample is from the basinal Bou Dabbous Formation.

or current imbrication were recognized in El Garia cores or outcrops. Patches of aligned nummulites are common (Figs 6a and 6c). Many nummulite tests rest at angles and some are stacked in rows. Angle of tilt ranges from a few degrees to vertical and the organization is continuous only for distances of centimetres. Tilted grains are associated with burrows, such as those related to echinoid and Thalassinoides type organisms or are associated with compaction. Dish-shaped grains commonly align during compaction as mechanical stability is obtained.

Aigner (1982) noted similar imbrication features in nummulite accumulations in the Eocene in Egypt and attributed them to a current origin, on the basis of work by Laming (1966). Imbrication in Tunisian nummulite accumulations does not appear similar to contact imbrication structures shown by Laming (1966, p. 945). His imbrication structures have good internal organization for over a metre distance and dip of grains is commonly less than 25°. Aigner (1986) recognized that displaced orientation by bioturbation of nummulites can produce an imbricated-like structure, but he felt that the

two processes can be separated. He stated that bioturbation fabrics 'should be easily distinguished from intervals of densely packed accumulations with abundant edge-wise and fan-shaped orientations of tests which are produced hydrodynamically by oscillatory flow'. Wells (1986) interpreted nonhorizontal orientation of nummulites to be caused by bioturbation in nummulite accumulations in Pakistan Eocene strata.

Previous investigators used differences in the ratio of the smaller megalospheric (A-type; Fig. 5a) nummulite to the larger microspheric (B-type; Fig. 5b) nummulites as evidence of hydrodynamic transport and sorting of coarse-grained sediment (e.g. Aigner 1985; Moody 1987). In this interpretation, the original, undisturbed ratio is fixed at near 10:1 A:B ratio, and deviation from this ratio is due to selective transport and redeposition of the A-types, leaving a lag enriched with B-types. Aigner (1985) cited De la Harpe (1883) and Blondeau (1972) as evidence of original, undisturbed Eocene nummulite assemblages having an A:B ratio of 10:1.

Wells (1986) presented some alternatives to how enriched accumulation of A or B nummulites can form other than by hydraulic washing and sorting. Accumulations of similar types of nummulites marked by depauperate faunas can be a product of a stressed habitat. In stressed environments normal nummulite A:B ratios should not be expected, but rather one type or another can dominate. During periods of favourable environment conditions, individuals mature and reproduce rapidly and vacate small tests, whereas under stressed conditions, such as low temperature, insufficient food, or low light, individuals may grow to greater size before maturing (Hallock & Glenn 1986). Wells (1986) also pointed out that some Foraminifera may reproduce asexually under good environmental conditions and sexually during times of stress. Environmental influences, therefore, appear to have a strong control on population size and A:B ratio. A complicating factor in recording A:B ratios is that it is generally done by size of tests. As shown in Aigner's (1985) nummulite population diagram (his Fig. 3, p. 132), A-nummulites are generally less than 7 mm and B-nummulites are greater than 7 mm. Many nummulites are assigned to the A-nummulite category solely based on size and not the recognition of a large proloculus. Juvenile B-nummulites may not be recognized in populations where environmental conditions were not conducive to their survival; they may be mistakenly described as A-types based on their size.

We believe that the large variations in A:B ratios are mainly the product of biological reproductive response to environmental conditions rather than a product of hydraulic sorting. This means that the significant variations in A:B ratios do not reflect transportation, as much as changing environments within the mosaic of facies characteristic of the mid-ramp setting.

We base this interpretation on three lines of evidence. First, El Garia nummulitic sediments have a depauperate fauna, which indicates a stressed environment where substantial biological variation of A:B ratio would be expected (following Wells (1986)). Second, we feel that A-dominated and B-dominated beds are too thick to be the product of size sorting and transportation. As noted earlier, uninterrupted A- or B-nummulite-enriched beds can be 10–20 m thick, much thicker than the beds described by Aigner (1982). Storm-generated beds on the deeper shelf are generally thin. Finally, the abundance of silt- and mud-sized carbonate between the nummulites in both the supposedly washed B-dominated facies (Figs 5b, 5c and 5e) and the transported A-dominated facies (Figs 5a and 5d) is inconsistent with their supposed origin by transportation. Why should A-type nummulites be washed out and mud- to sand-sized matrix be left behind? Much of the mud matrix in the enriched B-nummulite packstones has a geopetal structure (Fig. 6d) indicating that the mud filtered down into the interparticle pore spaces of gravels after storm events. Subsequent bioturbation commonly redistributed this mud in an irregular pattern. If burrowing accounted for reintroduction of the fine matrix, it should have also reintroduced A-types into the B-dominated intervals.

There is no evidence indicative of differential relief over the nummulite accumulations in the mid-ramp environment. We found no hard data supporting relative shoaling in any part of the accumulation. This observation was confirmed by evaluation of large outcrop exposures in the Dar Dakhallate and Kef el Guitoun areas. No evidence of dip reversal or steeper seaward dips was observed near or on the nummulite accumulations. Although these bodies can be referred to as 'banks', the amount of local depositional relief was small with respect to the water depth.

Outer-ramp setting

The El Garia nummulitic facies of the mid-ramp overlie and grade downdip into the Ousselat nummulithoclastic packstone and grainstone of the outer ramp. The Ousselat Member consists of poor to very well sorted, coarse silt-sized to medium sand-sized nummulithoclastic debris

(Fig. 6e) very similar to the matrix between whole nummulites in the El Garia accumulation, except here whole nummulites are rare. There is a pronounced gradation from coarser to finer debris down the ramp. Other grain types included echinoid fragments, rare discocyclinids, bivalves, small benthic Foraminifera, ostracods, globigerinids, and phosphate (Fig. 3). Rare, thin beds of small corals and Bryozoa were observed in outcrop. Moody & Ratcliffe (1993) noted that nummulithoclastic debris decreases in a basinward direction and is replaced by benthonic and planktonic Foraminifera, ostracods, and micrite. Burrows are the most common sedimentary structure. Hydrodynamic sedimentary structures are rare and are confined to thin graded beds.

This facies is interpreted as a deep-water (deep neritic), outer-ramp deposit (Figs 2 and 3). It is composed of sediment derived from the mid-ramp El Garia nummulitic accumulation and transported downslope by storm suspension, turbidity currents, and probably small debris flows. High-intensity storms that reworked the mid-ramp nummulite gravels generated a landward surge of water which produced an associated down-ramp counter current (Allen 1984; Buxton & Pedley 1989). The return flow probably carried much of the nummulithoclastic debris to the outer ramp. Moody & Ratcliffe (1993) described the thick deposits of nummulithoclastic debris as aprons seaward of high nummulite production. Thick sections of nummulithoclastic debris intertongue with nummulite mid-ramp deposits and basinal foraminiferal limestones (Moody 1987). This intertonguing probably reflects periodic transgression and regression.

Basinal setting

The Bou Dabbous Formation is composed of foraminiferal limestones deposited in upper bathyal water depths. These consist of fine-grained, burrowed, globigerinid packstones and wackestones intercalated with rare packstone deposits containing nummulite debris and echinoderm fragments (Fig. 6f). Sediment was deposited predominantly by suspension with subordinate gravity-flow deposition. This facies is the source rock for the El Garia nummulite reservoirs (Bailey *et al.* 1989; Hughes & Reed 1995).

El Garia diagenesis and porosity evolution

Because reservoir quality in the El Garia Formation is a function of grain types, pore types, grain size, sorting, cementation, and compaction, it is difficult to predict areas of high reservoir quality. Reservoir quality within El Garia facies is quite variable with most lime packstones and grainstones having moderate to high porosity, but relative poor permeability (generally less than 10 mD). The high amount of ineffective porosity in the El Garia Formation is caused by abundant intraparticle porosity in the living chambers (Fig. 5) and abundant microporosity (Figs 7a and 7b) in the walls of nummulite tests. The higher-quality packstones and grainstones have preserved interparticle porosity (Fig. 5) which can have permeabilities ranging from a few millidarcys to over a darcy.

Effects of grain types on porosity

Grain types and original mineralogy of El Garia sediments produced a significant influence on final pore networks. Nummulites, the dominant grain type, contain abundant intraparticle pores and micropores. Some of the microporosity is related to original fine canals in the chamber walls (Hottinger & Dreher 1974; Hottinger, 1978), but most of the microporosity is a diagenetic product of high Mg-calcite stabilization. Discocyclinids have similar microporosity. Larger Foraminifera tests disaggregate during extensive bioturbation or burial compaction. This process decreases intraparticle porosity. Echinoid fragments, another common grain type, have coarse-crystalline syntaxial calcite cement (Figs 7c and 7d), which reduces interparticle porosity near the grains. These major grain types were all high Mg-calcite, which only rarely produces mouldic porosity. Because they do not commonly dissolve during mineralogical stabilization, they do not produce calcium carbonate for cementation.

Diagenetic stages

El Garia diagenesis and pore network evolution in the mid- and outer ramp can be divided into three diagenetic stages: sea floor, shallow burial, and deeper burial. Figure 8 displays the stages of diagenesis and associated diagenetic features developed during each stage. Some diagenetic features were initiated during a shallower stage and continued to develop into the next stage.

Sea-floor processes. Sea-floor processes during El Garia deposition included physical and biological processes. Storm wave and bottom currents

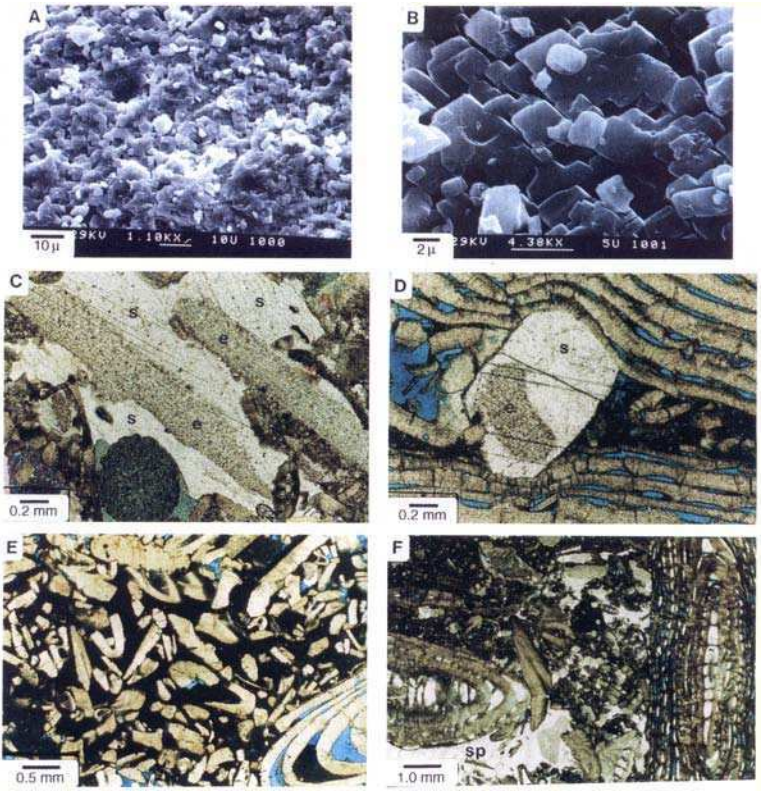

Fig. 7. Diagenetic features in the mid-ramp El Garia Formation. Samples are from offshore Tunisia. (**a**) Scanning electron micrograph of a nummulite test. The original high Mg-calcite in the test has recrystallized to microrhombic low Mg-calcite with abundant microporosity. (**b**) Close-up of upper left-hand corner of (**a**) showing aligned crystal structure of the microrhombic calcite. (**c**) Echinoid fragments (e) with coarse-crystalline syntaxial calcite (s) occluding interparticle pore space. (**d**) Syntaxial calcite (s) around echinoid grain (e). Syntaxial rim shows a compactional contact with the nummulite test, indicating that some syntaxial cement is precompaction. (**e**) Broken grains produced by bioturbation. (**f**) Irregular packing of poorly sorted sediments produced shelter porosity (sp). This sheltered void is occluded with medium- to coarse-crystalline equant calcite.

sorted the El Garia gravels and transported finer material down ramp. This enhanced interparticle porosity in the better-sorted gravels. Grain breakage (Fig. 7e) caused by physical processes and bioturbation reduced the intraparticle porosity. Bioturbation decreased sorting by remixing sediment layers previously sorted by physical processes. Bioturbation also created shelter pores in El Garia packstones, which appear as oversized irregular pores (Fig. 7f) that may be mistaken as dissolution porosity. Grain borings, some by sponges, are present in larger nummulite tests. Marine hardgrounds may have developed as evidenced by borings into lime mud.

In the sea-floor environment, the nummulite gravels contained abundant interparticle and intraparticle porosity, and some microporosity. Original porosity ranged from 40 to 70%. Nummulithoclastic sands, deposits on the outer ramp, contained interparticle and microporosity that ranged up to 40%.

Shallow-burial processes. The sediments deposited on the deep mid-ramp and outer ramp show no evidence of subaerial exposure. No near-surface meteoric waters affected them. This lack of meteoric diagenesis allowed the sediments to enter the subsurface without any early precipitated, grain stabilizing cements to inhibit compaction.

Burial mechanical compaction (Fig. 9a) is the most prominent diagenetic feature that affected El Garia gravels. Primary interparticle porosity

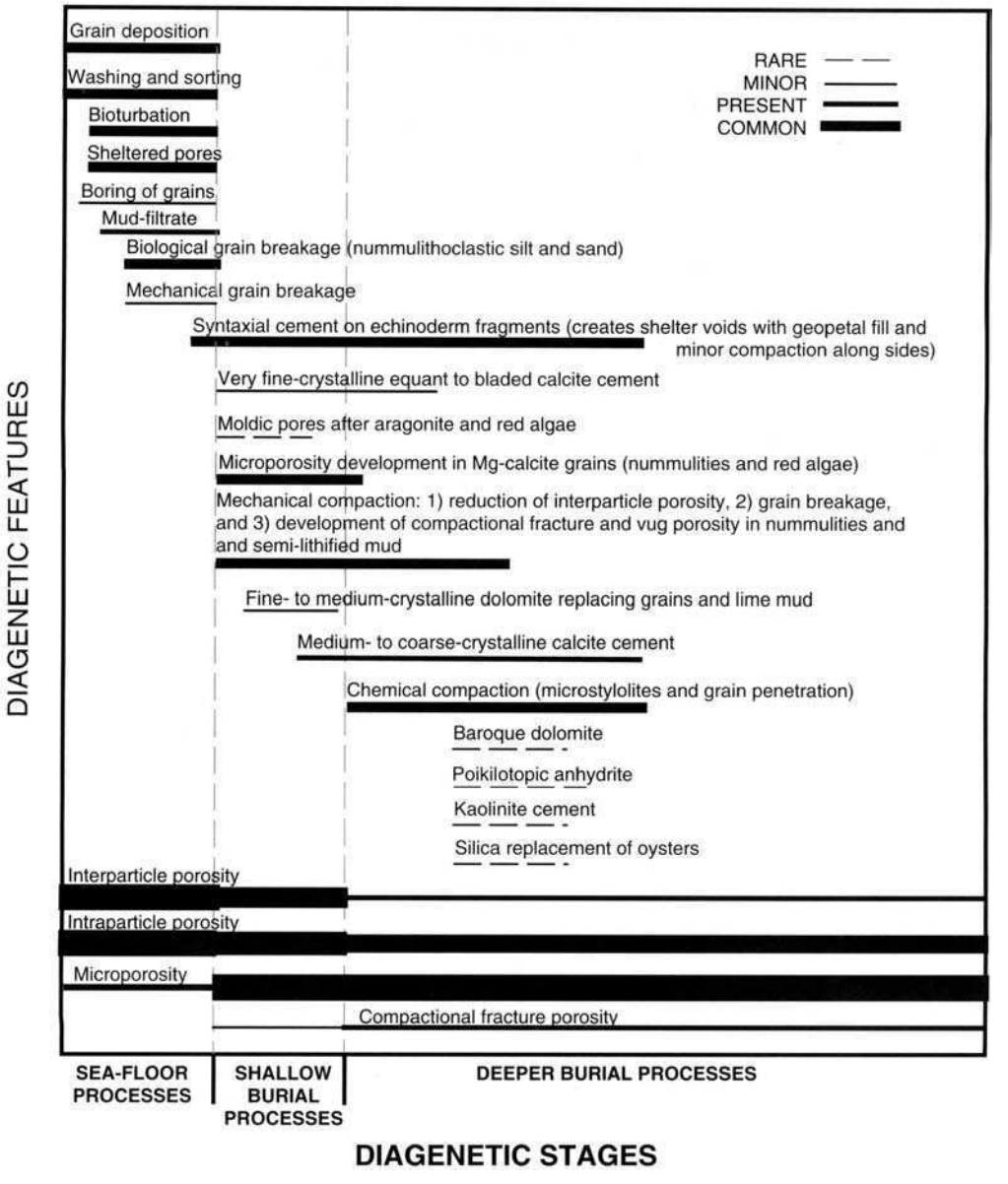

Fig. 8. Generalized diagram of diagenetic stages and associated diagenetic features for the Tunisia offshore, mid-ramp El Garia Formation.

was greatly reduced, resulting in much lower permeability. Mechanical compaction caused grain breakage, resulting in compactional fracture porosity (Fig. 9b) in nummulite tests and small fractures in semilithified mud. Vug-shaped pores were also created by compaction of semilithified muddy nummulite gravels (Figs 9c and 9d). Differential compaction split nummulite grains and mud apart in a manner that formed vugs with uneven outlines. Vugs similar to these may have been identified as burial dissolution porosity by several workers (Bishop, 1988; Bailey *et al.* 1989; Dridi & Sejil 1991). We recognized no burial dissolution porosity affecting lime mud or nummulites in any El Garia cores except in association with dolomitization. Rare mouldic

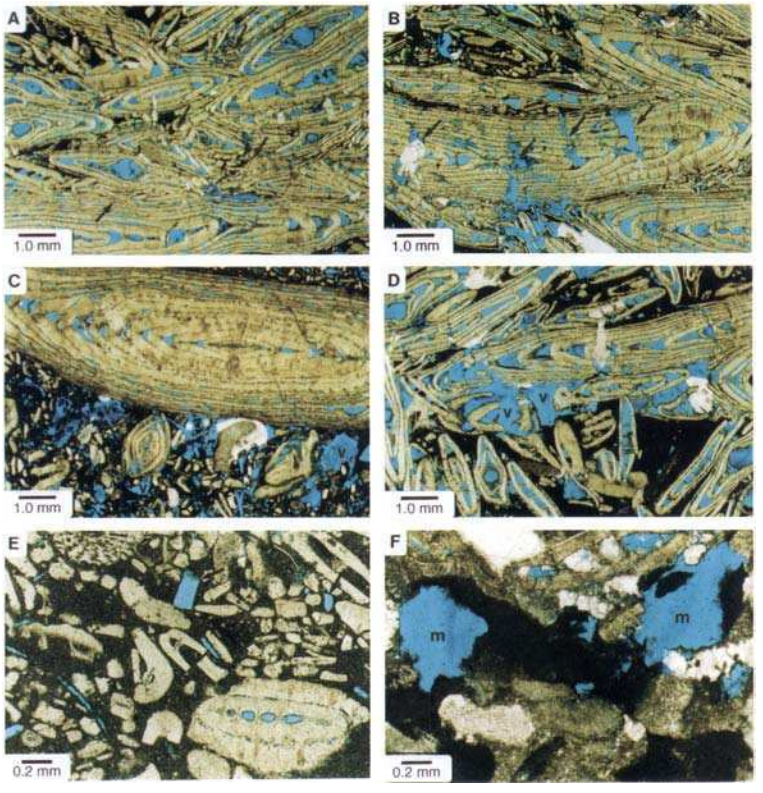

Fig. 9. Diagenetic features in the mid-ramp El Garia Formation. Samples are from offshore Tunisia. (**a**) Mechanical compaction crushed many of these nummulite tests (arrows). This reduced interparticle porosity. (Note variable crushing of grains.) (**b**) Compactional fracture porosity developed by mechanical compaction. This millimetre-scale fracture porosity connects intraparticle pores to the effective interparticle pore network (arrows). (**c**) Vug porosity (v) developed by mechanical compaction disturbing lithified grains and lime-mud. These vugs are not associated with subsurface dissolution. (**d**) Irregular shaped vugs (v) in muddy gravels produced by mechanical compaction. (**e**) Rare mouldic porosity (arrows) after mollusc fragments. (**f**) Rare mouldic porosity (m) after red-algal fragments.

pores formed in aragonite mollusc (Fig. 9e) and high Mg-calcite red algal fragments (Fig. 9), but this is a normal stabilization process produced by increased temperature and pressure with burial and is not an effect of aggressive subsurface fluids.

Microporosity formed in high Mg-calcite tests of larger Foraminifera. Scanning electron micrographs (Figs 7a and 7b) show the micropores to be related to diagenetic microrhombic equant calcite, which is a stabilization product of Mg-calcite during shallow burial (Loucks & Sullivan 1987) and/or deeper burial (Koepnick *et al.* 1994). Microporosity can contribute up to 50% or more of the pore network volume in many samples, but it does not substantially increase permeability.

Several forms of El Garia cementation were initiated by shallow burial processes, and these cement types continued to be precipitated into the deeper burial environment. The most important of these was syntaxial calcite cementation around echinoid fragments (Figs 7c and 7d). This is the only calcite cement that significantly affected porosity. It also inhibited compaction, indicating that it started to precipitate in the shallow subsurface. The amount of syntaxial cement is directly proportional to amount of echinoid fragments. Some packstones and grainstones have up to 20% echinoid fragments with 10 to 15% being fairly common.

Other cement types are rare to minor in abundance. Very fine-crystalline equant to slightly bladed calcite formed during or after compaction (Figs 10a and 10b). It rims both broken and unbroken nummulite grains. This cement type

did not inhibit compaction. Medium- to coarse-crystalline equant calcite (Fig. 10c) might have been initiated as a shallow burial cement, but most of it was probably precipitated in the deeper subsurface.

Fine-crystalline dolomite is present in several wells (Fig. 10d). In selected zones it can be relatively abundant. A 6m section in one well contains 40–90% dolomite. Dolomite crystals developed across boundaries of compacted grains, indicating that it is a syncompactional or post-compactional feature formed during burial (Fig. 10d). Most commonly, the dolomite reduces porosity by filling pores or it has no effect on porosity where it replaces grains or matrix mud. If the rock is highly dolomitized, however, it can form intercrystalline and connected-mouldic porosity (nummulite moulds) and create a permeable rock (Figs 10e and 10f). In some wells this zone is referred to as the 'drain' as noted in proprietary reports.

Deeper burial processes. Mechanical compaction continued and chemical compaction began as the sediments were buried into the deeper subsurface. Chemical compaction produced pressure solution seams between grains and stylolites that cut across grains (Figs 11a and 11b). Some samples show well-developed grain penetration (Fig. 11c).

Late cements include baroque dolomite, poikilotopic anhydrite, and kaolinite. Baroque dolomite is a well-documented burial cement that generally precipitates at temperatures from 60 to 150° (Radke & Mathis 1980). In the El

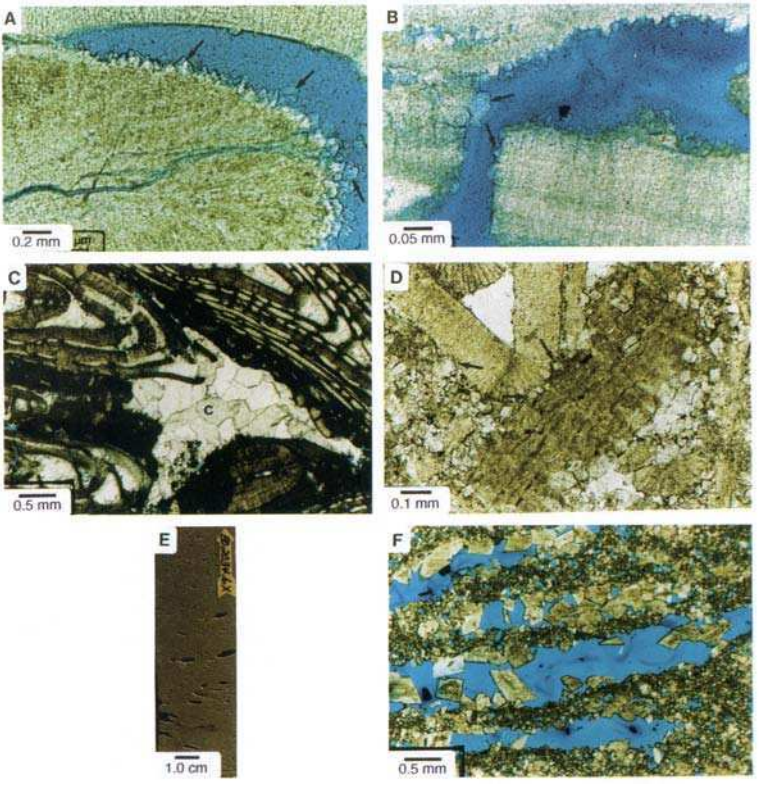

Fig. 10. Diagenetic features in the mid-ramp El Garia Formation. Samples are from offshore Tunisia. (**a**) Very fine crystalline bladed calcite (arrows) within nummulite chambers. Crystals are aligned with the crystal structure of the nummulite. This cement is most common in nummulite tests. (**b**) Compaction fracture with very fine crystalline bladed calcite (arrows) coating broken ends, indicating cement precipitated after compaction. (**c**) Medium- to coarse-crystalline equant calcite (c) filling interparticle pore space. (**d**) Fine-crystalline rhombic dolomite replacing nummulites and matrix. The dolomite appears to be after compaction because single rhombs (arrows) cut across compacted grain contacts. (**e**) The 'drain' composed of dolomite with large nummulite moulds. (**f**) The 'drain' dolomite has large mouldic pores connected by finer intercrystalline pores.

Garia gravels it was recognized in several wells filling interparticle and intraparticle pores (Fig. 10d). Poikilotopic anhydrite was seen in one well in the lowermost part of the El Garia section. Kaolinite (Fig. 10e) is rare and occurs in only a few wells. None of these cements had any appreciable effect on porosity or permeability.

Silica replacement of oyster fragments (Fig. 10f) in the form of chalcedony and megaquartz also occurred in the deeper subsurface. It most commonly affected oysters, but rare occurrences of silica replacing nummulites and echinoids were noted. Moody *et al.* (1992) interpreted silica replacement in the Compact Micrite, immediately above the El Garia Formation, to be a product of meteoric diagenesis in a near-surface mixing zone, but El Garia strata show no evidence of subaerial exposure. Silica replacement of oysters in the deeper subsurface has been documented in other studies (e.g. see Loucks (1977)). Silica diagenesis is present in all wells studied and the only apparent control on its distribution is the presence of oysters.

Pore networks and reservoir quality

Pore networks in original El Garia gravels consisted of interparticle and intraparticle porosity, and some microporosity. Porosities may have been as high as 70%. Mechanical compaction had the greatest affect on porosity loss, followed by syntaxial overgrowths on echinoderm fragments. Creation of abundant microporosity by the stabilization of high Mg-calcite and minor compactional fracture porosity by mechanical compaction increased porosity. Microporosity, however, is ineffective and did not add to permeability.

Economic reservoirs are encountered where effective primary porosity is preserved or where

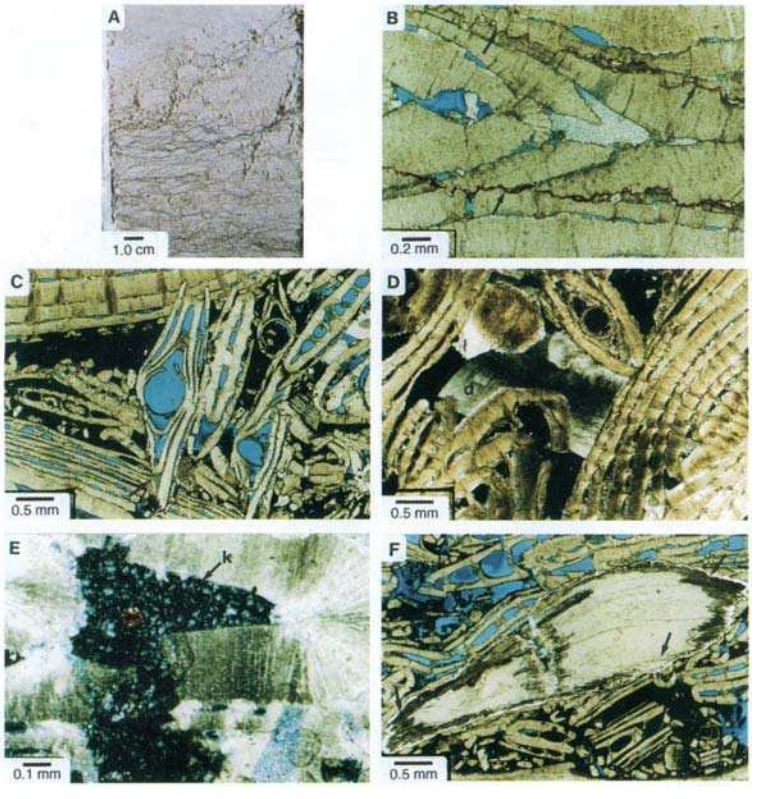

Fig. 11. Diagenetic features in the mid-ramp El Garia Formation. Samples are from offshore Tunisia. (**a**) Discrete stylolites and stylolite swarms. (**b**) Pressure solution seams (arrows) between highly compacted nummulite grains. (**c**) Compaction-produced, chemical-dissolution grain penetration (arrows). (**d**) Coarse-crystalline baroque dolomite (d) under polarized light. Baroque dolomite crystals are curved and produce undulatory extinction. (**e**) Kaolinite cement (k) in a nummulite chamber. (**f**) Ring of silica replacing oyster fragment (arrows).

intercrystalline and connected-mouldic porosity associated with dolomitization developed. Permeable nummulitic packstones and grainstones are favoured by the following factors: (1) low abundance of lime mud, (2) low abundance of nummulithoclastic debris, (3) low abundance of echinoderm fragments, (4) moderate sorting, (5) minor precipitation of late burial cements; (6) dolomitization.

Figure 12 shows the ranges of porosity and permeability in El Garia strata. Porosity averages 15.4% with a standard deviation of 5.1% and it ranges from 1.2 to 35.7%. Geometric mean of permeability is 5.6 mD and matches well with the mode of permeability (Figs 12b and 12d). Permeability ranges from 0.01 to 3400 mD. A scattergram of porosity permeability shows the effect of intraparticle porosity and microporosity (Fig. 12c). The high porosities of 15–25% have relatively low corresponding permeabilities. Most of the permeabilities are less than 10 mD. If the porosity was only the product of interparticle porosity, then the permeabilities would be in the hundreds to thousands millidarcy range (Lucia 1995)

Discussion

Ramp depositional setting

The Metlaoui ramp is similar to other ramp models (see Read 1985; Handford & Loucks 1993) relative to distribution of environmental processes. Ramps are characterized by gentle regional palaeoslopes with no sharp breaks in slope (Ahr, 1973; Read 1982, 1985). Because they have no sharp shelf break, the high-energy facies are located in the interior of the ramp and facies belts can be wide. According to Read (1985), deeper-water ramp facies of several tens of metres are characterized by muddy sands and gravels with whole and fragmented skeletal material reworked by storms and bioturbation.

The inner-ramp shoal complex (updip El Garia Formation), with landward restricted facies (Faid and Ain Merhotta formations), fits well with other ramp models. A generalized arid ramp model presented by Handford &Loucks (1993) shows a grain shoal belt with mudflats and salinas developed landward. Budd &Loucks (1981) presented a ramp model for

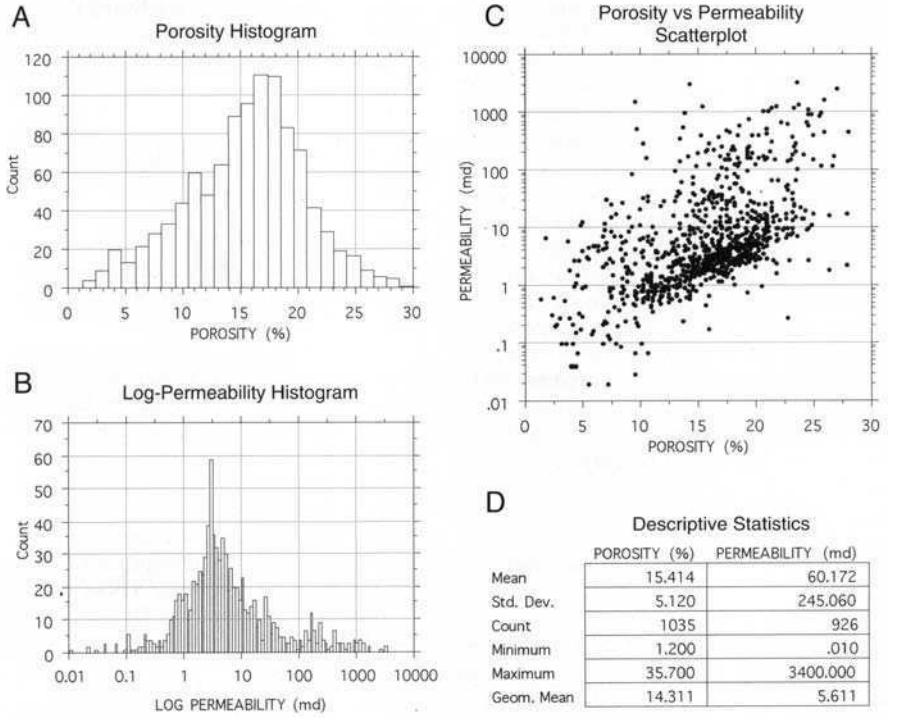

Fig. 12. Multiwell porosity and permeability statistics for offshore Tunisia mid-ramp El Garia Formation and outer-ramp Ousselat Member.

the Upper Jurassic Buckner and Smackover formations in south Texas. Thick, cross-bedded, ooid grainstone bars formed a barrier behind which low-energy lithofacies consisting of fine-grained carbonate, terrigenous sediment, and evaporites were deposited. The bar systems of inner ramps create restricted conditions landward and are responsible for the low fossil diversity, such as observed in the Ain Merhotta facies.

The main El Garia accumulation was deposited in a mid-ramp setting under lower-energy and -light conditions than the updip El Garia shoal complex. Large embayments cut into the mid-ramp producing local areas of outer-ramp to basinal environments. The mid-ramp, El Garia facies belt wraps around these embayments. Water depth may have also varied along strike because of the presence of local palaeotopographical highs. Sedimentation is not expected to be uniform in the mid-ramp environment because of these embayments and palaeotopographic highs. Because the major processes affecting the sediments were storm waves and bioturbation there is no apparent strong organization of facies within the accumulation. Relatively abrupt lateral and vertical variations in rock textures and nummulite A:B ratios are common within the strike-oriented body.

Cycles are not well developed within the El Garia Formation because of its deeper-water, mid-ramp depositional setting. A relative sea-level curve for the Lower Eocene by Haq *et al.* (1987) shows seven third-order sequences developed over a 5 ma time span. Sea level should have risen and fallen during each of these sequences. Water depth must have been great enough in the mid-ramp setting that none of the sediments were subaerially exposed during falls in sea level. Sea-level falls also do not appear to have been great enough to significantly affect sedimentation in the mid-ramp position. Several wells show no apparent cycles, whereas others show some sections where muddier sediments grade up into mud-free sediments. If these are cycles that formed in response to sea level, they do not appear to be correlative from well to well.

Depositional relief of mid-ramp nummulite accumulations

The mid-ramp accumulation of El Garia nummulites is commonly referred to as a 'bank' in Tunisia. Several workers proposed models that have fore-bank, main-bank, and back-bank facies, suggesting that the accumulation had relief significant enough to affect facies distribution (Examples: Arni 1965; Moody 1987). Aigner (1983) did note and demonstrate that nummulite build-ups in the Middle Eocene in Egypt could affect deposition of surrounding sediments. The El Garia nummulite accumulation in offshore Tunisia, however, does not have a high-relief bank morphology. Although the El Garia nummulite accumulation thickness can exceed 100 m, the slope across the accumulation at the time of deposition dipped seaward and no significant depositional relief was present. This is characteristic of mid-ramp settings. There is no special facies peculiar to the nummulite accumulations that would define a localized bank, and no strong facies organization that would suggest a back-bank to fore-bank transition. As noted above, abrupt lateral and vertical variations in facies are common. Even if there is evidence of some landward transport of sediment, it does not necessarily mean that slope has to dip landward. Storms can move sediments up a slope: a landward dip is not necessary. Also, no landward depositional dip was observed in any outcrop exposures of nummulite accumulations, nor is there evidence of landward dip in good-quality seismic data. Within the palaeobathymetric resolution, water depth over nummulite accumulations appears to be no shallower than that of landward deposits. Even if there was some local relief, it is estimated to have been at the metre scale at time of deposition.

Potential reservoir facies

Potential reservoir facies include inner-ramp El Garia packstones and grainstones, mid-ramp El Garia packstones and grainstones, and outer-ramp Ousselat grainstones.

Inner-ramp facies. The red algal–discocyclinid grainstones and packstones of the inner ramp should have good interparticle porosity with associated high permeabilites if not cemented. Because these sediments were deposited in shallow water, they may show extensive meteoric diagenesis. Early meteoric cements would inhibit compaction and promote preservation of effective interparticle porosity. These reservoirs are the furthest from the Bou Dabbous source area and may have had difficulty being charged.

Mid-ramp facies. The mid-ramp El Garia nummulite gravels contain proven, high-quality reservoirs, such as seen in the Ashtart field, the second

largest oil-field in Tunisia (Anon 1982; Anz & Ellouz 1985). There does not seem to be a well-developed facies distribution within the nummulite accumulation. The change from muddy or matrix-rich packstones to matrix-free grainstones appears to be somewhat random. This randomness is probably the result of storm processes affecting different part of the mid-ramp at different times with varying intensities. Palaeotopographical highs may have also influenced physical processes by producing localized variations in sediment texture. Strong variations in facies within the mid-ramp cause strong variations in reservoir quality both laterally and vertically. Lateral reservoir continuity can be variable, but data are not available in the literature to quantify continuity. The interval termed the 'drain' is thought to have excellent continuity in several offshore areas. The drain, however, may not be the same unit throughout the offshore area. The term is probably applied to any high-permeability unit in the lower El Garia section. It has been described as both limestone and dolomite. Vertical continuity in El Garia carbonates appears to be good. No continuous vertical permeability barriers were recognized in cores that would stratify reservoirs. Low-permeability streaks may impede vertical fluid flow locally but they probably do not have much lateral continuity.

Buried El Garia pore networks are a product of depositional fabric and mechanical and chemical diagenesis. Matrix-free sediments had the greatest potential to produce permeable interparticle pore networks in the subsurface, but compaction destroyed interparticle porosity in many rocks. Moderately sorted packstones and bimodal grainstones contain more interparticle porosity than well sorted grainstones because nummulite tests not separated by some matrix (especially well-sorted, B-rich nummulitic deposits) tended to align and compact during early burial. If too much matrix is present on the other hand, the matrix compacts excessively, destroying interparticle porosity.

Outer-ramp facies. Reservoir quality in the outer-ramp Ousselat nummulithoclastic debris is generally low. Significant compaction in both the packstones and grainstones destroyed interparticle porosity. Lime-mud matrix in the coarse silt and sand occluded interparticle porosity. In a few areas interparticle porosity is preserved, but commonly only microporosity is present. This member does not appear to have great potential for containing economic petroleum accumulations.

Exploration potential

The mid-ramp part of the El Garia Member contains the greatest reservoir potential. Exploring in the mid-ramp El Garia strata however, carries a high risk factor for locating permeable reservoirs. Porosity will generally be good, but permeability is variable. The large number of factors controlling permeability precludes a simple model for predicting location of high-quality reservoirs. Cores are essential for identifying facies and analysing reservoir quality. Porosity analysis from wireline logs cannot be used to determine permeability because of large volumes of ineffective intraparticle porosity and microporosity. Microporosity commonly contains large amounts of irreducible water, which affects wireline-log calculations. Calculated water saturations will not correspond to amount of water that will actually be produced. Sections that appear to have high water saturations may produce only oil, with the water being bound in the microporosity. Oil trapped within intraparticle pores may be difficult to produce because it is connected to the effective pore system by microporosity. This will affect recovery efficiency.

Exploration should be oriented to positioning a well into the main trend of the mid-ramp, nummulite accumulation. If nummulithoclastic-rich rocks are encountered it must be decided if the well is in the outer ramp or an mid-ramp, deep-embayment setting. This decision is important in determining whether to move updip or laterally to encounter the main nummulite accumulation. If the initial well encountered a thick nummulitic accumulation, but most of the section has low permeability, a decision on where to move is much more difficult because of the randomness of the reservoir facies in both dip and strike directions. An added complication is that different nummulite facies can be reservoirs depending on their diagenetic history. Diagenetic decrease in porosity must be distinguished from lack of porosity because of unfavourable depositional environments, so that exploration options can be adequately assessed.

Conclusions

The Metlaoui Group was deposited on a broad ramp that deepened to the northeast into the Mediterranean Sea. The ramp contains a series of broad facies belts that can be divided into inner-ramp (Faid, Ain Merhotta, and updip El Garia formations), mid-ramp (downdip El Garia Formation), and outer-ramp settings

(Ousselat Member). Seaward of the ramp, basinal sediments of the Bou Dabbous Formation were deposited.

The inner ramp is composed of three facies tracts: (1) Faid sabkha (most landward), (2) Ain Merhotta restricted shallow lagoon, (3) updip El Garia high-energy shoal complex (most seaward). Updip El Garia Formation in the outer part of the inner ramp is composed of red algal–discocyclinid grainstones and packstones, which are locally cross-bedded. Seaward from the inner ramp, the El Garia carbonates are dominated by nummulites. Textures are mud-poor packstones and poorly sorted or bimodal grainstones. Bioturbation is the only common sedimentary structure; no unambiguous fabrics indicative of hydrodynamic transport of whole nummulites are evident. There is no apparent strong subfacies organization within the accumulation. El Garia nummulitic facies of the mid-ramp overlie and grade downdip into outer-ramp Ousselat nummulithoclastic packstones and grainstones. There is a pronounced gradation from coarser to finer debris down the ramp. The Bou Dabbous Formation is composed of basinal sediments deposited in upper bathyal water depths.

Reservoir quality in the El Garia Formation is a function of grain types, pore types, grain size, sorting, cementation and compaction, and it is difficult to predict areas of high reservoir quality. Reservoir quality is variable, with most lime packstones and grainstones having moderate to high porosity, but only poor to fair permeability (generally less than 10 mD). The high amount of ineffective porosity in the El Garia Formation is caused by abundant intraparticle porosity in the living chambers and abundant microporosity in the tests of nummulites. The higher-quality packstones and grainstones have preserved interparticle porosity which can have permeabilities from the tens of millidarcys to several darcys. Permeable nummulitic packstones and grainstones are favoured by the following factors: (1) low abundance of lime mud; (2) low abundance of nummulithoclastic debris; (3) low abundance of echinoderm fragments; (4) moderate sorting; (5) minor precipitation of late burial cements; (6) dolomitization.

El Garia packstones and grainstones can form excellent hydrocarbon reservoirs but pronounced lateral and vertical textural changes affect reservoir quality. Uncertainty produced by the depositional and diagenetic variables must be taken into account when estimating risk for encountering economic reservoir quality.

We want to express our appreciation to ARCO International Oil and Gas Company for supporting this study and permission to publish some of the major conclusions. We thank N. Chine of SEREPT for making available several offshore El Garia cores. P. Thompson of ARCO Exploration and Production Technology aided in researching and in discussing the literature on larger Foraminifera. M. Scheihing of ARCO Exploration and Production Technology and J. Hollywood of ARCO International Oil and Gas Company reviewed the manuscript. This paper is based upon a conference held in Tunis, Tunisia.

References

AHR, W. M. 1973. The carbonate ramp: an alternative to the shelf model. *Transactions of the Gulf Coast Association of Geological Societies*, **23**, 221–225.

AIGNER, T. 1982. Event-stratification in nummulite accumulations and in shell beds from the Eocene of Egypt. *In*: EINSELE, G. & SEILACHER, A. (eds.) *Cyclic and event stratification*. Springer-Verlag, Berlin, 248–262.

—— 1983. Facies and origin of nummulitic buildups: an example from the Giza Pyramids Plateau (Middle Eocene, Egypt). *Neues Jahrbuch für Geologie und Palaontologie, Abhandlungen*, **166**, 247–368.

—— 1985. Biofabrics as dynamic indicators in nummulite accumulations. *Journal of Sedimentary Petrology*, **55**, 131–134.

—— 1986. Biofabrics as dynamic indicators in nummulite accumulations reply. *Journal of Sedimentary Petrology*, **56**, 320.

ALLEN, J. R. L. 1986. Some general physical implications of storms and their relevance to problems of storm sedimentation. *British Sedimentological Research Group Meeting: Storm Sedimentation, Cardiff, Abstract 3*.

ANON 1982. Worldwide production. *Oil and Gas Journal*, **80**(52), 123, 127.

ANZ, J. W. & ELLOUZ, M. 1985. Development and operation of the El Garia reservoir, Ashtart field, offshore Tunisia. *Journal of Petroleum Technology*, 481–487.

ARNI, P. 1965. L'évolution des Nummulitinae en tant que facteur de modification des dépôts littoraux. *Colloque International de Micropaléontologie (Dakar)*. Mémoires du BRGM, **32**, 7–20.

BAILEY, H. W., DUNGWORTH, G., HARDY, M., SCULL, D. & VAUGHAN, R. D. 1989. A fresh approach to the Metlaoui. *In*: *IIème Journées de Géologie Tunisienne Appliquée à la Recherche des Hydrocarbures*, Tunis, 2–3 November 1989, 281–307.

BISHOP, W. F. 1975. Geology of Tunisia and adjacent parts of Algeria and Libya. *Bulletin, American Association of Petroleum Geologists*, **59**, 413–450.

—— 1985. Eocene and Upper Cretaceous carbonate reservoirs in east-central Tunisia. *Oil and Gas Journal*, **38**(48), 137–142.

—— 1988, Petroleum geology of east-central Tunisia. *Bulletin, American Association of Petroleum Geologists*, **72**, 1033–1058.

BISWAS, B. 1976. Bathymetry of Holocene foraminifera and Quaternary sea-level changes on the Sunda shelf. *Journal of Foraminiferal Research*, **6**, 107–133.

BLONDEAU, A. 1972. *Les Nummulites*. Vuibert, Paris.

BUDD, D. A. & LOUCKS, R. G. 1981. *Smackover and Lower Buckner Formations, South Texas: Depositional Systems on a Jurassic Carbonate Ramp*. University of Texas at Austin, Bureau of Economic Geology Report of Investigations **122**, 38.

BUXTON, M. W. M. & H. M. PEDLEY, 1989. A standardized model for Tethyan Tertiary carbonate ramps. *Journal of the Geological Society, London*, **146**, 746–748.

COMPTE, D. & LEHMANN, P. 1974. Sur les carbonates de l'Ypresian et du Lutetien basal de la Tunisie centrale. *Compagnie Française des Pétroles, Notes et Mémoires*, **11**, 275–292.

DECROUEZ, D. & LATERNO, E. 1979. Les 'bancs a nummulites' de l'Eocene mesogeen et leurs implication. *Archives des Sciences*, **32**, 275–292.

DE LA HARPE, P. 1883. *Monographie der in Aegypten und der libyschen Wüste vorkommenden Nummuliten. Palaeontographica*, **30**, 155–218.

DRIDI, M. & SEJIL, A. 1991, Eocene. *In*: HMIDI, Z. & SADRAS, W. (eds) *Tunisian Exploration Review*. ETAP, 73–93.

FOURNIE, D. 1975. L'analyse séquentielle et la sédimentologie de l'Ypresian de Tunisie. *Bulletin de Centre de Recherches de Pau*, **9**, 27–75.

FOURNIE, D. 1978. Nomenclature lithostratigraphique des series du Cretace Superieur au Tertiare de Tunisie. *Bulletin des Centres de Recherches Exploration–Production Elf-Aquitaine*, **2**, 97–148.

HALLOCK, P. & GLENN, E. C. 1986. Larger Foraminifera: a tool for paleoenvironmental analysis of Cenozoic carbonate depositional facies. *Palaios*, **1**, 55–64.

HANDFORD, C. R. & LOUCKS, R. G. 1993. Carbonate depositional sequences and systems tracts—responses of carbonate platforms to relative sea-level change. *In*: LOUCKS, R. G. & SARG, R. (eds) *Carbonate Sequence Stratigraphy: Recent Advances and Applications*. American Association of Petroleum Geologists Memoir, **57**, 3–41.

HAQ, B. U., HARDENBOL, J. & VAIL, P. R. 1987. Chronology of fluctuating sea levels since the Triassic. *Science*, **235**, 1156–1166.

HOTTINGER, L. 1978. Comparative anatomy of elementary shell structures in selected larger foraminifera. *In*: HEDLEY, R. H. & ADAMS, C. G. (eds) *Foraminifera*, Vol. 3, Academic Press, London, 203–266.

—— 1983. Processes determining the distribution of larger foraminifera in space and time. *Utrecht Micropaleontology Bulletin*, **30**, 239–253.

—— & DREHER, D. 1974. Differentiation of protoplasm in Nummulitidae (foraminifera) from Elat, Red Sea. *Marine Biology*, **25**, 41–61.

HUGHES, W. B. & REED, J. D. 1995. Oil and source rock geochemistry and exploration implications. *In*: *Northern Tunisia, Proceedings of the Seminar on Source Rocks and Hydrocarbon Habitat in Tunisia*. ETAP, Tunis, 49–67.

KOEPNICK, R. B., WAITE, L. E., KOMPANIK, G. S., AL-SHAMMERY, M. J. & AL-AMOUDI, M. O. 1994. Sequence stratal geometries and burial-related microporosity development: controls on performance of the Hadriya reservoir (Upper Jurassic) Berri field, Saudi Arabia. *In*: AL-HUSSEINI, M. I. (ed.) *GEO '94, The Middle East Petroleum Geosciences*. Gulf PetroLink, Bahrain, 615–623.

LAMING, D. J. C. 1966. Imbrication, paleocurrents and other sedimentary features in the Lower New Red Bed Sandstone, Devonshire, England. *Journal of Sedimentary Petrology*, **36**, 940–959.

LOUCKS, R. G. 1977. Porosity development and preservation in a high-energy, shoal-water carbonate complex–Pearsall Formation, Lower Cretaceous, South Texas. *In*: BEBOUT, D. G. & LOUCKS, R. G. (eds) *Cretaceous Carbonates of Texas and New Mexico—Applications to Subsurface Exploration*. University of Texas at Austin, Bureau of Economic Geology Report of Investigations, **89**, 97–126.

—— & SULLIVAN, P. A. 1987. Microrhombic calcite diagenesis and associated microporosity in deeply buried Lower Cretaceous limestones (abstract). *Society of Economic Paleontologists and Mineralogists Midyear Meeting at Austin, TX*.

LUCIA, F. J. 1995. Rock-fabric/petrophysical classification of carbonate pore space for reservoir characterization. *Bulletin, American Association of Petroleum Geologists*, **79**, 1275–1300.

MOODY, R. T. J. 1987. The Ypresian carbonates of Tunisia–a model of foraminiferal facies distribution. *In*: HART, M. B. (ed.) *Micropaleontology of Carbonate Environments*. British Micropalaeontology Society Series, 82–92.

—— & GRANT, G. G. 1989, On the importance of bioclasts in the definition of a depositional model for the Metlaoui Carbonate Group. *Actes des IIème Journées de Géologie Tunisienne Appliquée à la Recherche des Hydrocarbures, Vol. 3*, Tunis, 2–3 November 1989, 409–427.

—— & RATCLIFFE, K. T. 1993. Microfacies and diagenetic controls on the reservoir potential of the Metlaoui Group carbonates (Eocene) of Tunisia (abstract). *In*: BURCHETTE, T. & HARWOOD, G. (eds) *Carbonate Petroleum Reservoirs: Models for Exploration and Development*. Petroleum Group, London.

——, SANDMAN, R. I. & FINCH, E. M. 1992. The Ypresian–Lutetian boundary, onshore Tunisia & its offshore subsurface analogue. *Actes des IIème Journées de Géologie Tunisienne Appliquée à la Recherche des Hydrocarbures*, **5**, 181–191.

RADKE, B. M. & MATHIS, R. L. 1980. On the formation and occurrence of saddle dolomite. *Journal of Sedimentary Petrology*, **50**, 1149–1168.

READ, J. F. 1982. Carbonate platforms of passive (extensional) continental margins: type, characteristics and evolution. *Tectonophysics*, **81**, 195–212.

—— 1985, Carbonate platforms facies models. *Bulletin, American Association of Petroleum Geologists*, **69**, 1–21.

REISS, Z. & HOTTINGER, L. 1984. *The Gulf of Aqaba: Ecological Micropaleontology*. Springer-Verlag, 354.

VERNET, J. P. 1971. *Étude sédimentologique de l'Éocene de Tunisie*. Rapport SEREPT.

WELLS, N. A. 1986. Biofabrics as dynamic indicators in nummulite accumulations—discussion. *Journal of Sedimentary Petrology*, **56**. 318–320.

Basin evolution and deposition during the Early Paleogene in Tunisia

A. ZAÏER[1], A. BEJI-SASSI[1], S. SASSI[1] & R. T. J. MOODY[2]

[1]*Laboratoire des Ressources Minérales, Faculté des Sciences de Tunis, Université de Tunis II, 1060 Tunis, Tunisie*

[2]*School of Geological Sciences, Kingston University, Kingston upon Thames, Surrey KT1 2EE, UK*

Abstract: The marine Paleocene and Ypresian deposits of Tunisia, within the El Haria Formation and the Metlaoui Group, have been intensively studied because of the commercial interest in phosphates and hydrocarbons. This paper presents the latest updates of isochron, lithofacies and palaeogeographical maps, and interprets the patterns identified in light of syn-sedimentary structure. This reveals a close association between structure, basin geometry and subsidence. Facies distribution during the Early Paleogene is thought to be structurally controlled along basement lineaments. These major fault systems were reactivated several times during the Mesozoic and Tertiary, with the last movements occurring as Neogene and post-Villafranchian events. The structural control of facies is most evident during the Ypresian, particularly along the 'North–South Axis' (Nosa) a sub-meridian orogenic segment of Central Tunisia. In this area the Ypresian deposits exhibit a preferred alignment with the Nosa exerting a notable influence on basin geometries and rates of local subsidence. In addition to two large islands indicated in the onshore area of Tunisia, a number of 'bald' highs are identified in the offshore, representing original submarine highs. The general pattern across Tunisia throughout the period is of a number of small tectonically controlled basins. The distribution of phosphorites, organic-rich shales and evaporites can be particularly linked to the development of restricted basins during the period.

Previous studies on the Early Paleogene of Tunisia (Pervinquière 1903; Solignac 1927; Flandrin 1948; Castany 1951; Visse 1952; Burollet 1956; Jauzein 1967; Comte & Dufaure 1973; Sassi 1974, 1980; Fournié 1978; Winnock 1980; Sassi *et al.* 1984, 1991; Bishop 1988; Bailey *et al.* 1989; Moody *et al.* 1989; Roberson 1989) detail the stratigraphy and regional paleo-geography of the Paleocene and the Early Eocene (Ypresian). However, the palaeogeographical reconstructions of previous workers vary considerably and the stratigraphic nomenclature of the Paleogene is poorly defined.

Facies thicknesses and distribution indicate a close link between Ypresian–Paleocene isopachs and tectonic lineaments. The structural elements appear to be influenced by ancient tectonic events, many of which were syn-sedimentary.

On a broad regional scale, the thickness of the Paleogene series appears to be strongly constrained by pre-existing structures and their recent evolution. Such structures are important in controlling the distribution of phosphorites in the west (Gafsa–Metlaoui Basin, Kalaa Khasba–Sra Ouertane Basin and Maknassy–Mezzouna Basin) and of organic-rich deposits in the east.

The structural framework

Throughout the geological history of Tunisia two main areas can be identified. These are the Saharan Platform and the central–northern domain. The latter is characterized by younger Mesozoic–Cenozoic sediments which were affected by the Alpine orogeny (Fig.1). Northern and central Tunisia are dominated by the Tunisian Atlas, which is divided into four or five major zones, each characterized by faults and folds of variable intensity (Fig. 2). The Tellian Atlas Zone is essentially a single thrust sheet found in the extreme north of the country (Fig. 3). The Medjerda Zone or the 'Zone of Domes', is the subject of considerable debate, with the long-accepted view of predominantly diapiric structure recently challenged by thrust and inversion theories (see Morgan *et al.* this volume). The central region of Tunisia is characterized by the broad open folds of the 'Central or Middle Tunisian Atlas' whereas in the south, in the Chott Jerid region, the structures are sub-tabular and less fractured. This area is termed the Saharan Platform Domain and it is associated with a thin sedimentary cover. To the east the Middle Atlas Zone is separated from the

ZAIER, A., BEJI-SASSI, A., SASSI, S. & MOODY, R. T. J. 1998. Basin evolution and deposition during the Early Paleogene in Tunisia. *In*: MACGREGOR, D. S., MOODY, R. T. J. & CLARK-LOWES, D. D. (eds) 1998. *Petroleum Geology of North Africa*. Geological Society, London, Special Publication No. 132, 375–393.

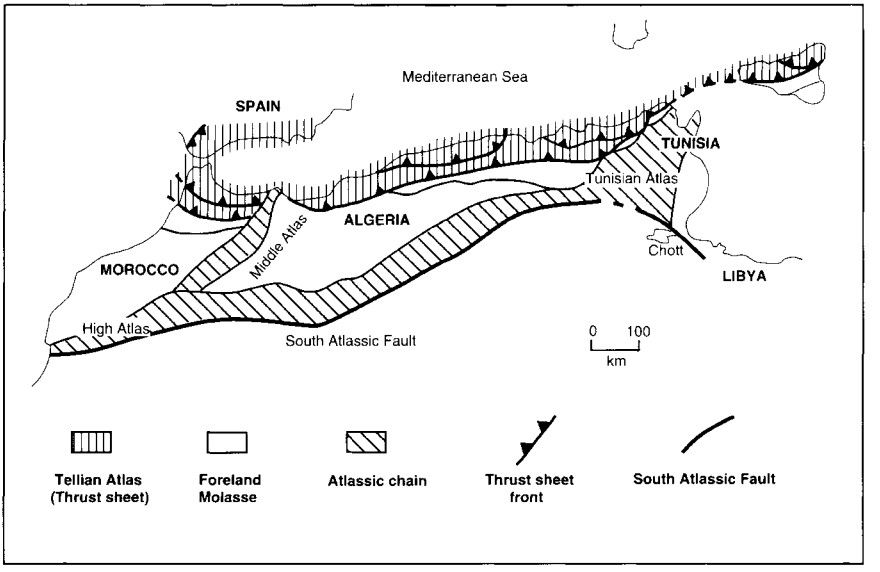

Fig. 1. The Atlassic mountain chains of the southwestern Mediterranean (after Durand-Delga & Fontboté 1980).

stable Pelagian Shelf by the North–South Axis (Nosa).

Structure along the northern African margin is strongly influenced by the collision of the African and Euro-Asian plates (Caire 1971; Durand-Delga & Fontboté 1980; Burollet & Desforges 1982). The relative movements between these two plates was not a simple N–S shortening. Pitman & Talwani (1972), Biju-Duval *et al.* 1977), Auboin & Debelmas (1980), Boillot *et al.* (1984) and Dercourt *et al.* (1985) have pointed out that the relative displacement of the two plates and kinematic forces have induced distension and compressional structures related to general movement at a specific point. During the Jurassic and the Early Cretaceous, the northern African continental margin was subjected to E–W distension (Chihi *et al.* 1984; Turki 1985; Philip *et al.* 1986; Martinez & Truillet 1987; Ouali *et al.* 1987; Bédir, 1988; Soyer & Tricart 1989; Saadi & Zargouni 1990; Delteil *et al.* 1991; Boukadi 1994), whereas in the Late Cretaceous, Tunisia was subjected to uni-directional NE–SW extension.

Throughout the Tertiary and Quaternary, the predominant structural style is compressive (Haller 1983; Turki 1985; Bédir 1988; Rigane 1991; Boukadi 1994) and tectonic events recorded during this period are a result of the Tunisian Atlas Orogeny. Perthuisot (1978), Letouzey & Trémolières (1980), Abbès (1983), Haller (1983), Yaïch (1984), Boukadi (1994) and Lanioli-Ouazaa (1994) recognized the significance of compression during this period. However, Rigane (1991) suggested that during the Ypresian, some regions of Tunisia were subjected to a transtensive regime of variable orientation. Martinez & Truillet (1987) considered that the deformation of the Early Eocene is rather poorly constrained whereas the Tertiary and Quaternary deformation appears to overprint earlier structural episodes (Delteil 1991). To constrain the structural framework of the region during the Early Paleogene, it is useful to retrace its geological history during the Late Cretaceous and so determine the pre-orogenic structures which controlled facies distribution and the rates of sedimentation and uplift (Haller 1983; Ellouz 1984; Turki 1985; Ouali *et al.* 1987; Zouari *et al.* 1990).

During the early Mesozoic, Tunisia was essentially a fault-bounded continental margin associated with Triassic uplift. Movements were induced within a NW–SE, N–S, E–W and NE–SW fault network, generating fault-controlled basins (Boltenhagen 1981; Turki 1985; Burollet & Ellouz 1986; Martinez & Truillet 1987; Boukadi 1994). Variations in sediment thickness and facies distribution are evident in the Atlas Domain, where the Triassic, essentially composed of shale and evaporites with subsidiary black dolomites and silts, is almost invariably overlain unconformably by younger sediments.

During the late Jurassic, a sandy limestone sequence was deposited in southern and central Tunisia, with the north being dominated by

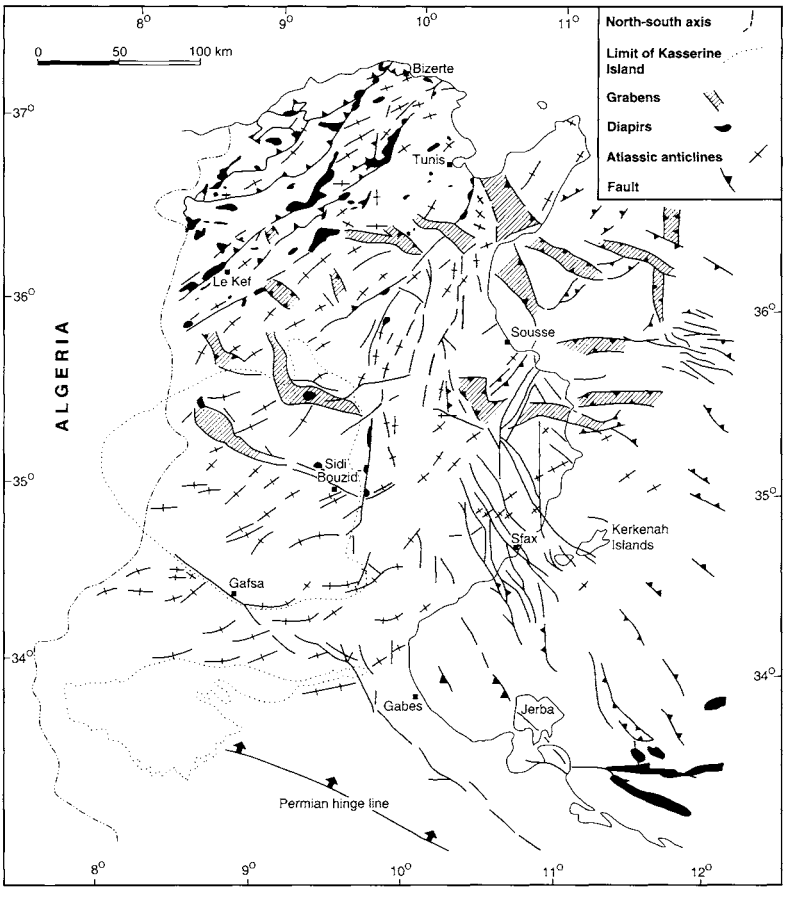

Fig. 2. Structural map of Tunisia (after Burollet 1991).

deep marine shales and limestones. Pre-orogenic structures were locally reactivated to influence facies distribution, e.g. the north or 'dorsale tunisienne' (Turki 1985), the Kef region (Chikhaoui 1988), the Nosa (Ouali 1985; Gourmelen *et al.* 1989; Soyer & Tricart 1989), and the Gafsa Chain (Zargouni 1985; Zouari *et al.* 1990; Boukadi 1994).

During the Late Cretaceous, the chalky lithofacies of the Abiod (Campanian–Maastrichian) covered a large area but localized depositional phenomena, associated with structural instability, have been identified by several workers (Jauzein 1967; Perthuisot 1978; Burollet & Desforges 1982; Marie *et al.* 1984; Yaïch, 1984; Zaïer, 1984; Burollet & Ellouz 1986; Chikhaoui 1988; Zouari *et al.* 1990; Negra 1994). These include: (1) intraformational erosive events, particularly at the base of the Abiod Formation (e.g. Maktar central–west Tunisia and Grombalia in the northeast); (2) turbidites and syn-sedimentary debris flows; at Maktar and Teboursouk and in the southern area of the Nosa at Maknassy–Mezzouna; (3) rapid thickness variations with localized 'depocentres', at Jebel Bou Dabbous (northwest of Kairouan) and in the subsurface near Sousse and Sfax. Localized sedimentation was controlled by syn-sedimentary normal faults during the Senonian. Specific faults are weakly deformed.

Diapirism is also thought to have been important in the tectonic history of northern Tunisia (Burollet 1973; Perthuisot 1978; Gourmelen 1984; Touati 1985). Research dealing with diapiric structures and their control over sedimentation (Gourmelen 1984; Perthuisot & Rouvier 1990, 1992) indicates that the first halokinetic movements were perceptible in the Jurassic, although the first significant uplift is detected in the Aptian (Perthuisot 1978; Lataar 1980; Smati 1986; Bouhlel 1993). The diapiric movements were thought to be associated with ancient

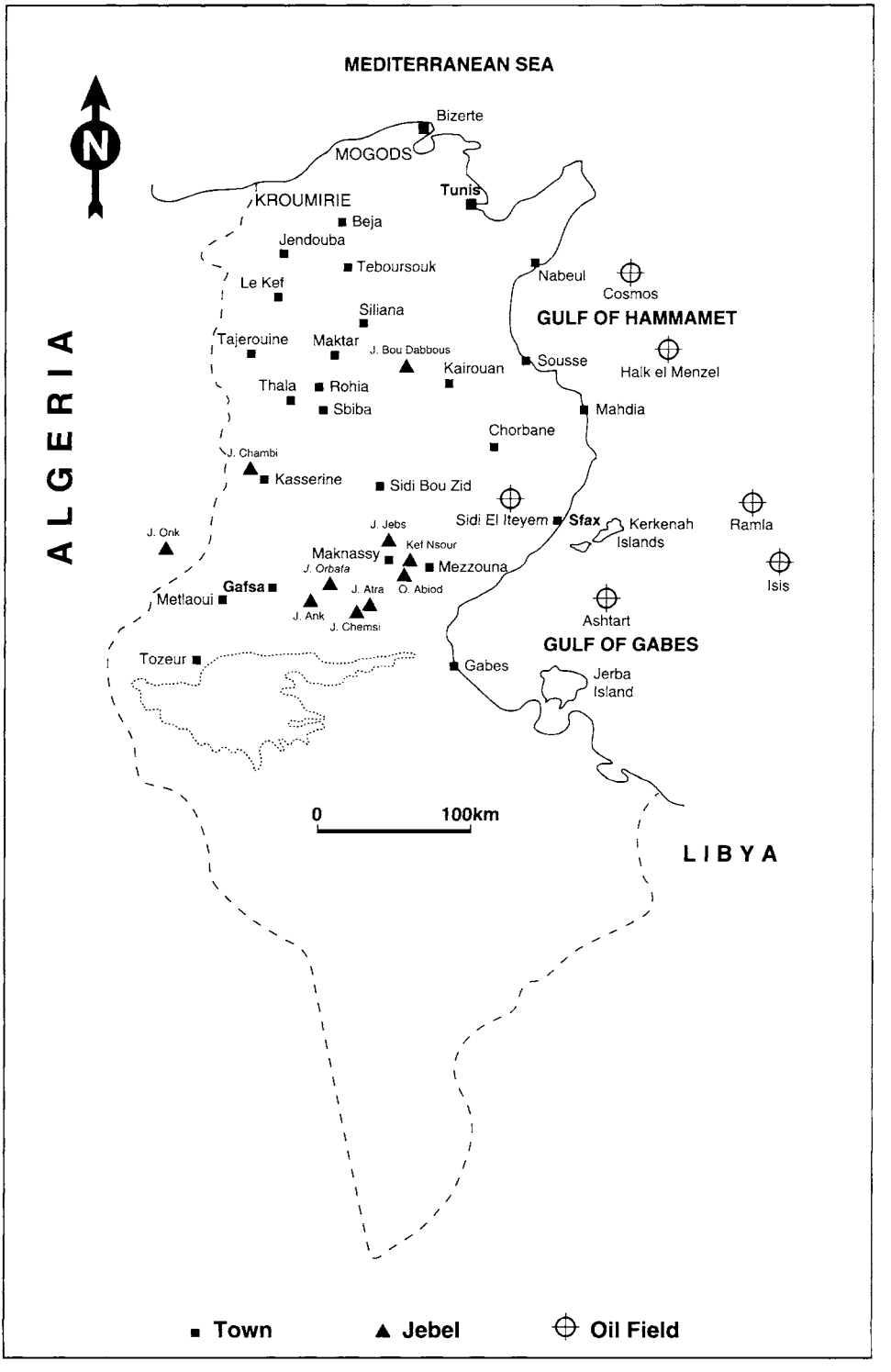

Fig. 3. Location map of towns, mountains and oilfields, mentioned in this paper.

lineaments reactivated by the African Plate movement. Perthuisot & Rouvier (1990, 1992) recorded that the diapirs continued to ascend during the Late Cretaceous and Early Tertiary, and affected local sedimentation patterns.

Arguments against diapirism were made by Baird *et al.* 1990) and Morgan *et al.* this volume). Morgan *et al.* have argued for a model of basin loading and up-gradient migration of Triassic shales and evaporites. This could easily account for the considerable variations in sediment thickness and sediment type in areas that lack salt. Recent seismic shot across the Medjerda zone supports this model of the 'leaking' of the Triassic up fault planes.

Palaeogeography and deposit evolution during the Early Paleogene

Before the Tertiary, Tethyan waters covered most of the Tunisian landmass, but during the Late Cretaceous, the Jeffara and Kasserine Islands, and other smaller areas, emerged in southern and central Tunisia. Indications of uplift and emergence are found in Jebel Kebar, J. Chambi and J. Chebket west of Sbeitla, and in Bouloufa, Jebel Idoudi and Bir Oum Ali west of Gabes (Abdeljaoued 1983; Sassi *et al.* 1984). Palaeosoils and dolocretes occur locally.

Coeval with the erosional events inferred above was the development of a deep gulf which was effectively separated from Tethys by the north–central Tunisian–Algerian basin (Sassi 1974; Winnock 1980; Bishop 1988). The Gafsa–Metlaoui Basin in the southwest was formed at this time (Berthon 1926; Flandrin 1948; Visse 1952; Sassi 1974; Moody *et al.*, 1989). During the Late Paleocene–Early Ypresian, these two basins, situated to the north and the south of the Kasserine Island, were the sites of phosphorite deposition (Burollet 1956; Comte & Dufaure 1973; Comte & Lehman 1974; Sassi 1974; Bishop 1988; Moody & Grant 1989; Sassi *et al.*, 1991).

The palaeogeography of the southern basin (Fig. 4) was such that only a restricted exchange took place between oceanic and 'intercontinental' waters. This resulted in a thick sequence of commercial phosphates being deposited before the essentially lumachellic facies of the Lutetian. Evidence for the gradual closure of this basin from the Early Oligocene exists in Jebel Ank and the Mezzouna area.

The lithostratigraphic nomenclature of the two basins lacks precise correlation. The discovery of major oilfields, such as Ashtart (Tunisia) and El Bouri (Libya), has resulted in numerous papers (Fig. 5) which have perhaps overcomplicated the original scheme set out by Burollet (1956). A revised, somewhat simplified, scheme is set out below (Fig. 5).

A detailed analysis of the Eocene–Paleocene sedimentary sequences (Fig. 6) provides important data on the geological history of each of the following basins.

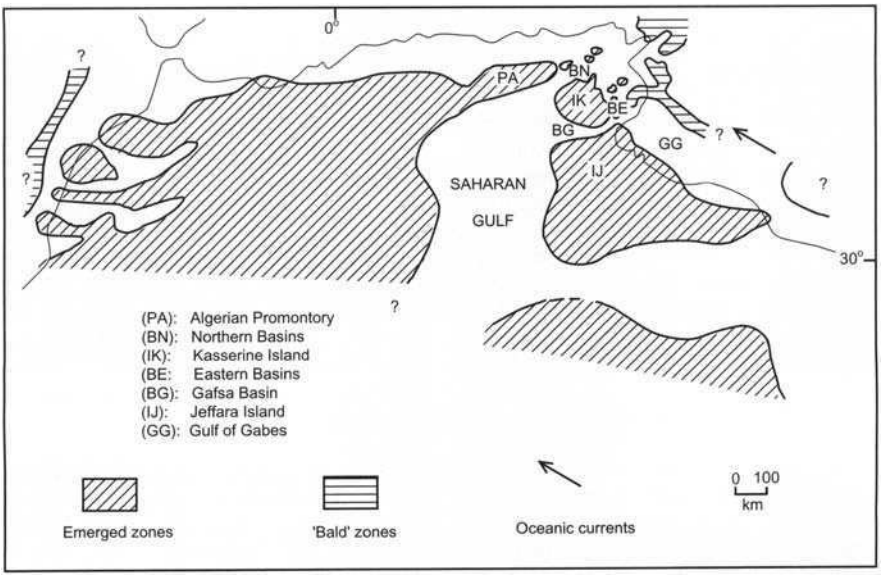

Fig. 4. Palaeogeographical map of North Africa during the Early Eocene (after Sassi 1974; Winnock 1980).

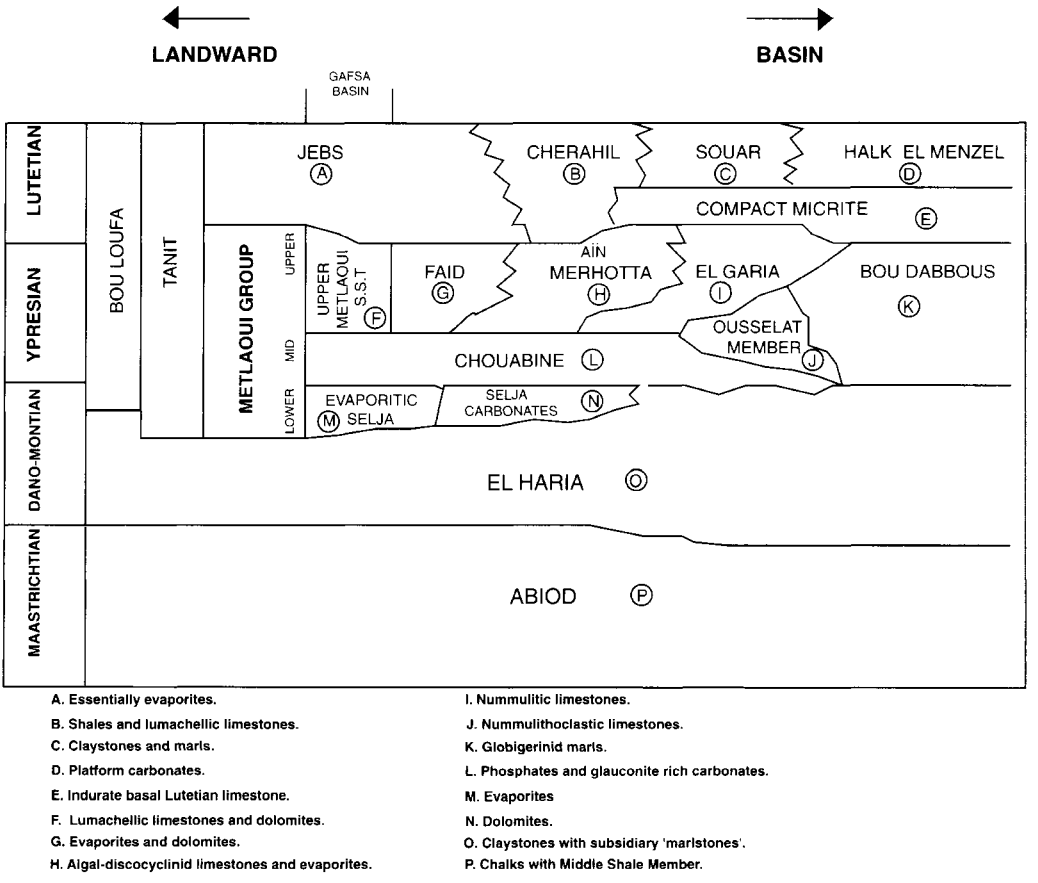

A. Essentially evaporites.
B. Shales and lumachellic limestones.
C. Claystones and marls.
D. Platform carbonates.
E. Indurate basal Lutetian limestone.
F. Lumachellic limestones and dolomites.
G. Evaporites and dolomites.
H. Algal-discocyclinid limestones and evaporites.
I. Nummulitic limestones.
J. Nummulithoclastic limestones.
K. Globigerinid marls.
L. Phosphates and glauconite rich carbonates.
M. Evaporites
N. Dolomites.
O. Claystones with subsidiary 'marlstones'.
P. Chalks with Middle Shale Member.

Fig. 5. Lithostratigraphic nomenclature of Upper Cretaceous–Lower Paleogene formations, based on models of Moody & Grant (1989) and Ben Ferjani *et al.* 1990).

Gafsa–Metlaoui Basin

The Gafsa–Metlaoui Basin (Fig. 7), situated between the Jeffara Island to the south and the Kasserine Island to the north, is characterized by a succession of shales, limestones, evaporites and phosphorites.

The top of the Upper Abiod Formation (Maastrichian) is marked by a well-developed hardground which is bored and stained red. It is overlain by a sequence of marls and shales, which are in turn overlain by limestones. These lithologies constitute the El Haria Formation which is of Middle Maastrichian–Paleocene (pro parte) age (Chaabani 1978, and 1995; Ben Abdessalam 1979) The base of the sequence may locally, be characterized by units rich in either phosphate or glauconite. The shale sequence may be missing locally with either phosphorite or glauconitic beds resting directly on the underlying Abiod limestones.

In the centre of the basin, the shales are overlain by Paleocene deposits (basal Metlaoui), consisting of bioclastic limestones which are locally lumachellic and gypsum rich. The lumachellic layers are often lens shaped and cross stratified. The sequence, termed the Selja Formation, can reach 100 m in thickness (Fig. 5). Laterally, on the margins of the basin (west, at J. Onk in Algeria, east at J. Atra, and south of J. Chemsi in Tunisia), the lower part of the Metlaoui Group is represented by lumachelles and dolomites (Sassi 1974). Dolomite, gypsum and oyster-rich shell banks are indicative of restricted environments.

The base of the Ypresian in the Gafsa Basin (Middle Metlaoui) (Fournié 1978; Chaabani 1995) is represented by the principal phosphorite series overlying a bored hard ground. The series, known as the Chouabine Formation (Fig. 5), varies in thickness from a few metres to *c.* 60 m. The formation is locally composed of nine

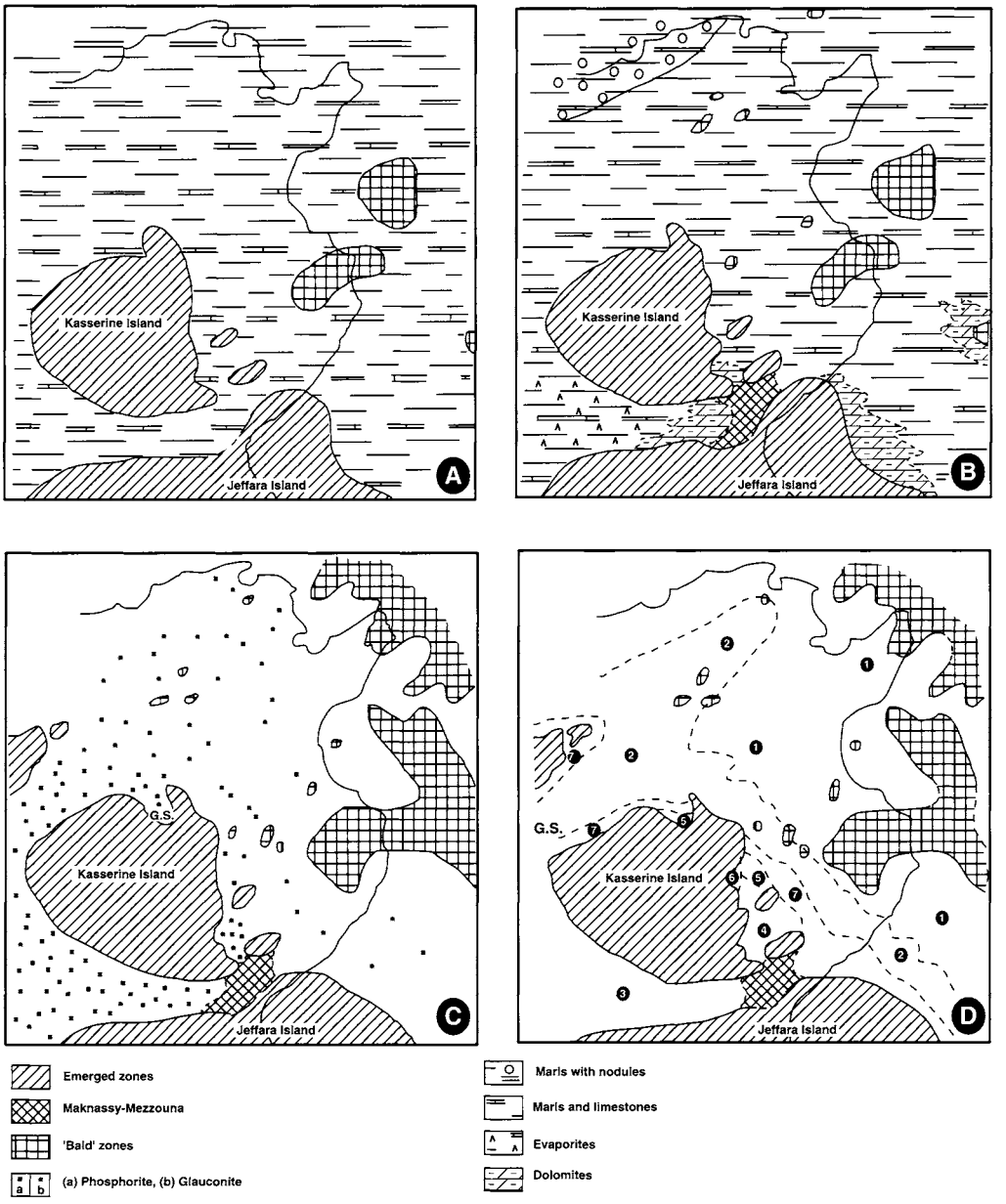

Fig. 6. Palaeogeographical evolution during the Early Paleogene. (**a**) El Haria Formation (*sensu lato*) (Paleocene *pro parte*). (**b**) El Haria Formation and laterally equivalent limestones (Late Paleocene 'Lower Metlaoui'). (**c**) Chouabine Formation and its lateral equivalent (Early Ypresian). (**d**) Upper Metlaoui (Ypresian *pro parte*). (The detailed distribution of facies 1–7 is presented in Fig. 7.) G.S., Gulf of Sbiba.

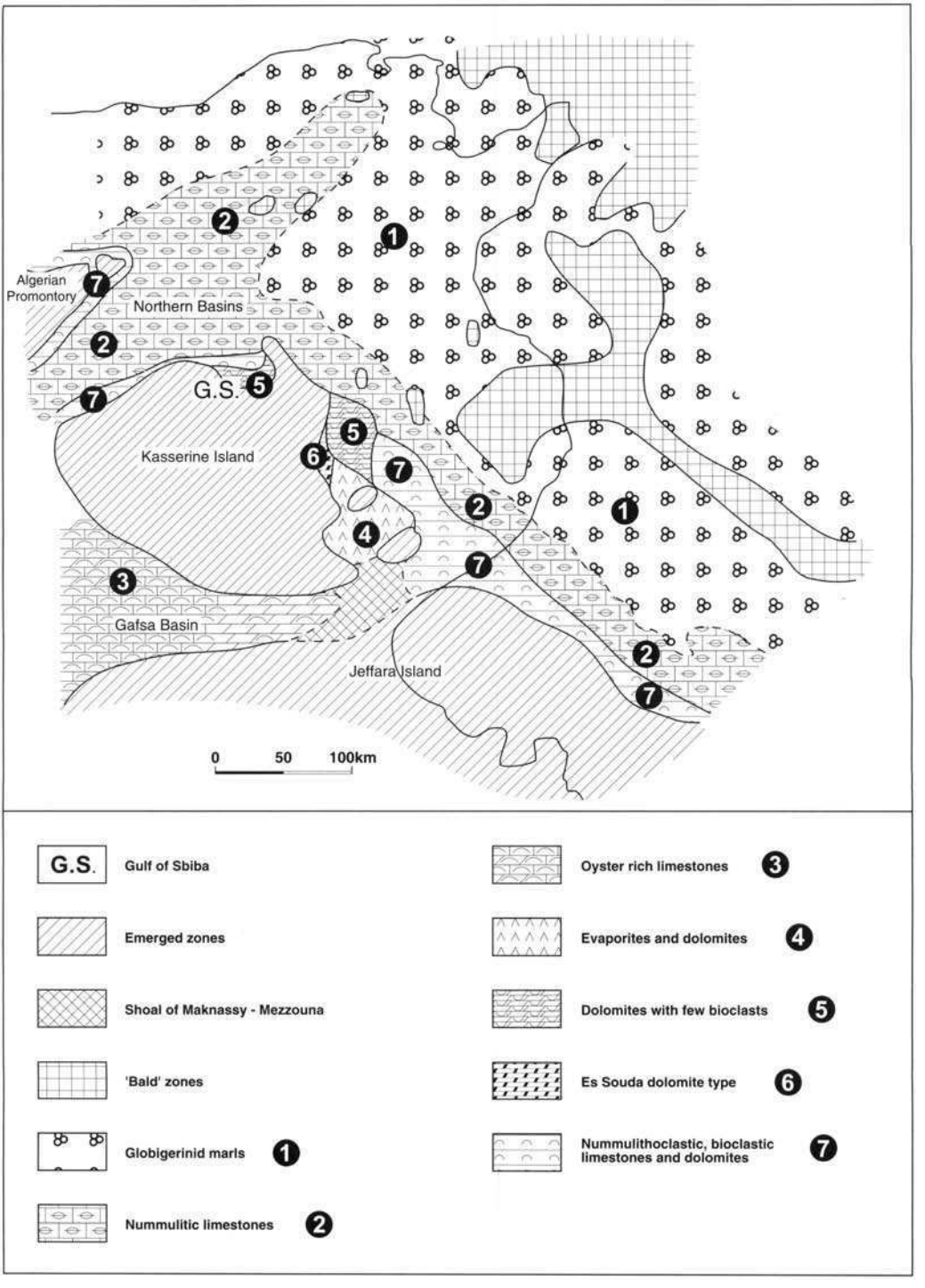

Fig. 7. Distribution map of Ypresian Metlaoui carbonates.

phosphatic units which alternate with beds of marly limestone and flint, which are variably enriched in phosphorite. In the eastern part of the basin (J. Chemsi), the amount of phosphorite decreases relative to the number of marl or carbonate horizons (Chaabani 1995), whereas to the west, silica (flint or opal) characterizes the principal levels within this formation (Sassi 1974, 1980).

The upper part of the Metlaoui Group is represented by oyster-rich limestones with phosphorite and chert-rich intercalations known as 'phosphate du toit'. Locally, the limestones may contain abundant flints (M'Rata and Onk) and are dolomitic proximal to the basin margin (to the east and also to the west) (Sassi 1974; Sassi *et al.* 1991 Chaabani 1995).

The Metlaoui carbonates are overlain by a sequence dominated by gypsum (Jebs Formation, Fig. 5) which is indicative of regional uplift and emergence during the Lutetian (Sassi 1974). Locally (J. Ank, eastern extremity of the basin), the Jebs Formation is overlain by a second phosphorite unit which, in turn, is overlain by several few metres of oolitic iron and oyster-bearing marls. These lithofacies support the thesis of a major transgression during the Late Priabonian–Early Oligocene.

Specific levels within the Paleocene–Ypresian succession of the Gafsa–Metlaoui Basin contain volcanic materials (Sassi 1974). They have a quartzo-feldspathic mineralogy with local concentrations of apatite, ilmenite and zircon. These materials indicate a rhyolitic acid volcanism, although the emission centre is not precisely located. However, Sassi (1980) and Winnock (1980) inferred that the volcanism could be situated in the eastern part of the basin or in the Gulf of Gabès (southeast of Tunisia). Hyaloclastites are a common feature of wells drilled in Upper Cretaceous sections offshore.

The Early Paleogene deposits of the Gafsa–Metlaoui Basin testify to the presence of an inlet located at its eastern extremity. This controlled communication to Tethys via the Maknassy–Mezzouna shoal (Fig. 6). The role of this inlet is most significant post El Haria, with the deposition of limestones and gypsum at the centre of the basin (Selja Formation, Late Paleocene (Lower Metlaoui Group) (Sassi 1974).

During phosphatogenesis, the inlet played an important role in regulating the amount of organic material entering the basin. Fluctuations in deposition are an indication of rhythmic or episodic sedimentation. Restricted communication with the open sea is also evident post-Metlaoui Group with evaporitic sedimentation resulting from a palaeotopographical bottleneck (Figs 6 and 7). The inlet closed during the Oligocene.

Isopachs for the Paleocene (El Haria Formation and the evaporites and/or limestones of the lower Metlaoui) are elongated in two directions (Fig. 8a and b), as are those of the Early Eocene (Middle and Upper Metlaoui). The first direction of elongation (NW–SE) characterizes the western part of the basin, whereas an E–W direction predominates in the east. The two trends are directly influenced by the presence of the Gafsa fault (NW–SE) and the broad E–W fault zone associated with the Orbata–Bou Hedma orogenic segment. These two structural entities more or less constitute the southern limits of the Kasserine Island at this time (Fig. 7).

The northern basins

During the Paleocene, prolonged marine sedimentation north of the Kasserine Island took place in a quiescent pelagic setting. The episode is marked by a thick marl–shale series (El Haria Formation) which is characterized by a rich and diverse planktonic microfauna at the base with a restricted number of species in the upper part (Burollet & Sainfeld 1956, Saïd 1978; Zaïer 1984; Salaj 1990). This is indicative of a regressive sequence. The deposits have the same characteristics as those of the underlying Maastrichian. The El Haria Formation may be of reduced thickness in areas proximal to the palaeoshoreline of the Kasserine Island. The formation thickens steadily away from the northern shoreline.

During the Late Paleocene–Early Ypresian, the area between Kasserine Island and the Algerian Promontory was essentially an embayment (Sassi 1974; Zaïer, 1984), with the deposition of organic rich phosphorites under moderately oxygenated conditions (Kalaat Es Snam, Kalaat Khasba, Sra Ouertane). Further to the north and northeast, the phosphorite series passes laterally into a sequence of marls and shales with less phosphorite but more glauconite. These sediments suggest a less confined and better oxygenated environment. Lithostratigraphically, the phosphorite layers and their lateral equivalents (Chouabine Formation) constitute the base of the Metlaoui Group. Above these mineral-rich horizons, the Metlaoui Group is carbonate rich with a diverse microfauna of Ypresian age (Comte & Dufaure 1973; Fournié 1978; Ben Abdessalam 1979; Saïd 1978; Bishop 1988).

The Ypresian carbonates of the northern basins can be subdivided into several different facies (Figs 2 and 7) with the El Garia Forma-

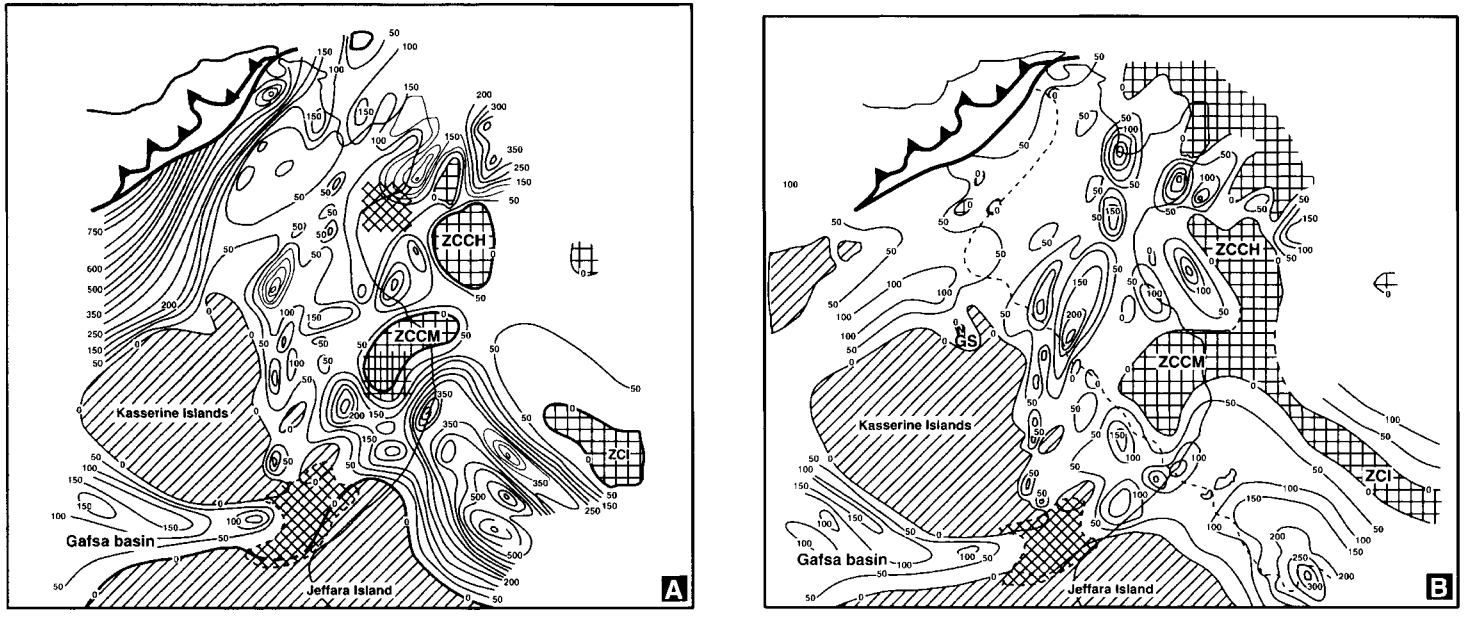

Fig. 8. (**a**) Isopach map of the Paleocene (El Haria Formation *pro parte* included in the lower part of the Metlaoui Group, south of the Kasserine Island). (**b**) Isopach map of the Ypresian Metlaoui Group carbonates (lower term included in Paleocene).

tion, Ousselat Member and Bou Dabbous Formation representative of ramp–basin sedimentation (Loucks *et al.* this volume). Isopach geometry indicates a NE–SW axis located in the area now known as the northern thrust sheet (Tell and Medjerda Zones). The overall NE–SW orientation is deflected to the NW in the Sbiba Gulf (which now corresponds to the Rohia Graben) (Fig. 8a and b). Several such deflections can be associated with fault-controlled embayments which are notably rich in organic material. Such embayments are well documented in the offshore Gulf of Gabès.

The rate of subsidence during the Ypresian is rather modest. Together, the analysis of the restored thickness and P_2O_5 content (of regional phosphorite deposits) (Zaïer 1984, 1990), reveal the independent nature of numerous small basins which are the product of localized tectonics and possible halokinesis during the Late Cretaceous–Paleocene (Fig. 9a–d)

The eastern basins

During the Paleocene the area east of the Kasserine Island was characterized by the deposition of a marl–shale sequence typical of the El Haria Formation. However, along the Nosa local variations exist (Comte & Dufaure 1973; Aubert & Berggren 1976; Fournié 1978) and field and subsurface data (Abbès 1983; Béji-Sassi 1984; Gourmelen 1984, Ouali 1985) indicate the presence of a multitude of small basins disposed in couplets or en echelon, parallel to the main structural lineament.

Within these basins the Ypresian Chouabine phosphates and their lateral equivalents are less developed than their homologues of the Gafsa–Metlaoui Basin. They are overlain by a dolostone–evaporitic succession (Jebel Kef Nsour and Oued Abiod, J. Faid, J. Rheouis and J. Nara), which is attributed to the upper part of the Metlaoui Group (Burollet 1956; Béji-Sassi 1984). The distribution of these facies is defined in Figs 2, 7 and 10. The El Garia nummulitic facies are the known reservoirs of the offshore Ashtart and Bouri fields, with the organic-rich Bou Dabbous representing the probable source to these fields. Several significant oil seeps also occur from Bou Dabbous lithologies in northern Tunisia.

In the southern area of Nosa (J. Jebs, Oued Abiod and Jebel Kef Nsour), dolomites occur at the transition with the overlying phosphorites. This succession is reminiscent of the sequence exposed at the eastern border of the Gafsa–Metlaoui Basin.

To the north, and along the eastern margin of the Kasserine Island, the transitional sequence disappears and the basal Metlaoui is represented by phosphates and glauconitic deposits of the Chouabine Formation. In the Gulf of Gabès, dolomites of Paleocene age locally overlie the El Haria Formation. These dolomites are the lateral equivalent of the basal phosphorite series and may be overlain by a total thickness of 240 m of Ypresian carbonates.

A sequence of evaporites rich in gypsum, locally dolomitic, outcrops southeast of the Kasserine Island in the enclosed basins of Maknassy–Mezzouna, in J. Jebs and J. Faid (Faid Formation). To the east and northeast, these deposits pass into the gastropodal–algal-rich carbonates of the Ain Merhotta Formation.

In the external platform, broad facies belts of nummulitic limestones and globigerinid marls characterize the eastern basins (Fig. 7). Owing to their exceptional organic content, the globigerinid limestones in this region constitute good-quality source rocks. The transition zone between the source facies and the porous–permeable nummulitic limestone (reservoir rock) is of considerable economic interest, with the Ousselat Member, nummulithoclastic apron deposits, forming a probable permeability barrier against the up-ramp nummulitic reservoir facies of the Ashtart and Sidi El Itayem fields. A clean chalky subfacies of the Bou Dabbous Formation could form an effective reservoir if sufficiently fractured.

The small basins east of the Kasserine Island along the length of the Nosa are separated by elevated or low-subsidence palaeohighs. Consequently, isopachs related to the constituent facies reflect the basin profile. The major structural control over the disposition of these areas of non- deposition is an E–W, NW–SE fracture system. Deposition was also probably influenced by major SE–NW oceanic currents which swept the Tethyan region (Figs 2 and 4).

The history of the basins east of the Kasserine Island and on the Pelagian Shelf can be documented as follows. The principal basins of Sidi El Itayem–Sidi Behara, Gremda and Ashtart situated in the Gulf of Gabès and the Sfax region are marked by the lateral transition between nummulitic reservoir and globigerinid source rocks. Each of these basins is oil rich with reservoir and source in excellent communication, as in the Ashtart field. Further to the north (Chorbane and Mahdia), a large E–W high lacking sediment deposition is identified during the Paleocene. In the Ypresian, this area expands and merges with two other 'bald' zones centred on Isis in the north east sector of

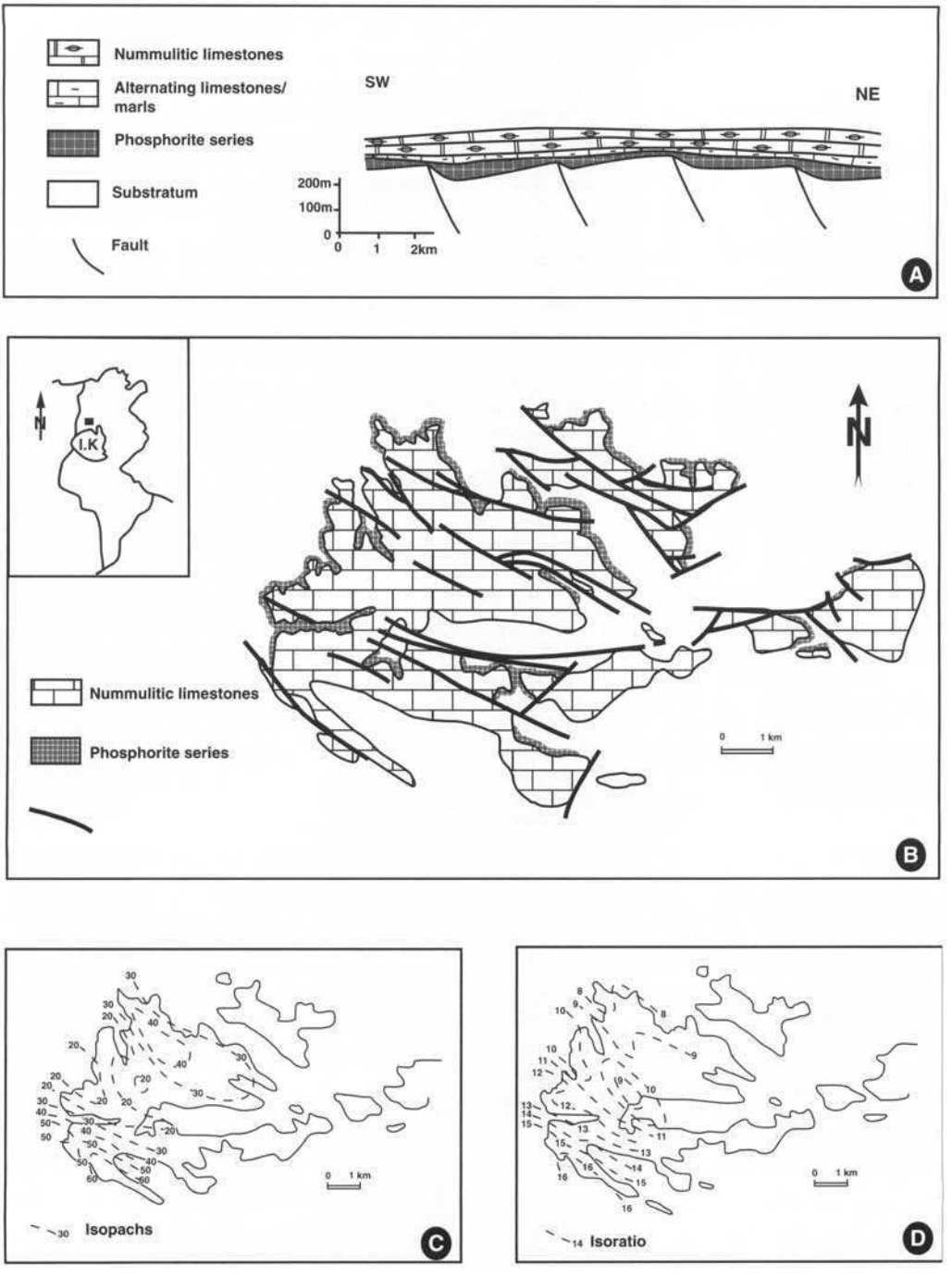

Fig. 9. (**a**) Structural interpretation of Sra Ouertane Basin during the Ypresian (northern part of the Kasserine island). (**b**) Simplified structural map of Sra Ouertane region. (**c**) Isopach map of phosphatic series in Sra Ouertane depocentre. (**d**) P_2O_5 iso-ratio curves map of phosphatic series in Sra Ouertane deposit.

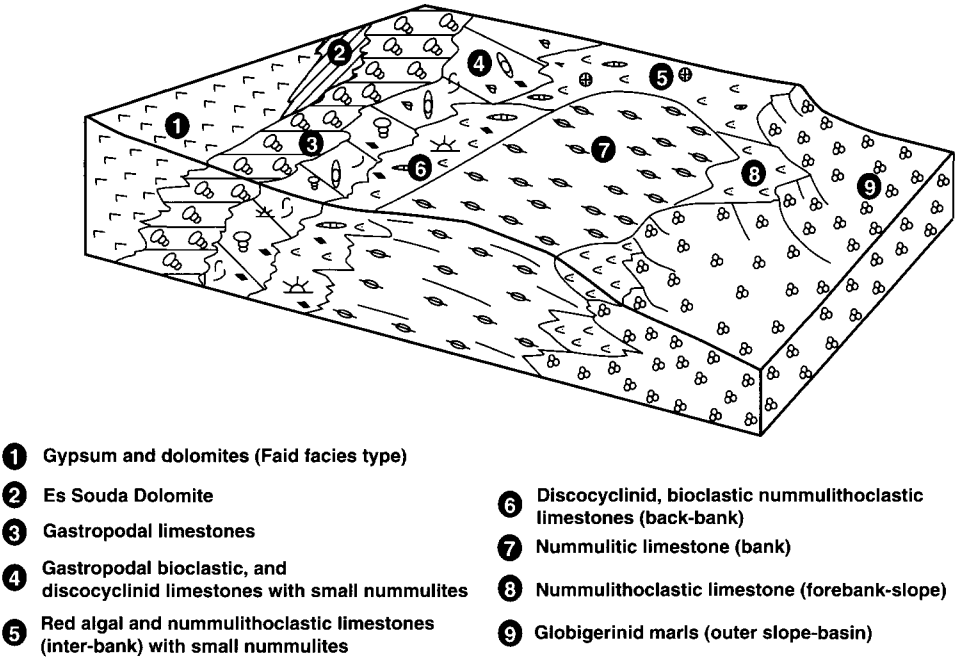

Fig. 10. Block diagram showing distribution of the Metlaoui Group facies along the eastern flank of the Kasserine island (modified after Moody & Grant 1989).

the Gulf of Gabes and Halk El Menzel–Cosmos, offshore northern Tunisia. During the Paleocene, rapid subsidence occurred in the Cap Bon and neighbouring areas. Stable or 'bald' zones evolved during the Ypresian to separate individual basins. The comparison of Paleocene and Ypresian isopach maps with tectonic data shows a limited association between the orientation of basin axes and the preferential direction of certain faults (Figs 8 and 11). Volcanic activity (calc-alkaline and acidic) similar to that in the Gafsa–Metlaoui Basin is found in the eastern basins (Béji-Sassi 1984; Béji-Sassi *et al.* 1996).

Structural framework and palaeogeography

Detailed sedimentological studies reveal that significant changes in facies type began during the Middle and the Late Maastrichian (Fig 5). The chalky limestones of the Abiod Formation pass upwards into the shales and marls of the El Haria Formation (Upper Maastrichian–Paleocene). Deep basinal sedimentation characterized this period. During the Early and Middle Paleocene, the predominant deposits were essentially marls and shales. Facies may vary slightly between regions, but they are referred in part or totality to the El Haria Formation. During the Late Paleocene, the same lithofacies occur to the north and south of the Kasserine Island. Elsewhere, to the east and west of the Gafsa–Metlaoui Basin, to the southeast of the Kasserine Island and along the palaeo-coastline of the Jeffara Island (Gulf of Gabès), the Late Paleocene is represented by shallower water carbonates. At the centre of the Gafsa–Metlaoui Basin, the equivalent lithofacies are evaporites, dolomites and lumachellic limestones.

During the Ypresian, proximal to the Kasserine Island, marine sedimentation commenced with phosphorites but away from the land mass, these give way to thick shale–limestone sequences with subsidiary phosphorites and glauconite-rich beds. These sediments are overlain by limestones, the character of which varies between regions, the type of facies being determined by local and regional palaeogeographical characteristics (Fig. 4).

Isopach maps of the El Haria and Metlaoui Formations have been presented by Burollet (1956), Jauzein (1967), Sassi (1974), Ellouz (1984), Bishop (1988) and Ben Ferjani *et al.* 1990). Although detailed, these maps do not take account of the relationships suggested in this paper between structure, sediment thickness and facies. A detailed examination of new data has enabled us to establish such links (Figs 8

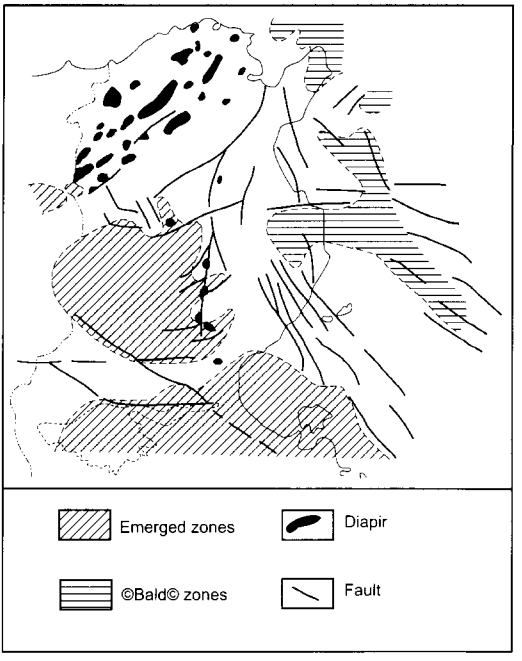

Fig. 11. Structural elements and palaeogeographical framework of Tunisia during the deposition of Ypresian facies.

and 11) and has resulted in the following observations: (a) direct links between structure and basin morphology exist in the areas of the Nosa, the Gafsa–Metlaoui basin, the Gulfs of Hammamet and Gabes and northern Tunisia, and (b) the reactivation of old fractures, halokinesis or soft sediment flow as a result of basin loading, can be closely associated with localized facies variation within these areas.

Boukadi (1994) has already described the importance of reverse faults related to the deposition of Paleocene marls in the Metlaoui region. The appearance of dolomites and evaporites during the Late Paleocene in the Gafsa–Metlaoui Basin suggests basin isolation, but fluctuations in later sedimentation reveal that a 'valve-like' inlet ensures a continued, although episodic link between this basin and Tethys. This inlet is essentially controlled by tectonic and/or halokinetic activity in the eastern extremity of the basin (Abdeljaoued 1983; Boukadi 1985; Zargouni 1985; Chaabani 1995).

Early Eocene deposits are characterized by phosphorite sedimentation along the boundary of the Kasserine Island and economic reserves are evaluated in millions of tons. Towards the open sea, the deposits are generally poorer in phosphorite and richer in glauconite. Béji Sassi (1984), Belayouni (1984) and Zaïer (1984, 1990) supported this model for the accumulation and preservation of sufficient quantities of organic matter to give rise to economic deposits.

In the Maknassy–Mezzouna Basin, the principal phosphorite accumulations are defined by major faults linked with the Triassic. These faults were probably active during the Ypresian and contributed to the basin confinement. To the north of the Kasserine Island, the isopach and iso-phosphorus (P_2O_5) content trends (Zaïer, 1984) of the various deposits correspond to the orientation of the major faults (Fig. 9b–d). The role of local structure in the formation and the accumulation of phosphorite is again underlined.

After the initial phase of phosphorite deposition, Ypresian carbonates were deposited in facies belts broadly distributed in a NW–SE direction (Fig. 7). On the carbonate ramp, to the north and east of Kasserine Island, bioclastic accumulations of large benthic Foraminifera (nummulites, discocyclinids and orbitoids) developed. Down ramp, deposits rich in globigerinids occur, whereas inland evaporitic deposits were deposited in enclosed basins (SE extremity of the Kasserine Island).

In the Gafsa–Metlaoui Basin, deposition is characterized by the lumachellic limestones. On the boundary of this basin and in the Saharan

Gulf, the Ypresian carbonates are dolomitized (Busson 1971; Sassi 1974). This was induced by the presence of restricted environmental conditions resulting from limited communication with the open sea.

Isopach reconstructions of Early Eocene deposits (Fig. 7b) indicate that facies distribution and basin geometry are similar to those of the Paleocene (Fig. 7a), although lithofacies distribution shows a less direct relationship to basin configuration. This is due to the additional influences of physico-chemical conditions and sediment input at this time. It should be noted that the bathymetry of specific basins is controlled by the eustatic changes in sea level and by tectonic and/or halokinetic movements. Thus, the nummulitic accumulations were deposited under a limited water depth. The exceptional and local appearance of some nummulitic lenses, above dolomitic or globigerinid facies, is explained by basin isolation resulting from tectonic and/or halokinetic control (Jebel Es Souda in Central Tunisia, subsurface Gulf of Gabes, and in northern Tunisia). In northern areas (Hedhil, Kef, Teboursouk) some workers (Kujawsky 1969; Sassi 1974; Ben Haj 1978; Perthuisot 1978; Ghanmi 1980) have described black quartz crystals, which appear to be Triassic in origin, associated with the nummulitic deposits and phosphorites. Their presence may support the theory of the periodic flow of Triassic evaporites and shales locally influencing facies variation.

Conclusions

A study of the Paleocene and Eocene series has permitted the precise location of the emergent zones and 'bald' zones at these times. It also confirms the presence of an inlet controlling communication between the Gafsa–Metlaoui Basin and Tethys. This inlet has controlled the distribution of facies between the Kasserine Island and the Jeffara Island, particularly from the Late Paleocene through to the Ypresian.

During the Paleocene–Eocene interval, the marine basins remained relatively stable although sedimentation patterns and bathymetry continued to evolve. Thus, zones characterized by pelagic deposits during the Paleocene become sectors of reduced subsidence during the Eocene. Localized 'bald' or emergent areas were swept by currents.

During the Tertiary, the African continent was separated from Tethys by an archipelago composed of the Kasserine–Jeffara Islands and other smaller islands. A general regression along its shoreline resulted in the appearance of several zones of uplift and shallowing. These limited the influx of marine water and resulted in the presence of several basins whose subsidence is limited (150 m), compared with the more easterly basins (350 m in the of Gabès Gulf).

During this period, the eastern coastline of Kasserine Island was the centre of biochemical–chemical deposition. The lack of detrital deposits suggests that the climate was hot and dry, and subject to chemical alteration, uplift and limited transport resulting in the development of palaeo-soils with 'dolocretes'. The palaeogeographical framework explains the development of lagoonal deposits along the boundary of Kasserine Island during the Ypresian.

Isopachs of Paleocene and Ypresian sediments clearly illustrate the existence of zones of variable subsidence. These indicate that the basins have an axial orientation analogous to that of the large faults of the period.

The existence of small basins, 'en echelon' along the Nosa with localized high rates of subsidence, emphasizes the complex nature of the structure. Burollet (1991) suggested that the Nosa formed along a deep meridian fracture of 'Pan-African' origin. The zone was characterized during the Cretaceous and Tertiary by a series of palaeohighs and/or grabens which were carried on a salt ridge. Ouali (1985) and Gourmelen (1984) proposed that at least one area of the Nosa is formed of several generations of tilted blocks. It appears therefore that the deposition was influenced by the halokinesis and/or the reactivation of faults.

Boukadi (1994) stated that when two major faults converge, the Triassic deposits are usually mobilized and that the mobility of Triassic salt is affected by frequent intrusive pulsations and extrusions. However, it is difficult to distinguish between the rate of halokinesis and other tectonic events noted by various workers (Burollet 1956, 1991; Abbès 1983; Gourmelen 1984; Yaïch 1984; Ouali 1985; Gourmelen *et al.* 1989). To the north of Kasserine Island, deposition during the Paleocene increased from the south to the north. During the Ypresian, a wide NE–SW zone developed which corresponds to the zone des diapirs' or Medjerda Zone. The zone is characterized by a low rate of subsidence and by the development of nummulitic limestones. The majority of research carried out in this region records a high level of halokinetic activity, with piercement immediately preceding or occurring during the Ypresian (Ben Haj 1978; Perthuisot 1978; Ghanmi 1980; Zaïer 1990). It is believed that the movement of Trias-

sic evaporites and shales induced heaving and created shallow water conditions conducive to deposition of nummulitic limestones. The movement of the Triassic deposits resulted in the modification of the basin geometry (Fig. 12).

The variation in thickness and facies distribution of Paleocene–Ypresian deposits is governed by the relative reactivation of ancient faults, which were developed by tectonic and/or halokinetic events during the Upper Cretaceous–Paleocene. However, the influence of tectonics on facies and sediment thickness in the 'zone des diapirs' and along the Nosa is amplified by later movement of Triassic sediments because of basin loading during the Upper Cretaceous–Paleocene.

The morphology of the basins and their ability to accumulate sediments reflect the continued structural control on sediment type. The type of deposit is related to bathymetric conditions and marine influence. This resulted in the deposition of Ypresian evaporites in small embayments along the eastern coast of Kasserine Island. These southern basins of the Nosa (southeast of Kasserine Island) were separated from the open sea by a succession of shallows and islets, which limited the exchange with the open-sea (Figs 6 and 7).

The authors of this paper would like to thank ETAP for providing the subsurface data used in the drafting of the palaeogeographical and isopach maps. They also thank A. Mabrouk and P. Sutcliffe of Kingston University, and H. Hemissi of the University of Tunis II for their helpful suggestions during review and translation of this work. This manuscript benefited from the suggestions and comments of E. Mercier and F. Orsag of the University of Paris Sud Orsay, H. Belayouni of the University of Tunis II and M. Slansky of the BRGM (France). Finally, we thank S. Bignold of Kingston University for his assistance with the cartography.

References

ABBÈS, C. 1983. *Étude structurale du Jebel Touila. Extrémité septentrionale du chaînon N S Sidi Khalif–Nara–El Houareb.* Thèse 3ème cycle, University of Tunis.

ABDELJAOUED, S. 1983. *Étude stratigraphique, sédimentologique et structurale de l'extrémité orientale de la Chaîne Nord des Chotts.* Thèse 3ème cycle, University of Tunis.

AUBERT, J. & BERGGREN, W. A. 1976. Paleocene benthic foraminiferal biostratigraphy and paleoecology of Tunisia. *Bulletin du Centre de Recherches de Pau*, **7**(1), 99–110.

AUBOIN, J. & DEBELMAS, J. 1980. L'Europe alpine: les chaînes périméditerranéennes: introduction. *In: Géologie des Chaînes Alpines Issues de la Téthys, Colloque C5, 26ème Congrès Géologique International, Paris*, 62–66.

BAILEY, H. W., DUNGWORTH, G., HARDY, M., SCULL, D. & VAUHAN, R. D. 1989. A fresh approach to the Metlaoui. *In: Actes des IIème Journées de Géologie Tunisienne Appliquée à la Recherche des Hydrocarbures.* Mémoire de l'ETAP, **3**, 281–307.

BAIRD, A. W., GROCOTT, J., SANDMAN, R. I., GRANT, G. G. & MOODY, R. T. J. 1990. A radical re-inter-

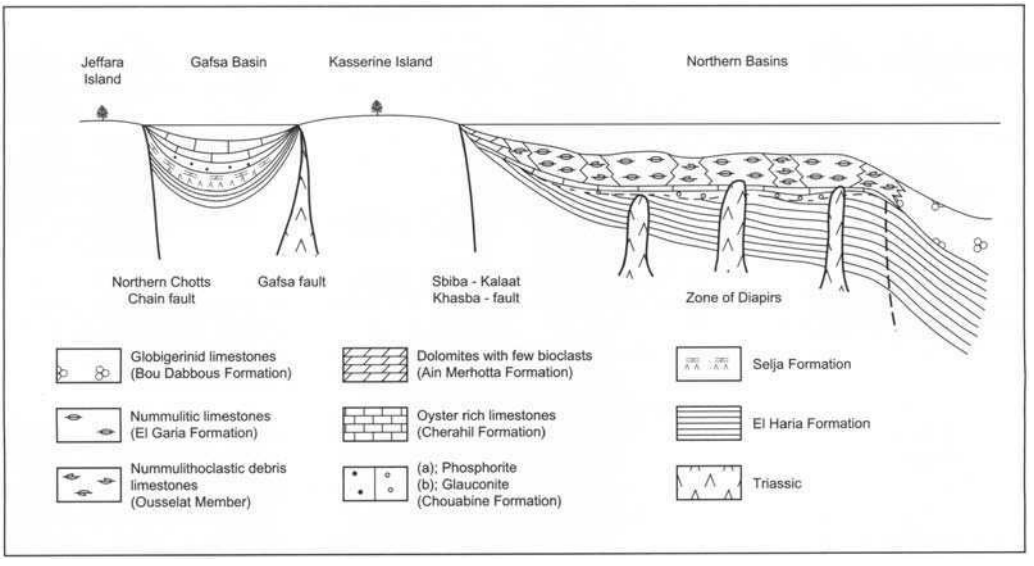

Fig. 12. North south section across the Jeffara Island, Gafsa Basin, Kasserine Island and northern basins during the Ypresian.

pretation of the Tunisian Atlas thrust belt and foreland basin system. *In: International Conference on Thrust Tectonics, Royal Holloway and Bedford New College, Programme and Absracts*, 81.

BÉDIR, M. 1988. Géodynamique des Bassins Sédimentaires du Sahel de Mahdia (Tunisie orientale) de l'Aptien à l'Actuel, Sismotectonique et Structurale. *Revue des Sciences de la Terre, Tunis*, **9**.

BÉJI-SASSI, A. 1984. *Pétrographie, Minéralogie et Géochimie des sédiments phosphatés de la bordure orientale de l'Ile de Kasserine (Tunisie)*. Thèse 3ème cycle, Université d'Orléans, 230 p.

——, LARIDI-OUAZAA, N. & CLOCCHIATI, R. 1996. Les inclusions vitreuses des ilménites, apatites et quartz des sédiments phosphatés de Tunisie: témoignage d'un volcanisme alcalin d'âge paléocène supérieur à éocène. *Bulletin de la Société Géologique de France*, **167**(2), 227–234.

BELAYOUNI, H. 1984. *Étude de la Matière Organique dans la Série Phosphatée du Bassin de Gafsa-Métlaoui (Tunisie). Application à la Compréhension des Mécanismes de la Phosphatogenèse*. Document du BRGM, **77**.

BEN ABDESSLAM, S. 1979. *Étude palynologique et micropaléontologique de la série phosphatée du bassin de Gafsa–Métlaoui (Tunisie). Application à la compréhension des mécanismes de la phosphatogenèse*. Thèse 3ème cycle, Université de Paris VI.

BEN FERJANI, A., BUROLLET, P. F. & MEJRI, F. 1990. *Petroleum Geology of Tunisia*. ETAP, Tunis.

BEN HAJ, A. M. 1978. *Étude géologique du Djebel Gorraa, (région de Téboursouk—Atlas tunisien)*. Thèse 3ème cycle, Université de Paris VI.

BERTHON, L. 1926. Les réserves de la Tunisie en acide phosphorique. *In: Les Réserves Mondiales en Phosphates*. Publication XIVème Congrès International Madrid, 1926, Publication 1928, Vol. 2.

BIJU-DUVAL, B., DERCOURT, J. & LE PICHON, X. 1977. From the Tethys ocean to the Mediterranean seas: a plate tectonic model of the evolution of the western Alpine system. *International Symposium, Structural History of the Mediterranean Basins*. Technip, Paris, 143–164.

BISHOP, W. F. 1988. Petroleum geology of East–Central Tunisia. *Bulletin, American Association of Petroleum Geologists*, **72**(9), 1033–1058.

BOILLOT, G., MONTADERT, L, LEMOINE, M. & BIJU-DUVAL, B. 1984. Le cadre géologique régional et les contraintes de la tectonique des plaques. *In: Les Marges Continentales Actuelles et Fossiles Autour de la France*. Masson, Paris, 157–178

BOLTENHAGEN, C. 1981. Paléogéographie du Crétacé moyen de la Tunisie Centrale. *1er Congrès National des Sciences del la Terre, Tunis 1981*, Vol. 1, 97–114

BOUHLEL, S. 1993. *Gîtologie, minéralogie et essai de modélisation des minéralisation à F–Ba–Sr–Pb–Zn–(S°)* associées aux carbonates (jurassique et crétacés) et aux diapirs triasiques: gisements de Stah-Kohol, Zriba-Guebli, Bou Jaber et Fej Lahdoum (Tunisie septentrionale). Thèse Doct. ès Sci., Université de Tunis II.

BOUKADI, N. 1985. *Évolution géométrique et cinématique de la zone d'interférence de l'Axe Nord-Sud et de la chaîne de Gafsa (Maknassy–Mezzouna et Jebel Bou Hedma), Tunisie*. Thèse 3ème cycle, Université de Strasbourg, 155 p.

—— 1994. *Structuration de l'Atlas de Tunisie: signification géometrique et cinématique des noeuds et des zones d'interférences structurales au contact des grands couloirs tectoniques*. Thèse Doct. ès Sciences, Université de Tunis II, 249p.

BUROLLET, P. F. 1956. Contribution à l'étude stratigraphique de la Tunisie Centrale. *Annales des Mines et de la Géologie (Tunis)*, **18**.

—— 1973. Importance des facteurs salifères dans la tectonique tunisienne. *Annales des Mines et de la Géologie (Tunis)*, **26**, 111–120.

—— 1991. Structures and tectonics of Tunisia. *Tectonophysics*, **195**, 359–369.

—— & DESFORGES, G. 1982. *Dynamique des bassins néo-crétacés en Tunisie*. Livre jub. G. Lucas; Mémoires Géologiques de l'Université de Dijon, **7**, 381–389.

—— & ELLOUZ, N. 1986. L'évolution des bassins sédimentaires de la Tunisie Centrale et Orientale. *Bulletin des Centres Recherche Exploration–Production Elf-Aquitaine*, **10**(1), 49–68.

—— & SAINFELD, P. 1956. *Notice explicative de la carte géologique au 1/50 000 de Tajerouine*.

BUSSON, G. 1971. *Principes, méthodes et résultats d'une étude stratigraphique du Mésozoïque saharien*. Thèse Doct. ès Sci. naturelles, Université de Paris VI.

CAIRE, A. 1971. Chaînes alpines de la Méditerranée centrale (Algérie et Tunisie septentrionale, Sicile, Calabre et Apennin méridional). *In: Tectonique de l'Afrique (Sciences de la Terre, 6)*. UNESCO, Paris, 61–90.

CASTANY, G. 1951. *Etude géologique de l'Atlas tunisien oriental*. Thèse Doct. ès Sci., Annales des Mines et de la Géologie (Tunis), **8**.

CHAABANI, F. 1978. *Les phosphorites de la coupe-type de Foum Selja (Métlaoui, Tunisie), une série sédimentaire séquentielle à évaporites du Paléocène*. Thèse 3ème cycle, Université Louis Pasteur Strasbourg.

—— 1995. *Dynamique de la partie orientale du bassin de Gafsa au Crétacé et au Paléogène. Etude minéralogique et géochimique de la série phosphatée éocène. Tunisie méridionale*. Thèse Doct. ès Sci. Université de Tunis II.

CHIHI, L., DLALA, M. & BEN AYED, N. 1984. Manifestations tectoniques synsédimentaires et polyphasées d'âge Crétacé moyen dans l'Atlas Tunisien Central (Région de Kasserine). *Comptes Rendus Hebdomadaires des Séances de l'Academie des Sciences, série II, 298*(4), 141–146

CHIKHAOUI, M. 1988. *Succession distention-compression dans le sillon tunisien, secteur de Nebeur, El Kef, Tunisie centre nord*. Thèse d'Univ. Université de Nice.

COMTE, D. & DUFAURE, P. 1973. Quelques précisions sur la stratigraphie et la paléogéographie tertiaires en Tunisie Centrale et Centro-Orientale du Cap Bon à Mezzouna. Annales des Mines et de la Géologie (Tunis), **26**.

—— & LEHMAN, P. 1974. *Sur les carbonates de l'Yprésien et du Lutétien basal de la Tunisie centrale*.

Compagnie Française des Pétroles, Notes et Mémoires, **11**, 275–292.

DELTEIL, J., ZOUARI, H., CHIKHAOUI, M., *et al.* 1991. Relation entre ouvertures téthysienne et mésogéenne en Tunisie. *Bulletin de la Société Géologique de France*, **162**, 1173–1181

DERCOURT, J., ZONENSHAN, L. P., RICOU, L. M., *et al.* 1985. Présentation de 9 cartes paléogéographiques au 1/20 000 000 s'étendant de l'Atlantique au Pamir pour la période du Lias à l'Actuel. *Bulletin de la Société Géologique de la France*, (8), I, 5, 637–652.

DURAND-DELGA, M. & FONTBOTÉ, J. M. 1980. Le cadre structural de la Méditerranée occidental. Géologie des chaînes alpines issues de la Téthys. *Colloque C5 du 26ème C.G.I.* Mémoire du BRGM, **115**, 65–85.

ELLOUZ, N. 1984. *Etude de la subsidence de la Tunisie atlasique, orientale et de la Mer pélagienne.* Thèse 3ème cycle. Université P. et M. Curie, Paris VI.

FLANDRIN, J. 1948. Contribution à l'étude stratigraphique du Nummulitique algérien. Bulletin du Service Géologique d'Algérie (2): Stratigraphie, Alger, **4**(19).

FOURNIÉ, D. 1978. Nomenclature lithostratigraphique des séries du Crétacé supérieur au Tertiaire en Tunisie. *Bulletin des Centres de Recherches Exploration–Production Elf-Aquitaine*, **2**(1), 97–148.

GHANMI, M. 1980. *Etude géologique du Jebel Kebbouch (Tunisie septentrionale)*, Thèse, 3ème cycle, Université Paul Sabatier, Toulouse.

GOURMELEN, C. 1984. *Serrage polyphasé de paléostructures distensives dans l'Axe Nord-Sud tunisien: le segment Bouzer-Rheouis.* Thèse de 3ème cycle. Université de Grenoble.

——, OUALI, J. & TRICART, P. 1989. Les blocs basculés mésozoïques dans l'Axe nord-sud de Tunisie centrale: importance et signification. *Bulletin de la Société Géologique de France*, (8), V(1), 117–120.

HALLER, P. 1983. *Structure profonde du Sahel tunisien. Interprétation géodynamique.* Thèse 3ème cycle, Université de Besançon.

JAUZEIN, A. 1967. Contribution à l'étude géologique des confins de la Dorsale tunisienne. *Annales des Mines et de la Géologie (Tunis)*, **22**.

KUJAWSKY, H. 1969. Contribution à l'étude géologique de la région des Hédil et du Béjaoua oriental. *Annales des Mines et de la Géologie (Tunis)*, **24**.

LAATAR, S. 1980. *Gisements de Pb-Zn et diapirisme du Trias salifère en Tunisie septentrionale: les concentrations péri-diapiriques du district minier de Nefate-Fedj el Adoum.* Thèse, 3ème cycle, Université de Paris VI.

LETOUZEY, J. & TRÉMOLIÈRES, P. 1980. Paleostress fields around the Mediterranean since the Mesozoic derived microtectonics: comparisons with plate tectonic data. *26ème Congrès de Géologie International, Paris, Colloque C5*, BRGM, Orléans, 261–268.

LONIOLI-OUAZAA, N. 1994. *Etude minéralogique et géochimique des épisodes magmatiques mésozoïques et miocènes de la Tunisie.* Thèse Doct. ès Sciences, Université de Tunis II.

LOUCKS, R. G., MOODY, R. T. J., BELLIS, J. K. & BROWN, A. A. 1998. Regional depositional setting and pore network systems of the El Garia Formation (Metlaoui Group, Lower Eocene) offshore Tunisia. *This volume.*

MARIE, J., TROUVÉ, P., DESFORGES, G., & DUFAURE, P. 1984. *Nouveaux éléments de paléogéographie du Crétacé de Tunisie.* Notes et Mémoires, Compagnie Française des Pétroles, **19**, 7–37.

MARTINEZ, C. & TRUILLET, R. 1987. Évolution structurale et paléogéographique de la Tunisie. *Memorie della Società Geologica Italiana*, **38**.

MOODY, R. T. J. & GRANT, G. G. 1989. On the importance of bioclasts in the definition of depositional model for the Metlaoui carbonate group. *Actes des IIème Journées de Géologie Tunisienne Appliquée à la Recherche des Hydrocarbures.* Mémoire de l'ETAP, **3**, 409–427.

MORGAN, M. A., GROCOTT, J. & MOODY, R. T. J. 1998. The structural evolution of the Zaghouan–Ressas Structural Belt, Northern Tunisia. *This volume.*

NEGRA, H. 1994. *Les dépôts de plate-forme à bassin du Crétacé supérieur en Tunisie centro-septentrionale (formation Abiod et faciès associés). Stratigraphie, sédimentation, diagenèse et intérêt pétrolier.* Thèse Doct. ès Sci. Université de Tunis II.

OUALI, J. 1985. Structure et évolution géodynamique du chaînon Nara–Sidi Khalif (Tunisie centrale). *Bulletin des Centres de Recherches Exploration–Production Elf-Aquitaine, Pau*, vol. 9, pp. 155–182.

——, MARTINEZ, C. & KHESSIBI, M. 1986. Caractères de la tectonique crétacée en distention au Jebel Kebar (Tunisie centrale): ses conséquences. *Cahiers ORSTOM, Géodynamique*, **I**(1), 3–12.

——, TRICART, P. & DELTEIL, J. 1987. Ampleur et signification des recouvrements anormaux dans l'axe Nord–Sud (tunisie centrale): données nouvelles dans le chaînon Nara–Sidi Khalif. *Eclogae Geologicae Helveticae*, **80**(3), 685–696.

PERTHUISOT, V. 1978. *Dynamique et pétrogenèse des extrusions triasiques en Tunisie septentrionale.* Thèse Doct. ès Sci., École Normale Supérieure, Paris.

—— & ROUVIER, H. 1990. Halocinèse et plates-formes en extension ou coulissement: le Maghreb oriental au Mésozoïque. Comparaison avec la rive septentrionale de la Téthys. *2ème Congrès National des Sciences de la Terre, Tunis*, 223.

—— & —— 1992. Les diapirs du Maghreb central et oriental: des appareils variés, résultats d'une évolution structurale et pétrogénétique complexe. *Bulletin de la Société Géologique de France*, **163**(6).

PERVINQUIÈRE, L. 1903. *Étude Géologique de la Tunisie Centrale.* De Rudeval, Paris.

PHILIP, H., ANDRIEUX, J., DLALA, M., CHIHI, L. & BEN AYED, N. 1986. Evolution tectonique mio-plio-quaternaire du fossé de Kasserine (Tunisie centrale): implications sur l'évolution géodynamique récente de la Tunisie. *Bulletin de la Société Géologique de France*, **II**(4), 559–568.

PITMAN, W. C. & TALWANI, M. 1972. Sea-floor spreading in the North Atlantic. *Geological Society of America Bulletin*, **83**, 619–646.

RIGANE, A. 1991. *Les calcaires de l'Yprésien en Tunisie centro-septentrionale: cartographie, cinématique et dynamique des structures.* Thèse Doct. d'Univ., Université de Franche-Comté.

ROBERSON, P. 1989. A geophysical approach to analysis of the Metlaoui group. *Actes des IIème Journées de Géologie Tunisienne Appliquée à la Recherche des Hydrocarbures.* Mémoire de l'ETAP, **3**, 199–233

SAADI, J. & ZARGOUNI, F. 1990. *Sédimentation syntectonique pendant le Crétacé inférieur dans la région d'Enfida (Tunisie nord-orientale).* Réunion Sci. de la Terre Société Géologique de France, 112

SAÏD R. 1978. *Étude stratigraphique et micropaléontologique du passage Crétacé-Tertiaire du synclinal d'Ellès (région de Siliana-Sers), Tunisie centrale.* Thèse 3ème cycle. Université de P. et M. Curie, Paris.

SALAJ, J. 1990. L'Harien (Paléocène moyen) et ses limites. *2ème Congrès National des Sciences de la Terre*, Tunis, 236.

SASSI, S. 1974. *La sédimentation phosphatée au Paléocène dans le Sud et le Centre Ouest de la Tunisie.* Thèse Doct. ès Sci., Université de Paris Sud Orsay.

—— 1980. Contexte paléogéographique des dépôts phosphatés en Tunisie. *In*: *Géologie Comparée des Gisements de Phosphates et de Pétrole.* Document de BRGM, **24**, 167–183.

——, TRIAT, J. M., TRUC, G. & MILLOT, G. 1984. Découverte de l'Eocène continental en Tunisie centrale: la formation de Jebel Chambi et ses encroûtements carbonatés. *Comptes Rendus de l'Academie des Sciences, serie II*, **299**(7), 357–364.

——, ZAIER, A., BÈJI-SASSI, A. & ABDELJAOUED, S. 1991. *Etude paléogéographique du Paléocène et de l'Eocène inférieur de la Tunisie.* Rapport inédit de projet de recherche, Document ETAP, Tunis.

SMATI, A. 1986. *Les gisements de Pb-Zn et de fer de J. Slata (Tunisie du Centre-Nord): minéralisations épigénitiques dans le Crétacé néritique de la bordure d'un diapir de Trias. Gisements de Sidi Amor Ben Salem et de Slata-fer.* Thèse Doct. 3ème cycle. Université P. et M. Curie, Paris VI.

SOLIGNAC, M. 1927. *Etude géologique de la Tunisie septentrionale.* Thèse Doct. ès Sci., Université de Lyon.

SOYER, C. & TRICART, P. 1989. Tectonique d'inversion en Tunisie centrale: le chaînon atlasique Segdal–Boudinar. *Bulletin de la Société Géologique de France*, **8**(4), 829–836.

TOUATI, M. 1985. *Étude géologique et géophysique de la concession Sidi-el-Itayem en Tunisie orientale, Sahel de Sfax.* Thèse Doct. ès Sci., Université de Paris VI.

TURKI, M. M. 1985. *Polycinématique et contrôle sédimentaire associé sur la cicatrice Zaghouan - Nebhana.* Thèse Doct. ès Sci. Université de Tunis, et Revue des Sciences de la Terre, Tunis, CST-INRST, **7**, 1988.

VISSE, L. D. 1952. Genèse des gîtes phosphatés du Sud-Est algéro-tunisien. *XIXème Congrès International, Alger, 1ère série*, 27.

WINNOCK, E. 1980. Les dépôts de l'Eocène au Nord de l'Afrique: aperçu paléogéographique de l'ensemble. *In*: *Géologie Comparée des Gisements de Phosphates et de Pétrole. Colloque International, Orléans, 6–7 November 1979.* Document du BRGM, **24**, 219–243.

YAÏCH, C. 1984. *Étude géologique des chaînons du Chérahil et du Khechem-el-Artsouma (Tunisie centrale). Liaison avec les structures profondes des plaines adjacentes.* Thèse 3ème cycle Université de Besançon.

ZAÏER, A. 1984. *Étude stratigraphique et tectonique de la région de Sra Ouertane (Atlas Tunisien Central). Lithologie, pétrographie et minéralogie de la série phosphatée.* Thèse 3ème cycle, Université de Tunis.

—— 1990. Tectonique anté-éocène et contrôle de la sédimentation dans le Centre ouest de la Tunisie. *2ème Congrès National des Sciences de la Terre, Tunis*, 271.

ZARGOUNI, F. 1985. *Tectonique de l'Atlas méridional de Tunisie. Evolution géométrique et cinématique des structures en zone de cisaillement.* Thèse Doct. ès Sci., Université de Strasbourg, et Revue des Sciences de la Terre, Tunis, CST-INRST, **3**, 1966.

ZOUARI, H., TURKI, M. M. & DELTEIL, J. 1990. Nouvelles données sur l'évolution tectonique de la chaîne de Gafsa. *Bulletin de la Société Géologique de France*, **8**(VI), 621–629.

This page intentionally left blank

The thin-skinned style of the South Atlas Front in Central Algeria

R. BRACÈNE[1], A. BELLAHCÈNE[1], D. BEKKOUCHE[1], E. MERCIER[2] & D. FRIZON de LAMOTTE[2]

[1]*Sonatrach Exploration, Côte Rouge, Algiers, Algeria*
[2]*Université de Cergy-Pontoise, Département des Sciences de la Terre, (CNRS-URA 1759), F 95011 Cergy-Pontoise Cedex, France*

Abstract: Seismic lines cutting through the southern front of the Sahara Atlas show that the front is not superimposed on a major basement fault. Folded Cretaceous rocks can be observed on these lines to overlie a décollement surface climbing from Triassic to Early Cretaceous, below which flat-lying sediments can be recognized. The structural style is thus interpreted to be thin skinned and the folds underlining the front as ramp- related features. The development of duplexes in the core of some anticlines explains the apparent thickening of Cretaceous and/or Jurassic strata revealed by boreholes. This thickening was previously interpreted to be related to now-inverted extensional half-grabens, a model which cannot now be supported. This new interpretation allows a reassessment of other parts of the Sahara Atlas system, the large-scale structural model for which is that of large half-graben system that has undergone inversion because of shortening between the High Plateau massif and the Sahara Platform.

North Africa is classically divided in four structural domains, which are, from south to north (Fig.1): the Sahara Platform; the Atlas Mountains; the High Plateaux (i.e. Meseta) which suffered an *en bloc* motion during the tectogenesis of the Atlas Mountains; the Tell (Algeria, Tunisia) and Rif (Morocco) orogenic domains, located at the former margin of the Tethys ocean. This tectonic framework is partly inherited from faulting which occurred at the beginning of Mesozoic times, as a result of the extension which led to the opening of the Atlantic and Tethys oceans (Dercourt *et al.* 1993; Ricou, 1994).

The Atlas Mountains of North Africa exhibit a Mesozoic to Cenozoic sedimentary sequence that was folded and faulted during tectonic events ranging from Tertiary to Quaternary. These mountains have been historically considered as an intra-continental chain in which cover folds are mainly caused by basement faulting (Durand-Delga & Fontboté 1980). This interpretation is based, in particular, on observations made in the High Atlas (Morocco), where the Mesozoic cover is thin and the basement is clearly involved in the structures (see Laville *et al.* 1977; Letouzey 1990).

The deformation front of the Atlas Mountains (southern limit) can be traced from Agadir to Tunis (Fig. 1). In the past, this front has been considered as a strike-slip fault inherited from a normal fault forming the southern boundary of the Atlas basin (Durand-Delga & Fontboté 1980).

In the eastern Atlas regions, the Mesozoic cover is thicker (up to 10000 m in the Aurès Mountains; Laffitte 1939) and a thin-skinned style, without major strike-slip component, has been inferred on the basis of balanced cross-sections and geometrical modelling (Frizon de Lamotte *et al.* 1990; Ghandriche 1991; Al Saffar, 1993; Creuzot *et al.* 1993; Addoum 1995; Mercier *et al.* 1995; Outtani *et al.* 1995;). These workers showed that the surface geometry of the frontal folds is consistent with active décollement levels situated within Triassic evaporites or even in Cretaceous strata (Outtani *et al.* 1995). However, these interpretations are still debated because of the lack of seismic profiles imaging a clear ramp-flat geometry in the core of the anticlines.

Such seismic profiles across the deformation front are available in the study area situated along the southern boundary of the Sahara Atlas between Abiod Sidi Cheik and Messad (Fig. 1). By using, in addition, fieldwork and forward modelling of balanced cross-sections, we propose a new tectonic interpretation of this segment of the South Atlas Front. We will show that the front is not superimposed on a major basement fault but constitutes a classical thrust front characterized by ramp-related folds.

Geometry of the southern boundary of the Sahara Atlas basin

The superimposition of the South Atlas Front on the southern limit of the Atlas Mesozoic basin is demonstrated in Eastern Morocco (Jossen &

BRACÈNE, A., BELLAHCÈNE, A., BEKKOUCHE, D., MERCIER, E. FRIZON DE LAMOTTE, D. 1998. The thin-skinned style of the South Atlas Front in Central Algeria. *In*: MACGREGOR, D. S., MOODY, R. T. J. & CLARK-LOWES, D. D. (eds) 1998. *Petroleum Geology of North Africa.* Geological Society, London, Special Publication No. 132, 395–404.

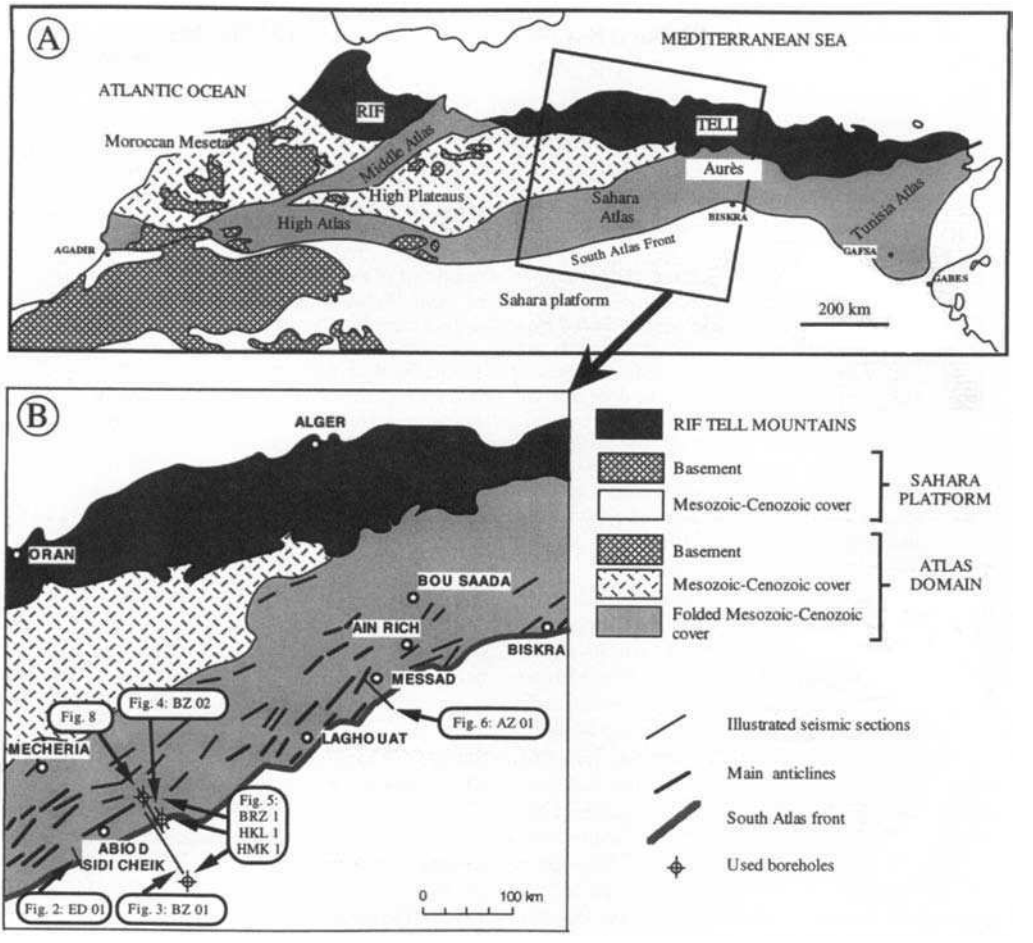

Fig. 1. (**a**) Schematic map of North Africa showing the main structural domains and the location of the study area. (**b**) Structural map of the Algerian Atlas region showing the location of seismic lines, boreholes and geological sections studied in this paper.

Filali-Moutei 1992) and in Northern Tunisia (Turki *et al.* 1988; Creuzot *et al.* 1992; Morgan et al., this volume). In the study area, such a geometry is not visible on seismic lines but has nevertheless been inferred by analogy from the adjacent regions, with thickening of geological sections in boreholes (Kazi-Tani 1970, Guiraud 1973; 1986; Vially *et al.* 1994) quoted as evidence for an original now-inverted half-graben geometry. On the contrary, our interpretation of seismic lines is that they illustrate a simple sedimentary wedge, with no major tectonic discontinuities or major extensional basin-margin faults identified (Fig. 2, profile ED 01; Fig. 3). Some small steeply dipping faults that are probably extensional are exposed in the same profile below the main detachment. However, they do not perturb greatly the layer-cake geometry.

Such profiles could appear inconsistent with the classical view of this zone, which emphasizes rapid variations in the thickness of the sedimentary pile. As we noted above, such a view generally arose from the interpretation of borehole data. For instance, close to the seismic profiles BZ 01 and BZ 02 (Figs 3 and 4), where no significant increase of the thickness of the Mesozoic is observed on seismic lines, two boreholes give the following thickness for the Cretaceous strata: at 80 km from the front within the platform (borehole HMK-1) the thickness is 789 m (from −254 to −1043m); at the front (borehole HKL 1) the thickness is 2918 m (from −45 to −2963 m).

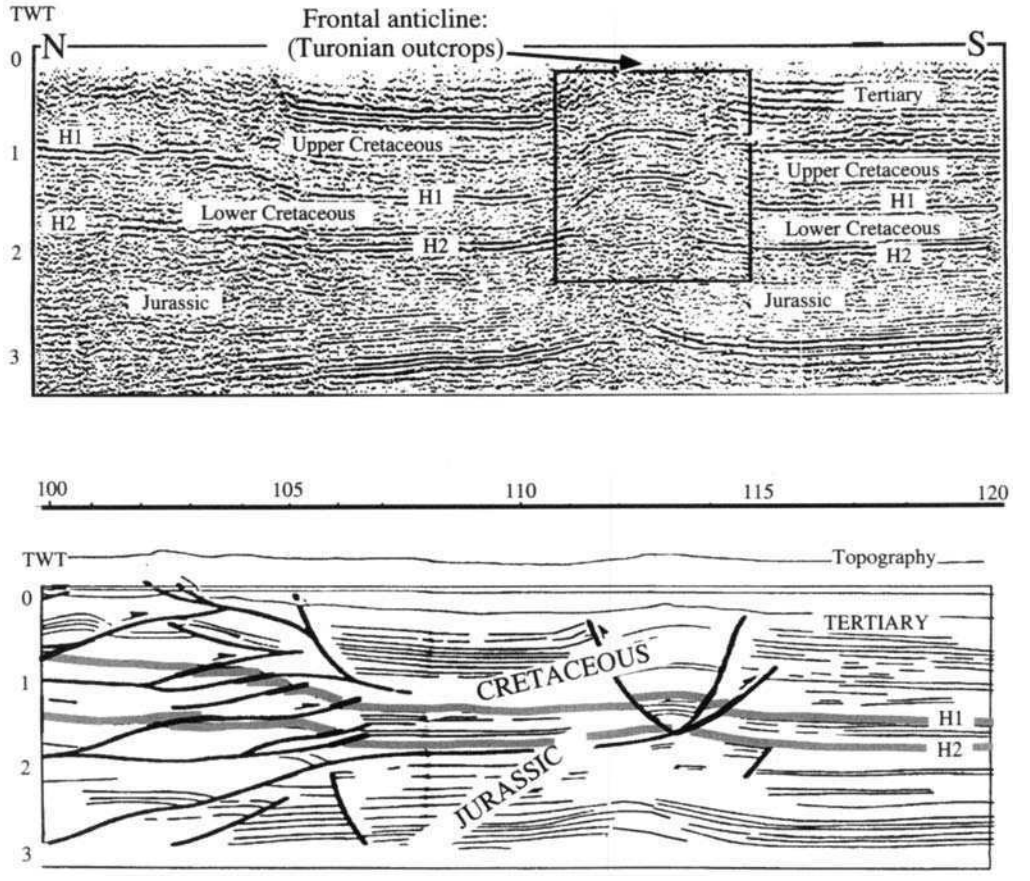

Fig. 2. Seismic line ED 01 (location shown in Fig. 1b). TWT, Two-way travel time (in seconds).

Additionally, the borehole BRZ 1 situated about 30 km north of the front, exhibits a Jurassic sequence which is incomplete but thicker than in the boreholes to the south (Fig. 5).

If we keep in mind that in the Sahara Atlas, as well as along the front, the boreholes are drilled on shallow anticlines, an alternative tectonic origin for the observed thickening arises, one which is more consistent with the geometries discernible on the seismic profiles. Examination of the BZ 02 seismic profile (Fig. 4) strongly suggests that the Cretaceous strata thickening (borehole HKL 1) is due to repetition of section on a blind imbricate in the core of the anticline. The application of this proposal to the whole region requires a reassessment of down-hole measurements of dips and micropalaeontological data. However, from the dataset currently available, our preferred model is that the Sahara Atlas Basin lies within a layer-cake sedimentary wedge and is not marked by a major basin margin fault zone. To link rapid thickening of the sedimentary pile and compressive structures (for instance, northern sectors of sections ED 01 (Fig. 3) and BZ 01 (Fig. 3)) a critical survey of the tectonic style is needed.

The structural style of the southern front of the Sahara Atlas

One of the main characteristics of the Sahara Atlas is that the faulted zones are underlain by Triassic evaporites. This suggests that the thick Triassic section greatly influences the deformation mode, which is probably dominated by detachment folding (Bracène 1992*a*, *b*). However, the folding style changes toward the front (Kazi-Tani 1970; Aissaoui 1984) where the kink-like geometry of the folds suggests a ramp-related style. Moreover, the Triassic evaporite does not crop out in this area.

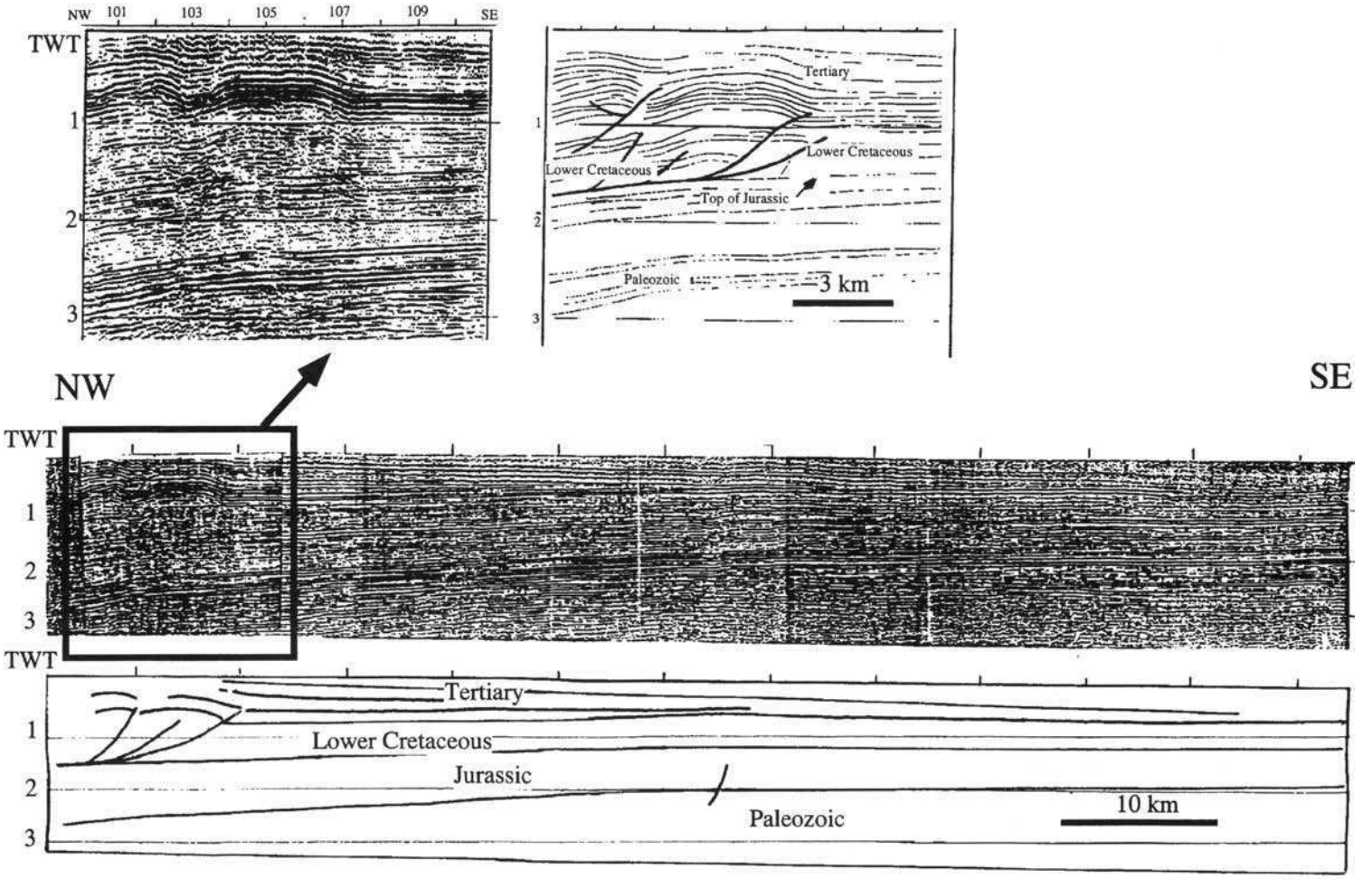

Fig. 3. Seismic line BZ 01 (location shown in Fig. 1b).

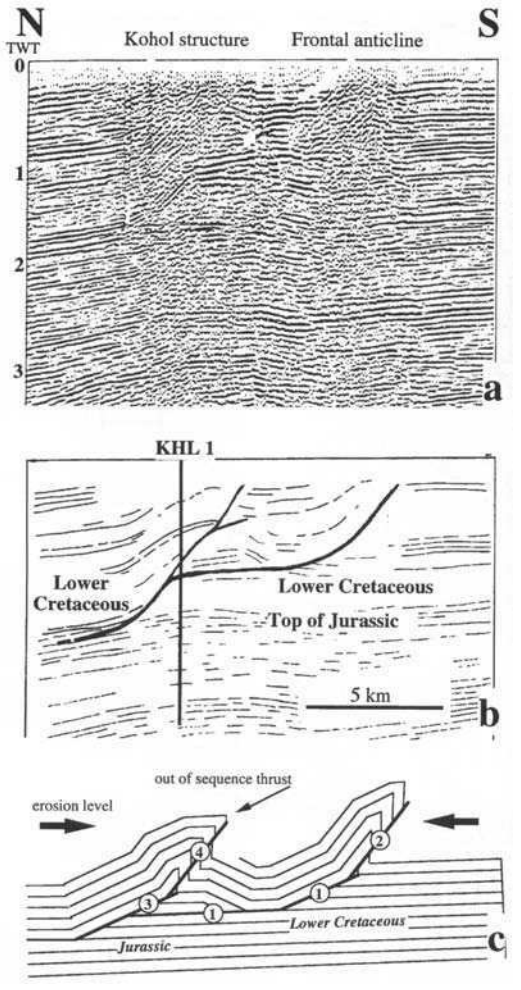

Fig. 4. Seismic line BZ 02 and geometrical modelling (location shown in Fig. 1b).

The kink-like geometry is confirmed by seismic profiles. The anticlines are built above ramps that branch from shallow décollements and the basement is indicated to be not involved in these folds. The ED 01 seismic profile (Fig. 2) shows that below the southernmost anticline, the frontal thrust fault branches from a décollement level situated at the Jurassic–Cretaceous transition. Turonian limestone outcrops in the core of the anticline. Northward, a ramp links this shallow décollement to a deeper one, probably situated within the Triassic. In the hanging wall, imbricate structure leads to the uplift, and to thickening by duplication of the overlying strata. Similar patterns are visible on the other sections presented here (see, in particular, the northern part of the section BZ 01, Fig. 3).

Consequently, we consider that, as in the eastern region (Ghandriche 1991; Addoum 1995; Outtani *et al.* 1995; Frizon de Lamotte *et al.*, 1997) the structural style at the Saharan Atlas Front is thin skinned. In the Messad region, west of Biskra (Fig. 1), the front is underlain by a major back thrust branching from a décollement situated at Jurassic level (seismic profile AZ 01, Fig. 6). It is worth noting that back-thrusting has been already observed at the thrust-front east of Biskra along the front of the Aurès Mountains (Ghandriche 1991; Addoum, 1995; Frizon de Lamotte *et al.* 1997).

Kinematics of the ramp-related folds

The complex geometry of the folds and surface geology exposed along the front cannot be adequately explain by a simple piggy back sequence (i.e. propagation from the hinterland). As shown in the two following case studies, the basic pattern is that of dual folds, with slip originating from the inner fault-bend fold accommodated within a more or less synchronous outer fault-propagation fold. However, out-of-sequence thrusting appears necessary in all transects.

The first kinematic model (Fig. 7) is based on field measurements and two boreholes crossing the Djebel Rhezala and Djebel Kohol anticlines. It has been performed with the help of the 'Rampe(EM)' software (Mercier 1992; Mercier *et al.* 1997). The model (Fig. 7) assumes that a set of out-of-sequence back-thrusts and fore-thrusts are developed in the inner anticline (Dj. Rhezala) as a consequence of blocking of the thrust propagation in the frontal structure (Dj. Kohol). A back-thrust at the junction between the forelimb and the roof of the Dj. Rhezala and a fore-thrust at the junction between the roof and the back limb are exposed in the field. In addition, the duplex forming the core of this anticline gives a consistent explanation for the apparent thickening of Cretaceous strata (borehole BRZ 1, see above). The timing of thrusts in the Dj. Rhezala anticline is close to that proposed by Vially *et al.* (1994) on the basis of sand box experiments.

The second kinematic model concerns also the Dj. Kohol anticline in an area further east along the structural strike (seismic profile BZ 02, Fig. 4). Along this section a new anticline is developed at the front of the major Kohol structure. Balancing of this section indicates that the Kohol anticline is an early fault-bend fold, in the back of which a late fault-propagation fold is developed. This later fold is itself cut out by a breakthrough

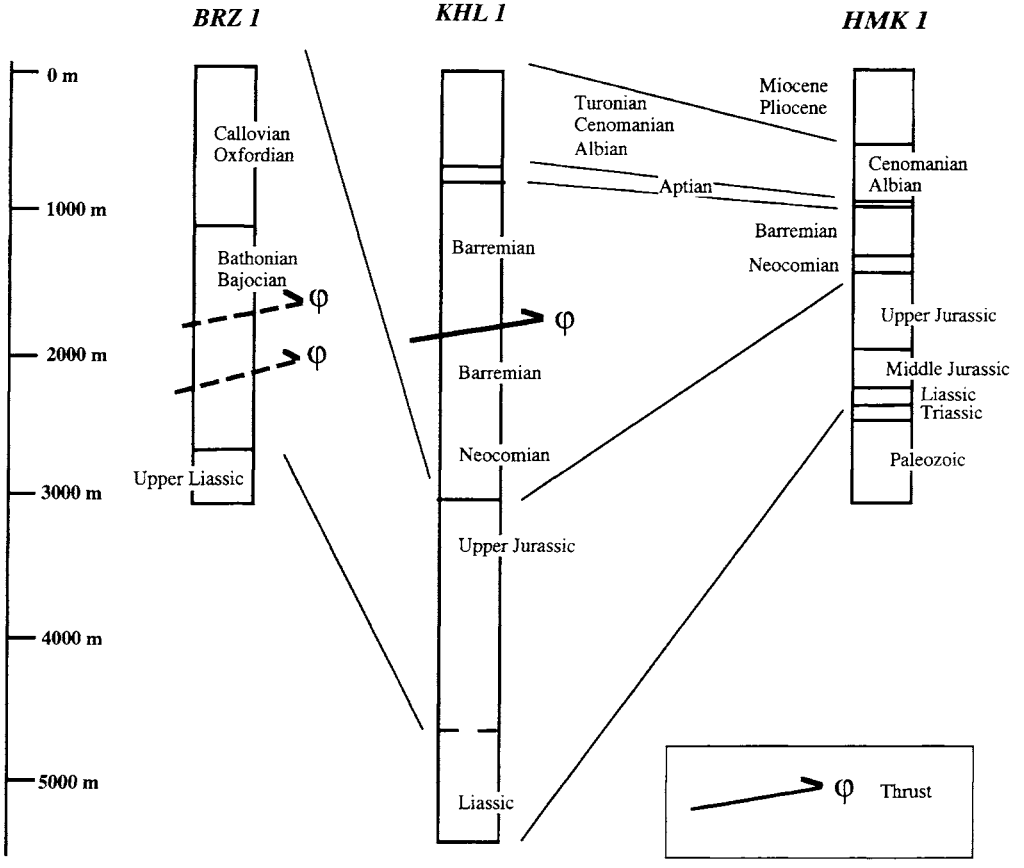

Fig. 5. Schematic diagram of studied boreholes (location shown in Fig. 1b).

out-of-sequence thrust. As in the first model, we believe that the complex thrust sequence leading to the present-day geometry of the Kohol anticline is due to difficulties in thrust propagation toward the platform.

Conclusion

Observed subsurface structure and thickening of geological intervals in boreholes in the southern front of the Sahara Atlas can be explained most rationally by a thin-skinned style. The thrust faults, which are mainly blind, show a typical staircase geometry and climb progressively from a basal décollement situated within Triassic beds to shallow detachments situated at the Cretaceous–Jurassic transition or even within the Lower Cretaceous. Kinematics of the folding is complex, with out-of-sequence thrust faults and duplexes developed, explaining the tectonic thickening of Cretaceous and or Jurassic strata in boreholes. The position of the deformation front is not determined by an inherited normal fault; on the contrary, the boundary between the Atlas basin and the Sahara Platform appear transitional. From this standpoint, the geometry of the Sahara Atlas Front is very different from that of the Eastern High Atlas (Morocco) and Northern Tunisian thrust fronts.

We emphasize this fundamental asymmetry of the Sahara Atlas basin, the geometry of which was, in our mind, close to that of a half-graben (Bracène, 1992b). During the Triassic and Liassic extensional periods, the major normal faults were situated along the present-day High Plateaux–Atlas boundary (Fig. 8). Subsequently, the Tertiary inversion of the Atlas and associated folding can be linked to the southward translation of the High Plateaux buttress towards the

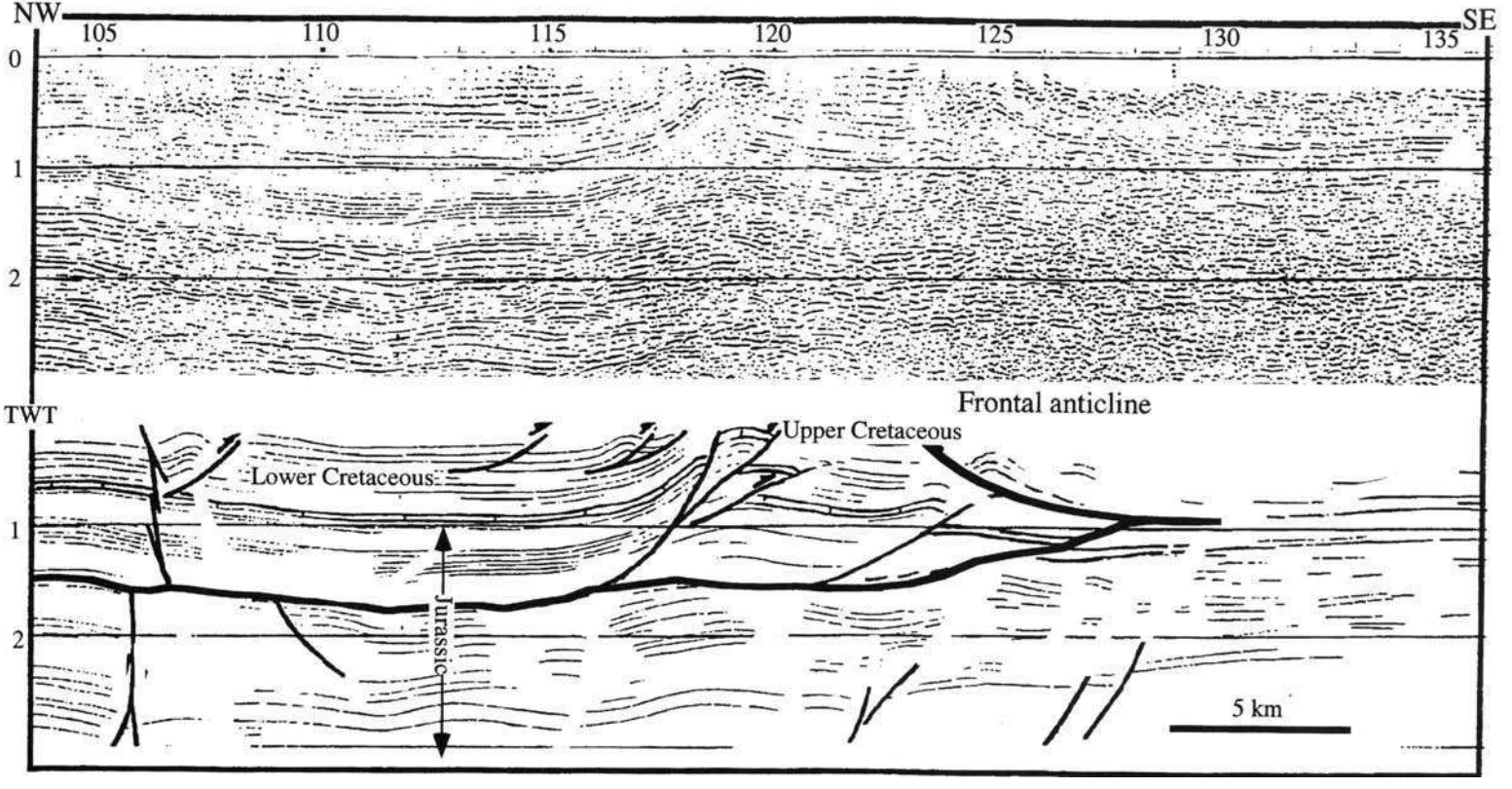

Fig. 6. Seismic line AZ 01 (location shown in Fig. 1b).

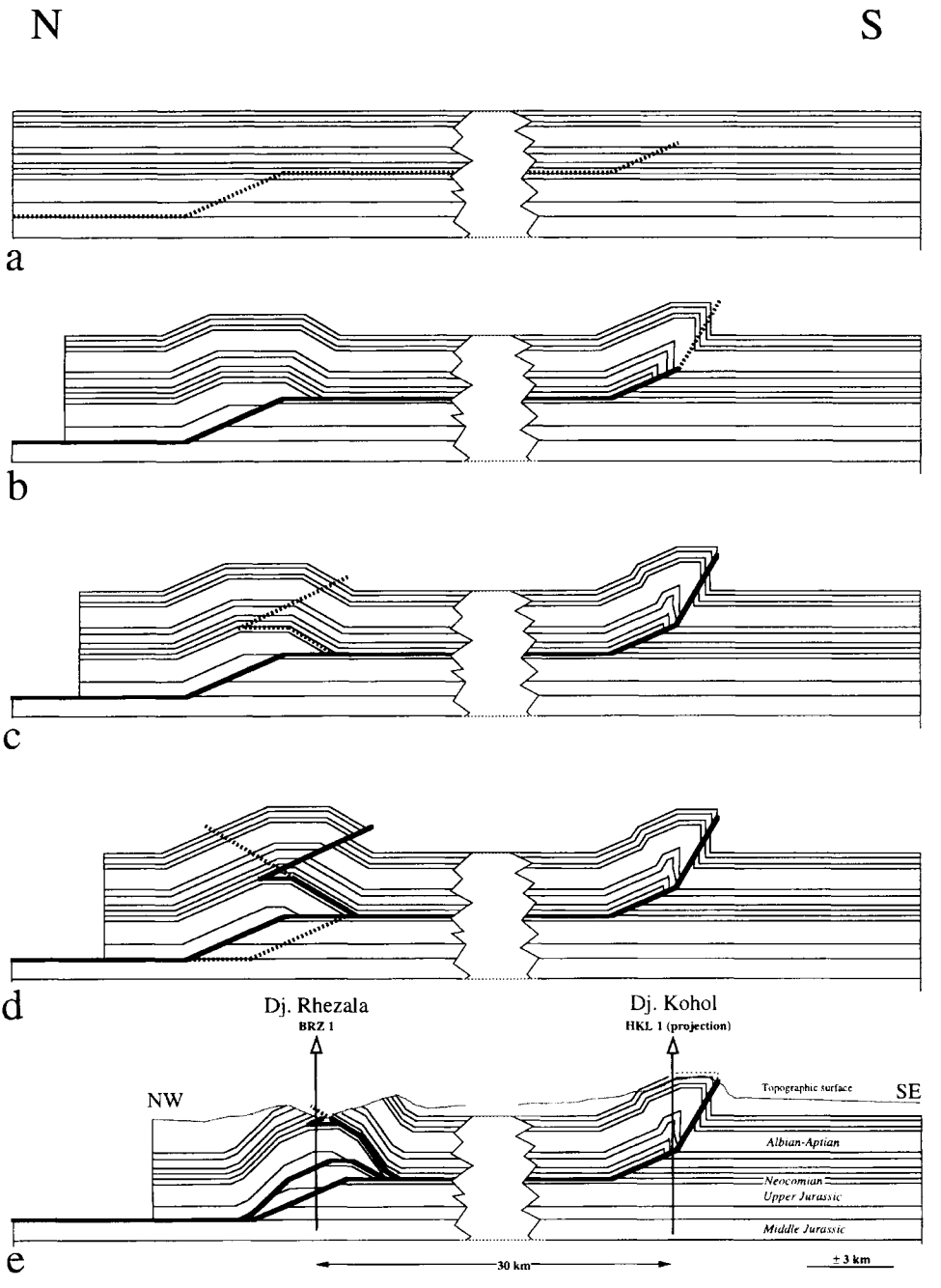

Fig. 7. Kinematic modelling of geological cross-section located near the BZ 02 seismic line (as for Fig. 4: location shown in Fig. 2). (Note that in this particular section, no deformation is transmitted forward at the front of Dj. Kohol.) (**a**) Initial stage. (**b**) Emplacement of a fault-bend fold and a fault-propagation fold (**c**) Breakthrough evolution of the frontal fault-propagation fold and blocking. (**d**) An out-of-sequence triangular zone occurs within the fault-bend fold as a consequence of blocking in the frontal anticline. A duplex and a back-thrust are developed in the core of the fold. (**e**)

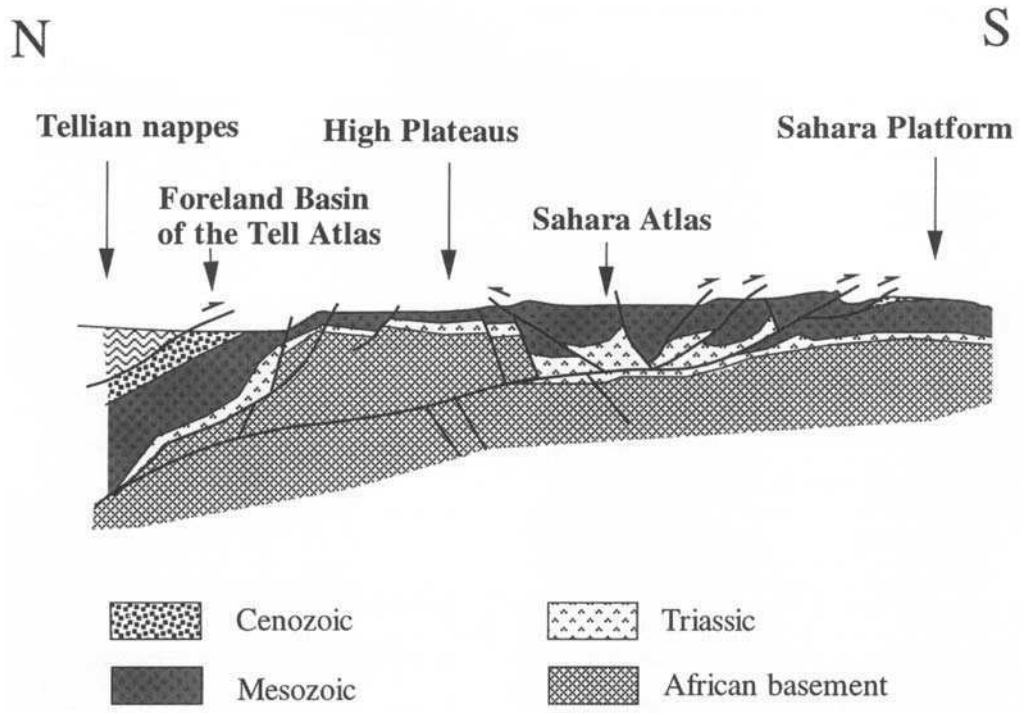

Fig. 8. A highly schematic section (without scale) illustrating the tectonic framework of the Sahara Atlas.

Sahara Platform (Fig. 8). Because of the absence of Neogene sedimentary rocks, it is difficult to differentiate the respective contribution of the Atlas (late Eocene) and Alpine (post Miocene) tectonic events known in the eastern regions (see Frizon de Lamotte *et al.* 1997). However, the seismic profile BZ 01 (Fig. 3) shows two important unconformities situated at the base and within Tertiary beds. This suggests a progressive deformation, which is, moreover, still active today.

The authors wish to thank M. Attar, Head of Sonatrach Division Exploration, who gave access to the seismic profiles and authorized publication; R. Moody, who encouraged the writing of this paper; and anonymous referees for their helpful comments. This paper is a contribution to the peri-Tethys programme (South Atlas Front project).

References

ADDOUM, B. 1995. *L'Atlas Saharien Sud-Oriental. Cinématique des plis-chevauchements et reconstitution du bassin du Sud-Est constantinois (confins algéro-tunisien).* Thèse Université de Paris-Sud, Orsay.

AISSAOUI, D. 1984. *Les structures liées à l'accident Sud atlasique entre Biskra et le Djebel Mandra. Évolution géométrique et cinématique.* Thèse 3ème cycle, Université Louis Pasteur, Strasbourg.

AL SAFFAR, M 1993. Geometry of fault-propagation folds: method and application. *Tectonophysics*, **223**, 363–380.

BRACÈNE, R. 1992*a*. Typologie des structures pilicatives dans l'Atlas saharien. *In: 9e Séminaire des Sciences de la Terre, Tlemcen Meeting, Abstracts Volume.*

—— 1992*b* Évolution géodynamique de la partie Occidentale de Nord de l'Algérie (Atlas Saharien Occidental). *In: 9e Séminaire des Sciences de la Terre, Tlemsen Meeting, Abstracts Volume.*

CREUZOT, G., MERCIER, E., OUALI, J. & TRICART, P. 193. La tectogenèse atlasique en Tunisie centrale: apport de la modélisation géometrique. *Eclogae Geologicae Helvetiae*, **86**(2), 609–627.

——, ——, —— & Turki, M. M. 1992. Héritage distensif et structuration chevauchante: rapports de la modélisation du chevauchement alpin de Zaghouan (Atlas Tunisien). *Comptes Rendus de l'Académie des Sciences, série II*, **314**, 961–965.

DERCOURT, J., RICOU, L. F. & VRIELYNCK, B. (eds) 1993. *Atlas Tethys Palaeoenvironmental Maps.* Gauthier-Villars, Paris.

DURAND-DELGA, & FONTBONTÉ, J. M. 1980. Le cadre structural de la Méditerranée occidentale. *In: 26th International Geological Congress, C5 'Geolo-*

gie des Chaînes Alpines Issues de la Téthys'. Paris, 67–85.

FRIZON DE LAMOTTE, D., GHANDRICHE, H. & MORETTI, I. 1990. La flexure saharienne: trace d'un chevauchement aveugle post-Pliocène de flèche plurikilométrique au Nord du Sahara (Aurès, Algérie). *Comptes Rendus de l'Académe des Sciences, série II*, **310**, 1527–1532.

——, MERCIER, E., OUTTANI, F., *et al.* 1997. Structural inheritance and kinematics of folding and thrusting along the front of the Eastern Atlas Mountains (Algeria and Tunisia). *In: Peri-Tethyan Platforms no. 3* Technip, Paris.

GHANDRICHE, H. 1991. *Modalités de la superposition de structures de plissement–chevauchement d'âge Alpin dans les Aurès (Algérie)*. Thèse, Université de Paris-Sud, Orsay.

GUIRAUD, R. 1973. *Evolution post triasique de l'avant pays de la chaîne Alpine en Algérie d'après l'étude du bassin du Hodna et des régions voisines*. Thèse Doct. ès Sci., Université de Nice.

JOSSEN, J. A. & FILALI-MOUTEI, J. 1992. A new look at the structural geology of the southern side of the Central and Eastern High Atlas mountains. *Geologische Rundschau*, **81**, 143–156.

KAZI-TANI, N. 1970. *Contribution à l'étude géologique de Dj. Fernane et des Monts de Ben S'rour. Étude sédimentologique et structurale*. Thèse 3ème cycle, Faculté d'Alger.

—— (1986). *Évolution géodynamique de la Bordure Nord Africaine. Le Domaine intra plaque Nord Algérien. Approche Mégaséquentielle*. Thèse Doct. ès Sci., Université de Pau.

LAFFITTE, R. 1939. *Étude géologique de l'Aurès*. Thèse Doct. ès Sci., Université de Paris.

LAVILLE, E., LESAGE, J. L. & SEGURET, M. 1977. Geométrie cinématique (dynamique) de la tectonique Atlasique sur le versant sud du Haut Atlas Marocain. Aperçu sur les tectoniques hercyniennes et tardi-Hercyniennes. *Bulletin de la Société Géologique de France*, **XIX**(3).

LETOUZEY, J. 1990. Fault reactivation, inversion and fold-thrust belt. *In: Petroleum and Tectonics in Mobile Belts*. Technip, Paris, 101–128.

MERCIER, E. 1992. Une évolution possible des chevauchements associés aux plis de propagation: le transport sur le plat (modélisation et exemple). *Bulletin de la Société Géologique de France*, **163**(6), 713–720.

——, OUTTANI, F. & FRIZON DE LAMOTTE, D. 1997. Late evolution of fault-propagation folds: principles and example. *Journal of Structural Geology*, **19**, 185–193.

——, ——, —— & GHANDRICHE, H. 1995. Comment on 'Geometry of fault-propagation folds: method and application'. *Tectonophysics*, **245**, 111–113.

MORGAN, M. A., GROCOTT, J. & MOODY, R. T. J. 1998. The structural evolution of the Zaghouan–Ressas Structural Belt, Northern Tunisia. *This volume*.

OUTTANI, F. ADDOUM, B., MERCIER, E., FRIZON DE LAMOTTE, D. & ANDRIEUX, J. 1995. Geometry and kinematics of the South Atlas Front (Algeria–Tunisia). An analysis emphasising the structural role of the fault-propagation folds. *Tectonophysics*, **249**, 233–248.

RICOU, L. E. 1994. Tethys reconstructed: plates continental fragments and their boundaries since 260 Ma from Central America to South-eastern Asia. *Geodinamica Acta*, **7**(4), 169–218.

TURKI, M. M., DELTEIL, J., TRUILLET, R. & YAÏCH, C. 1988. Les inversions tectoniques de la Tunisie centro-septentrionale. *Bulletin de la Société Géologique de France*, **IV**(8), 399–406.

VIALLY, R., LETOUZEY, J., BÉNARD, F., HADDADI, N., DESFORGES, G., ASKRI, H. & DOUDJEMA, A. 1994. Basin inversion along the North African Margin. The Saharan Atlas (Algeria). *In:* ROURE, F. (ed.) *Peri-Tethyan Platforms*. Technip, Paris, 79–118.

The structural evolution of the Zaghouan–Ressas Structural Belt, northern Tunisia

MARK A. MORGAN[1,2], JOHN GROCOTT[1] & RICHARD T. J. MOODY[1]

[1]*School of Geological Sciences, Kingston University, Penrhyn Road, Kingston upon Thames, Surrey KT1 2EE, UK*

[2]*Present address: Institut für Landschaftsplanung und Ökologie, Universität Stuttgart, Keplerstraße 11, D70174 Stuttgart, Germany*

Abstract: From Middle Jurassic to Late Cretaceous time the African–European Rift Zone (AERZ), a seaway connecting the western part of the Tethys Ocean to the embryonic Atlantic Ocean, was characterized by sinistral transtension. On the African margin of the AERZ this caused break-up of Tethyan Triassic and Lower Jurassic evaporite and carbonate platform sequences by linked, strike-slip and normal-slip fault displacements that delineated a system of sedimentary basins separated by horsts. The Zaghouan–Ressas Structural Belt (ZRSB) in northern Tunisia was initiated as a north-tapering horst in this system, bounded to the northwest by a pelagic basin (the Tunisian Trough) in which thick Lower Cretaceous sequences were deposited and to the east by a north–south trending system of reactivated Tethyan margin faults. Thickness variations in syn-rift stratigraphy led to lateral flow in underlying Triassic evaporitic sequences and the initiation of pillows and, perhaps, piercement diapirs. Mid- to latest Cretaceous post-rift sequences onlapped syn-rift fault blocks, but the post-rift period is complicated by a reversal in the displacement sense across the AERZ leading to dextral transpression and local fault inversion. In Paleocene and Eocene time, northern Tunisia was characterized by northeast–southwest extension accommodated by displacements on linked systems of reactivated AERZ-related and Tethyan margin faults at the southern margin of Mesogea. This was associated with drift of the Apulian microplate into eventual collision with the European margin to form the Western Alps. Further west, convergence of Africa relative to Europe was initially taken up by subduction of oceanic lithosphere in the remnant AERZ. The Oligo-Miocene evolution of the western Mediterranean reflects the destruction of this oceanic lithosphere and its successor oceanic basin, the Proto-Mediterranean. The Atlassic orogeny in northern Tunisia began in Oligocene time as a result of collision of microplates rifted off the European margin with the North African margin, and coincided with the progressive elimination of Proto-Mediterranean lithosphere from west to east along the African margin. Evidence of the contractional deformation is the development of an Oligocene–Miocene foreland basin in northern Tunisia and its deformation in the Atlas fold–thrust belt of mid- to Upper Miocene age. Within this tectonic framework, two models for the structural evolution of the ZRSB during the Atlassic orogeny are evaluated. The first recognizes the importance of facies variation in controlling thrust geometry, but is essentially a thin-skinned model in which detachment on incompetent Triassic strata forms the main control of structural style. The second model emphasizes reactivation of AERZ-related basin margin faults during contraction and accounts for the major folds in the ZRSB at Djebel Zaghouan and Djebel Ressas as forced folds formed by fault inversion. Anticlines at Hamman Zriba, and east of Grombalia, are also interpreted as fault-inversion folds formed in normal sequence on the external side of the ZRSB. Flow of Triassic strata into the cores of these folds may have been assisted by tectonic loading during fault inversion along the ZRSB. Subsequently, structures in the ZRSB were dissected by northeast–southwest-trending faults that propagated through the post-rift sequence during post-Miocene reactivation of syn-rift extensional faults. These faults accommodated dextral oblique-slip displacement and were linked to extension in northwest–southeast-trending graben that cut the ZRSB and the Intermediate Atlas Zone.

The structure of the Atlas Mountains in northern Tunisia is characterized by northeast–southwest-trending faults and large-scale folds of Mesozoic and Tertiary sedimentary rocks (Ben Ferjani *et al.* 1990; Burollet 1991). Elucidation of the respective roles of salt diapirism, thin-skinned fold-thrust tectonics and inversion tectonics in this part of the Maghrebian orogenic belt has proved controversial. The purpose of this paper is to trace the geological evolution of one of the most important structural lines in northern Tunisia, the Zaghouan–Ressas Structural Belt (ZRSB), and to evaluate the role played by Tethyan-margin extensional and strike-slip fault sys-

MORGAN, M. A., GROCOTT, J. & MOODY, R. T. J. 1998. The structural evolution of the Zaghouan–Ressas Structural Belt, northern Tunisia. *In*: MACGREGOR, D. S., MOODY, R. T. J. & CLARK-LOWES, D. D. (eds) 1998. *Petroleum Geology of North Africa*. Geological Society, London, Special Publication No. 132, 405–422.

tems during basin evolution and during mid- to late-Miocene Atlassic orogeny. In recent publications, researchers have emphasized the thin-skinned nature of the Atlassic contractional deformation in Tunisia and Algeria (Outanni *et al.* 1995; Anderson, 1996; Bracène *et al.* this volume). Although it is clear that a model invoking thin-skinned thrusting with a detachment in Triassic rocks is relevant and can successfully explain structures formed during shortening in these areas, we believe that this approach takes too little account of evidence that Tethyan margin extensional and strike-slip faults, reactivated during the Atlassic orogeny, have exercised a major control on structural style in northern Tunisia. In this respect, the North African margin may be similar to the deformed European margin of the Tethys Ocean in the importance of fault inversion in its structural evolution (Graciansky *et al.* 1989).

Northern Tunisia may be subdivided into six zones based on structure and stratigraphy. From the internal side (northwest) to the external side (southeast) of the fold belt these zones are the Tellian Atlas Zone, the Mejerda Zone, the Intermediate Atlas Zone, the Zaghouan–Ressas Structural Belt, the North–South Axis and the Pelagian or Sahel Platform (Fig. 1). The Tellian Atlas Zone is characterized by a major thrust sheet of Oligo-Miocene 'Numidian' flysch emplaced out-of-sequence on younger strata, mainly of Upper Cretaceous and Eocene age (Morley 1988). To the southeast of the Tell is the Mejerda Zone, also called the 'Zone of Diapirs' (Perthuisot 1981) characterized by extensive, northeast–southwest-elongate outcrops of Triassic rocks, apparently emplaced within younger strata. Absence of halite in the Triassic rocks of the Mejerda Zone make it extremely unlikely that classical salt diapirism has been responsible for the outcrop pattern, but the geology still awaits a satisfactory explanation. The boundary of the Mejerda Zone to the southeast is a thrust contact with the Intermediate Atlas Zone (Morelli & Nicolich, 1990). This Zone consists of northeast–southwest-trending, large-scale, symmetrical to southeast-overturned detachment or fault-inversion folds, and was dissected by northwest–southeast trending faults, active during basin evolution and during folding, which have been reactivated to form a system of Pliocene–Recent half-grabens (Morgan 1994).

The Zaghouan–Ressas Structural Belt (ZRSB) is a 3–5 km wide, northeast–southwest-trending domain of particularly intense folding and faulting located toward the external (southeast) side of the Intermediate Atlas Zone (Fig. 2). It is not a thrust-front structure as such, and Intermediate Atlas Zone folds are present east of the ZRSB but with decreasing amplitude toward the coast. The ZRSB has been regarded as the northern continuation of the North–South Axis (NOSA), an important structural line at the external side of the Intermediate Atlas Zone in central Tunisia (Fig 1; Boccaletti *et al.* 1988, Boccaletti *et al.* 1990; Anderson 1991) but this view is a simplification as will be shown here. To the east of the NOSA, the Sahel or Pelagian platform is regarded as the foreland of the Atlassic orogeny in Tunisia (Ouali 1985) although pre-existing fault systems in the platform were reactivated during this deformation (Bedir *et al.* 1992).

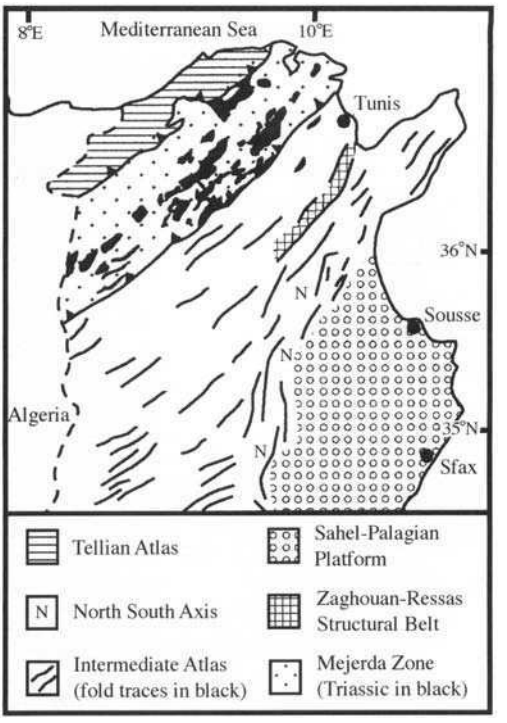

Fig. 1. Major geological subdivisions of northern and central Tunisia.

The structure of the ZRSB appears dominated by Atlassic shortening because Jurassic strata have been elevated up to 3 km above their regional height at Djebel Zaghouan (Fig. 2; Morgan & Grocott, 1993.) In fact, the ZRSB is more complex than this observation implies because faults that bound the Jurassic carbonates at Djebel Zaghouan are vertical, and therefore cannot easily be attributed to thrust tectonics. To investigate the history of structures that characterize the ZRSB, and their relationship to sedi-

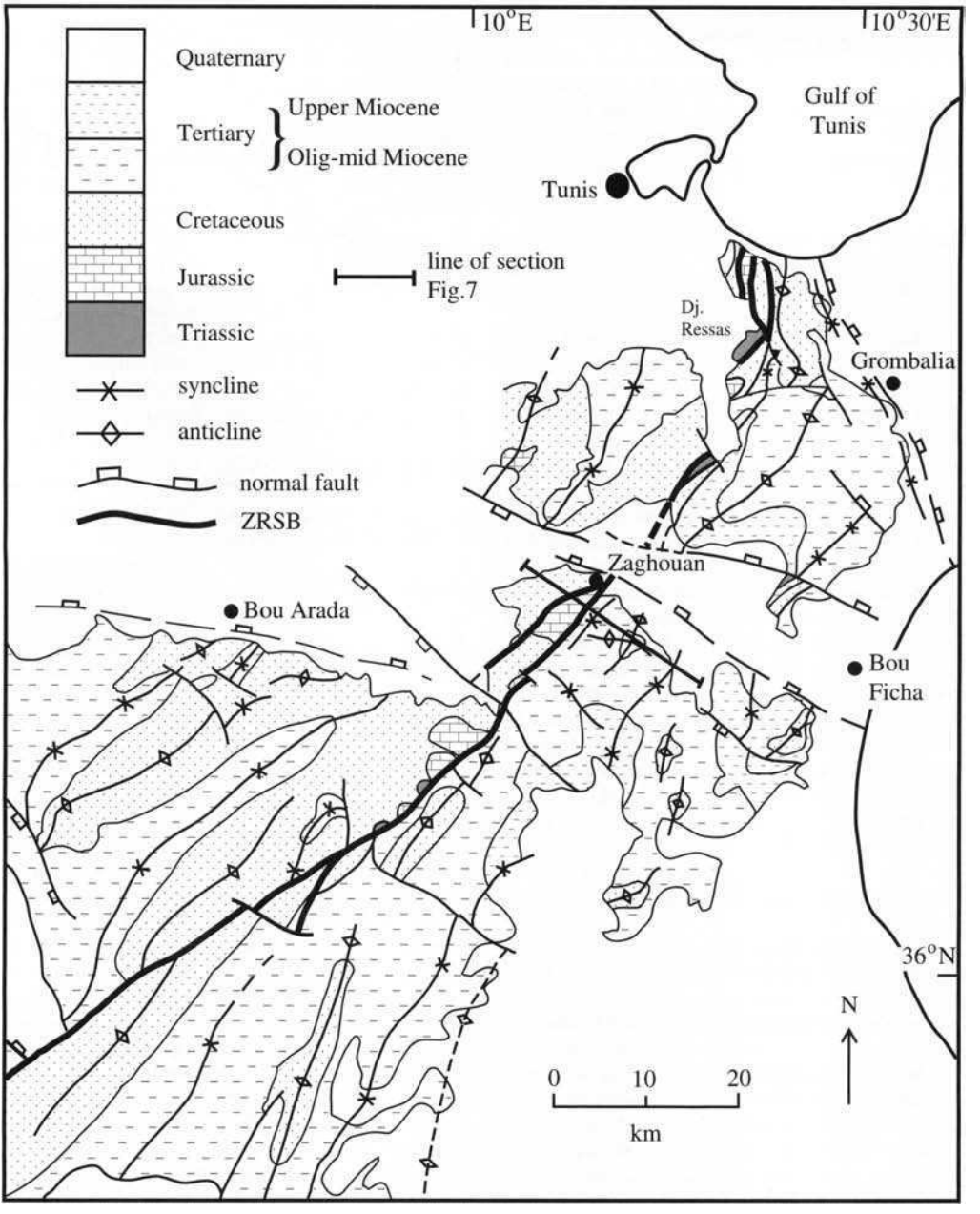

Fig. 2. Geological map of the Zaghouan–Ressas Structural Belt

mentation and contractional tectonics, we review first the tectonic framework of northern Tunisia from a North African perspective and then use this as a basis to evaluate the importance, during the Atlassic orogeny, of fault inversion as opposed to thin-skinned thrusting in the structural evolution of the ZRSB.

Tectonic framework

Triassic–Early Jurassic

In Triassic and Early Jurassic time the present site of Tunisia was located on the North African continental margin southwest of the Tethys Ocean (Dercourt *et al.* 1986, 1993; Ziegler 1988; Ricou 1994). This margin was characterized by extension, crustal thinning and subsidence (Coward & Dietrich, 1989). Triassic evaporites formed extensive deposits around the margins of the Tethys Ocean, and overlying shelf carbonates, pelagic limestones and turbidites of Jurassic age are indicative of deeper-water deposits and post-rift thermal subsidence (Laubscher & Bernoulli 1977). In eastern Tunisia, there is strong evidence for activity on north–south-trending normal faults and east–west-trending transfer faults at this time (Doglioni 1992), particularly along the line of the North–South Axis (Fig 3a; Ouali, 1985) and these faults probably defined the eastern margin of a Jurassic carbonate platform.

Middle Jurassic–Early Cretaceous

In Triassic and Early Jurassic time, the main influence on the tectonic evolution of the Mediterranean region was the development of the Tethys Ocean to the east. During the Middle Jurassic and Early Cretaceous, opening of the central Atlantic caused eastward motion of Africa relative to Europe and the development of a sinistral transform boundary west of Tethys (Fig. 3a) referred to here as the African–European Rift Zone (AERZ) and by Dercourt *et al.* (1986) as the Maghrebian–Ligurian trough. Accretion of new oceanic lithosphere was a feature of this rift system which may have been characterized by a triple junction northeast of Tunisia comprising a failed arm and two segments characterized by oceanic accretion (Morgan, 1994). We propose that opening of the AERZ was accommodated by dip-slip on northeast–trending extensional faults and sinistral strike-slip on northwest–trending transfer faults in northern Tunisia (Fig. 3a). The strike-slip faults may be reactivated basement lineaments that constrained the opening direction of the AERZ (J. Golonka, pers. comm. 1996).

The pattern of sedimentation in the central and western Mediterranean region throughout Middle and Late Jurassic time continued to be dominated by shelf carbonate deposition. At this time, northeast–southwest-trending, AERZ-related, dip-slip faults along the line of the ZRSB defined a basin–carbonate platform boundary at the southeast margin of a major pelagic basin (the Tunisian Trough of Burollet (1956); this paper, Fig. 3a). Sediment input into this and other pelagic basins of the AERZ was minimal, possibly because of arid climatic conditions, and this may have contributed to omission of Jurassic strata within the Tunisian Trough and extremely condensed sequences elsewhere (Fig. 4; Channel & Horváth 1976). The boundary of the Jurassic carbonate platform to the east was established during opening of the Tethys and we believe that north–south-trending Tethyan faults described above were reactivated as zones of strike-slip during rifting in the AERZ (Fig. 3a). The interference between faults related to the AERZ and faults related to the Tethyan margin, led to a rhomboid pattern (Fig. 3a) that has continued to control sedimentation in northern Tunisia to the present day.

In the Early Cretaceous, the AERZ–Tethyan basins located northwest and east of the Jurassic carbonate platform in Tunisia received mostly pelagic sediments, which reached a thickness of 2.5 km at Djebel Oost (Fig. 4; Turki 1988). It is tempting to regard this as essentially a post-rift, thermal subsidence-related sequence, representing the drift phase of a widening AERZ. However, widespread thickness and facies variations characterize Lower Cretaceous stratigraphy and indicate that fault systems, which initially compartmentalized the North African margin during Tethyan–AERZ rifting, continued to be active, defining horsts (palaeohighs) characterized by stratigraphic omissions or condensed sequences and relatively small, deep basins that received several kilometres of Lower Cretaceous sediments (Fig. 4). In the ZRSB, the thin or condensed Lower Cretaceous sequence preserved at Djebel Stah and the absence of Lower Cretaceous rocks at Hamman Zriba are consistent with the persistence of the Belt as a palaeohigh at this time. Variation in the thickness of Lower Cretaceous sequences in the Tunisian Trough may have caused lateral flow of Triassic evaporites leading to pillowing which, in addition to fault displacements, may be a mechanism explaining Lower Cretaceous facies and thickness variations in the Trough (Snoke *et al.* 1988).

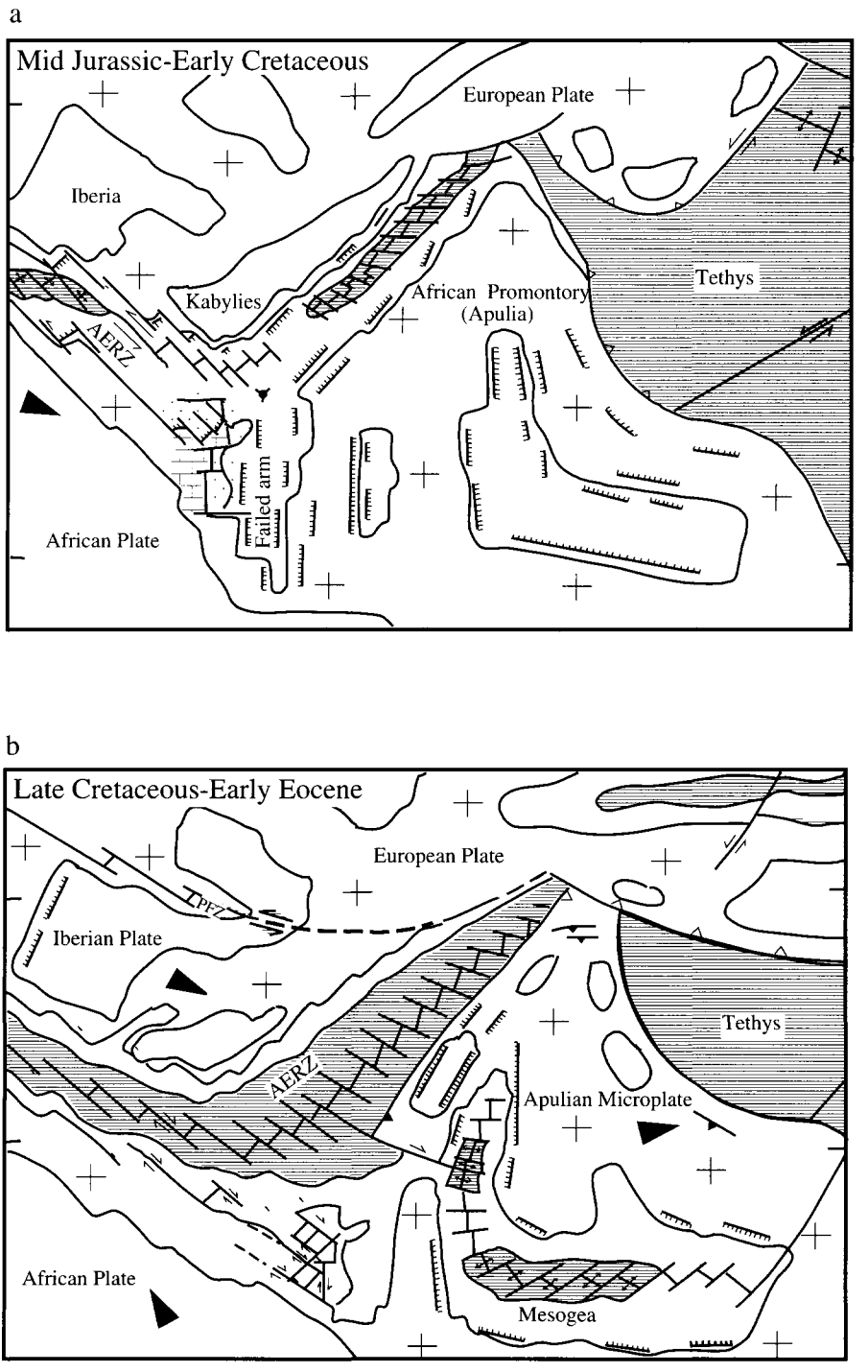

Fig. 3. Plate tectonic model for the Mediterranean area: (**a**) Middle Jurassic–Early Cretaceous; (**b**) Late Cretaceous–Early Eocene.
Details on the relative position of the African and European plates are taken from Dewey *et al.* (1973, 1989) and Livermore & Smith (1985).

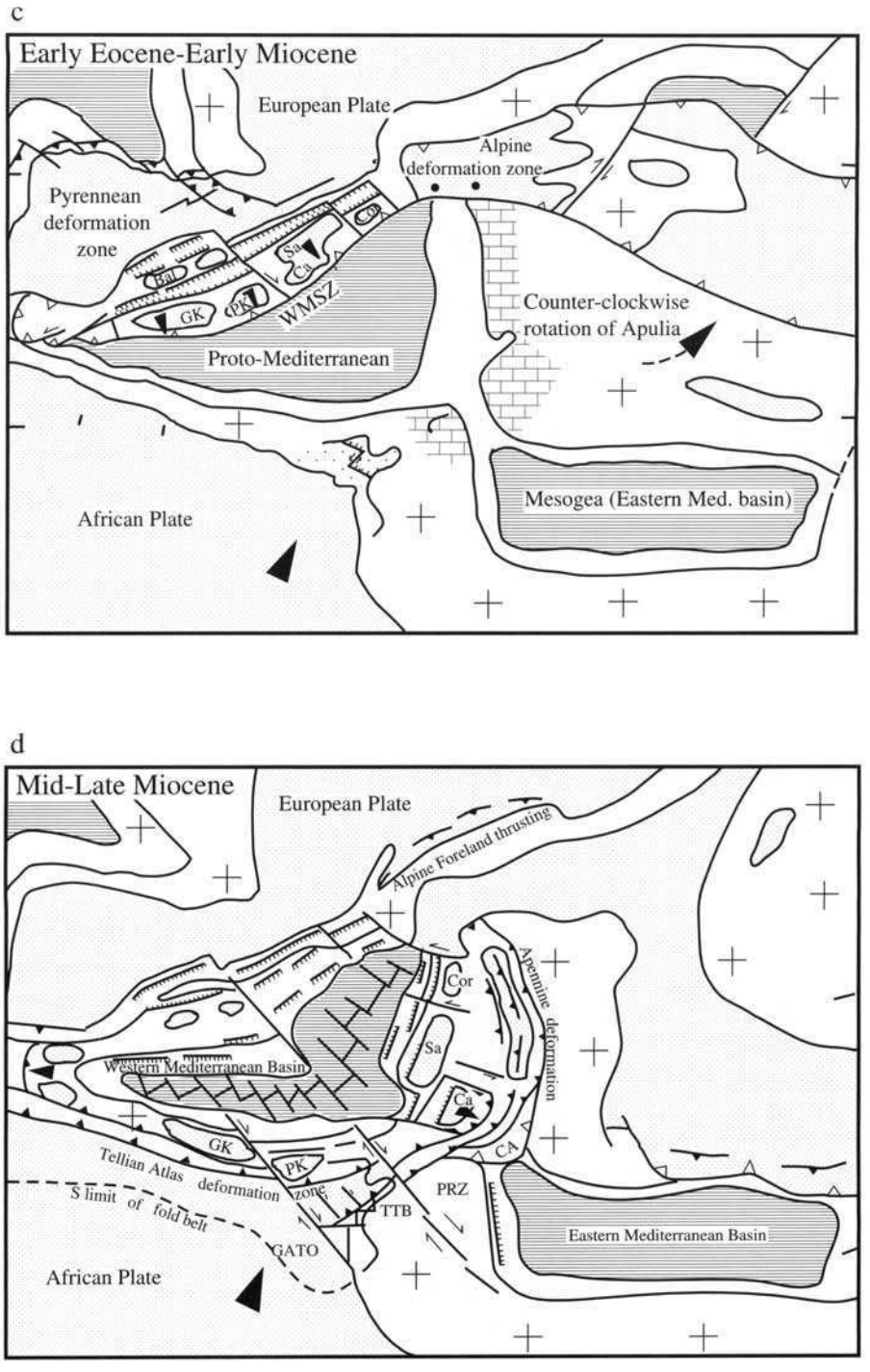

Fig. 3. (**c**) Late Eocene–Early Miocene; (**d**) Middle–Late Miocene.

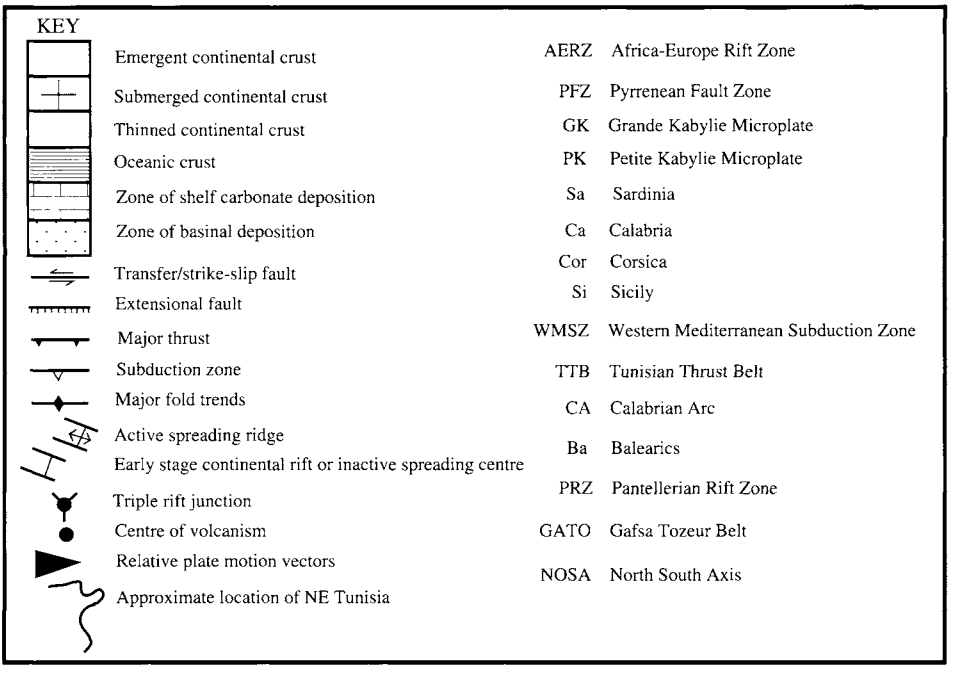

Fig. 3.

Late Cretaceous–Early Eocene

A fundamental change occurred in the drift of Africa relative to Europe in mid-Cretaceous time (*c.* 92 Ma), when the start of sea-floor spreading in both the South and North Atlantic resulted in northward drift of Africa and ended accretion of oceanic lithosphere in the AERZ (Dewey *et al.* 1989). From this time onward, a direct link between deformation in the western Mediterranean area and the motion of Africa relative to Europe is difficult to make, because the tectonics reflect the movement of microplates lying between the two continents. The displacement of these microplates, which is constrained mainly by geological arguments, is not simply a function of relative plate motion of the major plates, (Livermore & Smith, 1985; Hill & Hayward 1988; Dewey *et al.* 1989; Mantovani *et al.* 1990; Dercourt *et al.* 1993; Royden 1993; Ricou 1994).

Opening of the North Atlantic was marked initially by drift of Iberia to the southeast possibly in Albian time (c. 110 Ma, Coward & Dietrich 1989), but conceivably as late as the Campanian (*c.* 84 Ma; Dewey *et al.* 1989). The result was a reversal in the relative motion of Africa and the western European margin of the AERZ, now formed by the Iberian plate (Fig. 3b), leading to dextral transpression in the AERZ (Morgan 1994). Motion of Iberia was accommodated by displacement on the North Pyrenean fault and east-subduction of AERZ oceanic lithosphere beneath Apulia. Elimination of oceanic lithosphere in the northern segment of the AERZ, where it was narrowest, was followed by continental collision of Iberia with Apulia and led to Eoalpine (Late Cretaceous) deformation in the western Alps (Fig 3b Coward & Dietrich 1989). Drift of the Apulian microplate resulted in the formation of a new ocean basin between Africa and Apulia known as Mesogea (Dercourt *et al.* 1986), which was a precursor to the present-day eastern Mediterranean (Fig. 3b).

Upper Cretaceous to Eocene sedimentary sequences in Tunisia are characterized by thickness and facies variations similar in nature to those of Lower Cretaceous sequences. The variations are exemplified (Fig. 4) by deposition of 2–3 km of Upper Cretaceous strata at Djebel Dababdib (Snoke *et al.* 1988) and Djebel Goraa (Ben Hadj Ali 1977) but less than 500 m at Djebel Oost (Turki 1988), absence of these strata at Hamman Zriba (Turki 1988) and a very thin, condensed sequence near Grombalia east of the ZRSB. The implication is that fault displace-

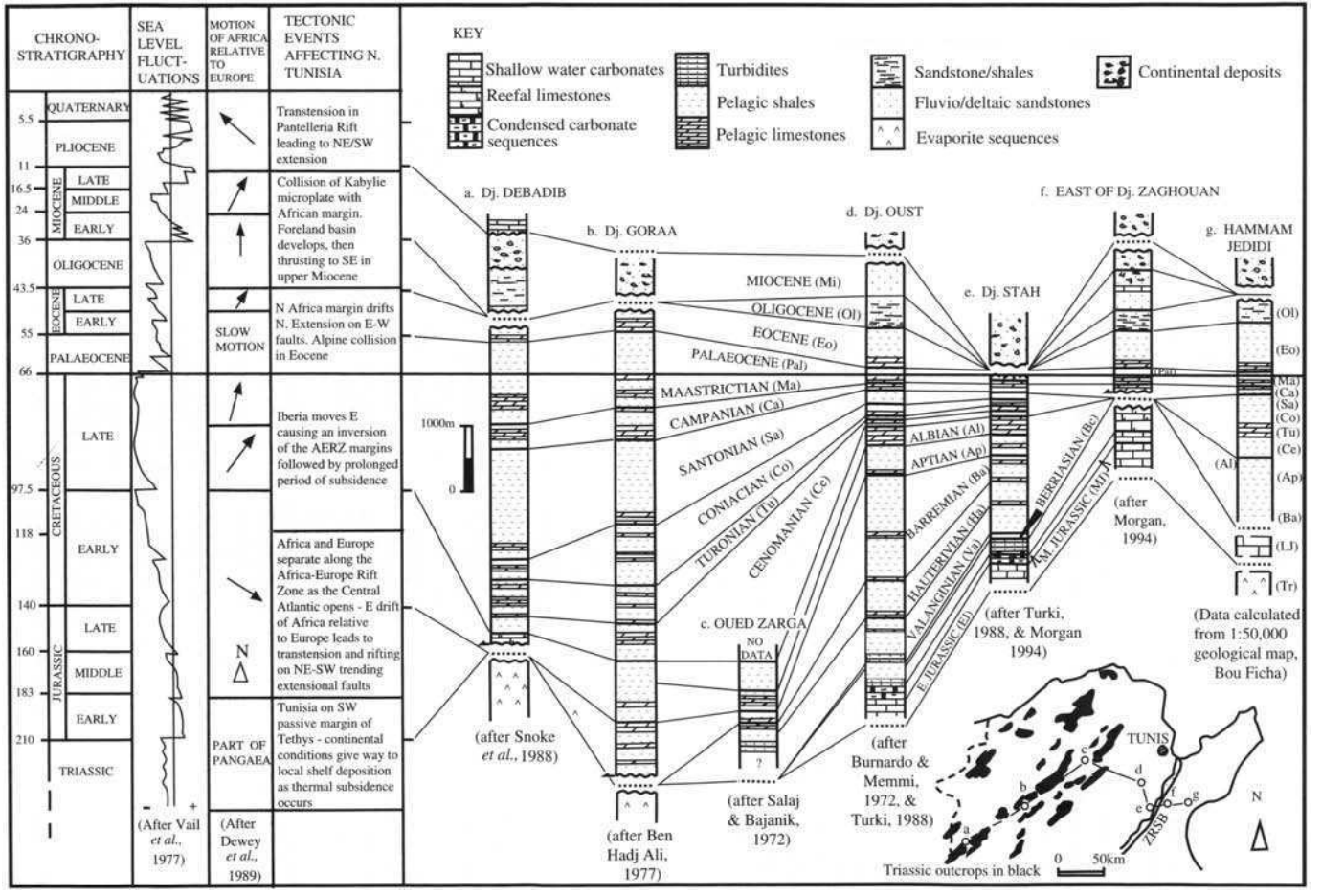

Fig. 4. Stratigraphic correlation diagram for northern Tunisia including details on sea level, relative plate motions and tectonic activity.

ments and uplift of horst blocks continued to strongly influence deposition in Tunisia during the Upper Cretaceous, although the basins and structural highs did not always correspond to those of the Lower Cretaceous.

The occurrence of palaeohighs with condensed sequences or non-deposition adjacent to small basins with thick, rapidly deposited sequences, is consistent with deposition within a strike-slip fault system. Consequently, we propose that inversion of the Triassic–Lower Cretaceous sinistral transtensive fault system during dextral transpression induced by the drift of Iberia could be responsible for Late Cretaceous sedimentary facies and thickness variation (Fig. 3b). Alternatively, southeast-subduction and roll-back of oceanic lithosphere of the narrow AERZ beneath Tunisia as well as beneath Apulia could have been responsible for transtension in the overiding plate (Fig. 3b). In addition, mobilization of Triassic evaporite–shale sequences because of thickness variations of the sedimentary packages may have led to pillowing or even piercement diapirism influencing further the characteristics of Upper Cretaceous sedimentary sequences (Perthuisot 1981).

Following collision of Iberia with northern Apulia in the Late Cretaceous, Africa continued to drift north slowly relative to Europe (Dewey *et al.* 1989). Late Cretaceous facies and thickness boundaries in northern Tunisia were controlled by reactivated northeast–southwest-trending AERZ margin faults (Salaj 1978; Ben Ferjani *et al.* 1990), but facies boundaries in early Eocene (Ypresian) rocks trend east–west or WNW–ESE (Moody 1987) implying that east–west Tethyan margin-related transfer faults (Fig. 3a) were reactivated at this stage to control sedimentation. This may be a reflection of sea-floor spreading in Mesogea leading to extension of the African margin and counter-clockwise rotation of Apulia which was eventually to result in the collision of this microplate with Europe in the late Eocene and deformation in the Western Alps (Fig 3c Platt *et al.* 1989).

Late Eocene–Early Miocene

The southeast-dipping and retreating Late Cretaceous subduction boundary located at the southeast margin of the AERZ (Fig. 3b) was eliminated when a fore-arc terrane rifted from the Apulian margin collided with the Ibero-Franco margin in the Late Eocene (Fig 3b and c; Rehault *et al.* 1984; Harris, 1985). This fore-arc terrane probably included what are today parts of Sardinia and Corsica but it is difficult to constrain the positions of Grande and Petite Kabylie, Calabria and the Balearics at this time and these microplate fragments may still have been part of the southeastern edge of the Iberian plate (Fig 3b; Dewey *et al.* 1989). Oceanic lithosphere was accreted in the back-arc basin that developed in the wake of these northwest-drifting microplates and formed the Proto-Mediterranean, an oceanic area to the west of Apulia. The Proto-Mediterranean was enlarged, together with Mesogea, during counter-clockwise rotation of Apulia into collision with the European plate to form the Western Alps (Fig. 3c Cohen 1980;).

West of Apulia, subsequent convergence between Africa and Europe was taken up by north-dipping subduction along the northern margin of the Proto-Mediterranean (Fig. 3c). Oceanic lithosphere in the Proto-Mediterranean was itself eventually eliminated by a process similar to that which brought about the destruction of the oceanic lithosphere of the AERZ. This time, north-dipping subduction beneath the European margin accompanied by roll-back to the southeast was involved (Horváth *et al.* 1981; Dewey *et al.* 1989). This induced opening of a back-arc basin and drift of a fore-arc terrane, containing present-day Corsica, Sardinia, Grande and Petite Kabylie and Calabria, toward the southeast and eventually into collision with the North African margin and Apulia (Fig. 3c and d). Oceanic lithosphere of the present-day western Mediterranean accreted behind this south-retreating subduction zone. The shape of the Proto-Mediterranean was such that fragments of the microplate located near the centre of the retreating subduction zone had farther to travel before collision occurred. The result of this was that deformation occurred initially in the northern Apennine region and the western edge of the North African margin. Contractional deformation then migrated to the south and east, respectively, from these two areas.

Collision of Petite Kabylie with the Tunisia margin led to the development of the Tunisian Atlas fold–thrust belt (Fig 3d Cohen 1980; Cohen *et al.* 1980). In the Mejerda Zone, onset of contractional deformation is marked by an angular unconformity at the base of the Oligocene and the development of an Oligo-Miocene foreland basin. This angular unconformity is not apparent everywhere in northern Tunisia. For example, in the Intermediate Atlas Zone east of the ZRSB (Fig. 2) there is a conformable transition from marine sedimentary rocks of Lutetian age to continental deposits of the

Oligo-Miocene foreland basin. Provenance of the Oligocene sediments was from the west and from the northeast (Van Houten 1980; Yaich 1992;), consistent with uplift earlier in Algeria and in the Apennines than in Tunisia and accretion of terranes progressively from west to east along the African margin and from north to south along the Apulian margin. In the foredeep sediments, particularly in Miocene and Mio-Pliocene sequences, drowning events are marked by the deposition of shallow-marine calc-arenite and thick, shale-dominated sequences (Moody & Sutcliffe, 1994). In the ZRSB, contractional deformation of the foreland basin sediments occurred in Upper Miocene time (post-Tortonian, pre-Messinian) and represents the main deformation responsible for the formation of the Atlas fold–thrust belt in Tunisia. In the internal zones (Mejerda Zone and the Tell) two major phases of Upper Miocene contractional deformation are recognized, an initial phase of folding and thrusting followed by emplacement of the out-of-sequence 'Numidian' thrust sheet which carried deep-water, Oligo-Miocene flysch deposits in its hanging wall at least 30 km to the southeast (Morley 1988). Collision of Petite Kabylie with northern Tunisia resulted also in strike-slip motion on transfer faults to the east and west of the thrust belt (Fig. 3d). These transfer faults define the important lineaments of the Gafsa–Tozeur Belt and the Pantelleria Rift Zone. They probably have their origins in the rifting phase of the AERZ and they may represent reactivated basement lineaments.

Models for the structural evolution of the Zaghouan–Ressas Structural Belt

In the following sections we present and evaluate two models for the Zaghouan–Ressas Structural Belt. The first is a thin-skinned detachment model which focuses on structures formed during Upper Miocene contractional deformation above a detachment controlled by evaporitic Triassic strata (Baird *et al.* 1990; Anderson 1991, 1996; Morgan & Grocott 1993; Outanni *et al.* 1995). The second is a fault-inversion model which takes into account basin evolution and particularly the influence of sedimentary facies variation on the deformation style which developed during contractional deformation. This model has much in common with recent interpretations of the European Tethyan margin where the inversion of formerly extensional structures during Alpine contractional deformation is emphasized (Coward & Dietrich 1989; Graciansky *et al.* 1989).

Fold–thrust detachment model for Zaghouan–Ressas Structural Belt

Stratigraphic template

An important constraint in drafting structural cross-sections through thrust belts is provided by the construction of a viable stratigraphic template (Ramsay & Huber 1987; Mitra 1993). Figure 5 shows a sequence of pre-Upper Miocene stratigraphic templates for the ZRSB southeast of Zaghouan. They are based on measured sedimentary logs (Fig. 4) and assumptions drawn from the tectonic framework outlined above.

The template for Middle–Late Jurassic time (Fig. 5a) shows the Jurassic carbonate platform of northern Tunisia cut by extensional faults related to the AERZ. Faults to the northwest of the site of the future ZRSB are located at the margin of the Tunisian Trough where thick sequences of Lower Cretaceous sediments were deposited (Fig. 5b). Faults shown to the southeast are reactivated Tethyan margin faults such as those along the North–South Axis. The site of the future Zriba anticline is a horst with no Cretaceous deposition until it was overlapped in the Upper Cretaceous and the Abiod Formation was deposited unconformably on Jurassic platform carbonates. It remains possible that the missing sediments were originally deposited above palaeohighs but were eroded in the post-Aptian–pre-Campanian period. In Fig. 5b, it is assumed that the opening of the North Atlantic and the drift of Iberia resulted in transpression of the Tunisian margin in the Upper Cretaceous, which caused partial inversion of earlier faults.

The Paleocene to Oligocene sequence is shown as a layer-cake for the Zaghouan-Zriba profile (Fig. 5c) because substantial thickness variations do not occur for this time interval along the line of section. To the northeast, along strike from the Hamman Zriba palaeohigh, thin, condensed Paleocene and Ypresian sequences exposed southwest of Grombalia (Fig. 2) imply that fault displacements and block movements were characteristic of this period elsewhere in the ZRSB, possibly related to extension on the southern margin of Mesogea as outlined above. The final, pre-Atlassic deformation template (Fig. 5d) shows partial inversion along the ZRSB in Early Miocene time.

It is clear that facies and thickness variations characterize Jurassic and Cretaceous stratigraphy. In a thin-skinned thrust model, such variation should exercise structural control on thrust propagation and on lateral continuity of the structures. In addition, it is evident from the distribution of lithologies and thicknesses that dif-

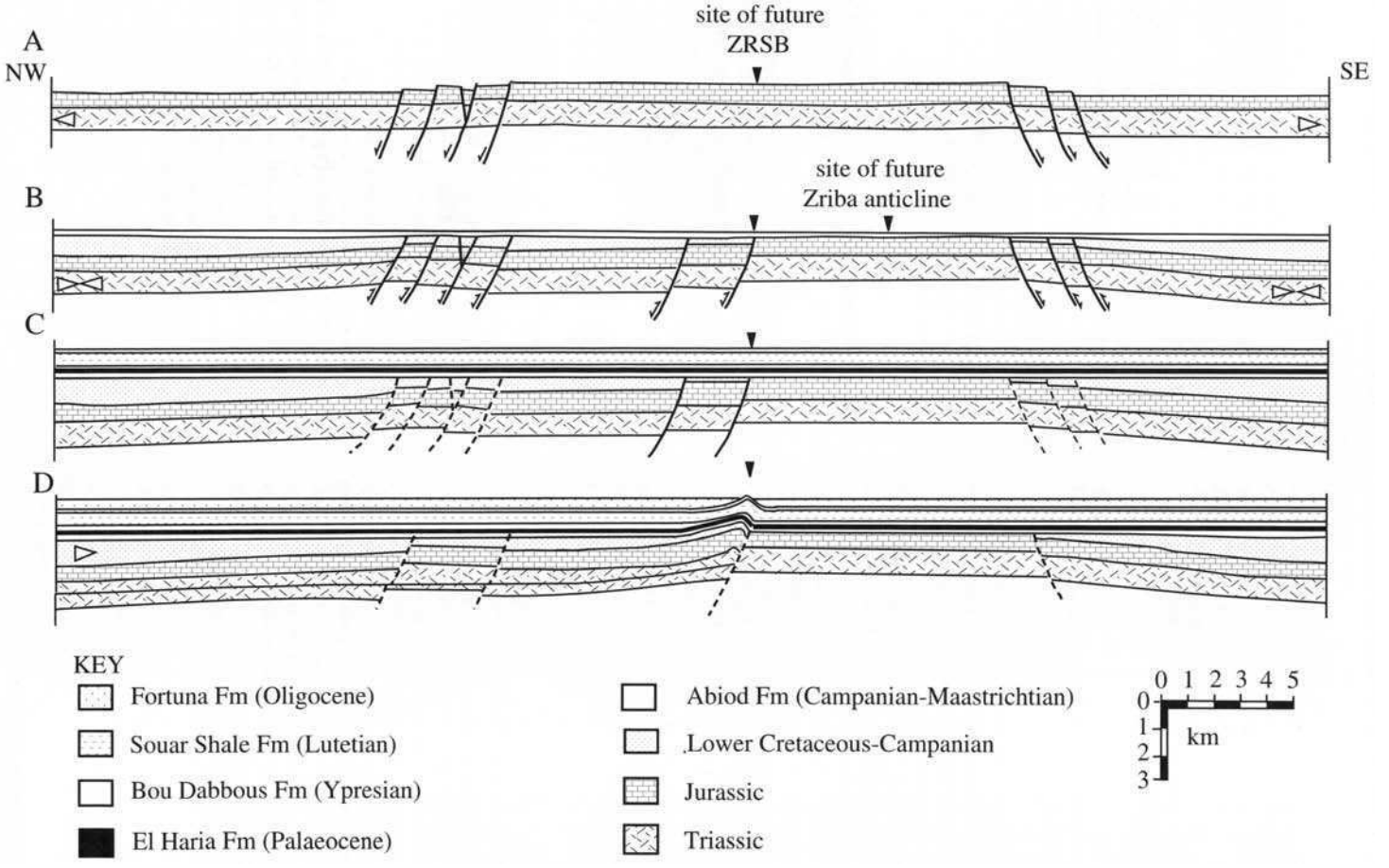

Fig. 5. Palinspastic restoration of the pre-thrusting stratigraphic template for the balanced cross-sections through Djebel Zaghouan: **(a)** Late Jurassic; **(b)** Cretaceous; **(c)** Late Oligocene; **(d)** Early Miocene.

ferential loading of the Triassic evaporite–shale sequences, from Early Cretaceous time, may have caused them to flow laterally. Consequently, development of pillow-structures, or even piercement diapirs, may have complicated further the pre-thrusting stratigraphic template. Nevertheless, the existence of weak Triassic evaporitic and shale sequences, and the virtual absence of exposed basement supports the adoption of a thin-skinned model to explain the structure of the Tunisian Atlas.

Cross-section through Djebel Zaghouan and Hamman Zriba

Figure 6 is a cross-section drawn through Djebel Zaghouan, southeast of Zaghouan town showing contractional structures above a detachment in Triassic evaporites. The stratigraphic template used is that in Fig. 5d. Tethyan margin–AERZ faults play a role in that they may have provided buttresses inhibiting foreland propagation of the detachment fault. In addition, assuming that the Tethyan margin faults may have been initiated before Jurassic–Early Cretaceous rifting, then facies variations across the faults in Triassic rocks are expected which may have encouraged thrusts to cut up-section. At Djebel Zaghouan, a ramp in thrust T1 is induced by a basement step above extensional fault E1 (Fig. 6). The development of the Zaghouan fold is interpreted as an anticline–syncline fold-pair formed during fault propagation and related to thrust T1. Fault propagation in the footwall of thrust T1 led to the development of a duplex which formed the core of the Hammam Zriba anticline. Formation of this duplex requires that the Triassic in the subsurface at Zriba is relatively competent, or is thin or absent over the crest of the Zriba palaeohigh. East of the ZRSB, thrust T1 enters a flat at the level of the Upper Cretaceous–Jurassic unconformity at Zriba accounting for the deformation observed at that contact. The Zriba, anticline may also be interpreted as a detachment fold cored by Triassic evaporites and this, rather than duplex structure, may account for the elevation of the Jurassic in the fold above its regional height in the foreland.

The absence of a hanging wall anticline at Zaghouan is accounted for using an out-of-sequence thrust, T5. This cuts the fault-propagation fold associated with thrust T1 and allows the planar beds in the back-limb of this fold to be juxtaposed against a fault-propagation syncline in the footwall of T5 (Fig. 6). As this thrust was probably emergent, a large amount of post-Lower Cretaceous section will have been rapidly eroded from the hanging wall, and consequently no attempt has been made to balance the cross-section by predicting the position of hanging wall cut off points for T5. The fault-propagation fold–antiformal stack along the ZRSB at Zaghouan was later dissected by northeast–southwest-trending, oblique-slip extensional faults giving rise to the steeply dipping, paired faults that define the belt for much of its length (Fig. 7). These faults may have propagated upward through the thrust-belt structures from beneath the Triassic detachment because of reactivation of deep segments of AERZ-related extensional fault system. Reactivation is probably of Pliocene–Recent age and linked to displacements responsible for the opening of the northwest–southeast-trending graben and half-graben structures during Pliocene–Recent time. (Fig. 5, Boccaleti *et al.* 1987; Jongsma *et al.* 1987; Reuther *et al.* 1993).

Fault-inversion model for the development of the ZRSB

Problems with the thin-skinned detachment model are: (1) the dual role required for the Triassic as both a fault-preference horizon and a competent horizon in which thrust-ramping occurs; (2) the need for an explanation of the reactivation of AERZ–Tethyan margin faults during late oblique-slip but not during earlier Atlassic shortening. In addition, there is a need for an interpretation which is consistent with stratigraphy and structures across the whole of northern Tunisia. An alternative explanation for the structure of the ZRSB can be made in terms of fault inversion (Fig. 8). The pre-contractional template is wider than in Fig. 4 and shows that differential loading of the Triassic during Lower Cretaceous sedimentation in the Tunisian trough may be responsible for pillowing of Triassic strata in the Mejerda Zone and even for piercement diapirism (see Graciansky *et al.* 1989). Another possibility is that the Triassic outcrops in the Mejerda Zone represent corners of rotated, extensional fault blocks (Baird & Clayton 1995) and that they were palaeohighs in much the same way as the Jurassic at Zriba or Zaghouan represent palaeohighs (Morgan 1994). The overlying Cretaceous to Miocene sedimentary sequences were deposited unconformably on these blocks rather than the relationship with the Triassic being diapirism related.

The inversion model shows similarities with the cross-sections drawn by Graciansky *et al.* (1989) for the Western Alps although the timing of events differs. The structure proposed

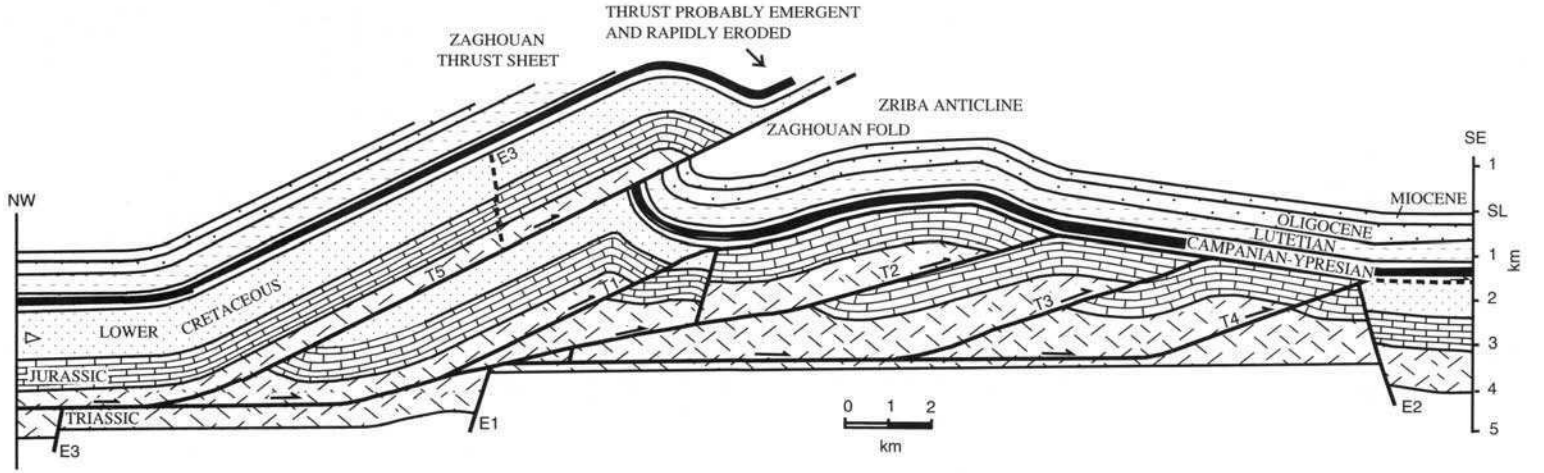

Fig. 6. Cross-section for Djebel Zaghouan–Zriba. The cross-section corresponds to the structure after Late Miocene deformation but before Post-Tortonian oblique extensional faulting, which has been restored. Faults E1–E3 are NW–S- trending AERZ-related extensional faults (Fig. 5). Thrusts T1–T4 formed in piggy-back sequence and T5 is an out-of-sequence thrust responsible for the uplift of the Jurassic at Djebel Zaghouan. The key is the same as in Fig. 5.

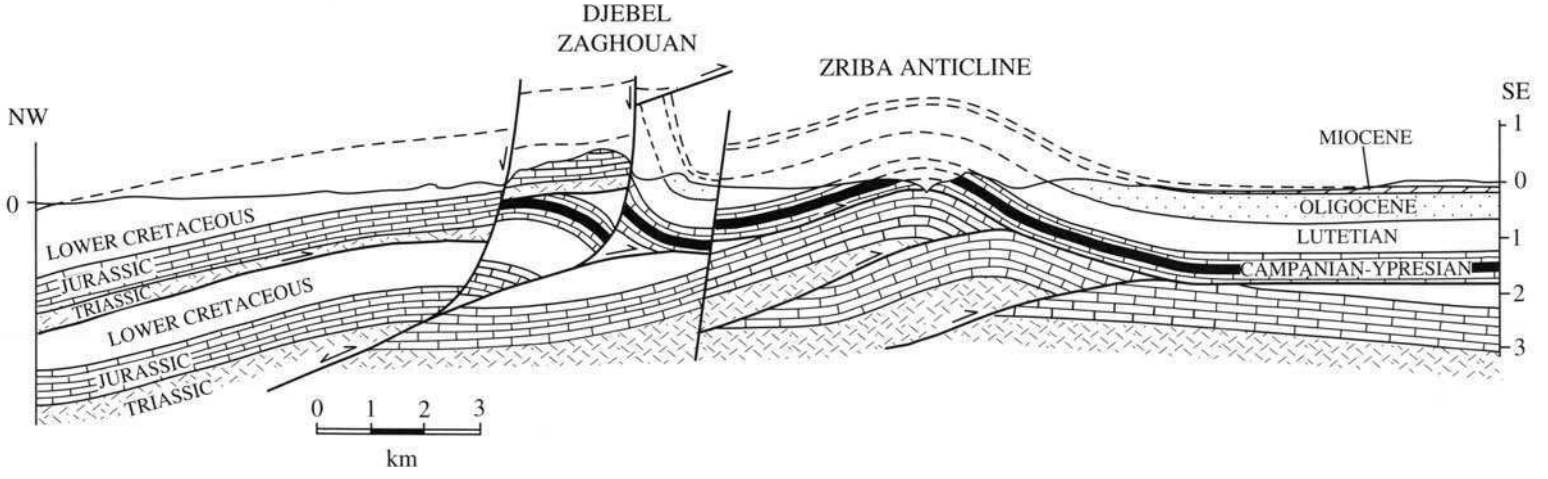

Fig. 7. Sketch cross-section for Djebel Zaghouan Zriba. This is the present-day cross section showing the topography and including Post-Tortonian oblique extensional faults. (Note that the subsurface interpretation is slightly different from that shown in Fig. 6.

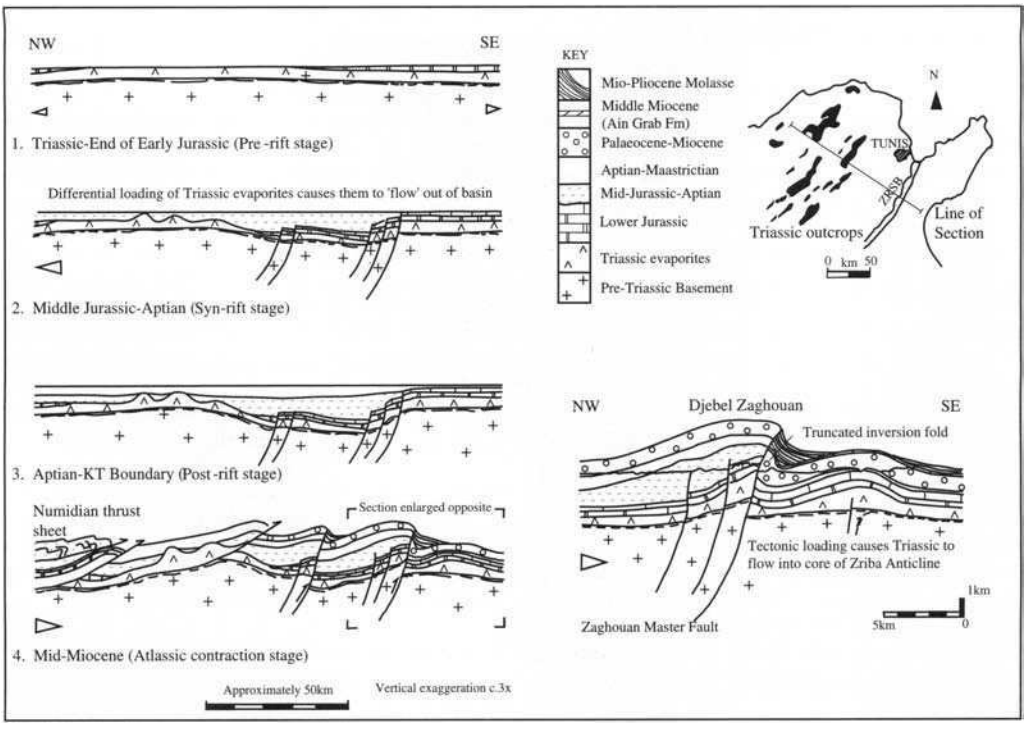

Fig. 8. A basin-inversion model for the origin of the Zaghouan–Ressas Structural Belt and the structural style of the Tunisian Atlas.

avoids the complexity of the thin-skinned model yet remains consistent with the surface geology. However, problems with the inversion model include the following: (1) the ZRSB boundary faults are steep to vertical at outcrop and imply inversion of very steep faults without the development of hanging wall short cuts; (2) the ZRSB boundary faults have strike-slip or oblique-slip kinematic indicators rather than dip-slip indicators consistent with fault inversion during Atlassic contraction; (3) assuming that inversion of growth faults that cut basement has occurred widely in northern Tunisia, then sub-Triassic basement should be more commonly exposed; (4) there is no inversion 'buttress' anticline exposed in the hanging wall of the putative inversion fault at Zaghouan.

Implications for petroleum geology

During the Jurassic and Early Cretaceous, fault systems on the southwest margin of the Tethys, and on the African margin of the AERZ, defined a system of pelagic basins separated by uplifted fault blocks characterized by slope and carbonate platform deposition and exemplified by the ZRSB. Lateral thickness and facies variations in the sedimentary sequences are typical of this system. In the Tunisian Trough, immediately northwest of the ZRSB, Lower and mid-Cretaceous reservoir rocks are absent and the succession is shale dominated and characterized by limited biotic production. Elsewhere in northern Tunisia excellent mid-Cretaceous source rocks (Mouelha Formation, Bahloul Formation) are widespread but their distribution is affected by Late Cretaceous inversion, which led to erosion of the sequences on uplifted fault blocks and/or above pillows of Triassic rocks. Where thick sequences were deposited, maturation may well have occurred locally in mid-Cretaceous time, but more work is required to define the geometry of the basins and horsts, the distribution of the source rocks and the timing of their maturation.

Inversion of AERZ-related faults occurred initially in Late Cretaceous time in response to initiation of sea-floor spreading in the North Atlantic and southeast drift of Iberia. In northern Tunisia, the depositional distribution and thickness of Abiod Formation reservoir carbonates (Campanian–Maastrichtian) was con-

trolled by fault-block displacements and possibly by related flow of Triassic strata to form pillows at this time (Fig. 3b). In the Eocene, extension of the Tunisian margin, and continued reactivation of AERZ fault trends in response to northward drift of Apulia (Fig. 3c), controlled the distribution of Metlaoui Group potential oil-source and reservoir rocks (Moody 1987).

In the internal zones a strong unconformity at the base of the Oligocene marks the onset of contractional tectonics and development of the foreland basin in northern Tunisia. The unconformity must reflect Cretaceous–Eocene deformation as a consequence of which, potential oil-source rocks have locally been removed by erosion before they reached maturation in parts of the Intermediate Atlas and Mejerda Zones. Where they were preserved, maturation of mid-Cretaceous source rocks that had not already reached the oil generation window during burial and Ypresian source rocks (Metlaoui Group–Bou Dabbous Formation) will be a function of the burial depth below Oligo-Miocene molasse. In the Tell and Mejerda Zones, maturation may also have been induced by thrust sheet emplacement in the Upper Miocene.

Conclusions

On balance, we believe that the Zaghouan–Ressas Structural Belt is a fault-inversion feature caused by reactivation of AERZ-related, northeast–southwest-trending basin-margin faults during the Atlassic Orogeny. The inversion is particularly great at the ZRSB because it was the site of large extensional displacements associated with the southeast margin of the Tunisian Trough and consequently buttressing effects, caused by a combination of a basement step and thickness and facies variations across the fault, were greatest. Fault inversion is preferred to an interpretation involving thin-skinned, detachment tectonics because the solution it produces is simple and the amount of shortening and stratigraphic duplication is much less. In addition, it is not necessary to argue that AERZ-related faults were selectively inverted; that is, that they were not inverted during Atlassic contraction, but were reactivated during neotectonic oblique-slip displacements. The objections to the inversion model outlined above cannot be sustained. The steepness of the ZRSB boundary faults at Zaghouan may be a consequence of steepening during contraction (Graciansky *et al.* 1989) and the oblique-slip indicators may reflect the latest, neotectonic, increments of deformation on the ZRSB, rather than the displacement direction of the faults during inversion. Sub-Triassic basement, though rare, is exposed at Djebel Hairech in the southwest part of the Mejerda Zone, near Jendouba, where Triassic sandstones overlie Permian(?) slates containing a pre-Atlas cleavage indicating that at least some Tethyan margin extensional faults cut down-section into metamorphic basement. This favours a thick-skinned model at the early stages of contraction, but as shortening increased, we envisage that detachment on Triassic strata played an increasingly important role in the evolution of the thrust belt, particularly in the internal zones. Finally, the cross-sections of Graciansky *et al.* (1989) from the Western Alps show that uplift of competent platform carbonates during fault inversion need not be accompanied by the growth of large-scale, fault-inversion anticlines (forced folds), so the absence of such a fold in the hanging wall at Zaghouan is not necessarily problematic for the inversion model.

It is also likely that inversion of AERZ-related faults has occurred in the more internal zones of the Tunisian Atlas fold–thrust belt. However, particularly in the Tell, contraction is greater and the inversion geometries and faults have been overprinted by hanging wall short cuts and/or possibly rotated into a thrust orientation. The Mejerda Zone is located at the boundary between the thin-skinned thrust structures of the Tell and the inversion tectonics of the Intermediate Atlas Zone (including the North–South Axis and the ZRSB). As such, it is an obvious focus for future study of the relationship between thick-skinned inversion tectonics and thin-skinned tectonics in the Atlas fold–thrust belt of Tunisia.

M.A.M acknowledges receipt of a Kingston University Research Studentship and financial support for fieldwork from Marathon Petroleum (Tunisia) Ltd. We have benefited from discussions with M. Rogers, K. Barnes, H. Belayouni, K. Corbett, D. Green, J. Golonka, R. Hodgkinson, J. Kendall, P. Price and A. Mabrouk. D. Frizon de Lamotte is thanked for a perceptive review of the manuscript.

References

ANDERSON, J. E. 1991. *Subsidence history and structural evolution of the western margin of the Pelagian Platform, Central Tunisia. PhD thesis, Kingston University.*

—— 1996. The Neogene structural evolution of the western margin of the Pelagian Platform, central Tunisia. *Journal of Structural Geology*, **18**, 819–833.

BAIRD, A. W. & CLAYTON, C. J. 1995. Tethyan aulacogen formation in northern Tunisia and its control of basin inversion mechanisms. *1st Symposium on the Hydrocarbon Geology of North Africa, Abstracts*, Geological Society, London, 9–10.

——, GROCOTT, J., SANDMAN, R. I., GRANT, G. G. & MOODY, R. T. J. 1990. A radical re-interpretation of the Tunisian Atlas thrust belt and foreland basin system. *International Conference on Thrust Tectonics, Royal Holloway & Bedford New College. Programme and Abstracts*, 81.

BEDIR, M., ZARGOUNI, F., TLIG, S. & BOBIER, C. 1992. Subsurface geodynamics and petroleum geology of transform margin basins in the Sahel of Mahdia and El Jem, eastern Tunisia. *Bulletin, American Association of Petroleum Geologists*, **76**, 1417–1442.

BEN FERJANI, A., BUROLLET, P. F. & MEJRI, F. 1990. *Petroleum Geology of Tunisia*. ETAP, Tunis.

BEN HADJ ALI, M. 1977. *Etude géologique du Djebel Goraa (région de Teboursouk Atlas Tunisien)*. Thèse de 3ème cycle, Université de Paris VI.

BOCCALETTI, M., CELLO, G. & TORTORICI, L. 1987. Neogene–Quaternary tectonics in the Sicily Channel. *Journal of Structural Geology*, **9**, 869–876.

——, —— & —— 1988. Structure and tectonic significance of the North–South axis of Tunisia. *Annales Tectonicae*, **2**, 12–20

——, —— & —— 1990. First order kinematic elements in Tunisia and the Pelagian block. *Tectonophysics*, **176**, 215–228.

BRACÈNE, R., BELLAHCÈNE, BEKKOUCHE, D., MERCIER, E. & FRIZON DE LAMOTTE, D. 1998. The thin-skinned style of the South Atlas Front in central Algeria. *This volume*.

BURNADO, R. & MEMMI, L. 1972. *La série infracrétacée du Jebel Oust (Tunisie)*. Notes Service de Géologie Tunisie, **38**, 49–61.

BUROLLET, P. F. 1956. Contribution a l'étude stratigraphic de la Tunisie centrale. *Annales Mines et Géologie, Tunis*, **18**, 1–352.

—— 1991. Structures and tectonics of Tunisia. *Tectonophysics*, **195**, 359–369.

CHANNEL, J. E. T. & HORVÁTH, F. 1976. The African/Adriatic Promontory as a palaeogeographic premise for the Alpine orogeny and plate movements in the Carpatho-Balkan region. *Tectonophysics*, **35**, 71–101.

COHEN, C. R. 1980. Plate tectonic model for the Oligo-Miocene evolution of the western Mediterranean. *Tectonophysics*, **68**, 283–311.

——, SCHAMEL, S. & BOYD-KAYGI, P. 1980. Neogene deformation in northern Tunisia: Origin of the eastern Atlas by microplate–continental margin collision. *Bulletin, Geological Society of America*, **91**, 225–237.

COWARD, M. P. & DIETRICH, D. 1989. Alpine tectonics: an overview. *In*: COWARD, M. P., DIETRICH, D. & PARK, R. G. (eds) *Alpine Tectonics*. Geological Society, Special Publication, **45**, 1–29.

DERCOURT, J., RICOU, L. E. & VRIELYNCK, B. (eds) 1993. *Atlas Tethys Palaeoenvironmental maps*. Gauthier-Villars, Paris.

——, ZONENSHAIN, L. P., RICOU, L. E., *et al.* 1986. Geological evolution of the Tethys belt from the Atlantic to the Pamirs since the Lias. *Tectonophysics*, **123**, 241–315.

DEWEY, J. F., HELMAN, M. L., TURCO, E. & HUTTON, D. H. W. 1989. Kinematics of the western Mediterranean. *In*: COWARD, M. P., DIETRICH, D. & PARK, R. G. (eds) *Alpine Tectonics*, Geological Society, London, Special Publication, **45**, 265–283.

——, PITMAN, W. C., RYAN, W. B. F. & BONNIN, J. 1973. Plate tectonics and evolution of the Alpine system. *Bulletin, Geological Society of America*, **84**, 3137–3180.

DOGLIONI, C. 1992. Main differences between thrust belts. *Terra Nova*, **4**, 152–164.

GRACIANSKY, P. C., DARDEAU, G., LEMOINE, M. & TRICART, P. 1989. The inverted margin of the French Alps and foreland basin inversion. *In*: COOPER, M. A. & WILLIAMS, G. D. (eds) *Inversion Tectonics*, Geological Society, London, Special Publication, **44**, 87–104.

HARRIS, B. L. 1985. Direction changes in thrusting in the Schistes Lustres in Alpine Corsica. *Tectonophysics*, **120**, 37–56.

HILL, K. C. & HAYWARD, A. B. 1988. Structural constraints on the Tertiary plate tectonic evolution of Italy. *Marine and Petroleum Geology*, **5**, 2–16.

HORVÁTH, F, BERCKHEMER, H. & STEGENA, L. 1981. Models of Mediterranean back-arc basin formation. *Philosophical Transactions of the Royal Society, London, Series A*, **300**, 383–402.

JONGSMA, D., WOODSIDE, J. M., KING, G. C. P. & VAN HINTE, J. E. 1987. The Medina Wrench: a key to the kinematics of the central and eastern Mediterranean over the past 5 Ma. *Earth and Planetary Science Letters*, **82**, 87–106.

LAUBSCHER, H. P. & BERNOULLI, D. 1977. The Mediterranean and Tethys. *In*: NAIRN, A. E. M., KANES, W. H. & STEHLI, F. G. (eds) *The Ocean Basins and Margins: The Eastern Mediterranian*, **4a**, Plenum Press, New York, 1–29.

LIVERMORE, R. A. & SMITH, A. G. 1985. Some boundary conditions for the evolution of the Mediterranean region. *In*: *Geological Evolution of the Mediterranean Basin*, Plenum Press, New York, 83–98.

MANTOVANI, E., BABUCCI, D., ALBARELLO, D. & MUCCIARELLI, M. 1990. Deformation pattern in the central Mediterranean and behaviour of the African/Adriatic promontory. *Tectonophysics*, **179**, 63–79.

MITRA, S. 1993. Geometry and kinematic evolution of inversion structures. *Bulletin, American Association of Petroleum Geologists*, **77**, 1159–1191.

MOODY, R. T. J. 1987. The Ypresian carbonates of Tunisia—a model of foraminiferal facies distribution: *In*: HART, M. B. (ed.) *Micropalaeontology of Carbonate Environments*. British Micropalaeontological Society Series, Ellis Horwood, Chichester, 82–92.

—— & SUTCLIFFE, P. J. C. S. 1994. The unroofing of the Medjerda Zone. *Proceedings of the Tunisian Petroleum Conference (Tunis, May 1994)*. Memoires de l'ETAP, **7**, 39–53.

MORELLI, C. & NICOLICH, R. 1990. A cross section of the lithosphere along the European Geotraverse southern segment (from the Alps to Tunisia). *Tectonophysics*, **176**, 229–243.

MORGAN, M. A. 1994. *The Structural Evolution of the Zaghouan-Ressas Structural Belt, NE Tunisia.* PhD thesis, Kingston University.

—— & GROCOTT, J. 1993. *The structural setting and evolution of the Zaghouan-Ressas structural belt in the Zaghouan area, Tunisian Atlas, northern Tunisia.* Mémoires de l'ETAP, **5**,193–209.

MORLEY, C. K. 1988. Out of sequence thrusts. *Tectonics*, **7**, 539–561.

OUALI, J. 1985. Structure et évolution géodynamique du chaînon Nara–Sidi Khalif (Tunisie Centrale). *Bulletin des Centres de Recherches Exploration–Production Elf-Aquitaine*, **9**, 155–182.

OUTTANI, F., ADDOUM, B., MERCIER, E., FRIZON DE LAMOTTE, F. & ANDRIEUX, J. 1995. Geometry and kinematics of the South Atlas Front, Algeria and Tunisia. *Tectonophysics*, **249**, 233–248.

PERTHUISOT, V. 1981. Diapirism in northern Tunisia. *Journal of Structural Geology*, **3**, 231–235.

PLATT, J. P., BEHRMANN, J. H., CUNNINGHAM, P. C., *et al.* 1989. Kinematics of the Alpine arc and the motion history of Adria. *Nature*, **337**, 158–161.

RAMSAY, J. G. & HUBER, M. I. 1987. *Techniques of Modern Structural Geology, Volume 2: Folds and Fractures.* John Wiley, New York.

REHAULT, J., BOILLOT, G. & MAUFFRET, A. 1984. Western Mediterranean Evolution. *Marine Geology*, **55**, 447–477.

REUTHER, C., BEN-AVRAHAM, Z. & GRASSO, M. 1993. Origin and role of major strike-slip transfers during plate collision in the central Mediterranean. *Terra Nova*, **5**, 249–257.

RICOU, L. E. 1994. Tethys reconstructed: plates, continental fragments and their boundaries since 260 Ma from Central America to South-eastern Asia. *Geodinamica Acta*, **7**, 169–218.

ROYDEN, L. H. 1993. Evolution of retreating subduction boundaries formed during continental collision. *Tectonics*, **12**, 303–325.

SALAJ, J. 1978. The geology of the Pelagian block: The eastern Tunisian platform. *In*: NAIRN, A. E. M., KANES, W. H. & STEHLI, F. G. (eds) *The Ocean Basins and Margins: The Eastern Mediterranean*, **4b**, Plenum Press, New York, 361–416.

—— & BAJANIK, K. 1972. Contribution à la stratigraphie du Crétacé et du Paléogène de la région de l'Oued Zarga. *Notes Service Géologie Tunisie*, **38**, 63–71.

SNOKE, A. W., SCHAMEL, S. & KARASEK, R. M. 1988. Structural evolution of Djebel Debadib anticline: a clue to the regional tectonic style of the Tunisian Atlas. *Tectonics*, **7**, 497–516.

TURKI, M. M. 1988. Polycinematique et controle sédimentaire associé sur la cicatrice Zaghouan–Nebhana. *Révue des Sciences de la Terre, Tunis*, **7**.

VAIL, P. R., MITCHUM, R. M. & THOMPSON, III, S. 1977. Seismic stratigraphy and global changes of sea level. *In*: PAYTON, C. E. (ed.) *Seismic Stratigraphy—Applications to Hydrocarbon Exploration.* American Association of Petroleum Geologists Memoirs, **26**, 2.4.

VAN HOUTEN, F. B. 1980. Mid-Cenozoic Fortuna Formation, northeastern Tunisia.: record of late Alpine activity of North African cratonic margin. *American Journal of Science*, **280**, 1051–1062.

YAICH, C. 1992. Dynamique des facies detritiques Oligo-Miocene de Tunisie. *Journal of African Earth Science*, **15**, 35–47.

ZIEGLER, P. A. 1988. Post-Hercynian plate reorganisation in the Tethys and Arctic—North Atlantic domains—Triassic and Jurassic rifting. *In*: MANSPEIZER, W. (ed.) *Developments in Geotectonics*, **22**, Elsevier, 711–755.

Critical factors in the exploration of an Atlas intramontane basin; the Western Hodna Basin of northern Algeria

KARIM MEKIRECHE[1], NORDINE SABAOU[2] & REDA-SAMY ZAZOUN[2]

[1]*D.E.S., Division Exploration, Sonatrach, Rue Capitaine Azzoug, Côte Rouge, A6000, Algiers, Algeria*

[2]*Direction de Geologie, Centre de Recherche et Développement, Sonatrach, Avenue du 1er Novembre, 35000 Boumerdès, Algiers, Algeria*

Abstract: The acquisition and evaluation of a substantial integrated surface outcrop and well database over the western Hodna Basin allows the identification of three critical factors (reservoir quality, source maturity and timing and hydrodynamic regime) to which well failures to date can largely be attributed. Reservoir quality is variable in Cretaceous sandstones, because of a high degree of quartz cementation, but improves to the south. Reservoir quality in Eocene limestones is related to the development of vuggy porosity and can now be mapped out from well control. Potential Cretaceous source rocks lie at moderate to high degrees of maturity, with expulsion probably preceding the Miocene phases of structure development. Tertiary palaeostress reconstructions from field studies indicate four main structural phases: (1) Late Cretaceous N–S to NW–SE oriented compression; (2) Oligo-Miocene distension; (3) N–S oriented Miocene (pre-Langhian) pull-apart; (4) Langhian compression related to the emplacement of the Tellian nappes. Seismic analysis illustrates some classic late-stage inversion structures. Organic matter seen in outcrops and cores within the Thanetian–Ypresian and lower Lutetian sections is composed mainly of type II kerogen and varies from undermature to marginally mature, leading to the development of shows in many wells that helped in the past to stimulate continued exploration. Study of the hydrology of the formation waters in drilled wells allows large areas of likely reservoir flushing to be delineated. Study of the three critical factors allows a high grading in terms of remaining exploration potential. Based on the interpretations derived from structural, palaeogeography, diagenetic and hydrodynamic studies, the basin can be divided into three areas, which are ranked on the basis of their prospectivity. Each of the factors also needs to be critically assessed in analogous regions of the Atlas, in which such good geological control may not exist.

The area reviewed in this paper covers the western section of the Hodna Basin, a small intermontane basin within the Atlas Mountains of Western Algeria (Fig. 1). The Hodna Basin and Mountains are located south of the Tellian nappe front and are bounded to the south by the inversions of the Saharan Atlas. The study area covers Blocks 139 and 105 within Algerian District 10, an area of over 7540 km^2.

Exploration in the area commenced in 1953–1954 following the discovery of the Oued Gueterini field in the Tellian nappes to the west, reservoired in Eocene carbonates. At this time, SN Repal focused on the Eocene in nine relatively shallow wells, all of which were dry. At a later stage, two wells were drilled to Cretaceous objectives (CHM and CH-1), but these were also dry. A second stage of exploration drilling was conducted in the early 1980s, when Sonatrach drilled three deeper wells to Cretaceous objectives (ID-2, KEF-1 and DRW-1), again without success. No wells have been drilled recently.

Our investigation is based on the results of the wells listed above, seismic profiles and outcrop investigations. Previous studies that are integrated into this analysis include geological mapping (Cruys 1953; Kieken 1962; Baldini 1963, 1966) and regional reviews (Savornin 1920; Drooger 1952; SN Repal 1952; Caire 1953; Emberger & Magné 1953; Guiraud 1973).

Stratigraphy

The stratigraphy of the region (Fig. 2) has been established through the compilation of field sections and from well penetrations. Thicknesses of different stratigraphic units have been estimated from the compilation of cross-sections based on field observations (Fig. 3) and well penetrations. The main field sections analysed are those at Djebel Djeddoug and Dokkara (Figs 3 and 4).

The stratigraphy shown in Fig. 2 is a synthesis of these data points. The pre-Aptian section is open marine and contains no significant potential reservoirs. The Aptian is represented by interbedded thick quartzitic shallow marine sandstones and dolomites, with minor marls. The overlying Albian contains shallow marine

MEKIRECHE, K., SABAOU, N. & ZAZOUN, R.-S. 1998. Critical factors in the exploration of an Atlas intramontane basin; the Western Hodna Basin of northern Algeria. *In:* MACGREGOR, D. S., MOODY, R. T. J. & CLARK-LOWES, D. D. (eds) 1998. *Petroleum Geology of North Africa.* Geological Society, London, Special Publication No. 132, 423–432.

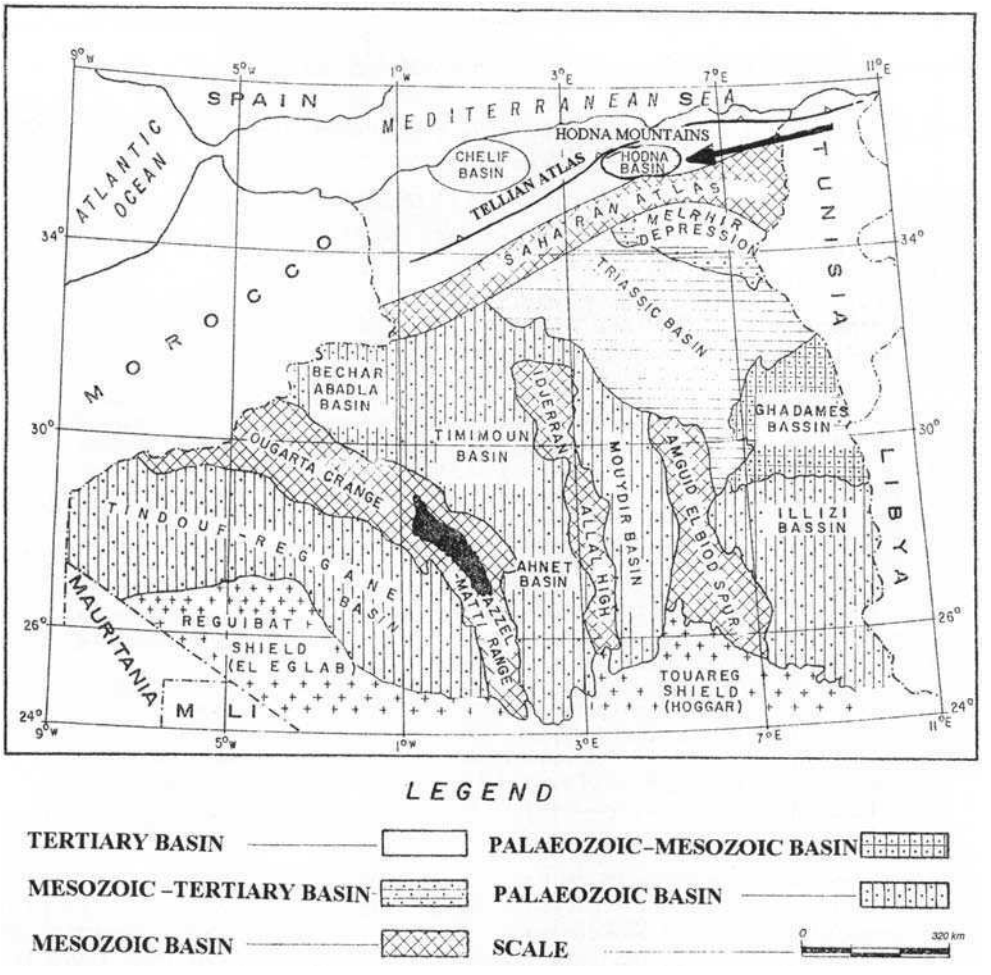

Fig. 1. Location map of the Hodna Basin and Mountains.

sandstones at the base, passing up into the Vraconian marls and shales. The Cenomanian begins with a sequence of grey–green marls interbedded with glauconitic limestones. These pass upwards into dolomites and black limestones in the late Cenomanian and Turonian. The Coniacian and Santonian are represented by gypsiferous marls and the Campanian by green marls and argillaceous limestones. The Cretaceous series is capped by Maastrichtian shelly limestone and an alternation of marls and reefal limestones. Facies throughout the Cretaceous are indicative of shallow-water deposition, as would be typical for the passive margin setting predicted at this time.

The Tertiary section ranges in age from Danian to Miocene. The Danian facies are similar to those of the underlying Maastrichtian. The Early Eocene contains marls, siliceous limestones and a phosphatic breccia bed, whereas the Late Eocene is composed of marls and gypsiferous shales. The Eocene–Oligocene boundary is marked by an unconformity and abrupt facies change, with the Oligocene composed of red continental sandstones with some calcareous beds and marls. The Miocene section, where present, is composed of sandstones in the east of the area and gypsiferous marls in the west.

These facies suggest that the region lay in a shelfal position at various points in its geological history (Kieken 1974), with sedimentation generally keeping pace with subsidence, except in periods of tectonic activity. Sedimentation and palaeogeography in this region of the Atlas

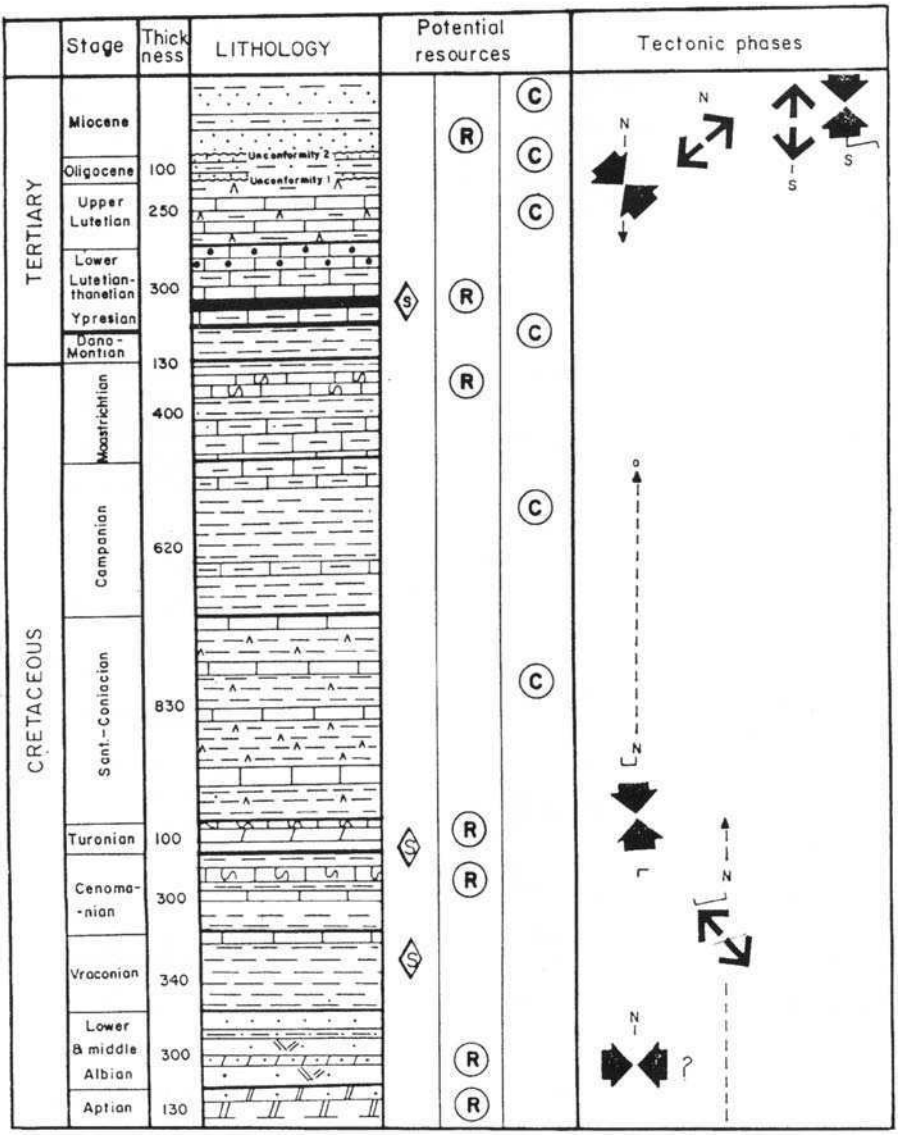

Fig. 2. Summarized statigraphy of the Hodna region, as established from outcrop geology and well penetrations. The main reservoirs (R) and source rocks (S) are labelled as are the main structural phases identified in this study. C, seal; bold arrows, $\sigma 1$; fine arrows, $\sigma 3$.

from the Triassic onwards are believed by Guiraud (1973) to have been heavily conditioned by the basement structure.

Structural analysis

Structural analysis of the basin combines the results of seismic analysis, which is concentrated on the Hodna Plain (Fig. 4), with fieldwork in the Hodna Mountains. Figure 3 illustrates sections constructed in the Tarmount area of the Hodna Mountains (location shown in Fig. 4). This area can be subdivided into four structural units as illustrated in cross-section view in Fig. 3 and map view in Fig. 4: (a) the Koudiat Griga–Mechat-El Garf Ridge, an anticline oriented ENE–WSW; (b) the Ras-El-Ma syncline, separated from the above by faults and bounded to the north by flexures; (c) the Djeddoug Mono-

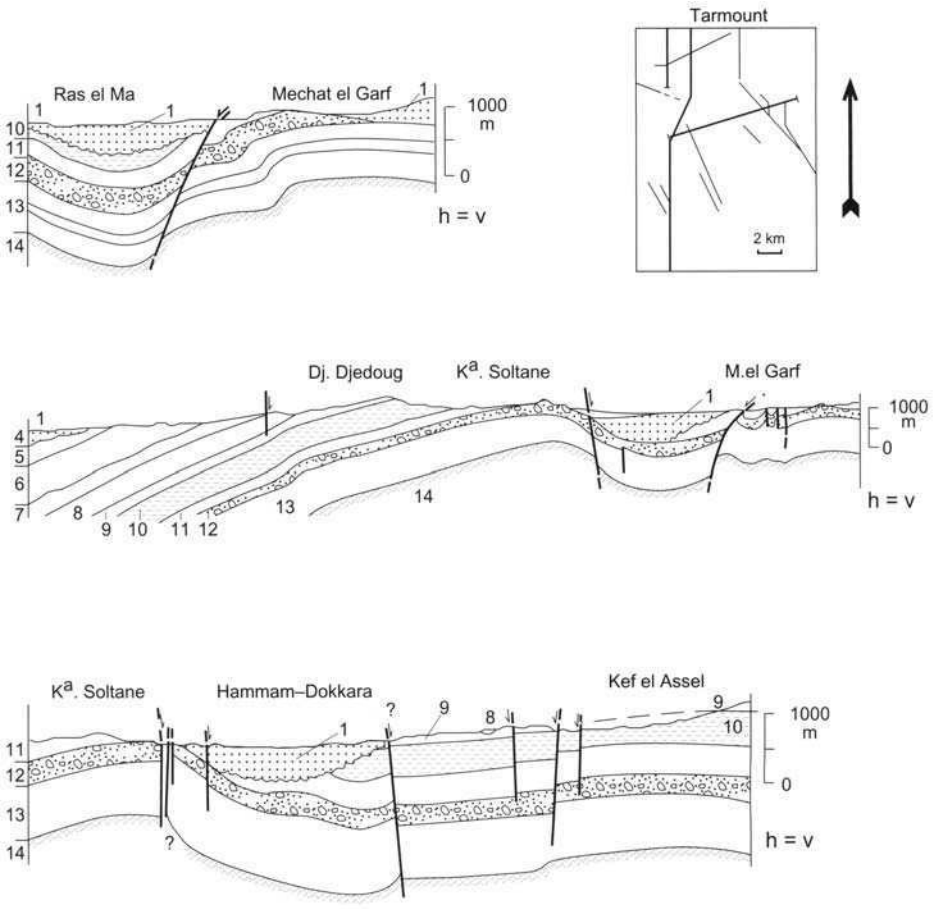

Fig. 3. Geological cross-sections constructed from field studies in the Tarmount region. The main structural elements discussed in the text are labelled. (For location, see Fig. 4.) Q, Quaternary; 1, Lower Miocene; 2, Upper Lutetian; 3, Lower Lutetian; 4, Paleocene; 5, Maastrichtian; 6, Campanian; 7, Santonian-Coniacian; 8, Turonian; 9, Cenomanian; 10, Vraconian; 11, Lower and Middle Albian; 12, Barremian; 13, Neocomian; 14, Upper Jurassic.

cline, which lies on trend with, and represents a continuation of the Koudiat–Soltane Ridge; (d) the Hamman–Dokkara Graben, bounded by strike-slip faults.

Seismic analysis shows that the sedimentary section present in outcrop in the Tarmount area dips steadily to the south into the basin and can be subdivided into three sequences, bounded by unconformities (Figs 5–7). Two Miocene sequences are recognized, with the younger sequences sometimes lying directly on eroded Cretaceous. The Oligocene forms a thin unconformity bounded sequence whereas the thick Eocene–Cretaceous section appears conformable throughout. In Fig. 6, the various unconformities are less well marked, with all sequences monoclinally dipping into the basin. The fault-bounded structure in the centre of Fig. 7 is a relatively small example of the inversion structures that are seen throughout the basin. Thickening of the Mesozoic and Oligocene section into an original half-graben can be recognized, followed by reversal of movement of the fault in the Miocene. Such late stage inversion features were tested unsuccessfully by many of the wells in the region (e.g. ID-2). The inversion seems to have been selective, with only the major faults affected. Such traps are now suspected to have formed too late to contain hydrocarbons, certainly from Cretaceous sources (see discussion on source below).

Structural analysis from these field observations tied to the seismic interpretation permits the identification of four discrete tectonic

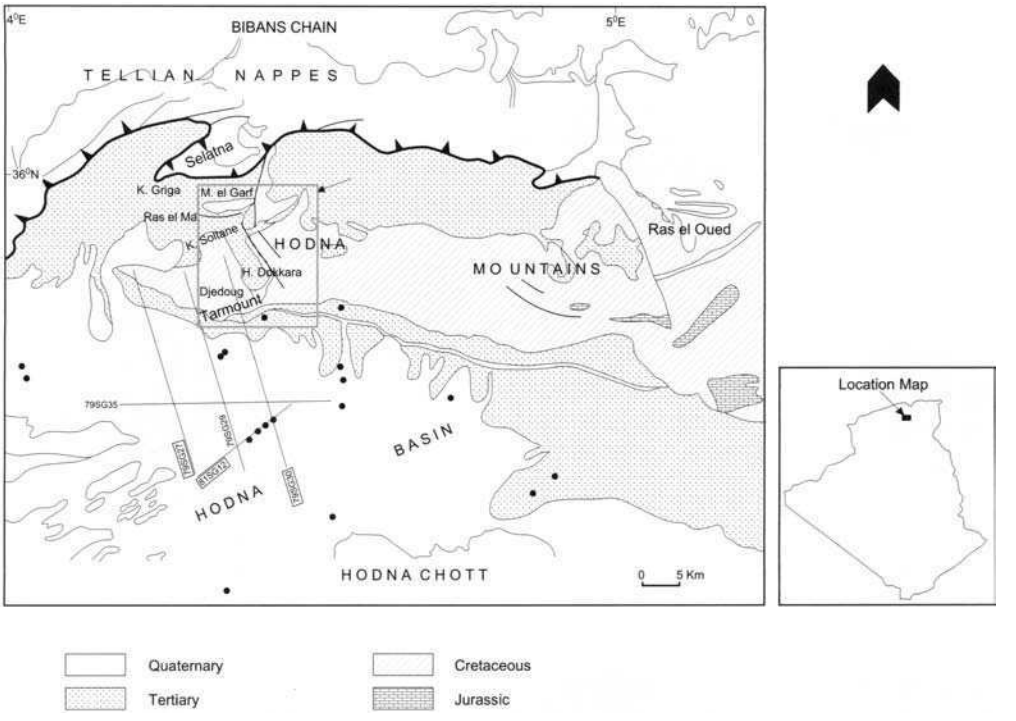

Fig. 4. Location map of the study area, showing main structural elements, and location of field sections and seismic sections shown in this paper.

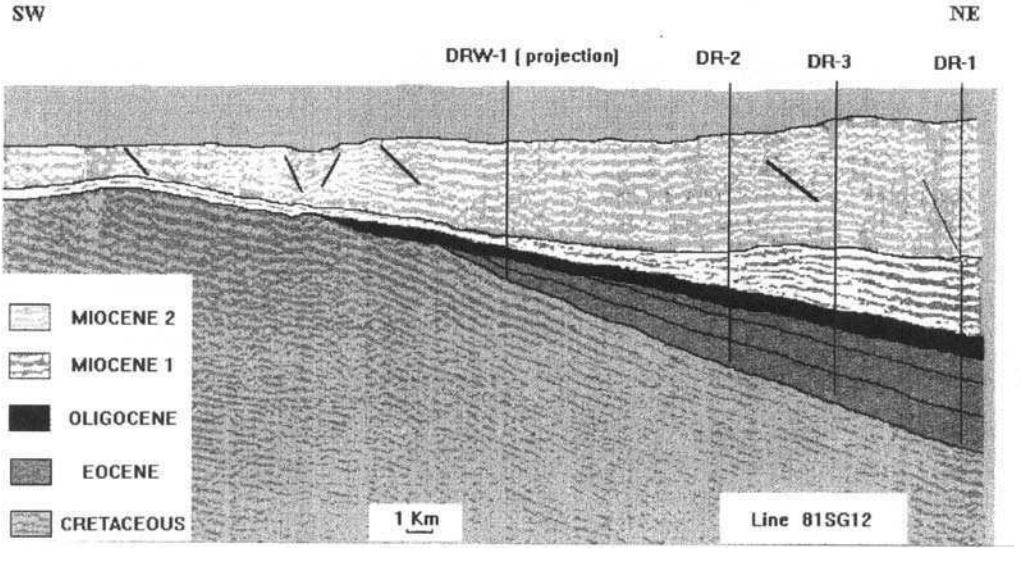

Fig. 5. Interpretation of Seismic Line 81SG12, located on the Hodna Plain and tying the Draa Ben Rabah wells. (Note the presence of a significant unconformity at the base of the Oligocene.)

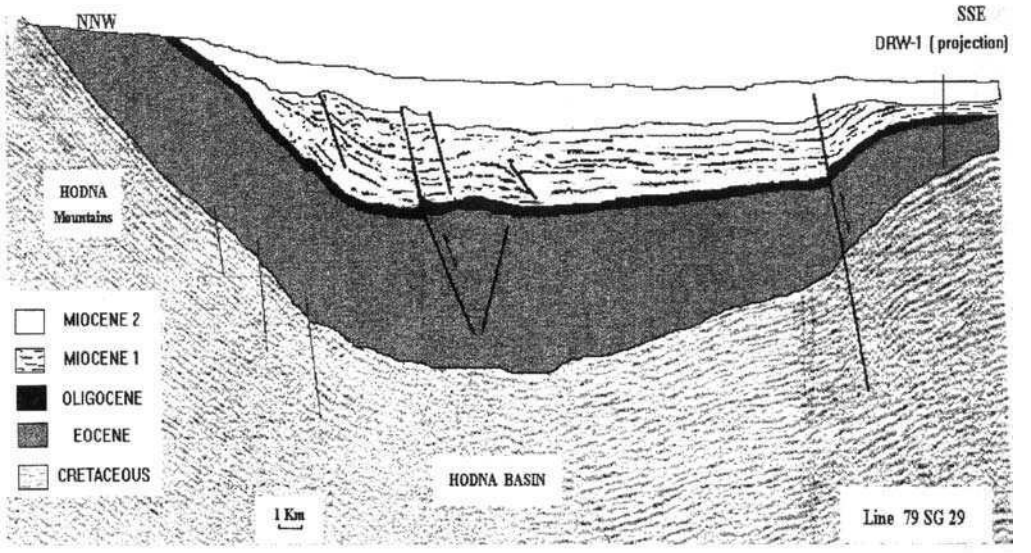

Fig. 6. Interpretation of Seismic Line 79SG29, tying the main depocentre on the Hodna Plain to the area of outcrop studies in the Tarmount area of the Hodna Mountains.

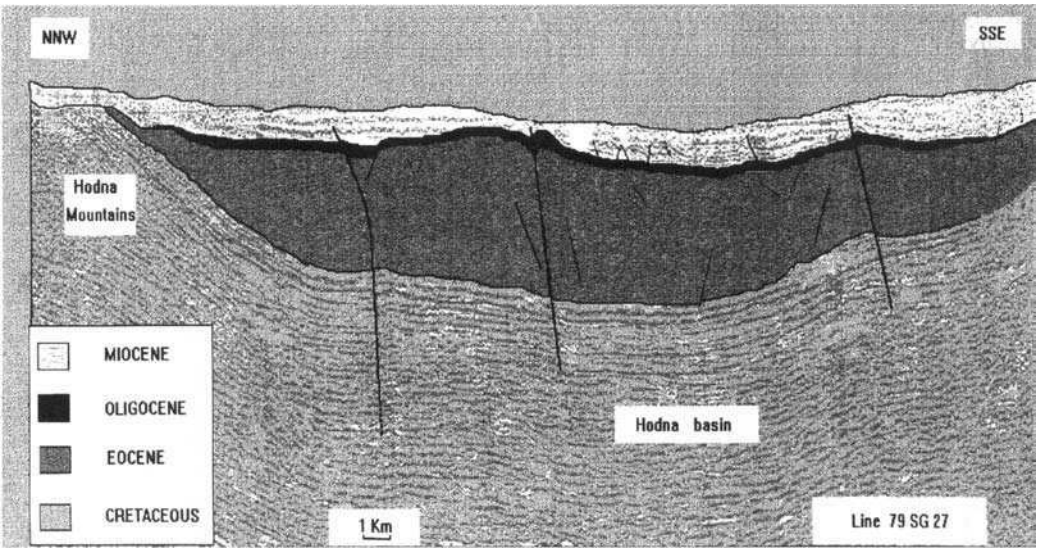

Fig. 7. Interpretation of Seismic Line 79SG27. (Note the small inversion structure in the centre of the profile.)

phases. The older events are frequently masked by younger lineaments, particularly those related to the Tellian (Miocene) phase:

(a) A Late Cretaceous (Turonian–Maastrichtian, Fig. 2) compressive episode, typified by N–S to NW–SE directed compression and E–W to NE–SW oriented structures, examples of which are the Koudiat–Soltane and Kef-El-Assel anticlines (Figs 3 and 4). Significant strike-slip movement is interpreted on these features. This event ties regionally to the Atlasic phase (Guiraud 1973).

(b) A Late Oligocene–Aquitanian extensional episode, with extension directed WSW–ENE to E–W. The N–S oriented Hamman–Dokkara Graben originated at this time.

(c) A further extensional period before the Langhian (Early Miocene), with a N–S directed

stress. An example of a structure originating at this time is the E–W trending Mechat–El Garf normal fault (Figs 3 and 4).

(d) An Early Langhian (Mid Miocene) period of compression, directed N–S to NNW–SSE, causing inversion of pre-existing normal faults. This event occurred synchronously with the emplacement of the Tellian nappe to the north and led to the formation of many of the anticlinal structures within the basin.

Many of the structures visible in seismic data in the region may have developed in multiple phases,for example, been initiated in the Santonian and accentuated in the Miocene.

Reservoir quality

Potential reservoirs occur in the form of coarse clastic formations in the Apto-Albian and Oligocene and of carbonates at various levels in the Late Cretaceous and Eocene. Most of these reservoirs are extensive with the development of reservoir quality the critical concern. The analysis of reservoir potential is based on original petrophysical analyses by SN RÉPAL in 1954, core analyses from a more recent set of Sonatrach wells (1984) and later work by our team on computerized porosity estimation though point counting on thin sections. The reservoir rocks analysed come from the Cretaceous (Aptian–Maastrichtian) section and Tertiary (Eocene) sections. The emphasis in the discussions here will be on the thickest reservoirs of the Apto-Albian sandstones and Eocene limestones. Younger reservoirs such as the Oligocene sandstones have not been studied, as these are unlikely to be sealed. The carbonate porosity classification used below is that of Choquette & Pray (1970).

Cretaceous reservoirs

The sample database available on Cretaceous reservoirs, particularly older levels, was relatively sparse compared with that on Eocene reservoirs. It is thus more difficult to confidently identify trends of porosity variation.

Thick dolomites occur in the Aptian (Fig. 2). During the early stages of dolomitization, dolomicrite was formed, which was later altered diagenetically to crystalline dolomites and dolosparites. Primary porosity is often enlarged and enhanced by leaching and through dolomitization: porosity types identified include vuggy, fracture and intercrystalline. Oil has been observed seeping from cores at this level in well ID-2 (Fig. 4), where porosity of these types ranges up to 8%.

The Albian sandstones were deposited in a shallow marine setting. These sandstones are present over a wide area and can reach considerable thicknesses (e.g. 180 m gross in ID-2). Both thicknesses and average porosities generally increase from north to south across the area, porosities rising from 3—6% below the Tellian nappe to 19% in KEF-1 and 20% in DRW-1. Much of this porosity is secondary, formed through dissolution of clay cement, with most of the primary porosity having been destroyed by compaction and quartz cementation. The porosity trend may be indicative of a trend of increasing burial and palaeoburial to the north, and suggests that exploration at this level should be focused towards the south. No shows have been observed at this level in any of the wells.

Cenomanian limestones show porosities ranging from 3.4% in DRW-1 to 6% in ID-2 and to 8% in KEF-1. Porosity is again largely formed through dissolution. Bioclastic limestones and dolomites of Turonian age also show low dissolution-derived porosities, while the overlying Senonian (Coniacian–Maastrichtian) contains bioclastic and oolitic limestones, with low fracture and mouldic porosities, averaging around 3%. These intervals clearly have very little reservoir potential, unless fractured.

Eocene reservoirs

The Lower Eocene (Thanetian–Ypresian–lower Lutetian) limestone reservoirs have been given greatest attention in the exploration of the region because of their frequent oil staining. The Eocene is the productive level in the Oued Gueterini field in the Tellian Atlas, 70 km to the northwest. These limestones also show the highest porosities and permeabilities of any of the potential reservoirs in the region. Porosity is most frequently of intercrystalline, interparticle and vuggy types.

Figure 8 illustrates the variations in porosity and permeability observed across the region within the Lower Eocene limestones. The highest porosities are seen in wells on the SE flank of the basin, within the Draa-ben-Rabah area (DR-1–2–3). Average values here are around 15%, with maxima ranging up to 38—40% in DR-2 and DR-3. Maximum permeability is 195 mD in DR-2. Porosity and permeability both fall off northwards and eastwards to more typical average values for the region of 5—10% porosity and 1—2 mD (Fig. 8), figures which would not

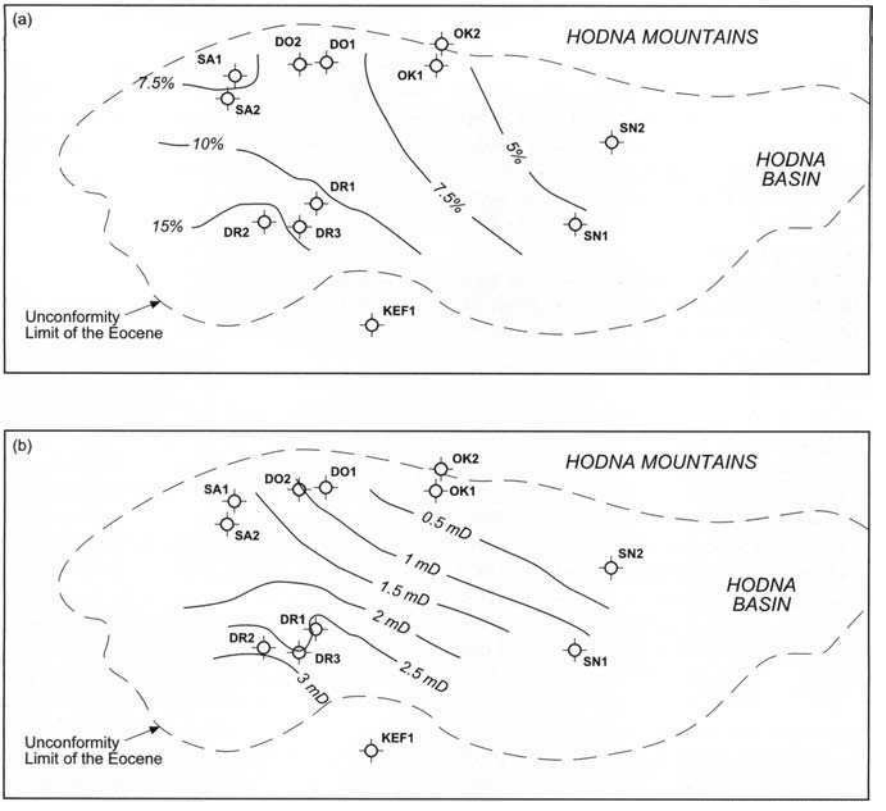

Fig. 8. Isoporosity (**a**) and isopermeability (**b**) contours across the western Hodna Basin based on porosities observed in cores, logs and thin sections from the various wells. (Note the consistent improvement in reservoir quality towards the southwest.)

give economic oil reservoirs unless the limestones were fractured. The lowest values occur in the eastern well SN 2, where porosity falls to 3—4%. Reasons for the areal variation in porosity are currently unknown.

High porosities are also locally seen within the phosphatic limestones of the Thanetian (maximum of 43% porosity at DO-2).

Source maturity and timing

As mentioned above, although there have been no discoveries in the study area, oil has been observed seeping from numerous Early Eocene limestone cores and also locally within Cretaceous limestones. Organic-rich intervals are present at a number of levels in the sequence, particularly in the Cenomanian–Turonian, possibly also in the Vraconian, and within the Thanetian–Ypresian phosphatic limestones. The Cretaceous source beds tie to highstands and oceanic anoxia, whereas the latter, by virtue of their close association with phosphatic deposits, are probably associated with upwelling events (Macgregor, 1996). These interpretations suggest that the development of these source rocks will be thin but widespread, as is observed. The Cenomanian–Turonian source rock reached thicknesses of 20—40 m and the Eocene source 10—20 m.

The Cretaceous sources appear to be mature to overmature. The vitrinite reflectance value of 0.6% at ID-2 probably ties to late Cretaceous burial; higher levels of maturity are apparent in wells to the north and northeast. Cretaceous sources may therefore expel much of their oil at an early stage relative to the development of traps, particularly those of Miocene origin. The Miocene-aged inversion structure drilled by ID-2 is an example of a closure whose development probably post-dates periods of hydrocarbon generation from Cretaceous sources. Exploration for Cretaceous sourced oil perhaps needs to be

focused on traps formed during the earlier (Late Cretaceous) structural phases identified in this paper.

The Eocene source beds, which by stratigraphic association are the probable source of most shows at this level, are typically submature to marginally mature (vitrinite reflectance Ro. $<0.6\%$). The shows that have been encountered in the Eocene may thus be indicative of a limited quantity of early generation products. Maturation of this source may well be tied to local Miocene depocentres or to thrust loading, as in the Tellian nappe area to the north (Macgregor 1996). Total organic carbon (TOC) in the Eocene ranges from 1.7% at OK-2 to 4.9% at SA-2. Because of the generally low degree of maturity, the quantitative potential associated with this source may, however, be very limited.

Further work remains necessary to fully understand the geochemistry of the various source rocks and to more adequately predict patterns of migration, re-migration and hydrocarbon destruction.

Hydrodynamic regime

Another important factor is likely to be hydrodynamic flushing, as fresh water (salinities less than 50 g/l) has been observed to have invaded most drilled Eocene sections on the flanks of the basin, particularly the northern flank. This indicates the existence of a hydrodynamic gradient that could have flushed low-relief oil accumulations. Salinity however increases into the basin, reaching maxima of 96 g/l at SA-2 and 130g/l at DR-1.

Conclusions

Previous disappointing well results in the western Hodna Basin can be rationally explained by a combination of three critical factors: reservoir quality, source maturity and timing, and hydrodynamic regime. Analysis of the geochemical, structural, stratigraphic, diagenetic and hydrodynamic controls on these three factors allows a high grading of the different parts of the basin, as summarized in map form in Fig. 9. The southwestern corner of the basin is rated of most interest, showing high porosities in Eocene reservoirs and being distant from areas of probable hydrodynamic flushing. The critical factor at Eocene level would appear to be the frequent immaturity of the Eocene source level. Prospectivity is assessed to fall off northwards and eastwards as reservoir quality at the key

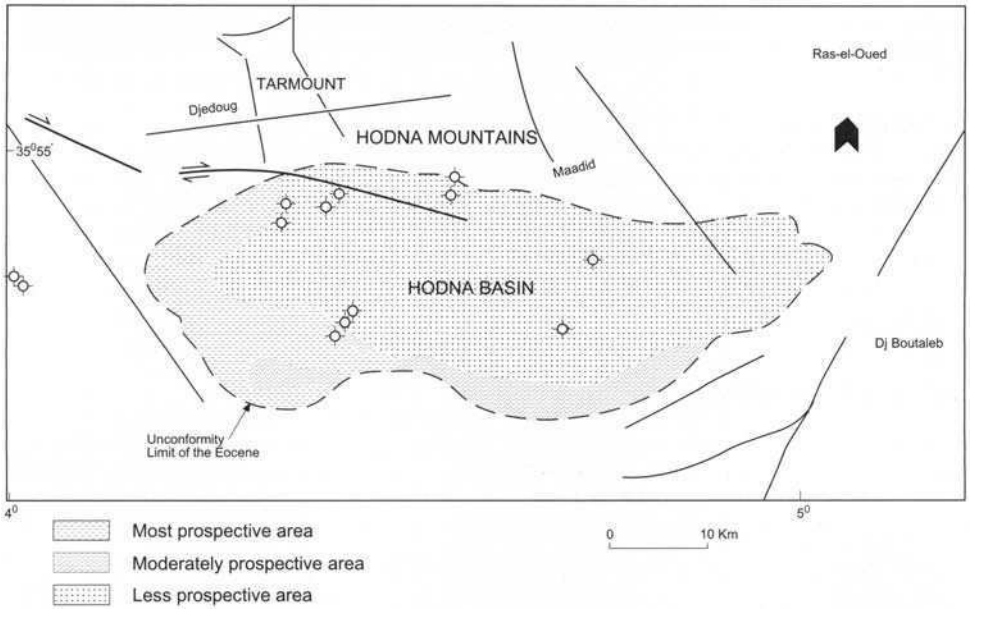

Fig. 9. Ranking of the prospectivity of the various regions of the Hodna Basin based on the analysis summarized in this paper. The SW flank is the most highly ranked, because of high Eocene reservoir quality and low probability of flushing.

Eocene level diminishes, and additionally falls towards the flushed northern flank of the basin, which is the most lowly ranked area. Areas of severe uplift and erosion, and therefore of possible reservoir breaching, such as the Hodna Mountains, are also poorly rated.

Cretaceous reservoirs such as the Albian sandstones remain conceivable objectives in this area, with reservoir quality and timing of sourcing relative to trap formation as critical factors. The most highly graded areas lie in the south of the area, where reservoir quality seems highest. A search for traps associated with the Triassic–Maastrichtian compressional phase may pay dividends here.

Further work is necessary to understand other key aspects of the prospectivity of the Hodna Basin, including source rock studies, more detailed analysis of hydrodynamic effects, and high-resolution seismic surveys to locate more favourable prospects than those drilled to date. The factors identified in this paper are likely to be of equal importance in exploring other parts of the Atlas fold belt and therefore need to be more carefully considered than in the past when making drilling decisions.

References

BALDINI, P. 1963. *Etude géologique de la feuille de Tarmount (1:50000)*. Permis de Djedoug-Hodna. SN REPAL Internal Report.

—— 1966. *Notice explicative de la carte géologique de Tarmount (1/50000)*. Service Géologique de l'Algerie

CAIRE, A. 1953. *Allochtone Sud-Telliene et Autochtone Présaharien au Nord du Hodna*. SN REPAL Internal Report.

CHOQUETTE, P. W. & PRAY, L. C. 1970. Geologic nomenclature and classification of porosity in sedimentation carbonates. *Bulletin, American Association of Petroleum Geologists*, **54**(2), 207–250.

CRUYS, H. 1953. *Study of the geology of the regions of Tocqueville and Bordj-R'dir* (in Dutch). Doctoral thesis, University of Utrecht.

DROOGER, C. W. 1952. Problèmes structuraux des Monts du Hodna. *Géologie en Mijnbouw, Leiden, New Series*, **8**, 291–297.

EMBERGER, J. & MAGNÉ, J. 1953. La terminaison en biseau du faciès à Nummulites de l'Yprésien à l'ouest de l'Oued Ksob, départment de Constantine (Algérie). *Comptes Rendus de l'Académie des Sciences, Paris*, **236**(21), 2091–2093.

GUIRAUD, R. 1973. *Evolution post-Triasique de L'Avant Pays de la Chaîne Alpine en Algérie d'après l'étude du Bassin du Hodna et des Régions Voisines*. Doctoral thesis, University of Nice–Avignon.

KIEKEN, M. 1962. *Notice explicative de la carte géologique de M'Sila (168), 1:50000*. Service Géologique de l'Algérie

MACGREGOR, D. S. 1996. Hydrocarbon systems of North Africa. *Marine and Petroleum Geology*, **13**(3), 329–340.

SAVORNIN, J. 1920. *Etude géologique de la région du Hodna et du plateau Sétifien*. Bulletin de la Service Conte Géologique de l'Algérie, 2ème Séries, **7**.

S.N. REPAL. 1952. *Régions Sud-Telliennes et Atlas Saharien*, Publication XIXème Congrès Géologique, International Algérie, Monographies Régionales, 1ère Série, **20**.

VILA, J. M. 1980. *La Chaîne Alpine d'Algérie Orientale et des confins Algéro-Tunisiens*. Doctoral thesis, University of Paris.

Index

Page numbers in *italics* refer to Figures or Tables.
Small variations in the transliteration of North African place names into American/English/French systems has not affected the alphabetical position of the names in the index. The most popular form of spelling is used in this list.